

**“In the Trenches”
at the University of Alberta**

Below

TJ
140
B45
A3
1996

ARCHIVES



EX LIBRIS
UNIVERSITATIS
ALBERTÆNSIS

97-25



**“In the Trenches”
at
the University of Alberta**

**by
Donald G.Bellow, PEng, FCAE, FCSME
Professor of Mechanical Engineering (1963-1996)**

for Jonathan and Denise

*Dedicated to my wife Jean whose love and understanding is as much responsible as
anything for the achievements that I take credit for in the pages that follow.*

1996

TABLE OF CONTENTS

	Page number
1. Introduction	1
2. The Early Years	1
3. The Department of Mechanical Engineering	8
4. Into the 70's	9
5. Equipment	9
6. Early Research Activities	10
7. International Industrial Research	11
8. Administration	13
9. Teaching	14
10. 75th Anniversary of the Faculty of Engineering	15
11. Life under the Deans	16
12. Out of the Trenches	18
13. Presidents of the University of Alberta	19
14. Concluding Remarks	27
15. Appendix I: APEGGA and CCPE	28
16. Appendix II: Honours and Awards	30
17. Appendix III: Graduate Students Supervised	30
18. Appendix IV: Letters	31
19. Appendix V: Newspaper Articles	32
20. Appendix VI: List of Technical Publications	33

INTRODUCTION

This is an account of what I have achieved in my career as an engineer (working at the University of Alberta), starting from my graduate student days which began in 1958, to when I was given an academic position in 1963, and to the time of my retirement from the U of A in August 1996. My intended readers were to be my immediate family and a few close friends who might be interested. I principally wanted my family to know how their sacrifices had enabled me to pursue the career that I followed, because at the time, it was often uncertain even in my own mind where I was heading. However, as I began to organize this review it occurred to me that I was in a unique position to observe and comment on the changes that have happened at the University over the past 38 years of my association with it. As I begin to plan the next phase of my life in retirement I am leaving the University at a time when it too is entering a new phase, the outcome of which is not yet clear, but will be different from what it was during the past four decades.

So what follows is a review of my time from the formative years of the Department of Mechanical Engineering through to its maturing years. And, having spent sixteen years in administration, the last seven years among the upper echelons of University Hall, I would be remiss in not making a few observations on how our University was run (and continues to be run) far from "The Trenches".

THE EARLY YEARS

When I first arrived on campus in 1958 there were individuals already on staff who would affect my career and the direction it would take, and who would be influential in shaping the Department of Mechanical Engineering. At the time, none of this was apparent. In 1958 there was no Mechanical Engineering Department at the University of Alberta although there were people who were working towards its formation. But before describing the later developments in the formation of the Department, and my view of the University from "The Trenches", let me recount how I came to be involved and what brought me to Alberta in the first place.

I was born in Winnipeg on Aug. 5, 1931.¹ I remember my early years in Winnipeg as being cold in winter and being hot in the summer, and forever wandering away from home and getting lost, and then being brought home in a Police Cruiser. After I had spent only a few months in kindergarten in Winnipeg my parents made a move to the B.C. Coast.

I travelled with my Mother in September 1937 since my Dad had gone out to Victoria in 1936 to be with his ailing father who had suffered a serious stroke. My mother was left with the chore of closing down the house in Winnipeg, selling off all the furniture and saying good-bye to her friends and relatives. Although I had just turned six my mother conspired with me to say that I was only five so that she could get a reduced train fare for me. When I was asked how old I was, as instructed by my mother, I replied that I couldn't tell them until the train arrived in Vancouver. The train ride was one which I will remember with great fondness. Everyone was so kind and friendly and there was so much to see as the prairie landscape with its golden fields of wheat moved past our window seat. My mother paid the porter 25 cents so we could sit out in the vestibule of the last car for an hour. This was travelling at its best!

Grandfather Bellow passed away in 1937 but in the meantime my father had found a good job in a woodworking mill in Victoria. After being shuttled around to a couple of schools, and we had been living in an equal number of rooming houses, my parents bought a house in the area of Tillicum Road and Gorge Road (73 Vincent Avenue), and we settled into living "on the Coast". Everything seemed to begin to fall into order as my father liked his job, which paid twice as much as he was

¹ My father, Walter William Bellow, was born in 1899 in Winnipeg. His father William Henry Belleau was born in Montreal and his mother, Edith Lee was born in England. My paternal grandfather anglicized the spelling of his name because he thought it would help him in the book binding business that he had established in Winnipeg. My mother, Lillie Christina Hnappdal, was born in Winnipeg in 1905 to Icelandic parents.

getting in Winnipeg, my Grandmother doted on me, and I started taking violin lessons and had performed my first solo at a concert for which my performance was lauded in the newspaper.² Also, I had the Nash girls next door as friends whom I had organized into digging a swimming pool (which was understandably never finished because it was located on solid rock) out in a vacant lot behind our house. But when war was declared in 1939 there was considerable fear on the West Coast that the Japanese would attack North America so my mother urged my father to look for work in Vancouver where she felt it would be safer from attack. My mother believed that if the Japanese wanted they could sink Vancouver Island anytime they wanted! So we relocated, but this time my father bought a City lot for \$300 and contracted to have a house built for \$5000 and we settled in on the south side of Kerrisdale (1618 - 60th Ave.) where I went to Maple Grove school from grades three to six (by the time I had reached grade three I had been in five different schools in three different cities). In Vancouver I attended Point Grey Junior High from grades seven to nine and at Magee High School from grades 10 to 13.

At Point Grey and at Magee I played the violin in the school orchestras. I had a very good violin teacher by the name of Henry Smythe (he was the principal viola player in the Vancouver Symphony) who prodded me to great heights in musical achievement. I placed first in Royal Conservatory examinations and was admitted into the Vancouver Junior Symphony. But the discipline exercised by my music teacher began to turn me off serious violin playing. As I was now earning money delivering newspapers, I bought a used clarinet for \$50 and signed up to take lessons. But the clarinet teacher was critical of my lack of practice and I quit after only five lessons. In Point Grey Jr. High there was a concert band led by the world famous (in Vancouver at least) conductor, Arthur Dalemont. He had taken boys bands all over the world in the 1920's and 30's. The only requirement for joining his band at Point Grey was that you had to have your own instrument and be able to turn up for practice at 7:30am. So with five lessons behind me and my own clarinet I began to take an interest in music once again and experienced the thrill of playing Big Band jazz which was popular in the 1930's and 40's. At Magee, Harry King was the music teacher, who had played trumpet with the Harry James Band, so I was further motivated. To carry this musical digression to its logical end I should say that when I reached University a few of us formed a jazz band and we hired ourselves out to fraternities and other groups. This brought in a few dollars each week, but playing the clarinet for a solid four hours each night left me exhausted for studying, and convinced me that I should seek a career other than one in music. By this time I had also learned a few basic chords on the piano, so whenever the occasion warranted it I would sit down and play the piano. I still do this but it is now for the aged in my mother's nursing home. This audience is appreciative of the musical interlude and most forgiving of my mistakes.

My first years at the University of British Columbia were challenging. I wanted to take engineering but my high school counselor had advised me against it. Instead I enrolled in a pre-architecture course but I soon realized that I had neither the artistic talent nor the ability to appreciate the artistry of others. I couldn't tell good art from bad art. Despite the encouragement of my instructors, B.C. Binning and Lionel Thomas, both of whom have works hanging in the National Gallery in Ottawa, I felt I was in the wrong place. So I decided to make a go of it in engineering. I had an advantage in that I liked math and I could get good marks in this subject. With a lot of hard work I got by the first couple of years and once into third year engineering I even managed to get some marks in the 80's. Part of the reason, or credit, for this was that my folks moved to a new house in Cloverdale and after unsuccessfully trying to commute for four months back and forth to UBC, I moved into the Acadia Camp dormitories on campus. This enabled me to concentrate on my studies instead of spending 2-3 hours per day driving to and from school. Also, and by no means least, I met my future wife Jean, and for the first time had a steady girl friend.³ Jean and I met on a blind date where a Sigma Phi Delta fraternity brother, Bill McCormick (he later became President of Sylvania Electric),

² I credit my father for whatever musical talent that I have. He was a top notch banjo player and performed in the early days of radio in Winnipeg during the Depression and in a dance orchestra at Winnipeg Beach in the summer. He also worked in my Grandfather's (Hnappdal) coal and wood yard and later in a mill which made butcher blocks.

³ Jean Marion Daye was born in a farm house near Camrose, Alberta, one of five children. Her father, Hugh Frederick Day was born in Chipman New Brunswick and joined the Canadian Expeditionary Force when he was 15 and fought on the battlefields of Europe during World War I. Upon returning to Canada he worked in logging camps in British Columbia where he met his wife Ivy Irene Walton. Jean's mom was born in Dauphin Manitoba to parents who had immigrated from England. Jean and her folks, along with two brothers and two sisters, moved to Vancouver in 1940.

had arranged to take out Jean's sister to a "sweater party" and said his date had a sister who was a nurse and had agreed to go along. These were the kind of parties engineers liked to attend, especially with nursing students. Jean was in her second year of nursing at St. Paul's Hospital in Vancouver. I don't think I made a very good impression on this first date because it was the first time Jean had ever gone into a beer parlour, which made her very nervous because she was under age, and I managed to put my truck into the ditch. But to my surprise, she went out with me again, and as they say, the rest is history.

The 1950's were good times to be an engineering student and I had no trouble getting summer jobs. The one I liked the most was being foreman on a weed-killing train during which, over three summers, I travelled every railway track in B.C., Alberta and Saskatchewan. I would have done this for a fourth year but the Chairman of the Department of Mechanical Engineering at UBC, Prof. W.O. Richmond, told me that if I didn't get a job in a factory or some work other than on the railroad, I would not get my degree. This was a faculty regulation. Without any difficulty I got a job at Westminster Paper. The downside of this was that it included a lot of shift work, but the upside was that I got to go out with Jean every weekend. Also, I learned more than if I had spent another summer on the railroad. Professors are always right!

My final year at UBC was most enjoyable. My marks were good and I began to go for interviews for a permanent job. There were 96 companies at UBC recruiting for mechanical engineers in 1956. My only requirement was that I did not want to work in B.C. but instead wanted to go to Ontario where the large manufacturing industries were located. I went to 14 job interviews and received firm offers of employment from 13. Ironically, the one rejection letter I received was from the company I had most wanted to join. Later I found out from one of my fellow students, Ralph Sultan, who accepted employment from this firm, that he left after a year because they put him in sales and didn't use his engineering background. They missed the boat, because Ralph later became the Chief Economist for the Royal Bank of Canada before moving into the resource industries. For myself, I accepted a position as a junior engineer at the Millhaven Plant of Canadian Industries Limited (C.I.L.), just outside Kingston, Ontario.

Jean and I were married on May 18, 1956 and five days later we took the train from Vancouver, via Portland through to Chicago and then up to Toronto and then on to Kingston. It was cheaper to travel in the U.S.A. than Canada at that time and, because more people were flying, we had a whole Pullman Car to ourselves. Upon arrival in Kingston we thought we had reached the end of the earth. We knew nobody, and nobody came to meet us. We had to ask directions to the town. We finally got a cab, and since we didn't have much money we asked to be taken to the "second best" hotel. Little did we know that in Kingston at that time there were no "second best" hotels, there were no "first class" ones either. But we managed through the weekend and found an apartment in a converted schoolhouse downtown right next to the Hotel Dieu Hospital where Jean was able to get a nursing job.

The C.I.L. plant in Millhaven was designed as a turn-key operation by Imperial Chemical Industries (I.C.I.) in England and was expected to work with a flip of the switch, which it did not. Thus, there were many production problems to be worked out. The plant was designed to make terylene fibres which, it was hoped, would be a strong competitor to nylon. This proved to be difficult because terylene was finding resistance in the market place. It was not competitive as a fabric for clothing.⁴ This was a case where a company had developed a product without having a clear idea of where its market was. But it was a good first experience for me as a junior engineer. I worked on an eclectic array of projects; investigating lubricants which would reduce the coefficient of friction on sewing machine threads, evaluating the thermal efficiencies of electrical steam boilers, determining the degradation of polymers due to laminar flow through screw pressure melters, evaluating the economics of incinerating waste, and many others. But I was not happy with my work at C.I.L. I believed I was capable of doing more and I wanted more challenges. I was frustrated with my supervisor who spent most of his time avoiding work and expected me to do the same. He told me I should learn to do "government work" which meant you did work for yourself on company time. To me this was, and is, dishonest. So before my first year had passed I began looking for other opportunities in the want ads.

⁴ For one, if water was spilled on to the fabric it left a permanent stain. Neckties given by the Company lasted only one trip to the drinking fountain.

One of my co-workers at C.I.L., another junior engineer, had moved to the 3-M (Minnesota Mining and Manufacturing) plant in London Ontario and claimed that living in London was more fun than living in Kingston. If I was going to leave Kingston, where incidentally we had met a lot of nice people, I wanted to get a job in a manufacturing plant and not one in another petrochemical industry. I knew there was a locomotive works in London, so I applied to General Motors Diesel Limited. GM invited me to London for an interview, and within a couple of weeks an offer of employment was in the mail. With Jean's concurrence I accepted the position of Project Engineer and we departed Kingston in July 1957. The drive to London across the north shore of Lake Ontario was during the height of Hurricane Hazel. The winds were fierce and the only thing that kept our car on the road was that it was loaded down with all of Jean's nursing books, my engineering books, and our recently acquired Book-of-the-Month Club Selections.

My project work at GM was very interesting. I did full scale structural testing of locomotive underframes using hundreds of electrical resistance strain gauges, remote cold weather testing of locomotives in Northern Quebec, wear studies on nylon bearings, and so on. The responsibility given to me by GM was as different as night is to day from my experience at C.I.L. GM expected me to work long hours and on weekends, but to my surprise they paid generous overtime. It would not be until many years later that my salary as an Assistant Professor would equal my average monthly salary at GM. Life in London was exciting and its proximity to the big cities of Detroit and Toronto and nearby Lake Huron made it a great place to live. We also had made a lot of nice friends. I even took a night course on investments at the University of Western Ontario. Nevertheless, I guess I was still young and restless so when I was given a performance appraisal at GM with the comment that I tended to probe too deeply into finding solutions to problems, I began once again to assess what I wanted to do. I liked the work at GM very much and believed I had a future with the company, although I didn't always agree with their corporate philosophies. But I did not want to quit so I asked for a leave of absence to do a graduate degree. GM agreed so I applied to UBC, Alberta and Saskatchewan. I still hadn't given up the idea of settling in the West. UBC sent a rejection letter. I think they remembered me as spending too much time playing the clarinet. I can't remember if I heard from Saskatchewan but I received a rejection letter from Dean Hardy saying there was no program available for me at the UofA as there was no Mechanical Engineering Department. This was a disappointment because in my travels on the weed killer train I had visited the UofA in 1954 and spent some time in the Library where I was given friendly and helpful assistance with a paper I was writing on gas turbines.

As it happened, GM sent me to the Allison Division in Indianapolis for a technical briefing on aluminum railway journal bearings. From Indianapolis I flew to Edmonton to begin to inspect and determine the cause of failure of bearings on 100 railway grain cars (that is 800 bearings). All of the bearings were inspected at the Calder Yards in sub freezing temperatures and I stayed in the new, but now torn down, Annex of the Macdonald Hotel for six weeks. The work was cold and tedious and being separated from Jean for so long was no fun either. But before returning to London I had the opportunity to meet with Dean Hardy and tell him that I wanted to do a graduate degree in engineering and that it didn't matter to me if it was not in Mechanical Engineering. I was interested in either fluid mechanics or heat transfer, both programs were being taught in one form or another at the UofA. Dean Hardy was sympathetic to my argument and told me to go along and see Dr. George Ford who was then the Head of the Department of Civil Engineering.

The meeting with Dr. Ford (it would be many years later before I could bring myself to call him George) was, as can be imagined by those who know him, very animated. However, and to my delight, George was enthusiastic about my wanting to do graduate work, and in due course followed up with an offer of a Sessional Lecturer position as a laboratory instructor in thermodynamics starting in Sept. 1958 in the Department of Electrical Engineering.

For the third time in less than three years Jean and I were on the move again, but as always, Jean was supportive of what I wanted to do, and continued to work as a nurse, and now began to support me while I took graduate studies. But coming to Alberta was not an unwelcome move for her as Jean was a native Albertan and in a way she was returning to her roots. For me, I was delighted with the offer of a teaching assignment at the UofA. The fact that the salary was a fraction of what I

was earning at GM did not matter either. Our car was paid for, our expense were low, I had long ago paid off my student loans at UBC and our only luxuries were to go to one movie a week and sometimes buy a bottle of wine for two dollars.

Upon our arrival in September 1958 Edmonton was in the throws of winter, but as we had previously located a place to stay in the Bel-Air Apartments near the Westmount Shopping Centre, we settled in very quickly. Jean got a job as a Head Nurse at the Misericordia Hospital and I shared an office in the old “sheep sheds” with Dave Panar, Eric Johnson, Gerry Sadler and Chris Rodkiewicz all of whom had appointments with the Department of Electrical Engineering headed by Professor Jim Harle.⁵ I enjoyed teaching thermodynamics, although to Civil Engineering students it was a tough sell at times. But what I enjoyed the most was the relaxed workplace atmosphere. Everyone got along with one another, the tasks were shared equally and fairly. There seemed to be no politics like I had known at CIL or GM. Much later I learned that first impressions can be deceiving.

In April of 1959 I was due to return to GM but could not see uprooting myself for just four months to then come back to the UofA to complete my degree. I wrote to GM asking for an extension of my leave of absence which they not only refused but interpreted as a letter of resignation. So the cord with GM was cut. I did not regret their decision nor did I ever regret working for them. I learned a great deal at GM which I was later able to pass on to my students. At the same time Dr. Ford informed me that there was no place for me at the UofA over the summer so I better go out and look for a job in industry! This was no problem. C.I.L. has a polymer plant in Edmonton and with my previous experience at C.I.L. in Millhaven, and my experience with stress analysis at GM, I was hired to work with an engineer named Roy Dean. Roy and I hit it off really well. We both shared a similar cynicism regarding corporate bureaucracies. We worked together on the proof testing of pressure vessels up to 1500 atmospheres. Roy was an engineer who had earned an external degree from the University of London and had a very practical outlook. He and his wife Ann were friends with whom we kept in touch even after they moved back to the U.K. and settled in Wales where Roy became the Deputy Director of the Nuclear Power Station on the Isle of Anglesey. We visited them on a number of occasions and they came over to see us in 1994. Unfortunately, Roy succumbed to cancer in 1995 at the age of 67.

Looking back at these early years it may seem that everything that I did was part of a master plan leading to a career in teaching. But this was not the case. I had no such plan and I didn't know where I was heading. It seems selfish in retrospect but I enjoyed the challenge at the time not thinking much of where it might lead me. It must be remembered that in the '50's and '60's I had no difficulty in getting a job so I wasn't worried about ever being unemployed.

My first graduate courses were from Dr. Ford in Elasticity, Dr. Tom Blench in Fluid Mechanics, a Metallurgy course from Dr. Jim Parr whom I remembered as a former instructor at UBC, and a Math course on Complex Variables. The name of this instructor I cannot recall, nor for that matter much of the course itself, but I do remember that the instructor was very kind because I passed the course. By the end of the summer of 1959 my interests were becoming more focused in the area of applied mechanics. At the same time Dr. George Ford informed me that there might be a chance that the UofA would form a Department of Mechanical Engineering and, if so, would I like my degree to be in Mechanical Engineering?⁶ I readily agreed, and Dr. Ford became my supervisor on a thesis entitled “The Anticlastic Bending Behaviour of Flat Plates”. This was a thesis topic which did not emanate from an industrial problem but was one for which I could use my industrial experience to some advantage. It was no surprise that strain gauges figured largely in the experimental part of the research.

⁵ Like most academics, Professor Harle had difficulty keeping his papers in order as they kept piling up on his desk. His solution was to use full width sheets of brown wrapping paper which he laid over the top of the pile whenever he wanted to start afresh without later having to sort through the previous mess of confusion.

⁶ The staff which formed the nucleus of the Department in 1959 consisted of, in the field of applied mechanics, Drs. George Ford and Stu Kennedy who were without a doubt the heart and soul of the department and who set high standards for the teaching and welfare of the students, along with Drs. John Duby and Jim Haddow who were noted for their desire to make the curriculum more mathematical and rigorous. On the thermo/fluids side there were Professors Dave Panar, Gerry Sadler, Eric Johnson and Chris Rodkiewicz. Each added his own specialization but Professor Panar was the *de facto* leader of the thermo group which was housed in the old “sheep sheds” where the Electrical Engineering building now stands. These were the eight staff members who made up the nucleus of the yet to be established Department of Mechanical Engineering in the Fall of 1958.

I finished my thesis in time for the 1960 Spring Convocation and graduated along with the first class of undergraduates in Mechanical Engineering. I remember my dissertation defense very well, because along with George Ford and Stu Kennedy, George had asked Dr. Max Wyman, Head of the Department of Mathematics, to act as the outside examiner. I was very worried about Dr. Wyman's presence because he was a world renowned mathematician, and an authority on Special Functions, about which I then knew nothing. As it turned out Dr. Wyman was very kind in his questioning and I passed.

At this point I had completed what I had intended to do. I knew Jean was anxious to do some travelling, but I was hooked on University life, and as there were two job openings at the Calgary Branch of the UofA, I and two other Sessionals applied for the positions. The prospects of a permanent teaching position and a move to Calgary seemed like the ideal job. But such was not to be. The Dean of Engineering, Dr. George Govier, had given the jobs to the other two candidates. In conveying the "bad news" to me Dr. Ford said that the "good news" was that they would accept me into a PhD program. As I had not expressed any interest in doing a PhD I did not see this as good news but merely as a consolation gesture. I talked it over with Jean and she agreed to go on working for a few more years if I wanted to further my studies, but made me promise that when it was all finished we would travel to Europe. I easily agreed at the time, but it would be 24 years later before I fulfilled this promise.

True to form, in the summer of 1960, Dr. Ford told me I had to go out and work in industry before starting my PhD program in the fall. This time I convinced Chemcell (later named Celanese) that I was an expert in thermodynamics (after all I had taught the course for two years!) and would undertake to conduct HVAC (heating, ventilating and air conditioning) studies on their synthetic fibres building where they were encountering air quality problems. At the same time I began to study German and review my high school French, because at that time all PhD candidates had to have some proficiency in two foreign languages other than English. As the Fall of 1960 approached Dr. Ford was in need of additional staff so he offered me a full time Sessional Lecturer appointment, teaching Strength of Materials and Thermodynamics, which I gladly accepted as it would allow me the time to work on my foreign languages as well as broadening my teaching expertise. This delayed the start of my PhD program for one year but I felt I could use the time to advantage on my foreign languages. At the same time I began to build a multi-channel digital data acquisition system which was modeled after one at NRC in Ottawa and became the second of its type in Canada. At the close of the 1960-61 academic term Dr. Ford informed me that I had been awarded a Queen Elizabeth Province of Alberta Scholarship of \$2600 for each of the years 1961-62 and 1962-63. I was elated because now I could devote full time to my studies.⁷

In due course I passed my two language exams (I had very considerate examiners). I got through all my courses and my thesis was well underway. Of all the courses the one given by Dr. Werner Israel, from the Department of Mathematics, was the most challenging because I was competing against the honors math students who made up the majority of the class. I set myself the goal that I was going to get the top mark, and I did as I got 100% on the final exam, but the time I spent to meet my objective almost wore me out. Nevertheless, I was able to finish my thesis by the Fall of 1963, although Dr. Ford thought I should have been able to have it finished by the Spring of 1963. As it was, I was in a group of four who received their PhD's in engineering, but mine was the first PhD degree awarded in Mechanical Engineering at the University of Alberta.

Our plan at the time was to take a trip to Europe when I had completed my PhD. But once again fate entered the picture when I was offered a tenure track position in the Department of Mechanical Engineering at the princely sum of \$8000 per year. With Jean's concurrence I accepted the offer, although Jean was beginning to wonder if we were ever going to get to Europe. However, for the first time in five years we began to think of Edmonton as our home.⁸

⁷ This scholarship was a complete and unexpected surprise for me. Unbeknownst to me Dr. Ford had recommended me to the Awards Committee.

⁸ Our son Jonathan Mark Bellow was born in 1965 and our daughter Denise Gisele Bellow was born in 1968. Jean and I are very proud that both children received degrees from the University of Alberta; Jonathan has a BSc and MSc in Geology and Denise has a BA in History and Political Science.

THE DEPARTMENT OF MECHANICAL ENGINEERING IN THE 60's

Life at the University in the 1960's was exciting.⁹ There was a feeling that the University was about to embark on a major expansion which would transform it into a premier institution. Many at the University said that if the province wanted its University to be recognized internationally, and not lose its good staff to the United States, it had to be prepared to put enough money into it. The Social Credit Government under Premier Ernest C. Manning responded and provided millions of dollars to the University over a number of years. There was money for everything; for equipment, for buildings, for salaries, for the Library, and for infrastructure. However, in Mechanical Engineering we still lacked adequate space. We were split between space in the Power Plant south of the Jubilee Auditorium, the old Power House, the new Civil/Electrical Building and the Chemical/Mineral Building. Nevertheless, the Department continued to expand under the leadership of George Ford. The academic roster began to have representation from all corners of the world with the likes of Professors Cheng, Colbourne, Craggs and Lock from abroad, and later, "prairie" boys like Professors Dale, Faulkner, Gilpin, Marsden, Sprague and Wilson. From the original eight (Ford, Kennedy, Panar, Haddow, Duby, Johnson, Sadler, and Rodkiewicz) who were attached to the Department of Mechanical Engineering, Professors Duby and Panar resigned to pursue successful careers in consulting. Professor Johnson resigned to study for a PhD at UBC and then obtained an appointment at the University of Calgary. One other member, who had a fine incisive mind, was Abe Eschel who went away to do a PhD and returned for a short time but then took up a position with IBM in the USA. So some came, some went, but most stayed, despite the harsh winters and the lack of decent facilities. However, there was an expectation that things were going to improve. The Department was developing a sense of purpose and spirit of enthusiasm, and had begun to build a reputation for providing a solid undergraduate program in engineering fundamentals, combined with a reasonable exposure to practical experience in the laboratories. Through the efforts of such people as Drs. Haddow, Cheng, Gilpin and Wilson the importance of good fundamental research began to take hold.

Our graduate program got off to a much slower start. As in most Canadian universities at that time, there were few Canadian engineering students who wished to take graduate work; jobs were plentiful in industry, industry was unwilling to pay any significant premium for a graduate degree, and salaries were considerably higher in industry than those paid to academics. The latter I knew from personal experience. In a conscious decision the Department tried to keep a reasonable balance between the number of foreign students and those from North America. This kept the graduate student numbers in the 20-30 range, whereas other departments accepted all those who met the minimum requirements, and consequently, had foreign graduate enrollments two or three times larger than ours. This affected our ability to get outside research support, and to a lesser extent, affected our credibility within our own Faculty. But in our own minds, at least, we believed we had a top notch undergraduate program; our research was being published in international peer-reviewed journals, and our grants from the National Research Council of Canada (later named NSERC) were adequate for our needs.¹⁰

Dr. Ford, forever our "fearless leader", continued to promote the need for a new building and made the case for Mechanical Engineering wherever and whenever he could. In the mid-'60's the capital budget for the University was phenomenal; there were three or four new building projects simultaneously underway at all times. In addition, the University was starting a major upgrading of its utility system, coupling it with the University of Alberta Hospitals, which would eventually become one of the largest district energy systems in North America serving a community of 50,000. The time was right to push for a Mechanical Engineering building. But Civil Engineering had the same idea,

⁹ Life was also uncomplicated. Students could park their cars anywhere for free and a plug-in only cost \$10 per year. And, there was only one Campus Security officer, a likable former policeman by the name of Lu Edmonds. He carried a gun but we thought if he ever took it out of its holster it would fall apart from rust.

¹⁰ Although I received many research contracts and grants from industry, I am particularly grateful for the financial support I received from the Natural Sciences and Engineering Research Council (Grant A-2705) over the years 1965-1996. I was honoured to be appointed to NRC's Mechanical Engineering Grant Selection Committee, 1972-75, and served as its Chairman in 1975.

and being a larger Department with a much longer history at the UofA, believed they should get the nod for a new building. However, the numbers supported Mechanical's case, and after due deliberation, Dean Hardy said that the first priority for a new building for the Faculty of Engineering would be for Mechanical Engineering.

Dr. Ford, with Dean Hardy's agreement, asked that I head up a design team to develop plans, in conjunction with an outside architectural firm, for a new Mechanical Engineering Building. In this capacity I laid out the general concept for the building; room sizes, interrelationships between rooms, and what the overall concept should be. I put my maximum effort into this project with tremendous enthusiasm, but it wasn't long before we ran into opposition from outside the Faculty, namely, the Campus Development Office, which had a suspicion of academics knowing anything about the design of a building, and the master planners from Toronto who were even further removed from understanding the building needs of a Mechanical Engineering Department. But by dint of persuasion we got almost everything we had asked for and we moved into our new quarters in 1972.¹¹ In my opinion it is one of the finest engineering buildings anywhere in the world.

When Dr. Ford was named (elected, because we had discovered the wonders of democracy) Dean of the Faculty of Engineering, Dr. Stu Kennedy was elected in his place as Chairman of Mechanical Engineering.¹² Under Stu's leadership, and with George as Dean we were poised for tremendous growth and consolidation of our activities. By and large this came to pass. Our staff was maturing in its research endeavors. Our graduate students, while not large in numbers, were doing impressive research and moving on to successful careers in universities and in industry. Much of this was supported by a well organized machine shop and technician group under the directions of Al Muir and Tom Villett, respectively. But the days of unlimited spending were over and the reality of no more new engineering buildings deepened the resentment of some of the other departments towards Mechanical Engineering. In any case the purse strings tightened and after four years as Chairman Dr. Kennedy had had enough and was anxious to return to his first love, teaching.

INTO THE '70's

I was elected Chairman of the Mechanical Engineering Department for a three year term beginning in 1975. I was elected for two successive three terms, serving as Chairman from 1975 to 1984. During that time Dr. Ford was replaced as Dean by Dr. Peter Adams, from the Department of Civil Engineering. Upon the directive from senior administration it was Dean Adams' task to lead us through a series of budget reductions. I was thankful that George and Stu had left some fat for me to take out. Subsequent Chairmen were not as fortunate and had to eliminate staff positions.

As Department Chairman throughout this period my major task seemed to involve filling academic vacancies. The results were rewarding for they enhanced the quality and broadened the experience of teaching and research in the Department. We added Professors David Budney, Tom Forest, Ted Gates, Roger Toogood, Andy Mioduchowski, Fernand Ellyin and John Whittaker. Others who were hired such as Drs. John Jones, John Lenard, and Bill Simms, left after a two or three years, for various reasons.

EQUIPMENT

When the Department was formed in 1959 it had no modern equipment. What it did have was old and steam-related. Some of the steam engines should have been preserved for their historical value but, unfortunately, they were consigned to the scrapyard long ago. In terms of modern equipment we were sorely lacking. In those early days the only equipment we seemed to have were BLH strain gauges and Ames dials. If you couldn't do your experimental work with these components you were pretty much out of luck. I recall that our first vacuum tube voltmeter was one we put together from a

¹¹ There were only three Tenders submitted for the construction of the building but all were within the budget approved by the Board. This enabled us to include many of the "extras" which otherwise would have been deleted had the project come in "high."

¹² The term Head had been abandoned for the less hierarchical term "Chairman". The university later adopted the more "politically correct" but inanimate term, "Chair".

"Heathkit". In an effort to get around this paucity of equipment I had to book time on the Universal Testing Machine in Civil, borrow the use of microscopes and specimen preparation equipment in Metallurgy, and borrow electronic filters from Physics. In each case I was met with resistance, outright refusal, or at best, given assistance grudgingly. Consequently, as soon as we received money for capital equipment we began to develop our own metallurgical preparation facility and the Materials Engineering Laboratory. Our first major purchase was the Tinius Olsen 400,000lb capacity testing machine in 1965, which is still in use today. Without a doubt our department now has one of the finest Materials Engineering Laboratories anywhere.

Mechanical Engineering can be loosely defined as the application of scientific and engineering principles to things that move and convert energy from one form into another. Mechanical Engineering can also be defined as the design, contrivance, or devising machines that produce effects which enable man to do things which he would otherwise be unable to do, or would take much longer in doing or at greater expense. Whatever definition is used, to me at least, Mechanical Engineering involves things mechanical, i.e., machines, and these things are practical. It follows that a Mechanical Engineering Department should teach practical things and demonstrate these in a practical way. This formed the basis of my philosophy for selecting equipment for the Materials Engineering Laboratory, for the Measurement Course, in equipping the Machine Shop, and in the design of the Mechanical Engineering Building.

As for our Machine Shop, in 1959 it consisted of a 9" South Bend Lathe, a bench grinder, a drill press and some hand tools. In 1960 Professor Jim Haddow returned from a study leave and directed his efforts to building up a reasonable size Machine Shop. We also hired some qualified machinists. But even then it was an uphill battle as questions were being asked why we needed a machine shop in the first place. When Dr. Haddow took a second sabbatical leave I was given responsibility for looking after the shop and was able to complete the job that he started, and was later able to incorporate the Machine Shop as a featured visual activity in the new building.

The equipping of the Materials Engineering Laboratory was a labour of love for me. Through the purchase of the Tinius Olsen, Gilmore, Amsler, Instron and MTS equipment, along with the custom designed equipment built by our qualified machinists and technicians, we have one of the best equipped laboratories I have ever seen around the world. Fortunately, when money was available in the 60's and 70's, we were able to acquire this world class facility, which was assisted in a major way by getting a new building and \$496,000 for new equipment. It would be impossible to find the money today for this facility. The thermo/fluids facilities were similarly enhanced under the guidance of Drs. Cheng, Gilpin, Lock and Wilson.

EARLY RESEARCH ACTIVITIES

With all the brand new equipment we were acquiring in the late 60's I was anxious to put it to good use, and because of my previous industrial experience, I wanted to start doing research for industry. But this was not as easy as it might have been. First of all there was a reluctance on campus for anyone to be involved with industry. There was a certain degree of paranoia that industrial research was for military purposes and somehow would end up supporting the war in Vietnam. Maybe there was some basis for this although I didn't think so at the time. One such project that I undertook was to evaluate the strength of parachute harnesses that were being used to drag cargoes out of the back doors of low flying C130 Hercules transport planes. The Canadian Armed Forces had a number of failures which left their payloads in piles of scrap on the northern tundra. I tested a number of the harnesses to determine the cause of the failures. The Dean instructed me to not write a report nor submit an invoice for the cost of the study. He would allow an Armed Forces Officer to witness the tests but the University's name could not be attached to the data.

In another instance I undertook to do work for the Steel Company of Canada. When they insisted that they pay for the research the only arrangement we were able to make was for them to give a grant to the University. I would have signing authority for this but there was to be no contract, nor were there to be any strings attached to how the money was to be spent. Fortunately, the University now has a more enlightened attitude to cooperating with industry.

My industrial experience at CIL and GM developed my appetite for problem solving, but I was able to pursue this to a greater depth at the University. Working at the University provided the opportunity for benefits from the best of both worlds; I could work on industrial problems and in the depth that I felt appropriate. I am particularly grateful to the Steel Company of Canada (Stelco) who engaged me as a Product Development Researcher for their Edmonton operations over a span of 25 years. To a lesser extent, but still important, was the financial support over the years that I received from the oil industries in Alberta. Some of the projects could have become so large as to have changed my career direction, and perhaps taken me out of academic life at the University. This did not come to pass, but two projects are worth mentioning, for they exposed me to the industrial scene on an international level.

INTERNATIONAL INDUSTRIAL RESEARCH

In 1980 Shell Canada and some partners formed a consortium to build a third tar sands plant in Fort McMurray. The company was called Alsands. At this time I was making the rounds of oil companies in Calgary trying to drum up interest in obtaining research dollars to support the broadening of my work in fatigue of metals and corrosion fatigue of oil field sucker rods. As fate would have it I was attending an APEGGA luncheon at the Banff Springs Hotel and was seated across the table from the senior Vice-President of Alsands, Mr. Ed Cjaza. He was very interested in what I was doing and how universities could assist industry in research and development. Consequently, he invited me to Calgary to attend a meeting with his senior engineers to scope out possible areas of research that we could do at the UofA. Along with Dr. Gary Faulkner we put on a "dog and pony" show in our areas of research. It was apparent that Alsands was primarily interested in the cold weather properties of steels that would be used to manufacture the huge bucket wheel excavators that would be used to mine the tar sands. The only country in the world that made such equipment was in Germany and Alsands was concerned that the German equipment might not meet the harsh conditions of the Athabasca tar sands. It was also a requirement of the Federal Government that 75% of the equipment had to be built in Canada using Canadian materials. Alsands invited me to take on the responsibility for approving the standards and specifications of all materials to be used in the manufacture of bucket wheel excavators. I accepted the challenge, although I really didn't comprehend the enormity of the task, nor what liabilities I was incurring. However, it wasn't too long before Alsands said that a team of engineers from M.A.N. (Maschinenfabrik Augsburg Nürnberg) would be visiting me to discuss future collaborative research.

My first meeting with German engineers took place in September of 1981 and was most interesting. They were very business like, very direct and appeared to have no time for humor. It was nothing like what I had experienced in the USA or in Canada, with GM or with CIL. I didn't know what to make of it all or what would follow. So when they suggested that I should come to Germany to visit their manufacturing facilities and review their technical capabilities first hand I thought that their invitation was nothing more than a courteous, but empty, gesture. But such was not the case, and I later learned that in business the Germans don't say one thing and mean another. Nevertheless, I was taken by complete surprise when I received a telephone call within a few weeks asking when it would be convenient for me to meet with them in Nürnberg. I replied that I wouldn't be available until the end of the term in April, and hearing nothing more from them I figured that was that. Much to my surprise, and delight, I received a telegram in March 1982 informing me that M.A.N had purchased a return airline ticket from Edmonton to Frankfurt and I should go to the Air Canada Ticket Office and pick it up. So prepared was I that I didn't even have a Passport!

My trip to Germany was organized with German efficiency. Unfortunately, I was suffering from the flu at the time and German hospitality was more than my constitution could handle. They kept bringing in fresh troops whose mission it seemed was to outdo my previous hosts' hospitality. Also, I was carrying tremendous guilt in not taking Jean along as this was my first trip abroad. An omission that, to this day, I am reminded about!

As might be expected, my visit to Germany was very interesting in a technical sense but more important in the personal contacts that were made over the course of ten days. Unfortunately,

while in Germany the Alsands project was cancelled due to rising costs and “cold feet” by prospective corporate partners. This decision dashed all hopes of M.A.N. building mining equipment for the Athabasca tar sands. When this news reached Germany, my host Dr. Hans-Jürgen Meyer and I were having dinner in a small Gasthaus situated on the Rhine near Mainz when Dr. Meyer was called to the telephone. When he returned to the table he told me the bad news. I asked what now? He said, “life goes on” - and it did.

Going back to 1980, Alsands had provided me with funds to support an MEng student, R. Carlson, to investigate the cold temperature properties of steels from European and North American suppliers. As my third term as Department Chairman was ending in 1984 I arranged to spend some of my Administrative Leave in Germany bringing together the fracture data produced by Carlson with some of the research work done in Germany by M.A.N.¹³ On this, my second visit to Germany, I was accompanied by Jean, Jonathan and Denise. I met and worked with Eugen Klotzbücher who was Head of Metallurgy and Quality Control for M.A.N.’s Railway and Crane Division located in Nürnberg. Eugen is a mechanical engineer with a strong background in metallurgy. He and I collaborated on a number of research papers on determining the critical flaw size in steels, based on the laboratory work we did at the UofA and the results of full scale structural testing in Germany. Since 1982 I’ve been to the M.A.N. works in Nürnberg about ten times on technical projects of mutual interest and count a number of M.A.N. engineers as personal friends, whom we visit when in Germany, and who in turn visit with us when they come to Canada. On two different occasions Jean and I have vacationed together with the Klotzbüchers in Italy.

What might have been a project of immense proportions with Alsands turned out, instead, to be a rewarding relationship with a large industrial company in Germany. Not only did it provide the opportunity for carrying out some practical engineering, but it also exposed me to German thoroughness and aggressiveness in business, which I was able to pass on to my students as models to emulate.

My interest in things German was matched by an interest in Japanese technology. Having been exposed to the North American automobile industry through my work at GM Diesel, I was impressed with the economic and technical advances the Japanese were making in the U.S.A. and in Canada. I was aware that one Japanese company, Sumitoma Heavy Metals Industry was making oil field sucker rods and down-hole tubular products. From Canadian companies who were purchasing these products the reports were that the equipment was excellent. This was impressive because Japan has no oil industry to speak of and therefore no local demand for these products.

In 1986 I presented two papers at an International Offshore and Arctic Engineering Conference in Tokyo. To take advantage of this, my first visit to Japan, I wrote to Sumitoma to request a meeting with representatives from their oil field tool manufacturing facility in Fukuoku. They agreed, and to my surprise, they were familiar with my published research on sucker rods and were as anxious to meet with me as I was to meet with them. The meeting took place in the Sumitoma headquarters in Tokyo, and was typical of the type of meeting where each side wanted to find out as much as possible from the other without divulging anything of importance. I had to be somewhat circumspect in what I said as I was still working on projects for Stelco for which I was bound by confidentiality agreements. In any case the meeting went well and they invited me to dinner. I said that I had my wife with me but they said that women were not included in businessmen’s dinners! I believe that this attitude is now changing in Japan. On more recent trips to Japan Jean has been included in all social events. Japan is a safe place for visitors and even though one stands out in the crowd one doesn’t feel out of place.¹⁴

In 1986 I received a request from Stelco to undertake a major survey of oil field production problems which were, or could, impact on the products Stelco was selling to the oil industry. A major

¹³ This Administrative Leave was the only leave I had taken from my teaching and research duties in 20 years.

¹⁴ One night Jean and I, along with Ted Gates, Tom Forest, from the Department, and Dr. Dan Matheson and his wife (friends from Calgary), set out to find a Japanese restaurant where the usual tourists would not be found. We started walking towards the Tokyo dock area and eventually we found a small place with a red lantern hanging outside. Despite the fact that none of us could speak Japanese nor could anyone in the restaurant speak English, through the liberal use of sign language and pointing to what looked good that other people were eating, we had a most enjoyable evening sampling hot sake, Japanese beer, and local cuisine.

Research Contract between Stelco and the UofA was signed. I arranged for the cooperation of eight oil companies and, with the help of a Research Assistant (I. Smuga-Otto), we surveyed the conditions and operating behaviour of 5500 producing oil wells in an area stretching from Northern British Columbia, through Alberta and into Southern Saskatchewan. During this exercise I became acquainted with a number of engineers in the oil patch, and one in particular, Mr. Allen Chui of ESSO Resources Canada Limited, which led to a number of Research Contracts with ESSO and successful applications for Research Grants from Imperial Oil's University Grant in Aid of Research Program. One result of this collaboration was that Allen and I wrote a joint paper on the wear of polymers used in down-hole oil field applications which we presented at an International Wear Conference in Nagoya, Japan in 1990. Since we were both going to Japan he suggested we visit his homeland in Hong Kong and he would show us around. Not only did Jean and I receive the royal treatment with a chauffeured Mercedes, but we were taken in a jet boat over to Macau for a dinner feast of gigantic proportions.

The wear conference in Nagoya was excellent and since I had written a few papers on wear I was getting to know a number of researchers in this field from all around the world. While in Nagoya we also visited the Kurimoto School of Business and were cordially greeted by Dr. Hiroshi Kurimoto who was very pleased to show off his excellent facilities and gave me a personally guided tour. From Nagoya we travelled to Osaka where we met up with Mr. N. Torrii of Sumitoma Heavy Metal Industries. This time Jean was included as an honored guest and subsequently we have become personal friends with the Torrii's. On our visit to Japan in 1995 the Torrii's insisted that we stay at their home so they could better show us Japanese hospitality and culture.

I have outlined in some detail my industrial experiences before and during my academic career for two reasons. First and foremost, I am proud to be a mechanical engineer, and as such I have felt most comfortable and had the most job satisfaction when doing engineering work. I have never thought of myself as an academic pursuing knowledge for the sake of knowledge itself. However, the next best thing to doing engineering is to talk about it, and having an academic appointment allowed me the opportunity to teach engineering and relate my own industrial experiences to students. The common thread in all of my research endeavours was the application of engineering to practical problems.

ADMINISTRATION

Given my dedication to engineering it needs to be explained why I spent 16 years of my career in Administration. As an employee, regardless of whether one is in academe or industry, one can always find fault with the management. Some are satisfied (or doomed) forever to criticize; others (and I include myself in this group) say if you don't like the ways things are being run then get involved and participate in making changes. In the milieu of collegiality that exists at the UofA another reason for becoming an administrator is to take one's turn at the helm. It is a matter of shared responsibility in keeping the ship on course.

I have often said, and still believe, that one of the most difficult administrative jobs on campus is that of being a Department Chairman. The Chairman has to be an arbitrator/mediator between the staff and the students, and between the Department and the Dean and other Senior administrators.¹⁵ Former Vice-President(Academic) George Baldwin told me that the best administrative job on campus is that of a Dean. If this is true it is because the headaches of dealing with irate students, frustrated staff, and budget cuts are all focused on the Department Chairman. It is in the Chairman's office that the "rubber hits the road".¹⁶ Despite this, it is the Chairman who has the opportunity to chart and navigate the future course of the Department. One cannot do this alone, and woe betide the Chairman who thinks differently. I had the support of my Department and I want to record my appreciation to my former colleagues for their cooperation and suggestions. I always felt that I was part of a team. On the other hand, I firmly believed that I was responsible for all the decisions that were made, and if fault were to be found it was mine and mine alone and not that of a committee or advisory group with whom I may have consulted prior to making the decision.

¹⁵ Throughout my terms as department chairman I was ably assisted by the departmental secretary, Ms. Helen Wozniuk and the departmental bookkeeper, first Mrs. Shirley Bernt and later Mrs Doris Amero.

¹⁶ President Myer Horowitz recognized this when he supported the formation of Chairmen's Council and made a point of meeting with its Executive Committee on a monthly basis.

One positive outcome from this period was the introduction of the Cooperative Education Program in the Faculty of Engineering for undergraduate students. Back in 1968 I was a panelist at a joint APEGGA/EIC Seminar on "Engineering Education in the 1980's and the Decades Beyond". I predicted that in the 1980's we would have a CO-OP style of education at the UofA for our undergraduate engineering students. I was well aware of the success of the CO-OP program at the University of Waterloo and was convinced that such a program could work equally well in Alberta. Later, when Dean Adams suggested we should develop a proposal for a CO-OP program for the Faculty of Engineering I readily agreed. Surprisingly, there was little support elsewhere in the Faculty at the time it was first discussed in the Executive Committee. In any case, I willingly accepted the task of developing the proposal, walking it through the Faculty, and convincing my own Department that they should be the first to implement the program should the necessary funding from the government be approved. The concept was enthusiastically accepted by the students. The Faculty were more cautious; some felt that it would lead to a trimester system and heavier teaching loads. Others thought the program was too costly, but eventually they all came around and gave their support. The program was officially approved with the necessary funding from Advanced Education in 1981 with implementation for 1982. I was given the additional task of being Chairman of the CO-OP Liaison Committee and worked closely with Mrs. Pat Kushnir who was named the first Director of the CO-OP Office, formerly called the Student Work in Engineering Placement Office (SWEP).

The CO-OP program was a success for the Department because it provided additional resources to expand from 18 staff members in 1975 to 26 in 1984 which allowed us to increase the size of our quota for undergraduate students. I considered this was essential to becoming a major Department within and outside our University and would enable us to develop the critical mass necessary to enlarge our graduate program. Maybe it helped, but it was many years later before the number of graduate students increased significantly; and this may have been due more to the economic recession which affected Alberta's oil industry. Be that as it may, the CO-OP Program has been an unqualified success with our students and has been welcomed by industry. It has also provided many important links between our Faculty and industry in Western Canada. Given its tentative start, its success is due to the enthusiastic and dedicated support of the staff in the CO-OP Office, whose management is headed by an Associate Dean, and of course the cooperation of the Faculty.

TEACHING

One of my first teaching assignments in 1964 was to develop a new course in Mechanical Measurements. In tackling this project I combined what I had learned as an undergraduate at UBC with what I found I needed to know and use when working in industry. My main objective was to provide a course in the fundamentals of measurement rather than a description of how to run laboratory equipment at a University. This was a new teaching concept in laboratory practice which was later copied by other universities.¹⁷ I taught this course for 10 years and participated in its transformation from a single lecture and three hour laboratory per week for two terms, to three lectures per week and a three hour lab for a single term. I am pleased to see that the basic philosophy of this course has not changed, and that improvements have been made drawing on the expertise of the course leaders who followed me.

One of the most difficult challenges facing a Department Chairman is to delegate teaching assignments which are equitable and fair to both faculty and students. In any group of academics there are those who are excellent teachers and there are those who excel at research, and there are as many variations as there are faculty. Compounding this was the task of finding suitable faculty to teach Design. But teaching Design is not the same as teaching a course with closed form solutions. I also learned that if someone is not interested in design one cannot be made to teach it. It might be called Design but it would come out as a course in Tensor Analysis! And yet, design is a fundamental requirement for mechanical engineers.

¹⁷ In 1981 I was pleased to be invited to my old alma mater (UBC) to present a lecture to the faculty in Mechanical Engineering on this new philosophy of teaching undergraduate laboratories.

When I was Chairman I attempted to hire someone who was an expert in the teaching of design. While we received many applications from candidates who were willing to teach design, or any other subject we cared to mention, their backgrounds were not in design. It wasn't until I had stepped down as Chairman and was assigned to teach a design course by Dr. Faulkner, who followed me as Chairman, that I came to realize what a challenge it is to teach design. There is so much material to cover in a short time that one has to be carefully selective about which topics to emphasize. It is a course that should only be taught by senior faculty who have had industrial experience. One of the best professors I was able to assign to this course was Dr. Franz Vitovec whom I invited to join our Department when he stepped down as Chairman of the Department of Mining and Metallurgy.¹⁸

Another course that I initiated and enjoyed teaching was Manufacturing Processes. As in design, one has to be very selective about which materials to cover and which to leave out. I tried to focus on the industries in Alberta, although this was somewhat confining in that Alberta has a limited manufacturing base. One feature of this course was that the students had to use the machine shop to make a center punch. This was the first time some of the students had ever made anything with their hands. The female students were especially proud of their handiwork, which they could show off to their brothers!

I also taught graduate level courses; Elastic Stability, Plates and Shells, and Experimental Stress Analysis. This latter was another course that I introduced to the curriculum.

As previously mentioned it was George Ford who set the high standards for teaching in our Department. He also believed that junior courses should only be taught by the most senior instructors and only those who had the interest and the patience to deal with first and second year students. Over the course of 35+ years I have seen the Department of Mechanical Engineering transform itself from primarily an undergraduate teaching department where each faculty member carried a very heavy teaching load to one where productivity was judged more on research output than on the amount and quality of teaching. I am in agreement with the peer review system, but time and time again as I sat on endless Salaries and Promotion Committees (for 11 years) I witnessed how poor teaching was excused if compensated with good research, but the reverse was never true. The University enters the next millennium during which student enrollments are expected to grow but with reduced funding. As I write these words our University seems to be focusing on research and the dollars it can bring in, but how good teaching will be recognized and rewarded is not clear. I maintain that the best "product" of our efforts is the quality of the students we graduate and the education they receive which allows them to make useful contributions to society and future generations.

75TH ANNIVERSARY OF THE FACULTY OF ENGINEERING

The year 1988 marked the 75th Anniversary of the Faculty of Engineering at the University of Alberta. Dr. Fred Otto, Dean of the Faculty, asked if I would organize a suitable celebration to commemorate this event. I agreed on the condition that I would have the enthusiastic support of all departments. I formed a Steering Committee consisting of Dr. I.G. Dalla Lana, liaison to the Technical Committee chaired by Dr. R.G. Bentson, Dr. J.G. MacGregor, liaison to the Editorial/Archives Committee chaired by Dr. A.E. Mather, Prof. P.M. Dranchuk, liaison to the Awards Committee chaired by Prof. G.W. Sadler, and Dr. P.R. Smy, liaison to the Social Committee chaired by Dr. J.N. McMullin. The Fund Raising Committee chaired by Dr. J.M. Whiting became a most important initiative of long term value for the Faculty.

We set our budget for around \$100,000. To be on the safe side and to keep within the budget, I was the only one with signing authority. The celebration took place over a two day period with an Open House, an Awards Luncheon, a Special Convocation, and a formal dinner and dance at the Convention Centre. The overall attendance was less than expected, despite the thousands of invitations

¹⁸ Dr. Vitovec was a brilliant engineer, and although he spent most of his academic career in Physical Metallurgy, he had a solid background in Mechanical Engineering. His move over to Mechanical Engineering was considered by his Metallurgical colleagues as a defection. They were also put out that they didn't get a replacement position until Dr. Vitovec retired five years later. However, the Mechanical Engineering students were the real winners because Dr. Vitovec provided them with a superb course in Design.

we sent to alumni, but for those who did attend it was a great success. At the Special Convocation, held in Convocation Hall in the Arts Building and presided over by Chancellor Tevie Miller and President Myer Horowitz, Honourary Doctors of Science were conferred on Edgerton King, former CEO of Canadian Utilities, Donald Stanley, founder of Stanley and Associates, and George Ford, Professor Emeritus of Mechanical Engineering. Our guest speaker at the Awards Luncheon was Dr. Jim Parr, a former faculty member of the Department of Mining and Metallurgy. Dr. Ford wrote and published the book "Sons of Martha" which relates the history of the Faculty, and despite the caution from the University's Fund Development Office that this was not a good time to start a Fund raising campaign, we went ahead anyway, and to date over \$12 million in donations has been received.

As I look back on this event I think it was very successful. The credit is due to those who worked on the Committees and behind the scenes. I also had an able assistant in Mrs. Betty Saelof. Apart from the inventory of "Sons of Martha" which the Deans will use for future gift giving, we kept within budget; our expenses of \$67,000 were exceeded by our revenues of \$78,000.

LIFE UNDER THE DEANS

The influence of Drs. Ford and Kennedy on my career has been mentioned. But also my career was influenced by the Deans under whom I served. The first was Dr. R.M. Hardy and my impression of him was that he was a cigar-smoking, portly and grandfather-like person. Apart from my initial meeting with him as a graduate student I had little contact with him, as was to be expected. However, it was known that his consulting activities kept him away from the campus a good part of the time. His firm R.M. Hardy and Associates was very successful, and it was not much of a surprise that in 1959 he resigned to take up consulting full time. With Dr. Hardy's departure the Faculty began to search for a new Dean. The process in those days was quite simple and did not resemble the convoluted search and electoral system that we have today. The Chairman of the Search Committee was the President, Dr. Walter Johns, and the Committee consisted of some senior Faculty from within Engineering and from other Faculties, along with the Dean of Graduate Studies. It didn't take long for the Committee to choose Dr. George Govier who was then the Head of the Department of Chemical Engineering.

Dr. Govier's style of leadership was precise. He was quick to make decisions and he did not procrastinate or shy away from controversial issues. For example, he used statistical analysis to monitor grade point results and required justification if the mark distributions varied from the norm. He set standards for promotion to Full Professor which were based on quality of teaching and research productivity and not simply on the basis of years of service, and he produced a long range plan for the Faculty, long before the University got around to doing this. He also assisted in the development of the Faculty of Engineering at the University of Calgary. But about this same time he was appointed by the Alberta Government to the Energy Resources Conservation Board whose head office was in Calgary. This resulted in Dr. Govier spending half his time in Calgary and the other half in Edmonton. But it left the Faculty with a part-time Dean, and it was not long before Dr. Govier resigned his position as Dean to take up full time duties as the Head of the ERCB in Calgary. Once again the Faculty was in the hunt for a new Dean!

Dr. Johns convened a Search Committee to begin the process. The first meeting was to establish the criteria for the selection process and set a date for the next meeting. Members of the Search Committee reported back to their respective Departments, and we all had a say in describing what type of person we thought would make a good Dean. At the second meeting of the Committee Dr. Johns was pleased to announce "Gentlemen, our search is over, Bob Hardy has agreed to come back and be your Dean again." The meeting adjourned as there was no further discussion. For some of us, at the time, this was not seen as a good decision. We were worried about Dr. Hardy's commitment to the Faculty knowing that he still was involved with R.M. Hardy and Associates. Fortunately this did not occur, and true to his word, Dr. Hardy considerably reduced his consulting activities and devoted himself to the needs of the Faculty.

By now my contacts with Dr. Hardy were increasing, notably because I was now handling the Department's capital budget and was starting the planning process for the new Mechanical

Engineering Building. I began to understand and appreciate the value of Dr. Hardy's contributions to the Faculty. Dr. Johns was right to get Dr. Hardy back into the Faculty. Such was the wisdom of Dr. Johns! I learned that Dr. Hardy was one who, despite appearances to the contrary, could be very precise in his decision making. I remember him as being fair and considerate. He was a great engineer who brought national and international recognition to our Faculty and to the University. His expertise was sought after in the construction of the many airfields built on the prairies for the Commonwealth Air-Training Program. He was attached to the airforce (RCAF) with the rank of Squadron Leader. Apart from his consulting expertise that was sought worldwide he will be best remembered for the students he taught in soil mechanics who went on to have successful careers in engineering and education. In 1971, after a total of 21 years as Dean, Dr. Hardy retired at the age of 65. He never stopped practicing engineering, and even though his consulting practice was now being managed by others, he kept up his involvement until he passed away at the age of 79 in 1985.

By 1970 the times had changed, Dr. Max Wyman had succeeded Dr. Johns as President, and the "power to the people" philosophy for the governance of universities in the United States was now reaching the U of A. We too began a period of democratization of administrative procedures and decentralization of administration.. No longer would a Dean Selection Committee be headed by the President (now it would be the Vice-President Academic), and no longer would the membership of the Selection Committee be appointed. It was elections everywhere! Departments would have run-off elections as to who would represent them on the Committee. And everyone was labeled pro-this or anti-that, depending of the issue of the day. It was with this background that a new Dean Selection Committee was established. Representatives chosen by the Faculty of Science, Graduate Studies and APEGGA were included. Undergraduate and Graduate Students also elected their representatives. The Committee was chaired by Dr. Kreisel who had become Vice-President Academic. Emotions ran high as there were four Department Chairmen who were considered eligible to be Dean (Drs. Ford, Robinson, Walker, and Professor Sinclair). Outside candidates were invited to apply, and some did. Dr. Robinson declared he was not interested in becoming Dean and the choice soon narrowed to Dr. Ford and Dr. Walker (from Electrical Engineering). Both were able candidates. However, on decision day when the vote was called, Dr. Kriesel declared that Dr. Ford had been elected.¹⁹ It was no surprise that the decision was greeted with delight by many in the Faculty but with dismay by others. A dissident group appealed to Dr. Wyman to have the vote rescinded but Dr. Wyman said that the Committee had acted properly and the decision would stand. It was after this that a group decided to change the election procedures within the Faculty so that no matter what a Selection Committee decides the Faculty has the opportunity of voting on whether they will accept or reject the recommendation of the Selection Committee. When this concept was proposed at an Engineering Faculty Council meeting it was passed and now is enshrined in the Faculty's election procedures. These rules also apply to the election of Department Chairmen.

Such was the mood of the Faculty when Dr. Ford took over as Dean in 1971 for a five year term. As a former student, work associate, and as a friend I was pleased that George Ford had the opportunity of leading the Faculty. George was a great teacher who put the welfare of the students first. Although he did not profess to be an active researcher, he strongly supported the Faculty of Engineering in developing its research potential. Unfortunately not everyone appreciated this, and George, never shy about calling a spade a shovel, was critical of those who put research above their responsibilities for undergraduate teaching. Like Drs. Hardy and Govier before, Dr. Ford was held in high esteem by members of the Engineering Profession. There isn't a former student of his who doesn't remember an anecdote about George and the positive impression he had on them.

When Dr. Ford's five year term was coming to a close he let his name stand for a second term. But the Faculty had other ideas. Some were still upset from the previous election and in the interval had campaigned for a new Dean, one who was an active researcher, one who would stand up to Central Administration, and one who would get a bigger share of the University's Budget. With these as criteria along with the new selection procedures, it was not surprising that one of those who had been a champion of these changes, Dr. Peter Adams, was elected Dean in 1976.

¹⁹ Although the proceedings of the Committee, and particularly how the votes were cast, were to be confidential, within a short time of the decision the Faculty at large knew how each person on the Committee had voted.

The Dean's Office began to reflect the ways of Dr. Adams. Prior to becoming Dean he had not served as a Department Chairman so that the interaction between the Dean's Office and the Chairmen was a new experience for him. Despite this, Dr. Adams brought forward some new initiatives such as the CO-OP Program already mentioned and the Centre for Frontier Engineering (CFER). Although I was active and participated in both these endeavours I did not agree with the direction that CFER was taking. I believed that CFER should have been a clearing house which would bring the problems from industry to the expertise at the University. It came to pass that CFER became a stand-alone facility out at the Edmonton Research Park. I still think it would have been better to have had CFER located on campus with closer ties to the University.

As the plans for CFER were entering the final stages of development it became known that Dr. Adams was to become its first president. Many in the Faculty thought that Dr. Adams should stay on as a part-time Dean while heading up CFER. However, Dr. Adams resigned his position as Dean in March 1984 to become President of CFER. To bridge the gap until a new Dean could be selected Dr. Ford was appointed Acting Dean. Once again Dr. Ford was in the Dean's office, but once again the Faculty was in the search for a new Dean.

The Orwellian year of 1984 was significant for me as it was the end of my nine years as Department Chairman, and the start of an Administrative Leave. Although I allowed my name to stand for Dean, I was pleased with the choice of Dr. Fred Otto, who served the Faculty with distinction in the Dean's Office for 10 years. In 1994 Dr. Otto declared he would seek a third five year term but for reasons best forgotten the Dean's Selection Committee rejected Dr. Otto in favour of another member of the Faculty. This action of the Committee was so controversial that the Committee's choice of candidate was rejected by the Faculty in the "Ratification Vote". This was an embarrassment to the Committee's candidate, to Dr. Otto, and to the entire Faculty of Engineering. The Faculty became encumbered in the entrails of its own bureaucratic procedures! The Selection Committee was discharged and a new Committee was formed. In the interim, Associate Dean David Lynch was appointed Acting Dean and following a second round, the Selection Committee recommended that Dr. Lynch be named Dean. This time the Faculty ratified Dr. Lynch as the Selection Committee's choice.²⁰

OUT OF THE TRENCHES

In February of 1989 I was visited in my office by Brian McQuitty, a Professor of Agricultural Engineering, but at that time, Associate Vice-President (Facilities) reporting to the Vice President (Administration), Dr. Allan Warrack. Professor McQuitty wanted to know if I would be interested in the Associate Vice-President's position as his five year term was coming to an end and he was going to take early retirement. My immediate reaction was to decline the offer as I had had enough of administrative life by then and was enjoying the role of just being a Professor. I was also building up my contacts with industry and the future looked very bright for me. Brian asked that I think it over before deciding. A week or so passed and I called Brian and suggested he tell me a little more about the position over a cup of coffee. After our discussion I said I would be interested in talking to Dr. Warrack if he was interested in having me. Dr. Warrack came over to our house one evening to discuss the position and our views of the university in general. We concluded that he and I could work well together. My only stipulation was that I was not willing to allow my name to stand if he was going to go through a search process and advertise for other candidates.²¹ He assured me he was not going to do

²⁰ For a more complete account of the history of the Faculty of Engineering the reader is referred to "Sons of Martha" authored by George Ford, and published by The University of Alberta Press. George's time and memory goes further back than mine.

²¹ I had two previous brushes with moving into senior administration. The first was when Dr. Baldwin asked if I would be interested in the newly established position of Vice-President Research. I replied that I was not interested and furthermore did not think the university needed such a person. I was later to be proved wrong in that Dr. Gordon Kaplan, who took on this responsibility, became a leading and effective spokesman for research at our University and gave research a high profile. The second brush was when I was asked by Dr. Baldwin to become his Associate Vice-President (Academic). Unbeknown to me he had asked others the same question and in the end chose Dr. Ron Bercov for the position.

this and the job was mine if I wanted it. I said yes and began a five year term as Associate Vice-President on June 1, 1989.²²

Life in University Hall was interesting and for me an opportunity to make changes. I was asked by Dr. Henry Kreisel, former Vice-President (Academic) and a fine man and an outstanding scholar, how I liked my new job and I said it gave me an insight as to how the other half lived. He replied, "you are now one of those, so you should know." One of my main functions was to develop the Capital Budget and allocate the funds where they were needed. Dr. Warrack gave me a free hand in all of this and I began to develop rapport with all the Deans. As well, the Directors of Physical Plant, Technical Services, and Planning and Development reported to me. All in all it was a very responsible position which I tackled with enthusiasm. By the time Dr. Davenport arrived on the scene my recommendations regarding capital matters were accepted without challenge, and as such, I believed I was doing a good job. A year and a half later Dr. Warrack's own five year term as Vice-President came to an end. A search for a replacement for Dr. Warrack was begun and Mr. Glenn Harris of the University of Western Ontario was chosen, but since he would not be able to take up his position until April 1, 1991 Dr. Davenport asked if I would serve as Acting Vice-President (Finance and Administration), with which I agreed. But with the stepping down of Dr. Warrack and the arrival of a new President, and then later a new Vice-President (Finance and Administration), my job as Associate Vice-President (Facilities) was no longer the same.

PRESIDENTS OF THE UNIVERSITY OF ALBERTA

In January 1994 Dr. Roderick Fraser was installed as the 11th President of the University of Alberta. Counting Dr. Fraser, I have served under seven of the eleven Presidents who have headed the administration of the UofA. Dr. Andrew Stewart was President when I arrived on campus in 1958 as a Sessional Instructor. I don't believe I ever met him but I came to know his successor quite well, Dr. Walter Johns, who was Vice-President at the time (there was only one Vice-President back in 1958).

Dr. Johns was a Professor of Classics and one whom I would classify as a gentleman and a scholar. As I recall he had a daughter living in Vancouver and as he knew that I had lived in Vancouver, on occasion he would send me newspaper clippings which he thought would be of interest to me. I was impressed that he would take the time and trouble to call me or write something of note for my attention, for I was a junior Assistant Professor in a Faculty far removed from his own.

When Dr. Johns took over as President in 1959 the University was embarking on a major expansion of its facilities, the likes of which it had never seen, nor probably will ever see again. It was also a time when staff salaries were escalating and the University was on the threshold of becoming a major research institution. It is not surprising that Dr. Johns was respected and well liked throughout the University. After all, he didn't have to cut anyone's budget! On the contrary, there seemed to be money for anything and everything.

When Dr. Johns was President I served on GFC and the Executive Committee of GFC and was the GFC's representative on the Senate. My recollection of Dr. Johns was that he was a patient man and not given to outbursts of frustration. Generally, I believe everyone had a high regard for Dr. Johns, as I did. This doesn't mean that everyone agreed with him on every issue. I for one disagreed with his acquiescence to student demands. For example, the Students' Union representatives on GFC were dissatisfied with the running of the food services and dormitories over in Lister Hall, a perpetual problem it seems. The students were adamant that they be allowed to take over the operation of all student residences. I argued at GFC Executive that the students did not have any experience in this type of business and furthermore, if they failed, the University would have to step in and bail them out. There was no down-side risk for the students. Dr. Johns saw things differently and he sided with the students. Within a couple of years the students had had enough and asked that the operation be turned back to the University including their financially troubled HUB Mall enterprise.

²² The transition from "the Trenches" was made easy for me because I was assigned the knowledgeable and helpful secretary Mrs. Doreen Jenkins who had served in the Vice-President's Office of Planning and Development for a number of years.

Dr. Johns had risen up through the ranks of Department Head, Dean, Vice-President and then President. After he stepped down as President, having served 10 years in this position, he continued to serve as a distinguished University Professor and later as a Professor Emeritus. As a tribute to the University he wrote the definitive (alas, devoid of any humor) History of the University of Alberta.²³

Following Dr. Johns as President was Dr. Max Wyman, who had previously served as Head of the Department of Mathematics and Vice-President (Academic). In my opinion Dr. Wyman has to be regarded as one of the best Presidents the University has ever had. He took on the Presidency at a time of growing student unrest and militancy and when the Faculty were fed up with all the construction activity that had been going on over the past ten years. I admired Dr. Wyman for his patience, soft spoken manner, and complete understanding of issues. He was a man of few words, but when he spoke, and it was always softly, everyone listened. He also delegated much responsibility and authority to his Vice-Presidents and the Administrative Staff. He did not pile trivia on his desk although he continued to pursue his mathematical research on his desk-top computer. One time when I was in his office, reflecting on the student power sweeping the University, I remarked that it seemed regrettable that the role of the President was being diminished. He said, "not so", in fact he was worried about the amount of power the President had, it was, in his words "the power of information".

As President, Dr. Wyman chaired GFC meetings and on the rare occasions when he wished to make a personal comment he would remove himself from the Chair and step down into the members' area. But through his understanding and vision, and much to the disappointment of many staff at the time, he enabled students to have parity with staff in representation on GFC. Whether this was a good idea in the long term or not I think that Dr. Wyman recognized the inevitability of student representation. His support for student parity headed off what might have become an ugly confrontation, the result of which would have given students the representation they demanded in any case, but would have left a legacy of bitterness.

The next President was Dr. Harry Gunning who came to the University in 1957 to become Head of the Department of Chemistry. Dr. Gunning quickly established himself as a "mover and a shaker." He didn't subscribe to the old ways of doing things if he thought there was a better and faster way of achieving his needs. For example, he thought that the University's purchasing system was archaic and unnecessarily slow. He demanded that his Professors be able to order directly from the suppliers, a practice that is still followed today and unique to Chemistry. He ran Chemistry autocratically but those in his Department were loyal to him and supportive of his efforts. However, when Dr. Gunning moved from being Head of Chemistry to the Office of President he found that managing the university, with its huge inertia, was not the same as managing his department. In particular, the recently democratized GFC had its own ideas on the role of the President.²⁴ By the time Dr. Gunning became President my term on GFC had ended, but I can relate a couple of instances which give some insight into Dr. Gunning.

When Dr. Johns was President a GFC Committee was struck to investigate the feasibility of establishing a Research Park in Edmonton. I believe Dr. Gunning was behind this initiative and he wanted the University to help promote the idea with the City. The Committee was chaired by Dr. Walter Neal, Vice-President of Planning, and included Dr. Gunning, Dr. Jack Sample, Head of Physics, and two junior professors, Dr. Gordon Williams from Geology, and myself. As the deliberations proceeded from meeting to meeting, Dr. Williams and I suggested that rather than try and convince the City of the need for a research park we should, instead, set up a research institute on campus. Such an institute would bridge the gap between the problems of industry with the expertise and facilities at the University. A further incentive to this option was that the Federal Government was willing to put in \$500,000 for start-up costs. But this idea was opposed by Drs. Gunning and Sample (the latter was in the process of becoming head of the TRIUMF Project at UBC). To resolve this impasse Dr. Neal requested that each side submit their respective positions in writing. The reports were duly drafted and circulated to members of the Committee. But before the issue could be resolved

²³ When Dr. Johns served as President he occupied University House (later named Alumni House) as his principal residence. He and his wife, Helen, hosted many teas and social events for the University. Jean was fortunate to attend a few such gatherings at the Johns' residence and recalls Mrs. Johns as being a gracious host befitting one who is the first lady of the University.

²⁴ Dr. Gunning became President without previously having been a Dean or a Vice-President.

Dr. Neal resigned from the University to return to Australia, so the Chairmanship, rather than going to his successor in the Vice-President's Office as I expected it would, went instead to Dr. Gunning. Dr. Gunning then named Dr. George Walker, Head of Electrical Engineering, to the Committee. Dr. Walker was against setting up any kind of research institute on campus. At the next meeting Dr. Gunning announced that the committee would recommend to GFC that the University support the establishment of a research park in the City. I responded by saying that I would present a minority report to GFC supporting the establishment of a research institute on campus and we would let GFC decide which of our proposals should be endorsed! But Dr. Gunning never took his proposal to GFC and he never called another meeting of the Committee. My proposal never got past the Committee. It came to pass that the Edmonton Research Park was established and Dr. Gunning became very active in it during its formative years, serving on its Board of Directors.

Eventually the University established a research institute along the lines suggested by Dr. Williams and myself. Although it is called the Industry Liaison Office, its mandate is similar to what we envisioned as developing; that is, to be a clearing house for research projects from which both the university and industry can mutually benefit. At the time, the main opposition to a research institute was that there was the fear that industry would determine the type of research that would be done at the university and the academic community would simply not stand for this.²⁵

One other incident which relates to Dr. Gunning was in March, 1978 when the Government announced it was going to cut back its grant to the University. As can be imagined, the students raised howls of protest and organized a march across the High Level Bridge to the Legislature. The picture in the newspaper showed Dr. Gunning leading the march. I thought at the time that his participation in the march was inappropriate, for if he felt strongly about this issue he could have had a meeting with the Minister of Advanced Education or the Premier at any time. In any case, the protest, and Dr. Gunning's participation, didn't accomplish anything as the Government went ahead with its planned cuts.²⁶

In my meetings with Dr. Gunning I was probably too brash for my own good but at the time I thought I was right; I wanted the University to become more involved in industrial research. But my opinion of Dr. Gunning is not negative. On the contrary, I credit Dr. Gunning as being one of the most influential persons in bringing the University of Alberta out of the shadows into the light where it began to gain international recognition as a first class research institution. When Dr. Gunning came to the University of Alberta he hired excellent staff and built up a first class Department of Chemistry and by example, he showed other Faculties what could be done. Unfortunately, he became President at the time of growing advocacy of the students and staff who were not prepared to accept the authority of the President, or any administrators for that matter, without question.

When Dr. Gunning took up the Presidency he moved into University House and had requested alterations be made and that the facility be expanded so that it could also become a meeting place for the University's intellectually elite. Such meetings were held among those of Dr. Gunning's acquaintance whom he deemed "scholars and thinkers". On such occasions Mrs. Gunning served as a gracious hostess.

Dr. Gunning served only one five-year term as President. His Vice-President (Academic) was Dr. Myer Horowitz who was a popular choice to become President. Dr. Horowitz had come to the University from a career teaching elementary and high school in Montreal and from McGill University where he served as Assistant Dean of Education. He rose up through the ranks in our Faculty of

²⁵ As this saga was unfolding, I learned that an internal memo was being circulated at the Alberta Research Council that named me as advocating the closure of the Alberta Research Council. I never suggested this, but I do remember saying that if the University were to establish a research institute then perhaps ARC may wish to re-define its role. To ensure that this idea was nipped in the bud, and fast, the Committee and myself were called to a special meeting which was chaired by the Minister in charge of ARC along with the President of ARC to state unequivocally that the Alberta Research Council was here to stay! It should be noted that the Alberta Government was the first in Canada to establish a provincial research council and they were not about to let this concept disappear.

²⁶ A humorous aside to all of this was that Dr. Gunning didn't "march" at all! He was chauffeured over to the north end of bridge, by Peter Tait, where he got out and waited for the protesters to catch up, whereupon he appeared at the head of the procession for the benefit of the TV cameramen and newspaper photographers.

Education, first as a Chairman and later to become Dean before moving over to University Hall in the Vice-President's Office. My association with Dr. Horowitz was not as a member of GFC but as a member of the Executive Committee of Chairmen's Council. This was a group that I did not pay much notice to until I realized that Dr. Horowitz sought the opinions of Chairmen on matters of concern to the University. I looked forward each month to our meetings with Dr. Horowitz because he had a genuine interest in making the University an outstanding institution and he shared with us what was going on in University Hall. Dr. Horowitz and his wife Barbara brought warmth and understanding to the Office of the President. Jean spent many enjoyable hours with Barbara and other wives of faculty members in quilting the University Crest which hangs in the north stairwell of University Hall.

Dr. Horowitz served two five-year terms as President even though he suffered, but recovered from, a serious heart attack part way through his second five year term. During his presidency he saw government funding begin to decrease while University expenses, through increased enrollment, continue to increase. Like Dr. Wyman before him, Dr. Horowitz believed that a university education was a right and not a privilege, and that the Government had a responsibility to provide adequate funding. Unfortunately, this was not an opinion shared by the Government. Dr. Horowitz's views found little support in the Conservative Government, and although Dr. Horowitz kept the lines of communication between the University and the Government always open, he was not content to keep his opinions private and, at times, took his message to the media, which strained relations with some Government Ministers.

On the other hand, Dr. Horowitz was immensely popular with the students; they renamed the Students' Union Theatre in his honour. And, to the extent that I am aware, his executive and administrative staff were loyal to him and held him in the highest regard. He kept himself well informed as to activities of his executive staff without intruding on their authority or responsibilities. There is no doubt that Dr. Horowitz was in control and this extended to the Board of Governors. He was a visionary who lent his support to new ideas, whether or not funding was available. He believed if the idea was a good one, funding would somehow be found to support it. An example of this was the Timms Collections Centre.

Albert William Timms made a sizable bequest to the University in the 70's which, along with matching Government money and favorable interest rates, provided in 1989 enough money to build a structure valued around \$10 million. Contrary to the belief of many, Mr. Timms did not specify what the building should be for, only that it be named after him. Dr. Horowitz believed there was a pressing need for a building to house the University's Collections and Archives. He knew that the Government would not likely fund a non-teaching facility. Dr. Horowitz reasoned that if such a building were ever to be built it would have to be from donated funds. Therefore, he decided that the best use of the Timms Estate was to build a Collections and Archives Building. Unfortunately, the project did not include any funds for ongoing operations including funding for the additional staff who would be needed to operate the new facility. A sod-turning ceremony was rushed through in June of 1989 so that Dr. Horowitz could preside over it before his term ended at the end of June. However, the tenders for construction did not come in until September, and were \$5 million over budget!²⁷

The Timms story does have a happy ending, and is related to another project initiated by Dr. Horowitz. This was the conversion of Corbett Hall for use by the Faculty of Rehab Medicine. Upon the initiative of Dr. Horowitz the University had successfully secured enough funds from the Government to build a new building exclusively for the Faculty of Extension (who previously occupied Corbett Hall), located on the east side of 112 Street. Corbett Hall also housed Studio Theatre and it was intended that a large lecture theatre in Corbett Hall be used jointly by both Rehab Medicine and Studio Theatre. As the planning process proceeded for a major renovation of Corbett Hall it became clear that it would not be possible to provide a suitable dual purpose lecture/performing arts theatre within the allocated budget, and the best solution would be to relocate Studio Theatre elsewhere on campus. This was not received very well by the Dean of Arts but Dr. Davenport accepted

²⁷ The main reason for the tenders coming in too high was that the planning team had lost sight of the budget. The architect blamed the extra costs on the fact that the building included an underground parkade. The contract with the architect required that he redesign the building to be within budget, at his cost, but the Board decided to scrap the entire project. The Board also declined to sue the architect to recover the design fees, which were over one million dollars.

the suggestion of using the Timms money to build a new facility for Studio Theatre. Once apprised that Studio Theatre would occupy the site originally planned for the Museums and Archives Building, the Faculty of Arts were once again supportive. However, the backlash from the Friends of the Museums did not abate. To his credit, Dr. Davenport insisted in taking all the "heat" himself.²⁸

My term as Associate Vice-President (Facilities) overlapped Dr. Horowitz's term as President for only one month, June 1989. I did not interact with him in my new position but I did get to attend many of the farewell parties held in his honour. My new boss, Dr. Allan Warrack, and the others on the third floor of U-Hall had a high regard for Dr. Horowitz, as I did. But I sensed that there was a feeling it was time for a change and everyone was looking forward (with mixed emotions) to the appointment of Dr. Paul Davenport who was to take up his position on Aug. 1, 1989.

The appointment of Dr. Davenport, an economist from McGill, broke with the tradition of appointing the Vice-President (Academic) to the Presidency. I was not alone in believing that Dr. Peter Meekison, Vice-President (Academic), was well liked and believed capable of being a good President. But the Board were concerned about fiscal matters and the ability of the University to keep within its diminishing resources. For this reason they wanted someone who had a strong economic background. And, as we found out later, they also wanted to exercise more control over the President. For whatever reason, they passed over the nomination of Dr. Meekison. The advanced information about Dr. Davenport was that although he was young, he was articulate, intelligent, and a quick study.

Dr. Davenport was enthusiastic about bringing the Operating Budget under control and spent much of his time immersed in spread sheets and budget forecasts. Dr. Davenport's first couple of years seemed filled with parties and barbecues hosted at his home. At the time I wondered about the value these efforts because I believe the President cannot be friends with everyone. Nevertheless, and to his credit, Dr. Davenport tried to get to know the University and have the University get to know him.

Dr. Davenport had a tough act to follow in Dr. Horowitz. If for nothing else, the Government funding was being severely cut back and he had a Board who wanted to get into the management of the University. It was a difficult time for Dr. Davenport. When Dr. Warrack's term was up at the end of Dec. 1991 he offered to stay on for another six months but Dr. Davenport declined his offer. I was sorry to see Dr. Warrack leave because he added quality and experience to the Administration. Dr. Warrack's previous role as a Minister in the Alberta Government was an asset to the University and I enjoyed working for him and seeing how he handled difficult and controversial matters. Also, and before his term was up, Dr. Davenport told Dr. James, the Vice-President (Research) that he didn't want him to stay beyond his five year term. By this time he believed his problems were due in part to the fact that he still had the senior management team of Dr. Horowitz and things would not get better until he had his own team in place.

In the reorganization of his administration Dr. Davenport created two new Vice-Presidential positions amid much criticism at a time when the Faculties and service units were required to take big budget reductions. He argued that he had eliminated two Associate-VP positions (External AVP and Community Relations AVP) and therefore had not added to the bureaucracy. With the appointments of Mr. John McConnell (VP Development and Community Affairs), Dr. Lois Stanford (VP Student and Academic Services), Mr. Glenn Harris (VP Finance and Administration) and Dr. Martha Piper (VP Research), Dr. Davenport now had his own team. Except for Dr. Peter Meekison (VP Academic) all the other VPs were of his choosing. Dr. Davenport was more relaxed with this team and I believe began to

²⁸ One project that did not end successfully was to build an Artists' Colony using donated funds located on some property at Seba Beech, near Lake Wabamun. Although some academic departments said such a facility could be used by their faculty, no department was willing to provide operating funds to maintain the facility. This project was in full flight when I came into the office of the Associate Vice-President (Facilities). I did not realize the difficulties inherent in this project until after I had authorized the transfer of some previously acquired ATCO portable housing units from Calgary be moved onto the site. To help recover some of the costs my recommendation that these units be removed and transferred to the Meanook Biological Research Station at Athabasca was not accepted. As this is written (1996), the University is trying to sell this unused, unfinished, and deteriorating facility.

work with a degree of enjoyment and accomplishment. His style was one of hard work and long hours. However, Dr. Davenport did not freely delegate and often preferred to do everything himself.²⁹

I was still responsible for the Capital Budget and making recommendations on how and where the money should be spent.³⁰ Before making my recommendations I first consulted individually with every Dean and Director over a series of two-hour meetings, usually during the summer months. In the course of these discussions the Deans and I naturally talked about a variety of subjects and particularly those issues that were troubling the Deans. On occasion when I reported to the President that certain views were being expressed, Dr. Davenport lamented that the Deans seemed to talk to me more than they did to him. I didn't think this was so unusual in as much as I had a long history at the University and knew most of the Deans long before they had become senior administrators.

I believe that Dr. Davenport had probably one of the most difficult Boards that any President has had to work with. This was unfortunate because the Board chose Dr. Davenport over Dr. Meekison and it was later to transpire that the Board did not support Dr. Davenport in his administration of the University. The Board seemed determined to micro-manage the University, without the involvement of the President or the Administration. At the urging of his Vice-Presidents, Dr. Davenport appealed to the Board to limit its involvement to policy-making and leave the managing of the University to the Administration, but the Board paid little heed. At times they acted much like the opposition in the Legislature. And, there appeared to be a shift in the role of the Board where they began to represent the views of Government to the University more than representing the views of the University to the Government. In fact, they seemed to have not understood, or lost sight of, those traditional values which go into making a great university and that everything does not end up on a balance sheet. They charged ahead with criticisms of the authority of GFC³¹, the need for tenure, the need for administrative leaves etc., all emotional subjects with the faculty, which are not sacrosanct in themselves, but if these issues are to be challenged they need to be reviewed in the widest possible manner with input from all levels. To be fair, not all Board Members agreed with this approach but there were few occasions where Board Members came to the defense of the Administration.³²

Dr. Davenport's five-year term was to be reviewed in 1993, and if all was favorable, he would be reappointed for a second five-year term beginning July 1, 1994. Dr. Davenport expressed his wish to continue as President for a second term but the Board/University Review Committee recommended a search be implemented. They invited Dr. Davenport to let his name stand. Clearly this was a vote of non-confidence in the President, and understandably, Dr. Davenport interpreted it as such and refused to allow his name to be considered. The decision of the Board/University Committee, and Dr. Davenport's response to it, raised protests from the student body (who by now counted Dr. Davenport as a friend) and a number of the academic staff. The end result was to throw the university community into a turmoil that lasted over a year.

The fifth and final year for Dr. Davenport was a year of uncertainty, both from the view of who would be his replacement, and having to deal with a President in whom the Board had no confidence. To prove that he was no "lame-duck" President, Dr. Davenport ruled with the authority of one who

²⁹ A case in point was when I was Acting Vice-President (Finance and Administration) from Jan 1-Mar 31, 1991 and it was my responsibility to prepare a draft of the 1992-93 Operating and Capital Budgets. This I set out to do, and within the time frame he set, but before I was finished he handed me a draft that he had drawn up of the budget. Although I wrote many letters for his signature which he did not change, he just could not accept an Operating Budget that he had not crafted as his own.

³⁰ I count a number of projects which I promoted to successful conclusions. Among these were the transformation of Studio Theatre from Corbett Hall into the Timms Centre for the Performing Arts, the removal of automobile traffic from 89th Avenue and the widening of the pedestrian walkway, the installation of the 13.3mw steam/turbine generator, the mitigation (without lawyers) of the design and construction deficiencies on the Butterdome, the completion of the Extension Centre, and the framework for an Environmental Management System. In all of these projects I had the able assistance of members of the Departments of Physical Plant and Planning and Development.

³¹ When GFC voted to cancel classes so that students and faculty could march on the Legislature in protest of the budget cuts the Board held Dr. Davenport personally responsible. A second GFC meeting was called wherein Dr. Davenport persuaded GFC to rescind its earlier cancellation of classes.

³² Even administrative successes were criticized. When I reported to the Board Building Committee that I had successfully negotiated a million dollar settlement to resolve the design and construction deficiencies on the Butterdome without resorting to litigation, I was told that I should have put it into the hands of lawyers.

did not have to live with the consequences of his decisions³³ and, by now, one who was looking forward to his next appointment, that of President of the University of Western Ontario. I don't think it was in the best interests for all concerned for Dr. Davenport to stay on for an entire year after the Board had effectively fired him. On the other hand, the Board had a contract to pay him for five years (plus a year of Administrative Leave), come what may. But I can't fault Dr. Davenport for the way he handled this whole affair. In fact, Dr. Davenport showed great class throughout this ordeal, which must have been very painful to him and his family. Given the opportunity, I believe Dr. Davenport would have done some things differently. His was a difficult job at a difficult time and no one can fault him for the dedication he gave to the University. It did not transpire that the Board was willing to allow him to serve a second five year term where the valuable experience he gained during his first term would have been an asset to the University. Instead, he became an excellent and successful candidate for the presidency at the University of Western Ontario.

I shall relate a couple of instances which were of concern to me and reflect on how things were handled during these difficult times. Ernie Ingles (Chief Librarian) and I were making a presentation to the Board Finance Committee to develop an off-campus storage facility for the Library, later named the BARD. The criticism that Ernie and I received was totally unexpected. Some members of the Committee said that the plan was ill-conceived, that not all the costs were included, that we were recommending leasing a facility (even though they knew there was no money to purchase the facility), and we hadn't struck a good enough deal with the owners (the Hong Kong Bank). Except for the leasing of the facility, all of the criticisms were without foundation. Eventually wiser heads prevailed and the project was approved. BARD was officially opened by the Minister of Advanced Education, Mr. Jack Ady. Also in attendance, and taking full credit for how this facility was an innovative venture which was going to save a lot of money, yet provide the University with much needed library storage space, were members of the Board!

Another example of the frustration those of us "In The Trenches" had to endure, as a result of the conflict between the Board and the President, was with the matter of salary increases. In 1993 the Board Compensation Committee (Executive Committee by another name) declared that there would be no salary increases, merit or otherwise, for the President and the Vice-Presidents. This was also to include the Associate Vice-Presidents (AVP's). The intention of the Board Compensation Committee was that they would not conduct any performance reviews of any of the Senior Administrators. At this time there were eight AVP's, four of them Administrative Professional Officers (APO's) who were not affected by this decree, and four academics who were; Dr. Roger Smith, Dr. Lynn Penrod, Dr. Robert Busch and myself. When I learned that the Compensation Committee's directive did not apply to Deans, being older and thus bolder, on my own I wrote to Dr. Davenport citing a section in the Academic Agreement that required the Board to conduct, or have conducted on its behalf, annual performance reviews. A few weeks later I learned that my letter had prompted the Compensation Committee to rescind its directive as applied to AVP's and, in fact, they had conducted performance reviews for each of the academic AVP's. We were each awarded a "merit increment" but these awards were to be "without any monetary value". I was astounded by this response. So I wrote another letter and asked Dr. Davenport just what message was the Board sending out to the academic community where, if an academic becomes an administrator, he/she can expect less salary than if they remained in teaching and research! Dr. Davenport took this letter forward to the Acting Chairman of the Board, Sandy Mactaggart, who apparently agreed with my position and attached a "monetary value" to our merit increments.

I worked more closely with Dr. Davenport than with any of the other Presidents. I wanted to see him do well and did whatever I could to support him. But his working style, his lack of history at the UofA, and his ongoing conflict with the Board, all combined to make problems for us, and for him a difficult five years as President. As he said at one of his farewell receptions, he had learned a lot and was leaving the UofA much better prepared for the Presidential Office than when he arrived!

Perhaps the biggest difficulty that Dr. Davenport faced, which was in no way related to his ability, was that he was unknown to the faculty, and as such, only his performance as President could be evaluated. There was no fall-back experience at the U of A he could draw upon, and there was no

³³ Two of his decisions were to eliminate one of the positions he had created, that of Vice-President (Academic and Student Affairs), and my position, Associate Vice-President (Facilities). The latter position was restored in 1996.

such U of A experience others could attest to in his defense. As a consequence of this, when the Board chose not to reappoint Dr. Davenport, the academic community raised little in the way of support to retain him as President.

What goes into making a good President? Why did Dr. Davenport have so much difficulty at the UofA? For one, he was just 41 years old. His background at McGill would appear to have been more that as an administrator than that of an academic. This may have tended to influence how he viewed issues.³⁴ In my mind at least, the President has to have strong academic credentials which include a respectable research career as well as many years teaching at all levels. On the other hand, Dr. Davenport's budgeting and analytical experiences were an asset in his role as President, and this is what probably attracted him initially to the Board. I don't believe the Board was particularly concerned about the academic experience of Dr. Davenport. What led to his departure was a breakdown in communication between the Board and himself, leading to the result that the Board lost confidence in the President. I believe the Board erred in not reappointing Dr. Davenport for a second five year term. At the same time it was clear that there had to be new members appointed to the Board who could contribute to the well-being of the University without the bellicose manner that prevailed.

Dr. Davenport's tenure at the University, while attended with a degree of turmoil and controversy, was in a way a watershed for the University. There is no doubt that severe budget constraints were occurring and that major reorganization within the University was required. Dr. Davenport, with the assistance of Dr. Meekison, developed the document entitled "Degrees of Freedom" (Nov. '93) and "Quality First" (Feb. '94), assisted by Dr. John McDonald who succeeded Dr. Meekison as Academic Vice-President, which set out significant restructuring recommendations involving many faculties. These documents were highly controversial and some recommendations were vehemently opposed by some Faculties. But in the end, the documents laid out a framework for the University to evaluate existing programs and created an environment where Faculties began to streamline and consolidate their programs to be more cost effective and efficient and to explore new methods of teaching delivery systems.

As I write this we are beginning the third year of the five-year term of Dr. Roderick Fraser, our 11th President. Has much changed? He is ten years older than when Dr. Davenport came to the UofA, and like Dr. Davenport, he is an economist, not that this is necessarily a requirement but probably reflects what the Board wants in a president. He came from Queen's where he was a Vice-President for Planning but he is a native Albertan who attended the University of Alberta. His management style is reported to be similar to that of Dr. Davenport in that he has a penchant for details and is convinced that the University's reputation will be established with the use of the proper performance indicators and that one measure of this is to score high in the annual Maclean's Magazine Survey of Universities. He is less visible than Dr. Davenport, partly because one of his objectives, that of fund development for the University, takes him away from the campus a good deal of the time. He has dropped the "confidants" of Dr. Davenport and has assembled a new secretarial group on the 3rd floor. However, when he first arrived I believe he erred by not encouraging the then Acting Vice-President (Academic), Dr. Roger Smith, to apply for the Vice-President's position. After conducting a review of other candidates, using the usual search (and destroy?) process he apparently had second thoughts and asked Dr. Smith to be a candidate. But by this time Dr. Smith had made other plans and said "no, thank you." This was unfortunate in my opinion and followed an earlier omission of Dr. Davenport when he was looking for a replacement for Dr. Warrack as Vice-President (Finance and Administration). Dr. Davenport was so convinced that his team had to come from outside the University that he passed over the candidacy of Dr. Smith for the finance position. In my opinion, had Dr. Smith been VP Finance he would have been a prime candidate for the Presidency. Such is the fate of decisions and what ifs.

³⁴ An example of this is when he accepted the suggestion of the Registrar to delete the names of all graduating students from the Convocation Program because it would save a few thousand dollars. He didn't take into account the negative impact such a decision would have on the newest crop of alumni and their potential for future gift-giving to the University.

Looking into the future we now have a Board which seems to be supportive of the President and the Senior Administration although there are still some members who seem to think the running of the University is just like running any other business. The University is in for some hard times ahead with reduced enrollments, decreased funding, and trying to respond to the challenge of delivering higher education in more meaningful and economical ways. Whether our existing senior administration, who are immersed in budget forecasts and performance indicators, will have a solution is anybody's guess. Time will tell. As I reflect back on my years at this university I have seen it grow from 4000 to 25,000+ students. It has grown in physical size as well. Each of these factors has presented huge challenges to the University. These challenges were met by a strong degree of cooperation and respect between the Administration and the academic community, and a supportive Board of Governors. These linkages will have to be reestablished, and strengthened, if the challenges of the future are to be met with equal success.

CONCLUDING REMARKS

From the forgoing I obviously could not resist the urge to wax philosophical in pondering the past when writing an essay of this sort. My comments are not intended to be critical of individuals as much as I offer as criticisms of the system where it pertains to the selection of administrators. I was brought up in the old tradition; hard work would be rewarded with responsibility (if one was so inclined), and this is how one would climb up the administrative ladder one step at a time. When individuals were given the opportunity to skip a few rungs, in my view, this led to difficulties. On the other hand, I believe all senior administrators (VP's and up) should have had extensive academic and administrative experience at the the University of Alberta. The learning curve is just too steep for outsiders to be up and running in just a couple of years and at the same time have an understanding of the University of Alberta. The University is large enough and amply staffed with excellent people who are capable of effective leadership. I have to accept that in today's world the practice is to seek individuals who are ready to take on senior administrative positions without having worked their way through the system, and more recently, seek candidates who are strangers to the University of Alberta. This is the way many corporations act, sometimes with disastrous results. I don't think this is a model to emulate at the University.

Appendix I describes my involvement with the Association of Professional Engineers, Geologists and Geophysicists of Alberta. While not a University activity, I am grateful for the time the University allowed me to be away from campus in order to participate in the affairs of APEGGA to the degree that I did. As a Past-President of APEGGA and as a Fellow of the Canadian Academy of Engineering I will be able to remain active in my profession in my retirement years.

Throughout my involvement with my profession I received some honours and awards. I have listed these in Appendix II.

In Appendix III I have listed the graduate students that I supervised. All of these students have gone on to distinguished careers in either industry or academe.

When one is an administrator one rarely is complimented on a job well done. Although being elected to three terms as Chairman is a form of some recognition. In any case I did receive some kind words which I have photocopied in Appendix IV. I wish I had kept more of them. The one from Professor Jan P. Den Hartog of M.I.T. was particularly appreciated, as I had used his books on vibration analysis and applied mechanics as a graduate student and later as a teacher. He was one of the top applied mechanics people of his day and ranks alongside the great Stephen P. Timoshenko. I was honored that my paper (co-authored with A. Semeniuk) was reviewed by such an eminent authority, and was touched by his comments.

In Appendix V, I have included a few newspaper clippings where I was mentioned.

Another purpose of this book was to outline some of my research activities spanning my working career at the University of Alberta. In Appendix VI is a compilation of the research papers that I published over my academic career from 1963 to 1996. Although my final seven years were spent in

University Hall, I continued to be involved in research, writing papers and supervising graduate students.

A glance at the variety of research subjects that follows may create the impression that I never could decide on what I wanted to do. It was deliberate. I just could never see myself researching variations of the same research topic for any length of time. For the same reason it is probably why I play three musical instruments with amateurish enthusiasm instead of one with professional proficiency. Readers who bother to review my research papers will see a shift from fairly theoretical research, stemming from my PhD thesis, to some almost exclusively experimental. Apart from some wanderings into the fertile fields of sports medicine (for a Mechanical Engineer at least) most of my research was based on problems suggested by the steel and petroleum industries in Alberta. For whatever their value, my research efforts are now exposed in their entirety. Some earlier papers seem to be missing or lost in obscurity; not an unknown fate, nor necessarily undesirable.

APPENDIX I: APEGGA and CCPE

The Association of Professional Engineers, Geologists and Geophysicists of Alberta (APEGGA), my professional association, was and still is very important to me and I owe it much for the opportunities it gave to me. However, my first professional involvement wasn't with APEGGA but with the Association of Professional Engineers of Ontario (APEO). One year after I graduated from UBC I applied to and was admitted into APEO. When I moved to Alberta to do graduate work I maintained my APEO membership because I was eligible for reduced out-of-province fees and more importantly, I could maintain my term life insurance policy which APEO was sponsoring at that time. There was also the possibility that I might have returned to Ontario once I had completed my studies. However, after accepting the faculty position at the UofA I applied for admission into APEGGA (then called APEA, The Association of Professional Engineers of Alberta) in 1964.

I resolved that if I was going to get anything out of APEGGA I was going to have to become involved. Accordingly, I volunteered to serve on any committee they chose for me. Soon after, I was appointed to the Continuing Education Committee. This was not an auspicious beginning. The Chairman of the Committee was convinced that, as far as he was concerned, continuing education meant that engineers should take a course on welding. There is nothing wrong with learning about welding but I envisioned that the committee would have a broader perspective on continuing education. In any case I can not recall how it came to pass but my next assignment was to serve on the Membership Committee. Again, this name was a bit misleading in that its main purpose was not to enlist eligible engineers to join the Association (a questionable activity to say the least), but to chase after those who were arrears in the payment of their dues. After overcoming some initial misgiving, I remained a member of this Committee for a number of years and eventually became its Chairman. I was instrumental in changing the focus of this Committee to serving the needs of the membership and renamed the Committee the Members Liaison Committee.

So that the Committee would not stray too far off course a senior staff member from the APEGGA office was assigned to the Committee as Recording Secretary. This is where I first met Clayton Milroy, P.Eng. who was then Deputy Registrar, and later for whom I had the highest regard. I also served on an Industrial Liaison Committee, Editorial Committee, the 1978 Convention Planning Committee in Jasper as the Vice-Chairman, and as Chairman of the 1988 Convention Planning Committee in Red Deer. Throughout this period my main contact in the APEGGA office was Clayton Milroy, although I also got to know others in the office including the Executive Director, Ivan Finlay, P.Eng.

In 1978 Clayton asked me if I would allow my name to stand for election to the APEGGA Council. This I agreed to do and was pleasantly surprised that I received enough votes to be elected to Council for a three year term 1978-1981. As a member of Council my committee involvement increased; I served on the Discipline Committee and eventually as its Chairman, the Enforcement Committee, the Act, Regulations and Bylaws Committee, and the Task Force on the Recognition of Technologists.

In 1980 once again I was approached by Clayton to run for office, but this time for one of the two Vice-President positions. I was not enthusiastic because there were two other excellent candidates (Bill Fraser and Ron Gray) who were senior officers in industry, and I had not finished my three year term as a Council member, and my candidacy could be perceived as being too ambitious. In any case I agreed to run but was not surprised at the outcome where I ran third. In 1981 my three year term on Council was up so when I was asked to run again I agreed. Again I lost. So that was it for me; or so I thought.

In 1982 I was awarded with the L.C.Charlesworth Award for one "who has served the profession diligently for many years and has made substantial contributions to the operation of the Association and the advancement of its professional status." This honour was further enhanced for me by the fact that Dr. George Ford, P.Eng. received it at the same time.

But this was not the end of my involvement with APEGGA for once again Clayton asked if I would allow my name to stand for Vice-President. This time I flatly refused as I did not think my pride could take another bruising with a further loss at the polls. But Clayton was not to be dissuaded and instead invited me over to the MacDonald Hotel for a couple of drinks where we were joined by Bill Fraser and Ron Gray. The three of them twisted my arm (and plied me with large martinis) and I finally agreed to run for the third and final time. But third time was lucky and I was elected 2nd Vice-President. Bob Savage was elected First Vice-President. The following year I ran again, which is expected of all 2nd Vice-Presidents (but is not always successful), and this time I won the majority of the votes to become First Vice-President, and by acclamation in the following year, President. All in all I served on the Executive Committee for four years and on Council for a total of seven years.

It was a very rewarding experience and a great honour for me to be President of APEGGA and represent Alberta's engineering profession throughout the province and across Canada. Jean accompanied me on all my visits to the Branches in Alberta and to the other Associations in Canada when attending their Annual Meetings. When my term on Council was ending, I held the position of Past President, I was nominated to serve as APEGGA's representative on the Board of Directors of the Canadian Council for Professional Engineers (CCPE).³⁵ I was elected to the first of three two-year terms. As APEGGA's representative on CCPE I, along with Jean, attended semi-annual meetings in Ottawa and annual meetings in a major city in one of the Provinces in Canada. Between our APEGGA and CCPE travels Jean and I visited every Province and the two Territories in Canada.

There is no doubt that Clayton Milroy had a large hand in my successful participation in APEGGA. I thoroughly enjoyed all the meetings I had with him. He had a sense of humour and as I knew that he was keen on the military we often talked about things military and him being an Honourary Colonel in the Canadian Militia. However, I was particularly grateful for the tremendous support he gave to me during my term as President. He typified what I believed to be what a professional engineer was all about. So it was with a great deal of sadness that it became apparent to all that he was not in good health and, too soon, succumbed to cancer in 1987. With his passing the Association lost one of its most esteemed and valuable members, and I lost a friend.

My six years on the Board of Directors of CCPE was interesting in that it was, in a way, a microcosm of the Canadian political scene. I was placed in a somewhat awkward position by APEGGA because the Council of the day was becoming quite militant and provincial in its outlook. As a result, I was instructed to take certain positions on the CCPE Board with which I personally did not agree. Nevertheless I enjoyed being on the Board of CCPE and served on the Nominating Committee, the Awards Committee, and the Audit Committee. Despite some differences of opinion from time to time I met many fine men and women who were serving our profession across Canada.

³⁵ I am indebted to Dr. Fred Otto for this nomination.

APPENDIX II: HONOURS AND AWARDS

- 1960-61 Province of Alberta Queen Elizabeth Scholarship
- 1961-62 Province of Alberta Queen Elizabeth Scholarship
- 1982 APEGGA; L.C. Charlesworth Award
- 1986 Fellow; Canadian Society for Mechanical Engineering
- 1986 APEGGA Life Membership Award
- 1986 Uof A; Twenty-five Year Service Award
- 1986 ASET; Certificate of Recognition
- 1988 ASME; Twenty-five Year Membership Award
- 1988 SESA; Twenty-five Year Membership Award
- 1991 Imperial Oil Research Excellence Award
- 1992 Fellow, Canadian Academy of Engineering
- 1994 UofA; Thirty Year Service Award
- 1996 Professor Emeritus of the University of Alberta

APPENDIX III: GRADUATE STUDENTS SUPERVISED

- 1965 B.R. Long, M.Sc., "Fatigue Crack Propagation in Mild Steel"
- 1966 M.G. Faulkner, M.Sc., "Bending Behaviour of Bi-Trapezoidal Plates"
- 1966 A. Semeniuk, M.Sc., "Stability of Cambered Bi-Trapezoidal Plates"
- 1967 J.G. Rae, M.Sc., "Vibration of Tapered Cantilever Plates"
- 1968 A.K. Saha, M.Sc., "Investigation of a Diaphragm Type Load Cell"
- 1969 V.E. Schneider, M.Sc., "A Comparative Evaluation of Hockey Helmets", jointly supervised with S.W. Mendryk
- 1969 D.D. Nelson, M.Sc., "Stiffness of Clamped Joints"
- 1971 A. Semeniuk, Ph.D., "Dynamic Response of Thin Elastic Arches"
- 1972 R.K. Jensen, Ph.D., "System of Standardized Biomechanical Force Measures", jointly supervised with S.W. Mendryk
- 1976 N.D. Cole, M.Eng., "Rolling Mill Cooling Bed"
- 1981 R.M. Carlson, M.Eng., "Cold Weather Steels"
- 1982 H.J. Gross, Ph.D., "Biomechanical Analysis of the Pole Vault", jointly supervised with J. Terauds
- 1983 D.J. Pridie, M.Sc., "A Study of the Charpy Test"
- 1983 A. Budhiman, M.Sc., "Fatigue Precracking and Fracture Toughness", jointly supervised with D.R. Budney
- 1984 M.A. Wahab, Ph.D., "Fatigue Life Estimation of Welded Structures", jointly supervised with M.G. Faulkner
- 1984 D.G. Syrotuik, Ph.D., "Torque Analysis of Nautilus Leg Extension Machine", jointly supervised with S.W. Mendryk
- 1988 R. Howe, M.Sc., "Bending Stresses Arising in Sucker Rod Ends"
- 1993 N.S. Viswanath, Ph.D., "An Analysis of the Wear of Polymers"
- 1994 G.H. Sonego, M.Sc., "Wear of Couplings with Oilfield Tubing"

APPENDIX IV: LETTERS

OFFICE of the PRESIDENT



EDMONTON,
Alberta, Canada

June 5th, 1963

Mr. Donald Grant Bellow
11464 - 132 Street
EDMONTON, Alberta

Dear Mr. Bellow:

I am happy to inform you that the Executive Committee of the Board of Governors, at their meeting on May 28th, 1963, approved your appointment as Assistant Professor of Mechanical Engineering, for a four-year probationary period, effective September 1st, 1963, at a salary of \$8,000 per annum.

I would like to take this opportunity to welcome you to the staff of our University and I also would like to mention that it is always a pleasure to have one of our own graduates join our staff.

Yours very truly,

Walter H. Johns per B.M.D.

Walter H. Johns
President

BHM/ems

cc: Dean G.W. Govier
Dr. G. Ford
Bursar

INTER-DEPARTMENTAL



CORRESPONDENCE

CONFIDENTIAL

TO Dr. D.G. Bellow, Dept. of Mechanical
Engineering
FROM Dean of Engineering

DATE June 22, 1970

Dear Dr. Bellow:

The recent salary letter which you received, and which was prepared in the President's office, did not specifically state that your salary increases for 1970-71 involve your promotion to the rank of "Professor". I therefore wish to advise you that the recommendation of the General Promotions Committee has been accepted by the Board and you will be promoted to the rank of "Professor" effective July 1, 1970.

May I congratulate you on your promotion and wish you every success in the future.

Sincerely yours

R. M. Hardy
Dean

RMH/11

cc: Vice-President (Academic)
Dr. G. Ford

INTER-DEPARTMENTAL



CORRESPONDENCE

Professor D. G. Bellow
TO Department of Mechanical Engineering

DATE June 30th, 1971

FROM The President

Dear Professor Bellow:

Sometimes I do not know whether to write a letter of regret or a letter of congratulations when people retire from the Executive Committee of General Faculties Council. As you know I myself cannot retire until my term of office as President is over. In any event, I would like to say how much I appreciate the contribution that you have made to the Executive Committee, and through this committee to the University as a whole.

Yours sincerely

M. Wyman
President

MW:im

J. P. DEN HARTOG
PROFESSOR OF MECHANICAL ENGINEERING Room 3-260
MASSACHUSETTS INSTITUTE OF TECHNOLOGY
CAMBRIDGE MASSACHUSETTS (02139).

18 Oct 1971

Prof. Bellon & Semeniuk

Gentlemen:

Hereby I beg your pardon for violating a trust. A certain Journal, receiving manuscripts sends them to diverse old gentlemen with the admonition "not to disclose his identity to the authors either directly or by implication". Of course I do nothing of the sort.

However ... in your H.S. you refer to one (of my many) youthful errors in connection with an algebraic assumption of a Rayleigh shape. You may believe me when I say I don't have the original notes any more and I am a bit lazy to start from scratch again after those many years. But I am curious just the same. If you still have your scratch sheets on the matter, a Xerox (or Canadian equivalent) copy of those would be highly welcome. Thank you for your continual courtesy & sincerely yours,
J. P. Den Hartog

MASSACHUSETTS INSTITUTE OF TECHNOLOGY
DEPARTMENT OF MECHANICAL ENGINEERING
CAMBRIDGE, MASSACHUSETTS 02139

J. P. DEN HARTOG
Professor of Mechanical Engineering

1 November 1971

Dear Professor Bellow:

I am very grateful to you for sending me the longhand calculations on my maiden paper. You did a lot of work on it indeed. I find that my accuracy in numerical work has not improved with the years.

When your paper gets printed I shall be glad if you could send me a reprint of it, because I only saw the M.S. and took no copy.

With best regards,

Yours sincerely

J.P. Den Hartog

July 27, 1972.

Professor J.P. Den Hartog,
Professor of Mechanical Engineering,
Massachusetts Institute of Technology,
Room 3-260, 77 Massachusetts Avenue,
Cambridge, Massachusetts. 02139

Dear Professor Den Hartog:

Please accept, with our compliments, the accompanying reprints of the paper entitled "Symmetrical and Unsymmetrical Forced Excitation of Thin Circular Arches" authored by Dr. Semeniuk and myself.

Yours very sincerely,

Donald G. Bellow, Professor
MECHANICAL ENGINEERING.

DGB:nw
enclosure

OFFICE OF THE CHANCELLOR



THE UNIVERSITY OF ALBERTA
EDMONTON 7, CANADA

T6G 2E1

July 4, 1972

Dr. D. G. Bellow,
Department of Mechanical Engineering,
Engineering Centre,
The University of Alberta,
Edmonton, Alberta,
T6G 2E1

Dear Dr. Bellow:

It is a matter of regret to me that your term of office as a member of the Senate of The University of Alberta ended on June 30, 1972.

May I take this opportunity of thanking you most sincerely for your participation in Senate matters during the past three years, and I hope that you will continue to take an interest in the Senate in the years to come.

Your name will, if you have no objection, be added to the list of Senate Alumni in order that you may receive, periodically, any information circulated on matters of interest to you regarding the Senate.

Sincerely yours,

L. A. DESROCHERS,
Chancellor

THE UNIVERSITY OF ALBERTA
EDMONTON, CANADA T6G 2J9



DEAN OF ARTS

R. G. Baldwin

Dec 20, 1973

Dear Don:

63
I've never got around to
congratulating you on what I thought
was an outstanding performance as
Chairman of the Role Committee. You
were patient, hard-working (heaven
knows), and above all sensitively
attuned to the concerns of your
Committee members. Bravo!

George

7/221

Louis A. Desrochers

1824 ROYAL TRUST TOWER
EDMONTON CENTRE
EDMONTON, ALBERTA
T5J 2Z2

April 16, 1975.

Dr. Donald G. Bellow,
Faculty of Engineering,
University of Alberta,
Edmonton, Alberta.

Dear Don,

I have just read about your appointment as Chairman of the Department of Mechanical Engineering and I congratulate you. It takes guts to assume administrative duties in the university world these days and I tip my hat to you.

Best wishes.

Yours sincerely,



LAD:bmg



Office of the President

The University of Alberta
Edmonton, Alberta
T6G 2J9
Telephone: 403 432-3212
403 432-3620

April 13, 1981

Dear Dan,

Congratulations on your
reappointment as Chairman.

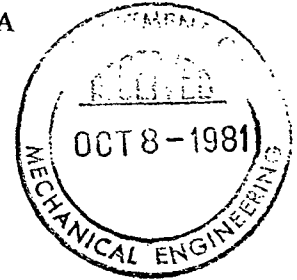
I am delighted that you
have agreed to continue to
serve.

Sincerely

Therese

THE UNIVERSITY OF BRITISH COLUMBIA
2324 MAIN MALL
VANCOUVER, B.C., CANADA
V6T 1W5

DEPARTMENT OF MECHANICAL ENGINEERING



October 5, 1981

Dr. Donald G. Bellow,
Chairman,
Mechanical Engineering,
The University of Alberta,
EDMONTON,
Alberta T6G 2G8.

Dear Don:

I would like to express the appreciation of all of us
for your very good seminar last week on the important question
of undergraduate engineering laboratory.

I am sure that you have provoked some good, if
uncomfortable thinking about several issues, and I hope our
future planning will show the benefits of your experience
and advice.

Under separate cover you should receive a cheque
for travel expense. Enclosed is a small honorarium cheque.

Yours sincerely,

A handwritten signature in cursive script, appearing to read "Phil".

Philip G. Hill, Professor and Head,
Department of Mechanical Engineering.

*Dr Bellow - your cheque for travel will come
direct from our Finance Dept.*

A handwritten signature in cursive script, appearing to read "J. G. Hill".

Teknica

Resource Development Ltd.

Telephone 403/269-4386 • Telex 03-826725 • Suite 600, 633-6th Avenue S.W., Calgary, Alberta, Canada T2P 2Y5

June 14, 1982

Dr. D.G. Bellow, P. Eng.
Department of Mechanical Engineering
University of Alberta
Edmonton, Alberta
T6G 2G8

Dear Don:

Congratulations on receiving the L.C. Charlesworth Award from APEGGA. I cannot think of anybody who has been more dedicated and more unselfish in their service to the Association. You are certainly very deserving and I wish you every continued success.

Cordially,



Roy O. Lindseth

ROL/sc





University of Alberta
Edmonton

Office of the President

Canada T6G 2J9

3-1 University Hall
Telephone (403) 432-3212

June 15, 1984

Dear Don,

Many thanks for
serving on the President's
Advisory Committee of
Chairmen. I appreciate
very much your valued
support.

Sincerely

Roy O. Lindseth

SUITE 1100, 736-6TH AVENUE S.W.

CALGARY, ALBERTA, CANADA

T2P 3T7

July 17, 1985

Mr. Don G. Bellow, P. Eng.
President
The Association of Professional Engineers,
Geologists
and Geophysicists of Alberta
University of Alberta
c/o Department of Mechanical Engineering
Edmonton, Alberta
T6G 2G8

Dear Don:

Let me extend congratulations upon your election to President of APEGGA. Your election crowns many years of diligent work for the profession.

I hope you find your term on the APEGGA Executive Committee to be stimulating and enjoyable.

With every good wish for a successful year, and best personal regards.

Cordially,



ROL/le



University of Alberta
Edmonton

Office of the President

Canada T6G 2J9

3-1 University Hall
Telephone (403) 432-3212

July 7, 1986

Dear Dan,

Congratulations. I

was very pleased to
read in yesterday's
newspaper that you've
been awarded a fellowship
by the Canadian Society for
Mechanical Engineering.

Best wishes always.

Sincerely
Thur



University of Alberta
Edmonton

Office of the President

Canada T6G 2J9

3-1 University Hall
Telephone (403) 432-3212

January 9, 1989

Dear Don,

Thanks - many thanks -
for agreeing to take
over as Associate Vice-President
(Facilities). I'm delighted.

Best wishes

Sincerely



University of Alberta
Edmonton

Canada T6G 2J9

Office of the
Vice-President (Research)

3rd Floor, University Hall

February 9/89

Dear Don

Congratulations on being appointed Associate Vice-President (Facilities). I must admire Allan Warrack's choice! With your wealth of experience in Engineering as Chairman of Meck E and in overseeing the construction of the Meck.E. building, you will be a great help over here.

By the way, I pointed out to Peter Meekison that there are three UBC engineering graduates in University Hall now.

Looking forward to working with you!

Bob



ADVANCED EDUCATION

Devonian Building, 11160 Jasper Avenue, Edmonton, Alberta, Canada T5K 0L3 Fax 403/427-4185

August 31st, 1992

Dr. Don Bellow
Associate Vice-President
(Facilities)
University of Alberta
3-16 University Hall
EDMONTON, Alberta
T6G 2J9

Dear Dr. Bellow:

Congratulations on your being inducted as a Fellow of the Canadian Academy of Engineering. It's an honour to be associated with such an eminent person.

Sincerely,

Lu Pastuszenko, P.Eng.
Director
Campus Development Services

LP:kjs





University of Alberta
Edmonton

Dr Paul Davenport
President

Canada T6G 2J9

3-1 University Hall, Telephone (403) 492-3212

September 8, 1992

Dr. D.G. Bellow
Associate Vice-President
(Facilities)
3-16 University Hall
Campus

Dear Don:

I see from the Laurels column in a recent edition of Folio that you have been inducted as a Fellow of the Canadian Academy of Engineering.

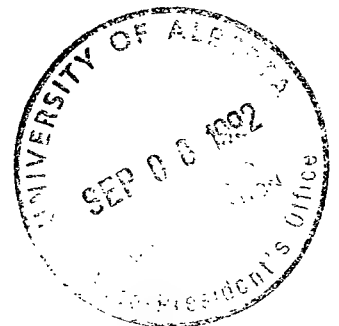
This is indeed an honour, and I offer my warmest congratulations and best wishes on your future endeavours.

Sincerely yours,

Paul Davenport

PD/mph

cc: Mr. G. Harris
Dr. F.D. Otto



June 28, 1996

Don,

It seems to me that the best universities
have depended on people like you for
their growth and development -
individuals who have been prepared
to step beyond the boundaries of
their departments and throw

themselves into the affairs of
their institutions and professions.

It has been a great pleasure working
with you. Please stay in touch

Cheers

Allen.



University of Alberta
Edmonton

Canada T6G 2J9

Office of the
Vice-President (Research and External Affairs)
Martha C. Piper

3rd Floor, University Hall

July 17, 1996

Dear Don,

I am so sorry that
I will be unable to
attend your reception - as
I will be out of town
on holiday . . . but I will
be thinking of you.

I have so enjoyed my
association and interaction
with you over the past
several years, and respect
immensely the contributions
you have made to the UoA.
I wish you only the very
best, and hope that I can
continue to draw upon your
wisdom from time to time.

Warmest regards,
Martha

Donny's Lament (to the tune of Danny Boy, with apologies)

Oh Donny Boy, the pipes, the pipes are bursting,
The roof it leaks, the paint begins to peel.
Ere long, I know, without more help from Gogo,
The wind and snow and bitter cold we'll feel.

Chorus:

So give us funds, the formula is folding.
The natural gas, its price to heaven soars.
Be quick, be quick, control the Board is wresting,
The Welsh run wild, and Stan the lion roars.

In better days the grounds they all were tidy,
No weeds there waved, nor dust lay round in heaps.
Yet now I fear, the leaves lie still and scattered,
For funds are short and Johnny's still too cheap.

Chorus:

So give us funds ...

The coffee's cold, the Printing House is closed,
In Engineering no Aggies more may roam,
Our quotas burst, and still the fees keep rising.
The Miners won, and so will not go home.

Chorus:

So give us funds ...

So contract out! the cry rings round the buildings,
And Seba Beach cries out for money more.
And in U. Hall they pack them in like sardines,
If this keeps up, we'll have to quit these shores.

Chorus:

Forget the funds, just let us keep on working,
'T'is all we hear, the APO's lament.
Quite soon we all be in need of Counselling
(If that's not gone), or be severely bent.

July 15, 1991

© PST, with help from RJF



University of Alberta
Edmonton

Faculty of Engineering
Office of the Dean

Canada T6G 2G8

5-1 Mechanical Engineering Building, Telephone (403) 492-3320
Fax (403) 492-0500

November 14, 1996

Dr. D.G. Bellow
Professor Emeritus
4915 - 115A Street
Edmonton, AB
T6H 3P7

Dear Don:

I am pleased to forward to you the statement of acknowledgement which was read into the Minutes of the meeting of Engineering Faculty Council on October 15, 1996. We wish you continued success and much happiness in the future.

May I also extend my personal thanks and congratulations for a job well done.

Sincerely yours

David T. Lynch
Dean

DTL/ae
Encl.



TransCanada

G.J. Maier P.Eng., FCAE
Chairman

TransCanada PipeLines

2900, 240 Fourth Avenue S.W.
Calgary, Alberta
Canada T2P 4L7

Telephone: (403) 267-8500
Fax: (403) 267-8502

February 24, 1997

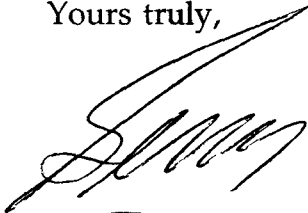
Mr. Don Bellow
4915 - 115A Street
Edmonton, Alberta
T6H 3P7

Dear Don:

I just received a copy of the **Colloquium** and noted with some sadness that you are leaving your position with the University of Alberta. While the write-up was very complimentary, I don't think it did you justice in that your contribution to the profession has been much greater than could be summarized on one page.

I am not sure what you have in mind for the future but, whatever you do, I know that it will be as successful as was your time at the UofA. In any event, you have my very best wishes.

Yours truly,


GJM/dr

Don Bellow's Legacy Lives On

When Don Bellow first arrived on the campus of the University of Alberta in 1958, he entered a graduate program in a department which had just been formed and had yet to graduate an undergraduate student. Don obtained his MSc in 1960 at the same time as the first undergraduate class was finishing. In 1963 he received the first PhD awarded by the Department of Mechanical Engineering and was appointed as an Assistant Professor in that same year.

During the early part of his career Don had a tremendous influence on the development of the Mechanical Engineering curriculum. He developed a number of design courses, graduate-level courses in stability and strain analysis, and perhaps the most outstanding example, a mechanical measurements course. Before the introduction of this course, mechanical measurements were studied in various laboratories associated with specific courses. Temperature was measured in the course on thermodynamics, strain was discussed in the strength of materials course, and flow measurements were covered in fluid mechanics. In the new course, Don brought all these measurements together and exposed students to theoretical concepts in measurement theory. A common measurements course has now been offered in our Faculty for nearly 25 years, and in fact, has been adopted by most universities in Canada. Don will long be remembered as a leader in the development of innovative curricula.

Don was appointed to the rank of Professor in 1970 and assumed many administrative duties. One which was unique and involved a great deal of perseverance and dedication, was the development of plans for a new building to house the growing Department of Mechanical Engineering. This building, innovative, flexible, and open in its design, soon became known as the premier Mechanical Engineering building in the coun-



Don Bellow

try. It gave the Department and Faculty something to be proud of in 1970, and to this day continues to stand the test of time. Don was also Chair of Mechanical Engineering from 1975 to 1984 — a period which saw the Department leading the way by offering the first Cooperative Education stream available at the U of A. This gave Mechanical

Engineering students the opportunity to combine their studies with 20 months of work experience before graduation.

Soon Don's administrative expertise extended beyond the Faculty, for he also served on

the University Senate and was appointed Associate Vice-President (Facilities) from 1989 to 1994. During his last two years at the University, he was a Special Assistant to the Vice President (Finance and Administration). In his professional capacity, Don has been

involved with the Association of Professional Engineers, Geologists, and Geophysicists (APEGGA) in numerous capacities, including President of the Association in 1984-85.

Throughout his career, Don pursued a rich variety of research activities and maintained strong ties with industry. His interests included machine components, in particular the behaviour of joints; welded joints; the development of improved threaded connections; and fatigue and wear of both joints and specific materials. His work led to a long-term association with Stelco and to the development of specific products for the oil industry. It is this industrial experience, combined with Don's academic strength, which benefited the graduate students fortunate enough to have him as their supervisor.

The legacy of Don Bellow will continue in the Department of Mechanical Engineering and the University. His contributions and memory will stay with us for a very long time.

It is with thanks and congratulations that we wish him the best in the future. ■

The legacy of Don Bellow will continue in the Department of Mechanical Engineering and the University. His contributions and memory will stay with us for a very long time.

From ???@??? Wed Nov 20 07:52:07 1996
 Received: from dassmtp.das.uwo.ca (dassmtp.das.uwo.ca [129.100.32.223]) by maildrop.srv.ualberta.ca (8.7.6/8.7.1) with SMTP id TAA37270 for <dbellow@gpu.srv.ualberta.ca>; Tue, 19 Nov 1996 19:21:56 -0700
 X-UIDL: 848501609.000
 From: Paul.Davenport@uwoadmin.uwo.ca
 Received: by dassmtp.das.uwo.ca (Smail3.1.28.1 #3)
 id m0vQ2IQ-00009PC; Tue, 19 Nov 96 21:21 EST
 Message-Id: <m0vQ2IQ-00009PC@dassmtp.das.uwo.ca>
 Date: Tuesday, 19 November 1996 9:20pm ET
 To: dbellow@gpu.srv.ualberta.ca
 Subject: Greetings from the West

Don,

It was good to hear from you. I have so many fine memories from U of A, and the best by far are those of the wonderful people I worked with at the University, including you. We had some good times together, on such issues as deferred maintenance in the residences, enormously complex renovation plans (remember the six-page charts!), and co-generation despite the loving attention of our friends at Edmonton Power!

Josette and I send our very best wishes to you and Jean and family--have a great retirement, and if you are ever in the London area, please come see us--the President's house has a beautiful guest bedroom, so we would have no problem putting you up for the night.

With best wishes,

Paul

----- (Forwarded letter 1 follows) -----
 Received: from bock.ucs.ualberta.ca by julian.uwo.ca with SMTP id RAA07385;
 Tue, 19 Nov 1996 17:05:42 -0500 (EST)
 Received: from [129.128.237.30] by bock.ucs.ualberta.ca with SMTP
 (8.6.5/UA) id PAA08988
 for <paul.davenport@uwo.ca>; Tue, 19 Nov 1996 15:05:39 -0700
 X-Sender: dbellow@pop.srv.ualberta.ca
 Message-Id: <v01510100aeb79594d175@[129.128.237.20]>
 Mime-Version: 1.0
 Content-Type: text/plain; charset="us-ascii"
 Date: Tue, 19 Nov 1996 15:04:06 -0700
 To: paul.davenport@uwo.ca
 From: dbellow@gpu.srv.ualberta.ca (Donald G. Bellow)
 Subject: Greetings from the West
 Reply-To: dbellow@gpu.srv.ualberta.ca

Dear Paul;

I'm sorry I missed you when you stopped by the office in the Fall. I would have liked to have talked with you.
 However, my main reason for sending you this note is to thank you for the kind words you sent via Glenn Harris on the occasion of my retirement from the University of Alberta. I was pleasantly surprised and deeply touched by your thoughtfulness.
 Please send my regards to Josette and the family.
 Sincerely,
 Don

From ???@??? Wed Nov 20 07:52:10 1996
 Received: from bock.ucs.ualberta.ca (bock.ucs.ualberta.ca [129.128.5.214]) by maildrop.srv.ualberta.ca

APPENDIX V: NEWSPAPER ARTICLES

May 15/70

U of A doing special tests for industry

By TOM CAMPBELL
Of The Journal

Mechanical engineering at the University of Alberta is co-operating with a steel manufacturer in conducting a research program with important overtones for the oil industry.

Dr. Donald Bellow, associate professor of mechanical engineering, has received a \$2,500 research grant from the Steel Company of Canada, Limited, for the investigation of fatigue properties of sucker rod couplings.

The couplings, used to link thousands of sections of sucker rod together in oil wells throughout Alberta, crack and break after an extended period of lifting hundreds of feet of rod, the piston and oil during pumping.

Although continuous sucker rod has been developed and is being used in some wells, especially very deep wells, most are still equipped with the conventional system of numerous rods and just as numerous couplings.

MOST COMMON

The most common break occur in the coupling which not only suffers the stress of the repetitive lifts, but is further weakened by threads which cut the metal surface and torque applied when the two rods are pulled together in the coupling.

Testing is being carried out for research purposes with the \$2,500 grant in the Old Power House near the Engineering Building on the U of A campus. Couplings are being manufactured at Stelco's Edmonton plant, Highway 14 East, for use in the test.

Dr. Bellow says he and his associates will be checking some 100 varieties of couplings supplied to them by Stelco. The couplings will be made of different alloys and processed by different methods.

PROVE VALUES

Threads in the couplings, for example, can be either cut, cut and burnished or rolled into the coupling. Although the more complex processes are supposed to make the couplings more fatigue resistant, the research should prove the values of each approach.

"The most significant thing about this project is that we, for the first time, are working on a long-term problem in industry which is very significant in our local area," says Dr. Bellow.

"In the past I have worked on many research projects for which I could not see the industrial application," Dr. Bellow said. "Perhaps they had use somewhere in the United States, but this time we can see where the findings will be used."

Stelco approached the university last year on the possibilities of doing research in certain areas. After several months of discussion the coupling problem appeared as the first research project.

Equipment acquired by the department in March 1969 is the key to the entire project. A \$45,000 machine, a closed loop servo-hydraulic fatigue tester, is doing the job.

The idea is to speed up the normal wear incurred in industry through the special tester. In this case years of use in an oilwell can be simulated within days by using the super accelerated experiment.

Four couplings are connected in series and fitted into the vertical fatigue tester. The slow and steady pumping action customary in the oil field has been replaced by a rapid fire six to eight strokes per second.

Stress, resulting in metal fatigue, has been intensified by applying loads varying from 38,000 pounds to 3,000 pounds during the cycle. The mean load runs at 20,500 pounds.

USE PRESSURE

The load is made possible by a 40 horsepower motor which applies 2,700 pounds pressure per square inch through the machine's hydraulic system.

Just to increase the rate of metal fatigue, the researchers cheat a little with the help of Stelco. The couplings are ground down to reduce the wall thickness.

This project provides more work which keeps the expensive equipment operating economically on a 24-hours-a-day basis.

"I hope this is the start of more co-operation between ourselves and industry," said Dr. Bellow. "I sure would like to be able to get the results of the research a little sooner, but several students are also using the machine for other post graduate mechanical projects."

GOOD INDICATION

"It is hoped fatigue data can be obtained in a reasonably short time," he said. "While testing is taking place in other than field conditions, it is believed that the results will give an indication which design will be most successful when subjected to field conditions."

Knowledge gained in this area can have far wider application than the oil industry, Dr. Bellow adds. The threaded joint, or nut and bolt, is still the basis of the industrial society.

More students on GFC?

"The whole principle of parity is at stake in the question of increased student representation on GFC," said Professor A. Cody at Monday's General Faculties Council executive meeting.

The special meeting discussed the report of an ad hoc Committee on Student Representation.

The proposed additional representation would bring the total number of members of GFC up to 127 from 79. Students would have parity with the academic staff, each body having a maximum of 49 members. The report does not distinguish between graduate and undergraduate students, however.

One executive member felt that the report should be sent back to the committee for the specific purpose of examining the future effectiveness of the body if the membership is increased.

Dr. D. G. Bellow was concerned that the increased size would make GFC even more unwieldy than it is at present. He suggested a review of the whole structure of university government.

"It is not just a question of adding students but it is changing the whole complexion of the body" he said. It was pointed out, however, that the committee had considered the disadvantages but felt that other considerations including urgency outweighed the disadvantages.

Professor Cody moved that the report be released to the students so that they can see the report and know what is at stake. He said that he would like to see submissions from interested students. The motion passed.

A further motion to have a deadline on submissions set at January 15 was passed after a heated discussion on the part of Zolton Melkvi, grad student rep on the executive council.

He accused the executive of feeling no sense of the urgency of the matter and letting it drag on until a less radical students' council is in office. A special meeting of GFC will be held in early February to discuss the report and to hear submissions.

GFC also passed a request for additional members from the non-academic staff on the Ad Hoc Committee on Law, Order and Discipline. The committee consists of five staff, five students (of which none presently sit), three non-academic staff members, and two grad students. As a member of the Non-academic Staff Association, Campus Patrol could, but does not, have a seat on the council.

GFC expansion causes problem

The push for more student representation in university affairs may have created cumbersome administrative bodies.

Some feel, for example, that the University of Alberta's general faculties council, which has grown from 81 members to 127, is an awkward structure.

Following bitter debate in February, GFC approved the principle of student-academic staff parity. The effect of this move was to increase student representatives from only three to 49.

The present composition of GFC is 49 student body representatives, 49 from the faculty, and 29 from the university administration and other groups.

To wrestle with the problem, the U of A has established a committee to study the role of GFC. Committee chairman is Dr. D. G. Bellow, professor of mechanical engineering.

One particular problem is that some student GFC members are no longer enrolled in the faculty which they were elected to represent, and students in that faculty resent the fact.

Another problem is that the sheer size of GFC creates a situation where debate on a given issue can be lengthy because of the number of representatives wanting to express their views.

Dr. Bellow says: "It's very true that we would like to see GFC operate as effectively as possible." It's his personal view that GFC "is too large."

The problem is not simple, Dr. Bellow points out, and the committee is trying to determine whether the original goals governing the establishment of GFC years ago, are being accomplished today.

Furthermore, the committee can't help but consider "the goals of the university for the future" in examining GFC's role, he adds.

Wyman Oct 8/70

GFC wants student reps back

by **Donna Brown**

General Faculties Council's executive committee agreed yesterday to settle the student participation question before considering tenure and campus security issues.

Tenure and campus security will each have to be discussed separately, suggested University President Max Wyman. "Each of the subjects we're talking about would require a special meeting," he said.

Dr. Wyman told the executive committee of GFC that he has written the brief on student participation and he expects "a fair amount of criticism."

"Such an important thing shouldn't be dealt with in haste," said Dr. Wyman.

It is expected that it will take six weeks for the students' union motion concerning student representation to go through both committees. Dr. Wyman said this action is primarily to satisfy the students.

The GFC executive committee said it would take them at least four or five months before they can get an answer for Academic Plan 9.

"I would feel that this plan should get a great deal of scrutiny," said Dr. Wyman. "The longer we postpone it, the longer before we get a final decision from the government of what this

university is going to be," he added.

One of the members proposed that there be some method to induce the students' union to come and speak at the meeting.

"I don't know what to do," said Dr. Wyman. "I would welcome them; I would hope they would come."

The students' union has two places on GFC but so far has been absent since withdrawing their reps last spring.

The Council agreed that it is not up to them to do anything special to have the students' union reps attend.

Dr. Wyman presented a report from the GFC Ad Hoc committee on tenure procedures. He told the council that there are a variety of difficulties which have hit the university on tenure procedure.

"I'm not too happy with the report on principle," said Dr. Wyman.

There are two types of suggested tenure: instant tenure by which the instructor could have tenure without a four year probationary period or until he is fired. The other is a contract appointment which would be a limited term.

Dr. Wyman remarked, "I don't know of any single university that has adopted it yet."

"We're going to end up re-writing the report," said Dr. D.

G. Bellow, "I can imagine there will be quite a number of individual and group submissions."

Council moved to circulate the report and pass it on to GFC.

A revised report by the GFC Committee on copyrights was discussed.

Dr. J. W. Mackie commented that it was not a very good report.

"This, I think, is an extremely difficult area," said Dr. Wyman. "This is going to be an administrative nightmare."

A motion by Dr. A. B. Cody sent the report forward to GFC.

A report on supplementary income earned by staff members was brought to the attention of the committee.

Every year the university receives complaints on possible misuse by the staff who set up business and work in government.

Dr. Wyman said that this question is "extremely difficult to carry out and legislate."

It was suggested that perhaps it should be felt up to the department chairman to ensure that the person is not abusing regulations.

"This is the kind of work we want staff people to do," said Dr. Wyman, "We want them to share their knowledge with the government and the community."

The matter will be forwarded to the GFC.

Nov 4/71

Drake sees flaws in Patterson helmet

By TERRY JONES
Of The Journal

The Patterson hockey helmet, currently being sold at \$5.00 by the Canadian General Electric Company on a non-profit basis, has drawn much publicity, almost all of it good.

The claim, however, isn't universal.

Clare Drake, coach of the University of Alberta Golden Bears and the Canadian college hockey all-star team, finds several things about the helmet package objectionable.

The helmet, upon Drake's request, is being tested by Dr. Don Bellow of the University of Alberta who has done most of the testing in this field in Canada.

The helmet is the work of Charlie Patterson who has spent the last decade developing helmets in his basement, and of late at York University in Toronto.

Drake said that each youngster registered with the Canadian Amateur Hockey Association has been sent a

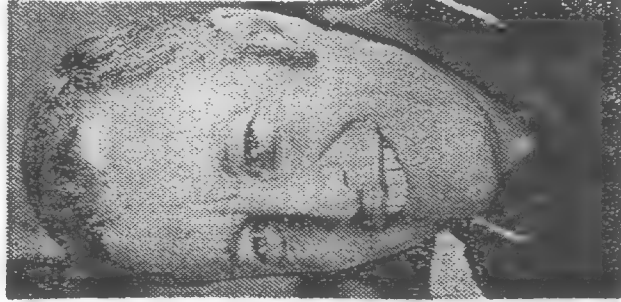
letter urging the youngsters to buy the helmet.

"It might prove to be highly misleading to parents looking for the best head protection for their hockey playing sons," said Drake.

The helmet, made of Lexan, the same material which is used in astronauts' head gear and an exclusive material to General Electric, is endorsed by the Canadian Amateur Hockey Association.

"The important protective aspects of hockey head gear have nothing to do with the helmet retaining its form at 300 degrees above zero as is being emphasized," said Drake.

"The important aspect in head protection is the absorption of force caused by unusual blows to the head that may result from falling into the boards, falling (particularly backwards) on the surface of the ice, a blow to the head caused by another player's stick or skates and being hit by a puck. It is not important how strong an impact the material will resist, but rather how much of the



CLARE DRAKE

force of the blow can be absorbed and its energies dissipated before it reaches the skull area.

"Two key areas for protection of blows to the head are the back of the skull and the temple area of the skull. There are other helmets on the market that give far better



CHARLIE PATTERSON

protection to these areas than the helmet being promoted in this instance as the best.

"It is disturbing to see that the CAHA would endorse this helmet and thus lend further credence to it. My purpose in pointing this out is not to condemn a

particular helmet, which, if it fits a particular boy and protects the greatest areas of vulnerability for that boy, may be the best helmet for him. However, I think it is important to make the public aware of obvious shortcomings in the helmet and that it is not, in fact, the best helmet available."

Drake said, that in his opinion, the best hockey helmet is best decided upon consultation with any number of reliable sporting goods retailers. "A proper fit is vital," he said.

The Patterson helmet is an extremely light-weight (because of the Lexan). It is like most helmets of a two-piece construction and is being sold as a public relations idea by the firm.

Drake said he considered it a good \$5.00 helmet but objected to it being promoted as the best helmet and as being worth anywhere from \$15 to \$30 as mentioned in the Canadian General Electric letter to the players and parents.

Dr. Bellow said he was not prepared to make any statements until he tests the helmet. "I question it being worth \$15 or \$20," he said.

"What Clare says is subjective at this point and I wouldn't like to comment on it until we have done the tests," said Dr. Bellow, who said that he considers Drake's comment noteworthy because of his experience as a hockey coach.

"I'm not going to say anything about the work of a man like Mr. Patterson who has spent a good part of his life on this helmet until we have completed the testing. And if we should find some deficiencies I think I would likely inform Mr. Patterson of them first," Dr. Bellow said he expects to begin the tests this week and hopes to have them complete within two weeks.

"In our previous testing we have generally found that the more expensive helmets are the better helmets," Dr. Bellow said.

Probe to decide if U polluting

The University of Alberta's technical staff will investigate whether the institution is contributing to air or water pollution.

The executive committee of the university's general faculties council agreed to ask the physical plant department, the division made up of engineers and other technical personnel who keep the campus functioning, to look into questions raised by H. V. Krusche, public health engineer with the province's environmental health services division.

"If we are in any way, shape or form, contributing to pollution, we ought to obviate it," said Dr. Max Wyman, president of the university.

The committee was considering a recommendation that an ad hoc committee of the GFC be set up to gather the answers

to Mr. Krusche's questions. But Dr. D. G. Bellow, head of mechanical engineering, suggested instead that the investigation be carried out by the technical staff.

The questions asked by Mr. Krusche were:

1. Where are "used up" chemicals disposed of? Are non-degradable chemicals broken up before disposal?

He wanted the question applied to the chemistry, chemical and petroleum engineering, pharmacology, medicine and agriculture departments.

2. What happens to test animals? Are they cremated or disposed in the city sewer?

3. What are the quantities of chemicals flushed down the city sewer?

4. What happens to non-re-usable radioactive materials used by the engineering departments, the cancer clinic and the University Hospital?

5. What "waste" is burned in the old University Hospital incinerator?

6. Has the air in the operating room at the University Hospital been tested for contaminants originating at the incinerator (stack is below operating room air intakes)?

7. Who is controlling the university construction crews so they do not make undue noise?

8. Who is responsible for the

safety of university personnel so that they are not exposed unknowingly to ionization radiation (microwave, laser beams, etc.)?

9. Is all the x-ray equipment in the whole area "leak proof"?

10. What happens to disposable injection needles?

Dr. Wyman supported the idea of a study by technical personnel rather than academics because "investigation of pollution is not an afternoon's work. I think it is the job of the physical plant department to make sure we are not polluting the air or the water."

Dr. David Friesen said that while there must be an immediate investigation, to gather information, the university must consider, in the long range, pollution control planning.

Dr. Bellow quipped that the present investigation "will not include architectural pollution."

Added Dr. Wyman: "I'd like to have noise pollution investigation gated, myself."

A panel on "Industry in Alberta — a Look Ahead to 1980", will be held Nov. 29 from 11 a.m. to 12:30 p.m. in the Chateau Lacombe. Panelists include F. K. Spragins, president and general manager, Syncrude Canada Limited; C. P. Ronden, manager, Engineered Plastics Limited; Dr. E. J. Wiggins, director, Research Council of Alberta, and D. G. Bellows, department of mechanical engineering, University of Alberta. The meeting is sponsored by the Engineering Institute of Canada.

ANOTHER CHAPTER

By TERRY JONES

Of The Journal

Like your favorite afternoon soap opera, The Great Hockey Helmet Debate continues.

Helmets for hockey players has been a newsworthy subject for most of a decade. It didn't, however, become the many faceted debate until last summer when the Canadian Amateur Hockey Association ruled that all players under its banner would be required to wear them.

Since then it has carried on much like the soap opera with several plots going at once, building to some sort of conclusion but never quite making it.

The usefulness of helmets is debated.

The Western Canada Hockey League didn't get around to abiding with the CAHA ruling until one-third of the schedule was over. Only a handful of players on the Edmonton Oil Kings, for example, would choose to remain helmeted if the decision was theirs. And, according to league secretary Tom Fisher of New Westminster, there is a movement within the WCHL to see the helmets come off.

It goes further than that.

Controversy surrounds a CAHA-endorsed helmet that is being sold on a non-profit basis by Canadian General Electric. When announced it drew rave reviews. Later the sporting good companies of whose sales it was biting into, pointed out what they considered to be shortcomings of the helmet. Further credence to their claims was added when University of Alberta hockey coach Clare Drake found the helmet objectionable in some areas and asked Dr. Don Bellow of the U of A to have it tested in the same manner he has tested other helmets.

Dr. Bellow completed his testing this week and he informs the world that the Patterson helmet is certainly not the best helmet but that it is a very good helmet for the money and that he would not hesitate to buy it for his own son.

The helmet debate goes still further.

The Canadian Standards Association, a non-profit organization which approves such safety headgear as construction hard hats, is at least \$1,000 away from completing tests to certify hockey helmets according to published reports. Because of the complexity and range of hockey accidents, tests used for hard hats are considered inadequate for hockey.

Without a standard for helmets, the public has little idea of what is and what isn't a good helmet.

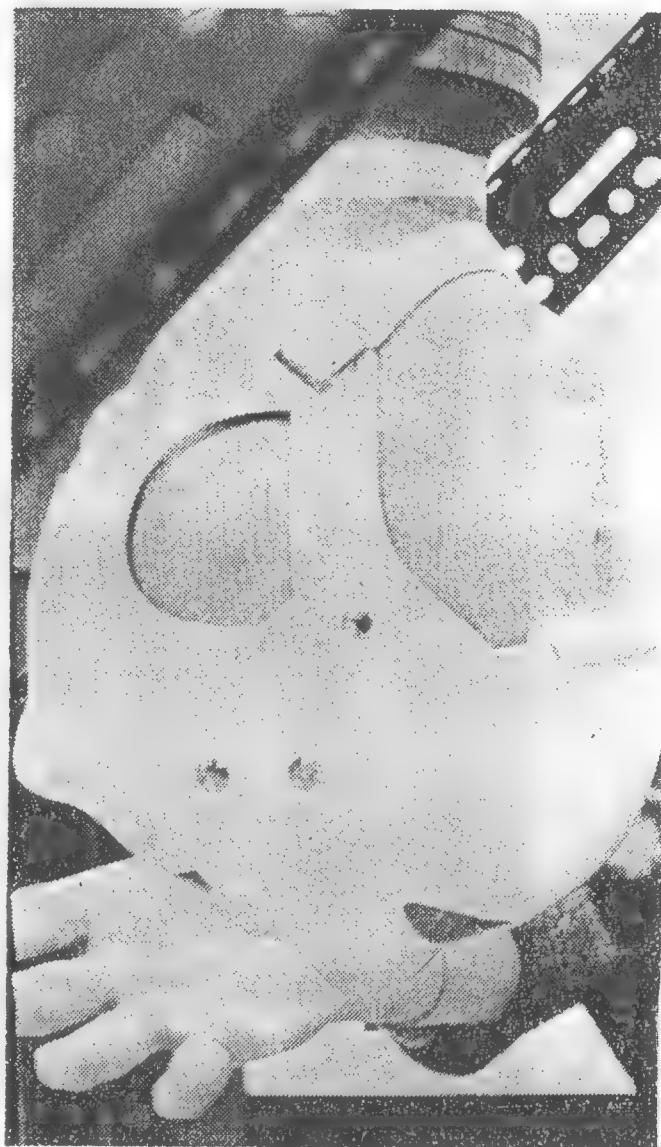
Sitting right in the middle of all this is Charlie Patterson, an instantly likeable character who is or was something of a Ralph Nader in the hockey helmet game.

He's a part-time inventor who continually bubbles with both energy and enthusiasm. Somehow he doesn't fit a controversial role.

But it was he who has done more than any other man in the hockey helmet game.

The amazing tale of the man who, inspired by an injury to his own son's head in a hockey game, began working in his basement in search of a perfect helmet has been told often.

It was he who generated national publicity with the



SOPHISTICATED TE

... Dr. Don Bellow of the University of A
helmets

message that the helmets worn by most of the 375,000 players involved are worthless.

Then, after the CAHA decision, press conferences around the country were held to announce the CAHA endorsed hockey helmet . . . the Charlie Patterson hockey helmet made of the material Lexan which is used in astronauts helmets and is an exclusive material to

IN HELMET DEBATE



TESTING EQUIPMENT

Bellert has done much of the testing of hockey in Canada

General Electric. It went on sale at \$5, the same cost it took CGE to produce it, the idea being that it was a good public relations idea.

The often-told Charlie Patterson story was rewritten. It told of the \$20,000 he had lost and how finally he had achieved success.

Or had he?

It wasn't long after the sporting goods people studied

the Patterson helmet and spelled out arguments for their own headgear.

Comments by Drake attracted national attention.

Drake objected to the promotion of the helmet as being the best and to a letter all youngsters registered with the CAHA received urging them to buy the helmet.

"It might prove to be highly misleading to parents looking for the best head protection for their hockey playing sons," said Drake. "Two key areas for protection of blows to the head are the back of the skull and the temple areas. There are other helmets on the market that give far better protection to these areas than helmets being promoted in this instance as the best."

Then came a strong vote for the helmet when Brian Shaw insisted that his Edmonton Oil Kings wear the Patterson models.

Dr. Bellow's research has been completed and Bellow, who has done a large amount of private helmet testing in Canada, admits to have been surprised by it.

"I was prepared to believe the Lexan material in the Patterson helmet would be great but I had certain doubts about the helmet itself. It's much better than I would have given it credit for.

"We did find that the material began to deform in some of our tests and that it has its breaking point. It is in the back of the helmet that the material deformed. I can't comment on how it stacks up from the side as we are unable to test in that area yet."

"Actually though it is not a bad helmet. I have tested it from the front and the back and it stands up well."

Would he buy it for his own son?

"That's an interesting question because I do have a son. If I was to buy him another helmet and one in the \$5 range I'd buy the Patterson helmet.

"I don't know if Mr. Patterson is aware of it but the best thing he did when he designed the helmet was give it a shell-like construction. The best helmets, our testing reveals, are the one piece helmets." The Patterson helmet is of a two-piece construction as are most on the market.

Dr. Bellow's agrees that standards are needed for helmets but wonders how interested the Canadian Standards Association is.

"I sent them a letter offering them all the information and testing techniques I use and I haven't even received a reply," he said.

He even wonders if people like himself maybe aren't going a little too far.

"Maybe we're looking at them in an environment that will never exist. Heck we're testing impacts up to 500 Gs. That would have the effect of a slap shot going better than 100 miles per hour."

As to the problem of whether or not helmets should be worn, especially in top amateur and professional ranks, the likely answer there is time.

With helmet wearing compulsory in amateur hockey it is quite likely that more and more players will take them into the professional game. And maybe someday everybody will be wearing helmets just like goaltenders today are wearing masks and asking themselves how they could have been so foolish as to not wear them in the first place.

New facility:

Basic engineering research at U. of A. will benefit construction

By Latif Durrani

EDMONTON—The construction industry can reap a rich harvest from the laborious basic research now being carried out at the Engineering Faculty of the University of Alberta here.

Efforts are being made in the field of acoustics, permafrost construction, aerodynamics of tall buildings and the design of a home suitable for mass production, said Dr. D.G. Bellow of the Engineering Faculty in a recent interview.

Dr. Bellow said that due to the "fantastic facilities" now available to students of basic research, results which could immensely benefit the construction industry can be expected.

On completion of the new Engineering 11 Building this summer, now under construction by Alta. West Construction Co., the department would be one of the most modern in Western Canada dealing with thermosciences, applied mechanics, mechanical design and industrial engineering, he claimed.

By July this year, Dr. Bellow said, it will be possible to perform transmission loss co-efficient test for building materials and wall design. The department is equipped with a large vibration and acoustic facility in which a variety of experiments and studies can be conducted.

A group of researchers is presently delivering into the structural characteristics of permafrost construction as well as other arctic heat transfer problems. A large frost tunnel is available in which ice formation studies are underway. Penetration of ice by means of a water jet which would have applications in arctic pile driving and oil pipelines is also a problem being investigated.

Aerodynamic characteristics of tall buildings in Edmonton and their effect on wind patterns is currently under examination with investigations into the contamination of air inlets by exhaust gases due to location and wind conditions.

The evaluation of the strength of wood from 40 degrees below zero to 70 above and the strength of gang nails are two under graduate projects relating to the building industry now under

study. These two projects, although ramifications will be felt throughout the construction industry, are primarily intended as teaching vehicles.

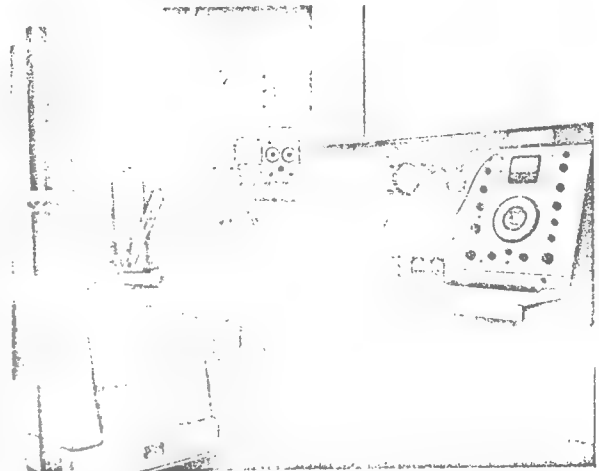
In discussing the design of mechanical systems for buildings in the Edmonton area, Dr. Bellow said that available data has been either extrapolated from somewhat warmer climates or it is not directly relevant to the conditions existing in Edmonton. To offset this information shortage, more up to date temperature and solar data is being compiled.

Another important project getting attention was the design of a mass production home. This involves, Dr. Bellow explained, designing a home with a view to individuality as well as flexibility for future expansion while at the same time being adaptable to mass production.

The project consists of the design of a home and a feasibility and economic study of the idea. The aim is to provide a quality home at a lower cost than what is being provided in the market place today.

The department will move into its new 76,000 sq. ft. building this summer. A wide variety of research facilities to be incorporated therein, include a solidification and thawing tunnel, cold rooms, radiant energy facilities, and all relating equipment necessary to conduct necessary tests.

Dr. Bellow said that the National Research Council provides the majority of the funds for both basic and applied research to the department. Funds are also granted by the university itself. Grants from the NRC annually total about \$20,000.



THE KIND OF equipment being used for research in the Department of Mechanical Engineering. Photo shows a thin elastic arch being subjected to a pulsating support displacement, by means of a 325 lb. force shaver table and system control.

Halifax Mail Star, N.S.

Circ. 114,524

July 13, 1973

Friday, July 13, 1973

Designed from inside out

EDMONTON (CP) — The and freedom.

University of Alberta's new mechanical engineering building was designed from the inside out.

"We decided how we wanted the space arranged and then enclosed it with a rain screen," says Donald G. Bellow, a professor from the department of mechanical engineering who was involved in the design.

In September, 1968, designers decided the building should be a teaching vehicle, not merely a place for teaching to take place, should reflect the importance of mechanical engineering and appear as part of the industrial expansion of Canada's north-west and give a feeling of space

It was to be a building designed for the future.

The building that resulted has a peculiar shape—three sections, none of them box-shaped, are visible through a reflective rain screen which mirrors the surroundings.

A Liberal amount of glass has been used. All of the classrooms have windows.

"It allows for a break in concentration . . . it's possible to see what's happening outside, whether it's raining or not," says Prof. Bellow.

Wherever possible, glass has been placed to allow students to see what is taking place in the laboratories and shops, which is

turn are placed where they are visible to people passing through the main pedestrian areas of the building.

Much of the duct work in the building has been exposed and color-coded to allow students to trace the building's service systems. Students are able to experiment with them and measure the flow through the pipes.

One half of one per cent of the capital funds for all buildings at the university goes for the acquisition of art work and designers selected art work that would fit into the general atmosphere of the mechanical engineering building.

On major art piece is of a graphic nature, bright red in color and has a flashing neon light. The other is a kinetic sculpture that moves as one passes by.

DONALD G. BELLOW,
Professor in Mechanical
Engineering, University of
Alberta.

U governing system backed by committee

By BOB GILMOUR
Of The Journal

The current two-branch system of government at the University of Alberta has received the approval of a special study committee.

A system of just one university governing body would be "undesirable," the committee said in a report Monday to general faculties council.

"As long as the university faculty and students wish to be involved in the decision-making process, the present system and size appear to satisfy this need."

The committee was appointed by general faculties council in 1971 to study the role of GFC in regards to size, composition and effectiveness.

Under the current two-level governing system, the general faculties council, comprising representatives from various university groups, decides academic matters. The board of governors deals with fiscal and administrative concerns.

The committee noted, however, a growing trend for academic decisions to be made in the light of their financial implications.

Instances also abound where a decision on finances can't be made without consideration of academic principles.

Although a one-body governing system is an attempt to combine both functions and would involve fewer people, it is undesirable, said the committee. Such a system is in effect at the University of Toronto.

"Where only a single body exists to deal with both academic and administrative problems, academic issues are likely to be slighted in favor of more pressing administrative and fiscal problems."

The committee urges, however, that there not be a complete separation of fiscal and academic matters and that "each tier of government should be aware of and free to criticize the operations of the other."

A big reduction in the size of the 127-member general faculties council would be unacceptable, it says. In fact, any reduction would pose more problems than leaving it unchanged.

Faculty and students wish to be involved in major decision-making and aren't ready to accept less participation, it says.

"Currently, at this university and elsewhere, the mood is for shared responsibility and co-operative action among the components of the institution."

The committee says it believes the current size of GFC satisfies the need for involvement.

The wish to be involved in decision-making, however, may not extend into the future, says the committee. A re-evaluation of the system is suggested in the next 10 years.

The committee also makes a number of recommendations about the current system which it says will improve

participation and the general effectiveness of GFC.

Major recommendations concern improvement of communication and procedures. Greater inter-action between GFC and its major committees is suggested.

One recommendation approved by GFC at its meeting Monday was that its size be expanded to include one elected member from the university extension department and three representatives from the university library academic staff.

This was done despite the warning of Dr. Donald Bellow, professor of mechanical engineering and head of the special study committee, that admitting library representatives would set a precedent for other university support groups asking to join GFC.

Among other recommendations approved were that GFC again review and debate the use of a question period; that its executive committee handmit annual reports; and that its executive committee handle implementation of approved policy matters.

Standing committees urged for GFC

General Faculties Council took action Monday to deal with the proliferation of committees. It decided to establish another committee to study the problem.

Councillors were considering a report on the role of GFC. The report suggested the formation of five standing committees, to which all GFC matter would be referred. 'Umbrella' committees suggested were: planning, academic operations, academic support, administrative support and personnel.

These large committees would in turn refer matters to sub-committees. Don Bellow, chairman of the special committee, noted that several GFC committees are inactive.

"I'm on one committee that hasn't met in three years, yet it's still on the books," Bellow said.

There are about 50 GFC committees still on the books.

The senate has also elected a special committee to study the role of the senate in university administration. The committee includes 12 people representing business, the university staff, and students.

Elected to the committee are: Prof. A. A. Ryan, Dr. D. G. Bellow, M. A. Adam, Don MacKenzie, Mrs. A. V. Calhoun, M. G. Hurtig, R. W. Chapman, Dr. G. M. Tuttle, Fil Frazer, Mrs. Ross Munro and D. J. Cardinal.

U of A appoints chairmen

Dr. Karel Puffer, academic vice-president at the Northern Alberta Institute of Technology, will head the University of Alberta's department of industrial and vocational education.

Dr. Puffer was one of three academic appointments announced Friday by the U of A board of governors.

Dr. Terry White will be the new chairman of the department of sociology and Dr. Don Bellow will head the department of mechanical engineering.

All three men's terms begin in July.

Dr. Puffer has been with NAIT since 1962. He received a bachelor of science in civil engineering from the U of A in 1955 and completed his master's and doctorate training at the University of Illinois.

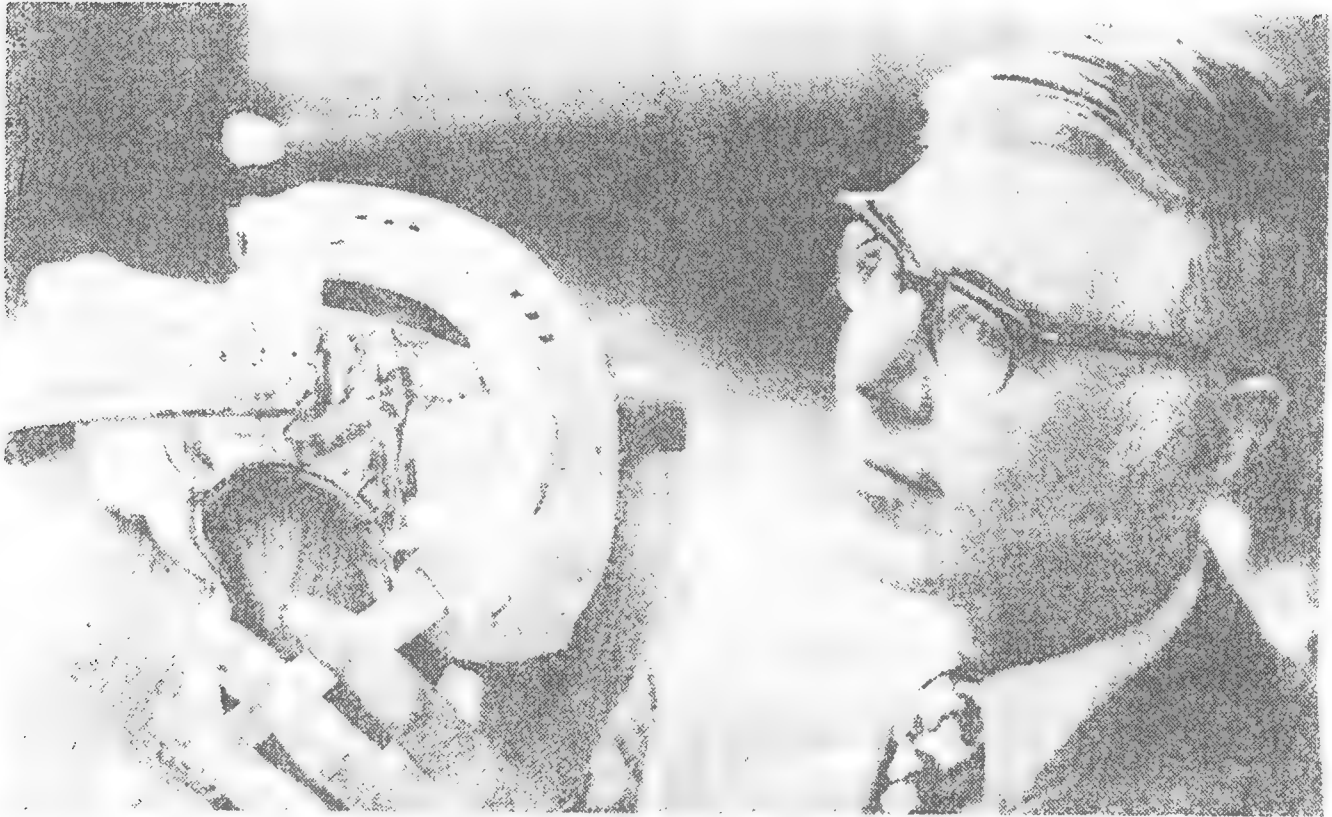
He succeeds Dr. J. E. Gallagher.

Dr. White is a 32-year-old assistant professor in the sociology department at the U of A and a consultant with the Social Science Research Council of Canada.

He replaces Dr. Charles Hobart, who returns to teach and do research in the department.

Dr. Bellow, who has been at the U of A since 1958, has worked extensively in industry and concentrates in the area of applied mechanics in his academic research.

He replaces Dr. J. S. Kennedy, who remains in the department in a teaching and research capacity.



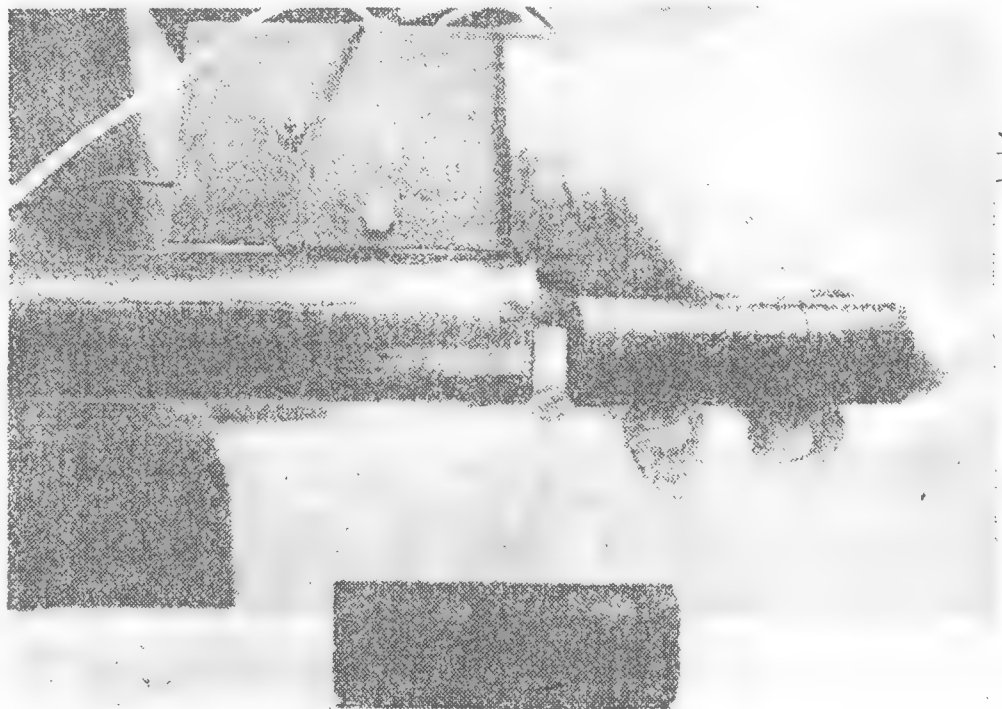
Dr. Don Bellow exhibits the test helmet

U of A open house Saturday

There's a blockhead doing research in the mechanical engineering department at the University of Alberta.

The thick-skulled dummy is testing the durability of hockey helmets in a research project designed to find out which models are safest.

On Saturday, he'll don a helmet and have his head bashed and battered to show people how researchers (led by Dr. Don Bellow) determine



The gun, with a projectile, used to batter helmet

energy absorption capabilities of different makes of helmets.

The demonstration is one of several hundred displays that will make up a day-long open house of science facilities at the U of A.

The open house is aimed primarily at graduating high school students interested in enrolling in a U of A science program.

But the three science faculties putting on the open house — engineering, science and agriculture and forestry — are also taking the opportunity to show the general public what is going on in the world of scientific research at the university.

The helmet testing study uses a wooden head with an implanted instrument to measure the force of impacts.

The project has shown so far that the best energy absorbers are molded, single-piece helmets with tight-fitting suspended padding.

Mechanical engineering also has displays on wind tunnel testing of model aircraft and trucks.

The scaled-down wind tunnel truck experiment has shown that truck trailers with bevelled fronts cut down wind resistance, giving a 12-per-cent reduction in

Mechanical engineering is just one of 25 different departments at the U of A that will be setting up displays on projects being carried out by their departments.

Zoology will use Joe, the (descended) skunk, to show how radio telemetry is used in tracking wild animals in the bush. A display on gopher hibernation, demonstrations on dissection and a film on fish behavior (made by science dean D.M. Ross and winner of several international awards) are included in the zoology presentations.

Botany is planning a display on edible and poisonous mushrooms, to let hungry hikers know what not to eat when hit by the "growlies" out in the woods.

Visitors will also have a chance to match wits with U of A computers in games such as tic-tac-toe and lunar landing simulations, with computer scientists explain-

ing the basics of the electronic brains.

Photographs of insects taken through the electron microscope will be displayed by entomology and plant science will demonstrate freeze-drying processes.

Twelve buildings will be open to the public during the open house,

which is expected to draw more than 5,000 people, mainly from northern Alberta. Hours are 10 a.m. to 4 p.m.

Past Presidents to study Council election procedures

A committee consisting of three Past Presidents will be appointed to review APEGGA legislation governing election of candidates to council.

The committee will examine Recommendation 8 of the Task Force on Future Regulation of the Profession, tabled last December. It states:

"The Task Force recommends that the Nominating Committee should ensure that there is always at least twice the number of nominees for the geology and geophysics candidates as there are positions to be filled to ensure that election by affirmative action is avoided."

Task Force Chairman D.G. Bellow, P. Eng., said in his February report to council that a concern has existed for some time that the current requirements of our legislation could inadvertently result in the election of candidates regardless of votes obtained.

The committee of Past Presidents is to present its recommendations to Council at the September, 1991, meeting.

In related business, Council set aside further action on Task Force Recommendation No. 5 until the finding of the Savage Committee and the Permit to Practice subcommittee of the Practice Standards Committee are presented. That recommendation reads:

"It is recommended that where APEGGA has identified engineering, geological or geophysical services are being offered directly or indirectly to the public, it seek a mechanism on how the Regulations can be fully enforced."

Recommendation No. 3 was also deferred until the findings of the Savage committee are established. That recommendation reads:

"It is recommended that when membership is being renewed each year that the member state that he/she is still practicing in the profession. This will require APEGGA to draft guidelines as to what constitutes practicing in the profession."

No more space for books in U of A library

CHARLES MANDEL

Edmonton

The University of Alberta's librarians no longer have the space to properly shelve the institution's huge research collection of books and periodicals.

The lack of space is causing damage to the collections and has U of A administrators scrambling to find a solution to the problem.

"We really need some new space. There's no question about that," says Deborah Dancik, acting head of the Humanities and Social Sciences Library.

Dancik, who looks after some 1.3 million books and another 10,000 volumes of bound periodicals, said she's already placed about 60,000 volumes in storage this year to make room for new materials.

The size of the U of A's collection is staggering. In 35,000 square metres of space divided between six main libraries and several smaller branches are approximately 3.5 million books and bound periodicals and another three million microforms. Every year, the U of A adds another 85-90,000 volumes to its collection.

On any given day, some 160,000 items from the libraries are circulating throughout the university. But the pressure builds at year-end when some 70,000 items are returned by students and professors. By the last week of April, up to 7,000 items a day come flooding into the libraries.

For the librarians, it becomes a challenge to find a place for the books. "If staff and students brought back everything that's

charged out, we'd probably be piling stuff on the floor," says Lyn Thompson, reference assistant with the Science and Technology Library.

"We have no place to store books," frets Ernie Ingles, U of A's director of libraries. "They sit in the aisles. They sit on top of the stacks. And they get damaged."

Books get shifted so often the spine breaks and the main text block breaks loose of its binding, says Dancik. Paper covers also get torn.

"So much of what we have is not replaceable," she says.

Another result of the crowding is loss of study space for students. As more books pour into the libraries, more shelving is erected. Says Dancik: "We don't have any place to put study spaces. Given our current enrolment, we really require another 2,300 (study) chairs."

The most immediate solution to the problem has been to shift library materials into storage. But while some materials can be retrieved in 24 hours, Ingles says in most cases the material is not easily accessible because it's not placed in storage in any order.

The answer to all this appears to be the acquisition of an off-campus facility which would hold about one million volumes in approximately 4,050 metres of space. Ingles says such an "auxiliary-stack facility" would be staffed by four people and would include a reading room.

As well, Ingles said he'd examine ways to ensure that materials requested by students and staff on the main campus could then be returned to the U of A quickly.

"We're looking at two ways," he said. "One is the possibility of faxing journal articles and that sort of thing, and the other is running a truck two or three times a day, back and forth."

One site currently under consideration for the new off-campus facility is a 2,050-square-metre-warehouse in the city's east end.

Don Bellow, U of A's associate vice-president of facilities, estimates the cost for an off-campus facility at about \$4 million, but notes that it could be at least a year before the funds become available.

"It's not a problem that's going to disappear," he says.

Charles Mandel is a freelance writer

THE PEGG

Vol. 14, No. 10, November 1986

Association of Professional Engineers, Geologists and Geophysicists

Job search support program gets go-ahead from APEGGA council

By Gail Poon

APEGGA's unemployed will be the prime benefactors of a \$50,000 aid package, introduced to assist engineers, geologists and geophysicists in their job search endeavors.

Recognizing the impact of Alberta's current economic climate, council agreed Sept. 17 to funnel reserve monies toward a job search support program proposed by the Career Development Advisory Committee (CDAC).

"Other associations are making efforts in this area to help their members. BC has spent a substantial amount helping unemployed members buy groceries. There is a feeling that those of us who have the budget should do something. This is something we can do," noted past president Dr. Don Bellow, P.Eng.

The job search support program is expected to run over an eight month period beginning this fall in both Edmonton and Calgary. Approximately 2/3 to 3/4 of the service will be concentrated in Calgary, according to CDAC chairman John Hep-ton, P.Eng.



Don Bellow, P.Eng.

The proposed program included four eight-week discussion sessions focusing on job search, skills training, motivation sessions and job search techniques which carry a price tag of \$6,000; two work stations in Calgary and one in Edmonton offering telephone — \$4,500; photocopying — \$3,000; resume typing — \$15,000; and individual consultation — \$15,000. Projected APEGGA staff costs are \$3,000 and a further \$3,000 has been allocated to a contingency fund.

To date, the CDAC has been approached by several firms experienced in relocation counselling.

Convention



New vest for retiring pres

Don Bellow, P.Eng., is vested during the long-standing traditional ceremony for the retiring president. Helping him is Bob Savage, P.Eng.

COUNCIL BRIEFS

Mindbender inquiry report

The board of inquiry which investigated the fatal June 14, 1986, rollercoaster accident at West Edmonton Mall, has overlooked an APEGGA recommendation.

In responding to the accident in the fall of 1986, APEGGA stressed the importance of having a professional engineer, registered in Alberta, take responsibility for the design, construction, maintenance and inspection of amusement rides of an unusual or unique nature.

"Instead, the board places the responsibility of ensuring public safety in the hands of the owner, who presumably, is required to set-up the necessary checks and balances for systems for which he may have no expertise," reads a report prepared by APEGGA Past-President Don Bellow, P.Eng., with input from Act, Regulations and Bylaws Committee Chairman Peter Savage, P.Geoph., and staff.

Owners cannot be faulted for this omission because they are businessmen and not engineers, the APEGGA report continues. However, it claims that by not stipulating that an Alberta registered professional engineer be responsible for the engineering the government will be allowing a serious omission — one that is not in the interests of public safety.

APEGGA council agreed Sept. 24 that the issue should be pursued with government officials.

Greater communication between council and committees needed

The 1986 committee chairmen's meeting provided participants with a chance to share tips and offer varying viewpoints on issues facing the association.

Highlighting the afternoon was a workshop session during which discussion focused on APEGGA's image, unemployment and registration. Incoming and outgoing chairmen, president Don Bellow, P.Eng., councillors and branch representatives were on hand as contributors to the APEGGA policy-making process.

"The committee system is the grassroots of our association. One of our goals is to improve the communication between Council and committees — to bridge that gap between them," said Dr. Bellow, whose APEGGA committee work has extended over many years. "When I was on committees, I often felt a degree of frustration with what we were doing and the reaction, if any, of Council to our efforts.

After serving on Council for six years, "I've found that committees are out of

touch with the thinking of Council, and Council has not always fully appreciated the concerns of the committees. This is not to place the blame on the committees nor on Council, but is more a reflection of a bureaucracy which is not always perfect."

Dr. Bellow said the "wild ideas" should come from committees and that Council has no time for grassroots thinking. He added, "the needs of Council are not always well communicated."

Included in a list of suggestions to chairmen were: maintain close contact with Council; don't be intimidated by Council; don't undertake too much; understand the terms of reference and the EGGP Act; and get Council reaction early.

"Develop three to five year plans and don't expect to come up with a brilliant idea each year," Dr. Bellow urged.

Also identified during the workshop was the need to raise the image of APEGGA within the eyes of its members and the public. Increasing dialogue with technical societies, studying the successes and failures of other associations, and taking stands on issues of public concern were some of the solutions offered.

"I'm not sure we have to do anything more than we are already doing. We have a distinct role and that is to administer the Act on behalf of the province of Alberta in the professional arena," Dr. Bellow rebutted.

"We have purposely kept out of politics. If you get involved, you tarnish your image. We have been called upon to take a political stand, but we are missing our mandate when we do that."



Retiring APEGGA president, Don Bellow, P.Eng. and his wife, Jean, (right) wish Margaret and Bill Blair, P.Geoph., the best for the next year as Mr. Blair assumes the president's chair for the 1986-87 term.



HONORARY LIFE: Don Bellow, P.Eng.

**University Student Liaison Committee -
U of A APEGGA/Geological/Geophysical
Student Society**

Dr. David Cruden, P.Geol., Honorary Chairman

Rob Klett

Steve Robertson

Tracy Bradley

Ken Matson

Roy Haggerty

Doug Voegtlin

Andrew Locock

Tracy Flohr

Ron Parent

Terry Mah

Jonathon Bellow

Dan Sturko

Kelly Arnold

Michelle Durand

Camela Dierker

Jeff Thurston

Tom O'Sullivan, Geol.I.T.

Tony Mah, Geol.I.T.

Dave Passfield, P.Eng., CIM

Calvin Nixon, P.Geoph.

Don Currie, P.Geol., CSPG

Mike Yakemchuk, P.Eng.

Neil Longson, P.Eng., Staff

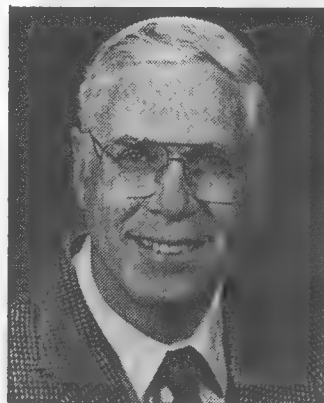
DISTRICT MEETINGS



Edmonton

Topic: The Japanese Experience - The Canadian Challenge

Japanese industries have been extremely successful over the past several years, while American industries have faltered. Ideas as to what can be learned from the Japanese experience will be presented. Specific examples will show that some of the best Japanese industrial practices originated in North America.



**Guest Speaker: Dr. Don Bellow,
P.Eng., Alberta Director,
Canadian Council of Professional
Engineers (CCPE)**

Dr. Bellow is an APEGGA Past President and currently serves the Association as its representative to the Canadian Council of Professional Engineers (CCPE). He was a recipient of the L.C. Charlesworth Award in 1982, which recognizes outstanding service to the Association and the advancement of its professional status. Dr. Bellow is a professor of mechanical engineering at the University of Alberta, having joined the faculty in 1963. He was Chairman of the Mechanical Engineering Department from 1975-1984. Active in numerous technical associations, Dr. Bellow is Chairman of the Steering Committee for the 75th anniversary celebration of the University of Alberta's Faculty of Engineering.

Date: Tues., Nov. 22, 1988

Place: Chateau Lacombe

**Time: 11:30 am/registration/reception; 12 noon/lunch;
12:40 pm/guest speaker**

Cost: \$15/members & guests; \$7/students

To pre-register, contact the Edmonton APEGGA office at 426-3990.

Aug '86



Bill Blair, P.Geoph., (left) begins his term as APEGGA president by taking the Oath of Office and signing a commemorative certificate. Retiring president Don Bellow, P.Eng., places the seal on the certificate.

Members enhance profession's image

Speaking to a resolution on image of the profession, put forward at the annual meeting in 1935, retiring president Don Bellow, P.Eng., stated that APEGGA's greatest and most productive contact with the public is through its members.

"Therefore it is our belief that our policy should strive to increase communication with the membership as a well-informed membership are by far our best public relations agents," he told delegates at the annual general meeting in Banff on June 6. Steps taken to address member concerns over the profession's image include: reinforcement of the communication department by staff with proven communication skills; early completion of a communication plan; cultivation of the concept of professional practice at the student level; review of the Code of Ethics; planning of seminars for members who assume responsibility for firms holding permits to practice; and, a comprehensive program of activities to mark the Engineering Centennial in 1987.

"We appreciate that this resolution was presented at the AGM last year so that we could highlight what activities were and are ongoing in the association in these areas of public image, value of professional services and the effects of good engineering," Dr. Bellow concluded.

LRT one year away from serving University campus

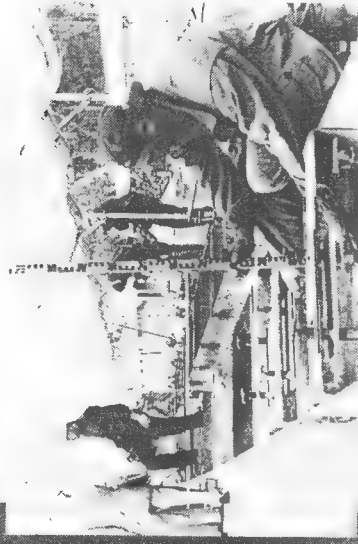
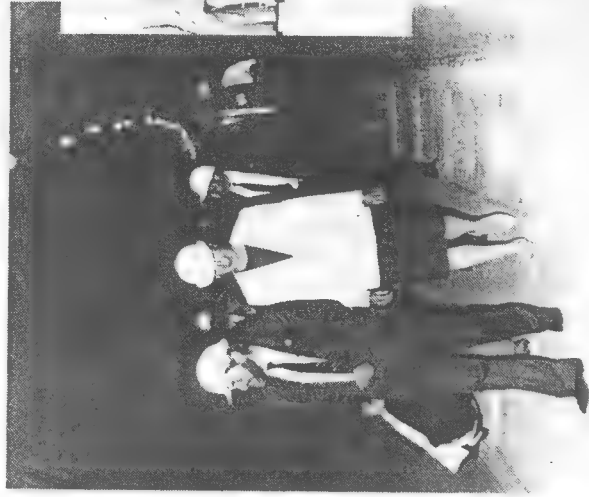
Coming to a campus near you. LRT service to University Station. And if all goes according to plan, that service could be at the University of Alberta's doorstep in one year's time.

"One year from now we intend to run the LRT to the University down this line," the Manager of the LRT Project Administration Branch, Rod Heise, told provincial, city and University officials 29 August. "This will mark the return of the 'trolley' or LRT to the southside."

A group of officials was given a tour of the project to mark the "365 day countdown" of the opening of the SLRT University Station, the largest station now on the City of Edmonton's LRT system.

Bob Kavanaugh, a Stanley Associates Engineering Ltd official, said the major civil engineering work on the Dudley B Menzies Bridge, the tunnel which travels under HUB Mall and the LRT University Station has been completed. More detailed work such as laying the rail, providing electrification and installing the signal system remains to be done.

Don Hickey, SLRT project manager of Stanley Associates, predicted that one year from now they would be able to say the project was on schedule and on or under budget. To date, the project is on schedule and under budget.



Beginning on the south river bank and travelling under HUB Mall, the tunnel to the LRT University Station is virtually complete. The major civil engineering work is done and now the rails, signals and electrical systems have to be installed.

Hickey said the project addresses concerns about cost effectiveness and humanistic needs, taking into account how Edmontonians feel about their river valley.

University of Alberta Associate Vice-President (Facilities) Don Bellow lauded the city for its vision and the province for its substantial support of the project (the province is footing 75 percent of the costs of construction). Dr Bellow said University Station is an important addition to the system, strengthening the links between "town and gown".

He said the University wants to develop 89 Avenue [where University Station entrances will be located] into a people space. The University looks forward to further developments of the LRT system down 114 Street, said Dr Bellow.

As part of the tour, a time capsule was placed in the LRT University Station wall. City, provincial and University officials placed assorted documents of the day in the capsule.

Campus smoking rules frequently ignored

University policy leaves officials without power to enforce

by Pat Kiernan

More than a year after the introduction of the University of Alberta's tough smoking policy, many people on campus continue to defy the rules.

Enforcement of the smoking policy is triggered by private complaints about specific violations. The vast majority of violations are never reported.

But university officials aren't sure the real solution will come from determined policing. Instead, they believe peer pressure and social acceptability ultimately determine the level to which students and staff comply.

Dr. Donald Bellow is the University's Associate Vice President of facilities. He describes the policy as regulating "not so much where you can't smoke, as where you can."

Students and staff are never likely to see a blitz against smoking policy violators. Bellow said in drafting the policy, administration decided not to go the route of the crackdown, "which would be fraught with difficulties, but rather to use the route of peer pressure and education." He notes that the policy has been very effective in most areas of campus.

Bellow said some complaints have been resolved through improved signs or ventilation. Smoking areas that are clearly identified are more likely to receive compliance from students and staff.

Bellow said the general philosophy on enforcement of the policy is that "education, peer pressure and intelligence will, in time, produce



Smokers in HUB among those who disregard signs.

the desired effect on campus." The effect he refers to is for non-smokers to be free of the annoyance and health risks caused by smokers.

Unless otherwise posted, the University is a non-smoking area. Designated smoking zones are clearly marked by a sign showing a cigarette in a green circle. The current policy has been in effect since September 1, 1988.

Occasionally, smokers become puzzled by the presence of ashtrays in non-smoking areas. Attempts have been made to remove those, but some remain. One university official said he's not surprised to see people lighting up in such confusing situations.

The primary enforcement of the University's smoking policy comes through Campus Security. Operations Manager, Ralph Oliver, said complaints are handled by his staff.

"We will then talk to the complainant, and get more information. And we'll try to identify the offender," said Oliver.

But there are no sanctions. Campus Security officers can take against the culprit. Oliver says enforcement is "by peer pressure, to convince that person to smoke where it's not offending other people. That's the only thing we can do." The smoking policy offers no provision for fines or other disciplinary measures.

Most action taken by Campus Security is in response to specific complaints. "We don't go around looking for offenders. But I'm sure that if we saw one, and it was quite an obvious thing, we might talk to them," said Oliver.

City of Edmonton officials say their jurisdiction over campus is limited by provincial legislation. Edmonton has a no-smoking bylaw enforceable with stiff fines, but prosecution has never taken place as a result of a University based complaint.

Bylaw Enforcement officers have spoken to university officials in response to specific complaints. In every case, they have always been met with a cooperative attitude. If that were to change in the future, they might attempt to prosecute, ultimately testing their jurisdiction through the courts.

There is a balance to be struck in dealing with smokers and non-smokers. The University has chosen not to ban smoking entirely, as some businesses, and many hospitals have done.

Bellow notes that smokers will continue with their habit "regardless of what we do. We should provide some area in which - if they do wish to smoke - they can do it in such a way that they don't offend the majority who do not smoke."

The effectiveness of the smoking policy is under constant scrutiny. A team of air quality consultants is currently working with the University. And the item continually appears on the agenda of the Occupational Health and Policy Committee.

"I think that in the near term, if we think a different approach needs to be taken, we will certainly investigate and consider that," said Bellow. But he points out "in most cases we feel the present policy is working reasonably well."

Extension Centre underway

by Bryan Hollands

Construction is underway on the new U of A Extension Centre at the north-east corner of 83 avenue and 112 street.

The cost of the building, designed by Hartwig Architecture Inc., is estimated at approximately 20.5 million dollars. Almost half of the funding (9.8 million) will be provided by the provincial government. The building is expected to be completed by August of 1991.

In an unusual move, some of the costs of construction will be covered by leasing commercial

space in the building to interested investors.

"We're trying to attract people who would find an advantage to being close to the University," said Don Bellow, assistant vp facilities.

"The Faculty of Extension itself will be leasing some space on a cost-recovery basis. The restaurant on the main floor will be run by Housing and Food Services."

Jamie Fleming, director of Investment and Real Estate for the University, sees no problem with leasing out space to commercial

investors in a building designed primarily for classroom use.

"The Faculty of Extension is more unique than other faculties. We feel that the uses we might find for tenants would be cooperative with the aims of the faculty. We've identified some who could benefit from being close to the faculty, and who would in turn, benefit the faculty."

Fleming said. Fleming cited professional clubs with interests related to Extension activities as "the most logical candidates." If enough professional clubs cannot be found, the space might be leased to other interested parties, such as the University Hospital and the government.

"It's a case of trying to mix and match," said Fleming. "We'd like to see the building full of uses that are complementary to Extension's mission."

Dr Wayne Lamble, acting Dean of the Faculty of Extension, sees the building as important to both the faculty's image on campus and its ability to function as a link between the University and the Community.

"Classroom space to us is quite critical, and is right now, a limiting factor. With the new building we expect our classroom space to double. We will be modernly equipped for adult students, with the proper seating, lighting and audio-visual technology," Lamble said.

A 297 space parkade attached to the building, is expected to be completed by February of 1991, several months prior to the rest of the building.

"There's a demand for parking," said Bellow of the parkade.



Ron Seors

What are these men building?

The construction taking place at 83 avenue and 112 street is for the new Extension Centre. the Faculty of Extension is currently housed in different locations across campus. The acting Dean, Wayne Lamble, believes the new building will be beneficial to the Faculty's image, as well as surrounding community.

Collection centre rejected, Fine Arts building approved

by Lesley Johnson

A plan has been approved for the Timms Centre for the Arts, almost a year after plans for the Timms Collection Centre were rejected.

The Facilities Development Committee (FDC), a subcommittee of the General Faculties Council (GFC) passed a general fit plan for the Centre, on October 5 of this year. The general fit plan for the Department of Drama details the amount of space required by the department, as the Centre is eventually intended to house Studio Theatre.

Alfred Timms, an Albertan farmer who made money in the oil industry, bequeathed his estate, now worth over four million dollars, to the U of A in 1974, with a request to have a building erected under his name.

Originally his donation, compiled with grants from the Alberta Department of

Advanced Education and the contributions of other private donors were thought to provide adequate funding for the proposed Timms Collection Centre.

The Centre was to have held the University's rare artifacts, art and archives of both educational and historical significance, in a showcase manner, available to both students and the public.

However, when the final budget proposal for the Timms Collection Centre exceeded the initial \$17.5 million budget by five million, excluding the estimated annual running costs of \$750,000, the Board of Governors halted plans for the Centre. The University Archives and Collections Department was disappointed as they had combined departments for the project and are in need of space for their collections.

The recipients of the Centre, the drama department, currently house their Studio

Theatre in the Myer Horowitz theatre in SUB. Previous to this, the theatre was in Corbett Hall, but because of renovations, it had to move. Once renovations are completed, Corbett Hall will only have Rehabilitation Medicine under its roof.

As well on October 5, Donald G. Bellow, associate vp facilities, appointed a consultant, Brinsmead Ziola, to work with the drama department in organizing a specific fit plan for the Centre. This plan will develop the initial layout designs in accordance with a set budget of \$11 million.

Ziola is with the Humanite Consulting Firm, the same firm who developed the general fit plan.

As no date for the completion if the Centre has been set, Bellow expressed some concern over the impact of the GST on building costs.

CAPITAL EQUIPMENT PURCHASES

A program exists to provide the carryover of unspent capital equipment funds into the next budget year. This carryforward is limited to the lesser of the expended balance, 15 percent of the departmental capital equipment budget, or \$50,000. Where the balance of unexpended funds is sufficient, commitments incurred by purchase orders placed before 31 December 1991 will be allocated a carryover equivalent to the amount of the commitment.

Where the balance of the unexpended and/or committed capital equipment budget is currently in excess of the foregoing limits, staff are urged to place the purchase orders for their further needs now to help ensure that delivery is effected before 31 December 1991. The program will not provide a carryover in relation to

commitments placed subsequent to 31 December 1991 other than in instances where a well-documented justification of circumstances merits exception.

Application for exceptions should be submitted to the attention of D Grover, Office of the Comptroller, 492-5894. Final approval on capital equipment carryovers remains with the Associate Vice-President (Facilities), DG Bellow.

Unexpended funds in excess of the limiting factors will lapse into the Vice-President Administration's Capital Equipment Contingency Account.

For additional information, see MAPPS 03 - 050 - 015 FLEXCAP - Flexible Capital Expenditures Program.

U of A proposes bus-loop move

by Karen Cho

The bus terminal that existed on 89th avenue before the start of LRT construction may be a thing of the past if a relocation proposal is accepted by the university administration.

The proposal was put forward by Don Bellow, vp facilities at the U of A, who believes that the University should think twice before moving the bus terminal back to its old location in front of the Dentistry-Pharmacy Building.

Bellow believes that by keeping the bus-loop away from the heart of campus the University will be better able to deal with pollution and pedestrian problems. He also argues that it will be aesthetically pleasing to have a green space in the middle of campus where the bus-loop used to be.

Students' Union Housing and Transportation commissioner, Jody Wilson disagrees with Bellow's assessment.

She argues that pollution and noise will exist wherever the bus-loop is located and that the present location on 87th avenue is actually more dangerous for pedestrians than the old location on 89th avenue.

While Wilson agrees that a green space on 89th avenue would be desirable, she says that the Univer-

sity should avoid unnecessary expenditures.

"In this day and age, money comes over aesthetics," she said.

In recognition of the fact that many people are dissatisfied with his proposal, Bellow pointed out that the relocation plan is still tentative.

"This is a tentative plan. We have to come up with a solution for general transit service to the University," he said.

According to Greg Latham, manager of Edmonton Transit, the whole question has to be looked into in greater depth before a final decision can be made.

"We don't know where the bus-loop is going to be but we're working on it," he said.

With this in mind, the University and the city have established a joint working committee to look into the question of bus-loop relocation.

Jody Wilson is concerned that the outcome of the committee's negotiations may leave students and members of the general public dissatisfied.

"I don't think that the University has looked into who they may be really inconveniencing," she said.

"I can definitely see their point, but I don't see a whole lot of pros that outweigh the cons."

~~Oct 4/90~~

Poop on new loop

What are the chances that vp facilities Don Bellow has a reserved parking spot a lot closer to the "aesthetically pleasing... green space in the middle of campus where the bus-loop used to be" than the bus-loop's present location?

Ian Lyttle
Engineering III

Tunnel vision in Edmonton

It's amazing how Edmonton's aldermen can turn a harmless field trip to a tunnel into a whole lot of political intrigue.

The occasion was a show-and-tell excursion to the south LRT line — which has emerged from the north bank, crossed the North Saskatchewan River on the Dudley B. Menzies bridge and mysteriously disappeared on the southside again. It's hoped that some day it'll come to the surface at an undisclosed destination south of the University of Alberta.

There was no other reason for the dog and pony show other than it's hoped that, one year from yesterday, the first train will rumble across the river and deposit its load of sweaty students on the U of A platform.

This is probably just a coincidence, but about the time the champagne corks are popping on Dudley's bridge, council's incumbent aldermen will be kicking-off their re-election campaigns. The LRT completion — as well as the official opening of the new city hall — will be just what the spin-doctor ordered to get Showdown '92 off to a flying start.

Yesterday's white hard-hat tour for media and assorted project and political brass — including provincial Transportation Minister Al "Boomer" Adair, who is really responsible for Edmonton's railroad — was to showcase engineering marvels like the Slurry Shield Tunnel Boring Machine.

And the equally impressive bridge — which apparently look home a coveted American Concrete Institute Award.

But no sooner had the entourage come out of the gloom at the university station, then the politics started.

Don Hickey, a spokesman for the project manager, Stanley Associates Engineering, beamed "the result has been very worthwhile."

He went on to praise the joint venture with the city's public works department as being "very effective."

This is the same warm and friendly relationship — where Stanley gets all the industry credit and the city staff engineers are largely left out in the cold — which public works manager Al Maurer tried to scuttle not so long ago.

Ald. Bruce Campbell came to Stanley's defence. He said by letting private sector engineers do the project it gives them the experience to "do this kind of work all over the world."

Campbell, who was speaking as a member of the South LRT Steering Committee, also lamented that he wished his group had become more involved in the "114 St. exercise."

NEIL

WAUGH



This, of course, is the ongoing controversy of where the LRT goes next. Residents of the neighboring Belgravia and McKernan neighborhoods have been waging a court and political battle to keep the LRT — and particularly the LRT tunnel entrance — out of their backyard.

An uneasy truce has been struck by moving the portal north of University Ave. to emerge on U of A lands — except this has only inflamed the University Hospital and other institutions in the area which don't want the hole in the ground either.

It's hoped that U of A vice-president Don Bellow will take seriously his promise yesterday of "continued co-operation" and allow the track to surface on the university lands.

The university has hardly been overly co-operative in the past. It's insistence that the SLRT go underground to the U of A is a lot of the reason why \$250 million has been poured into the project with very few kilometres of track to show.

Adair was quick to point out that 75 per cent of this cost came from provincial transportation grants.

"It's major proof by this government of a commitment to this city," Boomer boomed. The underlying political message here, of course, is that city voters have not been particularly committed to the ruling Tories in return for their LRT dollars. With the exception of two ridings, Edmonton is a Tory-free zone in the provincial legislature.

Even Ald. Catherine Chichak — who was pinch hitting for Mayor Jan Reimer — jumped into the act. She praised the project as very impressive to this point. And she got her name engraved on the brass plate that covered the time capsule that was embedded in the station wall yesterday. However, Chichak's plaque days may be severely limited if Ward 2 voters decide to punish her next fall for overlooking \$8,400 in back business taxes when she ran for council.

Yup, there's a lot more to the LRT than trains.

Edmonton Sun. Friday, August 30, 1991.

Solution to deficit may lie in sale of land says Premier

Gateway Mar 5/91

by Carolyn Ramsum

Premier Don Getty hinted in a recent press conference that the University should sell off some of its land to offset its severe budget difficulties.

Graduate Students' Association president, Stephen Downes, believes that by making this suggestion, Getty and John Gogo, Minister of Advanced Education, are "taking cheap shots instead of seriously examining university funding problems."

Nevertheless, according to Donald Bellow, acting vp administration, the University is considering Getty's proposal. Bellow believes, however, that the sale or lease of University lands would not raise as much money as people might think.

Bellow feels that a government figure which values University assets at \$1.75 billion is somewhat misleading. This figure, he says, includes the value of all buildings and other non-saleable capital at the U of A.

Bellow contends that the value of off-campus University property is closer to \$48 million. Almost all of this land, however, has been en-

gaged for teaching or research purposes.

The Board of Governors has recently reactivated its Real Estate Advisory Board to study the merits and/or drawbacks of the development of the W240. This tract of land — W240 — is adjacent to the University farm and is in the area between Landsdowne and

"(They're) taking cheap shots instead of seriously examining university funding problems."

Grandview.

The Faculty of Forestry and Agriculture use W240 as a field laboratory and research area. They have in the past expressed strong opposition to the development of this land.

Though nothing has been decided, Bellow says that even if the University does decide to develop the W240, there is no guarantee that the money would be put into the deficit-ridden operating budget. This is the budget that was hit last month by severe vertical and horizontal cuts.

Money made from land development could be put into the capital budget, Bellow explained. Government funding for the maintenance and repair of buildings has slipped 50 per cent over the last five years. Consequently, many buildings on campus require extensive renovations.

Downes said he would have no disagreement with putting funds raised from land development into the upgrading of student residences. These buildings are falling apart. He does object, however, to money raised through possible land development into the operating budget, as once it is spent, it is gone.

One of Bellow's concerns about any possible land development is that the government might reduce grants by the amount that was raised by the land development.

Bellow adds that the University is studying the option of land development because "we have to make the best possible use of our resources to demonstrate to the government that we are doing everything possible to meet our academic needs. And we hope that the government will respond positively."

Campus falling apart

by Karen Unland

Buildings at the University of Alberta are in desperate need of repair, says associate vp facilities Don Bellow.

According to Bellow, the University needs \$300 million to bring its buildings up to code specifications. He said the problem will have to be dealt with over ten to fifteen years.

"We have such a large deferred maintenance problem that we

would not be able to deal with this in any one year."

Bellow said that even though the maintenance problem will not be solved in one year, something has to be done now.

"The consequences of not spending any money is that it's just going to increase this sum or we're never going to get our heads above water."

Bellow said building practices of the 1960s caused the problem fac-

ing the University now. "There was no thought to putting away money for maintenance."

He said the Biological Sciences Building needs 100 million dollars and the Tory building is in similar straits. The residences need \$45 million to bring them up to standards.

The provincial government will be announcing its capital grant this spring.

Funding cuts affecting infrastructure *Sept 17/91*

by Christopher Spencer

The infrastructure of the university is crumbling — quite literally.

Significant reductions in government funding, and the deteriorating condition of many of the University's old buildings, have resulted in a dramatic backlog of renovation and reconstruction projects on campus. Donald Bellow, associate vice-president of facilities, estimates that the university will require \$500 million to satisfy all its

building and construction needs.

In the mean time, the University is embarking upon a programme of temporary repairs and stopgap measures in order to retain an acceptable level of office and classroom space.

With 3.5 million volumes currently occupying a physical space designed to hold between 2.3 and 2.7 volumes, the Library is among the University departments which is currently experiencing problems

related to the backlog of building construction. Compounding these problems is the deteriorating state of the Cameron Library, the exterior of which requires extensive renovation.

While the university administration would like to build a \$35 million addition to one of the existing libraries, it is prepared to settle for much less.

"The number one priority for the 1992-93 budget year is the development of an auxiliary stack facility for the Library," Bellow said Monday.

This reliance upon a temporary storage location is not popular among some members of the academic and library staff.

"The transportation of documents from a storage facility to the University campus will inevitably result in damage and loss of books and archives," contended English Professor Gary Kelly, a member of the "Save the Library Committee," during an interview with the *Gateway* last April.

Among the most expensive of the University's building priorities are Electrical Engineering (\$34.8 million), Computing Sciences (\$32.4 million), and Pharmacy (\$26.5 million). Unless the provincial government revises its policy of reducing funding to post-secondary education, it is unlikely that any of these projects will be completed, Bellow said.

"Each year we get a certain amount of capital from the government specifically for [construction projects involving] life, safety, and health. This year we got \$10.1 million, which is half of what we got five years ago."

The University may be forced to seek more funding from the private sector.

"The government has come up with a proposed capital funding paper in which they are suggesting to Universities that they investigate ways in which they could augment financing through other sources," Bellow said.

The controversy surrounding the allocation of limited resources to the tremendous backlog of building reconstruction may only just be beginning.

Dr. Lois Stanford, vice-president of student and academic services, is currently chairing a committee which may recommend, in late October, that some or all of the University residences, which require \$35 million in renovations, be closed.

Jody Robbins, Student's Union housing and transport commissioner, is fatalistic about the future of the residences.

"Whose to say that Lister will still be around in five years? Whose to say that Faculté Saint-Jean, or that any of the residences will still be around?"

U of A buildings suffering slow deterioration

Repair funds seen as inadequate

ALLEN PANZERI
Journal Staff Writer

Edmonton

The University of Alberta is witnessing a "creeping deterioration" of its buildings because of inadequate provincial funding to repair them, says the university's associate vice-president for facilities.

Don Bellow said buildings on campus are not in any danger of falling down, despite the collapse of a ceiling Tuesday during renovations in the 23-year-old clinical sciences building.

But he said there's not nearly enough money to pay for repairs that are desperately needed.

"We're not saying that buildings are about to fall down, but many of them just keep getting worse and worse, and the question becomes how long we're going to be able to live with them," he said Thursday.

"It's a creeping deterioration and what we're doing is putting money into repairs on a building we know is adequate at best."

Bellow said the clinical sciences building is safe and that once renovations are finished it will "be in reasonably good operating condition."

But he said the incident merely underlines the desperate condition of many buildings on campus — adding while the university is not facing an immediate crisis, it did face one two years ago when it had to borrow \$3 million for emergency repairs on its residences, which would otherwise have had to be shut down as unsafe.

"We are addressing the clinical sciences building, but there are other buildings on which we need to do work and the need is as great," Bellow said.

While there are a number of

"We're not saying that buildings are about to fall down, but many of them just keep getting worse and worse, and the question becomes how long we're going to be able to live with them."

— Don Bellow, associate vice-president, facilities

major needs on campus, the university has been forced to give approval only to high-priority projects that threaten health and safety because its provincial capital renewal grant has shrunk.

This year's grant of \$10.1 million is exactly the same as last year's, but five per cent less than the 1989-90 grant and 50 per cent less than the 1986-87 grant.

It's not likely to get any better next year, either.

"We believe that fiscal restraint is here to stay," Advanced Education Minister John Gogo's executive assistant Charlene Blaney said Thursday.

The province is currently developing a new capital funding plan and is seeking responses from post-secondary institutions.

Bellow said the university basically agrees with the province's suggestion that colleges and universities raise more money for facilities through private donations.

But he said the university is still essentially a "publicly funded institution and we have to rely on the government for those funds."

"We hope the government will recognize the problems we are facing."

May 1991

Capital budget: same sum, different year

A capital budget of roughly \$10 million for a University the size of the U of A is “ludicrously small”, John Bertie (Chemistry) told fellow Board of Governors members at the regular meeting 17 May.

“We are getting into a situation where we have departments with \$16 million of inventory, and they’re given \$150,000 a year towards the upkeep and the renewal of that inventory,” he said, responding to the Provincial Government’s allotment for the University’s capital renewal grant.

Dr Bertie said a capital, maintenance and replacement budget of about one percent of the inventory is “just appalling. It’ll destroy the University in very short order.”

The Board approved the 1991-92 capital renewal budget of \$10,121,000. Donald Bellow, Associate Vice-President (Facilities), informed the President and Vice-Presidents by letter that, “This is the same amount as was received for 1990-91 and is five per cent less than was received for 1989-90. This may not appear too much of a change until it is realized that the 1991-92 grant is 50 percent less than it was in 1986-87.”

The University plans to spend the money this way: \$350,000 will go to reduce the capital deficit which stood at \$2.5 million as of 31 March; \$5 million will be spent on equipment renewal; \$3,171,800 will be spent on renovations, and \$1.6 million will be spent on site and utilities maintenance.

The equipment renewal budget of \$5 million will be allocated as follows: primary programs will receive \$2,965,000; support services will receive \$700,000; computing support will receive \$1.3 million, and a contingency of \$34,650 will be included. Dr Bertie said, “I really appreciate the very clear effort that’s been made to put funds into the academic side of the University.”

The University will not be able to respond to all the requests for renovations and repairs. “Only the most urgent requests are addressed,” Dr Bellow outlined. “This has been the practice for some time and will be the practice again this year. Renovations projects which were requested, but not funded, in previous years have become critical this year and have risen to the top of the priority listing.”

This year Physical Plant requested \$4,250,000 for renovations, repairs and upgrading for essential projects of which only half are being funded, Bellow explained.

Advanced Education Minister John Gogo, in a letter to Board Chair Stan Milner, said the challenges presented by limited growth in provincial support will likely continue for some time.

The 1991-92 capital construction projects include: Corbett Hall, \$2,547,000; Extension Centre, \$793,000; PCB (polychlorinated biphenyl) removal, \$563,000; Clinical Sciences renovations, \$2,813,000; utilities upgrading, \$2,000,000; and animal care facilities upgrading, \$2,600,000.

Delay on 89th Ave. bus route riles U of A students' union

Vice-president miffed at lack of notification by city, U of A

SCOTT McKEEN
Journal Staff Writer

Edmonton

The city and university didn't have the courtesy to tell U of A students of plans to again run buses to a distant terminal on campus, says a spokesman.

Randy Boissonnault, student union vice-president, was miffed by the decision and the fact the association wasn't notified.

"We found out through the back door that this was happening," said Boissonnault.

He said the student union should have been notified as "a professional courtesy. It's the students who are affected," he said.

City spokesmen confirmed this week that the plan to return buses

to 89th Avenue has been delayed for a year. A temporary terminal will remain in the parking lot of the Jubilee Auditorium.

Construction of the LRT station on campus forced buses off 89th Avenue originally, and work reclaiming and landscaping the site has not been completed to allow for their return.

University Vice-President Donald Bellow bristled at the suggestion the university was to blame for the delay.

He said the city pushed the schedule back as the LRT construction site had not been cleared to allow for any of the landscaping.

As well, both the city and the university agreed that with the construction season ending and students returning to classes the work

was better done next spring.

Students were upset last winter at having to brave the long walks to classes from the terminal in the bitter cold.

Boissonnault said students have to take the walk into account in daily schedules and may have to leave home up to a half-hour earlier to make connections to get to classes on time.

Bellow said student representatives weren't brought into discussions on the terminal issues as it was being decided for "technical reasons, not emotion."

Edmonton Transit Manager Greg Latham said the return of buses on to 89th Avenue will be timed now for the fall of 1992, when the university LRT station is slated to open.

City steamed over bus site criticism

by Ron Kuipers

City of Edmonton Transit officials are becoming perturbed by what they feel is unfair criticism regarding the relocation of the University Transit Terminal.

Wayne Ramsbottom, director of Marketing and Planning for Edmonton Transit, said his group proposed several relocation sites for the terminal, "some of which were much closer to the main campus than the present site." However, all the proposals were flatly refused by university planners.

According to Ramsbottom, these proposals were refused because the University was concerned about losing space and harming the aesthetic quality of the campus as a whole. Ramsbottom said that one proposed site would have located the terminal "much closer to HUB Mall."

He summed up the city's frustration saying, "as director of marketing, I'm trying to encourage public transit use by one of its most important users (students). Yet, in effect, I am discouraging its use by having the terminal located in such a weird spot."

However, Dr. Don Bellow, university associate V.P. facilities, did not know about these alternative sites as he was recently appointed to his position. "I'm not aware of (these proposals)," he explained, adding that if Edmonton Transit wanted to use any available space near HUB Mall, they would be refused because of the resulting loss of university parking revenue.

Bellow was also quick to point out that city planners also rejected one of the University's proposals, which would see all buses circle the entire campus, dropping people off at intermittent points. Ramsbottom said the city rejected this proposal because "it would cost us a bundle on rescheduling cost alone." He also felt Saskatchewan Drive was unsuitable for heavy bus travel.

Whatever the case, Bellow said that the bus terminal will not be returned to its original location, and that a new solution must be found. "Despite the apparent difficulties," he explains, "we want to work closely with city planning officials to find an optimal solution for everyone involved."

Ron Sears

U of A needs \$500M for building upkeep, official says

GORDON KENT
Journal Staff Writer

Edmonton

The University of Alberta needs to spend up to \$500 million on an "unfathomable" backlog of building construction and renovation, a senior official said Friday.

"The government has to recognize the serious situation we're in," said Don Bellow, associate vice-president of facilities.

"We have a problem and it's not going to go away."

But the annual grant for capital projects covering repairs, renovations and new equipment has dropped from around \$20 million five years ago to about \$10 million this year, he said.

He acknowledged that it's a difficulty shared by other Alberta post-secondary schools.

But Bellow said it's worst at the U of A — the province's largest and oldest university.

"We have buildings that are slated for demolition, but I can't see how in this day and age we can

get rid of them because we need the space."

He supports a suggestion from Advanced Education Minister John Gogo that colleges and universities raise more money for facilities through donations.

Gogo said Thursday he has sent out a discussion paper to administrators proposing a higher ranking for projects that receive some funding outside government.

"We believe that the university, through its fund-raising efforts has got to get more from the private sector . . . because it's a major

beneficiary of the university," said Bellow.

High-priority areas at the U of A include more library space, which could cost \$35 million if an addition is built, Bellow said.

And residence renovations could also cost \$35 million, he said.

He'd like the province to come up with a plan for dealing with the construction crunch, such as paying for three-quarters of major projects for three-quarters of Edmonton's LRT.

"We're not even doing anything to keep even with where we are — there's a huge backlog."

Page 2 ♦ Thursday December 5, 1991 ♦ The Gateway

Substandard facilities upgraded

by Michael Curry

The University of Alberta is taking steps to upgrade animal care facilities described last year as being "substandard" and in a "crisis situation."

After receiving warnings in 1984 and 1987, the University was placed in a state of "total non-compliance" by the Canadian Council of Animal Care, jeopardizing millions of dollars in federal capital research grants. The University is now in a state of provisional non-compliance.

The primary reason for this action by the CCAC was the state of the animal research facilities in the Medical Sciences and Clinical Sciences Building, according to David Neil, director of Health Services Laboratory Animal Services.

Neil said the main problem was with the "totally inadequate" ventilation system in the Medical Sciences Building. He cited high levels of ammonia and carbon dioxide throughout the building, affecting both animals and employees.

"The fumes in some of these

rooms are unbelievable. The building in general was not designed to withstand the wear and tear of animals."

The University applied last year for \$8.4 million dollars from Advanced Education to upgrade the facilities to current standards. Renovations to the Medical Sciences Building should be completed by July 1993 with animals being temporarily relocated to the almost finished Heritage Medical Research Centre.

The renovation plans are being studied by the University Animal Welfare Policy Committee. Brian Dunford, chair of the committee, said the current facilities are unac-

ceptable, but he is optimistic about the new plans.

According to Neil, ventilation problems were affecting experimental results and causing disease to spread among the laboratory animals. However, Neil stressed that at no point were animal handling guidelines broken and that the University strictly adheres to humane practices. He said the University maintains contact with animal rights groups and the facilities are inspected twice a year by the Alberta Society for the Prevention of Cruelty to Animals.

Last year's CCAC report also listed the Clinical Sciences Building as being "non-compliant" but Neil said it is currently being phased out as an animal research facility. Most of the animals there will be moved to the Heritage Centre.

The Medical Sciences Building was built by the province in the early 1970s and presently accommodates rodents, dogs, cats and fish. The increase in the number of researchers and animals and more

of the building's problems, according to Don Bellow, U of A associate vp facilities.

"The major problem is that the standards have increased."

Bellow singled out the psychology animal laboratory as one of the more urgent cases in need of upgrading.

"By and large we are meeting standards."

Glenn Harris, chair of the facilities development committee, was unavailable for comment.

U of A needs \$500M for building upkeep, official says

GORDON KENT

Journal Staff Writer

Edmonton

The University of Alberta needs to spend up to \$500 million on an "unfathomable" backlog of building construction and renovation, a senior official said Friday.

"The government has to recognize the serious situation we're in," said Don Bellow, associate vice-president of facilities.

"We have a problem and it's not going to go away."

But the annual grant for capital projects covering repairs, renovations and new equipment has dropped from around \$20 million five years ago to about \$10 million this year, he said.

He acknowledged that it's a difficulty shared by other Alberta post-secondary schools.

But Bellow said it's worst at the U of A — the province's largest and oldest university.

"We have buildings that are slated for demolition, but I can't see how in this day and age we can

get rid of them because we need the space."

He supports a suggestion from Advanced Education Minister John Gogo that colleges and universities raise more money for facilities through donations.

Gogo said Thursday he has sent out a discussion paper to administrators proposing a higher ranking for projects that receive some funding outside government.

"We believe that the university, through its fund-raising efforts has got to get more from the private sector . . . because it's a major

beneficiary of the university," said Bellow.

High-priority areas at the U of A include more library space, which could cost \$35 million if an addition is built, Bellow said.

And residence renovations could also cost \$35 million, he said.

He'd like the province to come up with a plan for dealing with the construction crunch, such as paying for three-quarters of major projects like it does for Edmonton's LRT.

"We're not even doing anything to keep even with where we are — there's a huge backlog."

Page 2 ♦ Thursday December 5, 1991 ♦ The Gateway

Substandard facilities upgraded

by Michael Curry

The University of Alberta is taking steps to upgrade animal care facilities described last year as being "substandard" and in a "crisis situation."

After receiving warnings in 1984 and 1987, the University was placed in a state of "total non-compliance" by the Canadian Council of Animal Care, jeopardizing millions of dollars in federal capital research grants. The University is now in a state of provisional non-compliance.

The primary reason for this action by the CCAC was the state of the animal research facilities in the Medical Sciences and Clinical Sciences Building, according to David Neil, director of Health Services Laboratory Animal Services.

Neil said the main problem was with the "totally inadequate" ventilation system in the Medical Sciences Building. He cited high levels of ammonia and carbon dioxide throughout the building, affecting both animals and employees.

"The fumes in some of these

rooms are unbelievable. The building in general was not designed to withstand the wear and tear of animals."

The University applied last year for \$8.4 million dollars from Advanced Education to upgrade the facilities to current standards.

Renovations to the Medical Sciences Building should be completed by July 1993 with animals being temporarily relocated to the almost finished Heritage Medical Research Centre.

The renovation plans are being studied by the University Animal Welfare Policy Committee. Brian Dunford, chair of the committee, said the current facilities are unac-

ceptable, but he is optimistic about the new plans.

According to Neil, ventilation problems were affecting experimental results and causing disease to spread among the laboratory animals. However, Neil stressed that at no point were animal handling guidelines broken and that the University strictly adheres to humane practices. He said the University maintains contact with animal rights groups and the facilities are inspected twice a year by the Alberta Society for the Prevention of Cruelty to Animals.

Last year's CCAC report also listed the Clinical Sciences Building as being "non-compliant" but Neil said it is currently being phased out as an animal research facility. Most of the animals there will be moved to the Heritage Centre.

The Medical Sciences Building was built by the province in the early 1970s and presently accommodates rodents, dogs, cats and fish. The increase in the number of researchers and animals and more stringent regulations are the cause

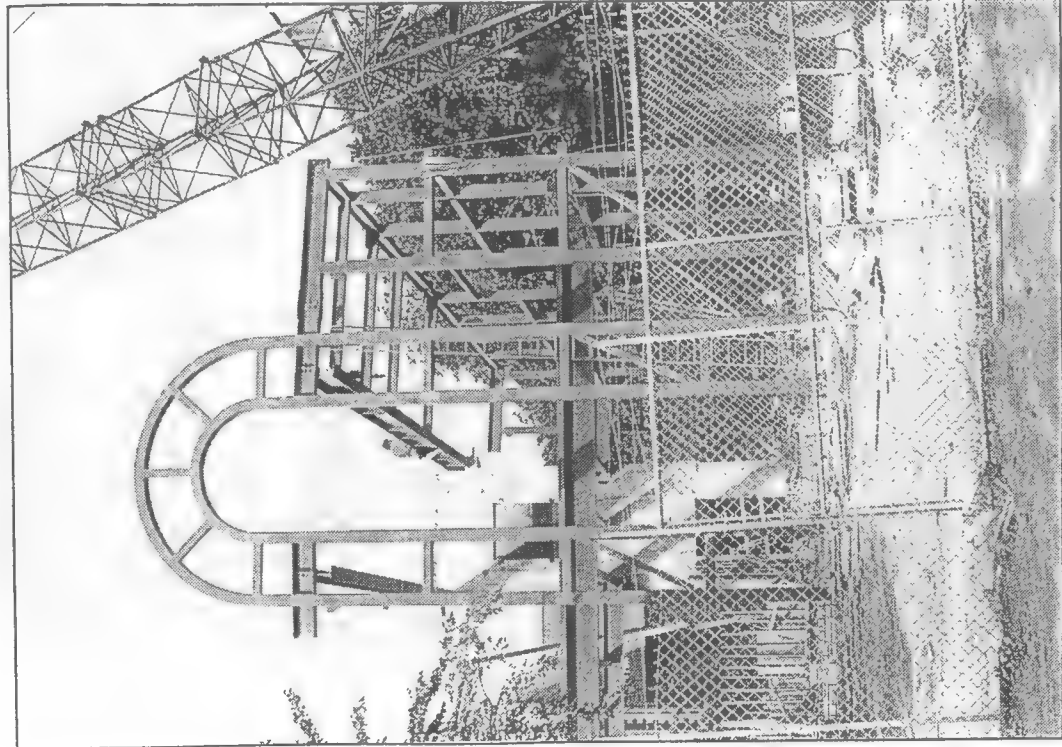
of the building's problems, according to Don Bellow, U of A associate vice-president.

"The major problem is that standards have increased."

Bellow singled out the psychology animal laboratory as one of the more urgent cases in need of upgrading.

"By and large we are meeting standards."

Glenn Harris, chair of the facilities development committee, was unavailable for comment.



Rachel Sanders

Construction and landscaping far from over at LRT site

Another winter of long walks

Bus loop not moving until September 1992

by Karen Unland

The bus loop will not be moving back to 89th Ave. until September 1992, despite earlier promises that the buses would be back this November.

The decision to delay the move was made two weeks ago when the public works department alerted the University that the proposed plan to reconstruct and landscape the old bus loop was impossible to complete this season.

Ron Neuman, manager of roadways for the City of Edmonton, says that the city and the university just ran out of time.

"We require about two to two-and-a-half months of construction time to do the work that is proposed."

Don Bellow, associate vp facilities, says that early Alberta winters are responsible for the holdup.

"We just ran out of time in view of the impending weather."

Bellow says that even if the necessary construction and landscaping could be completed before the snow flies, it would be costly and poorly done given the time con-

straints.

"It all seems better for technical reasons to delay [construction] until spring."

Students' Union officials were concerned that they were not informed of the decision earlier. Housing and Transport Commissioner Jody Robbins said that she

The fact of the matter is we weren't informed, which leads me to be upset."

According to Bellow, students do not usually participate in such decisions.

"I don't mean to convey that we're not concerned about students... it wasn't a deliberate attempt to cut the students out of the process."

Bellow believes that in the end students will benefit from the decision.

"The net result will be better than if we had relocated the buses this fall... One move off campus and one move back I think is simpler [and] less disruptive in the long run."

According to John Schnablegger, general manager of the transportation department for the City of Edmonton, the bus loop will definitely be moved by the fall of 1992.

"We have a contract with the University and are bound by that.... We will proceed with the construction of the roadway regardless [of future delays]."

"It wasn't a deliberate attempt to cut students out of the process."

found out about the change by accident at a Bikes on Campus committee meeting.

Randy Boissonnault, SU vp external, was unhappy about the way in which students were informed about the decision.

"We had very little lead time and found out through the back door that this was going to happen.... When something as monumental as the bus service to campus is changed it's logical that the Students' Union that represents these students should be informed."

DEPT. OF MECHANICAL ENGINEERING
Rm. 4-5 Mechanical Engineering Bldg.
University of Alberta
Edmonton
T6G 2G8

-DON BELLOW-

Friday, January 17, 1986 — THE LETHBRIDGE HERALD — B13

High liability premiums 'hurt the general public'

High liability insurance premiums are not in the best interests of the public, says Don Bellow, president of the Association of Professional Engineers, Geologists and Geophysicists of Alberta.

Bellow was on his annual president's trip to visit the local chapter of the association Thursday.

Recently, many groups from lawyers to the national Canadian Ski Team have complained about the skyrocketing cost of liability insurance.

"Going to court is perhaps part of doing business, but it appears to be more the case now than it has in the past," said Bellow in an interview. "But the main problem we see is that the insurance premiums for errors and omissions is going up astronomically high. It's becoming almost prohibitive for some companies."

At the same time the number of insurance underwriters willing to provide liability insurance has fallen from 14 to one or two companies in Canada.

Bellow said the association sees this as a national problem caused by large settlements in the United States and recently in Canada as well. "What I'm

raising here is this — is this in the public interest? If an engineering firm has to pay large premiums, clearly they're going to pass those premiums onto the clients."

Association executive-director Clayton Milroy said the problem is interna-

tional in scope and affects municipalities, doctors, everybody."

Bellow said he doesn't know what the solution is.

"When we've heard talks from lawyers, they blame it on the insurance underwriters. We here talk from the insurance underwriters who say it's the judiciary system and the judges. Perhaps the judges would blame it on the government and we've heard comment from the government that

says we can't do anything because this is what the public wants."

Bellow said he's suggesting representatives from all these groups get together and find an answer to the problem that's in the best interest of the public.

"I don't think the present system is in the best interest of the public. I think the public is the one going to suffer in the long run."



DON BELLOW

DON:

20-1-86.

FOR YOUR INFO.

THANKS AGAIN FOR A MOST ENJOYABLE VISIT.

Don Clark

●海外参加者リスト

注目される著名トライボロジストの横顔

(ABC順)

(解説は本人より送られてきた自己紹介文の和訳です)

Prof. Donald G. Bellow

(Canada)

Bellow教授は、プリティッシュ・コロ
ンビア大学で理学士の学位を、アルバー
タ大学で博士号を取得した。1963年以来、
アルバータ大学の職員を務めてきたが、
最近では機械工学の教授と副校長の特別補
佐(財務および管理)を務める。1975年～
1984年機械工学部の学部長、1989年～94年
までは副校長補佐。

研究テーマは鉄鋼業および石油工業に
関連した産業的な諸問題にしばられてき

た。潤滑油分野の諸要素の疲れ、腐食疲
れと摩耗において、広範にわたり実験作
業を実施した人でもある。

(東京大学 木村好次氏評)

「油井の摩耗問題という、きわめて国
際的なテーマを取り上げて、積極的な研
究をくりひろげている近年珍しい存在。
鉄道マニアでもある」



発表論文: Influence of Counterface and Configuration on Polymer Wear

Large animal surgery opens

Facility will reduce stress on animals and aid and abet their recovery

By David Holehouse

A grand opening celebration was held 9 October for the new large animal surgery at the University's Edmonton Research Station.

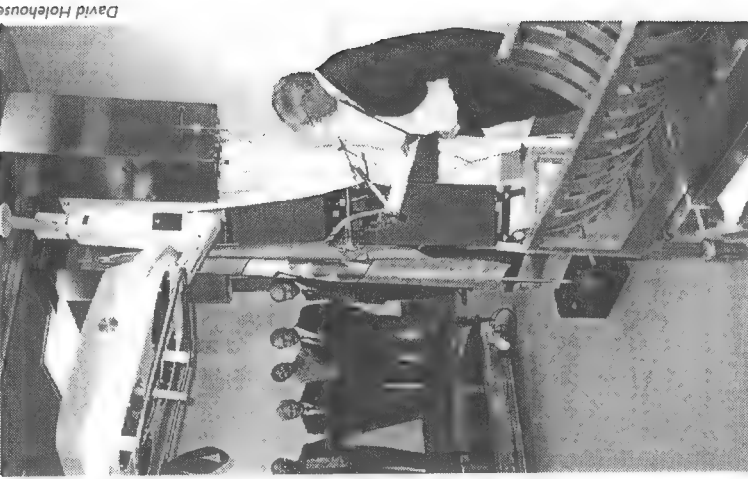
The ribbon-cutting was performed by Professor Emeritus Don Bellow, who, until his retirement this fall, was Associate Vice-President (Facilities). As a member of the animal welfare committee, he recognized the need for the new facility and marshalled \$832,000 in funding from the University. In addition, the Natural Sciences and Engineering Research Council gave \$127,000 towards new equipment.

The Department of Agricultural, Food and Nutritional Science supports the operation of the surgery with an operating budget and a full-time surgical technician. More than 300 large animal surgeries are performed each year on pigs, sheep, cattle and horses. The work provides training for graduate and undergraduate students

and enhances industry knowledge in the areas of metabolism, physiology and reproduction.

Bob Christopherson, Associate Dean (Research), Faculty of Agriculture, Forestry, and Home Economics, said the new facility will do much to reduce stress on animals, facilitate their recovery and improve sanitary conditions. Animals now have two pre-op preparation rooms where they can be acclimatized to the surgery temperature and prepped for surgery. The surgery itself has sophisticated lighting and sterilization equipment, as well as hydraulic surgical tables and a mobile anaesthetic machine. Once out of surgery, animals will go to one of two new post-operative rooms for recovery.

Opening of the surgery coincided with a visit by the Canadian Council of Animal Care assessment panel, which in 1990



Bob Christopherson takes his turn at the mike as the large animal surgery facility is opened.

identified some areas for improvement in the previous 15-year-old surgery.

The panel, which includes representatives of the Alberta SPCA and animal research organizations across the country, provides a peer review process involving a week-long visit, a report to the University, and follow-up on actions taken as a result of any recommendations. A written report on the assessment will be provided to the University in three months.

"The University of Alberta has a fantastic commitment with regard to the animal welfare issue," said Gilles Demers, associate director, Assessment, with the council. "I see the University as a leader in Canada. It has just established an ethics subcommittee and it has a [welfare committee] structure that is really well organized."

Trent Watts, chair of the assessment panel, said the peer review process is a model of its kind, one that is in many ways superior to a legislated approach. Legislation in the United States, for instance, does not cover the welfare of farm animals used in research, while the Canadian process covers all subjects from fish to fowl. ■

1996-97 McCalla Professorships

AGRICULTURE, FORESTRY
AND HOME ECONOMICS

Dr F Temelli, Agricultural, Food and Nutritional Science

ENGINEERING

Dr WD Grover, Electrical Engineering

LAW

for?

APPENDIX VI: LIST OF TECHNICAL PUBLICATIONS

1. Bellow, D.G., Kennedy, J.S., (1963) "Multi-channel Strain Analysis," Transactions, Engineering Institute of Canada, EIC-63-CE.
2. Haddow, J.S., Bellow, D.G., (1964) "A Note on the Convergence of Modified Fourier Series Applied to the Clamped Plate Problem," Journal of Applied Mechanics, Transactions of the American Society of Mechanical Engineers, 31, pp.558-559.
3. Bellow, D.G., Ford, G., Kennedy, J.S., (1964) "Anticlastic Behaviour of Flat Plates," Experimental Mechanics, 5, pp.227-232.
4. Bellow, D.G., Long, B.R., (1966) "Fatigue Crack Propagation in Mild Steel," Canadian Metallurgical Quarterly, 5(1), pp.19-34.
5. Bellow, D.G., Semeniuk, A., (1967) "Stability of Rectangular Plates with Cambered Bitrapezoidal Cross sections," Experimental Mechanics, 7(7), pp.309-312.
6. Bellow, D.G., Faulkner, M.G., (1967) "Bending Behaviour of a Rectangular Plate with a Trapezoidal Cross Section," Experimental Mechanics, 7(9), pp.392-397.
7. Bellow, D.G., Semeniuk, A., (1968) "The Inherent Instability of Rectangular Plates with Cambered Transverse Cross Sections," International Journal of Mechanical Sciences, 10, pp. 201-209.
8. Bellow, D.G., Mendryk, S., Schneider, V., (1970) "An Investigation into the Evaluation of Hockey Helmets," Medicine and Science in Sports, 2(1), pp.43-49.
9. Bellow, D.G., Nelson, D.D., (1970) "On the Experimental Investigation of the Stiffness of Clamped Machined Surfaces," 10(12), pp.506-513.
10. Bellow, D.G., Semeniuk, A., (1972) "Symmetrical and Unsymmetrical Forced Excitation of Thin Circular Arches," International Journal of Mechanical Sciences, 10, pp.201-209.
11. Bellow, D.G., Semeniuk, A. (1972) "Experimental Behaviour of Thin Circular Arches Subjected to Forced Excitation, Experimental Mechanics, 12(11), pp.489-495.
12. Bellow, D.G. (1972) "On the Design of a Mechanical Engineering Building," Engineering Institute of Canada Journal, 55(6), pp.25-29.
13. Faulkner, M.G., Bellow, D.G., (1972) "Improving the Fatigue Life of Butt Welded Medium Strength Steels," Proceedings of the 1st Symposium on Applications of Solid Mechanics," University of Waterloo Press, pp.613-628.
14. Bellow, D.G., Faulkner, M.G., (1972) "Fatigue of Threaded Sucker Rod Couplings," Journal of Canadian Petroleum Technology, 11(1), pp. 69-74.
15. Bellow, D.G., Faulkner, M.G., (1973) "Fatigue of Externally Threaded Machine Elements," 4th Canadian Congress of Applied Mechanics, CANCAM, Montreal, pp.115-116.
16. Smolik, O., Bellow, D.G., (1974) "On the Mixing of Photoelastic Immersion Fluids," Experimental Mechanics, 14(10), pp.400-402.
17. Jensen, R.K., Bellow, D.G., (1974) "Impulse Output Curves for Swimmers," 4th International Conference on Biomechanics, University of Pennsylvania Press, pp.197-202.
18. Bellow, D.G., Faulkner, M.G. (1974) "Corrosion Fatigue of Work Hardened Threaded Elements," Proceedings of the 2nd Symposium on Applications of Solid Mechanics, McMaster University, pp.123-142.
19. Bellow, D.G., Faulkner, M.G. (1974) "Fatigue of Internally Threaded Machine Elements," Transactions of the Canadian Society for Mechanical Engineering, 2(2), pp.63-69.
20. Faulkner, M.G., Bellow, D.G. (1975) "Improving the Fatigue Strength of Butt Welded Steel Joints by Peening," Welding Research Institute, 5(3), pp.64-72.
21. Jensen, R.K., Bellow, D.G. (1976) "Upper Extremity Contraction Moments and Their Relation to Swimming Training," Journal of Biomechanics, 9, pp.219-225.
22. Bellow, D.G., Faulkner, M.G. (1976) "Salt Water and Hydrogen Sulphide Corrosion Fatigue of Work Hardened Threaded Elements," Journal of Testing and Evaluation, 4(2), pp.141-147.
23. Bellow, D.G., Faulkner, M.G. (1978) "Development of an Improved Internal Thread for the Petroleum Industry," Closed Loop, 8(1), pp.3-12.
24. Bellow, D.G., Kumar, A. (1978) "Stress Analysis of Bent Sucker Rods," Journal of Canadian Petroleum Technology, 17(3), pp.76-81.
25. Budney, D.R., Bellow, D.G. (1979) "Forces Exerted by a Golfer," Science in Sports, Academic Publishers, pp.3-20.
26. Budney, D.R., Bellow, D.G. (1979) "Teaching Aids for the Golfer," Science in Sports, Academic Publishers, pp.21-36.

27. Budney, D.R., Bellow, D.G. (1979) "Kinetic Analysis of a Golf Swing," *Research Quarterly*, 50(2), pp.171-179.
28. Faulkner, M.G., Bellow, D.G. (1979) "Influence of Testing Frequency on the Fatigue of Butt Welded Steel Joints," *Welding International*, 9, pp.19-20.
29. Bellow, D.G., Kiss, G.C., Harrison, H.P. (1980) "Measurement of Cultivator Forces," *Proceedings of 5th Symposium on Application of Solid Mechanics*, University of Ottawa, NRCC 18370, pp.149-153.
30. Bellow, D.G., Faulkner, M.G. (1980) "Testing Factors which Influence Fatigue Life of Butt Welded Low Carbon Steels," *Pipeline and Energy Plant Piping*, Welding Institute of Canada, Pergamon Press, pp.367-374.
31. Bellow, D.G., Kiss, G.C. (1980) "Measurement of Tapping Torques," *Experimental Mechanics*, 21(5), pp.205-208.
32. Bellow, D.G., Pugh, R.W. (1981) "Cultivator Shank Manufacture and Evaluation, *Canadian Institute of Metallurgy Bulletin*, 75(837), pp.110-116.
33. Kiss, G.C., Bellow, D.G. (1981) "An Analysis of Forces on Cultivator Sweeps and Spikes," *Canadian Agricultural Engineering*, 23(2), pp.
34. Bellow, D.G. (1981) "Stress and Corrosion Fatigue Experiments on Oil field Components," *Society of Experimental Mechanics and Japan Society of Mechanical Engineers Joint Meeting*, Hawaii, Part 2, pp. 647-650.
35. Bellow, D.G. (1981) "Using Field Data in the Design of a Cultivator Implement," *Society of Experimental Stress Analysis and Japan Society of Mechanical Engineers, Joint Meeting*, Hawaii, Part 2, pp.651-655.
36. Budney, D.R., Bellow, D.G. (1982) "On the Analysis of Neutral Holes," *Experimental Mechanics*, 22(9), pp.348-353.
37. Budney, D.R., Bellow, D.G. (1982) "On the Swing Mechanics of a Matched Set of Golf Clubs," *Research Quarterly for Exercise and Sport*, 53(3), pp.185-192.
38. Patchett, B.M., Bellow, D.G. (1983) "Narrow Gap Welds Using Understrength Weld Material," *International Conference on Welding and Related Projects*, Welding Research Institute of Canada, Pergamon Press, pp.269-278.
39. Pugh, R.W., Bellow, D.G. (1983) "Tundish Stream Improvement Using a Water Model," *22nd Canadian Institute of Metallurgy, Conference Edmonton*.
40. Bellow, D.G., Pugh R.W. (1984) "Tundish Plate for Stream Shaped Control," *Canadian Patent* 1180532.
41. Bellow, D.G., Wahab, M., Faulkner, M.G. (1985) "Residual Stresses and Fatigue of Surface Treated Welded Specimens," *Advances in Surface Treatments II*, Pergamon Press, pp.85-94.
42. Bellow, D.G., Wahab, M., Faulkner, M.G. (1985) "Prediction of Fatigue, Crack Initiation and Propagation of Welded Structures," *Advances in surface Treatments III*, Pergamon Press, pp.27-40.
43. Bellow, D.G. (1985) "An Apparatus to Study Thermal Fatigue," *Proceedings Canadian Congress of Applied Mechanics, CANCAM, University of Western Ontario*, pp.A309-A310.
44. Bellow, D.G., Klotzbücher, E.F., Kraft, H.E. (1985) "On the Selection of Materials for Cold Service," *Society of Experimental Mechanics, Proceedings, Las Vegas*, pp.428-434.
45. Bellow, D.G., Budhiman, A., Budney, D.R. (1985) "The Effect of Precracking on Fracture Toughness Testing," *5th International Symposium on Offshore Mechanics and Arctic Engineering*, Tokyo, pp.193-196.
46. Bellow, D.G., Klotzbücher, E.F., Kraft, H.E. (1985) "The Effect of Material Size on Fracture Toughness," *5th International Symposium on Offshore Mechanics and Arctic Engineering*, Tokyo, pp.197-203.
47. Klotzbücher, E.F., Kraft, H.E., Bellow, D.G. (1987) "On the Selection of Steels for Mining " Equipment Operating under Arctic Conditions," *Proceedings of International Symposium on Continuous Surface Mining*, Edmonton, *Transactions, Technical Publications*, pp.245-255.
48. Morgenstern, V., Hewrrera, A., Patchett, B.M., Bellow, D.G. (1987) "Computer Control for Fracture Toughness Testing, *11th Proceedings, Canadian Congress of Applied Mechanics, CANCAM*, Edmonton, pp.A218-A219.
49. Bellow, D.G. (1987) "High Temperature Fatigue of Furnace Tray Alloys," *Proceedings, International Conference on Fatigue and Stress*, Paris, Pergamon Press, pp.182-189.
50. Bellow, D.G., Howe, R.K. (1988) "Bending Stresses in Otherwise Straight Sucker Rods," *Journal Canadian Petroleum Technology*, 27(5), pp.53-57.

51. Wahab, M., Bellow, D.G., Faulkner, M.G. (1988) "The Effect of Residual Stresses on the Improvement of Fatigue Life of Medium Strength Butt Welded Steel Structures," Conference on New Materials and Processes for Mechanical Design, Brisbane, Australian Institute of Engineers, 88(4), pp.16-20.
52. Wahab, M., Bellow, D.G., Faulkner, M.G. (1989) 'Measurement of Residual Stresses and their Uncertainties," Australasian Instrumentation and Measurement Conference, Adelaide, pp.39-44.
53. Bellow, D.G., Hood, J.E., Roberts, K.S. (1989) "Fatigue Life of Sucker Rods with Epoxy Coatings," Conference on Fatigue and Stress, Paris, Pergamon Press, pp.360-368.
54. Bellow, D.G. (1989) "The Role of Residual Stresses in the Development of Oilfield Sucker Rod Strings," Conference on Fatigue and Stress, London, Pergamon Press, pp.193-210.
55. Bellow, D.G., Smuga-Otto, I. (1989) "On the Selection of Steel Alloys for Corrosive Service," 8th International Conference on Offshore Mechanics and Arctic Engineering, den Hague, III, pp.199-205.
56. Bellow, D.G., Owens, D.C., Smuga-Otto, I. (1989) "Wear of Standard and Hard Metal Coated Couplings with Oilfield Tubing," Wear, 133, pp.83-93.
57. Bellow, D.G., Chiu, A., Owens, D.C. (1990) "Wear of Plastic Components used in Oil Wells," Proceedings of Japan International Tribology Conference, Nagoya, III, pp.1479-1484.
58. Bellow, D.G., Smuga-Otto, I., Owens, D.C. (1990) "Laboratory Simulation of Sucker Rod Corrosion Fatigue Type Failures," Canadian Western Region Conference of the National Association of Corrosion Engineers, Calgary.
59. Bellow, D.G., Smuga-Otto, I. (1991) "Corrosion Fatigue of Oil Field Sucker Rods," Canadian Western Region Conference of the National Association of Corrosion Engineers, Saskatoon, pp.388-394.
60. Bellow, D.G., Viswanath, N. (1993) "An Analysis of the Wear of Polymers," Wear, 137, pp.162-164.
61. Bellow, D.G. (1993) "Evaluating the Wear of Downhole Oilfield Components," 6th International Congress on Tribology, Eurotrib'93, Budapest, III, pp.416-423.
62. Bellow, D.G. (1995) "Wear and Toughness Parameters in the Selection of Grader Blades," Proceedings, Canadian Congress of Applied Mechanics, CANCAM, University of Victoria.
63. Viswanath, N., Bellow, D.G. (1995) "Development of an Equation for the Wear of Polymers," Wear, 181-183, pp.42-49.
64. Bellow, D.G., Sonuga, G.H. (1995) "The Effect of Sand Contamination on Sliding Wear," International Conference on Tribology, Yokohama, Vol. I, pp. 211-216.
65. Bellow, D.G., Viswanath, N. (1995) 'Influence of Counterface and Configuration on Polymer Wear," International Conference on Tribology, Yokohama, Vol. I, pp. 379-384.
66. Sonuga, G.H., Bellow, D.G. (1996) "Wear Behaviour of Coated Sucker Rod Couplings," 10th Surface Modification Technology Conference, Singapore, pp.

TRANSACTIONS
OF THE
ENGINEERING INSTITUTE
OF CANADA

PAPER NO:
EIC-63-CE&A 12

COMMUNICATIONS
ELECTRONICS &
AUTOMATION

MULTI-CHANNEL STRAIN ANALYSIS

by D.G. Bellow and J.S. Kennedy

VOL. 6
NO. C-5

NOVEMBER
1963

Authorized as Second Class Mail by Post Office Department, Ottawa.

MULTI-CHANNEL STRAIN ANALYSIS

by
D.G.Bellow and J.S. Kennedy

OBJECT

The purpose of this paper is to describe a 100-channel digital data processor recently constructed at the University of Alberta, and to show how this equipment, in conjunction with a digital computer, is used to analyze strain readings as indicated by "SR-4" electrical resistance strain gauges. The measurement of the curvature in the transverse direction of rectangular plates subjected to uniform moments along the short edges which produce large longitudinal deflections will be taken as a typical application of the digital processing equipment.

INTRODUCTION

When the output from each of a large number of strain gauges, thermocouples, or transducers has to be measured, it is a very tedious task if each measuring point (hereafter called channel) must be balanced by manually adjusting a Wheatstone bridge, potentiometer, or some other type of balancing instrument. Not only is this a time consuming operation but also errors, such as drift, may occur. In addition, in the case of strain analysis, it is not always possible to maintain a constant load on a test specimen or structure for an extended period of time. Thus, it is desirable to record the channels as rapidly as possible.

Another requirement when recording data from multi-channel systems is to have the data recorded in a convenient form which requires little or no further computation before it is to be analyzed. Computations involved in the reduction of strain gauge data are usually algebraic, such as adding, subtracting, averaging, or numerical integration; tasks which are readily adapted to a digital computer.

With the above requirements in mind, it was decided to construct a 100-channel digital data processor which would be compatible with a digital computer with no intermediate operator steps between sampling of the channels and final output of the computer.

DESCRIPTION OF EQUIPMENT

In correspondence with the National Aeronautical Establishment, National Research Council, Ottawa, the problem of multi-channel scanning and recording was discussed and it was suggested that a system be constructed around a Wheatstone bridge circuit consisting of a scanning unit, an analog-digital voltmeter, a program unit, and an output such as typewriter or tape perforator. All of these units were commercially available and were purchased from Data Instruments Division, Telecomputing Corporation. To complete the Wheatstone bridge circuit it was decided to construct a 100-channel balancing module similar to the one designed by N.R.C. The latter unit allows each channel to be initially set to zero for a no-load condition. This eliminates the need for recording initial values, and the subsequent algebraic calculations required to determine the strains.

Figure 1 shows the general arrangement of the equipment. The 100-channel balancing module is made up of two groups of 50 channels each. Figure 2 illustrates the electrical circuit of the balancing module. Balancing of each channel is achieved by deflecting a small cantilever beam (one for each channel) thereby changing the resistance of strain gauges mounted on the upper and lower surfaces of the beam. These two gauges serve as two arms of the Wheatstone bridge.

The scanning unit sequentially samples, manually or automatically up to 100 channels of information. The scanning rate can be as fast as 50 milliseconds per channel but is usually less when coupled to companion recording equipment. Commutation is achieved by magnetically actuated switches which have gold-plated contacts to minimize variations in contact resistance and also to reduce thermal effects to a minimum. The channel number is visually displayed on the front panel by neon lights.

After a channel is selected, the unknown voltage, or signal, is fed to the analog-digital voltmeter. This unit takes the unknown signal and automatically balances it against a standard voltage using a conventional Kelvin-Varley potentiometer circuit. Actual balance is accomplished by three magnetically operated stepper switches which vary the reference voltage in increments of hundreds, tens, and units. Balance is obtained when a null exists between the reference voltage and the unknown signal. A digital value of the voltage as well as its sign is displayed by neon lights on the front panel of the voltmeter. The sensitivity of the unit may be regulated by a range selector switch which enables the operator to make any input voltage, between 0.01v and 1.00v, produce a full scale reading. By means of this control the read-out may be "expanded" or "contracted" for a given input signal, thus facilitating calibration. This unit has an accuracy of 0.10 per cent full scale on any range and a maximum sensitivity of 10 microvolts per digit.

The program unit is used to control the operation of the scanner and the digital voltmeter, and will sequentially arrange the data and control the format of the data in the output devices. The program unit has a sequence selector plug board, shown in Figure 3, which, by suitable arrangement of jumpers, controls the method in which the data is sampled and its final output form.

Essentially, after a channel is switched, the digital voltmeter balances the unknown signal and this digital value along with any additional information such as channel number, run number, date, time, is programmed through the outputs. When all information is recorded either by typewriter or tape perforator, or both, a signal is sent to the scanner to advance to the next channel. This procedure is repeated until all channels have been measured and recorded.

The tape perforator and typewriter can record data independently or simultaneously depending on the requirement of the experiment. The electric typewriter is a standard IBM unit which has been modified with solenoid actuated digits

0 - 9, space, tab, minus sign, decimal, and carriage return. It is a serial input device which accepts information from the program unit.

Since there are two computers at the University's Computing Centre - A "Royal McBee LGP-30" and an "IBM 1620" - a decision had to be made as to which computer would be used, before the tape perforator could be selected and built. Either computer is adequate for strain analysis. The "LGP-30" was selected, because it was the least used of the two machines. Thus, the tape perforator was designed to be compatible with the 6-channel code of the "LGP-30". If, at a later date, the "IBM 1620" is preferred, all that is required for the conversion is the changing of a matrix board in the perforator.

Once the individual units, as described above, had been checked out they were all assembled and mounted in a metal console as shown in Figure 4. For portability, the cabinet was mounted on casters. Because the carriage return and other typewriter functions cause considerable vibration, the typewriter was mounted on a separate cabinet. The interior of the cabinet serves as storage for paper, tape, and calibration resistors.

APPLICATION OF EQUIPMENT

(a) Theory of the Problem

When a beam whose width, b , is of the order of its thickness, d , is bent to a radius, R , the strain in the longitudinal direction a distance y from the neutral axis is given by $e_z = \frac{y}{R}$, see Figure 5. Since there is no stress in the transverse direction (i.e. the beam is free to distort) the transverse strain is $e_x = -\mu e_z$, where μ is Poisson's ratio. This result was shown as early as 1864 by Saint-Venant.

Applying Hooke's Law and evaluating the moment on a cross section of the beam yields

$$M = \frac{EI}{R_z}$$

where M is the applied moment,

$\frac{1}{R_z}$ is the resulting longitudinal curvature,

EI is the flexural rigidity of the beam.

Hence, the longitudinal curvature is

$$\frac{1}{R_z} = \frac{M}{EI} \dots\dots\dots(1)$$

When a flat plate with two opposite edges simply supported and the other two free, is bent by moments applied along the supported edges, and the width parallel to the supports is infinite, distortion in the transverse direction is prevented. Hence, there is no strain in the transverse direction and the transverse curvature is zero. For this case the equations of elasticity yield

$$\sigma_x = \mu \sigma_z, \quad \sigma_z = \frac{e_z E}{(1 - \mu^2)}$$

and the bending moment per unit width parallel to the supports is

$$M = \frac{E}{(1 - \mu^2) R_z} \frac{d^3}{12}$$

The longitudinal curvature is given by

$$\frac{1}{R_z} = \frac{M(1 - \mu^2)}{EI} \dots\dots\dots (2)$$

Where I is the moment of inertia of a section of the plate one unit wide.

Equations (1) and (2) represent two extreme cases. For the general case the curvature may be given by

$$\frac{1}{R_z} = \frac{M\phi}{EI}$$

where ϕ varies from 1 for beam action to $(1 - \mu^2)$ for plate action.

In accordance with the above, it was desired to investigate the transition from beam action to plate action and in particular to observe the mode of transverse curvature and deflection.

Considering the distortions in the transverse direction, it is a well established fact that when the slope is small compared with unit, the curvature is closely approximated by the second spatial derivative of the deflection. Thus, the transverse curvature may be written

$$\frac{1}{R_x} = \frac{\partial^2 y}{\partial x^2} \dots\dots\dots (3)$$

Integrating equation (3) once with respect to the transverse distance, x, yields the transverse slope, and a second integration yields the deflection relative

to the starting point of integration. That is,

$$\frac{\partial^2 y}{\partial x^2} = \frac{1}{R}$$

$$\frac{\partial y}{\partial x} = \int \frac{1}{R} dx$$

$$y = \iint \frac{1}{R} dx dx$$

Thus it is possible to investigate the transverse distortions experimentally by observing the deflections, the slopes, or the curvatures.

(b) Experimental Investigations

In 1943 Ashwell and Greenberg¹ conducted experiments on large deflections of rectangular plates. They used dial gauges to measure the variation in deflection across the plate but found this method entirely unsatisfactory because even the small force which the dial gauge plunger exerted on the plate was enough to change the deflection. They could find no means of correcting this error and, as a result, they turned to an optical method. In this second method, the slope at various points across the plate was measured using small mirrors on the plate in conjunction with an optical collimator. This latter method enabled the authors to obtain reasonable results. This method, however, has several disadvantages, the main one being the test time required. Being entirely manual, it is a slow process and in addition the data must be recorded by hand. Also, since this method measures slopes at a point and not deflection, computation is required.

It has been shown² that strain gauges can be used to obtain a satisfactory analysis of transverse curvature and deflection. Currently the multi-channel digital data processor is being used to measure output from strain gauges which have been applied in the transverse direction of rectangular plates. This method overcomes the disadvantages of the optical method.

If the strains are known at the top and bottom surface of the plate at a point, the curvature at this point in the direction of the gauges is obtained by algebraically subtracting these strains and dividing by the thickness of the plate. As was pointed out previously this is only true for small deflections. However, although the deflection in the longitudinal direction can be quite large, the deflections in the transverse direction relative to the center point of that section are very small. To illustrate this, one need only bend a piece of shim stock or a post card and observe, if possible, the change in transverse deflection for large longitudinal deflections.

A Note on the Convergence of Modified Fourier Series Applied to the Clamped Plate Problem

J. B. HADDOW¹ and D. G. BELLOW²

THE purpose of this Note is to discuss the convergence of the Ritz method applied to a symmetrically loaded rectangular plate clamped at $x = \pm a/2$ and $y = \pm b/2$ if the deflected form is represented by the series

¹ Associate Professor of Mechanical Engineering, University of Alberta, Edmonton, Alberta, Canada. Assoc. Mem. ASME.

² Assistant Professor of Mechanical Engineering, University of Alberta, Edmonton, Alberta, Canada.

³ G. Pickett and S. Gopalacharyulu, "Modified Fourier Series for Clamped Beams and Plates," JOURNAL OF APPLIED MECHANICS, vol. 29, TRANS. ASME, vol. 84, Series E, 1962, p. 204.

⁴ L. V. Kantorovich and V. I. Krylov, *Approximate Methods of Higher Analysis*, P. Noordhoff Limited, Groningen, Holland, 1958, p. 284.

Manuscript received by ASME Applied Mechanics Division, January 20, 1964.

$$w_s = \sum_{m=1}^s \sum_{n=1}^s A_{mn} \left[\cos \frac{2m\pi x}{a} - (-1)^m \right] \times \left[\cos \frac{2n\pi y}{b} - (-1)^n \right] \quad (1)$$

Pickett and Gopalacharyulu³ have shown that the central deflection of a uniformly loaded square plate is given accurately by series (1) when 11 independent coefficients A_{mn} are evaluated by the Ritz method. Also, according to the criteria given by Kantorovich and Krylov,⁴ the Ritz method with series (1) should converge to the correct solutions for the deflected form and its first and second-order partial derivatives for the clamped-plate problem. However, for a uniformly loaded plate the series (1) cannot satisfy the plate equation

$$\nabla^4 w = \frac{q}{D}$$

at the edge of the plate even if s approaches infinity since $\nabla^4 w_s$ changes sign near the edge and

$$\int_{-a/2}^{a/2} \int_{-a/2}^{a/2} \nabla^4 w_s dx dy = 0$$

instead of tending to qa^2/D as s tends to infinity. The physical interpretation of this is that if a square plate were forced to assume the deflected form w_s with s large, an approximately uniform loading would be required in addition to the edge moments except for a region around the edge where a large negative distributed loading would be required. As s becomes larger the distributed loading around the edge tends to a line load which corresponds to the reaction of the support.

The foregoing considerations indicate that the convergence of the Ritz method with series (1), while satisfactory for the deflections, may be very slow for the moments especially on or near the edge of the plate. In order to examine the convergence for a uniformly loaded square plate the evaluation of the coefficients A_{mn} by the Ritz method and the determination of the resulting deflections and moments at various points were programmed for a digital computer. The deflections and moments (with Poisson's ratio taken as 0.3) were obtained from series (1) for $s = 3, 4, 5, 6, 8, 10$, and 12 and some of the values are shown in Table 1.

Table 1

Point	S	$w(D/q a^4)$	$M_x/q a^2$	$M_y/q a^2$
(0, 0)	3	0.0012626	0.025092	$M_x = M_y$
	4	0.0012586	0.021518	
	5	0.0012641	0.023827	
	6	0.0012633	0.022226	
	8	0.0012644	0.022505	
	10	0.0012649	0.022642	
(0.5a, 0)	12	0.0012651	0.022719	$M_x = 0.3M_y$
	3	0	-0.038922	
	4	0	-0.041473	
	5	0	-0.043284	
	6	0	-0.044490	
	8	0	-0.046094	
(0.3a, 0.3a)	10	0	-0.047088	$M_x = M_y$
	12	0	-0.047765	
	3	0.0002580	0.003287	
	4	0.0002597	0.002705	
	5	0.0002591	0.001504	
	6	0.0002594	0.001241	
(0.4a, 0.4a)	8	0.0002606	0.002126	$M_x = M_y$
	10	0.0002606	0.001708	
	12	0.0002607	0.001802	
	3	0.00002663	-0.003937	
	4	0.00002906	-0.003622	
	5	0.00003013	-0.003355	
(0.4a, 0.4a)	6	0.00003056	-0.003223	$M_x = M_y$
	8	0.00003078	-0.003226	
	10	0.00003080	-0.003353	
	12	0.00003081	-0.003416	

These results confirm that the convergence for the moments is slow especially at the edge of the plate. For example, with $s = 12$ the value of M_x at the center is about 7 percent less than the value given by the Hencky solution. For a rectangular plate it is necessary to solve 144 simultaneous equations for $s = 12$ to obtain the coefficients A_{mn} and 78 equations for a square plate. Evidently, if accurate values for the moments of a clamped rectangular plate are required, it is not practical to use the Ritz method with series (1).

This example indicates the importance of a judicious choice of series for use with the Ritz method. It is interesting to compare the slow convergence, for the moments, of the Ritz method using series (1) with the results obtained by Pickett⁵ using a polynomial representation of the deflected form.

⁵G. Pickett, "Solution of Rectangular Clamped Plate With Lateral Load by Generalized Energy Method," JOURNAL OF APPLIED MECHANICS, vol. 6, TRANS. ASME, vol. 61, 1939, p. A-168.

Anticlastic Behavior of Flat Plates

The mode of transverse distortion in a rectangular plate subjected to large longitudinal curvatures depends on the dimensionless parameter b^2/Rt . Using a numerical technique, experimental results are shown to agree with theory for b^2/Rt values up to 50

by D. G. Bellow, G. Ford, and J. S. Kennedy

ABSTRACT—The purpose of this paper is to show that the readings from strain gages can be used effectively to compute small transverse deflections in a rectangular plate and, further, show that the theory developed by Lamb for the rectangular-plate problem agrees with experiment.

A numerical procedure is developed, based on the trapezoidal rule, which determines the transverse deflections from the readings of strain gages mounted to the top and bottom surface of a rectangular plate subjected to large longitudinal curvatures. It is shown using the strain-gage technique that experiment agrees with Lamb's theory for b^2/Rt ratios up to 50.

List of Symbols

- b = width of beam or plate
- t = thickness of beam or plate
- E = modulus of elasticity
- R = radius of curvature of neutral surface in longitudinal direction
- R_x = radius of curvature of middle surface in transverse direction
- x, y, z = rectangular coordinates, where the x axis is in the transverse direction and passes through the centroid of the deformed cross section, the y axis is in the longitudinal direction, and the z axis is perpendicular to the x - y plane
- w = displacement of the middle surface in the z direction measured from the x axis
- ν = Poisson's ratio

Introduction

When a beam, whose breadth is of the same order of magnitude as its depth, is bent by uniform couples applied to its ends producing a given curvature in the longitudinal direction, there is a corresponding curvature in the transverse or lateral direction. Although the problem of flexure of beams was discussed as early as 1632 by Galileo, it was Saint-Venant¹ in 1864 who first recorded the mathematical analysis of the contraction and elongation of the transverse fibers of a beam bent longitudinally by

applied couples. The problem was further discussed in 1879 by Kelvin and Tait who reposed the problem in terms of a plate. In 1891, Lamb presented a solution to the problem which considered the behaviors of both beams and plates.

Previous attempts at experimental justification of Lamb's theory have met with varying degrees of success. In 1908, Searle² proposed some methods in which the distorted cross section could be observed, but in comparison with the measuring devices available today these experiments were rather crude. It was not until 1950, using an optical technique to measure the transverse slopes, that some verification was given for Lamb's theory by Ashwell and Greenwood.³ They showed that experiment agreed with theory, with some qualification, for b^2/Rt values between 7 and 12. They also investigated the use of dial gages but discarded the method as unsatisfactory.

It was believed the work of Ashwell and Greenwood should be extended into the region of large b^2/Rt ratios. The purpose of this paper is to show that strain gages can be used, with sufficient accuracy, to determine minute deflections in beams and plates and further, to apply this technique to show that Lamb's theory agrees with experiment for b^2/Rt ratios up to 50.

Theory

Consider a plate of width b and thickness t bent to a longitudinal curvature $1/R$ by uniform moments M_y applied to two opposite ends which lie in the x - z plane. If the deformed shape is to be truly cylindrical, that is, the transverse strips are to remain straight, moments $M_x = \nu M_y$ are required along the edges $x = \pm b/2$. Since such moments are not present, the plate tends to assume a curvature $-\nu/R$ in the transverse direction. This distortion causes the midline of the plate to move off the true cylindrical form, with the result that longitudinal membrane forces N_y are developed which tend to prevent this distortion. Initially, when $1/R$ is

D. G. Bellow, G. Ford and J. S. Kennedy are Assistant Professor, Professor and Associate Professor, respectively, Department of Mechanical Engineering, University of Alberta, Edmonton, Alberta, Canada.

Paper was presented at 1964 SESA Annual Meeting held in Cleveland, Ohio, on October 28-30.

very small, the effect of the longitudinal membrane forces is small and the transverse curvature is indeed $-\nu/R$, or very close to it. However, as $1/R$ is increased, the effect of the longitudinal membrane forces becomes appreciable and must be considered.

To investigate the transverse distortion, consider a transverse strip of width dy cut from the plate. The longitudinal membrane forces on either side of this strip arising as a result of the transverse distortion have, because of the longitudinal curvature, a resultant perpendicular to the plate surface. This amounts to a load distributed along the strip which at any point is proportional to the deflection of the strip at that point. The problem is therefore analogous to the problem of a beam on an elastic foundation.

The detailed derivation of Lamb's theory can be found in the literature⁴ so it will only be highlighted here. By considering an element $dx-dy$ cut from the deformed plate (see Fig. 1), it can be shown that the governing differential equation for the deflection of the transverse strip is given by

$$\frac{d^4 w}{dx^4} + 4\alpha^4 w = 0$$

where

$$4\alpha^4 = \frac{12(1-\nu^2)}{R^2 t^2}.$$

This equation neglects the effect on M_x of the change in the longitudinal curvature produced by the deflection w of the strip from the cylindrical surface. It can be shown that the term introduced by this effect is of higher order. Also, since there are no transverse membrane forces N_x , there will be no contribution to the differential equation from this source. The solution of this equation is

$$w = A \cosh \alpha x \cos \alpha x + B \cosh \alpha x \sin \alpha x + C \sinh \alpha x \sin \alpha x + D \sinh \alpha x \cos \alpha x. \quad (1)$$

At the free edges of the plate $x = \pm b/2$, there is no shear and no moment, that is,

$$[V_x]_{x=\pm b/2} = -D \left[\frac{\partial^3 w}{\partial x^3} + (2+\nu) \frac{\partial^3 w}{\partial x \partial y^2} \right]_{x=\pm b/2} = 0$$

$$[M_x]_{x=\pm b/2} = -D \left[\frac{1}{R_x} + \nu \frac{1}{R_y} \right]_{x=\pm b/2} = 0.$$

Now w is a function of x only, $1/R_x \doteq d^2 w/dx^2$, and $R_y = R - w \doteq R$, so the boundary conditions which must be satisfied by eq (1), for the transverse strip, are,

$$\frac{d^3 w}{dx^3} = 0 \text{ at } x = \pm \frac{b}{2},$$

$$\frac{d^2 w}{dx^2} = -\frac{\nu}{R} \text{ at } x = \pm \frac{b}{2}.$$

Rewriting eq (1) in a nondimensional form, and applying the boundary conditions, it follows that

$$\frac{w}{t} = \bar{A} \cosh \alpha x \cos \alpha x + \bar{B} \sinh \alpha x \sin \alpha x \quad (2)$$

where

$$\bar{A} = \frac{-\nu \sinh \alpha b/2 \cos \alpha b/2 - \cosh \alpha b/2 \sin \alpha b/2}{\alpha^2 R t \sinh \alpha b + \sin \alpha b}$$

$$\bar{B} = \frac{-\nu \sinh \alpha b/2 \cos \alpha b/2 + \cosh \alpha b/2 \sin \alpha b/2}{\alpha^2 R t \sinh \alpha b + \sin \alpha b}.$$

For a given Poisson's ratio, the term $\alpha b/2$ is directly proportional to the dimensionless ratio $\sqrt{b^2/Rt}$ and it is this ratio which determines the mode of transverse deflections. Solving eq (2) numerically, it can be shown that if b^2/Rt is less than 1.6, the transverse deflections describe an arc of radius R/ν , which is the problem discussed by Saint-Venant. This is beam action giving an anticlastic surface. However, b^2/Rt must be greater than 1000 before the surface can be considered cylindrical, which is the so-called plate action. Equation (2) shows that no matter how large b^2/Rt becomes, there is always some distortion at the free edges of the plate.

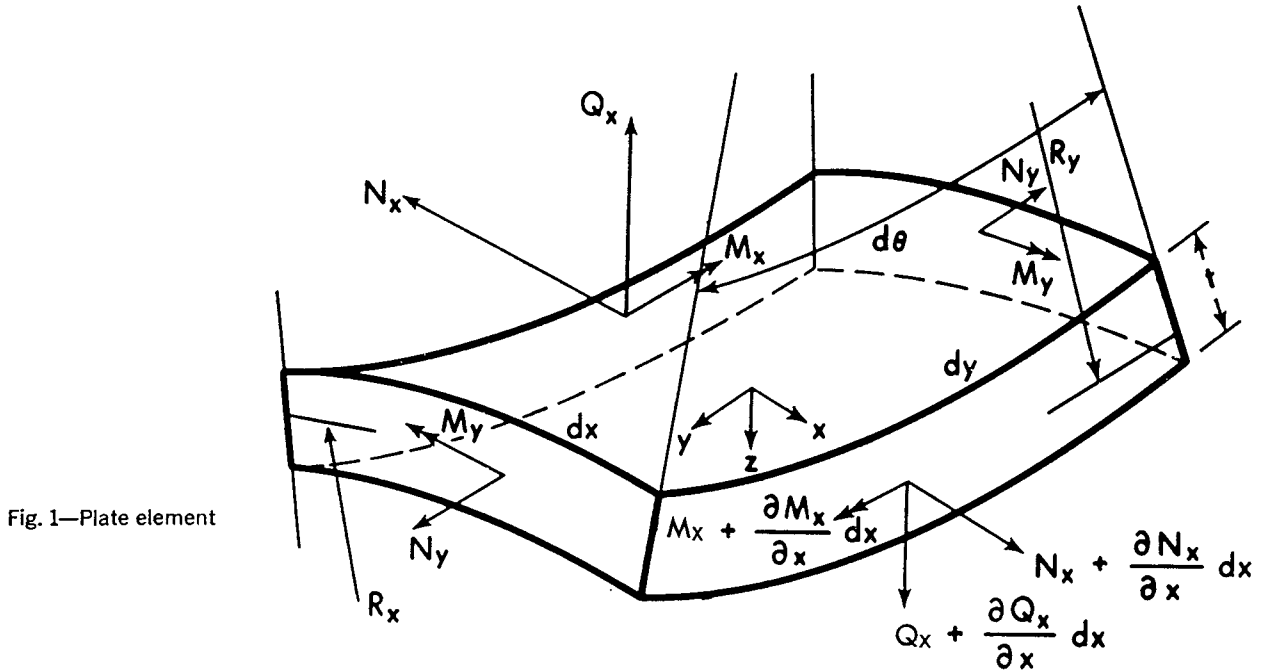


Fig. 1—Plate element

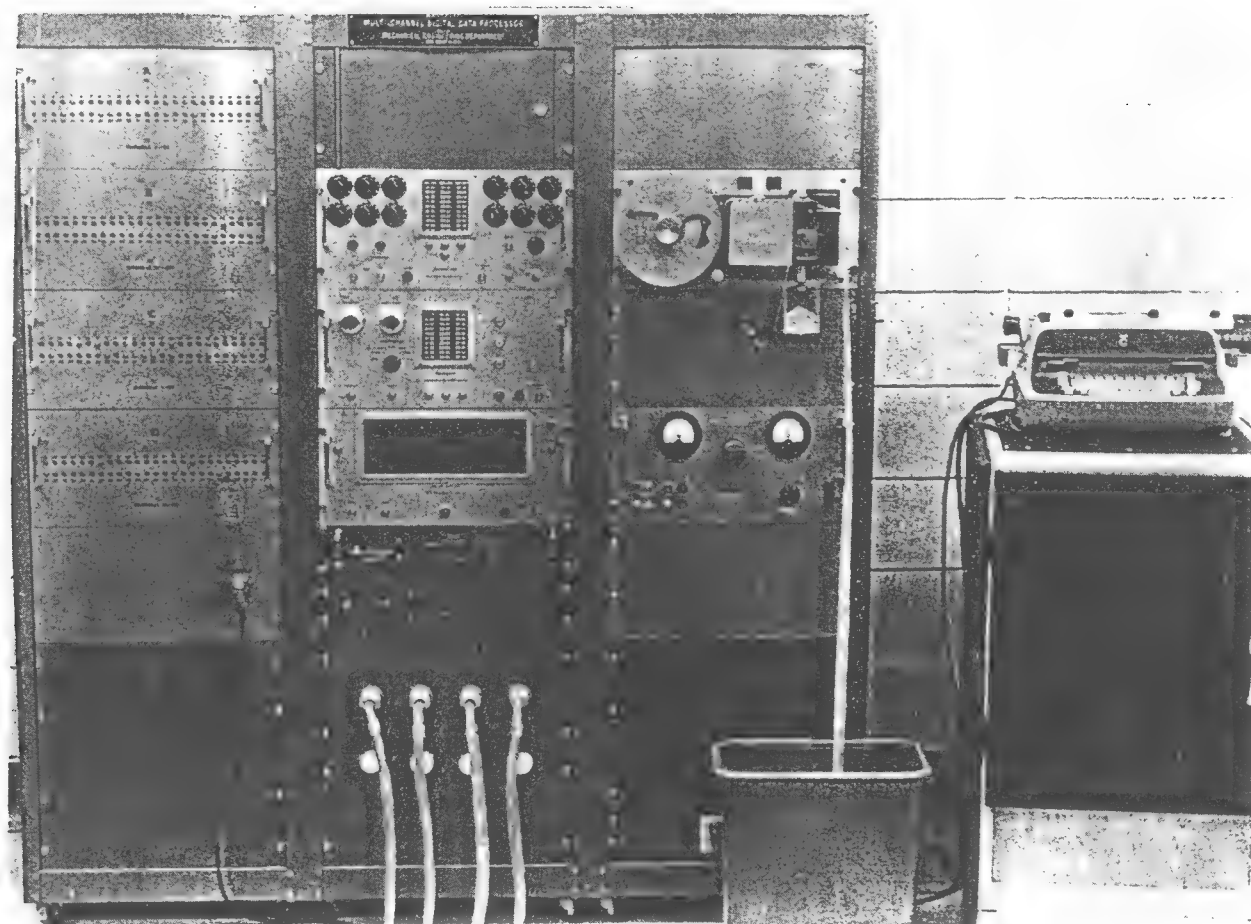


Fig. 2—Automatic strain recorder

Experimental Apparatus

The experimental procedure consisted in automatically recording the readings from strain gages mounted in the transverse direction along the midline of a rectangular plate on both top and bottom surfaces. A digital computer was used to calculate the deflected form of the transverse section from these readings using the trapezoidal rule as described in the next section.

An aluminum plate (Alclad 75 ST-6) $\frac{1}{8} \times 18 \times 144$ in. was placed on the simple supports of a loading frame which had an adjustable span length of 6.0 to 1.5 ft. Vertical loads were applied on the overhanging portion of the plate. Neglecting the weight of the plate, this loading arrangement produced pure bending of the plate between the supports; a necessary condition for the comparison of the results with the theory of Lamb.

Metal-film strain gages, Type C12-121 (Budd Instruments) were placed at $\frac{1}{2}$ -in. intervals across the midline of the plate in the transverse direction on both top and bottom surfaces. At the edges, Type C12-111 was used to obtain readings as close to the edge as possible. The gages were mounted

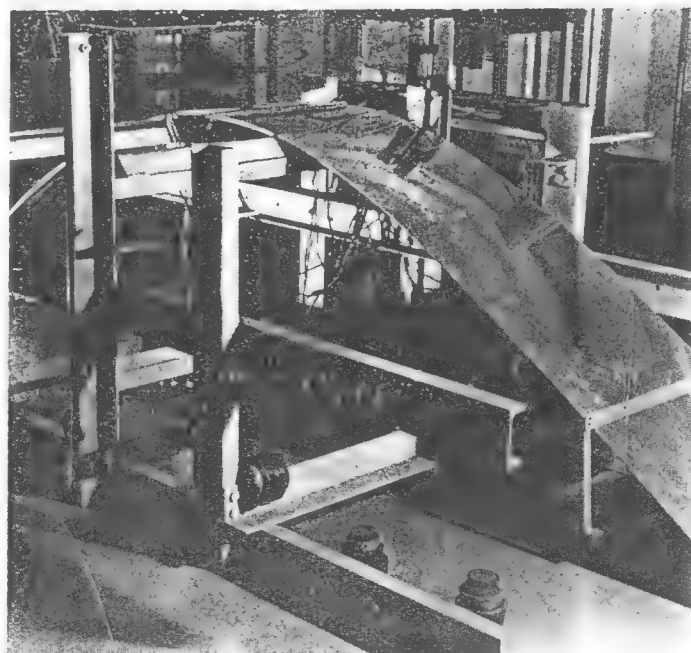


Fig. 3—Plate under test on loading frame

with Eastman 910 cement and waterproofed with Dow Corning GW-1 compound.

A multichannel digital data processor⁵ was used to automatically record the readings from the strain gages. The readings were recorded by a typewriter and a tape perforator. A general view of the recording apparatus is shown in Fig. 2 and a view of the plate and loading frame is shown in Fig. 3.

Analysis of Strains to Obtain Deflections

The curvature in the transverse deflection is given by the expression

$$\frac{1}{R_z} = \frac{d^2w}{dx^2}$$

assuming the slopes are small and the squares of the slopes are negligible compared with unity. Integrating this expression twice with respect to the transverse direction x yields

$$w(x) = \int_{c_1}^x \int_{c_2}^x \frac{d^2w}{dx^2} dx dx$$

where c_1 and c_2 are arbitrary constants.

Consider a transverse strip to which strain gages have been bonded on the top and bottom surfaces. At a point x_i , let the values recorded from the two strain gages be denoted by e_{Ti} and e_{Bi} , respectively. The strain at a point in a fiber, a distance z from the neutral surface, is directly proportional to the curvature at that point and is

$$e = \frac{-z}{R_z}$$

It is possible the strains recorded from the gages e_{Ti} and e_{Bi} include membrane as well as bending strains. Since the curvature depends only on the bending strains, it is required to subtract the average strain from either e_{Ti} or e_{Bi} . Thus,

$$\begin{aligned} e_{avi} &= \frac{e_{Ti} + e_{Bi}}{2} \\ e_{(bending)_i} &= e_{Bi} - e_{avi} = -(e_{Ti} - e_{avi}) \\ &= -\frac{e_{Ti} - e_{Bi}}{2} \end{aligned}$$

The bending strain at the surface $z = \pm t/2$ is

$$e_{(bending)_t} = \frac{-t}{2R_{zi}}$$

and combining the last two results yields

$$\frac{1}{R_{zi}} = \frac{e_{Ti} - e_{Bi}}{t} \quad (3)$$

where i denotes a particular point along the transverse strip.

The values of R_{zi} are evaluated at the measuring points x_i from eq (3). The difference in slopes between points x_{i+1} and x_i is given by

$$\left[\frac{dw}{dx} \right]_{i+1} - \left[\frac{dw}{dx} \right]_i = \int_{x_i}^{x_{i+1}} \frac{1}{R_z} dx \quad (4)$$

Using the trapezoidal rule, the right-hand side of eq (4) is evaluated as follows

$$\left[\frac{dw}{dx} \right]_{i+1} - \left[\frac{dw}{dx} \right]_i = \frac{1}{2} \left[\frac{1}{R_{zi+1}} + \frac{1}{R_{zi}} \right] (x_{i+1} - x_i) \quad (5)$$

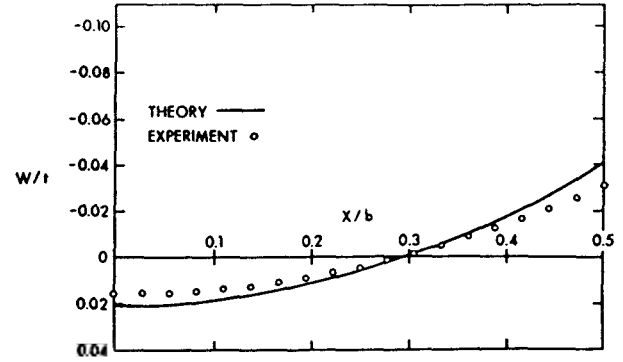


Fig. 4—Transverse deflections for $b^2/Rt = 1.5$

Since the slope at x_0 (the center line of the plate) is zero, the slope at the point x_i can be evaluated from the values of eq (5) by addition. The numerical integration is started at the center of the plate.

Once the slopes have been evaluated, a similar procedure is followed to determine the deflections. The difference in deflections between points x_{i+1} and x_i is given by

$$w_{i+1} - w_i = \int_{x_i}^{x_{i+1}} \frac{dw}{dx} dx$$

Using the trapezoidal rule, the right-hand side of this equation can be evaluated as follows

$$w_{i+1} - w_i = \frac{1}{2} \left\{ \left[\frac{dw}{dx} \right]_{i+1} + \left[\frac{dw}{dx} \right]_i \right\} (x_{i+1} - x_i) \quad (6)$$

The deflection at x_0 is taken as zero. By starting the numerical integration at x_0 , the center line of the plate, the deflection at any point along the transverse strip can be obtained by a repeated application of eq (6).

The deflections obtained from eq (6) are relative to $w = 0$ at x_0 . In order to compare the experimental results with Lamb's solution [eq (2)], the deflections must be found relative to the centroidal axis of the deflected transverse cross section.

The position of the centroidal axis can be calculated from the experimental w vs. x curve by applying the trapezoidal rule. The centroid of the deflected transverse cross section is given by

$$\bar{w}b = \int_{-b/2}^{b/2} w dx$$

and if n is the number of measuring stations, the width of the plate can be expressed by

$$b = (n - 1)h$$

where h is the distance between x_{i+1} and x_i . Thus,

$$\bar{w} = \frac{1}{2(n-1)} (w_0 + \sum_{m=2}^n 2w_{m-1} + w_n) \quad (7)$$

The true position of the w curve relative to the centroidal axis is given by eqs (6) and (7), that is

$$w_{true} = w - \bar{w}$$

A digital computer was used to evaluate the deflections from the strain readings using the above

equations. Transverse strains recorded on a perforated tape were fed directly into the computer.

Testing Procedure

The first series of tests was conducted with a fixed span length of 6.0 ft between supports. The overhanging portion of the plate was 3.0 ft at either end. The plate was tested first with one side facing up and then turned over and tested with the opposite side facing up, so as to evaluate symmetry and initial imperfections in the plate.

In the second series of tests, tests were conducted with various span lengths of 6.0 ft to 1.5 ft to investigate the influence of the support and loading conditions and, consequently, load the plate at higher b^2/Rt values.

Before testing the plate under load, it was first placed flat on a table and the initial strains were recorded for each gage location. These initial strains were subtracted from the strains recorded for a loaded condition using a digital computer. The plate was then set on the supports, for which conditions another set of readings was recorded. The load-hanger assemblies were then attached to the plate and weights were added to these hangers one at a time. For each loaded condition, the transverse strains were recorded simultaneously on a tape perforator and a typewriter, and the transverse deflections were obtained from the digital com-

puter which was programmed to use the trapezoidal method described above.

The b^2/Rt ratio was recorded for each loaded condition. The longitudinal radius of curvature was obtained by means of two longitudinally placed strain gages, one on top, the other on the bottom of the plate.

Experimental Results

From the experimental results, it was found that deformation of the midline of the plate cross section was the same, for a given b^2/Rt ratio, irrespective of which side was facing up. It was shown, from an additional transverse row of strain gages placed 3 in. from the support, that the deflected form of the transverse cross section was unaffected by the support conditions or the manner in which the loads were applied. Thus the test results plotted in Figs. 4 to 10 are valid for either side facing up and for any span to width ratio as low as $1/3$.

In Figs. 4 to 10, the axes have been made non-dimensional by dividing by b , the width of the plate in the case of the abscissa x , and dividing by t , the thickness, in the case of the ordinate w . Although only a single point was plotted for each measuring station, each loaded condition was tested at least six and sometimes nine or ten times. It was found, for a given b^2/Rt ratio, that all tests coincided almost exactly with one another and any

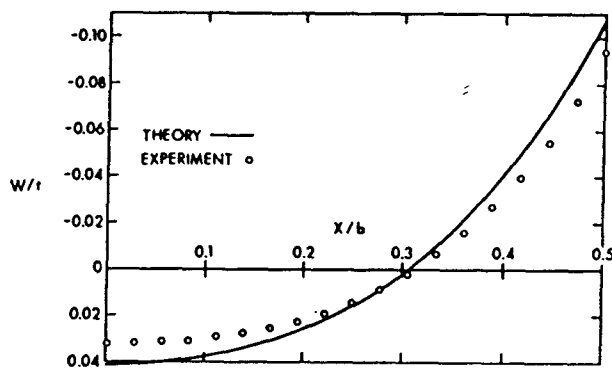


Fig. 5—Transverse deflections for $b^2/Rt = 8.5$

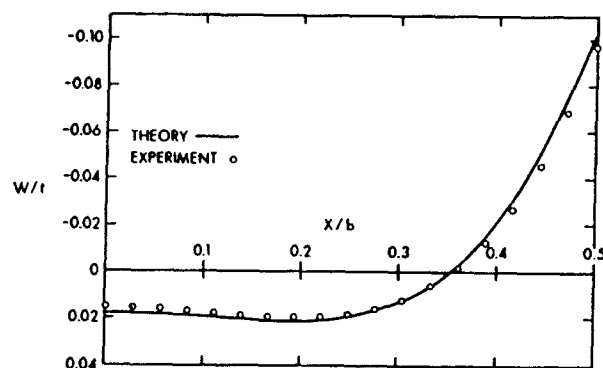


Fig. 7—Transverse deflections for $b^2/Rt = 18.0$

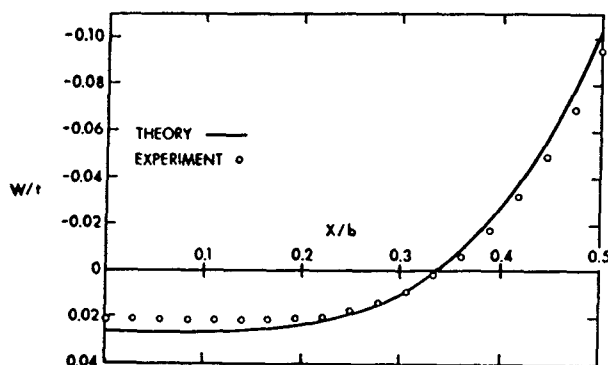


Fig. 6—Transverse deflections for $b^2/Rt = 14.6$

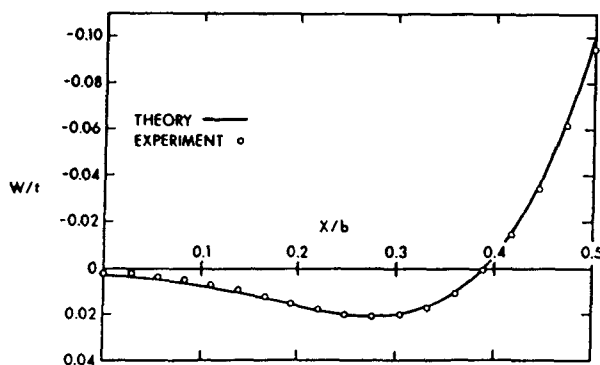


Fig. 8—Transverse deflections for $b^2/Rt = 29.8$

difference could not be observed on the plotted results.

The deflection at a point on one side of the plate was averaged with the value for the corresponding point on the other side, and the average value was plotted as shown in Figs. 4 to 10. Since there was very little antisymmetry in the deflected form, this averaging process was believed to be justified.

The theoretical curve from Lamb's solution is shown for each set of experimental values corresponding to the experimental b^2/Rt ratio and Poisson's ratio of $1/3$.

Experimental Error

Inaccuracies in the computed transverse deflections arose from three sources: calibration error, measurement error and truncation error.

The calibration error was made up from the variation in resistance of the strain gage, the variation in the gage factor, and the variation in the shunt or calibration resistance. For the strain gages used in this work, the calibration error was found to be within ± 0.72 percent which includes a 0.05 percent accuracy of the shunt resistance.

The error in measurement of the automatic strain recorder was found to be ± 0.6 percent full scale.

In using the trapezoidal rule, the leading term of the truncation error can be shown to be

$$\frac{h^3}{12} \left[\frac{d^2 w}{dx^2} \right]_i$$

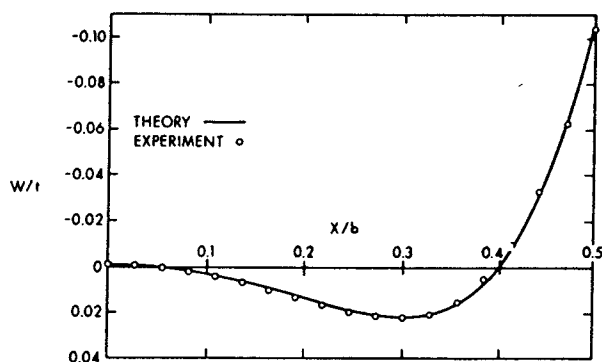


Fig. 9—Transverse deflections for $b^2/Rt = 39.4$

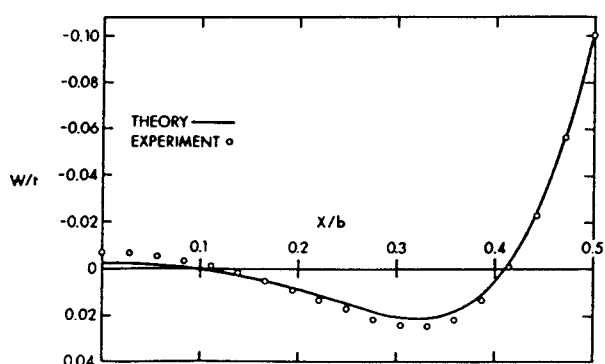


Fig. 10—Transverse deflections for $b^2/Rt = 49.7$

where h is the distance between adjacent measuring stations. Noting that the curvature is proportional to the change in slopes between two points x_{i+1} and x_i , this can be rewritten as

$$\frac{h^2}{12} \left[\frac{dw}{dx_{i+1}} - \frac{dw}{dx_i} \right]$$

or

$$\frac{1}{48} \left[\frac{dw}{dx_{i+1}} - \frac{dw}{dx_i} \right] \text{ in.}^2$$

where the distance between x_{i+1} and x_i is 0.5 in. Applying this result to the experimental curves, it was found that the truncation error in computing slopes was less than 0.04 percent. The truncation error in calculating the deflections was less than 0.06 percent and the error in calculating the position of the centroidal axis was less than 0.11 percent. These errors were calculated assuming a constant truncation error over the width of the plate. Summing the errors, it was found the computation of the values $(w - \bar{w})$ vs. x , using the trapezoidal rule, incurred an error of less than 0.21 percent.

The total error of measurement of the transverse deflection was found to be within ± 0.93 percent plus the error in strain measurement.

Conclusions

1. The experimental results generally agreed with theory as the transverse deflection passed from beam action, through the transition region and into the beginning of plate behavior, for b^2/Rt ratios up to 50. The discrepancies noted at low b^2/Rt ratios were probably due to error in strain measurement since for low b^2/Rt ratios the measured strains were small.

2. The support and loading conditions of the plate did not affect the mode of transverse deflection even when the supports were placed as close as 3 in. from the transverse strain gages. Thus no distortion was observed for an equivalent span to width ratio of $1/3$.

3. The trapezoidal rule is an adequate numerical method for determining deflections from strain-gage readings.

Acknowledgments

The authors express their sincere appreciation to the National Research Council (Ottawa) for their financial assistance for this project under Grant N.R.C. A-1234, to R. Marak who assisted in the building of the automatic strain recorder, and to P. M. Falconer who typed the manuscript.

References

1. Navier, L. M. H., "Résumé des Leçons, Troisième édition avec des notes et des appendices par M. Barré de Saint-Venant," Paris, 32-36 (1864).
2. Searle, G. F. C., "Experimental Elasticity," Cambridge (1908).
3. Ashwell, D. G., and Greenwood, E. D., "The Pure Bending of Rectangular Plates," *Engineering* (July 21 and 28, 1950).
4. Lamb, H., "On the Flexure of a Flat Elastic Spring," *Philosophical Mag., Series 5*, 31 (1891).
5. Bellow, D. G., and Kennedy, J. S., "Multi-channel Strain Analysis," *Transactions Engrg. Inst. of Canada, EIC-63-CE and A12* (Nov. 1963).

FATIGUE CRACK PROPAGATION IN MILD STEEL

D.G. Bellow and B.R. Long

Abstract

Tests were conducted to determine the rate of fatigue crack growth in terms of the applied stress and current crack length in mild steel sheet subjected to cyclic bending and static axial stresses. The results were compared with some of the theoretical relationships which have been developed for axial-loaded fatigue specimens. It was found that the rate of crack propagation was proportional to the fourth power of the amplitude of the alternating stress and was influenced by the value of the mean stress. It was also found that for constant stress cycles the rate of crack propagation was a constant, and independent of crack length.

Résumé

Des essais ont été faits pour déterminer le taux d'accroissement des fissures de fatigue par la mesure de la contrainte appliquée et de la longueur courante des fissures dans des feuilles d'acier doux soumises à la flexion cyclique et aux contraintes statiques axiales. Les résultats furent comparés à quelques unes des formules théoriques qui ont été développées pour des échantillons exposés à la fatigue par charges axiales. On a trouvé que la vitesse de propagation des fissures est proportionnelle à la puissance quatre de l'amplitude de la contrainte alternative et est influencée par la valeur de la contrainte moyenne. On a aussi trouvé que, en cas de cycles de contrainte constants, la vitesse de propagation des fissures était constante et indépendante de la longueur des fissures.

D. G. BELLOW, Associate Professor, Department of Mechanical Engineering, University of Alberta, Edmonton, Alberta.

B. R. LONG, Defence Scientific Service Officer, Defence Research Board, Suffield Experimental Station, Ralston, Alberta.

INTRODUCTION

The rate of fatigue crack propagation can be considered as a property of fatigue damage. Since many laws of crack propagation have been formulated, this paper aims to compare some of the theories which have been developed for axial-load type fatigue, with experimental fatigue results which have been produced by cyclic bending stresses and combined cyclic bending and static axial stresses.

REVIEW OF THE LITERATURE

In 1939 Orowan (1) suggested that the presence of minute flaws, inhomogeneities and microcracks could cause stress concentrations which, if sufficiently large, would lead to progressive work hardening eventually initiating a crack. He further suggested that a fatigue crack propagates in the same manner, with the stress concentration effect provided by the tip of the existing crack. Orowan predicted that the rate of crack propagation was dependent only on the applied stress range.

In 1946 Bennett (2) measured crack growth rates in cylindrical specimens subjected to rotary bending and found the crack length increased exponentially with the number of loading cycles.

Head (3) in 1953 proposed that the rate of crack propagation was a function of crack length, and in 1954 and 1956 Weibull (4,5) proposed that the rate of crack growth was a constant for a constant applied stress. In 1958 Frost and Dugdale (6) modified Head's theory to include the plastic zone ahead of the crack. Their results showed that the size of this plastic zone was proportional to the current crack length. They also concluded that the rate of crack propagation in mild steel was influenced by the applied stress range but independent of the mean stress.

In 1961 Liu (7) determined the dependence of the rate of growth on stress range and mean stress for aluminum. No results were presented for mild steel. In a theoretical investigation in 1963 Liu (8) found the rate of crack propagation was proportional to the crack length and the square of the amplitude of the stress range. However, in a discussion of this paper, Paris and Erdogan (9) suggested the index could be three or four based on actual measurements.

TESTING CONSIDERATIONS

All the fatigue results cited above (3-8) were obtained using axial-load type fatigue machines which produced a direct or plane stress condition

in the specimen. For the results of this paper mild steel specimens were subjected to a bending stress condition resulting in a stress gradient through the thickness of the specimen. Cracks forming on opposite surfaces on the specimen were expected to propagate independently of one another.

In axial-loaded test specimens subjected to a constant load amplitude, the nominal stress range based on the net remaining area increases as the crack extends. To reduce the number of variables involved it is convenient to have a constant nominal stress range. With this in view Frost, Dugdale and Liu used wide sheets of material and measured the crack growth over a small portion of the total width. They based the nominal stress on the gross area and assumed that the relatively small length of crack did not influence the nominal stress amplitude. Weibull disagreed with this assumption; when measuring crack growth due to axial loading, he reduced the amplitude of the applied load so that the stress based on the remaining area was constant.

When a cantilever specimen is subjected to bending stresses only, the maximum bending stress will be a constant so long as the minimum curvature is constant. The minimum curvature will be a constant provided the modal shape of the vibrating specimen remains the same. It was anticipated that the modal shape would remain constant for crack lengths extending across a major portion of the width of the specimen. Also, for a cantilever specimen subjected to cyclic bending stresses the average or mean stress at any point in the member over a cycle of loading is zero.

If a specimen is clamped at both ends and subjected to cyclic bending stresses the mean stress will not be zero over a cycle of loading. However, as a crack occurs in the specimen the mean stress as well as the maximum bending stress will remain constant as long as the modal shape of the vibrating beam remains the same. It was expected that the modal shape would not be significantly affected by a fatigue crack which extended across a major portion of the specimen width.

EXPERIMENTAL PROCEDURE

An electrodynamic shaker was used to induce bending stresses by means of resonant vibration. A mild steel specimen was mounted in one of the two test fixtures, which was bolted to the top of the shaker table. The frequency and amplitude were controlled so that the specimen vibrated at its lowest natural frequency. The desired alternating stress was maintained by controlling the appropriate amplitude of vibration of the test

specimen. Calibration curves relating amplitude to alternating stress were used. These curves were obtained by mounting dynamic electrical resistance strain gauges on the top and bottom surfaces of the specimens in the area in which the crack was expected to propagate, that is, between the two stress raisers. For both specimen geometries the amplitude-stress relationships were linear.

To check the effect of crack length on modal shape of the vibrating test specimens, dynamic electrical resistance strain gauges were mounted on the top and bottom surfaces along the centre line of the specimen adjacent the area in which the crack was expected to propagate. It was found for the cantilever beam that the maximum applied stress in the notched section varied by 2 per cent for $L/b = 0.4$ and increased to 5 per cent for $L/b = 0.7$, where L is the total crack length and $2b$ is the net width of the specimen, that is, distance between the two stress raisers, which for the specimens tested was 2 inches. For the specimens tested in the fixed-end apparatus the applied maximum stress increased by 7 per cent at $L/b = 0.4$ and by 13 per cent at $L/b = 0.6$.

The existence of a fatigue crack in the test specimen reduced the stiffness and consequently the natural frequency of the specimen. The amplitude and frequency of the shaker oscillator were continually adjusted to maintain the desired amplitude of vibration on the test specimen. For the cantilever configuration the specimens were vibrated at a frequency of 63 cps. As the crack extended, this frequency decreased. For example, for $L/b = 0.4$ the frequency had decreased by 6 per cent, and for $L/b = 0.6$, by 11 per cent. For the fixed-end configuration the testing frequency was between 100 and 120 cps depending on the amount of pretensioning.

The first phase of the experimental investigation was the determination of the rate of fatigue crack propagation for three ranges of alternating stress ($\bar{\sigma} = \pm 21, \pm 26, \pm 35$ ksi) with zero mean stress ($\sigma_m = 0$). The second phase of testing used a test fixture which clamped the specimen at each end. By means of screw adjustments at the ends of the fixture a mean stress of up to 6 ksi was induced in the specimen. Strain gauges were applied to each specimen to indicate when the desired mean stress was reached and to monitor this stress throughout the test. The desired alternating stress was obtained by use of a calibration curve. Specimens were tested under four different stress conditions: $\sigma, \sigma = \pm 21, 0; \pm 21, 3; \pm 21, 6; \pm 24, 0$ ksi.

Specimens were cut from 0.110-inch mild steel sheet (ASTM A-242). The longitudinal edges were machined parallel and the stress raisers were cut



Figure 1
Test fixtures for the
two series of tests.

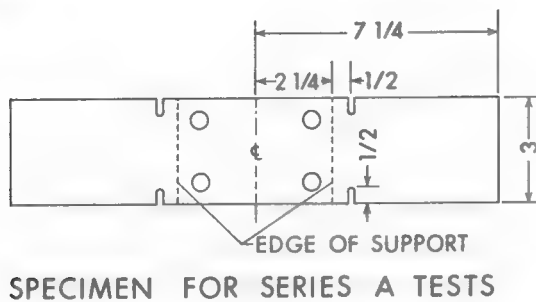
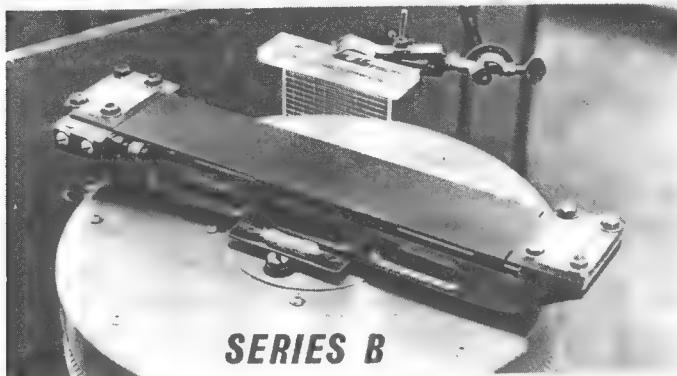
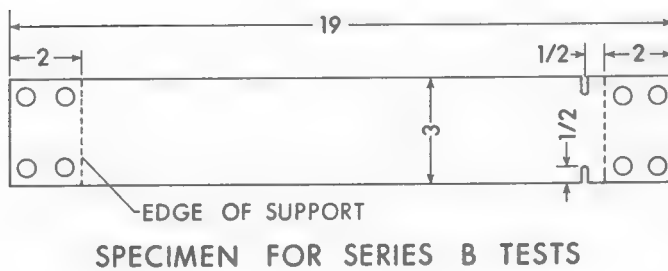


Figure 2
Specimen geometries
for two test phases.



with a milling cutter. The roots of the notches were inspected visually and, when necessary, buffed lightly to obtain a smooth contour. The surface between the stress raisers was polished lightly with a dressed wheel. It was assumed this surface treatment would not affect the crack growth [de Forrest (10)]. Photographs of the two test fixtures are shown in Figure 1 and the specimen geometries for the two phases of testing are shown in Figure 2.

Clamped in front of, but isolated from the test specimen was a piece of clear lucite on which a grid had been scribed. During a test the amplitude of the specimen was observed through this grid using the optical system and ground glass viewing screen of a 4×5-inch camera. The grid and specimen were illuminated with a stroboscopic light system. The scaled grid allowed the amplitude of vibration to be measured within ± 0.010 inch.

The extent of a crack at any time was measured with the use of 5X magnifier with a scale graticule. The grid of the graticule allowed measurements of crack lengths to within ± 0.004 inch. When there was some doubt as to the existence of a crack, a dye-penetrant was used. Crack lengths were measured at all the notches, two or four depending on the specimen used, and averaged. The cracks were measured only on the top surface of the specimen.

TEST RESULTS

Series A. Zero Mean Stress and Varying Stress Range

The test results of varying stress range and zero mean stress are plotted in Figure 3. As discussed above, strain gauges mounted on the surface of a test specimen indicated that the nominal stress did not measurably change for crack length ratios up to L/b of 0.4. Thus, each of the curves shown has a constant nominal stress range for L/b up to 0.4.

Figure 3 shows that as the stress range increases so does the rate of crack propagation. Also, for each stress range the rate of crack propagation is constant as long as the nominal stress remains constant (for $L/b \leq 0.4$).

A detailed examination of some of the fractured surfaces showed that all of the cracks initiated along a plane perpendicular to the surface of the specimen, but then for some of the fractures part of the fracture surface gradually rotated as much as 30 degrees. This rotation of the fracture plane caused the surface crack to deviate from the original line of propagation, resulting eventually in a new crack branching out from some point

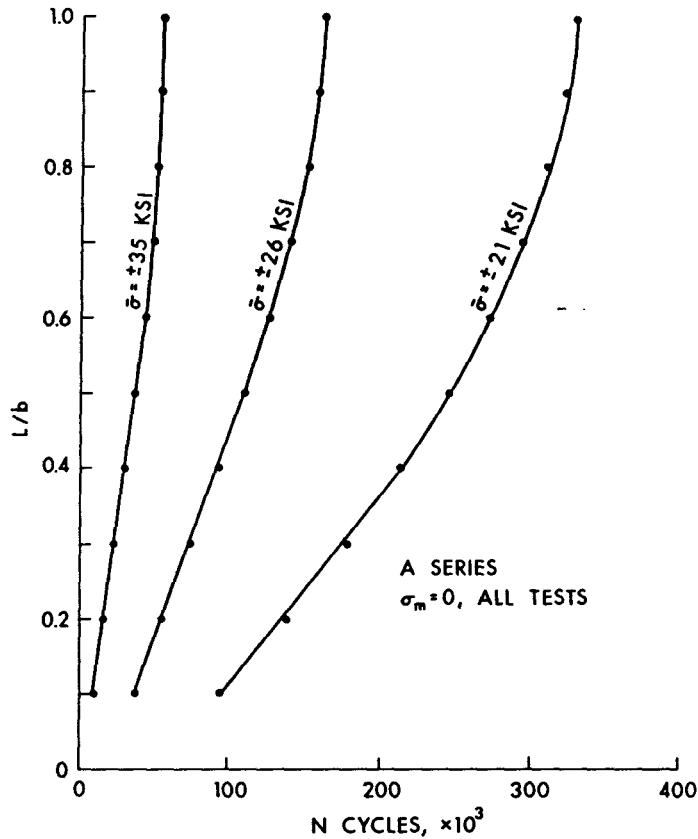


Figure 3. Zero mean stress and varying stress range.

behind the tip of the existing crack. There was considerable crack branching of the specimens subjected to a stress range of ± 35 ksi, very little at ± 26 , and none at all at ± 21 . The rotation of fractured surfaces has been observed by Weibull, Schijve and others (11).

A plot of a single test at $\bar{\sigma} = \pm 35$ ksi, $\sigma_m = 0$ is shown in Figure 4. For this specimen, rotation of the fracture plane was noticeable after each of the cracks had reached $L/b = 0.35$. For crack lengths greater than $L/b = 0.35$ the rate of crack propagation was observed to decrease. This decreasing rate continued until new cracks branched out and extended past the existing cracks. However, since the rate of crack propagation decreased only slightly for $L/b \leq 0.4$, the region over which the nominal stress remained constant, these results were averaged with those in which no crack branching was observed.

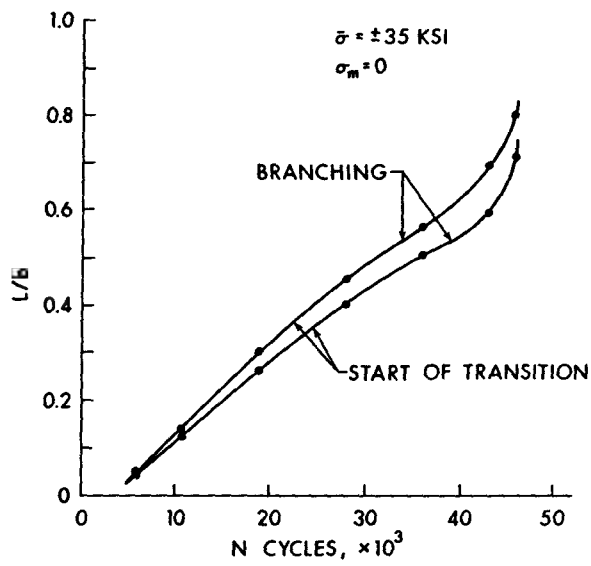


Figure 4
Single test $\bar{\sigma} = \pm 35$
ksi, $\sigma_m = 0$.

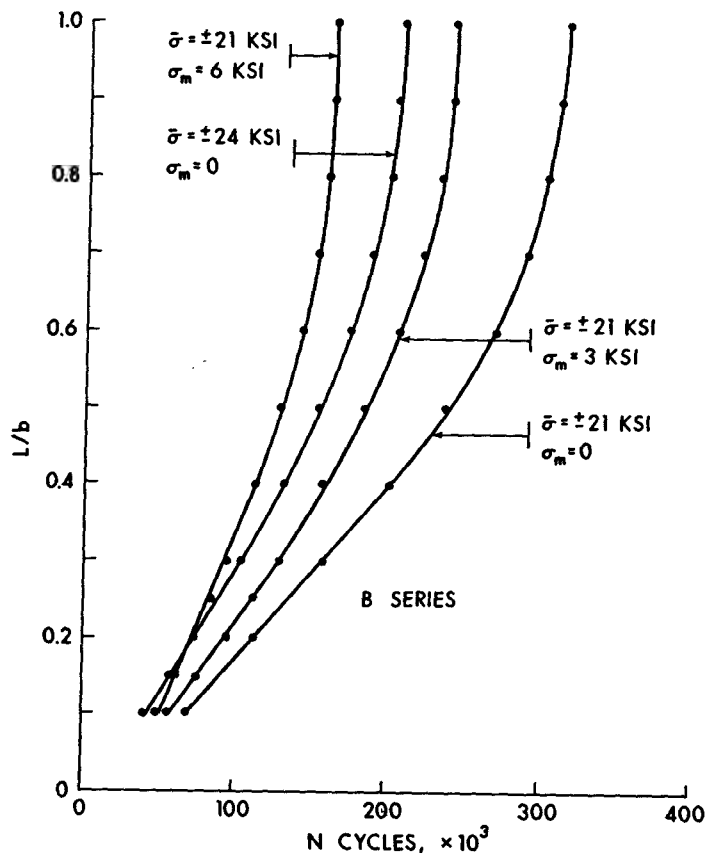


Figure 5
Varying mean stress and
varying stress range.

Series B. Varying Mean Stress and Varying Stress Range

The test results of varying mean stress and varying stress range are shown in Figure 5. Except for a different specimen geometry and holding fixture, the testing procedure for this series of tests was identical to that of the Series A tests.

The results in Figure 5 show that for a given stress range of ± 21 ksi the rate of crack propagation increases for an increasing mean stress. For the same peak stress of 24 ksi the curve of $\bar{\sigma} = \pm 24$ ksi, $\sigma_m = 0$ has a higher rate of crack propagation, throughout most of the life of the specimen, than the curve $\bar{\sigma} = \pm 21$ ksi, $\sigma_m = 3$ ksi. This indicates that the range of stress may be more important than the mean stress in determining the rate of crack propagation.

Again, as in the Series A tests, the rate of crack propagation was generally constant for L/b up to 0.4 for a given stress range and zero mean stress. A slight departure from linearity was noted in Series B for the nonzero mean stress tests over the range $0 < L/b < 0.4$ because these tests did not have a constant mean stress.

The rotation of the fracture surface which was noted in the Series A tests was not as evident in Series B. For $\bar{\sigma} = \pm 21$ ksi, $\sigma_m = 3$ ksi, the fracture surface angle was noticed to change at $L/b = 0.4$ reaching a maximum of 10 degrees at $L/b = 1.0$, i.e., at complete fracture of the specimen. For $\bar{\sigma} = \pm 21$ ksi, $\sigma_m = 6$ ksi, the fracture surface angle began to change at $L/b = 0.3$ reaching a maximum of 15 degrees at L/b of 1.0. For $\bar{\sigma} = \pm 24$ ksi, $\sigma_m = 0$, although no rotation was noted on some of the specimens, on others the rotation was as much as 26 degrees.

For the specimens in which crack branching occurred no variation in the rate of crack growth was observed.

DISCUSSION OF RESULTS AND COMPARISONS WITH THEORY

The rates of crack propagation for $L/b < 0.4$ for the average curves presented in Figures 3 and 5 are shown in the table. It is observed that for $\bar{\sigma} = \pm 21$ ksi, $\sigma_m = 0$ the rate of crack propagation given by both test series were in general agreement with one another even though the specimen geometries were different.

Effect of Stress Range and Mean Stress on the Rate of Crack Propagation

Test Series	Stress Range (ksi)	Mean Stress (ksi)	Rate of Crack Propagation for $L/b \leq 0.4$ (in./cycle)	Number of Tests
A	± 21	0	2.5×10^{-6}	14
	± 26	0	5.5	14
	± 35	0	14.6	14
B	± 21	0	2.3	5
	± 21	3	2.9	4
	± 21	6	4.7	6
	± 24	0	3.3	5

Comparison with Head's Theory

Head based his theory (3) on the fact that a straight line would result if the reciprocal of the square root of the crack length were plotted against the number of stress cycles. Assuming this linear relationship it can be shown that the rate of crack propagation is proportional to $L^{1/2}$. Head proposed that the constant of proportionality was a function of the applied stress and material stress-strain properties C and the length of plastic region ahead of the crack a . Thus he obtained

$$\frac{dL}{dN} = \frac{CL^{1/2}}{a^{1/2}} \quad 1$$

To check Head's theory, data from Figure 3 was used to plot $L^{-1/2}$ versus N as shown in Figure 6. In Figure 6, L is the length of the stress raiser plus the length of the fatigue crack. If L only represented the crack length, Head's theory would predict a zero rate of crack growth for zero crack length. Only the data from Figure 3 for $0 \leq L/b \leq 0.4$ was used in Figure 6 since the applied stress was a constant over this range.

Figure 6 shows that a straight line does not exist for any of the stress ranges tested. Of course, a straight line could be drawn for the $\bar{\sigma} = \pm 21$ ksi points but on the basis of the other curves the relationship between $L^{-1/2}$ and N does not generally appear to be linear, thus contradicting Head's original assumption.

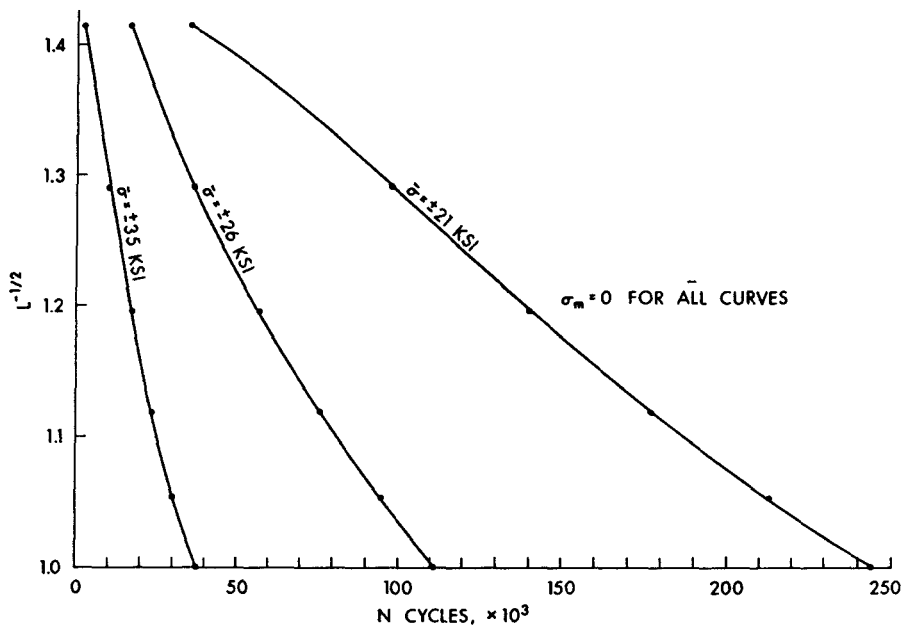


Figure 6. Comparison with Head's theory.

Comparison with Frost and Dugdale's Theory

The theory of Frost and Dugdale (6) and Liu (7,8) states that the rate of crack propagation is proportional to the crack length: $dL/dN = CL$. They suggested that the constant of proportionality C was a function of the alternating stress $\bar{\sigma}$, a material property n , and N_s , a factor affected by the mean stress. They obtained

$$\frac{dL}{dN} = \frac{\bar{\sigma}^n}{N_s} L \quad 2$$

Integrating this equation leads to the result that the crack length L increases exponentially with the number of stress cycles for constant stress range and mean stress. Thus, plotting L versus N on a semilogarithmic scale should be a straight line.

The results of Figure 3 for the range $0 \leq L/b \leq 0.4$ were plotted on a semi-logarithmic scale in Figure 7. Again, as in Head's work, L is the length of the stress raiser plus the length of the crack. While it might be argued

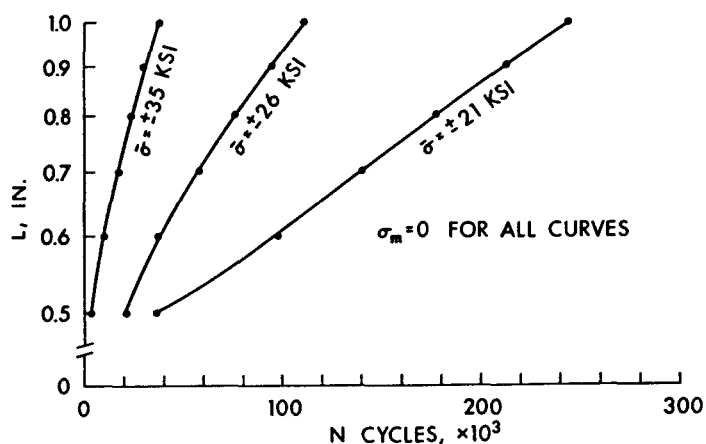


Figure 7
Comparison with Frost
and Dugdale's theory.

that a straight line could be drawn through the points for the $\bar{\sigma} = \pm 21$ ksi stress range, this is not true for the other stress ranges. On this basis it is concluded that a linear relationship generally does not exist for L versus N on a semilogarithmic scale. Thus, the rate of crack growth is not proportional to the length of crack. In using Equation 2, Frost and Dugdale restricted their crack length plus stress raiser to less than one-eighth the width of the specimen. In the present work the length of the stress raiser alone was one-third the width of the specimen. This may, in part, account for the disagreement between the present work and Frost and Dugdale's theory.

Comparison with Weibull's Theory

The theory of Weibull (4,5) states that the rate of crack growth is independent of the length of the crack but dependent on some function of the peak stress at the tip of the crack. Weibull proposed that the rate of crack propagation be given by

$$\frac{dL}{dN} = \frac{\bar{\sigma}^n}{N_s} \quad 3$$

where $\bar{\sigma}$ is the nominal stress amplitude, N_s is a constant depending on the mean stress, and n is a material constant. Thus for a constant stress range and mean stress the rate of crack propagation is a constant.

It was found for both test configurations that the rate of crack propagation was generally a constant, for a constant stress range and a constant mean

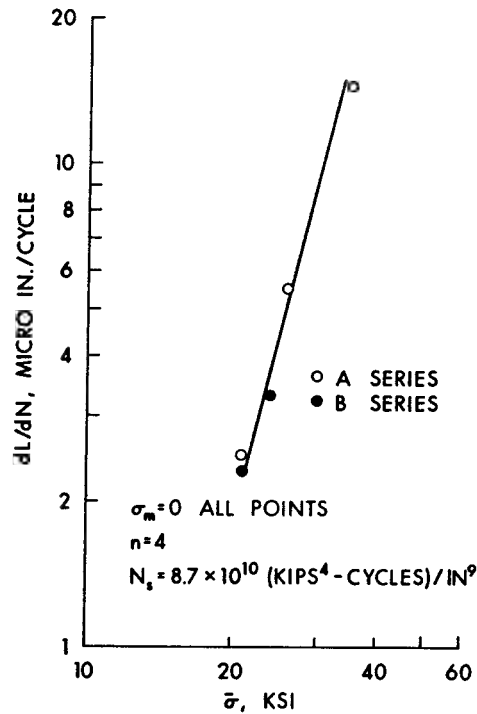
stress, over the range $0 \leq L/b \leq 0.4$ (see Figures 3 and 5). Some departure from linearity was noted for the nonzero mean stress tests over the range $0 \leq L/b \leq 0.4$ but this was because the mean stress and stress range varied by approximately 7 per cent over this L/b range.

In Figure 8, dL/dN versus the amplitude of the stress range $\bar{\sigma}$ has been plotted for a zero mean stress using the results in the table for both series of tests. Values taken from this graph show that in Equation 3,

$$n = 4 \text{ for mild steel, and} \\ N_s = 8.7 \times 10^{10} \frac{\text{kps}^4 - \text{cycles}}{\text{in.}^9}$$

where $\bar{\sigma}$ is measured in kps/in.² and dL/dN is in in./cycle.

Figure 8
 $\frac{dL}{dN}$ versus the amplitude
of the stress range $\bar{\sigma}$.



ADDITIONAL OBSERVATIONS

Assuming that the rate of crack propagation is defined by the actual stress existing in the region of the crack tip, and assuming a constant nominal stress on the remaining portion of the specimen, it follows that the rate of crack propagation will be constant for a constant stress concentration factor at the crack tip. If this factor increases in proportion to

the crack length, the crack length can be expected to increase exponentially with the number of stress cycles. The present investigation shows that the rate of crack propagation is constant and independent of the crack length for constant stress range and mean stress. Thus the stress concentration factor at the tip of the crack must remain constant.

Test Series B showed that the rate of crack growth was affected by the mean stress. Frost and Dugdale found the rate of crack propagation was independent of mean stress in mild steel, but dependent on mean stress in aluminum. The Series B tests also suggested that the range-of stress may be more important in determining the rate of crack propagation than the mean stress.

Figure 9 shows some of the fractured surfaces observed in the testing program. In Figure 10 a closeup view illustrates the type of fracture surface rotation observed in both test series. Both of these figures show a well defined line running along the middle of the cross section, indicating that the cracks propagated on opposite surfaces more or less independently of one another.

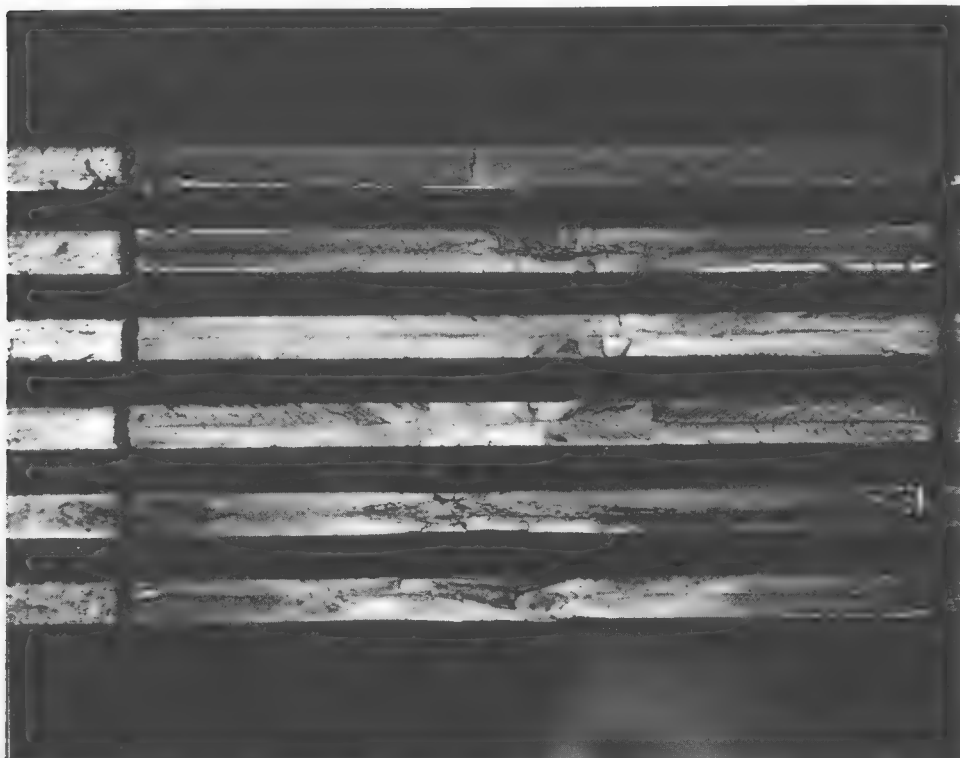


Figure 9. Fractured surfaces with little surface rotation.

CONCLUSIONS

For reversed bending tests in mild steel the following conclusions were reached:

1. For constant alternating stress amplitude and zero mean stress the rate of crack propagation was constant and independent of the crack length.
2. The rate of crack propagation was proportional to the fourth power of the alternating stress amplitude and the rate could be predicted by

$$\frac{dL}{dN} = \frac{\bar{\sigma}^n}{N_s}, \text{ where}$$

$\bar{\sigma}$ = alternating stress amplitude,

n = material constant, four for mild steel, and

N_s = constant depending on mean stress.

3. The value of the mean stress affects the rate of crack propagation but the alternating stress amplitude appears to affect it more.

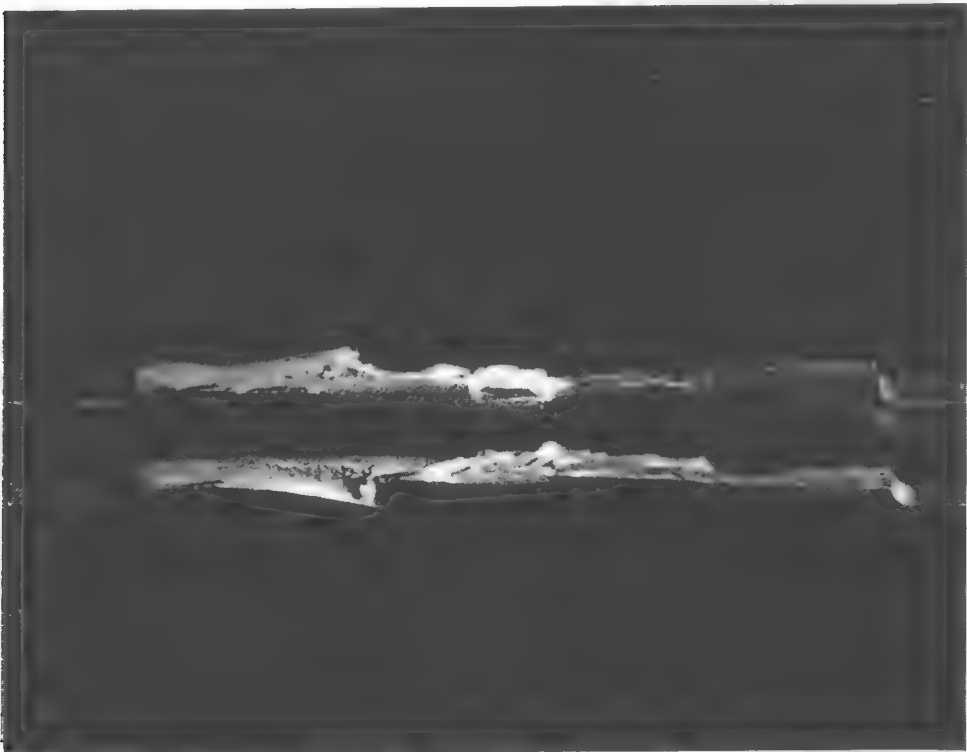


Figure 10. Detail showing surface fracture rotation.

ACKNOWLEDGMENT

The authors express their appreciation to the National Research Council of Canada for financial assistance received in support of this project under the grant number A-2705.

REFERENCES

- (1) Orowan, E. Proc. Roy. Soc., London. A171: 79. 1939.
- (2) Bennett, J.A. Proc. ASTM. 46: 693. 1946.
- (3) Head, A.K. Phil. Mag. 44: 925. 1953.
- (4) Weibull, W. SAAB. TN25. 1954.
- (5) Weibull, W. FFA. Rep. 65. 1956.
- (6) Frost, N.E., and D.A. Dugdale. J. Mech. Phy. Solids. 6: 92. 1958.
- (7) Liu, H.W. Trans. ASME. 83: 23. 1961.
- (8) Liu, H.W. Trans. ASME. 85: 116. 1963.
- (9) Paris, P., and F. Erdogan. Trans. ASME. 85: 121. 1963.
- (10) de Forrest, A.V. J. App. Mech. 58: A23. 1963.
- (11) Weibull, W. Current aero. fatigue problems. Pergamon Press, 1965. 201.

Stability of Rectangular Plates with Cambered Bitrapezoidal Cross Sections

A theory relating moment to curvature is presented by the authors. Also, they show, theoretically and experimentally, that these plates exhibit instability for certain combinations of edge thickness and camber

by D. G. Bellow and A. Semeniuk

ABSTRACT—This paper presents a theoretical moment-curvature relationship for rectangular plates having bitrapezoidal cross sections. It is shown that, for certain values of the cross-section camber and edge thickness, the plates exhibit a bending instability for some values of longitudinal curvature. Experimental results show good agreement between theory and experiment.

List of Symbols

- b = one-half plate width
- c = plate-edge thickness
- k = dimensionless parameter defining transverse camber
- M_y = moment per unit distance acting on a plane whose normal is in the y -direction
- N_y = membrane force per unit distance acting on a plane whose normal is in the y -direction
- R = longitudinal radius of curvature as measured to the neutral surface of the plate cross section
- t = total thickness of plate
- t_0 = one-half thickness of tapered portion of plate
- w = deflection in z -direction of midline of cross section from neutral surface
- w_0 = initial deflection of midline from neutral surface
- ζ = deflection in z -direction of midline of cross section from neutral surface due to applied moments
- x, y, z = rectangular coordinates

Introduction

The problem of finding a moment-curvature relationship for a flat plate of width $2b$ and thickness t having a rectangular cross section was investigated in 1879 by Kelvin and Tait.¹ In 1924, Timoshenko² suggested the moment-curvature relationship for a plate with a rectangular cross section could be written as

$$M = \frac{-EI}{R} \frac{(1 - \bar{k}\nu^2)}{(1 - \nu^2)},$$

D. G. Bellow and A. Semeniuk are Associate Professor and Sessional Lecturer, respectively, Department of Mechanical Engineering, University of Alberta, Edmonton, Alberta, Canada.

where M is the end moment causing the longitudinal curvature $1/R$, EI is the stiffness, ν is Poisson's ratio, and k is a parameter which depends on the dimensionless ratio b^2/Rt such that $\bar{k} = 1$ for $b^2/Rt < 0.4$ and $\bar{k} = 0$ for $b^2/Rt \gg 250$. Timoshenko further noted that there would be a gradual transition for k varying in the range $1 \geq \bar{k} \geq 0$.

The moment-curvature relationship becomes more complicated when the thickness of the cross section is some function of the transverse coordinate. In 1949, Flügge³ obtained theoretical moment-curvature relationships for rectangular plates having double wedge, rectangular, or bitrapezoidal cross sections. The bitrapezoidal cross section he considered had no camber. Fung and Wittrick⁴ discussed the bending of rectangular plates having tapered cross sections with and without camber. Their tapered sections were infinitely thin along the longitudinal edges. Although they discussed the stability problem, they presented no results.

The purpose of this paper is: first, to extend the theory to include instability of rectangular plates having a general bitrapezoidal cross section; and

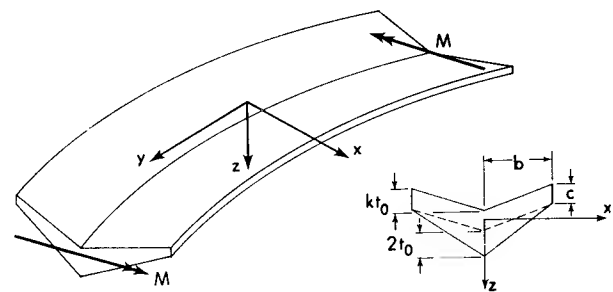


Fig. 1—Pure bending of rectangular plate showing bitrapezoidal cross section

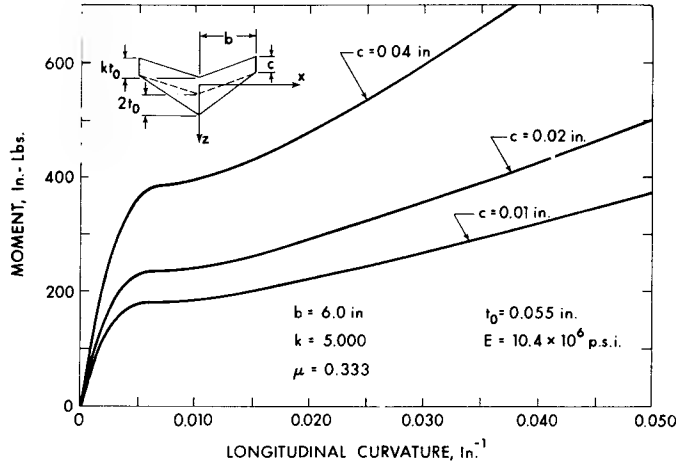


Fig. 2—Effect of varying edge thickness c for a constant camber $k = 5.0$

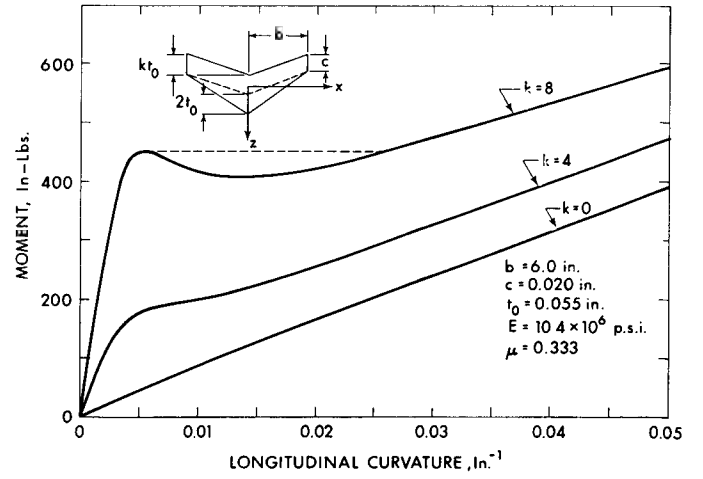


Fig. 3—Effect of varying camber k for a constant edge thickness $c = 0.020$ in.

second, to present experimental results with a discussion on the agreement between experiment and theory.

Theory

The general bitrapezoidal cross section considered and the manner in which the rectangular plate is loaded are shown in Fig. 1. By considering the equilibrium of an element cut from the plate and applying Hooke's law and geometrical relationships, the following governing differential equation is obtained:

$$\frac{d^2}{dx^2} \left(\frac{Et^3}{12(1-\nu^2)} \left[\frac{d^2w}{dx^2} + \frac{\nu}{R-w} \right] \right) + \frac{Ewt}{(R-w)^2} = 0 \quad (1)$$

For the section shown in Fig. 1, the thickness t may be expressed as

$$t = 2t_0 \left(1 - \frac{x}{b} \right) + c$$

for any positive x , where c is the edge thickness. In eq (1), w is the displacement in the z -direction of the midline of the transverse section as measured from the x -axis. Let $w = \zeta + w_0$, where ζ is the deflection due to the anticlastic effects of the curvature $1/R$, and w_0 is the initial deflection of the midline of the cross section measured relative to the centroidal axis. For the cross section shown in Fig. 1, w_0 is

$$w_0 = t_0 (1 + k) \left[1 - \frac{x}{b} - \frac{\beta + 2/3}{2\beta + 1} \right],$$

where $\beta = c/2t_0$. Using these results, eq (1) yields

$$\frac{d^2}{dx^2} \left(t^3 \frac{d^2\zeta}{dx^2} \right) + \frac{\nu}{R} \frac{d^2(t^3)}{dx^2} + \frac{12t(1-\nu^2)(\zeta + w_0)}{R^2} = 0 \quad (2)$$

where $R - w \doteq R$ since $R \gg w$. Introducing the

dimensionless terms $\xi = 1 - x/b$, and $\gamma = \xi + \beta$, eq (2) becomes

$$\frac{d^2}{d\gamma^2} \left(\gamma^3 \frac{d^2\zeta}{d\gamma^2} \right) + \lambda^4 \gamma \zeta = \frac{-6\nu b^2 \gamma}{R} - \lambda^4 \gamma w_0 \quad (3)$$

$$\text{where } \lambda^4 = \frac{3(1-\nu^2)b^4}{R^2 t_0^2}.$$

The general solution of eq (3) is

$$\zeta = \frac{1}{\eta} (Aber'\eta + Bbei'\eta + Cker'\eta + Dkei'\eta)$$

$$-w_0 - \frac{6\nu b^2}{R\lambda^4}, \quad (4)$$

where the prime denotes differentiation with respect to η , and $\eta = 2\lambda\gamma^{1/2}$. The last two terms of eq (4) represent the particular integral of eq (3).

The constants of integration can be obtained from the following four conditions; at the free edge, $x = b$, there is no shear and no moment, thus,

$$\left[\frac{d^3\zeta}{d\eta^3} - \frac{3}{\eta} \frac{d^2\zeta}{d\eta^2} + \frac{3}{\eta^2} \frac{d\zeta}{d\eta} \right]_{\eta} = 2\lambda\beta^{1/2} = 0,$$

$$\text{and } \left[\frac{d^2\zeta}{d\eta^2} - \frac{1}{\eta} \frac{d\zeta}{d\eta} + \frac{\nu b^2 \eta^2}{4\lambda^4 R} \right]_{\eta} = 2\lambda\beta^{1/2} = 0$$

respectively.

The deformation is symmetrical about the y axis, therefore,

$$\left[\frac{d\zeta}{d\eta} \right]_{\eta} = 2\lambda(1 + \beta)^{1/2} = 0;$$

and the resultant normal force in the y -direction is zero, hence,

$$\int_{\beta}^{1+\beta} \zeta \gamma d\gamma = 0.$$

A computer was used to solve these equations for the constants A , B , C , and D .

By considering moment equilibrium of an ele-

mental strip of width dx , the applied moment dM must balance the internal moments $M_y dx$ and $N_y w dx$, that is

$$M = 2 \int_0^b M_y dx + 2 \int_0^b N_y w dx.$$

Transforming this equation to a dimensionless form and setting

$$F' = A ber'_{\eta} + B bei'_{\eta} + C ker'_{\eta} + D kei'_{\eta}$$

the following expression results:

$$M = \frac{Ebt_0^3}{96\lambda^8(1-\nu^2)} \int_{\alpha}^{\epsilon} \left[\frac{\eta^7}{R} + \frac{4\nu\lambda^4}{b^2} (3\eta^2 F' - 3\eta^3 F'' + \eta^4 F''') \right] d\eta + \frac{bEt_0}{2\lambda^4 R} \int_{\alpha}^{\epsilon} \eta^3 \left[\frac{F'}{\eta} - \frac{6\nu b^2}{\lambda^4 R} \right]^2 d\eta \quad (5)$$

where $\epsilon = 2\lambda B^{1/2}$ and $\alpha = 2\lambda(1 + \beta)^{1/2}$.

Integration of eq (5) leads to the following:

$$\begin{aligned} M = & \left[\frac{bEt_0^3}{96\lambda^8(1-\nu^2)} \left(\frac{\eta^8}{8R} \right. \right. \\ & + \frac{4\nu\lambda^4}{b^2} \left[A(\eta^4 ber''_{\eta} - 7\eta^3 ber'_{\eta} + 24\eta^2 ber_{\eta} - 48\eta bei'_{\eta}) \right. \\ & + B(\eta^4 bei''_{\eta} - 7\eta^3 bei'_{\eta} + 24\eta^2 bei_{\eta} + 48\eta ber'_{\eta}) \\ & + C(\eta^4 ker''_{\eta} - 7\eta^3 ker'_{\eta} + 24\eta^2 ker_{\eta} - 48\eta kei'_{\eta}) \\ & \left. \left. + D(\eta^4 kei''_{\eta} - 7\eta^3 kei'_{\eta} + 24\eta^2 kei_{\eta} + 48\eta ker'_{\eta}) \right] \right] \\ & + \frac{Et_0 b}{2\lambda^4 R} \left(\frac{(A^2 + B^2)}{2} \eta (ber_{\eta} bei'_{\eta} - ber'_{\eta} bei_{\eta}) \right. \\ & + \frac{(A^2 - B^2)}{4} \eta^2 (2ber_{\eta} bei_{\eta} - ber_{\eta} bei_{2\eta} - ber_{2\eta} bei_{\eta}) \\ & + \frac{(C^2 + D^2)}{2} \eta (ker_{\eta} kei'_{\eta} - ker'_{\eta} kei_{\eta}) \\ & + \frac{(C^2 - D^2)}{4} \eta^2 (2ker_{\eta} kei_{\eta} - ker_{\eta} kei_{2\eta} - ker_{2\eta} kei_{\eta}) \\ & - \frac{AB\eta^2}{2} (ber_{1\eta}^2 - ber_{\eta} ber_{2\eta} - bei_{1\eta}^2 + bei_{\eta} bei_{2\eta}) \\ & - \frac{CD\eta^2}{2} (ker_{1\eta}^2 - ker_{\eta} ker_{2\eta} - kei_{1\eta}^2 + kei_{\eta} kei_{2\eta}) \\ & - \frac{(AC + BD)}{2} \eta (ber'_{1\eta} kei_{1\eta} - ber_{1\eta} kei'_{1\eta} - bei'_{1\eta} ker_{1\eta} + bei_{1\eta} ker'_{1\eta}) \\ & \left. - \frac{(AD - BC)}{2} \eta (ker'_{1\eta} ber_{1\eta} - ker_{1\eta} ber'_{1\eta} + kei'_{1\eta} bei_{1\eta} - kei_{1\eta} bei'_{1\eta}) \right) \end{aligned}$$

$$\begin{aligned} & + \frac{(AC - BD)}{4} \eta^2 (2ber_{1\eta} kei_{1\eta} - ber_{\eta} kei_{2\eta} - ber_{2\eta} kei_{\eta} + 2bei_{1\eta} ker_{1\eta} - bei_{\eta} ker_{2\eta} - bei_{2\eta} ker_{\eta}) \\ & + \frac{(AD + BC)}{4} \eta^2 (2bei_{1\eta} kei_{1\eta} - bei_{\eta} kei_{2\eta} - bei_{2\eta} kei_{\eta} - 2ber_{1\eta} ker_{1\eta} + ber_{\eta} ker_{2\eta} + ber_{2\eta} ker_{\eta}) \\ & - \frac{12\nu b^2}{\lambda^4 R} \left[A(\eta^2 ber_{\eta} - 2\eta bei'_{\eta}) + B(\eta^2 bei_{\eta} + 2\eta ber'_{\eta}) + C(\eta^2 ker_{\eta} - 2\eta kei'_{\eta}) + D(\eta^2 kei_{\eta} + 2\eta ker'_{\eta}) \right] \\ & + \frac{9\nu^2 b^4 \eta^4}{\lambda^8 R^2} \Big]_{\alpha}^{\epsilon}. \quad (6) \end{aligned}$$

Equation (6) was evaluated for different curvatures and parameters using a digital computer. The results are discussed below.

Theoretical Results

Figures 2 and 3 represent in graphical form the moment-curvature relationship as derived in eq (6). It is seen that, for some of the curves, the slope is always positive. However, for some combinations of edge thickness c and camber k the curves have a zero slope indicating a point of instability. For example, in Fig. 3, the curve $k = 8$, $c = 0.02$ in. shows that, for an increase in moment, there is an increase in curvature up to a critical value of the moment, in this case $M = 450$ in.-lbs. Theoretically, increasing the curvature from this critical value results in a decrease in moment required to maintain this curvature. If, however, the applied moment is maintained at the critical value, for an increase in curvature, the plate is in an unstable condition and will become stable again only when the curvature reaches a value of 0.025 in.⁻¹

It is evident from Fig. 2 that, for a constant camber, k , increasing the edge thickness c increases the value of the critical moment. In Fig. 3, it is seen that increasing the camber for a constant edge thickness also increases the value of the critical moment.

Experimental Considerations

The test plates were machined from 7075-T6 aluminum-alloy sheet having an elastic modulus of 10.4×10^6 psi and a Poisson's ratio of $1/3$. The taper was machined on the plates using a milling machine and the camber was produced using a sheet-metal press brake.

For the measurement of longitudinal curvature, electrical-resistance strain gages were placed along the center line (y -axis) on the top and bottom surfaces of the plate. Each gage on the top surface was connected to its counterpart on the bottom surface and wired up as two adjacent arms of a Wheatstone bridge. This doubled the sensitivity of the bending strains while eliminating the axial strains.

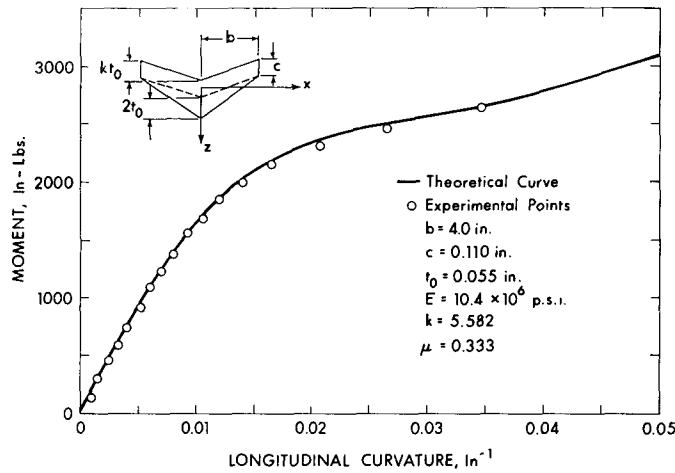


Fig. 4—Comparison of theory with experiment for a plate with $c = 0.110$ in., $k = 5.58$

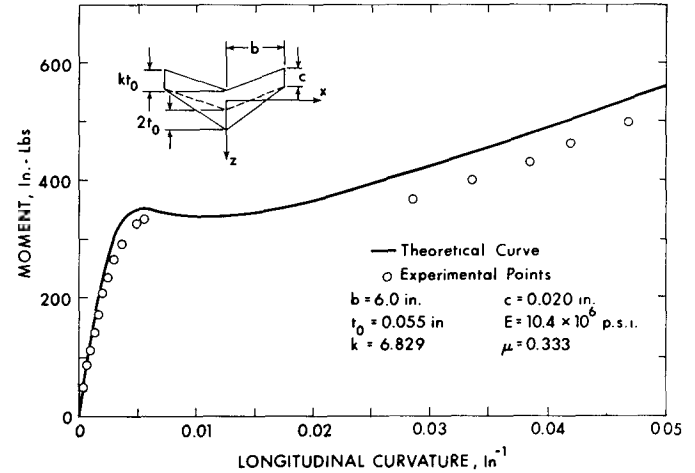


Fig. 5—Comparison of theory with experiment for a plate with $c = 0.020$ in., $k = 6.83$

Moments were applied by means of pulley-hanger assemblies rigidly fixed to each end of the plate. The pulley assemblies rested on channel sections, thus supporting the plate. Loads were attached to the rims of the pulleys allowing easy determination of the end moments. Because of the length of the plate, the distributed moment due to the weight of the plate was not negligible. In comparing the experimental results with theory, the moment at each measuring station of the plate was calculated on the basis of the end moment minus the moment due to the weight of the plate at the measuring station under consideration. Because of the large curvatures, the weight of the plate was not distributed uniformly along the length of the plate. This effect was taken into account in the moment equation given below:

$$M_c = qL(a - y) + qR[(R^2 - a^2)^{1/2} - (R^2 - y^2)^{1/2}] + qRy \left(\arcsin \frac{a}{R} - \arcsin \frac{y}{R} \right)$$

where

- q = weight per unit length of plate,
- y = horizontal distance from midline to measuring station under consideration,
- R = average longitudinal radius of curvature,
- L = half the length of the plate,
- a = half the distance between supports,
- M_c = moment due to weight of plate at measuring station.

Some typical experimental results are compared with theory in Figs. 4 and 5. In Fig. 4, the combination of k and c did not exhibit instability: thus, the moment followed a nonlinear bending relationship with the curvature. In Fig. 5, a critical moment was reached at a curvature of $1/R = 0.006$ in.⁻¹. At this curvature, the plate was unstable and, since the applied moment was kept constant, the plate snapped through to a curvature of 0.028

in.⁻¹, at which point an increase in curvature required an increase in applied moment. These results generally agreed with theory except that the experimental critical moment occurred five percent lower than predicted by theory.

Error of Measurement

As in all stability testing, the need for uniform materials and test conditions is of utmost importance. Any eccentricities in the specimen geometry or manner of loading will affect the critical conditions. For the experimental work of this paper, initial imperfections in the plate geometry were impossible to eliminate. Also, in the measurement of the camber k , it was found that it was not constant for every cross section of the plate. An average k was used in the calculations, but it was evident from the theory that a small deviation in k for $k > 5$ resulted in a significant change in the shape of the moment curvature curve.

Summary

A theory was developed relating moment to curvature for rectangular plates having a cambered bitrapezoidal cross section. It was shown experimentally and theoretically that such plates would exhibit instability for certain combinations of edge thickness c and camber k .

Acknowledgments

The authors express their appreciation to the National Research Council (Ottawa) for financial assistance received in support of this research.

References

1. Kelvin, Lord, and Tait, P. G., *Principle of Mechanics and Dynamics* Dover (1962).
2. Timoshenko, S. P., *Collected Papers*, McGraw-Hill, 366-370 (1953).
3. Flügge, W., "Large Deflections of Thin Wings," Technical Report No. 3, Air Forces Contract W33-038 AC-16697, Stanford University (1949).
4. Fung, Y. C., and Wittrick, W. H., "The Anticlastic Curvature of a Strip with a Lateral Thickness Variation," *Jnl. Appl. Mech.*, 21 (1954).

Bending Behavior of a Rectangular Plate with a Bitrapezoidal Cross Section

Experimental transverse deflections are compared with theory when a rectangular plate having a bitrapezoidal cross section undergoes a uniform longitudinal curvature

by D. G. Bellow and M. G. Faulkner

ABSTRACT—A theory is developed for the transverse deflections when a rectangular plate having a bitrapezoidal cross section is subjected to a uniform longitudinal curvature. The theoretical solutions are compared with earlier results presented by Lamb and Fung and Wittrick. Experimental results are compared with the theory and good agreement is obtained over the range of curvatures tested.

List of Symbols

- b = one-half the plate width
- c = thickness of the longitudinal edges
- k = nondimensional coefficient relating the amount of camber of the transverse cross section
- R = radius of curvature of the neutral surface in the longitudinal direction
- $2t_0$ = thickness of the tapered portion of the plate as shown in Fig. 1
- t = thickness of the plate as a function of x
- x, y, z = coordinate axes, where the x -axis coincides with the centroidal axis of the transverse cross section
- w = deflection of the midline of the cross section in the z -direction measured from the x -axis
- w_0 = initial deflection of the midline of the cross section measured from the x -axis
- $\alpha = 2\lambda(1 + \beta)^{1/2}$
- $\beta = c/2t_0$
- $\xi = 1 - x/b$
- $\gamma = \xi + \beta = \rho/2$
- $\epsilon = 2\lambda\beta^{1/2}$
- ζ = distortion of the midline of the cross section due to the longitudinal curvature $1/R$
- $\eta = 2\lambda(1 - x/b + \beta)^{1/2}$
- $\lambda^4 = [3(1 - \nu^2)b^4]/R^2t_0^2$
- ν = Poisson's ratio
- $\rho = t/t_0$

D. G. Bellow is Associate Professor, Department of Mechanical Engineering, University of Alberta, Edmonton, Alberta, Canada. M. G. Faulkner, formerly graduate student, Department of Mechanical Engineering, University of Alberta, is presently graduate student, University of California, Berkeley, Calif.

Introduction

In recent years, considerable attention has been given to the anticlastic bending behavior of rectangular plates with a rectangular cross section subjected to a uniform longitudinal curvature. Although the initial problem was solved by Lamb¹ in 1891, it was not until 1950 in a paper by Ashwell² and later by Fung and Wittrick³ in 1954, that the current interest in the problem was revived. In addition to plates having rectangular cross sections, Fung and Wittrick presented theoretical solutions for plates with linear thickness variations having different initial deflections. All of their plates tapered to a line edge. Although unknown to them at the time of their work, Flügge⁴ and Murray and Niles⁵ considered similar problems of tapered plates. Flügge analyzed plates with rectangular, double wedge and bitrapezoidal transverse cross sections. Murray and Niles also presented results for a biconvex transverse cross section. More recently, Conway and Farnham⁶ and Pao and Conway⁷ have theoretically considered the transverse deflections of plates having various tapers over the edge portion of the cross section.

The present paper is the result of work which had as its initial purpose the experimental verification of a tapered plate as investigated theoretically by Flügge, and Fung and Wittrick. However, it was found impractical to machine an infinitely thin edge on a tapered plate and thus the theory was modified to include the case of the bitrapezoidal plate as investigated by Flügge but allowing for a camber in the transverse direction. Experimental results are shown which indicate that the theory predicts, with reasonable accuracy, the transverse deflection of plates with bitrapezoidal cross sections.

Theory

Consider a rectangular plate, having a tapered cross section as shown in Fig. 1 (a), being subjected to a longitudinal curvature $1/R$ in a manner shown in Fig. 1(b). Applying the equations of force and moment equilibrium to an element of this plate, dx by dy , and using Hooke's Law, it can be shown¹ that the governing differential equation reduces to

$$\frac{d^2}{dx^2} \left[\frac{Et^3}{12(1-\nu^2)} \left(\frac{d^2w}{dx^2} + \frac{\nu}{R} \right) \right] + \frac{Ewt}{R^2} = 0 \quad (1)$$

where t is a function of x , $1/R_x \doteq d^2w/dx^2$, and E and ν are Young's modulus and Poisson's ratio, respectively.

Let $w = w_o + \zeta$ where w_o is the initial deflection of the midline of the cross section measured relative to the centroidal axis and ζ is the deflection due to the anticlastic effects of the curvature $1/R$. Assuming w_o is a linear function of x , eq (1) reduces to

$$\frac{d^2}{dx^2} \left(t^3 \frac{d^2\zeta}{dx^2} \right) + \frac{\nu}{R} \frac{d^2(t^3)}{dx^2} + \frac{12(1-\nu^2)t}{R^2} \times (\zeta + w_o) = 0 \quad (2)$$

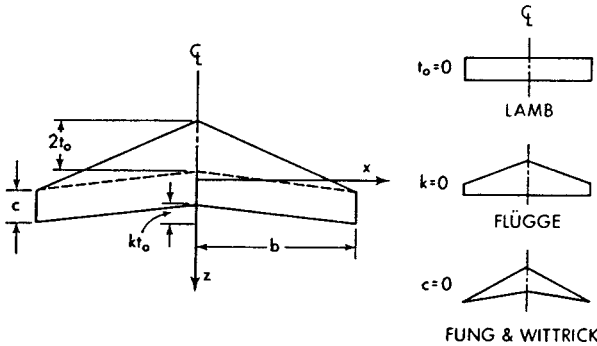
For the bitrapezoidal transverse cross section as shown in Fig. 1(a), the thickness t , and the initial deflection w_o of the cross section as measured from the centroidal x -axis may be expressed, for any positive x , as

$$t = 2t_o \left(1 - \frac{x}{b} \right) + c \quad (3)$$

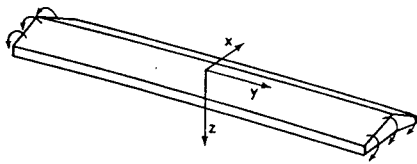
and

$$w_o = -t_o(1+k) \left[1 - \frac{x}{b} - \frac{\beta + 2/3}{2\beta + 1} \right] \quad (4)$$

respectively, where $\beta = c/2t_o$.



(a) GENERAL BITRAPEZOIDAL CROSS SECTION



(b) ORIENTATION

Fig. 1—Plate

If the edge thickness is zero (i.e., $c = 0$), the result is the double-wedge shape considered by Fung and Wittrick.³ If $t_o = 0$, then $t = c$ and the cross section is rectangular. This is the problem treated by Lamb¹ and Ashwell.² If $k = 0$, the result is the tapered cross section investigated by Flügge.⁴

Introducing the nondimensional variables $\xi = 1 - x/b$, $\rho = t/t_o$, $\gamma = \xi + \beta$, and $\gamma = \rho/2$ [from eq (3)], eq (2) reduces to

$$\frac{d^2}{d\gamma^2} \left(\gamma^3 \frac{d^2\zeta}{d\gamma^2} \right) + \lambda^4 \gamma \zeta = \frac{-6\nu b^2 \gamma}{R} - \lambda^4 \gamma w_o \quad (5)$$

where

$$\lambda^4 = \frac{3(1-\nu^2)b^4}{R^2 t_o^2}$$

A particular integral of eq (5) is given by

$$\zeta_o = -w_o - \frac{6\nu b^2}{R\lambda^4}$$

Combining this with the complementary solution,⁸ the general solution of eq (5) becomes

$$\zeta = \frac{1}{\eta} [Aber'\eta + Bbei'\eta + Cker'\eta + Dkei'\eta] - w_o - \frac{6\nu b^2}{R\lambda^4} \quad (6)$$

where $\eta = 2\lambda\gamma^{1/2}$.

At the free edge $x = b$, there is no shear and no moment, thus

$$[V_x]_{x=b} = -D \left[\frac{d^3w}{dx^3} \right]_{x=b} = 0$$

$$[M_x]_{x=b} = -D \left[\frac{d^2w}{dx^2} + \frac{\nu}{R} \right]_{x=b} = 0$$

Transforming these conditions to a nondimensional form yield, respectively,

$$\left[\frac{d^3\zeta}{d\eta^3} - \frac{3}{\eta} \frac{d^2\zeta}{d\eta^2} + \frac{3}{\eta^2} \frac{d\zeta}{d\eta} \right]_{\eta=2\lambda\beta^{1/2}} = 0 \quad (7)$$

$$\left[\frac{d^2\zeta}{d\eta^2} - \frac{1}{\eta} \frac{d\zeta}{d\eta} + \frac{\nu b^2 \eta^2}{4\lambda^4 R} \right]_{\eta=2\lambda\beta^{1/2}} = 0 \quad (8)$$

A third condition comes from the symmetry of the problem at $x = 0$

$$\left[\frac{d\zeta}{d\eta} \right]_{\eta=2\lambda(1+\beta)^{1/2}} = 0 \quad (9)$$

The fourth condition is obtained by observing that the resultant normal force in the y -direction must be zero, which is equivalent to

$$\int_0^b (w_o + \zeta) t dx = 0$$

and in nondimensional form reduces to

$$\int_{\beta}^{1+\beta} \zeta \gamma d\gamma = 0 \quad (10)$$

where $\int_0^b w_o t dx = 0$ since the x -axis is the centroidal axis of the cross section. Combining eq (6) with eqs (7) to (10) results in four algebraic equations

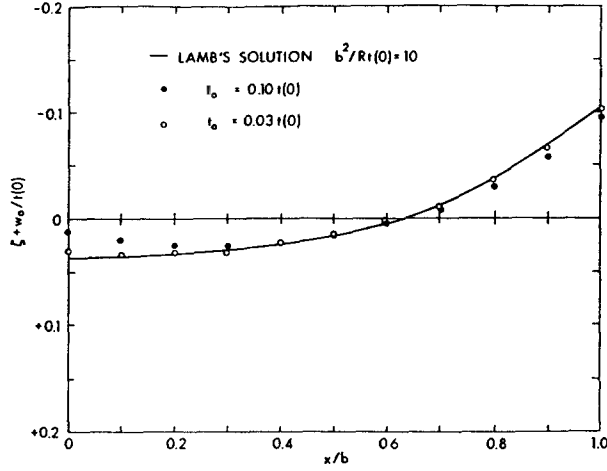


Fig. 2—Comparison of theory with Lamb's solution

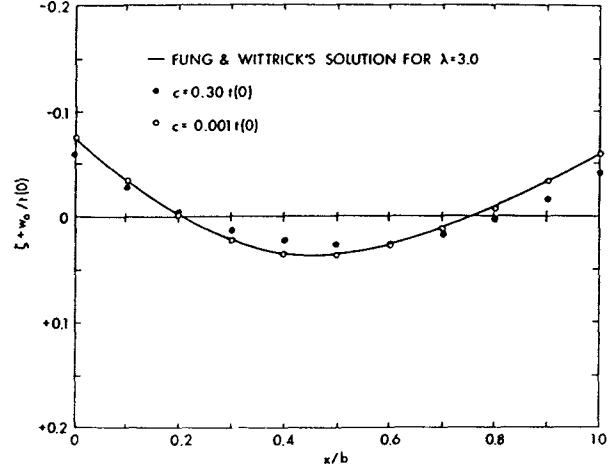


Fig. 3—Comparison of theory with Fung and Wittrick's solution

sufficient to determine the constants A , B , C , and D . Noting that $\alpha = 2\lambda(1 + \beta)^{1/2}$, and $\epsilon = 2\lambda B^{1/2}$, eqs (7) to (10) become

$$\begin{aligned} &A(-\epsilon^3 ber\epsilon - 24\epsilon bei\epsilon - 48ber'\epsilon + 8\epsilon^2 bei'\epsilon) + \\ &B(-\epsilon^3 bei\epsilon + 24\epsilon ber\epsilon - 48bei'\epsilon - 8\epsilon^2 ber'\epsilon) + \\ &C(-\epsilon^3 ker\epsilon - 24\epsilon kei\epsilon - 48ker'\epsilon + 8\epsilon^2 kei'\epsilon) + \\ &D(-\epsilon^3 kei\epsilon + 24\epsilon ker\epsilon - 48kei'\epsilon - 8\epsilon^2 ker'\epsilon) = 0 \quad (11) \end{aligned}$$

$$\begin{aligned} &A(4\epsilon bei\epsilon - \epsilon^2 bei'\epsilon + 8ber'\epsilon) + \\ &B(-4\epsilon ber\epsilon + \epsilon^2 ber'\epsilon + 8bei'\epsilon) + \\ &C(4\epsilon kei\epsilon - \epsilon^2 kei'\epsilon + 8ker'\epsilon) + \\ &D(-4\epsilon ker\epsilon + \epsilon^2 ker'\epsilon + 8kei'\epsilon) + \\ &\frac{\nu b^2 \beta \epsilon^3}{R\lambda^2} = 0 \quad (12) \end{aligned}$$

$$\begin{aligned} &A(-\alpha bei\alpha - 2ber'\alpha) + B(\alpha ber\alpha - 2bei'\alpha) + \\ &C(-\alpha kei\alpha - 2ker'\alpha) + D(\alpha ker\alpha - 2kei'\alpha) + \\ &\frac{t_0(1+k)\alpha^3}{2\lambda^2} = 0 \quad (13) \end{aligned}$$

$$\begin{aligned} &A(\alpha^2 ber\alpha - 2\alpha bei'\alpha - \epsilon^2 ber\epsilon + 2\epsilon bei'\epsilon) + \\ &B(\alpha^2 bei\alpha + 2\alpha ber'\alpha - \epsilon^2 bei\epsilon - 2\epsilon ber'\epsilon) + \\ &C(\alpha^2 ker\alpha - 2\alpha kei'\alpha - \epsilon^2 ker\epsilon + 2\epsilon kei'\epsilon) + \\ &D(\alpha^2 kei\alpha + 2\alpha ker'\alpha - \epsilon^2 kei\epsilon - 2\epsilon ker'\epsilon) - \\ &\frac{3\nu b^2}{2R\lambda^4}(\alpha^4 - \epsilon^4) = 0 \quad (14) \end{aligned}$$

Equations (11) to (14) were solved using an IBM 7040/1401 computer to determine the constants of integration A , B , C , and D . The values of the ber , bei , ker , and kei functions and their derivatives were calculated using a series for arguments $0 \leq \eta \leq 8$ and an asymptotic expansion for $\eta > 8$.⁹

While eq (6) is not generally applicable to all cases considered in Refs. 1 to 5, it can be shown to approach the known solutions for a plate having a rectangular cross section and for a plate having a cross section which tapers to a line edge. The use of eq (6) for a rectangular cross section is of

academic interest only because a more exact solution can be obtained easily by starting with eq (1) in a manner similar to Lamb.¹ However, eq (6) has been compared with Lamb's solution in Fig. 2 on the basis of the same $b^2/Rt(0)$ for $t_0 = 0.10t(0)$ and $t_0 = 0.03t(0)$ where $t(0)$ is the thickness of the cross section at $x = 0$. Obviously, if $t_0 = 0$, which would yield a rectangular cross section, eq (6) would no longer be valid since η would be infinite.

For the case of a rectangular plate whose transverse cross section tapers to a point at either free edge, c in eq (3) must be set to zero. When $c = 0$, $\eta = 0$ making $ker'\eta$ negative infinity. Along the free edges, the conditions of zero moment and

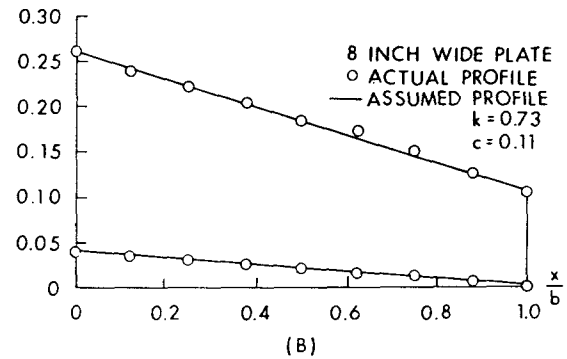
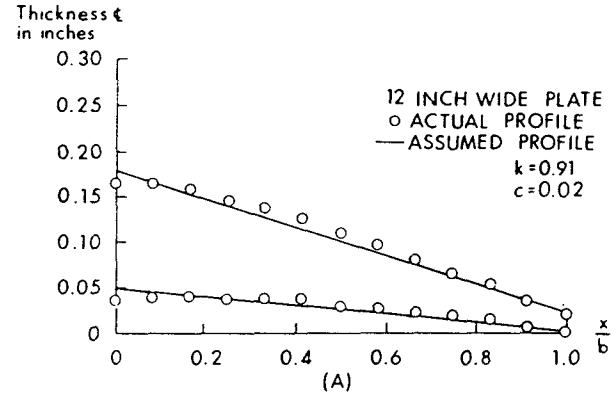


Fig. 4—Comparison of actual and assumed cross-section profiles

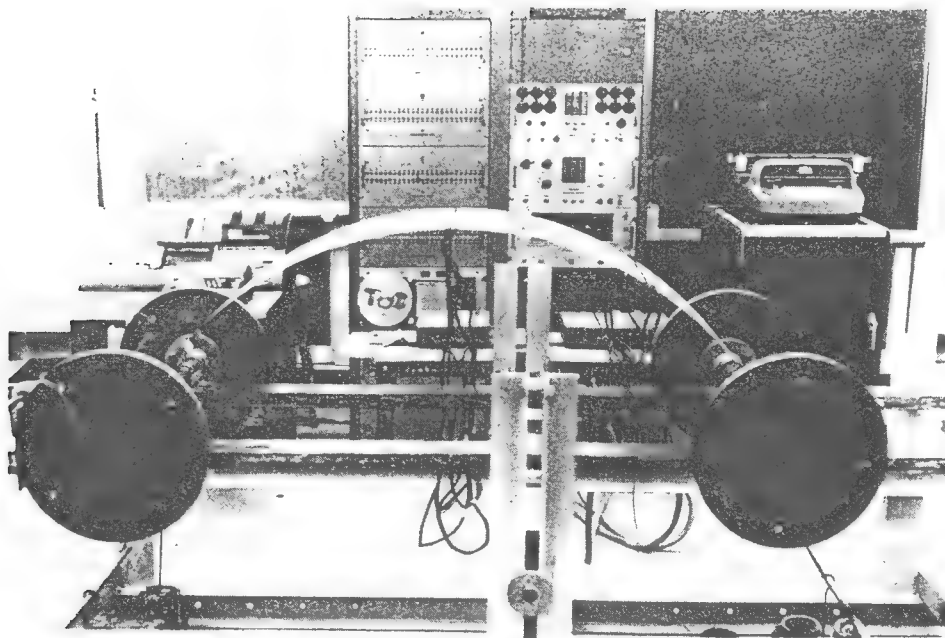


Fig. 5—Testing arrangement

zero shear have no meaning since the stiffness is also zero and other conditions must be employed.^{3, 7} In spite of these objections, eq (6) has been compared with the results of Fung and Wittrick³ in Fig. 3 on the basis of the same λ value. For $c = 0.001t/0$, there is good agreement between eq (6) and the theory of Fung and Wittrick.

The remainder of this paper discusses the experimental verification of eq (6) for four different λ values.

Experimental Equipment and Procedures

Two test plates were machined from flat rolled Alclad 7075-T6 aluminum sheet. A 12-in.-wide plate was cut from a 0.125-in.-thick sheet. The bitrapezoidal cross section was obtained using an end-mill cutter on a vertical milling machine. In the process of machining, the cross section warped as shown in the profile of Fig. 4 (a). An 8-in.-wide plate was cut from a 0.250-in.-thick sheet. The tapered cross section was obtained using a horizontal milling machine. The resulting profile in Fig. 4 (b) shows less cross-section distortion than obtained with the 12-in.-wide plate. In comparing theory with experiment, the profiles as indicated by the solid lines in Fig. 4 were used in computing w . For the 12-in.-wide plate, $k = 0.91$ and $c = 0.02$ and, for the 8-in.-wide plate, $k = 0.73$ and $c = 0.11$.

Electrical-resistance strain gages (Budd type C12-121) were mounted along the midline of the upper and lower surfaces of each plate, in the transverse direction. When the plate was loaded, readings from these strain gages were measured and recorded automatically using a digital data processor and an IBM 024 key punch. Using the numerical procedure based on the trapezoidal rule, as described by Bellow, Ford, and Kennedy,¹⁰ the strains were integrated by an IBM 7040 1401 to obtain the transverse deflections. In order that the truncation error be negligible in using the trapezoidal rule, it is necessary to use as many

measuring stations as possible. It was decided that 13 stations on each half cross section would give the required accuracy, while the application of this number of gages would not be difficult. As a result, the distance between gage centers was 0.50 in. for the 12-in. plate and 0.33 in. for the 8-in. plate. To obtain the gage spacing of 0.33 in. for the 8-in. plate, the gages were staggered. As well as these transverse gages, four longitudinal gages on each plate (two on top and two opposite on the bottom) were used to calculate the longitudinal curvature.

Figure 5 shows a general arrangement of the experimental apparatus. The desired longitudinal curvature was obtained by applying loads to the rims of the pulleys which were keyed to 1-in.-diam. shafts which, in turn, were bolted to each end of the test plate. A 6-in.-diam pulley was used with the 12-in. plate and a 15-in.-diam pulley was used with the 8-in. plate. The shafts at each end of the plate were supported in bearings which were free to roll along flat steel ways.

The testing procedure consisted of taking a set of zero readings from the strain gages with the plate resting on a flat surface. These initial readings were subtracted from those taken with the plate bent into a longitudinal curvature $1/R$ to obtain the absolute change in strain due to the curvature $1/R$. Each plate was loaded and the transverse strains were recorded for various λ values over the range $0 < \lambda < 4$. Each λ value was calculated using the longitudinal curvature measured, by strain gages, at the center of the plate.

The plates and the loads applied to them were symmetrical about the longitudinal axis. Thus, the experimental results of both halves of the transverse cross section were averaged and compared with the theoretical curves for half the cross section. In this way, two sets of experimental results were obtained from each test. The plates were loaded at least five times for each λ value tested. Thus, there were at least 10 sets of results to compare for each λ value.

Discussion of Results

Figure 6 shows a typical range of values obtained for the 12-in.-wide plate. The experimental results for the 8 in.-wide plate were more precise as a typical set of values shows in Fig. 7.

Figures 8 to 11 indicate that good agreement between experiment and theory was obtained for the 8-in.-wide plate and for the lower λ values of the 12-in.-wide plate.

The disagreement between theory and experiment for the 12-in.-wide plate for $\lambda \geq 3.0$ was believed to be due to the nonlinear warping of the cross section which occurred during machining. Examination of Fig. 4 (a) shows that there was some deviation between the assumed and actual cross-sectional profile of the 12-in.-wide plate while, in Fig. 4 (b), the assumed and actual profile of the

8-in.-wide plate was seen to be in close agreement. Since good agreement was obtained from tests on the 8-in. plate, it was concluded that the disagreement between experiment and theory observed for the 12-in. plate was due to the nonlinear warping of the transverse cross section.

For both plates tested, the total error of measurement was estimated to be less than ± 4 percent, of which the truncation error involved in the application of the trapezoidal rule was less than one-half of 1 percent.

Summary

1. The theory presented was shown to approach the known results of Lamb¹ and Fung and Wittrick.³
2. The theory predicted, with reasonable agree-

Fig. 6—Typical range of experimental results for the 12-in.-wide plate

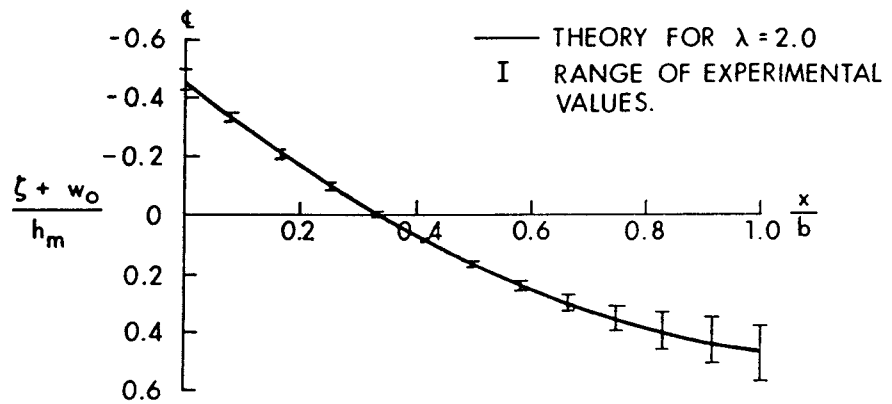


Fig. 7—Typical range of experimental results for the 8-in.-wide plate

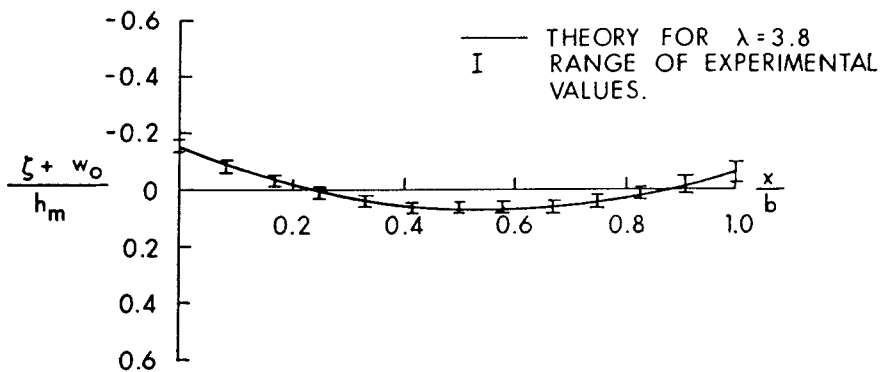
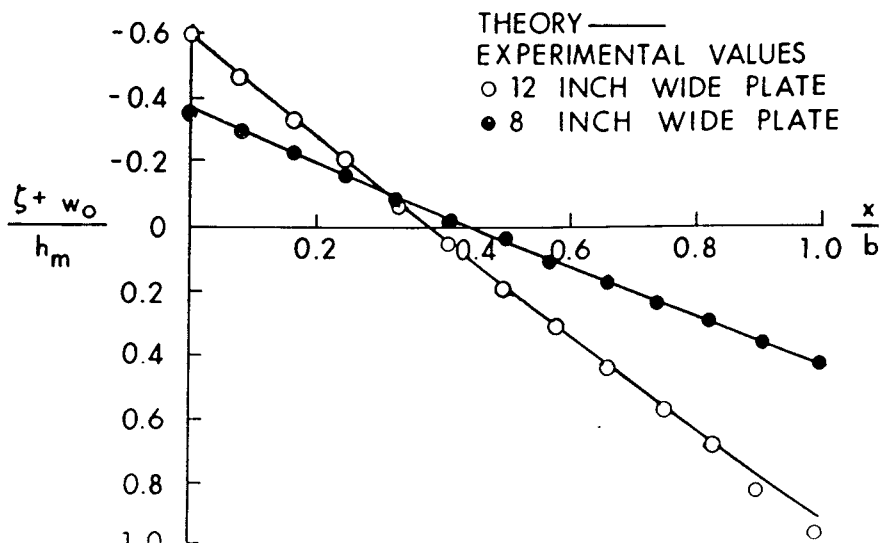


Fig. 8—Transverse deflections for $\lambda = 1.0$



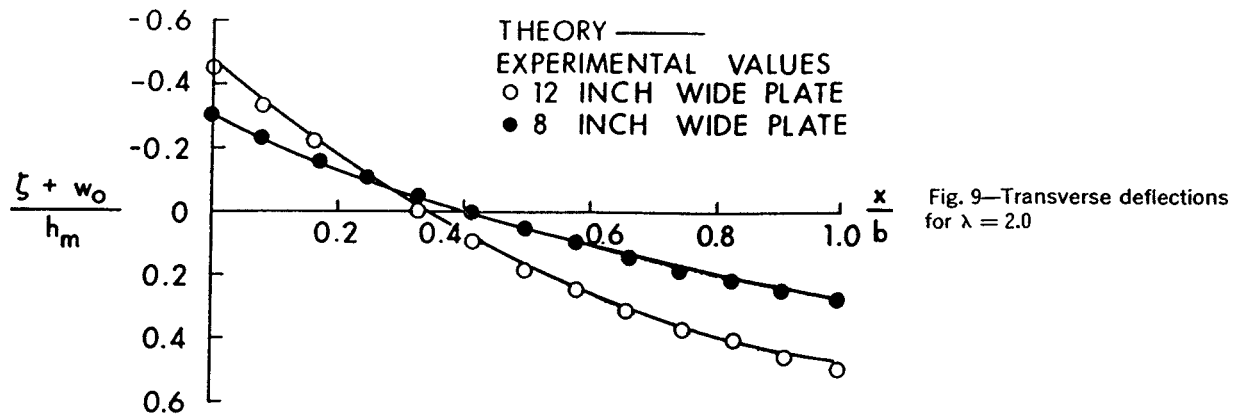


Fig. 9—Transverse deflections for $\lambda = 2.0$

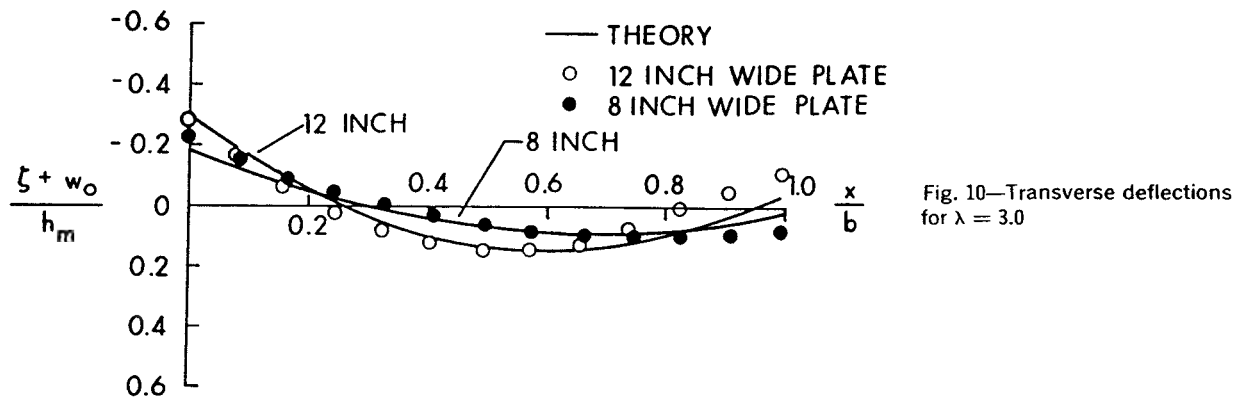


Fig. 10—Transverse deflections for $\lambda = 3.0$

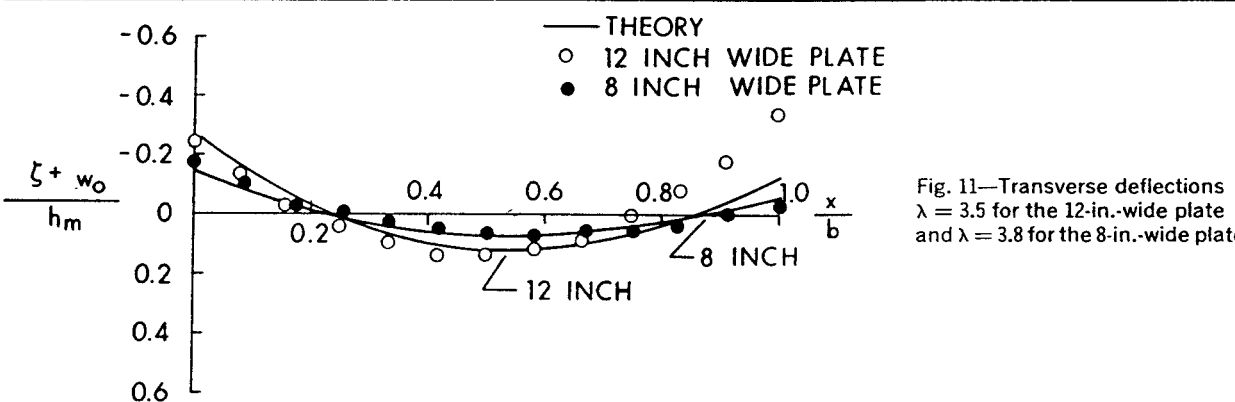


Fig. 11—Transverse deflections $\lambda = 3.5$ for the 12-in.-wide plate and $\lambda = 3.8$ for the 8-in.-wide plate

ment, the experimental transverse deflections for the range of λ values tested $0 < \lambda < 4$ for two rectangular plates, each having a different bitrapezoidal cross section.

3. The theory is equally valid if the plate is turned upside down. One only needs to multiply the right hand side of the expression for w_0 [eq (4)] by -1 and the results are obtained in a similar fashion to that described above.

4. For the range of λ values tested, the plates were always in a condition of stable equilibrium. It is possible for certain combinations of c and k that the plates will become unstable before reaching a particular λ value. This aspect of the problem is the subject of another investigation.¹¹

Acknowledgment

The authors express their appreciation to the National Research Council (Ottawa) for the finan-

cial assistance received in support of this project under Grant A-2705.

References

1. Lamb, H., "On the Flexure of a Flat Elastic Spring," *Philosophical Mag., Series 5*, **31**, 182-188 (1891).
2. Ashwell, D. G., "The Anticlastic Curvature of Rectangular Beams and Plates," *Jnl. Royal Aero. Soc.*, **782-788** (1950).
3. Fung, Y. C., and Wittrick, W. H., "The Anticlastic Curvature of a Strip with Lateral Thickness Variation," *Jnl. Appl. Mech.*, **21**, 351-358 (1954).
4. Flügge, W., "Large Deflections of Thin Wings," *Technical Report No. 3, Air Forces Contract W33-038, AC-16697, Stanford University* (1949).
5. Murray, T. R., and Niles, A. S., "Bending of Wide Beams of Doubly Symmetric Section," *Technical Report No. 4, Air Forces Contract W33-038, AC-16697, Stanford University* (1949).
6. Conway, H. D., and Farnham, K. A., "Anticlastic Curvature of Strips of Variable Thickness," *Intnl. Jnl. Mech. Sci.*, **7**, 451-458 (1965).
7. Pao, Y. C., and Conway, H. D., "An Optimum Study of the Anticlastic Deformations of Strips with Tapered Edges," *Intnl. Jnl. Mech. Sci.*, **8**, 65-76 (1966).
8. Flügge, W., *Stresses in Shells*, Springer-Verlag, 287-291 (1960).
9. McLachlan, N. W., *Bessel Functions for Engineers*, Oxford Press, 137-152 (1955).
10. Bellow, D. G., Ford, G., and Kennedy, J. S., "Anticlastic Behavior of Flat Plates," *EXPERIMENTAL MECHANICS*, **5** (7), 227-232 (July 1965).
11. Bellow, D. G., and Semeniuk, A., "Stability of Rectangular Plates with Cambered Bitrapezoidal Cross Sections," *EXPERIMENTAL MECHANICS*, **7** (7), 309-312 (July 1967).

THE INHERENT BENDING INSTABILITY OF RECTANGULAR PLATES WITH CAMBERED TRANSVERSE CROSS-SECTIONS

D. G. BELLOW and A. SEMENIUK

Department of Mechanical Engineering, University of Alberta,
Edmonton, Alberta, Canada

(Received 27 September 1967)

Summary—The problem of bending instability of a rectangular plate subjected to pure bending is analyzed for various types of transverse cross-sections. It is shown that for a plate to be inherently unstable it depends on the degree of transverse camber and the type of cross-section under consideration. Because of this it is demonstrated that not all cambered cross-sections necessarily result in bending instability. For a plate with a bitrapezoidal cross-section tapering to an edge thickness a relationship between the camber and edge thickness is presented for designing such a plate to ensure stability for all values of the longitudinal curvature.

NOTATION

b	half the plate width
c	edge thickness
\bar{C}	dimensionless curvature
\bar{C}_{cr}	critical curvature
E	Young's modulus
k	dimensionless parameter defining degree of transverse camber
M	moment required to produce a longitudinal curvature, $1/R$
\bar{M}	dimensionless moment
\bar{M}_{cr}	critical moment
M_y	moment per unit length acting on a plane whose normal is in the y -direction
N_y	membrane force per unit length acting on a plane whose normal is in the y -direction
R	longitudinal radius of curvature
t	total plate thickness
t_0	half the tapered thickness measured at the center of the plate
w	deflection in z -direction of midline of cross-section from neutral surface
w_0	initial deflection of midline from neutral surface
x, y, z	rectangular co-ordinates
ν	Poisson's ratio, taken as $\frac{1}{2}$
ζ	deflection in z -direction of midline of cross-section from neutral surface due to applied moments

INTRODUCTION

WHEN a flat beam or plate is subjected to pure bending by couples applied along the edges perpendicular to the longitudinal axis, the other two edges remaining free, the beam or plate develops an anticlastic surface, the shape of which can be predicted accurately. Among others, particular reference is made to the work of Ashwell¹ in 1950. When the beam or plate has an initial transverse curvature and is subjected to the same type of loading conditions,

the analysis for the shape of the distorted cross-section can also be determined readily. Ashwell² considered the case of a uniform thickness plate having a constant initial transverse curvature, Flügge³, and Fung and Wittrick⁴ considered plates having initial tapered transverse cross-sections and, more recently, Conway and Farham⁵ and Pao and Conway⁶ have studied the problem of strips having partially tapered cross-sections.

Under the prescribed loading conditions not all of the cross-sections mentioned above result in stable equilibrium for any combination of arbitrary loading and initial transverse curvature. Two types of instability can occur, depending on the initial transverse curvature and the longitudinal curvature produced by the applied loads. If the longitudinal and initial transverse curvatures are of the same sign, the plate will exhibit torsional instability; a phenomenon described by Goodier⁷. On the other hand, if the longitudinal curvature and the initial transverse curvature are of opposite signs, the plate will exhibit a type of bending instability, the occurrence of which will depend on the particular transverse cross-section, the initial transverse curvature and the longitudinal curvature. It is this latter type of instability which will be considered here.

Ashwell² in 1952 presented theoretical and experimental results for the bending moment required to produce a given longitudinal curvature for a uniform thickness plate having a constant lateral curvature. A later paper of Ashwell's⁸ considered uniform thickness plates having corrugations of various forms in the transverse direction. In 1967, Bellow and Semeniuk⁹ showed good agreement between theory and experiment for the bending instability of rectangular plates having a cambered bitrapezoidal cross-section.

The aim of the present paper is to investigate the bending instability of rectangular plates with both uniform and tapered cross-sections having an initial transverse camber and to determine what parameters influence such instability.

THEORETICAL CONSIDERATIONS

The rectangular plates considered in this analysis will be restricted to those having cross-sections which are symmetrical about the longitudinal axis and which have a zero initial longitudinal curvature. Also, only symmetrical initial transverse deflections or curvatures will be considered. The plates will be loaded in pure bending by applying moments along the edges perpendicular to the longitudinal axis, the other two edges will remain free. The moments will be applied such that the resulting longitudinal curvature will be opposite in sign to the initial transverse curvature. Finally, the usual assumptions made for linear elasticity will be employed.

By considering the equilibrium of an element cut from a plate subjected to pure bending, the governing differential equation for the distortion of a transverse cross-section can be shown to be

$$\frac{d^2}{dx^2} \left(t^3 \frac{d^2 \zeta}{dx^2} \right) + \frac{\nu}{R} \frac{d^2(t^3)}{dx^2} + \frac{12(1-\nu^2)}{R^2} (\zeta + w_0) t = 0 \quad (1)$$

where the co-ordinate axes have been taken in accordance with Fig. 1. The distortion due to the anticlastic effects of the curvature $1/R$ is denoted by ζ and the initial transverse deflection is denoted by w_0 . In a manner similar to that used by Ashwell¹, the same equation can be derived by considering a transverse strip like a beam on an elastic

foundation where the "foundation forces" are brought about by the radial components of the membrane forces. Also, the analogy between this problem and the deformation of a cylindrical shell has been pointed out by Conway and Farham⁵.

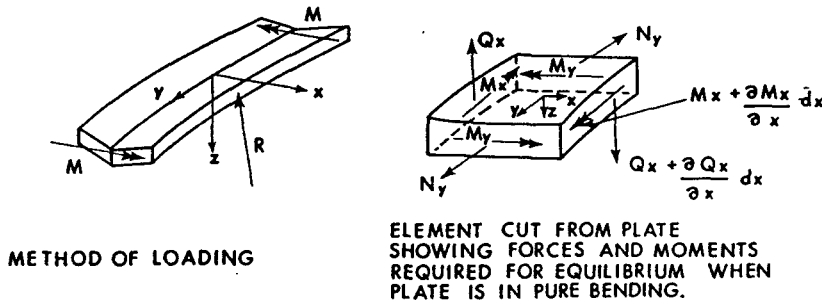


FIG. 1. Forces on plate and element cut from plate.

The solution of equation (1) consists in choosing the appropriate function of $t = t(x)$ and expressing the initial transverse deflection $w_0 = w_0(x)$ so that the x -axis coincides with the centroidal axis of the transverse cross-section. The four arbitrary constants of integration are obtained by satisfying the appropriate boundary conditions.

For the deflection equations and their method of solution reference is made to Ashwell² for a uniform thickness plate with a constant transverse curvature, to Fung and Wittrick⁴ for a plate which tapers to a line edge with an initial transverse camber, and to Bellow and Faulkner¹⁰ for a plate which tapers to a plane edge with an initial transverse camber.

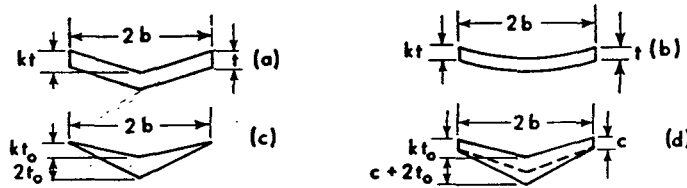


FIG. 2. Dimensions of transverse cross-sections considered.

To illustrate the method of analysis, and because it is not known to be obtainable elsewhere in the literature, the solution will be presented for a uniform thickness plate folded along the longitudinal axis as shown in Fig. 2(a). Since t is constant and $w_0 = (kt/2)(1 - 2x/b)$ for the cross-section in Fig. 2(a), equation (1) is simplified to

$$\frac{d^4 \zeta}{dx^4} + 4\lambda^4 \zeta = -2\lambda^4 kt \left(1 - \frac{2x}{b}\right)$$

and the solution becomes

$$\begin{aligned} \zeta = & A \cosh \lambda x \cos \lambda x + B \sinh \lambda x \sin \lambda x + C \cosh \lambda x \sin \lambda x \\ & + D \sinh \lambda x \cos \lambda x - \frac{kt}{2} \left(1 - \frac{2x}{b}\right) \end{aligned} \quad (2)$$

where

$$4\lambda^4 = \frac{12(1-\nu^2)}{R^2 t^2}$$

For the cross-section of Fig. 2(a) the boundary conditions are: the deformation is symmetrical about the y -axis, there is no moment or shear at the free edge, and there is

no resulting force in the y -direction. Thus, when the conditions

$$\frac{d\zeta}{dx} = 0 \quad \text{at } x = 0$$

$$\frac{d^2\zeta}{dx^2} = -\frac{\nu}{R} \quad \text{at } x = b$$

$$\frac{d^3\zeta}{dx^3} = 0 \quad \text{at } x = b$$

$$\int_0^b \zeta dx = 0$$

are applied to equation (2) the following four equations are obtained

$$-\frac{kt}{\lambda b} = C + D$$

$$\frac{\nu}{2\lambda^2 R} = A \sinh \lambda b \sin \lambda b - B \cosh \lambda b \cos \lambda b - C \sinh \lambda b \cos \lambda b \\ + D \cosh \lambda b \sin \lambda b$$

$$0 = (A - B) \sinh \lambda b \cos \lambda b + (A + B) \cosh \lambda b \sin \lambda b \\ + (C + D) \sinh \lambda b \sin \lambda b + (D - C) \cosh \lambda b \cos \lambda b$$

$$0 = (A - B) \sinh \lambda b \cos \lambda b + (A + B) \cosh \lambda b \sin \lambda b \\ + (C + D) \sinh \lambda b \sin \lambda b + (D - C) (\cosh \lambda b \cos \lambda b - 1) \quad (3)$$

Solving the equations in (3) for the constants A , B , C and D and substituting these into equation (2) results in the solution for the transverse deflection of a rectangular plate having a cross-section as in Fig. 2(a) when bent into a longitudinal curvature $1/R$.

In order to determine the bending moment required to produce the longitudinal curvature, both the moment M_y and the moment of the membrane force N_y about the centroidal x -axis must be integrated over the width of the cross-section. This results in the following expression:

$$M = 2 \int_0^b M_y dx + 2 \int_0^b N_y (\zeta + w_0) dx$$

or

$$M = -\frac{2Et^3}{12(1-\nu^2)} \int_0^b \left(\frac{1}{R} + \nu \frac{d^2\zeta}{dx^2} \right) dx - \frac{2Et}{R} \int_0^b (\zeta + w_0)^2 dx \quad (4)$$

where t = constant for the example chosen. Substituting equation (2) into (4) leads to the moment-curvature relationship below:

$$M = -\frac{Et^3}{6(1-\nu^2)} \left\{ \frac{b}{R} + \nu \lambda \left[(A + B) \sinh \lambda b \cos \lambda b - (A - B) \cosh \lambda b \sin \lambda b \right. \right. \\ \left. \left. + (C + D) (\cosh \lambda b \cos \lambda b - 1) + (C - D) \sinh \lambda b \sin \lambda b \right] \right\} \\ - \frac{Et}{8\lambda R} \{ (A^2 - B^2 - C^2 + D^2 - 2AB - 2CD) \sinh 2\lambda b \cos 2\lambda b \\ + 2(A^2 + B^2 + C^2 + D^2) \sinh 2\lambda b + (A^2 - B^2 - C^2 + D^2 \\ + 2AB + 2CD) \cosh 2\lambda b \sin 2\lambda b + 4(AD + BC) \cosh 2\lambda b \\ + 2[A(C + D) - B(C - D)] \sinh 2\lambda b \sin 2\lambda b \\ + 2[A(D - C) - B(C + D)] \cosh 2\lambda b \cos 2\lambda b \\ + 2(A^2 + B^2 - C^2 - D^2) \sin 2\lambda b + 4(BD - AC) \cos 2\lambda b \\ + 4\lambda b(A^2 - B^2 + C^2 - D^2) + 6A(C - D) - 2B(C + D) \} \quad (5)$$

where the constants A , B , C and D are determined by solving the equations in (3) simultaneously. Equation (5) along with the equations in (3) were evaluated on a digital computer for various values of the camber k . The results are plotted in Fig. 3, where

$$\bar{M} = \frac{4b^2 M}{Et^3}$$

and $I = 2bt^3/12$ for the cross-section when $k = 0$, yielding

$$\bar{M} = \frac{24bM}{Et^3}$$

and

$$C = \frac{4b^2}{Rt}$$

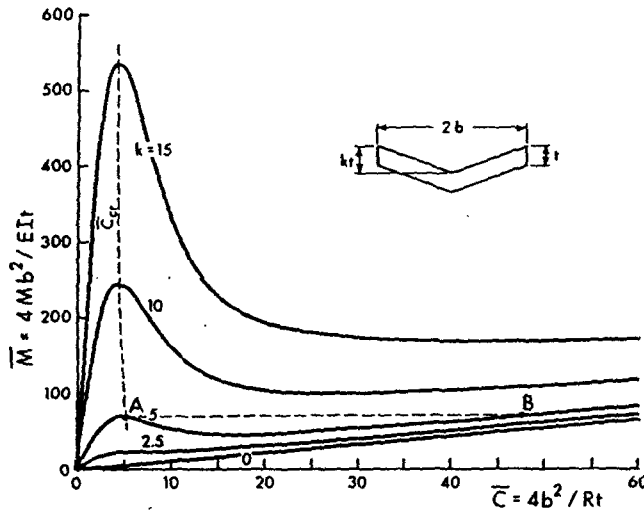


FIG. 3. Moment-curvature relationship for a folded plate with a uniform thickness for various values of transverse camber k .

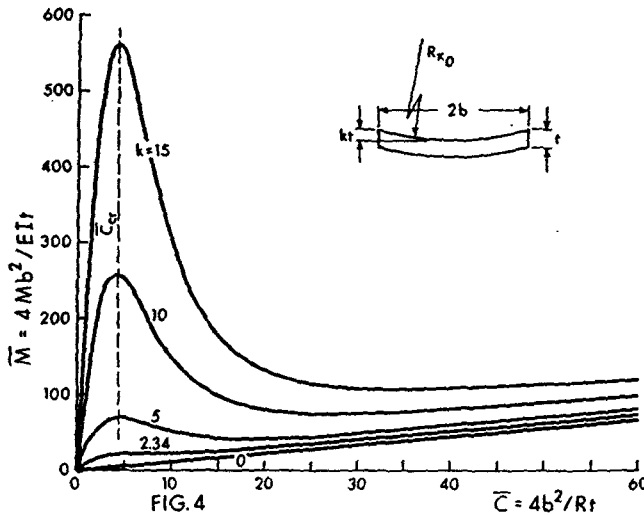


FIG. 4. Moment-curvature relationship for a uniform thickness plate with constant curvature for various values of transverse camber k .

In a manner similar to that described above, moment-curvature relationships were determined for all the cross-sections shown in Fig. 2. For the tapered sections in Figs. 2(c)

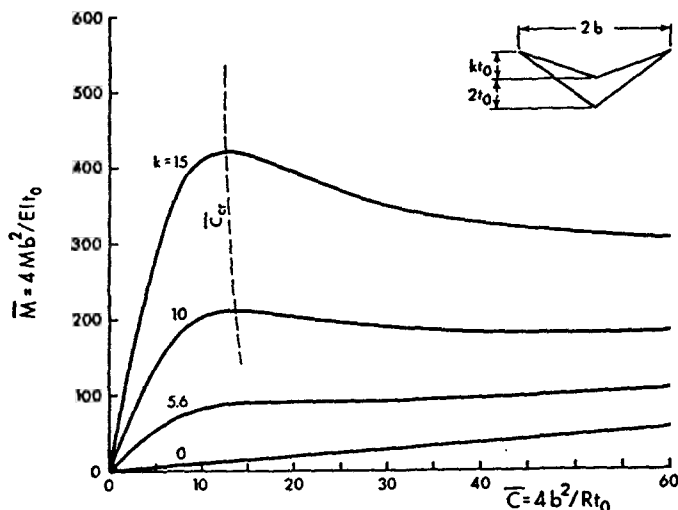


FIG. 5. Moment-curvature relationship for a plate with a tapered cross-section for various values of transverse camber k .

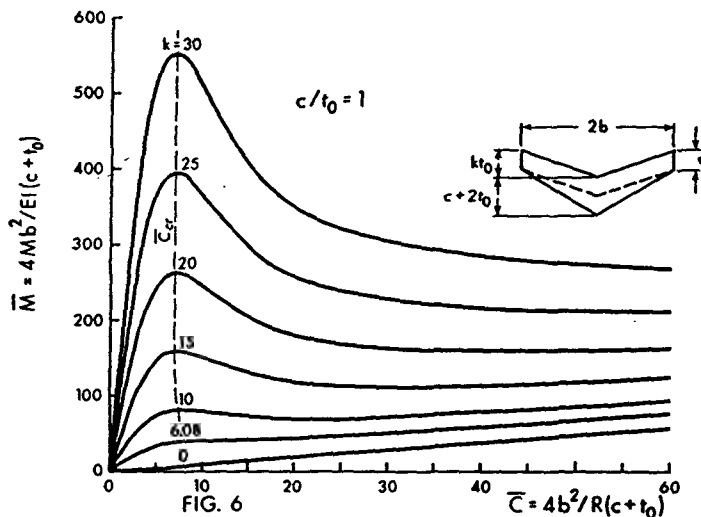


FIG. 6. Moment-curvature relationship for a plate with a bitrapezoidal cross-section for various values of transverse camber k at an edge thickness of $c/t_0 = 1$.

and (d) the solution of the differential equation (1) yields a Bessel equation which, when substituted into equation (4) and evaluated,⁹ results in a rather complicated expression for M , nonetheless, obtainable with patience. For these cross-sections the results were also obtained on a digital computer and are plotted in Figs. 4-7.

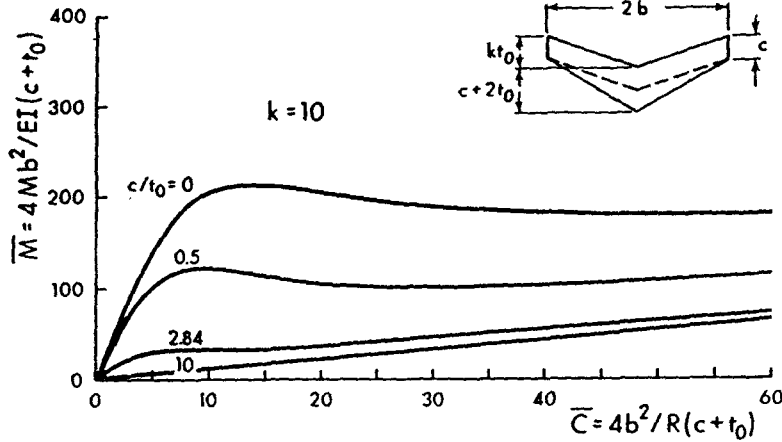


FIG. 7. Moment-curvature relationship for a plate with a bitrapezoidal cross-section for various values of edge thickness at a constant camber $k = 10$.

DISCUSSION OF MOMENT-CURVATURE RESULTS

The moment-curvature relationships for a uniform thickness plate folded along its longitudinal axis are shown in Fig. 3 for various values of the transverse camber k . For a flat plate $k = 0$, and when k is increased the applied moment \bar{M} required to maintain a given curvature \bar{C} is also increased. Furthermore, the general shapes of the \bar{M} - \bar{C} curves change, as k is increased, from ones whose slopes are always positive to ones whose slopes change sign; that is to say, as k is increased the \bar{M} - \bar{C} curves possess an extremum. The co-ordinates of an extremum will be denoted by $\bar{M}_{cr}, \bar{C}_{cr}$.

The existence of an extremum characterizes the instability of such a plate since increasing $\bar{C} > \bar{C}_{cr}$ results in a decrease in the value of \bar{M} . A plate will be classified as inherently unstable if an extremum point exists anywhere along the path of the \bar{M} - \bar{C} curve. It should be mentioned that in practice, unless one has a reaction-type loading, the negative slope portion of the \bar{M} - \bar{C} curve will never be experienced. This is because under a dead-weight type loading the instant $\bar{C} > \bar{C}_{cr}$ the plate will snap through to a new value of \bar{C} on the curve whose slope is positive again. This is indicated by the horizontal broken line between the points A and B in Fig. 3 and has been verified experimentally for the bitrapezoidal cross-section of Fig. 2(d) by Bellow and Semeniuk⁸.

It is clear from Fig. 3 that there will be one \bar{M} - \bar{C} curve for which the slope will change from a positive value, through zero, to a positive value again. This curve corresponds to the limiting value of k , since an increase in k results in a maximum at \bar{C}_{cr} and a decrease in k results in stable equilibrium for all values of \bar{C} . In order to determine the limiting value of k , the moment-curvature relationship must satisfy simultaneously the two conditions

$$\frac{d\bar{M}}{d(1/R)} = 0, \quad \frac{d^2\bar{M}}{d(1/R)^2} = 0 \quad (6)$$

In other words, equation (5) along with the expressions for A , B , C and D from the equations in (3) must be substituted into the above expression in (6), thus yielding two equations in the unknowns k and \bar{C} . From these two equations the limiting value of k can be determined. Obviously this is an almost impossible task, even for the relatively simple cross-section of Fig. 2(a). Instead, the procedure followed was to evaluate the moment-curvature relationship (5) over a large range of longitudinal curvatures for different values of k , and by closely examining the results with respect to satisfying the conditions in (6), the limiting value of k was determined.

Thus, it is shown in Fig. 3 that for the folded uniform thickness plate the limiting value of k is $k = 2.50$. Also, for $k > 5$ it is observed that \bar{M}_{cr} occurs at approximately the same value of $\bar{C}_{cr} = 4.2$.

A similar analysis can be made for the uniform thickness plate with constant initial transverse curvature (Fig. 2(b)), the results of which are plotted in Fig. 4. Again, the critical value of \bar{M} occurs at approximately $\bar{C}_{cr} = 4.2$, but the limiting value of k for which the plate is inherently unstable is $k = 2.34$, slightly less than for the folded plate in Fig. 3. Also, it is seen that for a given value of k the value of \bar{M}_{cr} is slightly greater than that observed for the folded plate. This may be explained in part by the fact that the moment of inertia of the cross-section for the curved plate is slightly greater than that for the folded plate having the same camber k . The curves in Fig. 4 can be compared with the work of Ashwell² by noting that $k = [b^2/2R_x t] = [C_x/8]$ for $k \ll b$, where C_x is the initial dimensionless curvature in the transverse direction.

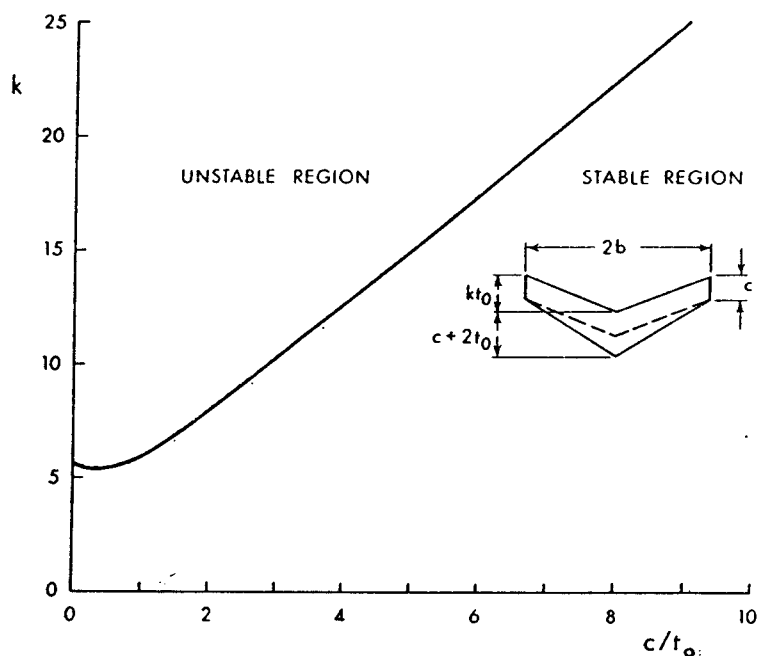


FIG. 8. Stability relationship between edge thickness and transverse camber for a plate with a bitrapezoidal cross-section.

The moment-curvature results for the cambered tapered plate cross-section of Fig. 2(c) are shown in Fig. 5. For this case the values of \bar{M} and \bar{C} have been calculated using t_0 as the average value of the plate thickness. From the results it is shown that the limiting value of $k = 5.6$. However, the value of \bar{C}_{cr} is not the same for each curve but rather is a function of the camber k . This is indicated by the vertical curved dotted line. However, for large values of k the dotted line straightens out indicating a $\bar{C}_{cr} = 12$ approximately for $k > 15$.

For a rectangular plate having a cambered bitrapezoidal cross-section of Fig. 2(d) the moment-curvature relationship is affected both by a change in the camber k and the edge thickness c . To illustrate this, Fig. 6 shows, for a value of $c/t_0 = 1.0$, the shape of the \bar{M} - \bar{C} curves for various values of k . For these results it is evident that \bar{M}_{cr} occurs at approximately $\bar{C}_{cr} = 7$ and the limiting value of k is 6.08. In Fig. 7 the \bar{M} - \bar{C} curves are plotted for various values of the edge thickness, c/t_0 , for a fixed value of the camber $k = 10$. The value of the critical curvature is not constant for various values of edge thickness, however, for $k = 10$ the limiting value of the edge thickness for which the plate is inherently stable is $c/t_0 = 2.84$. In each of the Figs. 6 and 7, \bar{M} and \bar{C} have been calculated using $(t_0 + c)$ as the average plate thickness.

Because of the interdependence of k and c/t_0 on the stability of the cambered bitrapezoidal plate with edge thickness the relationship between k and c/t_0 has been plotted

in Fig. 8. This curve represents c/t_0 vs. the limiting value of k . That is, any combination of c/t_0 and k below the curve results in stable equilibrium for all values of longitudinal curvature, while any point above the curve results in the plate being inherently unstable. When $c/t_0 = 0$ the limiting value of k is seen to be equal to 5.6. This agrees with the results in Fig. 5 obtained for the tapered section of Fig. 2(c).

A further observation can be made from Fig. 8 regarding stability. If a cambered plate is inherently unstable, keeping the camber constant, one only needs to increase the edge thickness an appropriate amount to bring the $(k, c/t_0)$ value to the right-hand side of the curve and the plate will then be stable for all values of longitudinal curvature.

CONCLUSIONS

1. It has been shown that rectangular plates having some type of initial transverse camber can exhibit a type of bending instability when subjected to pure bending. However, not all such rectangular plates with initial transverse camber will exhibit this instability. Moreover, it has been demonstrated that for such a plate to be inherently unstable the transverse camber k must exceed a certain limiting value; the value of which depends on the type of cross-section under consideration.

2. For a given cross-section, increasing the camber increases the stiffness and as a result increases the value of the critical moment. However, generally this does not appreciably affect the value of the longitudinal curvature at which instability occurs. For the cross-sections considered the one exception to this was the bitrapezoidal cross-section which tapered to a line edge (Fig. 2(c)). For this case, increasing the camber k increased the critical moment \bar{M} , while slightly decreasing the critical value of the longitudinal curvature.

3. For a cambered bitrapezoidal cross-section with edge thickness (Fig. 2(d)) it was shown that by increasing the edge thickness c for the same camber k it is possible to make a plate which is stable for all values of longitudinal curvature. A graph was presented showing k vs. c/t_0 which is useful in designing such plates for complete stability.

Acknowledgement—The authors express their appreciation to the National Research Council (Ottawa) for the financial support of this research under grant number A-2705.

REFERENCES

1. D. G. ASHWELL, *Jl R. aeronaut. Soc.* 54, 708 (1950).
2. D. G. ASHWELL, *Proc. R. Soc. A* 214, 98 (1952).
3. W. FLÜGGE, Tech. Report No. 3, Air Forces Contract (U.S.) W33-038 AC-16697 (1949).
4. Y. C. FUNG and W. H. WITTRICK, *J. appl. Mech.* 21, 351 (1954).
5. H. D. CONWAY and K. A. FARHAM, *Int. J. mech. Sci.* 7, 811 (1965).
6. Y. C. PAO and H. D. CONWAY, *Int. J. mech. Sci.* 8, 65 (1966).
7. J. N. GOODIER, *J. appl. Mech.* 9, A-103 (1942).
8. D. G. ASHWELL, *Jl R. aeronaut. Soc.* 56, 782 (1952).
9. D. G. BELLOW and A. SEMENIUK, *Exp. Mech.* 7, 309 (1967).
10. D. G. BELLOW and M. G. FAULKNER, *Exp. Mech.* 7, 392 (1967).

An Investigation into the evaluation of Hockey Helmets

D. G. BELLOW*, S. MENDRYK**,
AND V. SCHNEIDER**

**Department of Mechanical Engineering,*

***Faculty of Physical Education, University of Alberta,
Edmonton 7, Alberta, Canada*

ABSTRACT. A testing apparatus and technique is described for the evaluation of the impact absorption characteristics of hockey helmets. Ten hockey helmets were tested. The test consisted of placing a hockey helmet on a wooden headform suspended from the ceiling by cables, and impacting the helmet and headform assembly by a pendulum at predetermined impact velocities. The effectiveness of a helmet was evaluated by measuring the peak acceleration, calculating the maximum kinetic energy absorbed, and considering the shape of the acceleration-time-curve obtained from a piezoelectric accelerometer embedded in the headform. It was demonstrated that the testing technique and apparatus was capable of detecting differences between one helmet and another, between one position and another position on the same helmet, and that the results were repeatable. It was suggested that three parameters be used for evaluating the protectiveness of a helmet. These are; the general shape of an acceleration-time-curve, the peak acceleration, and the maximum kinetic energy absorbed in the headform.

INTRODUCTION

A review of the literature (2,3,4,5,6,7,8,9) shows that the design and evaluation of athletic protective headgear has been the object of many investigations.

That these investigations are continuing indicates the growing concern people have for the ensured safety of athletes in competitive sports. Of the recent publications, attention has either been focused on the mechanisms of head and neck injuries in general, or on an examination of the protective characteristics of football helmets in particular. This paper is an attempt to reassess the evaluation of athletic protective headgear and suggest a testing technique and means upon which hockey helmets should be compared and evaluated.

Increased interest and participation in ice hockey in Canada, the United States, and Europe has resulted in the need for an appraisal of the relative effectiveness of hockey helmets. Head and facial injuries are most common in ice hockey and are usually of a minor nature (10). However, possible severe consequences of head injuries necessitates adequate protection even though the incidence of serious head injury is rare. In fact, the wearing of a helmet does not preclude serious and fatal injury as evidenced by a recent report (1) of the fatalities of two minor league hockey players who were wearing helmets. Hockey helmets must be adequately evaluated in order to determine the optimum design for protection under any and all game conditions as well as considering the comfort of the wearer.

Submitted for publication October, 1969.

EXPERIMENTAL EQUIPMENT AND PROCEDURES

Introduction

The first stage of this investigation was to design an experimental apparatus and develop suitable testing procedures so that a comparative study could be obtained on the impact resistance of protective headgear which would produce meaningful results. In particular one of the primary aims in the design of the experimental apparatus was to obtain a test setup which would produce results which would be repeatable.

Experimental Apparatus

A general view of the apparatus is shown in Figure 1. Essentially this consists of an impact frame to which a striker arm is mounted, a headform support and cable arrangement, and a release mechanism for the striker arm. This testing setup does not differ greatly from previous investigations, and while it may be adapted to any type of protective headgear, it was designed specifically for a comparative evaluation of hockey helmets. To this end the striker arm was fitted with a small piece of wood taken from a hockey stick which would represent an impact by a hockey stick or rink boards on a hockey helmet. This would at least ensure a realistic coefficient of restitution between the helmet and striker arm. The striker arm made contact with the headform at the center of percussion of the striker arm so that no impact would be transmitted to the pillow-block bearings and the impact frame. The head-

form, which was supported from the ceiling on cables approximately 10 feet long, was carved from laminated oak to accommodate $7\frac{1}{4}$ in. size hockey helmets. An accelerometer was placed in the headform on the opposite side from which the striker arm made contact with the helmet. The release mechanism was a simple relay which allowed the striker arm to fall from different predetermined heights with no vibrations.

Energy is not conserved in the impact process. Only the kinetic energy absorbed in the headform was measured. No consideration was given to how the energy before impact was dissipated during impact or after impact. The comparative study was developed on the premise that for any given velocity of the pendulum just prior to impact, the helmet showing the lowest energy absorbed (as measured in headform deformations) would be the superior helmet compared with the others tested.

Figure 2 shows how the accelerometer was attached to the wooden headform. The headform was attached to the metal supporting plates which allowed the helmet to be hit at different positions. The accelerometer which was used was a uniaxial piezoelectric type, (Bruel and Kjaer 4332) and therefore the helmets were tested at the front and back positions only (i.e. positions which, when impacted, produced accelerations in the direction of the axis of maximum sensitivity of the accelerometer). The accelerometer was always placed diametrically opposite the point of impact. In order that the helmet may be hit at the side and at 45° positions a different headform arrangement would

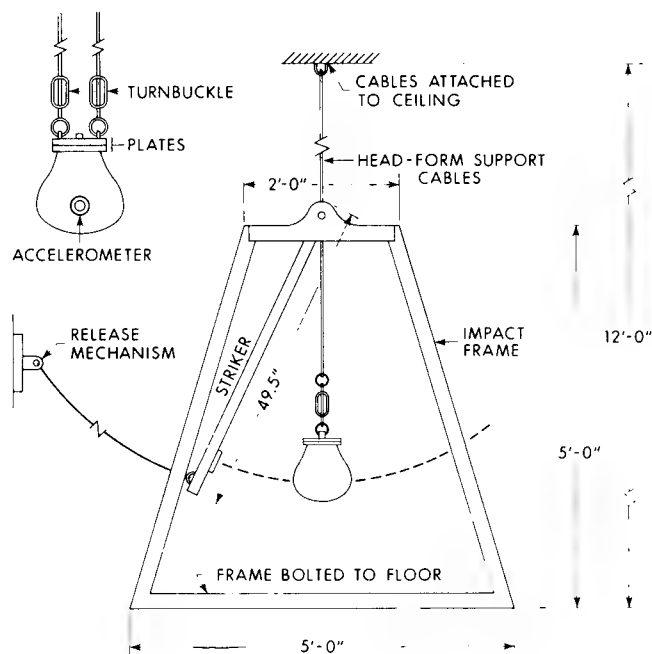


Figure 1 — Experimental Apparatus

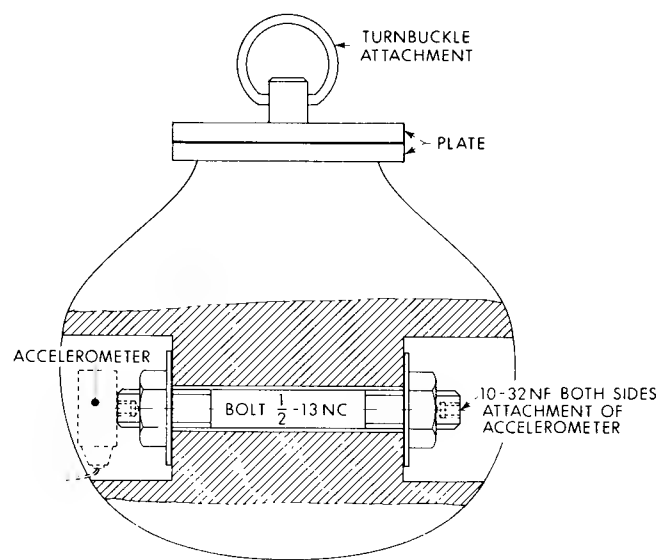


Figure 2 — Headform and Accelerometer

have to be used with the incorporation of a triaxial accelerometer. The triaxial accelerometer would permit the determination of the principal direction and principal magnitude of acceleration.

The output signal from the accelerometer was connected to a Bruel and Kjaer 2616 preamplifier and the resulting signal displayed on the screen of a Tektronix 564 storage oscilloscope. The oscilloscope was adjusted for single sweep operation and the output signal from the accelerometer was used to automatically trigger the horizontal sweep. The resulting acceleration-time-curve was then photographed for permanent record and later analysis.

Testing Procedures

Each helmet was carefully fitted to the wooden headform, and attention was given to ensure that each helmet covered the same portion of the headform. Prior to a blow being delivered, the headform, helmet, and pendulum were aligned so that when the pendulum made contact with the helmet, the pendulum would be in a completely vertical position and at its maximum velocity. If required, the headform and helmet assembly could be raised or lowered by means of the adjustable clamps attached to the cable suspension system. For each helmet, for each position, and for each velocity tested, three oscilloscope traces were recorded. Thus, for one helmet to be tested at the front and back positions, for five different impact velocities, 30 readings were taken.

The hockey helmets tested are listed in Table 1. This Table indicates that the helmets differed in weights and styles as well as in the type of construction. Hockey helmet design varies from one-piece construction similar to football helmets to the common two and three-piece types. Because of the single axis sensitivity of the accelerometer used in this test, blows were not impacted on the helmet other than the front and back positions. The manufacturer of each helmet has not been identified because it is not the intent of this paper to judge the "best" helmet but rather to suggest a suitable evaluation procedure.

ANALYSIS AND RESULTS

Introduction

For each of the acceleration-time-curves obtained, the peak or maximum acceleration was recorded and the area under the acceleration-time-curves was integrated. It was believed that the assessment of the impact absorbing qualities of a helmet should be based on the kinetic energy absorbed by the helmet or transmitted to the head as well as the peak acceleration absorbed by the helmet or transmitted to the head. In this test the peak acceleration absorbed by the helmet or the kinetic energy absorbed by the helmet was not determined, but instead, the peak acceleration and kinetic energy measured in the headform was obtained. Thus for any given impact conditions the helmet or helmets which indicated the lowest amount of energy absorbed and the lowest peak acceleration measured in the headform would be deemed superior to the remaining helmets tested. Typical acceleration-time-curves as photographed from the oscilloscope are shown in Figure 3.

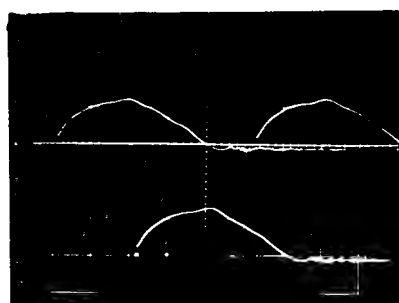
For all of the results obtained, no evidence of fatigue was observed on the helmets. This was to be expected since the number of blows for a given impact area were relatively small, and the stresses involved were within the elastic range of the materials. However, on some of the helmets the material used to line the surfaces was of a visco-elastic nature and as a result exhibited a time effect in the elastic recovery after the helmet was subjected to an impact. This was overcome by allowing the helmet sufficient time, generally 5 to 10 minutes, to regain its original configuration before subjecting it to another impact.

In order to test the helmets so that the acceleration absorbed in the headform was within the range of 0 to 50 g's, the pendulum velocity was varied between 0 and 70 in/sec. The object of this study was to comparatively evaluate one helmet with another within the range of accelerations which are known to be tolerable by humans (4). Thus, for the helmets tested, a player wearing any of these helmets would not have suffered any head injuries when subjected to the test impacts.

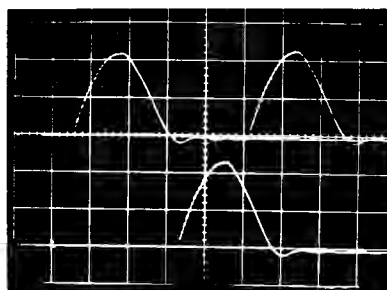
TABLE 1. Helmet Details

Helmet	Approximate Retail Price	Weight oz.	Plastic Material Thickness	Finish		Design
				Exterior Covering	Interior Finish	
A	\$ 6.00	10	1/8"	None	1/4" P.F.	2 piece
B	6.00	9.5	1/8"	None	3/16" P.F.	3 piece
C	10.00	12	1/8"	None	3/16" R.	3 piece
D	20.00	15	1/8"	1/16" R.&L.	3/16" R. & L.	3 piece
E	7.00	8	1/16"	None	R.	2 piece
F	20.00	20	3/16"	None	*	1 piece
G	5.00	10	1/8"	None	3/16" P.F.	2 piece
H	9.00	11.5	1/8"	None	1/4" P.F.	2 piece
I	19.00	15	1/8"	1/8" P.F.	1/4" P.F.	2 piece
J	10.00	11	1/8"	None	1/4" R.	2 piece

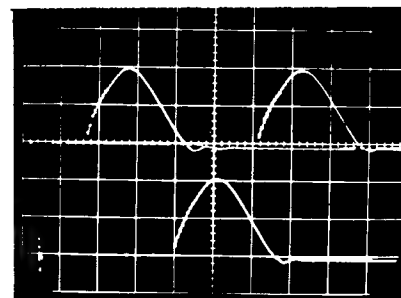
L. Leather: R. Rubber-like substance (Rubatex): P.F. Plastic Foam (Polyethylene): * Football type helmet suspension system



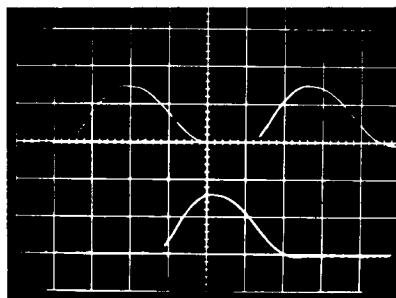
Helmet: "A"
Vertical: 0.5 volt/cm.
Horizontal: 5 ms./cm.



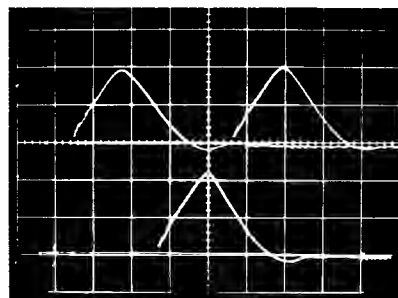
Helmet: "B"
Vertical: 0.5 volt/cm.
Horizontal: 5 ms./cm.



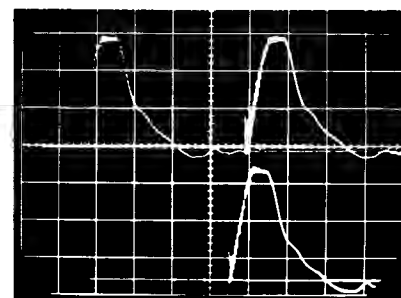
Helmet: "C"
Vertical: 0.5 volt/cm.
Horizontal: 5 ms./cm.



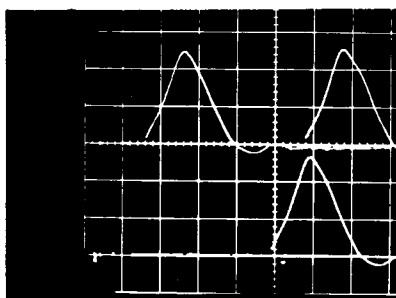
Helmet: "D"
Vertical: 0.5 volt/cm.
Horizontal: 5 ms./cm.



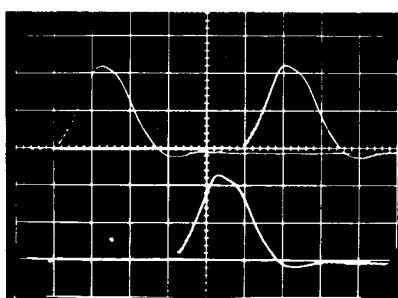
Helmet: "E"
Vertical: 0.5 volt/cm.
Horizontal: 5 ms./cm.



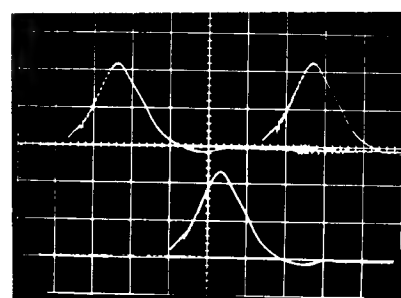
Helmet: "F"
Vertical: 0.2 volt/cm.
Horizontal: 10 ms./cm.



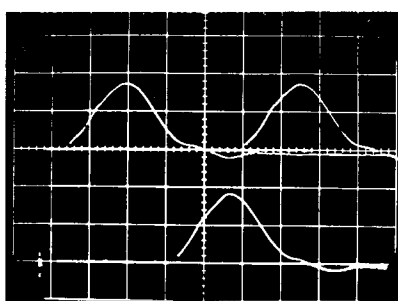
Helmet: "G"
Vertical: 0.5 volt/cm.
Horizontal: 5 ms./cm.



Helmet: "H"
Vertical: 0.5 volt/cm.
Horizontal: 0.5 ms./cm.



Helmet: "I"
Vertical: 0.5 volt/cm.
Horizontal: 5 ms./cm.



Helmet: "J"
Vertical: 0.5 volt/cm.
Horizontal: 5 ms./cm.

Figure 3 — Typical Acceleration-time-curves

Peak Acceleration

Peak acceleration was obtained from the acceleration-time-curves by measuring from the base line (zero acceleration) to the maximum amplitude. Because the photograph of the graticule was slightly smaller than actual size, a correction factor of 1.075 was applied to the amplitude of the acceleration scaled from the photograph. This value in cm was multiplied by the vertical sensitivity of the oscilloscope in volts/cm and divided by the sensitivity of the accelerometer in volts/g. The resulting value was the peak acceleration expressed in g units, where $g = 386 \text{ in/sec}^2$.

Kinetic Energy

Measuring the area under the acceleration-time-curve yielded the maximum velocity attained by the headform, and when this value was squared and multiplied by half the mass of the headform and helmet assembly, the maximum kinetic energy absorbed in the headform was obtained.

The integration of the acceleration-time-curves was made by measuring the area under the curve with a planimeter. A correction factor had to be applied to the areas obtained from the photographs. This consisted of multiplying the areas by $(1.075)^2$ or 1.16. By multiplying the corrected area under the curve (cm^2) by the horizontal (secs/cm) and vertical (volts/cm) sensitivity of the oscilloscope and dividing by the accelerometer sensitivity (volts/g), the maximum velocity, expressed in in/sec, was determined.

RESULTS

The results of the analyses of the acceleration-time-curves are presented in Figures 4 to 7. In Figures 4 and 5, peak acceleration as measured in the headform is

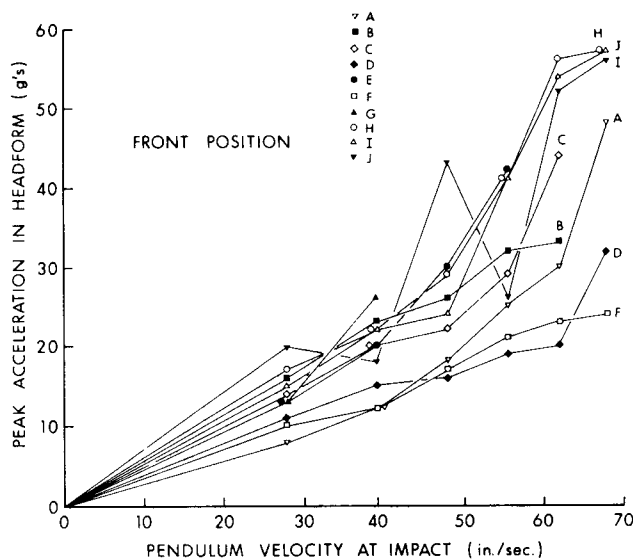


Figure 4 — Peak Acceleration; front position

plotted versus the pendulum velocity at the instant of impact. Figure 4 shows the results when the pendulum struck the front of the helmets, and Figure 5 shows the results when the pendulum struck the back of the helmets.

In Figures 6 and 7 the maximum kinetic energy measured in the headform is plotted versus the impact velocity of the pendulum. Figure 6 shows the results when the pendulum struck the front position of the helmets and Figure 7 when the pendulum struck the back of the helmets.

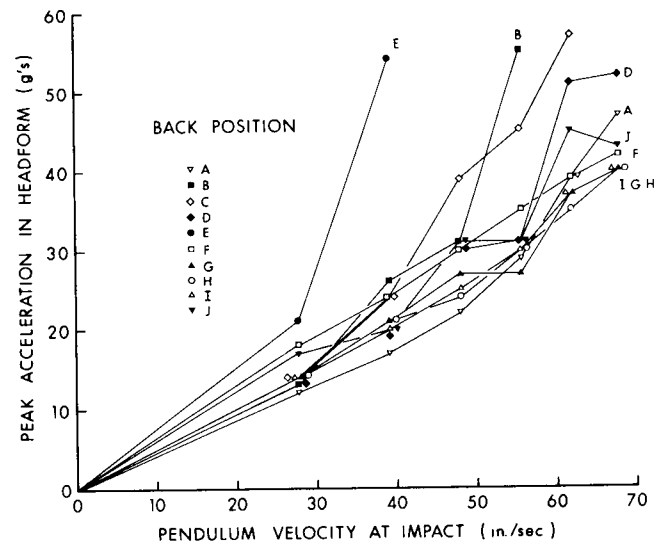


Figure 5 — Peak Acceleration; back position

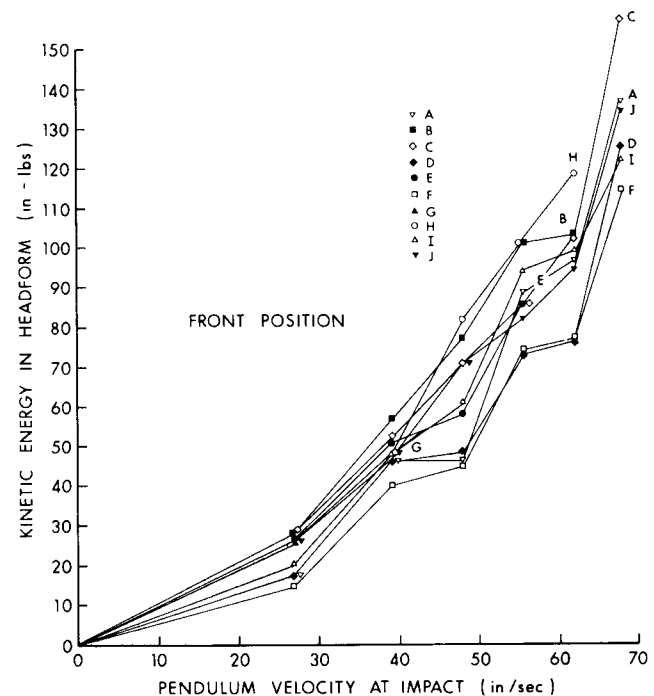


Figure 6 — Kinetic Energy; front position

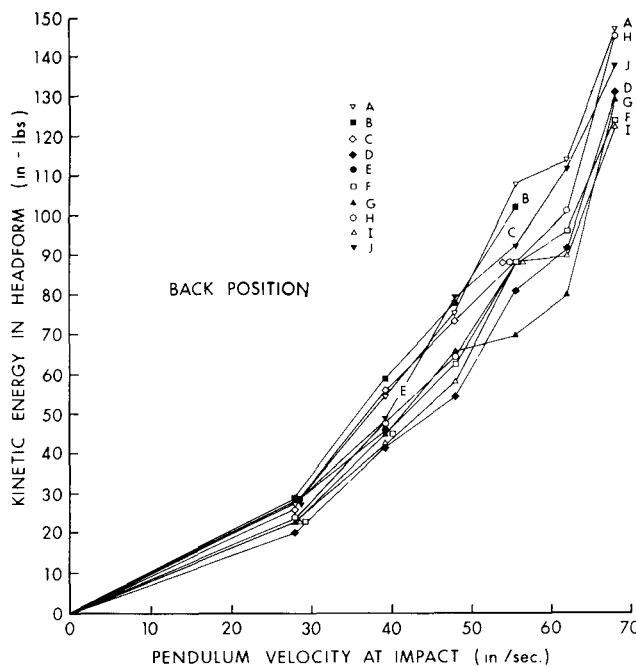


Figure 7 — Kinetic Energy; back position

DISCUSSION

In Figure 3 acceleration-time-curves have been selected for each of the helmets when impacted at the front position with a velocity of the pendulum of 39.2 in/sec. These curves are typical of all of the results obtained for the other velocities tested. Below each set of curves is indicated the vertical and horizontal sensitivities of the oscilloscope setting. That the testing technique was precise is shown by observing that each of the curves in a specific group are identical. It is evident from these curves that different helmets respond differently to the same impact blow. For example, some of the curves are similar in shape to a sinusoid while others are more saw-tooth in shape. It was also observed that at the higher velocities some of these differences in shapes of acceleration-time-curves were even more pronounced. For example, some acceleration-time-curves showed two peaks occurring for a single impact blow.

Another observation from the curves in Figure 3 is that it is possible for two helmets to have the same peak acceleration and yet because one curve has a broader base relative to another, greater kinetic energy has been absorbed in the headform. Such is the case between the "F" and "A" helmets. Both have the same peak acceleration of 10.2 g's but the energy transmitted to the headform through the "A" helmet is 15 percent greater than that transmitted to the headform through the "F" helmet. This illustrates that the measurement of peak acceleration is not a complete assessment of the impact absorption qualities of a helmet and there is a need also to integrate under the acceleration-time-

curve to obtain a measurement of the kinetic energy absorbed.

In Figures 4 and 5 peak accelerations recorded by the accelerometer are shown when the blows were impacted on the front and back of the helmets. In general the peak accelerations were lower for the same impact velocity when the helmets were impacted at the front than when impacted at the back. More importantly in Figure 4 and 5 it is shown clearly that differences in helmets can be detected on the basis of peak acceleration. Some helmets show a decrease in the slope of the peak acceleration versus velocity curves with increase in impact velocity, while others show an increase.

The importance of testing a helmet at more than one position is shown by comparing the results of Figure 4 with the results of Figure 5. For example the "F" helmet which appears to be superior to the other helmets tested for the front position was not as good as some of the other helmets when tested in the back position. While certain comparisons can be made from these curves as to the effectiveness of a particular helmet, it must be remembered that there were only two positions on each helmet that were tested and that it would be erroneous to conclude that one helmet was superior to another. The results are presented here only to show the manner in which helmets can be evaluated and to indicate that the testing technique has merit.

Similar comparisons can be made for the helmets on the basis of the kinetic energy absorbed in the headform as shown in Figure 6 and 7. Thus, the helmet which shows the lowest amount of kinetic energy absorbed in the headform obviously has absorbed more kinetic energy and therefore is deemed to be superior to one which transmits most of the kinetic energy into the headform. As in the peak acceleration curves, the kinetic energy absorbed in the headform as a function of the impact velocity, shows that different helmets respond to the same impact velocity differently.

There is less scatter with the results plotted in Figures 6 and 7 than those recorded for the peak accelerations in Figures 4 and 5. This is due in part to the fact that the curves represented in Figures 6 and 7 are based on integrated values which tend to average out the predominant features of an acceleration-time-curve. Because of this there was little difference in the kinetic energy absorbed in the helmets between the front and back positions, although for some helmets, the differences could be considered significant.

SUMMARY

A testing apparatus and technique has been described for the evaluation of the impact absorption characteristics of athletic headgear. To illustrate the effectiveness of the testing method, ten hockey helmets were tested. The results showed that the technique and apparatus was capable of detecting differences between one helmet and another and that the results were repeatable.

Three methods for evaluating the effectiveness of a hockey helmet were investigated: the general shape of an acceleration-time-curve, the peak acceleration, and the area under the acceleration-time-curve. It was shown that to evaluate helmets on the basis of peak acceleration alone was not adequate in that two helmets could be absorbing different kinetic energies and yet still have the same peak acceleration. Also, a certain amount of information can be obtained by just comparing the shapes of the acceleration-time-curves. For instance, a numerical figure either in peak acceleration or kinetic energy absorbed would not indicate whether a particular acceleration-time-curve had two peaks, whether the peak acceleration was held for a length

of time, or whether it occurred for only an instant. Therefore, it is important to evaluate helmets on the basis of three factors, shape of acceleration-time-curves, peak acceleration, and the area under the acceleration-time-curve which relates to the kinetic energy absorbed.

The experimental results showed that there could be differences in a single helmet depending on what position the helmet was being impacted. It is evident from the results that to completely evaluate the effectiveness of a helmet a considerable amount of testing will have to take place involving a great number of test positions on the helmet.

REFERENCES

1. FEKETE, J. F. Severe Brain Injury and Death Following Minor Hockey Accidents: The Effectiveness of the Safety Helmets of Amateur Hockey Players. *Canad. Med. Ass. J.* 99:1234-1238, 1968.
2. FENNER, HAROLD A. Football Injuries and Helmet Design. *Gen. Pract.* 30:106-113, 1964.
3. GURDJIAN, E. S., H. R. LISSNER, V. R. HODGSON, W. G. HARDY AND L. W. PATRICK. Evaluation of the Protective Characteristics of Helmets in Sports. *J. Trauma.* 40:309-324, 1964.
4. GURDJIAN, E. S., H. R. LISSNER AND L. M. PATRICK. Protection of the Neck and Head in Sports. *JAMA* 182:509-512, 1962.
5. KOVACIC, CHARLES. Impact-Absorbing Qualities of Football Helmets. *Res. Quart.* 36:421-426, 1965.
6. NELSON, RICHARD C., JOHN F. ALEXANDER, HENRY J. MONTOYE AND WAYNE D. VAN HUSS. An Investigation of Various Measures Used in Impact Testing of Protective Head Gear. *J. Sports Med.* 4:94-101, 1964.
7. PATRICK, L. M. Head Impact Protection. Head Injury Conf. Proc. Lippincott: 41-48, 1962.
8. Proc. of the National Conf. on Head Protection for Athletes. Chicago. 1962.
9. SNIVELY, GEORGE C., CHARLES KOVACIC AND C. O. CHICHESTER. Design of Football Helmets. *Res. Quart.* 32:221-228, 1961.
10. TOOGOOD, TED AND W. G. LOVE. Hockey Injury Survey, *J. Can. Assoc. HPER.* 32:20-23, 1966.

On the Experimental Investigation of the Stiffness of Clamped Machined Surfaces

Experiments conducted to determine the effects of surface texture and normal load on the stiffness of joints formed by two machined surfaces are discussed by the authors

by D. G. Bellow and D. D. Nelson

ABSTRACT Experiments were conducted to determine the effects of surface texture and normal load on the stiffness of joints formed by two machined surfaces. The experiments involved deformation measurements and examination of the contact surfaces of joints subjected to normal loads. It was shown that surface-displacement results can be affected by assuming that the compressive strain in the joint specimen is the same as in an equivalent solid piece. The elastic stiffness of joints were found to increase with an increase in the maximum nominal surface pressure. Results were also shown to illustrate that the elastic stiffness of a joint is affected by the loading history. Surface-profile measurements indicated that the topography of a joint surface changed with normal load, and that the deformation of a surface profile was related to the permanent change measured by extensometers placed across the joint interface.

Nomenclature

x = displacement across surface, and distance into profile as defined in Fig. 15
 δ = extensometer deflection, in.
 ϵ = axial strain, in./in.
 l = extensometer gage length
 NSP = nominal surface pressure
 CLA = center-line average
 A = bearing area
 F = feed rate
 R = tool-tip radius

Introduction

Whenever separate machine elements are mechanically clamped together to form joints within a structure, the joints themselves will contribute to the deflection under load and can cause a significant reduction in the overall stiffness of the machine structure. The reduction in stiffness due to a joint can be examined by comparing the combination of two components in mechanical contact with a single

component of the same material and dimensions.¹ If a compressive load is applied to the joined parts in a direction normal to the contact surfaces, deflection between gage points on either side of the joint will be larger than the deflection over the corresponding gage length of an equivalent solid component under the same normal loading.

The stiffness of a joint may be affected by the surface texture, the nominal shape of the contact surfaces (i.e., spherical, flat, etc.), the presence of debris, adhesive, or lubricant on the contact surface, the loading conditions and the type of materials used forming the joint. Since the surface texture has a primary influence on the deflection of a joint under static normal load, the scope of this study has been limited to the evaluation of the effects of surface texture on the stiffness of clamped, clean, machine elements loaded in a direction normal to the joint surface.

The behavior of a machined surface has been investigated in two different ways: by relating the normal load to the deformation of the surface profile, and by relating the normal load to the deflection across the joint interface. Using an optical technique, Kragelsky and Demkin² obtained favorable agreement between theory and experiment for the load as a function of the contact area using cylindrical machined specimens of lead, copper and aluminum pressed against a flat glass prism. Measuring the deformation between gage points placed on either side of the joint 0.0063-in. apart, Ling³ found that joint stiffness increased with normal load for ground surfaces of steel, brass and aluminum. Measurements made by Thornley, *et al.*,¹ showed that, while surface roughness affected joint stiffness, it did so only up to some minimum surface pressure.

When two joint surfaces are first brought together, the contact is not uniform because the load is concentrated at the tips of a few asperities. As

D. G. Bellow is Professor, Department of Mechanical Engineering, University of Alberta, Edmonton, Alberta, Can. D. D. Nelson is Engineer, Atomic Energy of Canada Limited, Pinawa, Manitoba, Can.
Paper has been accepted for presentation at a future meeting of the SESA.

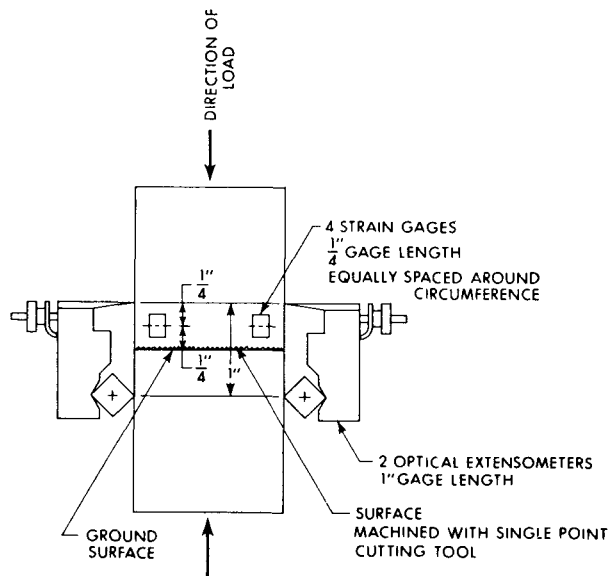


Fig. 1—Arrangement of extensometers and strain gages

the load increases, these asperities deform or are displaced allowing other parts of the surface to make contact, as was shown experimentally by Kragelsky and Demkin.² The load-deflection results of Connolly and Thornley, *et al.*,^{1, 4} indicate that considerable plastic deformation took place in their experiments, yet they did not report any changes in the surface profile. In setting up this study, it was suggested that the elastic behavior of a joint may be affected by a permanent rearrangement of the surface asperities. Furthermore, if the recoverable deformation was affected by the loading history of the joint, then it might be possible by means of large preloads to increase the joint stiffness. Consequently, the aims of this study were:

- to measure joint stiffness without introducing an equivalent solid piece and, hence, determine whether joint stiffness is sensitive to measurement technique;
- to establish, if possible, a relationship between deformation measurements across the joint and deformation of the surface profiles; and,
- to determine whether the loading history affects the stiffness of a joint.

In addition, since none of the cited references

related load-deflection results to bearing area as defined by Abbott and Firestone,⁵ an attempt would be made in this study to see if this was possible using a stylus-type profilometer. A relationship between load and bearing area could be useful in predicting joint stiffness.

Experimental Procedures

Three series of tests were conducted to evaluate the joint behavior of cylindrical steel specimens when pressed together under a static normal load. In each test, one surface was rough and one was smooth. This was done to ascertain which asperities first came into contact with the smooth surface and to enable detection of changes in surface profile; a more difficult if not impossible task if both surfaces were of equal roughness. Each surface had a hardness of approximately Vickers 245.

The two cylinders forming the joint were placed in a universal testing machine and compressive loads were applied through a ball-and-socket attachment at the moveable platten of the testing machine. Specimens were loaded and unloaded in increments and the loads, strains and extensometer readings were recorded. Strain gages and extensometers were placed on the specimens according to Fig. 1.

From the load measurements, the nominal surface pressure (NSP) was obtained by dividing the load by the cross-sectional area of the cylindrical specimens. The surface displacement x across the joint was calculated from

$$x = \delta - \epsilon l$$

where

δ = average reading from the extensometers

l = extensometer gage length (1.0 in.)

ϵ = average reading from the strain gage

To check that the strains were uniform between the extensometer gage mark and the joint surface, a series of three $1/16$ -in. gage-length electrical-resistance strain gages were placed end to end. It was found that little or no strain gradient existed.

Surface profiles and CLA values were obtained using a "Talysurf-4" surface-measuring instrument. This unit employed a diamond stylus which traversed across the surface of the specimen. All the surface profiles were obtained using a straight-line unit attached to the "Talysurf-4" which provided

TABLE 1—SPECIMEN DETAILS

CLA/cut-off length	Test series	OD, in.	ID, in.	Length, in.	Cross-sectional area, in. ²	Depth of cut, in.	Feed rate	Material	Machining process
225 μ in./0.100 in.	I	1.884	1.000	1.75	2.00	0.010	0.012 in./stroke	CR AISI 1018	Shaper
750 μ in./0.058 in.	II	1.500	0.990	2.00	0.997	0.005	0.028 in./rev.	GS AISI 1045	Lathe
190 μ in./0.030 in.	III	1.500	0.990	2.00	0.997	0.005	0.010 in./rev.	GS AISI 1045	Lathe

CR, cold-rolled; GS, ground steel

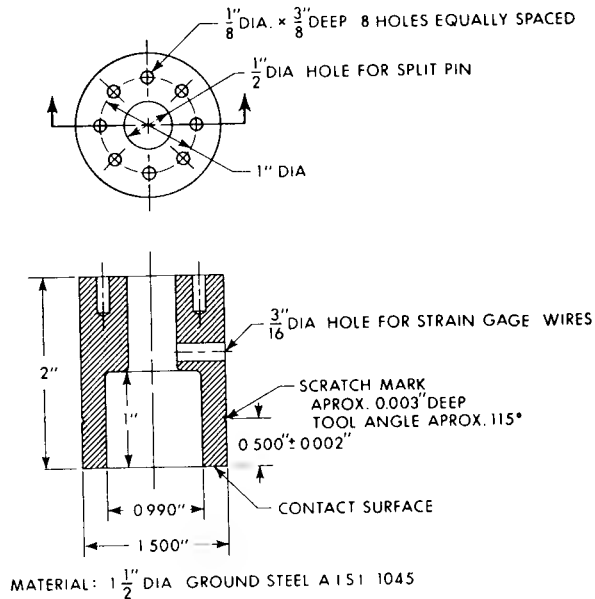


Fig. 2—Joint specimen for tests II and III

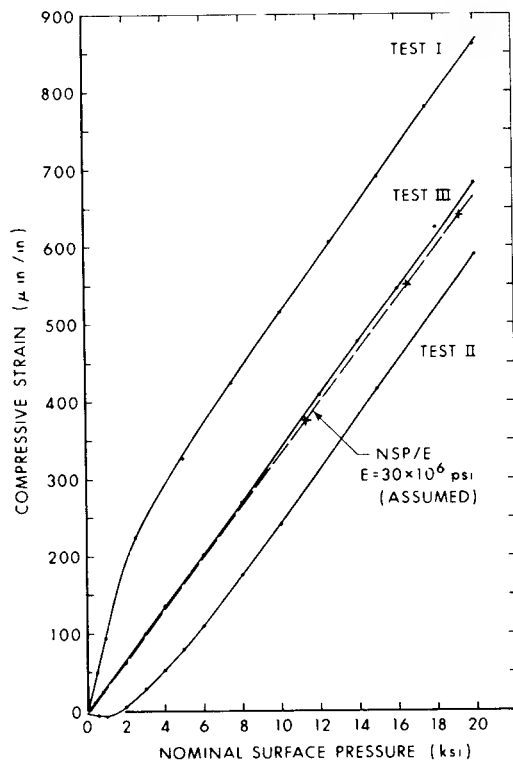


Fig. 3—Average strain-gage results after 20-ksi nominal surface pressure

a datum which was independent of the surface of the specimen. Because of the ultra-rough surfaces investigated in Test II, the *CLA* values were obtained using a Brüel and Kjaer roughness meter, otherwise the "Talysurf-4" was used in all other tests.

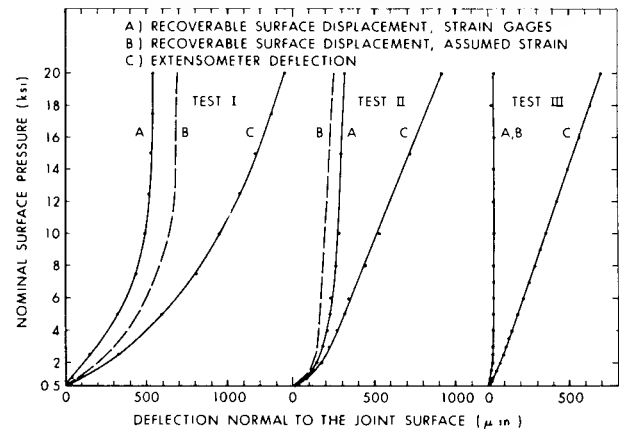


Fig. 4—Recoverable surface displacement based on strain-gage results and assumed strain

Bearing-area curves were obtained for all rough surfaces. The method, described by Abbott and Firestone,⁵ and used in this work, defines the bearing area as that fraction of the total length of a line which cuts the profile parallel to the nominal surface of the specimen. The bearing area was obtained at several levels in the profile record and plotted as a function of the displacement, normal to the nominal surface, measured from the outermost asperity of the profile. While the bearing area is not necessarily the same as the contact area for a joint surface under load, it is another way of assessing a surface profile.

The details of the specimens tested are given in Table 1 and are shown in Fig. 2. From the results of Test I, it was found that the irregular spacing and shape of the surface asperities made it impossible to obtain a surface profile which would be representative of the entire joint surface. Thus, the specimens in tests II and III were produced so that the most prominent feature of the surface profile would be the circular arc left by a single-point cutting tool. In order to achieve this, the specimens of II and III were machined at the maximum permissible speeds for the equipment used. The cross-sectional area of the specimens in tests II and III were half that used in Test I. It was hoped that the smaller cross-sectional area would reduce the effort in finding which asperities were deforming under load. Also, since the surfaces of tests II and III were machined on a lathe in a facing-off process, the wall thickness of the cylinders was kept small so as to approximate a constant machining speed.

Specimens in tests II and III were loaded through soft-brass rings having the same cross section as the contact surfaces. This was done in addition to the spherical seating arrangement to avoid any bending which might occur in the loading process.

In order that the profiles taken from the same traverse line across the surface could be compared for different loadings, a special fixture was ground flat on both the top and bottom surfaces, and locating holes were drilled perpendicular to the top sur-

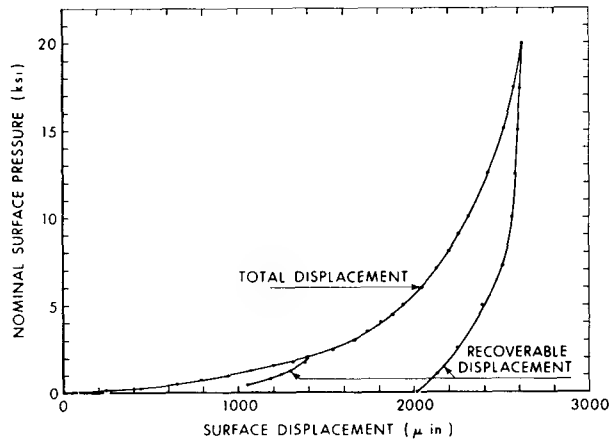


Fig. 5—Loading envelope, Test I

face and in line with the direction of the stylus traverse. A jig was made which allowed accurate spacing of $1/8$ -in.-diam locating holes drilled in the base of each specimen. Two pins were then used to locate each specimen to the fixture, thus allowing a profile of the same traverse line to be examined before and after loading.

The surface displacements for tests II and III, were obtained in the same manner as in Test I. All of the loading in Test I was completed without separating the joint surfaces or removing the specimens from the testing machine. The specimens in tests II and III were removed from the testing machine to obtain surface profiles at a maximum NSP of 4.0 and 10.0 ksi.

Results and Discussion

Strain Readings

The strain results from Test I indicated some difference between what was expected assuming an equivalent solid specimen. Therefore, for Test II, strain gages were placed on the inside surface as well as the outside. The results from Test II showed that there was a considerable difference between inside and outside gages, indicating bending or a barreling effect in the walls of the test cylinders. However, in Test II when both inside and outside sets of results were averaged, they agreed quite closely with what would be expected from an equivalent solid specimen.

From the results of tests I and II, the assumption of an equivalent solid piece was not necessarily consistent with strains recorded on the outer surface. It was concluded that the geometry of the specimens was influencing the results in these tests. However, for the specimens of this study, surface displacement was calculated on the basis of the strain readings recorded on the surface of the test cylinders since the extensometers measured deflections between gage

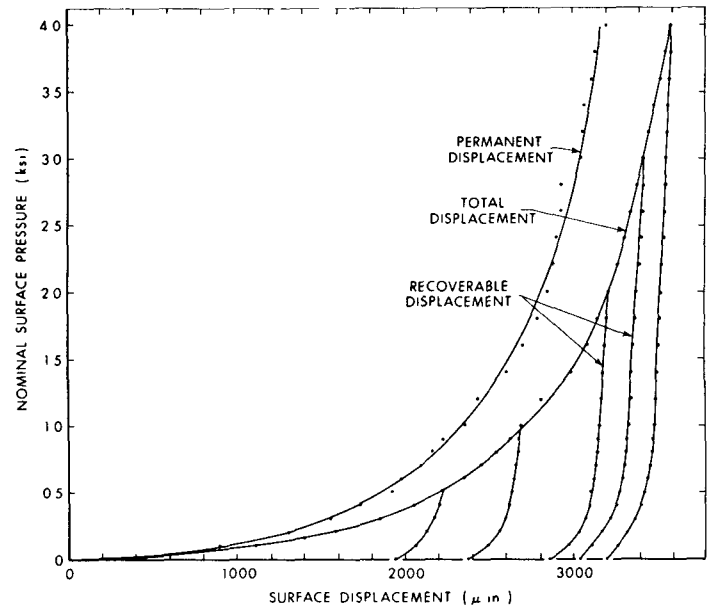


Fig. 6—Loading envelope, Test II

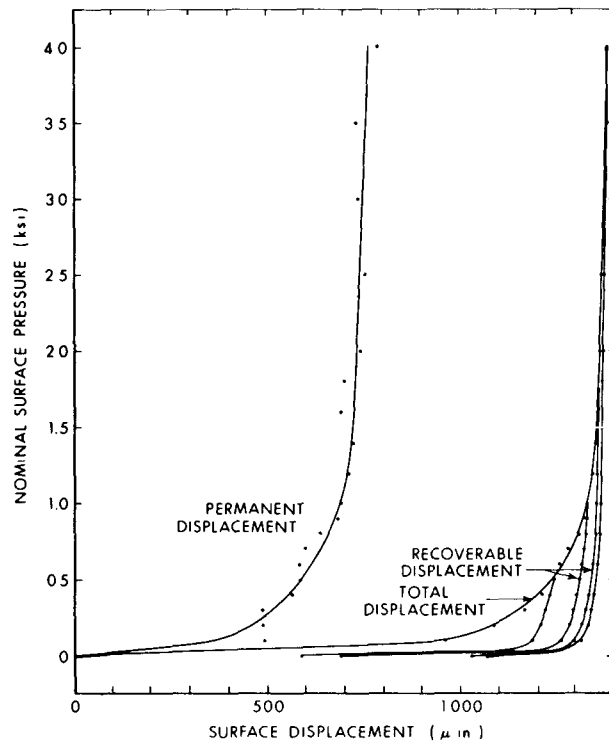


Fig. 7—Loading envelope, Test III

marks on the outer surface. For Test III, strain gages were placed on the outer surface only.

For all three tests, the averaged outer surface strains are plotted in Fig. 3. The dashed line is what would be expected from an equivalent solid piece. To check the manner in which the strain

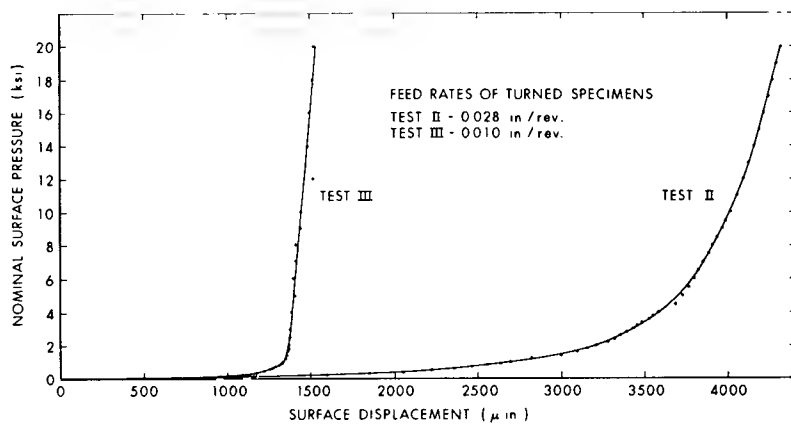


Fig. 8—Total surface displacement, tests II and III

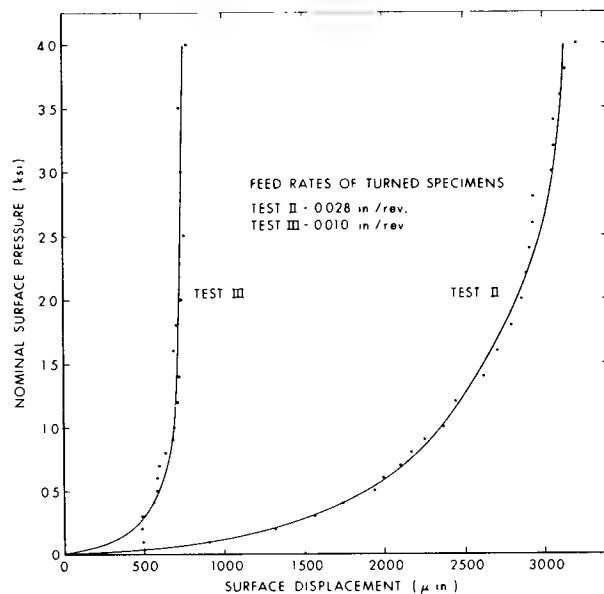


Fig. 9—Permanent surface displacement, tests II and III

gages were applied, strain gages were applied to a solid cylinder having the same dimensions as tests II and III. Some of the values are plotted, as crosses, and are shown to fall on top of this dashed line. This was to be expected if the gages were applied correctly.

The strain results of Fig. 3 were used to compute the recoverable displacement, which are compared with extensometer deflections in Fig. 4. The surface displacement was obtained from the equation $x = \delta - \epsilon l$. The B-curves in Fig. 4 represent recoverable surface displacements assuming uniform strain over the cross sections as given in Fig. 3. As is evident in Fig. 4, this assumption had a noticeable effect in tests I and II and no effect in Test III. The differences noted in tests I and II indicate that the surface displacement is quite sensitive to measurement techniques. From these results, it is quite evident that compressive strains normal to the contact surface are not necessarily uniform

over the cross section of the joint specimen.

Loading Curves

The loading curves for the three test series shown in Figs. 5–7 are similar in shape to those obtained by Connolly and Thornley.^{1, 4} As indicated by the total-displacement curves, the stiffness of the joints increased with load when loaded for the first time. The total surface displacement included both elastic and plastic deformation. The permanent-displacement curves in Figs. 6 and 7 indicate the plastic deformation which occurred when the joints were loaded for the first time.

The same results for tests II and III are plotted in Figs. 8 and 9 to indicate the differences in total and permanent surface displacement caused by different feed rates. These differences in displacements were the result of the different surface topography of the specimens. Test II had fewer tool marks (large asperities) than Test III, resulting in greater deformation of the surface than in Test III for the same *NSP*.

Permanent Changes in Surface Profile with Load

Thornley, et al.,¹ indicated for surfaces having roughnesses of about 700 μ in. peak to peak that there was little or no profile deformation for *NSP* values less than about 78.0 ksi. It was suggested that deformation must take place below the surface since no significant changes could be observed from the surface profiles.

For tests II and III, profile records were taken of both mating surfaces forming the joints after nominal surface pressures of 0, 4.0, 10.0, and 20.0 ksi. The tool marks of the turned specimens of Test II were approximately 3000 μ in. peak to peak, while those of Test II were about 800 μ in. peak to peak. The Test III results indicated there was only a slight change in the profile shape with load. However, for the rougher surface of Test II, there was evidence of a change in profile for both the turned and ground specimens, more noticeable on the mating ground surface. This change in profile for Test II was noticeable at an *NSP* as low as 4.0 ksi.

Thus, if the surface is rough enough, then changes in surface profiles can be detected and recorded.

It was believed that it should be possible to relate the profile deformation to the deformation recorded from the extensometers placed across the joint interface. Figure 10 compares the change in profile with the change in permanent surface displacement after an *NSP* of 4.0 ksi. The change in profile was taken to be the sum of the average change in the maximum peak-to-peak height of the tool marks, plus the average change in the maximum depth of the indentations on the ground surface. Four profiles from different positions on each specimen were taken at an *NSP* of 10.0 ksi and 20.0 ksi and the averages were plotted in Fig. 10. The good agreement in the case of Test II demonstrates that it is possible to relate permanent joint deflection to the deformation of the surface profile. The difficulty of this technique is making sure the recorded profiles are representative of those which make contact with the mating surface. This is especially true if the surface is quite irregular.

Bearing Area

If the surface topography is well defined, such as in the case where the surface was machined with a single-point cutting tool at a high machining rate, then it is possible to approximate the bearing area from a theoretically assumed surface profile. In the Appendix, a theoretical formula has been derived which relates bearing area *A*, to feed rate *F*, tool-tip radius *R*, and *x*, the distance into the surface from the tip of the tool marks. The results of Test II have been plotted in Fig. 11 and compare favorably with the theoretical curve. Associated with this approach, Ansell and Taylor⁶ stated that the *CLA* value could also be predicted from well defined profiles using the formula $CLA = F^2 \cdot (18\sqrt{3R})$ (see Appendix). For Test II, this formula indicated

a *CLA* of 800 μ in. compared with a *CLA* of 750 μ in. measured experimentally with a cutoff length of 0.058 in.

Since the bearing area is expressed as a curve for a particular profile and not a number, as is given by the *CLA* it is not possible to directly relate bearing area to *NSP*. While profile changes with *NSP* were noted on some specimens, the changes were not large enough to obtain differences in bearing-area curves as a function of the *NSP*. In fact, if this were possible a relationship between bearing area and *NSP* would only be possible for fixed values of *x*, the distance into the profile from the outermost asperity assumed to make first contact with the mating surface. Another way of approaching this problem would be to assume that the distance *x* into the profile is, in some way, related to the displacement of the joint surface. This idea was tried for Test II by combining the total-displacement curve of Fig. 8, eliminating *x* and plotting *NSP* vs. bearing area. The resulting curve was nonlinear and, at best, highly speculative.

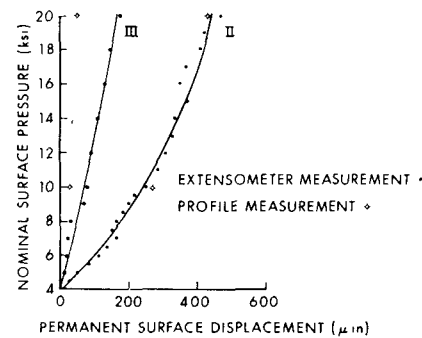


Fig. 10—Comparison of extensometer measurement with profile measurement, tests II and III

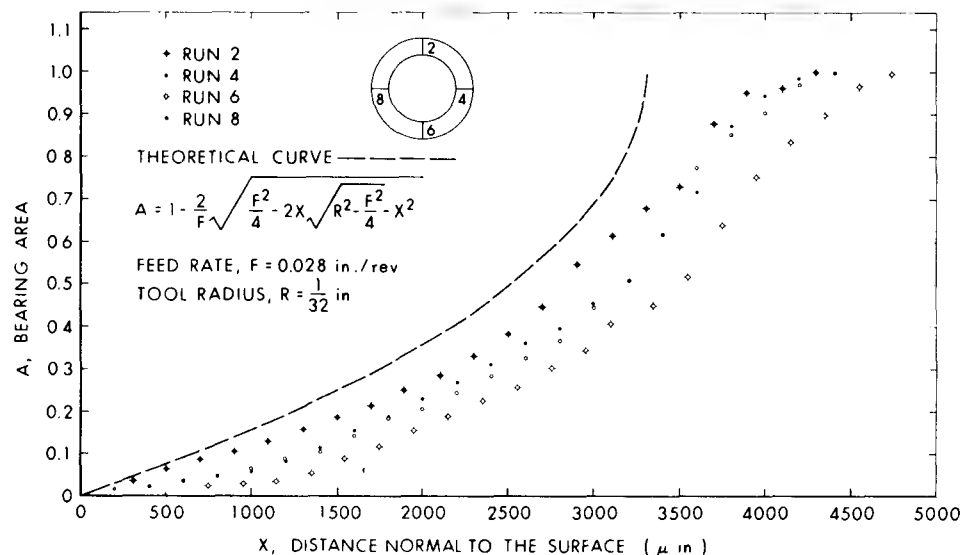


Fig. 11—Bearing area, Test II

Recoverable-surface-displacement Results

Recoverable-surface-displacement results were obtained for all test series and are plotted in Figs. 12 to 14. For Test I, Fig. 12, the results were obtained by loading the joint up to an *NSP* of 2.0 ksi and plotting the recovery curve as shown down to an *NSP* of 0.5 ksi and, at this point, calling the surface displacement zero. Initially, a datum of 0.5 ksi was considered necessary to prevent shifting at the joint interface. In Test III, the datum was reduced with no noticeable shifting at the joint interface. The results in Fig. 12 clearly indicate that the stiffness of the joint increases for increase in maximum *NSP*.

Figure 13 shows the recoverable-surface-displacement results for Test II referred to a datum of 0.5 ksi. Figure 14 illustrates the same trend noted in tests I and II on the characteristics of the recoverable surface displacement. Also noticeable is the decrease in recoverable displacement with increase in maximum *NSP*. These results of Test III, referred to a datum of 0.1 ksi, along with the results of tests I and II indicated that the maximum *NSP* influences the stiffness of the joint as well as the elastic recovery. This is in contradiction to previous observations^{1, 4} which have indicated that unloading curves were congruent over the same load range and that loading history does not affect the elastic recovery of a joint. The reason for this discrepancy is probably due to the fact that the

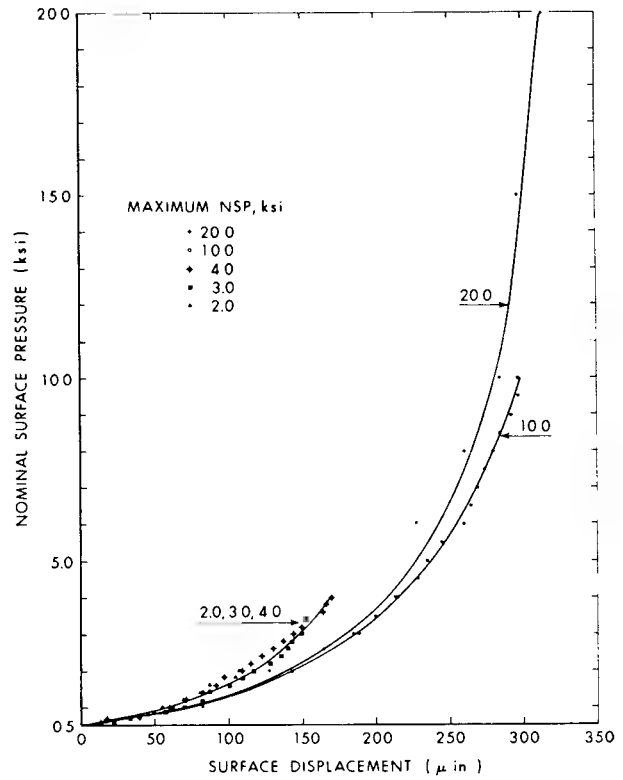


Fig. 13—Recoverable surface displacement, Test II

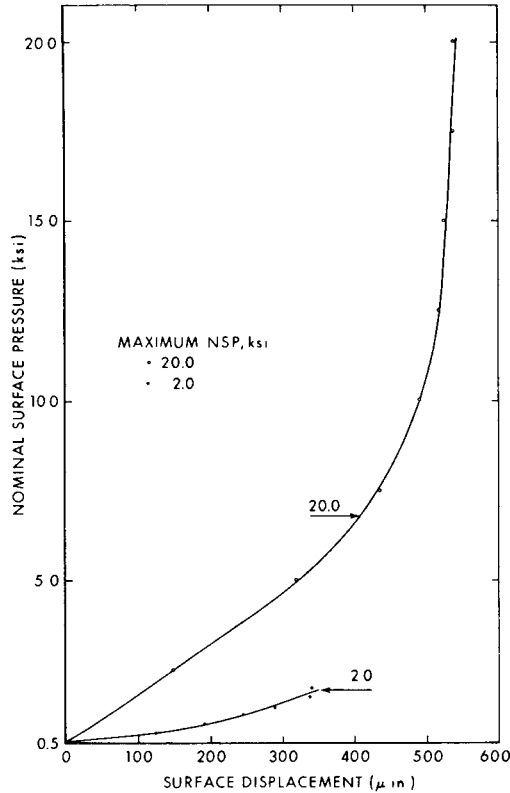


Fig. 12—Recoverable surface displacement, Test I

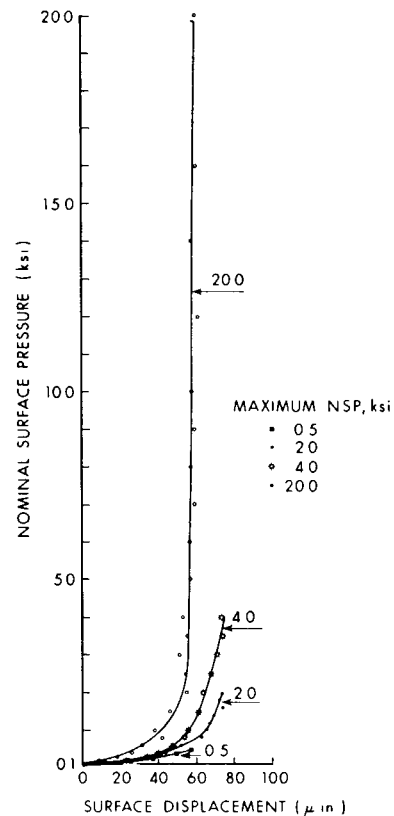


Fig. 14—Recoverable surface displacement, Test III

observations of previous investigations have been based on a maximum *NSP* of 4.0 ksi and higher, where the differences in stiffness and elastic recovery are not as pronounced.

Summary

1. From the strain-gage results, it was shown that the deformation of a solid material between the contact surfaces and the extensometer gage marks was a significant portion of the total extensometer measurement. The irregular topography of the contact surfaces caused a nonuniform loading and the compressive strains were not uniform over the cross section of the joint specimen. Surface-displacement results were affected by assuming a uniform compressive strain over the cross section of the joint specimen.

2. The surface topography of joint surfaces changed with normal load. Detection of the change was limited by the nature of the joint specimens and the technique used to obtain the surface profile.

3. For a rough surface, the permanent change in the profiles of the joint surfaces was approximately equal to the permanent surface displacement after a maximum nominal surface pressure of 4.0 ksi.

4. The recoverable surface displacement was affected by the loading history of the joints. The elastic stiffness of the joints increased with an increase in the maximum nominal surface pressure. This change in stiffness was probably due to plastic deformation at or near regions of contact.

5. It was not possible to relate bearing area to the surface displacement of the joint using a stylus-type profilometer.

Acknowledgment

The authors express their sincere appreciation to the National Research Council (Ottawa) for the financial assistance received in support of this research under Grant No. A-2705.

References

1. Thornley, R. H., Connolly, R., Barash, M. M. and Koenigsberger, F., "The Effect of Surface Topography Upon the Static Stiffness of Machine

Tool Joints," *Intl. Jnl. Mach. Tool Des. Res.*, 5(1-2), 57-73 (Sept. 1965) (1965).

2. Kragelsky, I. V. and Demkin, N. B., "Contact Area of Rough Surfaces," *Wear*, 3(3), 170-187 (May-June 1960).

3. Ling, F. F., "On Asperity Distributions of Metallic Surfaces," *Jnl. Ap. Phys.* 29 (8), 1168-1174 (Aug. 1958).

4. Connolly, R. and Thornley, R. H., "Determining the Normal Stiffness of Joint Faces," *Jnl. Eng. Ind.*, ASME Paper 67-Prod 6, (1967).

5. Abbott, E. J. and Firestone, F. A., "Specifying Surface Quality," *Mech. Eng.*, 55 (9), 569-572 (Sept. 1933).

6. Ansell, C. T. and Taylor, J., "The Surface Finishing Properties of a Carbide and Ceramic Tool," *Advances in Machine Tool Design and Research*, Pergamon Press, New York, 225-243 (1963).

APPENDIX

CLA Value

The following derivations assume that the surface finish is uniform and the profile follows the circular contour of a single-point cutting tool as shown in Fig. 15. The depth of tool mark d is related to the feed rate F and radius of cutting tool R as

$$d = R - \sqrt{R^2 - F^2/4}$$

The depth x at any position f of the profile follows as

$$x = R - \sqrt{R^2 - f^2}$$

and $x \simeq f^2/2R$, neglecting 4th-order terms and higher as being small compared with one.

The nominal surface line $x = \bar{x}$ is determined from

$$\int_0^{F/2} (x - \bar{x}) df = 0$$

which yields

$$\bar{x} = F^2/24R$$

and, if $x = \bar{x}$ at $f = f_1$ then $f_1 = F/2\sqrt{3}$.

The CLA value is defined as

$$\begin{aligned} CLA &= \frac{2}{F} \int_0^{F/2} |x - \bar{x}| df \\ &= \frac{2}{F} \left\{ \int_0^{f_1} (\bar{x} - x) df + \int_{f_1}^{F/2} (x - \bar{x}) df \right\} \\ &= F^2/18\sqrt{3}R \end{aligned}$$

Bearing Area

For convenience, a different coordinate system was chosen for determining the bearing area, as shown in Fig. 15. The datum was chosen so that the bearing area A is zero at the first point of contact, i.e., $A = 0$ at $x = 0$. Assuming a uniform surface roughness, then the bearing area is given as

$$A = \frac{F - 2f}{F}$$

and relating to a single-point cutting tool where

$$f = \sqrt{R^2 - (x + R - d)^2}, \quad d = R - \sqrt{R^2 - F^2/4}$$

thus,

$$A = 1 - \frac{2}{F} \sqrt{F^2/4 - 2x\sqrt{R^2 - F^2/4} - x^2}$$

This expression for A is plotted vs. x in Fig. 11 and the resulting curve compared with the experimental values obtained from the actual surface profiles.

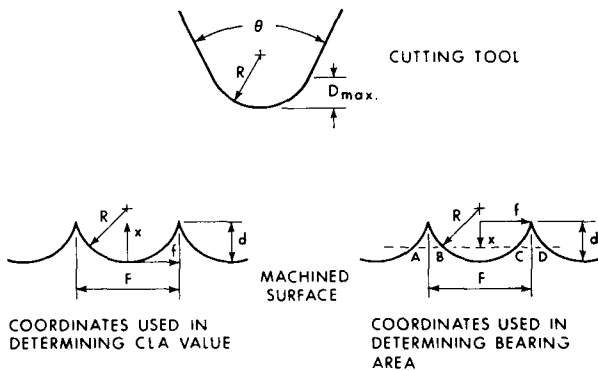


Fig. 15—Geometry of cutting tool and machined surface

SYMMETRICAL AND UNSYMMETRICAL FORCED EXCITATION OF THIN CIRCULAR ARCHES

D. G. BELLOW and A. SEMENIUK

Department of Mechanical Engineering, University of Alberta,
Edmonton 7, Alberta, Canada

(Received 19 August 1971)

Summary—Closed-form steady-state solutions are presented for in-plane excitation of thin circular arches subjected to cyclic symmetric and unsymmetric support movement. Arches with pinned-end and clamped-end boundary conditions are considered. The steady-state solutions consist of a series of the free modes of vibration.

Comparisons are made between the closed-form solution, for the frequency parameters of the free modes of vibration, with some approximate techniques available in the literature.

NOTATION

C_{ni} constants determined from the boundary conditions
 $D_i(t)$ time-dependent function, where

$$D_i(t) = -\frac{1}{2\alpha m} \int_{-\alpha}^{\alpha} V_i \left(\frac{\partial P_R}{\partial \phi} - P_T \right) d\phi$$

E Young's modulus of elasticity
 E_i constant for symmetrical excitation, where

$$E_i = \frac{1}{\alpha} \int_{-\alpha}^{\alpha} V_i(\phi) \sin \phi d\phi$$

F_i constant for unsymmetrical excitation, where

$$F_i = \frac{1}{4\alpha \sin \alpha} \int_{-\alpha}^{\alpha} V_i(\phi) [1 - 2 \cos(\phi + \alpha)] d\phi$$

$g(t)$ function describing support movement
 G amplitude of support movement
 H arch thickness
 I second moment of area of arch cross-section
 m arch mass per unit length
 $P_R(\phi, t)$ external radial load per unit arch length
 $P_T(\phi, t)$ external tangential load per unit arch length
 R radius of curvature
 t time variable
 $u(\phi, t)$ radial displacement
 $U_i(\phi)$ i th radial mode shape
 $v(\phi, t)$ tangential displacement
 $V_i(\phi)$ i th tangential mode shape
 α arch opening half-angle
 ϕ angular co-ordinate
 λ_n frequency parameter, where $\lambda_n^2 = \omega_n^2 m R^4 / EI$
 ω_n n th natural frequency
 Ω frequency of support excitation
 $\eta(t)$ time-dependent function

INTRODUCTION

THE GOVERNING differential equation for free vibration of an inextensible arch was first obtained by Lamb.¹ Since then, several approximate techniques have been employed to obtain a solution for the dynamic response of an arch. The Rayleigh quotient was used by Den Hartog² to obtain the characteristics of the fundamental mode for both the extensional and inextensional case. Eppink and Veletsos³⁻⁵ investigated the response of an arch to a dynamic pressure load by analyzing the arch as a framework of rigid bars and flexible joints. The Rayleigh-Ritz method in conjunction with Lagrangian multipliers was used by Nelson^{6,7} to calculate the characteristics of the first four free modes of vibration. Again, the Rayleigh-Ritz method was employed by Volterra and Morell⁸⁻¹¹ to include arches with center lines other than circular. By use of the transfer matrix technique, the solution of the free vibration of a circular arch was investigated by Lang and Reed.¹²

Closed-form solutions for the free vibration of an arch or ring have been provided by Archer,¹³ Morley,¹⁴ Hoppe,¹⁵ Takahashi¹⁶ and Love.¹⁷ The contribution of non-linear terms in the governing differential equation was investigated by Antmann and Warner.¹⁸ Except for Archer's transient solution for the case when one support of an arch was given a time-dependent displacement, the above studies consisted of finding the natural frequencies and mode shapes for freely vibrating arches. However, Lang^{19,20} derived the orthogonality condition for the free modes of vibration for an arch and proposed a steady-state solution as a series in terms of these free modes of vibration. While Lang presented the steady-state solution in integral form, it was not evaluated for any particular type of loading.

The main purpose of this paper is to study the dynamic response of an arch, in the plane of the initial curvature of the arch, when subjected to two different types of cyclic support movement. One case involves both supports moving simultaneously and in phase. The other case has one support stationary while the other support is moving cyclically. The steady-state solution will consist of a series of the free modes of vibration.

Because of the approximate techniques available for determining the free modes of vibration, and because the steady-state solution consists of a series of these modes, comparisons are made for the resonant frequency parameters as calculated by the approximate techniques with the values obtained from the closed-form solution.

THEORY

Fig. 1 shows the co-ordinate system employed for the arch and an element cut from this arch showing the relevant forces and moments. Employing the usual assumptions considered for linear elasticity, and neglecting the effect of damping on the steady-state solution, the equations of motion derived from the arch element in Fig. 1 reduce to the following:

$$\frac{EI}{mR^4} \left(\frac{\partial^5 u}{\partial \phi^5} + 2 \frac{\partial^3 u}{\partial \phi^3} + \frac{\partial u}{\partial \phi} \right) + \frac{\partial^3 u}{\partial \phi \partial t^2} - \frac{\partial^2 v}{\partial t^2} = \frac{1}{m} \left(\frac{\partial P_R}{\partial \phi} - P_T \right). \quad (1)$$

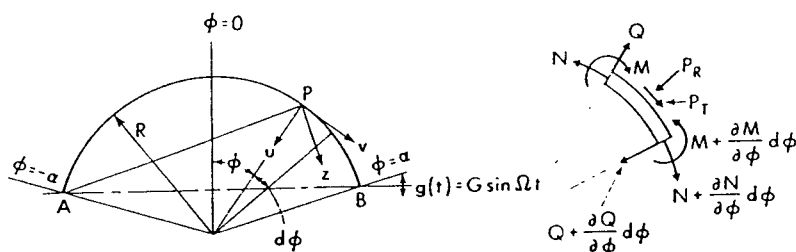


FIG. 1. Co-ordinate system and arch element.

The condition of inextensibility

$$\partial v / \partial \phi = u$$

is used to separate equation (1) into

$$\frac{EI}{mR^4} \left(\frac{\partial^6 v}{\partial \phi^6} + 2 \frac{\partial^4 v}{\partial \phi^4} + \frac{\partial^2 v}{\partial \phi^2} \right) + \frac{\partial^4 v}{\partial \phi^2 \partial t^2} - \frac{\partial^2 v}{\partial t^2} = \frac{1}{m} \left(\frac{\partial P_R}{\partial \phi} - P_T \right) \quad (2)$$

and

$$\frac{EI}{mR^4} \left(\frac{\partial^6 u}{\partial \phi^6} + 2 \frac{\partial^4 u}{\partial \phi^4} + \frac{\partial^2 u}{\partial \phi^2} \right) + \frac{\partial^4 u}{\partial \phi^2 \partial t^2} - \frac{\partial^2 u}{\partial t^2} = \frac{1}{m} \left(\frac{\partial^2 P_R}{\partial \phi^2} - \frac{\partial P_T}{\partial \phi} \right). \quad (3)$$

As a check on the validity of equation (3), it reduces to the governing equation for a straight beam as $R \rightarrow \infty$.

The procedure for solution is to evaluate $v(\phi, t)$ and then calculate $u(\phi, t)$ from the condition of inextensibility. Equation (2) can be separated into

$$V_n^{VI} + 2V_n^{IV} + (1 - \lambda_n^2) V_n^{II} + \lambda_n^2 V_n = 0 \quad (4)$$

and

$$\ddot{T}_n + \omega_n^2 T_n = 0,$$

where $\lambda_n^2 = \omega_n^2 m R^4 / EI$, $(\cdot)^I \equiv d(\cdot) / d\phi$ and $(\cdot) \equiv d(\cdot) / dt$, etc. Taking the solution to equation (4) as

$$V_n(\phi) = \sum_{j=1}^6 C_{nj} \exp(r_{nj} \phi) \quad (5)$$

yields the following cubic equation in r_n^2

$$r_n^6 + 2r_n^4 + r_n^2(1 - \lambda_n^2) + \lambda_n^2 = 0.$$

The solution to this cubic is easily obtained once the value of λ_n^2 is established. A detailed description of the homogeneous solution can be found in the papers of Archer¹³ and Lang.¹⁹ The constants C_{nj} ($j = 1, 2, \dots, 6$) of equation (5) are determined from the boundary conditions and n is the mode number.

The particular, or steady-state, solution to equation (2) can be taken as

$$v = \sum_{i=1}^{\infty} V_i(\phi) \eta_i(t) \quad (6)$$

which is a summation of the free modes of vibration. Substitution of this into equation (2), multiplying by $V_j d\phi$ and integrating over the opening angle of the arch, yields

$$\sum_{i=1}^{\infty} \left[(\ddot{\eta}_i + \omega_i^2 \eta_i) \int_{-\alpha}^{\alpha} (V_i^I V_j^I + V_i V_j) d\phi \right] = - \int_{-\alpha}^{\alpha} \frac{V_j}{m} \left(\frac{\partial P_R}{\partial \phi} - P_T \right) d\phi. \quad (7)$$

The orthogonality condition for the free modes is given by

$$\int_{-\alpha}^{\alpha} (V_i^I V_j^I + V_i V_j) d\phi = 0, \quad i \neq j$$

and when $i = j$ the normalized modes are given by

$$\frac{1}{2\alpha} \int_{-\alpha}^{\alpha} (V_i^T V_i^T + V_i V_i^T) d\phi = 1. \quad (8)$$

From the orthogonality condition it is seen that the i th and j th modes uncouple in equation (7), and by use of equation (8) the following is obtained

$$\ddot{\eta}_i + \omega_i^2 \eta_i = D_i(t) \quad (9)$$

where

$$D_i(t) = -\frac{1}{2\alpha m} \int_{-\alpha}^{\alpha} V_i \left(\frac{\partial P_R}{\partial \phi} - P_T \right) d\phi.$$

It now remains to determine P_R and P_T for symmetrical and unsymmetrical cyclic support displacement and hence, solve equation (9) for these two specific cases.

SYMMETRICAL EXCITATION

Symmetrical excitation of the arch is interpreted as meaning both supports are moving identically, in phase with one another, and in the plane of the initial curvature of the arch. Such excitation develops inertia loads in the radial and tangential directions as follows:

$$P_R = -m\ddot{g}(t) \cos \phi,$$

$$P_T = -m\ddot{g}(t) \sin \phi,$$

where $g(t) = G \sin \Omega t$, is the support movement. The solution of equation (9), for symmetrical excitation, can now be written as

$$\eta_i(t) = \left[\frac{G\Omega^2 E_i}{\omega_i^2 - \Omega^2} \right] \sin \Omega t + B_{i1} \sin \omega_i t + B_{i2} \cos \omega_i t \quad (10)$$

where

$$E_i = \frac{1}{\alpha} \int_{-\alpha}^{\alpha} V_i(\phi) \sin \phi d\phi.$$

From equations (10) and (6) the steady-state radial and tangential displacements can be written as

$$\frac{u}{G} = \sum_{i=1}^{\infty} \frac{\Omega^2 E_i U_i}{\omega_i^2 - \Omega^2} \sin \Omega t, \quad (11)$$

$$\frac{v}{G} = \sum_{i=1}^{\infty} \frac{\Omega^2 E_i V_i}{\omega_i^2 - \Omega^2} \sin \Omega t. \quad (12)$$

The transient components have been neglected in equations (11) and (12) as having negligible contribution in the case of an actual arch due to the presence of damping.

UNSYMMETRICAL EXCITATION

When support A in Fig. 1 is held stationary while support B vibrates vertically in the plane of the initial curvature of the arch, a condition of unsymmetrical excitation exists. This causes a rotation $\xi(t)$ of the arch about A which can be expressed as

$$\xi(t) = g(t) \overline{AB},$$

where $g(t) = G \sin \Omega t$ and $G \ll \overline{AB}$. For an arbitrary point P on the arch the displacement z perpendicular to the line joining A to P is given by

$$z(\phi, t) = \overline{AP} \xi(t)$$

or

$$= 2R \sin \left(\frac{\phi + \alpha}{2} \right) \xi(t).$$

Taking the radial and tangential components of this displacement, differentiating twice to obtain the accelerations, the radial and tangential inertia loads can be obtained, where

$$P_R = -\frac{m\ddot{g}(t) \sin(\phi + \alpha)}{2 \sin \alpha},$$

$$P_T = -\frac{m\ddot{g}(t) [1 - \cos(\phi + \alpha)]}{2 \sin \alpha}.$$

Substituting these into equation (9), $\eta_i(t)$ becomes

$$\eta_i(t) = \frac{G\Omega^2 F_i}{\omega_i^2 - \Omega^2} \sin \Omega t + C_{i1} \sin \omega_i t + C_{i2} \cos \omega_i t,$$

where

$$F_i = \frac{1}{4 \alpha \sin \alpha} \int_{-\alpha}^{\alpha} V_i(\phi) [1 - 2 \cos(\phi + \alpha)] d\phi.$$

Again neglecting the transient component, the steady-state solution for unsymmetrical excitation becomes

$$\frac{u}{G} = \sum_{i=1}^{\infty} \frac{\Omega^2 F_i U_i}{\omega_i^2 - \Omega^2} \sin \Omega t, \quad (13)$$

$$\frac{v}{G} = \sum_{i=1}^{\infty} \frac{\Omega^2 F_i V_i}{\omega_i^2 - \Omega^2} \sin \Omega t. \quad (14)$$

METHOD OF EVALUATION

The theoretical equations were evaluated for both pinned-end and clamped-end boundary conditions. When either of these boundary conditions are applied to equation (5), six homogeneous algebraic equations with six unknown constants C_{nj} are obtained. For a non-trivial solution for this set of equations the determinant of the coefficients, which contained the natural frequency parameter λ_n , must be zero. To avoid the difficulty of expanding the six by six determinant, an iterative procedure was chosen to evaluate λ_n . For each mode, values for λ_n were arbitrarily chosen and the determinant was evaluated. Adjustments to the value of λ_n were then made so that the determinant was zero or near zero. The calculated λ_n was identified by evaluating its modal shape. For the lower modes it was possible, by this iterative process, to obtain a λ_n value which made the determinant zero. However, for the higher modes this was not possible but the value of the determinant was found to oscillate between a positive and negative value for small changes in only the sixteenth significant figure of the assumed value of λ_n . Thus, it was concluded that the iterative procedure used was sufficiently accurate for evaluating the homogeneous solution of equation (5).

The steady-state solution was evaluated by summing a sufficient number of terms as required by equations (11) or (13). It was found that summing eight terms in the series yielded values for u/G accurate to three significant figures for forcing frequencies up to the fourth mode. For forcing frequencies above the fourth mode, more than eight terms must be taken in equation (6) to obtain three figure accuracy. However, this may lead to computational difficulties. For example, in using the computer program developed for this study it was found, for certain values of α , that an ill-condition was set up in the computer when a steady-state solution was attempted near the eighth mode of free vibration.

PRESENTATION OF RESULTS

Fig. 2 shows the plot of λ_n vs. α for the first nine modes of free vibration. This indicates the variation of the resonant frequency parameter with respect to the arch opening angle for pinned-end conditions. A similar plot for clamped ends is shown in Fig. 3. As might be expected, the difference in the resonant frequency parameter λ_n , between pinned ends and clamped ends, diminishes with increasing mode number. As the mode number increases, the number of radial nodal points increases and the effect of the boundary conditions decreases.

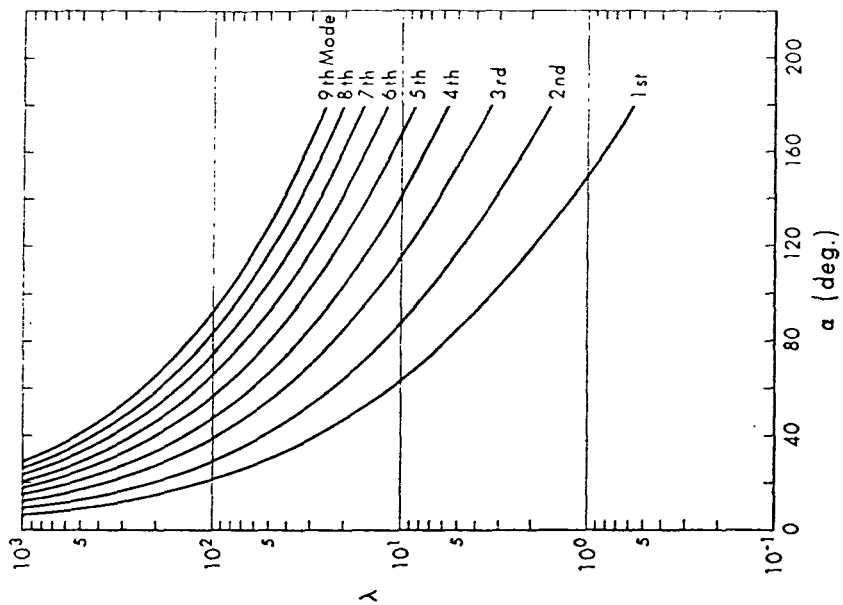


Fig. 3. Dimensionless natural frequency; clamped end.

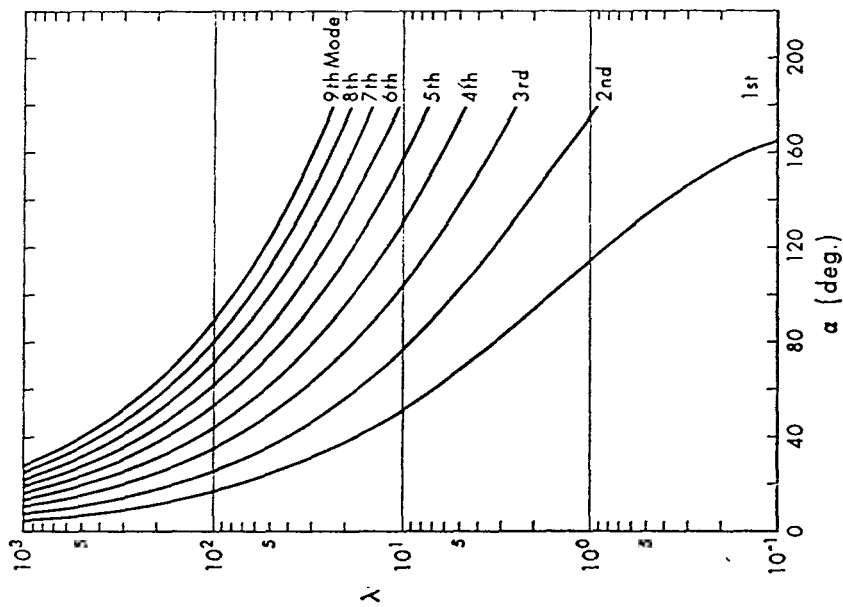


Fig. 2. Dimensionless natural frequency; pinned end.

It was not possible to non-dimensionalize all of the parameters used in calculating the dynamic response of the arches. Thus, for all curves drawn, $\alpha = 100^\circ$, $R = 5.09$ in. and $H = 0.032$ in. Only the radial displacement is shown, and for convenience, it is plotted relative to a straight line rather than relative to the undeformed circular arch. The tangential displacement can be obtained from the inextensibility condition. Figs. 4 and 5

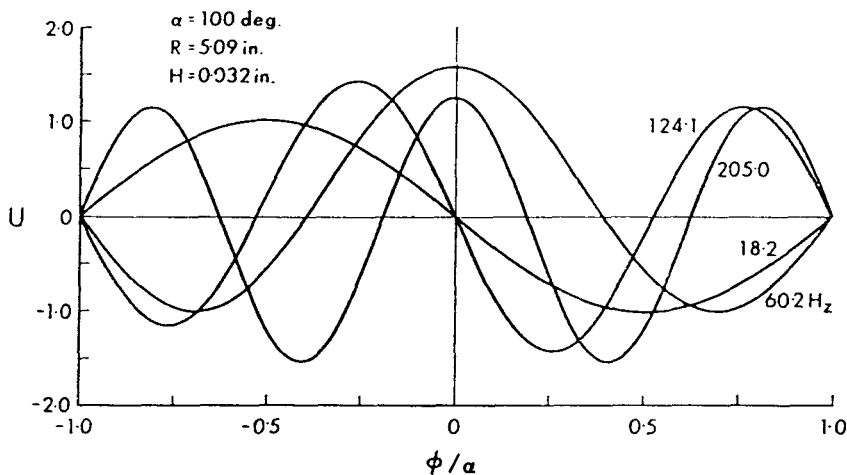


FIG. 4. Normalized radial displacement; pinned end.

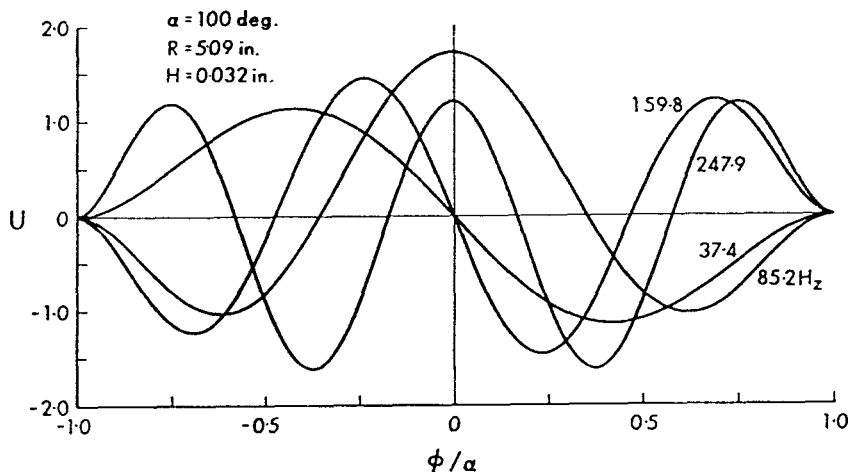


FIG. 5. Normalized radial displacement; clamped end.

show the normalized radial displacements for the first four mode shapes for pinned-end and clamped-end boundary conditions, respectively.

The plotted radial displacements shown in Figs. 6–9 include the radial component of the support displacement. Thus, for symmetrical excitation, equation (11) becomes

$$\frac{u}{G} = \left[\sum_{i=1}^{\infty} \frac{\Omega^2 E_i U_i}{\omega_i^2 - \Omega^2} + \cos \phi \right] \sin \Omega t,$$

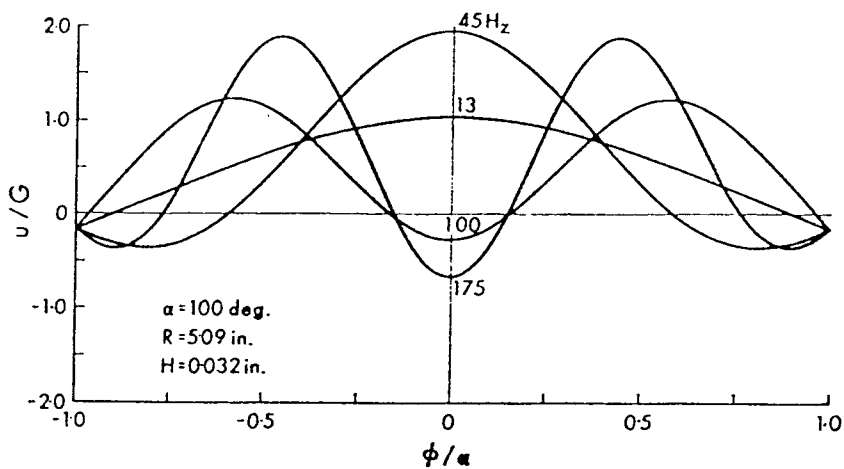


FIG. 6. Symmetrically forced; pinned end.

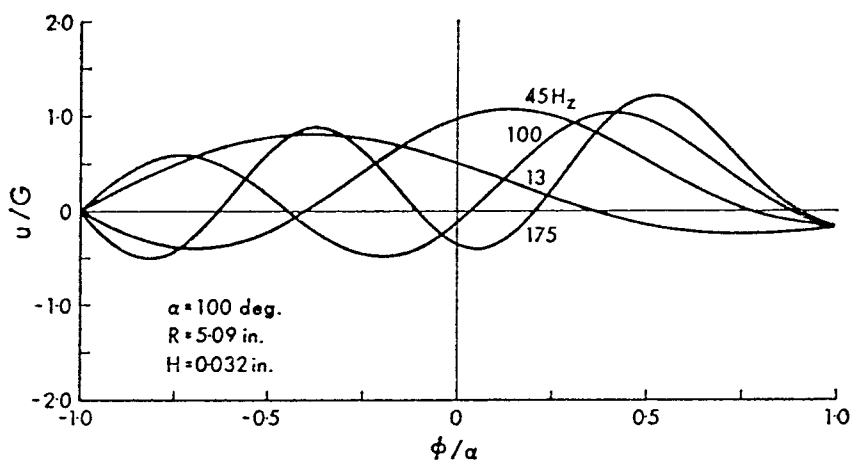


FIG. 7. Unsymmetrically forced; pinned-end.

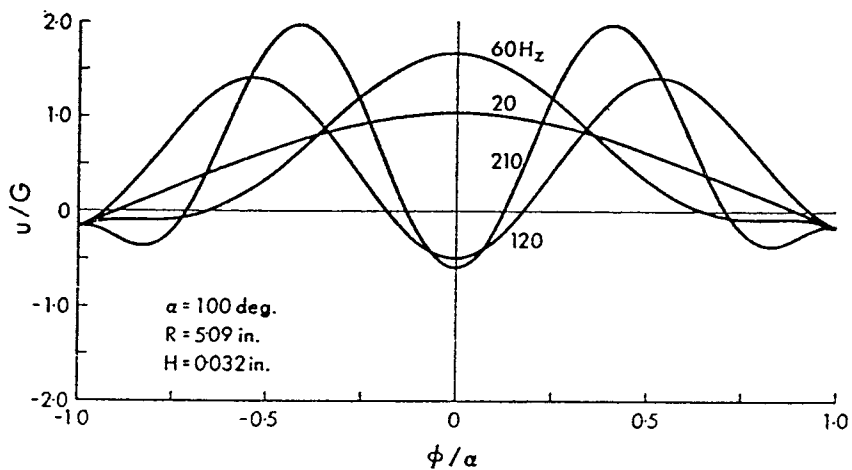


FIG. 8. Symmetrically forced; clamped end.

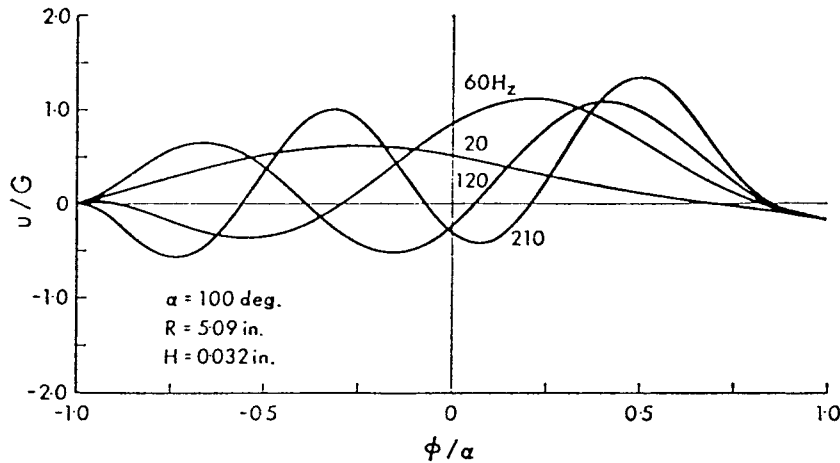


FIG. 9. Unsymmetrically forced; clamped end.

and for unsymmetrical excitation, equation (13) becomes

$$\frac{u}{G} = \left[\sum_{i=1}^{\infty} \frac{\Omega^2 F_i U_i}{\omega_i^2 - \Omega^2} + \frac{\sin(\phi + \alpha)}{2 \sin \alpha} \right] \sin \Omega t.$$

In Figs. 6-9 four different forcing frequencies were chosen for both pinned-end and clamped-end boundary conditions under symmetrical and unsymmetrical excitation. The forcing frequencies were selected so that the lowest was below the first resonant frequency, one was between the first and second, another between the second and third, and another between the third and fourth resonant frequencies.

In the case of symmetrical excitations, Figs. 6 and 8, it is seen that only symmetrical modes are present. While for unsymmetrical excitation, Figs. 7 and 9, the symmetrical as well as the anti-symmetrical modes are present. Under unsymmetrical excitation the arch undergoes both a rotation and a displacement.

APPROXIMATE TECHNIQUES FOR DETERMINING NORMAL MODES

The theory presented in this paper provides a solution for the forced vibration of an arch to include both symmetrical and unsymmetrical excitation of pinned-end and clamped-end boundary conditions. Since the solution of the forced vibration problem consists of a series of the normal modes, it is of interest to compare the normal mode results obtained by previous investigators using approximate techniques with the closed-form solution used in this paper.

In applying the Rayleigh quotient to obtain the fundamental frequency of a pinned-end arch, whose opening half-angle is $30^\circ < \alpha < 135^\circ$, Den Hartog² suggested that a single parameter polynomial expression for the shape function would yield a better approximation than what would be obtained from assuming a single sine term. In the original paper of Den Hartog there is an error in the expression for λ_1 (Den Hartog's C_1) which was obtained from the polynomial shape function. However, following the procedure of Den Hartog the corrected formula is

$$\lambda_1 = \frac{1}{(2\alpha)^2} \left[\frac{(2\alpha)^4 - 79.2(2\alpha)^2 + 1584}{1 + 0.07769(2\alpha)^2} \right]^{1/2}. \quad (15)$$

Table 1 shows a comparison of the fundamental frequency for various half-angles, as calculated from the closed-form solution, with equation (15) and the values tabulated by

TABLE 1. FUNDAMENTAL FREQUENCY FOR A PINNED-END CIRCULAR ARCH

	Opening half-angle							
	20	40	60	80	100	120	140	160
Closed-form solution	78.558	17.964	6.927	3.218	1.613	0.818	0.389	0.145
Sinusoidal displacement function of Den Hartog	78.558	17.965	6.928	3.219	1.614	0.818	0.389	0.145
Corrected formula for polynomial displacement function of Den Hartog	79.179	18.098	6.977	3.243	1.630	0.831	0.412	0.161

Den Hartog based on a sinusoidal shape function. This table indicates that a closer upper bound is obtained by using the sinusoidal function rather than using the polynomial as suggested by Den Hartog.

For a clamped-end arch, Den Hartog employed a two-parameter polynomial for the shape function. When these results are compared with those obtained from the closed-form solution, it is found that the agreement is better than 0.2 per cent; and, as would be expected, the approximate technique yielding slightly higher values for the fundamental frequency than obtained from the closed-form solution.

Using the Rayleigh quotient in combination with Lagrangian multipliers, Nelson⁶ calculated the first four resonant frequencies of a pinned-end circular arch. Table 2 shows a comparison of Nelson's results, taken from graphs presented in his paper, with the

TABLE 2. RESONANT FREQUENCIES OF PINNED-END CIRCULAR ARCH

		Opening half-angle			
		45	90	135	180
λ_1	Nelson	13.8	2.27	0.474	0
	Closed form	13.764	2.267	0.474	0
λ_2	Nelson	32.5	6.93	2.39	0.901
	Closed form	32.404	6.923	2.366	0.901
λ_3	Nelson	62.0	14.1	5.44	2.46
	Closed form	61.673	13.978	5.349	2.447
λ_4	Nelson	97.8	23.3	9.32	4.61
	Closed form	96.446	22.820	9.267	4.597

closed-form solution. As in Den Hartog's solution for the fundamental frequency, it is seen that the Rayleigh quotient also gives very close upper bounds for the higher modes for a circular arch pinned at its ends.

While not specifically stating it, a lower bound technique for determining the resonant frequency of arches was illustrated in a paper by Eppink and Veletsos.³ These authors analyzed the dynamic response of arches by replacing the continuous arch with a series of rigid bars and flexible joints. For the specific arch opening half-angle of 43.6°, Table 3

TABLE 3. RESONANT FREQUENCIES OF PINNED-END CIRCULAR ARCH; $\alpha = 43.6^\circ$

Resonant frequency									
	λ_1	λ_2	λ_3	λ_4	λ_5	λ_6	λ_7	λ_8	λ_9
Closed-form solution	14.794	34.630	65.840	102.856	151.049	205.149	270.355	341.519	423.751
Eppink and Veletsos	14.8	36.4	65.8	103.1	150.9	205.1	269.6	340.1	420.6

shows a comparison of this numerical technique with the closed-form solution for the first nine resonant frequencies. It is observed that the technique employed by Eppink and Veletsos yields very close lower bounds for the resonant frequencies. Two discrepancies for λ_2 and λ_4 were noted where their numerical technique gave values higher than obtained from the closed-form solution. This is attributed to round-off error.

CONCLUSIONS

A theory has been presented for the evaluation of the dynamic response of thin circular arches subjected to inertia loads caused by cyclic symmetric and unsymmetric support displacement. For forcing frequencies near the fourth mode, an eight-term series in terms of the free modes of vibration, yielded the steady-state solution accurate to three significant figures.

The closed-form solution for the free modes of vibration is compared with the approximate techniques suggested by Den Hartog, Nelson, and Eppink and Veletsos. It is shown that these approximate techniques give very close bounds to the closed-form solution.

Acknowledgement—The authors express their appreciation to the National Research Council (Ottawa) for the financial support of this research under Grant No. A-2705.

REFERENCES

1. H. LAMB, *Lond. Math. Soc. Proc.* **19**, 365 (1887).
2. J. P. DEN HARTOG, *Phil. Mag.* **5**, 400 (1928).
3. R. T. EPPINK and A. S. VELETOS, Air Force Special Weapons Center, TR 59-9, New Mexico (1959).
4. R. T. EPPINK and A. S. VELETOS, *ASCE 2nd Conf. on Electronic Computation* 477 (1960).
5. R. T. EPPINK and A. S. VELETOS, Air Force Special Weapons Center, TR 60-53, New Mexico (1960).
6. F. C. NELSON, *Int. J. mech. Sci.* **4**, 517 (1962).
7. F. C. NELSON, *J. Franklin Inst.* **278**, 20 (1964).
8. E. VOLTERRA and J. D. MORELL, *J. appl. Mech.* **27**, 82, 744 (1960).
9. E. VOLTERRA and J. D. MORELL, *J. appl. Mech.* **28**, 624 (1961).
10. E. VOLTERRA and J. D. MORELL, *J. acoust. Soc. Am.* **33**, 1787 (1961).
11. E. VOLTERRA and J. D. MORELL, *J. appl. Mech.* **34**, 1046 (1967).
12. T. E. LANG and R. E. REED, TR 32-252, Jet Prop. Lab., Calif. (1962).
13. R. R. ARCHER, *Int. J. mech. Sci.* **1**, 45 (1960).
14. L. S. D. MORLEY, *Q. J. mech. appl. Math.* **9**, 491 (1958).
15. R. HOPPE, *J. reine angew. Math.* **73**, 158 (1871).
16. S. TAKAHASHI, *J.S.M.E.* **6**, 666 (1963).
17. A. E. H. LOVE, *A Treatise on the Mathematical Theory of Elasticity*. Dover, New York (1944).
18. S. ANTMAN and W. H. WARNER, *J. Soc. Indust. Appl. Math.* **13**, 1007 (1965).
19. T. E. LANG, TR 32-261, Jet Prop. Lab., Calif. (1962).
20. T. E. LANG, TR 32-261, Jet Prop. Lab., Calif. (1963).

Experimental Behavior of Thin Circular Arches Subjected to Forced Excitation

Experimental results agree closely with the theory presented for the steady-state solution of a thin circular arch, pinned at the ends, and subjected to symmetrical and unsymmetrical support excitation

by D. G. Bellow and A. Semeniuk

ABSTRACT—Experimental evidence is presented to verify the steady-state solution for a thin circular arch, pinned at the ends, and subjected to symmetrical and unsymmetrical support excitation. The steady-state solutions consist of a series of the free modes of vibration. It is shown how these solutions are developed when both supports of the arch are moving simultaneously and in phase with one another. The unsymmetrical case, where only one support is moving, is also considered.

The arches chosen for testing had a radius-to-thickness ratio of 121 to 179. The arch-opening half-angles varied from 90 to 125 deg. The arches were vibrated on an electrodynamic-shaker table. Dynamic arch amplitudes were measured using a specially designed micrometer probe. Comparison of theory with experiment was considered good; the average error in prediction of resonant frequencies was less than three percent. For the forced excitation, the modal shapes agreed quite closely with that predicted by theory.

It was found that experimental arches were quite sensitive to variations in the arch radius and that, in general, for all arches tested, the degree of agreement between theory and experiment was more sensitive to changes in the opening half-angle rather than the R/H value. A further observation was that, for some poorly constructed arches, it was found that out-of-plane vibrations occurred at approximately 16 times the fundamental flexural frequency.

Nomenclature

- C_{ni} = constants determined from the boundary conditions
- $D_i(t)$ = time-dependent function
- E = modulus of elasticity
- E_i = constant for symmetrical excitation
- F_i = constant for unsymmetrical excitation
- $g(t)$ = function describing support displacement
- G = amplitude of support movement
- H = arch thickness
- I = second moment of area of cross section
- k = radius of gyration of cross section
- m = arch mass per unit length
- $P_R(\phi, t)$ = external radial load per unit arch length
- $P_T(\phi, t)$ = external tangential load per unit arch length

D. G. Bellow is Professor of Mechanical Engineering, University of Alberta, Edmonton 7, Alberta, Canada. A. Semeniuk is Research Officer, Atomic Energy of Canada Limited, Pinawa, Manitoba, Canada. Paper was presented at 1972 SESA Fall Meeting held in Seattle, Wash. on October 17-20.

- R = radius of curvature
- t = time
- $u(\phi, t)$ = radial displacement
- $v(\phi, t)$ = tangential displacement
- α = arch-opening half-angle
- ϕ = angular coordinate
- λ_n = frequency parameter
- ω_n = n th natural frequency
- Ω = frequency of support excitation
- $\eta(t)$ = time-dependent function

Introduction

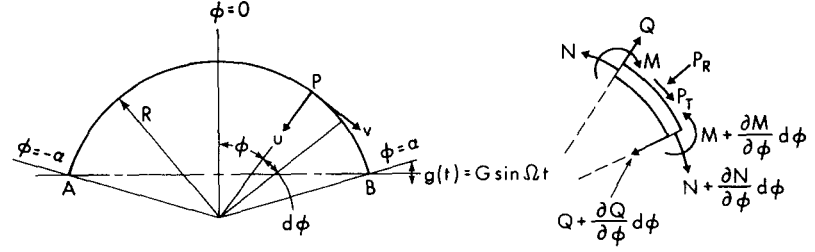
The governing differential equation for the free vibration of thin, elastic, inextensible arches was first determined by Lamb¹ in 1888. In more recent times, a method of solution was suggested by Lang^{2,3} for solving the problem of an arch subjected to a cyclic disturbing force. Extending this method, the present paper provides a theoretical solution for a thin circular arch subjected to symmetric and unsymmetric cyclic support displacement.

While some experimental results have been presented for the free vibration of complete rings, there has been little experimental evaluation of a steady-state solution for an arch. The purpose of this paper is to compare experiment with theory for the dynamic response of an arch, in the plane of the initial curvature of the arch, when subjected to two different types of cyclic support movement. One case involves both supports moving simultaneously and in-phase. The other case has one support stationary while the other is moving cyclically. The steady-state solution consists of a series of the free modes of vibration. A brief description of this solution is given for an arch pinned at its ends. For a more complete description of the theoretical solution, and for its application to an arch clamped at its ends, Ref. 4 should be consulted.

Theory

Figure 1 shows the coordinate system employed for the arch and an element cut from this arch showing the relevant forces and moments. Employing the usual assumptions considered for linear elasticity, and neglecting the effect of damping on the steady-state solution, the equations of motion derived from

Fig. 1—Coordinate system for arch



the arch element in Fig. 1 reduce to the following,

$$\frac{EI}{mR^4} \left(\frac{\partial^5 u}{\partial \phi^5} + 2 \frac{\partial^3 u}{\partial \phi^3} + \frac{\partial u}{\partial \phi} \right) + \frac{\partial^3 u}{\partial \phi \partial t^2} - \frac{\partial^2 v}{\partial t^2} = \frac{1}{m} \left(\frac{\partial P_R}{\partial \phi} - P_T \right). \quad (1)$$

The condition of inextensibility $\frac{\partial v}{\partial \phi} = u$ is used to separate eq (1) into

$$\frac{EI}{mR^4} \left(\frac{\partial^6 v}{\partial \phi^6} + 2 \frac{\partial^4 v}{\partial \phi^4} + \frac{\partial^2 v}{\partial \phi^2} \right) + \frac{\partial^4 v}{\partial \phi^2 \partial t^2} - \frac{\partial^2 v}{\partial t^2} = \frac{1}{m} \left(\frac{\partial P_R}{\partial \phi} - P_T \right) \quad (2)$$

and

$$\frac{EI}{mR^4} \left(\frac{\partial^6 u}{\partial \phi^6} + 2 \frac{\partial^4 u}{\partial \phi^4} + \frac{\partial^2 u}{\partial \phi^2} \right) + \frac{\partial^4 u}{\partial \phi^2 \partial t^2} - \frac{\partial^2 u}{\partial t^2} = \frac{1}{m} \left(\frac{\partial^2 P_R}{\partial \phi^2} - \frac{\partial P_T}{\partial \phi} \right). \quad (3)$$

The procedure for solution is to evaluate $v(\phi, t)$ and then calculate $u(\phi, t)$ from the condition of inextensibility. Equation (2) can be separated into

$$V_n^{VI} + 2V_n^{IV} + (1 - \lambda_n^2) V_n^{II} + \lambda_n^2 V_n = 0 \quad (4)$$

and

$$\ddot{T}_n + \omega_n^2 T_n = 0$$

where

$$\lambda_n^2 = \omega_n^2 \frac{mR^4}{EI}, \quad ()^I \equiv \frac{d()}{d\phi}, \quad \text{and} \quad ()^{\cdot} \equiv \frac{d()}{dt} \text{ etc.}$$

The shape functions for eq (4) can be obtained by setting

$$V_n(\phi) = \sum_{i=1}^6 C_{ni} e^{r_{ni}\phi}. \quad (5)$$

Substituting eq (5) into eq (4) yields the following cubic equation in r_n^2

$$r_n^6 + 2r_n^4 + r_n^2(1 - \lambda_n^2) + \lambda_n^2 = 0.$$

Once the value of λ_n is established, the solution of the cubic can be obtained.³

The constants C_{ni} in eq (5) are determined from the boundary conditions and "n" is the mode number. Equation (5) represents six simultaneous algebraic equations in six unknowns. Setting the determinant of the coefficients to zero yields the eigenvalues for

the arch whose boundary conditions have been prescribed.

The steady-state solution of eq (2) can be taken as the summation of the free modes of vibration, or

$$v(\phi, t) = \sum_{i=1}^{\infty} V_i(\phi) \eta_i(t).$$

Substituting this into eq (2), multiplying by $V_j d\phi$, and integrating over the opening angle of the arch yields

$$\sum_{i=1}^{\infty} \int_{-\alpha}^{\alpha} \left\{ \frac{EI}{mR^4} (V_i^{VI} + 2V_i^{IV} + V_i^{II}) \eta_i + (V_i^{II} - V_i) \ddot{\eta}_i \right\} V_j d\phi = \int_{-\alpha}^{\alpha} \frac{V_j}{m} \left(\frac{\partial P_R}{\partial \phi} - P_T \right) d\phi$$

and by use of the homogeneous equation this reduces to

$$\sum_{i=1}^{\infty} \left[(\ddot{\eta}_i + \omega_i^2 \eta_i) \int_{-\alpha}^{\alpha} (V_i^I V_j^I + V_i V_j) d\phi \right] = - \int_{-\alpha}^{\alpha} \frac{V_j}{m} \left(\frac{\partial P_R}{\partial \phi} - P_T \right) d\phi.$$

This equation is uncoupled by the use of the orthogonality condition

$$\int_{-\alpha}^{\alpha} (V_i^I V_j^I + V_i V_j) d\phi = 0 \quad i \neq j,$$

and with the use of the normalizing condition

$$\frac{1}{2\alpha} \int_{-\alpha}^{\alpha} (V_i^I V_i^I + V_i V_i) d\phi = 1 \quad i = j,$$

reduces to

$$\ddot{\eta}_i + \omega_i^2 \eta_i = D_i(t) \quad (6)$$

where

$$D_i(t) = - \int_{-\alpha}^{\alpha} \frac{V_i}{2\alpha m} \left(\frac{\partial P_R}{\partial \phi} - P_T \right) d\phi.$$

The right-hand side of eq (6) is to be determined for two particular types of support displacement.

Symmetrical Support Excitation

Symmetrical support excitation is interpreted to mean that both supports are moving identically, in phase with one another, and in the plane of the initial curvature of the arch. If the supports are moving

vertically according to $g(t) = G \sin \Omega t$, where G is the amplitude and Ω is the frequency of the excitation, then the following radial and tangential inertia loads are developed:

$$P_R = -m \ddot{g}(t) \cos \phi$$

$$P_T = -m \ddot{g}(t) \sin \phi.$$

Substituting these into eq (6) and solving for the steady-state solution, produces

$$\frac{u}{G} = \sum_{i=1}^{\infty} \frac{\Omega^2 E_i U_i}{(\omega_i^2 - \Omega^2)} \sin \Omega t \quad (7)$$

and

$$\frac{v}{G} = \sum_{i=1}^{\infty} \frac{\Omega^2 E_i V_i}{(\omega_i^2 - \Omega^2)} \sin \Omega t,$$

where

$$E_i = \frac{1}{\alpha} \int_{-\alpha}^{\alpha} V_i(\phi) \sin \phi d\phi.$$

The transient components in eq (7) have been neglected as having negligible contribution due to the presence of damping.

Unsymmetrical Support Excitation

When support A in Fig. 1 is held stationary while support B vibrates vertically in the plane of the initial curvature of the arch, a condition of unsymmetrical support excitation exists. The appropriate radial and tangential inertia loads can be shown to be

$$P_R = -\frac{m \ddot{g}(t) \sin(\phi + \alpha)}{2 \sin \alpha}$$

$$P_T = -\frac{m \ddot{g}(t) [1 - \cos(\phi + \alpha)]}{2 \sin \alpha}$$

and the steady-state solution eq (2) for unsymmetrical excitation becomes

$$\frac{u}{G} = \sum_{i=1}^{\infty} \frac{\Omega^2 F_i U_i}{\omega_i^2 - \Omega^2} \sin \Omega t. \quad (8)$$

$$\frac{v}{G} = \sum_{i=1}^{\infty} \frac{\Omega^2 F_i V_i}{\omega_i^2 - \Omega^2} \sin \Omega t.$$

where

$$F_i = \frac{1}{4 \alpha \sin \alpha} \int_{-\alpha}^{\alpha} V_i(\phi) [1 - 2 \cos(\phi + \alpha)] d\phi$$

and, as before, the transient components have been neglected.

Equations (7) and (8) yield radial displacements due to arch deformation only and do not include any support displacement. To account for support displacement and provide a means for comparing with experiment, eqs (7) and (8) are modified to yield absolute displacements⁴ according to

$$\frac{u}{G} = \left[\sum_{i=1}^{\infty} \frac{\Omega^2 E_i U_i}{(\omega_i^2 - \Omega^2)} + \cos \phi \right] \sin \Omega t \quad (9)$$

in the case of symmetrical excitation, and

$$\frac{u}{G} = \left[\sum_{i=1}^{\infty} \frac{\Omega^2 F_i U_i}{(\omega_i^2 - \Omega^2)} + \frac{\sin(\phi + \alpha)}{2 \sin \alpha} \right] \sin \Omega t \quad (10)$$

in the case of unsymmetrical excitation.

Design of the Experiment

Experimental arches were cut from 6061-T6 aluminum sheet and formed into the desired radius with a 3-roll roller. Pinned-end conditions were obtained by bolting a split 0.5-in.-diam steel shaft to each end and allowing this shaft to rotate freely in a ball-bearing support. The outer races of the bearings were firmly attached to an aluminum-channel section which was mounted to the armature of an electrodynamic-shaker table. The base of the arch was excited with the amplitude and frequency being controlled and monitored by means of the shaker-system controls.

The amplitude of the displacement of the arches and that of the support was measured by use of a specially designed micrometer probe. This probe was fitted with a spring-loaded tip to avoid any disturbance applied to the arch when the probe made contact. The probe itself was mounted to an arm which was pinned at one end and was adjustable to any radial position. A simple make-or-break electrical circuit was used to indicate when the probe came into contact with the arch. This device permitted a precise measurement of the absolute radial displacement of any point on the arch. The accuracy of this measurement was checked against an optical cathetometer and it was found to be within ± 0.005 in.

For testing purposes, the choice of arch geometry was constrained by the maximum force output of the shaker table plus the resolution of the amplitude-measuring probe. After considerable experimentation with various arch geometries, it was found that arches with opening half-angles in the range $90 \leq \alpha \leq 125$ deg and with a radius-to-thickness ratio in the range $120 \leq R/H \leq 180$ permitted testing in the frequency range 5 to 125 Hz. Thus, the test arches were designed to have the fundamental resonant frequency above 5 Hz and have the second resonant frequency less than 125 Hz. Even abiding by these general restrictions, for some of the arches it was possible to obtain a measurable response up to the fourth mode. However, it was found that, if the arches were too flexible, it was impossible to control the modal behavior and restrict the vibrations to the initial plane of curvature. On the other hand, if the arches were too stiff, the shaker table was incapable of exciting measurable amplitudes.

Another point which was of importance was that the channel section to which the arches were mounted had to be stiff enough so that it did not resonate in the frequency range used to test the arches. This was possible if an aluminum-channel section was chosen with the dimensions $11 \times 3 \times 1\frac{1}{2}$ in. This fixed the distance between supports at 10.02 in. In order for the opening half-angle of the arch to be in the range $90 \leq \alpha \leq 125$ deg, the radius of the arch had to be $5 \leq R \leq 6$ in. With the opening half-angle and radius prescribed, the thickness of the arch was chosen to satisfy the con-

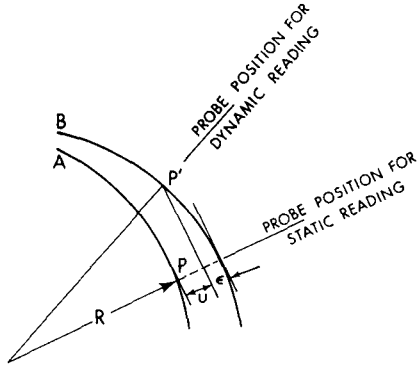


Fig. 2—Displacement measurement

dition of inextensibility, i.e., $R/k^2 > 1/n^2$ where k is the radius of gyration of the cross section. Consequently, the thickness of the arches tested was 0.032 and 0.042 in. The width for all arches was 1.0 in.

Preliminary testing on some of the arches constructed showed that the amplitude of vibration was sensitive to variations in arch radius. To reduce the effect of variation in the arch radius, test arches were chosen whose radius did not vary by more than half the thickness of the arch. The theoretical solutions were then based on the radius which gave the best circular fit to the actual profile of the arches tested. The value of the opening half-angle for the arches was calculated on the basis of this radius and the distance between arch supports of 10.02 in.

Although the presence of damping was acknowledged, its effect was assumed to be negligible and was neglected in the theoretical analysis. To ensure that damping had little effect on the experimental arches used to investigate the steady-state solution, forcing frequencies were chosen to be sufficiently removed from the resonant arch frequencies. It is at resonance that the effects of damping are most pronounced.

Since the arch vibrated about its static position,

the amplitude of the radial displacement was obtained by taking the difference in readings between the dynamic and static values. For example, in Fig. 2, an arbitrary point P is shown with the arch in the static position A and under a dynamic load moves to point P' , indicated by B . If both the static and dynamic displacements were measured with the probe at one position only, an error ϵ would occur in moving from P to P' in that the arch undergoes both a tangential and a radial displacement. Thus, the probe was moved to P' before the radial component of the dynamic displacement was recorded. Generally, the angular displacement between P and P' was less than two degrees. Experimental displacements were measured at 20-deg intervals along the circumference of the arch.

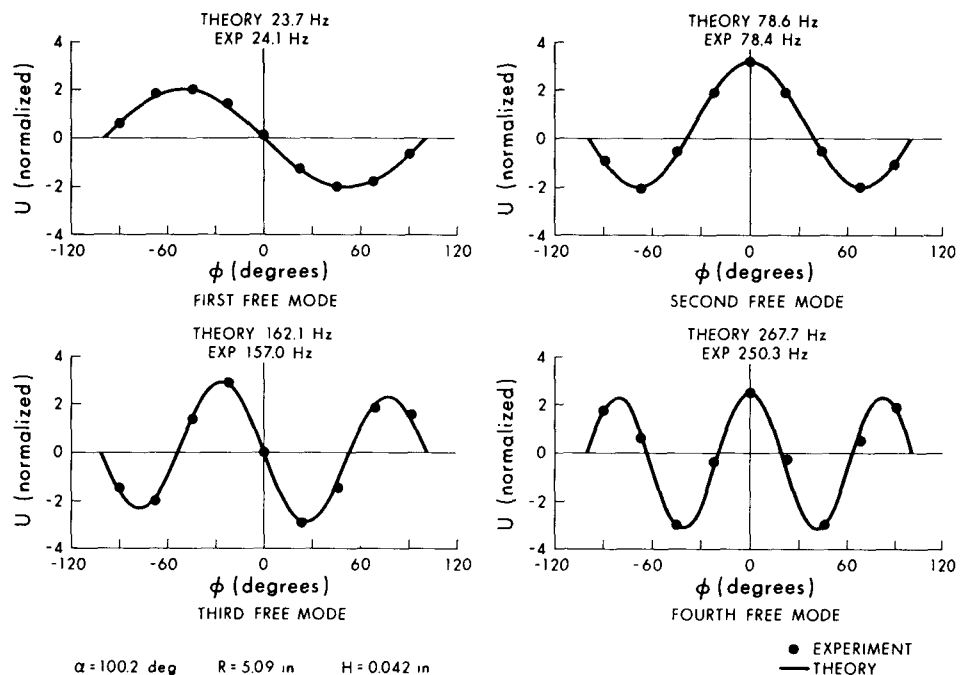
Presentation of Results

Since the theoretical solution consists of a summation of the free modes of vibration, the behavior of the arches was studied when operating at resonant conditions. It was observed that the odd-numbered modes were obtained by unsymmetrical support excitation while symmetrical excitation produced the even-numbered modes.

A comparison between theory and experiment for the first four modes of free vibration is shown in Fig. 3 for an arch with $R/H = 121.2$ and in Fig. 6 for an arch with $R/H = 179.4$. Although not shown in this paper, arches with $R/H = 133.3$ and 157.8 were also tested and their results were consistent with those observed for the arches of Figs. 3 and 6. Experimental values are plotted as points while the solid line represents the theory.

The experimental modal shapes shown in Figs. 3 and 6 were obtained by exciting the arches at their resonant frequencies. The condition of resonance was obtained by adjusting the shaker-table frequency for maximum deflection of the arch. The resonant frequency was resolved within ± 0.3 Hz. At resonance, the shaker-table amplitude was less than 0.005 in. yielding magnification ratios on the arch in excess

Fig. 3—Normalized radial displacement, $R/H = 121.2$



of 40. Under these conditions, it was assumed the arch was essentially in a state of free vibration and the experimental modal shapes shown in Figs. 3 and 6 were obtained. For symmetrical support excitation the experimental data were normalized with respect to the point at $\phi = 0$. For unsymmetrical excitation, the data were normalized with respect to the largest displacement.

The theoretical steady-state solution for symmetrical support excitation is compared with experiment in Figs. 4 and 7. For unsymmetrical support excitation, theory and experiment are compared in Figs. 5 and 8. These results are presented for four different, nonresonant, forcing frequencies. For each of these

forcing frequencies, a series of four readings, each with a different support displacement, was taken for each position on the arch. The support displacements were divided into four equally spaced increments between the two extremes used for the particular test. An average value was calculated for the absolute arch displacement divided by the support displacement, i.e., u/G .

Discussion of the Results

The average difference between theory and experiment for the resonant frequencies, for all modes and all arches tested, was less than 3 percent; with a maximum of 6.5 percent and a minimum of zero re-

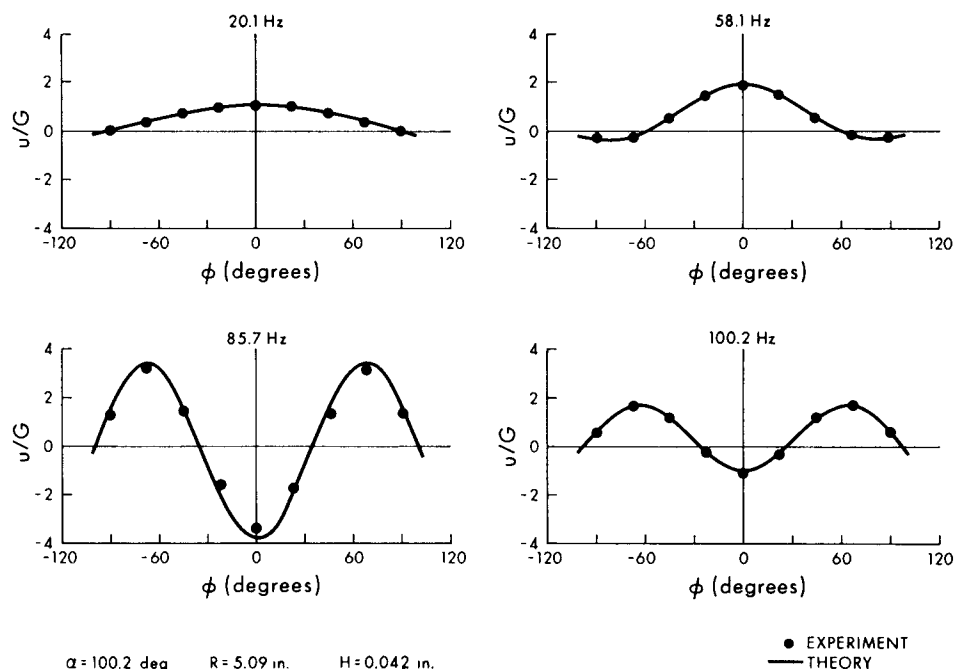


Fig. 4—Steady-state solution—Symmetrical support excitation, $R/H = 121.2$

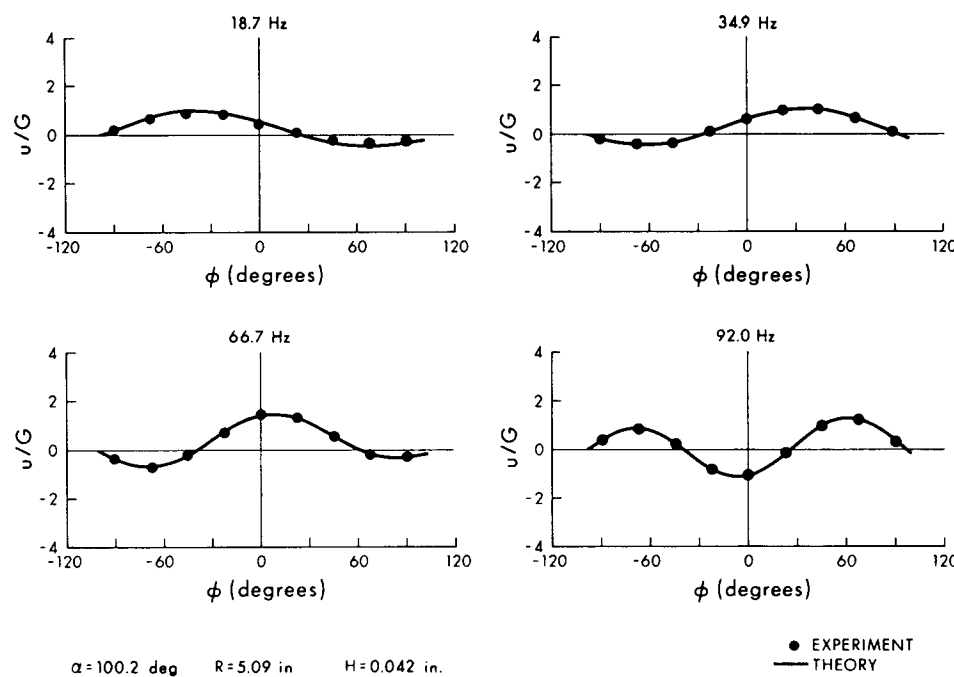


Fig. 5—Steady-state solution—Unsymmetrical support excitation, $R/H = 121.2$

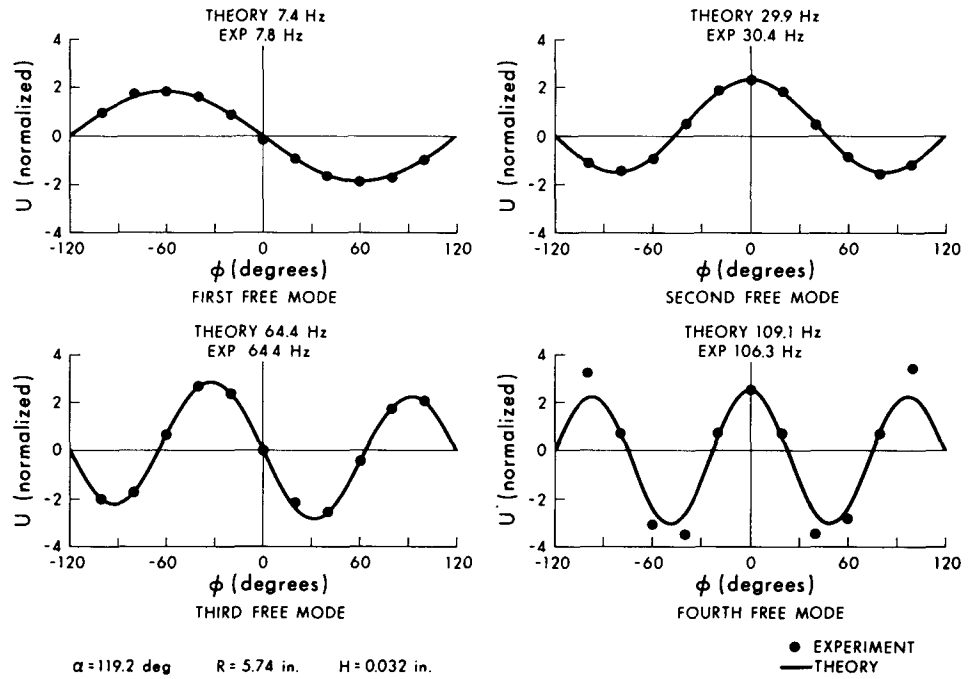


Fig. 6—Normalized radial displacement, $R/H = 179.4$

corded. However, this variation in frequency had little effect on the modal shapes where, as resonance, these shapes were quite consistent with that predicted by theory. Some differences were noted at the fourth mode for the arch $R/H = 179.4$ but, in general, the agreement was considered good.

For both symmetrical and unsymmetrical forced excitation, the steady-state solutions given by eqs (9) and (10) agreed quite closely with the results obtained from experiment. Slightly better agreement

was noted for the unsymmetrical excited arches. It is suggested, since only one support was moving in the unsymmetrical case, any abnormalities of arch behavior were perturbed only half the amount that they would have been perturbed under symmetrical excitation.

Although not particularly evident from the results selected for presentation in Figs. 4 to 8, a general observation based on all arches tested was that the degree of agreement between theory and experiment

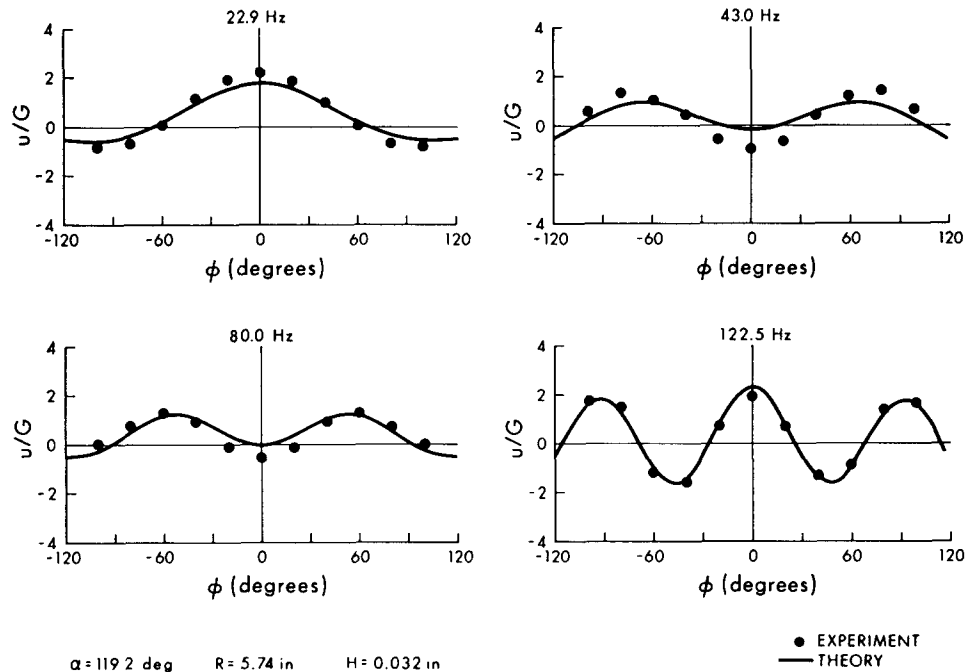


Fig. 7—Steady-state solution—Symmetrical support excitation, $R/H = 179.4$

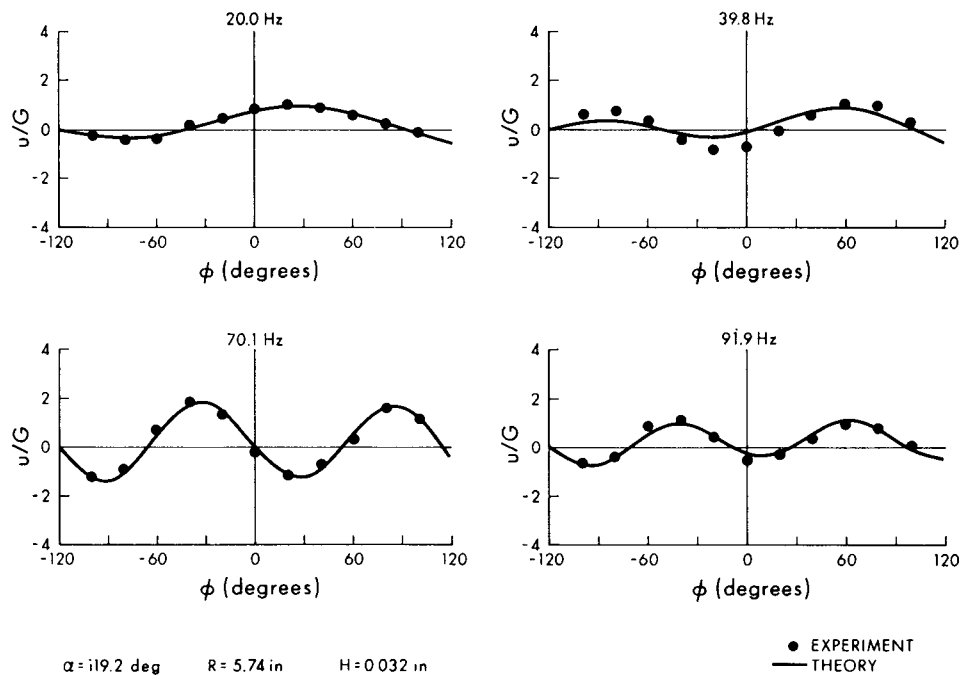


Fig. 8—Steady-state solution—Unsymmetrical support excitation, $R/H = 179.4$

was more sensitive to the choice of α than to the choice of R/H for the range of α and R/H values considered. Better agreement was obtained for those arches whose α was small.

Throughout the experimental program, every attempt was made to excite the arches in a controlled and predictable manner. Even taking all the precautions to avoid complicated arch behavior, it was observed, however, that out-of-plane vibrations occurred with some arches at forcing frequencies approximately 16 times the fundamental flexural frequency. This agreed with the observations of Volterra and Morell.⁵ It was believed these out-of-plane modes were present due to the inability to perfectly align the plane of the initial curvature of the arch with the plane of support excitation. Such a misalignment would introduce a rotation which would excite these out-of-plane modes.

In the theory and in performing the experiments, the effect of damping on the dynamic response of the arch was considered to be negligible. This assumption was evaluated by attaching a displacement probe (LVDT) to the crown of the arch and another to the base support. Under symmetrical excitation, displacements from both probes were traced simultaneously using an optical galvanometer. These traces indicated that the phase angle between the crown of the arch and the support was either 0 or 180 deg, the value depending on where the frequency of the shaker was in relation to the resonant frequencies of the arch. If damping were present in an amount which should have been included in the theory, then it should have been possible with this measurement to detect phase angles other than 0 and 180 deg. This was not the case and, therefore, the assumption of negligible damping was confirmed. While this measurement was made only at the crown of the arch, it was assumed that other points of the arch behaved in a similar manner.

Conclusions

Experimental evidence has been presented to indicate that the theory developed for the forced symmetrical and unsymmetrical support excitation of thin circular arches is valid. While the experimental values were obtained for arches with pinned-end conditions, it is suggested that the theory could also be modified to include fixed-end conditions and that similar agreement between experiment and theory should be expected.

It was found that, to obtain reasonable experimental results, utmost care and refinement had to be taken in the manufacture of the arches as well as in the performing of the experiment. It was found that experimental arch behavior was quite sensitive to small changes in curvature and to changes in the opening half-angle. Also, it was noted that out-of-plane vibrations could occur at 16 times the fundamental flexural frequency if the plane of the initial curvature of the arch did not coincide with the plane of support excitation.

Acknowledgment

The authors wish to express their sincere appreciation and thanks to the National Research Council of Canada for the financial assistance received in support of this research project under Grant A-2705.

References

1. Lamb, H., "On the Flexure and the Vibrations of a Curved Bar", *London Math. Soc. Proc.*, **1** (19), 365-376 (1887).
2. Lang, T. E., "Vibration of Thin Circular Rings, Part I, Solutions for Modal Characteristics and Forced Excitation", *Tech. Rep. 32-261*, J.P.L., Caltech, (1962).
3. Lang, T. E., "Vibration of Thin Circular Rings, Part II, Modal Functions and Eigenvalues of Constrained Semicircular Rings", *Tech. Rep. 32-261*, J.P.L., Caltech, (1962).
4. Bellow, D. G. and Semeniuk, A., "Symmetrical and Unsymmetrical Forced Excitation of Thin Circular Arches", *Int. J. Mech. Sci.*, **11** (3), 185-195 (1972).
5. Volterra, E. and Morell, J. D., "Lowest Natural Frequencies of Elastic Hinged Arcs", *Acous. Soc. of Amer.*, **32**, 1787-1790 (1962).



Design of a Mechanical Engineering Building

25

Donald G. Bellow,
MCSME, Professor,
Department of
Mechanical Engineering,
University of Alberta,
Edmonton

71-CSME-60
EIC-72-MECH 4

Introduction

Designing for the Mechanical Engineering Building at the University of Alberta started in September 1968. At this time it was learned that the building could contain up to 75,000 net square feet at a cost per gross square foot of around \$28.00. The total project cost, including design, construction, and move-in, was not to exceed \$4,000,000. In addition, it was declared that the building had to be designed with respect to the university's long range development plan. This meant that the building had to be in keeping with the growth pattern at the university, and had to provide a pedestrian way between adjacent buildings.

The Department of Mechanical Engineering had been actively engaged in planning for facilities ever since its inception as a department in 1959. Many projections were made on the basis of future student enrollment, both undergraduate and graduate, and the participation of staff in research programs. Consideration was also given to the general development of the Mechanical Engineering Department in relationship to the Faculty of Engineering, its relationship to similar departments at other universities, and its relationship to the industrial community.

As soon as the design group was established, the department was requested to produce a statement of its purposes to serve as a guide for the physical planning of the building. Some time was taken in preparing this and it was gratifying to the department that this document received careful attention by all those concerned with arriving at a concept for the building. This document, entitled "A Philosophy for Mechanical Engineering", embodied all of the purposes and aspirations that the department had for a new building. Ideas concerning the teaching process, research aims, and service responsibilities were detailed in this document. Included was a proximity matrix to indicate the desired room interrelationships and room specifications.

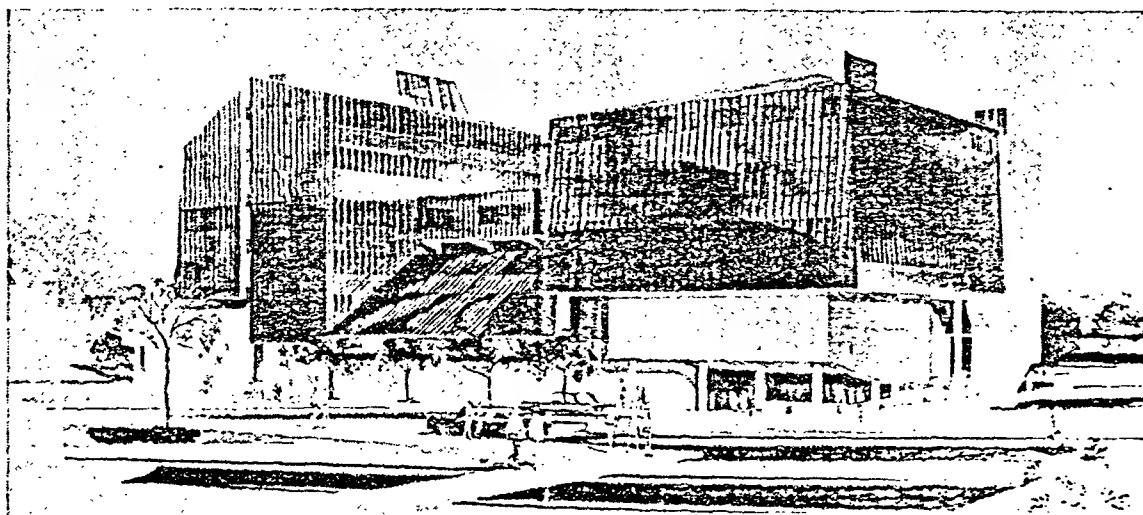
The designers suggested that a study be made of

new mechanical engineering buildings elsewhere on the continent. This procedure had been used by other design groups and the university had accepted this as a desirable, if not necessary, part of the design process. The department rejected this on the grounds that a solution to their problems and needs would not be found elsewhere. Rather than copy aspects of buildings which appealed to the department, it was believed that the building should be designed to reflect the philosophy practiced by the Department of Mechanical Engineering in achieving its goals in education and research. Specifically, it was believed the following concepts were of great importance in arriving at such a design:

- The building should reflect the importance of mechanical engineering in the world today.
- The industrial character of the building should be exploited to give a sense of space and freedom associated with such a dynamic subject as mechanical engineering.
- The building should express its function in an interesting and exciting way.
- The building should itself be a teaching vehicle and not just a space in which teaching takes place.
- The building should appear to be part of the industrial expansion and northern development of Canada's great northwest.

It was anticipated that if these concepts were embodied in the design of the building a more meaningful solution to the special needs of mechanical engineering would be achieved. The faculty wanted a building designed for the future, and not one which could have been designed in the past. This did not mean that change for the sake of change was desired, but on the contrary, it was believed that in many instances university architecture had become stereo-typed beyond the point where economics was still a consideration. It had seemed that it was simpler to repeat the same architecture rather than to develop new architecture which would better fit the changing needs of the university community.

Figure 1
Artist's rendition of the
mechanical engineering
building



On the Concept of Openness

The sense of space and freedom was considered to be important. It was believed one of the best ways of achieving this, as well as obtaining the desired interrelationships within the building, was to use a liberal amount of glass. So that the occupants would feel a part of their environment, it was decided to openly display all laboratories housing major pieces of equipment, the mechanical room containing the building's air handling and service systems, and the machine shop.

The main entrance serves as a display area and as such expresses the theme of mechanical engineering. Also, the hallways contain enough space so as to provide areas for use of displays, planters, and art forms. The whole purpose is to have the building create an inspiring environment in which to work.

Lighting has been placed on the exterior of the building to highlight the architectural features. In the interior, lighting will be used to draw attention to the equipment in the large laboratories which will be visible from the hallway systems.

Classrooms

One of the most important considerations in a university building is its design and use of classroom space. The department has experienced many different types of classrooms in its brief history. Some fixed ideas have arisen as to what is a workable classroom and what is not. However, on this there is no unanimity of opinion.

While admitting to not being practitioners of new teaching methods, the faculty did not wish the building to inhibit experiments in teaching. It was intended that the classroom space be designed to encourage experimentation in the teaching process. Thus, two 100 seat tiered lecture theatres were designed; one of which is of the traditional type with fixed seating, but has the feature of continuous tables in front of the seats so that students can spread their work out with some degree of freedom. In the other there is no fixed seating, but there are three different levels which are essentially platforms upon which seating can be arranged in any way the lecturer desires. When the traditional type lecture space is desired, the chairs can be arranged in a symmetrical fashion and the lecturer can position himself at the front of his class. However, he can also move his podium to a more central location in the classroom and deliver his lecture from a position amongst the students. This arrangement should promote more interchange of ideas between faculty and students and thus improve the level of understanding in the classroom. The same space can also be used as a design laboratory when scheduling demands it. For example, by arranging the seating on each level as a separate entity it will be possible to conduct three design groups, whose projects differ in detail but not in philosophy, simultaneously within the one general area. In this way a rather expensive space becomes a multi-purpose space.

Two other large classroom areas have been

designed to achieve maximum utilization of the space. On one level a 2,700 sq. ft. area has been divided into two smaller areas by use of folding walls. On demand, this space can be used as a single, or as two separate units. By pulling back the walls it will be possible for classrooms to overflow into the hallway system when more space is required. On another level, a 3,500 sq. ft. area is completely open wherein classrooms will be partitioned off by a suitable arrangement of tables and chairs. In these areas, special attention has been paid to acoustics, with carpets on the floors and acoustic tiles backed by plaster board on the drop ceiling.

Other teaching areas within the building have been placed in the vicinity of frequently used undergraduate laboratories. Such placement will serve a dual role; as lecture rooms serving a specific laboratory, and as study rooms in the off periods during the day and evening.

Undergraduate and Research Laboratories

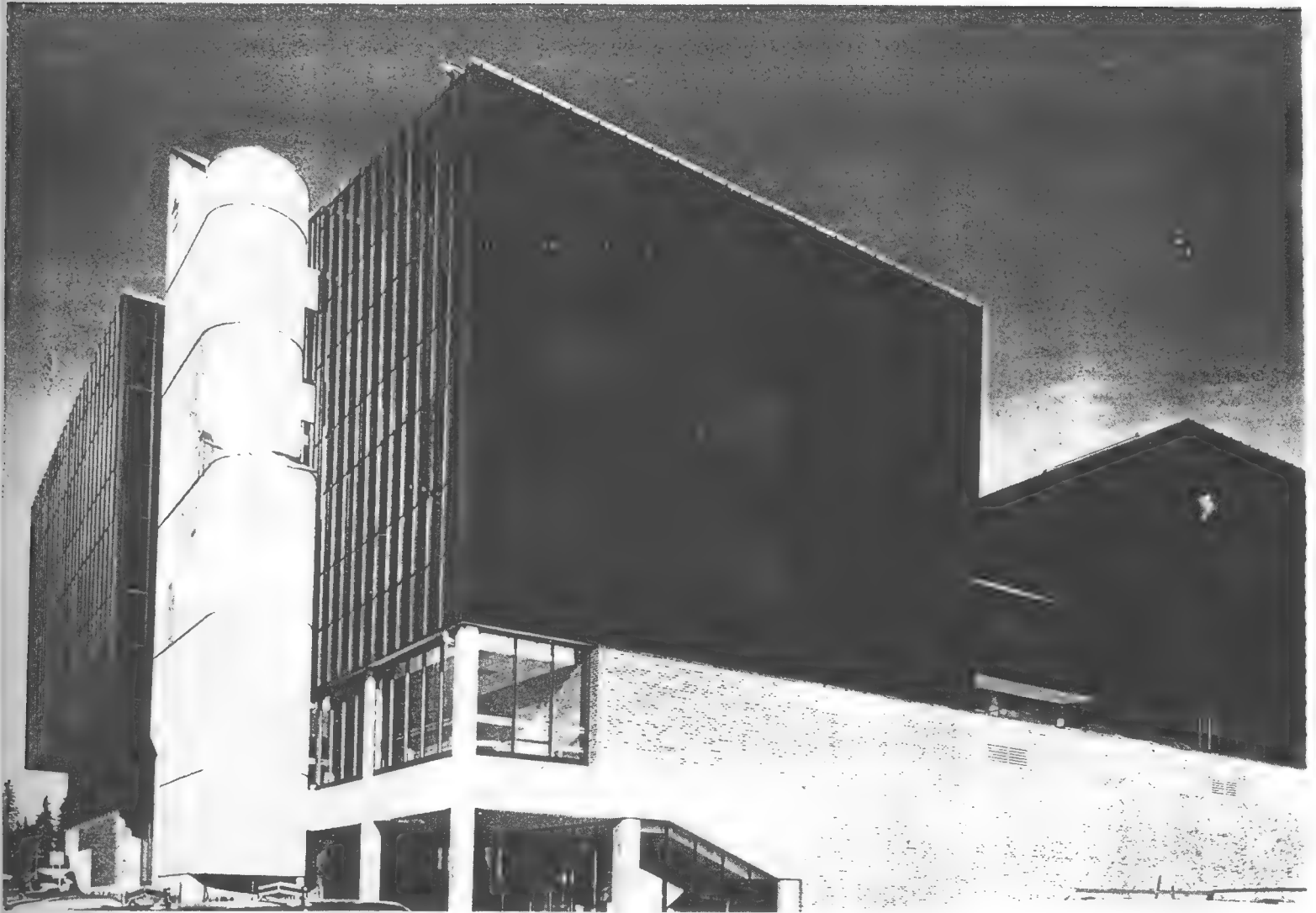
Laboratory experiments play an important role in the educational program of mechanical engineering. It is only in the laboratories that students see practical applications and demonstrations of the theoretical principles taught in the lecture rooms. In a sense, the laboratories are used to express the dynamic character of mechanical engineering. Wherever possible, the laboratories are visible through windows in the hallways. This has been incorporated in the large and frequently used undergraduate laboratories, and especially for those which are occupied with interesting and dynamic looking equipment.

It is intended to place undergraduate experiments side by side with research projects. In doing this, a two-fold purpose will be achieved; one, it will acquaint the undergraduate students with the kind of research that is being done in mechanical engineering, and two, it will give the graduate students an opportunity of explaining their research to the undergraduate. While there are some research projects which are of such a delicate nature that it would be unwise to place them in the vicinity of pedestrian traffic, wherever possible a compatible mixture of research and undergraduate laboratories will be attempted.

The effect of combining undergraduate and research laboratories has been to reduce the quantity of smaller rooms within the building. This has been welcomed by the designers as a means of making the building more efficient. It is anticipated that this will make the teaching and learning process also more efficient.

The Use of the Building as a Teaching Tool

The entire building is to serve as a teaching and learning experience for the students. The building has been designed to be a teaching vehicle and not just a space in which teaching takes place. It is intended that students, in the course of their laboratory instruction, will obtain an appreciation for measurements on industrial and commercial



THE MECHANICAL ENGINEERING BUILDING

THE UNIVERSITY OF ALBERTA

MECHANICAL ENGINEERING BUILDING



THE UNIVERSITY OF ALBERTA

The University of Alberta is proud to announce the official opening of their new Mechanical Engineering Building on April 27, 1973. Not only is this a special occasion for the Department of Mechanical Engineering, but it also marks the 60th Anniversary for the Faculty of Engineering at The University of Alberta.

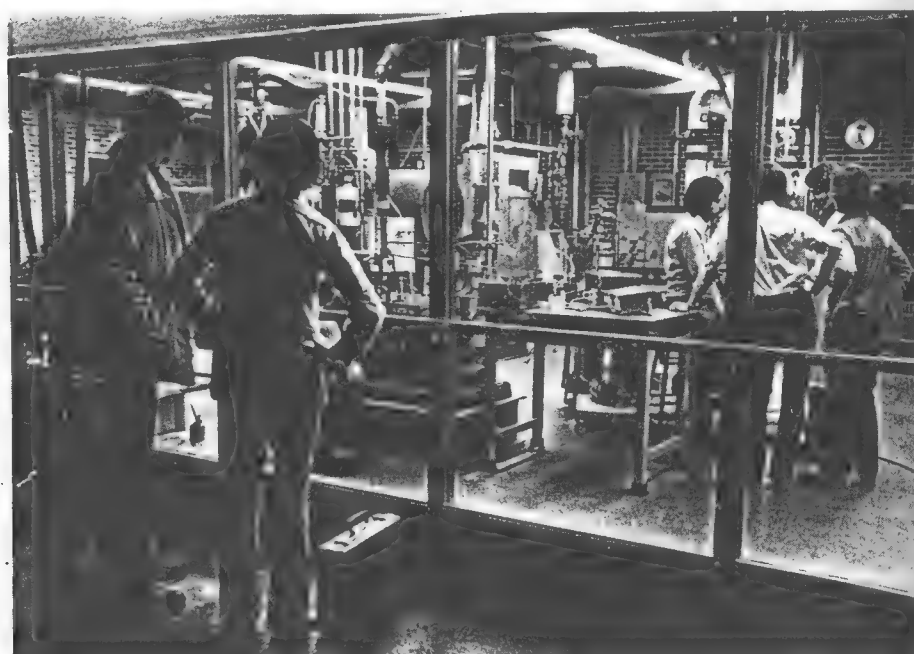
When formed in 1913 the Faculty of Applied Science, which later became named the Faculty of Engineering, granted degrees in Engineering and Architecture. In 1913, Engineering encompassed Civil, Electrical and Mining. Subsequent developments saw the introduction of Chemical, Metallurgical, and Petroleum Engineering. In 1959 the Mechanical Engineering Department was formed with its first graduands receiving their degrees in 1960. Since that time the Department of Mechanical Engineering has developed undergraduate and graduate programs in three broad areas: Applied Mechanics, Industrial Engineering, and Thermoscience.

During its brief history the Department of Mechanical Engineering has developed and grown to the point where it now has one of the largest undergraduate enrollments in Canada. Concurrent with its undergraduate growth the Department has developed strong research programs in the areas of Applied Mechanics, Fluid Mechanics and Thermoscience. Much of the

research carried out in the Department is applied and is conducted in close liaison with industry and government.

In the past, the physical facilities of the Department have fallen short of what was considered to be adequate to keep pace with its academic growth. For example, during the past twelve years the Department has moved five times. This is not extraordinary for a Department at this University but it is unusual for one which has research and teaching laboratories. With this experience now in the past the Department is pleased that for the first time all of its facilities are housed in one building.

When it was first announced that planning could commence for a new building the Department reacted with enthusiasm. The Faculty wanted a building to reflect the philosophy



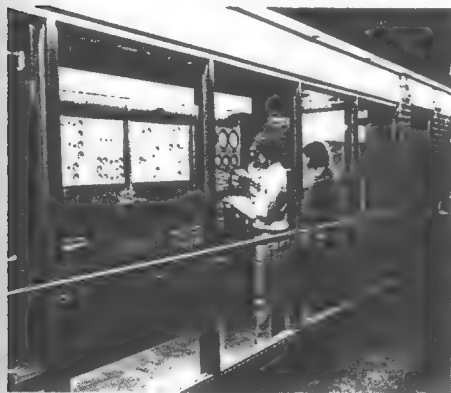
practised by the Department of Mechanical Engineering in achieving its goals in education and research. Specifically it was believed that in arriving at a satisfactory design solution the following concepts were to be considered.

—The building should itself be a teaching vehicle and not just a space in which teaching takes place.

—The building should reflect the importance of Mechanical Engineering in the world today.

—The industrial character of the building should be exploited to give a sense of space and freedom associated with such a dynamic subject as Mechanical Engineering.

—The building should express its function in an interesting and exciting way.



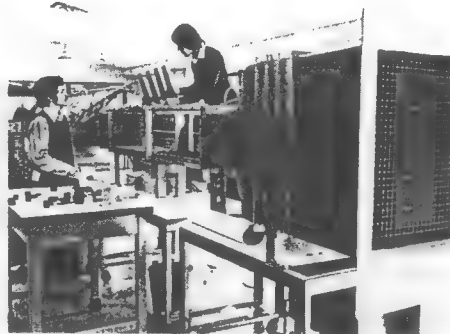
On the Concept of Openness

The sense of space and freedom was considered to be important. It was believed that the best way of achieving this, as well as obtaining the desired interrelationships within the building, was to use a liberal amount of glass. In order that the occupants would feel a part of their environment, it was decided to openly display all laboratories housing major pieces of equipment, the mechanical room containing the building's air handling and service systems, and the Machine Shop.

From practically every point inside the building a visual contact with the outside is possible. After prolonged study and concentration a visual break is often desirable if not necessary. The extensive use of exterior windows provides for this in an effective and aesthetic manner.

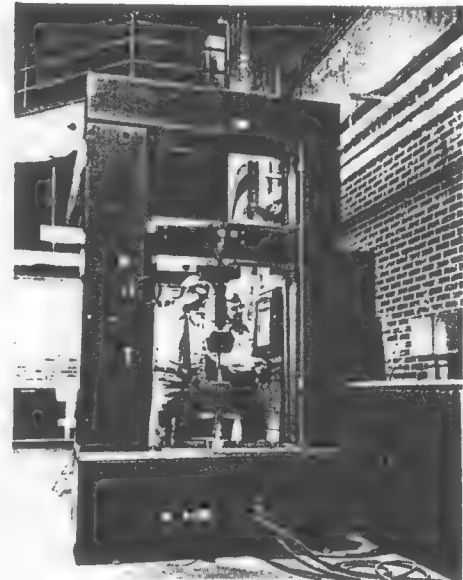
Classrooms

It was intended that the classroom space be designed to encourage experimentation in the teaching process. Two one hundred-seat tiered lecture theatres were designed; one of which is of the traditional type with fixed seating, and the other in which there is no fixed seating but with three different levels allowing seating to be arranged in any way the lecturer desires. This same space can be used as a design laboratory when scheduling demands, thus making it a multi-purpose space. On the fourth floor over 2,700 sq. ft. of classroom space has been divided into two areas by the use of folding walls. This space can be used as a single large area or as two separate units. By folding back the walls it is possible for classrooms to overflow into the hallway system when even more space is required. In these areas special attention has been given to acoustic treatment to the floors, ceiling, and folding walls.



Undergraduate and Research Laboratories

Laboratory experiments play an important role in the educational program of Mechanical Engineering. It is mainly in the laboratories that students see practical applications and demonstrations of the theoretical principles taught in the lecture rooms. In one sense the laboratories are used to express the dynamic character of Mechanical Engineering. Wherever



possible, the laboratories are visible through windows in the hallways. This has been incorporated in the large and frequently used undergraduate laboratories, and especially for those which house interesting and dynamic equipment.

Undergraduate experiments are placed side by side with research projects in many of the laboratories. In doing this a two-fold purpose has been achieved:

—It allows the undergraduate students to be acquainted with the kind of research that is being done in Mechanical Engineering,

—It gives the graduate student an opportunity of explaining his research to the undergraduate.

The effect of combining undergraduate and research laboratories has been to reduce the quantity of smaller rooms within the building, a concept welcomed by the designers as a means of making the building more efficient. It also provides the opportunity for making the teaching and learning process more effective.

The Building as a Teaching Tool

The entire building serves as a teaching and learning experience for the students. The building has been designed to be a teaching vehicle and not just a space in which teaching takes place. It is now possible for students, in the course of their laboratory instruction, to obtain an appreciation for measurements on industrial and commercial systems and not just on laboratory apparatus.



Whether formalized or not, students are now able to see what goes on in the Machine Shop and can trace all of the building service systems from one point to another in the building. In addition, the building serves as a piece of experimental apparatus by providing examples for the measurement of noise levels and the effectiveness of various types of acoustic treatment. Also, the vibrations of the various areas in the building can be monitored and measured by students in the course of normal laboratory instruction. The main consideration for making the building as open as it is, is for the students to be able to walk through the various hallways and see the various activities associated with Mechanical Engineering. The Faculty believes that

this informal learning process is extremely important and would not be possible in a building with laboratories and service facilities hidden behind brick walls and closed doors.

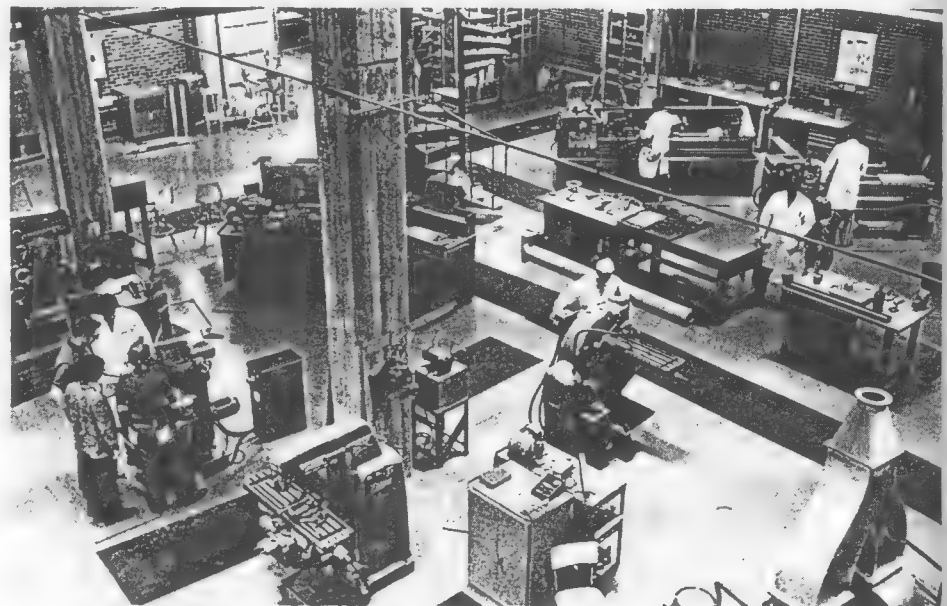
Building Layout

The building was designed so that noisy and vibration producing equipment would be located as far as possible from the administrative offices, classrooms, and rooms which house delicate and sensitive equipment. In achieving this the building evolved into three different sections. The East Tower houses the laboratories. The central section contains the Machine Shop, the Materials Engineering Laboratory, and the building's mechanical systems. Most of the laboratories housing equipment have been enveloped with sound absorbing masonry walls. Heavy machines which produce vibration have been located on Level One on foundations isolated from the superstructure. The West Tower is a people tower in which the offices and classrooms are located. To enclose the exterior of the building a reflective rain screen has been chosen which allows the building to mirror its surroundings. The purpose of this is to show that not all buildings on campus must be identical, or be constructed of identical materials, to blend into a common theme.

The main pedestrian walkway through the building is provided on Level Two allowing access to the main lecture theatres and an overview of the Machine Shop and the Materials Engineering Laboratory. In future this main pedestrian walkway will connect with adjacent buildings and thus become a link in a covered walkway system as provided for in the University's Master Plan.

The Department believes they have a building which itself will play a role in the learning process, a building which will serve as an example of good design not only for the University but for the industrial community, a building which is functional like a mechanical engineering building should be, a building which looks like a mechanical engineering building, and a building which will enable the Department to achieve the excellence it has set for itself.

The building was designed by the architectural firm of Dupuis, Dunn and Donahue Ltd. with design consultant J. W. Long and Associates. The engineering consultants were Reid, Crowther and Partners Ltd. The contract for the building was awarded to Cana Construction Ltd. (Edmonton) for a total cost of \$3,366,100. It contains approximately 78,000 net sq. ft.



Applications of Solid Mechanics

Proceedings of the Symposium held at the
University of Waterloo, June 26 and 27, 1972.

Editors:

R. G. Charlwood

D. S. Weaver

B. Tabarrok

IMPROVING THE FATIGUE LIFE OF BUTT-WELDED MEDIUM STRENGTH STEELS

M.G. Faulkner and D.G. Bellow

University of Alberta

SUMMARY-While the static strength of butt-welded medium strength steel (60-90 ksi yield) approaches the yield strength of the unwelded steel, the fatigue strength is usually reduced to approximately one-half of its original value. Many methods of improving the fatigue strength of the weld have been proposed. The purpose of the present work was to compare the improvements obtained by grinding the weld bead flush and by steel shot peening the weld. The work was done on Stelco Columbium 60 with an automatic submerged arc weld. The results obtained were compared with those of previous investigators.

The results show, that with careful grinding, the fatigue strength can be brought up to that of the parent material. This is due both to the reduction of the stress concentration and the introduction of residual stresses in the surface layer.

The steel shot peening process after welding improved the fatigue strength by 45 percent. This improvement is approximately what would be expected by smoothing the weld using additional passes. It is shown that the effectiveness of this treatment is dependent on the depth of cold working of the surface layer.

INTRODUCTION

It is well known that the static strength of butt-welded medium strength steels (60-90 ksi yield) approaches the yield strength of the unwelded steel. The fatigue strength, however, is usually reduced considerably after welding. Many proposals have been put forward for improving the fatigue life of these welds since often these determine the overall performance of a structure. Two of the most common methods are:

- (a) improvement of the weld profile
- (b) introduction of a favorable residual stress pattern.

These two methods are interrelated; for example, by grinding the weld bead in a butt-welded sample changes the notch geometry but also introduces some residual stresses into the surface layer. The most common improvement techniques used include grinding the weld bead flush, hammer or shot peening, preloading and local compression in which a region adjacent to the weld is compressed to form a residual stress pattern. The technique of smoothing the weld bead by using additional weld passes has also been employed. Of the methods listed, grinding and shot peening are probably the most extensively used.

While the effects of these latter techniques have been studied by various investigators their results tend to vary considerably. A comparison of some of these techniques has been given by Harrison [1] and by Gurney [2], however, the comparisons were not always based on the same materials and/or testing techniques.

It is the purpose of the present study to compare the effects of grinding and shot peening on the fatigue life of a weldable medium strength steel. The results are compared to previous investigators who used these as well as other techniques. It is suggested that, with the knowledge of the

FATIGUE LIFE OF STEELS

improvement possibilities, a decision on which technique to use in a given situation can be made.

TEST SPECIMENS AND TESTING TECHNIQUES

Stelco Columbium 60 steel was used as it is a steel with good weldability and a relatively high (greater than 60 ksi) yield strength. The test specimens were made by welding two 5 in. wide, 1/4 in. thick plates of steel which were in the as-rolled condition. The welding process chosen was automatic submerged arc to control, as far as possible, some of the welding variables. The details of this process as well as the material properties of the weld and plate material are given in Table I.

The welds were all fluoroscoped to check for flaws and then cut into 3 in. wide strips with the weld transverse to the cut. In the cases where surface treatment of the weld was done, this was completed before the specimen was cut from this 3 in. strip to the shape shown in Figure 1. The first specimens tested were radiographed as well but when no flaws could be seen this inspection was discontinued.

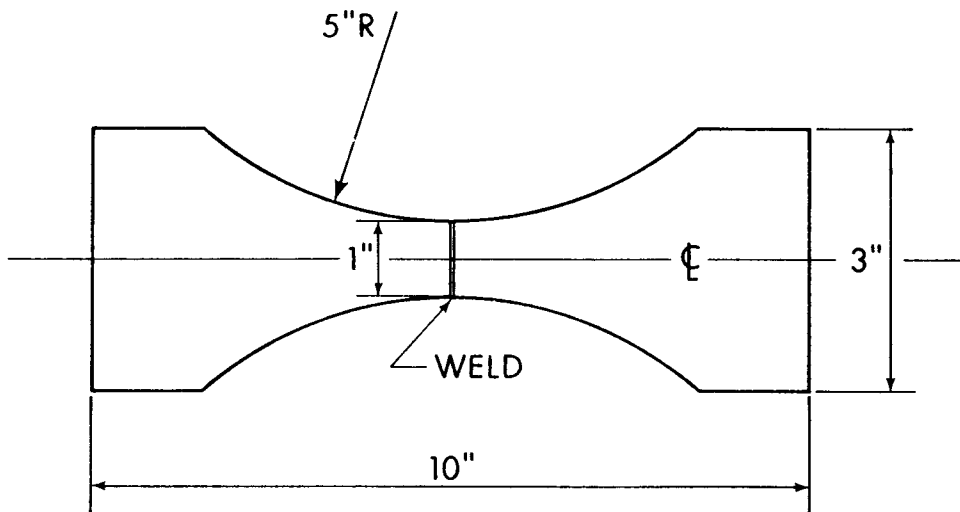


Figure 1 - Fatigue Specimen

FATIGUE LIFE OF STEELS

The ground specimens were machined using a 46 grit, grade J wheel, grinding parallel to the weld. The surface CLA values parallel and perpendicular to the weld after grinding were 1.5 μ -in. and 5.9 μ -in. respectively. The welds were ground to three different depths. In the first case care was taken to insure that the grinding was as close to the parent material surface as possible without removing any of the mill scale from the parent material or the toe of the weld. In the second case, the grinding removed a small amount of the scale but the weld-material interface was still visible. There was no net decrease in section in either of these cases. The third case of grinding undercut the thickness of specimen by approximately 0.005 - 0.010 in.

Two peening processes were considered; the first process using glass beads 0.007 - 0.012 in. in diameter, was used on only one group of 12 specimens, the second peening process used a "Rotoblast" wheel with steel shot 0.025 - 0.045 in. in diameter. The velocity of this shot was approximately 250 ft/sec. This peening was done for 8, 15 and 30 min. on coupons of the parent material to evaluate length of peening time versus the depth of working on the material. It was found that after 8 minutes the maximum work-hardening depth had been obtained and increasing the length of time only gave better coverage. The surface roughness on the steel shot peened surfaces was CLA 26 - 34 μ -in.

The fatigue testing was done on an Amsler 10 Ton Vibrophore at approximately 190 Hz. The specimens were loaded in pulsating tension with the mean load set at half the maximum for the stress level selected. The fatigue life was indicated when the machine automatically stopped due to a decreasing mean load.

The depth of working of each of the surface finishing processes was evaluated by cutting the specimen at a small angle to the surface. The hardness was measured on this inclined surface using a KNOOP diamond indenter with a 100 gm load. The depth of hardness obtained in this manner was checked against that obtained by taking surface hardnesses with various loads from 25 - 1000 gm.

RESULTS OF TESTING AND DISCUSSION

Fatigue Results

A summary of the results obtained for the fatigue testing of the welded plate, parent material and the various treatments of both are shown in Figure 2. The median values of at least twelve specimens are plotted for each point on the S-N curves. The results shown for the ground, and the ground and steel shot peened cases have had the complete grinding in which a net decrease of the thickness occurred. When considerable scatter occurred more than twelve specimens were tested, a situation which occurred when the stress concentration due to the weld bead was reduced. The standard deviation which occurred in each series in which all the specimens cracked is shown in Table II.

In almost every case of cracking of the welded specimens the crack started at the weld toe and always on the surface. As seen from Figure 3 this is the heat-affected zone (HAZ) and the welding resulted in a smaller grain size in this region. This is the same result as found by Signes et al [3]. However, in their case it was also noticed that a significantly greater amount of non-metallic inclusions were also present in this region.

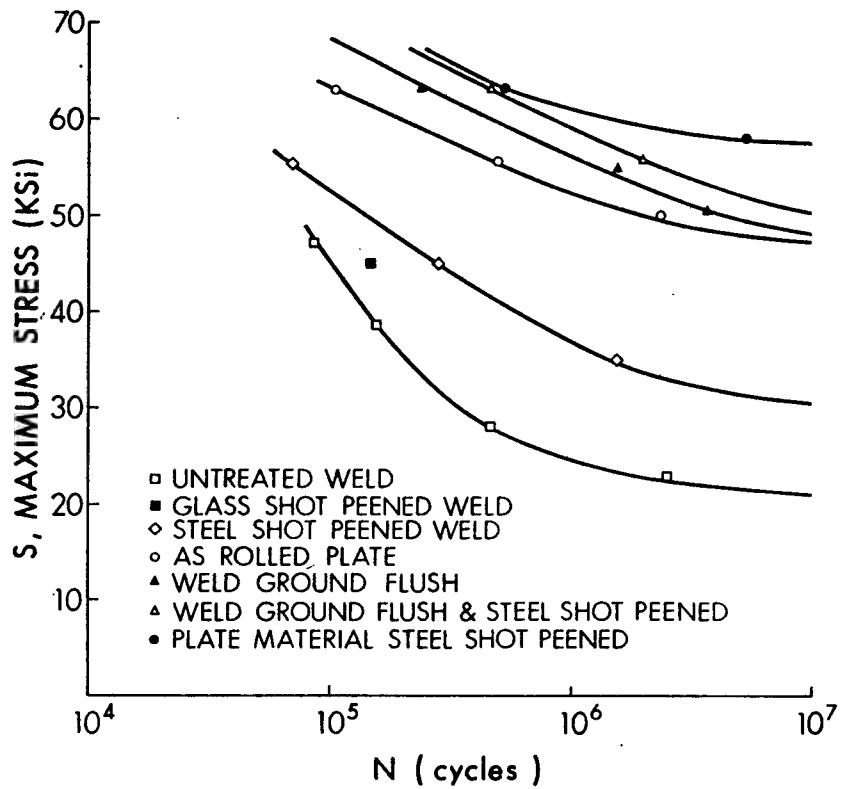


Figure 2 - Effect of Improvement Techniques on Fatigue Life

FATIGUE LIFE OF STEELS

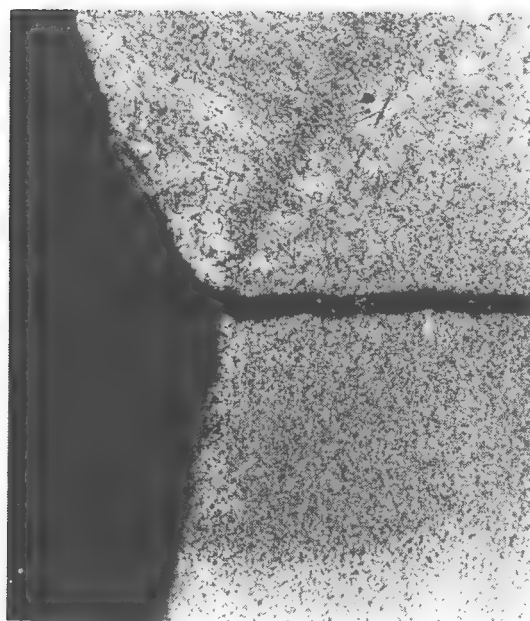


Figure 3 - Typical Weld and Fatigue Crack

In only three cases did the crack initiation not occur on the weld-parent material interface, indicating that the weld itself was not weak in fatigue. Other investigators [4] found that the point of initiation moved from the HAZ to the weld when the stress concentration was eliminated by grinding.

It is interesting to note that in all of the welded specimens that cracked during testing, the crack always started on the filler pass side of the weld. Examination of the weld metal in Figure 3 shows dendritic grain growth in the filler pass weld metal as well as a slightly larger HAZ bordering the weld. The enlarged HAZ could be the reason for this weakness since this is the most critical region. In addition, the hardness of the filler pass weld metal was higher (205 KHN) than that of the surrounding parent material and first pass weld (185 KHN).

The results show that, while Columbium 60 is meant to be a medium strength steel with good welding properties, there is a 100 percent improvement in fatigue strength possible with the weld steel. At 2×10^6 cycles the fatigue strength in the untreated welded plate was 23 ksi while for the plate itself it was 50 ksi.

It is also seen that this improvement is possible provided care is taken in the weld surface treatment. The complete grinding of the weld increased the fatigue strength to 53 ksi at 2×10^6 cycles. However, without the complete grinding Figure 4 shows the scatter of results that occurred. It is possible in this case for the grinding to be almost ineffectual if not done completely. The reason for this is that the critical HAZ was surface ground in some cases but not in others. While complete grinding reduces the effect of this zone, this is at the expense of a slight reduction in section. This improvement in fatigue strength

FATIGUE LIFE OF STEELS

by removing the weld bead has been demonstrated by Kenyon et al [5] and Frost and Denton [4] for steels with approximately the same mechanical properties as the Columbium 60. Their results show that removal of the weld bead results in fatigue strengths approaching that of the parent material. However, in the latter case the initiation point moved to the center of the weld. Less improvement has been reported by Dunsby and Walker [6] for maraging steels.

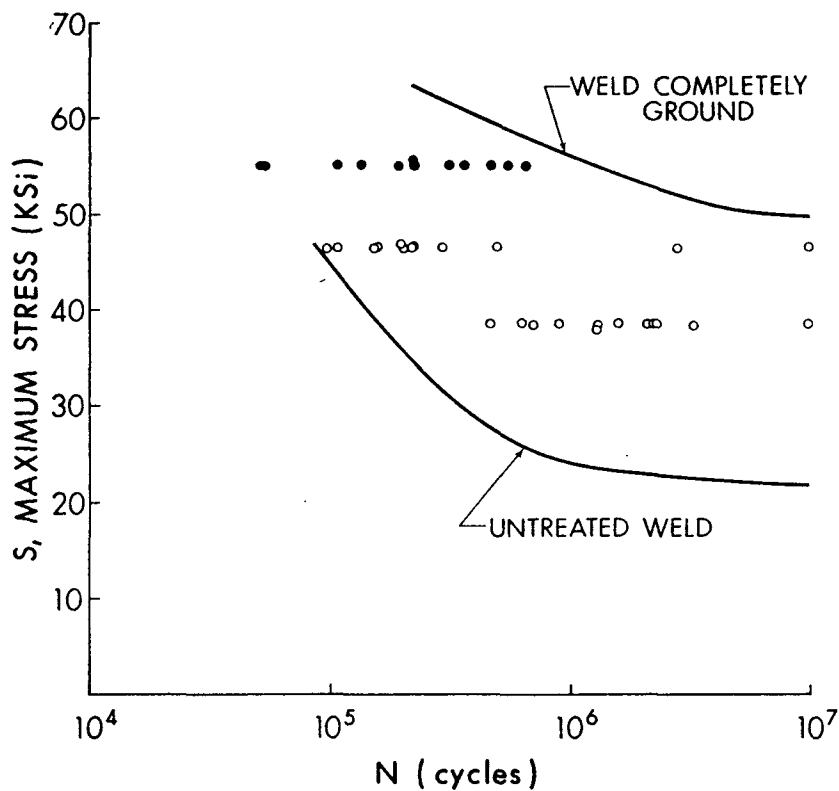


Figure 4 - Effect of Weld Grinding on Fatigue Life

For improvement of the weld by shot peening, Figure 2 shows the steel shot yielded an increase in fatigue strength from 23 ksi to 33.5 ksi, a 45 percent improvement. This improvement is greater than can be obtained by simply peening the parent material, in which case the fatigue strength rose from 50 ksi to 59 ksi, an 18 percent improvement. The larger improvement in the welded case is due to the fact that the stress concentration of the weld has been reduced as well as introducing compressive stresses in the surface layer.

Previous investigators have considered the improvement in fatigue strength due to the peening of welds. Guerrero [7] reported on work in which the fatigue life in pulsating tension was improved approximately 25 percent above that of the untreated weld. Baron and Brine [8] obtained a 35 percent improvement for steel comparable in properties to that of Columbium 60.

While the results of only one series of tests of the glass shot peening is shown in Figure 2 it indicated that this technique would result in an improvement in the fatigue strength at 2×10^6 cycles (at 2×10^5 cycles the improvement was 20 percent). The smaller increase for this procedure as opposed to the steel shot peening is believed attributable to the smaller depth of hardening caused by the glass shot. The surface hardness and the variation in hardness with depth are shown in Figure 5. The glass bead peening work hardens the parent material to a depth of .004 - .005 in. while the steel shot blast increases the hardness to .010 in. In this instance, doubling the depth of increased hardness doubles the percentage increase in fatigue strength as shown in Figure 2. This may also be the reason why previous investigators have reported improvements from 30 to 100 percent [9]. In part this variation may be

FATIGUE LIFE OF STEELS

due to materials and welding techniques. However, the differences in work-hardening are probably a major reason as well. While it is possible that extreme amounts of peening could be detrimental, in the present investigation there was no evidence that this occurred.

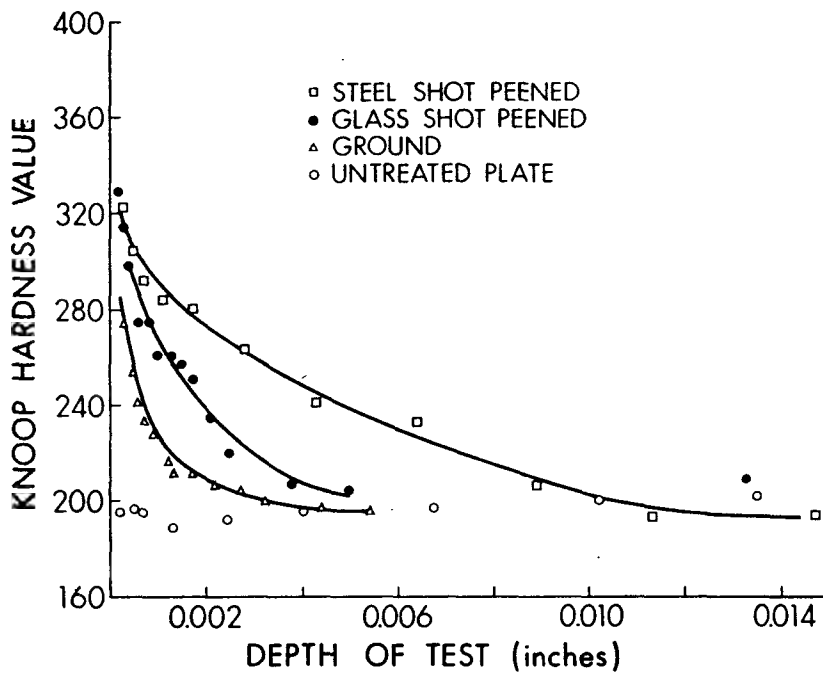


Figure 5 - Effect of Improvement Techniques on Depth of Cold-Working

The fact that the peening process alters the geometry of the notch makes it akin to grinding as well as other notch reduction techniques. Kenyon et al [5] obtained a 50 percent improvement by adding an extra bead using an argon torch and mild steel filler rod. In this way, the weld profile blended smoothly with the plate and the notch at the toe was eliminated. A similar procedure was used by Kanazawa et al [10] on medium strength steel (85 ksi tensile strength) who obtained an increase of approximately 35 percent. One would expect this amount of improvement from the steel shot peening as well. Recently Chadwick [11] reported improvements of 40 percent by explosively peening maraging steel; again approximately the amount of improvement possible by smoothing the weld.

Figure 2 also shows the results of first grinding completely, then steel shot peening. The improvement compared to the completely ground is small (53 ksi versus 56 ksi). Again this small increase is due to the increased depth of hardness caused by the steel shot compared to the grinding technique (Figure 5). While the surface hardness may be increased to approximately the same value, the depth depends on the treatment. In neither the ground nor the ground and steel shot peened surfaces is the improvement as much as would be expected if the plate material had these treatments applied to it.

CONCLUSIONS

While the results above are for butt-welded Columbium 60, it is believed that they would apply to most butt-welded medium strength steels.

- (1) It is possible to improve the fatigue strength of submerged arc welded medium strength steels to approach that of the rolled plate by grinding the

FATIGUE LIFE OF STEELS

weld bead flush. This is possible only through careful grinding since any notch left unground can reduce the fatigue life until it is little better than the untreated welded plate.

- (2) The steel shot peening process after welding can improve the fatigue strength by 45 percent. This is about the improvement one could expect by smoothing the weld bead by an additional weld pass.
- (3) The effectiveness of the surface working techniques is dependent on the depth of cold working obtained by the process. While it may be possible that too much surface working is detrimental this was not observed in this work.
- (4) In specimens welded with two passes, the second or filler pass was most critical from the fatigue point of view. It may be possible to increase fatigue life appreciably by working only the filler pass side.

REFERENCES

- 1. J.D. HARRISON 1965, *Commonwealth Weld Conf.* London, 327.
- 2. T.R. GURNEY 1968, *Fatigue of Welded Structures* Cambridge University Press.
- 3. E.G. SIGNES, R.G. BAKER, J.D. HARRISON and F.M. BURDEKIN 1967, *Br. Weld. J.* 14, 108.
- 4. N.E. FROST and K. DENTON 1967, *Br. Weld. J.* 14, 157.
- 5. N. KENYON, W.B. MORRISON and A.G. QUARRELL 1966, *Br. Weld. J.* 13, 123.
- 6. J.A. DUNSBY and A.C. WALKER 1969, *National Research Council of Canada Mechanical Eng. Report MS-122.*
- 7. U. GUERRA 1966, *Br. Weld. J.* 7, 513.
- 8. H.G. BARON and F.E. BRINE 1965, *Commonwealth Weld. Conf.* 322.
- 9. F.E. BRINE, D. WEBBER and H.G. BARON 1968, *Br. Weld. J.* 15, 541.
- 10. S. KANAZAWA, T. ISHIGURO and M. MIZUI 1970, *IIW Doc.* XIII-575-70.
- 11. M.D. CHADWICK 1971, *Metal Const. and Br. Weld. J.* 2, 374.

Table I
Material Properties and Welding Details

Chemical Compositions					
	C	Mn	P	S	S _i Columbium
Columbium 60	0.2%	1.2%	0.04%	0.05%	-- 0.005%
Oxweld #36 Rod	0.14%	2.0%	0.017%	0.024%	0.05% --
Mechanical Properties					
	Yield (psi)		Ultimate (psi)		Elongation
Columbium 60	77,000		80,000		--
Oxweld #36 Rod	75-90,000		--		20-30%
Welding Details					
1. Welding Process	- submerged arc welding, double side, using flux				
2. No. of Welding Wires	- two, tandem				
3. Welding Wire	- Linde, Oxweld #36, 1/8" diameter				
4. Flux	- Linde, Oxweld 585				
5. Tip Height	- 7/8" from work piece				
6. Distance between Electrodes	- 5/16"				
7. Speed	- 56 in/min				

FATIGUE LIFE OF STEELS

TABLE II
Standard Deviation of Fatigue Specimens

	Maximum Stress (ksi)	Median Life (x 1000 cycles)	Standard Deviation (x 1000 cycles)
1. Untreated Weld	47.0 38.5 28.0 23.0	86.0 153.5 457.0 2,464.0	25.6 97.0 402.2 1,131.0
2. Glass-Shot Peened	45.0	148.0	30.1
3. Steel-Shot Peened	55.5 45.0 35.0	70.0 280.5 1,565.0	85.2 122.0 1,808.0
4. As-rolled Plate	63.0 55.5	104.5 499.0	119.6 1,132.0
5. Welds Ground Flush	63.0	236.0	78.4
6. Welds Ground Flush & Steel Shot Peened	63.0	469.5	155.9
7. Plate Material Steel Shot Peened	63.0	525.5	624.9

Fatigue of Threaded Sucker-Rod Couplings

D. G. BELLOW, Professor,
M. G. FAULKNER, Assistant Professor,
Department of Mechanical Engineering,
University of Alberta,
Edmonton 7, Alta.

ABSTRACT

Accelerated laboratory tests on the fatigue characteristics of sucker-rod couplings were carried out on a closed-loop hydraulic testing system. The purpose was to evaluate a number of different thread designs currently being used in the manufacture of sucker-rod couplings. The thread forms tested included the simple cut, a keyhole cut and burnished, cut and cold worked and fully cold worked.

The results show that the fatigue life increases as the degree of cold-working increases. It is also seen that the effects of accelerating the testing are insignificant.

INTRODUCTION

THE FAILURE OF SUCKER-ROD JOINTS is of considerable interest to those involved in petroleum production. To eliminate or minimize such failures many attempts have been made both in producing new rod and coupling designs and eliminating the coupling altogether. The literature shows a number of papers dealing with the subject of joint failures, specifically related to im-

proving the pin connection. There is apparently very little written on the coupling itself, but there are a multitude of coupling designs commercially available for use in joining sucker-rods. The question arises as to which of these designs is the best. Thus, to aid in the design and selection of a coupling, the purpose of this paper is to evaluate the fatigue life of a number of different thread designs which are being used in the manufacture of sucker-rod couplings.

Coupling design has, for the most part, been consistent with the pin design to which it must mate. Coupling thread design has evolved from the simple cut thread, to a keyhole, burnished, cut and cold worked, and recently to a fully cold worked or rolled thread. Apart from the simple cut thread and keyhole thread, all other thread designs incorporate some degree of cold working in the thread-forming process.

To the consumer the coupling represents but a part of the cost of a rod. However, to the manufacturer, not all coupling designs can be made with the same ease and quality control and, hence, same cost.

The majority of coupling failures are the result of fatigue damage. This damage can be accelerated by improper joint make-up in the field, operating in a hostile environment such as sour wells, manufacturing couplings from materials with poor fatigue characteristics, and the manner in which the thread has been formed inside the coupling. The problems of improper joint make-up have been explored in the paper by Hardy.⁽¹⁾ In this same work, reference is made to the influence of corrosion on the fatigue life of sucker-rod materials. Although the scope of the present investigation excludes evaluation of the fatigue life of coupling materials, its main purpose is to evaluate the fatigue life of thread designs found in sucker-rod couplings and compare these results with the fatigue life of the unnotched coupling material.

TESTING PROGRAM

In any testing program involving fatigue, one of the two major problems to be overcome is to control all but one of the variables involved. The other is to accelerate the testing so that results can be obtained in as short a time as possible without biasing the results.

To conduct laboratory fatigue tests on couplings at the same rate of load application as experienced in the field would take a very long time and would be a very costly experimental program. Because the main question to be answered is how does one coupling thread configuration compare with another, it was deemed permissible to increase the frequency of load application to the maximum of the testing equipment available in the laboratory.

The testing machine used in fatiguing of the sucker rod couplings was a closed-loop servo-hydraulic system produced by Gilmore of Cleveland. This machine



D. G. BELLOW



M. G. FAULKNER

D. G. BELLOW, born in Winnipeg, Manitoba, obtained his early education in Victoria and Vancouver, graduating from U.B.C. in 1956 with a B.A.Sc. in mechanical engineering. After working in industry in Ontario he returned to the west and obtained an M.Sc. (1960) and Ph.D. (1963) in mechanical engineering from the University of Alberta. In 1963, he was appointed Assistant Professor in the Mechanical Engineering Department and in 1970 he was promoted to the rank of full Professor. Professor Bellow's research interests are in the area of applied mechanics and he has published papers on fatigue, dynamics and experimental mechanics.

M. GARY FAULKNER was born in Edmonton and received his early education in that city. After receiving a B.Sc. in mechanical engineering from the University of Alberta in 1963, he worked in the production and drilling field of the oil industry in Alberta and West Texas. Returning to the University of Alberta, he received an M.Sc. in mechanical engineering in 1966 and a Ph.D. in 1969 from the University of California, Berkeley. Since that time, he has been an Assistant Professor at the University of Alberta and has published in the general field of applied mechanics.

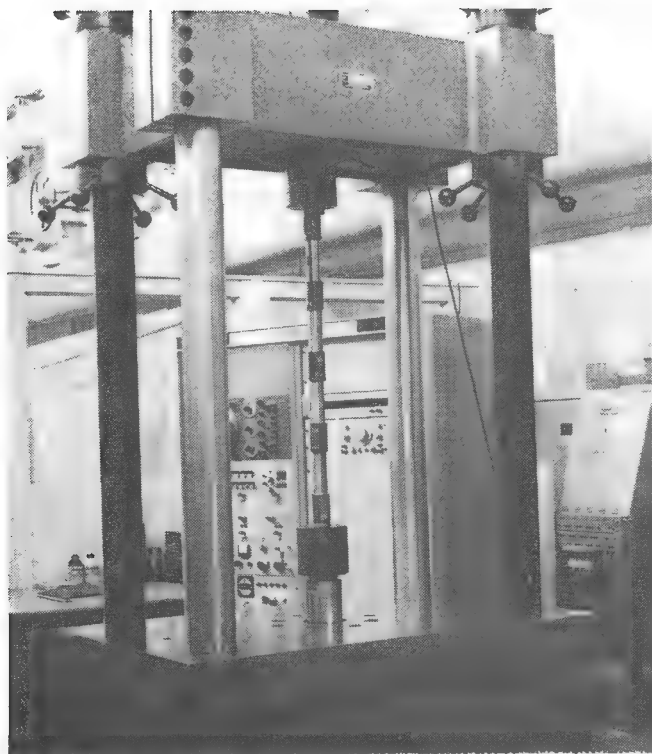


FIGURE 1 — Couplings under test.

TABLE 1 — DETAILS OF COUPLING THREAD CONFIGURATIONS

Series	Description	Details of Producing Thread
A	Cut thread	<ul style="list-style-type: none"> — Coupling I.D. machined to 0.955 — 0.976 in. — Threads cut to API-11B dimensions for 3/4-in. rod size
B	Cut and burnished	<ul style="list-style-type: none"> — Coupling I.D. machined to 0.955 — 0.976 in. — Pre-cut tap dimensions major diameter 1.0760 — 1.0765 in. — Burnish to API-11B dimensions for 3/4-in. rod size
C	Cut and Cold worked	<ul style="list-style-type: none"> — Coupling I.D. machined to 0.990 in. — Cut thread to 90 deg. included angle — Cold-work to 60 deg. included angle to API-11B dimensions for 3/4-in. rod size
D	Fully cold worked	<ul style="list-style-type: none"> — Coupling I.D. machined to 1.015 in. — Cold-work thread to API-11B dimensions for 3/4-in. rod size
E	Keyhole	<ul style="list-style-type: none"> — Coupling I.D. machined to 0.955 — 0.976 in. — Thread cut to API-11B dimensions for 3/4-in. rod size — Keyhole at root of thread cut to radius of 0.014 ± 0.003 in. Major and pitch diameter dimensions conform to API-11B dimensions

Note: All couplings tested were made from AISI 8635 steel and were quenched and tempered, as a single batch, to a hardness of Rockwell C 16-23. The outer diameters were then ground down to 1.325 in.

has a dynamic load capability of $\pm 50,000$ lbs in axial tension or compression and a frequency range from 0 to 30 Hz. The space available between the crossheads permitted the simultaneous testing of four couplings in series as shown in Figure 1. Also shown in this figure is the control console which was used to predetermine the load levels and testing frequency, monitor the number of cycles to failure, and monitor the wave-form of the load application.

The testing program consisted of making up a "string" of four couplings and five pins as shown in Figure 1. The couplings and pins were threaded together until the shoulder of the pin was hand-tight against the end face of the coupling. The joint then was torqued with a wrench so that the relative circumferential displacement between pin and coupling was 1/4 in. This was done for each joint. The completed "string" was then inserted into the testing machine and a pre-stress of 6,100 psi tension was applied. This stress was to simulate a dead load that is present when the coupling is in service in a well. The "string" was subjected to an alternating axial tensile stress such that the minimum stress never fell below 6,100 psi but the maximum was set for each particular test. Couplings were tested at maximum stresses from 40,000 psi to 77,000 psi. The frequency of load application for all tests was 8 Hz or 480 cycles per minute.

The initial testing program was set up to determine whether differences in fatigue life for different thread configurations in couplings could be detected. The first series of tests consisted of axially loading a set of couplings the threads of which were cut according to A.P.I.-11B dimensions.⁽²⁾ The nominal coupling size was 3/4 in., with an external diameter of 1-5/8 in.

There were two wrench flats on the couplings, 1-1/4 in. long and 1-1/2 in. apart. The rods which were used to join the couplings, in all tests, were made to fit the 3/4-in. coupling. They were 2-7/8 in. long and the outside diameter was 1-3/8 in. For ease in string make-up, two flats, 1-1/4 in. long and 1-1/4 in. apart, were machined on the surface.

The first set of test results was negative in that no couplings broke, only the pins. To overcome this the couplings were ground down to 1.375 in. O.D. Couplings at this diameter broke only when the testing machine was operating at or near its maximum, i.e. 50,000 lbs. As a protracted experimental program was

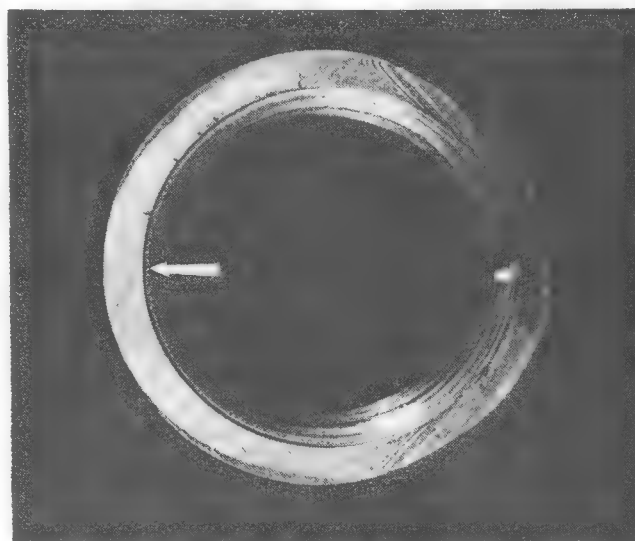


FIGURE 2 — Typical fatigue failure.

envisioned it was believed desirable to reduce the coupling O.D. to enable the testing machine to operate at lower loads. Also, due to the dynamic characteristics of the testing machine, at the high loads the frequency of load application dropped off. However, if the O.D. of the couplings was reduced too much, then for some of the couplings the fatigue fracture did not propagate completely through to the outside surface, leaving part of the cross section to carry the load. This reduced area then yielded, as evidenced by necking of the coupling at this point. So that the first fatigue crack would propagate through to the outside surface an O.D. of 1.325 in. was found to be acceptable. This outside diameter permitted all couplings to be tested at a frequency of 8 Hz within a nominal stress range of 6,100 - 77,000 psi. The nominal stress was calculated by dividing the axial load by the net cross-sectional area of the coupling based on the major thread diameter. The cross-sectional area of the coupling was 0.4914 in.² for a major thread diameter of 1.063 in. and outside diameter of 1.325 in. This can be compared with the pin, with a cross-sectional area of 0.6916 in.² based on a minor thread diameter of 0.9384 in.

All couplings tested were made from AISI 8635 and subjected to the same quench and tempered heat treatment to produce a surface hardness of 16-23 Rockwell C as recommended by API. The couplings were manufactured full size for 3/4-in. rod, as they would be for market. They then were ground down to 1.325 in. O.D. This grinding increased the surface hardness to 25-26 Rockwell C. It was believed that this increase in surface hardness would not influence the fatigue results, as all fatigue cracks originated on the inside of the coupling at the root of the thread. This, of course, was an important consideration because the testing was designed to evaluate the different thread configurations used in coupling designs and not test the effectiveness of surface treatment on the outside of the coupling. The outside surface roughness for all couplings was in the range of C.L.A. 20-31 μ -in. A description of the various thread configurations tested is given in Table 1.

PRESENTATION AND DISCUSSION OF RESULTS

Figure 2 shows the typical type of fatigue failure observed for all couplings tested. The arrow superimposed on the photograph indicates where the crack initiated. The striated fatigue surface, indicated by the light and dark bands, is the result of discontinuous crack propagation. All couplings broke at the point which coincides with the first thread of the pin. As many couplings failed opposite the location of the first thread of the top pin as failed opposite the location of the first thread of the bottom pin.

The fatigue results for all the couplings are plotted in Figures 3 to 7. The arrows through some of the points indicate that the couplings were unbroken at this particular stress level and number of cycles. All other points represent a coupling failure. For each stress level in each series, twelve couplings were tested and the median value was calculated. A smooth curve was then drawn through these medians.

In Figure 8 the results of Figures 3 to 7 are summarized. For convenience, Figure 8 is a log-log plot to indicate that, for the most part, all the results plot as a straight line, although there are slight differ-

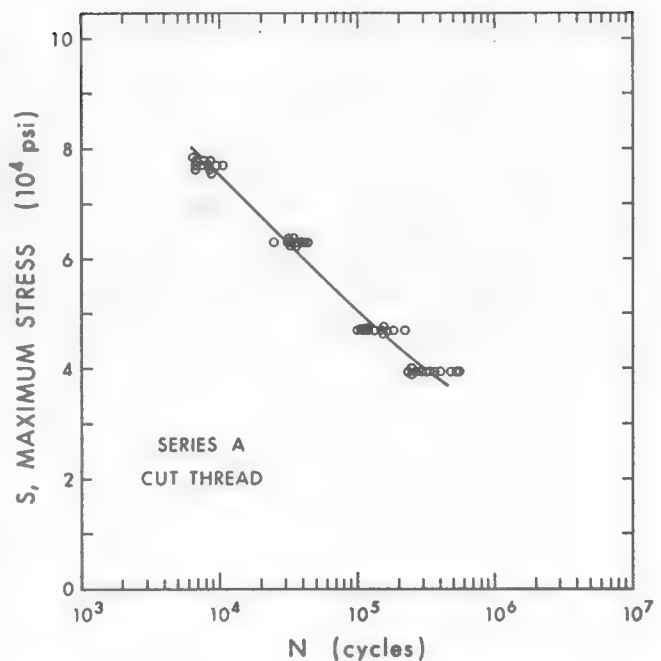


FIGURE 3 — S-N data for Series A cut thread.

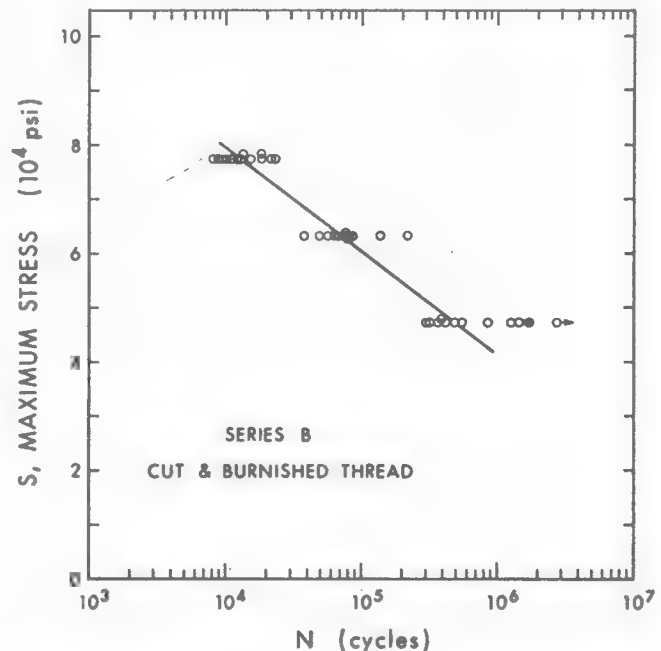


FIGURE 4 — S-N data for Series B cut and burnished thread.

ences in slopes. It is obvious from Figure 8 that the longest fatigue life was obtained from the Series-D coupling which had a fully cold-worked thread. The poorest fatigue life was obtained from the Series-E coupling which had a keyhole thread; although, statistically, there is little significant difference between the Series-E and the Series-A, which is a simply cut thread. Obviously, rounding the root of thread as was done in the keyhole thread, Series-E, did not improve its performance over that of the simply cut thread. The results in Figure 8 also show that burnishing the thread, as was done with the Series-B coupling, improves the fatigue life. However, burnishing was not as effective as partially cold-working the thread as was done for the Series-C coupling.

The test results indicate that the best fatigue life was obtained from a coupling the thread of which has been fully cold-worked. This point was further illustrated when, in obtaining the data, some concern was expressed over the scatter of the data. In particular, in Figure 5 for the Series-C coupling it was observed that, at a stress of 63,000 psi, one coupling broke at 10^5 cycles and another broke at 10^6 cycles. To determine the reason for this, these couplings were sectioned along a longitudinal axis, polished and deep-etched to show the extent of cold-working. Upon examination under a microscope it was observed that the coupling which broke at 10^6 cycles has approximately

30 per cent greater cold-working than the coupling which broke at 10^5 cycles.

Although in any fatigue work scatter of results is unavoidable, the fatigue life of the couplings tested was very sensitive to the degree of cold-working. It was believed that in the forming of threads by processes other than cutting alone, the degree of cold-working was not necessarily uniform for a given series of couplings tested. This would account for greater scatter in results for all series tested than observed for a simply cut thread as in Series-A. It was found that at 63,000 psi the standard deviation of Series-C was 94 per cent of the median while for

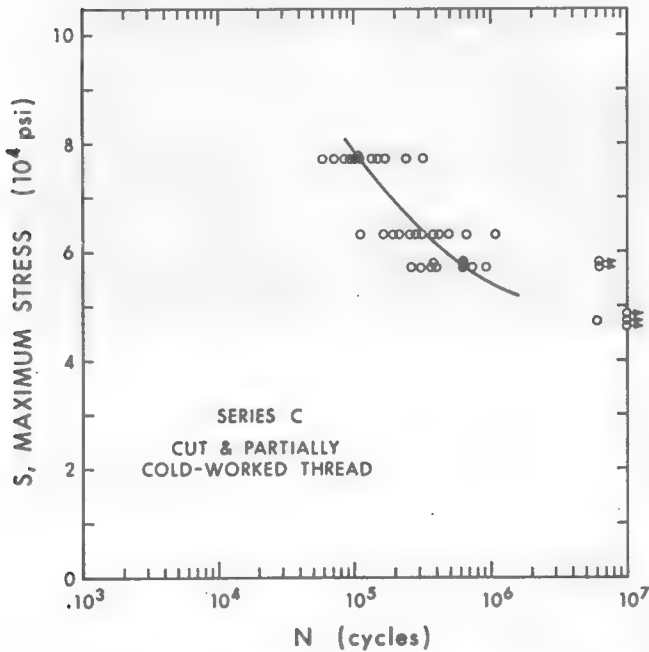


FIGURE 5 — S-N data for Series C cut and partially cold worked.

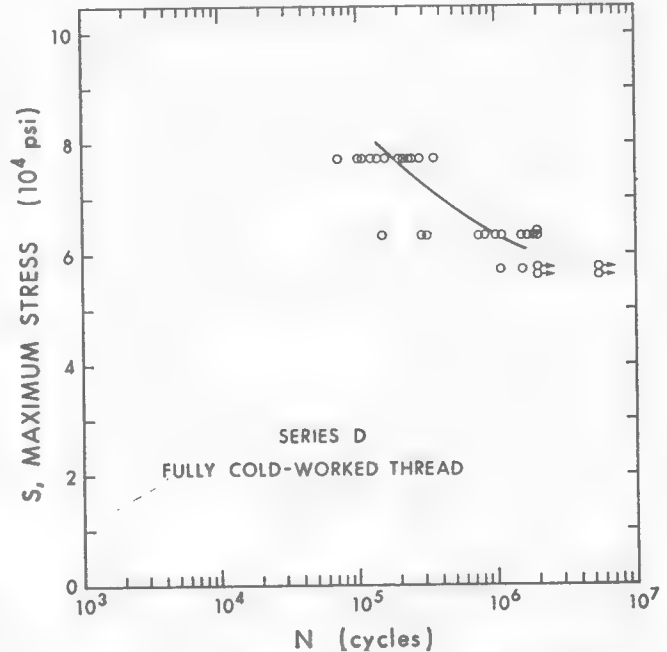


FIGURE 6 — S-N data for Series D fully cold worked.

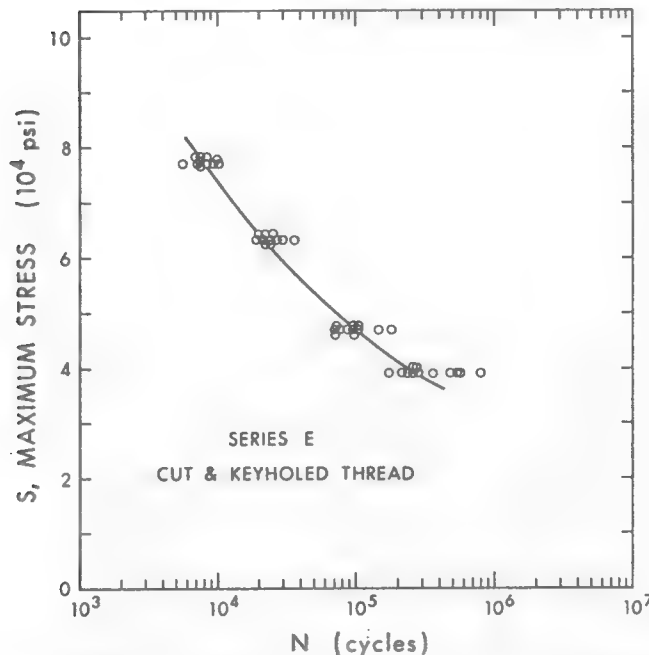


FIGURE 7 — S-N data for Series E cut and keyholed thread.

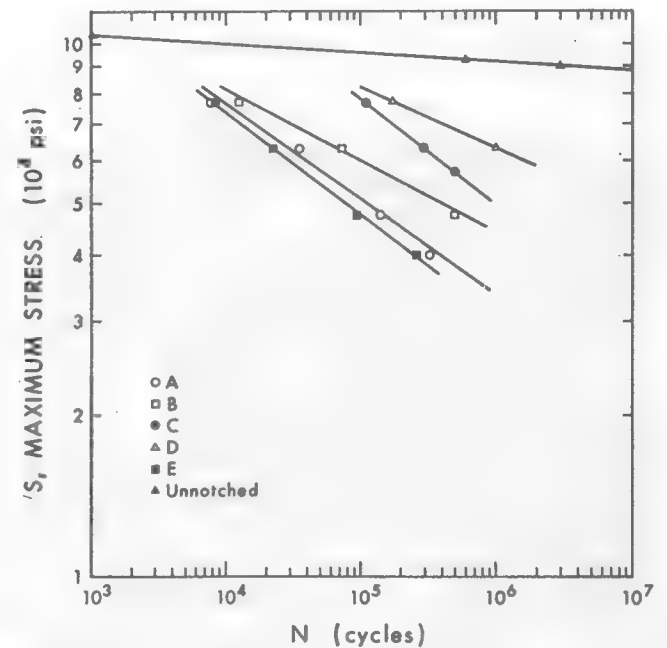


FIGURE 8 — Comparison of Series A-E thread configurations.

Series-A it was only 14 per cent of the median. Obviously, improved quality control procedures are required in order to reduce the wide variation in depth of cold working and, hence, the variation in fatigue life.

It was assumed that the results would not be affected by the testing frequency. However, it is known that in aircraft fatigue, low-frequency testing is more severe than high-frequency testing under the same loading conditions. In the present situation all couplings were cycled at 480 cycles per minute. This rate was chosen to allow completion of the testing in a reasonable time. However, in a field pumping situation, the frequency of load application can be as low as 10 cycles per minute and lower, depending on the depth of the well. To evaluate whether the frequency of testing was influencing the results, 12 Series-B couplings were tested at a maximum stress of 77,000 psi and at a frequency of load application of 10 cycles per minute. It was found that the median life of 12 couplings tested at 10 cycles per minute was 13,020 cycles compared with 12,410 cycles for 12 other couplings, taken from the same population, when tested at 480 cycles per minute. A student t-test was performed on these two sets of data and it was observed that the probability is very high that testing frequency does not influence the fatigue results in the range 10-480 cycles per minute.

The stress versus fatigue life of the unnotched coupling material is shown in Figure 8. These results were obtained by applying an alternating axial tension-tension stress to standard A.S.T.M. fatigue specimens. The fatigue notch factor,⁽³⁾ K_f , can be obtained by calculating, for a given number of cycles, the ratio of the fatigue strength of the unnotched material to the fatigue strength of a particular coupling. For each of the couplings the fatigue notch factor is plotted versus the number of cycles in Figure 9. It is seen from this figure that the lowest K_f occurs for the fully cold-worked coupling, Series-D, and that the highest K_f occurs for the keyhole thread, Series-E. It has been reported⁽⁴⁾ that for threaded drill-pipe joints a K_f of 4.2 - 4.6 is possible at a life of 10^7 cycles. If the data of Figure 9 are extrapolated to this life, then the present investigation indicates that the fatigue notch factor would lie in the range of 1.6 - 3.9 for all couplings tested. The life of 10^7 cycles is somewhat significant in that a pumping rate of 10 cycles per minute would be equivalent to approximately two years of operation. Thus, after two years of operation at 10 cycles per minute, a cut or keyhole threaded coupling will have a fatigue notch factor of close to four, whereas during the same period and conditions the fatigue notch factor for a fully cold-worked coupling is less than two. It should be mentioned that the fatigue notch factor is not the same as a stress concentration factor. Generally, a stress concentration factor is calculated or measured on the basis of stresses due to applied loads and does not take into account the presence of residual stresses, which may be present due to cold-working of the material. Obviously, the results of this investigation demonstrate that the presence of residual stresses greatly improves the fatigue life of a sucker-rod coupling. This confirms the experience of certain operators; for instance, O'Neil⁽⁵⁾ reported improvement in the field life of couplings which had some degree of cold working.

It would be expected that the thread configurations tested under laboratory conditions would behave in a similar manner in the field, providing the threads of

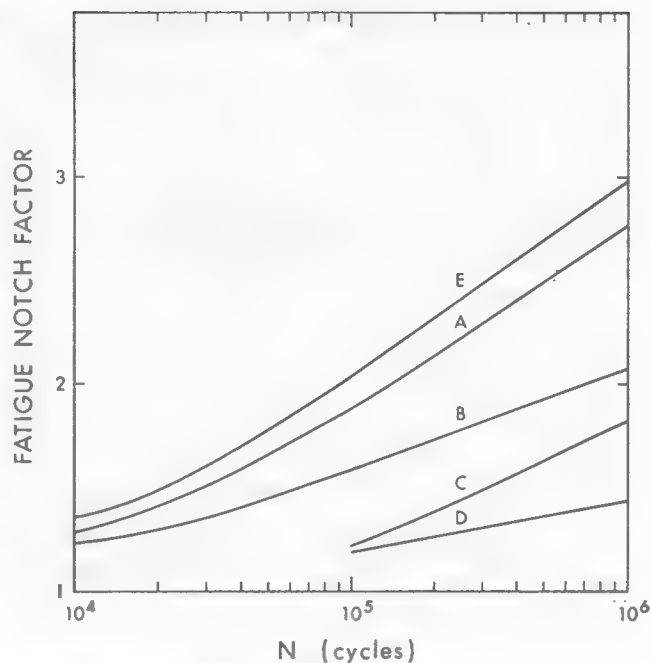


FIGURE 9 — Fatigue notch factor.

the couplings were protected with adequate seals and corrosion inhibitors. However, if adequate protection against corrosion cannot be taken then the conclusion that a fully cold-worked coupling would give the longest fatigue life may not be borne out in the field. The reason for this is that severe cold working of the threads can cause breaking of the grains and introduction of micro-cracks near the surface of the threads which will promote corrosion. Further work needs to be done to evaluate the apparent superiority of the fully cold-worked thread when placed in a corrosive environment.

SUMMARY

1. It is shown that fatigue of sucker-rod couplings can be accelerated in the laboratory by reducing the outside diameter of the couplings and by increasing the frequency of load application. Moreover, these changes do not inhibit the ability to detect differences in the fatigue life of couplings of different thread designs.

2. Fatigue results of five different couplings were obtained. It was observed that fatigue life was improved with cold working of the thread; the best fatigue life was recorded for those couplings with a thread formed entirely by cold working. It was also found that rounding the radius of the root of the thread, as in a key-hole thread, did not improve the fatigue life over that of a simply cut thread. Finally, it was concluded that the fatigue life of sucker-rod couplings was quite sensitive to the degree of cold-working that had been introduced in the manufacture of the thread.

3. For all couplings the fatigue notch factor was obtained. At a fatigue life of 10^7 cycles it was suggested that the fatigue notch factor for a simply cut thread was four whereas for a fully cold-worked thread this factor was less than two.

project. Thanks are also extended to E. Fenske and D. Park, who first suggested this project and arranged to provide all the material, and also to W. Brockington who provided us with almost instant service whenever he was asked. Finally, appreciation is acknowledged to H. Schroeder, who conducted most of the testing.

REFERENCES

- (1) Hardy, A. A., Sucker-Rod Failures; Drilling and Production Practice, A.P.I., pp. 214-225, 1952.
- (2) API Production Division, Specification for Sucker Rods, Standard 11B, January 1970.
- (3) A Guide for Fatigue Testing and the Statistical Analysis of Fatigue Data; A.S.T.M. Tech. Pub. No. 91-A, 2nd Edition, 1963.
- (4) Franz, W. F., A Three-Dimensional Photoelastic Stress Analysis of a Threaded Drill Pipe Joint. The Petroleum Engineer, Vol. 23, No. 2, Part I, pp. B-60-65, Feb. 1951.
- (5) O'Neil, R. K., Conoco Stops 70% of Rod Breaks in Wyoming Field; World Oil, pp. 75-78, March 1970.

Acknowledgements

The authors wish to express their sincere appreciation to the Steel Company of Canada Ltd. for the financial assistance which was given to this project.

Reprinted from The Journal of Canadian Petroleum Technology, January-March, 1972, Montreal
Printed in Canada

FATIGUE OF INTERNALLY THREADED MACHINE ELEMENTS

Dr. D.G. Bellow, Professor
Dept. of Mechanical Engrg.,
University of Alberta,
Edmonton, Alberta

Dr. M.G. Faulkner
Associate Professor,
Dept. of Mechanical Engrg.,
University of Alberta,
Edmonton, Alberta

INTRODUCTION

Threaded machine elements are a common fastening unit which have wide application in industry. As a result there has been considerable work done in determining fatigue strength for threaded connections. The majority of the theoretical and experimental studies have, however, been concerned with bolt and external thread design. Many of the earlier references to this work appear in the review article of Thurston [1].

In this investigation fatigue characteristics were determined for internally threaded machine elements. Specifically these were of the type used for oilfield sucker-rod couplings. The testing was done first to evaluate various thread designs [2] and second to evaluate the merits of using extruded coupling blanks instead of rolled and machined ones. In addition, the fatigue life of couplings made from two different steel chemistries, namely AISI 1045 and AISI 8635, were compared. While all the testing was done on sucker-rod couplings it is believed that the results are applicable to other internally threaded machine elements.

TESTING PROCEDURE AND RESULTS

The thread forms tested include the simple cut, cut and burnished, cut and cold

worked and keyhole. Couplings with these thread forms manufactured on either rolled and machined blanks or extruded blanks were loaded in axial fatigue on a servo-hydraulic testing machine. The minimum stress was held constant at 6100 psi while the maximum varied. For each maximum stress level 12 couplings were tested and the median of these used in the S-N curves.

All of the couplings were tested at a frequency of 8 Hz. Since these couplings in actual practice are loaded at a frequency of about 10 cycles per minute a set of 12 specimens were fatigued at this frequency to see if the change from 480 cycles per minute to 10 would affect the results. Employing student's t-test indicated there was no appreciable difference between the fatigue life of the couplings at these two speeds.

The results of the testing are shown in Figures 1 and 2. In Figure 1 the fatigue life of the various thread forms manufactured on the machined blanks are compared. In Figure 2 the effect of extruded blanks as well as the differences between AISI 8635 and AISI 1045 steels are shown. For comparison the results of the tests on the machined blanks with cut, cut and burnished and fully cold worked threads are included and shown as

solid lines.

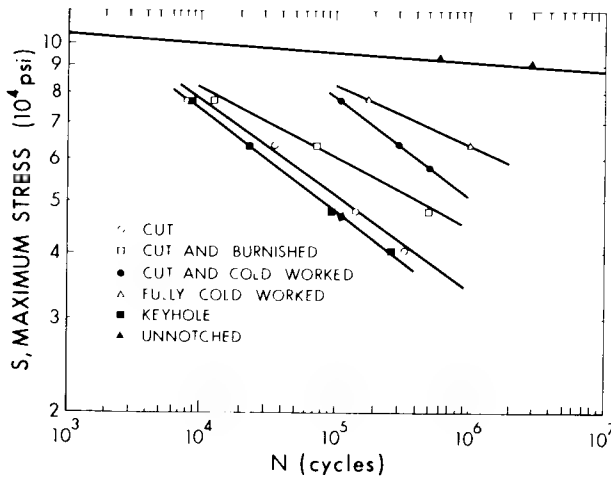


Fig. 1

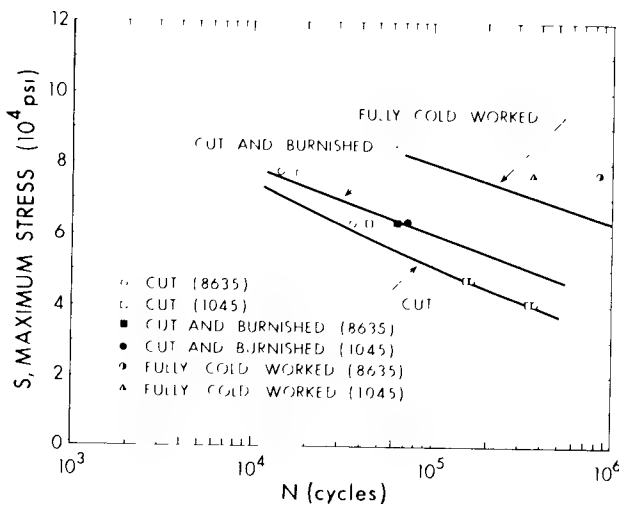


Fig. 2

CONCLUSIONS

1. It was observed that fatigue life was improved with cold working of the thread; the best fatigue life was recorded for those couplings whose thread was formed entirely by cold working. It was also found that rounding the radius of the root of the thread, as in a keyhole thread, did not improve the fatigue life over that of a simple cut thread.

2. There was little significant difference between the fatigue life of a coupling whose thread was formed by a simple cutting process, even with burnishing the cut thread, whether the coupling blank was extruded or not prior to cutting of the thread, and whether AISI 1045 or AISI 8635 steel was used.

3. The fatigue life of a fully cold worked threaded coupling was extended by using coupling blanks which had been extruded prior to the thread forming process. The results also showed that, for such a thread, AISI 8635 was superior to AISI 1045 for the coupling material.

4. While it is possible that excessive cold working of the threads could cause cracking of the material and thereby actually reducing its fatigue strength, this was not observed in this work.

REFERENCES

- [1] R.C.A. Thurston, "The Fatigue Strength of Threaded Connections", *Trans. A.S.M.E.* **73**, pp. 1085-1092 (1951).
- [2] D.G. Bellow and M.G. Faulkner, "Fatigue of Threaded Sucker-Rod Couplings", *J. Can. Pet. Tech.* **11**, pp. 69-74 (1972).

On the Mixing of Photoelastic Immersion Fluids

Paper describes a technique which can be used to obtain a desired refractive index of an immersion fluid without resorting to a trial-and-error method

by O. Smolik and D. G. Bellow

ABSTRACT—It is shown that an equation can be used to determine the exact quantities of components to yield a specified refractive index for an immersion fluid. The results obtained from this equation are compared with values obtained experimentally for two different immersion fluids, IMF163 and Hallowax. The paper also discusses the kinds of errors that are introduced when a mismatch in refractive index occurs between model material and immersion fluid. Graphs are presented which show the effect of temperature on the refractive index, the degree of refraction of the light beam when the refractive indices are different between immersion fluid and birefringent model, and the effect of the angle of incidence.

Nomenclature

- n = index of refraction of immersion-fluid mixture
- n_1, n_2 = indices of refraction of components in the mixture
- n_F = index of refraction of fluid
- n_M = index of refraction of photoelastic model
- V = volume of fluid
- α = angle of incidence
- β = angle of refraction
- λ = wavelength of light source

Introduction

In scattered-light photoelasticity and other techniques employing the use of an immersion fluid, it is essential that the index of refraction of the immersion fluid be equal to that of the birefringent model. If this is not the case, and the light-beam angle of incidence at the surface of the model is other than normal, then an error is introduced in determining the location of a point within the specimen. The aim of

this paper is to describe a simple means by which the index of refraction of the immersion fluid can be adjusted without resorting to a trial-and-error method. The paper also discusses the errors that are introduced in the analysis when a mismatch in refractive indices exists between model and fluid. A relationship is derived which indicates the magnitude of the error which will be incurred in the analysis when the mismatch is known.

Photoelastic immersion fluids are often binary mixtures of either IMF163* or Hallowax to which is added mineral oil to achieve a required index of refraction. A trial-and-error method for this mixing process is well known^{1,2} and consists of passing a light beam through a prism constructed from the birefringent model material located in the immersion fluid. If the index of refraction of the model is identical to that of the immersion fluid, the light beam will not be refracted in passing from the immersion fluid through the model. While successful, this method requires experience in knowing just how much mineral oil to add. Too much or too little requires further mixing and testing. This can present a problem when mixing a large batch for the first time or if mixing is done only occasionally.

It is suggested that an alternate approach to this problem is available which will not only enable accurate predictions of the quantities required to obtain a specified index of refraction for the immersion fluid, but which will also enable one to evaluate the errors that will be incurred if a mismatch between fluid and model exists.

The degree of purification or measure of concentration of one component in a binary mixture can be determined if the refractive indices of the individual components in the mixture are known. It can be shown³ that the relationship between quantities of components and their indices of refraction is given by

O. Smolik and D. G. Bellow are Research Assistant and Professor, respectively, Department of Mechanical Engineering, University of Alberta, Edmonton, Alberta, Canada.

Paper was presented at 1973 SESA Fall Meeting held in Indianapolis, IN on October 16-19.

Original manuscript submitted: March 23, 1973. Final version received: December 2, 1973.

* IMF163 is available from Vishay Intertechnology Incorporated, Malvern, PA or Intertechnology Ltd., Don Mills, Ontario, Canada.

$$\frac{100(n-1)}{d} = \frac{p_1(n_1-1)}{d_1} + \frac{(100-p_1)(n_2-1)}{d_2}$$

where n is the refractive index, p is the percent weight, d is the density, and the subscripts refer to the components. If the densities of the components are equal to the densities of the mixture, this equation can be simplified to

$$n - n_2 = \frac{V_1}{V_1 + V_2} (n_1 - n_2) \quad (1)$$

where V is the volume. The evaluation of this equation is presented in the next section.

Optical Properties of Immersion Fluids

Two immersion fluids were prepared: IMF163 and Hallowax. These were each diluted using mineral oil (Saybolt Viscosity 125/135). In Table 1, calculated values of the refractive index are compared with experimentally measured values obtained using an Abbe refractometer for various mixture concentrations. The Abbe refractometer measured refractive index relative to the velocity of light in air using light of the D-line ($\lambda = 589.3$ nm). All measurements were made at 20°C.

From Table 1, it is seen that the values obtained from eq (1) agreed quite closely with those measured experimentally, the error being less than 0.04 percent for IMF163 and less than 0.07 percent for Hallowax. If the wavelength of the light used to determine the refractive indices of the components is appreciably different from the wavelength used in the photoelastic apparatus, then the concentration $V_1/(V_1 + V_2)$ will be in error. In the example discussed here, the wavelength used to determine the refractive indices of the components was $\lambda = 589.3$ nm as compared with the laser light used in the photoelastic apparatus having a wavelength of $\lambda = 632.8$ nm. This difference in wavelengths is not sufficient to cause an appreciable error in calculation of the correct concentration. This lack of error is because the change in reciprocal dispersion between the immersion fluid and the photoelastic material is insignificant over the bandwidth of wavelengths involved. For wavelengths outside the range illustrated by the example, then, a correction may have to

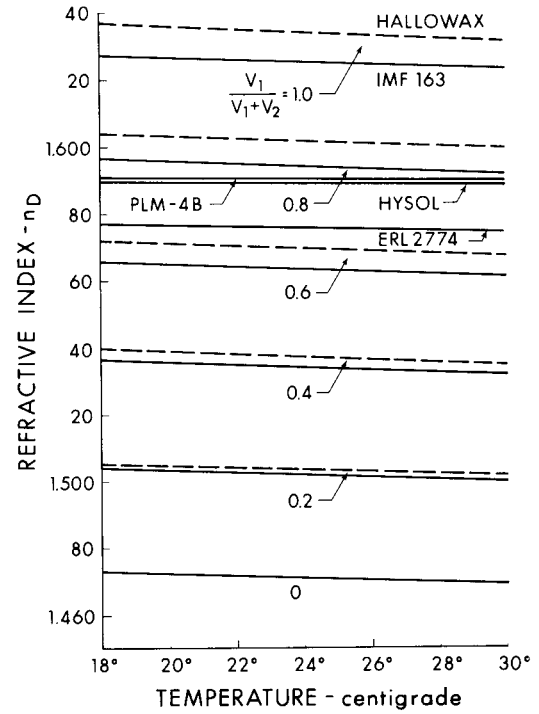


Fig. 1—Refractive index as a function of temperature for various mixture concentrations

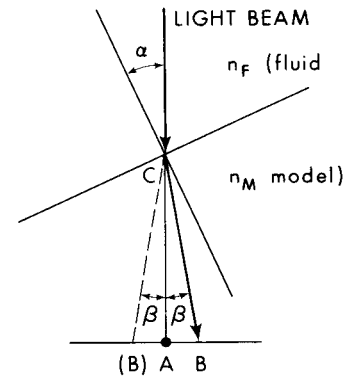


Fig. 2—Refraction of light beam owing to a difference in refractive indices n_F, n_M

TABLE 1—COMPARISON OF MEASURED REFRACTIVE INDICES WITH THEORETICAL VALUES FOR IMF 163 AND HALLOWAX AS A FUNCTION OF THE MIXTURE PURITY

$\frac{V_1}{V_1 + V_2}$	IMF 163		Hallowax	
	n_{calc}	n_{meas}	n_{calc}	n_{meas}
0	1.4724	1.4724	1.4727	1.4727
0.2	1.5033	1.5026	1.5054	1.5055
0.4	1.5343	1.5341	1.5381	1.5391
0.6	1.5652	1.5650	1.5708	1.5711
0.8	1.5962	1.5957	1.6035	1.6036
1.0	1.6271	1.6271	1.6362	1.6362

be made to the concentration as given by eq (1). A correction can be made with the use of a modified form of Cauchy's equation which uses empirical data and relates refractive indices obtained at one wavelength to the refractive index at a new wavelength.³

Another factor which can affect the index of refraction is the operating temperature. In Fig. 1, the refractive indices of two immersion fluids of various concentrations are compared with some common model materials as a function of temperature over the range $18 \leq T \leq 30^\circ\text{C}$. This figure shows that, while all materials experience a decrease in the index of refraction for an increase in temperature, the modeling materials are less affected by a temperature change than the immersion fluids. For the range of

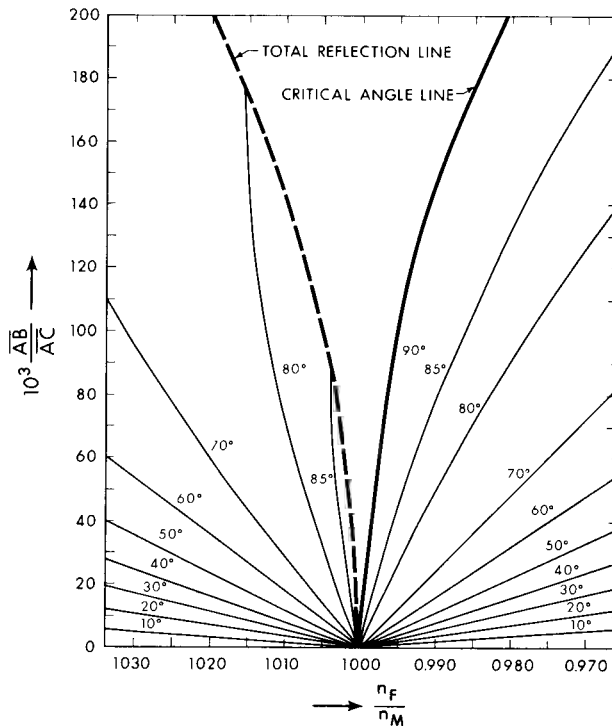


Fig. 3—Refractive error $\overline{AB}/\overline{AC}$ as a function of the ratio of refractive indices n_F/n_M

temperatures shown in Fig. 1, the change in the index of refraction for the model materials is approximately 0.12 percent, while for the immersion fluids it is approximately 0.3 percent. While it appears that the temperature effect is small, it can be significant in a test when measuring stresses using a large angle of incidence.

Figure 2 illustrates the magnitude and type of error which is introduced into the experimental readings when a small difference in the refractive indices exists between immersion fluid and model material. In this figure, a light beam is refracted an angle β in passing from the immersion fluid having a refractive index n_F into a model material having a refractive index n_M . The normal to the surface of the model is inclined an angle α to the light beam in the immersion fluid. If the point A in the model is to be investigated and a difference in refractive indices exists (i.e., $n_F \neq n_M$), then, by the use of Snell's law, it can be shown that the light beam will pass through point B instead, and the error \overline{AB} expressed as a function of the distance into the model \overline{AC} is given by

$$\frac{\overline{AB}}{\overline{AC}} = \tan \left[\alpha - \arcsin \left(\frac{n_F}{n_M} \sin \alpha \right) \right]. \quad (2)$$

If $n_F = n_M$ then $\overline{AB} = 0$. If $n_F \neq n_M$ then $\overline{AB} \neq 0$, and if the region \overline{AB} is subjected to a high stress gradient, then it is possible that a significant error will be introduced into the readings if they are measured at B when they are assumed to be taken at A. \overline{AB} can be positive or negative depending on whether

n_F/n_M is greater or less than 1. Figure 3 illustrates the application of eq (2). A mismatch of indices of refraction has been chosen over the range $0.967 \leq n_F/n_M \leq 1.033$ and for $0 < \alpha < 80$ deg. For example, if $\alpha = 70$ deg and $n_F/n_M = 1.03$, then $\overline{AB}/\overline{AC}$ will be 0.095. If $\overline{AC} = 75$ mm then \overline{AB} will be 7.1 mm, a significant distance in a model over which the fringe order can change.

A further appreciation for the effect of a mismatch in indices of refraction coupled with the angle of incidence can be observed in Fig. 3 from the area bounded by the two heavy curved lines in the center of the figure, one solid and one dashed. Light will only enter the model if the conditions are such that the points either lie to the left of the dashed line (total-reflection line), or, on or to the right of the solid line (critical-angle line). A further observation is that the critical-angle line coincides with an angle of incidence of 90 deg when $n_F/n_M \leq 1$. The total-reflection line is the loci of various angles of incidence which are other than 90 deg except at the surface of the model. Thus, it is possible to get no light entering the model even though the angle of incidence is less than 90 deg. For a condition of n_F/n_M which places a point on the critical-angle line, the light beam theoretically will enter the model even though the angle of incidence is 90 deg. However, this will result in a large error, as shown in Fig. 3.

It is important to know if a mismatch between fluid and model exists and whether $n_F/n_M < 1$. If n_F/n_M is known, then Fig. 3 can be used to correct for the errors that will occur. It has been stated above that the effect of temperature on index of refraction is more pronounced with immersion fluid than model material. If testing is at a temperature other than at which the immersion fluid was mixed, a mismatch in indices of refraction will result. This can lead to errors in analysis unless accounted for by eq (2) or a graph such as Fig. 3.

A further observation in this work is that eq (1) can also be used to determine an unknown index of refraction of a model material, providing the indices of refraction are known for the components of the immersion fluid. By keeping track of the volumes of the components of the immersion fluid, the trial and error method^{1,2} can be used to determine the correct mixture of immersion fluid to allow a light beam to pass unrefracted from the fluid into the model. Knowing both the quantities and indices of refraction of the components of the immersion fluid, eq (1) can be solved for the index of refraction for the model material.

Acknowledgment

The authors wish to thank the National Research Council of Canada for the financial support received on behalf of this project under grant number A-2705.

References

1. Hickson, V. M., "Photoelastic Determination of Free Boundary Stresses on Frozen Stress Models by an Oblique Incidence Method," *J. Appl. Phys.*, 2(9), 261-269 (1951).
2. Swinson, W. F. and Bowman, C. E., "Application of Scattered-light Photoelasticity to Doubly Connected Tapered Torsion Bars," *EXPERIMENTAL MECHANICS*, 6(6), 297-305 (1966).
3. Weissberger, A., "Physical Methods of Organic Chemistry," 3rd ed., Interscience Publishers, Inc., 1(11), 1158 (1960).

International Series
on Sport Sciences, Volume 1

BIOMECHANICS IV

Proceedings of the Fourth International Seminar
on Biomechanics, University Park, Pennsylvania

Impulse and work output curves for swimmers

R. K. Jensen
Laurentian University, Sudbury

D. G. Bellow
University of Alberta, Edmonton

The purpose of this study was to determine whether impulse and work output curves for shoulder extension against an appropriate resistance (a) are different for different levels of front-crawl swimming ability and (b) change as a result of swimming training.

The motion of a body segment underwater produces a drag force that is proportional to the square of the velocity of the segment moving through the water (Gallenstein and Huston, 1973, Seireg and Baz, 1971; and Seireg, Baz, and Patel, 1971). Body segment motion is due to the rotational forces created by muscle contraction and external forces. Differences in swimming ability between individuals can be explained partially in terms of differences in the availability of the rotational force caused by muscle contraction. If the swimming action is attributed wholly to shoulder extension in the sagittal plane, with the body segment considered as a rigid body rotating about a fixed, noncentroidal axis (the shoulder joint), then the equilibrium equation taken about the joint axis is:

$$M_a = I_o \alpha + F_g (\cos \phi) r_g - F_b (\cos \phi) r_b + M_d \quad (1)$$

- where M_a is moment caused by muscle contraction; I_o is moment of inertia of segment about joint axis; α is angular acceleration; F_g is weight of the segment; ϕ is segment angular displacement; r_g is radius to center of gravity of body segment; F_b is buoyancy force on the segment; r_b is radius to center of

This research was supported by General Research Grant 55-32285 from the University of Alberta.

UNIVERSITY PARK PRESS

Baltimore • London • Tokyo



buoyancy; and M_d is drag moment. This model is a gross simplification corresponding approximately to tethered swimming, but it does provide insight into the rotational forces involved.

Swimming speed does not depend on the availability of rotational force at a particular instant or angle.

Sinusoidal variations of horizontal momentum are evident (Miyashita, 1971), and the forms and the magnitudes of this curve determine the time taken to cover the swimming distance. Variations in horizontal momentum can be attributed to the impulses for the body segments. Impulse for the contraction moment for the simple model postulated is given by:

$$\text{Imp}_{1 \rightarrow 2} = \int_{t_1}^{t_2} M_a dt \quad (2)$$

where Imp is impulse and t_1 and t_2 are limits of time argument.

The total work that the swimmer expends in propelling himself over the distance is also of considerable importance and is the sum of the work outputs for each segment. Work output for a single action can be calculated from the contraction moment and is the sum of the work ($w_{1 \rightarrow 2}$) required for drag and for moving the body segment:

$$W_{1 \rightarrow 2} = \int_{\theta_1}^{\theta_2} M_a d\theta \quad (3)$$

where θ_1 and θ_2 are limits of the displacement argument.

EXPERIMENTAL APPARATUS AND TEST

The conditions envisaged in the above model can be simulated in the laboratory. The problem was to build a testing device that was compact and that permitted accurate and precise measures of the experimental parameters under conditions that were uniform for all subjects. A rotary torque actuator (Roto Actuator, Model DS4-4) was fitted with hydraulic tubing and valves to bypass the stator and with a lever arm and handle to propel the vane (Jensen, 1973). Rotation of the actuator caused fluid to flow through a valve. Application of the momentum equation to the constriction caused by the valve showed that the resistance moment was proportional to the square of the angular velocity. It was assumed that the action of the body segment paralleled that of the lever arm, and the joint axis was aligned at all times with the fixed instrument axis. The equilibrium equation is given by:

$$M_a = I'_o \alpha + F_z (\cos \theta) r_z + M_r \quad (4)$$

where I'_o is moment of inertia of segment and instrument about joint axis; F_z is weight of segment/lever/handle; r_z is radius to center of gravity of seg-

ment/lever/handle; and M_r is resistance moment caused by instrument. A comparison with Equation 1 shows that there are differences between the two models, but the instrument developed was compact and could be used conveniently to test a large number of subjects and movements.

Bending strain for the lever arm was calibrated in terms of moment of force, and angular displacement was measured with a LVDT. The results were digitized electronically, and the analysis was fully computerized. Accuracy and precision were found to be high for the instrument. Impulse (Equation 2) and work output (Equation 3) were calculated for efforts started at 150° from the anatomical position, with the subject supine and stabilized. A uniform valve setting was used, and test reliability across trials was judged to be adequate.

A sample composed of 42 boys, 8–11 years of age, was divided into three ability levels on the basis of 50-m front-crawl speed (*A*, higher, *B*, medium, *C*, lower ability). The sample then was paired randomly into an experimental group that underwent 6 wk of training, 3 sessions per wk, and a control group. Test 1 was for 3 wk and Test 2 was for 6 wk after the start of training. A further testing session was conducted at the start of the training period to familiarize the subjects with the test. Four trials per test were conducted, and the best trial was selected.

RESULTS AND DISCUSSIONS

The impulse and work output curves calculated were of the means of the best trials for each of the 12 experimental subgroups (Tests 1 and 2, experimental, control, Abilities A, B, and C). Comparisons between curves were made using a one-tailed *t* test and a probability of 0.05.

Comparisons between levels of ability were made using the results of Test 2 for the control group. The three mean curves (Figure 1) were distinct for both impulse and work output. Comparisons of the differences between mean points indicated that Curve A was greater than Curve C and that, for the initial segments of the curves, Curve A was greater than Curve B (degrees of freedom = 12). The remaining differences were not significant. It can be said, then, that the test does distinguish between levels of swimming ability.

Comparisons of the ability level curves for the experimental group indicated that the Group B curves were probably greater than the corresponding control group curves. In Figure 2, a comparison has been made between experimental and control curves for Tests 1 and 2. The curves for the experimental group showed that, during the initial 0.28-sec period, the second test was significantly greater than the first test. Also, for the second half of the work output curves, the experimental curve was greater than the control curve on Test 1. All other differences were not significant. These

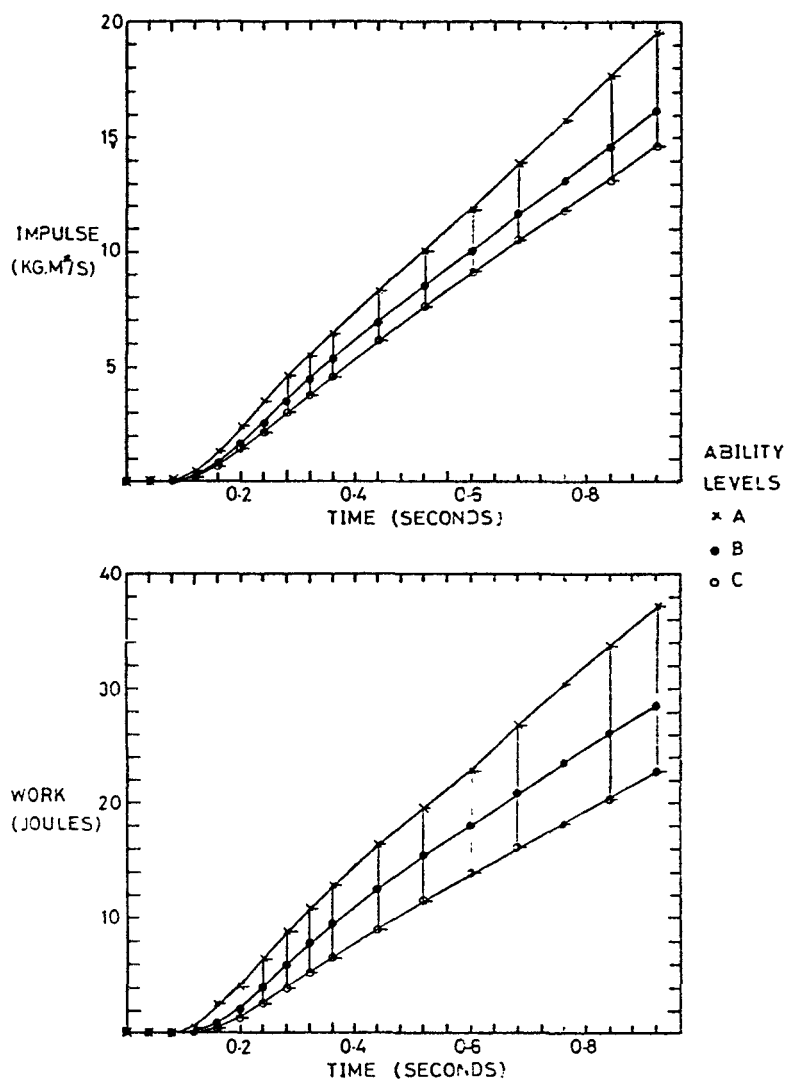


Figure 1. Control group ability level curves for Test 2. Bars between data points indicate a nonsignificant difference at the 0.05 level.

results were not supported by results from Ability Groups A and C, but suggest that the B group may have had a greater capacity for change.

CONCLUSIONS

An apparatus has been presented that provides a resistance moment similar to that for a simple underwater arm movement. It has been shown that differ-

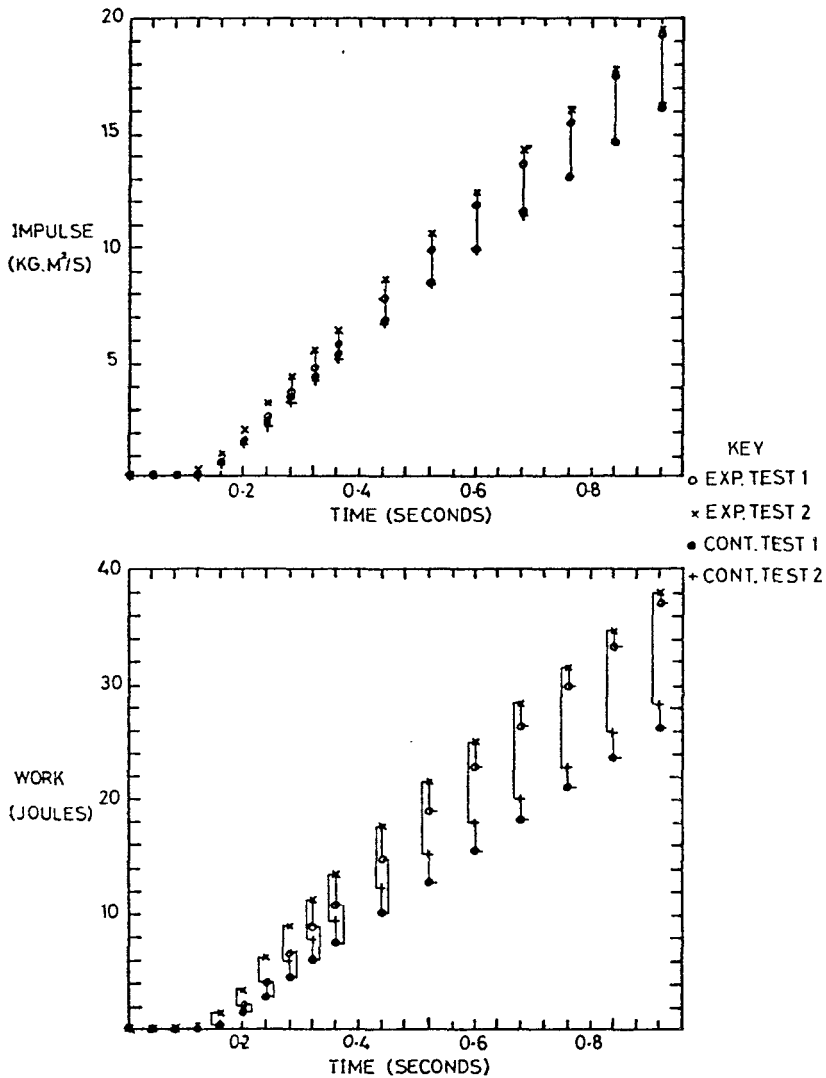


Figure 2. Comparison of curves for the B Subgroups. Bars between data points indicate a nonsignificant difference at the 0.05 level.

ences between individuals can be detected, and some changes that could be attributable to training have been demonstrated. Further investigations with more subjects and more intensive training are warranted.

REFERENCES

- Gallenstein, J., and R. L. Huston. 1973. Analysis of swimming motions. *Hum. Factors* 15: 91-98.

- Jensen, R. K. 1973. Dynametric measurement of static and dynamic responses. Paper presented at CAHPER, Calgary, July.
- Miyashita, M. 1971. An analysis of fluctuations of swimming speed. *In*: L. Lewille and J. P. Clarys (eds.). First International Symposium on Biomechanics of Swimming. pp. 53-58. Université Libre de Bruxelles, Brussels.
- Seireg, A., and A. Baz. 1971. A mathematical model for swimming mechanics. *In*: First International Symposium on Biomechanics of Swimming. pp. 81-103. Université Libre de Bruxelles, Brussels.
- Seireg, A., A. Baz, and D. Patel. 1971. Supportive forces on the human body during underwater activities. *J. Biomech.* 4: 23-30.

Author's address: Dr. Robert K. Jensen, School of Physical and Health Education, Laurentian University, Sudbury, Ontario (Canada)



PROCEEDINGS Vol. 1

Second Symposium

APPLICATIONS OF SOLID MECHANICS

SPONSORED BY CSME, CSCE, ASME

June 17 and 18, 1974

Faculty of Engineering
McMaster University

HAMILTON, ONTARIO, CANADA L8S 4L7

CORROSION-FATIGUE OF COLD WORKED
THREADED CONNECTIONS

DONALD G. BELLOW
Prof. Mech. Eng.
University of Alberta

M. GARY FAULKNER
Assoc. Prof., Mech. Eng.
University of Alberta

SUMMARY

An experimental procedure is described which was used to evaluate the fatigue life of internally threaded connections, such as sucker-rod couplings, when in the presence of a 3.5 percent NaCl solution. The threaded connections were machined on quenched and tempered coupling blanks made from AISI 1045 and AISI 8635; two medium strength steels having ultimate strengths of 109 ksi and 106 ksi respectively. The effects of corrosion fatigue on the depth of cold working was evaluated by testing couplings whose threads had been formed by three different processes. These consisted of simply cutting the thread, cutting and then burnishing the thread, and rolling or fully cold working the thread. All threads were manufactured to API specifications for a 3/4 inch nominal size sucker-rod.

It was found that at a life of 10^5 cycles the endurance stress of a simple cut thread in the presence of 3.5 percent NaCl solution was reduced by 7-8 percent compared with the in-air tests, and for the rolled or fully cold worked thread this decrease was 18-19 percent. Notwithstanding the above, the actual endurance stress for the rolled thread was still superior to all other thread forms tested, with slightly better results obtained for couplings made from AISI 8635 than from AISI 1045. The most surprising result of the investigation showed that while burnishing a simple cut thread could improve the endurance stress by 23 percent when fati-

gued in air, virtually no benefit was obtained when fatigued in the presence of a 3.5 percent NaCl solution. It is explained that this is because the first stage of the corrosion fatigue process quickly penetrates through the work hardened layer of the thread, producing a sharp stress concentration from which a fatigue crack can originate and propagate uninhibited by any residual stresses left by the thread forming process. While the results of this work were obtained for a particular problem encountered in the petroleum industry, it is believed they will be equally valid for applications of medium strength bolted connections in the aircraft and maritime industries as well as other applications where such connections are subjected to cyclic loading in the presence of a saline environment.

INTRODUCTION

Many oilfields contain large quantities of salt water which unavoidably are pumped out of the wells with the crude oil. This salt water can cause premature failure of all unprotected components. Sucker-rods and couplings are especially vulnerable to this corrosive attack because they are simultaneously subjected to a cyclic loading through the pumping action in the wells. This paper describes a laboratory test method which was used to determine the effect of salt water corrosion in combination with axially cyclic loading of internally threaded connections of the type commonly found in the petroleum industry and known as sucker-rod couplings.

In an earlier work [1] the authors showed that the fatigue life, in air, of internally threaded couplings was influenced by the manner in which the threads were formed. Threads which had been formed by a cold working process were found to be significantly superior to those which were simply cut or had only superficial work-hardening of the thread surface. This work was extended [2] to evaluate the effects on the fatigue life of two different steels as well as evaluating the benefits of using extruded versus machined blanks prior to the thread forming process. All of this work was conducted in air in the laboratory, and while it was able to show which thread forming process was superior under axial loaded fatigue conditions, it did not give any insight into how the couplings would behave when cyclically loaded in a hostile or corrosive environment. The aim of the present paper is to provide these results and compare them with the in-air tests of earlier investigations[1,2] along with similar investigations into the corrosion fatigue and stress corrosion of medium and high strength materials by other authors.

EXPERIMENTAL PROGRAM

Corrosion fatigue is a mechanism which affects the life of a component more severely than simply exposing to a corrosive environment and then subjecting to a fatigue loading. However, the effects of corrosion are very much time dependent, and in combination with fatigue, the cyclic rate must be chosen to enable sufficient time for the corrosion mechanism to develop before component failure occurs. In the previous work [1] the cyclic rate of loading was set at 8 Hz, or 480 cpm. In actual petroleum pumping situations, the cyclic rate is in the neighborhood of 10 cpm. It was also found [1] that there was no significant difference in fatigue results obtained in air when cycled at 480 cpm or at 10 cpm. Therefore, for the present investigation the cyclic rate of loading was set at 10 cpm. It was believed that this rate, which corresponded to field conditions, would be slow enough to enable a significant corrosion mechanism to develop. This cyclic rate would also allow comparison to be made with the in-air results of previous studies [1,2].

Sucker-rods and couplings are manufactured in many different sizes. It was found that the 3/4 in. nominal size rod and coupling was a convenient size for testing and was common enough so that the results obtained would be applicable to most petroleum field situations. Since the main objective was to evaluate the effect of internal thread manufacturing techniques, it was found necessary to reduce the outside diameter of the coupling from 1.625 in. to 1.325 O.D. This resulted in a cross sectional area for the coupling of 0.4914 in.² compared with 0.6916 in.² for the mating pin. The reduction in outside diameter of the coupling enabled higher stresses to be applied to the coupling than the mating pin. The test facility cyclically loaded four couplings and five pins in series; couplings being joined together by mating pins (sucker-rods).

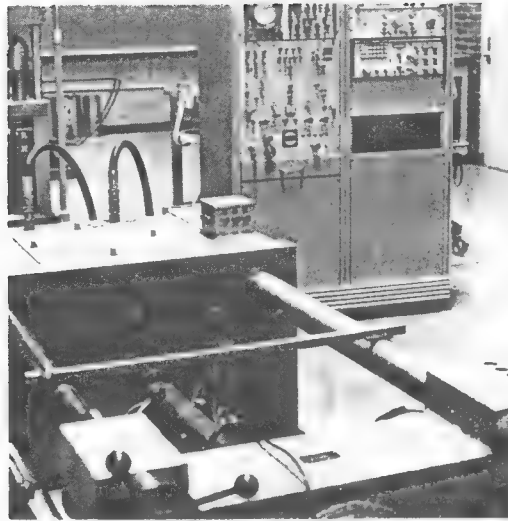


Figure 1 Photograph of testing facility

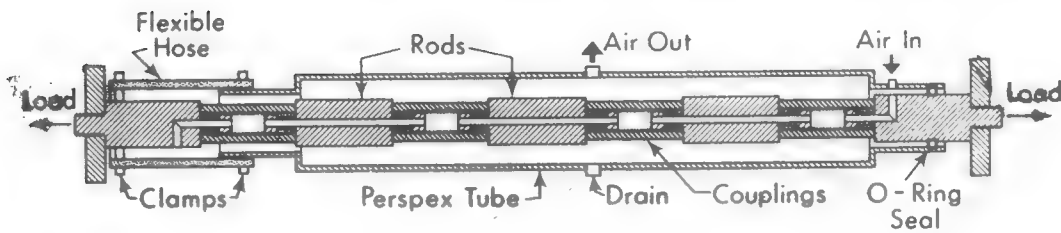


Figure 2 Corrosion chamber

A corrosion chamber was designed to fit between the cross heads of a closed loop servo-hydraulic testing machine, Figure 1. A schematic of the chamber is shown in Figure 2. For purposes of this test, a 1/4 in. hole was drilled through the center of each pin, except those at the ends. The end pins, which fitted into the threaded fixtures of the testing machine, were partially drilled through. These end pins also had a radial hole drilled on one side which allowed the corrosive medium to contact the inside as well as the outside surfaces of the couplings. Corrosive fluid was circulated through the center of the pins by means of an air jet situated opposite the radial

hole in one of the end pins. The air jet entrapped fluid on the outside of the couplings and forced it into the center cavity of the pin-coupling string. The air jet also provided a constant source of oxygen to maintain the corrosion activity in the chamber. The air jet had a diameter of 1/8 in. and air was supplied at a pressure of 5 psig. The outer case of the chamber consisted of a 3 in. diameter Perspex tube. The ends were sealed with clamps to prevent leakage with one end being provided with a slip-on hose assembly to enable easy make-up and breakdown of the assembly.

Couplings were mated to the pins by hand tightening and then the joint was torqued with a wrench so that the relative circumferential displacement between coupling and pin was 1/4 in. [1]. This pre-torquing, which is consistent with practice, was to produce a tensile stress in the pin with a consequent reduction in alternating stress on the threads of the pin and the coupling. Pre-torquing also prevents joints from loosening during cyclic loading.

After inserting the couplings in the corrosion chamber, the entire assembly was placed within the frame of the testing machine. The coupling-pin assembly was then subjected to a base or minimum tensile load of 3000 lbs. which induced a nominal stress in the coupling of 6.1 ksi. The maximum stress was set for each particular test and was in the range of 43 to 77 ksi.

The corrosion medium was a 3.5 percent NaCl solution made up with distilled water. This concentration is similar to that found in many oil-field situations. In order to keep the pH of the solution relatively constant, a fresh solution was used at the beginning of each test, or when a coupling failed, and also at regular 24 hour intervals. It was found that the salinity increased slightly to 3.8 percent in 24 hours. This was attributed to evaporation. In the same time interval the pH of the solution decreased from 9.5 to 7.5. It was believed the decrease was due to a

reaction between the carbon dioxide (contained in the air entrainment) and the hydrogen ions in solution (as a result of the corrosion process) yielding carbonic acid (H_2CO_3).

The couplings were made from two types of steel; AISI 1045 and AISI 8635. All coupling blanks were machined and the threads were formed after quench and tempering according to the schedule in Table I. It has been found [3] that rolling a thread after heat treatment increases the fatigue life and that the beneficial effects increase with increase in the ultimate strength of the material. Additional in-air tests were conducted for purposes of comparison with the corrosion results and previous in-air results [1] to evaluate if any changes existed in manufacturing techniques between different heats of couplings. Three thread manufacturing techniques were used to produce the internal threads; A, which is a simple cut thread with no additional work hardening of the surface, B, a cut and burnished thread, and D, a rolled or fully cold worked thread. The details of the manufacturing techniques are given in Table I.

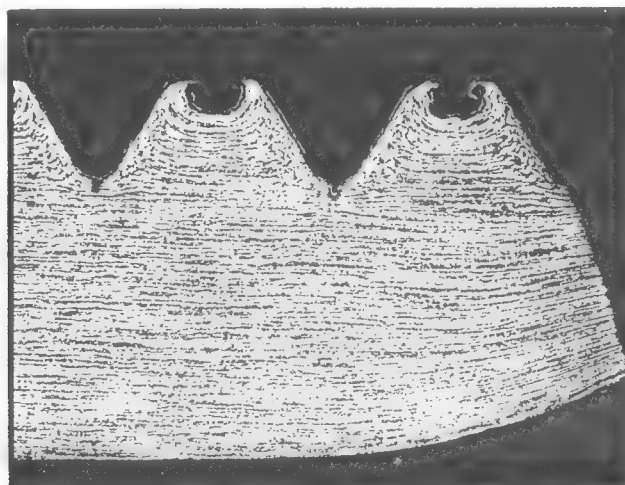


Figure 3 Cross section of threads showing corrosion fatigue cracks

Table I
Thread Details for Couplings from
AISI 1045 and AISI 8635

Series	Description	Manufacturing Technique
A	Cut-thread	<ul style="list-style-type: none">- Coupling quenched and tempered to Rockwell C 16-23.- Coupling ID machined to 0.955 - 0.976 in.- Threads cut to API-11B dimensions for 3/4 in. nominal rod size.- Outer diameter ground down to 1.325 in.
B	Cut thread	<ul style="list-style-type: none">- Heat treatment as for A series.- Coupling ID as for A series.- Precut tap dimensions major diameter 1.0760 - 1.0765 in.- Burnished to API-11B dimensions for 3/4 in. nominal rod size.- Final dimensioning as for A series.
D	Fully cold worked thread	<ul style="list-style-type: none">- Heat treatment as for A series.- Coupling ID machined to 1.014 - 1.016 in.- Cold work thread to API-11B dimensions for 3/4 in. nominal rod size.- Final dimensioning as for A series.

Threaded couplings which failed under the combined action of corrosion and fatigue were sectioned and examined. Figure 3 shows a typical failed coupling where cracks originated at the roots of all threads. Such failures have been identified [4] as corrosion-fatigue, a process which is considered to take place in two stages. During the first stage rounded pits are formed mainly due to the effects of corrosion which, in the situation under investigation, occurs as a result of oxygen concentration cell corrosion in the highly stressed areas at the roots of the threads. The second stage consists of an extension of the pits further into the metal. As these pits increase in size and the cracks grow, the rate of propagation decreases allowing new pits to form and grow before final fracture occurs as a result of fatigue propagating one of the cracks from these pits. Even though a multiplicity of cracks occurred in any one coupling, final failure generally occurred as a result of the crack in the coupling thread, opposite the first thread of the pin, propagating to failure. This area is considered to be the most highly stressed area of the coupling-pin combination and was the location of all the failures of the in-air tests.

TEST RESULTS

The corrosion-fatigue S-N curves for AISI 1045 and AISI 8635 are plotted in Figures 4 and 5 respectively. Each of the plotted points is the median of at least twelve tests. The scatter in the fatigue results can be evaluated from Table II which gives the medians, standard deviations, and 95 percent confidence limits for each of the plotted points.

In all cases, it was observed that the S-N curves obtained from corrosion-fatigue had steeper negative slopes than the corresponding in-air results. It is fairly well established in the literature [4] that most materials evaluated under corrosion-fatigue do not exhibit any endurance limit. The same is true for specimens containing a notch. Thus in Figures 4 and 5, straight lines have been

Table II
Fatigue Test Results

Coupling Series and Material	Maximum Stress ksi	Median Cycles to Failure x 10 ³ Cycles	Confidence Limits x 10 ³ Cycles Lower Upper	Standard Deviation x 10 ³ Cycles	
A-1045 In-Air	47 63	64 11.3	56 11.0	78 11.9	14 1.9
A-1045 3.5% NaCl	47 63	41 6.7	38 4.6	45 7.6	5.4 1.6
A-8635 In-Air	47 63	79 19	69 16	102 24	26 3.4
A-8635 3.5% NaCl	47 63	53 10.5	42 8.3	59 12.3	9.9 2.2
B-8635 In-Air	47 63	228 35	153 29	245 42	73 7.6
B-8635 3.5% NaCl	47 63	56 14.7	51 12.3	65 16.7	12.9 2.2
D-1045 In-Air	63 77	158 7.3	75 6.1	404 8.7	206 2.2
D-1045 3.5% NaCl	63 77	26 3.1	23 3.0	53 7.6	15.4 2.3
D-8635 In-Air	63 77	900 39	449 26	3,250 62	1,390 13.7
D-8635 3.5% NaCl	63 77	74 16	50 12	105 18	34 8.6

drawn through the points and no attempt was made to indicate an endurance limit at an infinite number of cycles.

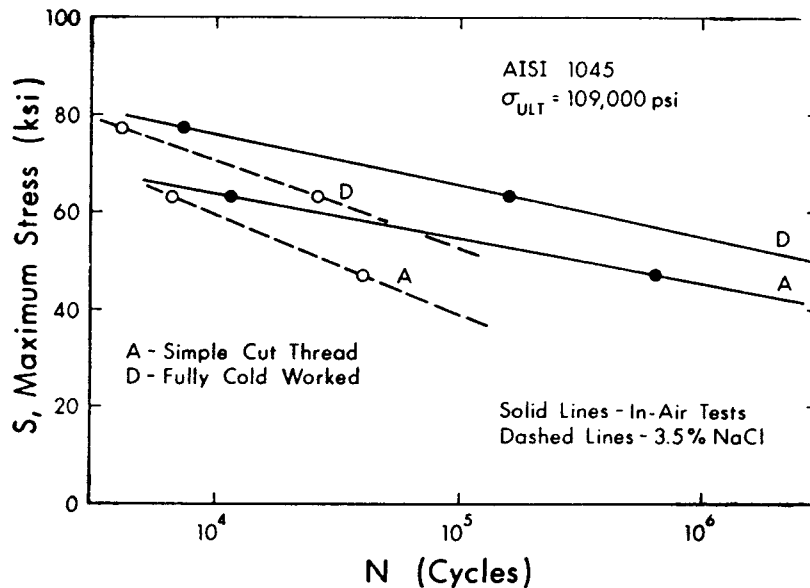


Figure 4 S-N curves for couplings machined from AISI 1045

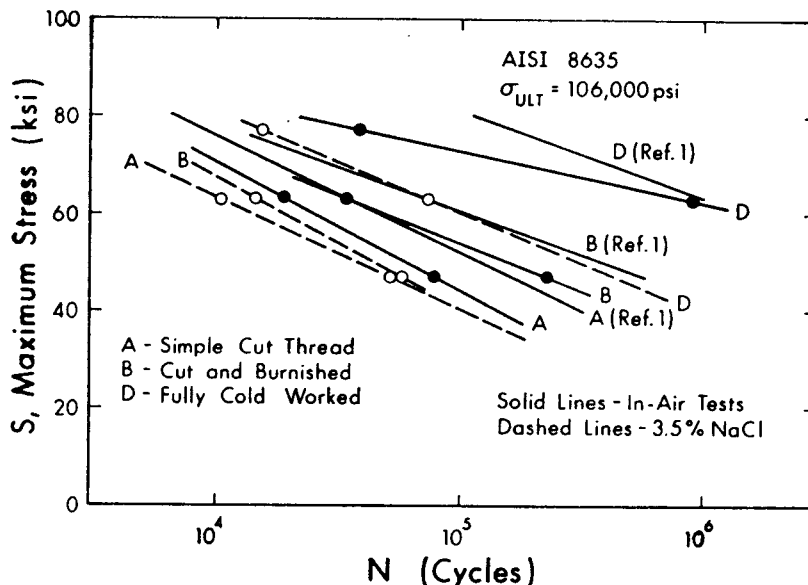


Figure 5 S-N curves for couplings machined from AISI 8635

For couplings machined from AISI 1045 the results plotted in Figure 4 show a decrease in the fatigue life when exposed to a 3.5 percent NaCl environment. Similar differences can be noted in Figure 5 for couplings manufactured from AISI 8635. In evaluating the effect of environment on the fatigue life it is customary to compare stresses on the basis of a fixed number of cycles. For the results in Figures 4 and 5 it was practical to choose a fatigue life of 10^5 cycles. In Table III the corrosion-fatigue stresses at 10^5 cycles, along with the reduction

in corrosion-fatigue stress, are presented for all couplings tested.

It is evident from Table III that the greatest reduction in corrosion-fatigue stress was 26 percent for the B series, cut and burnished thread machined on an AISI 8635 blank. The least reduction was observed for the A series, simple cut thread, and the reduction was about the same for both AISI 1045 and AISI 8635, eight and seven percent respectively. The highest fatigue stress for both in-air and in the presence of a 3.5 percent NaCl solution was observed for the D series machined from an AISI 8635 blank; 73 ksi in air and 60 ksi in 3.5 percent NaCl. In addition, while the fully cold worked thread suffered an 18 percent reduction in the corrosion-fatigue stress at 10^5 cycles, at 60 ksi it was still superior to all other couplings tested in air with the exception of the F series machined from an AISI 1045 blank. Thus, these results confirm the findings of the in-air tests reported on previously [1,2] in that a thread which has been formed entirely by a cold working process has superior resistance to fatigue than threads formed by any of the other techniques evaluated.

The in-air results of previous tests [2] indicated little difference in the fatigue life, at a given fatigue stress, of a coupling whose thread was formed by a simple cutting process, whether the coupling material was AISI 1045 or AISI 8635. This observation is unchanged when the couplings are fatigued in the presence of a 3.5 percent NaCl environment as seen from Figures 4 and 5 and Table III. Similarly, it was found for the fully cold worked thread that there was little difference in the percentage reduction in the corrosion-fatigue stress between using AISI 1045 and using AISI 8635 as a coupling blank material. Nevertheless, a fully cold worked thread produced on a blank made from AISI 8635 has the best fatigue life in either air or 3.5 percent NaCl.

As noted before, from in-air testing, improvement in

Table III
Endurance Stress at 10^5 Cycles

Material	Thread	Endurance		Percent Reduction
		in-air ksi	3.5% NaCl ksi	
AISI 1045	A - simple cut	43	39.5	8
	D - Cold worked	66.5	53	19
AISI 8635	A - Simple cut	44	41	7
	B - Cut & burnished	54	40	26
	D - Cold worked	73	60	18

Table IV
Fatigue Life at 47 ksi Maximum Fatigue Stress

Material	Thread	Life at 47 ksi		Percent Reduction
		in-air $\times 10^4$ cycles	3.5% NaCl $\times 10^4$ cycles	
AISI 1045	A - Simple cut	64	4	94
	D - Cold worked	550	22	96
AISI 8635	A - Simple cut	7.9	5.2	34
	B - Cut & burnished	23.0	5.8	75
	D - Cold worked	>1000	450	>96

fatigue life appeared to be a function of the degree of cold working of the thread. The salt-water corrosion-fatigue tests confirm this only in part. For example, in-air results have shown that the fully cold worked thread, D-series, had a longer fatigue life at a given stress than the cut and burnished thread, B-series, and the cut and burnished thread was in turn, superior to the simple cut thread, A-series. However, when the same couplings were subjected to fatigue in the presence of the 3.5 percent NaCl solution it was found, as can be seen from Table III, that there was no improvement in life for a burnished thread over that of a simple cut thread. In fact, the greatest reduction of 26 percent in the corrosion-fatigue stress was observed for the cut and burnished thread, B-series. It is suggested the reason for this is that in burnishing a thread the degree of cold working is only slight and that the corrosion pits which are formed during the first stage of the fatigue-corrosion process quickly penetrate through the beneficial work hardened layer and the threaded coupling then behaves during the second stage of the corrosion process as if its thread were a simple cut. If improvement in the fatigue life of a threaded element is to be obtained through work hardening of the surface of the threads, the depth of work hardening must be sufficiently great so that when the corrosion pits are formed the tips of these pits are contained within the work hardened layer. If the tips of the corrosion pits are allowed to penetrate through the work hardened layer, then fatigue cracks will propagate uninhibited during the second stage of the fatigue corrosion process. It appears that this is what happened with the B-series cut and burnished thread and explains why the fatigue life of these couplings was about the same as for the A-series which were simple cut when both were fatigued in the presence of a 3.5 percent NaCl solution. The in-air results, of course, which do not have the corrosion stage, showed that the small amount of work hardening of the cut

and burnished thread did provide an increase of about 23 percent in fatigue life over that of a simple cut thread.

Another method of assessing the results of Figures 4 and 5 is to compare fatigue lives of the couplings at a specified stress level. This was done for a maximum nominal stress of 45 ksi and the results were tabulated in Table IV. The same conclusions can be drawn from this table as were made from Table III. However, the reduction in number of cycles is more pronounced than the reduction in corrosion-fatigue stress and this may not be so evident from the figures until it is noted that cycles to-failure are plotted on a log scale.

All the results obtained for corrosion-fatigue were compared with in-air results on couplings manufactured from the same heat of steel and batch heat-treatment. Although the manufacturing techniques and other factors should remain constant from heat to heat, the specifications for an individual heat are only required to lie within certain ranges of composition as specified by AISI. Therefore, while two heats may both lie within the ranges of specifications the individual compositions can differ. Coupled with the fact that there may be slight differences in the heat treatment of the couplings, the manufacturing techniques used to form the threads can vary, all of which can contribute to variations in the fatigue life. It is interesting to observe in Figure 5 the differences in fatigue lives that exist between the in-air current series of tests and the results from a different heat and batch heat-treatment [1]. A greater difference is noted for the fully cold worked thread, D-series, than for the simple cut thread, A-series. This is understandable in as much as the greatest variation in the thread forming process will occur for a cold worked thread where tool wear is of great significance. It is suggested that the differences observed for the simple cut thread, is due more to variations in the heats of the two steels than either the heat treatment or the manner in

which the thread was formed.

DISCUSSION

The results of the present investigation can be compared with some related experiments on medium and high strength steels ($\sigma_{ult} = 100-200$ ksi) reported by others. For example, the benefits that can accrue by rolling the threads after heat treatment of threaded connections to improve the corrosion-fatigue strength, was also found to improve the stress-corrosion life for high strength bolting ($\sigma_{ult} = 260$ ksi) by Lyn, Laurilliard, and Hood [5].

One concern in the present investigation was the variation of the pH of the solution during the corrosion process, although it was attempted to keep this as close to neutrality as possible. According to the investigations of Radd, Crowder, and Wolfe [6] the pH must be greater than 11 before oxygen concentration cell corrosion is effectively stopped. They noted very little difference in fatigue life of AISI 1036 tested in a saline solution whose pH was in the range 6.6 to 10. Further evidence of this was reported by Pettit, Hoepfner, and Hyler [7] who evaluated the effects of environment of Type 135 drill-pipe steel ($\sigma_{ult} = 159$ ksi) used in off-shore drilling applications. They found little difference in the fatigue life in deaerated sea-water, fresh-water drilling mud with a pH of 9, and two sea-water drilling muds of pH 9 and pH 12. In view of these studies [6,7] it is probable that a variation in pH of 6.9 to 9.9 in the present investigation should not have influenced the fatigue life of the specimens evaluated.

The corrosion-fatigue tests were conducted at a cyclic rate of 10 cpm. The work of Pettit et al [7] evaluated the effects of corrosion-fatigue testing frequency in the range 12 - 1200 cpm. They found little difference in fatigue life in the range 12 - 60 cpm but noted the fatigue life improved at a testing frequency of 1200 cpm.

Although the present investigation did not evaluate the effects of differences in heat treatment of the coupling

blanks, it was suspected that variations in the heat treatment could contribute to the differences noted between the current test results and those reported earlier [1]. Of particular interest is a paper by Mehizadah, McGlasson, and Landers [8] in which they investigated the corrosion-fatigue of AISI 1035 in the presence of a 5.0 percent NaCl solution. It was reported that normalized crystal structures behaved similarly to quenched structures and they suggested that the fatigue strength could be expected to vary with the corrosion resistance of the material for severe corrosive environments, whereas for high strength steels, they suggested the fatigue strength should increase with strength under mild corrosive attack. In a paper dealing with stress-corrosion, McGlasson and Greathouse [9] observed that quenched and tempered low chemistry steels appeared to have superior stress corrosion resistance compared with normalized high chemistry steels. More recently, Dvoracek [10] evaluated, under the action of corrosion-fatigue, a number of commercially available sucker-rod materials in which it was reported that in the presence of a 3 percent NaCl solution, oxygen depleted, there was little difference in the results whether the specimens were quenched and tempered, normalized, or normalized and tempered. However, when H_2S was added to the environment, it was found that a normalized or normalized and tempered structure gave a better fatigue life than a quenched and tempered structure.

It is evident from the work cited above [8,9,10] that any comment on the effect of heat treatment on the resistance to corrosion-fatigue must be made with a knowledge of the chemistry of the steel and corrosive environment under investigation. It is believed there is insufficient evidence to rule out the possible effects of heat treatment on the resistance to corrosion-fatigue, and in particular, differences between batches of the same heat treatment on the fatigue life of air. However, in an attempt to explain the differences observed between earlier results [1] and

the present investigation for the fully cold worked thread, as employed in the D-series couplings, it is suggested that the fatigue life is more sensitive to the manner in which the thread was formed and changes in chemistry, although within specified limits, than due to possible unobserved variations in the heat treating process.

CONCLUSIONS

This paper has presented the results of fatigue of medium strength internally threaded components when in the presence of 3.5 percent NaCl environment. The following conclusions can be made;

1. The longest fatigue life was obtained for threads which had the greatest degree of cold working induced during the thread forming process.

2. Burnishing a simple cut thread to improve the fatigue life is practical when placed in a non-corrosive environment but in the presence of a 3.5 percent NaCl solution such treatment was found to have no beneficial effect on the fatigue life.

3. Couplings manufactured from AISI 8635 appeared to yield superior fatigue life to those manufactured from AISI 1045 for both in-air and in the presence of a 3.5 percent NaCl solution.

4. A cycle rate of 10 cpm appears satisfactory to show differences in the corrosion-fatigue life of internally threaded couplings in the presence of a 3.5 percent NaCl solution.

5. While within specifications, small variations in the chemistry of the steel, coupled with small changes in manufacturing techniques of the thread form, can have a significant effect on the fatigue life.

ACKNOWLEDGEMENTS

Financial support for this project was received from the Steel Company of Canada and the National Research Council (Grant A-2705). To these organizations the authors express their sincere appreciation. Also special thanks are extended to Messrs. E.F. Fenske, J. Marshall, and W.D. Brockington at Stelco who assisted in providing the materials and services necessary for the completion of this stage of the project.

REFERENCES

1. Bellow, D.G., and Faulkner, M.G., Fatigue of Threaded Sucker-Rod Couplings, J. Can. Pet. Tech., Vol. 11, No. 1, Jan-Mar 1972, pp. 69-74.
2. Bellow, D.G., and Faulkner, M.G., Fatigue of Internally Threaded Machine Elements, Proc. Fourth CANCAM, 1973, pp. 115-116.
3. Baumgartner, T.C., and Sproat, R.L., Basic Design and Manufacturing of Aircraft Fasteners for Use up to 1600°F, Fastner Symposium, Stand. Steel Press, 1957.
4. Forrest, P.G., Fatigue of Metals, Pergamon Press, 1962.
5. Lin, C.S., Laurilliard, J.J., and Hood, A.C., Stress Corrosion Cracking of High Strength Bolting, ASTM, STP 425, 1967, pp. 84-98.
6. Radd, F.J., Crowder, L.H., and Wolfe, L.H., Effect of pH in the Range 6.6 - 14.0+ on the Aerobic Corrosion Fatigue of Steel, Corrosion, Vol. 16, No. 8, 1959, pp. 415t - 418t.
7. Pettit, D.E., Hoepfner, D.W., and Hyler, W.S., Evaluation of Methods used to Alleviate Corrosion Fatigue in Type 135 Drill-Pipe Steel for Offshore-Drilling Applications, ASTM, STP 462, 1970.
8. Mehdizadeh, P., McGlasson, R.L., and Landers, J.E., Corrosion Fatigue Performance of a Carbon Steel in Brine Containing Air, H₂S and CO₂, Corrosion, Vol. 22, No. 12 1966, pp. 325-335.

9. McGlasson, R.L., and Greathouse, W.D., Stress Corrosion Cracking of Oil Country Tubular Goods, Corrosion, Vol. 15, No. 8, 1959, pp. 437t-442t.
10. Dvoracek, L.M., Corrosion Fatigue Testing of Oil Well Sucker Rods, Materials, Vol. 12, No. 9, 1973, pp. 16-19.

Fatigue of Internally Threaded Machine Elements*

D. G. Bellow, MCSME
Professor

M. G. Faulkner, MCSME
Associate Professor

Department of Mechanical Engineering
University of Alberta
Edmonton, Alberta

Fatigue characteristics were determined for internally-threaded machine elements. Specifically these were of the type used for oilfield sucker-rod couplings. The testing was done first to evaluate various thread designs and second to evaluate the merits of using extruded coupling blanks instead of rolled and machined ones. In addition the fatigue lives of couplings made from two different steel chemistries, namely AISI 1045 and AISI 8635, were compared.

It was found that the fatigue life increased with the degree of cold working used in the thread forming process. There was little significant difference between the fatigue life of a coupling whose thread was formed by a simple cutting process, whether the coupling blank was extruded or not prior to the thread cutting and whether AISI 1045 or AISI 8635 steel was used. However, considerable improvement in the fatigue life of couplings was found for a fully cold-worked thread when that thread was formed on an extruded blank. Furthermore, for the fully cold-worked thread, better fatigue life was obtained for those couplings made out of extruded blanks from AISI 8635 than from extruded blanks made from AISI 1045.

While the testing was all done on sucker-rod couplings it is believed that the results are applicable to other internally-threaded machine elements.

Introduction

Threaded machine elements are common fastening units which have wide application in industry. One such application in the petroleum industry is the use of threaded couplings joining sucker-rods. Long strings of sucker-rods reach far below the surface of the earth and continuously pulsate up and down operating a pump at the bottom of the well. This pulsating action, while only approximately 10 cycles per minute, subjects the sucker-rods and couplings to axial fatigue loads. The purpose of this paper is to discuss the fatigue characteristics of the couplings which join the sucker-rods together; the results may be applied to other threaded machine elements subjected to axial loads in fatigue.

At the present time, there are a number of different designs used in internally-threaded oilfield sucker-rod couplings. These range from a simple cut thread used in a rolled machined blank to a fully cold-worked thread in an extruded blank. In order to evaluate the relative merits of the various forming processes an investigation of the fatigue characteristics of current sucker-rod coupling designs was initiated. In practice of course, these couplings are exposed to a hostile environment, are often improperly made-up, and can be subjected to bending as well as axial loads. As a first step, the behaviour of the thread designs during laboratory tests in air can indicate which design has the best fatigue characteristics. Other factors such as a hostile environment and improper joint make-up can then be examined in the light of these results.

Previous investigations of the fatigue characteristics of threaded connections have been concerned mainly with external threads. These include the review articles of Thurston⁽¹⁾ and Hardy⁽²⁾. Hardy specifically discussed sucker-rod joints and recommended the use of a rounded root thread to reduce coupling breakage. Full size testing of drill pipe-to-tool joint connections was done by Bachman⁽³⁾; however, the testing was done in a rotating beam machine. Improvements in the tool joint, such as vanishing threads and welded connections, were also considered.

In a previous study the authors⁽⁴⁾ discussed the influence of cold working of the thread on the fatigue notch factor. This work is extended in the present paper to evaluate the differences in fatigue life between a coupling made from an extruded blank and a coupling made from a machined blank. Also, the fatigue characteristics of two different materials used in coupling manufacture are evaluated.

Testing Program

The fatigue machine used was a closed-loop servo-hydraulic system having a load capability of $\pm 50,000$ lbs. in axial tension and compression and a frequency range from 0 to 30 Hz. The vertical space available between the cross heads permitted the simultaneous testing of four couplings in series. The load levels, testing frequency, number of cycles to failure and the wave-form of the load application were controlled and monitored by the system's electronics.

The testing program consisted of making up a "string" of four couplings and five rods. The joints were torqued together according to recommended field practice. Figure 1 shows a

*Manuscript received Aug. 18, 1972, and in revised forms, June 4, 1973 and Nov. 12, 1973. No. 72-CSME-29, EIC Accession No. 1297.

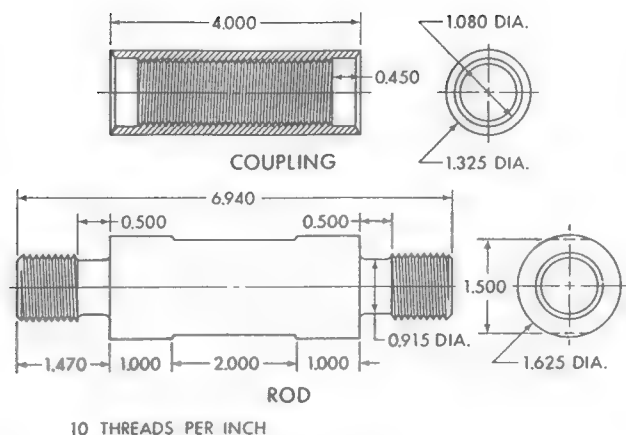


Figure 1 Details of Coupling and Rod

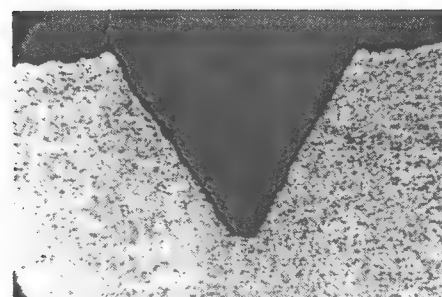
coupling and a rod before mating. This consisted of threading the pins and couplings together until the shoulder of the pin was hand tight against the end face of the coupling. The joint was then torqued with a wrench so that the relative circumferential displacement between pin and coupling was $\frac{1}{4}$ in. This was done for each joint, the purpose of which was twofold⁽⁵⁾:

(1) to produce a tensile load in the pin portion of the joint so that the effect of fluctuating loads will be reduced.

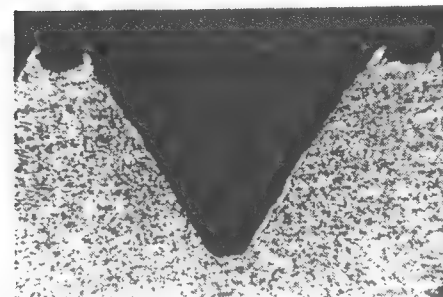
(2) to increase the frictional forces between pin and shoulder of the coupling to prevent unscrewing during the course of normal pumping operation.

The completed "string" was then inserted into the fatigue machine and a prestress of 6100 psi tension was applied. This stress was to simulate the typical dead load that is present when the coupling is in service in an oil well. The "string" was subjected to an alternating axial tensile stress such that the minimum stress never fell below 6100 psi with the maximum set for each particular test. The same testing procedure was used for all couplings evaluated.

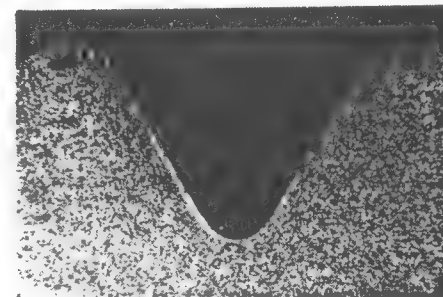
Fatigue failures in the field have indicated that cracks initiated on the inside of the couplings at the root of the thread, opposite the location of the first thread of the pin. One of the primary considerations was that the fatigue failure of the couplings tested in the laboratory would replicate as nearly as possible the failure mechanism observed in the field. So that the couplings would break rather than the pins, and to enable the testing machine to operate at lower loads, and hence at a reasonable frequency of load application, it was necessary to reduce the outside diameter of the coupling from its original value of 1.625 in. to 1.325 in. It was found⁽⁴⁾ that an outside diameter of 1.325 in. permitted a fatigue crack to originate on the inside of the coupling at the root of the thread and in the vicinity of the first thread of the pin. This outside diameter permitted all couplings to be tested at a frequency of 8 Hz or 480 cycles per minute, within a nominal stress range of 6100 to 77,000 psi. The nominal stress was calculated by dividing the axial load by the net cross sectional area of the coupling based on the major thread diameter. The cross sectional area of the coupling was 0.4914 in.² for a major thread diameter of 1.063 in.⁽⁶⁾ and an outside diameter of 1.325 in. (see Figure 1). This compares to the pin whose cross sectional area was 0.6916 in.² based on a minor thread diameter of 0.9384 in. Table 1 shows the chemical composition, and mechanical properties, of the two materials AISI 8635 and AISI 1045.



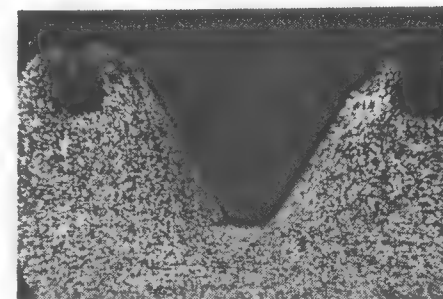
A - Simple Cut Thread
Rockwell C20



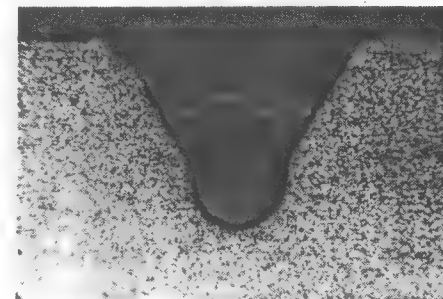
B - Cut and Burnished
Rockwell C22



C - Cut and Partially Cold Worked
Rockwell C37



D - Fully Cold Worked
Rockwell C35



E - Keyhole
Rockwell C22

Figure 2 Profiles of Thread Forms Tested, AISI 8635 x 30

Table 1 Chemical Compositions and Mechanical Properties

	C	Mn	P	S	Si	Ni	Cr	Mo
AISI 1045	0.43-0.50	0.60-0.90	0.040	0.050				
AISI 8635	0.33-0.38	0.70-0.90	0.040	0.040	0.20-0.35	0.40-0.70	0.40-0.60	0.15-0.25
				Yield Strength ksi			Ultimate Strength ksi	
	AISI 1045			105			105	
	AISI 8635			106			112	
	1/2 Charpy V-Notch Test Av. Energy Absorbed (ft-lbs)							
				0°F	40°F	55°F	72°F	
	AISI 1045			5	17	18	21	
	AISI 8635			3	7	9	14	

Discussion of Results – Machined Blanks

The first phase of the testing program consisted of producing five different thread designs on couplings machined from AISI 8635. All these couplings (over 300 were tested) were batch quenched and tempered to Rockwell C16-21. The

process consisted of heating the couplings to 1550°F for 20 minutes and then quenching in oil. The couplings were then tempered for one hour at 1300°F. This produced a fine grain martensite structure throughout. The thread forms were then produced in the couplings to fit a 3/4 in. nominal-size rod. The outside diameters were centerless-ground from 1.625 to 1.325

Table 2 Details of Test Couplings and Thread Configurations

Series Designation	Blank Type	Material A.I.S.I.	Thread Type	Thread Production Details
A	Machined	8635	Cut	<ul style="list-style-type: none"> – Coupling I.D. Machined to 0.955 – 0.976 in. – Thread cut to API-11B dimensions for 3/4 in. rod size
A-2	Extruded	8635	Cut	
A-3	Extruded	1045	Cut	
B	Machined	8635	Cut and burnished	<ul style="list-style-type: none"> – Coupling I.D. machined to 0.955 – 0.976 in. – Precut tap dimensions major diameter 1.0760 – 1.0765 in. – Burnish to API-11B dimensions for 3/4 in. rod size
B-2	Extruded	8635	Cut and burnished	
B-3	Extruded	1045	Cut and burnished	
C	Machined	8635	Cut and cold worked	<ul style="list-style-type: none"> – Coupling I.D. machined to 0.990 in. – Cut thread to 90 deg. included angle – Cold-work to 60 deg. included angle to API-11B dimensions for 3/4 in. rod size
D	Machined	8635	Fully cold-worked	<ul style="list-style-type: none"> – Coupling I.D. machined to 1.015 in. – Cold-work thread to API-11B dimensions for 3/4 in. rod size
D-2	Extruded	8635	Fully cold-worked	
D-3	Extruded	1045	Fully cold-worked	
E	Machined	8635	Keyhole	<ul style="list-style-type: none"> – Coupling I.D. machined to 0.995 – 0.976 in. – Thread cut to API-11B dimensions for 3/4 in. rod size – Keyhole at root of thread cut to radius of 0.014 ± 0.003 in. Major and pitch diameter dimensions conform to API-11B dimensions

in. O.D. The grinding increased the surface hardness to Rockwell C25-26. It was believed this increase in surface hardness would not influence the fatigue results as all fatigue cracks originated on the inside of the coupling at the root of the thread. The outside surface roughness for all couplings was in the range C.L.A. 20-30 μ -in. A description of the various thread configurations tested and thread manufacturing details is given in Table 2. Figure 2 gives a comparison of the profiles of thread forms A-E. For B, C, and D it can be seen that there is evidence of cold working at the root of the thread. For C and D additional cold working is observed at the top of the thread. Below each micrograph is listed the hardness obtained at the root of the thread. These hardnesses can be compared with the base material hardness of Rockwell C16-21, which averaged Rockwell C19 for the couplings selected and micrographed (Figure 2). The effect of the cold working of the threads on the C and D couplings can be measured in hardnesses, at the root of the threads, of Rockwell C37 and 35 respectively.

The fatigue results for the couplings manufactured from

machined AISI 8635 blanks are listed in Table 3. For each stress level in each series, 12 couplings were tested and the median value was calculated and plotted in Figure 3. The actual results are shown in(4). As given in Reference 7 the confidence interval for 12 specimens for a 95 percent confidence level ranges from the third lowest value obtained to the third highest. This estimation of confidence interval does not assume any particular frequency distribution. Along with the confidence intervals, the standard deviation was evaluated for the data assuming a normal distribution and these are listed in Table 3. The distribution was not tested for normalcy. Figure 3 is a log-log plot to indicate that all the results plot as straight lines although there are slight differences in slopes. The longest fatigue life was obtained from the D coupling, which had a fully cold worked thread, while the shortest life was obtained from the E coupling which had a keyhole thread. On the basis of the median values and confidence limits there was little significant difference between the E coupling and the A, which was a simple cut thread. Rounding the root of the thread as was done in the keyhole did not improve its performance over that of the simply cut thread. The results in Figure 3 also show that burnishing the thread, as was done

Table 3 Fatigue Test Results

Coupling Series	Maximum Stress x 10 ³ psi (Minimum stress = 6100 psi)	Median cycles to failure x 10 ³ cycles	95% Confidence Limits		Standard Deviation x 10 ³ cycles
			Lower	Upper	
A	40.7	326	249	470	113
	46.8	144	116	169	34
	63.1	35	33	39	5
	77.3	8	7	9	1
A-2	40.7	365	209	699	258
	46.8	168	140	248	52
	63.1	36	33	42	7
	77.3	15	14	17	2
A-3	40.7	363	202	545	217
	46.8	156	140	179	23
	63.1	44	41	50	4
	77.3	18	16	22	3
B	46.8	508	352	1767	455
	63.1	73	58	86	47
	77.3	12	9	19	6
B-2	63.1	64	53	79	14
B-3	63.1	72	54	77	17
C	57.0	505	363	∞	221
	63.1	300	198	501	275
	77.3	113	86	170	77
D	63.1	1005	318	1668	649
	77.3	175	117	240	82
D-2	77.3	855	514	2066	858
D-3	77.3	368	258	578	219
E	40.7	278	240	537	194
	46.8	95	72	108	31
	63.1	23	21	26	4
	77.3	8	7	9	1

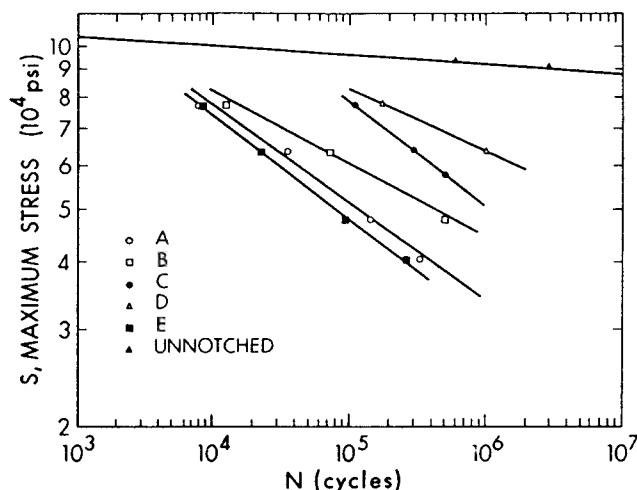


Figure 3 Comparison of Fatigue Life for Series A-E Thread Configurations – Machined Blanks, AISI 8635

with the B coupling, improved the fatigue life. However, burnishing was not as effective as partially cold working the thread as was done for the C coupling.

It has been reported⁽⁴⁾ that for couplings manufactured from machined blanks the fatigue notch factor K_f ⁽⁷⁾, at a life of 10^7 cycles, was four for a simple cut thread and less than two for a fully cold-worked thread. This can be compared with a fatigue notch factor greater than four for threaded drill-pipe joints⁽⁸⁾.

The fatigue life of the couplings tested was very sensitive to the degree of cold working. It was observed that in the forming of threads by processes other than cutting alone, the degree of cold working was not necessarily uniform for a given series of couplings tested. For example, it was found that at 63,000 psi the standard deviation of C was 92 percent of the median while for A it was only 14 percent of the median (see Table 3). The scatter in data for the cold worked threads is evident from the wide confidence limits as shown in Table 3.

Extruded versus Machined Blanks

The second phase of the testing was designed to evaluate whether or not the fatigue life could be extended for fully cold-worked couplings by replacing the machined blank with an extruded one. An additional objective was to determine if there was any significant difference in using AISI 1045 in place of AISI 8635 as the coupling material.

The details of the couplings tested in the second phase are given in Table 2. The couplings used in this series were cold extruded and then stress relieved at 1200°F to form a pearlite-ferrite crystal structure. One hundred and forty-four couplings were tested. S-N curves were obtained for couplings having a simple cut thread produced on blanks of AISI 8635 and AISI 1045; A-2 and A-3 respectively. The failure mechanism for couplings made from these extruded blanks was the same as that for couplings made from machined blanks. Also, there appeared to be no difference in the failure mechanism between AISI 1045 and AISI 8635.

The fatigue results for couplings manufactured from extruded blanks are shown in Figure 4-9 and listed in Table 3. Figure 10 compares the results for couplings manufactured

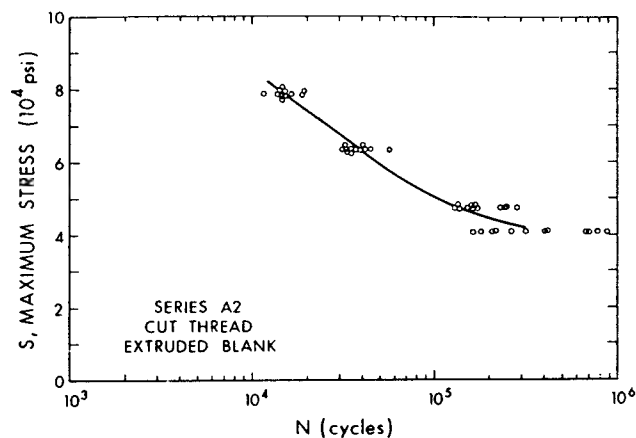


Figure 4 Results for Simple Cut Thread on Extruded Blank, AISI 8635

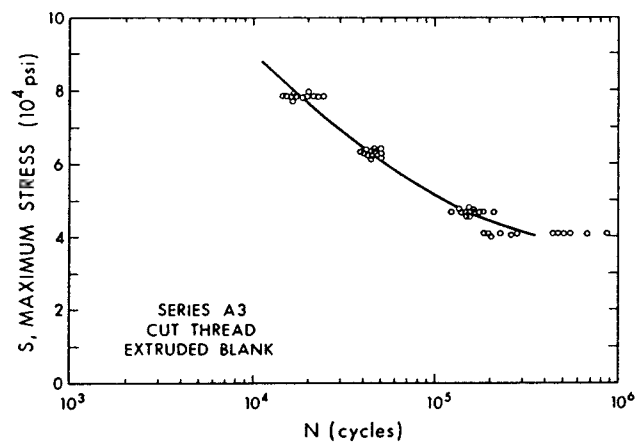


Figure 5 Results for Simple Cut Thread on an Extruded Blank, AISI 1045

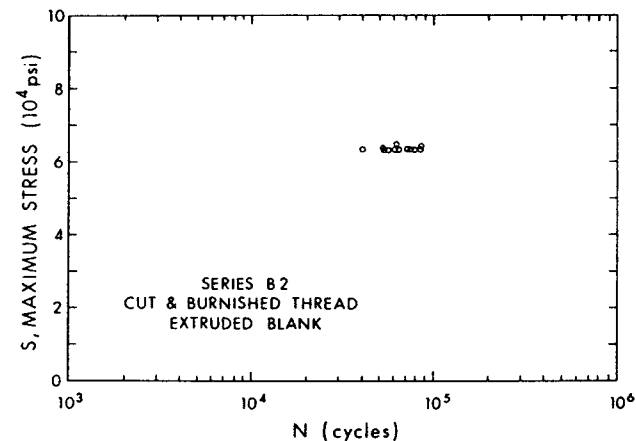


Figure 6 Results for a Cut and Burnished Thread on an Extruded Blank, AISI 8635

from extruded blanks with couplings manufactured from machined blanks. For the simple cut thread (A, A-2, and A-3) it is seen that there is little difference between using an extruded blank and using a machined blank, and that the difference between the use of AISI 1045 and AISI 8635 is insignificant. The exception to this is that; at a stress of 77,000 psi, a slight improvement is observed when using an extruded blank A-2 over a machined blank A.

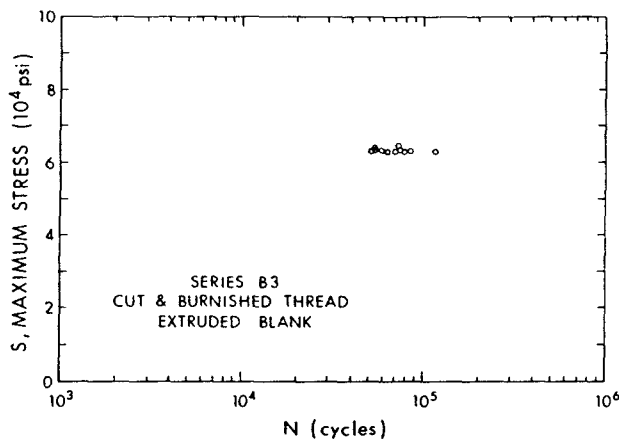


Figure 7 Results for a Cut and Burnished Thread on an Extruded Blank, AISI 1045

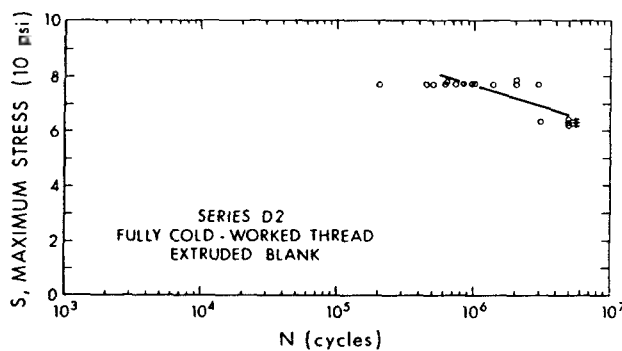


Figure 8 Results for a Fully Cold-Worked Thread on an Extruded Blank, AISI 8635

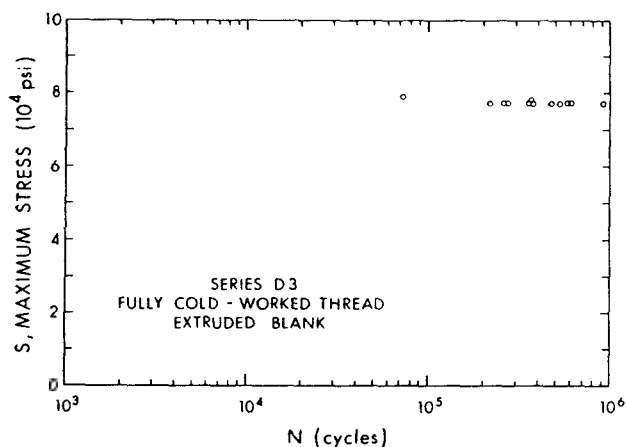


Figure 9 Fatigue Results for a Fully Cold Worked Thread on an Extruded Blank, AISI 1045

While only one series of tests at one stress level for each steel chemistry was produced for the cut and burnished thread on an extruded blank, there appeared to be little difference between the B-2 using AISI 8635 and B-3 using AISI 1045. While the median value for the B-3 was higher than the B-2 (72,000 cycles as compared with 64,000 cycles for the B-2) the 95 percent confidence limits were similar.

Figure 10 shows that at an maximum stress of 77,000 psi there is improvement in fatigue life for a fully cold-worked

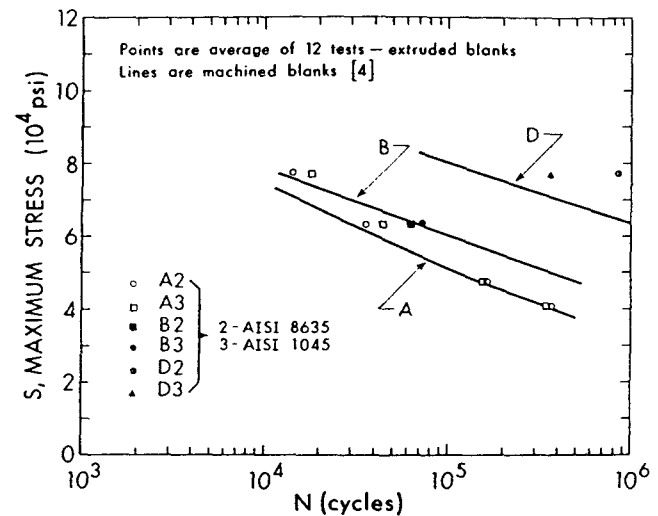


Figure 10 Comparison of Fatigue Life Between Machined Blanks and Extruded Blanks

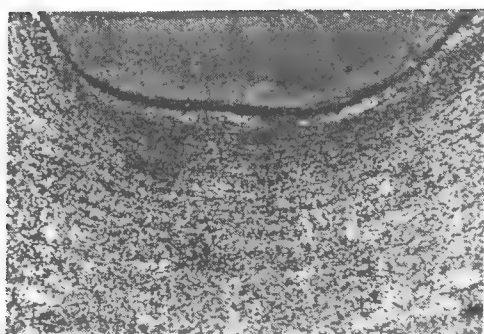
thread formed on an extruded blank. In fact, of all the couplings tested, the only significant improvement in fatigue life by using extruded blanks was for the fully cold-worked thread, D-2 and D-3. Also, of the two chemistries of steel, it would appear that a cold-worked thread formed on an AISI 8635 steel yields a longer fatigue life than the same thread configuration formed on an AISI 1045 steel. Just how much improvement must be speculative since the couplings of the D, D-2 and D-3 did not all come from the same batch heat treating process. However, from Figure 10 an improvement factor of six, at 77,000 psi, appears to be evident.

To explain why a coupling made from an extruded blank is better than one made from a machined blank, photomicrographs of the root of the threads are shown in Figure 11. This figure compares, for the fully cold-worked thread, a D coupling machined from AISI 8635 and extruded couplings made from AISI 8635 and AISI 1045, D-2 and D-3 respectively. It is seen that for D-2 and D-3 the extrusion process develops a preferred orientation of the pearlite-ferrite crystal structure in the longitudinal direction of the coupling. Added to this, the cold working of the threads produces grain orientation around the root of the thread, the area in which all fatigue cracks originated. This lowers the fatigue strength reduction factor. In the fine grain tempered martensite structure of the D machined couplings there is no preferred grain orientation except at the root of the thread. Furthermore, the effect of the cold working of the thread forming process for D appears to be less than observed for D-2 and D-3. Referring to Figure 3, this difference is not significant in the case of A, A-2, and A-3 and B, B-2, and B-3, and it is suggested that with a cut thread, or a cut and burnished one, the fatigue strength reduction factor is too severe to be significantly reduced by extruding the blank prior to the thread forming process.

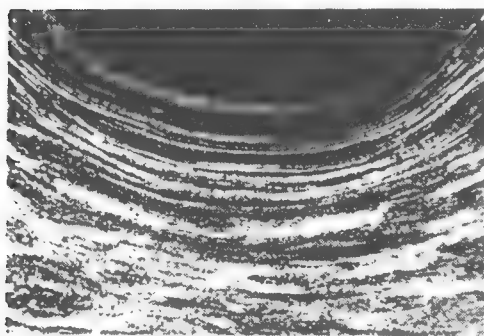
Conclusions

The conclusions listed below are based on the median values of test results. Where the data scatter is considerable, as in the case of the cold-worked threads, the confidence limits also indicate the differences or similarities given below.

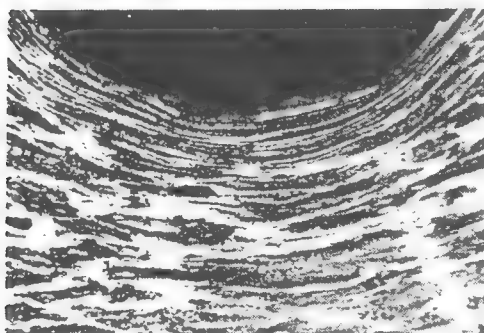
1. Fatigue results of five different couplings made from machined AISI 8635 blanks were obtained. It was observed that fatigue life was improved with cold working of the thread; the longest fatigue life was recorded for those couplings whose



D- Machined Blank
AISI 8635



D-2 Extruded Blank
AISI 8635



D-3 Extruded Blank
AISI 1045

Figure 11 Photomicrographs of Machined and Extruded Blanks x 200

thread was formed entirely by cold working. It was also found that rounding the radius of the root of the thread, as in a keyhole thread, did not improve the fatigue life over that of a simple cut thread. It was concluded that the fatigue life of sucker-rod couplings was quite sensitive to the degree of cold working that had been introduced in the manufacturing of the thread.

2. There was little significant difference between the fatigue life of a coupling whose thread was formed by a simple cutting process, even with burnishing the cut thread, whether or not the coupling blank was extruded or not prior to cutting of the thread, and whether or not AISI 1045 or AISI 8635 steel was used.

3. The fatigue life of a fully cold-worked threaded coupling was extended by using coupling blanks which had been extruded prior to the thread forming process. The results also show that, for such a thread, AISI 8635 is superior to AISI 1045 for the coupling material.

4. While it may be possible that excessive cold working of the threads could cause cracking of the material and thereby actually reducing its fatigue strength, this was not observed in this work.

Acknowledgements

The authors wish to express their sincere appreciation and thanks to The Steel Company of Canada for the financial assistance given to this project. Thanks are also extended to Mr. E. Fenske, who first suggested the project and to Mr. W. Brockington, who provided all the coupling materials. Finally, our appreciation is acknowledged to Mr. H. Schroeder of the University's Department of Mechanical Engineering, who carried out the experimental work.

References

1. Thurston, R.C.A., *Trans ASME*, 73, 1085-1092, 1951.
2. Hardy, A.A., *Drilling and Production Practice*, API, 214-225, 1952.
3. Bachman, W.S., *Pet. Eng.*, 23, B36-51, 1951.
4. Bellow, D.G. and Faulkner, M.G., *J. Can. Pet. Tech.*, 11, 69-74, 1972.
5. Miller, D.R., *API Midyear Standards Conference*, 1950.
6. *Standard 11B*, API Production Division, 1970.
7. Special Technical Publication 91-A, ASTM, 1963.
8. Frantz, W.F., *Pet. Eng.*, 23, B60-65, 1951.

Improving the fatigue strength of butt welded steel joints by peening

M.G. Faulkner and D.G. Bellow



INTRODUCTION

It is generally accepted for design purposes that the fatigue strength of steel plate increases progressively with the ultimate tensile strength (UTS) of the steel. Up to a UTS of about 150 000 psi (1020N/mm²) the fatigue strength increases almost proportionately with the UTS. However, if medium to high strength steels are butt welded, the fatigue strengths which are measured for fatigue lives above 10⁵ cycles are no higher than those shown by mild steel.¹ Higher strength steels then have little advantage where the structure may be subjected to varying stresses in service.

The higher strength steels do show a fatigue strength advantage over mild steel under low cycle conditions or if the butt welds are dressed or treated in some manner. It is believed that the stress concentration at the weld toe is primarily responsible for the reduced fatigue behaviour. As a result, a number of investigators²⁻⁴ have been concerned with postwelding techniques aimed at reducing the effect of this notch. These include grinding the weld bead flush, using additional weld passes, local machining of the weld, and residual stress techniques such as prior overloading and peening. A summary of the various techniques and the improvements possible has been reported by Gurney.⁵

The most common of the residual stress techniques is to peen with a high velocity stream of metal particles or with a tool operated by a pneumatic hammer. Although peening is one of the easiest methods to use, the improvements in fatigue strength can vary from 10 to 100%.⁵ It is difficult to compare results from different investigators since the welding details as well as the material may vary. It is believed, however, that one major reason for the discrepancy between the reported results is the degree of peening or peening intensity used in the various studies. Although it is thought that a minimal amount of peening will not show a great improvement, too much peening could lead to rapid deterioration of the joint since it would induce surface cracking. Previous authors^{6,7} have suggested an optimum peening process for plate materials; however, because of the overriding influence of the stress concentration factor at the root of the weld, whether or not an optimum exists for the welded joint is not known.

The main purpose of this article is to relate increased fatigue strength of the welded joints to the peening intensity of the process used. The ultimate goal is to determine the peening intensity which gives the best fatigue behaviour. To this end four different peening processes were compared on the basis of improvements in the fatigue life and the peening intensity measured by determining the depth to which the parent material was work-hardened.

TEST PROCEDURE

The fatigue testing was done using specimens similar to those shown in Fig. 1. These test specimens were made from Stelco Columbium (niobium) 50 steel by

welding together two 5in. (127mm) wide, 0.25in. (6.3mm) thick steel plates. The plate was in the as-rolled condition; however, the plate edges were prepared by machining them straight and bevelling the edges at 45° to a depth of about 0.06in. (1.5mm). Automatic submerged-arc welding was used so as to control, as much as possible, the welding variables. Details of this process as well as the material properties of the weld metal and plate material are given in Table 1.

The welds were all fluoroscoped to check for flaws and then cut into 3in. (76mm) wide strips with the weld transverse to the cut. Where surface treatment was done by peening, it was completed before the specimen was cut to the shape shown in Fig. 1.

Four different peening processes were evaluated:

- 1 Air-blasted glass beads 0.007-0.012in. (0.2-0.3mm) in diameter.
- 2 Steel shot 0.025-0.045in. (0.63-1.1mm) in diameter from a Pangborn 'Rotoblast' wheel. The velocity of the shot was approximately 250ft/sec (76m/sec).
- 3 Pneumatic multiple-rod hammer peening using a needle scaler.* This tool had nineteen flat-ended needles of 0.12in. (3.1mm) in diameter. Operating pressure was 90psi (6.2 bar).
- 4 Pneumatic hammer peening using a single-point scaler.** This tool was equipped with a flat-ended round punch, the diameter of which was 0.25in. (6.3mm). Operating pressure was 90psi (6.2 bar).

Visual checks were always made to ensure that the coverage in the critical points of the weld and the surrounding region was as uniform and complete as possible. The time of exposure to each process was measured to be 20-30sec/in² (3-5sec/cm² approx.) of surface area treated. The surfaces of the specimens treated by the four techniques mentioned above and the CLA are shown in Fig. 2.

The specimens were tested in pulsating tension, the maximum stresses being shown in Table 2. Fatigue testing was carried out at approximately 190Hz in an Amsler Vibrophore. Testing of each specimen was terminated by setting the load limits on the fatigue machine so that when a visible crack occurred the machine automatically stopped. The crack always occurred at the weld toe and on the surface (see Fig. 2a) propagating inwards. This meant that the crack was in the heat-affected zone where the welding resulted in a smaller grain size and a slight increase in hardness.⁴

The usual way to measure the peening intensity is to use the Almen strip test;⁸ however, this does not always give a reasonable indication of the peening intensity for very intensive peening. This has been pointed out previously by Horger and Neifert.⁹ As a result, the actual depth of work-hardening was evaluated by cutting the specimen at a small angle to the surface (approximately 10°). The hardness v. the depth was measured on this inclined surface

* Manufactured by Sioux Tools Inc.

** Manufactured by Fuji Air Tools Co. Ltd.

using a Knoop indenter with a 300g load. The depth of work-hardening was then obtained by plotting these hardness measurements v. the actual depth and estimating the depth at which the hardness approached that of the parent material.

RESULTS AND DISCUSSIONS

A summary of the results obtained from the fatigue testing is shown in Table 2 and Fig. 3. In Fig. 3 the points plotted correspond to the median values in Table 2. Also plotted in the Figure are the fatigue results of the parent material with steel-shot peening which are from Ref. 4. It is seen that up to twenty-one specimens were used because of the high degree of scatter. The scatter was greater for the welded specimens than for the parent material and was probably a result of the variations in the notch geometry at the weld toe.

The results show that, although there is a vast difference in the fatigue behaviour of the parent material and the as-welded plate, considerable improvement is possible with proper peening. The improvements (in fatigue strength at 2×10^6 cycles) obtained by the four peening processes are shown in Table 3 where the percentage improvement as well as the depth of work-hardening for each process are shown.

It is seen that the greatest improvement in the welded specimens occurred with the multiple-rod peening. This is especially true at lower fatigue lives, but at longer fatigue lives the steel-shot blasted, multiple-wire hammer peened, and single-point hammer peened curves approached one another. This indicated that for fatigue lives greater than 10^6 cycles, once a certain peening intensity (depth of work-hardening) was reached, increasing it further increased the fatigue strength only marginally. It is believed that the reason the multiple-rod tool was more effective than the single-point one was because the radius of the single-point hammer was much larger than that of the individual rods in the multiple-point tool and thus could not work the weld toe as effectively.

For the unwelded plate both the multiple-rod and single-point hammer peening resulted in smaller improvements than with the steel-shot blast. The steel-shot blast intensity was also measured by the Almen strip and was found to give 0.012A, i.e. an arc height of 0.012in. (0.3mm) on an A strip. This peening intensity was close to the optimum suggested by Straub⁷ for 0.25in. (6.3mm) steel plate. The more intense peens which were applied by the pneumatic hammers resulted in some surface cracking and therefore were not an effective surface treatment. This did not show up in the welded specimens, probably because the effect of any surface cracking was masked by the presence of the stress concentration at the weld toe.

It appears that for welded material a more severe peen is desirable than for unwelded plate of the same size. This may be explained by the fact that the weld toe is much more susceptible to fatigue failure than the as-rolled plate and therefore requires more attention. Work by Signes et al¹⁰ indicates that two factors are responsible for initiating failure in the weld toe region. Firstly, most welds have an undercut in this region of 0.003-0.005in. (0.08-0.13mm) in depth, and secondly there is a buildup of impurities in this region. Brodrick⁶ indicates that the depth of the work-hardened layer should be two to five times the depth of any surface defects. This means that the depth should be up to 0.025in. (0.63mm). From Table 3 it can be seen that the multiple-rod peen is

the process which gives somewhat above this value and also gives the greatest improvement in the fatigue strength.

CONCLUSIONS

The results above were obtained using Columbium (niobium) 50; however, it is believed that they would apply to most butt welded medium strength steels.

- 1 To obtain the best improvement in the fatigue strength of butt welded joints it is necessary to use a more severe peen than would be used for plate material alone.
- 2 For the Columbium 50 steel, the greatest improvement in the fatigue strength was obtained with the multiple-rod pneumatic hammer. This treatment resulted in a work-hardened layer of 0.035in. (0.9mm) thick and an increase in fatigue strength (at 2×10^6 cycles) of approximately 65%.
- 3 Although peening treatment which yields a larger depth of work-hardening than necessary does not give as great an improvement in fatigue strength, it does improve the fatigue behaviour over what it would be without any treatment.

ACKNOWLEDGEMENTS

The authors would like to thank The Steel Company of Canada for supplying the material as well as performing the welding. Financial support from the National Research Council of Canada under grant Nos A-7514 and A-2705 is also gratefully acknowledged.

REFERENCES

- 1 FROST, N.E. and DENTON, K. 'The fatigue strength of butt welded joints in low alloy structural steels'. Brit. Weld. J., 14 (4), 1967, 157-63.
- 2 BARON, H.G. and BRINE, F.E. 'A note on the improvement in fatigue properties of butt welds produced by shot peening or prestretching'. 2nd Commonwealth Welding Conference, Inst. of Welding, London, 1965, 322-6.
- 3 HARRISON, J.D. 'Techniques for improving the fatigue strength of welded structures'. 2nd Commonwealth Welding Conference, Inst. of Welding, London, 1965, 327-33.
- 4 FAULKNER, M.G. and BELLOW, D.G. 'Improving the fatigue life of butt welded medium strength steels'. Symposium on Applications of Solid Mechanics, University of Waterloo, 1972, 613.
- 5 GURNEY, T.R. 'Fatigue of welded structures'. Cambridge University Press, 1968.
- 6 BRODRICK, R.F. 'The selection of optimum conditions of mechanical prestressing'. SP-181, Soc. of Automotive Engineers (Mechanical pre-stressing), 1960, 4-7.
- 7 STRAUB, J.C. 'Choosing the optimum method, intensity and coverage of shot peening'. SP-181, Soc. of Automotive Engineers (Mechanical pre-stressing), 1960, 8-10.
- 8 SAE. 'Manual on shot peening'. SAE J808a.
- 9 HORGER, O.J. and NEIFERT, H.R. 'Improving fatigue resistance by

- shot peening'. Soc. for Experimental Stress Analysis, Vol. II, (1), 1944, 178-90.
- 10 SIGNES, E.G. et al. 'Factors affecting the fatigue strength of welded high strength steels'. Brit. Weld. J., 14 (3), 1967, 108-16.

Table 1 Material properties and welding details

		Chemical compositions, %				
		Mn	P	S	Si	Columbium*
Columbium* 50	0.2	1.2	0.04	0.05	-	0.005
Oxweld no. 36 rod	0.14	2.0	0.017	0.024	0.05	-

		Mechanical properties				
		Yield,		Ultimate,		Elongation, %
		psi	N/mm ²	psi	N/mm ²	
Columbium* 50	77 000	520	80 000	545	-	
Oxweld no. 36 rod	75-90 000	510-615	-	-	20-30	

Welding details		
1	Welding process	- submerged-arc welding, double-sided, using flux backing
2	No. of welding wires	- two, tandem
3	Welding wire	- Linde, Oxweld no. 36, 0.125in. (3.17mm)
4	Flux	- Linde, Oxweld 585
5	Tip height	- 0.8in. (22.2mm) from workpiece
6	Distance between electrodes	- 0.3in. (8mm)
7	Speed	- 56in/min (1.42m/min)

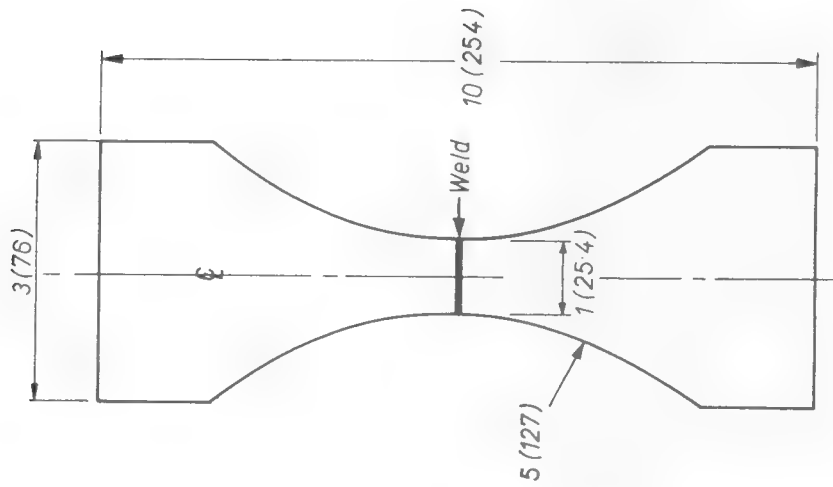
* Niobium

Table 2 Summary of fatigue results

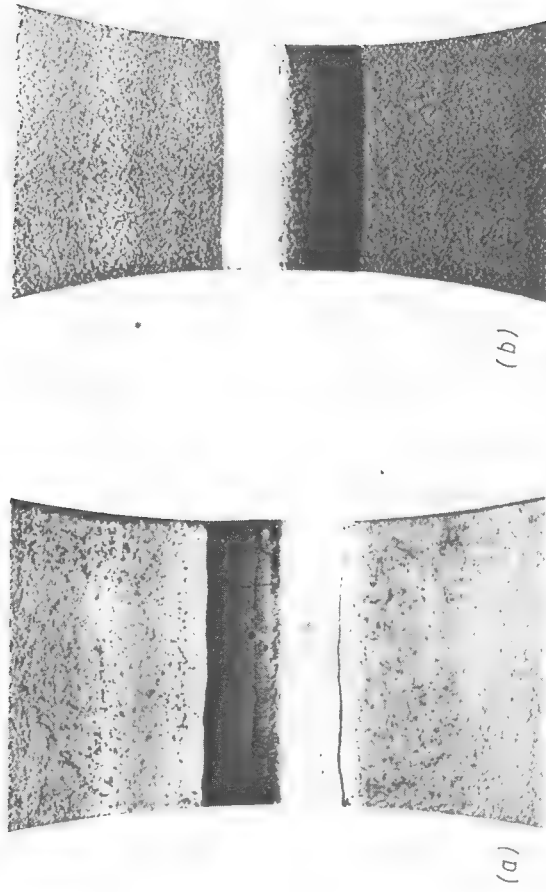
Treatment	No. of specimens tested	Maximum stress		Median life (x 1000 cycles)	95% confidence limits (x 1000 cycles)	
		ksi	N/mm ²		Lower	Upper
Untreated weld	12	23.8	164	1324	899	3793
	12	30.8	212	406	232	798
	12	36.9	254	282	219	298
	12	46.1	318	113	65	188
Glass-shot peened (welded)	12	30.8	212	1903	366	10000+
	12	36.9	254	301	164	1605
	12	46.1	318	122	84	195
Steel-shot peened (welded)	17	36.9	254	1417	922	3674
	18	41.5	286	333	218	851
	18	46.1	318	200	128	434
Multiple-wire hammer peened (welded)	12	36.9	254	10000+	1825	10000+
	18	39.2	270	1076	694	1375
	18	41.5	286	683	399	1557
	12	46.1	318	508	247	1244
	12	52.3	360	275	101	332
Single-point hammer peened (welded)	12	36.9	254	1036	575	2034
	21	41.5	286	420	279	639
	21	46.1	318	323	258	477
As-rolled plate (no weld)	18	49.2	339	1463	833	10000+
	18	61.5	424	237	198	669
	18	67.7	467	108	60	222
As-rolled plate steel-shot peened (no weld)	12	63.0	434	526	442	658
	12	58.0	400	4918	1384	10000
As-rolled plate multiple-point	12	49.2	339	10000+	10000+	10000+
	12	55.5	383	972	376	2415
	11	61.5	424	313	246	674
As-rolled plate single-point hammer peened	12	55.5	383	869	554	2174
	12	61.5	424	202	116	457

Table 3 Comparison of fatigue strength at 2×10^6 cycles

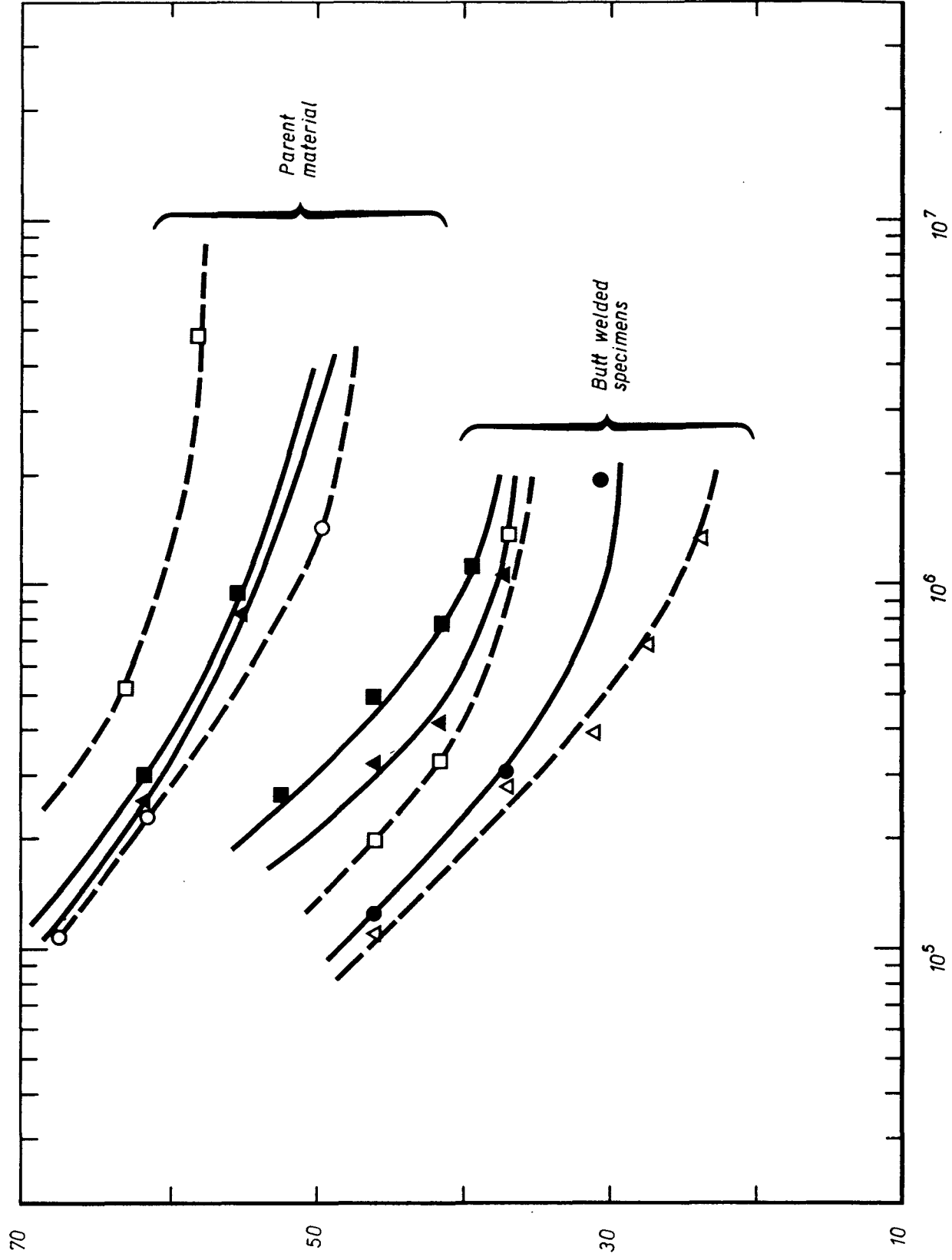
Welded specimens					
Surface treatment	Fatigue strength		Percentage improvement	Depth of work-hardening	
	ksi	N/mm ²		in.	mm
Untreated weld	22.8	157	-	-	-
Glass-shot blasted	29.2	201	28	0.005	0.127
Steel-shot blasted	35.2	243	54	0.015	0.4
Multiple-point hammer peened	37.6	259	65	0.035	0.9
Single-point hammer peened	36.3	250	59	0.060	1.5
Parent material					
As-rolled plate	48.5	335	-	-	-
Steel-shot blasted	58.5	403	21	0.015	0.4
Multiple-rod hammer peened	52.0	359	7	0.035	0.9
Single-point hammer peened	51.0	351	5	0.060	1.5



1 Fatigue specimen; dimensions in in. (mm)



2 Surface of specimens after peening: (a) glass-shot blasted; CLA 250 μ in. (6.3 μ m), (b) steel-shot blasted; CLA 350 μ in. (8.9 μ m), (c) multiple-rod hammer peened; CLA 500 μ in. (12.7 μ m), and (d) single-point hammer peened; CLA 300 μ in. (7.6 μ m)



3 Effect of peening processes on fatigue life. \triangle — as-welded; \circ — untreated plate; \square — steel-shot blasted; \bullet — glass-shot blasted; \triangle — single-point hammer peened; \blacksquare — multiple-rod hammer peened

UPPER EXTREMITY CONTRACTION MOMENTS AND THEIR RELATIONSHIP TO SWIMMING TRAINING*

ROBERT K. JENSEN

School of Physical & Health Education, Laurentian University, Sudbury, Ontario, Canada

and

DONALD G. BELLOW

Department of Mechanical Engineering, University of Alberta, Edmonton, Alberta, Canada

Abstract—A rationale is presented for relationships between the contraction moments at the shoulder and elbow joints and the forces acting on the adjacent body segments during the propulsive phase of front crawl swimming. It was hypothesised that the magnitude of the contraction moments necessary to sustain large hydrodynamic forces would be such that with swimming training the contraction moments would increase, and that the faster swimmers would have larger contraction moments. In order to reduce the complexity of the kinetic analysis it was assumed the contraction moments could be measured using a device which allowed for rotation without translation and provided an appropriate resistance moment. The contraction moment produced bending strain on a lever arm and the signal was integrated to give impulse and work output. Tests were carried out on a sample of 42 boys. Half of the group underwent a period of swim training and it was found that the medium ability swimmers did increase the initial segments of the impulse and work output curves. Tests on the remaining swimmers showed that the higher ability swimmers had impulse and work output curves which were significantly greater than for the lower ability swimmers.

INTRODUCTION

Changes in the moment of force due to muscle contraction can be induced through the use of external forces such as weights and springs. The external forces are used to provide a training moment opposite in sense to the muscle contraction moment, and provided the load is sufficient functional changes occur in the muscles. There has been a trend however, toward replacing or supplementing the use of external forces of this type with skills which conceivably provide external and inertial forces sufficient to act as a training stimulus. The major advantage of skill-based training is that the individual is usually motivated to continue the activity for extended periods of time and simultaneously acquires proficiency in the skill. The major disadvantages are that quantitatively, the training loads are usually unknown and the effects of training on the contraction moments are not known. The purpose of this study was to investigate the relationships between the skill of front crawl swimming and the upper extremity contraction moments considered to be of importance to the skill, viz. shoulder extension and elbow extension.

It was postulated that if there are relationships between the skill of front crawl swimming and the contraction moments for shoulder and elbow extension, they could be demonstrated in two ways. Firstly, swimmers in a training programme would tend to increase their contraction moments. Secondly, faster swimmers would tend to have greater contraction

moments. These results would be of use in providing insight into the relative contribution of upper extremity contraction moments to front crawl swimming. Furthermore, the techniques for evaluating the contraction moments could be used to test the effect of various swim training programmes on the contraction moments.

In swimming, the horizontal forces consist of a propulsive force and a resistive force. The resistive force is that due to frictional, eddy and wave resistance caused by having the body move through the water. The propulsive force is attributable to the hydrodynamic and inertial forces produced by the motion of the segments of the upper and lower extremities. In accordance with Newton's Second Law of Motion the resultant horizontal force is equal to the time rate of change of horizontal momentum.

A number of studies have been conducted in which the hydrodynamic forces and/or the joint moments of force have been estimated. In each case it has been necessary to use simplified models of the segmental rotations. Plagenhoef (1971, pp. 121–127, 152–158) computed peak contraction moments of 98 Nm for shoulder extension and 49 Nm for elbow extension but assumed that the hand was held stationary by a force of 62 N. Gallenstein and Huston (1973) and Huston and Passerello (1971) calculated but did not publish segmental drag forces and joint moments of force. Drag and inertial moments for shoulder flexion about a fixed axis were evaluated by Baz (1970) using a cylindrical model of the arm. The results of this experiment were used in the evaluation of supportive forces about the feet during transient arm actions in

* Received 20 December 1974.

Secondly, the angular velocities developed in the segments depend upon the contraction moments at shoulder and elbow. These velocities largely determine the drag forces on the segments. The above equations show that the horizontal reaction force at shoulder (R_{x1}) depends upon the corresponding drag and inertial forces for the two segments. As the horizontal shoulder reaction force is considered the primary source of propulsion it was hypothesised that the faster swimmers would have greater contraction moments.

The two segment model (Fig. 1) was considered too complex for controlled measurement. Changes in the contraction moments over a 3-week period were being investigated. Any attempt to measure the drag, inertial, weight and buoyancy terms would have been inaccurate and imprecise due to the assumptions which would have had to be made and the limitations of the measurement techniques. It was decided that the changes in contraction moments could be more effectively investigated by controlling the above terms. The planar movement of each segment was treated individually and as if the joint axis was fixed so that equations for noncentroidal rotation could be applied. In constructing a laboratory testing device emphasis was placed in providing an appropriate drag moment.

DESCRIPTION OF APPARATUS

The apparatus was designed to provide a resistance moment proportional to the square of the angular velocity. A rotary torque actuator (Roto Actuator, Model S-4-4) with a lever arm attached to one end of the axle was used to provide a hydraulic resistance (Fig. 2). Rotation of the axle caused a vane within the actuator to produce a flow of hydraulic fluid which was directed past a stator via a bi-directional valve. The flow of hydraulic fluid through the constriction as caused by moving the lever arm can be shown, by application of the momentum equation, to produce a resistance force proportional to the square of the angular velocity. Preliminary tests were conducted to select an appropriate valve setting. A comparison was made with normalized displacement

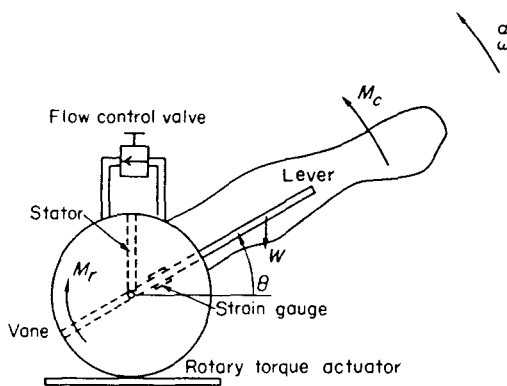


Fig. 2. Schematic of the apparatus.

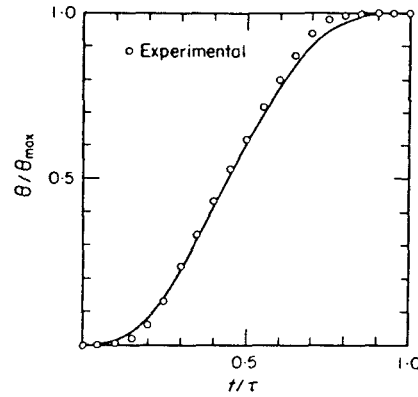


Fig. 3. Experimental and theoretical (Seireg *et al.*, 1971) normalized displacement/time curves.

time curves calculated by Baz (1970) from tests on an underwater model of the arm. These results are shown in Fig. 3. Except for buoyancy effects and the increased mass and inertia due to the lever arm, the hydraulic actuator simulated the resistance to motion of a swimmer's arm in water as demonstrated by Baz (Jensen and Bellow, 1973).

The bending strain produced by the subject's arm on the lever handle was measured directly by means of a pair of strain gauges mounted near the axle. Force calibration consisted of suspending known weights from the handle. Angular displacement was measured by a linear voltage differential transformer (LVDT) activated by a cord attached to the axle. The linear range of the transducer was calibrated by using a large protractor. Instrument precision was evaluated and the variance over a 24 hr trial was effectively zero.

The bending strain and displacement signals were amplified, monitored on an *XY* recorder, and recorded on magnetic tape.

DATA ANALYSIS

When the body segment of the subject is attached to the lever arm it can be idealized as in Fig. 2. The resulting equilibrium equation for non-centroidal rotation of a rigid body about a fixed axis is

$$M_c = M_r + (W_l r_l + W_s r_s) \cos \theta + (I_l + I_s) \alpha \quad (9)$$

where the terms on the r.h.s. are the resistance moment due to the torque actuator, the moment due to the weight of the lever, the moment due to the weight of the segment, and the inertia of the lever and the inertia of the segment about the axis of rotation.

The principle of impulse and momentum was used to examine the relationship between the contraction moment (M_c) and the angular momentum for the segment. The impulse for the contraction moment was

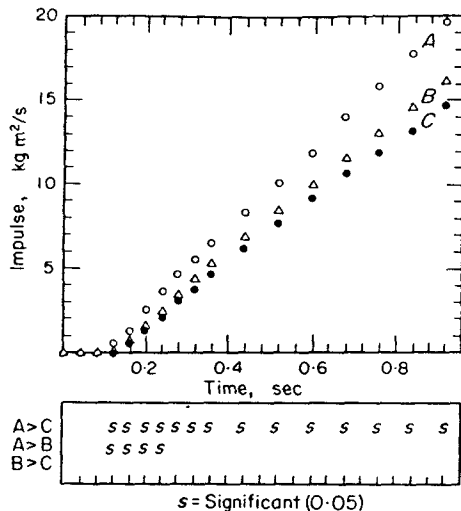


Fig. 8. Shoulder extension impulse curves for the three untrained subgroups.

swimmers, the experimental group, then trained three times per week for six weeks and the remaining swimmers, the control group, did not train. Prior to the training period a session was conducted to familiarize the subjects with the tests. Testing session 1 (E1, C1) was held three weeks and testing session 2 (E2, C2), six weeks after the start of training, giving an inter-test training period of three weeks.

RESULTS AND DISCUSSION

The results of the experiment are presented in Figs. 4 through 11. The form of the contraction moment curves is evident from Fig. 4, an elbow extension, and Fig. 5, a shoulder extension. The curves tended to be similar in magnitude and demonstrated a rapid

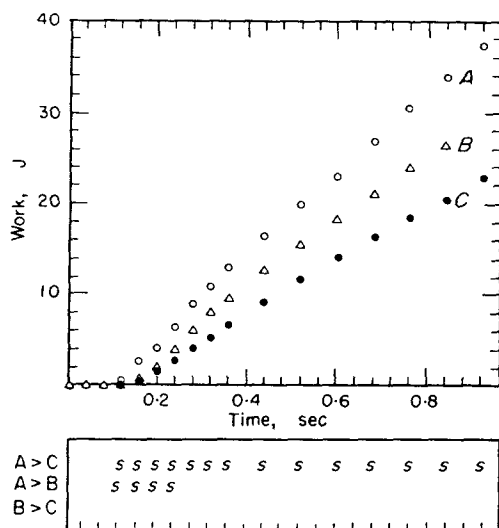


Fig. 9. Shoulder extension work output curves for the three untrained subgroups.

rise to an initial peak followed by a period of sustained force.

The performance curves for each of the six subgroups consisted of the mean of the individual impulse curves and work output curves ($n = 7$). Comparisons were made using a "t" test and a probability level of 0.05, to see if the curves for the experimental group were significantly affected by the training. The curves for the higher (A) and lower (C) level swimmers were not significantly affected, but the shoulder extension curves for the medium (B) level swimmers showed an increase with training (Figs. 6 and 7). Four of the data points for both impulse and work output were significantly greater on the second testing day (E2) than on the first day (E1). The differences for the control subgroup (C2 vs C1) were nonsignificant. These results indicate that swimming training can affect the work output and the momentum for the initial segment of the shoulder extension movement. The changes could be due to the swimmers in the B subgroup having reasonable swimming skills but having had little previous practice in swimming. It is possible that with a more extensive period of intensive training the changes would be more pronounced.

The relationships between the level of swimming ability and the performance curves were examined by evaluating the differences between subgroups. The results of the second testing session for the control group were used in order to ensure that the differences were not due to the training program. In each case the curve for the A subgroup was significantly greater than for the C subgroup (Figs. 8–11). Thus the higher level swimmers were more capable of producing work and momentum for shoulder extension and elbow extension, than were the lower level swimmers. This could account for the difference in swimming ability. Differences between the other curves were not as pronounced. The initial four data points of the A subgroup curves for shoulder extension were significantly greater than the B subgroup curves (Figs. 8 and 9). It is of interest that it was this segment of the curve which changed as a result of training (Figs. 6 and 7). Elbow extension work output for the B swimmers tended to be greater than for the C swimmers (Fig. 11). All other differences were nonsignificant at the 0.05 level. Although power was not calculated it can be seen from the figures that the slopes of the work output curves were different. It is evident from these results that there is a relationship between the level of swimming ability and contraction moments for the upper extremity. The biomechanical relationship is in all probability due to firstly, the capacity of the swimmer to develop the angular momentum for the segments and thus the required hydrodynamic forces, and secondly, the capacity to produce work and power using the contraction moments for shoulder extension and elbow extension.

These results are limited by the experimental procedures used and the nature of the sample. Further

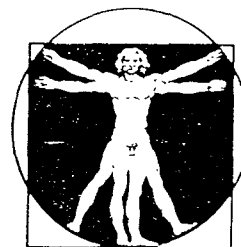
M_r	apparatus resistance moment	r	radius to center of gravity
M_w	weight moment	r_b	radius to center of buoyancy
R	proximal axis resultant force	s	segment
V	velocity	t	time
W	segment weight	α	angular acceleration
W_{1-2}	work	ω	angular velocity
a	acceleration of the centroid	θ	angular displacement
d	segment length	ρ	density
l	lever arm	ν	kinematic viscosity
m	segment mass		

SCIENCE IN SPORTS

A DYNAMIC MODEL FOR THE GOLF SWING

David R. Budney
University of Newcastle
Australia

Donald G. Bellow
University of Alberta
Edmonton, Alberta



ICSS

The evolution of the golf swing is continually influenced by the availability of modern materials for golf balls and clubs, increased understanding of the mechanics of the golf swing, improved knowledge of the required physical and mental preparation for the game, and a general increase in interest in achieving the ultimate in performance. The modern golf swing is probably more powerful and accurate than it has ever been. Despite this progress the precise manner in which the golfer uses his energy to develop club head speed is not well understood. The anatomy of the golfer includes muscles of various sizes and types throughout his body, many of which must be involved in the golf swing to some extent and some of which are called upon for more strenuous exertion. A panel of "experts" (Dickson, Jacobs, et al., 1977) discussed the primary source of power noting that wrist action, arm swinging motion or leg action are believed to be the main power source. Without performing relevant experiments, Cochrane and Stobbs (1968) concluded that all of these muscle groups, as well as the back and shoulders, are called upon to contribute to the power applied in the golf swing.

In a previous attempt (Williams, 1967) at modelling the golf swing, the club was considered as a point mass system and it was assumed that the torque applied through the hands of the golfer was zero. In another analysis (Jorgensen, 1970) the torque applied by the golfer's body to the arm was assumed to be constant throughout the swing. Lampsa (1975) attempted to optimize the exertion of the golfer to attain increased club head speed. Unfortunately, the prescribed golf swing which resulted was not discussed in relation to the methods of the best competing golfers; nor was there any attempt to relate the prescribed swing method to human physical abilities or limitations.

Differences of opinion with respect to certain instructional points exist amongst golf teachers. For instance, Cochrane and Stobbs

ACADEMIC PUBLISHERS

Del Mar

(1968) stated that a deliberate delayed wrist action (in relation to body movement) is necessary for a powerful golf swing while Nicklaus (1974) stated that it is impossible to apply wrist action too early in the swing if body mechanics are properly applied from the beginning.

The purpose of this paper was to develop a mathematical model based on real golf swings and to use this model to analyze various aspects of the swing such as power sources and application of forces. With reference to the model, many points commonly found in golf instruction were discussed. Because the results from only one golfer's swing would necessarily restrict the conclusions that could be made, golfers of different levels of ability were employed as subjects for this investigation. For each golf swing, the power associated with arm swing motion and wrist rotation were continuously plotted and compared. Similarly, the final energy of the golf club was proportionally attributed to two separate sources: wrist power and arm power. The manner of energy transfer from the golfer to the club was shown to be different for the professional golfer from the amateur golfer. The concept of the delayed wrist action was examined and discussed. Some unexpected benefits from the model were obtained due to the ability of the model to detect loss of energy or negative work by the golfer.

MATHEMATICAL MODEL

The mathematical model used to describe the dynamic characteristics of a golf swing was based on the free body diagram shown in Figure 1 which considers that the arms and golf club act in the same plane. It

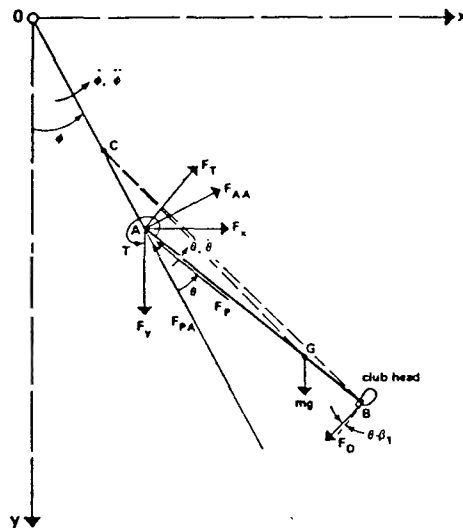


Figure 1. Mathematical model of a golf swing.

was assumed that the forces exerted by the hands can be resolved into two components (F_x and F_y) and a torque (T). F_D represents the drag force which was taken proportionally to the square of the club head velocity. The photographs of this investigation, as those of other investigations (Cochran and Stobbs, 1968; Williams, 1967; Jorgensen, 1970; Lamps, 1975) demonstrated that the hands travel in a plane circular path permitting the two arm pendulum model to be used. The center of the hands applied to the club A travelled about the center of rotation O, such that OA is of constant length for all values of ϕ . The position of A relative to O was determined by the angle ϕ and the distance \overline{OA} where point O occurred approximately in the vicinity of the golfer's neck. The angle the club made with the line segment \overline{OA} is θ . Thus, the angular velocity of the club at any instant of time was given by the first derivative of the angular position, or $(\dot{\phi} + \dot{\theta})$ and the angular acceleration was given by $(\ddot{\phi} + \ddot{\theta})$. The following analysis treated the golf club as a rigid body and assumed shaft flexibility to be negligible.

The distance from point A to the center of gravity of the golf club G was denoted by " l ". Thus, the coordinates of G for any instant of time could be written as:

$$\begin{aligned} x &= a \sin \phi + l \cos(\phi + \theta) \\ y &= a \cos \phi + l \sin(\phi + \theta) \end{aligned} \quad (1)$$

These equations can be differentiated to obtain the appropriate velocities and accelerations in the x and y directions respectively. Similar expressions describing the motion of the club head can be obtained by replacing " l " with " b " in Equation 1.

The governing equations of motion for the golf swing were obtained by applying force and moment equilibrium to the system shown in Figure 1. Because the swing plane was different from the vertical plane by an angle α , only the in-plane component of the weight, or $(mg \cos \alpha)$, applied to these equations. Thus, for force equilibrium

$$\begin{aligned} F_x - F_D \cos(\phi + \beta_1) &= m\ddot{x} \\ F_y + mg \cos \alpha + F_D \sin(\phi + \beta_1) &= m\ddot{y} \end{aligned} \quad (2)$$

where β_1 was the angle that the line connecting the instantaneous center (I.C.) with the club end (B) made with \overline{OA} . F_D was the force due to aerodynamic drag and acted in opposition to the direction of velocity at that point. It was assumed the drag of the golf shaft was negligible compared with that of the club head.

Moment equilibrium, taken about the center of gravity (G), was given by:

$$T - F_T l - F_D (b - l) \cos(\theta + \beta_1) = I_G (\ddot{\phi} + \ddot{\theta}) \quad (3)$$

where I_G was the moment of inertia about the center of mass. The forces F_x and F_y caused by the hands were resolved into components along the shaft F_p , and perpendicular to the shaft F_T . That is,

$$F_T = F_x \cos(\phi+\theta) - F_y \sin(\phi+\theta)$$

$$F_p = -F_x \sin(\phi+\theta) - F_y \cos(\phi+\theta)$$

If ω was defined as the angular velocity of the club, " r_c " as the distance from C to G, and " c " the distance from I.C. to A, as shown in Figure 1, then from kinematic considerations it followed that

$$\omega = \dot{\phi} + \dot{\theta} = \frac{V_A}{c} = \frac{V_G}{r_c} = \frac{V_{G/A}}{l}$$

where $V_{G/A}$, the velocity of G with respect to A, was given as

$$V_{G/A} = l(\dot{\phi} + \dot{\theta})$$

Since $V_A = a$, it followed from the above that

$$c = a \left\{ \frac{\dot{\phi}}{\dot{\phi} + \dot{\theta}} \right\} \quad (4)$$

The drag force F_D was expressed as:

$$F_D = C_D V^2$$

where $C_D = CA$.

C was the drag coefficient and A was the frontal area of the club head. The velocity V at the club head was given by:

$$V = r_b \omega$$

and

$$r_b^2 = c^2 + b^2 + 2bc \cos\theta \quad (5)$$

or

$$F_D = C_D(\dot{\phi} + \dot{\theta})^2 (c^2 + b^2 + 2bc \cos\theta)$$

When equation 5 was substituted into equations 2 and 3 and with the use of the equations in 1, a complete dynamic analysis was obtained with knowledge of the relationship of ϕ and θ for any instant of time.

The energy developed in swinging a golf club resulted from the work done by the hands in providing translational motion to the grip plus the work done by the hands in rotating the club. This analysis did not include the work done by the golfer in accelerating his own body

members nor did it take into account the contribution of the golfer's legs and body toward imparting momentum to the hands. Neither the feet nor the body made any contact with the golf club; it was only through the hands that the necessary forces were applied to the club to propel it through its intended path of motion. When the golfer shifted weight from one foot to the other or if he twisted his body, work had to be expended in order to accomplish this. While this weight transfer served the purpose of providing forward body momentum to compound the effort of the arms and hands in swinging the golf club, the fact remained that the hands were the only part of the golfer's body applying forces to the golf club.

An extension to this research would be to evaluate the total mechanics of the body motion in order to determine the total work done by a golfer in swinging a club. If such were done, it would then be possible to quantify the effects of weight shift in the feet, body motion, as well as arm power and wrist power.

Work was defined as force times distance. The work done by the hands was the force component F_{AA} , perpendicular to the arms, multiplied by the distance travelled in the direction of this force; plus the torque T multiplied by the angle through which the hands rotated the club. That is,

$$W = (F_{AA} a + T \int d\phi + T) d\theta \quad (6)$$

The first term in equation 6 was thought of as the work done by the "arms"; the second term the work done by the "wrists".

Power was the rate of work done for any instant of time; thus it followed from equation 6 that

$$P = F_{AA}(a\dot{\phi}) + T(\dot{\phi} + \dot{\theta}) \quad (7)$$

EXPERIMENTAL ANALYSIS

In order to apply equations 1 to 7 to the swing of the golfer it was necessary to obtain displacement-time data for a typical swing. This was accomplished by having a golfer hit a ball in a laboratory test facility. The paths of the arms and the club were photographically recorded using a single exposure and a stroboscopic light source which flashed at 100 Hz throughout the duration of the swing. The camera position was on a line through the hub of the swing (point O) perpendicular to the swing plane. A general view of the test facility is shown in Figure 2 and a typical photograph of test data is shown in Figure 3.

As the time intervals in Figure 3 were fixed and known for any position of the golf swing, it was a simple task to obtain the angle of the arms ϕ and the angle of the club relative to the arms θ as a function of time. For a typical golf swing, these data were plotted



Figure 2. Experimental test facility.

as curves in Figure 4. Since it was intended to solve equations 1 to 7 for a variety of golfers using drivers as well as irons, a program was written for a computer to solve these equations directly from given ϕ , θ , t data. Thus, a first step was to obtain equations for ϕ and θ as functions of time. That is, best fit equations had to be found for the curves typically shown in Figure 4. It was determined that a reasonable fit could be obtained if a fourth order polynomial was used of the form

$$x = a_0 + a_1t + a_2t^2 + a_3t^3 + a_4t^4$$

where the coefficients of a_1t , etc., were determined using a Chebyshev polynomial for discrete intervals. The "goodness of fit" was judged from Figure 4 where some representative points, calculated from the polynomials, are shown. Once the equations for ϕ and θ were obtained, the

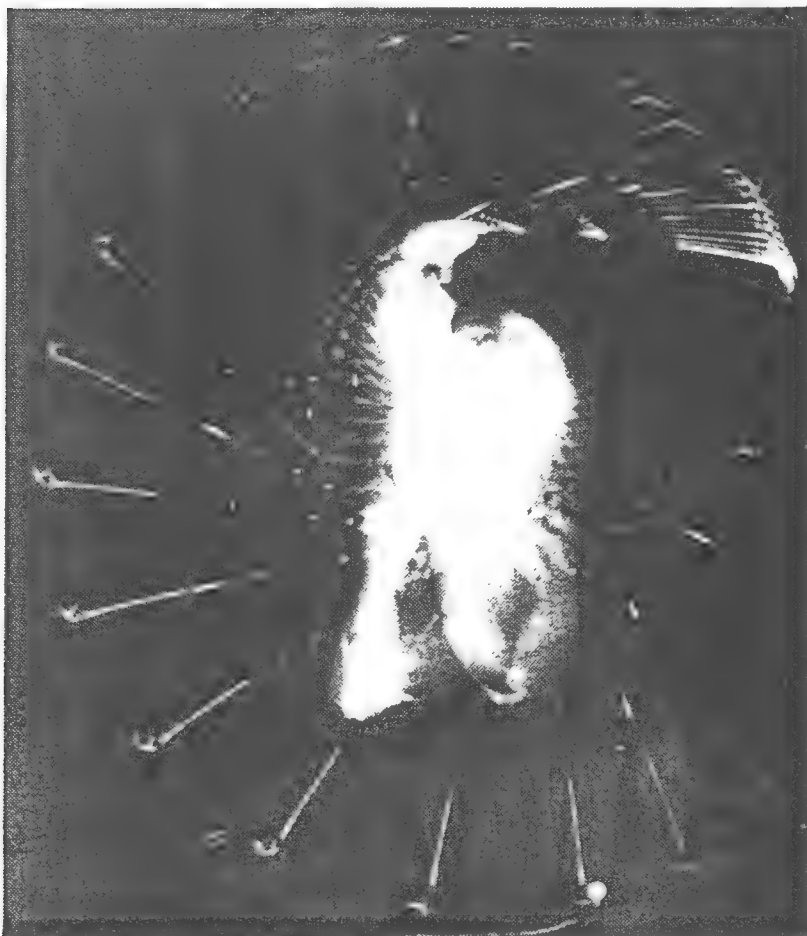


Figure 3. Photographic data of golf swing.

velocities and accelerations were calculated by differentiation. From the swing plane data shown in Figure 3, the dimension "a" and total time for the swing was measured. The dimensions "b" and "c" were measured from the golf club. The period of oscillation of the golf club, when suspended at the end of the grip, was measured. This enabled the moment of inertia of the club about its center of gravity to be calculated.

RESULTS

It was determined that a distinct benefit of a mathematical model is that every possible relevant parameter can be calculated and graphed (in this case by computer) for consideration by the analyst. To

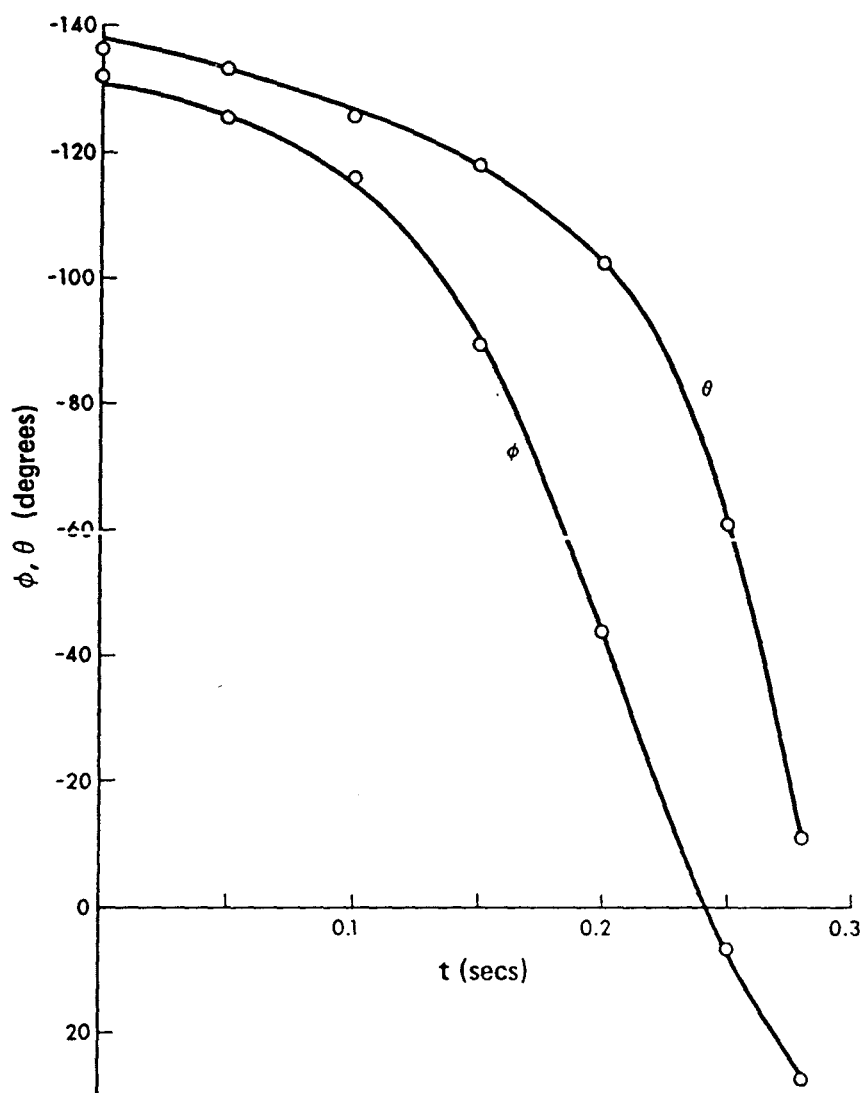


Figure 4. Golf swing data, ϕ and θ , for one golfer.

illustrate the method, two of these parameters are presented. The calculations have been classified as follows:

Golf Swing Dynamics

1. Detailed results for a golf swing.
2. Comparison of golfers.

Detailed results for a golf swing - The subject for this part of the analysis was a golf professional using a "MacGregor" driver with a "True Temper Dynamic" stiff shaft.

In Figure 5, the various forces applied by this golfer to the club were shown as functions of time where the start of the downswing

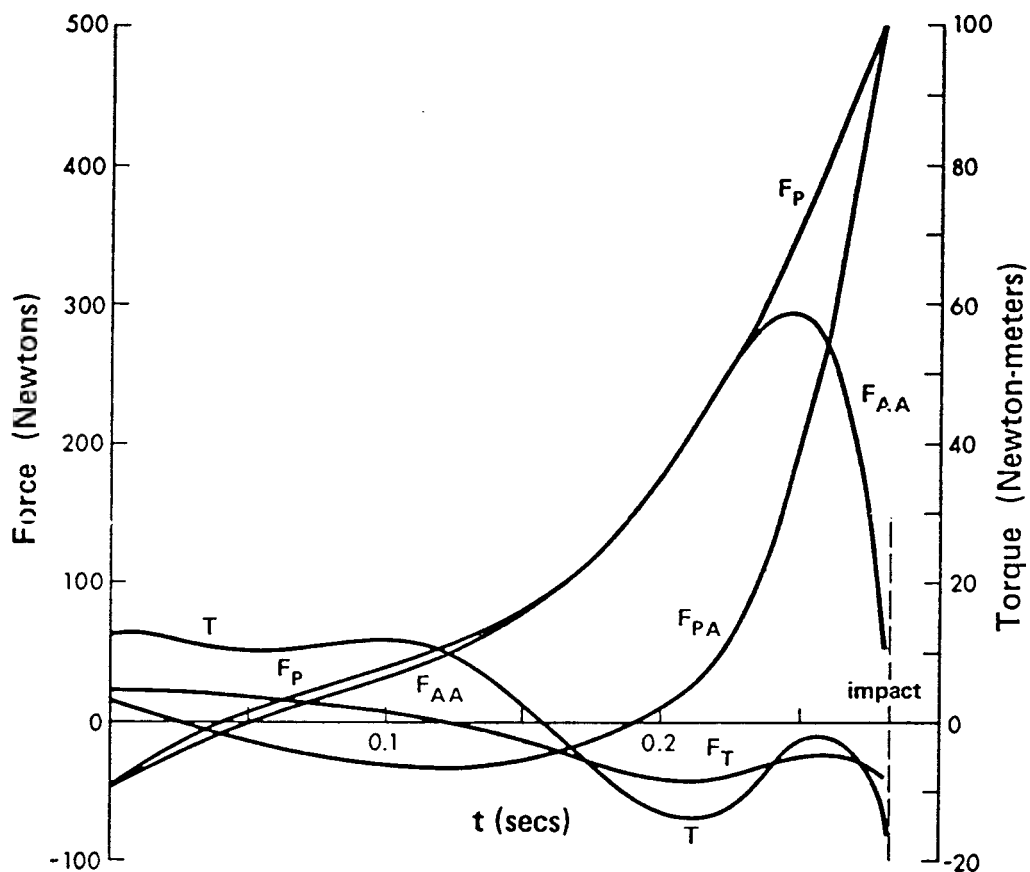


Figure 5. Forces applied by one golfer.

was on the left and impact with the ball occurred on the right side of the graph. The forces were shown as components parallel to and transverse to the golf club (F_p and F_T). An alternative resolution of the same forces can be made in terms of components toward the hub of the swing O and transverse to the "arm" OA (Figure 1). These were referred to as the forces parallel (F_{PA}) and transverse (F_{AA}) to the arm respectively, although the directions did not quite coincide with the arm orientation. The value of the torque T applied by the hands was also shown in Figure 5.

The generalized forces that accelerated the club head toward the ball were the force F_{AA} and the torque T (Figure 1). F_{PA} is the centrifugal force and does no work. In figure 5, it was shown that the subject golfer achieved a maximum force of 295 N (66 lb) at 0.035 seconds prior to impact and that this force was applied as an impulse over the last third (approximately 0.08 sec) of the swing duration before impact. Figure 5 also demonstrated that this golfer applied a positive torque by his hands at the beginning of the swing and that this torque became negative toward impact, reaching a value of -14 Nm at impact. This result implied that the golfer was retarding the acceleration of the downswing by hand action while he was positively accelerating the club by swinging his arms. The early part of this delayed uncocking may have been deliberate and beneficial according to some instructors, but toward impact this retarding action was not desirable. Fortunately for this golfer, the amount of energy lost through this retardation had only minimal negative effects on the energy developed through the arm swinging motion. There were two possible explanations for the negative torque applied by the hands. First, the angular velocity of the golf club at impact was 44.3 rad/sec (7.05 rev/sec) and the angular velocity of the club relative to the arm was 36.6 rad/sec (5.82 rev/sec); an angular velocity that could have been taxing the golfer beyond his ability even though it was applied over a short duration in time. In other words, the golfer may well have generated an angular speed for his golf club that his hands could not follow, or at least could not continue to apply a positive torque while following. The golfer's mechanics at this stage are usually described as the release which is the rolling of the right hand over the left hand.

Second, although not necessarily separate, the position of the hands tended to be higher or more in line with the golfer's shoulder and club head at impact than it was at address. This alignment was brought about by the centrifugal force of the golf club. The impact position required the golfer to be "pointing" the club lower with respect to the arms than found comfortable at the address position. Because of the inability of the wrists to conform to the straight line configuration that the centrifugal force tended to develop, the hands applied a torque tending to lift the club and causing the shaft to bend. A photograph of the golf club at impact taken from the golfer's side demonstrated this curvature. It is not difficult to imagine that prior to impact, as this torque was developing, a component of it retards the in-plane angular acceleration of the golf club. This point, as well as the effects of

shaft flexibility, are discussed more extensively in another paper presented by the authors where experiments showed the existence of such a couple.

The centrifugal force F_{pA} was the component of force perpendicular to the circumferential force F_{AA} . Figure 5 showed that F_{pA} was relatively small for much of the swing duration but increased rapidly just prior to impact, showing a value at impact of 500 N (112 lb) and apparently reaching its maximum after impact. As stated earlier, the angular velocity of the club itself at impact was 44.3 rad/sec or 7.05 rev/sec, a speed requiring substantial hand mobility. At this moment the tendons at the wrist were also required to exert grip pressure substantial enough to withstand a centrifugal force of 500 N. It is well known (Cochran and Stobbs, 1968) that the mobility and effort required of the wrists at this point in the swing are conflicting requirements.

The force applied to the golf grip was also shown in Figure 5 as components parallel to, F_p , and transverse to, F_T , the club. The force transverse to the club was always small compared with the other forces shown indicating that the total force was applied nearly parallel to the shaft.

The golfer's power (rate at which the golfer increases the total energy of the golf club) is shown in Figure 6. The total power consists

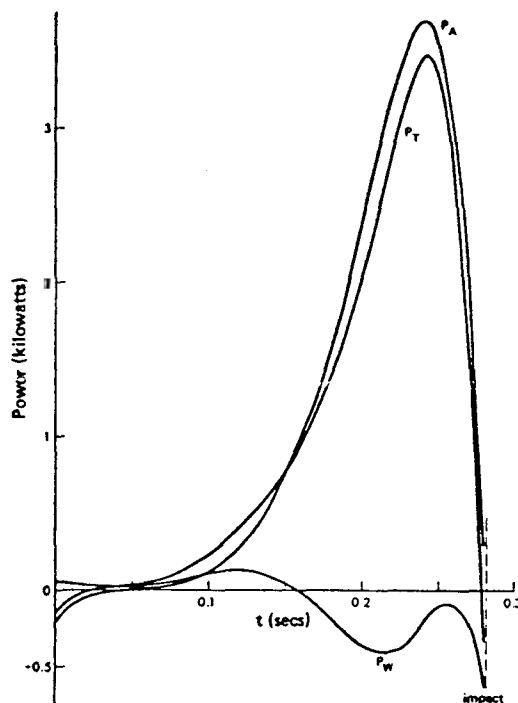


Figure 6. Power applied by one golfer.

of the arm swing power and wrist power as stated in equation 7. Both power components, as well as the total power, were obviously small for the first half of the golf swing. It was also apparent that the total power was applied in the form of an impulse over the last half of the swing. The maximum arm power developed was 3.6 kw (4.8 Hp) at approximately 0.04 seconds prior to impact and decreasing rapidly from that time. The wrist power was positive for most of the swing but became negative toward impact. Figures 5 and 6 demonstrate that the wrists retarded the acceleration of the golf club briefly before impact.

The power developed by the golfer serves to increase the total kinetic energy of the golf club of which the kinetic energy of the club head is only a part. Figure 7 represents, as functions of time, the

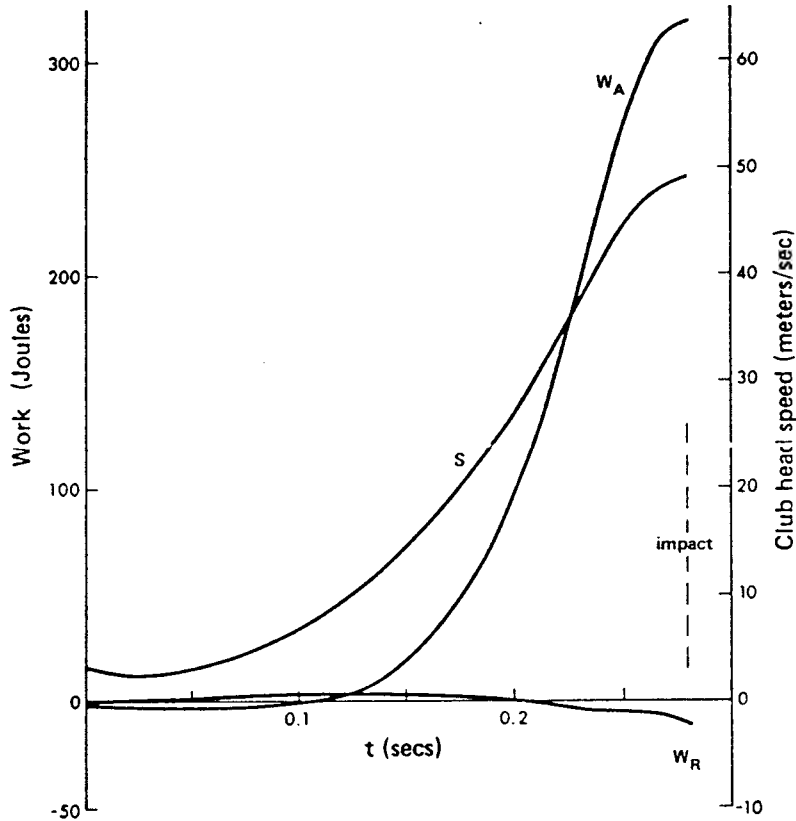


Figure 7. Club head speed and work done by one golfer.

Golf Swing Dynamics

total work done by the golfer and the club head speed. Additionally, the work done by each contributing generalized force was plotted. Again, the shape of the arm swing graph was very similar in shape to the total work curve, since the final energy of the club head arose mostly from arm swing motion. The wrists were "working" early in the swing but were shown to be contributing negatively for the last 0.075 second.

In this case, the total energy of the golf club consisted of 310 Joules arising from arm swing and -10 Joules due to wrist work. Clearly the arm swinging motion was most responsible for developing club head speed. As expected, the rate of increase of club head speed decreased rapidly toward impact as the work rate decreased.

Comparison of golfers - Each golfer demonstrated characteristics in his swing that were unique to himself. Figures 8 and 9 demonstrate

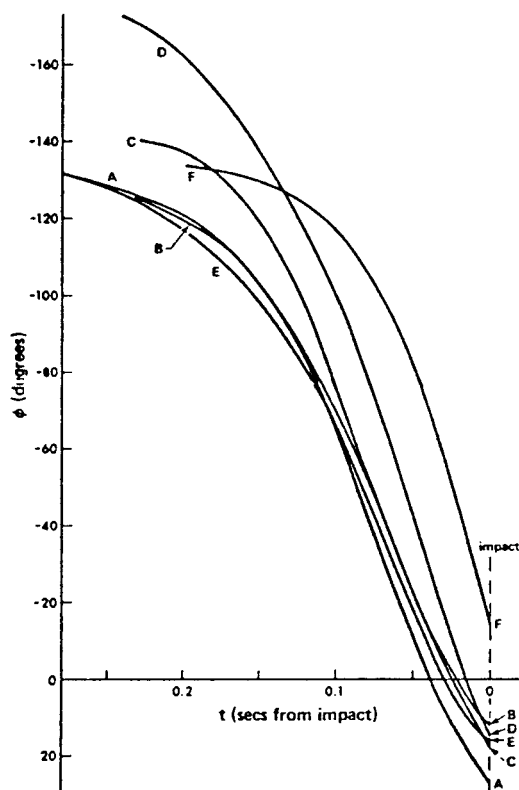


Figure 8. Variations in ϕ for different golfers.

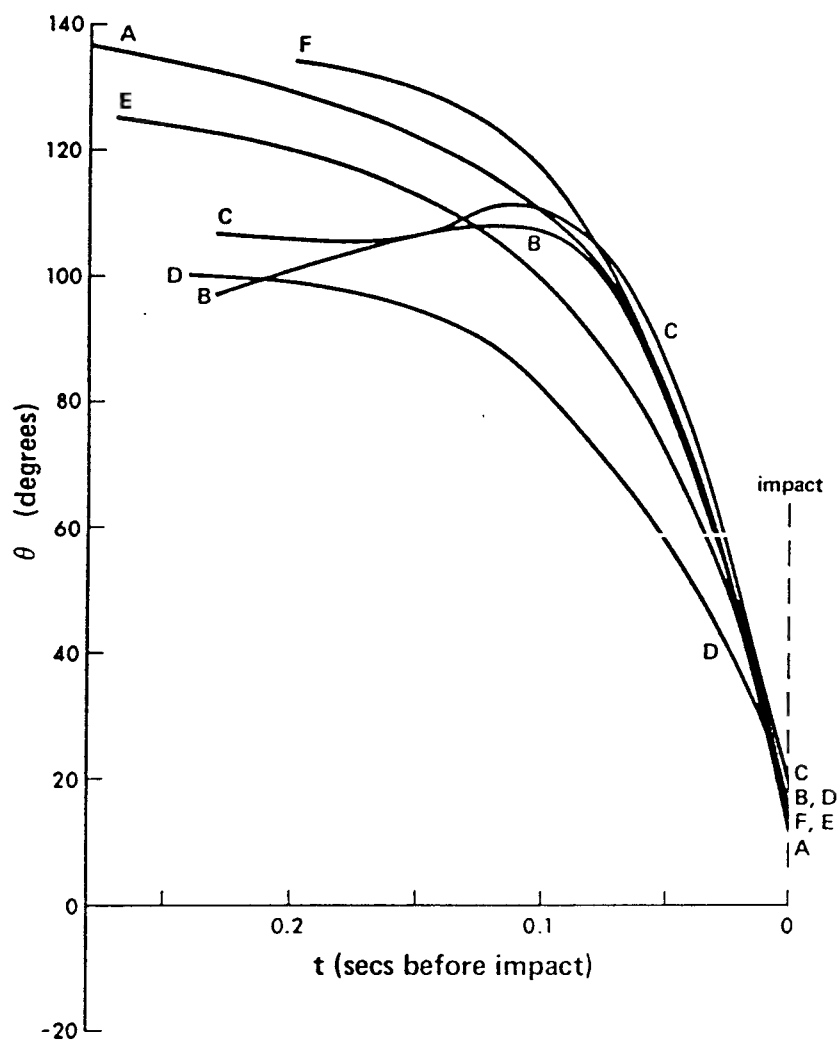


Figure 9. Variations in θ for different golfers.

ϕ and θ variations with time for some golfers whose abilities were described in Table I. The subjects consisted of three professional golfers and three amateurs of varying abilities. Swing durations, total length of backswing (initial angles) and the general shape of each curve was different for each golfer. Another aspect that differed from golfer to

golfer was the slope of the ϕ curve (angular velocity of the arm) toward impact.

TABLE 1
GOLF SWING SUBJECTS

Code	Description	Club Head Speed at Impact (m/s)	Torque at Impact (Nm)	Work done by Arm Swing (Joules)	Wrist Work (Joules)	Total Work (Joules)
A	Golf Professional	49.2	-14.1	310.1	-10.3	299.8
B	Professional B.J. Hunt (Ref. 2)	44.5	-15.1	233.9	9.3	243.2
C	Professional G. Wolstenholms (Ref. 2)	42.7	-45.9	244.3	-23.5	220.8
D	13 Handicap Golfer	48.9	10.4	273.5	11.0	284.5
E	Non-Golfer	43.2	10.1	195.4	18.1	213.5
F	Female Golfer	42.8	41.0	178.3	37.3	215.6

The total work done by each golfer as well as the portions of work done by each generalized force are quoted in Table 1. Comparing the last three columns, it is evident that the work done by the arm swinging motion accounted for most of the work done. It was also apparent that the wrist torque contribution to total work was sometimes useful; and for some golfers, this work was negative, preventing the total benefit of arm swing work from being realized. Related to this problem, the calculated value of torque at impact is shown in Table 1. Golfers A and C are shown to do net negative work by wrist torque.

Comparing arm swing power of the various subjects (Figure 10) it

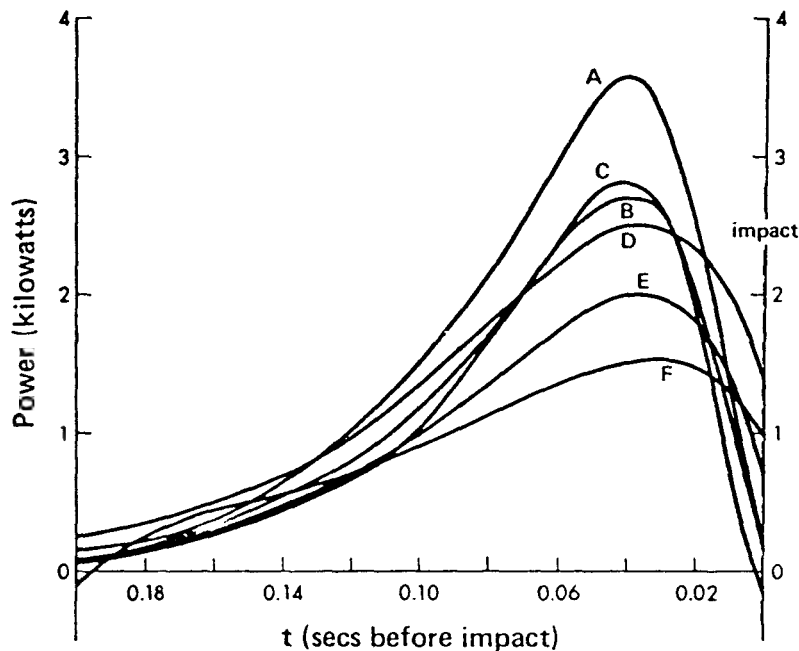


Figure 10. Variations in arm swing power for different golfers.

was evident that the professionals, particularly A and C, developed greater peak power in this fashion than did the amateur golfers, particularly E and F. The overall shape of these power curves indicated that the professional golfers applied power in the form of an impulse that was greater in magnitude but of shorter duration than for the amateur golfer. This suggested that the more competent golfer takes advantage of physical ability to apply maximum effort for only a short time. It would be of interest to make similar comparisons of golfers representing a variety of abilities but who have similar physical characteristics such as age and muscular development. Golfer C was determined to achieve maximum club head speed of 43.4 m/s prior to impact which reduced to 42.7 m/s at impact. All other subjects achieved maximum club head speed

at impact.

CONCLUSIONS

By solving the equations of motion for the golf club at positions starting from the top of the backswing until impact, the golfer's exertion parameters such as forces, torque and power, were determined. It was shown that for all subjects, arm swing motion was responsible for most of the energy imparted to the golf club. It was also shown that wrist torque was less a factor but varied considerably from golfer to golfer. This result agreed with the teaching of a well known golf professional (Dickinson, Jacobs, et al., 1977) who stated that arm swing motion was the most important factor for power development in the golf swing but that all other sources must be well coordinated to add to this power.

The qualitative variation of wrist torque contribution between golfers was attributed to the considerable angular velocity of the shaft at impact. The hands of the golfer must be capable of applying a positive torque at high speed toward impact or they may easily tend to decelerate the club head. Calculations showed that the centrifugal force at impact reached 500 N (112 lb) at exactly the moment when wrist mobility was required. The need for tightened wrist tendons at impact may have been responsible as well for the development of negative torque. Another factor responsible for negative wrist torque was the requirement that the wrists uncock at impact so the alignment of the arm and club are straighter than at address.

Contrary to the opinions expressed by some, it was shown that wrist torque is not zero throughout the swing. Delayed wrist uncocking, sometimes stated as a desirable feature of a powerful golf swing, was shown to be unnecessary. It was also shown that most subjects did not achieve maximum club head speed prior to impact.

The mathematical model of the swing has been shown to be useful in providing more insight into the golf swing as well as verifying some instruction points hitherto based on feel rather than analysis.

The authors express appreciation to the National Research Council of Canada for the financial support provided under the auspices of Grant no. A-2705. Thanks are also expressed to golf professionals Messrs. G. McHattie and A. Olynyk for their participation and helpful comments.

REFERENCES

- Cochran, A. and J. Stobbs. "The Search for the Perfect Swing".
Heinemann Press, 1968.

Budney and Bellow

- Dickinson, G., J. Jacobs, et al. "Power Comes from the Legs Right? Wrong". Golf Magazine, Vol. 19, No. 9, Sept. 1977, 39-42.
- Jorgensen, T. Jr. "On the Dynamics of the Swing of a Golf Club". American Journal of Physics, Vol. 38, 5:644-651, May 1970.
- Lamps, M.A. "Maximizing Distance of the Golf Drive: An Optimal Control Study". Journal of Dynamic Systems, Measurement and Control, Trans. A.S.M.E., Vol. 97, 4:362-367, Series G, 1975.
- Nicklaus, J. "Golf My Way". 1974. Heinemann Press.
- Williams, D. "The Dynamics of the Golf Swing". Quarterly Journal of Mechanics and Applied Mathematics, Vol. XX, Pt. 2:247-264, 1967.

TEACHING AIDS FOR GOLFERS

David R. Budney
University of Newcastle
Australia

Donald G. Bellow
University of Alberta
Edmonton, Alberta

Although the golf swing has improved over the years, the methods employed by golf instructors are generally unchanged. Observation of the student by the instructor provides the basis for discussion of the fundamentals of the golf swing. The success of such a relationship between students and teachers cannot be doubted as this method of instruction has endured.

Although most features of the student golfer's swing are apparent to the instructor through observation, certain swing faults are not easily detected. Other aspects are difficult to communicate since the "feel" of an alteration to the swing mechanics is subjective. The purpose of this paper was to demonstrate that instrumentation techniques and photographic arrangements can provide useful information during a golf lesson. The measurements dealt with in this paper relate to grip pressure, shaft bending and photographic recording of club head trajectory. The results were available immediately following the swing and serve to quantify various parameters that are otherwise subjective or difficult to detect.

Grip pressure measurement - Immediately prior to impact, the golfer is required to demonstrate sufficient wrist mobility so as not to impede rapid uncocking of the wrists. At the same time, it is necessary that the grip pressure exerted by the golfer be sufficient to withstand a centrifugal force of the order of 450 Newtons (100 lb) (Budney and Bellow, 1978). Grip pressure is developed by activating the muscles in the lower arms through the tendons in the wrists. Consequently, increasing the grip pressure decreases the mobility of wrist activity (Cochran and Stobbs, 1968). These conflicting requirements of wrist behavior near impact demonstrate that the grip pressure applied by the golfer is an important factor which contributes to a successful golf swing.

Prominent golfers and golf instructors (Watson, 1978; Toski and Flock, 1978) agree that the last three fingers of the left hand should have the most significant pressure application to the grip of the golf club. These experts also advise that right hand grip pressure should be much less and should remain constant during the swing. It has been advocated (Toski and Flick, 1978) that there be no pressure at all in the right thumb and forefinger. Since grip pressure is not quantified, interpretation of these statements is highly subjective.

During the course of a golf lesson, the instructor normally detects insufficient grip pressure in the last three fingers of the left hand by noticing that the palm separates from the grip of the club. Excessive grip pressure is demonstrated by muscle tension in the arms and a lack of smoothness in the swing. However, the duration of the swing from address to impact is less than one second and the duration of the downswing is only about one quarter of a second. Hence the visual observation of symptoms of problems related to grip pressure is a challenging task for the instructor. It is difficult to convey the "feel" of correct grip pressure; what may be moderate grip pressure to the instructor may feel light to the golfer. Anatomical differences could further complicate such difficulties.

Vossler (1978) states that the right hand supplies the power whereas the left hand squares (aligns) the club. Cochrane and Stobbs (1968) state that, for a right-handed golfer, the entire swing is controlled by the left hand with the right merely reinforcing the left hand's efforts.

One objective of this paper was to show, with the use of an instrumented golf club, how grip pressure measurements can be effectively employed by a golf instructor to quantify and discuss the effects of grip pressure on the control of the golf swing.

Shaft bending - Another aspect of the golf swing considered here was the amount of shaft bending that occurs prior to and during impact. Shaft bending has been attributed by some (Budney and Bellow, 1978; Lampsa, 1975) to the application of a negative torque and is demonstrated by the curvature of the golf club in Figure 1. Negative torque is counter-productive with respect to the intent of the golfer to accelerate the head of the golf club. The extent to which torque is employed to deliberately accelerate the club head is a debated point among golf teachers (Dickinson, Jacobs et al., 1977). It has been said that the torque applied by the hands is negligible (Williams, 1967). This paper discusses a method which has been successfully employed to monitor bending of the shaft in order to determine the torque applied by the hands and its influence on the golf swing.

Club head trajectory photographs - The use of video recorders for instruction has proved to be invaluable. The immediate replay of the golf swing enables the instructor to discuss points being made about the swing. One important factor of the swing that is missed by videotape, is the path of the club head through the impact zone. The club

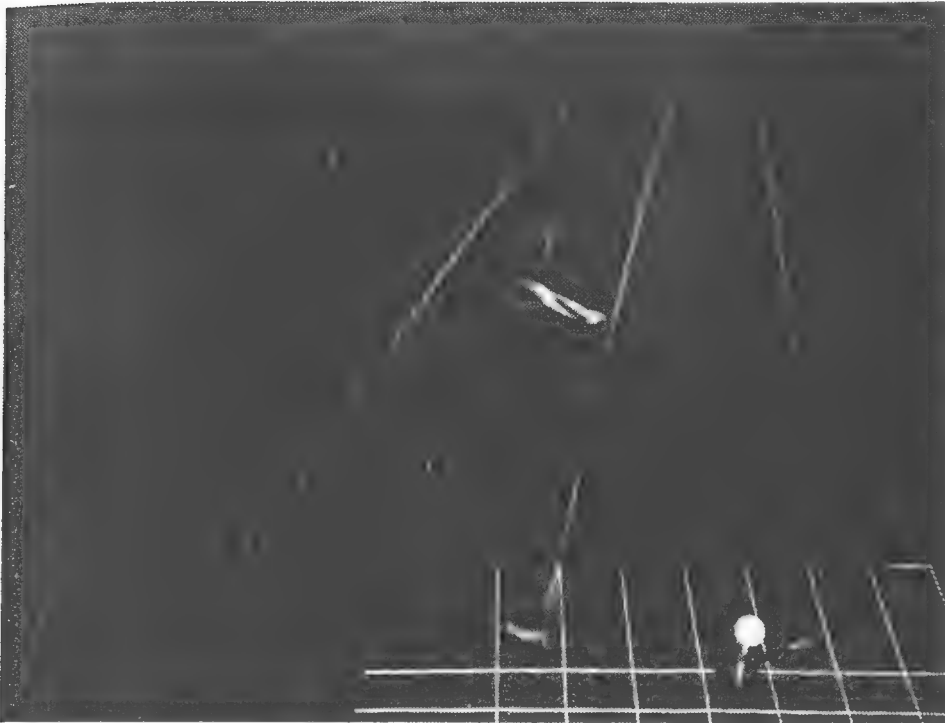
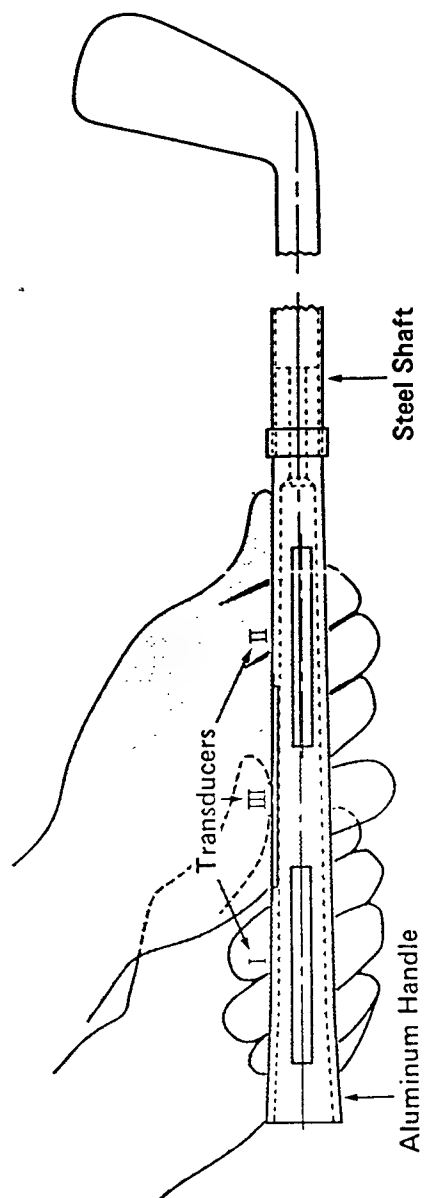


Figure 1. Illustration of golf club bending.

head orientation, the club head direction and the impact location of the ball on the club face are all important with respect to the subsequent flight of the ball. The rate of change of club face orientation and the rate of change of club head direction are important with respect to the "timing" of the swing. This paper shows, through the use of inexpensive still photography, how these data can be obtained and effectively used by a golf instructor.

METHOD

Grip pressure - A steel shafted driver was instrumented to respond to grip pressure applied at three locations, as shown in Figure 2. The three locations were:



Teaching Aids for Golfers

1. The region under the last three fingers of the left hand. It has been suggested (Watson, 1978; Toski and Flick, 1978) that this pressure zone is the most significant for controlling the club during the swing.
2. The region experiencing pressure exerted by the pincer action at the base of the three fingers of the right hand. This region was expected to experience the right hand thrust late in the swing (Vossler, 1978).
3. The area under the left thumb. Due to anatomical characteristics, it was expected that the left thumb limited the degree of wrist cocking that each golfer could achieve. Pressure on the thumb was expected to demonstrate any problems in this respect.

Exact location of the transducers was determined by measurements of hand locations for numerous professional and amateur golfers. As hand location on the golf grip is one of the subjective aspects of the game, these locations were not satisfactory for everyone tested, but did meet the requirements for all professional and low handicap golfers. The grip of the test club included a hollow handle made of 6061 aluminum with openings for the transducers which consisted of simply supported beams of the same material. Metal foil electrical resistance strain gauges on the bottom surface of each beam transmitted a signal to the recording instruments when a force was applied on the outer surface of the beam.

One of the requirements of the design involved ensuring that the weight of the device equalled that of the grip (usually rubber composition) that it replaced. Another requirement, which led to this particular design, related to the need to eliminate mechanical friction in the system. To satisfy this and the need for the grip to have suitable "feel", the handle was covered with a thin layer of latex rubber secured by contact cement.

Strain gauges were located on the shaft next to the club head to detect bending upon impact. This method prevented weight difficulties associated with the use of accelerometers.

Electrical leads from the transducers passed over the golfer's shoulder to the recording instrumentation as shown in Figure 3. Separate circuits for each transducer were powered by a multi-channel bridge amplifier. The dynamic signals were permanently recorded using an oscillograph. Stroboscopic photography operating at 100 Hertz was used to make a simultaneous visual recording of the swing to relate events on the grip pressure graph.

Shaft bending - A no. 3 iron was instrumented to detect bending in two perpendicular planes as illustrated in Figure 4. Bending of the shaft in the plane perpendicular to AA produced curvature of the type that occurs early in the downswing for most golfers. It was



Figure 3. Laboratory arrangement for grip pressure measurement.

expected that torque applied to the shaft bending the club in a plane perpendicular to BB, would arise late in the swing (toward impact) if the club was being accelerated toward the ball. A negative torque at this time was claimed (Budney and Bellow, 1978; Lamps, 1975) to occur by mathematically modelling real golf swings. To measure the torque applied by the hands, strain gauges were located 20 cm from the end of the grip, just beyond the hands.

The experimental arrangement consisted of wires passing over the golfer's shoulder to the same instrumentation as for grip pressure measurement.

Club head trajectory - A 4 x 5 Graflex view camera with a Polaroid back was centred two meters directly above the golf ball. Stroboscopic lighting at 400 Hertz was employed to obtain the horizontal projections of the golf club along its path. The reference grid lines were strings spaced 10 cm apart parallel to and perpendicular to the intended line of the ball's flight. In order to protect these materials, the grid

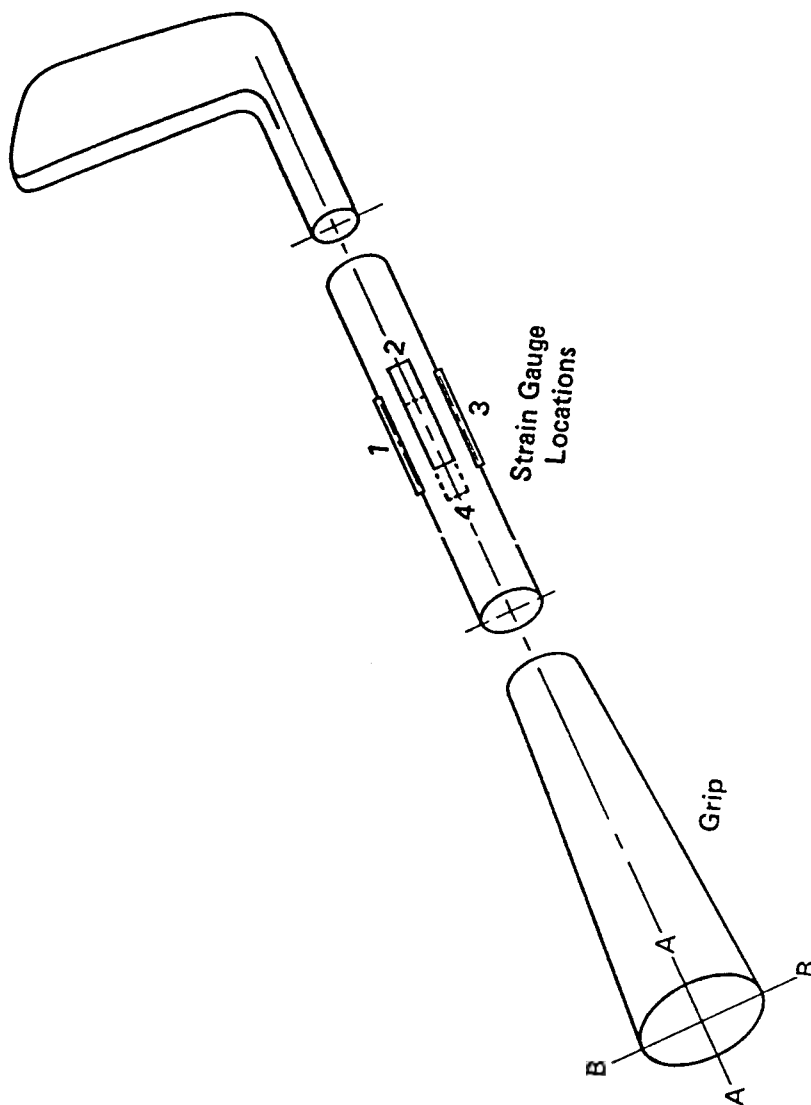


Figure 4. Club bending strain gauge configuration.

and the cloth on which it rested, were placed 10 cm below the level of the golfer's feet. The golf ball required an elevated tee (see Figure 8 for typical club head trajectory photographs).

RESULTS

Figures 5 and 6 illustrate the grip pressure characteristics of three golf professionals and three amateur golfers. Grip "pressures" were interpreted in terms of an equivalent point load applied to the center of each beam transducer. Time was measured in relation to the moment of impact with the ball. Hence the start of the backswing was indicated by a local maximum pressure approximately 0.8 to 1.0 seconds prior to impact. The time from the top of the backswing to impact was slightly different for each golfer; however, for the sake of convenience, 0.25 seconds were used for all golfers.

Referring to Figure 5, golfers A and C demonstrated grip pressure application that was consistent with the recommendations of Watson (1978) and Toski and Flick (1978). Throughout the backswing and commencing the downswing, the last three fingers of the left hand applied more pressure than the other fingers contacting the club, although there was a rise in pressure on the left thumb for golfer A at the top of the backswing. On the downswing, for all three golf professionals, both the left thumb and the right hand pincer fingers applied an impulsive force to the club, reaching a peak at 0.05 or 0.06 seconds prior to impact. This pressure reduced to nearly zero by impact. The pressure in the last three fingers of the left hand was maintained until after impact and was responsible for withstanding the centrifugal force.

The grip pressure characteristics of golfer B were different in that the pressure applied by his right hand and left thumb were higher at the top of the backswing. Figure 5 also demonstrates that golfer B decreased the pressure applied by the last three fingers of his left hand toward impact; a fault that was subsequently corrected. For each of these golfers, the maximum pressure impulse of the right hand appeared to be slightly higher than the pressure impulse applied by the left thumb. Although not apparent in Figure 5, recordings involving higher chart speed showed that the right hand pressure impulse occurred slightly after the left hand impulse for these golfers. This combined left thumb-right hand impulse accounts for the circumferential thrust of the arms (Budney and Bellow, 1978) which was the greatest contributor to development of club head speed.

Golfer D (13 handicap) differed from the professional golfers in the following respects (see Figure 6):

1. pressure on the left thumb was significantly higher at the top of the backswing and did not decrease to zero at impact.
2. peak pressure on the left thumb occurred at 0.07 seconds prior to impact, much earlier than for the golf professionals.

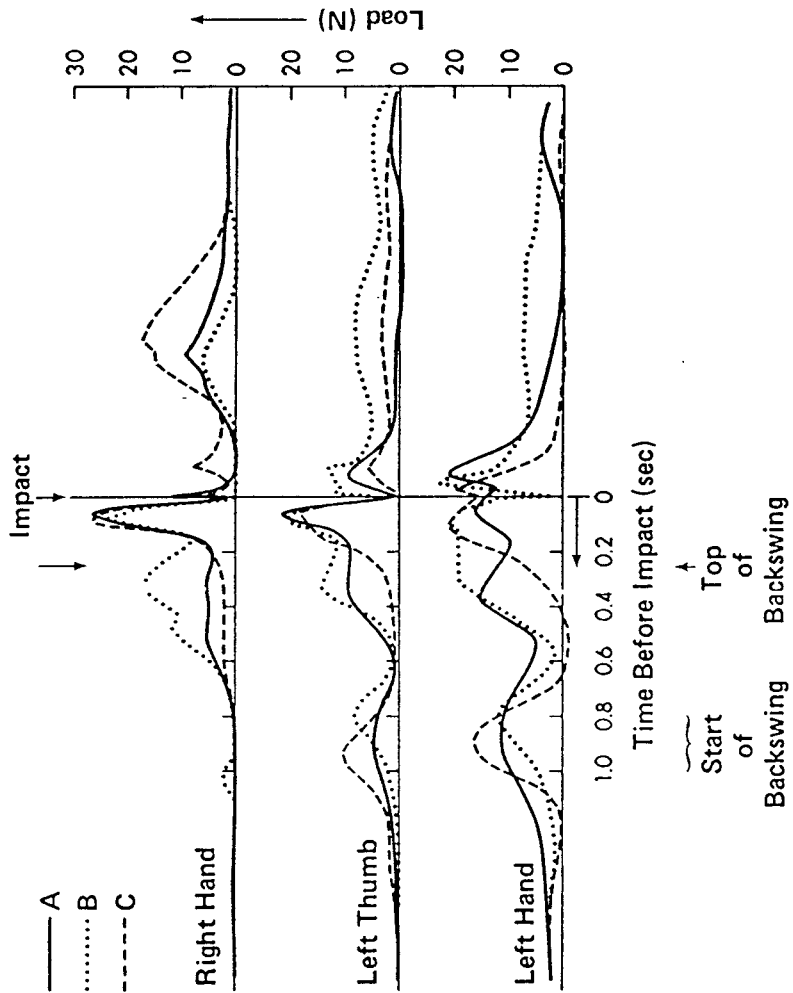
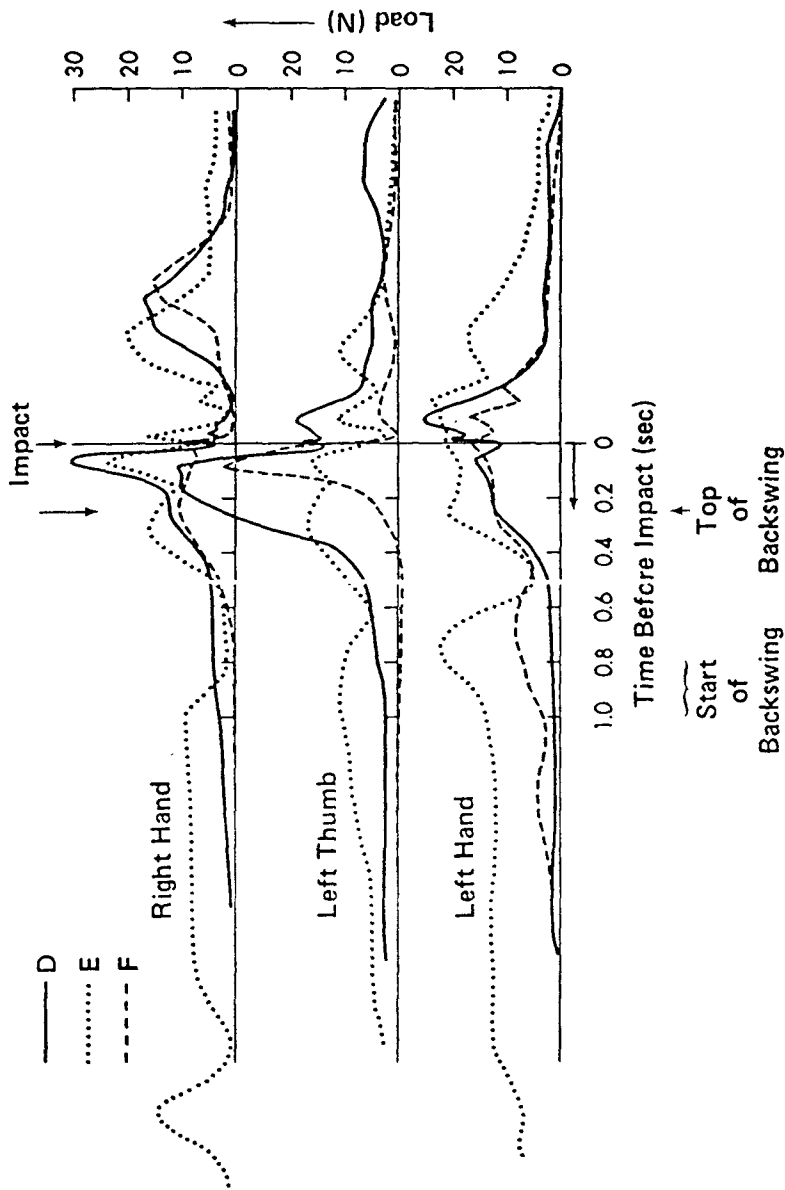


Figure 5. Grip pressure characteristics (professionals).



Teaching Aids for Golfers

Golfer E (21 handicap) differed from the professional golfers in that:

1. grip pressure at address was much higher
2. peak pressure application occurred at 0.09 seconds prior to impact; earlier than for the professionals.

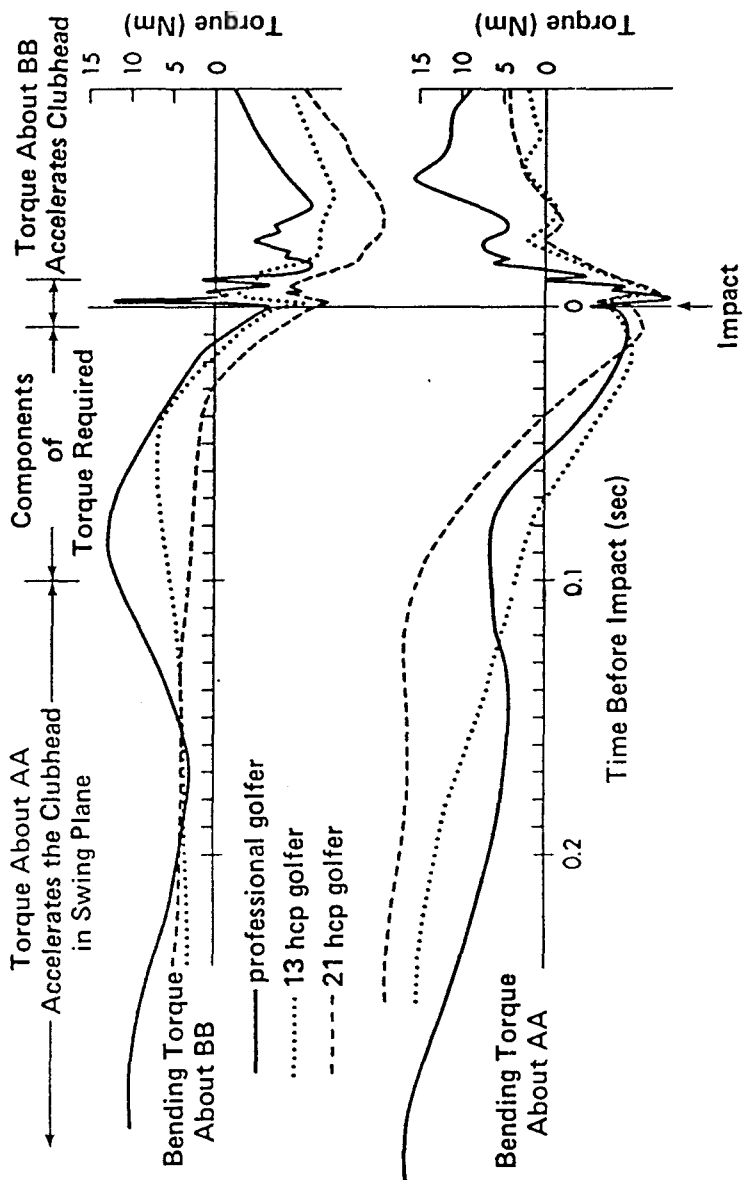
Golfer F (9 handicap) differed significantly from the professional golfers in that his peak right hand pressure did not occur at the same time the left thumb pressure impulse was applied. A modification involving this golfer's deliberate attention to holding the club more securely with his right hand subsequently produced a right hand pressure impulse. His maximum left thumb pressure application also occurred earlier than for the professionals.

Comparison of three golf professionals with six amateurs demonstrated that the less competent golfer accelerated the club by swinging his left arm considerably earlier than the more competent golfer. Two other types of faulty grip pressure characteristics were determined for some subjects although the results are not shown here.

It was determined that some golfers applied no pressure with the last three fingers of the left hand at impact; the club was held at this instant with the right hand. Grip pressure measurements also clearly demonstrated that some golfers were controlling the club with the right hand instead of the left to commence the backswing.

Shaft bending - Figure 7 describes the variation of shaft torque with time for three golfers, including one professional. The torque was indicated only for the gauge position 20 cm from the end of the shaft, next to the hands of the golfer. In the early part of the swing, bending about AA accelerated the club in the plane of the swing. Figure 7 demonstrates that, at this stage, the professional golfer had the least torque in this plane. At impact, torque about BB related to acceleration of the club head toward the ball. Immediately prior to impact, all three golfers exerted a negative torque about BB. The torque applied by the professional golfer (-6.5 Nm) was less than the torque applied by the two amateurs (-7.8 Nm and -12.4 Nm). Since the orientation of the club face with respect to the swing plane changed rapidly for the last 1/10 second, it was necessary to take components of the two torques to determine the actual torque accelerating the club head in the swing plane. This small complication, as well as the interpretation of results from the other strain gauges on the shaft, was regarded as scope for a separate analysis.

Club head trajectory - Typical club head trajectory photographs are shown in Figure 8. Data from photographs of this type are shown in Table 1. The angle between the target direction and the path of the club head was defined as γ and the time rate of change of this angle was $\dot{\gamma}$. Positive γ implied that the club head approached the target line from the side on which the golfer stood. The angle between



Teaching Aids for Golfers

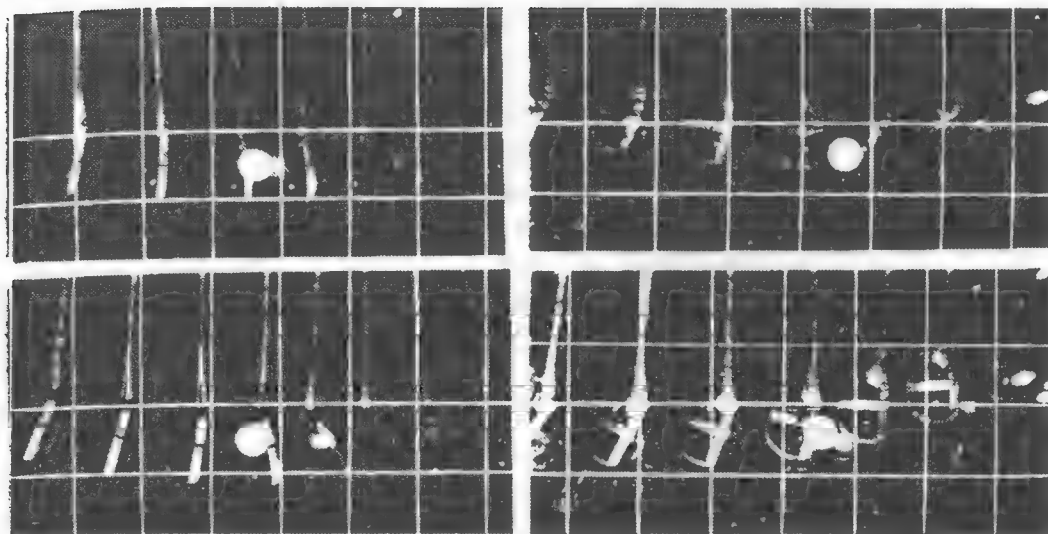


Figure 8. Club head trajectory photographs.

the normal to the target line and the leading edge of the club head was defined as δ and the time rate of change of this angle was defined as $\dot{\delta}$.

TABLE 1

TRAJECTORY AND ALIGNMENT

Golfer	Club	$\gamma(\text{deg})$	$\delta(\text{deg})$	$\dot{\gamma}(\text{deg/sec})$	$\dot{\delta}(\text{deg/sec})$
Professional C	Driver	-1	8	1590	2630
Professional B	6 Iron	5	0	870	2850
13 hcp)	6 Iron	-1	0	1250	2550
9 hcp)	6 Iron	1	1	950	2450
21 hcp)	6 Iron	-3	-5	- 370	2550

The parameter of interest from Table 1, which was believed to have potential as a teaching aid, was the angle of approach γ . For the five golfers tested, the γ values illustrated that golfer B approached the ball from inside the target line and golfer H (A chronic slicer) approached the ball from outside the target line. Golfer H received immediate advice from the golf professional and his subsequent swings demonstrated a club head trajectory much closer to the target line. The δ values demonstrated that golfer C had an "open" club face at impact whereas golfer H had the club face "closed" considerably. The rate of change of club face alignment appeared to be much the same for all golfers' however, the rate of change of trajectory varied considerably. Golfer C demonstrated the most rapidly changing trajectory, suggesting that variations in the "timing" of his swing could have the greatest consequences. The trajectory photographs clearly demonstrated off center contact between the club and the ball resulting in rotation of the club head as well as loss of distance.

CONCLUSIONS

Results from the methods employed in this investigation demonstrated differences between professional and amateur golfers and served as the basis for correction of certain swing faults. Based on grip pressure measurement, it was shown that professional golfers controlled the club much differently than amateurs. Specific grip pressure characteristics were easily detected and analyzed in relation to popular instruction concepts. The shaft bending experiments demonstrated that resisting torque late in the swing differed for each golfer, existing least for the professional golfer. Club head trajectory photographs showed that accurate information can be obtained quickly and inexpensively and can be applied to eliminate swing faults.

The authors wish to thank the National Research Council of Canada for the financial support of this project provided by Grant no. A2705 and to golf equipment manufacturers Dunlop-Slazangers and the Colgate-Palmolive Sports Group for donating the equipment used in this study. The authors also wish to express their gratitude to golf professionals Gordon McHattie, John Munro and Alex Olynyk for freely donating their time and advice.

REFERENCES

- Budney, D. and D.G. Bellow. A Dynamic Model for the Golf Swing.
International Congress of Sports Sciences, July 25-29, 1978, Edmonton.

- Cochran, A. and J. Stobbs. 1968. The Search for the Perfect Swing. Heinemann Press.
- Dickinson, G. J. Jacobs et al. 1977. Power Comes from the Legs, Right? Wrong. Golf Magazine, Vol. 19, no. 9, Sept., pp.39-42.
- Lamps, M.A. 1975. Maximizing distance of the golf drive: an optimal control study. Journal of Dynamic Systems, Measurement, and Control, Trans. A.S.M.E., Vol. 97, Series G, no. 4, pp.362-367.
- Toski, B. and J. Flick. 1978. How to become a complete golfer. Golf Digest, vol. 29, no. 4, April, pp.89-120.
- Vossler, E. 1978. Slice no more. Golf Magazine, vol. 20, no. 5, May, pp.68-73.
- Watson, T. 1978. Tom Watson's Key Swing Thoughts. Golf Digest, vol. 29, no. 2, Feb., pp.98-105.
- Williams, D. 1967. The dynamics of the golf swing. Quarterly Journal of Mechanics and Applied Mathematics, vol. XX, pt. 2, pp.247-264.

Stress analysis of bent sucker rods

D. G. BELLOW and A. KUMAR
Department of Mechanical Engineering
University of Alberta

ABSTRACT

This paper describes an elastic analysis which can be applied to bent sucker rods to determine the effect of this imperfection on the stress behaviour or load-carrying capacity of the rod. It is shown that if the location of the bend in the rod is close to the sucker rod coupling, then high stresses can occur on the surface of the bend and this can seriously reduce the working capacity of the rod. Also, it is shown that for rods with bends in them a significant compressive stress can occur at the bend even though the rod is subjected to a large axial load. Experimental results are shown to agree quite favourably with the theory.

The problem of residual stresses in the rod is also discussed and a mechanism for analyzing this problem is described along with some experimental results.

Introduction

A sucker rod passes through many operations and handling procedures from the time it originally takes its shape

in the manufacturing industry until it is placed in a well in the field. To what extent do bends in a sucker rod influence the life of that rod when placed down a well? When a rod is permanently bent, plastic deformation has taken place; this not only reduces the flexibility of the rod, but, in the area of the bend, the residual stresses can accelerate corrosion.

The object of this paper is to describe a means of evaluating the significance of bends on the elastic behaviour of a sucker rod and provide a design formula for use in determining an acceptable degree of bend. Some experimental results are also presented which show the extent of plastic deformation that has occurred as a function of observable bends in a rod.

Theoretical Considerations

In the theoretical analysis, it was assumed that the initial shape of a bent rod could be represented by two straight lines, A-C and C-B, which meet at an apex called the bend position. The bend position is identified by dimension "a" and its location from one of the ends "c", as shown in Figure 1. It was also assumed that such a rod was bent before final heat treatment and therefore no residual stresses would be present when an axial load was applied. Thus, the analysis is a simple one of elastic behaviour of an initially bent circular rod. When the rod has been bent after heat treatment, there will be residual stresses and the total stress picture must be obtained by considering the elastic stresses added to the residual stresses. This is discussed in the treatment of the experimental program.

The procedure for the elastic analysis was based on attempting to provide a mathematical model which could be checked by experiment. Because the experimental apparatus available for loading a sucker rod was limited to one of the testing machines in the laboratory, it meant that the segment of the rod had to be kept within 6 feet. However, it was believed that if reasonable agreement between theory and experiment could be reached for a segment of a rod of this length, the theoretical results would then be applicable to any rod length.

It is assumed that the rod is subjected to an axial force P and, depending on the end conditions (i.e. the effects of straight rods coupled at A and B), moments M_A and M_B and lateral forces R_A and R_B may prevail. It is further assumed that the limiting cases for the end constraints at A and B are:

- (1) the ends cannot rotate, therefore the moments at A and B are not equal to zero; or
 - (2) the ends are free to rotate, giving $M_A = M_B = 0$.
- Any other end constraints will lie within these limits.

Because of the discontinuity of shape at C, the analysis

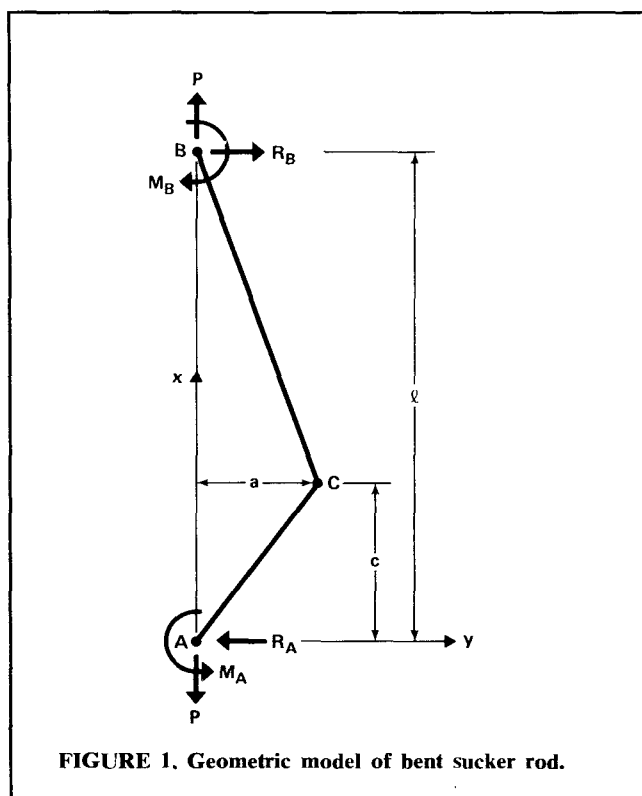


FIGURE 1. Geometric model of bent sucker rod.

of the rod must be divided into two parts — A to C and C to B. The initial deflections are as follows:

$$y_0 = \frac{ax}{c} \text{ for } 0 \leq x \leq c$$

and

$$y_0 = \frac{a(l-x)}{l-c} \text{ for } c \leq x \leq l$$

$$y_0 = a \text{ at } x = c.$$

The final lateral deflection, from which the strains or stresses can be computed, is the initial deflection y_0 plus the deflection due to the axial load y_1 , i.e., $y = y_0 + y_1$.

It can be shown (see Appendix) that the general solution of this problem is in the form

$$y = \bar{A} \sinh kx + \bar{B} \cosh kx - \frac{M_A}{P} + \frac{M_A - M_B}{P} \frac{x}{l} \quad (0 \leq x \leq c) \quad \dots \dots \dots (1)$$

$$y = \bar{C} \sinh kx + \bar{D} \cosh kx - \frac{M_A}{P} + \frac{M_A - M_B}{P} \frac{x}{l} \quad (c \leq x \leq l)$$

where the constants \bar{A} , \bar{B} , \bar{C} and \bar{D} are determined from the boundary conditions which exist at the ends A and B and the continuity of slope and deflection at $x=c$. A more detailed analysis of determining the boundary conditions is provided in the Appendix. The purpose here is to determine the stress at bend C and compare results for the two extremes of boundary conditions chosen. Knowing the lateral deflection of the rod for a given imperfection, it is a simple matter to calculate the bending moment at any cross section of the rod. The stress will consist of an axial component plus a bending component,

$$\sigma = \frac{P}{A} \pm \frac{Mr}{I} \quad \dots \dots \dots (2)$$

where M is obtained from the relationship (see Appendix)

$$M = -P(y_0 + y_1) - M_A + \frac{(M_A - M_B)}{l} x \quad \dots \dots \dots (3)$$

Equation 2 is plotted in Figure 2 for both rigid and simple end support conditions. The stress at $x=c$, the location of the bend, is shown as a function of the nominal stress in the rod assuming no bend for a number of different values of a/d ratios. It is seen from this figure that for values of $c/l > 0.1$ (i.e., for a 25-ft rod, for bends no closer to the couplings than 2-1/2 ft), the assumption of the type of boundary conditions has little effect on the magnitude of the stress at the bend. It is also shown that the stress at the bend becomes significant when it is close to the coupling. Figure 2 can be used to estimate the stress in the bend if the degree and location of the bend is known. For estimation purposes, it is suggested that the worst case occurs when the ends are considered to be simply supported; accordingly, the dashed lines in Figure 2 should be used in the analysis when the bend is closer than 2-1/2 ft to the coupling.

Another way the theoretical results can be applied is shown in Figure 3. For purposes of this example, it was assumed that a 3/4-in. rod had been subjected to a 20,000-lb axial load. The three lines indicate the maximum eccentricity permissible assuming the allowable working stress is not to exceed a predetermined value. Three such allowable stresses have been chosen and, for the conditions assumed, it is shown that as the bend approaches the coupling, the allowable value of the eccentricity decreases. Similar curves can be generated for rods of other diameters by substituting the appropriate parameters into Equation 2.

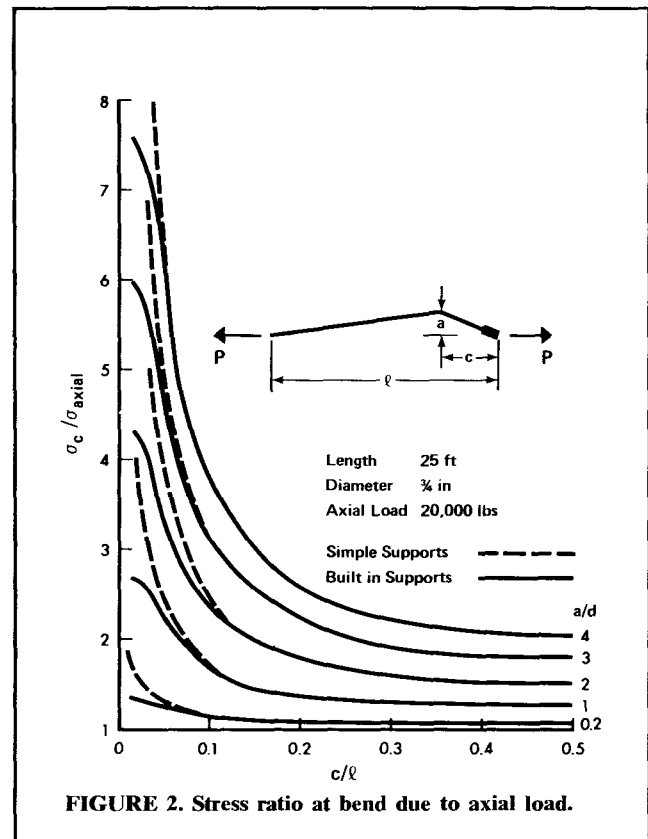


FIGURE 2. Stress ratio at bend due to axial load.

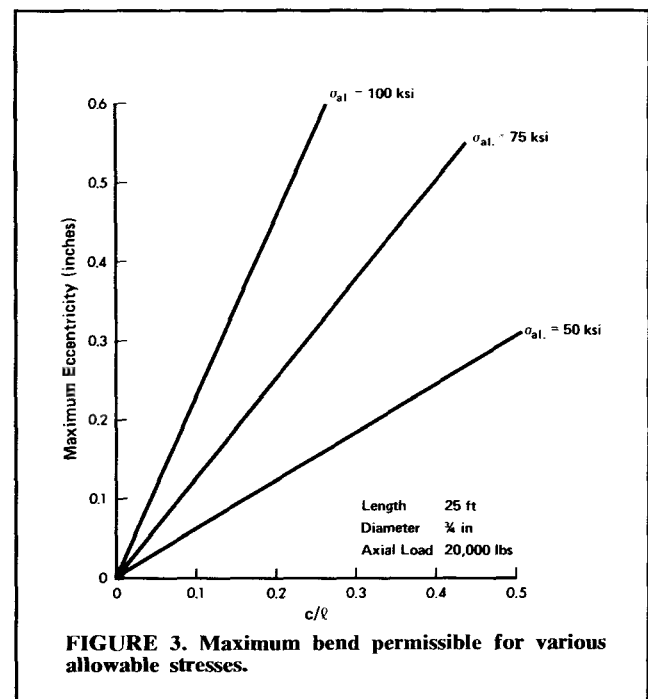


FIGURE 3. Maximum bend permissible for various allowable stresses.

Experimental Results

To illustrate the applicability of the theory, a number of sucker rods were instrumented with electrical resistance strain gauges. These rods had been bent prior to the final heat treatment. Because of the limitations of the testing machine used in the laboratory, the rods were shortened to an over-all length of 6 ft, with one end plain and the other with the usual coupling-pin configuration. Strain gauges were mounted at three different locations along

the length of the rod — on either side of the bend, half-way between the bend and the coupling, and halfway between the bend and the other end. Figure 4 shows the general test arrangement with the rod under axial tension in the testing machine.

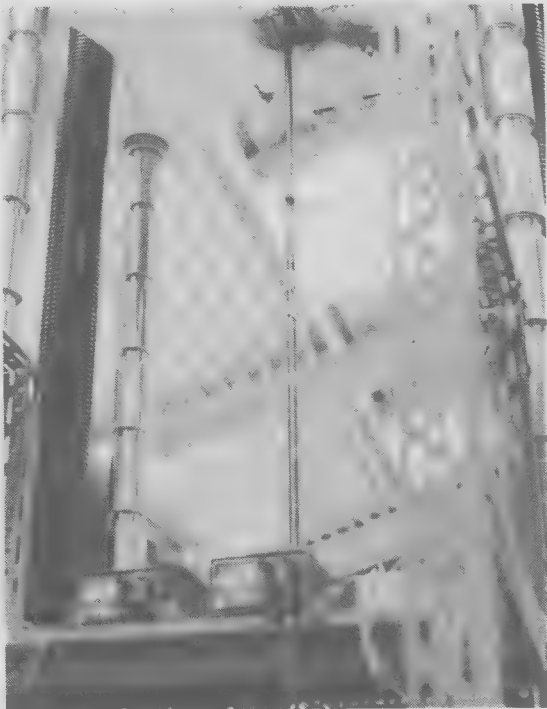


FIGURE 4. Photograph of rod under test.

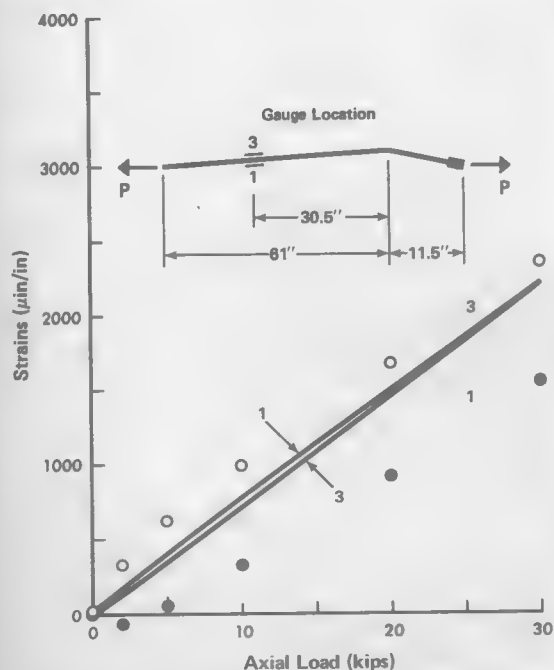


FIGURE 5. Experimental results — gauge location remote from bend.

The degree of bend in the rods was measured by placing each on a surface table and measuring, with the aid of thickness gauges, the extent of imperfection. The axial test consisted of loading each of the rods and recording the strains for each load condition. The total elongation was also measured by means of an extensometer specially designed for this purpose. Inasmuch as the testing machine gripping system imposed different end conditions than those expected in a field situation, the theory was modified to account for a fixed end condition at the plain end and a flexible or simple support condition at the coupling end. Thus, referring to Figure 1, the boundary conditions at end A became $M_A=0$, with the result that this term drops out of Equations 1 and 3. Solving these modified equations for new constants of integration allows the value of strain to be computed at any point along the rod as before.

The experimental results are plotted in Figures 5-7 as points. For specific values of a and c , the theoretical strains were plotted as curves. From these figures, it is shown there is reasonable agreement between theory and experiment not only in magnitude of strain, but in the general form of the strain behaviour as a function of increasing load. Thus, it is concluded that the theory outlined above and explained in more detail in the Appendix is a reasonable approach to predicting the values of stress in a rod which contains an imperfection in shape of the kind considered.

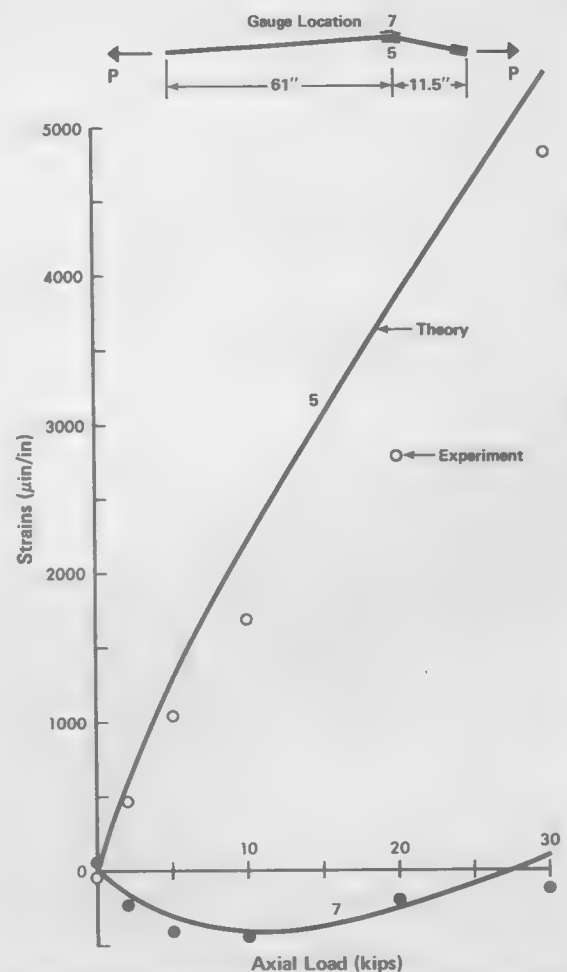


FIGURE 6. Experimental results — gauge location at the bend.

Some additional observations from the experiments that can be made is that for rods with an initial imperfection it was found that, as the axial tensile load was applied, a compressive strain occurred on the outside of the bend and this compressive condition existed until the rod was loaded to near its working capacity. For example, as seen in Figure 6, the compressive strain on the outside of the bend prevailed even with a 30-kip axial load. When such a situation occurs, the tensile stress is considerably larger on the inside of the bend than that given by the nominal stress of the rod (i.e., the nominal stress is the axial load divided by the nominal cross-sectional area of the rod), and it is at this point that the stress would first exceed the working stress of the rod. For some examples tested in the laboratory, the maximum working stress in bent rods occurred between 70 and 90 per cent of the normal working capacity of the rods. Thus, if bent rods are loaded so that the working stress is not to exceed a predetermined value, the carrying capacity of the rod will be reduced. On the other hand, if the load is applied as if the rod is straight, then, on the inside of the bend, the axial stress will exceed the allowable working stress.

Residual Stresses

When a sucker rod is bent out of shape after final heat treatment and the bend is such as to have caused plastic deformation in at least the outer fibers of the rod, there will be residual stresses present in the rod. The actual stress distribution under an axial load in a field situation will be the sum of the stresses determined from the elastic analysis plus these residual stresses. If the residual stress magnitude is large, then this could lead not only to

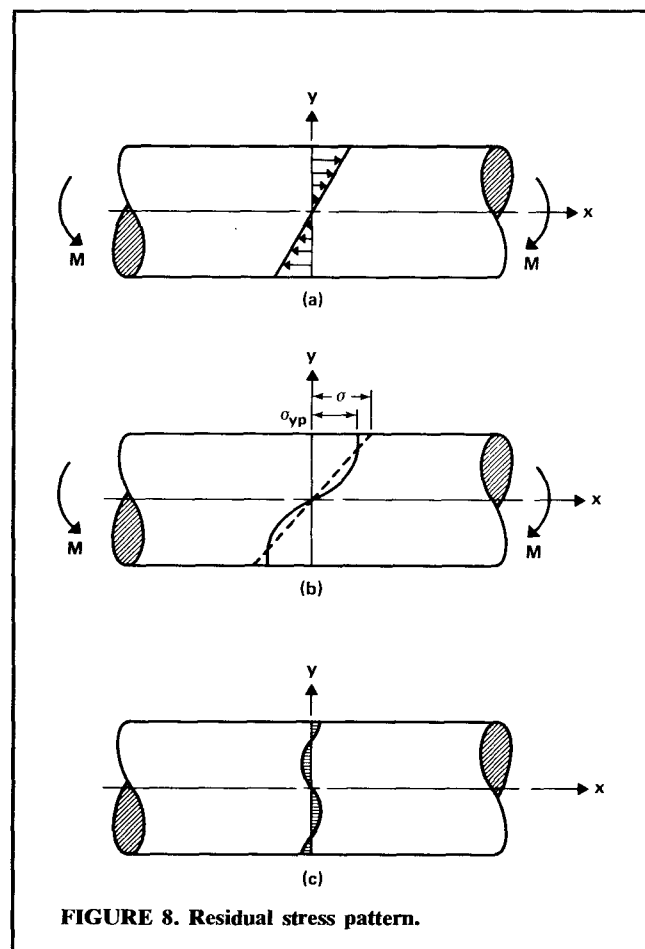
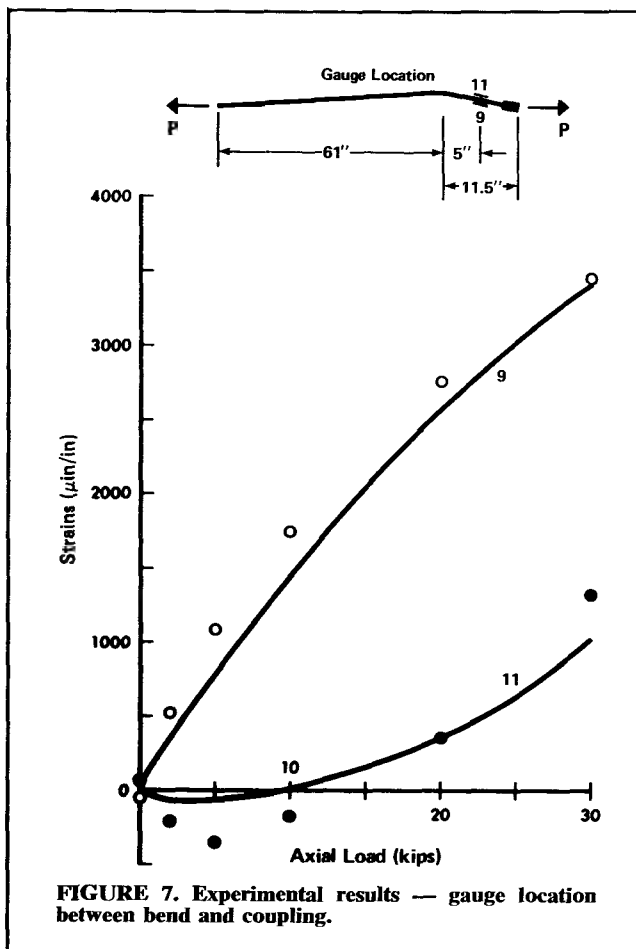
significant reduction in load-carrying capacity, but the residual stresses could accelerate stress corrosion. In the following section, it is shown how the residual stresses can be analyzed and a discussion of the results of an experiment is given.

When a rod is subjected to simple bending, an elastic stress distribution is caused, as shown by a solid straight line in Figure 8a. It follows that the moment required to cause a stress of σ on the outer fiber is given by

$$M = \int_{h/2}^{h/2} \sigma y \, dA$$

Now, when the moment increases so that the stress on the outer fiber exceeds the yield stress, in order for the above equation to remain valid an elasto-plastic stress distribution, as shown in Figure 8b, must exist. When the moment causing this stress distribution is removed, the rod can be thought to be subjected to a negative elastic stress, as shown by the dashed line in Figure 8b. Superimposing these two distributions yields the residual stress pattern in Figure 8c. The actual measurement of the distribution in Figure 8c is not easy, especially in the field, although there are a number of techniques that can be employed using methods of trepanning or drilling of holes in combination with electrical resistance strain gauges.

In the manner described above, consider a sucker rod with a circular cross section which has been bent to the extent that plastic deformation has occurred in the outer fibers, as indicated by the shaded portions in Figure 9. Assuming no work hardening of the material, the stress in the shaded portions will be the yield stress for the material σ_{yp} . It follows that the moment M required to cause this stress distribution is given by



$$M = \sigma_{yp} \left(\frac{4r^3}{3} \sin^3 \alpha + \frac{l}{r \cos \alpha} \left[\frac{\pi r^4}{4} - \frac{r^4}{4} \left(2\alpha - \frac{\sin 4\alpha}{2} \right) \right] \right)$$

and

$$\epsilon = \frac{y}{R} \text{ and } \frac{l}{R} = \frac{\sigma_{yp}}{r E \cos \alpha}$$

where l/R is the curvature of the bend in the rod. Substituting these expressions into the beam equation yields

$$\frac{d^2 y_p}{dx^2} = \frac{-M}{\beta EI} \quad (4)$$

$$\text{where } \beta = \frac{16}{3\pi} \sin^3 \alpha \cos \alpha + \left[1 - \frac{1}{\pi} \left(2\alpha - \frac{\sin 4\alpha}{2} \right) \right]$$

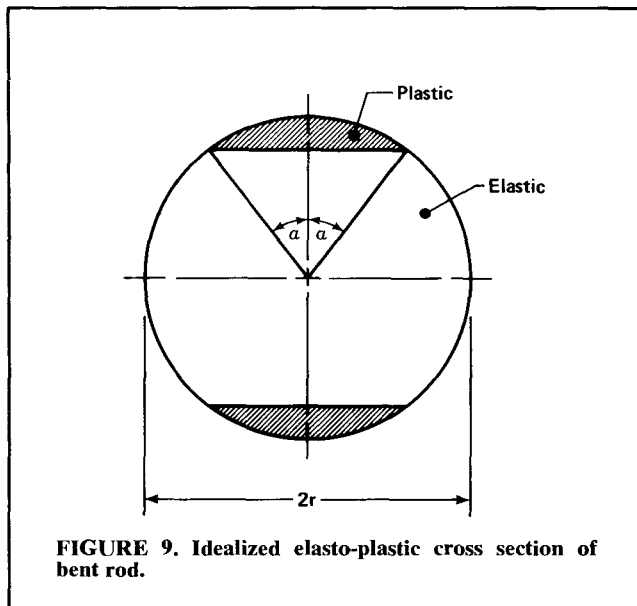


FIGURE 9. Idealized elasto-plastic cross section of bent rod.

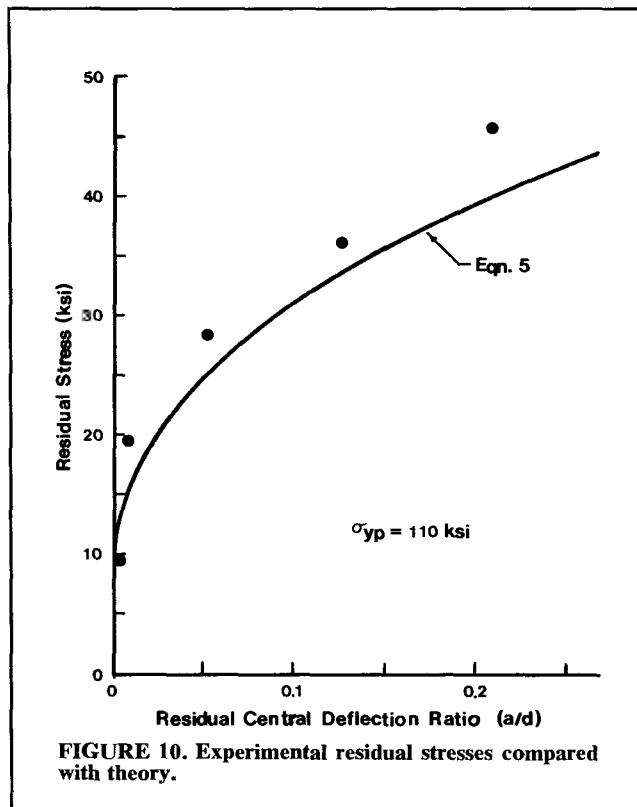


FIGURE 10. Experimental residual stresses compared with theory.

Equation 4 was solved using a finite-difference method for various values of load. The residual deflection is given by

$$y_{Res.} = y_{Plastic} - y_{Elastic} \quad (5)$$

An experiment was performed on a 66-inch rod, 3/4 inch in diameter, to check the above theory. The rod was held at the ends by simple supports and a concentrated load was applied at the center. Electrical resistance strain gauges were applied to opposite sides of the rod where the lateral load was to occur. For each load increment the strains were measured as ϵ_L , and after the load was released ϵ_0 . The residual central deflection of the rod was recorded after each load increment. From an idealized elastic-plastic stress-strain curve for the material, the yield-point strain, ϵ_Y , was determined. The plastic strain at load was calculated as

$$\epsilon_p = \epsilon_L - \epsilon_Y$$

For the case being considered, $\epsilon_0 < \epsilon_p$ and thus the difference $(\epsilon_p - \epsilon_0)$ was used to determine the residual stress at the surface of the rod as

$$\sigma_{res} = E(\epsilon_p - \epsilon_0) = E(\epsilon_L - \epsilon_Y - \epsilon_0)$$

The values of residual stress were plotted and compared with equation 5, as shown in Figure 10. The agreement between theory and experiment is favourable.

Conclusions

A mathematical technique has been described which predicts, with reasonable accuracy, the values of stress in a slightly bent sucker rod when it is subjected to an axial load. It is shown that the load carrying capacity of a sucker rod can be significantly reduced if there is a bend in the rod and that the state of stress of the rod is more critical the closer the bend is to the coupling end. For sucker rods that are bent in the field, the residual stresses that result can be significant. A technique is described whereby the extent of residual stresses can be estimated.

It is believed that, with an analysis such as described in this paper, standards can be developed which will determine under what conditions bent sucker rods can or should be used. This will prevent sucker rods of reduced load-carrying capacity from being used in critical situations.

Acknowledgment

Appreciation is expressed to the National Research Council of Canada for financial support in aid of this project under the auspices of Grant No. A-2705.

Appendix

Static equilibrium of the imperfect rod shown in Figure 1 requires that

$$R_A = -R_B = \frac{M_A - M_B}{l}$$

and the bending moment, for any cross section along the length, is given by

$$M = -P(y_0 + y_1) - M_A + \frac{M_A - M_B}{l} x \quad (1)$$

The deflection (y_1), due to the axial load (P) is obtained from

$$EI \frac{d^2 y_1}{dx^2} = -M \quad (2)$$

Combining equations (1) and (2) and letting $k^2 = P/EI$ yields.

$$\frac{d^2 y_1}{dx^2} - k^2 y_1 = k^2 \frac{ax}{c} + \frac{M_A}{EI} - \frac{(M_A - M_B)}{l} x \quad (0 \leq x \leq c)$$

and

$$\frac{d^2 y_1}{dx^2} - k^2 y_1 = \frac{k^2 a(l-x)}{l-c} + \frac{M_A}{EI} - \frac{(M_A - M_B)}{l} x \quad (c \leq x \leq l)$$

The general solution to these equations is given by

$$y_1 = \bar{A} \sinh kx + \bar{B} \cosh kx - \frac{ax}{c} - \frac{M_A}{P} + \frac{(M_A - M_B)x}{Pl} \quad (0 \leq x \leq c)$$

$$y_1 = \bar{C} \sinh kx + \bar{D} \cosh kx - \frac{a(l-x)}{l-c} - \frac{M_A}{P} + \frac{(M_A - M_B)x}{Pl} \quad (c \leq x \leq l)$$

The constants \bar{A} , \bar{B} , \bar{C} and \bar{D} are found from the end conditions at A and B and the continuity of slope and deflection at $x=c$. Two types of boundary conditions are evaluated below.

(i) *Both ends built-in*

Substitution of the general solutions into four conditions

- (i) $y_1 = 0$ at $x = 0$
- (ii) $y_1 = 0$ at $x = l$
- (iii) $y_1|_{LHS} = y_1|_{RHS}$ at $x = c$
- (iv) $\left. \frac{dy_1}{dx} \right|_{LHS} = \left. \frac{dy_1}{dx} \right|_{RHS}$ at $x = c$

and solution of the resulting equations leads to the following values of constants \bar{A} , \bar{B} , \bar{C} and \bar{D} :

$$\bar{A} = \frac{M_B}{P \sinh kl} - \frac{M_A}{P \tanh kl} + \frac{al}{kc(l-c)} \times \frac{\sinh k(l-c)}{\sinh kl}$$

$$\bar{B} = \frac{M_A}{P}$$

$$\bar{C} = \frac{M_B}{P \sinh kl} - \frac{M_A}{P \tanh kl} - \frac{al}{kc(l-c)} \times \frac{\sinh kc}{\tanh kl}$$

$$\bar{D} = \frac{M_A}{P} + \frac{al}{kc(l-c)} \sinh kc$$

D.G. Bellow

Donald G. Bellow, born in Winnipeg, Manitoba, obtained his early education in Victoria and Vancouver, graduating from the University of British Columbia in 1956 with a B.A.Sc. in mechanical engineering. After working in industry in Ontario, he returned to the West and obtained an M.Sc. (1960) and a Ph.D. (1963) in mechanical engineering from the University of Alberta. In 1963, he joined the Faculty of Engineering at the University of Alberta and is currently Professor and Chairman of the Department of Mechanical Engineering. His research interests are in the general area of applied mechanics and he has co-authored a number of papers on the fatigue properties of sucker-rod couplings.



Employing two additional conditions

(i) $\frac{dy_1}{dx} = 0$ at $x = 0$ and

(ii) $\frac{dy_1}{dx} = 0$ at $x = l$ results in the following two equations for the determination of unknown moments M_A and M_B

$$\frac{M_A}{P} \left[\frac{1}{l} - \frac{k}{\tanh kl} \right] + \frac{M_B}{P} \times \left[\frac{k}{\sinh kl} - \frac{1}{l} \right] = \frac{a}{c} - \frac{al}{c(l-c)} \times \frac{\sinh k(l-c)}{\sinh kl}$$

$$\frac{M_A}{P} \left[\frac{1}{l} - \frac{k}{\sinh kl} \right] + \frac{M_B}{P} \times \left[\frac{k}{\tanh kl} - \frac{1}{l} \right] = \frac{al}{c(l-c)} \times \frac{\sinh kc}{\sinh kl} - \frac{a}{l-c}$$

(ii) *Both ends simply-supported*

For simply-supported ends

$$R_A = R_B = M_A = M_B = 0$$

The first four boundary conditions used in the previous case enable the constants \bar{A} , \bar{B} , \bar{C} and \bar{D} to be determined. Hence, it follows that

$$\bar{A} = \frac{a}{kc(l-c)} \frac{\sinh k(l-c)}{\sinh kl}$$

$$\bar{B} = 0$$

$$\bar{C} = \frac{a}{kc(l-c)} \frac{\sinh kc}{\tanh kl}$$

$$\bar{D} = \frac{a}{kc(l-c)} \sinh kc$$

The total deflection $y = y_0 + y_1$ and the bending moment M can be determined at every cross section of the rod for both types of boundary conditions. The stress at any cross section is computed with the aid of the equation

$$\sigma = \frac{P}{A} \pm \frac{Mr}{I}$$

NOMENCLATURE

a	= degree of bend
A	= cross-sectional area of rod
c	= location of bend from coupling
d	= diameter of rod, $d = 2r$
E	= Young's modulus
I	= second moment of area
l	= length of rod
M, M_A, M_B	= bending moments applied to rod
P	= axial load
R	= radius of curvature of bend
y	= final lateral deflection of rod $y = y_0 + y_1$
y_0	= initial lateral deflection of rod
y_1	= lateral deflection of rod due to axial load
ϵ	= bending strain
σ	= stress
σ_{yp}	= yield stress

Keywords: Stress analysis, Sucker rods, Stress behaviour, Pumping, Bending, Axial loads.

A. Kumar

Anil Kumar received a B.S. degree (1969) from the University of Delhi, and an M.S. (1969) and Ph.D. (1974) from the University of Wisconsin. He worked at the University of Alberta as a post-Doctoral Fellow in 1975-77.

closed loop

The Magazine of Mechanical Testing

February 1978



Published by MTS Systems Corporation

closed loop

The Magazine of Mechanical Testing
February 1978 Vol. 8, No. 1

Contents

Development of an Improved Internal Thread for the Petroleum Industry 3

Repairing underground oil well components is a costly operation; not only is valuable production time lost but a mobile service rig must be called to the site to pull the components from the shaft so the repairs can be made. Obviously, any underground component should be built to provide the longest possible service life.

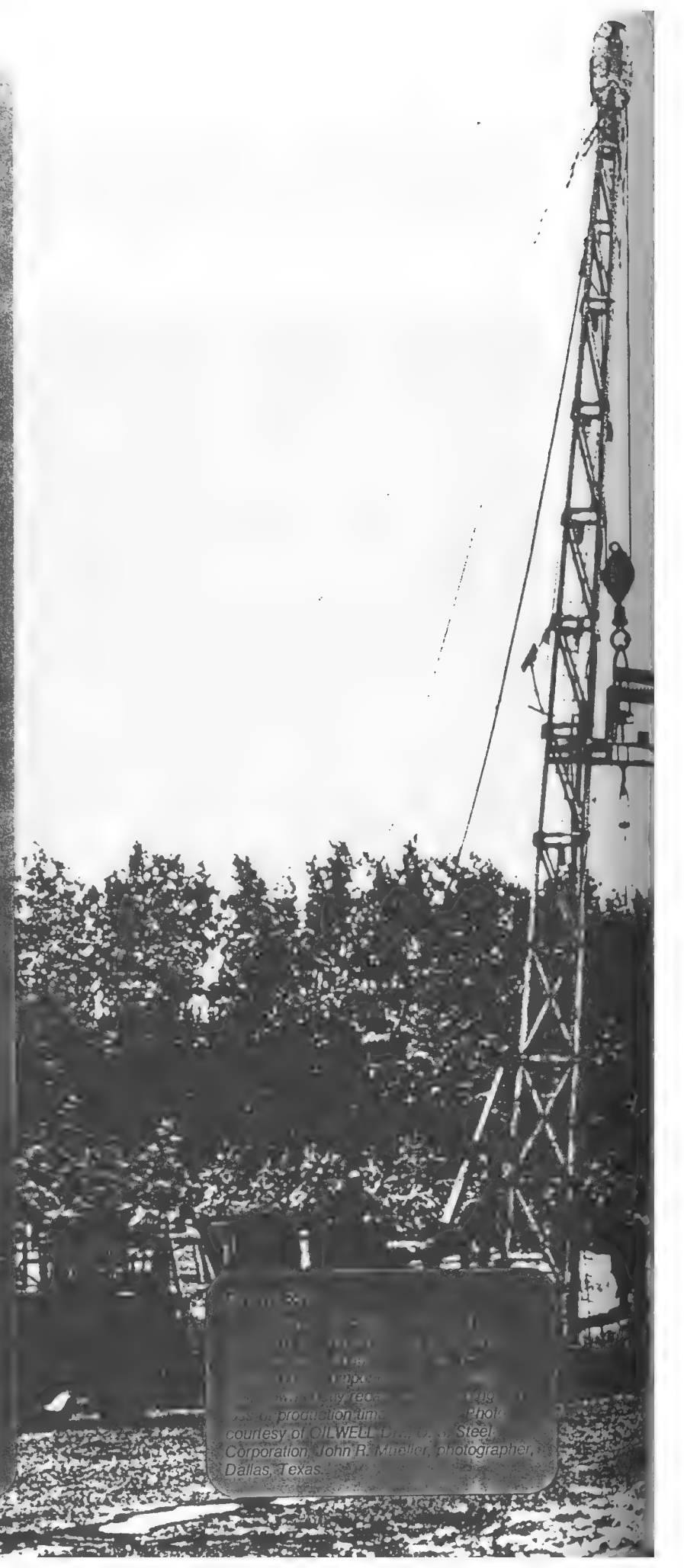
The University of Alberta, Department of Mechanical Engineering, conducted a test program with the objective of developing an improved design for an underground oil well component (the threaded joint of sucker rods) especially susceptible to the effects of cyclic loading in a hostile environment such as an oilfield with significant quantities of salt water and hydrogen sulfide, common oilfield contaminants.

Although sucker-rod joints have received considerable attention before this investigation, most previous study has been directed to improving the pin condition of the rod with little concern for the actual design of the coupling. The project described was specifically directed to develop an improved design for the threaded joints for coupling sucker rods.


Subsequent Yield Surfaces for Annealed Mild Steel Under Servo-Controlled Strain and Load Histories: Aging, Normality, Convexity, Corners, Baushinger and Cross Effects 13

The growing need for conservation of the world's energy resources gives impetus for research into extending the service life of mechanical components to the limits of their material capability. Researchers at Brown University undertook a project designed to develop techniques for characterizing materials under multiaxial stresses and to provide a data base to help enable engineers in developing a new design methodology incorporating consideration of multiaxial stresses.

This report is a technical report of the Mechanical Testing Systems Corporation. The material is the property of the Mechanical Testing Systems Corporation and is not to be distributed outside the company without the written permission of the company. Requests for subscriptions should be addressed to: Dept. MTS Systems Corporation, P.O. Box 117, Minneapolis, Minnesota 55424.



This report is a technical report of the Mechanical Testing Systems Corporation. The material is the property of the Mechanical Testing Systems Corporation and is not to be distributed outside the company without the written permission of the company. Requests for subscriptions should be addressed to: Dept. MTS Systems Corporation, P.O. Box 117, Minneapolis, Minnesota 55424.



Development of an Improved Internal Thread for the Petroleum Industry

by

Donald G. Bellow, Professor and Chairman,
and M. Gary Faulkner, Professor,
Department of Mechanical Engineering,
University of Alberta, Edmonton, Alberta, Canada

In most oil fields, crude oil must be pumped to the earth's surface from pools located many hundreds, and frequently many thousands, of meters underground. One oil field pump commonly used for this purpose is shown in Figure 1 and consists of a plunger inside a tube approximately 5-10 feet (1.5-3 m) in length (length determined by stroke design) with ball valves located at each end. The pump's plunger reciprocates vertically inside the pump barrel causing crude oil to enter at the bottom on the downward stroke and exit at the top on the upward stroke. The process continues with each stroke pumping more oil out the top of the pump and up through the casing or tubing. The pump's driving mechanism is located at the surface of the well and is shown in Figure 2. It consists of a "horsehead" and walking beam driven by a suitable power source. Attached to the "horsehead" is a series of rods 25 feet (7.6 m) in length coupled together to form what is called a sucker-rod string.

The actual installation of a producing well is accomplished by drilling the hole, inserting the casing piece by piece and finally, assembling the sucker-rod string by connecting the rods and couplings. If the pump or sucker-rod string should malfunction at any time and require repairs, a mobile service rig must be called to the well site, an operation resulting in loss of valuable production time from the well in addition to service rig costs which could be several thousand dollars. Obviously, the components that are lowered into the well should be built to provide the longest possible service life, making recall of the mobile service rig a rare occurrence.

One area that has received considerable attention in efforts to lengthen the service life of oil well components is the threaded joints of the sucker-rod string. Most previous work has been directed to improving the pin condition (the threaded end of the rod) with little consideration given to improving the design of the coupling. The objective of the project described in this article was to develop an improved

threaded coupling for joining the sucker-rods. The basic problem was to determine a thread design which would best survive large cyclic stresses in hostile environments since many oil fields contain significant quantities of contaminants such as salt water (NaCl solution) and hydrogen sulfide (H_2S). Premature failure of components can occur in these environments during cyclic loading due to the environmental effects of corrosion fatigue.

Historically, all threaded sucker-rod components have been produced using a single point cutting tool in the case of an external thread and simple cutting die in the case of an internal thread. In the effort to design components with a longer service life, many ideas were proposed. Suggestions such as using a keyhole at the root of the thread, burnishing the thread, partially rolling or fully rolling the thread and using extruded material instead of hot rolled material were all considered and eventually discarded, primarily because the required manufacturing processes were relatively difficult and expensive. Various manufacturers claimed superior performance for their product based on the data obtained in field studies; but the data, in many cases were incomplete and inconclusive.

One early attempt to evaluate, under a single set of field conditions, a number of different thread designs was made in the Redwater district in Central Alberta, Canada. For this test, various thread designs were assembled in a sucker-rod string at a producing well site. Since no failure had yet occurred, the string was pulled eighteen months later; and each component was inspected for signs of deterioration. Some components showed more wear than others, but the results were inconclusive and no quantitative assessment could be made. The project was then moved to the

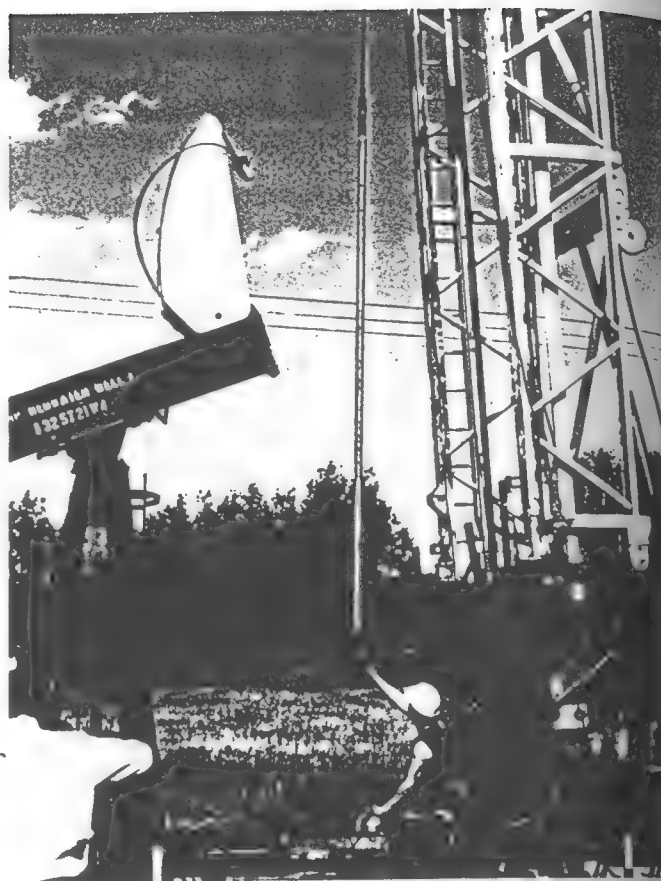


Figure 1. Oil pump and service rig at field test site, Redwater Alberta.

Figure 2. "Horsehead" and walking beam located at surface of well.



laboratory where the test program could be accelerated and where such variables as load, time and corrosive environment could be controlled. The specific objective of the project was to determine the relative merits of different threaded elements in a number of selected environments. The testing program was divided into three phases: testing in air, testing in a 3.5 percent NaCl solution, and testing in a saturated H_2S environment.

Testing in Air

The first testing program was designed to accelerate the fatigue process as much as possible and to obtain, under a set of controlled stress amplitudes, an indication of the relative merits of five different internal thread designs: simple cut, keyhole, cut and burnished, cut and partially rolled and fully rolled as shown in Figure 3. All testing was done in air at a frequency of 8 Hz. The sucker-rod string

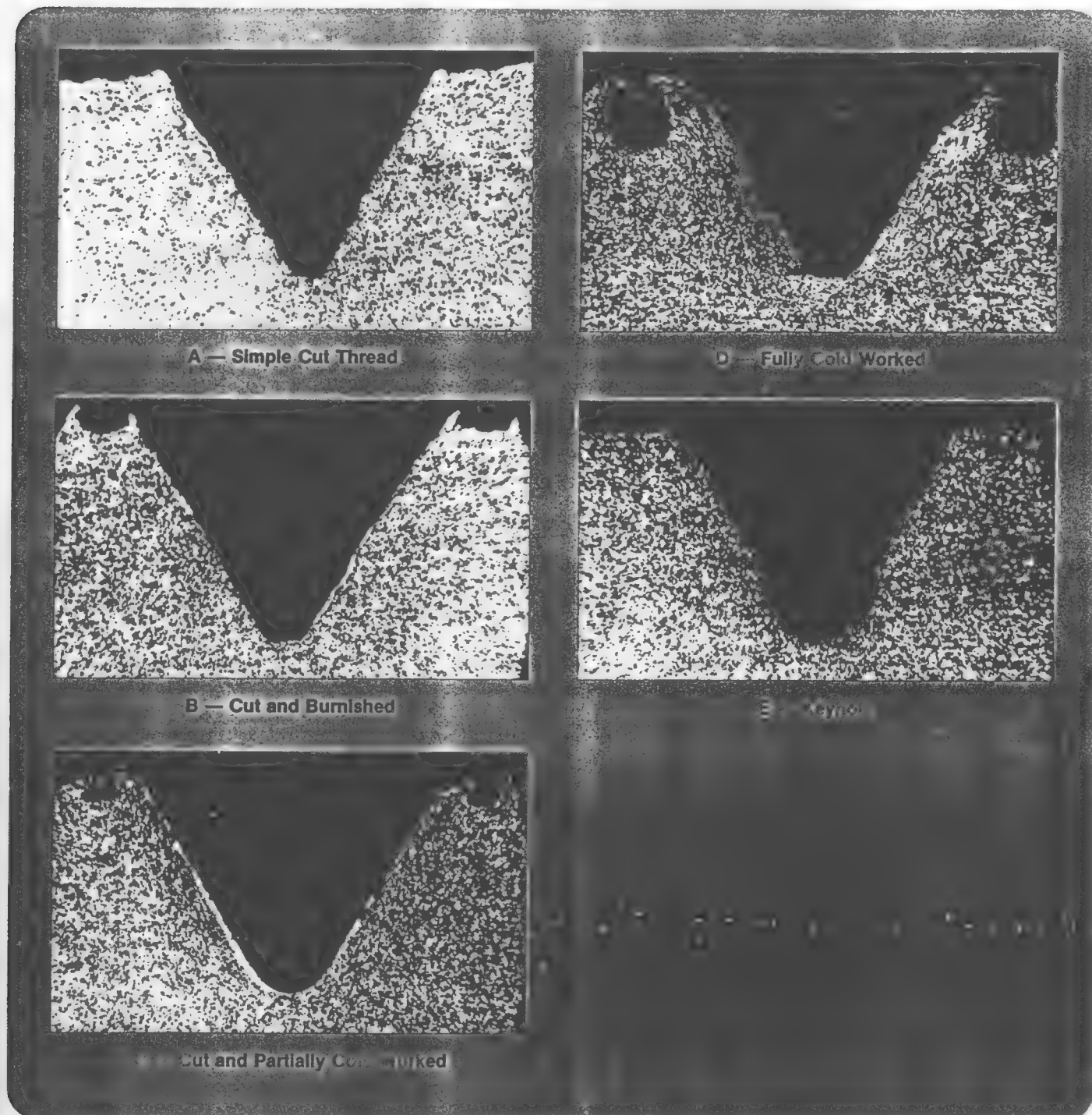


Figure 3. Profiles of five different thread designs.

used for the laboratory testing consisted of a series of couplings and pins shown in Figure 4 which were assembled between the crosshead and actuator of an MTS closed-loop servohydraulic testing machine. The shiny elements are the couplings which were reduced in diameter from the original 1-3/4" (44.5 mm) to 1-3/8" (34 mm) O.D. (The threads were for a standard 3/4-inch diameter sucker-rod manufactured to specifications set by the American Petroleum Institute.) The reduction was to localize failures in the couplings and was achieved by centerless grinding. It did not influence initiation of the fatigue cracks which always occurred on the inside of the coupling at the root of one of the threads located opposite the first thread of the pin on the sucker rod. When the sucker-rod string was assembled in the testing machine, a prestress of 6.1 ksi (42 MPa) tension was applied to simulate a typical dead load when a coupling is in service. The string was subjected to an alternating stress such that the minimum stress was always 6.1 ksi (42 MPa) and the maximum was set

at specific values for each particular test in the range of 40 ksi (275 MPa) to 77 ksi (530 MPa). A summary of the in-air testing is shown in Figure 5. The fatigue life of each of the thread designs can be compared with the unnotched material. All specimens tested were made from AISI 8635, quenched and tempered to Rockwell C16-23. All test results shown are the median of a minimum of twelve samples.

A subsidiary testing program² was conducted to determine if the fatigue life of the coupling could be extended by replacing the machined blank with an extruded blank and also to determine if there was any significant difference between AISI 1045 and AISI 8635 as the coupling material. Although AISI 8635 is more commonly used throughout the petroleum industry, AISI 1045 was also evaluated since it is more readily available and possibly less expensive. The results (Figure 6) show little difference between the fatigue life of a coupling whose thread was formed by a simple cutting process, even with burnishing the cut thread,

Figure 4. Laboratory sucker-rod string.



Closed Loop

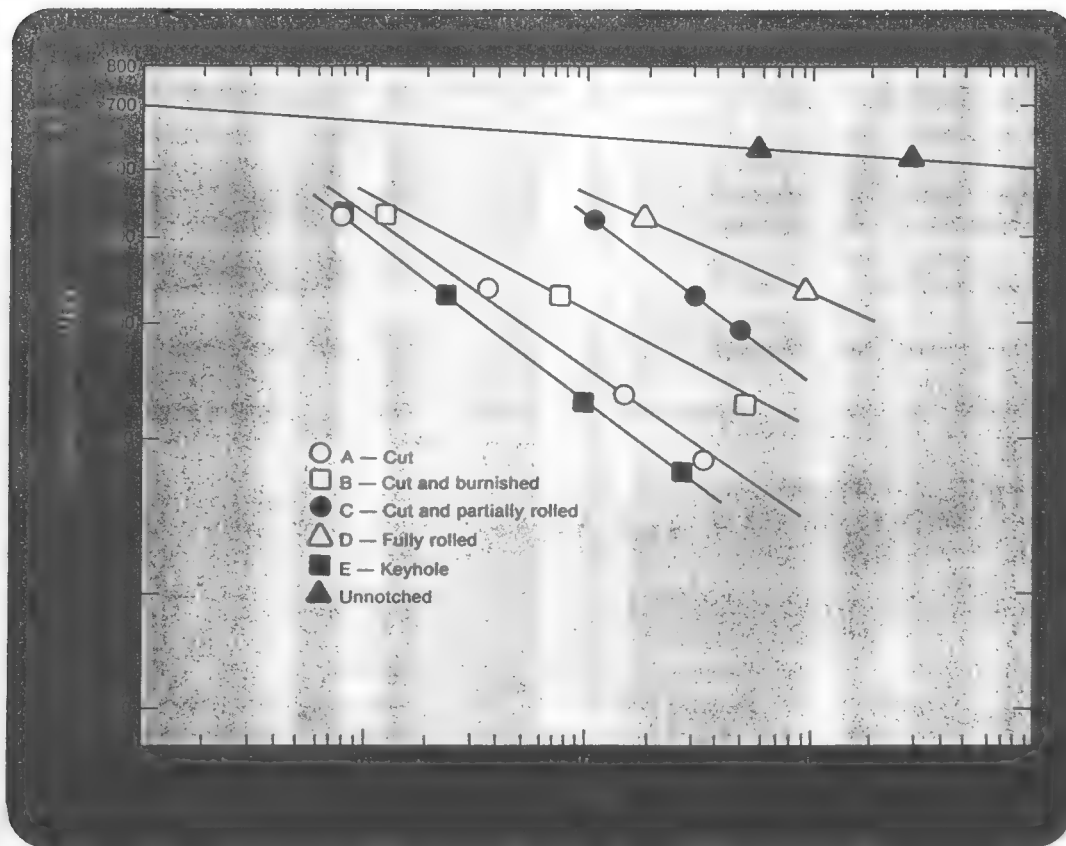


Figure 5. Summary of in-air test results.

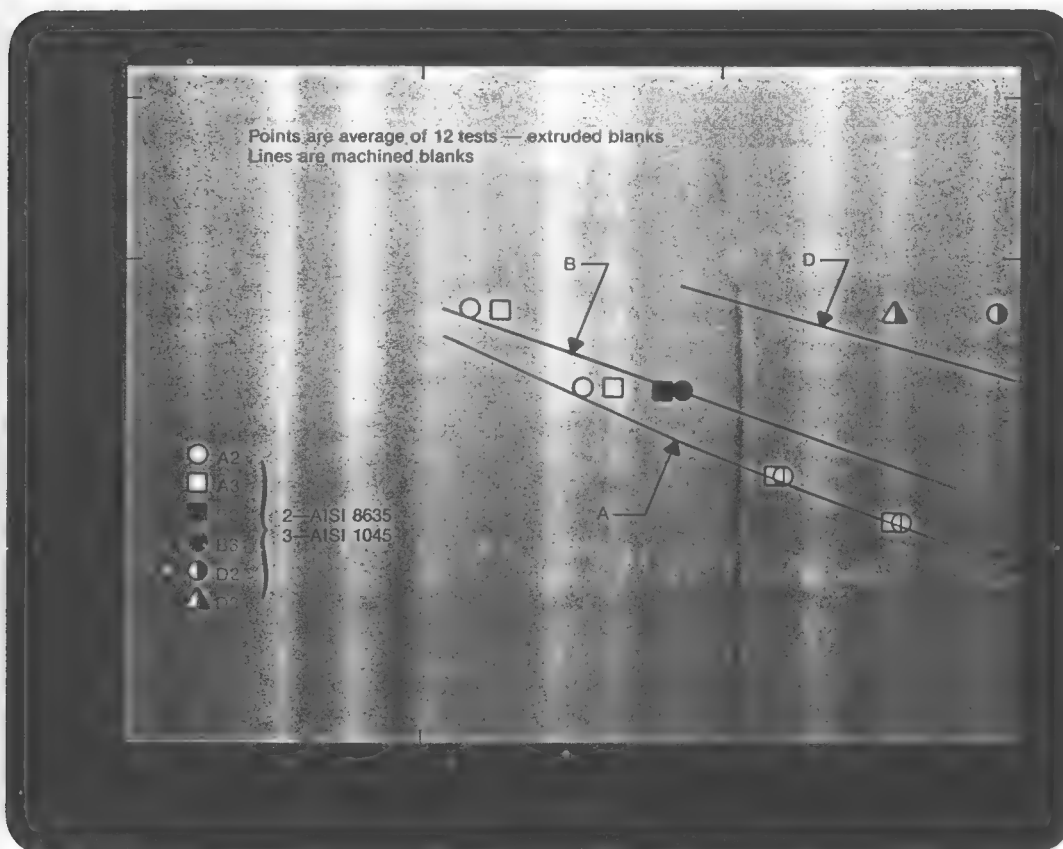


Figure 6. Comparison between extruded and machined blanks and between AISI 1045 and AISI 8635.

whether the coupling was extruded prior to cutting of the thread, and whether AISI 1045 or AISI 8635 was used. However, the fatigue life of a fully cold-worked threaded coupling could be extended by use of blanks which had been extruded prior to the thread forming process. Also, for such a thread, AISI 8635 was found to be superior to AISI 1045 for the coupling material.

All fatigue testing was conducted at 8 Hz or 480 cpm. In actual oil field pumping situations, the pumping frequency is much less with 0.2 Hz being quite common. To evaluate if the testing frequency was influencing the results, a series of couplings was tested at 0.2 Hz and the results were compared using standard statistical theory with the results under identical load conditions run at 8 Hz. No significant difference in the mean between the two test results was indicated.

The in-air testing program verified that the fully rolled or cold-worked thread had superior fatigue life to all other thread forms examined. While this was an important conclusion, it remained to be demonstrated if the fully rolled thread would retain its relative superiority in a hostile environment. Thus, the next set of results was obtained by cyclically loading sucker-rod couplings in a 3.5 percent NaCl solution.

Salt Water Tests

The Redwater field tests had been conducted in a "sour" well — one containing crude oil with a high concentration of hydrogen sulfide — and no effort was made to separate the effects of the hydrogen sulfide from any salt water effects. Since many wells also contain significant quantities of salt water mixed with the oil, an important objective of the test program was to separate the effects of the salt water from the effects of the hydrogen sulfide. Consequently, the first medium chosen for the corrosion fatigue testing was an aerated 3.5 percent NaCl solution, a salinity comparable to that of many North American oil fields.

Corrosion fatigue is a mechanism which affects the life of a component more severely than simply exposing it to a corrosive environment and then subjecting it to a fatigue loading. However, the effects of corrosion are time dependent, and in combination with fatigue, the cyclic rate must be chosen to enable sufficient time for the corrosion mechanism to develop before component failure occurs due to

mechanical fatigue alone. Since there is little difference in fatigue life in air whether tested at 8 Hz or 0.2 Hz, and since the cyclic rate in actual pumping situations is around 0.2 Hz, all corrosion fatigue tests were run at 0.2 Hz. It was assumed that this rate would be slow enough to enable a significant corrosion mechanism to develop and would allow comparison with the previously obtained in-air results.

The corrosion chamber was designed³ so that a corrosive medium could circulate through the center of the coupling (a practice to be avoided in the field but which provided an effective means of accelerating the corrosion fatigue process) as well as around the exterior surfaces. The corrosive medium was circulated through the system by an air jet used to entrain the fluid. The corrosion chamber for the salt water tests is shown in Figure 7. The testing machine frame was laid on its side so that any spillage would not affect the frame. Figure 8 shows the corrosion chamber positioned between the crosshead and base plate of the testing machine. Table 1 summarizes the 3.5 percent NaCl corrosion fatigue test results.

In evaluating the effect of environment on fatigue life, it is customary to compare stresses on the basis of a fixed number of cycles because an endurance limit may not exist for notched specimens and specimens fatigued in corrosive environments. Consequently, a life of 10^5 cycles was used to determine the relative merits of the different thread designs under the combined action of corrosion fatigue. Table 1 shows that the greatest reduction in corrosion fatigue stress was 26 percent for the B Series (cut and burnished thread machined on an AISI 8635 blank). The least reduction was observed for the A Series (simple cut thread). However, while the fully rolled thread suffered a 19 percent loss in corrosion fatigue stress at 10^5 cycles, its behavior in salt water at 60 ksi (414 MPa) was still superior to all other thread designs even when they were tested in air.

The most surprising result in this program was that the B Series (cut and burnished thread) indicated a 26 percent reduction in endurance stress in 3.5 percent NaCl at 10^5 cycles. This was unexpected because it was assumed on the basis of the in-air tests that the degree of improvement in the fatigue life of a threaded coupling was a function of the degree of cold working that had been used in the formation of the thread. To explain this apparent contradiction, one must first be understood that corrosion fatigue occurs in two

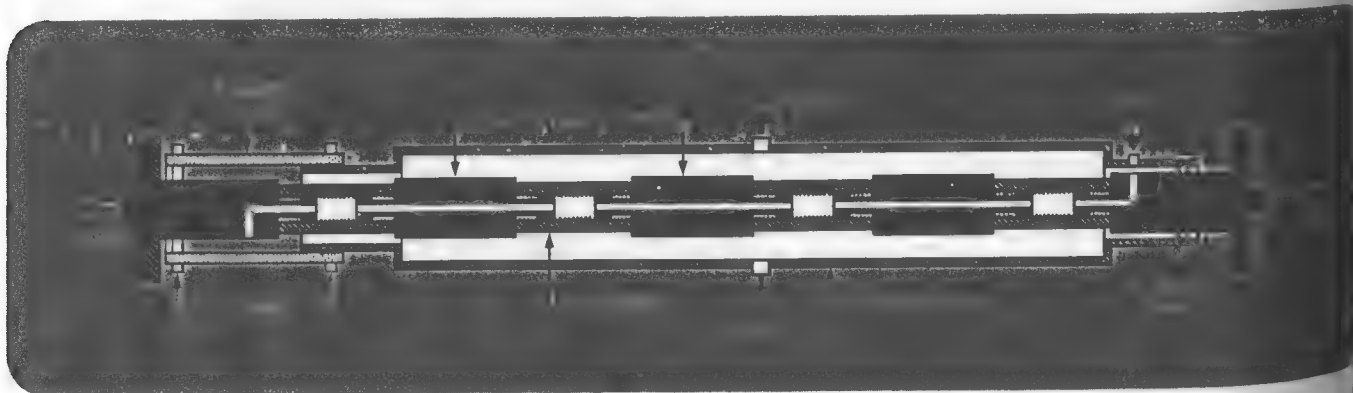


Figure 7. Salt water corrosion chamber.



Figure 8. Corrosion chamber located between crosshead and base-plate of testing machine frame.

stages. During the first stage, the surface is chemically etched, causing the formation of rounded pits, especially in the vicinity of high stresses such as the roots of threads. This process is accelerated if there are residual stresses present such as the work-hardened surfaces for the B, C and D Series couplings. As these pits deepen, they form a very high stress concentration point from which cracks can initiate due to mechanical failure. Once a crack has been initiated, the second stage of failures occurs, that of mechanical fatigue. Thus, if improvement in the fatigue life of a threaded element is to be obtained through work hardening of the surface of the threads, the depth of work hardening must be sufficiently great so that when corrosion pits are formed, they are contained within the work-hardened layer. If the corrosion pits were allowed to penetrate through this layer, then fatigue cracks would propagate uninhibited during the second stage of the corrosion fatigue process. This apparently occurred with the cut and burnished thread and explains why the fatigue life of these couplings was similar to the simple cut thread when both were fatigued in a 3.5 percent NaCl solution. The in-air results, however, showed that a small amount of work hardening of the cut and burnished thread did provide an increase in endurance stress over that of a simple cut thread.

Hydrogen Sulfide Tests

The National Association of Corrosion Engineers has proposed a corrosion medium⁴ to be used in sulfide stress cracking studies. This medium consists of a 5 percent NaCl solution in distilled water with a 0.5 percent solution of acetic acid. H₂S gas is bubbled into this solution at a constant rate. It was believed that with this solution in contact with the threaded elements under cyclic loading, the action of hydrogen sulfide would be similar to what might be present under field conditions. To overcome the potential hazards of using such a medium, an elaborate corrosion chamber and safety control system were constructed⁵. A schematic of this system is shown in

Material	Thread Type	Endurance Stress		% Reduction When Tested In Air
		Air MPa (ksi)	3.5% NaCl MPa (ksi)	
AISI 1045	A - Simple Cut	297 (43)	272 (39.5)	8
	D - Fully Rolled	459 (66.5)	365 (53)	19
AISI 8635	A - Simple Cut	303 (44)	283 (41)	7
	B - Cut and Burnished	372 (54)	276 (40)	26
	D - Fully Rolled	510 (74)	414 (60)	19

Table 1. Endurance stress at 10⁶ cycles for 3.5% NaCl environment.

Figure 9 and a general photograph of the overall testing apparatus is shown in Figure 10. This system provided the means to introduce H_2S gas into the hydrogen sulfide solution, and at the same time, circulate it around and through the threaded elements which were undergoing axial fatigue. The axial corrosion chamber was similar to that used for the 3.5 percent NaCl tests except that in place of the perspex tube, a stainless steel tube with a rubber bellows was used.

For this testing program, the simple cut thread and fully cold rolled thread were evaluated using AISI 8635 as the base material. Figures 11 and 12 summarize the corrosion fatigue results. For comparison, the results obtained under a 3.5 percent NaCl solution are also provided. Both Figures 11 and 12 show that the threaded elements deteriorated the most under the action of H_2S corrosion fatigue. For comparison of the two thread types Table 2 gives the endurance stress based on a fatigue life of 10^5 cycles. It is clear that the fully rolled or cold worked thread is superior. Even when the endurance stress was reduced by 38 percent when fatigued in the H_2S environment, the fully rolled thread had a higher endurance stress than a simple cut thread when fatigued in air.

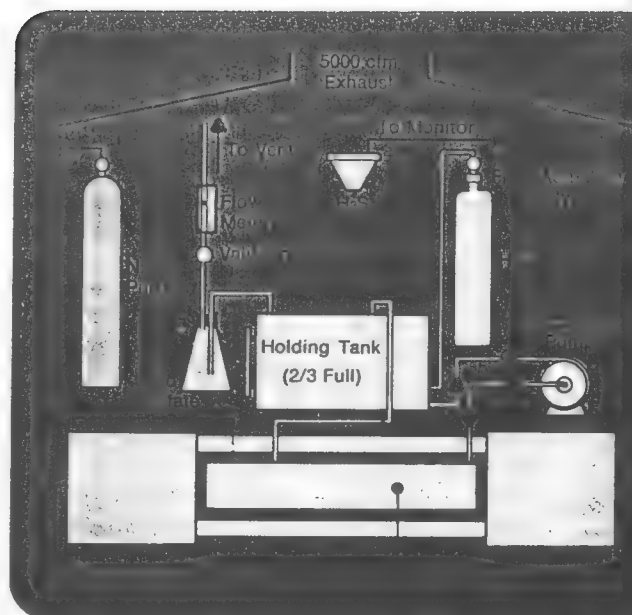


Figure 9. Schematic of H_2S corrosion fatigue facility.

Figure 10. Overall view of corrosion fatigue apparatus.

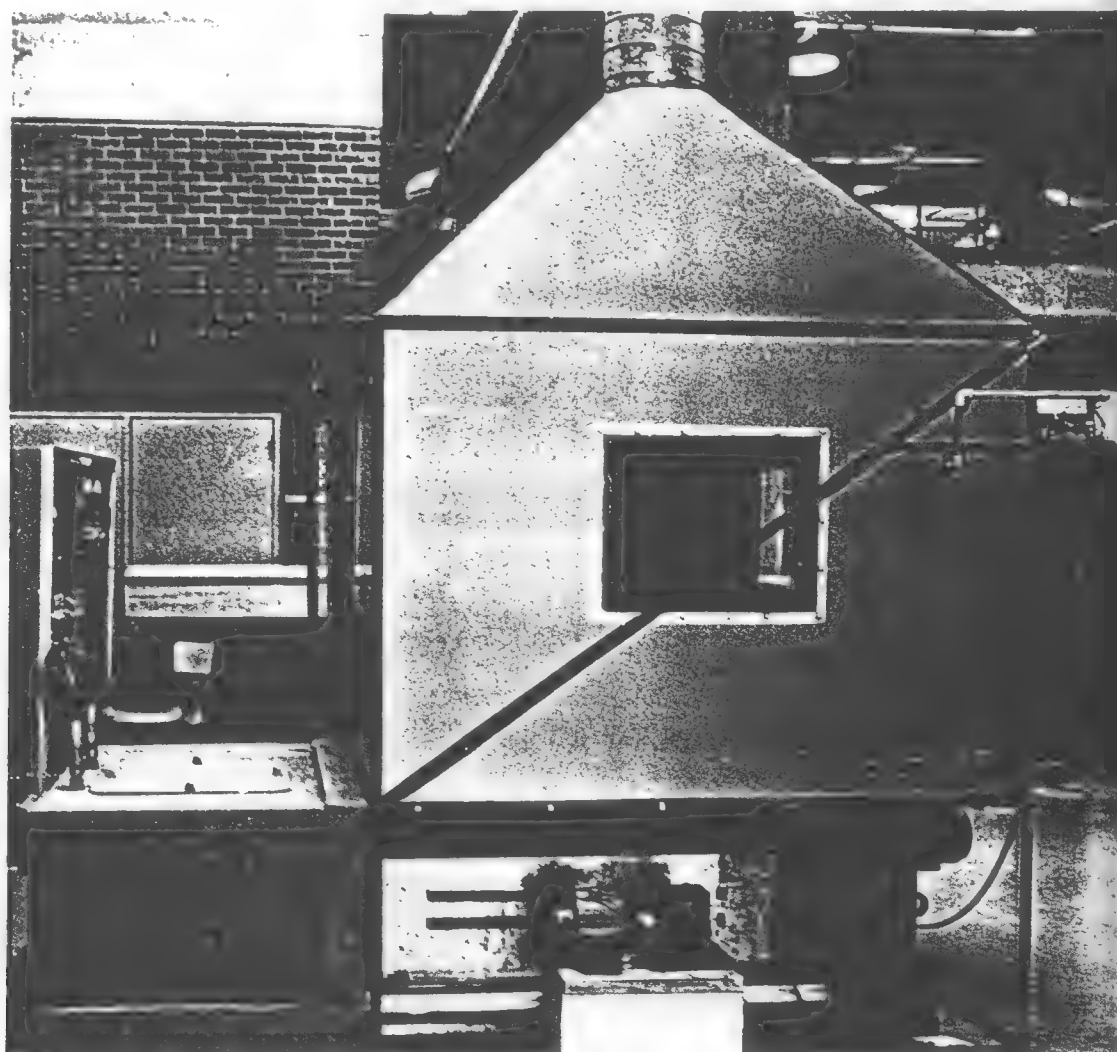


Figure 11. Corrosion fatigue results for simple cut thread.

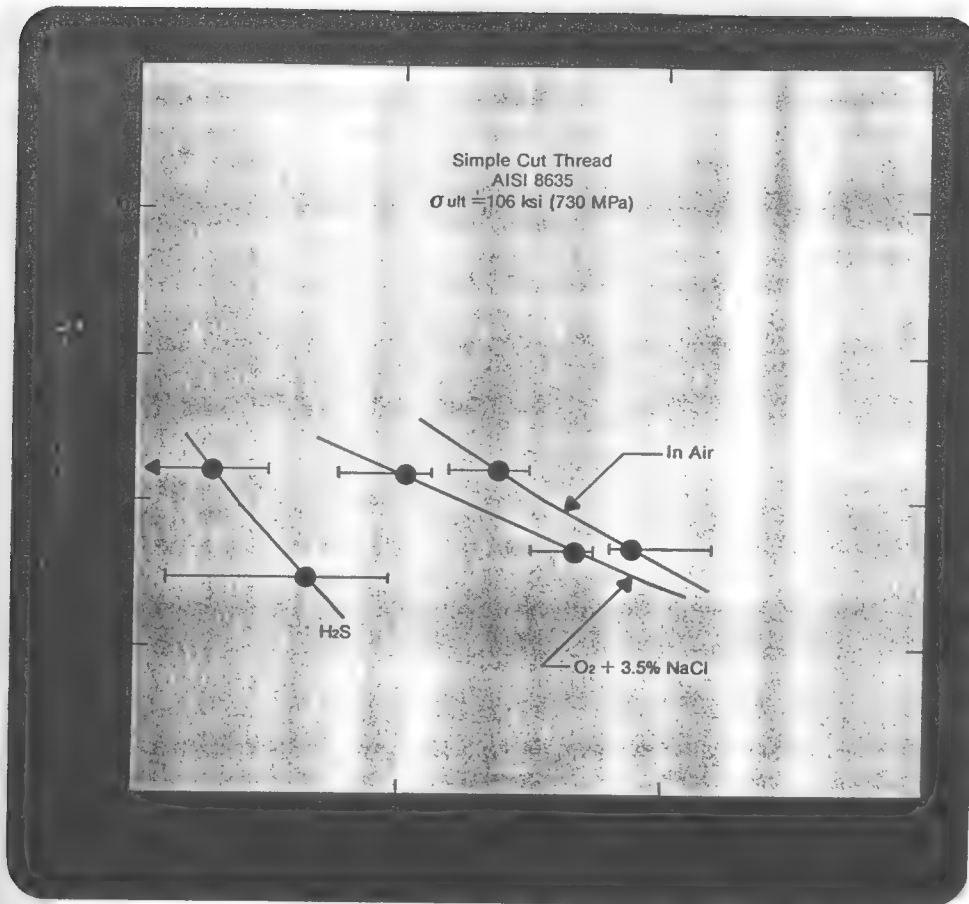
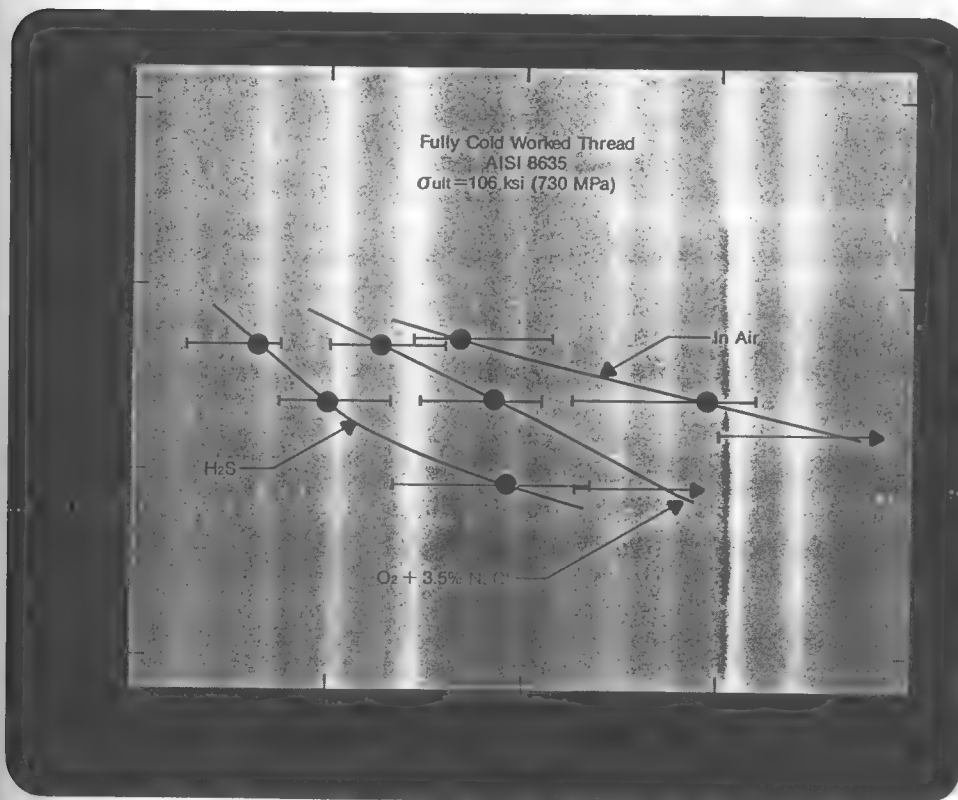


Figure 12. Corrosion fatigue results for fully cold rolled thread.



Testing Environment	Endurance Stress at 10 ⁵ Cycles MPa (ksi)	Reduction from Fully Rolled Thread When Testing in Air - %
Fully Rolled Thread — AISI 8635		
Air	510 (74)	0
N ₂ + CH ₃ COOH + 5% NaCl	434 (63)*	15
O ₂ + 3.5% NaCl	414 (60)	19
H ₂ S + CH ₃ COOH + NaCl	317 (46)	38
Simple Cut Thread - AISI 8635		
Air	303 (44)	41
O ₂ + 3.5% NaCl	290 (42)	44
H ₂ S + CH ₃ COOH + 5% NaCl	< 276 (40)*	> 73
*Estimates		

Table 2. Endurance stress at 10⁵ cycles for four different environments.

Summary

The objectives of this testing program were achieved. An accelerated testing program was developed under controlled laboratory conditions which provided a precise method of comparatively evaluating a series of different thread designs under a variety of environmental conditions. The results showed that the fully rolled or cold-worked thread was the superior thread design compared to all other types evaluated. While the production of fully rolled internal threads provided some manufacturing difficulties, notably variations in quality control and excessive tap wear, the superiority of the rolled thread was established. As a result of this testing program, for one manufacturer at least, the fully rolled thread became the standard internal thread for all sucker-rod couplings produced.

Acknowledgments

The authors express their sincere appreciation to the Steel Company of Canada Limited for their assistance with this

project and to the National Research Council of Canada who supported this project under the auspices of grants nos. A-2705 and A-7514.

References

1. Bellow, D. G. and Faulkner, M. G., "Fatigue of Threaded Sucker-Rod Couplings," *Jour. Can. Pet. Tech.*, Vol. II, No. 1, Jan-Feb. 1972, pp. 69-74.
2. Bellow, D. G. and Faulkner, M. G., "Fatigue of Internally Threaded Machine Elements," *Trans. Can. Soc. Mech. Eng.*, Vol. 2, No. 2, 1973-74, pp. 63-69.
3. Bellow, D. G. and Faulkner, M. G., "Corrosion Fatigue of Cold Worked Threaded Elements," *Proc. 2nd Symp. on Appl. of Solid Mech.*, Univ. McMaster Press, 1974, pp. 223-142.
4. "Proposed NACE Standard for Testing of Metals for Resistance to Sulfide Stress Corrosion," T-1F-9, National Assoc. of Corrosion Engs., 1971.
5. Bellow, D. G. and Faulkner, M. G., "Salt Water and Hydrogen Sulfide Corrosion Fatigue of Work-Hardened, Threaded Elements," *Jour. of Testing and Eval. JTEVA*, Vol. 4, no. 2, 1976, pp. 141-147.

D. G. Bellow¹ and M. G. Faulkner¹

Salt Water and Hydrogen Sulfide Corrosion Fatigue of Work-Hardened, Threaded Elements

REFERENCE: Bellow, D. G. and Faulkner, M. G., "Salt Water and Hydrogen Sulfide Corrosion Fatigue of Work-Hardened, Threaded Elements," *Journal of Testing and Evaluation*, JTEVA, Vol. 4, No. 2, March 1976, pp. 141-147.

ABSTRACT: This work describes the results of a laboratory testing program undertaken to evaluate the merits of work-hardened, threaded machine elements when subjected to axial fatigue in the presence of a corrosive environment. The experimental apparatus is described, including details of the corrosive mediums. The most damaging corrosive medium consisted of a salt water solution through which hydrogen sulfide gas was bubbled. Lower corrosion fatigue damage was noted for aerated salt water and the least occurred for a deaerated salt water solution. The corrosion fatigue results are compared with results obtained in air for simple cut threads and fully cold-worked or rolled threads formed on AISI 8635 steel. The results show that at a life of 10^5 cycles the fully cold-worked threaded element had an endurance stress of 74 ksi (510 MPa) compared with 44 ksi (303 MPa) for the simple cut threaded element. Under the combined action of corrosion fatigue in the presence of a hydrogen sulfide saline solution these values were reduced to 46 ksi (317 MPa) and less than 20 ksi (138 MPa), respectively, which indicated that the fully cold-worked, threaded element was superior to all thread forms evaluated under a variety of environmental conditions.

KEY WORDS: corrosion, fatigue, work hardening, threads, threaded elements, durability, stresses, hydrogen sulfide, salt water, oxygen cell corrosion, hydrogen embrittlement

Many oilfields contain large quantities of contaminants which are unavoidably pumped out of the wells with the crude oil. The contaminants, which can vary from one well to another, consist of mixtures of water, salt, carbon dioxide, and hydrogen sulfide (H_2S). When threaded machine elements such as sucker rods and couplings are subjected to cyclic loading in the presence of any or all of these contaminants, premature failure can occur as a result of corrosion fatigue. Initially, an attempt was made to evaluate the effects of a corrosive environment on the fatigue life of such threaded connections at a producing oil well site. The test well had a concentration of 3% H_2S gas in solution in the crude oil. After cycling a variety of threaded elements at a rate of 10 cycles/min for a period of 18 months, no failures had occurred. Since these findings were inconclusive beyond the fact that certain test components showed more deterioration than others, it was deemed desirable to accelerate the testing program in the laboratory to obtain a relative indication of the merits of the different threaded elements in a num-

ber of selected environments. This paper describes the results of the laboratory testing program.

It has been observed [1] that the fatigue life of a threaded element can be improved by cold working the threaded element onto the base material after heat treatment. Also, it has been shown [2] that resistance to stress corrosion cracking of high strength bolts ($\sigma_{ult} = 260$ ksi or 1793 MPa) can be improved by cold working or rolling the threads after heat treatment. In the 1960s the petroleum industry introduced the rolled thread on the pin end of the sucker rod and for the internal thread of the mating coupling. In this application the rolled thread was acclaimed [3] as providing greater hardness and strength at the critical root area of the thread, giving a smoother thread form and reducing the susceptibility to corrosion. However, the extent of improvement of a rolled thread over that of other types and the effects of corrosion fatigue were yet to be established.

One of several studies [4] undertaken to evaluate the effects of work hardening on the fatigue life of internally threaded machine elements of the type used in sucker rod couplings consisted of evaluating the fatigue notch factor K_f for elements whose threads were produced by five different manufacturing techniques: simple cut, simple cut with a keyhole at the root of the thread, simple cut and burnished, cut and partially rolled, and a fully cold-worked or rolled thread. The results clearly showed the superiority of the fully cold-worked thread which has a fatigue notch factor of 1.4, whereas for the simple cut thread the fatigue notch factor was almost double at 2.8 (Fig 1).

In another study [5], two different types of steels were evaluated: AISI 1045 and AISI 8635 (see Table 1). It was found that there was some difference in the fatigue life between the two steels when a simple cut thread was used, but the greatest improvement was observed for the fully cold-worked thread formed on AISI 8635. All the testing was conducted in air; the evidence indicated that the fatigue life of threaded elements could be improved by cold working the thread, the amount of improvement being a function of the depth of work hardening achieved during the thread forming process. For all thread forms evaluated the coupling blanks were machined and then heated to 1550°F (843.4°C), quenched in oil, and then tempered for one hour at 1300°F (704.4°C) to form a fine-grained, martensitic structure. All threads were formed after heat treatment of the blanks.

This program also evaluated the effects of the fatigue properties of the grain orientation in the base material prior to the thread forming process. Threads were formed on base materials that had been annealed and then machined and on base materials that had been extruded prior to the thread forming process.

¹ Professor and associate professor, respectively, University of Alberta, Edmonton, Alberta, Canada.

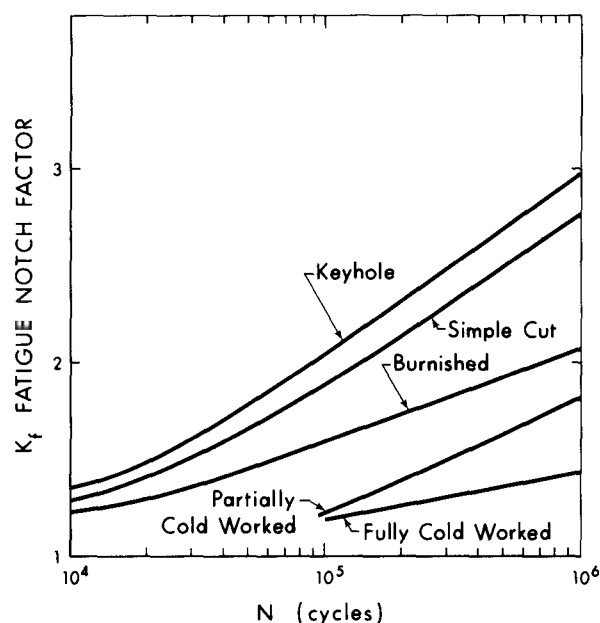


FIG. 1—Fatigue notch factor K_f for five thread forms (AISI 8635), Ref 4.

The results, summarized in Fig. 2, show that there was little difference between the fatigue life of a coupling whose thread was formed by a simple cutting process, even with a slight degree of cold working as in the case of burnished thread, whether the coupling blank was extruded or not, and whether or not AISI 1045 or AISI 8635 steel was used. However, the fatigue life

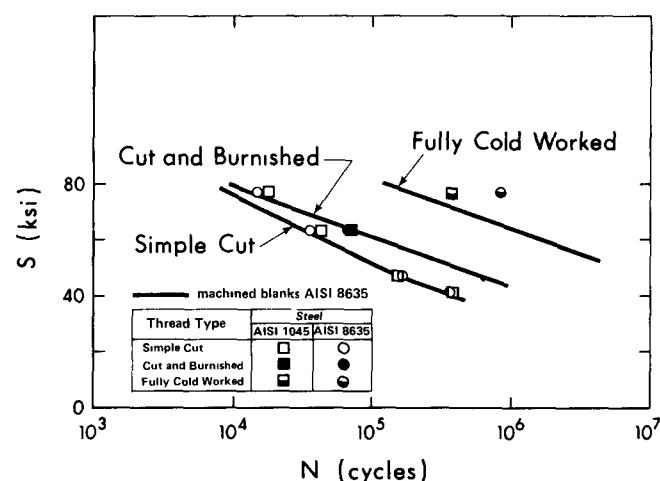


FIG. 2—Comparison of fatigue life between machined blanks and extruded blanks (AISI 1045 and AISI 8635), Ref 5.

slightly better results were obtained when AISI 8635 was used as the base material.

There have been many studies discussing the factors influencing the effects of corrosion on the static and fatigue strength of metals. To name a few, there are reports on the effect of environment [6-8], pH level [9-11], microstructure and heat treatment [7,12,13], and chemistry [14,15]. Although France [9] investigated the effects of plastic deformation on the corrosion of steel most studies have been based on results obtained from standard test specimens rather than on work-hardened machine elements.

Salt Water Tests

The influence of salt water corrosion fatigue on the endurance stress of threaded elements was the first mechanism to be evaluated in the laboratory. While corrosion fatigue affects the life of a component more severely than simple exposure to a corrosive environment, the effects of corrosion are very much time dependent. For laboratory purposes the cyclic rate at which the load is applied can be controlled, but it must be set at a sufficiently low value to enable an effective corrosion mechanism to develop before component failure occurs due to the effects of mechanical fatigue alone. In the previous work reported in the literature [4,5] a cyclic rate of 8 Hz (480 cycles per minute) was applied to the threaded elements. It was shown [4] that there was no significant difference (using a standard t test) in the fatigue results in air when cycled at rates of 8 Hz or 0.1 Hz, the latter being approximately the rate used in petroleum pumping situations. To coincide with field conditions and at the same time allow sufficient time for an effective corrosion fatigue mechanism to be established, all corrosion fatigue tests were conducted at 0.1 Hz.

It was believed by many in the industry that of the sucker rod-coupling combination, the coupling would be the most vulnerable to fatigue even though, according to specifications established by the American Petroleum Institute,² the net cross-sectional area of the coupling exceeds that of the mating pin of the sucker rod. To localize failures in the coupling for laboratory purposes, the net cross-sectional area was reduced from a nominal 0.6916 in.² (4.4619 cm²) (3/4-in. or 19.05-mm rod size) to 0.4914 in.² (3.1703 cm²). The reduction in outside diameter was achieved by centerless grinding and did not influence initiation of fatigue cracks, which always occurred on the inside of the coupling at the root of one of the threads located opposite the first thread of the pin.

The corrosion chamber designed for salt water was described in Ref 15 and consisted of a cylindrical chamber into which a coupling-rod string was inserted. An air jet was built into the corrosion chamber to maintain a constant supply of oxygen to support the corrosion mechanism as well as to circulate the

TABLE 1—Chemical composition of base material.

AISI Type	$\sigma_{ultimate}$, ksi (MPa)	C	Mn	P	S	Si	Ni	Cr	Mo
1045	109 (751.5)	0.43-0.50	0.60-0.90	0.040	0.050
8635	106 (730.8)	0.33-0.38	0.70-0.90	0.040	0.040	0.20-0.35	0.40-0.70	0.40-0.60	0.15-0.25

of a fully cold-worked, threaded coupling was extended by using an extruded blank rather than a machined blank and

² API Production Div., Specification for Sucker Rods, Standard 11B, Jan. 1970.

corrosion medium around the threaded elements. The corrosion medium was a 3.5% sodium chloride (NaCl) solution in distilled water with an initial pH of 9.5 which decreased to a pH of 7.5 in a 24-h test period. All corrosion fatigue tests were conducted at room temperature, $24 \pm 3^\circ\text{C}$ (70 to 80°F).

A summary of the salt water corrosion fatigue results for AISI 8635 is shown in Fig. 3, where it is seen that at a life of

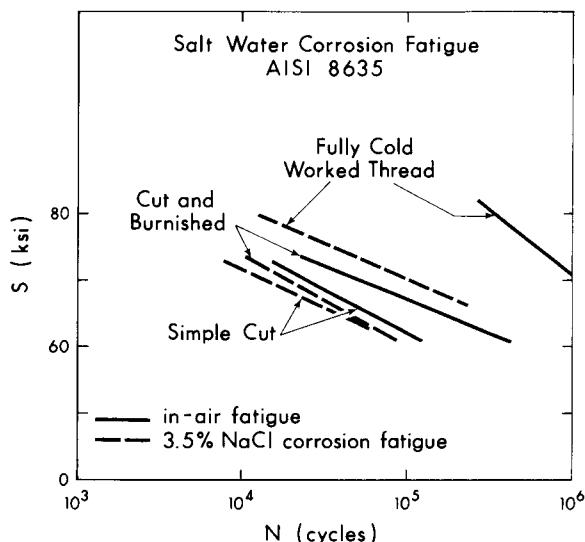


FIG. 3—Salt water corrosion fatigue tests (AISI 8635), Ref 6.

10^5 cycles, the reduction in endurance stress for the simple cut thread when compared with the in-air results was approximately 6%, and for the fully cold-worked thread the reduction was approximately 19%. Similar observations were obtained for coupling blanks made from AISI 1045 steel [14]. Even though the percentage reduction was greater for the fully cold-worked thread, the actual endurance stress of the fully cold-worked thread was greater than that for the simple cut thread. For the cut and burnished thread no significant improvement was observed over that of the simple cut thread when cyclically loaded in the salt water solution.

This result was unexpected in that, when tested in air, the cut and burnished thread showed a 23% improvement over that of the simple cut thread. The poor performance of the cut and burnished thread was explained [14] by considering that the corrosion fatigue mechanism takes place in two stages. During the first stage, a chemical etching away of the surface in the vicinity of high stress areas causes rounded corrosion pits to form. As these pits deepen due to crevice corrosion, they form very high stress raisers from which cracks can initiate due to mechanical fatigue. Once such cracks occur, then the failure mechanism is more mechanical fatigue. When corrosion pits are allowed to penetrate through the work-hardened layer induced on the surface of the threads, fatigue cracks will propagate uninhibited during the second stage of the corrosion fatigue process. If improvement in the fatigue life of a threaded element is to be obtained through work hardening of the thread surfaces, then the depth of work hardening must be sufficiently great to ensure that when the corrosion pits are formed, they are contained within the work-hardened layer. The insufficient depth of work hardening of the burnished thread allowed the

corrosion pits to penetrate into the annealed portion of the base material.

Hydrogen Sulfide Tests

The National Association of Corrosion Engineers proposed [15] a corrosion medium to be used in sulfide stress cracking studies. This medium consisted of a 5% NaCl solution in distilled water with a 0.5% solution of acetic acid yielding a starting pH of about 4. Into this solution H_2S gas was bubbled at a constant rate.

Although this technique posed certain safety problems it was believed that the contact the hydrogen sulfide would make with the threaded elements was similar to what might be anticipated under field conditions. A corrosion apparatus, shown schematically in Fig. 4, was designed to provide a means by

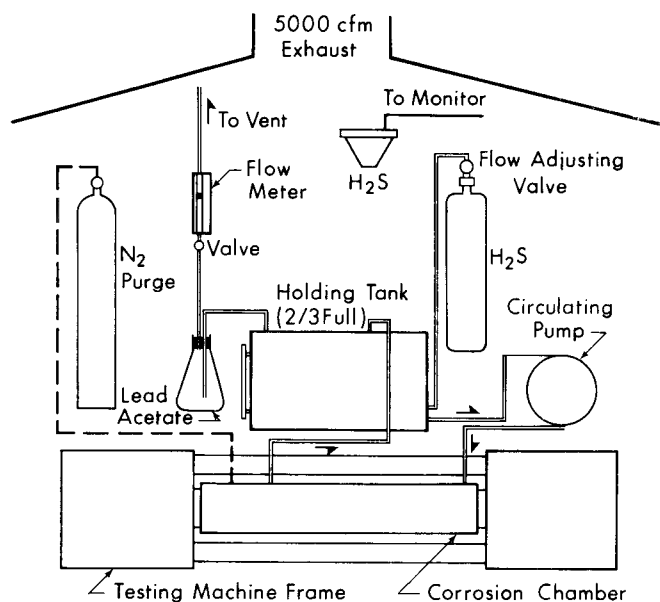


FIG. 4—Hydrogen sulfide corrosion fatigue apparatus.

which H_2S gas would be introduced into solution and, at the same time, circulate this solution around and through the threaded elements which were undergoing axial fatigue.

Figure 5 shows the stainless steel (Type 316) corrosion chamber into which the threaded test couplings and mating pins were inserted. This was placed between the crossheads of the testing frame of a closed-loop servohydraulic fatigue machine. The entire frame and all corrosion chamber components, except the electrical motor of the circulating pump, were enclosed in a sheet steel corrosion room, the top of which was connected to a 5000 ft³/min (140 m³/min) continuous exhaust fan. The room air was continuously monitored for H_2S contamination and when a certain minimum value was exceeded an alarm would ring and completely shut down the apparatus.

The corrosion fatigue test was started by purging the apparatus with nitrogen to completely remove any entrapped air and then saturating it with H_2S for 15 min. Once the cyclic loading began this saturation was maintained by continuously bubbling H_2S through the solution at a rate of approximately 5 to 10 ml/min

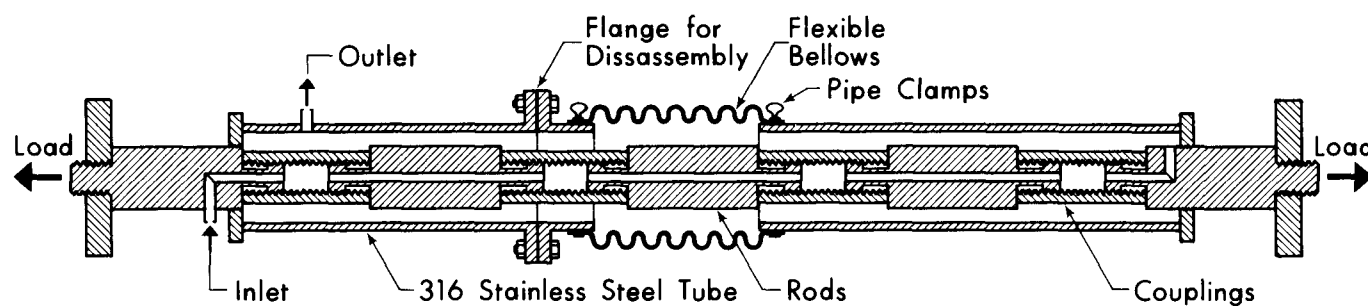


FIG. 5—Hydrogen sulfide corrosion chamber details.

throughout the duration of the test. The testing temperature was $24 \pm 3^\circ\text{C}$ (70 to 80°F).

The H_2S solution had a nominal starting pH of 4, but for some batches it varied within the range 3.6 to 4.4. During any given test program the pH remained relatively constant, never varying by more than a quarter of a point from the initial value.

Test couplings and pins were assembled to form a string of four couplings and five pins (see Fig. 5). Each coupling-pin joint was hand tightened and then torqued with a wrench so that the relative circumferential displacement between the shoulder of the coupling and the shoulder of the pin was $\frac{1}{4}$ in. (6.35 mm). The axial cyclic load was applied so that the alternating tensile stress varied from a minimum of 6.1 ksi (42.06 MPa) to a maximum stress in the range 40 to 77 ksi (275.8 to 530.9 MPa). The minimum stress was chosen to simulate a dead load that is present when a coupling-pin combination is in service in a well.

The test was run until a fatigue crack initiated in one of the four couplings causing the displacement amplitude to exceed predetermined limits set on the electronic control system of the fatigue machine. When these limits were exceeded the machine shut down, shutting off the H_2S gas supply and stopping the circulating pump of the corrosion chamber.

Results

The H_2S corrosion fatigue testing program evaluated simple cut threads and fully cold-worked threads produced on machined coupling blanks made from AISI 8635 steel. The stress-cycles to failure (S-N) curves for the simple cut thread are shown in Fig. 6 and for the fully cold-worked thread, in Fig. 7. For comparison, the fatigue results for the coupling tested in a 3.5% NaCl solution are also shown. The curves have been drawn through the median of at least twelve test couplings. The horizontal bars indicate the scatter of data for a given test condition.

Both Figs. 6 and 7 show that the threaded elements deteriorated most under the action of H_2S corrosion fatigue. In Fig. 7 one plotted point (at a maximum stress of 77 ksi or 530.9 MPa) is shown when the H_2S gas was replaced with N_2 in the 5% NaCl and 0.5% CH_3COOH solution. This environment was not as severe as the aerated 3.5% NaCl solution, clearly showing the effect oxygen has on the corrosion process.

Figure 6 shows that when the simple cut thread was axially loaded between 6.1 and 63 ksi (59.8 and 617.8 MPa), the number of cycles to failure in air was reduced 58% when the thread was cycled in the presence of a 3.5% NaCl solution and that

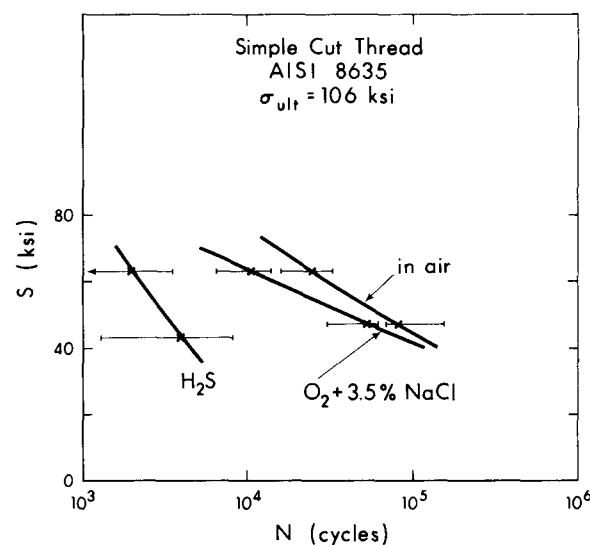


FIG. 6—S-N curves for the simple cut thread under the action of corrosion fatigue (AISI 8635).

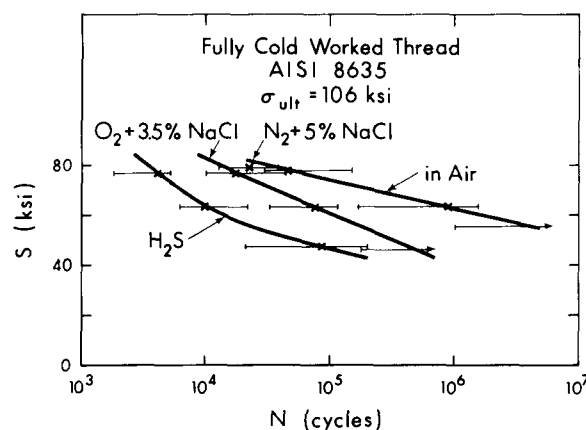


FIG. 7—S-N curves for the fully cold-worked thread under the action of corrosion fatigue (AISI 8635).

this number of cycles was further reduced by 92% when the thread was cycled in the presence of H_2S . Similar observations in Fig. 7 show that for the fully cold-worked thread the reduction in life from that in air was 93% for the NaCl solution and 98% for the H_2S environment. As might be expected, the cold-worked thread was more susceptible to corrosion fatigue and

yet, at 63 ksi, the cold-worked thread had a superior life to that of the simple cut thread under similar conditions of load and environment. For comparison, a life factor (or factor of merit) was defined as the ratio of the number of cycles to failure for a particular thread form under specified environmental conditions to the number of cycles to failure for the simple cut thread when tested in air. Even though the life factor for the fully cold-worked thread was reduced from 37 to 3 when tested in the NaCl solution (Table 2), it still had a life three times greater than that of the simple cut thread when tested in air.

TABLE 2—Life factors for cut thread and fully cold-worked thread at 63 ksi (434.4 MPa) for AISI 8635 steel, based on unity life for cut thread tested in air.

Thread Type	Environment	Life Factor
Cold worked	air	37
Cold worked	3.5% NaCl + O ₂	3.1
Simple cut	air	1.0
Simple cut	3.5% NaCl + O ₂	0.43
Cold worked	H ₂ S + CH ₃ COOH + 5% NaCl	0.41
Simple cut	H ₂ S + CH ₃ COOH + 5% NaCl	0.08

For notched specimens or specimens subjected to a corrosive environment, an endurance limit does not exist. Under such circumstances an endurance stress is defined as the stress at a specified finite life on the S-N fatigue curve. From the data plotted in Figs. 6 and 7 the endurance stresses were obtained at a life of 10⁷ cycles, and these values have been presented in Table 3. The percentage reduction in endurance stress was calculated on the basis of the fully cold-worked thread when fatigued in air. The results show the superiority of the cold-worked thread, and even though the endurance stress at 10⁷ cycles was reduced by 38% when fatigued in the H₂S environment, it still had a higher endurance stress than a simple cut thread when fatigued in air. From Figs. 6 and 7 it is apparent that different percentage reduction values would be computed if a different fatigue life were chosen. Nevertheless, the relative merits of each thread type, when fatigued in a particular environment, would probably be about the same as given in Table 3.

The effect of H₂S in combination with fatigue loading can be observed from the photomicrograph shown in Fig. 8. This figure shows the attack that took place at the root of a fully



FIG. 8—Photomicrograph of cold-worked thread when fatigued in hydrogen sulfide; original magnification, $\times 200$.

cold-worked thread. Unlike the more rounded pitting action that occurs with a salt water environment (Fig. 9), the H₂S attack produced sharp notches as well as what appears to be delaminations or stress corrosion cracks in the longitudinal direction of the coupling. At first it was thought these cracks were peculiar to the hydrogen environment but they were also observed, to a lesser extent, with the aerated NaCl environment. Although no fatigue cracks causing component failure were observed at the ends of the delaminations, such corrosion contributes to an overall deterioration of the thread structure.

Discussion

If a thread is fully cold worked, or rolled, onto a base material after all heat treatment has taken place, there is a marked improvement in the fatigue life of that element over that of a simple cut thread. The results shown in Table 2 indicate that the improvement in fatigue life is 37 times greater than what would be expected from a simple cut thread. However, while the fully cold-worked thread suffers greater corrosion damage than does the simple cut thread, the fully cold-worked thread has the capacity to withstand severe corrosive attack and be

TABLE 3—Endurance stress based on a fatigue life of 10⁸ cycles.

Testing Environment	Stress at 10 ⁸ Cycles, ksi (MPa)		Reduction from Cold- Worked Thread Testing in Air, %
Fully cold-worked thread			
Air	74	(510.2)	0
N ₂ + CH ₃ COOH + 5% NaCl	63 ^a	(434.4)	14.9
O ₂ + 3.5% NaCl	60	(413.7)	18.9
H ₂ S + CH ₃ 1/4 cooh + 5% NaCl	46	(317.2)	37.8
Simple cut thread			
Air	44	(303.4)	40.5
O ₂ + 3.5% NaCl	41.5	(286.1)	43.9
H ₂ S + CH ₃ COOH + 5% NaCl	<20 ^a	(137.9)	>73

^a Estimates.

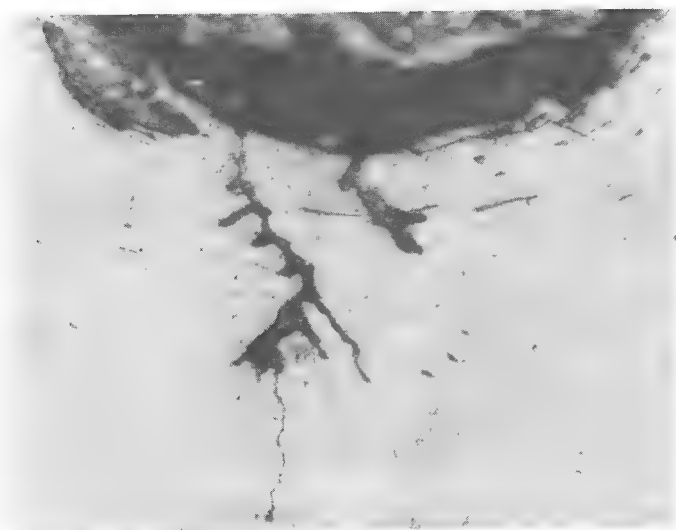


FIG. 9—Photomicrograph of cold-worked thread when fatigued in salt water; original magnification, $\times 200$.

superior to that of a simple cut thread under the same environmental conditions.

For the salt water corrosion tests the pH varied in the range $7.5 < \text{pH} < 9.5$, well below the α -point [10], thereby providing an environment conducive to oxygen cell corrosion. For the hydrogen sulfide tests, the pH was in the range of $3.8 < \text{pH} < 4.4$, which would indicate, according to Gutzeit [11], that the environment was conducive to causing severe hydrogen embrittlement.

Mehdizadeh et al [6] reported that for an AISI 1036 steel a 5% NaCl and H_2S environment produced only a mild corrosive attack. They found that an endurance limit was obtained in the absence of air. The experiments reported in this paper do not confirm these observations; in fact, it was found that the 5% NaCl and H_2S environment was by far the most corrosive medium evaluated. Mehdizadeh observed bending fatigue in the corrosive environment, whereas the work reported in this paper was on axial fatigue. The differences in observations may also be because the steels were not the same in both studies.

Although a discussion of the quality control of the product is somewhat outside the scope of this paper, it was observed that the degree of cold working for the rolled thread could vary from specimen to specimen. When this happened it caused more scatter in the fatigue data than was anticipated. This problem was traced to the manufacturing technique where it was found that the tap wear, which was greater for the fully rolled thread than for the simple cut thread, was causing inconsistent depth of cold working at the root of the thread. Once recognized, the problem was soon overcome with improved production practices.

Conclusions

Based on the results presented in this paper plus those summarized from previous studies and reported in more detail elsewhere, the following conclusions can be made. While these conclusions are based on threaded elements formed on either AISI 1045 or AISI 8635 steel, it is believed the results are applicable to a general class of threaded elements made from

medium strength steels when subjected to cyclic loading in the presence of either a salt water environment or an H_2S environment.

1. For the ranges of pH observed in the testing program it was found that the corrosion fatigue mechanism of salt water is different from H_2S . The former was essentially an etching away of the metal surface in the vicinity of high stress areas, producing rounded pits. H_2S in combination with fatigue produced sharp pits which caused considerably greater deterioration of the fatigue life of the threaded element.

2. Hydrogen sulfide in combination with fatigue may cause severe delaminations along lines of high residual shear stress in threads which have been formed by a cold working or rolling process.

3. Of all the thread types evaluated, the fully cold-worked thread had the highest endurance stress under the action of either salt water corrosion fatigue or H_2S corrosion fatigue.

Acknowledgments

The authors wish to express their appreciation to Messrs. E. F. Fenske and J. H. Marshall of The Steel Company of Canada Ltd. who arranged for the supply of materials and financial assistance received in support of this project. Financial support from the National Research Council of Canada under grant Nos. A-2705 and A-7514 is also gratefully acknowledged.

References

- [1] Baumgartner, T. C. and Sproat, R. L., "Basic Design and Manufacturing of Aircraft Fasteners for Use up to 1600°F" in *Fasteners Symposium*, Standard Steel Press, 1957.
- [2] Lin, C. S., Laurilliard, J. J., and Hood, A. C., "Stress Corrosion Cracking of High Strength Bolting" in *Stress Corrosion Testing, ASTM STP 425*, American Society for Testing and Materials, Philadelphia, 1967, pp. 84-98.
- [3] Crosby, G. E., "Fully Rolled Thread: Breakthrough in Rod Couplings," *Petroleum Engineering*, July 1970, p. 70.
- [4] Bellow, D. G. and Faulkner, M. G., "Fatigue of Threaded Sucker Rod Couplings," *Journal of Canadian Petroleum Technology*, Vol. 11, No. 1, Jan.-Feb. 1972, pp. 69-74.
- [5] Bellow, D. G. and Faulkner, M. G., "Fatigue of Internally Threaded Machine Elements," *Transactions of the Canadian Society for Mechanical Engineering*, Vol. 2, No. 2, 1973-1974, pp. 63-69.
- [6] Mehdizadeh, P., McClasson, R. L., and Landers, J. E., "Corrosion Fatigue Performance of a Carbon Steel in Brine Containing Air, H_2S and CO_2 ," *Corrosion*, Vol. 22, No. 12, Dec. 1966, pp. 325-335.
- [7] Dvoracek, L. M., "Corrosion Fatigue Testing of Oil Well Sucker Rods," *Material Protection and Performance*, Vol. 12, No. 9, Sept. 1973, pp. 16-19.
- [8] Prowse, R. L., and Wayman, M. L., "Effect of Environment on the Fatigue Behavior of Medium Carbon Steel," *Corrosion*, Vol. 30, No. 8, Aug. 1974, pp. 280-284.
- [9] France, W. D., "Effects of Stress and Plastic Deformation on the Corrosion of Steel," *Corrosion*, Vol. 26, No. 5, 1970, pp. 189-199.
- [10] Radd, F. J., Crowder, L. H., and Wolfe, L. H., "Effect of pH in the Range 6.6 - 14.0 + on the Aerobic Corrosion Fatigue of Steel," *Corrosion*, Vol. 16, Aug. 1960, pp. 121-124.
- [11] Gutzeit, J., "Corrosion of Steel by Sulfides and Cyanides in Refinery Condensate Water," *Materials Protection*, Vol. 7, No. 12, Dec. 1968, pp. 17-23.
- [12] Snape, E., Schaller, F. W., and Forbes Jones, R. M., "A Method of Improving Hydrogen Sulphide Accelerated Cracking Resistance of Low Alloy Steels," *Corrosion*, Vol. 25, No. 9, 1969, pp. 380-388.

- [13] Hill, M., Kawasaki, E. P., and Kronbach, G. E., "Evidence of the Sensitivity to Rapid Failure in an H₂S Environment," *Materials Protection and Performance*, Vol. 11, No. 1, Jan. 1972, pp. 19-22.
- [14] Bellow, D. G., and Faulkner, M. G., "Corrosion Fatigue of Cold Worked Threaded Elements," *Proceedings, 2nd Symposium on Applications Solid Mechanics*, University of McMaster Press, 1974, pp. 123-142.
- [15] "Proposed NACE Standard for Testing of Metals for Resistance to Sulphide Stress Corrosion," T-1F-9, *National Association of Corrosion Engineers*, 1971.

Kinetic Analysis of a Golf Swing

DAVID R. BUDNEY AND DONALD G. BELLOW

A dynamic model of the golf swing is used to analyze the effect changes of "swing weight" and club type have on the forces, power, and work exerted by a golfer. The dynamic model demonstrates the significance of various equipment types as well as some modifications to the equipment. The model is also used to show how club head speed and the forces exerted by the golfer are changed by a slight modification to the kinematics of a real golf swing. On the basis of mathematical analysis, it is shown that the effect of drag on a golf swing is negligible, and that adding weight to the handle of a club to maintain "swing weight" has little effect on the forces exerted by a golfer. It is also shown that for the same club head speed, a graphite driver requires less effort than an ordinary driver.

It has been shown (Budney & Bellow, 1978) that a dynamic model of the golf swing can be successfully employed to evaluate arm forces, wrist torque, and power as applied by a variety of golfers ranging from amateurs to professionals. This same model can also be used to evaluate the various methods employed by manufacturers and professionals alike to improve the golf swing. For example, the golf equipment industry produces a "matched" set in terms of a particular "swing weight," which is a prescribed first moment of mass of the club about a point 12 inches from the grip end of the golf club. It is a common practice to compensate for a club head that is deemed too heavy by adding weight to the handle to bring the club to within the tolerances prescribed for a "matched set." However, it is yet to be shown whether or not this procedure is relevant with respect to parameters that describe the physical effort required by the golfer.

Some manufacturers design the heads of clubs to reduce aerodynamic drag. While this obviously has advertising appeal, the actual influence of aerodynamic drag on

David R. Budney is a lecturer with the Department of Mechanical Engineering, University of Newcastle, N.S.W., Australia, 2308. Donald G. Bellow is professor and chairman of the Department of Mechanical Engineering, University of Alberta, Canada, T6G 2G8. The authors express their appreciation to the National Research Council of Canada for financial support received under grant No. A-2705.

the golf swing has not yet been critically analyzed. These and other techniques used by the industry to improve hitting power or accommodate different types of golf swings have their ardent supporters. A systematic and objective technique is required that will quantify the merits of each of these concepts so that the golfer can better judge whether or not the suggested improvements are substantive.

The purpose of this paper is to apply a dynamic model (Budney & Bellow, 1978) to a number of modifications that have been or can be made to the golf club and to evaluate the effect of these changes on the kinetics required by the golfer. The dynamic model will also be used to show the effect a slight modification to the kinematics of a known golf swing can have on club head speed and general efficiency of the application of forces to the golf club.

Theoretical Background

The basis for the dynamic model is contained in Figure 1, where it is assumed that the path of the golf swing consists of a two-element pendulum with the hands located at A, permitting the club to travel about the center of rotation O. For all values of ϕ , \overline{OA} was assumed to be constant. This was verified later by close examination of stroboscopic photographs of actual golf swings. The angle the club makes with \overline{OA} is given by θ . For any golf swing, values of ϕ and θ in terms of time throughout the downswing can be determined from stroboscopic photographs. From these data, velocities and accelerations are readily obtained.

Because the swing plane is not vertical, the camera position was chosen carefully for each golfer so as to be centered on a line perpendicular to the plane of the swing. The angle the swing plane makes with the vertical was denoted by α . Also, from observations made in the laboratory, it is reasonable to assume the motion of the golf swing is confined to a single plane.

In the analysis of Figure 1 it has been shown (Budney & Bellow, 1978) that the equations of motion of the golf club require that the forces parallel and perpendicular to the arm are given by F_{PA} and F_{AA} respectively, where

$$F_{PA} = m(g \cos \alpha \cos \phi - \ddot{x} \cos \phi - \ddot{y} \sin \phi) + F_D \sin \beta_1 \quad (1)$$

and

$$F_{AA} = m(g \cos \alpha \sin \phi - \ddot{x} \sin \phi + \ddot{y} \cos \phi) + F_D \cos \beta_1, \quad (2)$$

where F_D is the drag force acting on the club head, m is the mass of the club, β_1 is illustrated in Figure 1, and \ddot{x} and \ddot{y} are the accelerations in the x and y directions of the mass center of the club, designated as point G in Figure 1. The accelerations \ddot{x} and \ddot{y} are obtained by twice differentiating the coordinate equations

$$x = a \sin \phi + l \sin(\phi + \theta)$$

and

$$y = a \cos \phi + l \cos(\phi + \theta),$$

where a is the length of \overline{OA} (from the center of rotation to the hands) and l is the distance from point A to the center of gravity G. The torque (T) applied by the wrists to the club at point A can be shown to be given by

$$T = I_G(\ddot{\phi} + \ddot{\theta}) + ml[\ddot{y} \cos(\phi + \theta) - (\ddot{x} - g \cos \alpha) \sin(\phi + \theta)] + F_D b \cos(\theta - \beta_1), \quad (3)$$

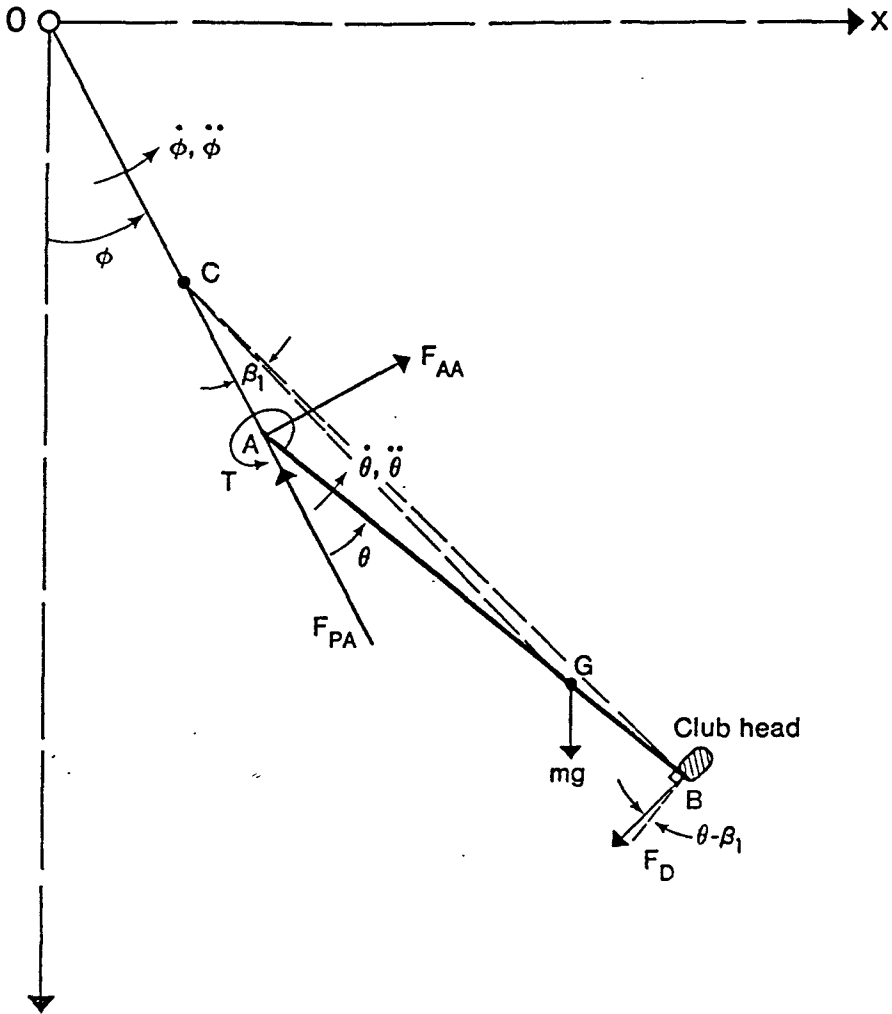


Figure 1—Dynamic model of a golf swing.

where I_G is the moment of inertia about the center of mass of the club at G and b is the distance \overline{AB} in Figure 1. This analysis assumed the golf shafts were perfectly rigid. It was found that the amount of energy required to bend the shafts to the extent observed during the downswing was negligible compared with the energy imparted to the head of the club.

Equations 1 to 3 were programed for solution on a computer for known ϕ vs. t (time) and θ vs. t obtained from stroboscopic photography. The procedure (Budney & Bellow, 1978) involved determining suitable fourth-order polynomial equations necessary to represent accurately the data of ϕ vs. t and θ vs. t . This was especially important since these equations had to be differentiated twice to obtain accelerations. Knowing ϕ , θ , and the physical parameters of the golf club it was a simple matter to determine forces, torque, and club head speed for any instant of time throughout the duration of the swing up to impact.

Work output and power exerted by the golfer can also be computed from the ϕ and θ curves. Work is defined as the force times the distance traveled in the direction of the force, and power as the rate of doing work. Thus, for the golf swing, work can be obtained from

$$W = \int (F_{AA}a + T)\dot{\phi}dt + \int T\dot{\theta}dt \quad (4)$$

and for power

$$P = P_A + P_W,$$

where P_A is the power developed from the arms and is given by

$$P_A = (F_{AA}a + T)\dot{\phi}.$$

Power from the wrists is given by

$$P_W = T\dot{\theta}.$$

These equations were applied to swing kinematics of a golf professional to show how various changes in club parameters affect the energy exerted by the golfer.

Results

Each golfer has a unique swing which can be identified by the shape of the ϕ or θ vs. time curves, power vs. time, or forces vs. time. In some cases it has been shown that, late in the downswing, some golfers retard the acceleration of the golf club by applying a negative torque with the hands. To illustrate this and other aspects, taking into account cause and effect relationships with various "swing weights," a stroboscopic photograph of the golf swing of G. Wolstenholme as reported by Cochran and Stobbs (1968) was used. This swing is a good example of the retarding torque phenomenon, and it is shown how this swing can be modified to eliminate this characteristic.

In Figure 2 the ϕ vs. time and θ vs. time characteristics of Wolstenholme's golf swing are represented by the solid lines. Figure 3 illustrates the variation of the generalized forces applied by this golfer as a function of time for this swing (solid lines). For purposes of illustration, it was assumed the golfer used a standard driver (mass 0.3795 kg or 14 ounces) with a D2 "swing weight" (mass moment of 244 ounce inches).

Solving Equation 2 showed that this golfer produced a maximum circumferential force of 284 N (66 pounds) at .032 seconds before impact with a negative torque applied at impact (-46 Nm or -34 foot pounds). It is shown in Figure 2 that the club head speed was 42.7 m/s at impact, having decreased from 43.4 m/s .009 seconds prior to impact. In this case, the negative torque served to decrease club head speed. Modified kinematics (for ϕ only) were used to demonstrate that this negative torque can possibly be eliminated and club head speed, as a result, can be significantly increased. The modification is shown by the broken line in Figure 2, where ϕ was forced to decrease for part of the downswing and was then prescribed to increase briefly before impact (where deceleration of the arms was previously evident). The same final value of ϕ was achieved, so the golfer should achieve the same posture at impact as for the initial swing. Final club head speed was calculated to be 54.5 m/s,

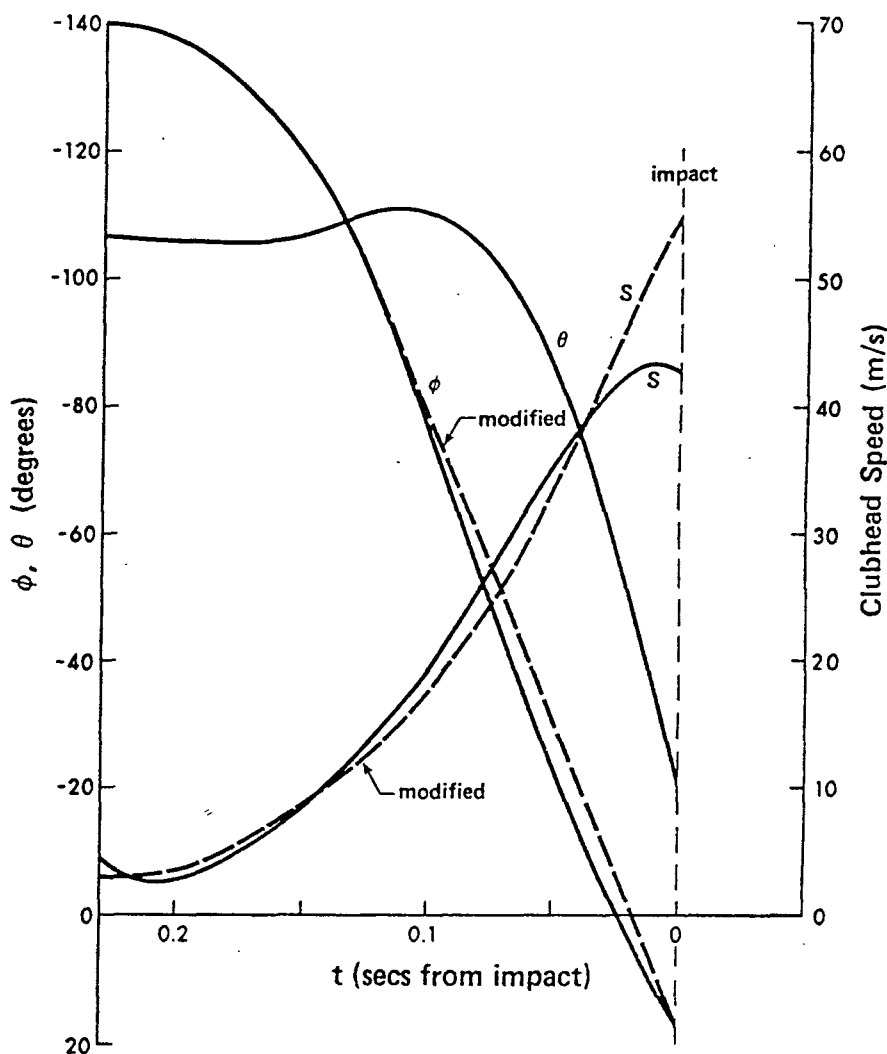


Figure 2— ϕ , θ relationships for G. Wolstenholme (Cochran & Stobbs, 1968).

representing an increase of almost 30%. The modified club head speed is shown as the dash line in Figure 2.

To achieve an increase in club head speed as shown in Figure 2 the relevant forces also had to change. These forces are shown by the broken lines in Figure 3. The maximum circumferential force increased from 284 N (66 pounds) to 368 N (83 pounds) and the centrifugal force at impact from 398 N (89 pounds) to 478 N (130 pounds), and the required torque at impact changed from -46 Nm (-34 foot pounds) to 58 Nm (43 foot pounds). Although not shown on the graphs it was determined the maximum power exerted by the golfer increased from 2.75 kw (3.7 hp) at .045 seconds prior to impact to 5.35 kw (7.3 hp) at .014 seconds prior to impact. The torque remained positive throughout the swing. These results suggest that the delayed wrist uncocking, or late hit, which requires a negative torque, theoretically

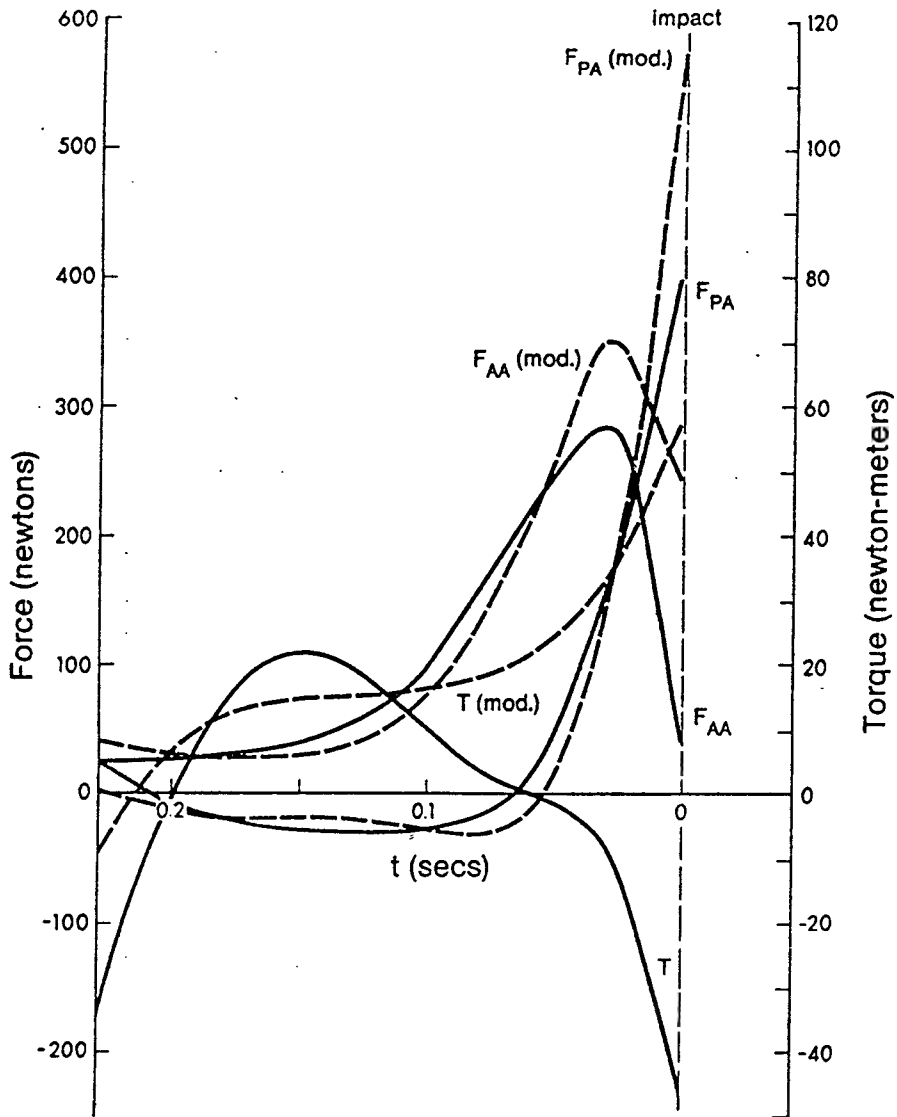


Figure 3—Generalized forces applied during golf swing to impact.

is not necessary for a powerful golf swing. Any attempt to incorporate these theoretical considerations into a real golf swing would be limited by human musculoskeletal capabilities. The modification calls for increased exertion in terms of force and torque but requires a decreased arm swing velocity.

The second part of this analysis demonstrates the effects of swinging golf clubs of various weights and also describes the effect of swinging a driver with a lighter weight graphite shaft. For each golf club considered, the assumed kinematics were given by the solid lines in Figure 3. Only the mass and mass distribution were changed for each club. In a real situation, changing some parameters undoubtedly would

result in a change in the kinematics. This cause-and-effect phenomenon would be an interesting investigation and is at this time regarded as scope for additional work.

The first golf club considered, club 1, was a typical driver with the standard D2 "swing weight" as supplied by a manufacturer. The values in parentheses represent results for the same club assuming no aerodynamic drag. The second driver, club 2, was identical to the first except that .2 ounce (5.7 gm) was added to the club head to change the "swing weight" from D2 to D5, a change that is considered significant by the golf industry. Club 3 was the same club again with enough mass added to the end of the grip to restore it to the original "swing weight." This club was included to consider the practice of some manufacturers of adding weight to the grip to reduce the club to the desired "swing weight" allowing for a club head that is too heavy. Club 4 driver had a lightweight graphite shaft. Club 5 was a modern lightweight driver with a steel shaft.

Comparison of the values in brackets with the original values from club 1 allowed the following observations in relation to the elimination of aerodynamic drag:

1. The maximum circumferential force changed from 284.2 N to 283.0 N, a decrease of .4%. Similarly the maximum required torque experienced a .5% decrease of 21.7 Nm.
2. The maximum arm swing power changed from 2.84 kW to 2.83 kW, a reduction of .4%, while maximum total power decreased 2.5% to 2.68 kW.
3. The required work to achieve the same final club head velocity was decreased 2.8% to 214.7 Joules.

These calculations demonstrated that although aerodynamic considerations appeared to have only a slight influence on the maximum exertion required of the golfer, the energy dissipated by drag amounted to 2.8% of the total energy expended by this golfer. This percentage would be more for the golfer who achieves a higher club head speed and would be correspondingly less for the more leisurely golf swing. Only a portion of this lost energy could be regained by possibly improved aerodynamic designs.

By increasing the swing weight of the driver (club 2), the maximum circumferential force increased 2.3% to 290.7 N, and the required maximum torque also increased 2.3% to 22.3 Nm. The maximum arm swing power and maximum total swing power both required increases of 2.1%, to 2.90 kW and 2.81 KW respectively. The total energy required to swing the golf club was increased from 220.8 Joules to 229.7 Joules, a 2.2% change. Since the club head with greater mass at the same velocity has a higher kinetic energy, the ball should start off after impact with a higher initial velocity for club 2. However, it may not be possible for the golfer to apply this extra power, and thus it may well be that the desired final velocity cannot be attained. Extending this analysis to optimize the mass of the club head for a particular golfer is beyond the scope of this investigation.

Comparison of the values for club 2 suggested that the procedure of applying the added weight to the grip was unnecessary. The exertion parameter experiencing the greatest change is the maximum circumferential force, which was reduced only .2%, from 290.7 N to 290.1 N.

The mass of club 4, with the graphite shaft, was .359 kg, 5.4% less than the number 1 steel-shafted club. The distance from the center of the hands to the center of gravity of the golf club was 688 mm, 17 mm more toward the club head than the corresponding distance for the first driver. The lighter graphite shaft enabled the manufacturer to place increased mass in the club head since the mass of the shaft

had been reduced while still matching the club "swing weight." The results reported in Table 1 showed that all the parameters that measured the physical exertion of the golfer were reduced for this club. The maximum torque was reduced by 7.8% to 20.1 Nm, the maximum circumferential force was reduced 2.5% to 267.6 N, the maximum arm swing power and the maximum total power were both reduced by 6%, and the total work done was decreased from 220.8 Joules to 206.8 Joules, a reduction of 6.3%. These reductions were significant in that they occurred for a golf club with greater mass at the head while not sacrificing club head speed. This suggests that if the standard driver were deemed suitable for this golfer, the graphite driver may well have the mass of its club head increased even more. This would classify the club as heavy according to the "swing weight" scale but could be designed so that the parameters measuring the physical exertion of the golfer are more similar to those using a steel-shafted golf club.

Golf club 5 was a modern lightweight steel-shafted driver, comparable in total weight with the graphite driver. Whereas the graphite driver had a reduced shaft weight which permitted a heavier club head than the standard driver, club 5 had a shaft, grip, and club head that were all lighter than for club 1. Hence, the exertion parameters for this lightweight club were also less than for the standard driver, but the energy of the club head at impact would be less because of the lesser club head mass.

Conclusions

A detailed analysis of the characteristics of a golf swing has shown how certain swing faults or defects can be objectively detected and corrected. Using the known kinematics of a golf swing, the analysis was extended to determine the effect of different types of clubs on the kinetics of the swing. The mathematical model also showed that aerodynamic drag had a negligible effect on the work or power exerted by the golfer and that methods employed to reduce aerodynamic drag appear to be more cosmetic than substantive. It was also shown how adding weight to the grip of a driver to maintain "swing weight" had a negligible effect on the forces applied by the golfer;

Table 1—Requirements for Swinging Different Golf Clubs

Golf Club	Mass (kg)	Length (m) "b"	Moment of Inertia (kg m ²)	Max- imum Circ. Force F_{AA} (N)	Max- imum Cent. Force F_{PA} (N)	Max- imum Torque (Nm)	Max- imum Arm Swing Power (kw)	Max- imum Total Power (KW)	Total Work Done (Joules)
1. Standard Driver	0.3795	0.671	0.0638	284.2 (283.0)*	397.7 (398.4)*	21.8 (21.7)*	2.84 (2.83)*	2.75 (2.68)*	220.8 (214.7)*
2. Driver with Increased Swing Weight	0.3852	0.6755	0.0643	290.7	406.3	22.3	2.90	2.81	225.7
3. Driver with Weight Added to Grip to Restore Original Swing Weight	0.3874	0.671	0.0656	290.1	406.0	22.3	2.90	2.81	225.7
4. Graphite Driver	0.3590	0.688	0.0586	267.6	374.5	20.1	2.67	2.58	206.8
5. Lightweight Driver	0.3574	0.679	0.0663	271.5	378.9	22.2	2.69	2.68	216.7

* Assumes no aerodynamic drag.

reduction of the weight of the club head was considered more realistic. The analysis showed the merits of a graphite driver wherein the same club head speed could be achieved with less effort than that obtained using a standard driver. Similarly, less effort was shown to be required for the modern lightweight driver, although the benefits were not as significant as for the graphite driver.

References

- Budney, D. R., & Bellow, D. G. *A dynamic model for the golf swing*. Paper presented at the 5th International Congress of Sports Sciences, Edmonton, Canada, 1978.
- Cochran, A., & Stobbs, J. *The search for the perfect swing*, Heinemann Press, 1968.

Submitted: 19 July, 1978

Accepted: 19 December, 1978

Influence of testing frequency on the fatigue of butt welded steel joints

By M.G. Faulkner and D.G. Bellow



1. INTRODUCTION

Butt welded joints in service may be subjected to loading frequencies from a few cycles per day to a few hundred cycles per second. In addition laboratory testing of these weldments has been performed at frequencies generally between 2 and 200Hz. Because of the large variation in frequency it is important to know whether or not frequency influences the fatigue life of a particular weldment. This needs to be considered when comparing results obtained from different testing laboratories at different cycling rates as well as in design for particular conditions.

There is a widely held belief that the frequency of testing has little effect on the fatigue life for the range of testing frequencies normally encountered in the laboratory. This is a result of studies such as that reported by the ASTM Task Group (1). This report indicated that in the range 3-120Hz there was no frequency effect provided that steps were taken to ensure that the specimen temperature did not rise and there was no simultaneous corrosion effect. These conclusions were based on tests of a particular material rather than a welded joint. Studies conducted by Lomas et al (2) on various steels at 750-15 000Hz indicated that as the testing frequency increased there was an increase in endurance limit up to about 1200-1800Hz, followed by a progressive decrease. Jones and Higgins (3) did not find an appreciable frequency effect in their tests of fillet welds in mild steel. Their testing was done with narrow band random loading at frequencies centred between 100-2500Hz. The only previous study which considered the frequency effect for butt welded steel joints was that by Gyorgyi (4) in which effects of both temperature and frequency were studied to a limited extent. While this study included a limited number of specimens tested at each stress level and testing frequency, it did show a distinct frequency effect with approximately a 22% increase in fatigue life when the frequency was increased from 8 to 117Hz.

From the literature it is clear that there is a variety of opinions on the effect of testing frequency and, in particular, whether or not there is a pronounced effect on the results obtained in testing butt welded specimens. Thus the objective of the present study was to consider in more detail the effect of testing frequency on the fatigue strength of butt welded steel joints. The testing frequencies used in this investigation ranged from 2 to over 200Hz, which is believed to be the range most commonly used in laboratory testing.

2. METHOD OF INVESTIGATION

The specimens used in this study were made by welding together two 127mm wide, 6.4mm thick plates of Stelco Columbium 50 steel. The plates, which were in the as-rolled condition, were prepared for welding by machining the edges straight then bevelling them at 45°. The welding process used was

automatic submerged arc, to make it possible to control, as much as possible, the welding variables. The specimens, material and welding details are the same as used in the authors' previous paper (5) and are shown in Table 1. The welds were fluoroscoped to check for flaws, then cut into 76mm wide strips with the weld transverse to the cut. Finally, the 76 x 254mm strips were machined to the shape shown in Fig.1.

It is known that specimen dimensions, both thickness and width, influence the fatigue results, as the residual stress distribution in the welded area will be different for different sizes of specimen. In the present investigation the width to thickness ratio is 4:1. The results of various investigations reported by Gurney (6) indicated that this geometric effect was a less significant factor when testing was purely under tensile loading. The present work was carried out using pulsating tension to minimise the influence of these size effects on the results.

To obtain the frequency range 2-250Hz, the fatigue testing was done on two different fatigue machines — the higher speed tests on an Amsler at frequencies of approximately 128-140, 180-187 and 230-240Hz, the lower speed on an MTS resonant fatigue machine. The frequencies used were 2, 20, 70-75 and 125-140Hz. As both machines were able to be operated near 135Hz, the data obtained from one could be compared with those from the other to check consistency between the two.

As mentioned above, all the testing was in pulsating tension; the maximum loads were chosen to give nominal stresses at the weld of 331, 265 and 193N/mm². It was assumed that changes in frequency or loading produced no significant changes in the measuring or controlling systems of the testing machines. As a check a non-welded specimen on which electrical resistance strain gauges were mounted was inserted into both the MTS and Amsler machines and run at the frequencies and loads used in this investigation. The output from this specimen was monitored on an oscilloscope and it was found that the output waveform was a consistent sinusoid and the loads were within the measurement accuracy ($\pm 5\%$) of the strain gauge system.

The welded specimens were prepared using a first pass then a filler pass on the opposite side of the plates. It was found that some warping of the specimens occurred. To evaluate what effect this warping would have on the stresses near the weld, strain gauges were mounted at each toe of the weld on both sides of the plate. One side of the specimen with two strain gauges is shown in Fig.2. The specimen was proof-loaded to a nominal stress of 300N/mm². It was found by careful gripping of the specimen that the bending stresses measured were less than 10-15% of the axial load. It was also found that with improper gripping the bending stress component would result in stresses which varied from the mean axial load by $\pm 75\text{N/mm}^2$. In the testing reported below, care was taken to minimise the effect of these bending stresses.

The test on each specimen was terminated when the testing machine automatically shut off. In the case of the Amsler this occurred when a visible crack had started, in the case of the MTS on complete rupture of the specimen; but visual observation indicated that only a few thousand cycles elapsed between the beginning of a crack and final breakage. This was a small fraction of the total life, i.e. less than 5%. A statistical test (see below) of the life of the cracked versus the life of the fully-broken specimens showed no significant

difference. Thus it was assumed that it was permissible to neglect this difference in the final analysis of the results.

The fatigue crack always occurred at the weld toe and on the surface propagating inward. Figure 3 shows the weld cross-section with the crack in the weld toe, while Fig.4 is a scanning electron micrograph showing the fatigue striations on the fracture surface. As can be seen, the crack propagated in the heat affected zone (HAZ) where metallurgical examination indicated that the welding resulted in a smaller grain size and a corresponding increase in hardness. Figure 3 shows the weld made in two passes — first pass and filler pass. The crack usually began on the filler pass side of the weld, which may be attributed to the fact that the HAZ on the filler pass side was slightly larger and the hardness of the weld somewhat higher than on the first pass side.

All the fatigue tests were conducted in a laboratory in which the room temperature was $20 \pm 3^{\circ}\text{C}$ and the relative humidity was approximately constant at 35%. To ensure that the effects being measured were not being influenced by local heating in the test specimen during testing, the temperature at the root of the weld was monitored over the life of one specimen. This specimen was tested at the highest speed (240Hz) and at the highest maximum stress (331N/mm^2). The temperature on the surface rose less than 5°C from the start of the test until a crack began. After the initial crack became visible the temperature rose rapidly until failure, when the total rise was approximately 20°C .

To determine whether or not the differences found in the testing between two series at the same stress level but at different testing frequencies were significant, the data from the series were compared using the student 't' test. Also, data from the same stress level and testing frequency but from different machines were tested to ensure that differences could not be attributable simply to a change in the testing machine used. The statistical analysis of the data was carried out according to ASTM Special Technical Publication 91-A (7). The t-tests were calculated assuming that the data followed a log-normal distribution with the significance level chosen as 5%.

The number of specimens tested at each frequency and for each machine was set at a minimum of 14. This number should allow nearly a 90% chance of finding differences of more than a standard deviation between the two samples (7). With 14 specimens the 95% confidence limits would be between the specimen with the third lowest number of cycles to failure and the third highest. This allowed for two runouts for any one series and still provided finite upper confidence limits. These limits (which are noted below) compared favourably with those calculated after testing and using the log-normal distribution assumption.

3. RESULTS AND DISCUSSION

The first tests were carried out on the two machines at the same stress level and testing frequency. Statistical analysis gave no indication of any difference between the results obtained from the MTS and the Amsler machines. Following this the data obtained at a given stress level but for different frequencies of testing were compared with the results at the same stress but at a frequency of 125-145Hz on the MTS. This frequency was chosen firstly because it was approximately midrange and secondly because it was obtainable on both machines.

The results of the tests are summarised in Table 2. This Table identifies the machines used, the median life for each series, and the 95% confidence limits for each test series. In addition, the results of the statistical comparison are summarised in the last column. These tests showed that at 265 and 331N/mm² the results from the two highest and the lowest testing frequencies are significantly different from the 125-140Hz data. At 193N/mm² no significant differences were found even between the lowest testing frequency (71Hz) and the highest (240Hz).

Figure 5 shows the median life and confidence interval for each of the tests. The medians obtained at each particular maximum stress level have been joined to indicate the effect of increasing the frequency of testing. This effect is most noticeable at the intermediate stress of 265N/mm². Here the median life shows more than a threefold increase between the 2 and the 232Hz testing frequency. The same trend is shown at the highest stress but the increase in median fatigue life is only approximately twofold between 2 and 232Hz.

Replotting the data in the form of the more standard S-N curve (Fig.6) suggests that the curves for each testing frequency would converge at low fatigue lives (<10⁴ cycles) as well as at long lives (>10⁶ cycles). Frequency has a distinct influence only in the range 10⁴-10⁶ cycles. This is also the region in which S-N curves tend to have their steepest slope.

It seems, at the higher stress levels, that the stress concentration because of the weld raises the stress at the weld toe to near the yield point of the material and failure occurs after a relatively low number of cycles. At the other end of the range (>10⁶ cycles) the frequency effect disappears because the stress at the weld toe is approaching the endurance limit of the material. The number of cycles necessary to cause failure is quite high and insensitive to the changes in testing frequencies which were used.

The usual reasons given for the existence of a frequency effect are specimen heating because of high internal damping, corrosion-fatigue interaction, and effects of strain rate and creep. None of these effects appears to be present in the current investigation. The temperature did not rise appreciably for the highest stress level and highest testing frequency. The other reasons mentioned would be more evident at the longer fatigue lives since they are time dependent. However, since no frequency effects were seen in the tests which were conducted over the longest time interval these effects cannot be occurring to any significant extent.

4. CONCLUDING REMARKS

Frequency will noticeably affect the fatigue strength of butt welded joints of the type investigated only over a limited range of fatigue life, i.e. from approximately 10⁴ to 10⁶ cycles. For most design purposes this poses no particular problem as the fatigue life which is to be designed for is usually much greater than 10⁶ cycles. For the frequencies tested there was no significant difference at 10⁶ cycles even between the lowest and the highest frequency.

The frequency of testing did cause a statistically significant difference when the testing was conducted for fatigue lives between 10⁴ and 10⁶ cycles. This is also the range in which Gyorgyi (4) did the majority of his testing, but the limited number of specimens tested makes it difficult to compare statistically his results for two different frequencies. The differences found both by

Gyorgyi and in the current work show that comparison of fatigue studies in which the lives are approximately between 10^4 and 10^6 cycles must take into account the frequency of testing.

ACKNOWLEDGEMENTS

The authors would like to thank The Steel Company of Canada for supplying the welded steel specimens and to acknowledge the support of the National Science and Engineering Research Council under grants A2705 and A7514.

REFERENCES

1. MOORE, H.F., WILSON, B.L., HOWELL, F.M. and GOHN, G.R. 'Report of the task group on effect of speed of testing on fatigue test results'. Proceedings ASTM, 50, 1950, 421-424.
2. LOMAS, T.W., WARD, J.P., RAIT, J.R. and COLBECK, M.A. 'The influence of frequency of vibration on the endurance limit of ferrous alloys at speeds up to 150 000 cycles per minute using a pneumatic resonance system'. IME-ASME International Conference on Fatigue of Metals, 1956, 375-385.
3. JONES, A.W. and HIGGINS, M.G. 'The effect of testing frequency on the fatigue strength of fillet welds in mild steel in narrow band random loading'. Conference on the 'Fatigue of welded structures', Cambridge, 1970, paper 23, 290-295.
4. GYORGYI, F. 'Influence of loading frequency and other factors on fatigue test results of butt welded joints'. IIW Document XIII-383-65, 1965.
5. FAULKNER, M.G. and BELLOW, D.G. 'Improving the fatigue strength of welded steel joints by peening'. Welding Research International, 1975, 5, 63-72.
6. GURNEY, T.R. 'Fatigue of welded structures'. Cambridge, 1968.
7. ASTM Special Technical Publication No. 91-A (second edition). A guide for fatigue testing and the statistical analysis of fatigue data, ASTM, 1963.

TABLE 1. Material properties and welding details

	Chemical compositions, wt %					Mechanical properties			
	C	Mn	P	S	Si	Columbium*	Yield stress, N/mm ²	UTS, N/mm ²	Elongation, %
Columbium* 50	0.2	1.2	0.04	0.05	-	0.005	520	545	-
'Oxweld' number 36 rod	0.14	2.0	0.017	0.024	0.05	-	510-615	-	20-30

Welding details	
1	Welding process
2	Number of welding wires
3	Welding wire
4	Flux
5	Tip height
6	Distance between electrodes
7	Speed
* Niobium	

Submerged arc welding, double sided, using flux backing

Two, tandem

Linde, Oxweld number 36, 3.17mm

Linde, Oxweld 585

22.2mm from workpiece

8mm

1.42m/min

TABLE 2

Test	Maximum stress, N/mm ²	Testing machine	Testing frequency, Hz	Number of specimens	Median life, thousands of cycles	95% confidence limits, thousands of cycles		Significant difference from MTS at 125-140Hz
						Lower	Upper	
1	331	MTS	2	14	62	45	69	Yes
2		MTS	20	17	67	61	103	No
3		MTS	76	14	73	42	113	No
4		MTS	128	14	87	57	107	-
5		Amsler	128	14	68	62	108	No
6		Amsler	187	14	114	86	182	Yes
7		Amsler	231	14	126	105	142	Yes
8	265	MTS	2	14	127	86	175	Yes
9		MTS	20	14	166	134	236	No
10		MTS	71	14	175	126	206	No
11		MTS	130	14	232	177	305	-
12		Amsler	183	20	358	275	538	Yes
13		Amsler	232	14	513	313	786	Yes
14	193	MTS	71	14	1206	713	1833	No
15		MTS	144	14	1426	771	2391	-
16		Amsler	145	14	1582	841	2431	No
17		Amsler	180	15	1557	913	5624	No
18		Amsler	240	14	1482	1057	2352	No

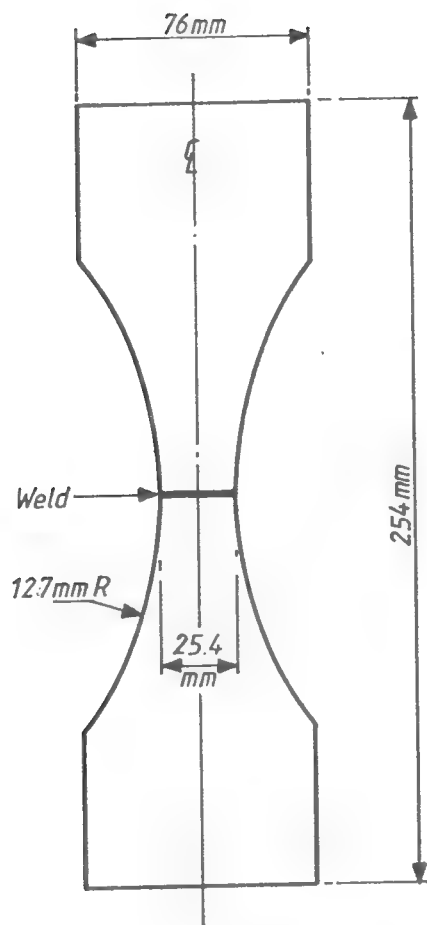


Fig.1. Butt welded specimen.

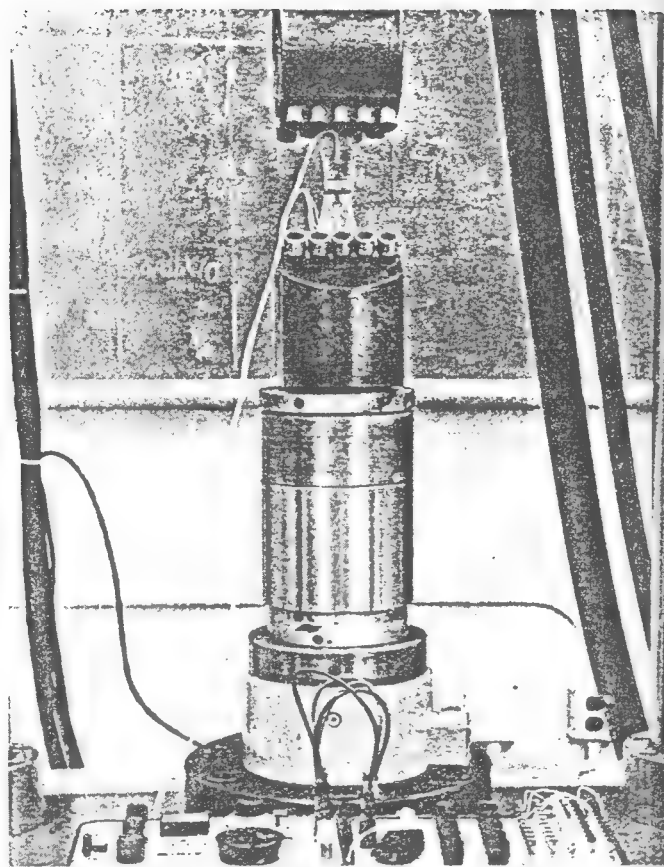


Fig.2. Specimen under test.

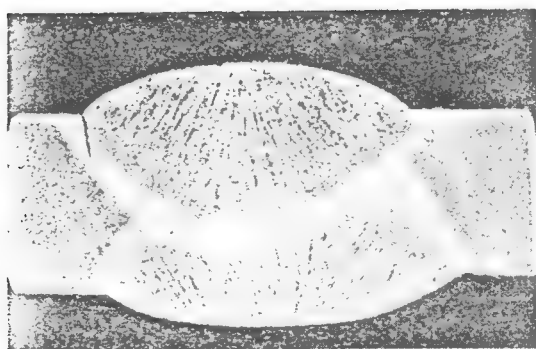


Fig.3. Typical weld and figure crack.

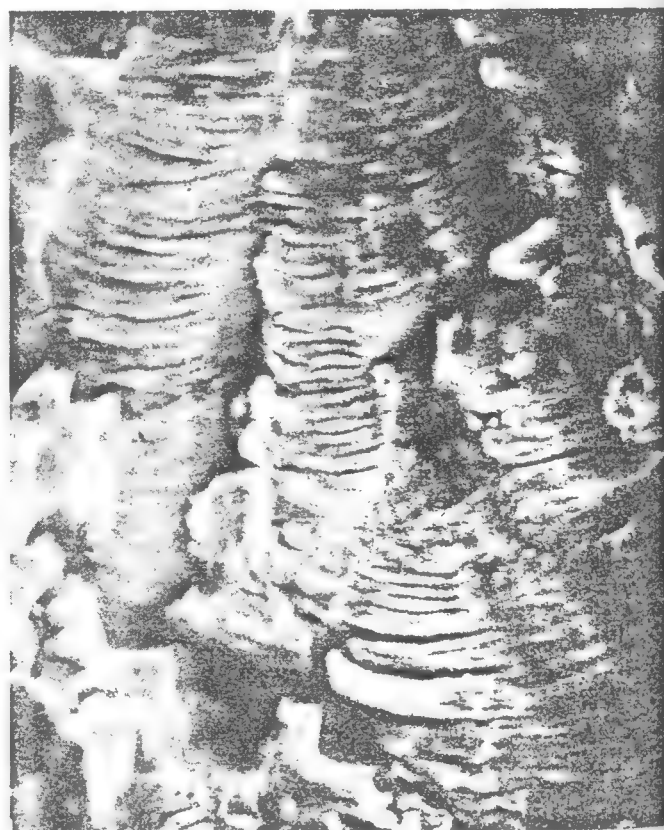


Fig.4. Fracture surface (x 5000).

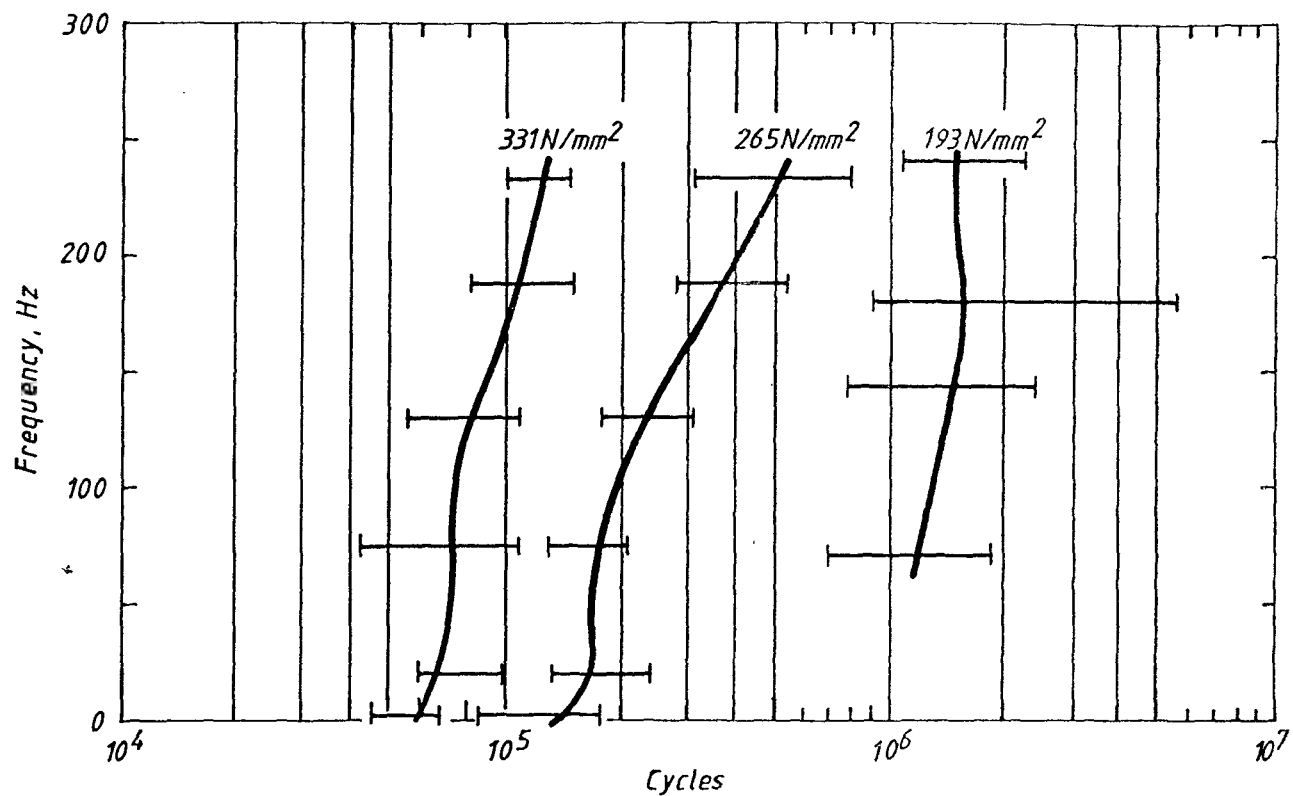


Fig.5. Effect of testing frequency on fatigue life.

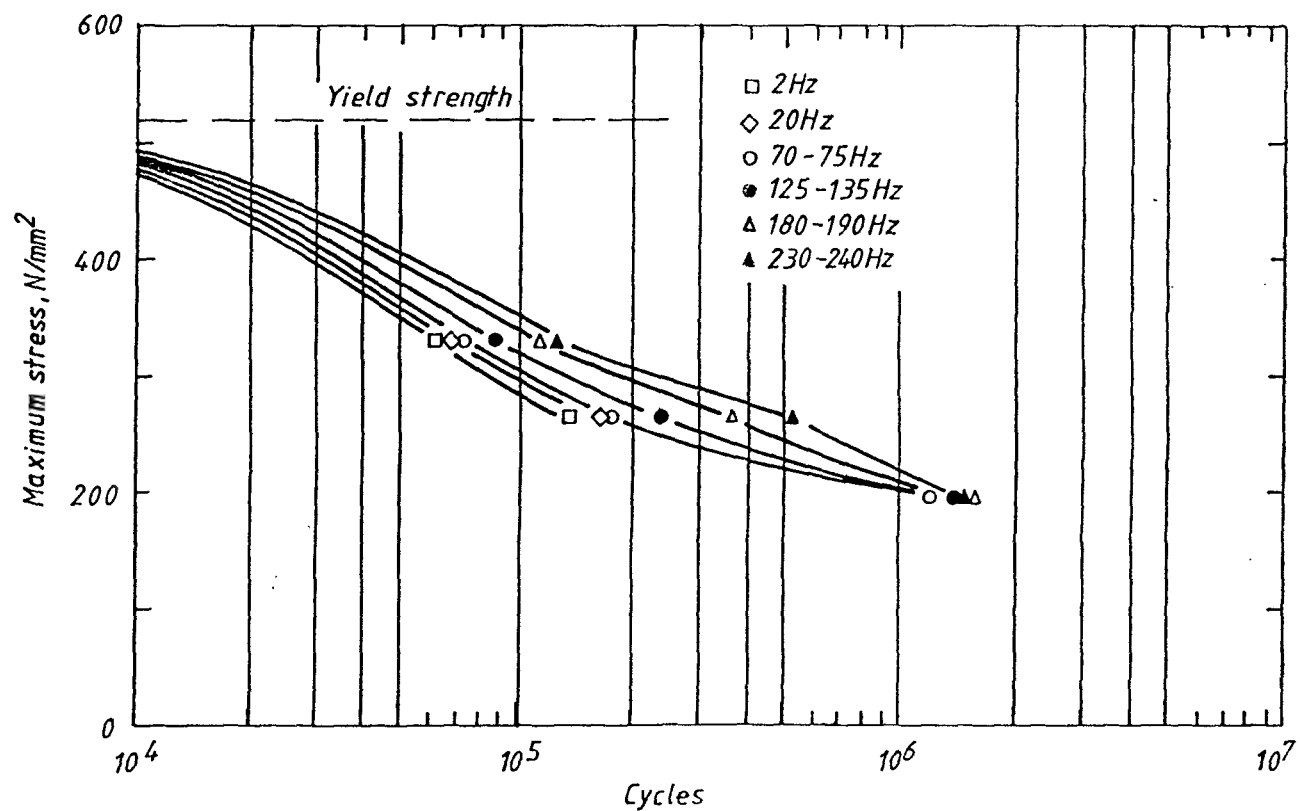


Fig.6. S-N curves for various testing frequencies.



M.G. Faulkner and D.G. Bellow

INFLUENCE OF TESTING FREQUENCY ON THE FATIGUE OF BUTT WELDED STEEL JOINTS

Abstract

The effect of testing frequency between 2 and 230-240Hz on the fatigue strength of butt welded steel joints was investigated. Testpieces consisting of two Stelco Columbium 50 steel plates, 127mm wide and 6.4mm thick, were automatic submerged arc welded with strictly controlled variables. Pulsating tension test results were compared for welded and non-welded specimens. Fatigue cracking always occurred in the heat affected zone at the weld toe, a region of smaller grain size and increased hardness. Fatigue strength of the joints was noticeably affected over only a limited range of fatigue life, and design considerations would be unaffected.

Keywords

BUTT WELDS; FATIGUE STRENGTH; FREQUENCIES; TESTPIECES; PULSATIONS; AUTOMATIC CONTROL; SUBMERGED ARC WELDI; CRACK INITIATION; DESIGN; HEAT AFFECTED ZONE; GRAIN SIZE; HARDNESS; MICROALLOYED STEELS; FATIGUE LOADING; LIFETIME

EFFET DE LA FREQUENCE DES ESSAIS SUR LA FATIGUE DE JOINTS D'ACIER SOUDES EN BOUT

Sommaire

L'effet de la fréquence des essais entre 2 et 230-240Hz sur la résistance à la fatigue de joints d'acier soudés en bout fut étudié. Des éprouvettes formées deux plaques d'acier Stelco Columbium 50 de 127mm de large et 6,4mm d'épaisseur furent soudées à l'arc submergé automatique avec des variables strictement contrôlés. Les résultats de l'essai de traction pulsée furent comparés avec des éprouvettes soudées et non soudées. La fissuration par fatigue se faisait toujours dans la zone HAZ au bout de la soudure, région de grosseur de grains plus petite et de dureté accrue. La résistance à la fatigue des joints ne fut affectée de façon appréciable que sur une gamme limitée de vie de fatigue, et les considérations de design restaient in affectées.

Mots clefs

SOUDURE BOUT A BOUT; RESISTANCE FATIGUE; FREQUENCE; EPROUVETTE; IMPULSION; COMMANDE AUTOMATIQUE; SOUDAGE SOUS FLUX; AMORCAGE FISSURE; CONCEPTION; ZONE THERMIQUEMENT AFFECTEE; GROSSEUR GRAIN; DURETE; ACIER A DISPERSOIDE; SOLLECITATION FATIGUE; DUREE VIE

EINFLUSS VON PRUFFREQUENZ AUF DIE ERMUDUNG VON STUMPFNAHTSTAHLSCHEISS- VERBINDUNGEN

Kurzbericht

Es wurde der Effekt von Prüffrequenz zwischen 2 und 230-240Hz auf die Dauerfestigkeit von Stumpfnahstahlschweisverbindungen untersucht. Prüfstücke, bestehend aus zwei 127mm breiten und 6,4mm dicken Stelco-Columbium-50 - Stahlblechen, wurden mit streng kontrollierten Einflussgrößen automatisch unterpulvergeschweisst. Man verglich Stromstosszugspannungsprüfresultate von geschweissten und nichtgeschweissten Versuchssproben miteinander. Ermüdungsrissbildung zeigte sich stets in der Wärmeeinflusszone (HAZ) am Nahtübergang, einem Bereich von kleinerer Korngrösse und erhöhter Härte. Die Dauerfestigkeit der Schweissnahtverbindungen wurde nur über einen begrenzten Teil der Zeitfestigkeit merklich beeinflusst, und Entwurfserwägungen würden unbeeinflusst bleiben.

Schlüsselwörter

STUMPFNAHT; DAUERFESTIGKEIT; FREQUENZ; PROBE; PULSIEREN; STEUERUNG; UP-SCHWEISSEN; RISSEINLEITUNG; GESTALTUNG; WÄRMEEINFLUSSZONE; KORNGROSSE; HÄRTE; MIKROLEGIERTER STAHL; DAUERBEANSPRUCHUNG; LEBENSDAUER



National Research
Council Canada

Conseil national
de recherches Canada

PROCEEDINGS
COMPTES RENDUS

FIFTH CINQUIÈME
SYMPOSIUM

ENGINEERING APPLICATIONS
APPLICATIONS TECHNIQUES
OF DE LA
MECHANICS MÉCANIQUE

University of Ottawa
16th and 17th June

Université d'Ottawa
16 et 17 juin

1980

MEASUREMENT OF CULTIVATOR FORCES

Donald G. Bellow, Gerald C. Kiss

Department of Mechanical Engineering, University of Alberta, Edmonton, Alberta

H. Page Harrison

Department of Agricultural Engineering, University of Alberta
Edmonton, Alberta

ABSTRACT - This paper describes the apparatus, testing, and evaluation procedure for determining the loads and frequencies measured on a cultivator implement under a variety of input conditions. It is shown that the depth of cultivation is more a factor on the measured loads than is the forward speed. It is also shown that at a depth of 0.20 m the loads are quite large although the stresses on the cultivator shank used in the test were still within acceptable limits.

RÉSUMÉ - Cette communication décrit l'équipement et le processus d'évaluation et d'essai pour déterminer le chargement et les fréquences des machines à cultiver sous une variété de conditions et de circonstances. Nous démontrons que la profondeur de cultivation est le principal facteur à considérer pour les chargements mesurés plutôt que la vitesse en avant. Nous démontrons également qu'aux profondeurs de 0.20 m ou plus les chargements sont assez considérables. Toutes fois, la tension soutenue par la jambe de la machine à cultiver ne dépasse pas les limites acceptables.

INTRODUCTION

The use of cultivator sweeps or shovel tools for seed bed preparation and weed control is widespread in the agricultural industry. In some regions cultivators equipped with chisels or spikes are used for deep penetration in place of a standard mould-board plough. This depth has increased to 0.10 to 0.20 m due to the availability of large tractors. Under such severe operating conditions the cultivator shanks and holder assemblies are required to withstand stresses greatly in excess of what was originally intended. Thus, it is desirable to determine how existing cultivator designs are behaving under these more severe loading conditions and assess whether or not changes in design are required.

The main purpose of this paper is to describe the experimental equipment and procedures used to measure the loads imposed on cultivator shanks fitted with cultivator sweeps singly and in off-set tandem operation. A six element load sensing frame was designed to measure the forces and couples acting on a cultivator shank under a variety of soil conditions, depths of tillage, and tractor speeds. The operation of this apparatus, the collection of data, and the testing procedure is discussed along with the results from one particular test site.

EXPERIMENTAL EQUIPMENT

Mobile Test Frame

A mobile test frame to carry a cultivator shank and holder assembly was designed to fit onto a 3-point hitch of a tractor. Figure 1 shows a schematic of the load frame indicating the position

of the six load cells. Each load cell was connected to the floating arm by a universal bearing. This ensured no interaction between the load measured along one axis with that being measured along another axis. The floating arm assembly incorporated a shear pin to ensure the safety of the system in case the cultivator hit an immovable object. For purposes of evaluating the effects of multiple sweeps in an off-set tandem arrangement (i.e., one leading and one trailing) a duplicate shank and holder assembly was attached to the front and to the right of the trailing sweep. The leading sweep was not instrumented. The holder assembly of the trailing sweep was modified to eliminate the spring load support. The original intent of this spring system was to allow the shank to pivot up and away from immovable objects and consequently limited the drawbar forces developed. The modification made the cultivator shank attachment rigid and allowed for a greater depth of cultivation.

The load cells consisted of circular rods made from 2024T4 aluminum 20 mm (3/4 in.) in diameter machined down in the center to 12 mm (0.5 in.) and threaded at both ends. Four electrical resistance strain gauges were attached and wired up in a four-arm bridge circuit to maximize the output. In addition, strain gauges were mounted to the cultivator shank approximately 60 mm (2.5 in.) from where the shank connected to the holder assembly. This was to enable direct measurement of strain on the cultivator shank and also, if necessary, to serve as a back-up system to the six element load cell configuration.

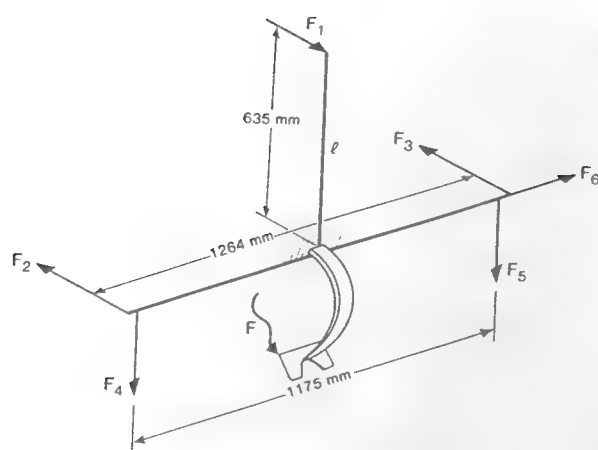


Figure 1 Load Frame Schematic

A general view of the test facility being towed behind a tractor is shown in Figure 2. The gauge wheels enabled the depth of cultivation to be predetermined by operating a ratchet linked to the wheels. By changing the wheel position in relation to the test frame, desired tool depths could be preselected. The three point hitch was used only to lift the complete test frame off the ground to ease transportation. Also, attached to the axle of one gauge wheel was a small DC generator which provided an output proportional to the forward speed. The recording equipment was housed in the air conditioned van seen in the background of Figure 2 with a 30 m (100 ft.) umbilical cord connecting the load cells and strain gauges to the signal conditioning equipment in the van.

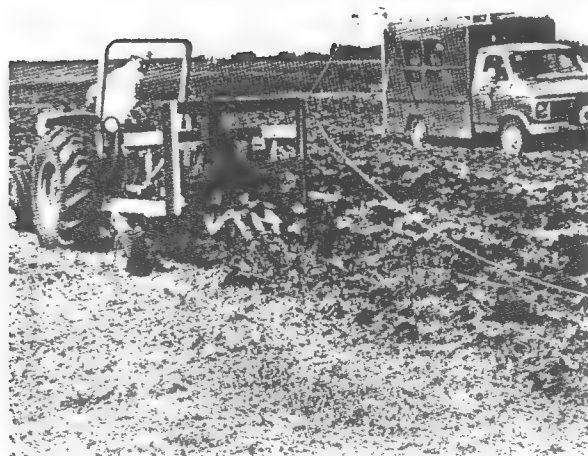


Figure 2 Test Facility in Use

Recording Equipment

The mobile van was equipped with a gasoline engine driven 60 Hz AC generator with sufficient capacity to drive all recorders and ancillary equipment. For the strain gauges on the cultivator shank and the load cells, DC signal conditioning was provided by means of power supplies and amplifiers. The outputs from the strain gauges were fed simultaneously onto a seven track FM tape recorder and a ultra-violet (U-V) chart recorder. It was initially determined that all data be recorded on magnetic tape to enable ease of data analysis with the use of a computer. However, in order to ensure no loss of data during the field trials all data was also monitored and recorded on an U-V recorder. The voice channel on the FM tape recorder and the event recorder on the U-V recorder were used to synchronize the inputs. The speed of the cultivator was monitored and recorded on an X-Y recorder. The depth of cultivation was measured with a ruler at selected points along the ploughed furrow.

Data Analysis

Inasmuch as it was intended to measure cultivator forces under a variety of field conditions, tractor speed, and depth of tillage it was planned that the best possible way of coping with the vast quantity of data would be to record on magnetic tape, process the data through an analog to digital converter, and analyze on a computer. Thus, the first step in the data process was to convert from analog to digital (A-D) using an A-D converter. In considering conversion from analog to digital the sample rate had to be prescribed. If the sampling rate is too slow then important data will be missed. On the other hand if the sampling rate is too fast then lengthy tapes and recording of unnecessary data will result. For Fast Fourier Transform (FFT) digital spectral analysis a sampling rate of at least twice the highest expected frequency should be selected. Several trial runs showed most of the analog signals recorded were contained in the bandwidth DC to 55 Hz. A sampling rate of 167 times per second was chosen as being appropriate.

A computer program was written to analyze each run to first output, in graphical form, the raw data as obtained from each load cell. Figure 3 compares the output from one load cell for a typical test run with the output as received on the U-V recorder. While the computerized data is somewhat smoother, as to be expected, generally there is favorable agreement between the output in both magnitudes and location of the major perturbations. This led to confidence in basing all of the analysis on the computerized data and the U-V records were used only as a means of providing an occasional check. The computer program was also written to analyze the output for each load cell for each test run, record the peak values, means, standard deviations, probability densities, and calculate the resultant forces acting on the tip of the shovel tool in the horizontal, vertical, and lateral directions.

In order to obtain an assessment of the frequency of load application as measured by each load cell the analog data from the FM tape recorder was processed through an FFT digital spectrum analyzer which allowed for a visual display of the power spectral density as a function of frequency for each test run.

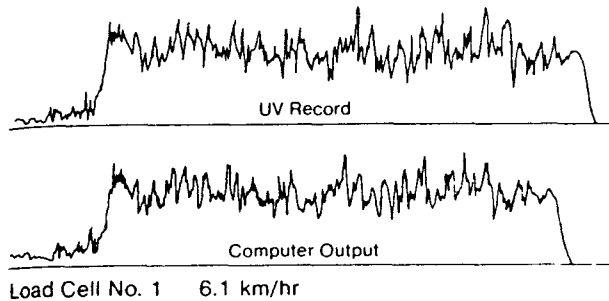


Figure 3 Computerized and U-V Outputs

TESTING PROCEDURE

Variables

Although space does not permit all of the data to be presented here, five different test sites in Alberta ranging from Lethbridge in the South to Edmonton in the North and Vegreville in the East were evaluated. With one exception each test site was considered to be a severe test for any tillage tool. At each test site a number of test runs were conducted with the following variables controlled;

1. Single sweep free with shovel tool (spring system in operation).
2. Single sweep solid with shovel tool (spring system locked out).
3. Dual sweep solid with shovel tools.
4. 1) repeated but with cultivating spike instead of shovel tool.
5. Depth of tillage.
6. Speed of tractor.

In addition, moisture content and dry bulk densities were measured at the same time the trials were conducted. A gamma radiation source and detector recorded data at one inch intervals from the soil surface down to the deepest cultivation depth achieved.

Operation

A test run was begun by backing the tractor away from the van the length of the umbilical cord (approx. 30m) connecting the load cells to the recording devices housed in the van. The depth of cultivation was set and, upon a signal from the recording engineer in the van, the tractor accelerated to the desired forward speed. The tool

was lowered into the ground by operating the three point hitch until the weight of the test frame was born by the gauge wheels. Data was recorded until the tractor proceeded past the van the length of the umbilical cord, resulting in a total distance travelled of 50 to 60 m. As one test run was providing sufficient data the run was not repeated unless a malfunction in recording the data or input conditions had been observed. Additional runs were conducted for different input conditions, resulting in a total of 30 to 40 trials per test site.

RESULTS

Effect of Tractor Speed

Although it was initially intended to evaluate the effects of ploughing speed it was found during the field trials that it was not possible to plough effectively at speeds less than 6 km/hr, nor would speeds below this be practical or economical for a farmer. On the other hand it was found that for speeds in excess of 12 km/hr the tractor tended to bounce and become difficult to control. While the test runs were varied in some cases between 6 and 12 km/hr it was found that the forces on the cultivator shank varied less with tractor speed in this speed range, and in some cases varied very little with tractor speed, than the forces that were observed to vary as a function of the depth of cultivation. Thus the data plotted in Figures 4 and 5 to show the effects of the depth of cultivation on the forces and stresses on the cultivator shank were assumed to be at a constant tractor speed of 8.0 ± 1.0 km/hr.

Load Cell Outputs

The loads plotted in Figure 4 are mean values obtained from four different runs with the vertical bars representing one standard deviation of the random data. In other words, the mean values represent the DC components or steady forces applied to the shank at a given depth whereas the vertical bars represent the cyclic force or AC component. The latter is equivalent to the root mean square (RMS) value about the mean. For assessment of cultivation forces on implement performance an analysis of mean loads is a generally acceptable approach. However, for assessment of the cultivation forces on cultivator shanks or implement holder assemblies then an analysis of the fluctuating loads would be more appropriate.

The results plotted in Figure 4 show that load increased with depth. The lateral load, as measured on the trailing sweep, and not generally present with a symmetrically shaped tool, was because of the unsymmetrical disturbed/undisturbed soil left by the forward sweep. On other data where only a single sweep was used the lateral load was considerably less than that shown in Figure 4 unless the shovel tool was observed to glance off or hit a rock. From Figure 4 it is seen that at a cultivation depth of 0.2 m the draw

bar forces were large at 3.5 kN/sweep (790 lbs/sweep). When multiple sweeps are employed the depth of cultivation will be severely limited by the tractive power available.

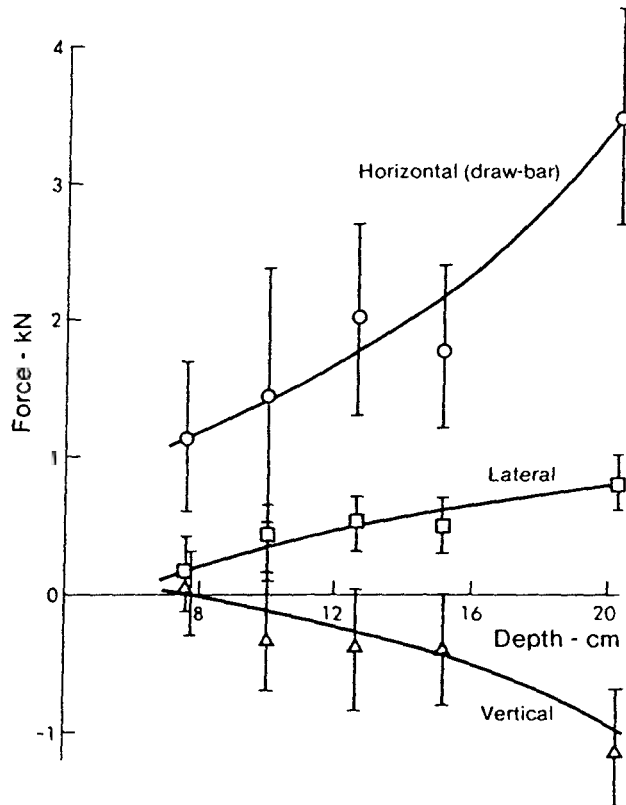


Figure 4 Outputs from Load cells

With any random data, such as obtained from the outputs of the load cells during field runs, it is possible to evaluate the output signals to establish a statistical probability of certain amplitudes occurring in any given test run. From the computer program the probability density function was obtained for each selected test run and test runs of similar input conditions were compared to evaluate the degree of randomness of the data. In Figure 5 the probability density functions are plotted for two test runs conducted at the same depth but at different speeds. These plots show the similarities in the testing conditions and, because they were run at different speeds, provide further evidence that the speed variation was not a significant factor in the measured loads for the particular soil conditions tested.

Stress on the Shank

In Figure 6 the average stresses measured 0.06 m from the fixed end of the cultivator shank are presented. The vertical bars denote the RMS cyclic stress about the mean. It is evident that for the 0.02 m depth the longitudinal stress was 317 ± 64 MPa (46 ± 9 ksi) whereas the lateral stress, at the same point, was considerably lower

at 17 ± 12 MPa (2.4 ± 1.7 ksi). Even though at this depth of cultivation the system seemed to be under heavy loads, the average stresses in the shank were within reasonable limits and the fluctuating stresses less than the endurance limit 415 MPa (60 ksi) for the material (AISI 8635).

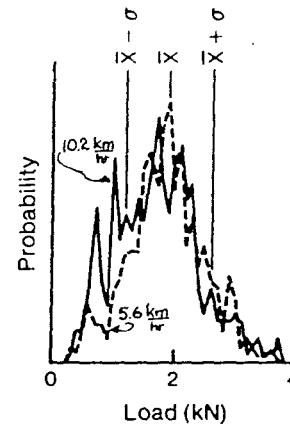


Figure 5 Probability Densities

Frequency Analysis

The data recorded directly on FM tape was processed through an FFT analyzer to determine the dominant frequencies of the recorded random signals. The analysis of two load cells, numbers one and six (see Figure 1) of power spectral density versus frequency is shown in Figure 7. Similar frequencies are recorded in Table I.

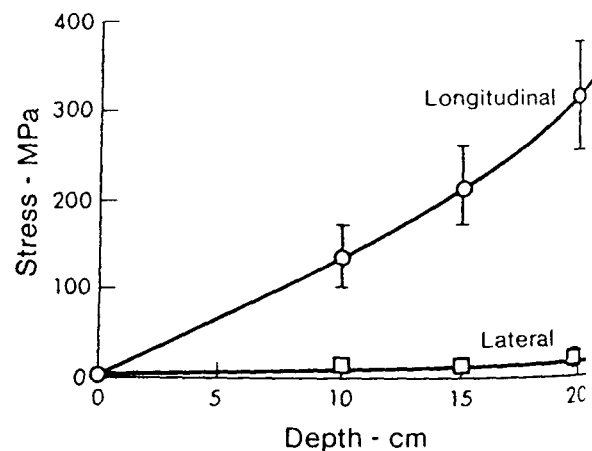


Figure 6 Stress on Cultivator Shank

Although in some cases there appears to be a range of dominant frequencies, generally the frequency of vibration of the cultivator shank at a depth of 0.15 m and speed of 7.4 km/hr in the tested soil conditions produced low cyclic vibration in the range of one to nine Hertz. It is evident from Table I that with one sweep the range of dominant frequencies for the horizontal forces are generally less than that observed

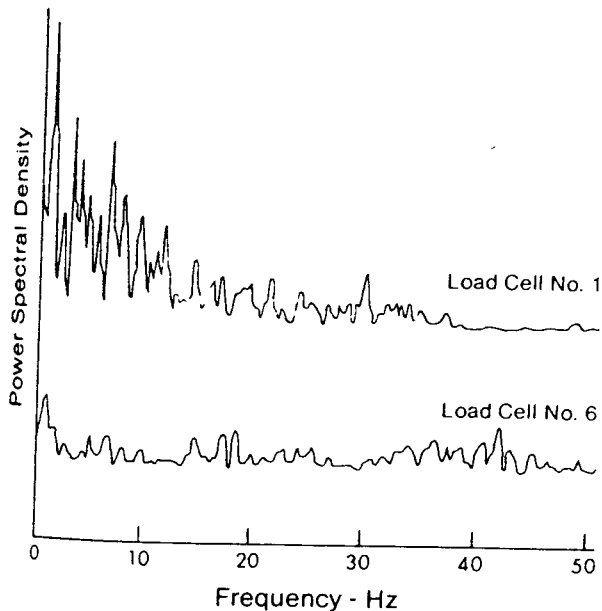
with two sweeps in operation. Whereas, for the vertical and lateral forces, the range of frequencies are generally higher with the one sweep than with the two sweep operation. This suggests that the partially ploughed ground left by the forward sweep reduces the range of dominant frequencies of the vertical and lateral loads on the trailing sweep, while increasing the frequency range slightly for the horizontal loads acting on the trailing sweep.

Table I

Load Cell	Dominant Frequencies - Coaldale (Alta.)		
	Test Condition		
	One Sweep (free*)	One Sweep (solid)**	Two Sweeps (solid)
1	1-7 Hz	3-4.75 Hz	1.25-6.75 Hz
2 & 3	1-9	0.75-4.75	1-6.75
4 & 5	1.15-9	1.38-8.25	1.75-2
6	1-5	1.5-3.25	1-2

*Spring of holder assembly in operation

**Spring of holder assembly locked out

Figure 7
FFT Analysis

SUMMARY

An apparatus and testing procedure has been described which is being used successfully to measure loads on cultivator shanks while ploughing under actual field conditions. It is shown that both the magnitude of the load and the frequency of application can be monitored and the data processed in a manner which enables an ana-

lysis to detect differences in depth of ploughing and differences in measured loads whether a single sweep or tandem sweep is in operation.

The analysis also showed that the effects of forward speed on the measured loads in the range 6 to 12 km/hr was not significant and for the particular test site evaluated, the effect of depth of cultivation on the measured loads was more pronounced.

It was found that uneven terrain, bouncing of the tractor, and compression of the depth gauge tires all contributed to an uneven depth of cultivation. An improvement in the testing apparatus would be to incorporate a means to record depth continuously as a function of forward speed.

This paper presents the results from a single test site. Further work is currently underway to analyze the results obtained from four other test sites evaluated during 1979 with the purpose of relating the measured forces to the differences in soil conditions noted from one test site to another.

ACKNOWLEDGEMENTS

The authors express their sincere appreciation to the Alberta Agricultural Research Trust and The Steel Company of Canada Limited for their joint financial support of this program. Thanks are also due to Mr. R. Holowach, Mr. F. Sawyer, and Mr. Richard Mills who assisted in operating the equipment during the field trials.

Measurement of Tapping Torques

Paper describes two simple load dynamometers which have been used successfully to measure tapping torques under both laboratory and production operating conditions

by D.G. Bellow and G.C. Kiss

ABSTRACT—Two dynamometers are described which have been successfully used to measure the torques of tapping internal threads in hardened-steel cylinders. It is shown that the results from a dynamometer attached to a tapping machine in a production operation compare favorably with the results obtained in the laboratory using a lathe to which a simple torque dynamometer can be fitted. For purposes of illustration, the results of using a cut tap and a rolled tap are presented and discussed.

Nomenclature

ϵ_s = apparent strain— $\mu\epsilon$
 ϵ = torsional strain— $\mu\epsilon$
 R_g = gage resistance—ohms
 R_s = shunt resistance—ohms
 k = gage factor
 T = torque—ft-lb (Nm)
 r = radius of tap shank—in. (mm)
 G = modulus of rigidity of shank material— 11.5×10^6 psi (79.3 GPa) for steel

Introduction

The measurement of torque from a rotating shaft is both a straightforward and, yet, complicated procedure. It is straightforward because, with the use of suitably mounted electrical-resistance strain gages, the analysis of calculating torque from strain readings is quite simple. What often complicates the procedure, however, is transmitting the electrical signals from a rotating shaft to the fixed position of a recorder. The use of slip rings to overcome this problem is widespread, but there can be problems, such as noise superimposed on the signal, which can lead to difficulties. These were some of the problems foreseen when it was required that a convenient, yet reliable, system be found for measuring the torque required to produce internal threads under a variety of speeds and machining conditions.

In an extensive report on measuring drilling forces, Galloway¹ used dynamometers to which the stock to be drilled could be clamped. Thus, the reactive torque of the workpiece was measured. Another report by Loewen

*et al.*² described similar types of load cells for measuring drilling torques and which used electrical-resistance strain gages attached to a torque tube. While these devices were adequate for the experiments described, they required the testing to be carried out under laboratory rather than production conditions. There is merit in setting up a test in the laboratory but there is nothing more convincing than a test performed under actual field or production conditions.

The objective of this paper is to describe two simple load dynamometers which have been used successfully to measure tapping torques under both laboratory and production operating conditions. Some features to be incorporated in the design of the dynamometers were that they be convenient to use and be adaptable to different sizes of drills or taps. For evaluation purposes, it was desired to measure the torque required to produce a 1-in. (25-mm)-diam internal thread under production conditions.

The measurement of tapping torques can be accomplished by determining the active torque on the tap or the reactive torque in the workpiece. For the primary applications specified for this project, it was deemed too costly and complicated to modify the clamping device on a production machine to act as a dynamometer and, thus, it was prescribed that the tap be instrumented to measure the active torque of the thread-cutting process. Once it was decided to instrument the tap, the next step was to get the output signal from the tap to the recording instrument. This was accomplished in two ways; one was to use a small FM transmitter clamped to the shank of the tap, the other was to use a lathe where the workpiece rotated and the tap remained fixed. The construction of these dynamometers and the results obtained are described below.

FM Telemeter

The use of an FM telemetering device for transmitting signals from rotating machine elements to remote locations is not new. However, the application of this device to the transient recording of torque is a departure from conventional methods hitherto used in measuring tapping forces. While the cost of an FM transmitter and receiver is not insignificant (presently, \$2500 U.S.), this represents the major cost in this torque-measuring system. As the FM transmitter is a versatile piece of equipment, the initial cost can be justified on the basis that it can be used for other measuring systems and need not be used exclusively for torque measurement.

For the results of this investigation, an Inmet Model

D.G. Bellow (SLSA Member) is Professor and Chairman, Department of Mechanical Engineering, and G.C. Kiss is Research Associate, Department of Mechanical Engineering, University of Alberta, Edmonton, Alberta, Canada T6G 2G8.

Original manuscript submitted: September 1979. Author notified of acceptance: June 1980. Final version received: July 23, 1980.

T-208B transmitter and Inmet Model R10-B receiver were used. The transmitter measured 1 1/4 in. (44 mm) in diameter by 1 1/2 in. (38 mm) long. The transmitter was fitted with a rechargeable Ni-Cd battery which provided the bridge-excitation voltage as well as the power required for transmission of the signal to the receiver. The transmitter weighed 2 oz (57 grams). With the use of four active gages in a Wheatstone-bridge configuration, the strain sensitivity of the unit was 125 $\mu\epsilon$ for full-scale output. Accuracy was ± 2 percent and linearity better than ± 1 percent over a frequency range of dc to 2000 Hz. The

transmitter and receiver were tuneable anywhere in the FM band (88-108 MHz) and operated with a subcarrier frequency of 10 kHz.

It was determined that the anticipated torques required to produce a 1-in. (25-mm) internal thread would be sufficient to produce enough strain on the surface of the tap shank that no machining of the shank or alterations of the tap would be required. Four electrical 350-ohm resistance strain gages, oriented at 45 deg to the longitudinal axis, and wired up in a four-arm Wheatstone-bridge configuration were attached to the shank of the tap. Under test conditions, it was found that the measured strain from these gages was greater than 125 $\mu\epsilon$ so as to saturate the amplifier of the FM receiver. Thus, two resistors (75 Ω and 270 Ω) were added to decrease the full-scale sensitivity, effectively desensitizing the output signal. The instrumented tap with FM transmitter clamped to the shank and general electrical arrangement are shown schematically in Fig. 1.

The calibration of the FM-transmitter dynamometer was carried out by using a shunt resistance across one of the active gages to produce an apparent strain

$$\epsilon_s = \frac{R_g}{k(R_s + R_g)} \quad (1)$$

where R_g is the gage resistance, R_s is the shunt resistance, and k the gage factor for the strain gages in use. The output measured on an ultra-violet oscillograph chart recorder for a specified shunt resistance across one gage was one-quarter of the output if all gages were active. Thus, the output measured on the recorder under actual tapping conditions was divided by four.

For four active gages, it can be shown that the resulting torque can be calculated from

$$T = \pi r^3 G \epsilon \quad (2)$$

where G is the modulus of rigidity of the tap material, r is the radius of the tap shank, and ϵ is the strain in one of the active arms. This formula [eq (2)] assumes that a four-arm active bridge is used with the gages wired to be additive.

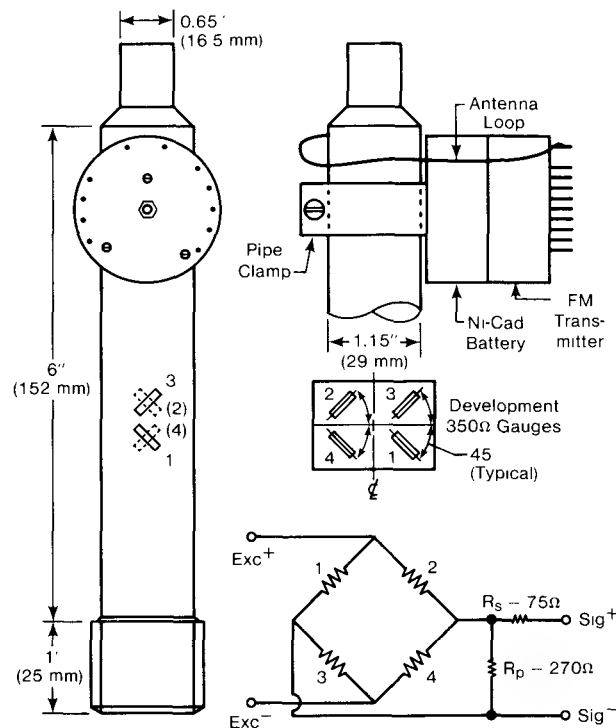


Fig. 1—FM transmitter and strain gages on tap shank

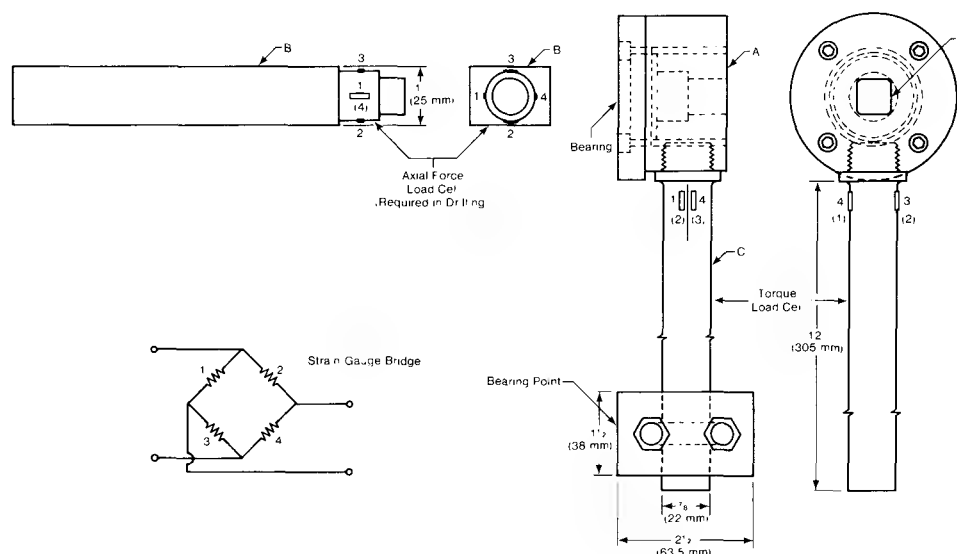


Fig. 2—Lathe-tool dynamometer

Fig. 3—Dynamometer in place in lathe



Lathe Dynamometer

The second dynamometer developed for measuring tapping torques was one which was designed to be used on a lathe in the laboratory. This was to enable tapping torques as measured under production conditions to be compared with those measured in the laboratory. A lathe dynamometer also allowed for greater flexibility in selecting tapping speeds than that permitted on a production-line tapping machine, and enabled the results to be obtained without disrupting a production schedule.

Figure 2 shows a general arrangement of the lathe dynamometer wherein the square end of the shank of the tap fitted into a square socket of the load cell at A. The rectangular shank B fitted into the tool-post holder of the lathe carriage. The torque arm of the dynamometer had four 350-ohm strain gages mounted to measure the bending strain of the arm. The clamp (bearing point) was supported by the lathe carriage. The carriage was set to move at the feed rate consistent with the thread being produced, but the carriage did not provide any axial thrust on the tap as the tap was self feeding. A general view of the dynamometer in place on the lathe measuring the torque of tapping is shown in Fig. 3.

The lathe dynamometer was calibrated with the dynamometer in place shown in Fig. 3 except that instead of the arm C resting on the lathe carriage it was suspended at an angle of 180 deg to that shown in Fig. 3 and weights were attached to the bearing point (see Fig. 2). Calibration curves were plotted for both the FM-transmitter dynamometer and the lathe dynamometer with the results for each case being linear. Typical output gains were 15-25 ft-lb (20-34 Nm) per centimeter of output on the oscillograph recorder. Although not a factor in self-threading taps, the end thrusts could be measured, as for the case in drilling, by the axial gages mounted to the tool-post shank as shown in Fig. 2.

Results

For evaluation purposes a 1-in. (25-mm) API-10 rolled-thread tap and a 1-in. (25-mm) API-10 conventional cut-thread tap were used to produce internal threads in cylinders made from AISI 8635 steel quenched and tempered to a hardness of Rockwell 28C. To compare the results obtained from the FM-transmitter dynamometer with the lathe dynamometer, the strain-gaged tap with transmitter was fitted into the lathe dynamometer and, for a rolled thread, the output signals were obtained

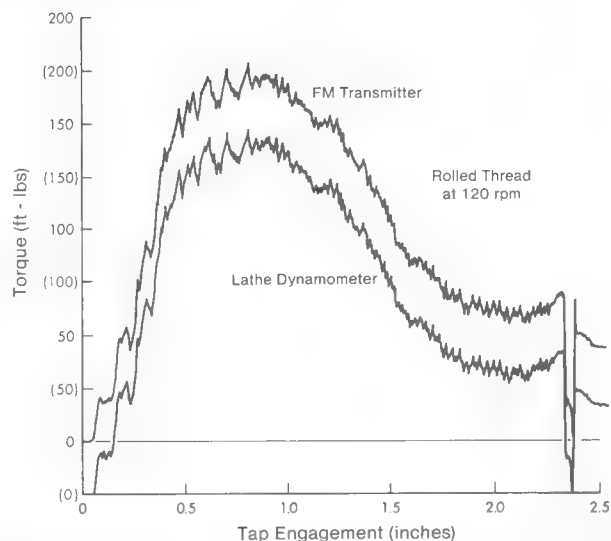


Fig. 4—Comparison between lathe dynamometer and FM transmitter

simultaneously on an oscillograph recorder. Figure 4 shows that the output from both dynamometers compared favorably with one another as to general form and output when a 1-in. (25-mm) API-10 rolled thread was produced at 120 rpm.

Figure 5 compares the torque profile for a cut tap with that of a rolled tap for a 1-in. (25-mm) API-10 thread. These profiles were obtained using a lathe dynamometer during which a thread was being produced inside a 4-in. (100-mm)-long cylinder. It is clearly evident that the cutting action of the rolled tap was different from that of the cut tap. Notably, the maximum torque of 120 ft-lb (164 Nm) for the cut tap was less than the maximum torque of 140 ft-lb (190 Nm) required for the rolled tap. It was also observed that the cut tap built up to a maximum torque when the thread of the cylinder was 60 percent complete followed with a rapid drop-off in torque as the end of the tap came out the other side of the cylinder. For the rolled tap, the torque built up quickly and remained relatively constant for almost the entire length of the thread through the cylinder (100 mm).

Tapping torques as a function of tapping speed for a

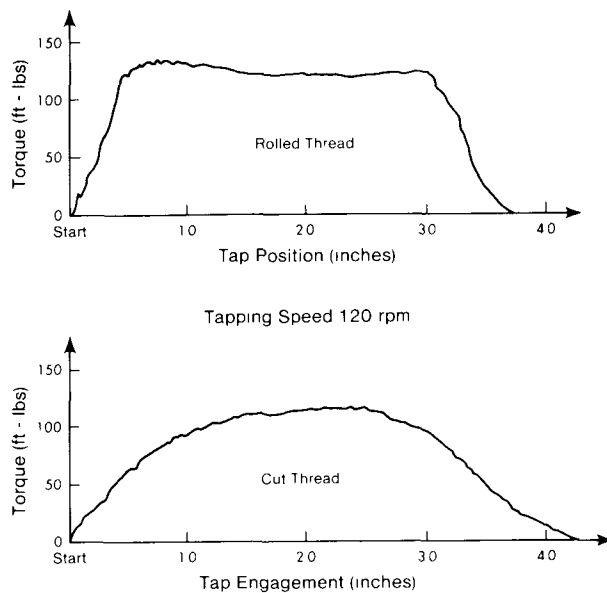


Fig. 5—Thread profiles

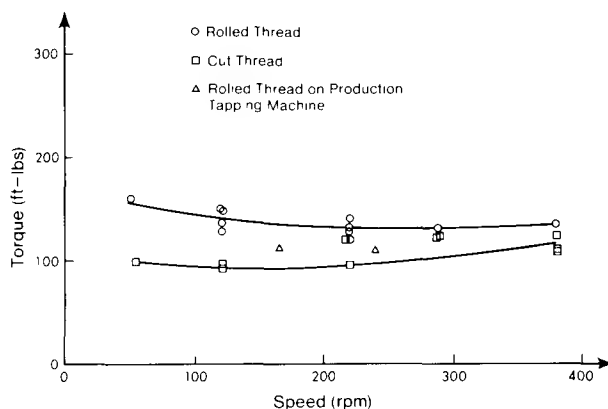


Fig. 6—Tapping torques for cut and rolled threads

1-in. (25-mm) API-10 thread are shown in Fig. 6. A number of test results were plotted with a smooth curve drawn to represent an average value. The results for the rolled and cut threads were obtained using the lathe dynamometer, whereas the two plotted points at 165 and 240 rpm were obtained using the FM transmitter on a vertical tapping machine for a rolled thread during a regular production run. All speeds were measured under tapping load. It is interesting to note that the torque required to produce a thread on a vertical tapping machine was less than that required to produce a similar thread on the lathe using the same tap and cutting speed. It is believed this is because the vertical tapping machine provided a better flood of lubrication and the vertical arrangement provided for a more direct path of chip removal. From Fig. 6 it is seen that, at a cutting speed of 120 rpm, it required approximately 35 percent more horsepower to produce a rolled thread than to produce a cut thread.

It was found that operating the FM transmitter in a

production factory led to poor reception of the signal due to excessive electrical interference from welding machines, radio-controlled overhead cranes, and nearby electrical machinery. As the tap rotated in the tapping machine, almost the entire signal was lost when the antenna of the transmitter was obscured by the shank of the tap from a line of sight to the receiving antenna. This problem was largely overcome by looping the antenna of the transmitter around the tap body as shown in Fig. 1.

The threading taps used in this investigation under production conditions were used to produce threads in 4-in. (100-mm)-long cylinders. The taps required no end thrust but were allowed to run through the length of the cylinder and drop out the other end. For the case of the lathe dynamometer, this practice was continued but, with the FM transmitter attached to the shank of the tap, the threading process had to be stopped before the tap completed its run to prevent damage to the strain gages and transmitter. This was not considered to be a major problem in that sufficient data for analysis could be obtained before the tap completed its runout.

In obtaining the results plotted in Fig. 6 it was found, for some taps and rotational speeds, excessive tool chatter prevented any meaningful output signal to be measured from either of the dynamometers evaluated. For example, with a cut tap having a single taper lead it was found that tool chatter occurred at speeds 220 rpm and over. However, for cut taps with two taper leads in series readable output signals were obtained for rotational speeds up to 480 rpm (the maximum speed evaluated) although some chatter was observed as the tap was first engaging the metal. These tests were repeated using worn taps; taps which would no longer be used in production. In these cases, it was found that the output signals from the dynamometers were clear and readable and similar to those shown in Figs. 4 and 5. From the tests performed in this study, it would appear that tool chatter was more a factor of the tapping speed and tap type rather than on the condition of the tap.

Summary

This paper describes two types of dynamometers which can be used successfully to measure tapping torques. It is shown that the results from both dynamometers are comparable and that the dynamometers described can be used to effectively detect a variety of tapping characteristics such as maximum torque and torque profile for a given length of thread produced. A lathe dynamometer has the advantage that it can be used for measuring tapping conditions under a greater range of speeds than possible on production tapping machines. Where confirmatory testing is required, the FM-transmitter dynamometer described is a simple device which can be used for this purpose.

Acknowledgments

The authors wish to thank The Steel Company of Canada Limited and the National Research Council (Grant A-2705) for their cooperation and support in this investigation.

References

1. Galloway, D.F., "Some Experiments on the Influence of Various Factors on Drill Performance," *Trans. A.S.M.E.*, **70**, 191-231 (1957).
2. Loewen, E.G., Marshall, E.R. and Shaw, M.G., "Electric Strain Gage Tool Dynamometers," *Proc. S.E.S.A.*, **8** (2), 1-16 (1951).

Pipeline and Energy Plant Piping: Design and Technology

Testing Factors Which Influence Fatigue Life of Butt Welded Low Carbon Steels

D.G. Bellow and M.G. Faulkner

Dept. Mech. Eng., Univ. of Alberta
Edmonton, Alberta, Canada

ABSTRACT

Frequency of testing and specimen size can affect the fatigue life of transverse butt welded low carbon steels subjected to a pulsating tensile load. It is shown that for a fatigue life in the range between 10^4 and 10^6 cycles the effect of frequency of testing is an important factor and should be taken into account while for a fatigue life greater than 10^6 cycles the effect of frequency of testing was insignificant. The width of the specimen was also found to affect fatigue strength wherein a reduction of 17 percent was observed when the specimen width increased from 25 mm to 102 mm. It was also shown that specimen shape was not a factor of influence in evaluating fatigue data for pulsating tensile loaded butt welded steel specimens.

KEYWORDS

Butt welds, low carbon steel, fatigue life, fatigue strength, testing frequency, specimen size, shape.

INTRODUCTION

As is well known, the fatigue limit of simple transverse butt welds depends on the welding process, the type of filler rod, the care with which the weld was produced, the shape of the weld, and whether or not any post heat or mechanical treatment was carried out. But what is not as well understood is the influence of the testing parameters used in generating and evaluating fatigue life data. For example, butt welded joints in service may be subjected to load frequencies varying from a few cycles per day to many hundred per minute. If the frequency of testing for fatigue life influences the measured values then the testing frequency should match the anticipated in-service load cycle conditions. It has been suggested (ASTM, 1963) that in the range 3-120 Hz for plain specimens there should be no frequency effect provided the temperature of the specimen being tested remains constant and there are no corrosion effects. In another case (Lomas and colleagues, 1956) it was observed that at frequencies in the range 750-15000 Hz that the endurance limit first increased with frequency up to 1200-1800 Hz and then decreased with further increases in testing frequency. These results were reported for non-welded specimens. Jones and Higgins (1970) found no appreciable

367

WELDING
INSTITUTE OF
CANADA



INSTITUT
DE SOUDAGE
DU CANADA

Pergamon Press

Toronto • Oxford • New York • Sydney • Paris • Frankfurt

effect of frequency on fillet welds in mild steel whereas Györgyi (1965) found some effect in the range 8-117 Hz. More recently Faulkner and Bellow (1979) have shown that for stress levels which give rise to fatigue lives of 10^6 cycles or more, the effect of frequency of testing must be accounted for in the fatigue life range of 10^4 to 10^6 cycles.

In preparing for a fatigue test the geometry of the specimen must be carefully selected. Trufyabor (1958) reported that, for reversed bending tests, that increasing the size of the test specimen, in both thickness and width tended to decrease the fatigue strength. This was attributed to the effects of residual stresses. In another investigation Frost and Denton (1957) observed no differences in fatigue lives for 3/8 in. (8.7 mm) and 3/4 in. (19 mm) wide specimens. Whereas, reductions of eight percent were reported by Gurney (1979) when specimen thickness was increased from 16 to 25 mm. For pulsating tension loads on transverse butt welds Trufyabor (1963) reported reductions of up to 25 percent when the cross section changed from 70 x 14 mm to 200 x 30 mm. Györgyi (1965) found that with increasing specimen width and thickness the fatigue strength decreased. Unlike the case for plain specimens it is generally agreed that there will be some reduction in fatigue life as the specimen size increases, the amount of which will depend on the degree of notch sensitivity at the toe of the weld, the material type, and consistency of surface finish as the specimen size increases.

For typical fatigue work of butt welded plain materials rectangular specimens 7-13 mm wide by 450-900 mm long are suggested (Gurney, 1979). Although much has been written (Weibull, 1961) on the influence of shape on the fatigue strength of a specimen, rectangular specimens for fatigue work are generally satisfactory because the notch factor at the toe of the weld is sufficient to ensure failure at the weld. If post mechanically treated welds are to be evaluated where the notch factor is reduced then dog-bone specimens are used. Apart from the added cost of making these latter specimens, the fatigue results obtained from dog-bone specimens should be the same as for plain rectangular specimens for the same cross sectional area at the location of the butt weld.

From the results of previous investigations it is clear there are a variety of opinions as to the effect of frequency of testing and specimen size on the fatigue life of butt welded steel specimens. The objectives of this paper are to describe the effects of testing frequency in the range 2-200 Hz and specimen width 25-102 mm on the fatigue life of butt welded steel specimens.

SPECIMEN PREPARATION

The material used in this study was made by welding 1 m long by 127 mm wide and 6.4 mm thick steel plates. The plates were in the as-rolled condition and were beveled at 45° before welding along the 1 m edge using a double-sided submerged arc welding process. Oxxweld No. 36 welding wire 3.17 mm diameter was used in combination with Oxxweld 585 flux. Welding speed was 1.42 m/min with the tip height 22.2 mm from the workpiece and 8 mm from the electrode. The material properties are listed in Table 1.

For evaluating the effects of testing frequency, dog-bone specimens were machined according to the shape shown in Fig. 1. For evaluating the effects of specimen width, plain rectangular shaped specimens of the sizes indicated in Fig. 1 were chosen. All welds were fluoroscoped to check for flaws and visually inspected. Any specimens showing obvious signs of undercutting at the toe of the weld, or where the specimens were welded offset or at angle, were discarded. Specimens were then selected at random for the testing program.

TABLE 1 Properties of Testing Materials

Material Use	Mechanical Properties		Chemical Composition				
	Yield(MPa)	Ultimate(MPa)	C	Mn	P	S	Nb
Frequency tests	520	545	0.13	0.60	0.014	0.018	<0.01
Specimen width tests	305	445	0.30	0.79	0.010	0.028	<0.01
Oxweld #36 rod	510-615	---	0.14	2.00	0.017	0.024	--

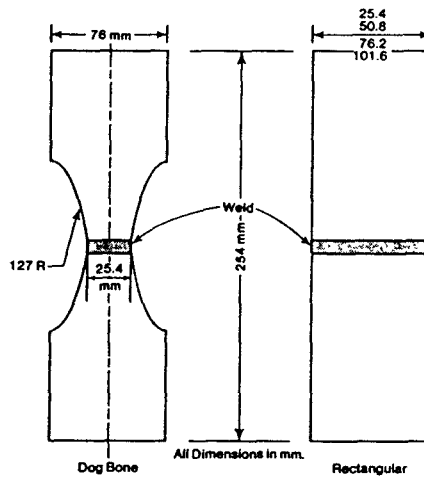


Fig. 1. Specimen geometries

FATIGUE MACHINES

In order to evaluate the effect of testing frequency in the range 2-250 Hz two different fatigue testing machines were used. The low speed tests, 2-140 Hz, were performed on an MTS closed looped resonant hydraulic fatigue machine. The high frequency tests, 128-250 Hz, were conducted on an Amsler Vibrophore. Both machines were operated at 128 Hz to allow the results of one machine to be compared with the results of the other under similar load and frequency conditions. All the testing was conducted in pulsating tension with the maximum loads chosen to give nominal stresses at the weld in the range 175-331 MPa depending on the specific test under investigation. All specimens were gripped using hardened serrated clamps. Both testing machines were checked as to frequency and load accuracy using a strain gauged plain specimen and monitoring the wave form, magnitude and frequency on an oscilloscope. The loads checked to be within ± 5 percent of the strain gauged specimen. The wave form was sinusoidal and frequency of load measured was within ± 1 Hz for both machines.

TESTING PROCEDURE

To ensure complete uniaxial application of load a special jig was designed such that when it was clamped to either side of the weld, it enabled the clamping screws of the grips to be tightened to minimize the bending stresses that could be introduced into the specimen under load. This system was checked with a welded specimen to which strain gauges were attached and it was found that bending stresses were kept to within 10 percent of the axial load whereas without this jig it was easy to introduce bending stresses as high as 30-40 percent of the axial load.

For the specimens run on the Vibrophore the tests were terminated when the machine shut off, usually upon the appearance of a visible crack. The difference between the number of cycles when the Vibrophore shut-off and the number of cycles to complete failure was less than 5 percent and of no statistical significance. For the dog-bone specimens run on the MTS, failure usually occurred with complete rupture of the specimen before the machine shut off. For the wider rectangular shaped specimens, all of which were tested on the MTS, the machine shut down when a visible crack occurred before complete rupture of the specimen.

All fatigue cracks occurred at the weld toe on the surface propagating inward. For the wider specimens surface cracks tended to occur at the center of the specimen as seen in Fig. 2 for a 102 mm wide specimen. Figure 3 shows an SEM photo of a fractured surface of a 102 mm wide specimen obtained at a magnification of 1300.

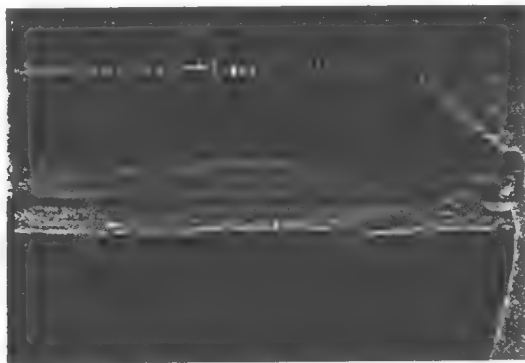


Fig. 2. Fractured surface for 102 mm wide specimen

A minimum of fourteen specimens were tested for each load frequency condition. This number allowed for a better than 90 percent chance in finding differences of more than a single standard deviation between two samples (ASTM, 1963).

To test the differences, if any, between results obtained on the Vibrophore with results obtained from the MTS for the same conditions of load and frequency, data was compared using the student t-test. It was found (Faulkner and Bellow, 1979) there was no significant difference in the results and that it was valid to compare the results obtained from the two machines.

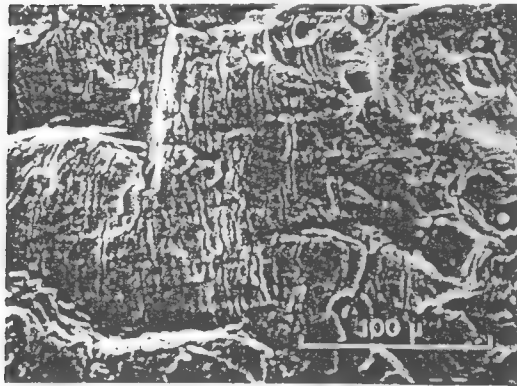


Fig. 3. SEM of fatigued surface

RESULTS

Effect of Testing Frequency

Figure 4 shows the effect of frequency on fatigue life. These results have been reported in more detail elsewhere (Faulkner and Bellow, 1979). The curves have been drawn through the median fatigue lives obtained at each noted stress level. The most notable effect of testing frequency was observed at 265 MPa where a threefold increase in fatigue life occurred between the 2 and 232 Hz testing frequencies. A similar effect was observed at the 331 MPa stress level where the fatigue life increased by a factor of two for the same testing frequency range. For the lowest stress level evaluated in this test, 193 MPa, the effect of testing frequency was less pronounced. The range in which the testing frequency appeared to be most influential was for fatigue lives between 10^4 and 10^6 cycles. This coincides with the range for which the steepest slope of the S-N curve occurs.

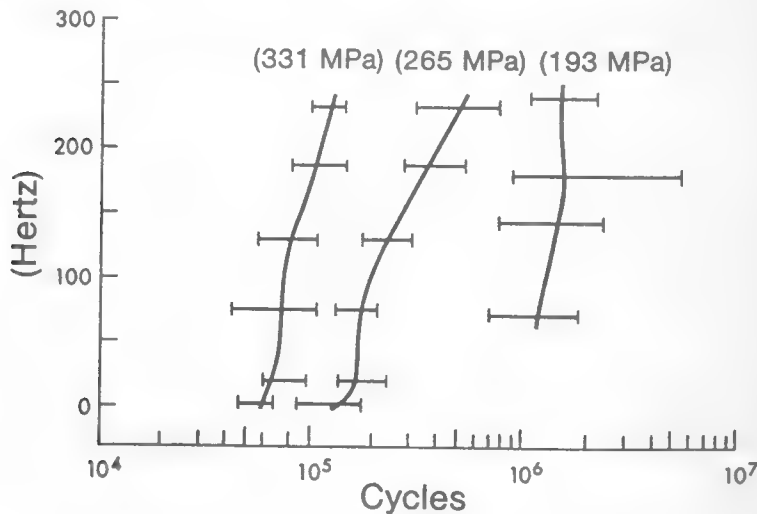


Fig. 4. Effects of testing frequency on fatigue life

Effect of Specimen Width

Except as noted in Table 1 where the material used for evaluating the effects of specimen width was different than that used to evaluate the effect of frequency, all other testing parameters were the same for all tests. Specimens were 254 mm long, 6.4 mm thick and four series of widths, 25.4, 50.8, 76.2, 101.6 mm. The testing was carried out on the MTS machine in the frequency range 90-117 Hz. This frequency range resulted from the fact that the testing machine was operated in a resonant mode and as the stiffnesses of specimen sizes varied, a finite number of weights had to be added or deleted to maintain the frequency in the desired range for a given specimen width. It was not always possible to operate the machine at the same frequency for different specimen widths. However, based on the previous work described above, it was believed that this frequency range would not affect the test results.

The results of the effect of specimen width are shown in Table 2. The median life, and confidence limits are given for each test series. On an S-N graph these data were plotted by connecting the best fit curve through the median points for each specimen width tested. The fatigue strength was then obtained from this graph at a life of 10^6 cycles and plotted as a function of specimen width as shown in Fig. 5. The fatigue life of the plain specimen, without a butt weld, was estimated as one-half the ultimate tensile strength for the parent material as reported in Table 1. In Fig. 5, it is seen that as the specimen width increased the fatigue strength decreased, and in particular, there was a 17 percent decrease in fatigue life when the specimen width increased from 25 mm to 102 mm. It would not appear that, for specimen widths greater than 100 mm, any further reduction in fatigue strength would occur. This is in agreement with Györgyi (1965) who reported a 16 percent decrease in fatigue strength between specimen widths of 20 and 600 mm.

TABLE 2. Effect of Specimen Width on Fatigue Life

Maximum Stress MPa(ksi)	Testing Frequencies Hz	Specimen Width mm(in.)	No. of Specimens Tested	Median Life $\times 10^3$ cycles	95% Confidence Limits	
					Lower	Upper
300(43.5)	110	76(3)	14	64	54	70
	110	51(2)	14	55	36	84
	110	25(1)	14	68	43	86
265(38.4)	100	102(4)	15	94	70	118
	92	76(3)	15	133	109	177
	110	51(2)	15	117	105	138
	115	25(1)	15	116	102	165
193(28)	100	102(4)	14	448	300	808
	90	76(3)	15	529	354	615
	105	51(2)	15	590	435	917
	110	25(1)	15	857	617	1447
175(25)	110	102(4)	14	540	416	793
	110	76(3)	14	793	617	1272
	115	51(2)	14	675	536	1037
	117	25(1)	14	839	447	1464

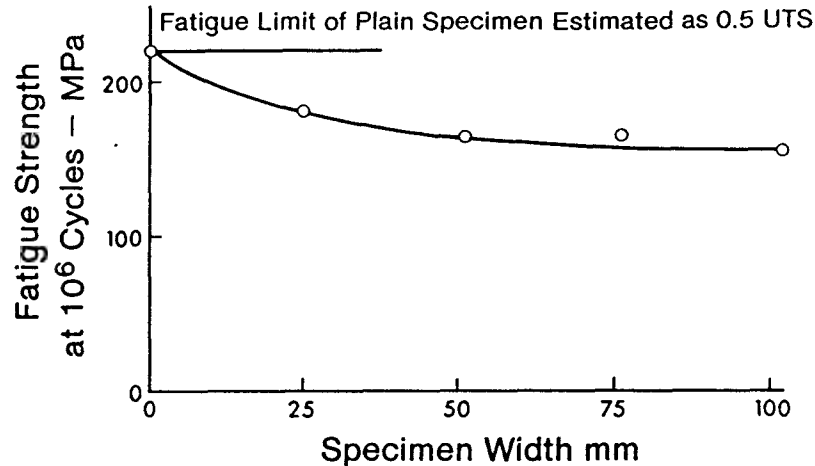


Fig. 5. Effect of specimen width on fatigue life

Effect of Specimen Shape

To evaluate the effects of specimen shape the two configurations shown in Fig. 1 were tested where the width at the weld was 25 mm. The specimen thickness was 6.4 mm in each case. The testing frequency was 145 Hz and maximum stress of 265 MPa. It was found, statistically, that there was no difference in fatigue life between the two specimen types. A total of 14 specimens were tested for each shape.

Generally, it is more economical to use a rectangular shaped specimen than a dog-bone shape because less machining is involved. Nonetheless, for the smaller specimens the surface area at the grips may not be sufficient to adequately clamp the specimen under pulsating load. Another factor to be considered as well, is if the effect of the notch at the toe of the weld is removed, then it will not be possible to ensure failure at the weld if rectangular shaped specimens are employed. This problem is overcome by the use of dog-bone specimens.

SUMMARY

Frequency of testing was shown to affect the fatigue strength of butt welded joints in the range of 10^4 to 10^6 cycles. At 10^6 cycles no significant difference in fatigue life was noted due to testing frequency in the range 79-240 Hz.

For a constant testing frequency it was found that the fatigue strength of a butt welded specimen at 10^6 cycles was reduced by 17 percent when the specimen width was increased from 25 mm to 102 mm.

No significant difference was observed in fatigue life between a dog-bone and a rectangular shaped specimen for the same cross sectional width and maximum pulsating tension load.

ACKNOWLEDGEMENTS

The authors express their sincere appreciation to The Steel Company of Canada Ltd. who supplied the material and carried out the welding of the test specimens. Support from the National Science and Engineering Research Council (Ottawa) under grants A-2705 and A-7514 is also appreciated.

REFERENCES

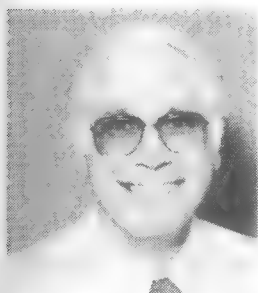
- Anon. (1963). A guide for fatigue testing and the statistical analysis of fatigue data. Special Technical Publication, No. 91-A, ASTM.
- Faulkner, M.G., and D.G. Bellow (1979). Influence of testing frequency on the fatigue of butt-welded steel joints. Weld Res. Int. 9, 12-20.
- Frost, N.E., and K. Denton (1957). The fatigue strength of specimens cut from welded plates of high tensile ferritic steel of fusion welding quality. MERL Rep. PM210 AB Div. No. 2/57.
- Gurney, T.R. (1979). Fatigue of Welded Structures. 2nd ed. Cambridge University Press, 104.
- Györgyi, F. (1965). Influence of load frequency and other factors on fatigue test results of butt welded joints. IIW Document XIII, 383.
- Jones, A.W., and M.G. Higgins (1970). The effect of testing frequency on the fatigue strength of fillet welds in mild steel in narrow band random loading. Conf. of Fatigue of Welded Structures. Cambridge, 23, 290-295.
- Tryfayakor, V.I. (1958). Welded joints and residual stresses. Br. Weld, J. 11, 491-8.
- Tryfayakor, V.I. (1963). Problems in the procedure for fatigue tests on welded joints. Avt. Sv. 1, 1-8.
- Weibull, W. (1961). Fatigue Testing and Analysis of Results, Pergamon Press.

Cultivator shank manufacture and evaluation

D.G. BELLOW
University of Alberta
R.W. PUGH
Stelco Inc., Edmonton, Alberta

ABSTRACT

This paper will describe how cultivator shanks are made in one company and how the manufacturing was studied with a view to increasing product consistency and reducing manufacturing cost. The product, which is used extensively in the agriculture industry, was analyzed to determine which geometric parameters optimized its design and whether there was justification for the great variety of styles and shapes that are available in the market. Finally, an extensive series of field trials were undertaken which showed that it is advantageous to the manufacturer to be better aware of the loads and forces that his product is subjected to by another industry.



D.G. Bellow

Doug Bellow graduated in mechanical engineering from the University of British Columbia in 1956 with a B.A.Sc. He worked for Canadian Industries Ltd. in Kingston, Ontario and General Motors Diesel Ltd., London, Ontario. He obtained an M.Sc. degree in mechanical engineering in 1960 at

the University of Alberta and a Ph.D. degree in the same subject in 1963 from the University of Alberta.

He was appointed to the University Faculty in the fall of 1963 as an Assistant Professor and currently holds the position of Professor and Chairman of the Department of Mechanical Engineering. The latter position he has held since 1975. Throughout his academic career, he has worked with other industries and in particular with Stelco Inc. since 1968, where he has done contact and consulting work primarily for their Edmonton Steel Works and Finishing Works plants.



R.W. Pugh

Robert W. Pugh graduated from the University of British Columbia in metallurgical engineering in 1965. He then worked as a process metallurgist for the Sydney Steel Company in Sydney, Nova Scotia between 1966 and 1968. He joined Stelco Inc. as a research engineer in Hamilton in 1968

and moved to their Edmonton Works in 1975. He currently holds the position as senior research investigator for Stelco Inc. at its Edmonton operations.

Keywords: Technology, Cultivator shanks, Stelco, University of Alberta, Manufacturing, Tensile stress, Steel.

Introduction

Stelco maintains a Research Group for its Western Region operations headquartered in Edmonton, Alberta. Because of the small staff, a location that is isolated with respect to its Burlington, Ontario centre and a diverse set of processes and products, a university relationship has developed which may be different from that which would be developed at a larger integrated Steel Works. This paper outlines the type of cooperative studies carried out by Stelco Inc. in Edmonton and the University of Alberta.

To meet the research needs covering a wide variety of steelmaking processes and steel products produced in Edmonton would require more staff and equipment than the sales volume in the West justifies. The gap is filled by cooperation with university personnel. This cooperation has provided these benefits to Stelco Inc:

- access to specialized test equipment and a trained staff to operate it; and
- assistance from experts in the areas of product testing and problem solving.

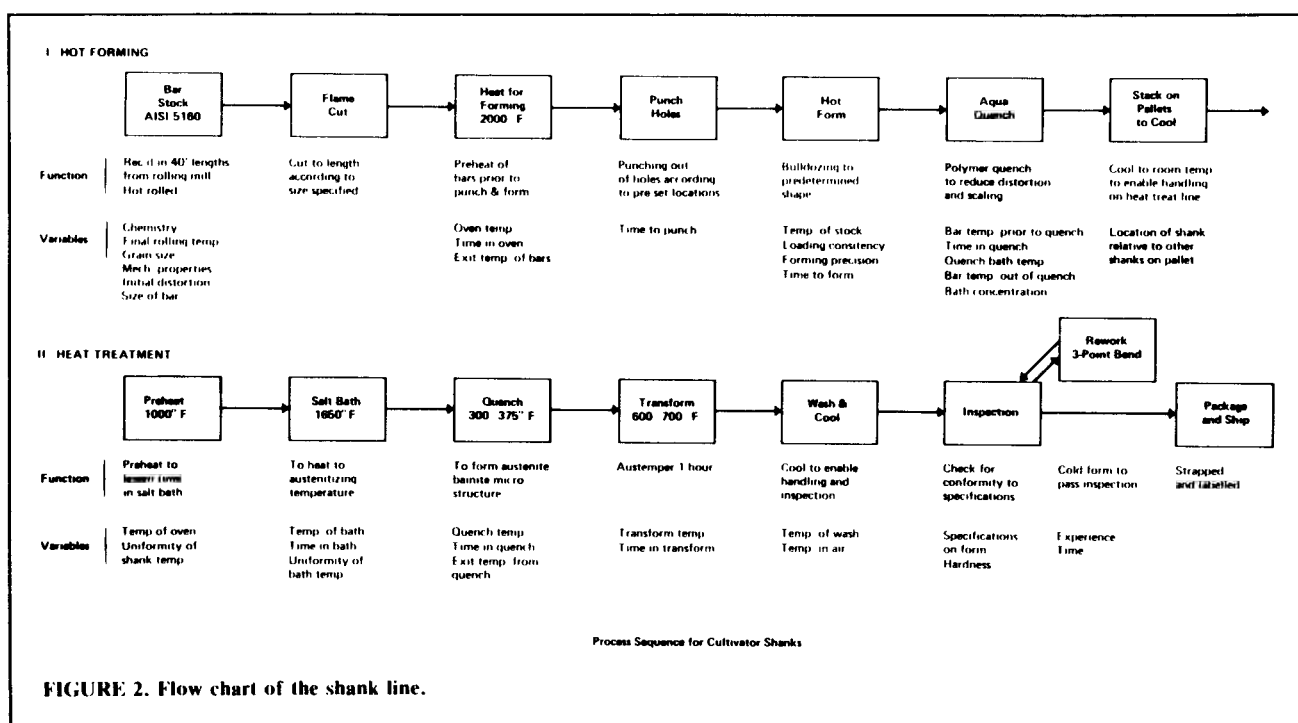
Moreover, the close proximity of the university to the plant allows frequent meetings and ensures that practical solutions are developed and implemented. A good example of the ongoing university/industry relationship developed is the joint work on improving cultivator shanks.

Manufacture of Cultivator Shanks Background

Cultivator shanks are curved spring elements made from bar stock of various sizes in a punch-and-forming operation followed by an appropriate heat treatment process. In Figure 1 is shown a row of cultivator shanks mounted behind a large



FIGURE 1. Cultivator shank unit.



tractor. A cultivator implement in some cases may contain as many as 45 cultivator shanks in a span 27.5 m wide. These types of implements are used to till the soil, which in farms in Alberta range up to 8000 ha.

As a result of a program of product diversification in 1967, the Edmonton Finishing Works of Stelco Inc. began to produce cultivator shanks. At first these shanks were produced using equipment available in the plant at the time, consisting of a spike furnace, a punch and a bulldozer adapted to produce the product. The hot-formed shanks were heat treated to form a tempered martensite microstructure.

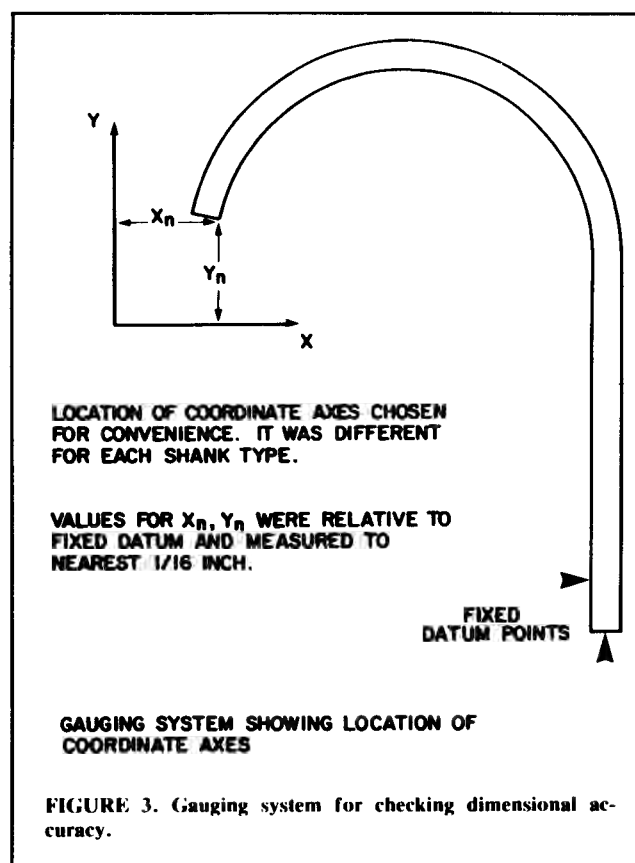
After a year of operation, an austempering heat-treat line was added to increase heat-treat capacity and produce a quench-and-tempered bainite structure. In 1975, an automated punch and press was added to the hot form line as the first step in increasing over-all line capacity. Production had gone from 100 t in 1968 to 2500 t in 1976 and levels of 4000 t were anticipated for 1979. However, control of cultivator shank shape was a major problem. Up to 35% of the production required some reworking to meet dimensional specifications and up to a further 23% had to be scraped together.

An in-plant study was carried out by Dr. Don Bellow, Mechanical Engineering Department, University of Alberta, to determine how to control this shank distortion.

Investigation

A preliminary analysis of the manufacturing process revealed that some 30 variables could lead to distortion of the final shape. A flow chart of the process was constructed and is shown in Figure 2. Each sequence of operation was detailed along with the variables which could affect the dimensional shape of the product. It was apparent at this preliminary stage that, throughout the process, temperature and time were subject to a range of controls. For example, temperature was monitored continuously at only one station, whereas there were five other stations at which temperature was assumed to be controlled, but not monitored.

At the spike furnace, the bar stock is cut to length by flame torch and is fed into a walking beam apparatus which allows the shanks to be heated above the austenitizing temperature. The shanks are then hot-punched and formed to the C-shape in the bulldozer. The shanks were then manually picked up with tongs and placed in a polymer quench tank. After coming out of the quench tank, they were stacked on pallets waiting to



be loaded into the batch process of the heat treatment line.

To determine the causes for shank distortion, unnecessary reworking and rejection, the investigation took place in three steps. The first step was to gather information on the process as it was then being operated, specifically with respect to measuring temperatures and times of each manufacturing sequence. The second step was to analyze the data and determine what caused this distortion in the shape of the shank. The third step was to adjust the system and make recommendations on

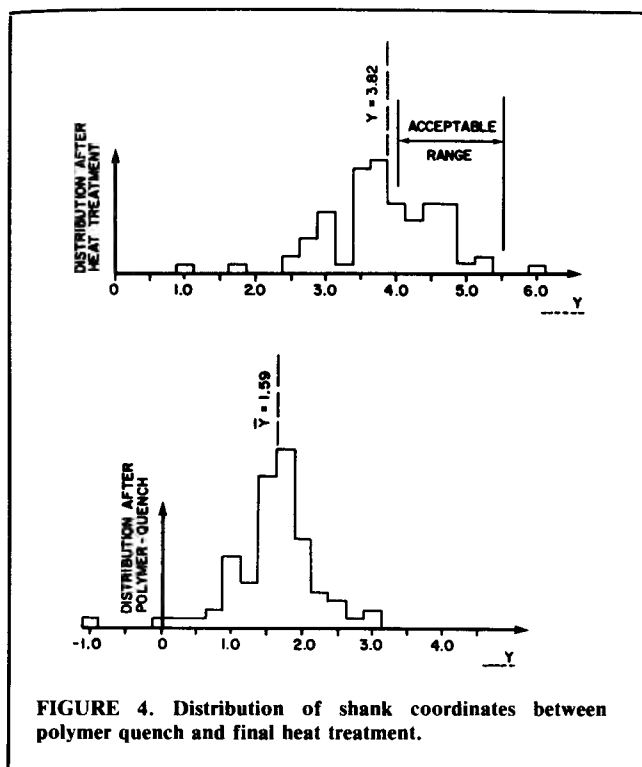


FIGURE 4. Distribution of shank coordinates between polymer quench and final heat treatment.

what controls would be necessary to maintain a consistent product.

Cultivator shank distortion was monitored using a rectangular coordinate system to measure the free-end position of the shank to the nearest ± 1.5 mm. The gauging system that was used is shown in Figure 3. Both absolute and relative changes were recorded and analyzed for a variety of shank sizes and production runs. Shanks were checked for distortion after the quench tank on the hot form line and after final heat treatment on the heat-treat line so the effect of both processes on distortion could be determined. Bar charts, averages and standard deviations were calculated along with other statistical and analytical methods where appropriate.

A typical set of data taken at the time are shown in Figure 4. In this case, some 68% of the finished shanks were rejected because they failed to meet the dimensional tolerances specified on the shop drawings. Clearly, the mean of the Y-coordinate did not lie within the acceptable range and the spread in dimensions exceeded the acceptable limits by a factor of three. This also showed that no amount of change in the conditions in the heat treatment line would reduce the spread in tolerances noted at the end of the hot forming line. This was in contradiction to some operators' beliefs that errors in dimensions as a result of the hot forming line could be corrected by appropriate temperature changes in the heat treatment line.

Another illustration of the type of data that were analyzed was to determine the influence of stacking the shanks after the polymer quench at the end of the hot form line. A test was performed which placed each shank individually on the cold shop floor (where the cooling rate was considered to be uniform) versus stacking the shanks one on top of the other (where the cooling rate was nonuniform). Figure 5 shows how the standard deviation was reduced when the shanks were subjected to uniform cooling.

Conclusions

On analysis of all the test results, of which only a few have been reported here, the following conclusions were reached:

- Control of distortion of the shape of cultivator shanks was a direct function of the degree of uniformity of the rate of cooling after hot forming and prior to heat treatment.

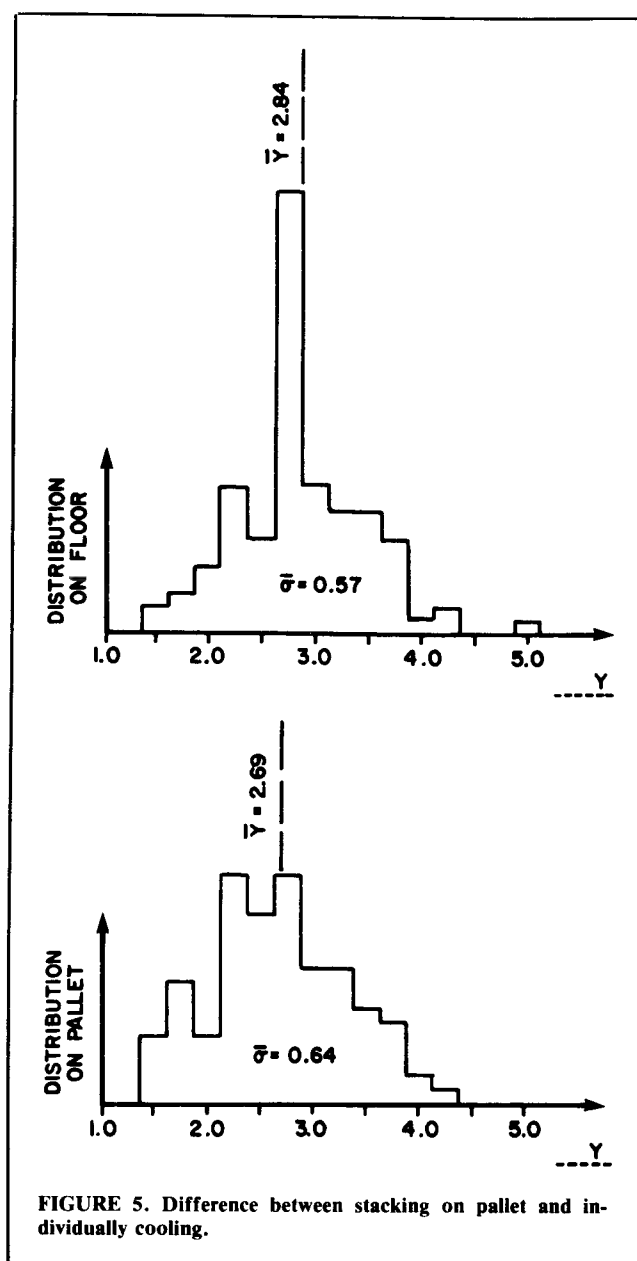


FIGURE 5. Difference between stacking on pallet and individually cooling.

- Lack of uniform cooling after hot forming could not be corrected by changing the conditions during the heat treatment process.

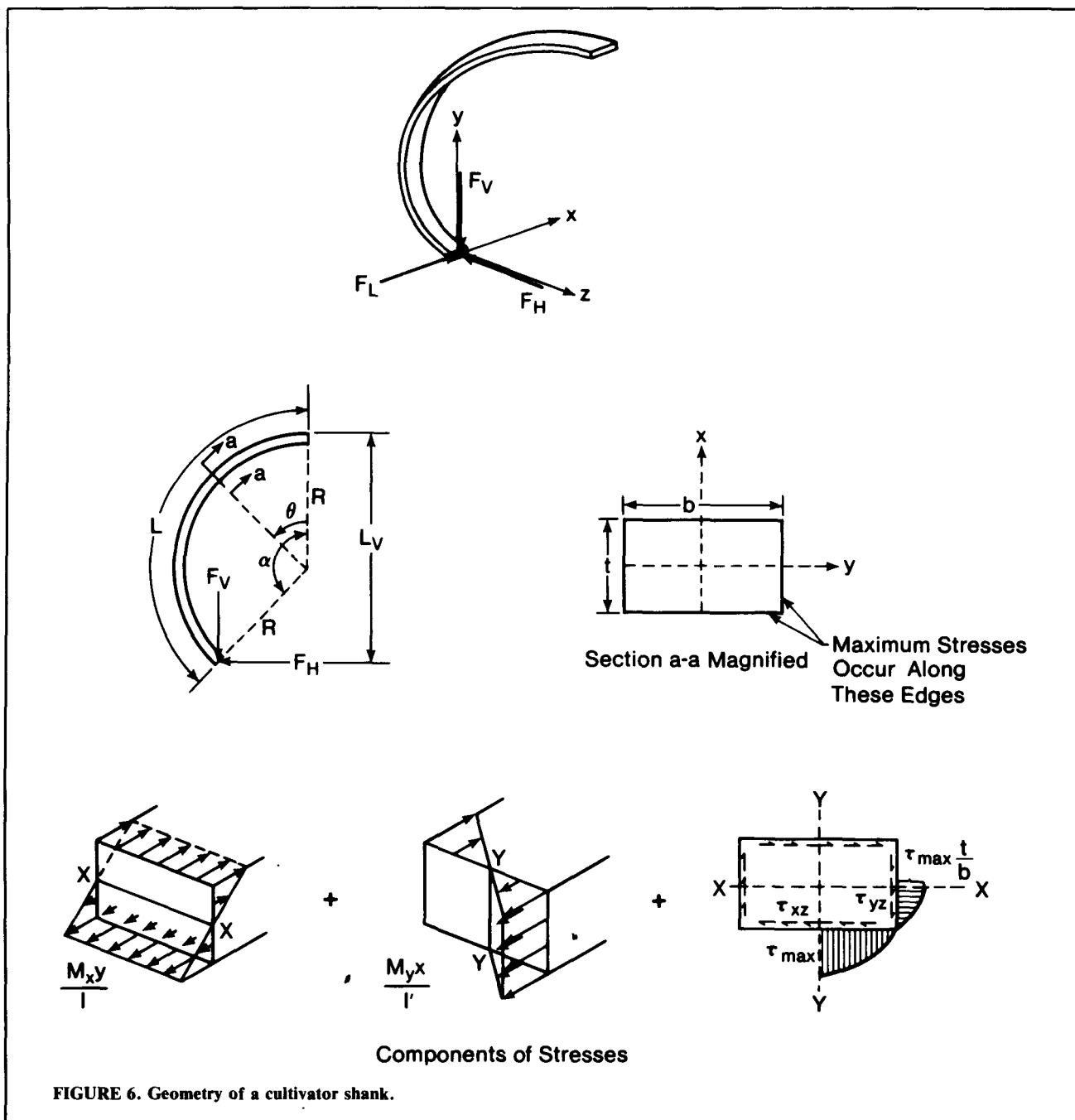
- The change in shape during the heat treatment process could be predicted to a high degree of accuracy.

Recommendations and Implementations

A number of recommendations followed from the analysis of all the test data and production information provided. However, the most important area which required attention was to provide a uniform cooling rate for the shanks at the end of the hot form line.

To accomplish this, it was suggested that an automated quench system be incorporated at the end of the hot form line. The hot formed shanks could drop automatically from the bulldozer onto a sloping chain conveyor belt submerged into the polymer quench tank. The rate of cooling could be controlled by regulating the speed of the conveyor loop and this would ensure that the shanks would always receive the same cooling rate for a given set of conditions.

As an adjunct to this recommendation, the requirements of an automated quench tank were set as a design project for a fourth year engineering group of students at the University of

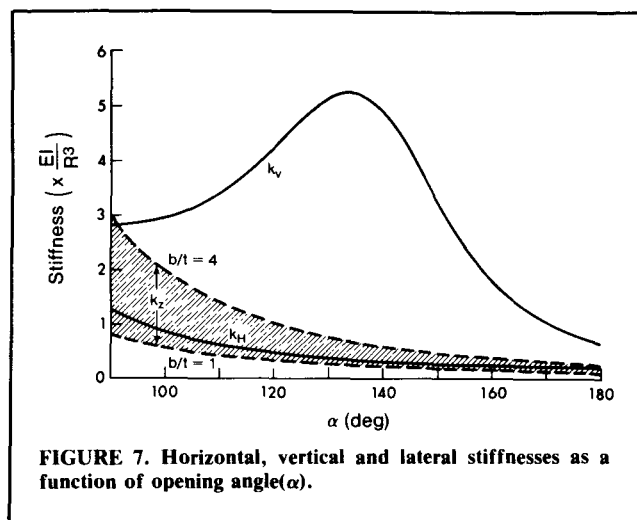


Alberta. The completed design project, which took into account such features as a liquid cooling system to maintain a constant temperature of the quench tank as well as selecting the components for the conveyor system, was presented to Stelco's Engineering Department. The net result is that Stelco Inc. designed and built a completely automated quench system integrated into the production line.

Design of Cultivator Shanks

Background

During the in-plant study, it was noticed that many production problems were related to the large number of different shank designs. Some 23 shank types were produced with width-to-thickness ratios varying between 1 and 4 and opening angles varying between 100 and 150 degrees. Fewer types would allow longer runs with only minor startup problems, less tooling, fewer varieties of stock, etc. It was also felt that a better understanding by the user of stiffness and stress in a shank under a given set of load conditions would lead to designs with



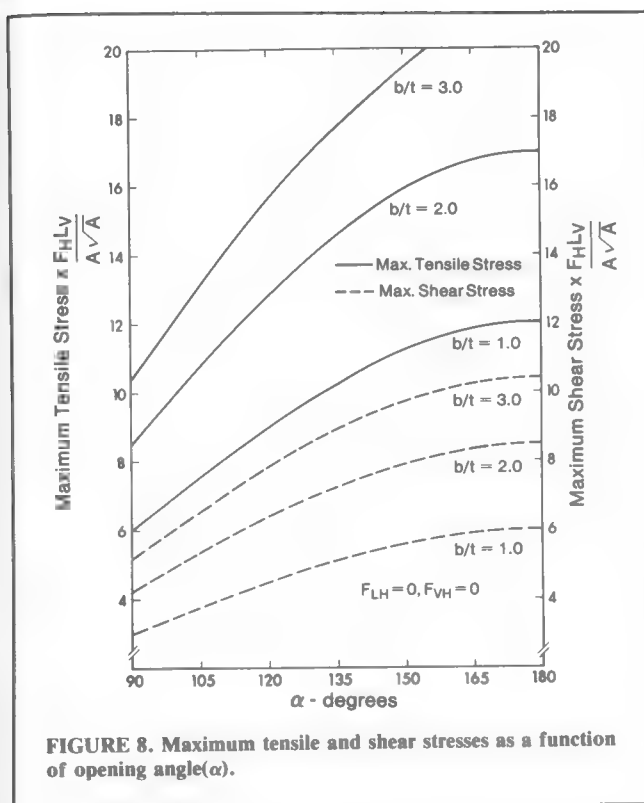


FIGURE 8. Maximum tensile and shear stresses as a function of opening angle(α).

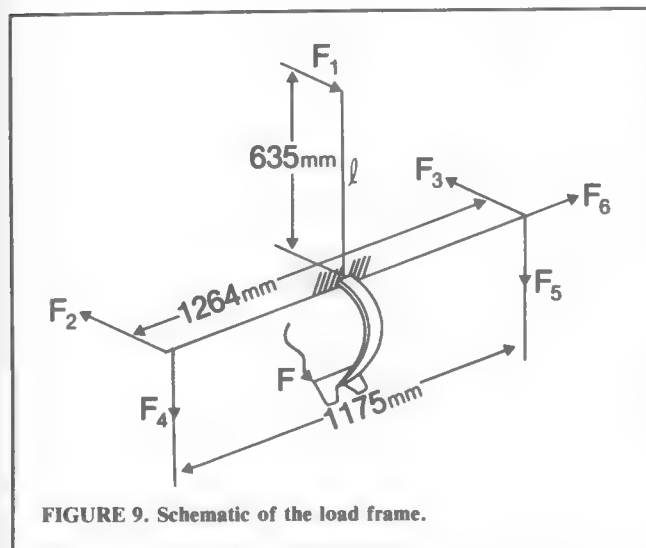


FIGURE 9. Schematic of the load frame.



FIGURE 10. Field trial in progress.

optimum width-to-thickness ratios and opening angles.

In order to relate these factors, a theoretical study was initiated at the university.

Stiffness

To optimize the shape of a cultivator shank, stiffness and stress are not mutually exclusive objectives. For a complete analysis, both factors were considered and were the subjects of two separate investigations. For analytical purposes, the geometrical measures shown in Figure 6 were chosen to describe the shape of the cultivator shank.

Without going into the mathematical details, it can be shown that the primary stiffnesses can be determined in each of the lateral, vertical and horizontal directions. The stiffnesses have been plotted as a function of the opening angle (α) in Figure 7, where it is shown that the vertical stiffness is greater than the horizontal or lateral stiffness and that the horizontal or lateral stiffnesses decrease as the opening angle (α) increases. However, there is an optimum opening angle for maximum vertical stiffness in the vicinity of 134 degrees.

Stress

The maximum tensile stress occurs on the inside or concave surface of the shank. It can be shown that the stress along the edge is made up of the maximum bending stress due to the shank bending about the horizontal axis or X-axis, plus the maximum bending stress due to the shank bending about the vertical axis, or Y-axis. These stresses must also be combined with the shearing stresses along the edges. In order to illustrate how the geometry of the shank influences the maximum stress on the inside surface, it will be assumed that the cross-sectional area (A) is constant, but the b/t ratio will be varied. The opening angle will be chosen typically in the range of 90 to 180 degrees. The maximum tensile stress as a function of opening angle is plotted in Figure 8 for the case of no vertical or lateral load. It is seen that the maximum tensile stress increases with opening angle (α) and the increase is greatest for the largest b/t ratios. In the same figure, it is seen that the maximum shear stress magnitudes are less sensitive to opening angle than was observed for the maximum tensile stresses. Similar results were obtained when the b/t ratio was less than one.

The foregoing analysis showed that while there were some differences in geometric parameters depending on whether stiffness or stress was being optimized, there were also similarities. If it is desired to design a cultivator shank to reduce the maximum stress, then the shank will not be optimally stiff, but will be close to it. Generally, a shank should have its opening angle in the range of 130 to 150 degrees and the b/t ratio should be close to unity; i.e., a square shank. As a check on the above analysis, 23 different commercially produced shanks were measured. Of these, 16 fell within the optimum range of α , but only six had a b/t ratio close to 1.3 for maximum stiffness.

Conclusions

It was clear from this analysis that manufacturing cultivator shanks to specifications set by the customer did not always yield a shank which was optimally designed. This could lead to problems, especially in the case where the customer was depending on the product to perform satisfactorily in service. There were no industry-wide specifications governing the shape of cultivator shanks. This analysis also pointed out the possibility for Stelco Inc. to manufacture cultivator shanks to its own specifications which would be superior to many being produced at the present time.

Evaluation—Field Trails

Background

On the basis of the theoretical analysis, spurred on by some field breakage, it was concluded that a knowledge of the actual loads experienced by cultivator shanks in service was necessary. There did not appear to be any published literature

available in this area, especially under conditions of dry, hard soil and deep shank penetration. A government-industry, jointly funded study was initiated in 1978 under the auspices of the Alberta Agricultural Research Trust to conduct field tests under a variety of operating conditions.

Objectives

The main purpose of this phase of the project was to determine how existing cultivator designs function under severe loading conditions and to assess whether or not changes in design are required. A further objective was to determine a rational basis for predicting actual field loads as a function of tillage depth and tractor speed.

Results

A mobile test frame was designed to fit onto a three-point hitch of a tractor. Attached to this frame was a cultivator shank assembly to which a shovel or spike could be mounted. The entire assembly was supported by six load cells to measure forces and couples in each of three directions. Under actual cultivator conditions, data from each of the six load cells were recorded on magnetic tape in a remote van. The schematic of the load frame is shown in Figure 9, with a general view in Figure 10 of the apparatus in use during a field trial.

Extensive experimental data were gathered during the course of the evaluation of five test sites in Alberta in 1979. All the data were recorded on FM magnetic tape, digitized and analyzed on a computer.

The force in kilo Newtons versus cultivation depth in cm for one test site is shown in Figure 11. The vertical bars indicate the scatter in results, with the circles representing the mean of the data. The lateral and vertical loads were considerably less than anticipated, and in general the lateral load was less than 10% of the horizontal load and the vertical load, which was always downward, was less than 20% of the horizontal or draft load. The maximum tensile stress of the shank was recorded for each of the five test sites evaluated and is shown in Figure 12. It is seen that under some of the severe operating conditions experienced, the working stress exceeded the yield stress and, if such a condition was allowed to prevail, would lead to premature failure of the shank.

Tractor speed also influenced the forces of cultivation, as did the location of the shank, i.e., whether leading or trailing, or whether a spike or shovel was attached to the free end of the shank. The moisture and density of the soil as well as its composition also influenced the results.

In Figure 13, the results of test runs from all test sites were collected, averaged and plotted for the horizontal loads produced with a sweep attached to the cultivator shank in each of the leading and trailing positions as well as a spike attached to the shank. The curves are the best fit for the data plotted and are given by the equations shown in the graph. These equations, which show existing similar data to be on the conservative side, enable the loads to be predicted for a given depth of tillage. Coupled with the results for optimized stiffness and minimum stress calculations, it should now be possible to design a shank which will best meet all requirements and a product for which the reliability can be safely predicted.

Conclusion

The analysis of extensive field data has made it possible to predict the actual field loads to be anticipated under a given set of operating conditions. This data will aid designers and manufacturers in producing a product which will make the best use of the material and will assist in developing some standards for the industry.

Summary

The work described shows the types of benefits that can accrue from an industry, university and government cooperative venture. Certainly Stelco Inc. has obtained real benefits here. The plant data have been used to redesign the shank line for increased throughput and quality. The performance data are

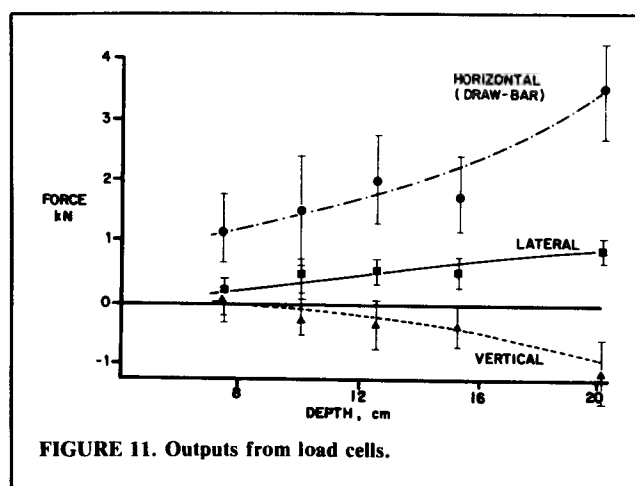


FIGURE 11. Outputs from load cells.

Location	Tool	Depth (cm)	Longitudinal Stress (MPa)
Travis Farm, Claresholm, Alberta	One Sweep Solid	20.3	778 ± 77
	Two Sweeps Solid*	20.3	355 ± 101
	One Spike Solid	20.3	534 ± 77
Agriculture Canada, Lethbridge, Alberta	One Sweep Solid	15.2	316 ± 85
	Two Sweeps Solid*	15.2	483 ± 22
	One Spike Solid	25.4	992 ± 161
Fournier Farm, Coaldale, Alberta	One Sweep Solid	20.3	521 ± 17
	Two Sweeps Solid*	20.3	278 ± 5
	One Spike Solid	25.4	634 ± 18
Agriculture Canada, Vegreville, Alberta	One Sweep Solid	15.2	400 ± 120
	Two Sweeps Solid*	15.2	497 ± 149
	One Spike Solid	25.4	781 ± 234
U of A Farm, Ellerslie, Alberta	One Sweep Solid	20.3	626 ± 16
	Two Sweep Solid*	20.3	331 ± 3
*Trailing Sweep Measured			Endurance Limit Stress = 415 MPa

FIGURE 12. Maximum cultivator shank stresses.

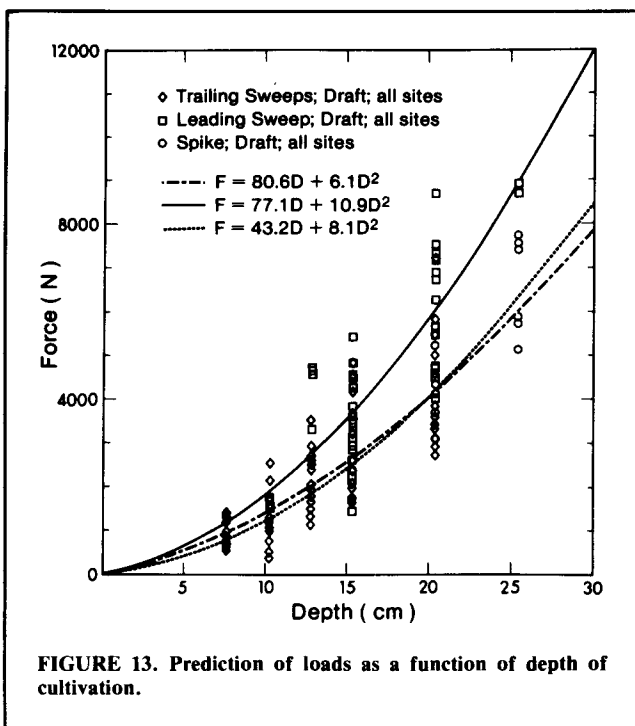


FIGURE 13. Prediction of loads as a function of depth of cultivation.

fundamental for any claims adjustment and for any future Stelco design.

As for current and future cooperative projects, Stelco Inc. already has studies underway at the University of Alberta in the areas of sucker rod fatigue and tundish design. The only change in format has been for Stelco personnel to handle the plant aspects of the work and leave the testing or experimental aspects of the projects to the university personnel. This allows each group to supply expertise in their own area.

This particular project illustrates that, in some areas at least, a knowledge of the use of the finished product is important, even though only one component may be manufactured in a specific plant. Further, the primary manufacturer, by default, may have to take the initiative in setting up standards for the industry to ensure that his product meets appropriate specifications and is acceptable to the users. With the results of the investigation described in this text, much of the mystery and art which has been part of the design and manufacture of cultivator shanks to date should give way to a more methodical and scientific approach—an approach which will provide the user with a superior product while enabling the manufacturer to minimize his costs.

Postscript

Dr. Don Bellow's association with Stelco goes back to 1968, when he was asked to do some testing on sucker rod couplings. However, in the summer of 1975 he was invited to become

familiar with the Edmonton Steel Works and all its operations, from the scrap being used to the electric furnace operation through to the continuous casting system. In addition, the specific problem of studying and making recommendations for the improvement of the quality control of cultivator shanks was given as a project. He attended weekly production meetings in the steel mill, where he felt that he was accepted as an employee. He was given free access to company information and, although much of it was company confidential, no fuss was ever made in giving the data to him.

As a result of this experience, Dr. Bellow believes "if university-industry cooperation is to achieve maximum benefit, there must be mutual trust on both sides right from the beginning. Equally important, especially for one such as myself who had no prior knowledge of the steel industry, is the familiarization process afforded by weekly meetings with production and management personnel. I cannot emphasize too strongly the benefits such meetings have in giving a general overview of a company's operations, its successes, its problems, the management/production/research interface, and the general attitude and philosophy of its people. It is a two-way street because at the same time these meetings also served the purpose of providing a forum for the company to evaluate the academic. Stelco Inc. must be given full credit for orchestrating this the way it worked out, and I must say for my part at least it provided a foundation upon which I felt I could make a positive contribution to the research effort of the company".

AN ANALYSIS OF FORCES ON CULTIVATOR SWEEPS AND SPIKES

G. C. Kiss and D. G. Bellow

Department of Mechanical Engineering, University of Alberta, Edmonton, Alta. T6G 2G8

Received 11 August 1981

Kiss, G. C. and D. G. Bellow. 1981. An analysis of forces on cultivator sweeps and spikes. *Can. Agric. Eng.* 23: 77-83.

This paper describes the results of extensive field measurements of the lateral, vertical and draft forces that are caused by cultivation. Two types of cultivator tools were evaluated: sweeps both in a leading and overlapped trailing position, and a spike. It is shown that draft forces increased with depth of tillage as did the vertical force, but the latter to a lesser degree. Where a trailing sweep was overlapped by a leading sweep the lateral force on the trailing sweep measured as much as 20% of the draft force. There was little correlation of forces with speed in the range of 6-12 km/h tested. All tests were conducted in dry hard packed soils classified as clay-loam.

INTRODUCTION

When cultivator sweeps or shovel tools are used for deep soil penetration in place of standard moldboard plows, the loads imposed on the cultivator components can be large and, in some cases, may be more than the manufacturer anticipated in the original design. This has resulted in the need for a better understanding of what forces exist under such severe operating conditions so that, if necessary, appropriate changes in design can be made. This paper describes the results of a series of field tests in Alberta over five different and widely separated localities in which the forces were measured on cultivator sweeps, in both a leading and trailing overlapped condition, and on spikes.

Numerous investigations into the interaction of simple cultivation implements and soil have been carried out and various two- and three-dimensional mathematical models have been proposed. Much of this data has been obtained in the laboratory under closely controlled conditions and while it has assisted in a better understanding of the mechanisms of cultivation there has been less application to actual cultivator operations including the interaction between pairs of sweeps acting in tandem. With the increased use of the cultivator for primary and secondary tillage, it is suggested that more data be available to enable designers to understand better the actual loading conditions under which these implements are to function.

Clyde (1936) reported that field testing of cultivators consisted of measuring vertical and longitudinal forces. Shovel tools, 51 mm in width, were tested at depths less than 127 mm with presumably no wing overlap and at the same speed. Draft loads from 93 to 512 N were measured with the vertical about 19% of the draft load. Nichols and Reaves (1958) pointed out that the angle of the tine of

subsoilers was important and reported that designers of subsoilers believed that there was a material reduction in draft for angles in the vicinity of 15 degrees. Additional work on the influence of factors affecting draft were published by Payne (1956) and Tanner (1960). For tine widths of 50, 75 and 100 mm, O'Callaghan and Farrelly (1964) found that draft increased with depth of tillage in the range of 50-100 mm, although for shallow depths (less than 50 mm) the results were inconclusive. Tanner (1960) also found that the direction of the vertical force was downward when the lift angle was 20 degrees, but had an upward component when the lift angle was greater than 60-75 degrees.

There has been considerable interest in developing mathematical models for the soil conditions from which forces on cultivation tools can be deduced. A recent paper by McKyes and Ali (1977) proposed a three-dimensional model for simple tools and obtained good correlation between the predicted draft for a swept blade and field data.

The manner in which speed influences the draft has also received considerable attention in the literature. McKibben and Reed (1952) reported that the effect of speed on draft was also influenced by the clay and moisture content as well as the kind of tillage tool in use. Rowe and Barnes (1961) suggested that draft could increase between 20 and 80% when the speed was doubled from 5 to 10 km/h. They believed this to be the result of the fact that at higher speeds the shear strength of the soil increased with higher rates of shear, but that the increase was not as great with soils having a high clay content. In the speed range of 4.8-9.6 km/h, Payne (1956) found the draft to increase by 11-16% for flat-plate tines whereas for sweep shovels in loam soils, Reed (1966) found the draft increased 4-13% for the

same speed range. McKibben and Reed (1952) also found, for the same speed range, the draft to increase by 16%. Stafford (1979) showed that the relationship between draft and speed was affected by moisture content and the nature of the soil failure, but for speeds in excess of 18 km/h draft was independent of speed.

A set of equations predicting the draft force of chisel plows and field cultivators has been published by the American Society of Agricultural Engineers (ASAE) (1980). The draft force was represented as a linear function of speed and a second degree polynomial function of depth. No mention was given to vertical or lateral forces or the effect that overlap might have on the applied loads to a cultivator sweep situated behind the front row of a cultivator assembly.

The objectives of this investigation were to measure the forces of cultivation for cultivator sweeps and spikes under a variety of depth and speed conditions in dry hard soils and to discover to what extent lateral and vertical forces are significant with respect to the draft forces. Additionally, the distribution of loads between a leading and trailing sweep with overlapping wings and frequency response of a sweep-shank were to be evaluated. By meeting these objectives it was hoped to confirm existing data or establish new data for the prediction of the loads of cultivation on sweep and spike cultivators. It is believed that these data will be of value to both designers and manufacturers of cultivator implements.

EXPERIMENTAL PROGRAM

Description of Apparatus

A mobile test frame was designed and constructed to carry a cultivator shank and holder assembly and fit onto a three-point hitch of a farm tractor (Bellow et al. 1980; Harrison 1974). This enabled the

cultivator assembly to be centrally attached to an active frame which was isolated from a passive frame by six load cells. A general schematic of the load frame showing the forces that were measured is shown in Fig. 1. Each load cell consisted of four electrical resistance strain gauges mounted on an aluminum rod forming a four-arm Wheatstone bridge circuit. In order to calculate the stress imposed on a cultivator shank, as well as serving as a check on the load cells, two electrical resistance strain gauges were mounted on the inside radius of the cultivator shank.

Depth of cultivation was selected by adjustment of gauge wheels in relation to the passive frame. Speed was monitored by a DC generator attached to one of the gauge wheels. To evaluate the interaction between trailing and leading sweeps a duplicate uninstrumented cultivator sweep assembly was mounted to the passive frame 400 mm in front of and 300 mm to the right of the instrumented trailing sweep. This caused a 25% overlap in sweeps (100 mm). A tandem arrangement of spikes was not tested as no overlap occurred in this case. Cultivator sweeps 406 mm wide and 51-mm-wide spikes were used for all field trials. The spring release mechanism incorporated in the design of the cultivator assembly tested was modified so that tripping-out was prevented enabling large loads to be applied and to maintain the sweep or spike at a

reasonably constant depth. From laboratory experiments it was found that for loads up to 9 kN the depth did not change by more than 10 mm. However, the cultivator shank was less stiff in the horizontal direction and for the same load range was found to deflect up to 100 mm. This would increase the rake angle of the sweep or spike, but was not believed to affect it significantly. The unloaded rake angle for the sweep was about 20 degrees and for the spike was about 17 degrees.

The force, strain and speed signals were transmitted from the tractor via a 30-m umbilical cord to a recording van housing signal conditioners, an FM tape recorder and an ultraviolet (UV) chart recorder. A general view of a typical test in progress is shown in Fig. 2.

Testing Procedure

Moisture content and dry bulk density of the soil were measured at each test site using a gamma radiation source and detector. Measurements were taken at 25-mm intervals from the soil surface down to the deepest cultivation depth achieved. Except for the Ellerslie test site (no. 5) the field conditions were judged to be dry and hard packed. In this study only the percent moisture, percentage clay, sand, loam and density were used to characterize the soil conditions.

A test run consisted of accelerating the tractor to a selected speed, lowering the tool to engage the soil to a pre-set depth

and travelling the distance permitted by the umbilical cord (approximately 50 m). Recording of data took place throughout the entire sequence. Three, approximately equally spaced speeds between 6 and 12 km/h were selected for each depth using the sweeps. A single speed of 9 km/h was used for the spike. A shear pin in the active frame was designed to fail at a load of 13 kN to protect the load cells. In some situations this pin failed before maximum depth of cultivation was achieved.

At each test site three different cultivator systems were evaluated; single instrumented sweep, single instrumented spike and dual sweeps with trailing sweep instrumented. As the test run proceeded the outputs from the load cells were monitored visually on the UV recorder. If conditions did not appear satisfactory a second or third run at the same depth and speed were performed. Each test run was approximately 50 m and this generally served as an ample length from which repetitive data could be analyzed.

DATA ANALYSIS

The analog data tape recordings were digitized at a rate of 167 times per second. This rate was chosen after a number of runs had been analyzed on a fast fourier transform (FFT) analyzer that showed that most of the output signals were contained in the DC to 55 Hz bandwidth. Digital FFT spectral analysis prescribes that a sampling rate be used which is at least twice the highest frequency expected.

A number of analytical procedures were programmed into a computer so that the digitized data could be analyzed directly for the mean and standard deviation of each load cell from which the draft, vertical and lateral forces were computed. Although the software for this was assembled without difficulty, considerable care had to be taken to select those portions of test runs for which the apparatus was considered to be operating under constant conditions of depth and speed. This was achieved by reviewing a computer-generated plot of the digitized load cell outputs along with the speed recordings on a CRT screen so that regions could be defined where the data analysis was to be performed.

The three forces on the tool were plotted against depth and speed and either linear, geometric (power), exponential or polynomial curves were fitted and correlated to the data.

RESULTS AND OBSERVATIONS

Soil Classification

The soil textural classification for five sites tested is plotted in Fig. 3, according

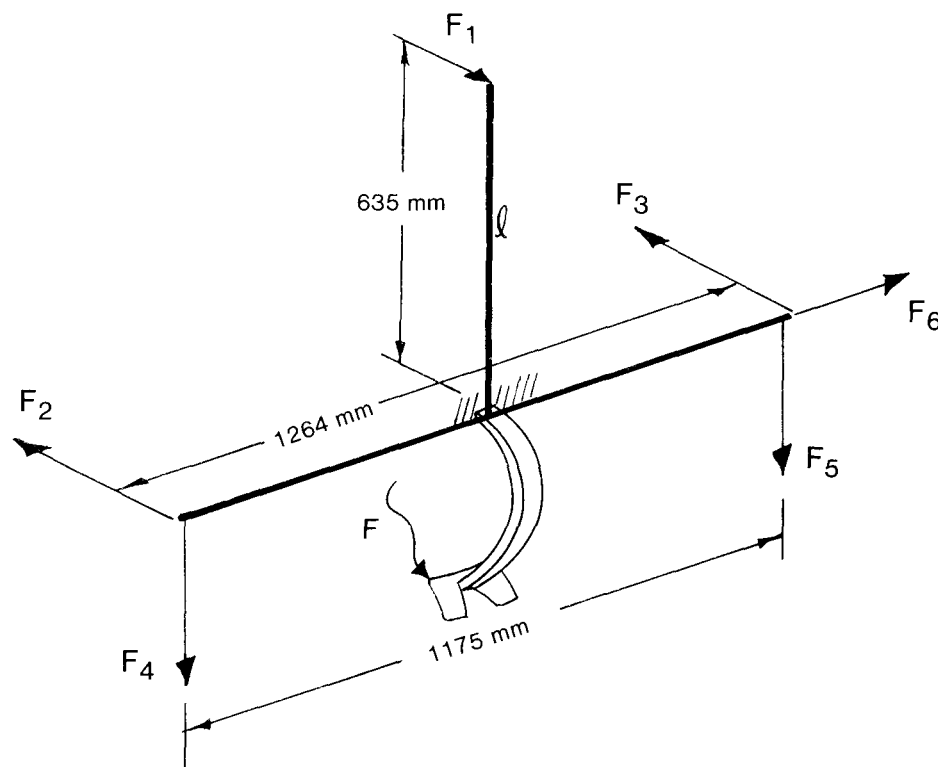


Figure 1. Load frame showing load cell locations and sweep location.



Figure 2. Test underway.

to the U.S. Department of Agriculture classification system. The results are an average of several core samples taken down to the deepest cultivation depth achieved.

With the exception of site no. 5, each site was considered a severe test for any tillage tool. Site no. 4 was a summer-fallow field, but all the others were stubble fields. Except for site no. 5 which was a silty-clay-loam soil, all soils fell into the

clay-loam category. It is seen from Fig. 3 that there was a small variation in clay content between all sites.

Table I shows the average dry density and moisture content measured at each test site. Again, excepting site no. 5, variation of dry density was less than 6% and moisture content varied less than 25% among the other four test sites.

Although an attempt was made to select locations of differing soil characteristics

TABLE I. MOISTURE AND DENSITY AT TEST SITES

Test site	Locality (Alberta)	Moisture content	Dry density (kg/m ³)
1	Claresholm	11.2	1438
2	Lethbridge	9.6	1371
3	Coaldale	10.1	1386
4	Vegreville	14.1	1507
5	Ellerslie	48.9	907

(all in a dry moisture condition), it was observed that four were of a similar nature and only site no. 5 was noticeably different. It was therefore decided to plot results from all sites together, noting any anomalies caused by inclusion of the data from site no. 5.

Effect of Depth

The results of each test run were analyzed as forces vs. depth and forces vs. speed. These results are plotted typically as shown in Fig. 4. Figure 4 shows that the draft force increased with depth for a leading sweep, a trailing sweep and a spike. The solid lines are fitted polynomial curves computed by a least squares regression of force on depth. Inclusion of a linear term was neglected as it only increased the correlation in the order of 1% for all cases and was not considered significant.

Draft forces for a leading and trailing sweep and for a spike are plotted as points in Fig. 4. The solid lines are "best fit" polynomials through these points with the generated equation for each particular curve shown. The degree of correlation between the curves and the experimental data is shown in brackets. The dotted curves represent the theoretical prediction as proposed by the American Society of Agriculture Engineers (1980) for chisel plows and field cultivators in firm clay-loam soil. A speed of 9 km/h was used for the ASAE curves. It should be noted that the ASAE data give equations for force per tool including rolling resistance and were based on the draft forces measured at the hitch divided by the number of tools being used. As a result, the ASAE data do not discriminate between the draft force of a leading versus a trailing sweep nor do they separate the draft of a spike from that of a sweep.

Comparing the experimental results to the ASAE equation it can be seen that the ASAE curve predicts a draft force 10% lower for a leading sweep, 19% higher for a trailing sweep and 26% higher for a spike. For comparison, the data for the trailing and leading sweeps were averaged and plotted as the second dashed line in Fig. 4. As might be expected, on the basis

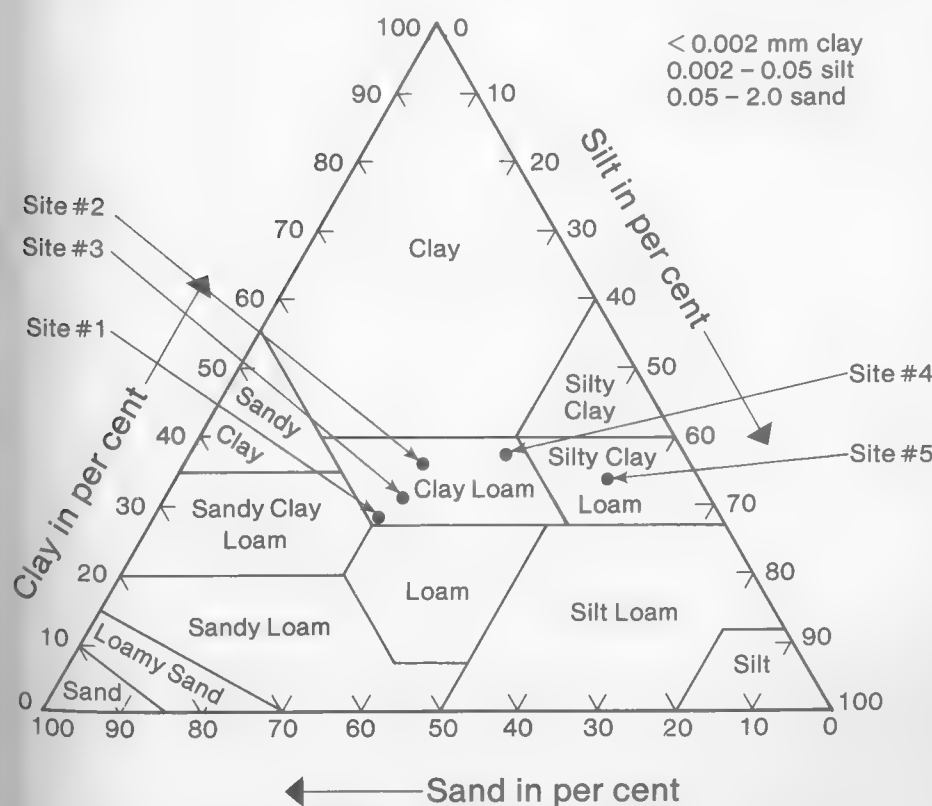


Figure 3. Soil classifications.

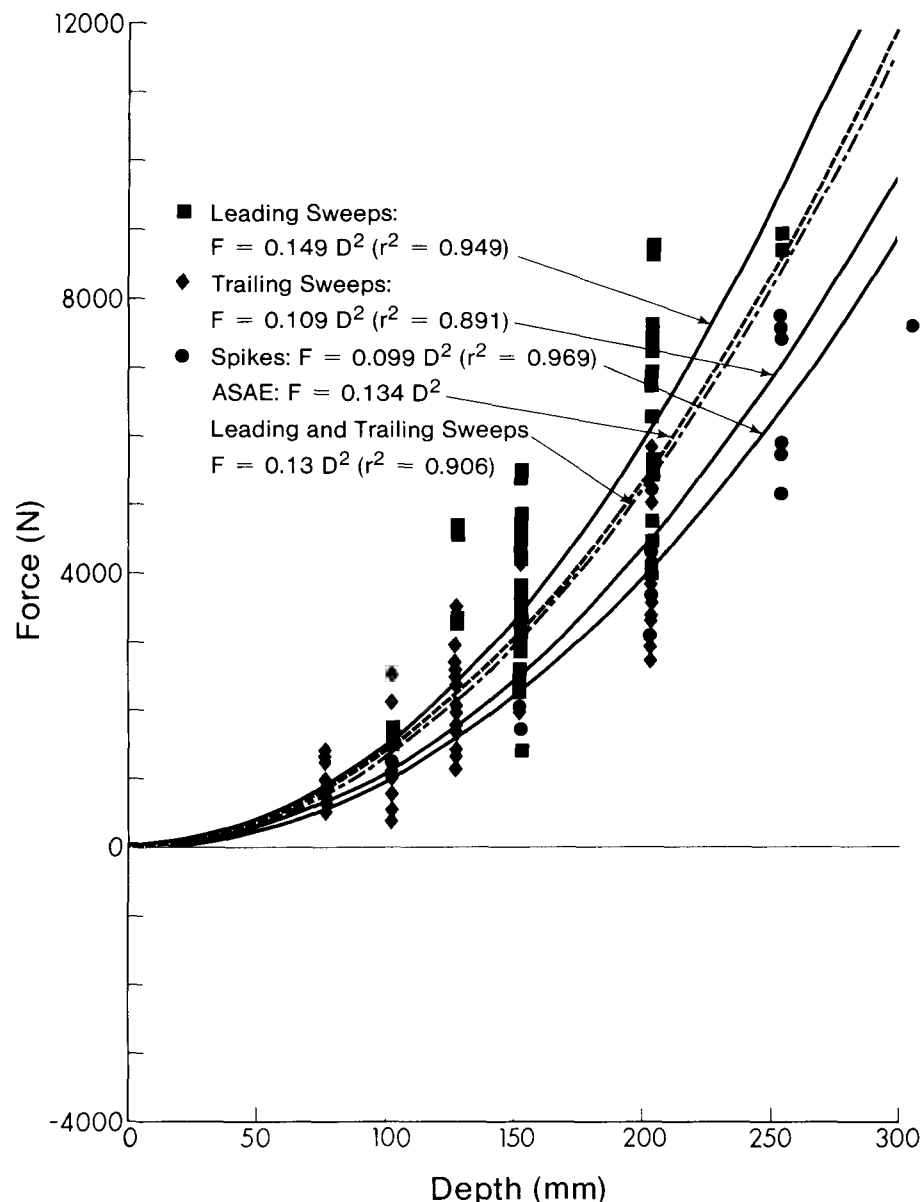


Figure 4. Draft forces for leading and trailing sweep and spike vs. depth.

of the average data, the results were very close to that predicted by the ASAE formula, within 3%, although the correlation was somewhat poorer. A final observation was made by comparing the curves for leading and trailing sweeps where it was noted that the draft force on the trailing sweep was 27% less than that measured on the leading sweep. Also, a comparison between the sweep and spike tested showed the draft on the spike to be 34% less than that on the leading sweep.

The variation of vertical force with depth is shown in Fig. 5 and is seen to increase downward with depth for a leading sweep and spike. Upward vertical forces can be produced on a trailing sweep at shallow depths and were observed during the course of this investigation, but usually the vertical force was directed downwards. For the rake angle of the tools

evaluated in this study these observations are in agreement with Tanner (1960). Although it is shown that there was no difference in vertical force between a trailing sweep and a spike, the correlation was not as good as obtained for the leading sweep. It was also observed that the vertical force on a trailing sweep and or spike was 34% of the vertical force measured on the leading sweep. Comparing results in Figs. 4 and 5 shows that the vertical force of the leading sweep was 20% of the draft force of the leading sweep. The vertical force of the trailing sweep was 9% of the draft force of the trailing sweep.

The variation of lateral force with depth is shown in Fig. 6 and was nearly zero for a leading sweep and spike. This is as expected as these tools encounter a symmetrical loading application. It was assumed that misalignment of the active frame con-

tributed to the small lateral forces shown. However, because the path of cultivation left by the leading sweep overlapped that of the trailing sweep, the trailing sweep experienced an unsymmetrical load distribution which caused a side or lateral force to be applied to the trailing sweep. This lateral force has been generally neglected by other investigators, but the data plotted in Fig. 6 show that the lateral force of the trailing sweep increased with depth and was measured to be 20% of the draft of the trailing sweep. This factor is important and should be included when considering a stress analysis of a cultivator shank and holder assembly.

Effect of Speed

Another objective of this investigation was to determine the nature of the relationship between speed and force on a cultivator sweep. However, variation of tractor speed was restricted to the practical range of speeds at which a farmer might operate his machinery. The draft, vertical and lateral forces were plotted against forward speed for the leading and trailing sweep for each depth tested and linear regression curves were fitted to the data. Although not shown here, it was found that the effect of forward speed was less pronounced than the effect of depth of tillage. In fact there was little, if any, correlation observed between either the vertical or lateral force with speed for the sweep evaluated. This was indicated by a zero slope of the regression lines.

For draft load vs. speed, the slope of the regression lines were generally positive and indicated a tendency for the draft force to increase with speed, but a large amount of scatter in the data caused the correlation to be quite low. Although there are a number of references in the literature which report a linear relationship between speed and draft (Telischi et al. 1956; Rowe and Barnes 1961) these results have been obtained using soil boxes under closely controlled laboratory conditions. The results of the present investigation do not confirm these observations and it is believed this was due to lack of control on such variables as moisture, density and depth. It should be noted, however, that the testing program outlined in this paper was sensitive to measuring changes in draft due to changes in depth, yet when the speed was doubled from 6 to 12 km/h, at a constant depth, no appreciable change in draft was recorded for the sweep evaluated. On the basis of this investigation, and within the limits of the testing variables, it was concluded that the forces acting on sweeps under actual tillage con-

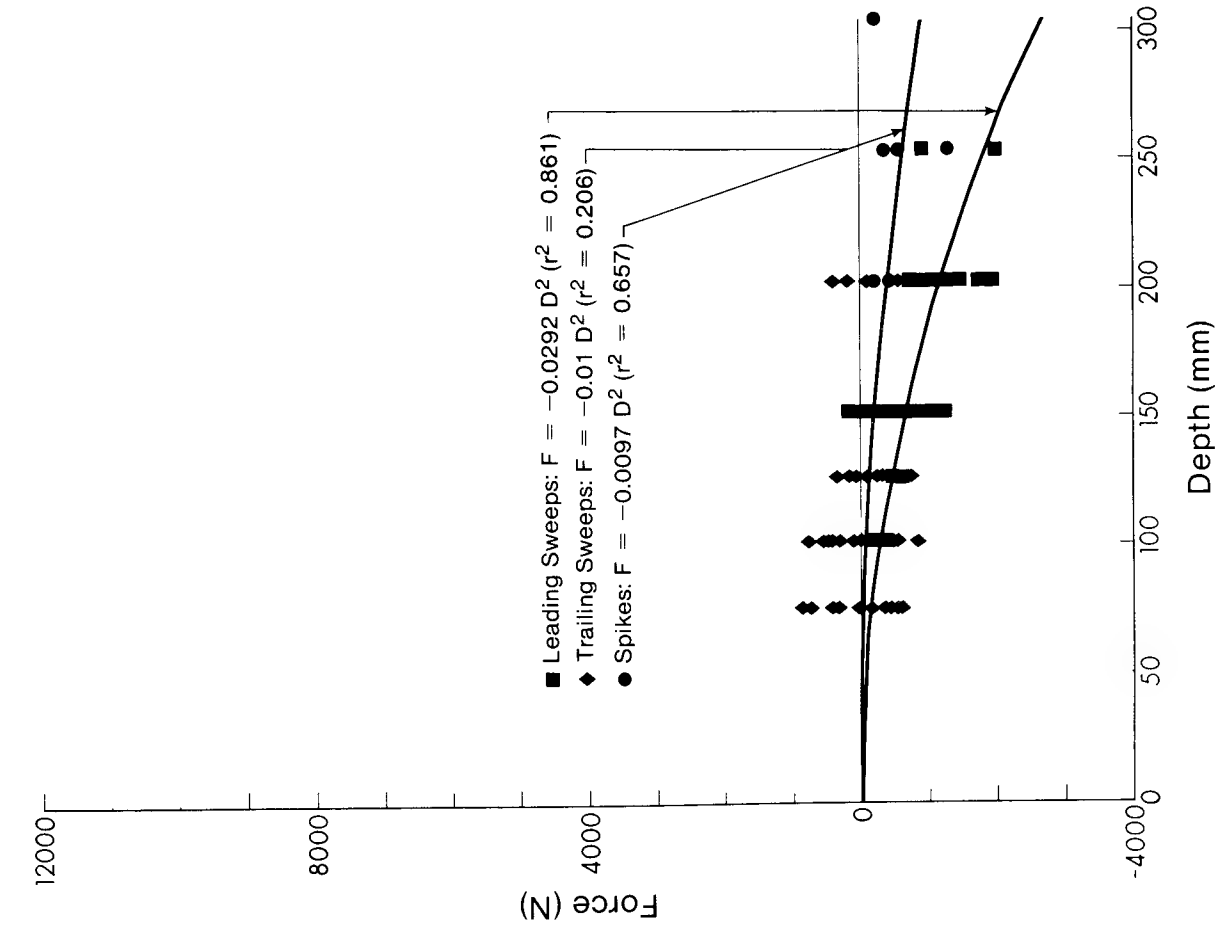


Figure 5. Vertical forces for leading and trailing sweep and spike vs. depth.

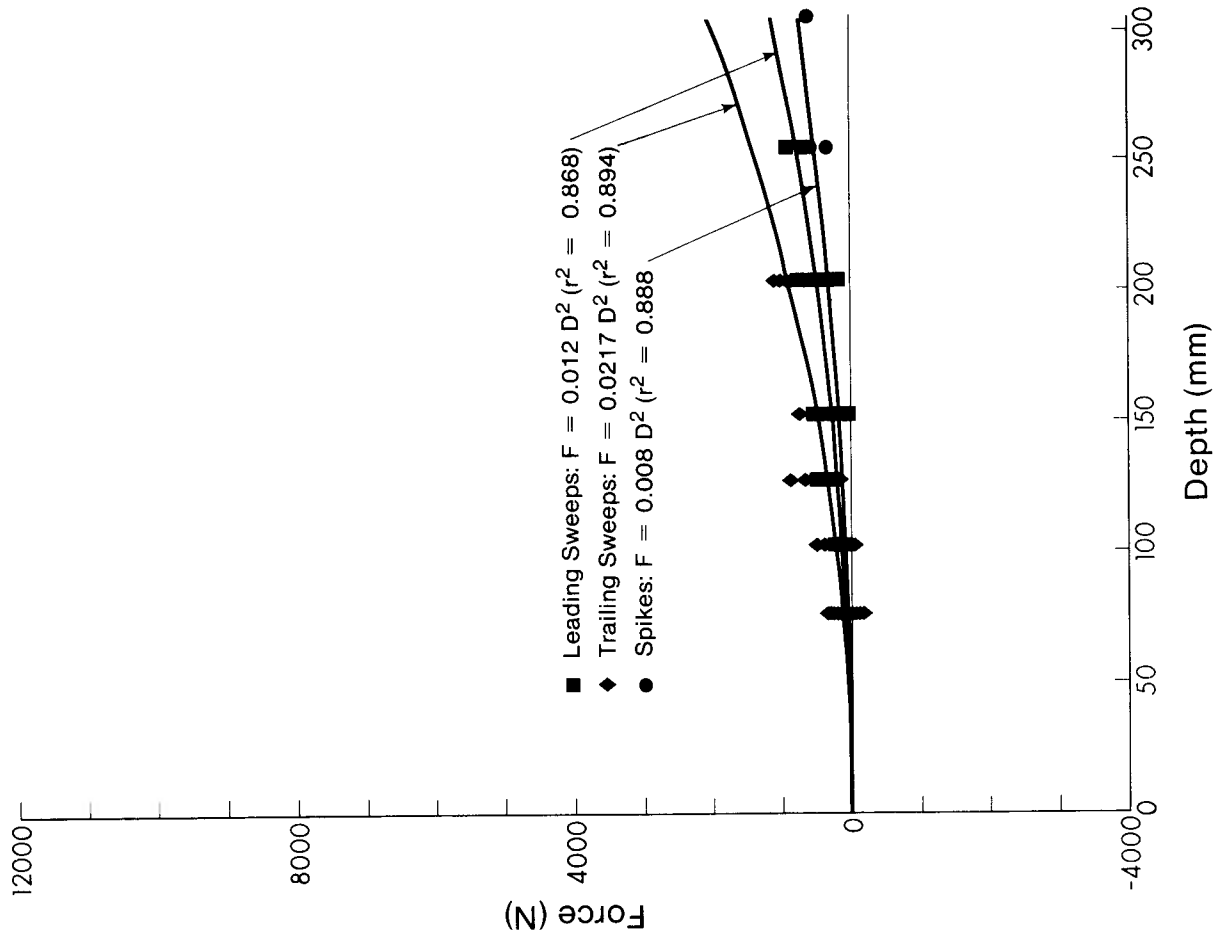


Figure 6. Lateral forces for leading and trailing sweep and spike vs. depth.

ditions are a function of the depth of tillage and not affected by variation in speed in the range 6-12 km/h.

Effect of Soil Composition

An overall average of the draft force for the leading sweeps at a constant depth of 150 mm at each test site was plotted against the percent of sand, silt and clay contained in the soil and is shown in Fig. 7. It is seen that as the percentage of sand increased the draft force decreased, whereas the draft force increased as the silt increased. Also, as the percentage of clay increased the draft force increased. These observations are consistent with others such as Telischi et al (1956) and Stafford (1979). Similar trends were noted for the trailing sweep, but the draft force of the spike was found to be insensitive to soil

component changes. It was also noted that all vertical and lateral forces were relatively insensitive to changes in the soil composition.

Frequency Analysis

Because concern was expressed by some farm equipment manufacturers that some components of cultivation implements, and in particular cultivator shanks, could break or were breaking due to fatigue it was desired to investigate the frequency of load application experienced by such implements under the variety of test conditions described above.

A digital fast fourier transform algorithm (Newland 1975) was used to analyze the output of each load cell to give a graph of power spectral density vs. frequency. A table of predominant frequ-

encies was compiled noting the speed and depth of each run. An examination of all runs suggested that two separate vibrational mechanisms occurred. A lower band of frequencies from 1 to 9 Hz was usually present, but no predominant frequency could be detected for runs conducted under similar test conditions. This low band was likely related to the formation of rupture planes in the soil as the tool advanced. Beyond this bandwidth there were certain higher frequencies that consistently appeared from one run to the next and were independent of depth or speed. This occurred only in the vertical and lateral directions where the predominant frequency was 33 Hz for the vertical force and 24 Hz for the lateral force. The draft force did not exhibit significant similar higher frequency vibrations. It was observed that these high frequency components were usually of less than half the amplitude strength of the low band.

In order to attempt an explanation of the occurrence of the higher frequencies, a cultivator sweep and shank were mounted to an electrodynamic shaker table so that resonant frequencies could be measured. The horizontal (draft), vertical and lateral resonant frequencies as measured from the shaker table were 21 Hz, 66 Hz and 26 Hz, respectively. In comparison, the analysis of the field data showed that there was no predominant horizontal (draft) frequency of vibration whereas peak frequencies at 33 Hz for the vertical and 24 Hz for the lateral were recorded. The lateral frequency of 24 Hz compared favorably to the 26 Hz measured on the shaker table, but the peak of 33 Hz for the vertical observed from field data was not confirmed with the data obtained on the shaker table. Although it was not possible to confirm on the shaker table the resonant frequencies recorded in the field, the data obtained from the shaker table showed the variety of resonant frequencies that are inherent in the cultivator shank. The fact that some of these resonant frequencies were not present in the field was due to the influence of the soil reaction on the vibrating system. The tests did show, however, that under certain conditions of soil, depth and speed the cultivator shank assembly can vibrate in a resonant condition that could, if the shank were also highly stressed, lead to premature failure by fatigue.

CONCLUSIONS

Extensive measurements on the forces involved in using sweep cultivators and spikes were undertaken at five different test sites at which depth and speed were varied with the following conclusions.

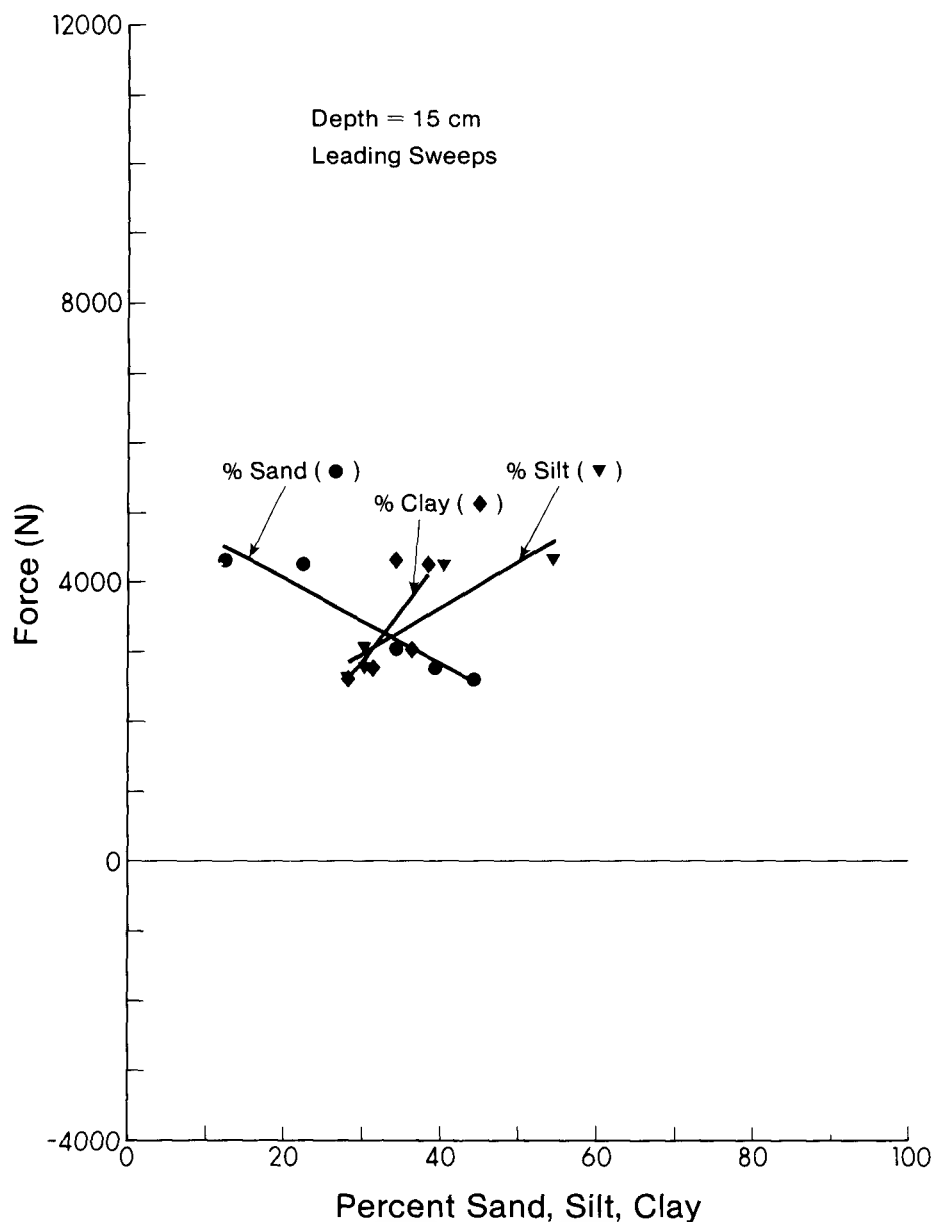


Figure 7. Average draft forces for leading sweep vs. soil classification.

1. Draft force increased with depth of cultivation and could be approximated with an equation similar to that published by the American Society of Agricultural Engineers. Additional regression analysis is given to show the load distribution between leading and trailing sweeps and spikes.

2. The draft force of a trailing sweep was approximately 27% less than measured on the leading (and overlapping) sweep and the draft force of a spike was approximately 34% less than the draft force of a leading sweep.

3. Lateral and vertical forces were measured up to 20% of the draft force. However, lateral forces were generally small or non-existent for leading sweeps and spikes.

4. Tool forces did not appear to be affected by speed in the range 6-12 km/h for the cultivator sweep evaluated.

5. Predominant frequencies of vibration of the implements tested were observed in the range 1 to 9 Hz, although some peaks were noted at higher frequencies.

ACKNOWLEDGMENTS

The authors wish to thank the Alberta Agriculture Research Trust, Stelco Inc. and the Natural Sciences and Engineering Research Council (Grant A2705) for the financial support received in aid of this project. Thanks are also due to Professor H. P. Harrison and Mr. R. Holowach of the Department of Agricultural Engineering at the University of Alberta for their interest and cooperation.

REFERENCES

- AMERICAN SOCIETY OF AGRICULTURAL ENGINEERS YEARBOOK. 1980. Standard ASAE D230. 2: 243.
- BELLOW, D. G., G. C. KISS, and H. P. HARRISON. 1980. Measurement of cultivator forces. Proc. 5th Symp. Eng. Mech. NRCC 18370: 149-153.
- CLYDE, A. W. 1936. Measurement of forces on soil tillage tools. Agric. Eng. 17: 5-9.
- HARRISON, H. P. 1974. Instrumentation of multi component sensor. Paper No. 74-5525, Am. Soc. Agric. Eng., St. Joseph, Mich.
- McKIBBEN, E. G. and I. F. REED. 1952. The influence of speed on the performance characteristics of implements. Soc. Auto. Eng. Nat. Tractor Meeting, Milwaukee, Wis.
- McKYES, E. and O. S. ALI. 1977. The cutting of soil by narrow blades. Terramech. 14: 43-58.
- NEWLAND, D. E. 1975. An introduction to random vibrations and spectral analysis. Longham, London, England.
- NICHOLS, M. L. and C. A. REAVES. 1958. Soil reaction: to subsoiling equipment. Agric. Eng. 39: 340-343.
- O'CALLAGHAN, J. R. and K. H. FARRELLY. 1964. Cleavage of soil by tined implements. J. Agric. Eng. Res. 9: 259-270.
- PAYNE, P. C. J. 1956. The relationship between the mechanical properties of soil and the performance of simple cultivation implements. J. Agric. Eng. Res. 1: 23-50.
- REED, W. B. 1966. Techniques for determining an equation for the draft of cultivators using several independent variables. Paper No. 66-123, Am. Soc. Agric. Eng., St. Joseph, Mich.
- ROWE, R. J. and K. K. BARNES. 1961. Influence of speed on elements of draft of a tillage tool. Trans. ASAE (Am. Soc. Agric. Eng.) 4: 55-57.
- STAFFORD, J. V. 1979. The performance of a rigid tine in relation to soil properties and speed. J. Agric. Eng. Res. 24: 41-56.
- TANNER, D. W. 1960. Further work on the relationship between rake angle and the performance of simple cultivation tools. J. Agric. Eng. Res. 5: 307-315.
- TELISCHI, B., H. F. MCCOLLY, and E. ERICKSON. 1956. Draft measurement for tillage tools. Agric. Eng. 37: 605-608.

Published in SESA/JSME Proceedings,
Hawaii, Part 2, 1981

STRESS AND CORROSION FATIGUE EXPERIMENTS ON OIL FIELD COMPONENTS

Donald G. Bellow
Department of Mechanical Engineering
University of Alberta
Edmonton, Alberta, Canada

Abstract:

Crude oil is pumped from the ground using a series of rods joined by couplings to form a sucker rod string. This paper describes the results of some experiments used to evaluate the corrosion fatigue resistance of these down hole components. It is shown that the life of a sucker rod can be reduced by an order of magnitude in the presence of an 8.4% NaCl solution and that in this environment the corrosion fatigue life is not adversely affected if the rod is ground subsequently to shot blasting.

Introduction:

Conventional crude oil is commonly pumped from pools located many hundreds and often thousands of meters below the surface of the earth. The pumping system usually consists of a double acting pump located at the bottom of the well and is operated, through a series of sucker rods and couplings called a sucker rod string, by a walking beam apparatus located on the surface. The walking beam apparatus provides a reciprocating action to the plunger of the pump. This method of pumping crude oil has its origins going back to the first century where the same principle was used in pumping water by the Romans. While the concept has remained the same there have been many improvements to the components over the years and much of this improvement has been guided by the American Petroleum Institute which has set standards for sucker rod sizes and configurations. However, now that oil production is at or near capacity world-wide there are many wells which are posing serious difficulties for pumping in this conventional sense. And, although improvements have been made to the design and manufacture of sucker rods and couplings over the years, this is still a topic under active investigation as manufacturers and producers alike attempt to find the most economical and durable sucker rod string which can be used.

The manufacture of a sucker rod consists of heating the rod and through a series of impacts the end is upset forged which provides the general shape shown in Fig. 1. Some difficulties can arise in this process where scale can be lodged between the sucker rod and forging dies causing imperfections and indentations on the forged surface. Although the sucker rod is subsequently heat treated and shot blasted these surface imperfections can still be present. Whether or not the imperfections pose a potential problem or whether they should be ground out, and whether the grinding itself would adversely affect the life of the rod were questions that needed to be answered. As a first step in this investigation an experimental program was devised to determine whether or not grinding after shot blasting had an adverse affect on the corrosion fatigue behaviour of the sucker rod.

Environment:

Many oil fields contain large quantities of contaminants such as salt water, carbon dioxide, and hydrogen sulphide which is pumped out of the well with the crude oil. These contaminants come in contact with the pump and sucker rod string and can lead to premature failure due to corrosion fatigue. When components fail in a well it can be a costly repair not only because of the lost production time but also because special service rigs must be brought to the well site to "fish out" the broken parts and replace with a new or repaired sucker rod string. To avoid this producers require down hole components which will be resistant to corrosive attack and be able to withstand the high cyclic stresses imposed by the pumping process.

It has been shown¹ that when sucker rod couplings are subjected to a salt water environment or salt water in combination with hydrogen sulphide that the fatigue life is markedly reduced. Although hydrogen sulphide is a contaminant found in many oil fields it is also lethal even in small concentrations so special precautions must be taken if it is introduced as an environment in the laboratory. In a previous paper² details were given for a hydrogen sulphide corrosion chamber. However, it has also been shown³ that much can be learned about the resistance to corrosion fatigue by testing in a salt water solution alone which,

of course, has none of the toxic hazards of hydrogen sulphide. The work which is currently underway is using salt water as a corrosive medium. The results thus obtained can be compared with field results from wells where the main contaminant is salt water.

Sucker Rod Joint:

A typical sucker rod joint is shown in Fig. 1 where the joint configuration shows the upset forged ends of the sucker rods threaded into the coupling. This joint occurs every 7.6m (25 ft) along the length of the sucker rod string. For a well of 3000m in depth the sucker rod string will contain as many as 400 of these joints. The joints are made up in the field by first hand tightening and then torquing with a wrench so that there is a 6mm (1/4 in) circumferential displacement between the shoulders of the sucker rod and the coupling on each face of the coupling. The purpose of this is to pre-load the threads in the coupling into compression so that under cyclic tensile load they will be subjected to lower tensile stresses in the vicinity of the thread roots which are where fatigue cracks will originate. A tight joint is also necessary to maintain metal-to-metal contact between the sucker rod and the coupling to prevent corrosive contaminants from coming into contact with the threads. Finally, the joint must be tight to prevent loosening during the cyclic loading and twisting that occurs during the pumping operation.

A sucker rod joint consisting of two short sucker rods (pony rods) and a coupling were instrumented with strain gauges along the outside of the rods and on the outside of the coupling. In Fig. 2 the stresses computed at these gauge locations are plotted for two conditions; when the sucker rod string was torqued but unloaded, and when the sucker rod string was undergoing a typical maximum load of 89kN (20 kips). These results illustrate that through the joint the stress distribution varies considerably, as does the cross sectional area. It is also seen that because of the initial compressive stresses set up in the coupling by the torquing of the joint the coupling stresses under an axial load are generally lower than those measured on the sucker rod. The stresses on the sucker rod are maximum in the transition zone between the straight portion of the sucker rod and the upset forged end. In Fig. 2 only the maximum axial tensile stresses have been plotted. Actually, bending stresses up to 30% greater than these plotted in Fig. 2 were recorded. These bending stresses were the result of slight misalignments of the sucker rod string. If similar misalignments were to occur in the field then for a heavily loaded sucker rod string the bending stresses would be most severe in the upset forged end and could explain why a number of failures have been observed in this particular portion of the sucker rod. The subject of bending stresses and bent sucker rods has been investigated theoretically in a previous work⁴ in which it was shown that if a bend in a rod is located in the vicinity of a coupling very high bending stresses can result.

Corrosion Fatigue:

Much has been written on methods of accelerating corrosion fatigue experiments. If experiments are accelerated then there is difficulty in interpreting the results for actual field situations. On the other hand if actual field conditions are used, the experiments are often protracted and expensive. There are tradeoffs no matter which method is chosen. The experimental conditions of environment and load ranges and rates must be set for each specific case. For the program described in this paper an aerated solution containing 8.4% NaCl was used as this was typical of some corrosive wells in which failures of sucker rods had occurred in as short a time as 10 working days.

A plexiglass corrosion chamber was built to house two pony rods and a coupling to fit between the cross heads of a closed loop servo-hydraulic testing machine as shown in Fig. 3. Air was bubbled into the chamber at the bottom to keep the corrosive medium supplied with oxygen and fully agitated. The corrosive medium was replaced every 24 hours. The minimum stress level was set at 42 MPa (6.1 ksi) whereas the maximum was set for each particular test within the range 276 MPa (40 ksi) to 379 MPa (55 ksi).

Some sixty pony rods of nominal 3/4 in. (19 mm) diameter, which were produced in the normal manner, were selected for the testing program. Half of the rods were ground after shot blasting (G-series) and half were left in the as-shot blasted condition (P-series). The normal painting was removed for both rod sets. A visual inspection indicated none of the test rods contained any forging defects.

Corrosion Fatigue Results:

The results from the corrosion fatigue experiments are shown in Fig. 4 with the location of the failures shown in Fig. 5. The results in Fig. 4 indicate that for rods cycled in 8.4% NaCl at a maximum stress of 379 MPa (55 ksi) the rods with the upset portion ground (G-series) had a median life of 1.9×10^5 cycles whereas the unground rods (P-series) had a median life of 1.6×10^5 cycles. Using Student's t-test it was found that at a stress level of 379 MPa (55 ksi) there was no evidence to support the hypothesis that the averages of the P and G series were the same. On the other hand at 276 MPa (40 ksi) Student's t-test showed there was no difference in the average lives of the P and G series. Since the G-series yielded a higher life at 379 MPa (55 ksi) than the P-series it was concluded that the effect of grinding the upset

forged end subsequent to the shot blasting operation did not reduce the corrosion fatigue life.

The corrosion fatigue results in Fig. 4 can be compared with the in-air results at a maximum stress of 379 MPa (55 ksi) which showed that the rods with the ground surface (G-series) had a median life of 2.1×10^6 cycles whereas the rods where the surface was not ground (P-series) had a median life of 4.4×10^6 cycles. These results indicate that in the absence of a corrosive environment there was some deterioration in fatigue life with a rod which had been subsequently ground after shot blasting although there was considerable overlap in scatter in the results of both the P and G series.

It is also interesting to note the location of the failures of the sucker rods as shown in Fig. 5. Regardless of whether the rods were ground or not the failures occurred mostly in the upset portion of the rod. Of 19 failed specimens, one failed in the threads, 13 (or about 70%) failed in the upset forged section, and five failed outside the upset section and beyond any area which had been ground. From the strain gauge results the effect of bending stresses in the upset portion of the rod may be more of a contributing factor to crack initiation than any defects or surface grinding.

For the rods run at 379 MPa (55 ksi) the life ranged from a low of 1.2×10^5 cycles in the unground rods (P-series) to a high of 2.45×10^5 cycles for the ground rods (G-series). As all rods were tested at a cyclic rate of 10 cpm this translated into a field life of between 10 and 17 days. For the sucker rods tested at 276 MPa (40 ksi) fatigue lives ranging from 2.8×10^5 cycles to a high of 4.93×10^5 cycles would yield field lives of between 19 and 34 days. These projected field lives were consistent with the failure data recorded in actual oil fields which had high concentrations of salt water with the crude oil and where the sucker rod string was highly stressed.

Summary:

1. The effects of bending can cause high stresses in the upset forged end of the sucker rod.
2. There was no evidence to indicate that grinding the upset forged end subsequent to shot blasting reduced the resistance to corrosion fatigue.
3. Seventy percent of all fatigue failures occurred in the upset forged end of the sucker rod.
4. Fatigue lives of 10-30 days measured in the laboratory compared closely with failure data reported from wells with high concentrations of salt water.

Acknowledgement:

Appreciation is expressed to the Natural Sciences and Engineering Research Council (Grant A2705) for financial support in aid of this project.

References:

1. Bellow, D.G. and Faulkner, M.G., "Corrosion Fatigue of Cold Worked Threaded Connections", Proc. 2nd Symp. on Appl. of Solid Mech., Univ. of McMaster Press, pp 123-142 (1974).
2. Bellow, D.G. and Faulkner, M.G., "Salt Water and Hydrogen Sulfide Corrosion Fatigue of Work Hardened Threaded Elements." J. Test. and Eval. JTEVA, 4 (2) pp 141-147 (1976).
3. Bellow, D.G. and Faulkner, M.G., "Development of an Improved Internal Thread for the Petroleum Industry", Closed Loop, 8 (2) pp 3-12 (1978).
4. Bellow, D.G. and Kumar, A., "Stress Analysis of Bent Sucker Rods", Jour. Can. Pet. Tech., 17(3) pp 76-81 (1978).

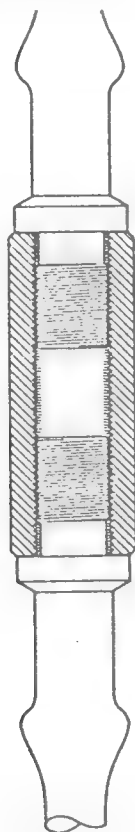


Figure 1. Sucker Rod Joint

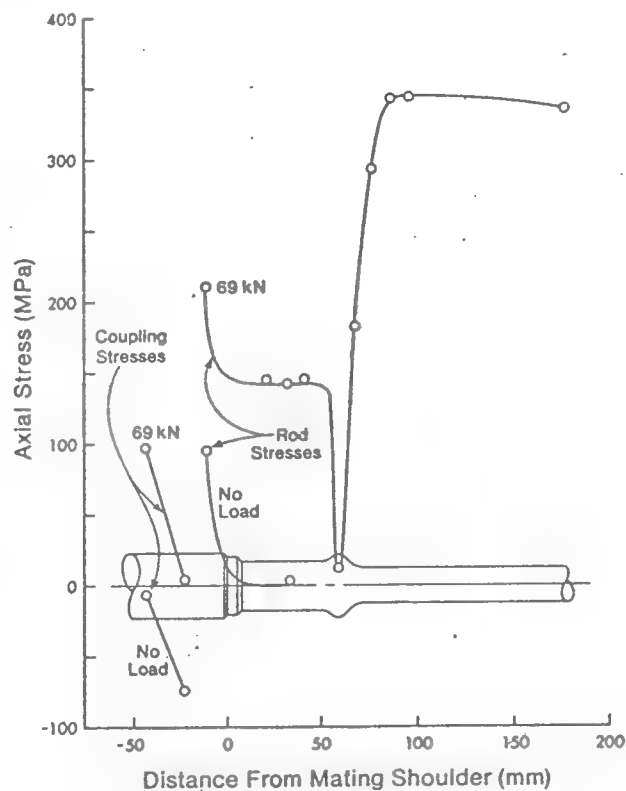


Figure 2. Stress Distribution across a Sucker Rod Joint

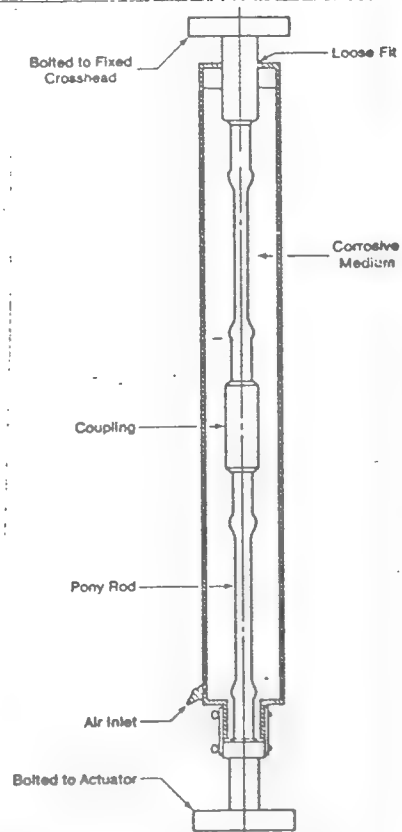


Figure 3. Corrosion Fatigue Test Chamber

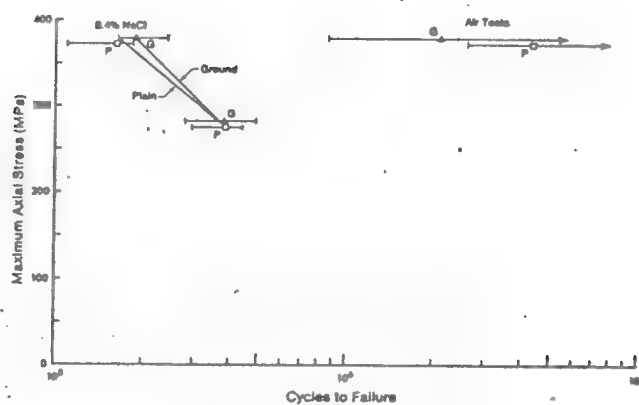


Figure 4. 8.4% NaCl Corrosion Fatigue Results

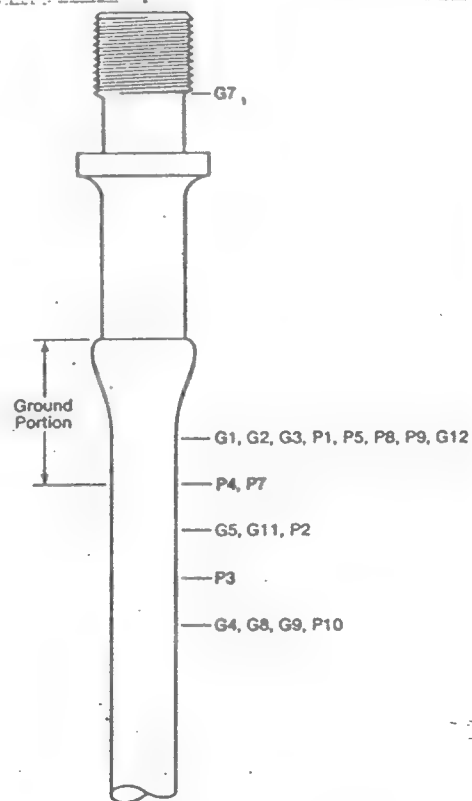


Figure 5. Location of Failures (8.4% NaCl)

USING FIELD DATA IN THE DESIGN OF A CULTIVATOR IMPLEMENT

Donald G. Bellow
Department of Mechanical Engineering
University of Alberta
Edmonton, Alberta, Canada

Abstract:

It is shown how the results of field tests can be combined with a theoretical analysis to evaluate the stresses on a cultivator shank. Experimental data is compared with the theory. Information is also provided on the dynamic aspects of a cultivator shank sweep unit under actual cultivating conditions.

Introduction:

A common method of cultivation in agriculture is for a tractor to pull a series of curved spring steel elements to which are attached spikes or chisel tools. A typical cultivator unit is shown in Fig. 1. In actual practice these units are arranged side by side and in more than one row sometimes stretching 27 m (90 ft) in width. When such implements are used for seed bed preparation and weed control the depth of tillage is generally limited to 50 to 100 mm (2 to 4 in.) such that the loads imposed on the cultivator units are not severe. However, if such implements are used in very dry hard packed soils containing a high clay content or if the implements are used for deep penetration, down to 200 mm (8 in.) or more, then the loads may be greater than what the manufacture originally intended and may lead to premature failure of the cultivator shank or the holding mechanism. The purpose of this paper is to show how field data can be combined with a theoretical analysis to design a cultivator shank to withstand the large loads severe operating conditions can impose.

In designing a cultivator shank for deep tillage or severe operating conditions stiffness and the maximum allowable stress are of prime importance. Factors such as impact strength and fatigue must also be considered and once a specific design has been chosen then these latter factors must be evaluated using test procedures established for this purpose.

Theoretical Analysis:

In Fig. 2 a cultivator shank unit is assumed to be subjected to point loads at the end of the shank consisting of in-plane loads F_H and F_V and an out of plane lateral load of F_L . Because of the cultivator tool attached to the end of the shank couples can also act on the end of the shank, but for purposes of analysis it is assumed that the main loads acting on the shank can be represented by the three force system shown in Fig. 2.

The stiffness of a cultivator shank has been analysed¹ as a function of opening angle α with typical results shown in Fig. 3. These results show that the stiffness is directly proportional to the second moment of area and the modulus of elasticity and inversely proportional to the cube of the radius. The lateral stiffness is also influenced by the b/t ratio. The stiffnesses shown do not include the cross terms involving displacements in the other two directions. These were omitted as being negligible. The relevant expressions for stiffness are as follows:

$$k_H = \frac{EI}{R^3(\alpha + \frac{\alpha \cos 2\alpha}{2} - \frac{3 \sin 2\alpha}{4})} \quad (1)$$

$$k_V = \frac{EI}{R^3(\alpha - 2 \sin \alpha - \frac{\alpha \cos 2\alpha}{2} + \frac{3 \sin 2\alpha}{4})} \quad (2)$$

$$k_L = \frac{EI}{R^3 \left[\frac{t^2}{2b^2} \left(\alpha - \frac{\sin 2\alpha}{2} \right) + \frac{E}{128G} \left(\frac{3\alpha}{2} - 2\sin\alpha + \frac{\sin 2\alpha}{4} \right) \right]} \quad \left(\frac{b}{t} \geq 1 \right) \quad (3)$$

Equations 1 - 3 have been plotted in Fig. 3 where it is seen that k_y is greater than either k_H or k_L and that k_H and k_L decrease as the opening angle α increases but that there is an optimum α for maximum vertical stiffness in the vicinity of 134° .

For an analysis of stress in the cultivator shank it can be shown that for the load condition shown in Fig. 2 that the maximum stress will occur either along the outside edge $x = -b/2$ or the inside radius $y = t/2$.

Considering an arbitrary section of the shank at θ measured from the fixed end, the moment caused by F_V and F_H can be expressed as

$$M_x = F_V R (\sin\theta - \sin\alpha) + F_H R (\cos\theta - \cos\alpha).$$

The out of plane force F_L causes both bending and twisting moments which can be expressed as

$$M_y = F_L R \sin(\alpha - \theta)$$

$$T = F_L R [1 - \cos(\alpha - \theta)].$$

Using these expressions it can be shown that the tensile stress acting along the inside radius $y = t/2$ is given by

$$\sigma_z = \frac{6F_H R}{A\sqrt{Ar}} \left\{ r[(\cos\theta - \cos\alpha) + f_{VH}(\sin\theta - \sin\alpha)] + f_{LH} w \sin(\alpha - \theta) \right\} \quad (4)$$

and for the shear stress, assuming a parabolic distribution,

$$\tau_{xz} = \frac{F_H f_{LH} R}{A\sqrt{Ar}} [1 - \cos(\alpha - \theta)] [3r + 1.8] (1 - w^2) \quad (5)$$

where $A = bt$, $r = b/t$, $w = 2x/b$, $f_{VH} = F_V/F_H$ and $f_{LH} = F_L/F_H$.

Similarly for the outside edge $x = -b/2$ it can be shown that

$$\sigma_z = \frac{6F_H R}{A\sqrt{Ar}} \left\{ ur[(\cos\theta - \cos\alpha) + f_{VH}(\sin\theta - \sin\alpha)] + f_{LH} \sin(\alpha - \theta) \right\} \quad (6)$$

$$\tau_{yz} = \frac{F_H f_{LH} R}{A\sqrt{Ar}} [1 - \cos(\alpha - \theta)] [3r + 1.8] (1 - u^2) \quad (7)$$

where $u = 2y/t$.

For given values of f_{VH} and f_{LH} eqns. 4 - 7 were programmed to compute the tensile and shear stresses for a given cross section (θ specified) along $x = -b/2$ and $y = t/2$ respectively. The stresses were evaluated at a series of 20 points along the edge $x = -b/2$ between $y = 0$ and $y = t/2$ and similarly at another 20 points along the inside radius $y = t/2$ between $x = 0$ and $x = -b/2$. The largest tensile and shear stresses were evaluated for each cross section starting at $\theta = 0$ and for each one degree thereafter until the maximum stress values were obtained. The computer determined the angle θ for which the stresses were maximum and indicated at which points on the cross section they occurred.

A number of different shank geometries and load combinations f_{VH} and f_{LH} were evaluated and it was found that the maximum tensile and maximum shear locations varied as did the cross section position (θ). Generally the maximum tensile stress was at or in the vicinity of the corner of the inside radius of the shank and at or near the fixed end of the shank. This was also confirmed from the fact that failures in the field were found to be at the fixed end of the shank and from observing failures in the laboratory where

fatigue cracks initiated at the corners on the inside radius.

The Use of Field Data:

An extensive field experiment was undertaken in dry clay-loam soils² where the loads of cultivation were measured for both sweeps and spikes under a variety of depths and plowing conditions. The test results showed³ that the forces of cultivation were a function of the depth but generally insensitive to speed in the range 6-12 km/h. It was also found that the vertical force was about 19% of the draft force and for a trailing sweep in an overlapped position the lateral force was 19% of the draft force. For the leading sweep the lateral force was less than 10% of the draft force. A summary of draft forces is shown in Fig. 4 which includes the relevant equations which best fit the experimental data. With these results it is possible to establish values for F_H , f_{LH} and f_{VH} and provide a realistic interpretation of eqns. 4 - 7. This has been done in Fig. 5 where $f_{LH} = 0.1$, $f_{VH} = 0.2$. If the value of F_H is taken for a specific depth of cultivation from Fig. 4, then the tensile and shear stress can be determined from Fig. 5. Using this data the geometric properties of a cultivator shank can be chosen which can optimize the design to meet the manufacturer's specifications and anticipated loads.

A Practical Example:

It is assumed that a manufacturer wishes to check the load capacity of a 25 x 50 mm ($b/t = 2$) cultivator shank to which a sweep will be attached. The shank has a nominal radius of 300 mm (12 in.) and an opening angle of 145°. The depth of cultivation is assumed to be 200 mm (8 in.). From Fig. 4 for dry clay-loam soils it is seen that at a depth of 200 mm the draft force on average was 6 kN. For $f_{LH} = 0.1$, $f_{VH} = 0.2$ the maximum tensile and shear stress from Fig. 5 are calculated to be approximately 600 MPa and 300 MPa respectively. During the field trials³ it was found that strain gauges, mounted to the inside radius of the shank at the upper end, indicated tensile stress magnitudes in the range 500 to 700 MPa at a depth of cultivation of 200 mm which is in close agreement with the theoretical predictions. It should be noted that these stress amplitudes were larger than the endurance limit of 415 MPa for the material so that if operation were sustained at these levels premature failure would result.

Dynamic Analysis:

The experimental data was analyzed for frequency content where it was found that a variety of vibrational modes were excited as the cultivator unit was being pulled through the ground. There were low amplitude horizontal frequencies recorded in the range 1 - 9 Hz whereas the lateral and vertical frequencies appeared to be first excited at 33 Hz and 24 Hz respectively.

To give an appreciation of the complex vibrational behaviour a cultivator shank and sweep unit was attached to the table of an electrodynamic shaker system. An accelerometer was placed along each of the three axes, horizontal, vertical and lateral with the system being driven with 0.44 g input in each of these directions in turn. The combination of all the results are shown in Fig. 6 including the dominant frequencies as measured from the field data and shown as vertical lines. Clearly, the field data does not correspond completely with the shaker data indicating a theoretical analysis would have to take into account the effects of the soil action on the tools. However, it is evident that from Fig. 6 the lowest frequency experienced by the cultivator unit was about 7 Hz in the horizontal direction. This corresponds with the fact that the horizontal stiffness as given by k_H in Fig. 3 was the lowest of all three stiffnesses for $b/t = 2$. Figure 6 also shows that the next two lowest frequencies were 21 Hz and 26 Hz which were probably associated with vertical and lateral vibration modes.

For a more comprehensive analysis of the vibrational characteristics of the cultivator unit the effects of soil behaviour on the tool must be considered and whether or not this is warranted will depend on to what extent the higher modes of vibration of a shank pose severe operating conditions. The fact that cultivator shanks can break in the field due to fatigue would suggest that the fundamental horizontal frequency, noted as 7 Hz in Fig. 6, which would be coupled with the largest dynamic amplitude (k_H is the least), would be the vibrational condition that should be considered most serious by the manufacturer.

Summary:

A methodology is given whereby manufacturers can combine data obtained from experiments in the field with a theoretical analysis to determine the optimum size and shape of a cultivator shank for use under severe operating conditions.

A discussion on the dynamic behaviour of a cultivator shank sweep unit is given wherein the results of field experiments are compared with those obtained in the laboratory. It is suggested that a theoretical analysis of the dynamic characteristics of this unit would be difficult and would have to include the effects of the soil acting on the tool. However, the experimental data indicates that the lowest natural

frequency in the horizontal direction is the one which manufacturers should be most concerned about.

Acknowledgements:

Appreciation is expressed to the Alberta Agriculture Research Trust, the Natural Sciences and Engineering Research Council (Grant A2705) and Stelco Inc. who provided financial support for this project. Thanks are also due to Mr. W. Chen and Mr. G.C. Kiss whose efforts, at various stages of this work, were of significant value.

References:

1. Bellow, D.G., and Chen, W., "On the Design of a Cultivator Shank", Proc. 4th Symp. Eng. Appl. Solid Mech., Ont. Res. Found., pp. 250-272, 1978.
2. Bellow, D.G., Kiss, G.C., and Harrison, H.P., "Measurement of Cultivator Forces", Proc. 5th Symp. Eng. Appl. Solid, Univ. of Ottawa, NRCC 18370, pp. 149-153, 1980.
3. Kiss, G.C., and Bellow, D.G., "An Analysis of Forces on Cultivator Sweeps and Spikes", Jour. Can. Agric. Eng. 3(2), 1981.

DO NOT TYPE OUTSIDE THESE LINES

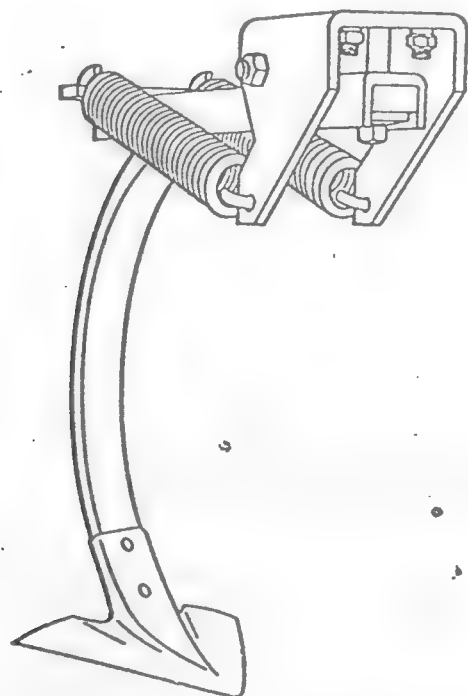


Fig. 1. Typical cultivator shank with sweep attached.

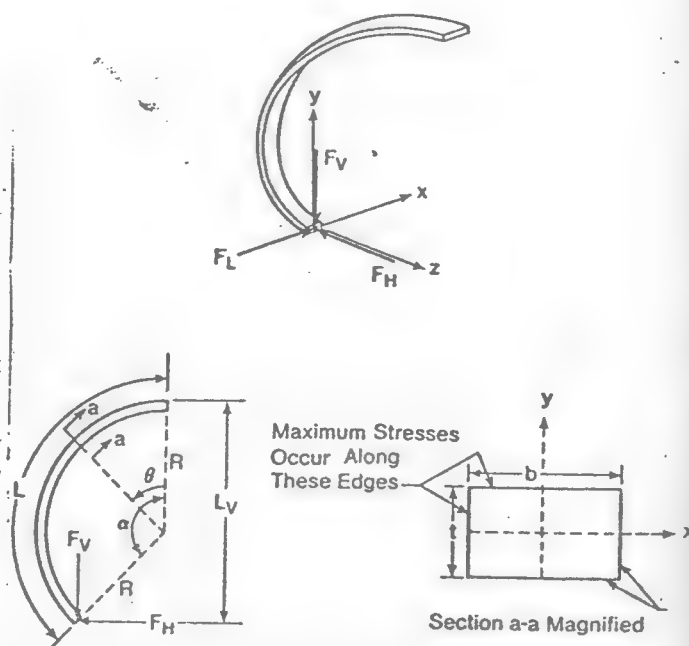


Fig. 2. Geometric parameters of a cultivator shank.

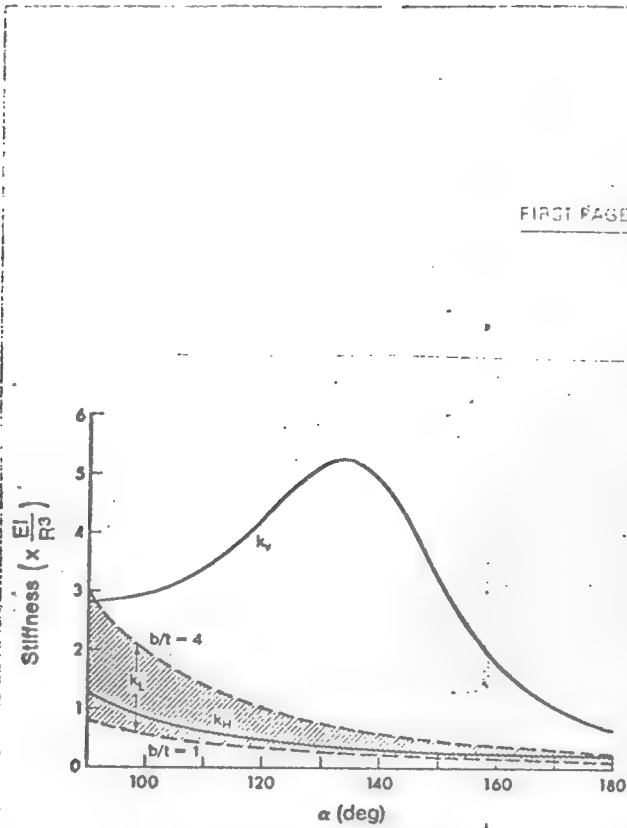


Fig. 3 Stiffness as a function of opening angle α .

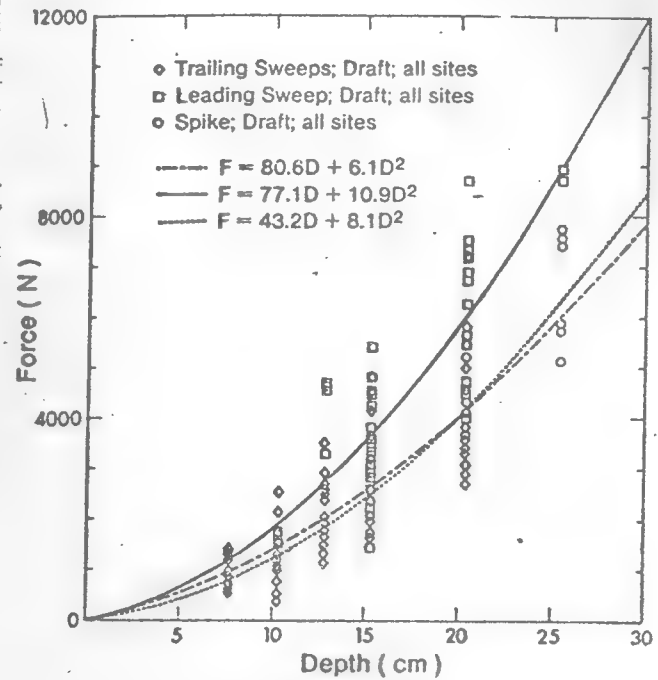


Fig. 4. Field test results for draft in dry clay-loam soils.

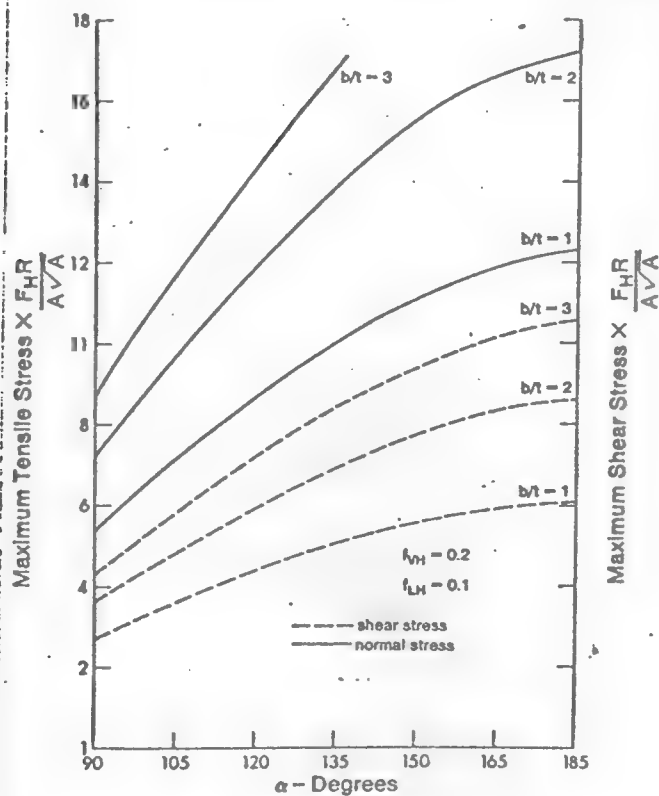


Fig. 5. Maximum tensile and maximum shear stress.

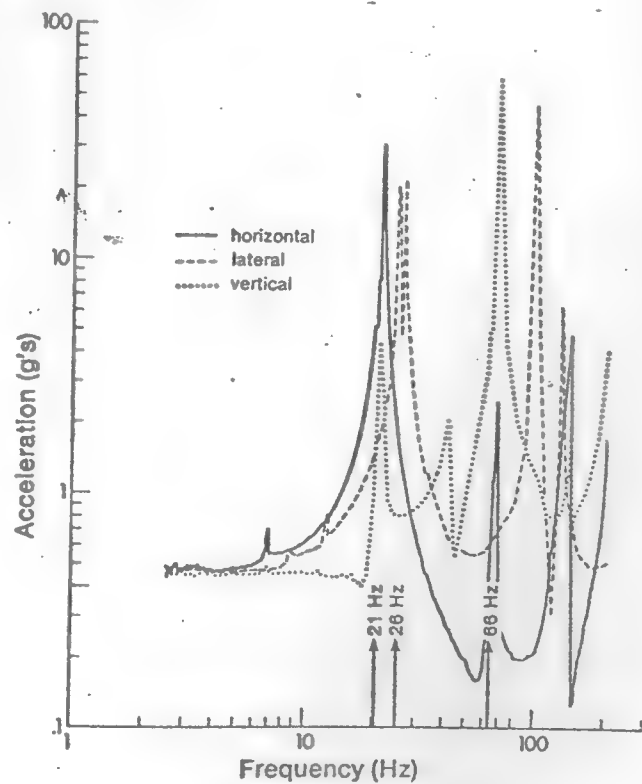


Fig. 6. Vibrational behaviour of a cultivator-sweep unit.

On the Analysis of Neutral Holes

Neutral-hole theory is extended to account for bending stresses in the reinforcement. Effectiveness of neutral reinforced openings in panels subject to uniaxial tension is investigated by photoelastic analysis

by D.R. Budney and D.G. Bellow

ABSTRACT—When an opening must be located in a tension panel the inevitable stress concentration that results can be reduced if the edge of the opening is reinforced. While there is a variety of solutions for providing reinforcements which reduce stress concentrations in the panel, none of these consider the state of stress that exists in the reinforcement.

This paper extends the theory of neutral holes to consider bending of the reinforcement as well as to allow for the use of a different material in the reinforcement. Photoelastic experiments demonstrate the effectiveness of neutral holes for uniform uniaxial tension panels for which the opening consists of parabolic sections.

List of Symbols

- ϕ = Airy stress function
- $\sigma_x = \frac{\partial^2 \phi}{\partial y^2}$
 $\sigma_y = \frac{\partial^2 \phi}{\partial x^2}$
 $\sigma_{xy} = -\frac{\partial^2 \phi}{\partial x \partial y}$ } plane stress components
- ψ = inclination of boundary to x-axis
 P = axial force in reinforcement boundary
 t = panel thickness
 σ_0 = uniaxial-tensile stress in y-direction
 P_v, P_h = vertical and horizontal components of force in reinforcement
 A_r = area of reinforcement cross section
 E_r = reinforcement modulus
 E_p = panel modulus
 ν_p = Poisson's ratio for panel
 ϵ_ψ = strain parallel to boundary of reinforcement
 r = arbitrary parameter for size of reinforcement
 A_t = area of cross section of vertical reinforcement
 σ_t = stress in vertical reinforcement member
 A_c = area of cross section of compressive reinforcing member
 σ_c = stress in compressive reinforcing member
 M = bending moment in reinforcement
 σ_r = mean tensile stress in reinforcement

f = stress-optical coefficient

n = fringe order

Introduction

The reduction of stress concentrations in tension panels using reinforcements is a common problem confronting designers of structures. Although many such problems have an inherent restriction on the shape of the opening, in some cases the designer may have latitude to design the opening, such as when it is necessary only to accommodate electrical or hydraulic conduits. For the case of a panel subjected to uniaxial tension, annular-ring reinforcements create stress concentrations at new locations while reducing stress concentrations at other locations.^{1,2} Such a reinforcement experiences extensive bending which accounts for high stress levels in the reinforcement for some geometries.

Various solutions to plane-stress problems involving reinforced openings assumed that the reinforcement is compact,²⁻⁴ that is, the cross section of the reinforcement is so small that bending stresses within the reinforcement do not exist. Hence, the reinforcement is assumed to be loaded in uniaxial tension. Neutral reinforced openings⁵ were also determined for particular stress fields based on the same assumption of compactness. Neutral openings can be designed so that the presence of the opening (and the reinforcement) does not alter the uniform stress field in the panel; the stress concentration is unity. All of the above analyses deal with the stress distribution in the panel and do not consider the stress distribution in the reinforcement. Numerical methods and experiments^{6,7} have shown, however, that stress concentrations occur at the inside of annular-ring reinforcements. Photoelastic analysis has shown that neutral reinforced openings are effective in reducing the stress concentration in the panel to levels just above unity.⁸

This paper extends Mansfield's theory of neutral holes to account for bending stresses in the reinforcement as well as to provide an explanation for the portion of reinforcement that cannot be used for the case of uniaxial tension. The theory is also extended to account for a stiffer material in the reinforcement permitting the design of more compact experimental models.

An experimental investigation of the neutral-hole concept for uniaxial tension was performed by photoelastic analysis.

Theory

A panel subject to uniform plane stress has an opening placed in it as shown in Fig. 1. It is assumed that the opening and the reinforcing bead do not alter the state of

D.R. Budney and D.G. Bellow (SESA Member) are Associate Professor and Professor & Chairman, respectively, Department of Mechanical Engineering, The University of Alberta, Edmonton, Alberta, Canada T6G 2G8.

Original manuscript submitted: January 3, 1979. Date authors notified of acceptance: July 18, 1980. Final version received: August 20, 1981.

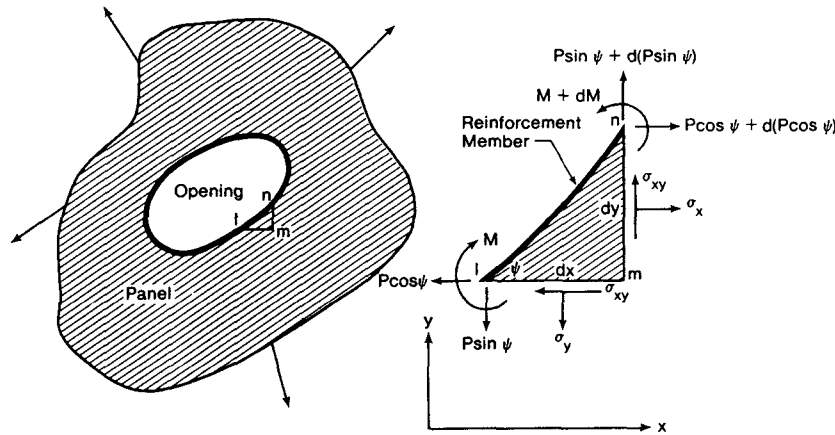


Fig. 1—Element of tension panel including reinforcement

uniform stress in the panel. The uniaxial load P in the reinforcement $l-n$ is inclined at an angle ψ to the horizontal axis. It is assumed, initially, that the reinforcement carries a bending moment M . It is assumed that any shear stiffness in the element shown exists in the panel element $l-m-n$ only and that the reinforcement shear stiffness is negligible.

By equilibrating the forces acting on the element $l-m-n$

$$d(P \sin \psi) = t(\sigma_y dx - \sigma_{xy} dy)$$

and

$$d(P \cos \psi) = t(\sigma_{xy} dx - \sigma_x dy)$$

Employing the Airy stress function ϕ ,

$$\frac{1}{t} d(P \sin \psi) = \frac{\partial^2 \phi}{\partial x^2} dx + \frac{\partial^2 \phi}{\partial x \partial y} dy \quad (2)$$

and

$$\frac{1}{t} d(P \cos \psi) = -\frac{\partial^2 \phi}{\partial x \partial y} dx - \frac{\partial^2 \phi}{\partial y^2} dy$$

Integrating eqs (2),

$$\frac{P \sin \psi}{t} = \frac{\partial \phi}{\partial x} + a$$

and

$$\frac{P \cos \psi}{t} = -\frac{\partial \phi}{\partial y} - b$$

where a and b are arbitrary constants of integration. Eliminating P/t from these equations,

$$\tan \psi = -\frac{\frac{\partial \phi}{\partial x} + a}{\frac{\partial \phi}{\partial y} + b} \quad (4)$$

Substituting $\frac{dy}{dx}$ for $\tan \psi$,

$$\left(\frac{\partial \phi}{\partial x} + a\right) dx + \left(\frac{\partial \phi}{\partial y} + b\right) dy = 0 \quad (5)$$

which is the differential of

$$\phi + ax + by + c = 0 \quad (6)$$

where c is also a constant of integration. By selection of different values of constants a , b and c , eq (6) represents an infinite number of shapes of a neutral hole for a particular state of stress defined by the stress function ϕ . It is shown later in this paper than no loss of generality occurs by letting the constants a , b and c all be zero. Hence the expression

$$\phi = 0 \quad (7)$$

is a condition which must be satisfied for the reinforcement and opening to exist without disturbing the uniform stress field in the panel.

Again referring to Fig. 1, by taking moments about m and eliminating higher order terms,

$$dM = P \sin \psi dx - P \cos \psi dy \quad (8)$$

But from eq (3),

$$P \sin \psi = t \frac{\partial \phi}{\partial x}$$

and

$$P \cos \psi = -t \frac{\partial \phi}{\partial y} \quad (9)$$

Hence eq (8) becomes

$$dM = t \frac{\partial \phi}{\partial x} dx + t \frac{\partial \phi}{\partial y} dy = t d\phi$$

It follows from eq (7) that

$$dM = 0 \quad (10)$$

Equation (10) demonstrates that a reinforcement boundary which does not alter the uniform state of stress in the panel, has a constant bending moment along it.

The area of the cross section of the reinforcement can be determined by

$$A_r = \frac{P}{\sigma_r} = \frac{P}{E_r \epsilon_\psi} \quad (11)$$

where σ_r is the mean tensile stress in the reinforcement, E_r is the modulus of the reinforcement material and ϵ_ψ is the strain in the panel parallel to the boundary. From eq (9),

$$P = t \left[\left(\frac{\partial \phi}{\partial x} \right)^2 + \left(\frac{\partial \phi}{\partial y} \right)^2 \right]^{1/2} \quad (12)$$

Transforming the stress field in the panel to components parallel and perpendicular to the boundary, and using Hooke's Law,

$$E_p \epsilon_\psi = \cos^2 \psi (\sigma_x - \nu_p \sigma_y) + \sin^2 \psi (\sigma_y - \nu_p \sigma_x) + 2 \sin \psi \cos \psi (1 + \nu_p) \sigma_{xy} \quad (13)$$

where E_p and ν_p are the modulus and Poisson's ratio of the panel material. Substituting eqs (12) and (13) in eq (11), and using eq (9) to eliminate $\sin \psi$ and $\cos \psi$,

$$A_r = \frac{\frac{E_p}{E_r} t \left[\left(\frac{\partial \phi}{\partial x} \right)^2 + \left(\frac{\partial \phi}{\partial y} \right)^2 \right]^{3/2}}{g(\phi) - \nu_p h(\phi)} \quad (14)$$

in which

$$g(\phi) = \frac{\partial^2 \phi}{\partial x^2} \left(\frac{\partial \phi}{\partial x} \right)^2 + \frac{\partial^2 \phi}{\partial y^2} \left(\frac{\partial \phi}{\partial y} \right)^2 + 2 \frac{\partial^2 \phi}{\partial x \partial y} \left(\frac{\partial \phi}{\partial x} \right) \left(\frac{\partial \phi}{\partial y} \right)$$

and

$$h(\phi) = \frac{\partial^2 \phi}{\partial x^2} \left(\frac{\partial \phi}{\partial y} \right)^2 + \frac{\partial^2 \phi}{\partial y^2} \left(\frac{\partial \phi}{\partial x} \right)^2 - 2 \frac{\partial^2 \phi}{\partial x \partial y} \left(\frac{\partial \phi}{\partial x} \right) \left(\frac{\partial \phi}{\partial y} \right)$$

Neutral Reinforcement for Uniaxial Tension

The most general stress function for uniform uniaxial tension σ_0 applied in the y -direction ($\sigma_x = \sigma_{xy} = 0$) is

$$\phi = \frac{1}{2} \sigma_0 x^2 + ax + by + c \quad (16)$$

Setting a and c to zero, the base of the parabola is placed at the origin, permitting any parabola size to be selected depending on the choice of b . By choosing the function in the form

$$\phi = \frac{\sigma_0}{2} (x^2 - ry) \quad (17)$$

r is the constant of integration which may be selected arbitrarily to proportion the reinforcement to the size of the model. (A trivial solution is obtained by setting r to zero, thus defining a boundary which is a vertical edge parallel to the applied stress σ_0 .)

Using the appropriate derivatives from eq (17) in the expression for the area of the reinforcement (eq 14)

$$A_r = \frac{\left(1 + \frac{4y}{r}\right)^{3/2} r t}{2 \left(\frac{4y}{r} - \nu_p\right)} \frac{E_p}{E_r} \quad (18)$$

The stress in the cross section is obtained by dividing the loads given by eq (12), in which the appropriate partial derivatives are used, by the area given by eq (18). Thus it can be shown that the normal stress in the reinforcement is

$$\sigma = \sigma_0 \frac{E_r}{E_p} \left(1 - \frac{\nu_p}{\frac{4y}{r} + 1}\right) \quad (19)$$

Equation (19) illustrates that the reinforcement stress is positive, and if the reinforcement and panel were made of the same material, the reinforcement stress would be less than the nominal stress (σ_0) in the panel. As y becomes very large, the contour becomes vertical and the reinforcement stress becomes $\sigma_0 E_r/E_p$. That is, in this region, the reinforcement approximates a tensile rod with applied stress σ_0 , and there is no bending. According to eq (10), it follows that there is no bending moment in the reinforcement at any other location.

Equation (18) exhibits a singularity at a value of y equal to $\nu_p r/4$ at which point the reinforcement transmits a finite-tensile force but is required to experience zero strain so as to be compatible with the neighboring panel material. Towards the origin, from this value of y , the force is positive but the strain in the same direction is negative. This phenomenon is totally incompatible with real material behavior as is shown by the suggestion that A_r is negative for values of y between zero and $\nu_p r/4$ in eq (18). This region of reinforcement cannot be used as part of a reinforcement for the opening.

By incorporating four symmetrical segments of a parabola, an opening is developed as shown in Fig. 2. At A , the horizontal force components ($P \cos \psi$) are self equilibrating and the unbalanced vertical force is $2P \sin \psi$. It can be shown that

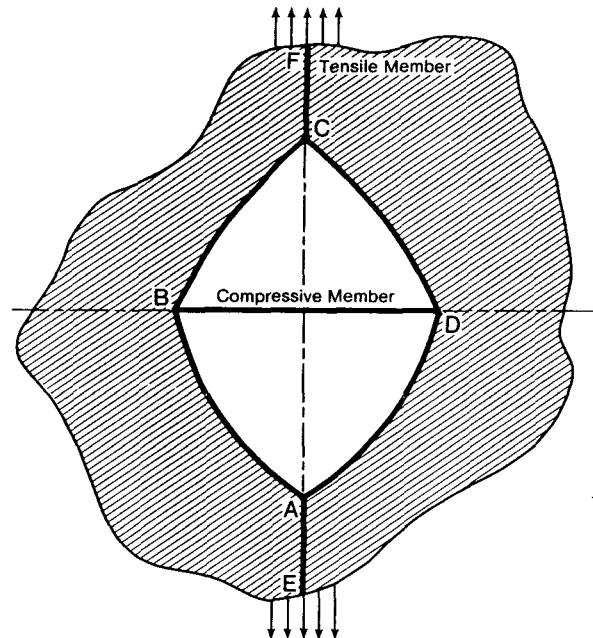


Fig. 2—Reinforced-opening configuration for uniaxial tension

$$2P \sin \psi = 2t \frac{\partial \phi}{\partial x} = 2t \sigma_0 x_0$$

where x_0 is the half width of the material removed. Therefore, the cross section of the tension member AE requires an area

$$A_t = \frac{2t \sigma_0 x_0}{\sigma_t}$$

Since the strain in this member is the same as the strain in the panel, it follows that

$$A_t = 2t x_0 \frac{E_p}{E_r}$$

Similarly, at D , there is an unbalanced horizontal force of

$$2P \cos \psi = -2t \frac{\partial \phi}{\partial y} = \sigma_0 tr$$

The cross section of the member BD would thus require an area

$$A_c = \frac{\sigma_0 tr}{\sigma_c} \quad (20)$$

where σ_c is the compressive stress in BD . Since the horizontal strain in the panel due to σ_0 is $\nu_p \sigma_0 / E_p$, the compressive stress in BD is

$$\sigma_c = E_r \nu_p \frac{\sigma_0}{E_p} \quad (21)$$

From eqs (20) and (21), the required cross section of BD is

$$A_c = \frac{tr}{\nu_p} \frac{E_p}{E_r}$$

Experimental Procedure

Whole-field photoelastic experiments were performed on a transmission polariscope to assess the uniformity of stress in the panel and compare the results with theory.

The photoelastic material used for the experiments was PSM-5 from Photolastic Inc. To minimize the effect of creep, one hour mechanical and stress-optical properties for this material were determined. That is, moduli-time relationships were determined by applying a constant load to a tensile specimen and recording strains at 5-min intervals as measured from electrical-resistance strain gages bonded to the photoelastic material, for a total period of two hours to verify that the creep rate was insignificant after one hour. The load was then removed and the specimen was allowed to recover. (Recovery time was twice the load time.) The entire procedure was repeated for each of four loads for each material. All tests were performed at 20°C. Stress-strain curves were then obtained for each material on the basis of a one-hour loading interval. The modulus of the photoelastic material was determined to be 2390 MPa. The elastic modulus of the aluminum reinforcement material was determined to be 62950 MPa.

One-hour stress-optical coefficients were obtained by using a standard transmission polariscope using a procedure similar to that used to evaluate the one-hour modulus. The stress-optical coefficient was determined to be 9.04 kN/m/fringe.

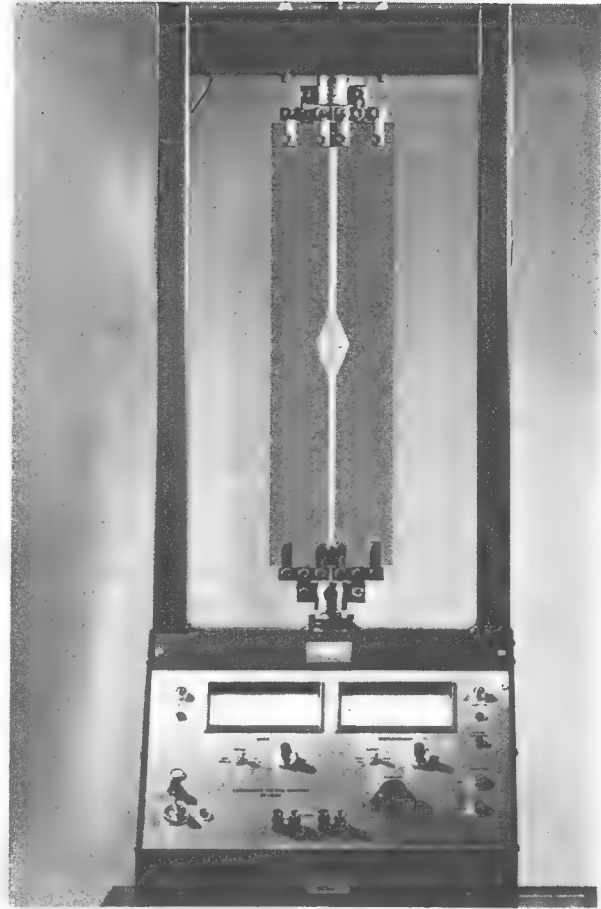


Fig. 3—General view of test panel in loading frame

The test panel consisted of a model with aluminum reinforcement bonded to the outside of an epoxy sheet. The panel was 490 mm × 142 mm and 6.66 mm thick. The aluminum reinforcement was 0.84 mm thick and was bonded to both sides of the epoxy panel. This configuration was intended to reduce the second moment of area of the reinforcement and to minimize the bulk at the locations where the different reinforcing members were joined, permitting the experiment to better approximate the mathematical model.

The experimental procedure consisted of using a standard circular-transmission polariscope. The testing frame consisted of a load cell and electrically driven screw jack. A tensile load was applied to the test panels through a linkage system to ensure a uniform stress distribution across the width of the panel (see Fig. 3). In addition to whole-field photographs of fringe patterns, a grid system was employed to assist in obtaining fringe data over the entire panel in the vicinity of the reinforcement and hole and also along a line midway between the center of the plate and plate-holding fixture.

Results

The light-field isochromatic fringe pattern for the plate when subjected to a tensile load of 2940 N is shown in Fig. 4. This figure clearly illustrates the uniformity of



Fig. 4—Light-field isochromatics for tension panel with neutral hole at a load of 2940 N



Fig. 5—Zero-deg isoclinic. Dark field throughout panel indicates principal stresses are vertical and horizontal near load frame. Applied load is 2940 N

fringe order in the vicinity of the reinforced hole whereas in the vicinity of the loading fixture fringe orders up to 3.5 are evident. To further illustrate the uniformity of the stress field in the panel, the zero-degree isoclinic pattern is shown in Fig. 5. Because the entire panel—except for the ends where the load was applied—experiences uniaxial tension, the whole field of the model was dark. The white lines identifying the edges of the plate were added after the photograph was taken.

Tardy compensation was used to obtain fractional fringe orders. A typical set of results has been reproduced in Fig. 6 for an applied load of 2380 N. The fringe orders of the quadrant shown are the averaged results obtained

from measurements from all four quadrants. At any point, the difference between fringe orders taken from different quadrants did not exceed 0.02 fringes. These fringes can be compared with the constant value of 1.56 obtained along the line midway between the reinforced opening and the plate end. Taking this value as the nominal fringe order, stress concentrations were determined by fringe-order ratios. The maximum-stress concentration occurred adjacent to the reinforcement and was $1.65/1.56$ or 1.06. It should be noted that at the reduced cross section of the panel, adjacent to the hole, the fringe order was less than 1.56, indicating the stresses in this portion of the panel were influenced by bending of

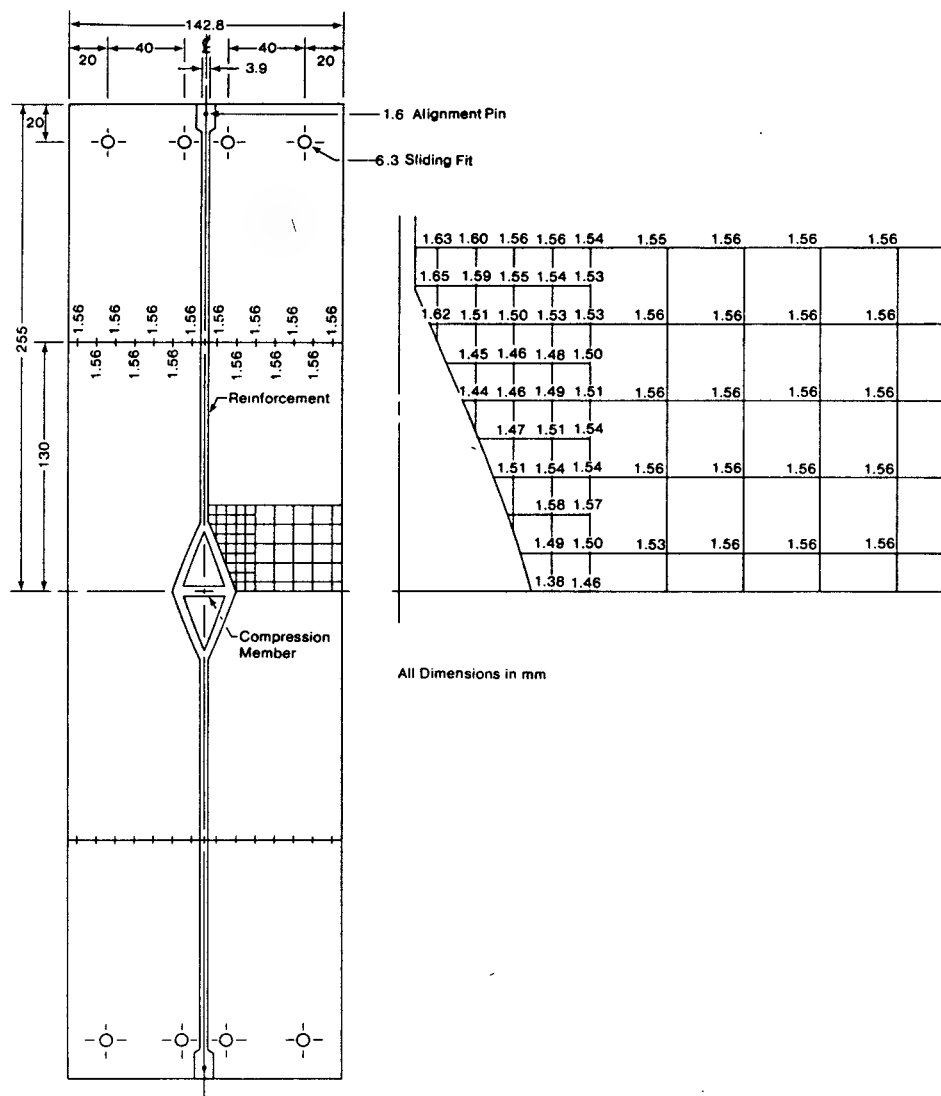


Fig. 6—Fringe orders measured at a load of 2380 N. Fringe orders shown are average values for four quadrants

the reinforcement, which superimposed compressive stresses at this location.

Conclusions

Neutral-hole theory was extended to show that the bending moment in the reinforcement was constant and zero for the case where the panel was subject to uniform uniaxial tension and the reinforcement was parabolic.

Photoelastic experiments were used to demonstrate the effectiveness of neutral reinforced openings in panels subject to uniaxial tension. The experiments demonstrated that, in applications where the shape of the opening is not required to be circular, it is possible to place a reinforced opening in a tension panel in such a fashion that the maximum stress in the panel is virtually no greater than the nominal stress.

Acknowledgment

Appreciation is expressed to the National Science and Engineering Research Council of Canada for financial

support in aid of this project (Grants Nos. A-2705, A-1376).

References

1. Beskin, L., "Strengthening of Circular Holes in Plates Under Edge Loads," *J. Appl. Mech.*, A140-A148 (1944).
2. Wells, A.A., "On the Plane Stress Distribution in an Infinite Plate With a Rim-Stiffened Elliptical Opening," *Quarterly J. Mech. and Appl. Math.*, 3 (1) (1950).
3. Radok, J.R.M., "Problems of Plane Elasticity for Reinforced Boundaries," *J. Appl. Mech.*, 22, 249-254 (1955).
4. Wittrick, W.H., "Analysis of Stress Concentrations at Reinforced Holes in Infinite Stress," *The Aeronautical Quarterly*, 11, 233-247 (1960).
5. Mansfield, E.H., "Neutral Holes in Plane Sheets - Reinforced Holes Which are Elastically Equivalent to the Uncut Sheet," *Quarterly J. Mech. and Appl. Math.*, 6 (3), 370-378 (1953).
6. Budney, D. and Svensson, N.L., "Reinforced Openings in Plastically Deforming Plates: A Finite Difference Analysis," *The J. Strain Analysis*, 9 (2), 118-129 (1974).
7. Levy, S., McPherson, A.E. and Smith, F.C., "Reinforcement of a Small Circular Hole in a Plane Sheet Under Tension," *J. Appl. Mech.*, 15, 160-168 (1948).
8. Budney, D. and Bellow, D.G., "Photoelastic Analysis of Neutral Holes," *Proc. 4th Symp. Engrg. Appl. of Solid Mech.*, 1, Ontario Research Foundation, 106-126 (1978).

RESEARCH QUARTERLY
FOR EXERCISE AND SPORT
1982, Vol. 53, No. 3, pp. 185-192

On the Swing Mechanics of a Matched Set of Golf Clubs

DAVID R. BUDNEY and DONALD G. BELLOW
University of Alberta-Edmonton

Some golf equipment manufacturers produce matched sets of golf clubs using an empirical method based on first moments of mass as well as shaft stiffness, whereas others claim to match sets on the basis of moment of inertia and dynamic considerations of shaft stiffness. This paper considers the significance of the mass distribution feature of club matching with regard to the parameters relating to physical exertion by the golfer. It is shown that dynamic considerations require a mass variation through the set almost identical to the variation prescribed by static swing weighting, and that conventionally static balanced golf clubs differ in mass by less than five percent from that suggested using a dynamic balance. It is also shown that the maximum driving force is relatively the same for a specific golfer using a variety of golf clubs but that the driving forces of the professionals were higher than those recorded for the amateurs.

Key words: golf clubs, matched set, golf swing, dynamic, static, swing weight, kinematics, force, power, torque.

It has been shown (Budney & Bellow, 1979a) using the plane compound pendulum model of the golf swing, that arm swing motion contributes most of the power developed in the golf swing, and that wrist torque has only a minor contribution. The previous analysis was performed on the golf swings of a number of professional golfers using drivers. An object of this investigation was to obtain similar information for the other golf clubs in a set.

A panel of professional golfers and golf teachers (Snead, Jacobs, Flick, Wiren, Toski, Middlecoff, Ransom, Runyan & Merrins, 1976), without defining any parameters to serve as a measure of exertion, stated that the golf swing was the same for woods and irons, but that in a given round of golf either the woods or the irons could be employed effectively, but not both. They then stated that possibly the best matched set of

golf clubs may not have yet been designed. One of the panelists stated that he thought the energy applied through the swing of the shorter clubs was less than for the swing of the longer clubs in the set. In a recent golf instruction book it is stated by one author that the swing should be identical for all clubs and, by yet another author, that it is necessary to swing each club at a different speed (Toski & Flick, 1978). Reasons for these beliefs were not given. This investigation will discuss the extent to which modifications in the golf swing are due to the length of the club, differences of mass and mass distribution for each club, or preferences of the subject in relation to power and/or accuracy.

Although professional golfers could disagree, it may not be possible to design a better matched set than currently exists because the golfer may not be sensitive to slight changes in mass distribution suggested by an analysis of this type. Another possibility worthy of consideration is that some golfers vary their kinematics through the matched set differently than do other golfers. Depending on the subject's sensitivity, it may be that club matching should be applied differently for different golfers. It would need to be determined eventually whether such alterations make a real difference, or whether accuracy and consistency are independent of golf club mechanical characteristics. If all golf swings, from driver to nine iron, involved the same kinematics and generalized forces and power, then all swings would feel the same and reproducibility should lead to great accuracy. This investigation attempts to quantify measures of physical exertion through a matched set of golf clubs to try to provide specific information related to the understanding of the golf swing, and to remove some subjectivity in describing the "feel" of the golf swing for different clubs.

The accepted practice in matching golf clubs by manufacturers is by common "swing weight" for all clubs in the set. Swing weight is usually defined as the first moment of mass of the golf club about a point 30.5 cm (12 in.) from the grip end of the golf club. Hence, the shorter golf clubs in the set (such as the 9-iron) would require a heavier club head than the longer clubs (such as the driver). The swing weight concept is an empirical method of "matching" clubs statically. However, it has not been shown to bear any relationship to the exertion by the golfer except perhaps for a monotonic change in "feel" through the set (Cochrane & Stobbs, 1968). Manufacturers employing a simple balance normally match golf sets to the nearest 70 gm cm (1 oz. in.) which implies a tolerance of 0.85 gm (0.03 oz.). It is questionable whether a golfer is sensitive enough to perceive such differences, although there is probably some psychological value to the knowledge of high accuracy in this regard. A few manufacturers match golf equipment according to moment of inertia, although it remains to be shown whether matching on this basis is any more significant than doing so by swing weight.

The Model

The golf swing, like most other human activities, involves three dimensional motion. However, it is well known that the motion of the head of a golf club is planar, from the start of the downswing until impact, and that the simultaneous motion of the grip end of

the club is nearly in the same plane (Cochrane & Stobbs, 1968). In this paper it is assumed that the motion of the club is planar, with the view that a full three dimensional analysis would provide only second order effects related to the results of the investigation. The mathematical model employed is identical to that used in previous investigations (Budney & Bellow, 1979a, 1979b). Hence the development of the equations is not repeated here, but the final equations and associated symbols are defined.

The basis for the dynamic model employed is contained in Figure 1—a view of the assumed plane of motion of the golf club from a location perpendicular to the plane. The path travelled by the club in the plane is defined by a two element pendulum, where the hands move about the fixed center of rotation O, and the club rotates about the hands. When the golfer is so viewed from a location perpendicular to the plane of motion of the club, point O can be seen to be in the vicinity of the golfer's neck. The plane of the swing is inclined by an angle α with respect to a vertical plane, where α is different for each golfer and for each club.

For all values of ϕ , \vec{OA} was assumed to be constant and given as "a." The angle between the club and \vec{OA} was given by " θ ." The distance from A to the mass center of the club was given by " ℓ ." For any golf swing, values of ϕ and θ in terms of time throughout the downswing can be determined by high speed cinematography or stroboscopic photographs. From these data, velocities and accelerations are readily obtained.

In an earlier paper (Budney & Bellow, 1979a) equations were developed, using as a model the two-arm pendulum shown in Figure 1, for the forces parallel to the arms (F_{PA}), torque (T), work (W) and power (P), and the circumferential force (F_{AA}) produced during the downswing in the golf stroke. It was shown that the circumferential force (F_{AA}) is the primary force in developing the power of the swing, and that the terms on the right side of Equation (1) can be considered to be a measure of the resistance to power development, given by

$$F_{AA} = m(g \cos \alpha \sin \phi - \ddot{x} \cos \phi + \ddot{y} \sin \phi) + F_D \cos \beta_1 \quad (1)$$

where F_D is the drag force acting on the clubhead, m is the mass of the club, β_1 is illustrated in Figure 1, and \ddot{x} and \ddot{y} are the accelerations in the x and y directions of the mass center of the club, designated as point G in Figure 1. If the coordinate equations for x and y are twice differentiated and substituted into Equation (1), and the higher order terms of gravity and

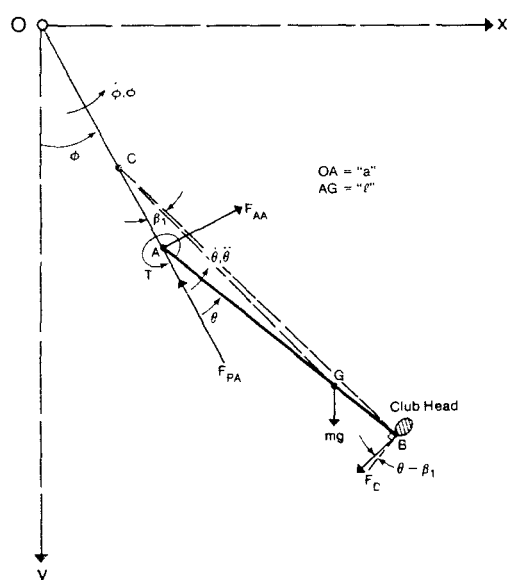


Figure 1—The model

aerodynamic drag are ignored, the resulting expression is obtained for F_{AA}

$$F_{AA} = -m(a\ddot{\phi} - \ell[(\dot{\phi} + \dot{\theta})^2 \sin\theta - (\ddot{\phi} + \ddot{\theta}) \cos\theta]) \quad (2)$$

Considering equation (2) at the instant in the swing when F_{AA} is a maximum, it is apparent that first moments of mass ma and $m\ell$ are the factors which resist the force most responsible for energy development. If the kinetics of the swings are identical for all clubs, and if the maximum force F_{AA} is identical also, the only parameters that can be permitted to be different for different golf clubs are m and ℓ in equation (2) which can be written:

$$m \left\{ \ell - \frac{a\ddot{\phi}}{(\dot{\phi} + \dot{\theta})^2 \sin\theta - (\ddot{\phi} + \ddot{\theta}) \cos\theta} \right\} = \frac{F_{AA}}{(\dot{\phi} + \dot{\theta})^2 \sin\theta - (\ddot{\phi} + \ddot{\theta}) \cos\theta}$$

or

$$m(\ell - q') = \text{const} \quad (3)$$

where

$$q' = \frac{a\ddot{\phi}}{(\dot{\phi} + \dot{\theta})^2 \sin\theta - (\ddot{\phi} + \ddot{\theta}) \cos\theta}$$

q' can be evaluated from cinematographic film data for the required position in the golf swing. At the specific instant in the swing when F_{AA} is a maximum, q' is a constant if the kinematics are identical for all swings.

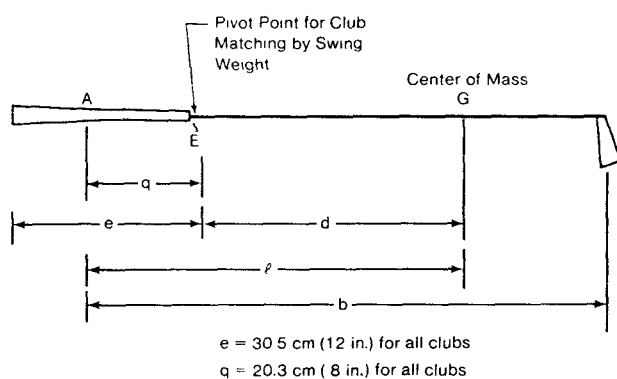


Figure 2—Club matching parameters

Comparison of Static and Dynamic Matched Sets

Conventional matching is based on identical first moments of mass for all clubs in the set about a point 30.5 cm (12 in.) from the grip end (point E in Figure 2).

If one club with mass m_1 and centroidal distance d_1 has a mass moment of $m_1 d_1$, then

$$m_2 d_2 = m_1 d_1, \quad (4)$$

where m_2 is the mass of the next club and d_2 is the centroidal distance of that club. Usually equation (4) is assured by the manufacturer by adjusting the mass of the clubhead; however, some manufacturers add mass to the grip end of the golf club to achieve the balance. This method of matching has been established empirically during the history of the game based on personal preferences of the better participants in the game and the desire of manufacturers to establish standards. The magnitude of the moment of mass is usually 17,590 gm cm (244 oz. in.) and varies from 17,150 gm cm (238 oz. in.) for a lightweight set (usually ladies') to 18,160 gm cm (252 oz. in.) for a heavy set for stronger professional golfers.

Letting S be the static moment value for a matched set, from Figure 2

$$S = m(\ell - q) \quad (5)$$

where ℓ is the length and q is 0.203 m (8 in.). Equations (3) and (5) are clearly similar in form.

In the Appendix it is shown that if m_1 is the mass of a specific club in the set and if m_2 is the recommended mass of a second club in the set by static swing weighting (Equation 5), the adjustment to m_2 prescribed by dynamic matching (Equation 3) is

$$\Delta m = (m_2 - m_1) \left\{ \frac{q' - q}{b - q'} \right\}. \quad (6)$$

The preceding equations were programmed for solution on a computer for known ϕ vs. t and θ vs. t obtained from either high speed film or stroboscopic photography. The procedure (Budney & Bellow, 1979a) involved determining suitable fourth order polynomial equations which were used to represent the data of ϕ vs. t and θ vs. t . Knowing ϕ , θ and the physical parameters of the golf club, the forces, torque and clubhead speed were determined for any instant of time throughout the duration of the swing up to impact.

Methodology

Either high speed cinematography or stroboscopic photography can be used to obtain the assumed planar kinematics of the golf club. Figure 3 is a reconstruction of the golf swing of a professional golfer using a driver from a 16 mm photographic record. The camera, which was a Milliken DBM 54 with a f2.2 12–120 mm Angenieux zoom lens, was located on a line perpendicular to the plane of the swing at a distance of ap-

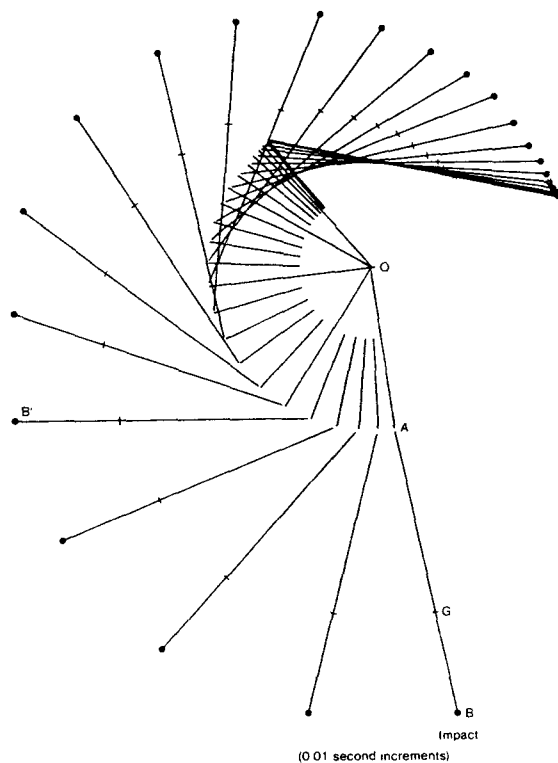


Figure 3—Model sequence for professional golfer

proximately 25 meters from the golfer. Since the inclination of the swing plane was different for each golfer and for each club, the camera location was set to suit each individual swing plane and was adjusted so that the swing plane of the golfer filled the 16 mm frame of the film. Framing rates of 100 and 200 frames per second were used. The 16 mm film used was Kodak Ektrachrome video news film type 7239. The magnification from film image to projected image, from which the angles of the swing were measured, was approximately 40 times.

It is well known that sophisticated curve smoothing techniques are required for the best estimation of derivatives from digital information. One of the most effective techniques used for smoothing digital data is the polynomial spline method. Simple polynomial regression can cause a phase shift as well as distort the magnitude of displacements and their derivatives, particularly toward the ends of the data interval. However, differences in calculated acceleration between ordinary polynomial curve fitting and spline fitting for the simple brief motion considered in this investigation were less than one percent in the central region of the interval where the critical dynamic parameters were of greatest importance. For this investigation or-

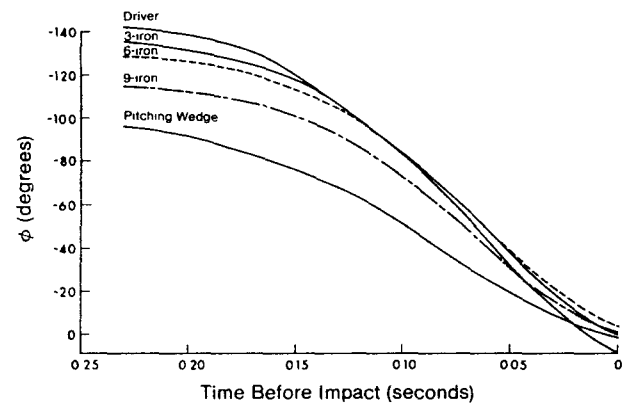


Figure 4— ϕ (arm position) for different golf clubs swung by a professional golfer

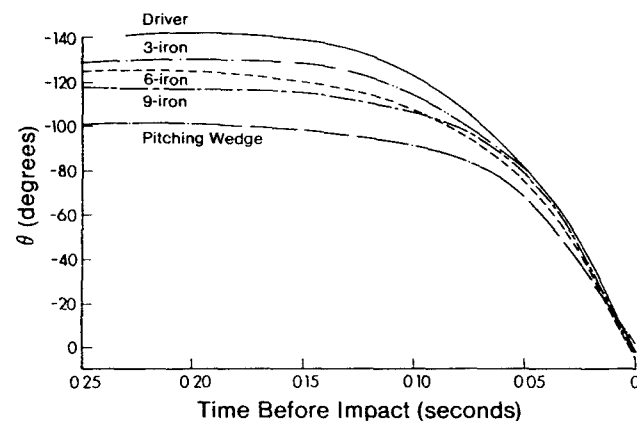


Figure 5— θ (wrist angle) for different golf clubs swung by a professional golfer

inary polynomial curve fitting for the parameters ϕ and θ proved satisfactory.

All the data presented is on the basis of one trial, as this was considered sufficient for each golfer. This was concluded when calculations based on repeated trials produced virtually identical results, indicating that athletes' performances were repeatable.

The subject golfers chosen were two professional golfers involved at the time of testing in competitive play, and two amateurs who were active, and consistent, golfers.

Results

Figure 4 demonstrates the variation of ϕ for a professional golfer for the swings of five different golf clubs. The downswing duration was about 0.23s for all swings. The length of the backswing (initial value of ϕ)

increased with club length. Figure 4 demonstrates that for all of these swings, arm swing motion first accelerated and then decelerated toward impact. It is also apparent that at impact the speed of the arms was greatest for the driver and decreased for each club approximately according to the length of each club. Final ϕ values are listed in Table 1. Wrist angle (θ) is shown for the same golf swings in Figure 5. Initial values of θ were greatest for the longest club (driver) and least for the shortest club, and these values stayed nearly constant for almost half the swing duration. Figure 5 also indicates that the final velocity ($\dot{\theta}$), as indicated by the slopes of the curves, was nearly identical for the driver and the 3, 6 and 9-irons; this angular velocity which consists of adduction of the wrists as well as supination of the left forearm was much less for the pitching wedge, as this was the only club being used in this investigation to hit less than "full shots." For the first four clubs (see Table 1) the nearly identical final values of $\dot{\theta}$ serve as evidence of the physical limitation of mobility of the wrists mentioned in a previous article (Budney & Bellow, 1979a, 1979c).

Figures 4 and 5 describe the kinematics of the two-arm pendulum model of the swing, and compare the arm position and the wrist angles for different golf clubs. The circumferential force producing motion shown in Figure 6 was applied in much the same manner for each of the golf clubs used by the subject golfer. The maximum force occurred earliest and was greatest (335N) for the driver, while it occurred later for the 9-iron, reaching a maximum value of 300N. The 3-iron and 6-iron curves fell between these two extremes. Maximum values were applied approximately 0.04s prior to impact, at which time the club-

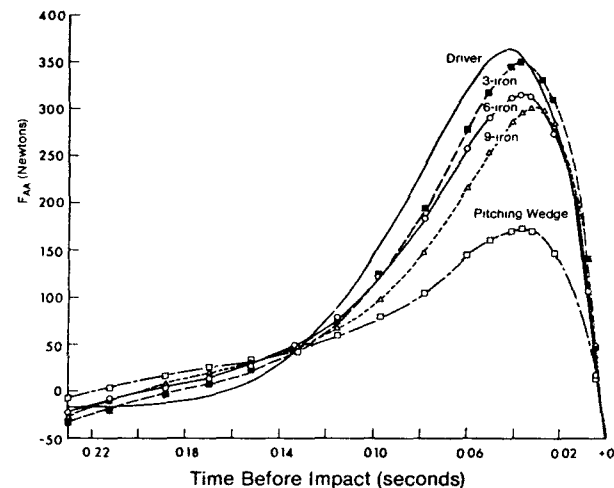


Figure 6—Circumferential force for different golf clubs

head was in position B' in Figure 3. Considerably reduced effort was shown for the swing of the pitching wedge.

The clubhead speed of the driver at impact was greatest and for the 9-iron was least, as was expected (Table 1). The total kinetic energy in the golf club, including the shaft, was 315 J for the driver and decreased to 263 J for the 9-iron. For the driver, this was made up of 304 J due to arm swing motion and 9 J due to wrist torque. The proportions changed monotonically toward the 9-iron for which arm swing motion produced 220 J and wrist torque produced 43 J. Thus, arm swing motion could be seen to contribute more than wrist torque although the net contribution toward developing kinetic energy was less for the shorter irons. The professional golfer represented in Table 1

Table 1
Comparison of Swing Mechanics for Five Different Golf Clubs
Swung by a Professional Golfer

Club	Mass of Club (kg)	Arm-Swing Angular Velocity at Impact ($\dot{\phi}$) (rad/s)	Wrist Angular Velocity at Impact ($\dot{\theta}$) (rad/s)	Max Arm-Swing Force F_{AA} (N)	Clubhead Speed at Impact (m/s)	Total Golf Club Energy at Impact (J)	Work Done by Arm Swing Motion (J)
Driver	0.380	10.3	36.2	363	52.6	315	304
3-Iron	0.417	6.9(10.3) ^a	35.9(36.2)	353(361)	46.0(44.8)	308(293)	279(299)
6-Iron	0.433	6.1(10.3)	35.5(36.2)	317(367)	42.9(43.3)	279(288)	251(311)
9-Iron	0.451	4.4(10.3)	34.9(36.2)	302(371)	40.0(41.4)	263(289)	220(311)
Pitching Wedge	0.485	1.4	20.0	173	28.6	14.6	118

^a Numbers in parentheses refer to values obtained if each club experienced kinematics identical to those of the driver.

Table 2
Comparison of Wrist Angular Velocities (rad/s)
Of Two Professional and Two Amateur Golfers at Impact

Club	Professionals		Amateurs	
	P1	P2	A1 (13 hcp) ^a	A2 (9 hcp)
Driver	36.2	30.4	22.4	27.2
3-Iron	35.9	28.9	22.8	26.9
6-Iron	35.5	30.2	22.9	29.3
9-Iron	34.9	29.5	23.6	27.2

^a hcp = handicap

applied less energy during the swing for those golf clubs for which accuracy was regarded as more important than power.

Table 1 displays in parentheses a separate set of values for the irons for which the kinematics (ϕ and θ vs time) of the driver were applied in the model analysis. Comparison of exertion parameters were made when identical swings were applied to the different golf clubs. These results provided forces (F_{AA}) for the irons much nearer to that for the swing of the driver, and slightly increased clubhead speed for the irons. Total final energy for each club was increased but was still less than for the driver. Work done by arm swinging motion could be seen to have increased substantially. For the 9-iron, for instance, this work increased from 220 to 311 J. Since the final energy was only 289 J, the kinematics of the driver resulted in negative net work done by the wrist couple of 22 J whereas it was a positive 43 J for the actual swing of the 9-iron.

A convenient and easily understood measure of the output of the golf swing is the release or unhinging velocity of the golf club at the instant of impact with the ball. In Table 2, the unhinging or release velocity ($\dot{\theta}$) at impact is compared for two professional golfers and two amateurs. Values shown in rad/s include wrist movement as well as supination of the left hand and

pronation of the right hand. It is apparent that these angular velocities were nearly identical for each golfer with all clubs but were characteristically different from one golfer to another. Particularly, the two professional golfers demonstrated greater skill in achieving higher release velocities than the two amateur golfers. The largest difference was between professional P1 who averaged 35.5 rad/s and amateur A1 who averaged 22.5 rad/s. Generally the professionals had a 30 percent higher swing velocity than did the amateurs. However, each golfer appeared to have his own unique limitation of mobility, with the result that each was unable to keep his hands moving at the same pace as the angular velocity of the club. In these circumstances the hands of the golfer apply a negative torque to the club, causing it to decelerate.

It is evident from Table 3 that where professional P1 demonstrated decreased total energy expended for his shorter clubs, golfer P2 applied more energy for the swing of his shorter clubs. Both professional golfers applied less maximum power for the swing of their drivers than for their 3-irons. For the shorter irons subject P1 applied slightly less power than did subject P2. Golfer P1 demonstrated diminishing maximum circumferential force, whereas golfer P2 applied lower maximum force for his driver than for his irons.

Equations (3) and (4) have been plotted in Figure 7 to demonstrate the similarity between existing static and the dynamic club matching methods suggested in this paper. With the driver selected as the basis for comparison, the dynamic club matching concept suggests reduced mass for the shorter irons; the greatest being 0.016 kg for the 9-iron, a reduction in mass of only 3.5 percent. The 3-iron requires the least reduction, 0.0074 kg or 1.8 percent less than that prescribed by static swing weighting. Dynamic matching appears to produce good qualitative as well as quantitative agreement with traditional static swing weighting concepts. However, matching by static swing

Table 3
Comparison of Some Exertion Parameters
For Two Professional and Two Amateur Golfers

Club	Professional P1			Professional P2			Amateur A1 (13 hcp)			Amateur A2 (9hcp)		
	Energy at Impact (J)	Max Total Power (kw)	Max F_{AA} (N)	Energy at Impact (J)	Max Total Power (kw)	Max F_{AA} (N)	Energy at Impact (J)	Max Total Power (kw)	Max F_{AA} (N)	Energy at Impact (J)	Max Total Power (kw)	Max F_{AA} (N)
Driver	311	3.64	363	271	2.65	278	285	2.53	266	214	2.62	304
3-Iron	308	3.88	353	279	3.08	314	269	2.39	253	259	2.97	356
6-Iron	282	3.46	317	295	3.54	295	342	3.24	303	255	2.65	343
9-Iron	268	3.41	302	297	3.67	310	282	2.66	281	190	2.27	305

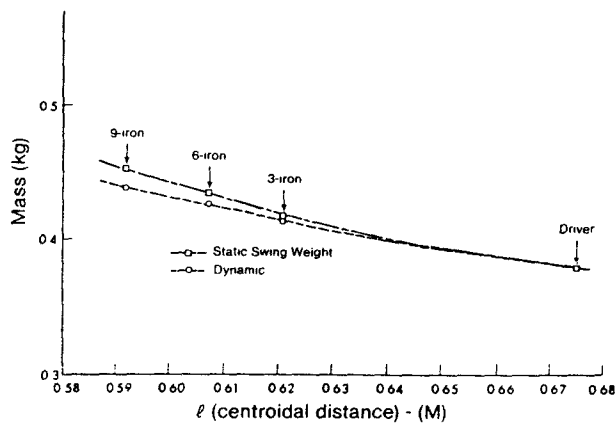


Figure 7—Comparison of club matching concepts

weight requires greater mass for the shorter irons. With the driver, golfers attempt to maximize clubhead energy at impact. With the shorter irons, the object of accuracy is more easily effected by a slower swing. In order that the golfer feel similar resistance at a reduced swing rate, the mass of the clubhead is increased, so that the forces developed are not severely lowered by the reduced accelerations. The golfer at least maintains some "feel" in terms of resistive force, if not for kinematics. A recent instructional book (Toski & Flick, 1978) suggests that the swing of all golf clubs should be conducted at the same pace, although the definition of pace was not included. If it was meant that identical kinematics should be used, then dynamic club matching would be of considerable significance. However, as each golfer probably displays his own unique variation of swings for a set of golf clubs, the results of this investigation suggest that alternatives to the current swing weight scale could be employed. If a golfer tended toward identical kinematics for all swings, the mass of shorter irons could be reduced in relation to constant swing weight. Alternatively, if a golfer preferred to swing his short irons considerably slower than his longer clubs, even greater clubhead mass than that prescribed by swing weight matching may be preferred. Whatever the variation from current matching, the simple swing weight balance used in the trade could well be used to establish a new monotonic mass variation through the set to suit the individual according to the dynamic considerations presented here.

Conclusion

Results show that professional golfers exhibit a monotonic variation of kinematics, forces and power for their normal swing of a conventional matched set of golf clubs. Further, it was shown that if the same

kinematics were applied to all clubs in the set, parameters which represented physical exertion by the golfer still exhibited a monotonic variation.

Final unhinging angular velocities were nearly identical for all clubs swung by each golfer, although each golfer appeared to have his own limitation in this regard. This observation supports the contention that the hands retard motion by applying negative torque. Also, as each golfer swung his shorter golf clubs, all measures of his physical exertion were less than those for his driver swing. There appeared to be no discernible relation of exertion parameters to the manner in which the mass distribution changed from club to club, as is suggested by the traditional matched set concept.

Based on the approach that identical kinematics as well as identical maximum circumferential force serve as the basis for club matching, it was shown that the manner in which mass should vary from club to club was the same as for static swing weighting, and qualitative differences were small. Conventional static balanced sets varied in mass from dynamically balanced sets by no more than 3.5 percent. Application of these results could be used to vary the mass of clubheads by the same formula but with different ratios, to enable personal preferences on variation of swing speed through the set to be accommodated.

References

- Budney, D. R. & Bellow, D. G. A dynamic model for the golf swing. *Science in Sports*. Del Mar, CA: Academic Publishers, 1979a, 3-20.
- Budney, D. R. & Bellow, D. G. A kinematic analysis of a golf swing. *Research Quarterly*, 1979b, 50, 171-179.
- Budney, D. R. & Bellow, D. G. Teaching aids for golfers. *Science in Sports*. Del Mar, CA: Academic Publishers, 1979c, 21-36.
- Cochrane, A. & Stobbs, J. The search for the perfect swing. London: Heinemann Press, 1968.
- Snead, S., Jacobs, J., Flick, J., Wiren, G., Toski, R., Middlecoff, C., Ransom, H., Runyan, P. & Merrins, E. Should you swing woods and irons differently? *Golf Digest*, 1976, 27 (4), 154-155.
- Toski, R. & Flick, J. *How to become a complete golfer*. Simon and Schuster, Norwalk, CT, 1978.

Appendix: Comparison of Static and Dynamic Club-Matching Concepts

As a basis for comparison, it is assumed that the driver is common to both systems of club-matching. Letting m_1 be the mass of the driver and d_1 be the distance from the center of mass to the static balance

point E (Figure 2), according to club-matching by static swing weight, the mass m_2 of any other club in the set is obtained from

$$m_2 d_2 = m_1 d_1 = S. \quad (A1)$$

The purpose of the equations developed here is to determine the additional mass Δm to be applied to the head of the second club which has been balanced statically according to equation A1 to bring about dynamic balancing based on equation (5).

Taking moments about E in Figure 2,

$$m_2 d_2^D = m_2 d_2 + \Delta m (b - q) \quad (A2)$$

where b is the distance from A to the clubhead of the second club, q is 0.203 m for all clubs, and d_2^D is the centroidal distance for the second club as determined by dynamic matching.

From equation (3), dynamic club-matching requires

$$k = m(\ell = q'). \quad (A3)$$

From Figure 2 this becomes

$$k = m_1 d_1 - m_1 [q' - q]$$

or, using (A1),

$$k = S - m_1 [q' - q].$$

For any other club in the set

$$m_2^D (d_2^D - [q' - q]) = S - m_1 [q' - q]$$

where m_2^D is the mass of the second club and d_2^D is the centroidal distance for the second club as determined by dynamic matching. Rearranging,

$$m_2^D d_2^D = S + (m_2^D - m_1) [q' - q]. \quad (A4)$$

Combining equations (A4) with (A1) and (A2)

$$\Delta m (b - q) = (m_2^D - m_1) [q' - q].$$

Since $\Delta m = m_2^D - m_2^S$, this equation can be rearranged to

$$\Delta m = (m_2^S - m_1) \left\{ \frac{q' - q}{b - q'} \right\}. \quad (A5)$$

Equation (A5) represents the mass to be added to the club head of each club in the set for the set to be matched dynamically.

Submitted: January 28, 1980

Accepted: January 13, 1982

David R. Budney is an Associate Professor and Donald G. Bellow is Professor and Chairman of the Department of Mechanical Engineering, University of Alberta, Canada, T6G 2G8. The authors express their appreciation to the Natural Sciences and Engineering Research Council of Canada for financial support received under grant No. A-2705 and to the United States Professional Golf Association for providing the venue and other valuable assistance in making the photographic study possible. Particular thanks are extended to golf professionals Mike Long and Vince Cali, who were willing subjects at a time when they were preparing for a tournament of considerable importance to them.

WELDING IN ENERGY-RELATED PROJECTS

WELDING
INSTITUTE OF
CANADA



INSTITUT
DE SOUDAGE
DU CANADA

NARROW GAP WELDS USING UNDER STRENGTH WELD MATERIAL

Barry M. Patchett and Donald G. Bellow
University of Alberta, Edmonton, Alberta T6G 2G8

ABSTRACT

In the production of narrow gap welds cracking can often occur due to the low ductility of the high strength weld material as specified in the ASME Code. To overcome this problem a lower strength weld material with increased ductility is used in combination with various weld thickness to plate thickness ratios (aspect ratio). The purpose of this paper is to describe the experimental results which were obtained in evaluating the behaviour of under strength weld material in narrow gap welds in A516 Gr70 plate. Aspect ratios between 0.5 and 1.0 have been evaluated using 25 mm thick plate. The arc welding procedure used both an inert gas and mildly oxidizing gas. The strength of the weld was evaluated by tension tests performed on stress relieved specimens taken across the weld and along the direction of the weld. The results showed that the ultimate strength of the weld, which had an ultimate tensile strength 25% less than that of the base metal, actually increased by eight percent as the aspect ratio was reduced from 1.05 to 0.55.

KEYWORDS

Narrow gap welds; understrength butt welds; aspect ratio; tensile strength; plastic flow stress.

INTRODUCTION

Many pressure vessel fabrication codes, including the ASME Boiler and Pressure Vessel Code, require that the strength of the weld metal used in weld joints must exceed the minimum specified parent metal strength. Since the Code design criteria are based on ultimate tensile strength, an A516 Gr 70 joint must exceed 480 MPa (70 ksi) even after all heat treating cycles, including intermediate stress relief treatments and any extra heat treatments due to repairs. In very large pressure vessels, the number of intermediate heat treatments, including repairs, can lead to total heat treating times in excess of 10 hours. Many weld metals will experience a significant drop in yield and ultimate tensile strength during such

heat treatments, often to the extent that the UTS drops below the minimum code criterion.¹ A higher strength electrode can be used to offset the loss of strength, but often at the expense of increased susceptibility to root pass cracking in restrained joints. It is therefore desirable to know if low strength or "undermatching" weld metal can be tolerated in fabrications, and is so, under what conditions of joint design and differential in both yield and ultimate tensile strength from base metal levels. Work by Satoh and Toyoda (1975, 1979) has shown that significant undermatching between weld metal and base metal strength can be tolerated in high-strength low alloy steels if narrow-gap joint configurations are used. This is due to the constraint on plastic deformation in the thin layer of weld metal by the stronger base metal which puts a triaxial stress on the lower strength metal. The early experiments by Satoh and Toyoda (1975) used a flash welding technique for most of their results, in order to obtain very low width to depth ratios in the weld metal, which they called the "relative thickness". They found that if the relative thickness is 0.25 or less, and the flat bar tensile test specimen width is five times the plate thickness, then the ultimate tensile strength of the complete weld joint will equal or exceed the specified base metal strength if the undermatching of the weld metal is 15% or less. To be specific, the low alloy base plate has an ultimate tensile strength of about 830 MPa - this strength was achieved in the joint using an E62016 (9016) electrode of about 660 MPa strength. Joint strength matching base metal strength can be assured if the strength disparity is 10% or less. Later work by Satoh and Toyoda (1979) showed that the lower strength weld metal not only minimized cracking in root passes but also allowed lower preheating temperatures by as much as 25°C. However, high-strength low alloy steels have very high yield strength, particularly as a percentage of ultimate tensile strength. The steel used by Satoh and Toyoda, for example, had a yield to ultimate ratio of 0.93, whereas typical C-Mn pressure vessel steels have ratios of about 0.55 to 0.70. C-Mn weld metals, on the other hand, have rather high yield to ultimate ratios which often exceed 0.75 (Wheatley and Baker, 1962). Therefore the behaviour of low-strength weld metals in low alloy steels is unlikely to be applicable to C-Mn steels and furthermore the high yield characteristics of C-Mn weld metals may improve performance in undermatching situations.

Narrow-gap welding procedures and processes have advanced rapidly in recent years. The most popular processes are the SAW and GMAW processes. The SAW process is most often used in an overlapping fillet weld (or dipass) procedure to fill a relatively narrow-gap of 20-25mm in width (Grist and Armstrong, 1980) but flux removal problems can occur in very narrow-gaps using a monopass (or one bead width) procedure. The GMAW process can be adopted to monopass procedures with gaps as narrow as 10mm in plates up to 300mm thick (Kimura et al 1979). The process has been used to fabricate a number of pressure vessels in C-Mn steels such as A533 GrB Cl 1 and A516 Gr70 and low alloy steels such as A387 Gr22 Cl 1 (Malin, 1983). However, these joints were all made with overmatching consumables, with no attempt to assess the effects of narrow-gap procedures on the tensile deformation characteristics of the weld joint.

Previous studies have therefore shown that narrow-gap welding processes are commercially viable, that C-Mn and low alloy steels can be fabricated into large pressure containing structures, and that undermatching weld metal can provide

¹ The loss in strength follows the Holloman-Jaffe parameter and can be predicted with reasonable accuracy if temperature and time cycles are known.

$$P = T(20 + \log t) \quad T = ^\circ\text{K}$$

$t = \text{time in hours}$

joints of tensile strength equal to the specified base metal strength in high-strength low alloy steels if a suitable weld aspect ratio (or weld gap to plate thickness ratio) is achieved. There is little knowledge available in the tensile deformation response of undermatching C-Mn weld metals in narrow-gap welds for thick plates of widely used pressure vessel steels such as A516 Gr70. The present work is a first step in assessing undermatching weld metals in C-Mn steels to see if their use is possible in large fabrications to minimize welding cracking difficulties while maintaining acceptable strength.

EXPERIMENTAL PROCEDURES

Plates 25 and 50mm thick made of A516 Gr70 steel and approximately 0.5 x 0.7m were butt welded together by a gas metal arc using a mildly oxidizing gas. For the low strength welds an AWS E112 electrode was used. One set of tests used a Kobe C-Mn twist wire which produced weld metal strengths exceeding the minimum strength specified for the base metal.

Before welding, the gap was set so that a range of aspect ratios could be evaluated. For an aspect ratio of 1.0 the welds were produced with three overlapping passes. For an aspect ratio of 0.75 two overlapping passes were used and for aspect ratios of 0.5 or less a single pass was used.

The tensile specimens were sawn out of the welded plate material and were stress relieved for one hour at 650°C. The specimens were milled to shape with the final surfaces being ground. Clip-on electrical resistance strain gauge transducers were attached to each tensile specimen. One transducer with a gauge length of 10mm was used to measure strains in the weld, one with a gauge length of 25mm was used to measure strains on the base metal and one with a gauge length of 50mm was used to measure strains across the weld which included a combination of weld metal and base metal strain behaviour. Specimens were cut in two widths, 38mm and 76mm, in order to determine the influence of specimen width on the test results.

The tensile specimens were loaded in a 400,000 lb. (1,780 kN) universal testing machine. The load was recorded simultaneously with the strain from each of the three transducers, digitized at 3.5 sec. intervals, and stored on a perforated tape. The tape was then analyzed by a computer which produced analog plots of stress vs log plastic strain and the log of the slope of the stress-strain curve vs plastic strain.

RESULTS

In Figs. 1-3 the stress-strain behaviour of the weld metal is compared with that of the base material. Figure 1 shows that the base metal had a lower yield than that of the weld metal, which arises from the high yield-to-ultimate strength ratio in C-Mn weld metal, even though the ultimate strength of the weld metal was 25% below the base metal strength. On average the yield and ultimate stresses for the base metal and welds are given in the Table.

TABLE Base Metal and Weld Metal Yield and Ultimate Stresses

Material	Yield (MPa)		Ultimate (MPa)	
	longitudinal	transverse	longitudinal	transverse
A 516 Gr70	405	299	545	496
weld metal	363	321	410	420
twist wire	-	405	-	522

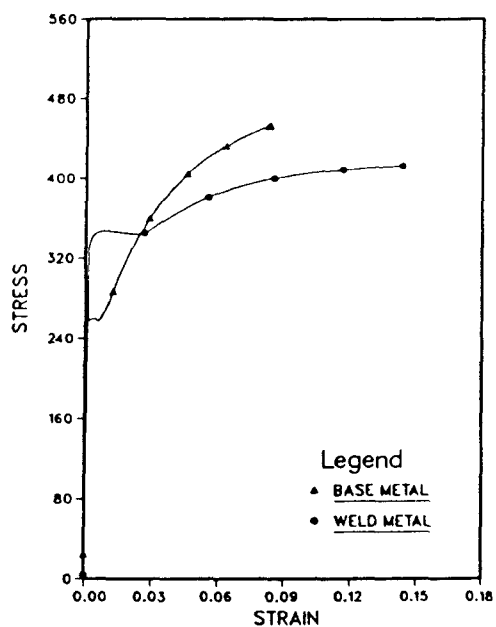


Fig. 1 Stress-strain curves of weld metal and base metal.

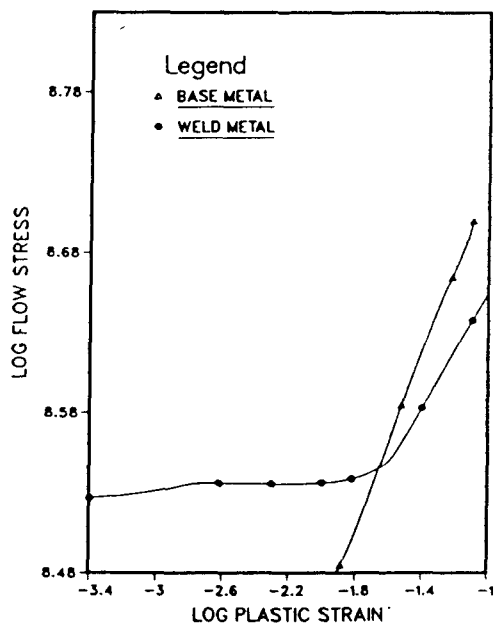


Fig. 2 Log flow stress vs log plastic strain for weld metal and base metal.

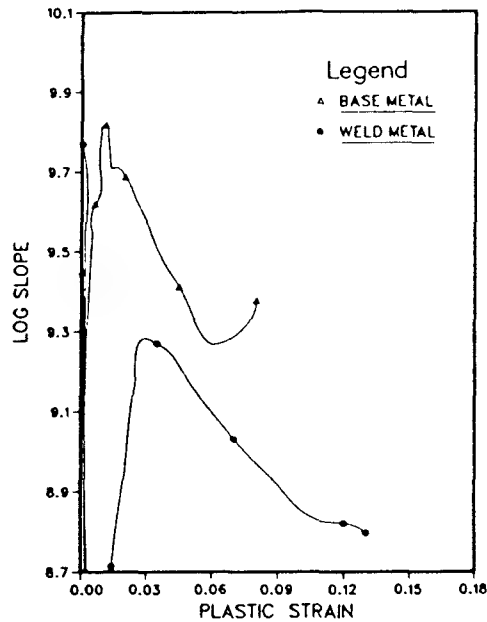


Fig. 3 Log slope of stress-strain curves vs plastic strain for weld metal and base metal.

Figures 2 and 3 illustrate the difference in the plastic strain behaviour between the base metal and the weld metals. It is seen that the base metal work hardens more than the weld metal as would be expected from the alloy content of the two metals. The work hardening rate, as shown in Fig. 3, indicates that the base metal had a peak log slope of 9.8 at a plastic strain of 1.0% whereas the weld metal had a peak log slope of 9.3 at a plastic strain of 3.0%.

A typical weld according to the ASME Boiler Code was obtained using a Kobe C-Mn twist wire. This weld was as strong as the base metal as required in the code. Figures 4 - 6 show the stress-strain behaviour of the "normal strength" weld for a gap of 13 mm. In Fig. 4 the strength of the base material (lower curve) was less than that of the weld material (upper curve) or across the weld as shown by the intermediate curve. These observations are amplified in Fig. 5 where the plastic flow stress was greater for the weld metal than that for the base metal. In Fig. 6 the degree of work hardening of the weld metal is seen to be 10.1 at a very low plastic strain which was greater than that for the base metal at approximately 9.8. It is also seen that as the plastic strain increased the slope for the weld metal fell more rapidly than it did for the base metal.

Similar graphs were plotted for the understrength narrow gap welds for which a typical set for the 13mm gap are shown in Figs. 7 - 9. Figure 7 shows that the base metal and weld metal yielded at 340 MPa and 330 MPa respectively. From Fig. 8 it is evident that the work hardening of the weld metal took place at a greater plastic strain than did the base metal but that log slope in Fig. 9 reached a peak of 9.55 indicating that the weld strength was approaching that of the base metal. For comparison, the peak log slope for the under strength weld metal for the 19mm gap weld tested was 9.4 and for the 25mm gap weld was 9.3, thus establishing the trend that as the weld gap decreased the degree of work hardening in the weld increased. Of course, part of this increase in weld strength as the gap narrowed

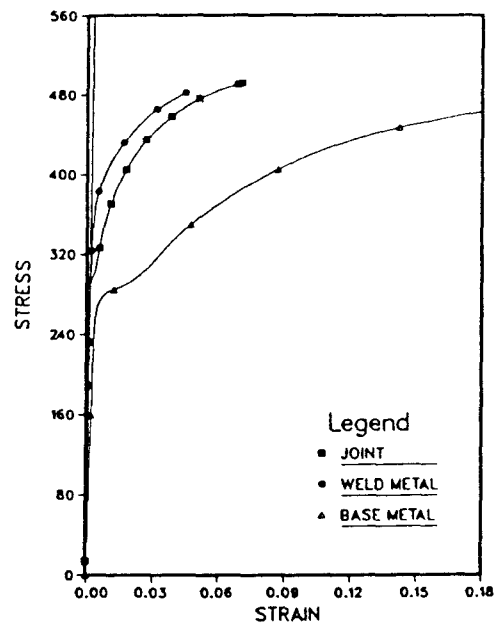


Fig. 4 Stress-strain curve for "normal strength" weld (twist-wire).

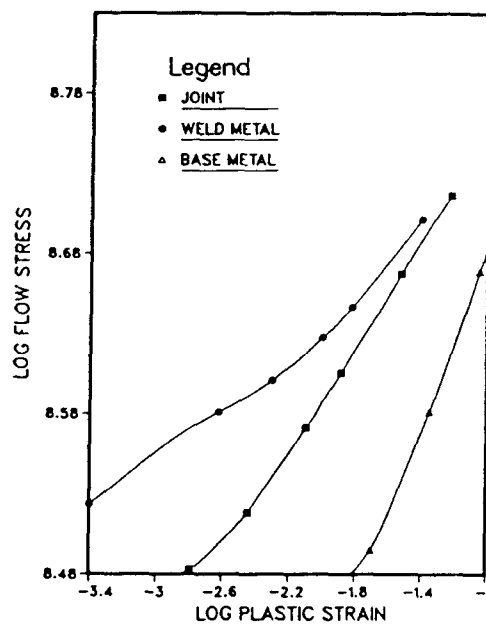


Fig 5. Log flow stress vs log plastic strain for "normal strength" weld (twist-wire)

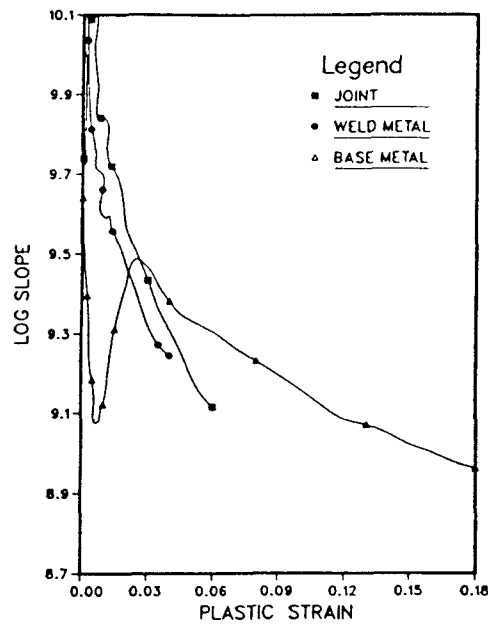


Fig. 6 Log slope of stress-strain curve vs plastic strain for "normal strength" weld (twist-wire).

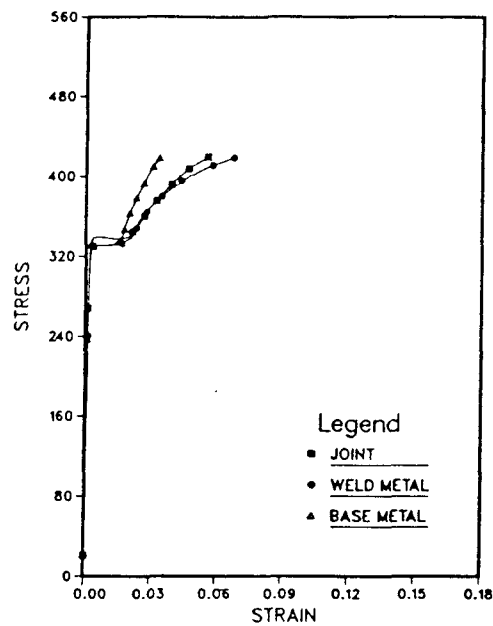


Fig. 7 Stress-strain curves for 13 mm narrow gap weld.

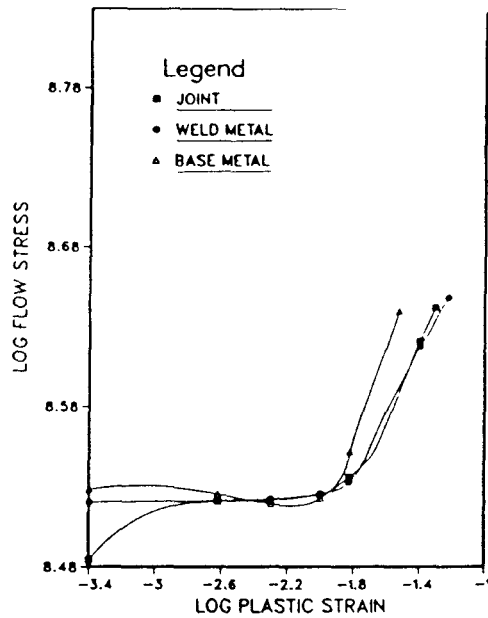


Fig 8. Log flow stress vs log plastic strain for 13 mm narrow gap weld.

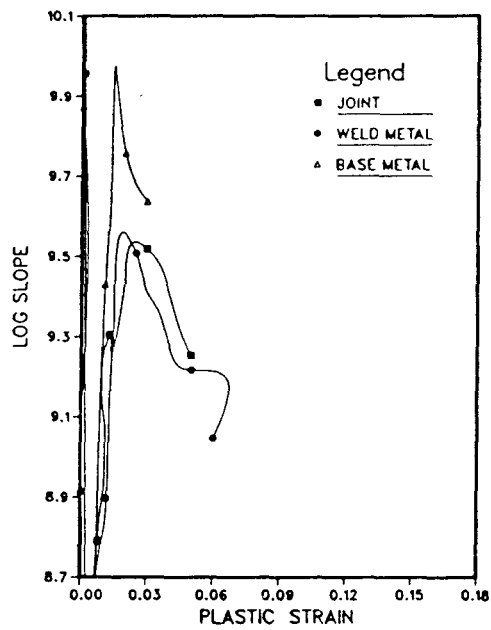


Fig. 9 Log slope of stress-strain curve vs plastic strain for 13 mm narrow gap weld.

can be attributed to dilution of the weld with the base metal, while the rest is due to the plastic constraint of the narrow gap weld metal imposed by the surrounding plate material.

The strength of the weld as a function of the aspect ratio has been plotted in Fig. 10. It is evident that as the gap of the weld decreased, for a given plate width, the ultimate strength of the weld increased and approached that of the base metal. The yield strength of the weld metal was relatively unaffected by changes in the aspect ratio.

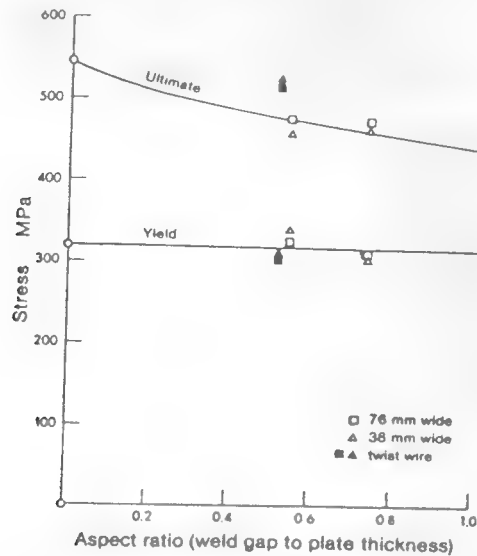


Fig. 10. Weld strength as a function of aspect ratio.

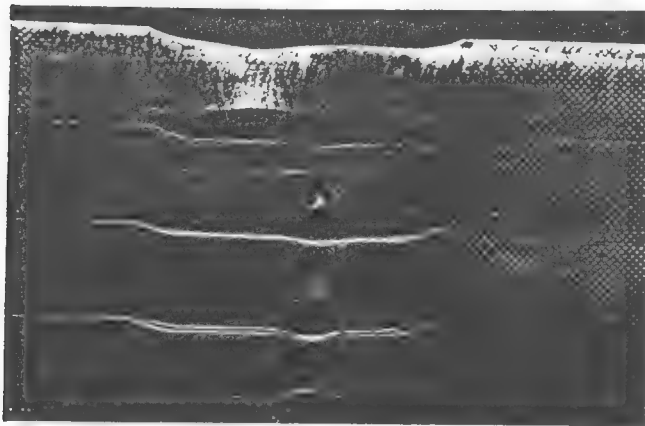


Fig. 11 Photograph showing pulled tensile specimens.

Although only two test specimen widths were evaluated, 38 and 76mm, in general there was an increase in strength of about three percent for the 76mm wide specimen compared with the 38mm wide specimen. This observation was consistent with that observed by Satoh and Toyada (1975) who reported that the strength of the weld increased up to a specimen width of five times the thickness and remained relatively constant for specimen widths greater than $5 \times t$.

A photograph of pulled welded tensile specimens is shown in Fig. 11. At the bottom of the photograph a weld gap of 25mm shows the yielding that took place in the weld whereas, as the two specimens above this show, as the weld gap narrowed the degree of yielding in the weld was decreased. For comparison, a "normal strength" weld is shown in the top picture where the base metal yielded whereas the weld retained its original shape.

CONCLUSIONS

While this paper presents the first step in a continuing program to investigate the feasibility of understrength narrow gap welds the initial results are encouraging. It was shown that the ultimate strength of the weld increased by eight percent as the aspect ratio was reduced from 1.05 to 0.55. Further improvements in weld strength are expected for aspect ratios less than 0.55 which implies that the benefits will be primarily associated with base metals of 50mm thickness or more. There is also scope for trials with a weld metal of intermediate strength between the present weld metal and the base material, e.g., with an ultimate strength drop of about 10 - 15% rather than the 25% achieved in this work.

ACKNOWLEDGEMENTS

The authors express their appreciation to Messrs. G. Lorimer, C. Bicknell and T. Sharratt who assisted in the experimental work. Appreciation is also expressed for the financial assistance from NSERC through grant 2705-A and from D.S.S. (E.M.R) through contract 14 SU. 23440-0-9197.

REFERENCES

- Grist, F.J. and F.W. Armstrong (1980). Welding Journal, 59 (6), 30.
- Kimura, S., I. Ichihara and Y. Nagi (1979). Welding Journal, 59 (7), 44.
- Malin, V.Y. (1983). Welding Journal, 62 (4), 22 and 62 (6), 37.
- Satoh, K. and Toyoda (1975). Welding Journal, 54 (9), 311.
- Satoh, K. and Toyoda (1979). Welding Journal, 58 (2), 26.
- Sawada, S., K. Hori, M. Kawahara, M. Takao and I. Asano (1979). Welding Journal 58 (9), 17.
- Wheatley, R.M. and R.G. Baker (1962). British Welding Journal, 9 (6), 378.

TUNDISH STREAM IMPROVEMENT USING WATER MODELS

Robert W. Pugh
Stelco, Inc.

Donald G. Bellow
University of Alberta

Presented at the 22nd Annual Conference of Metallurgists
in Edmonton, August 23, 1983

Paper No. 22.1

INTRODUCTION

The Stelco Edmonton Steel Works (ESW) shop produces steel in two 80 ton UHP arc furnaces which is cast on a single three-strand billet caster. The product mix is predominantly rebar and structural grades but some low alloy and special bar quality grades are made, notable AISI 1536 grade for oil-field sucker rods.

Varying surface and internal quality has been noted, especially on the more critical grades. One factor which influences surface and internal quality is stream shape. A smooth laminar stream picks up very little oxygen as it falls from the tundish to the mold and entrains very little air as it impacts into the steel in the mold (Figures 1 (a) and (b)). On the other hand, a ragged turbulent stream picks up and entrains more air giving more reoxidation products and worse surface and internal quality (Figures 2 (a) and 2 (b)). The main purpose of this study, which was initiated in 1979, was to determine what modifications could be made to the pouring system to ensure quiescent or laminar flow conditions in all the tundish streams. A second purpose was to provide a visual demonstration for operating personnel on the effect of various ladle and tundish conditions on stream shape.

The use of water models to evaluate fluid behaviour in steelmaking is well known and widely documented. Successful water models have been used in applications ranging from evaluating the flow characteristics in the casting of ingots to evaluating the effects of the use of baffles in the flow in tundishes. Because of the dimensional similitude between water and molten steel, the results observed from a water model are generally applicable to an actual steelmaking facility.

A full-scale water model of the E.S.W. three-strand tundish, mold and ladle pouring system was constructed at the University of Alberta and tested. As a result of the success of the studies on the three-strand tundish water model, and with a view to a possible plant expansion, a four-strand tundish model was constructed. This model was made with moveable interior walls so that a pouring box could be incorporated along with other tundish configurations and sizes.

This paper will describe some of the work carried out on the three and four-strand tundish models. Stream shape and air entrainment were determined from three photographs, each taken one second apart, of the stream and mold areas. For some studies, dye fluid and polyethylene chips were used to determine the flow into the nozzle wells.

THREE-STRAND TUNDISH

The three-strand tundish configuration was simulated complete with ladle and slide-gate, plexiglass tundish and nozzle wells and plexiglass mold boxes (Figure 3). The system was designed as a closed loop with the water from the mold boxes returned to the ladle by means of a pump. Valves, located on the bottom of each mold box, enabled the liquid level in the mold box to be set and maintained at an appropriate level. The slide gate was calibrated and monitored with a LVDT which allowed for a precise level to be set in the tundish.

The initial trials were carried out to determine the effect of operating conditions (eg., ladle steel level, tundish steel level, ladle nozzle position, etc.) on stream shape. It was found that high tundish levels (~ 400 mm) gave the worst stream shape. Any condition which caused turbulence in the tundish (eg., ladle stream flowing) worsened stream shape. With a quiescent tundish, smooth streams would develop but vortexes often occurred over the nozzles causing materials floating on the surface, such as slag, to be drawn into the stream even when there was a reasonable level of liquid in the tundish (see Figure 4). In most cases, the vortex developed first over the strand 3 nozzle (farthest from the steel entry point into the tundish) but could occur over all three nozzles when the ladle flow was shut off. The problem was to improve stream shape and also to prevent the formation of vortexes.

Because of the effect of both tundish and ladle metal level on stream shape, all subsequent tests were run with either a 400 mm tundish level and 0.6 m ladle level or a 160 mm tundish level with a 2.75 m ladle level.

A number of different configurations were tried in an attempt to improve the flow out of the nozzles. Some of the changes made in the ladle stream entry area included solid-shrouded ladle streams, solid and perforated pouring basins (see Figure 5), solid, perforated (see Figure 6), and V-notched weirs in front of the pouring box, and air curtains across the front of the pouring box. Changes made in the tundish area itself included air curtains around nozzles, X and star vanes in the nozzles, tubes and castellations above nozzles, modified well shape and modified tundish volumes. Some of the configurations produced encouraging results and, as shown in Figures 7 (a) and (b), some produced discouraging results:

From all of the results, it was apparent that weirs, dams, etc. could all lead to some improvement in flow out of the nozzles although the degree of improvement was, at times, difficult to quantify. What was quite evident, however, was that in order to obtain quiescent flow out of the nozzles, the flow into the nozzle wells had to be orderly. Figure 8 shows schematically what type of flow can occur upstream of the nozzle. In this case, as was observed using a dye penetrant, the main flow entered the nozzle well predominantly from one side. When this occurred the flow out of the nozzle was erratic and turbulent. On the other hand, when the flow was caused to enter the nozzle well in a symmetrical radial fashion, then the flow out of the nozzle was always quiescent and laminar in appearance.

During these trials, a novel method of streamlining flow into the nozzle was developed. Details of this method are not being disclosed because of an impending patent. Tests with "flow streamliners" were carried out on the water model under a variety of casting conditions. As shown in Figures 9 (a) and 9 (b), without the "flow streamliner", tundish stream shape was ragged and large amounts of air were entrained in the mold. With "flow streamlining" (Figures 10 (a) and (b)) for the same tundish conditions, the tundish stream was smooth and minimal amounts of air were entrained. In all cases, the "flow streamliner" improved stream shape and reduced the amount of air entrained. In addition, streamlining the flow prevented swirling and the development of vortexes in the liquid above the nozzles under quiescent tundish conditions.

FOUR-STRAND TUNDISH

Thermal stresses can lead to tundish distortion, especially if the tundish is long or an irregular shape. In contemplation of a future plant expansion, a four-strand tundish was built for water model experimentation to determine the effect of shape and size of flow characteristics out of the nozzles. A tundish with best stream shape and minimal thermal distortion was desired.

A general view of the completed four-strand tundish model is shown in Figure 11. On a plan view, it was rectangular in shape but adjustable interior walls allowed a variety of tundish configurations to be tried as shown in Figure 12. The small x marks the point where the ladle flow entered the tundish. As can be seen from the slide, both wide and narrow tundishes were evaluated including one where the back walls were angled forward as shown in Configuration B. Configuration A was just a large rectangular shape whereas Configuration C had side walls preventing the flow from the ladle being directed into the nozzle boxes on strands 2 and 3. In Configuration C₂, the flow from the ladle was directed back to the rear wall. Configuration D was a narrow tundish without a pouring box and Configuration E was a narrow tundish with a pouring box. This latter configuration was similar in shape to the three-strand tundish except the flow from the ladle was directed symmetrically between strands 2 and 3.

As might be expected, making changes to the shape of the tundish were not easily detected in changes to the flow characteristics out of the nozzles. Generally speaking, however, the large tundish shape appeared to provide more quiescent flow conditions out of the nozzles than when the tundish was narrow. This was true even in the case where a pouring box had been added to the narrow tundish. It was also observed that angling the rear walls inwards had some beneficial effects on the downstream side. Also, it was found that placing guard walls or baffles out from the front wall of the tundish, as in Configuration C, provided improvement in the flow downstream of the nozzles.

Trials were also carried out on all tundish configurations using the "flow streamlining" method mentioned earlier. In all cases improved stream shape and reduced air entrainment were observed (see Figures 13, 13 (a) and 14, 14(a)). Thus the design of the four-strand tundish is simplified significantly. The main criteria is minimal thermal distortion; stream shape can be controlled by the use of "flow streamliners".

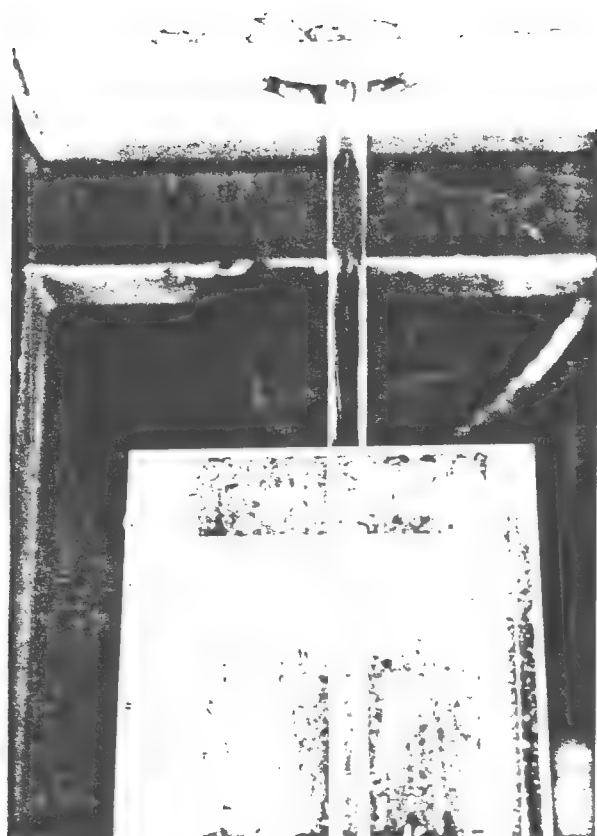
PLANT TRIALS

The ultimate test of any water model development is plant trials with steel as the casting medium. Plant trials were carried out in 1982 with the "flow streamliner" placed in strand 1 of the three-strand tundish. This strand consistently had a worse stream shape than strands 2 and 3 in the water model trials and in plant operation. With the "flow streamliner" in place, the stream shape on strand 1 (see Figure 15) was better than the other strands (see Figure 16 of strand 2). This improved stream shape was noted in all trials carried out to develop material and installation practices for the

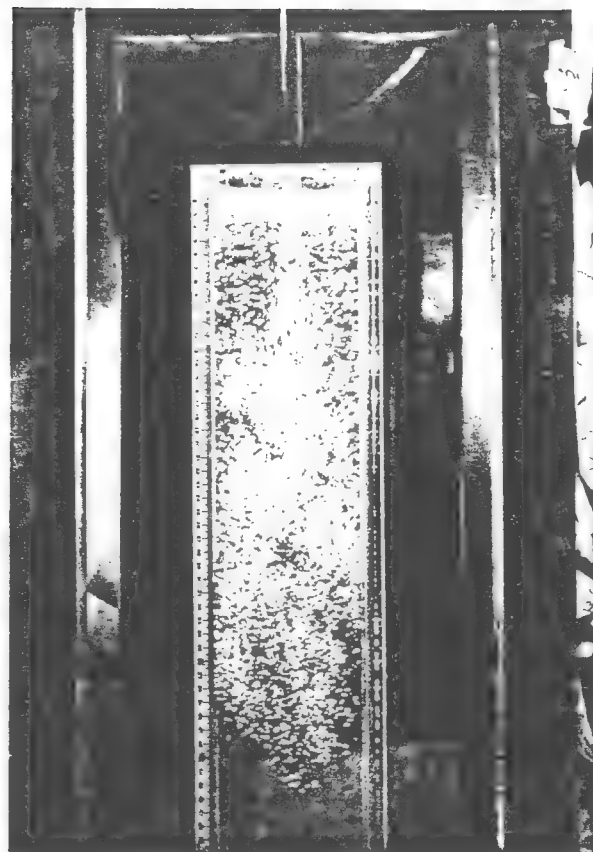
"flow streamliner". At the present time, the device will survive single and two heat casts. Further work is underway to ensure survival on multiple heat casts and to document the difference in cleanliness level between strands cast with the "flow streamliner" and strands cast without the "flow streamliner".

CONCLUSIONS

Water model studies of a three and four-strand steel casting system have been carried out. From visual observations of the tundish stream shape and mold box air entrainment level for a variety of casting configurations it has been noted that tundish stream shape is strongly affected by flow conditions just ahead of the tundish nozzle. This has been used on the water model to develop a "flow streamlining" process which improves tundish stream shape and reduces mold box air entrainment level for any tundish configuration. This process also reduces the tendency for vortexing and slag entrainment above the tundish nozzles. The process is currently being adapted for use in the three-strand steel plant tundish.



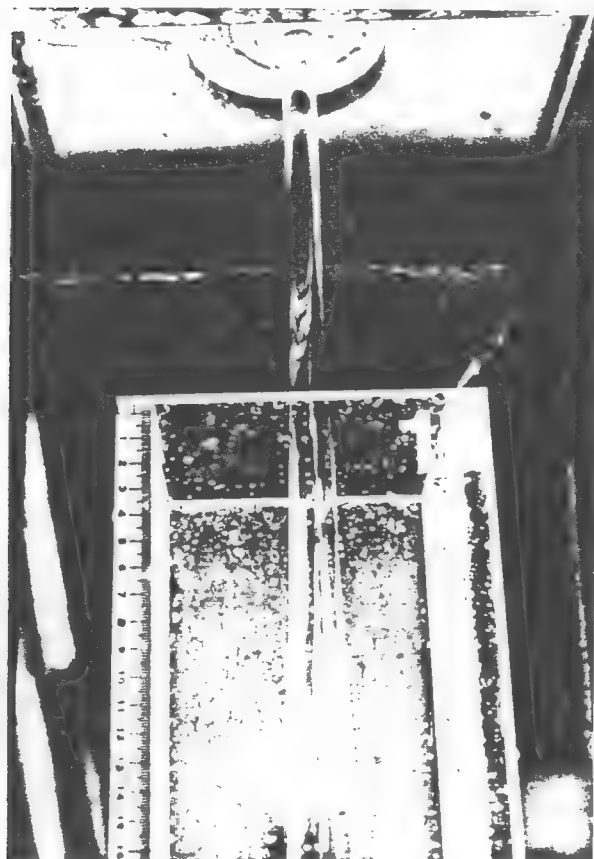
STREAM



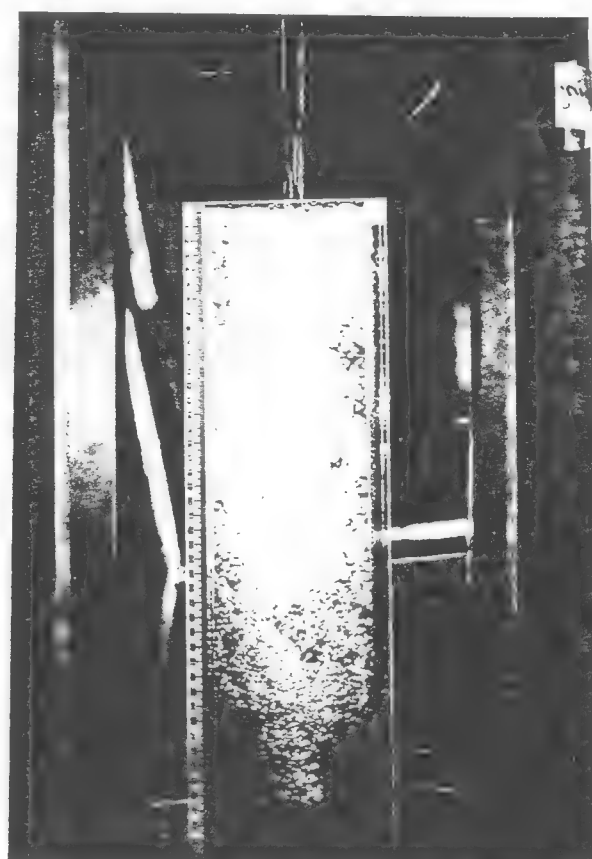
MOLD

FIGURE 1A & 1B

SMOOTH LAMINAR STREAM ENTRAINS VERY LITTLE AIR IN MOLD



STREAM



MOLD

FIGURE 2A & 2B

RAGGED, TURBULENT STREAM ENTRAINS MORE AIR IN MOLD

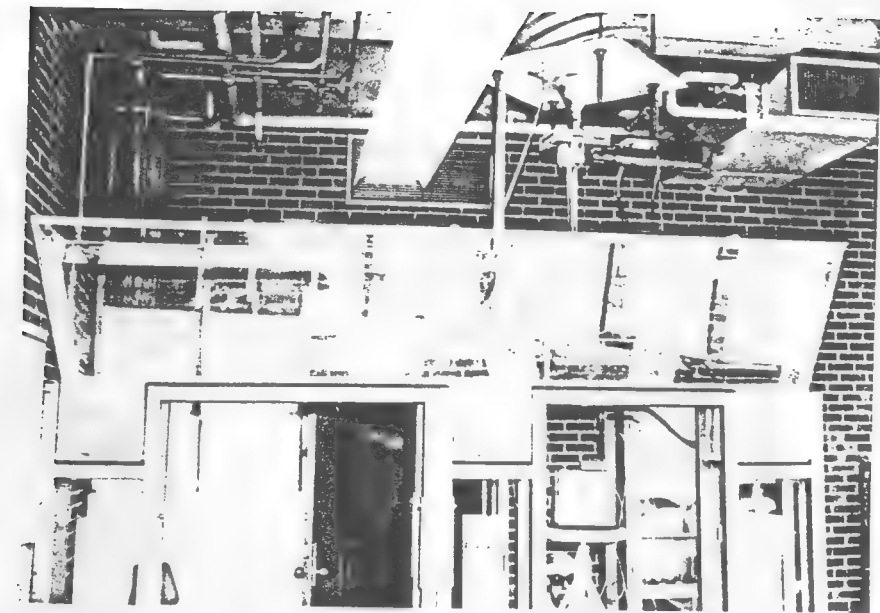


FIGURE 3 THREE STRAND TUNDISH WATER MODEL



FIGURE 4 VORTEX DEVELOPED IN A QUIESCENT TUNDISH

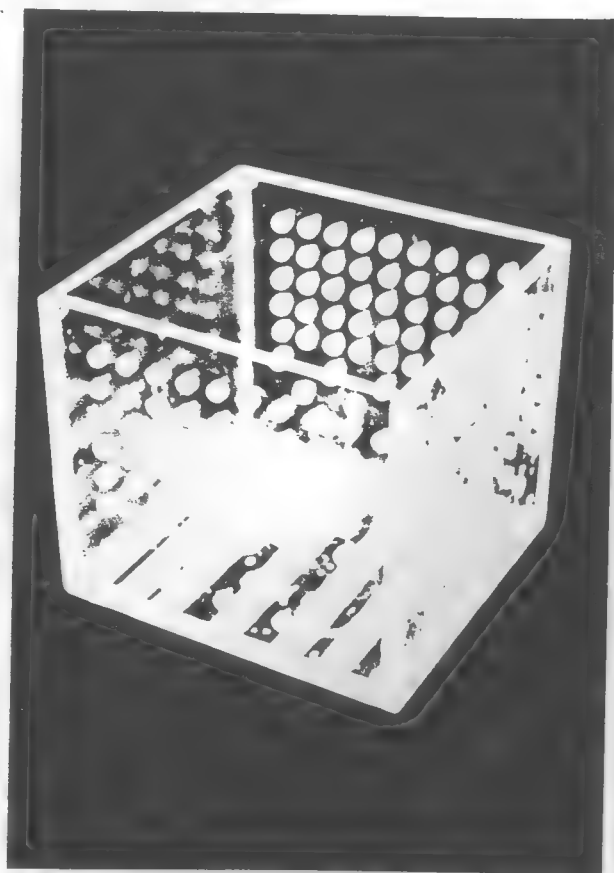


FIGURE 5 PERFORATED POURING BASIN

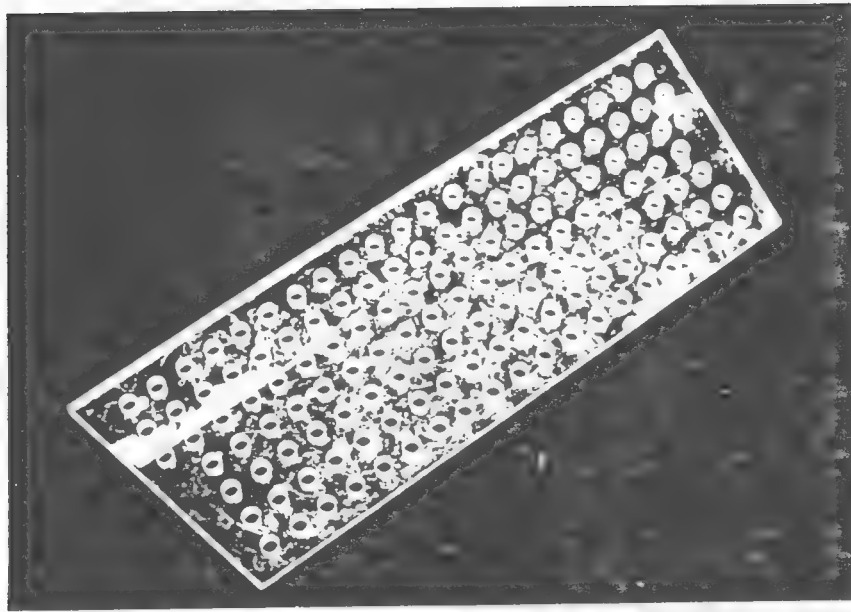
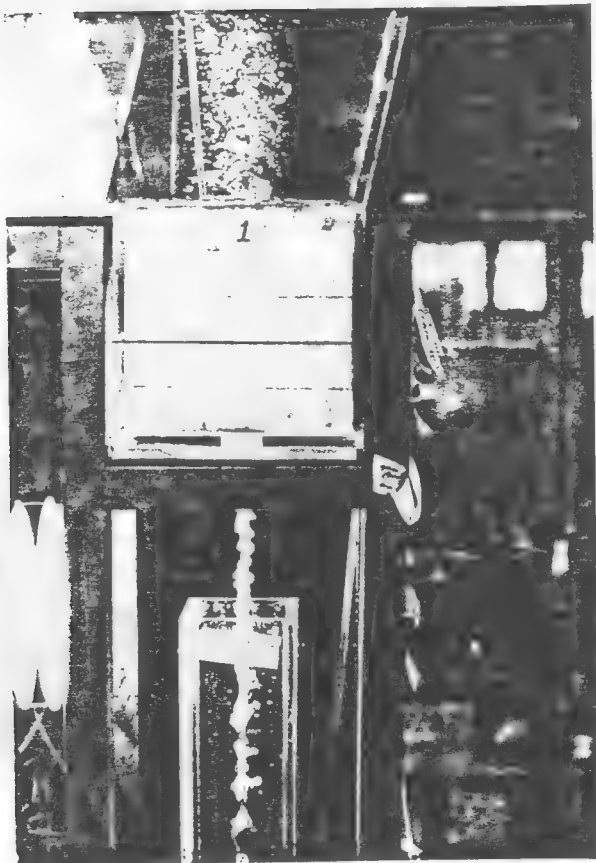
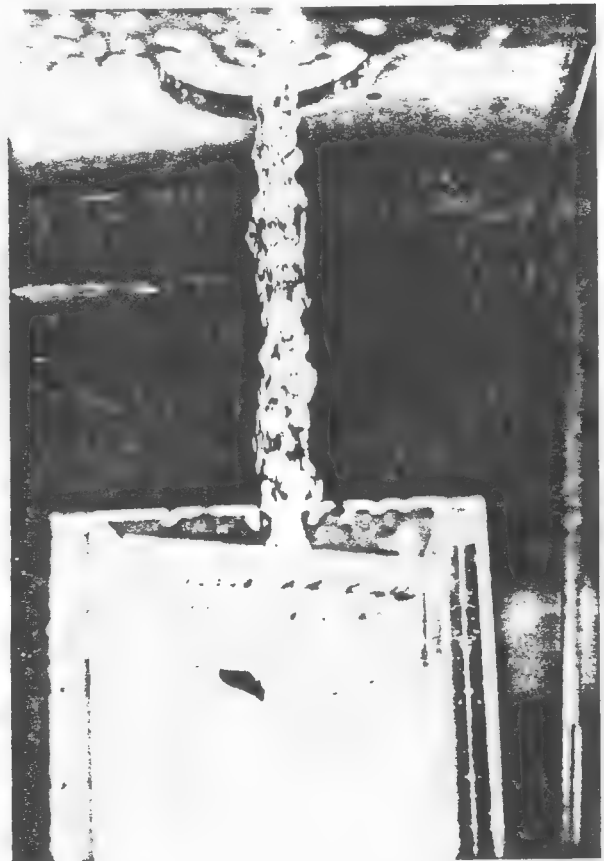


FIGURE 6 PERFORATED WEIR USED IN FRONT OF POURING BOX



STREAM



MOLD

FIGURE 7A & 7B

EFFECT OF AIR CURTAIN ON STREAM SHAPE AND AIR ENTRAINMENT IN MOLD.

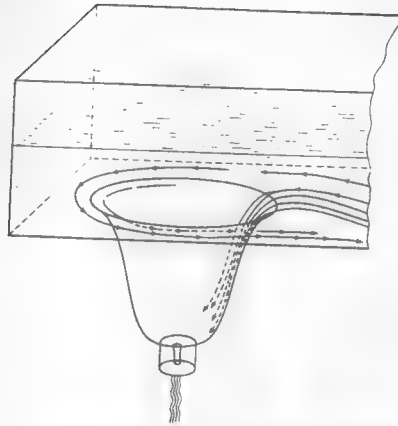


FIGURE 8 SCHEMATIC OF FLOW PATTERN AT ENTRANCE TO NOZZLE BOX



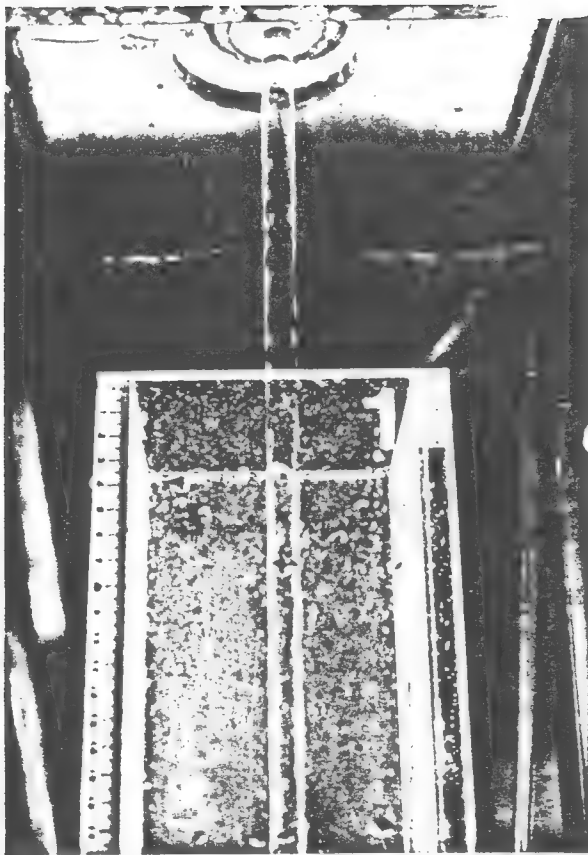
STREAM



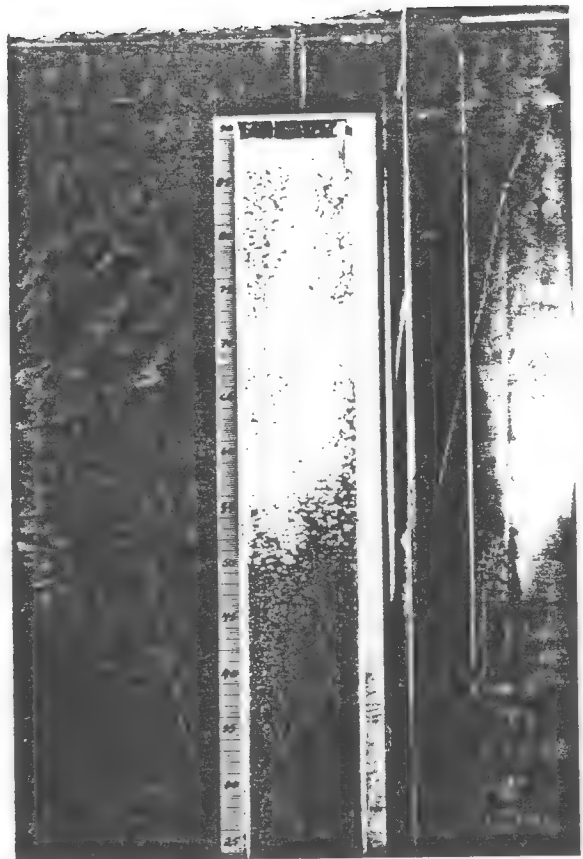
MOLD

FIGURE 9A & 9B

STREAM SHAPE AND AIR ENTRAINMENT WITHOUT "FLOW STREAMLINER",
ON THREE STRAND TUNDISH



STREAM



MOLD

FIGURE 10A & 10B

STREAM SHAPE AND AIR ENTRAINMENT WITH "FLOW STREAMLINER",
ON THREE STRAND TUNDISH

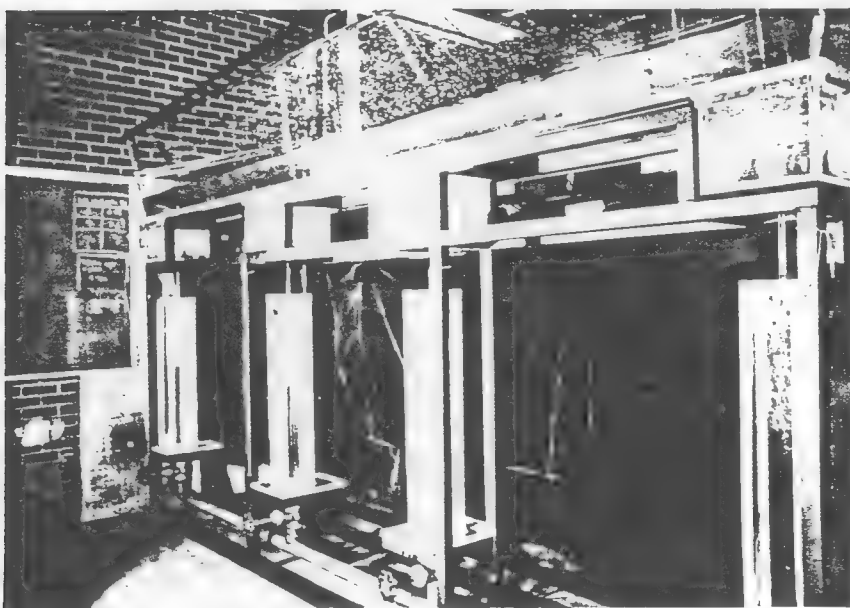


FIGURE 11

FOUR STRAND TUNDISH WATER MODEL

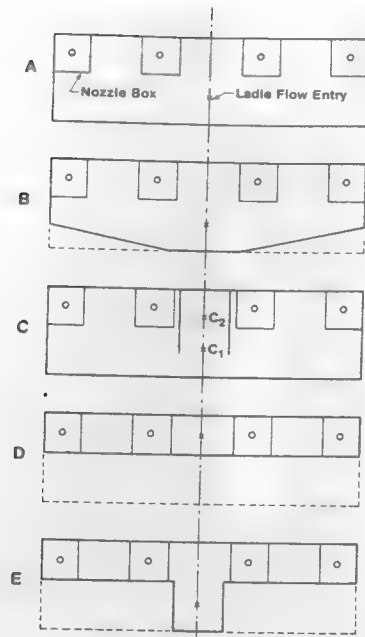
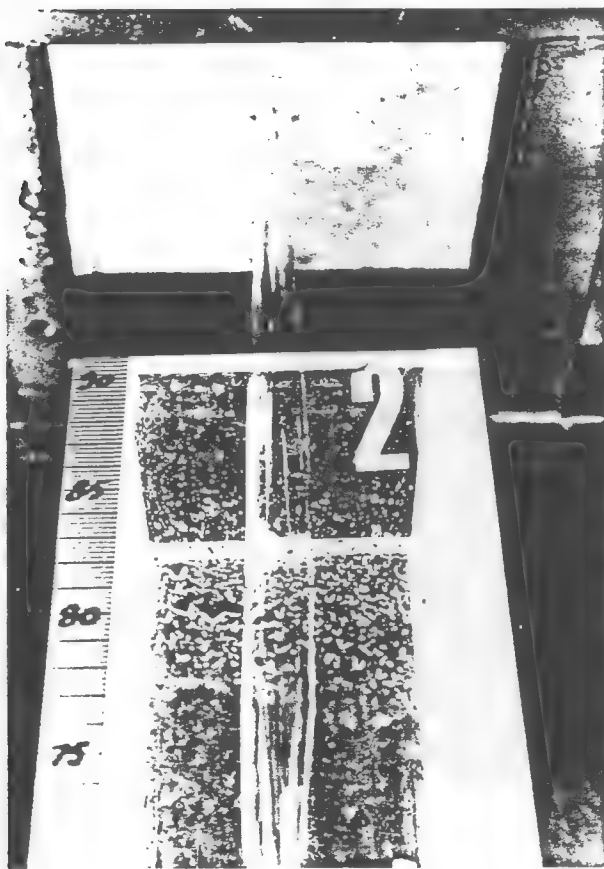
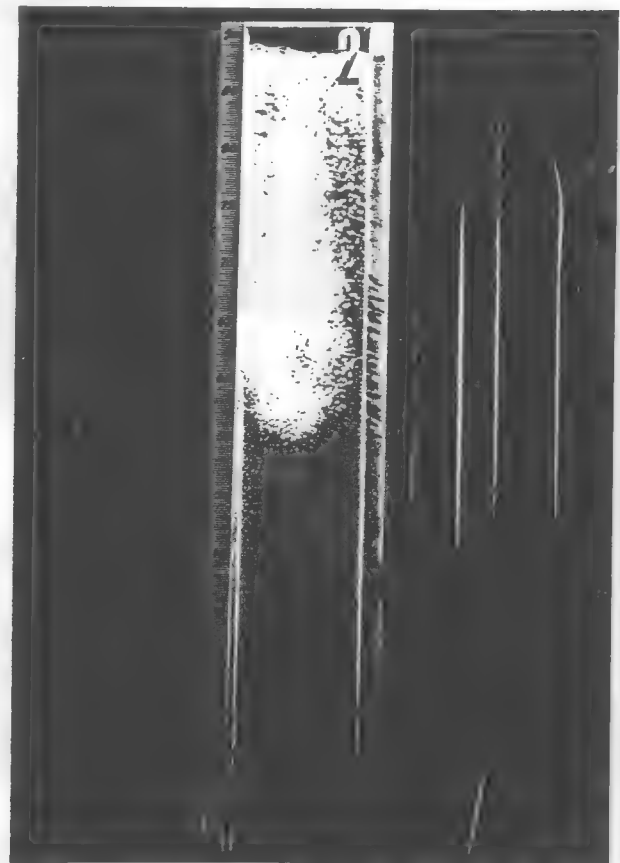


FIGURE 12 FOUR STRAND TUNDISH CONFIGURATIONS

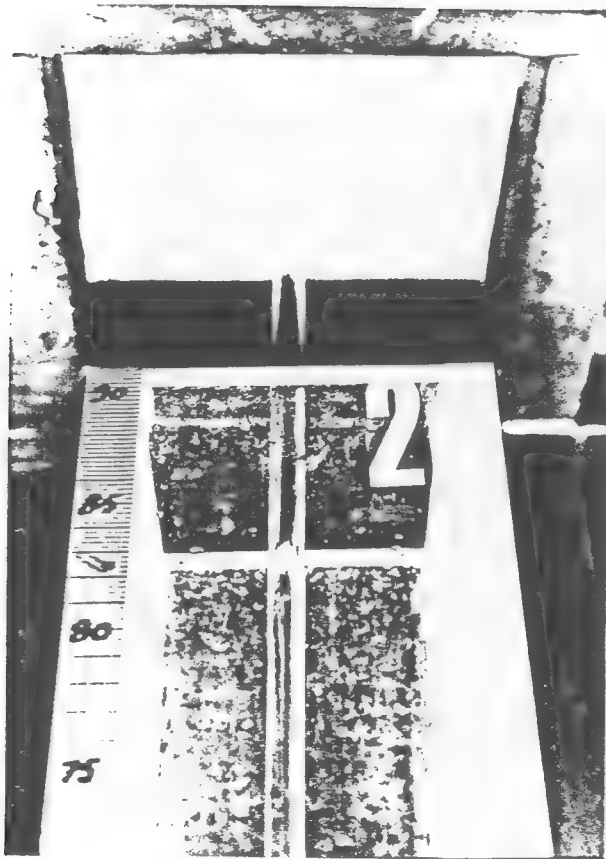


STREAM



MOLD

FIGURE 13a & 13b STREAM SHAPE AND AIR ENTRAINMENT WITHOUT "FLOW STREAMLINER" ON FOUR STRAND TUNDISH.



STREAM



MOLD

FIGURE 14A & 14B

STREAM SHAPE AND AIR ENTRAINMENT WITH "FLOW STREAMLINER" ON FOUR STRAND TUNDISH.

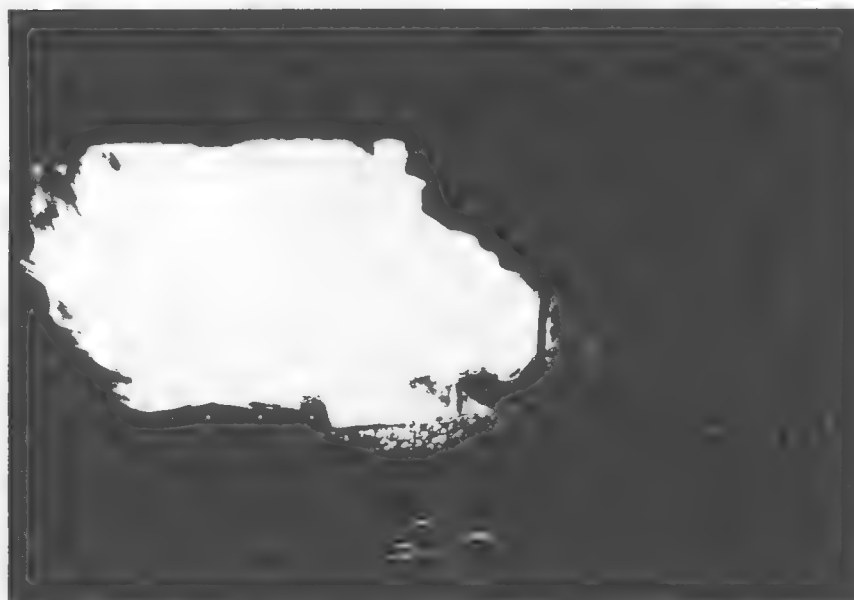


FIGURE 15

STREAM ON STEELPLANT TUNDISH WITH "FLOW STREAMLINER"

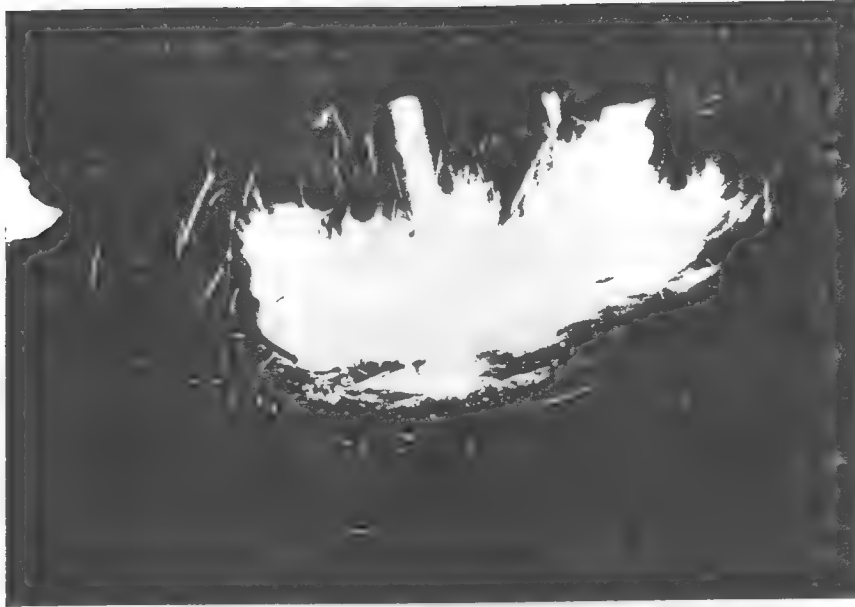


FIGURE 16 STREAM ON STEELPLANT TUNDISH WITHOUT "FLOW STREAMLINER"



Consumer and
Corporate Affairs Canada

Consommation
et Corporations Canada

(11) (A) No. **1 180 532**

(45) ISSUED 850108

(52) CLASS 22-57

(51) INT. CL. ³B22D 11/10

(19) (CA) **CANADIAN PATENT** (12)

(54) Tundish Plate for Stream Shaped Control

(72) Bellow, Donald G.;
Pugh, Robert W.,
Canada

(73) Granted to Stelco Inc.
Canada

(21) APPLICATION No. 411,316

(22) FILED 820913

No. OF CLAIMS 19

Canada

TUNDISH PLATE FOR STREAM SHAPE CONTROL

10 This invention relates generally to the casting industry, and has to do particularly with an improvement applicable to tundishes for use in the continuous casting of steel.

BACKGROUND OF THIS INVENTION

15 In the continuous casting of steel, especially billet casting, the shape of the tundish stream has a strong effect on the surface quality of the billet, the internal quality of the billet, and caster performance. A tundish stream that swirls or breaks up into droplets
20 between the tundish and the mold will entrain more air and lead to increased slag patches on the surface of the billet and inclusions in the interior of the billet. Either of these could cause increased quality rejects. In addition, increased slag quantities on the billets
25 leads to higher breakout frequency. The slag patches reduce heat transfer in the mold, causing thinner shells which are unable to support the weight of the liquid steel core. Such breakouts reduce productivity and increase maintenance costs.

30 In addition, a wildly swirling tundish stream can cause further casting difficulties, particularly on smaller billet sizes. The metal can hit either the mold wall or the top of the mold and solidify, requiring termination of the cast, and again resulting in reduced
35 productivity and increased maintenance costs. Swirling of the stream can occur under a variety of operating conditions. It is strongly affected by any action which causes movement in the liquid above the tundish nozzle. For example, when the ladle nozzle is opened fully to

bring up the level in the tundish, the tundish streams swirl appreciably, especially the stream closest to the steel entry point in the tundish. This swirling tends to be worse when the liquid level in the tundish is higher.

5 Another problem in continuous casting is the entrainment of slag. At lower tundish levels, especially under very quiet tundish conditions (the same type that gives very good stream shape), vortexes form above the nozzle and entrain slag into the casting stream. This
10 can give either large surface slag patches on the billets, large internal inclusions, or in some cases a change in steel chemistry by reversion of elements in the slag (e.g., MnO reverting to Mn in the steel).

Ceramic shrouds have been developed in order to
15 contain the metal stream to ensure that it hits the desired area in the mold. However, ceramic shrouds have several disadvantages. They do not allow access to the casting stream (for shut-off or lancing in the case of blockage), they are difficult to install, their use is
20 restricted to the larger billet sizes (because of clearance between outside and the mold wall), and special startup practices are often required to clear the skull that forms on the outside and can bridge the gap between shroud and mold wall. In addition, such shrouds make it
25 more difficult to control the level of steel in the mold.

Other systems are available to prevent or restrict stream oxidation. All of these involve the use of an inert gas around the casting stream. All require equipment fitted on the mold or tundish to feed or
30 contain the gas around the tundish stream and, as such, interfere to some extent with access to the stream. Also, because gas is involved, air flow in this area (often used to remove fumes) must be controlled.

Devices are known which reduce vortexing and
35 slag entrainment, these being gas-purged porous nozzles. However, their use tends to produce worse stream shape.

GENERAL DESCRIPTION OF THIS INVENTION

In view of the foregoing discussion, it is apparent that it would be desirable to achieve a

streamlined shape for a tundish stream, without swirling or break-up, while at the same time reducing vortexing and slag entrainment in the tundish. By reducing swirl and break-up, stream oxidation will be restricted.

5 It is therefore an aspect of this invention to provide a device for use with a tundish, and a process utilizing this device, which will produce a tight, smooth tundish stream that enters the mold in a small area and reduces breakout frequency in the billet.

10 A further aspect of this invention is to obtain a minimum of reoxidation in the stream or by air carried into the steel where the stream hits.

 A still further aspect of this invention is to reduce the amount of slag entrained in the casting stream
15 by vortexing in the tundish.

 In general terms, this invention consists in providing a plate with a number of holes or perforations, the plate being positioned in the path of the molten metal as it moves from the tundish to the nozzle at the
20 bottom of a nozzle well. Preferably, the plate is located at the top of each nozzle well.

 From tests reported below in this specification, it can be concluded generally that the plate acts as a kind of barrier separating the liquid
25 conditions in the tundish from those in the well. Its presence inhibits the formation of a tundish vortex under quiet tundish conditions, and shields the well from disturbance under agitated tundish conditions. As the liquid metal passes through the holes of the plate, some
30 slight agitation immediately below the plate can be expected to occur, but such agitation appears to settle into laminar flow as the liquid nears the nozzle.

 More particularly, this invention provides a continuous casting process for metal, including several
35 steps. The molten metal is teemed into a tundish, and then passed into a nozzle well and toward a nozzle at the bottom of the well. During its passage from the tundish to the nozzle, the molten metal is passed through a perforated plate located above the nozzle, thereby to

promote laminar flow below the plate. Finally, from the well, the molten metal is passed through the nozzle to form a stream entering a continuous casting mold.

This invention further provides a perforated
5 plate for use with an apparatus for the continuous casting of metal. The apparatus comprises a tundish having at least one nozzle well with a nozzle at the bottom of the well, and a continuous casting mold into which molten metal can stream from the nozzle. The
10 perforated plate is positioned in the path of molten metal passing from the tundish to the nozzle, but is spaced above the nozzle, whereby the molten metal must pass through the plate perforations to reach the nozzle.

In a preferred embodiment, the plate has at
15 least six holes and is located substantially at the top of the well. The plate must retain its strength and erosion resistance at molten metal temperatures.

GENERAL DESCRIPTION OF THE DRAWINGS

Five embodiments of this invention are
20 illustrated in the accompanying drawings, in which like numerals denote like parts throughout the several views, and in which:

Figure 1 is a sectional view through a tundish and continuous casting mold with the plate of this
25 invention in place;

Figure 1a is a partial sectional view through a tundish without a plate, showing a vortex in the liquid steel;

Figures 2 through 6 show five preferred
30 embodiments of this invention;

Figures 7 through 9 show configurations which were also tested; and

Figure 10 is a section through a conventional wafer nozzle.

35 DETAILED DESCRIPTION OF THE DRAWINGS

Attention is first directed to Figure 1, which shows a tundish 10 having side walls 12, end walls 13 and 14, a bottom wall 16, a well 18, and a nozzle 20 at the bottom of the well 18. The tundish contains molten steel

(or other molten metal) 22 up to a level identified by the numeral 24, and a layer of slag 26 is located above the level 24. In some situations, the slag layer may be thin or non-existent. The inside wall 29 of the well 18
5 defines a well chamber through which the molten metal passes in moving from the tundish to the nozzle 20.

Located below the well 18 is a continuous casting mold 30 having cooling chamber 32 for cooling water or the like. As can be seen in Figure 1, a stream
10 33 carries molten steel downwardly from the nozzle 20 to the mold 30.

In the continuous casting process, the billet 36 is formed on a continuous basis, and continuously moves downwardly from the mold 30. As it does so, it
15 gradually solidifies from the outside inwardly, so that the solidified side "wall" of the billet gradually thickens as it moves downward from the mold 30. The gradually thickening wall is identified by the numeral 38 in Figure 1.

20 Dissolved in the steel are elements (deoxidizers) designed to combine with the oxygen which comes out of solution as the steel solidifies. With a swirling or broken up stream, these elements will combine with the oxygen in the air that is either around the
25 stream or entrained in the mold as the stream penetrates, leading to excessive quantities of slag (e.g., MnO , SiO_2 , etc.). This slag can either float to the top of the steel in the mold and form a layer 40 or be entrapped in the solidifying steel shell. The layer
30 of slag on the top of the steel can lead to either breakout problems or surface quality problems as it solidifies against the continuous casting mold. The slag entrapped in the solidifying steel shell leads to worsened internal quality.

35 Attention is now directed to Figure 1a, which illustrates two of the typical problems encountered with the continuous casting process for steel. In Figure 1a, it is seen that the stream 33a tends to flare outwardly

as it descends, thus entraining air into the steel and leading to the problems discussed earlier.

Within the tundish 10 in Figure 1a, the steel 22 has begun to form a vortex 42 above the nozzle 20, and as a result of this vortex slag in the slag layer 26 is being drawn downwardly and into the steel stream 33a.

It should be pointed out that these two problems, while illustrated simultaneously in Figure 1a, do not necessarily occur together in prior art processes.

Returning to Figure 1, it will be seen that, in accordance with this invention, a plate 44 having a plurality of holes 46 is provided in the path of steel moving from the tundish to the nozzle 20. More particularly, the plate 44 is located substantially flush with the bottom of the tundish 10, and at the top of the chamber defined by the internal wall 29 of the tundish well 18.

TEST DATA

In order to evaluate the following plate conditions with a view to determining the characteristics of an optimum perforated plate, a program of water model simulation tests was carried out at the University of Alberta. It is well understood that water model simulations can provide useful data from the evaluation of systems designed for other liquids. By using a full size model, the Reynolds number and Froud number are substantially the same for the two systems. The key term in these expressions is kinematic viscosity (absolute viscosity \div density). The kinematic viscosity of steel and water is about the same. Since the viscosity of most liquid metals is close to that of liquid steel, any metals whose density is similar to steel (e.g., copper, tin, zinc, etc.) should also show the improvement noted for water.

Figures 2 through 9 illustrate various plate configurations which were tested. The main plate characteristics under investigation were the following:

1. Plate Location

2. Plate Thickness
3. Hole diameters
4. Number of Holes
5. Hole arrays

5 Some of the testing involved wafer nozzles, for which a word of explanation is in order.

 Attempts in the past to use strong deoxidizers such as aluminum have led to nozzle blockage problems. A wafer nozzle (seen in axial section in Figure 10) will
10 pour aluminum deoxidized steels but gives much poorer stream shape than regular nozzles. This leads to a worsened condition with respect to slag formation because of the high affinity of aluminum for oxygen. It was decided to test a wafer nozzle in combination with
15 different hole arrays, hole diameters and plate thicknesses for a perforated plate, to determine whether the combination could improve the flow characteristics out of a wafer nozzle.

 In selecting which plate configurations were to
20 be evaluated, certain factors were kept in mind. Firstly, shop practice required the plates to have a centre hole which is 1 1/8 inch diameter or larger. Also, because of possible strength limitations in the proposed plate material, as few holes as possible should
25 be used. The spacing of holes could well be critical to the life of the perforated plate in practice. In addition, the plate would be more likely to be 1 1/2 inch thick in practice, especially if it were intended to extend the existing fibre liner board over the nozzle
30 well. Finally, it was decided to evaluate the performance of the plate when located some distance down into the nozzle well, as well as at the top of the well.

 In the material below, each of the investigated characteristics are dealt with in separate sections, and
35 at the end of each, appropriate conclusions are drawn.

A. Effect of Plate Location in the Nozzle Box

For these tests it was necessary to reduce the number of holes in the plates so that, in all plate
5 locations, all holes would function.

Four different hole arrays were evaluated, and the plates were placed both flush with the bottom of the tundish, and about 4 inches (10 cm) below the bottom of the tundish. The observations follow.

10 a) Four 1 inch holes, $\frac{1}{4}$ inch plate

It was observed that the four hole configuration yielded very poor flow conditions downstream of the nozzle. Conditions were worse at a tundish head of 42 cm, and were also worse when the plate was placed
15 4 inches closer to the nozzle. The hole array was that shown in Figure 7.

b) Five 1 inch holes, $\frac{1}{4}$ inch plate

The hole array for this test was that shown in Figure 8. For this test, it was observed that the flow was quite erratic with the flow conditions worse at a
20 tundish head of 42 cm, and also worse with the plate placed 4 inches down into the nozzle well.

c) Six 1 inch holes with hole plugged, $\frac{1}{4}$ " plate

This test used the plate shown in Figure 9. The plate had a circular six hole array, with the centre hole plugged. It was observed that the flow downstream of the nozzle was poorer with the plate
25 placed 4 inches closer to the nozzle, and also that the flow was more erratic at a tundish head of 42 cm. In comparing the two different five hole arrays (one including a centre hole), it would appear that, with the plates flush with the bottom of the tundish, the flow conditions were somewhat improved with the array having no hole in the centre. A second comparison
30 was made between a six hole array as illustrated in Figure 2 and the six hole array illustrated in Figure 3. Here again it was seen that the plate with no centre hole showed some improvement in downstream
35 flow conditions.

d) Six 1 inch holes and effect of plate location

It was noted that the downstream flow conditions worsened when the plate was placed closer to the nozzle. However, the six hole plate exhibited better downstream flow conditions than the five hole plate, although none of these flow conditions could be considered ideal, nor were they as good as were achieved with the use of more holes.

Conclusions

The placing of the perforated plate in the nozzle well below the bottom of the tundish tended to produce poor downstream flow conditions out of the nozzle. Four, five and even six hole plate configurations produced poorer downstream flow conditions than plates with a greater number of holes. For a five hole plate, the downstream flow conditions were somewhat improved if there was no centre hole in the array. Also, for six 1-inch holes, the downstream flow conditions were better when the plate had no centre hole. It would be expected that the presence or absence of the centre hole would have less of an effect as the number of holes in the plate increased.

B. Effect of Plate Thickness

For this evaluation, plate thicknesses of 2, 1½, 1 and ½ inches were tested using 6, 7 and 9 one-inch diameter holes. These plate configurations are shown in Figures 3, 4 and 5.

a) Six hole plate, circular array, no centre hole

At a 16 cm tundish head, the flow characteristics of the stream out of the nozzle all appeared about the same regardless of which plate thickness was used. The streams appeared to be somewhat ragged but none was wildly splaying. The density and penetration of the air bubbles all appeared to be the same. Thus, at a 16 cm tundish head the effect of plate thickness

in the range from 0.5 inches to 2 inches appeared to be insignificant.

At the 42 cm tundish head, there was an increase in erratic flow patterns for all plate thicknesses

- 5 evaluated with perhaps less turbulence noted for the $\frac{1}{2}$ and 1 inch plates than for the other two thicker plates. Changing the plate thickness did not seem to alter the depth of bubble penetration into the mold box.

- 10 b) Seven hole plate, circular array, with centre hole
Using a 16 cm tundish head, the flow out of the nozzles for plate thicknesses of 1, $1\frac{1}{2}$ and 2 inches was more laminar in appearance than observed with the use of $\frac{1}{2}$ inch plate. The depth of bubble penetration
15 appeared to be least with the $1\frac{1}{2}$ inch plate, but was also most dense for this plate.

With a 42 cm tundish head, there did not seem to be any difference in flow conditions regardless of which plate thickness was used.

- 20 c) Nine hole plate, square array with centre hole
At a 16 cm tundish head the nine hole plate array yielded improved downstream flow conditions over those observed for the six or seven hole arrays evaluated above. For the nine hole array (Figure 5),
25 the $1\frac{1}{2}$ inch plate appeared to give the least density of bubbles in the mold box. The laminar appearance of the streams out of the nozzle was unaffected by plate thickness in the range of 0.5 inches to 2 inches.

- 30 At a 42 cm tundish head, there was noted a slightly more laminar-like stream with a 1 inch plate than with the others, but generally all streams appeared to be tight and laminar in appearance. The depth of penetration of bubbles in the mold box was about the
35 same for all plate thicknesses with possibly less density of bubbles observed with the use of a $1\frac{1}{2}$ inch plate thickness.

Conclusions

5 Generally, the plate thickness appeared to have less influence on the downstream flow characteristics than did the number of holes used in the array. The results appear to indicate that a nine hole array is clearly superior to the seven or six hole arrays evaluated.

10 The density of bubbles in the mold boxes was less at a 16 cm tundish head than at a 42 cm tundish head. The effect of plate thickness, although difficult to evaluate, showed that a $\frac{1}{2}$ inch plate produced poorer results at a 16 cm tundish head for a seven hole plate array, and $1\frac{1}{2}$ inch and 2 inch plates produced
15 slightly poorer stream shapes with a six hole array at a 42 cm tundish head. It would appear that the $\frac{1}{2}$ inch plate may not be suitable for all hole arrays whereas the $1\frac{1}{2}$ inch plate may be close to or at the optimum thickness for a number of different hole
20 arrays.

C. Effect of Hole Diameter

Two different hole arrays, seven and nine, were used to evaluate the effects of hole diameters of 1, $1\frac{1}{2}$
25 and $1\frac{1}{2}$ inches. All plates were $1\frac{1}{2}$ inch thick.

a) Seven hole circular array

At a 16 cm tundish head, the stream shape out of the nozzle was better for the $1\frac{1}{2}$ or $1\frac{1}{2}$ inch diameter holes than for the 1-inch hole size. However, the
30 penetration of air bubbles in the mold boxes was least for the one-inch holes.

For a tundish head of 42 cm, the stream shape was best for the $1\frac{1}{2}$ inch diameter holes. Also, the depth of penetration was least with the plate having $1\frac{1}{2}$
35 inch holes. The plate configuration is shown in Figure 4.

b) Nine hole square array

At a 16 cm tundish head, the stream shape for the different hole diameters was about the same with

possibly more laminar flow for the $1\frac{1}{4}$ or $1\frac{1}{2}$ inch holes than for the 1 inch holes. The penetration of air bubbles in the mold boxes was least for the 1-inch diameter holes and most for the $1\frac{1}{2}$ inch diameter holes.

At a 42 cm tundish head, the stream shape was good for all three hole sizes with slightly better results for the $1\frac{1}{2}$ inch hole size. The density of bubbles in the mold boxes was about the same for all three hole sizes evaluated.

Conclusions

Generally it appears that while hole size affected the stream flow conditions out of the nozzle, the effect was not a pronounced one. Hole diameter appeared to be a stronger factor with the seven hole array than with the nine hole array. This would be expected in that the percentage increase in hole area would be greater with fewer holes in the plate.

Again, it appeared that the nine hole array produced more laminar flow conditions than did the seven hole array. The plate with $1\frac{1}{4}$ inch holes appeared to give good downstream flow characteristics.

D. Tests with a Wafer Nozzle

Wafer nozzles are well known in the art of steel making, and a typical cross section of a wafer nozzle is shown in Figure 10.

Previous to the making of this invention, a wafer nozzle was tested in a continuous casting process. However, it was found that the flow out of the wafer nozzle, although 22% reduced compared with that of the regular nozzle, had wildly erratic flow characteristics. Because the wafer nozzle has advantages when used in conjunction with a deoxidation practice, it was desirable to evaluate some of the "better" perforated plates to see whether they could be used to improve the downstream flow conditions out of a wafer nozzle. Three different hole arrays and three hole diameters were evaluated. The 16

hole plate was $\frac{1}{4}$ inch thick, whereas the other plates were $1\frac{1}{4}$ inch thick.

a) Sixteen 1-inch diameter hole square array

5 A sixteen one-inch diameter hole array as seen in Figure 6 was evaluated with a wafer nozzle and compared with a regular nozzle. At both a 16 and a 42 cm tundish head, the flows out of the nozzles were tight and laminar in appearance. However, the density of air bubbles in the mold box was
10 considerably less for the wafer nozzle than for the regular nozzle. It has been noted that for the same tundish head, the flow out of the wafer nozzle was about 22% less than out of a regular nozzle. Therefore a more valid
15 comparison, although still only approximate, would be to compare the flow out of the wafer nozzle at a head of 42 cm to the flow out of a regular nozzle at 16 cm. When this was done, it was still evident that there was less density of bubbles in the mold box
20 with the wafer nozzle than with the regular nozzle.

b) Nine 1-inch hole square array

The use of the nine hole plate as seen in Figure 5 improved the flow out of the wafer nozzle. In comparing the wafer nozzle with the regular nozzle,
25 it should be remembered that there was 22% less flow out of the wafer nozzle than out of the regular nozzle for the same tundish head. At a 42 cm tundish head there was more penetration in the mold box than at the 16 cm tundish head. Even accounting for the
30 differences in flow rates it appeared there was less density of bubbles in the mold box with a wafer nozzle than with a regular nozzle.

c) Seven hole array - effect of different hole diameters

35 At a 16 cm tundish head, increasing the hole diameter from one to $1\frac{1}{4}$ to $1\frac{1}{2}$ inches reduced the density but increased the depth of bubble penetration in the mold box. The flow out of the nozzles appeared to be about the same for all hole sizes evaluated.

With the tundish at 42 cm the flows out of the nozzles were about equal for all hole diameters but the density of bubbles in the mold box was least for the 1½ inch holes. The depth of penetration of
5 bubbles in the mold box was greatest with the 1½ inch diameter holes.

Conclusions

Probably more than with the regular nozzle, the merits of a nine hole array over that of the seven
10 hole array were observed in this set of tests. The nine hole array in combination with a wafer nozzle produced much less density of air bubbles in the mold box than with the seven hole array. The 1½ and 1½ inch hole diameter appeared to yield laminar flow
15 conditions downstream of the nozzle.

Preferred Materials

Tests with plates fabricated from tundish liner boards (a silica refractory material called Profax by its manufacturer) have withstood erosion in the
20 tundish at the steel plant. Any refractories commonly used in steel teeming systems (e.g. alumina, zirconia, magnesia, alumina-graphite) could be used.

25

30

35

CLAIMS:

1. A continuous casting process for metal, including the steps:

- a) teeming the molten metal into a tundish,
- b) passing the molten metal into a nozzle well and toward a nozzle at the bottom of the well,
- c) during its passage from the tundish to the nozzle, passing the molten metal through a plate having a plurality of holes and located above the nozzle, thereby to promote laminar flow below the plate, and
- d) from the well, passing the molten metal through the nozzle to form a stream entering a continuous casting mold.

2. The process claimed in claim 1, in which the plate has at least six holes and is located substantially at the top of the well.

3. The process claimed in claim 1, in which the plate has at least seven substantially cylindrical holes of substantially the same diameter, and is located at least about six hole diameters above the nozzle.

4. The process claimed in claim 1, in which the plate has between about six and about ten cylindrical holes of the same diameter, the plate being located above a level which is six hole diameters above the bottom of the well.

5. The process claimed in claim 1, claim 2 or claim 4 in which the plate has at least seven cylindrical holes of which the diameter is between about one inch and about $1\frac{1}{2}$ inches.

6. The process claimed in claim 1, claim 2 or claim 4, in which the plate thickness is between about $\frac{1}{4}$ inch and about 2 inches.

7. The process claimed in claim 1, claim 2 or claim 4, in which the hole size is large enough to prevent freezing of the liquid metal as it first pours through the plate and small enough to promote laminar flow in the well.

8. The process claimed in claim 1, claim 2 or claim 4, in which the metal is steel.

9. For use with an apparatus for the continuous casting of metal:

a tundish having at least one nozzle well with a nozzle at the bottom of the well,

and a plate having a plurality of holes and located above the nozzle in a location such that molten metal in the tundish must pass through the holes in the plate to reach the nozzle.

10. For use with an apparatus for the continuous casting of metal, the apparatus comprising a tundish having at least one nozzle well with a nozzle at the bottom of the well, and a continuous casting mold into which molten metal can stream from the nozzle:

a plate having a plurality of holes and positioned in the path of molten metal passing from the tundish to the nozzle, but spaced above the nozzle, whereby the molten metal must pass through the holes in the plate to reach the nozzle.

11. An apparatus for the continuous casting of metal, comprising:

a tundish having at least one nozzle well with a nozzle at the bottom of the well,

a continuous casting mold into which molten metal can stream from the nozzle,

and a plate having a plurality of holes and positioned in the path of molten metal passing from the tundish to the nozzle but spaced above the nozzle, whereby the molten metal must pass through the holes in the plate to reach the nozzle.

12. The invention claimed in claim 9, claim 10 or claim 11, in which the plate has at least six holes and is located substantially at the top of the well.

13. The invention claimed in claim 9, claim 10 or claim 11, in which the plate has at least seven substantially cylindrical holes of substantially the same diameter, and is located at least about six hole diameters above the nozzle.

14. The invention claimed in claim 9, claim 10 or claim 11, in which the plate has between about six and about

ten cylindrical holes of the same diameter, the plate being located above a level which is six hole diameters above the bottom of the well.

15. The invention claimed in claim 9, claim 10 or claim 11, in which the plate has at least seven cylindrical holes of which the diameter is between about one inch and about $1\frac{1}{2}$ inches.

16. The invention claimed in claim 9, claim 10 or claim 11, in which the plate thickness is between about $\frac{1}{2}$ inch and about 2 inches.

17. The invention claimed in claim 9, claim 10 or claim 11, in which the hole size is large enough to prevent freezing of the liquid metal as it first pours through the plate and small enough to promote laminar flow in the well.

18. The invention claimed in claim 9, claim 10 or claim 11, in which the metal is steel.

19. The invention claimed in claim 3, claim 10 or claim 11, in which the plate has nine holes in three rows of three each, the plate being located substantially flush with the tundish bottom, the holes being cylindrical and having a diameter of at least 1 inch.

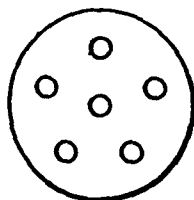
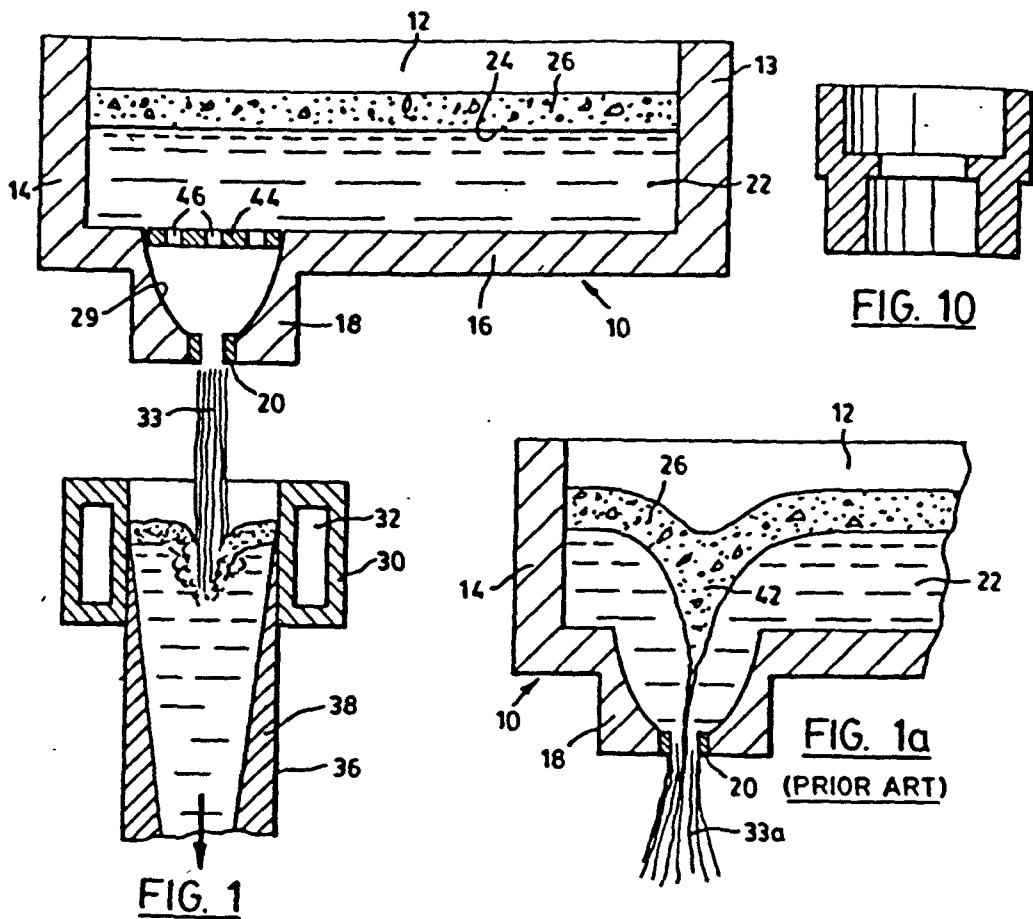


FIG. 2

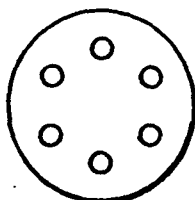


FIG. 3

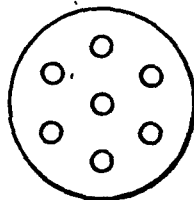


FIG. 4

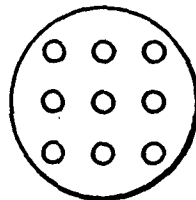


FIG. 5

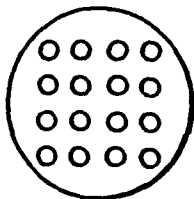


FIG. 6

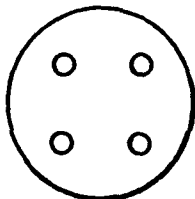


FIG. 7

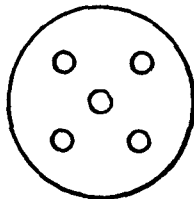


FIG. 8

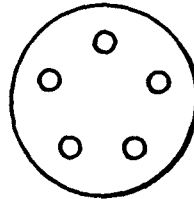


FIG. 9

Patented by H. K. K. K.

INTER - OFFICE LETTER
NOTE DE SERVICE

stelco

SUBJECT/OBJET TUNDISH PLATE FOR STREAM SHAPE CONTROL	OUR FILE/NOTRE NO DE DOSSIER S-306 Cda.	WORKS OR OFFICE/USINE OU BUREAU Stelco Tower - 20
	YOUR FILE/VOTRE NO DE DOSSIER	DEPARTMENT/ATELIER OU SERVICE Law
		DATE February 18, 1985

TO/A
R. W. Pugh

Copy to:

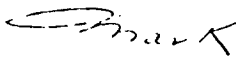
**R. N. Lawler
F. J. Pearce**

It has been said that the continued growth and health of any industrial organization depends upon the ingenuity of the people who work in that organization. The attached Canadian patent 1180532 on your tundish plate is a testament to your ingenuity.

I believe that the health and well being of our Company ten years from now can be forecast from the quality and the quantity of the inventions being made today. Thank you for contributing to this process.

I have attached an additional copy of Canadian patent 1180532 for Don Bellow. I think it would be more meaningful if you forwarded it to him on Stelco's behalf.

Once again I would like to thank you not only for the technical assistance you provided during the entire patenting process, but also for the positive manner in which you provided it. I look forward to working with you on future projects.



M. A. Renzetti

MAR:KN
Attach.

ADVANCES IN SURFACE TREATMENTS

Technology — Applications — Effects

A. NIKU-LARI

*Director, Institute for Industrial Technology Transfer,
24 Rue des Mimosas, Gournay s/Marne,
F93460 France*

Volume 2



PERGAMON PRESS

OXFORD · NEW YORK · TORONTO · SYDNEY · FRANKFURT

RESIDUAL STRESSES AND FATIGUE OF SURFACE TREATED WELDED SPECIMENS

D. G. Bellow, M. Wahab and
M. G. Faulkner

Department of Mechanical Engineering, University of Alberta, Canada

ABSTRACT

An experimental program was undertaken to evaluate the effect of induced compressive stresses due to various peening and thermal treatments on the fatigue life of a butt welded medium strength steel (Cb-50). Residual stresses were measured using x-ray diffraction and the results were compared with hardness values taken at the surface and through the thickness of the specimens. It was found that of all post weld treatments studied the stress peened specimens gave the most improvement in fatigue strength over that of the as-welded condition and approached 82% of the fatigue strength of the base metal at a fatigue life of 2×10^6 cycles. On the other hand annealing only showed an improvement of 14% over that of the as-welded condition.

It was found that a good linear correlation existed between the induced residual stresses at the toe of the weld and the fatigue strength evaluated at 2×10^6 cycles. However, for residual stresses of less than 130 MPa very little improvement in fatigue strength was evident.

Surface residual stresses were compared with Almen strip readings and the depth of work hardening. It was found that the Almen strip readings did not give as consistent an indication of work hardening as did measurement of the residual stresses.

KEYWORDS

Butt-welds, stress peening, shot peening, single and multiple point hammer peening, annealing, fatigue strength, residual stresses.

INTRODUCTION

The development of residual stresses in welded constructions is intrinsic to the welding process. These residual stresses often cannot be entirely removed by post-heating. While some investigators (Munse, 1964) have contended that residual stresses do not have any significant influence on fatigue life, others such as Dugdale (1959) have demonstrated a substantial effect in the case of small notched specimens. Furthermore, it has been known for some time (Buhler and Buchholtz, 1933; Horger and Neifert, 1945) that residual stresses are redistributed during the course of cyclic tension.

Residual stresses are caused by local yielding in an otherwise elastic body and for most welded structures they are confined to the neighbourhood of the welds. A model for following the development of residual stresses has been suggested by Parlane (1981). This model explains that the magnitude of the residual stresses is a function of the temperature difference between base material and the weld butt and can vary, depending on the conditions, up to the yield stress.

The investigation of the effect of residual stresses requires the study of the influence on the endurance and/or fatigue limit and the influence of the cyclic stresses on the redistribution of the residual stresses. Parker (1957), Tall (1964), Munse (1964), Gurney and Maddox (1973), Harrison (1981) among others have observed that the fatigue strength of stress relieved butt welded joints was improved over those in the as-welded condition. In particular, Harrison (1981) showed that when the applied stress range was purely tensile the residual stress had little effect but that if the stress cycle passed through zero the compressive components appeared to be more damaging.

The welding process is a complex one and depends on many variables. Thus, to investigate the influence of residual stresses on the fatigue life of welded joints the experiments must be done under closely controlled conditions. Most of the studies on the fatigue life of welded joints reported in the literature have shown that appropriate mechanical and/or thermal treatments have improved the fatigue life but the manner in which the residual stresses interact with the applied cyclic stress and the changes that occur during cycling is less known. The object of this paper is to show how the cyclic loading in the fatigue cycle affects the distribution of residual stresses in butt welded joints. In a subsequent paper a mathematical model will be developed for prediction of the crack initiation and propagation phases taking into account the residual stress behaviour noted here.

EXPERIMENTAL

The experiments were designed to obtain the base material properties for the prediction of total fatigue life and to determine the experimental data (S-N curve) for mechanically and thermally treated welded joints. High cycle pulsating tension tests were performed and the magnitude of the residual stresses and the effect of these on the fatigue life was observed. Fatigue testing was conducted on an MTS closed-loop servo-controlled hydraulic test system.

Fatigue Specimens

The high cycle fatigue specimens were made by welding two 127 mm wide by 6.35 mm thick plates out of as-rolled Columbium-50 steel (0.02% C, 1.2% Mn, 0.04% P, 0.05% S and 0.005% Cb). This steel was selected for its weldability and relatively high yield strength. The plate edges were machined straight and bevelled at 45° to a depth of about 1.6 mm. An automatic submerged arc welding process was used for a double-vee butt weld. The welding electrode was an Oxweld #36 (0.14% C, 2.0% Mn, 0.017% P, 0.024% S and 0.05% Si). The welds were all flouroscope, and some ultrasonically, to check for flaws and then sawn into 76 mm wide strips with the weld axis transverse to the saw cut. The longitudinal edges of the welded specimens were machined parallel using a milling cutter.

Surface Treatments

The surfaces of the welds as well as the adjacent base metal were subjected to the following mechanical surface treatments:

- (1) single point hammer (6.4 mm diameter)
- (2) multiple point hammer (19 needles of 3.2 mm diameter each)
- (3) glass shot beads (0.2-0.3 mm diameter)
- (4) steel shot (0.6-1.2 mm diameter)

The exposure time for the single and multiple hammer peening was between 25 and 35 s per 650 mm^2 of surface area covered. The duration of exposure for the glass and steel shot was six and eight minutes respectively. Visual checks were made to ensure the weld toe and adjacent base metal was evenly covered. To assist in this a dye penetrant along with an ultraviolet light was used. Full coverage of the surface during peening removed the coating so that incomplete coverage was detected by the ultraviolet light. In addition to using standard size Almen strips the depth of peening was measured by sectioning near the toe of the weld a plane inclined approximately 10° to the peened surface and measuring hardness using a Knoop indenter and 300 g load (Faulkner and Bellow, 1972).

A fifth technique for inducing compressive residual stresses was achieved by tensile preloading. The welded specimens were preloaded to approximately 90% of the yield of the base metal. Electrical resistance strain gauges were applied to the base metal adjacent to the weld to ensure that the base metal remained elastic. The rate of preloading was 7.5 kN min^{-1} . Stress measurements were made using an x-ray diffraction technique.

Another surface treatment evaluated was stress peening where the specimens were preloaded first to 90% of the yield of the base metal and then peened. A variation of this was also tried by first peening and then preloading. In both these cases the stresses were measured before and after the treatment.

To study the effect of annealing on the fatigue life some specimens were annealed at 550°C for 30 min. and slowly cooled (5 to 6 hrs).

Fatigue Testing

Specimens were mounted in the fatigue machine and a uniaxial cyclic tension load was applied. The dynamic peak load was controlled and the test was stopped automatically, due to a change in strain response, when a small fatigue crack occurred. The initiated crack was checked with dye penetrant and ultraviolet light. The test was then started again to obtain the propagation life of the specimen until complete fracture occurred.

Measurement of Residual Stresses

All stress measurements were performed using the Thomas-B double exposure x-ray diffraction technique (Sproull, 1946; Cullity, 1978). The x-ray method was calibrated with strain gauges and other techniques yielding good correlations between the various methods as shown in Fig. 1. Before each specimen was tested in fatigue the residual stresses were measured at the toe of the weld. Additional stress measurements were made for selected specimens at various stages in the fatigue life and at the end of fatigue cycling. Residual stresses were also measured across the thickness of the base metal and across the thickness of the butt welded specimens to examine the presence of any stress gradient. To compensate for the selective action of the x-rays at least three exposures to each setting were taken.

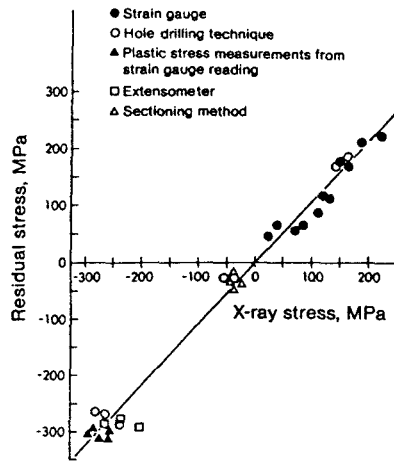


Fig. 1. Calibration of x-ray stress measurements with other techniques.

Hardness Tests

Hardness tests were carried out on peened and unpeened welded specimens. The peening intensity, as measured by surface hardness, and the depth of work hardening were measured with a Knoop indenter. Micro-hardness readings were obtained at the weld toe, untempered weld metal and the tempered weld metal zones for the untreated specimens using a Vicker's indenter and a 300 g load.

RESULTS

Distribution of Welding Residual Stresses

The distribution of residual stresses was measured across the welding joint. Since most fatigue cracks originated on the "second pass" side of the weld this was the side on which most stress measurements were made. Typical residual stress patterns for three specimens are shown in Fig. 2.

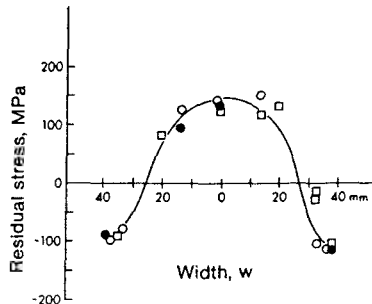


Fig. 2. Residual stress distribution near the toe of the weld.

From this figure it is clear that the residual stresses are maximum tensile (140–170 MPa) across the weld and decrease to compressive stresses between 100–120 MPa 30 mm away from the center of the weld.

In another test three untreated specimens were cycled at different stress levels 0–145 MPa for 0.5×10^5 cycles, 0–165 MPa for 10^5 cycles, and 0–265 MPa for 10^5 cycles and the test terminated before fatigue cracks initiated to evaluate the effect of cycling on the redistribution of the original residual stress pattern observed in Fig. 2. These results are shown in Fig. 3. Although the number of cycles and dynamic loads were different in each case the results show that the residual stress pattern changed, depending on dynamic load, during fatigue cycling and that for the 165 MPa dynamic load the pattern had changed at 10^3 cycles.

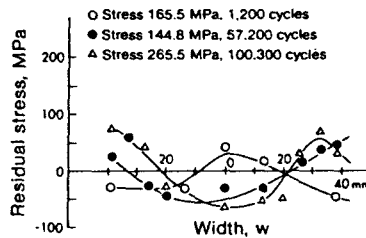


Fig. 3. Distribution of residual stresses after fatigue cycling.

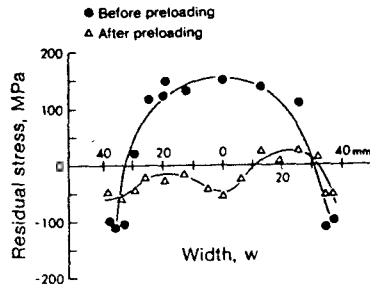


Fig. 4. Change in residual stress pattern after preloading.

Measurement of residual stresses through the thickness of the weld were made where it was found that the compressive stresses existed to a depth of about 0.08 mm whereas on the surface of the base metal compressive stresses between 21–35 MPa were measured.

Compressive Stresses of Surface Treated Welds

To evaluate the effect of tensile preloading residual stresses were measured near the toe of the weld before and after preloading. A typical result is shown in Fig. 4 where an initial tensile residual stress of 150 MPa changed to a compressive stress of about 50 MPa after preloading. Other tests showed the same result except that there was less uniformity in stress distribution observed after than before preloading.

Residual stresses were also measured on specimens before and after mechanical surface treatment. Figure 5 shows the manner in which the tensile residual stresses across the weld were modified to almost uniformly compressive stresses after peening. The single and multiple point hammer peening yielded residual compressive stresses of 150 MPa and 170 MPa respectively whereas the glass and steel shot compressive residual stresses were measured at 60 MPa and 110 MPa respectively. For comparison the residual stresses for an annealed specimen were near zero. The results of stress peening showed a compressive residual stress of 170 MPa and no difference was noted whether the specimen was peened and then preloaded or preloaded and then peened.

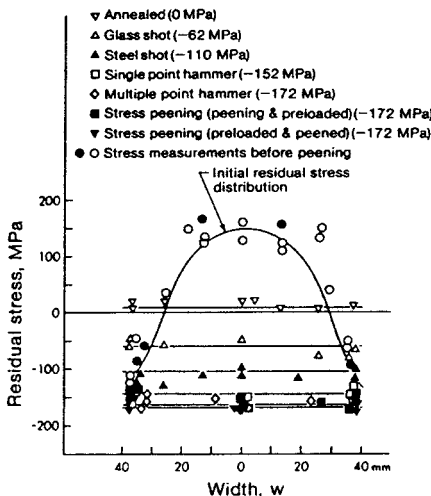


Fig. 5. Compressive stresses by various methods.

Fatigue Results

A summary of fatigue results is shown in Fig. 6. Each curve was drawn through the mean of at least four tests at each test load and for each curve the test was run at four and sometimes five different stress levels. From these results it is seen that at a life of 2×10^6 cycles the fatigue strength of the as-welded condition was 145 MPa or 43% of the base metal which was at 340 MPa. Table 1 summarizes the fatigue strengths at 2×10^6 cycles in order of improvement from the as-welded condition to the base metal.

From Fig. 6 and Table 1 it is evident that stress peening improved the fatigue strength from the as-welded condition more than any other treatment studied. From the residual stress patterns in Fig. 5 it was shown that there was little distinction in stress peening whether the specimen was peened before or after tensile preloading. This same result was noted in the fatigue results and thus in Fig. 6 and Table 1 both results were combined and noted as "stress peened". The next best surface treatments were achieved with the multiple point and single point hammer peening and steel shot. Each of these showed about the same improvement 70-79% over the as-welded condition. As might be expected the benefits of glass shot, while measurable at 40% better than the as-welded condition, were not as pronounced as for the heavier peened surfaces. Finally, annealing and preloading produced only small improvements of 14-17% over the as-welded condition.

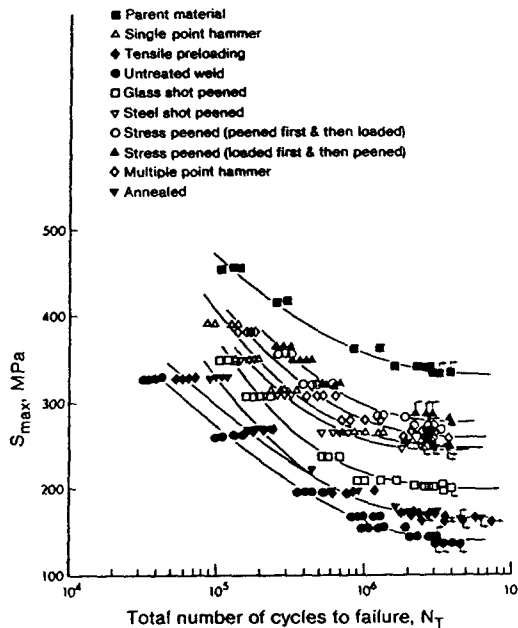


Fig. 6 Comparison of fatigue tests.

TABLE 1 Fatigue Strengths at 2×10^6 Cycles

Treatment	MPa @ 2×10^6 cycles	% Improvement over as-welded	% of base metal
Base metal	340	134	100
Stressed peened	280	93	82
Multiple point	260	79	76
Single point	250	72	74
Steel shot	245	70	72
Glass shot	200	40	59
Tensile preload	170	17	50
Annealed	165	14	49
As-welded	145	0	43

From the data plotted in Fig. 6 an induced stress value was calculated as the absolute value of the difference between the initial residual stress at the toe of the weld (150 MPa) and the induced compressive stress due to various forms of post welding treatment. The fatigue strength was evaluated at 2×10^6 cycles. The induced stress was plotted against the improvement in fatigue strength over the as-welded condition and shown in Fig. 7. A fourth order polynomial curve was fitted through the data and the equation is shown in Fig. 7. In addition, two straight lines were drawn through the data, one was drawn as a "best fit" straight line through the measured data but not including the origin, the other was drawn assuming the origin was a valid experimental point. For the two straight lines, with and without taking the origin as a

data point, the correlation co-efficients were 0.91 and 0.96 respectively. As might be expected the results show that as the induced compressive stress due to post welding treatment increases so does the fatigue strength.

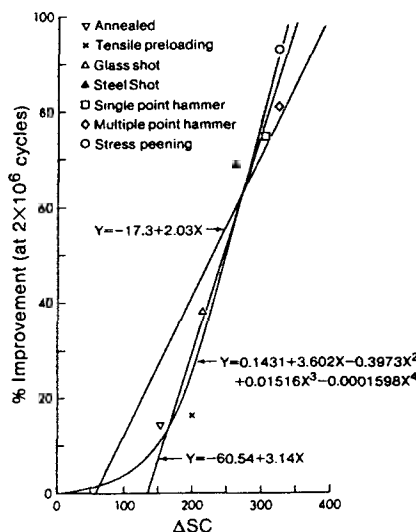


Fig. 7. Improvement in fatigue strength as a function of induced stress.

If the linear correlation of the data (without including the origin) is accepted as valid then for induced stresses of less than 130 MPa there is no improvement in fatigue strength over the as-welded condition.

Depth of Work Hardening

It is interesting to note the depth of work hardening as a consequence of the various post-treatments studied. The data showing the Knoop hardness (300 g load) versus the depth from the surface are plotted in Fig. 8. The glass shot produced a depth of work hardening of 0.2 mm, for steel shot the depth was 0.43 mm, for multiple and single point peening the depth was 0.69 mm and 0.76 mm respectively and for both forms of stress peening the depth of work hardening was 0.7 mm.

A consistent trend was found between the residual stress levels and the depth of work hardening. Although the depth of work hardening was slightly more (0.76 vs 0.69 mm) for single point than for multiple point hammer peening the improvement in fatigue strength by multiple point hammer peening was greater. This was probably the result of insufficient peening applied at the weld toe due to the large radius of the peening hammer. However, the compressive residual stress level was higher for multiple point hammer peening than for single point hammer peening.

As it is quite common to measure peening intensity by means of Almen strip tests a comparison between Almen strip readings and depth of work hardening is shown in Fig. 9. Also shown in Fig. 9 is the induced compressive residual stress versus the depth of work hardening. These two plots show that the depth of work hardening correlates better with residual stress than with the Almen strip values. Evident from Fig. 9 is the fact that the depth of work hardening

approached a constant value of 0.9 mm at an induced compressive stress of 170 MPa.

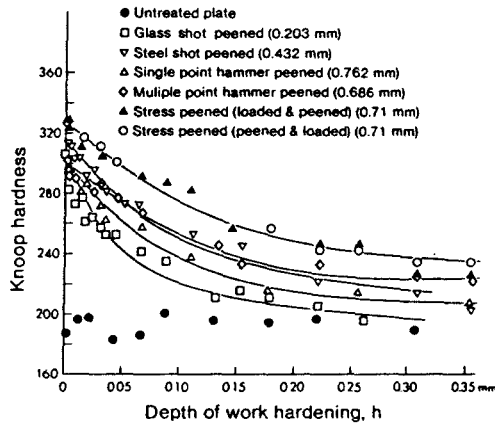


Fig. 8. Hardness versus depth of work hardening.

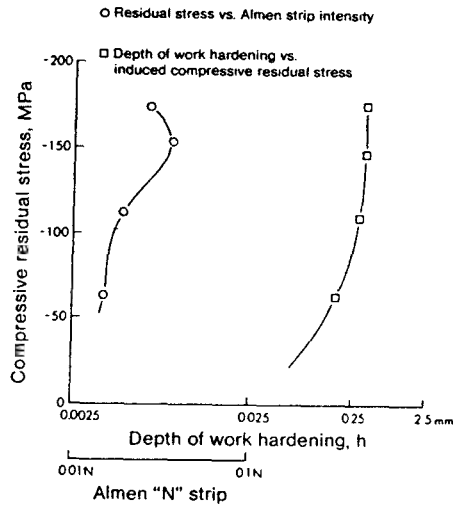


Fig. 9. Depth of work hardening and Almen strip intensity versus induced residual stress.

CONCLUSIONS

A series of experiments were conducted to evaluate the influence of residual stresses on the fatigue life of a butt-welded medium strength steel. A variety of post weld mechanical and thermal treatments were evaluated and it was found by stress relieving and inducing compressive residual stresses the improvement

in fatigue strength at a life of 2×10^6 cycles could be as much as 93% over the as-welded condition. Of the post weld treatments evaluated stress peening provided the most improvement whereas annealing provided the least at only 14% over the as-welded condition.

The depth of work hardening due to peening increased exponentially and approached a constant depth of 0.9 mm as the surface residual stress of 170 MPa was attained.

Finally, it was found that there was a good linear correlation between the induced compressive stress due to post weld surface treatment and the fatigue strength evaluated at 2×10^6 cycles. For residual stresses less than 130 MPa no beneficial effect in fatigue life is to be expected.

ACKNOWLEDGMENTS

The authors wish to thank the sponsors of this experimental program, Natural Sciences and Engineering Research Council (Canada), for the financial assistance received under grants A-2705 and A-7514. Thanks are also due to Messrs. T Villett, J Foy, A Muir, B Cielin and M Schubert of the Mechanical Engineering Department for their assistance in the experimental programs.

REFERENCES

- Buhler, H., and H. Bucholtz (1933). The effect of residual stresses on the dynamic bending strength, Mitt. Forsch. Inst., 3 (8), 235-248.
- Cullity, B. D. (1978). Elements of X-ray Diffraction. Addison-Wesley.
- Dugdale, D. S. (1959). Effect of residual stresses on fatigue strength. Weld Res. Suppl., 45-48.
- Faulkner, M. G., and D. G. Bellow (1972). Improving the fatigue of life of butt-welded medium strength steels. Proc Appl. of Solid Mech. Univ. of Waterloo.
- Gurney, T. R. and S. J. Maddox (1973). A reanalysis of fatigue data for welded joints in steel. Weld. Res. Int., 3(4), 1-54.
- Harrison, J. D. (1981). The effect of residual stresses on fatigue behaviour. Weld. Inst. Mono., 9-16.
- Horger, O. J., and H. R. Neifert (1945). Shot peening to improve fatigue resistance. Soc. Exp. Stress Anal., 1-10.
- Munse, W. H. (1964). Fatigue of Welded Steel Structures. Welding Research Council, New York.
- Parker, E. R. (1957). Stress relieving of weldments. Weld. Res. Suppl., 433-440.
- Parlane, A. J. A. (1981). Origin and nature of residual stresses in welded joints. Res. Stresses and Their Effect. Welding Institute, pp. 1-4.
- Sproull, W. T. (1946). X-Rays in Practice. McGraw-Hill.
- Tall, L. (1964). Residual stresses in welded plates - a theoretical study, Weld. Res. Suppl. 10-23.

ADVANCES IN SURFACE TREATMENTS

Technology — Applications — Effects

A. NIKU-LARI

*Director, Institute for Industrial Technology Transfer,
Gournay sur Marne, France*

Volume 3



PERGAMON PRESS

OXFORD · NEW YORK · BEIJING · FRANKFURT
SÃO PAULO · SYDNEY · TOKYO · TORONTO

PREDICTION OF FATIGUE CRACK INITIATION AND PROPAGATION OF WELDED JOINTS

D. G. Bellow*, M. Wahab** and M. G. Faulkner*

**Professor of Mechanical Engineering, University of Alberta, Edmonton, Alberta,
Canada T6G 2G8*

***Former graduate student, Department of Mechanical Engineering,
University of Alberta, Canada T6G 2G8*

ABSTRACT

Total fatigue life was considered as a combination of a crack initiation phase and a crack propagation phase. The initiation phase was based on an extension of the local strain fatigue life model which included the effects of residual and mean stresses. In order to determine the local notch root stress-strain condition a relationship between the fatigue notch and stress concentration factors was developed. Using elastic superposition and modifying Neuber's equation residual stresses at the weld toe were simulated. For the fatigue crack propagation phase Forman's equation was used which included the effects of residual stresses. The residual stress distribution at the weld toe was based on experimental observations.

The theory was compared with fatigue experiments conducted on butt welded steel specimens subjected to various forms of surface and mechanical treatments. The results showed good agreement between theory and experiment for all treatments evaluated.

KEYWORDS

Butt welds, residual stresses, fatigue life, crack initiation, crack propagation

INTRODUCTION

While there have been many studies on the fatigue life of welded joints most of these have been experimental. Some work has been done on predictive models for crack initiation and propagation but these have not included the influence of residual stresses although recent experiments have shown how the fatigue life can be influenced by residual stresses (Bellow, Wahab and Faulkner, 1984). The purpose of this paper is to develop an analytical model for predicting the fatigue crack initiation and propagation phases which will include the effects of residual stresses and their redistribution during the total fatigue life. The theory will be compared with experiments conducted on a butt welded medium strength steel (Columbium 50).

Estimates of the fatigue crack initiation may be based on the strain-life properties and cumulative damage criterion while the propagation life may be based

on fracture mechanics concepts as suggested by Topper and Conle (1972), Mattos and Lawrence (1977) and Morrow and Socie (1981). Crack initiation is influenced by the basic material properties, the effect of residual stresses at the weld toe, cyclic fatigue material properties and the accumulation of damage. An equation developed by Forman, Kearney and Engle (1967) can be used for predicting the propagation phase with appropriate modifications to include the effective stress ratio, loading histories and crack opening concepts. The summation of the crack initiation phase and the crack propagation phase determines the total fatigue life.

CRACK INITIATION

The crack initiation phase is assumed to be based on the fact that the most highly strained region can be represented by a filament of material whose mechanical response is similar to that of a smooth fatigue specimen. The initiation of a fatigue crack can be considered to occur by the rupture of this filament (Topper, Wetzel and Morrow, 1969). This model requires knowledge of the material properties and the stress-strain history of the notch root.

To enable an estimation of the crack initiation phase knowledge of local stress-strain behaviour is required. Several authors (Stowell 1968, Hardrath and Ohman 1951, Irwin 1960, Neuber 1961, Dixon and Straunigan 1964 and Huang 1972) have suggested approaches for relating the nominal stress-strain to local (i.e. at the weld toe) stress-strain behaviour. Of these Neuber's formulation has been used because of its simplicity.

Neuber (1961) suggested that the elastic stress concentration factor K_t is equal to the geometric mean value of the stress concentration factor K_σ and the strain concentration factor K_ϵ , that is,

$$K_t = (K_\sigma K_\epsilon)^{1/2}. \quad (1)$$

Hammouda, Smith and Miller (1979) showed that equation (1) could be modified to

$$K_t^2 = \frac{\Delta\sigma\Delta\epsilon E}{\Delta S^2} \quad (2)$$

where $\Delta\sigma$ and $\Delta\epsilon$ are the local stress and strain at the notch and ΔS and Δe remote from the notch. Extending equation (2) to fatigue and substituting the fatigue notch factor K_f for K_t it follows that

$$K_f = (K_\sigma K_\epsilon)^{1/2}$$

or rewriting in terms of the dynamic ranges of stress and strain

$$K_f = \left(\frac{\Delta\sigma\Delta\epsilon}{\Delta S\Delta e} \right)^{1/2} \quad (3)$$

or

$$K_f^2 \Delta S^2 / E = \Delta\sigma\Delta\epsilon$$

where $\Delta S = \Delta e E$.

For large radius notches K_f is nearly equal to K_t and for sharp notches K_f is a conservative estimate for K_t .

Equation 3 relates the nominal stress-strain behaviour at the weld toe and allows

an estimate of the crack initiation life of a smooth specimen to be made.

Stress Concentration Factor

For the case of butt welded specimens the estimate of the stress concentration factor must be made on the basis of the geometry of the weld toe. Lawrence (1973) specified the flank angle θ and edge preparation angle ϕ and established a relationship with the ratios h/w and h/t where h and w are the height and width of the weld bead and t is the thickness of the base metal. The stress concentration factor is also a function of the radius at the weld toe. Mattos and Lawrence (1977) proposed

$$K_t = 1 + A \sqrt{t/r} \quad (4)$$

where A depends on the weld macrogeometry.

Fatigue Notch Factor

The fatigue notch factor K_f is the ratio of the notched to unnotched fatigue strength at some finite life. While several equations relating K_f to the stress concentration factor K_t have been proposed the equation developed by Neuber (1961) is convenient to use

$$K_f = 1 + \frac{(K_t - 1)}{[1 + (\rho^*/r)^{1/2}]} \quad (5)$$

where r is the radius of the weld toe and ρ^* is an experimentally determined material parameter which Graham (1968) showed could be determined from the ultimate strength of the material S_u , which for steel is

$$\rho^* = 23.8 \times 10^3 / S_u^{1.6} \quad (\text{S.I. units}).$$

From equation (4) it is evident that as r decreases K_t increases and from equation (5) it can be shown that as r decreases K_f increases and approaches a constant value of 2.0.

The difficulty in obtaining a value of K_f is that the radius of the weld toe is not known precisely. It was found that a 20 percent increase in the K_f value occurred when the root radius decreased from 0.25 to 0.025 mm but only a seven percent increase occurred when the root radius was decreased from 0.025 mm to 0.0025 mm. Thus, as the root radius becomes smaller the K_f value is less sensitive to changes in the radius. On the basis of this as well as measurements of some typical welds a root radius of 0.025 mm was chosen which yields a K_f value of 1.85.

Cyclic Stress-Strain and Hysteresis

Landgraf, Morrow and Endo (1969) defined the cyclic stress-strain curve as the locus of the tips of the stable hysteresis loops from several tests at reversed constant strain amplitudes. The equation for the cyclic stress-strain curve was given as

$$\epsilon = \sigma/E + (c/K')^{1/n'} \quad (6)$$

where K' is the cyclic strength coefficient and n' is the cyclic strain hardening exponent.

It has been suggested by Wetzel (1968) that the hysteresis loop can be represented by a power function. Assuming the same exponent n' as in equation (6) the hysteresis loop can be obtained by substituting one point on the stress-strain curve $(\Delta\epsilon/2, \Delta\sigma/2)$ into equation (6) giving

$$\Delta\epsilon/2 = \Delta\sigma/2E + (\Delta\sigma/2K')^{1/n'} \quad (7)$$

Local Strain Analysis with Residual Stresses

In order to apply Neuber's theory to welds with residual stresses it is necessary to know the local stress and local strain range, $\Delta\sigma$ and $\Delta\epsilon$. The simulation of the notch stress-strain behaviour with initial residual stress at the weld toe $\sigma_{r,i}$, nominal mean stress S_m and nominal stress range ΔS is shown in Fig. 1 (Reemsnyder, 1981).

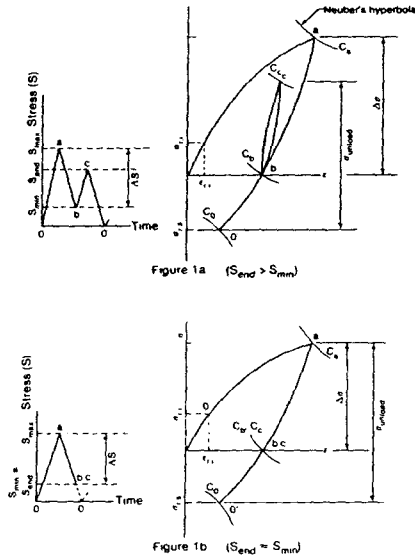


Fig. 1. Notch-root stress and strain (Reemsnyder, 1981).

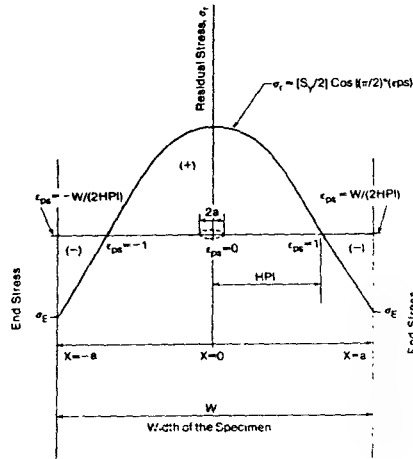


Fig. 2. Idealized distribution of stresses at weld toe.

At the start of the first fatigue cycle the notch stress at point 0 in Fig. 1a represents the state of initial residual stress at the toe of the weld. At the maximum stress S_{max} , σ and ϵ are established at the intersection of the cyclic stress-strain curve and Neuber's hyperbola Ca; point a in Fig. 1a. It can be shown that it follows from Neuber's rule that

$$S_{max} + \sigma_{r,i}/K_\sigma = E [e_{max} + e_{r,i}/K_\epsilon]$$

assuming linear elastic behaviour. Combining this last equation with equation (6) and solving for K_f gives

$$K_f = \frac{K_\sigma S_{max} [1 + E/K'^{1/n'} (K_\sigma S_{max})^{(1-n')/n'}]^{1/2}}{S_{max} + \sigma_{r,i}/K_\sigma} \quad (8)$$

Knowing the material properties, applied maximum stress range and the K_f value this equation can be solved using the Newton-Raphson iterative method.

Reemsnider (1981) developed a similar equation to equation (8) which yields a lower value for the notch root stress.

$$K_f = K_0 \left[1 + (E/K')^{1/n'} \right] (K_0 S_{\max} + c_{r,i})^{(1-n')/n'} \quad (9)$$

Using $S = 172$ MPa, $E = 200$ GPa, $n' = 0.278$, $c_{r,i} = 152$ MPa, $K' = 126$ 2MPa and $K_f = 1.851$, equation (8) produces a value of $K_0 = 1.521$ whereas for Reemsnider's equation $K_0 = 0.85$. Using the basic definition of $K_0 = \sigma/S$ equation (8) produces a local notch root stress of 262 MPa. For the same case Reemsnider's equation produces a local notch root stress of 145 MPa which is less than the applied stress of 172 MPa.

In his paper Reemsnider (1981) showed that when the nominal stress at the end of the cycle $S_{end} > S_{min}$ the notch root stress-strain behaviour follows the $\Delta\sigma$ - $\Delta\epsilon$ curve (equation (7) and Fig. 1a) with origin at point "b" and intersecting Neuber's hyperbola at "c". Using Neuber's rule he showed that

$$\sigma_{end} \epsilon_{end} = K_f^2 (S_{end} - S_{min})^2 / E$$

and

$$K_f^2 (S_{end} - S_{min})^2 / E = \sigma_{end}^2 / E + 2^{(n'-1)/n'} \frac{\sigma_{end}^{(n'+1)/n'}}{K'^{1/n'}}$$

which can be solved iteratively for σ_{end} .

The residual stress at the notch subsequent to cyclic loading $\sigma_{r,s}$ can be determined by unloading the notch to zero nominal stress. The notch stress-strain then follows the $\Delta\sigma$ - $\Delta\epsilon$ curve as shown in Fig. 1a with origin at point "c" until they intersect Neuber's hyperbola C_0' . From Neuber's rule it follows that

$$\sigma_{unload} \epsilon_{unload} = K_f^2 (S_{end})^2$$

which Reemsnider (1981) showed could be written as

$$K_f^2 S_{end}^2 / E = \sigma_{unload}^2 / E + 2^{(n'-1)/n'} \frac{\sigma_{unload}^{(n'+1)/n'}}{K'^{1/n'}}$$

which can be solved iteratively for σ_{unload} . The notch residual stress can then be found as

$$\sigma_{r,s} = \sigma_{max} - \Delta\sigma + \sigma_{end} - \sigma_{unload} \quad (S_{end} > S_{min}) \quad (10)$$

For the case where $S_{end} = S_{min}$ and applying Neuber's rule it can be shown from Fig. 1b that

$$K_f^2 S_{max}^2 / E = \sigma_{unload} \epsilon_{unload}$$

which, when substituted into equation (7) yields

$$K_f^2 S_{\max}^2/E = \sigma_{\text{unload}}^2/E + 2^{(n'-1)/n'} \frac{\sigma_{\text{unload}}^{(n'+1)/n'}}{K_f^{1/n'}} \quad (11)$$

The residual stress subsequent to cyclic loading is given by

$$\sigma_{r,s} = \sigma_{\max} - \sigma_{\text{unload}} \quad (S_{\text{end}} = S_{\min}). \quad (12)$$

The residual stress at the weld toe may be simulated by considering a nominal stress remote from the weld σ_r/K_t equal to the residual stress σ_r due to the welding. The nominal stress range ΔS is then added to this which then can be substituted in Neuber's equation. The first cycle is bounded by

$$K_f^2 (\Delta S / (1 - R_{\text{eff}}) + \sigma_{r,i} / K_t)^2 = \Delta \sigma \Delta \epsilon E \quad (13)$$

where R_{eff} is the effective stress ratio which accounts for the effect of initial stress. For the next cycle, Neuber's equation becomes

$$K_f^2 (\Delta S + \sigma_{r,s} / K_t)^2 = \Delta \sigma \Delta \epsilon E. \quad (14)$$

The initial residual stress $\sigma_{r,i}$ changes to a new value $\sigma_{r,s}$ depending on the properties and loading conditions.

Strain-Life

Manson and Hirschberg (1964) have shown that the resistance of a metal to total strain cycling can be considered as the summation of the elastic and plastic strain resistances

$$\Delta \epsilon / 2 = \sigma_f' (2N_f)^b / E + \epsilon_f' (2N_f)^c \quad (15)$$

where σ_f' = fatigue strength coefficient
 ϵ_f' = fatigue ductility coefficient
 b = fatigue strength exponent
 c = fatigue ductility exponent
 $2N_f$ = number of strain reversals

When a mean stress σ_0 is present Graham (1968) showed that

$$\Delta \epsilon / 2 = (\sigma_f' - \sigma_0) (2N_f)^b / E + \epsilon_f' (2N_f)^c.$$

Cumulative Fatigue Damage

The fatigue damage in terms of the elastic strain amplitude was shown by Basquin (1910) to be given by

$$[1/2N_f]_{\epsilon} = [(\Delta \sigma / 2) / \sigma_f']^{-1/b}.$$

If $(\sigma_{\max} + \sigma_{r,i}) \geq \sigma_{ys}'$ is the first cycle then the plastic damage criterion applies, otherwise elastic conditions prevail. According to Martin (1973) the damage due to mean stress σ_0 is given by

$$\left[\frac{1}{2N_f} \right]_0 = (\epsilon_f')^{1/c} \left[\{ (\Delta\sigma/2) K' \}^{-1/n'c} \right] \left[(1 - \sigma_{0,2N}/\sigma_f')^{1/n'c} - 1 \right]$$

where the mean stress relaxation criterion (Jhansale and Topper, 1973) is given by

$$\sigma_{0,2N} = \sigma_{0,i} (2N-1)^K$$

where $\sigma_{0,2N}$ = mean stress at reversal 2N

$$\sigma_{0,i} = \text{initial mean stress} = \frac{(1+R)S/2}{(1-R)}$$

K = strain dependant relaxation coefficient.

For mild steel Higashida, Burk and Lawrence (1978) suggested

$$K = -31,900 \frac{\Delta\epsilon/2}{E\epsilon_{tr}} \text{ MPa}^{-1}$$

The total damage per reversals $D_{i,t}$ can be calculated as

$$D_{i,t} = (1/2N_f)_\xi + (1/2N_f)_0$$

or

$$D_{i,t} = (1/2N_f)_p + (1/2N_f)_0$$

The crack initiation life is assumed to end when the linear cumulative damage rule is satisfied (Miner, 1945; Palmgren, 1924)

$$\sum_{i=1}^{2N_I} D_{i,t} = 1.0 \quad (16)$$

where $2N_I$ is the number of reversals necessary to initiate a crack.

Fatigue Crack Propagation Life

In this study the fatigue crack propagation life for a butt weld was estimated by assuming that the crack tip stress intensity factor range ΔK is the controlling variable for analyzing crack extension rates. This takes into account the effective load ratio R_{eff} . The equation of Forman, Kearney and Engle (1967) can be written as

$$\frac{da}{dN_p} = \frac{C_R (\Delta K_{eff})^m}{(1-R_{eff}) K_c^{-\Delta K_{eff}}} \quad (17)$$

where a = half crack length

N_p = crack propagation life

K_c = stress intensity factor

K = YS/\sqrt{a}

ΔK = range of stress intensity factor

m, C_R = crack growth exponent and coefficient respectively

R_{eff} = effective stress ratio

Y = factor depending on crack length and specimen geometry.

The effective stress ratio R_{eff} takes into account the effect of residual stresses in fatigue and can be expressed as

$$R_{eff} = \frac{K_{min}}{K_{max}} = \frac{\sigma_{r,i} + S_{min}}{\sigma_{r,i} + S_{max}} .$$

From equation (16) the cycles required to propagate a crack of initial size a_i to a final crack length of a_f are

$$N_f = \int_{a_i}^{a_f} \frac{(1-R_{eff})K_c - \Delta K_{eff}}{C_R \Delta K_{eff}^m} da . \quad (18)$$

The variation of the rate of crack propagation da/dN_p with the range of stress intensity factor ΔK is approximately sigmoidal in shape and bounded by the threshold range of stress intensity factor ΔK_{th} and the critical stress intensity factor K_c . To estimate ΔK_{th} Garwood (1978) proposed that

$$\Delta K_{th} \approx (190 - 144R) N_{mm}^{-3/2}$$

where R is the nominal stress ratio S_{min}/S_{max} .

The initial crack length a_i is taken as the crack length upon completion of the initiation phase. The threshold crack length a_{th} can be estimated from ΔK_{th} and ΔS according to Mattos and Lawrence (1977)

$$a_{th} \geq [1/(\pi A^2)] \Delta K_{th}^2 / \Delta S .$$

From a_{th} an approximation for a_i can be obtained. Alternatively, Lawrence, Ho and Mazumder (1981) suggested a_i could be obtained from

$$a_i = \frac{1.295 t^{0.5}}{A S_u} \text{ MPa} .$$

For the butt weld subjected to axial and bending stresses the stress intensity factor can be obtained by superimposing the above effects

$$\Delta K = \Delta K_A + \Delta K_B + K_R \quad (19)$$

where ΔK_A and ΔK_B are the stress intensity factors for axial and bending loading respectively. These factors can be written in terms of the axial and bending loads remote from the weld and in terms of the weld geometry and plate thickness (Lawrence, 1973)

$$\Delta K_A = \Delta S_A \sqrt{\pi a} f(c/t, \theta, \phi)$$

$$\Delta K_B = \Delta S_B \sqrt{\pi a} f(b/t, \theta, \phi) .$$

For an estimation of the residual stress intensity factor K_R Kanazawa, Oba and Machida (1961) suggested

$$K_R = \int_{-a}^a \sigma_r G dx$$

where G is given by

$$G = \left[\frac{2 \sin \pi(a+x)/w}{w \sin 2\pi a/w \sin \pi(a-x)/w} \right]^{0.5}$$

The actual shape of the distribution of the residual stress at the weld toe was obtained experimentally and reported earlier by the authors (Bellow, Wahab and Faulkner, 1984). In Fig. 2 the distribution has been idealized from experimental data and can be represented in non-dimensional form as

$$\epsilon_{ps} = (X + CDIFF)/HPI$$

where CDIFF is the distance between the center of the specimen and the center of the crack, X is the distance from the center of the crack to the intersection of the residual stress distribution and HPI a constant. The distribution of residual stress from $\epsilon_{ps} = -1$ to $+1$ can be taken as

$$\sigma_r = (S_y/2) \cos\{(\pi/2)\epsilon_{ps}\}.$$

For the straight line portion from $\epsilon_{ps} = 1$ to $W/2HPI$

$$\sigma_r = (\epsilon_{ps} - 1) \frac{\sigma_E}{W/(2HPI) - 1}$$

and from $\epsilon_{ps} = -1$ to $-W/2HPI$

$$\sigma_r = (\epsilon_{ps} + 1) \frac{\sigma_E}{W/(2HPI) - 1}$$

The above non-dimensionalized equations give the residual stress distribution along the toe of the weld. Numerical integration over the crack length was performed for K_R by using Simpson's Rule as the crack propagated from the initial crack length a_i to the final length a_f . Combining the effects of axial, bending and residual stress the intensity factor ΔK from equation (19) can then be solved.

The range of effective stress intensity factor can be written in terms of crack opening and the range of stress intensity as

$$\Delta K_{eff} = C_f \Delta K$$

The crack opening at any stress ratio can be expressed as

$$C_f(R) = \frac{\Delta K - \Delta K_{open}}{\Delta K} \quad \Delta K_{open} < \Delta K$$

$$\text{or} \quad C_f(R) = 0.4 \text{ to } 1.0 \quad \Delta K_{open} \geq \Delta K$$

$$\text{and} \quad C_f(R=0) \approx 0.5 \text{ for steel}$$

where $\Delta K_{\text{open}} = K_R + \Delta K_B + (S_{\text{max}} - S_{\text{op}}) f(c/t, \theta, \phi)$

where the crack opening stress S_{op} can be obtained from (Elber, 1976)

$$S_{\text{min}} = 1.25 [(1.6 S_{\text{max}} S_{\text{op}} - 0.79 S_{\text{max}})^{0.5} - 0.1 S_{\text{max}}].$$

From Socie (1975) the crack growth coefficient can be found from

$$C_R = C [C_f(R)/C_f(R=0)]^m$$

where C is the crack growth rate constant.

Theoretical Calculations

Fatigue lives of weldments were obtained by using the foregoing theoretical model. The K_f value was derived from Neuber's equation (5), using $\theta = 90^\circ$, $\phi = 45^\circ$ and $r = 0.025$ mm. The theoretical stress concentration factor K_t was computed from equation (4) for $A = 0.27$. The values of K_G and K_E were obtained for each level of S_{max} by using equations (8) and (9).

The effect of residual stresses initially and subsequent to the first cycle was accounted for by the modified Neuber's equations (13) and (14). The elastic, plastic and mean stress effects were calculated on a cycle for cycle basis until the cumulative damage law (equation (16)) was satisfied which led to the crack initiation life of the weld.

The crack propagation life was obtained from the crack growth rate constant C , crack growth exponent m and fracture toughness stress intensity factor K_f which were in turn determined from tests conducted on the base metal (BM) and weld metal (WM). The properties of the heat affected zone (HAZ) were assumed to be equivalent to those for the weld metal. The "adjusted material properties" were the average values between the properties of base metal and the weld metal. The total fatigue life was determined from the sum of the crack initiation and crack propagation phases.

EXPERIMENTAL

Comparison of Theory with Experiment

The experimental procedure, equipment, test specimens and measurement techniques have been described in a recent publication by the authors (Bellow, Wahab and Faulkner, 1984). In this recent publication the residual stress profiles were measured at the weld toes of butt welded specimens which had been subjected to a variety of surface peening and mechanical treatments. In the discussion below only the experimental results pertaining to crack initiation and crack propagation are shown.

In Fig. 3 the experimental fatigue results for an untreated butt weld are presented. Three theoretical solid lines are shown which were based on assuming the properties of the base metal, the weld metal and the average of the two. It is clear from Fig. 3 that the latter gives a better correlation with experiment and thus has been used in all subsequent comparisons.

Figure 4 shows the crack initiation and crack propagation lines for the untreated butt weld. It can be seen that at low stress ranges and for a life beyond 1.5×10^6 cycles the number of cycles to initiate a crack consumed the largest part of the total life whereas at lives less than 1.5×10^6 cycles the

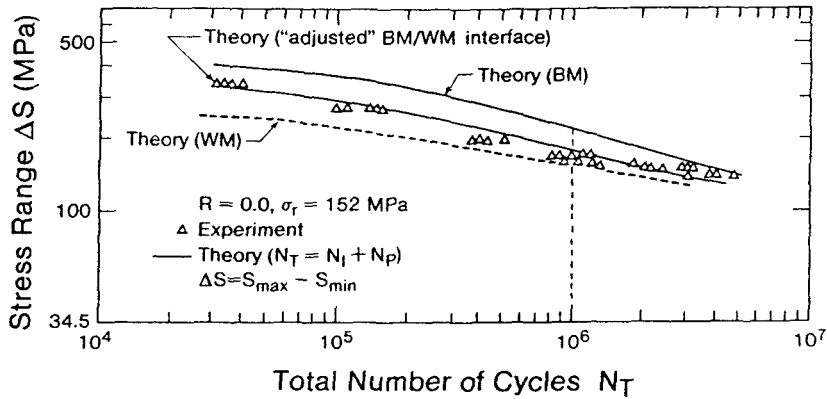


Fig. 3 Theory and experiment of as-welded specimens

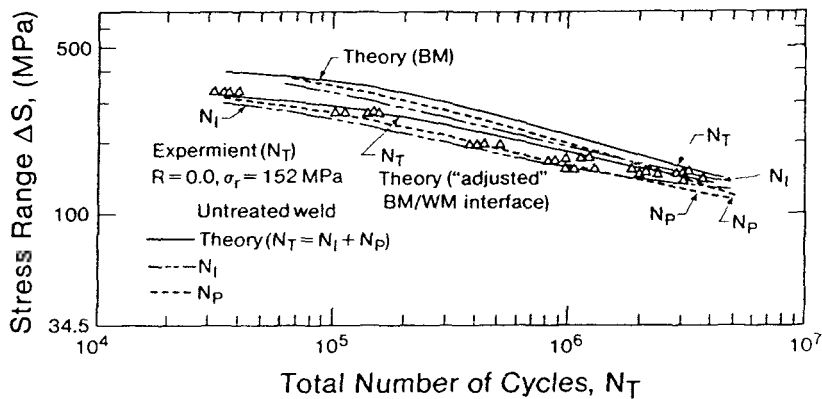


Fig. 4 Theory and experiment for crack initiation, crack propagation and total fatigue life for as-welded specimens

propagation phase was the larger. Figures 5 and 6 are plots of the nominal stress range ΔS as a function of the total life N_T for butt welded specimens which were subjected to a variety of surface treatments as indicated. For each case the residual stress at the toe of the weld was measured by x-ray diffraction and shown on the graphs. Overall the experimental results compared well with theory for residual stresses in the range of 14 MPa to -172 MPa.

From the experiments it was observed that the initiation phase was influenced by the cyclic material properties and loading history. This is illustrated in Fig. 7 where the initiation phase as a percentage of total life is plotted for the base metal, weld metal and heat affected zone metal. The initiation phase varied between 20 and 50 percent for the base metal, 20 to 60 percent for the weld metal and 25 to 50 percent for the HAZ in the cyclic range of 10^5 to 2×10^6 cycles. Although there was a variation in the percentages noted it is clearly evident that the crack initiation phase significantly contributed to the total fatigue life and cannot be ignored as has been reported by some in the literature.

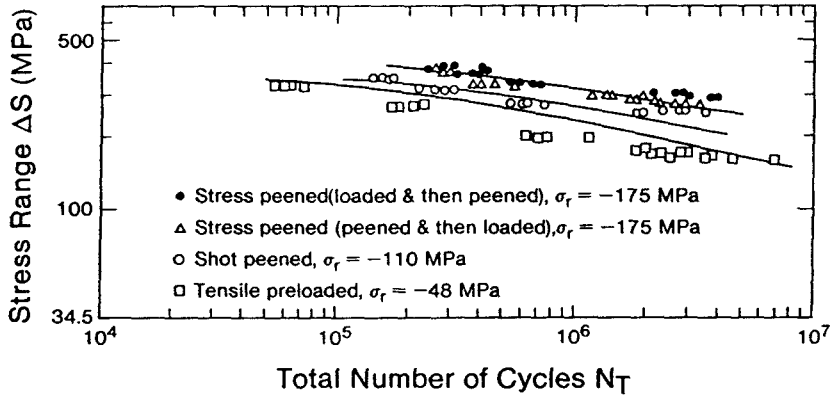


Fig. 5 Theory and experiment for stress peened, shot peened and tensile preloaded butt welded specimens

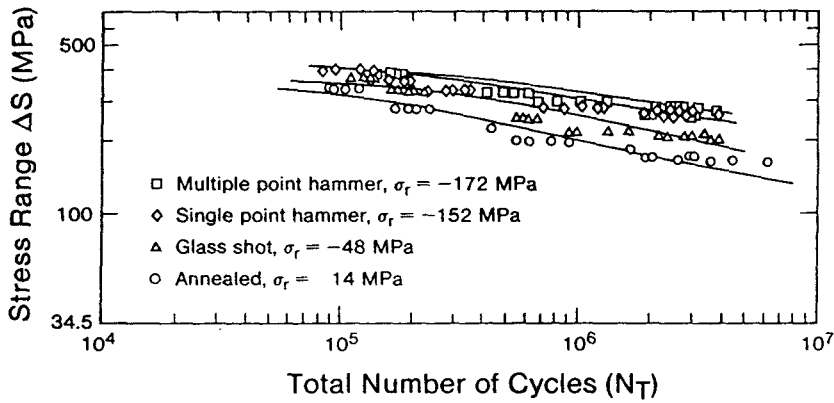


Fig. 6 Theory and experiment for annealed, glass shot, single point and multiple point peened butt welded specimens.

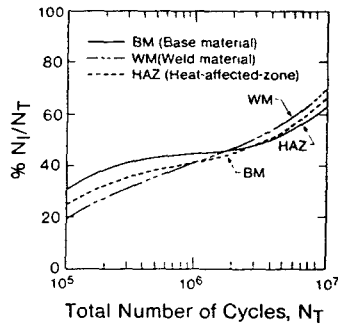


Fig. 7 Crack initiation as a percentage of total life for BM, WM and HAZ materials

SUMMARY

The estimation of the crack initiation phase was based on the work of Neuber and the crack propagation phase was based on the work of Forman. The combined effects of axial, bending and residual stresses were considered in determining the crack propagation phase. The results of these calculations were compared with experiments on butt welded specimens subjected to various kinds of surface and mechanical treatments.

It was found that the effect of residual stresses at the toe of a weld can be simulated by using elastic superposition of the residual stress and the elastic stress concentration factor and modification of Neuber's equation.

The resulting total life predictions based on "adjusted" (weld-parent interface) material properties were in close agreement with experimental results. The percentage error was within five percent for the as-welded condition at 10^6 cycles.

The ratio of crack initiation to total life was dependent on the cyclic and fatigue properties of the material and on the range of fatigue life under consideration.

ACKNOWLEDGEMENT

The authors wish to thank the Natural Sciences and Engineering Research Council (Canada) for the financial assistance received in support of this study under grants A-2705 and A-7514.

REFERENCES

- Basquin, O. H. (1910). The exponential law of endurance tests, *Proc. ASTM*, 10, 625-630.
- Bellow, D. G., M. Wahab and M. G. Faulkner (1984). Residual stresses and fatigue surface treated welded specimens. *Advances in Surface Treatments-II*, Pergamon Press, 85-94.
- Dixon, J. R., and J. S. Straunigan (1964). Effect of plastic deformation on the strain distribution around cracks in sheet materials. *Jour. Mech. Eng. Sci.*, 6 (2), 132.
- Elber, W. (1976). Equivalent constant amplitude concept for crack growth under spectrum loading. *ASTM STP 595*, 236-250.
- Forman, R. G., V. E. Kearney and R. M. Engle (1967). Numerical analysis of crack propagation in cyclic loaded structures. *Jour. Basic Eng.*, 89, 459-464.
- Garwood, S. J. (1978). Cumulative damage of welded structures. *Weld. Inst. Report*.
- Graham, J. A. (1968). *Fatigue Design Handbook*, SAE, 4 (3.2).
- Hammouda, M. M., R. A. Smith and K. J. Miller (1979). Elastic-plastic fracture mechanics for initiation and propagation of notch fatigue life. *Fat. of Eng. Mat'ls and Structures* 2, 139-154.
- Hardrath, H. F. and L. Ohman (1951). A study of elastic and plastic stress concentration factors due to notches and fillets in flat plates. *NACA Tech. Note 2566*.
- Higashida, Y., J. D. Burk and F. V. Lawrence (1978). Strain controlled fatigue behaviour of ASTM A36 and A514 grade F steels and 5083-O aluminium weld materials. *Weld. Jour.*, 57 (11), 334-344.
- Huang, W. C. (1972). Theoretical study of stress concentration of circular holes and inclusions of strain hardening materials. *Int. Jour. Solids and Structures* 2, 142-192.
- Irwin, G. R. (1960). Fracture testing of high strength steel materials under conditions appropriate for stress analysis. *NRL Report 5486*.

- Jhansale, H. R. and T. H. Topper (1973). Engineering analysis of the inelastic stress response of a structural metal under variable cyclic strains. *ASTM STP 519*, 246.
- Kanazawa, T., H. Oba and S. Machida (1961). *Soc. of Naval Architects of Japan Jour.*, 109, 359-369.
- Landgraf, R. W., J. Morrow and T. Endo (1969). Determination of the cyclic stress-strain curve. *Jour. of Mat'ls JMLSA*, 4 (1), 176.
- Lawrence, F. V. (1973). Estimation of fatigue crack propagation life in butt-welds. *Weld. Jour.* 52, 212.
- Lawrence, F. V., N. J. Ho and P. K. Mazumder (1981). Predicting the fatigue resistance of welds. *Annual Review Mat'ls Sci.* 11, 401-425.
- Manson, S. S. and M. H. Hirschberg (1964). *Fatigue an Interdisciplinary Approach*. Syracuse Univ. Press, New York, 1331.
- Martin, J. F. (1973). Fatigue damage analysis of irregular shaped structures subject to representative loads. *Fracture Control Program Report 10*, Univ. of Illinois.
- Mattos, R. J. and F. V. Lawrence (1977). Estimation of fatigue crack initiation life in welds using low cycle fatigue concepts. *S.A.E. SP424*.
- Miner, M. A. (1945). Cumulative damage in fatigue. *Jour. Ap. Mech.* 12 (3), 159-164.
- Morrow, J., and D. F. Socie (1981). The evolution of fatigue crack initiation life prediction methods. *Mat'ls. Exp. and Design in Fatigue*, Proc. of Fatigue '81, Univ. Warwick, 3-20.
- Neuber, H. (1961). Theory of stress concentration for shear strained prismatic bodies with arbitrary non-linear stress-strain law. *Jour. Ap. Mech.*, 65, 544-550.
- Palmgren, A. (1924). Die lebensdauer von kugellagern. *VDI Zeitschrift* 68 (14), 339-341.
- Reemsnyder, H. S. (1981). Evaluating the effect of residual stresses on notched fatigue resistance. *Matls. Exp. and Design in Fatigue*, Proc. of Fatigue '81, Univ. of Warwick, 273-295.
- Socie, D. F. (1975). Estimating the fatigue crack initiation and propagation lives in notched plates under variable loading histories. *TAM Report 417*, Univ. of Illinois.
- Stowell, E. Z. (1968). The calculation of fatigue life in the presence of stress concentrations. *Nucl. Eng. Design*, 8, 313-316.
- Topper, T. H., R. M. Wetzel and J. Morrow (1969). Neuber's rule applied to fatigue of notched specimens. *Jour. Matls.* 1 (4), 200-209.
- Topper, T. H. and A. Conle (1972). An approach to the analysis of the non-linear deformation and fatigue response of components subjected to complex service load histories. *Proc. Symp. of Exp. Mech.* Univ. of Waterloo, 419-422.
- Wetzel, R. M. (1968). Smooth specimen simulation of the fatigue behaviour of notches. *Jour. of Matls*, 3, 646-657.

An Apparatus to Study Thermal Fatigue

Donald G. Bellow
Professor
Dept. of Mechanical Engrg.
University of Alberta
Edmonton, Alberta, Canada

Introduction

The purpose of this paper is to describe an apparatus which can be used to study the thermal fatigue behaviour of metals. There are a number of ways in which thermal fatigue can be evaluated but all use essentially the same principle; that is, a test sample is clamped at the ends and a heat source is cyclically applied to the middle of the specimen between a maximum and minimum temperature until such time as a specimen breaks.

While there have been a number of electrically heated thermal fatigue systems used successfully these are costly and the thermal fatigue cycle is slow. It was desired to construct a low cost thermal fatigue apparatus which would closely model the conditions experienced in a gas fired heat treatment furnace.

Experimental Apparatus

A gas fired furnace was developed which is shown in schematic form in Fig. 1. The thread ended specimen was screwed tightly into the end fixtures which were held rigidly by the cross-heads of an Instron universal testing machine. In order to protect the cross heads and the load cell, water jackets were placed on either side of the specimen. This also had the effect of keeping the specimen ends cooled so that the yield stress in this area would not be affected by temperature and lead to

premature failure of the specimens in the threads.

A temperature controller was connected to an infrared thermometer aimed at, but remote from, the center of the specimen. The thermal cycle was started by igniting the two gas jets causing the temperature of the specimen to rise rapidly to a preset limit in the controller which then shut off the jets. Cold air (ambient temperature) was then directed at the specimen causing it to quickly cool. The temperatures versus time as well as load versus time was recorded. When the lower preset temperature was reached the gas jets were automatically re-ignited and the process was continued until a specimen failed.

Test Results

A typical load versus temperature curve is shown in Fig. 2. This was observed after a few cycles occurred and after the thermal upsetting had stabilized. This figure shows that upon heating the specimen relaxes with the load dropping off to zero at 810°C. Further heating puts the specimen into compression, because of the end constraints. Upon cooling, the specimen begins to contract and the load passes through zero at 565°C where upon it begins to go into tension.

For this study it was believed that the

stress at the maximum and minimum temperatures were critical and that the alloys tested should be compared on this basis. The stress shown in Fig. 3 was calculated at the narrowest cross-section adjacent to the thermally upset portion at the center of the specimen.

For the alloys tested the chromium content ranged between 17.6 and 22.2% whereas the nickel varied between 4.5 and 36.8%. Specimen A, with a combination of 4.5% Ni and 4.25% Co, gave better thermal fatigue life than did Specimen B which had 8% Ni and 0% Co. Specimen D which had 36.81% Ni and 17.76% Cr was the poorest. Although the tests are based on only a few alloys it appeared that additional nickel did not lead to better thermal fatigue life.

Summary

The results of this testing program have shown that the testing apparatus described can be used successfully to determine the thermal fatigue life of high temperature alloys. In particular, it has been shown that differences can be detected in the thermal fatigue life of five different alloys and that a high nickel content, does not in itself, yield improved thermal fatigue characteristics.

Acknowledgements

The author expresses appreciation to Stelco Inc. for permission to use the data in this report and to Mr. John Foy of the Mechanical Engineering Department who assisted in the experimental program.

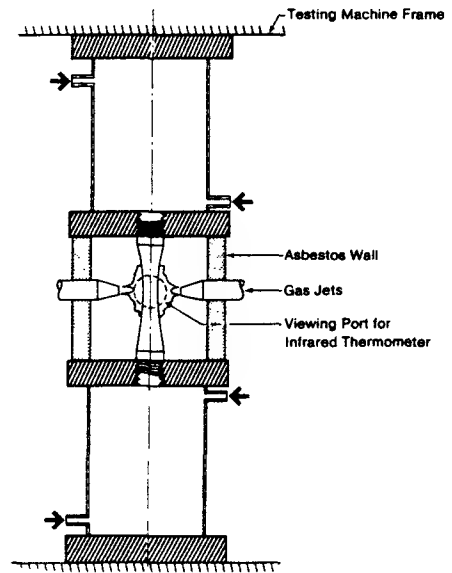


Fig. 1 Thermal Fatigue Apparatus

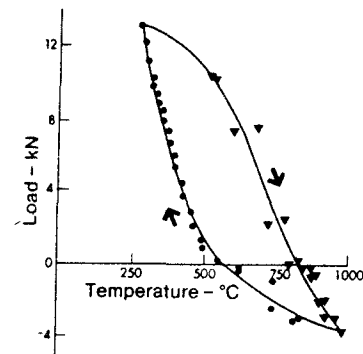


Fig. 2 Thermal Fatigue Cycle

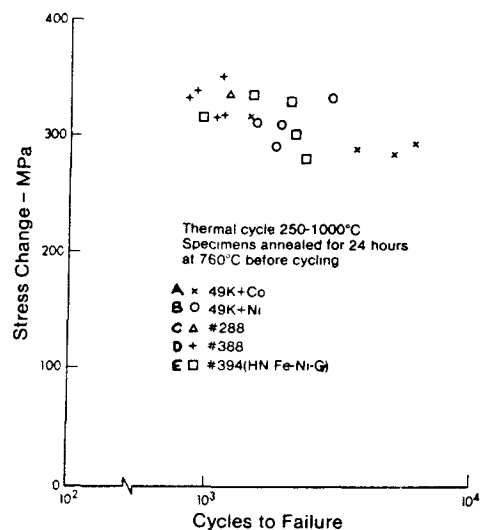


Fig. 3. Thermal Fatigue Life of Five Alloys



**University of Alberta
Edmonton, Canada**



**Maschinenfabrik Augsburg Nurnberg
Nurnberg, West Germany**

On the Selection of Materials for Cold Temperature Service

**Donald G. Bellow
Eugene F. Klotzbucher
Hans E. Kraft**

**Reprinted from Proceedings of 1985 SEM
Spring Conference on Experimental Mechanics
June 1985, pp 428 – 434**

ON THE SELECTION OF MATERIALS FOR COLD TEMPERATURE SERVICE

Donald G. Bellow¹
Eugene F. Klotzbücher²
Hans E. Kraft³

Abstract:

This paper describes the results of two parallel testing programs to assess the suitability of steels used for materials handling equipment under conditions of low temperatures. This involved comparing the transition temperatures established on Charpy V-notch specimens with nil ductility transition temperatures. The influence of the thickness of the materials was studied. Finally, impact test results are presented for full-size sections.

Introduction:

Manufacturers of equipment for use in Arctic regions are confronted with special problems in selecting suitable materials. Conventional stress-bearing steel structures and mechanical equipment tend to suffer a critical loss of toughness at decreasing temperatures. Plain and low-alloy structural steels may therefore fail due to brittle fracture under certain conditions.

A measure of the "toughness" of a material is generally provided by the energy absorbed in the notched-bar impact test. The standards of various countries specify different specimen sizes and notch shapes for the notched-bar impact test which makes it difficult to compare test results. While the Charpy V-notch test according to ASTM E23-81 (1981) has found increasing acceptance, all types of specifications have in common that the energy absorbed varies with the test temperature according to a characteristic curve. Associated with this transition temperature is the susceptibility of the steels to brittle fracture.

A very common problem is that brittle fracture may occur at stress levels that are far below the yield point. In calculating the stresses it is usual practice to determine only those stresses that result due to the action of the loads arising during the operation of the component. Stress concentrations at discontinuities, stresses due to temperature differences and residual stresses are often neglected. It is possible in combination with the operating stresses that plastic deformation can occur which has not been accounted for. However, the material is capable of accommodating plastic deformation only if it still has sufficient ductility, i.e. toughness. Special care is required in the design, engineering and manufacture as well as during inspection to avoid notch effects and faults that are liable to provide a source of brittle fracture (Pense, 1984).

This paper describes tests carried out by the manufacturer, Maschinenfabrik Augsburg-Nürnberg AG (M.A.N.) in collaboration with the University of Alberta to provide the basis for the selection of materials to be used in the construction of materials handling equipment for use in the northern climates of Canada.

Fracture studies:

A vast amount of work on the fracture behaviour of materials has been published in recent decades. Mention may be made of the pioneering work published by Robertson (1953) and Wells (1956, 1963) in the U.K. and by Pellini and Puzak (1954, 1958, 1962, 1963) in the U.S.A. on crack arrest and crack initiation. Further references will be found in ASTM E208 (1969).

On the strength of previous experience, M.A.N. preferably uses the drop weight test to determine the nil ductility transition temperature (NDT-temperature) according to ASTM E208-69 (1969) for the investigations. The NDT-temperature determined in this test is defined as the temperature below which brittle fracture is

¹Professor of Mechanical Engineering, University of Alberta, Edmonton, Alberta, Canada

²Dipl. Eng., Head of Metallurgy Department, Maschinenfabrik, Augsburg, Nürnberg, West Germany.

³Dipl. Eng. Maschinenfabrik, Augsburg, Nürnberg, West Germany

liable to occur and propagate. However, the NDT test is relatively costly and one which cannot be applied to all material thicknesses. Therefore, an attempt was made to establish a correlation between the drop weight test and the conveniently made notched-bar impact test using the Charpy V-notch (CVN) specimen according to ASTM E23-81 (1981). In addition, drop weight tests were made on notched and unnotched full-size lengths of thin-walled U-sections for vehicle frames. Again in this case, an attempt was made to establish a correlation with the notched-bar impact test.

Test program:

Comparative studies were made by M.A.N. and the University of Alberta (U.A.) on German materials that are customarily used in the construction of materials handling equipment such as bucket wheel excavators and conveyor belt transporters. The materials included plates made of fine-grain structural steels for steel fabrication, forged round bars (plain and low-alloy) and cast steel (plain and low-alloy) used mechanical equipment. The materials tested are shown in Table 1 which indicates the mechanical properties and the chemical compositions.

Tab. 1 German steels evaluated Joint program M.A.N. - University of Alberta

Designation	Name	Standard	Condition	Type	Diameter (D) or Thickness (T) (mm)	Yield Strength (MPa)	Tensile Strength (MPa)	Chemical Composition										
								(in weight %)										
A	TTSE28	DIN 17 102	Normalized	plate	20 T	320	430	0,08	0,24	1,27	0,025	0,01	-	-	-	0,05 ³⁾	-	-
B	TTSE36	DIN 17 102	Normalized	plate	20 T	402	536	0,15	0,37	1,47	0,017	0,009	-	-	-	0,035	0,042	-
C	28CrMo4	SEW 680 ⁴⁾	Q + T ¹⁾	round bar	200 D	478	656	0,27	0,22	0,76	0,02	0,014	1,11	0,23	-	-	-	-
D	42CrMoS4	DIN 17 200	Q + T	round bar	200 D	550	756	0,43	0,35	0,57	0,019	0,021	1,14	0,17	-	-	-	-
E	34CrNiMo6	DIN 17 200	Q + T	round bar	400 D	697	883	0,37	0,28	0,54	0,01	0,007	1,54	0,26	1,55	-	-	-
F	17CrNiMo6	DIN 17 210	2)	round bar	350 D	608	1010	0,18	0,23	0,56	0,009	0,032	1,69	0,27	1,47	-	-	-
G	Ck45	DIN 17 200	Normalized	round bar	100 D	358	659	0,49	0,25	0,72	0,007	0,012	-	-	-	-	-	-
H	GS-52.3	DIN 1681	Normalized	casting plate	80 T	334	569	0,31	0,53	0,83	0,006	0,009	0,12	0,02	0,06	-	-	-
I	GS-28CrMo4	SEW 685 ⁴⁾	Q + T	casting plate	100 T	461	641	0,26	0,42	0,70	0,004	0,011	1,04	0,26	0,06	-	-	-
J	GS-34CrNiMo6	SEW 515 ⁴⁾	Q + T	casting plate	150 T	697	871	0,32	0,48	0,64	0,007	0,01	1,5	0,21	1,5	-	-	-
K	GS-42CrMo4	SEW 510	Q + T	casting plate	100 T	474	711	0,41	0,53	0,81	0,005	0,01	1,12	0,26	0,07	-	-	-

1) Quenched and tempered

2) Heat treated corresponding to case hardening

3) Also 0.05 V

4) Stahl-Eisen-Werkstoffblatt

At M.A.N. the transition temperatures of CVN specimens were determined on the basis of three specimens per temperature. The transition temperature was defined according to two different criteria, energy absorption of 27 J (TT 27), and fracture appearance transition temperature (FATT 50). Also drop-weight tests were conducted according to the Pellini test where six specimens were used in each case to determine the nil ductility transition temperature (NDTT). The microstructure was examined in the regions where the specimens were broken. At the University of Alberta the transition temperatures by means of the Charpy V-notch were determined both by evaluating the energy absorption at 27 J and by measuring the lateral expansion of the fractured specimens as well as FATT 50. A minimum of three specimens were evaluated per temperature.

The notched-bar specimens were cut as longitudinal specimens directly under the plate surface in the case of plates and at a depth of 1/6 of the material thickness in the case of forgings and castings. The drop weight specimens were also prepared as longitudinal specimens cut at the surface in the case of plates and castings and at a depth of 1/6 of the material thickness in the case of forgings.

With increasing sizes of forgings, the transition temperatures tend to rise owing to the lesser penetration of heat treatment. With a view to obtaining more information on this effect, notched-bar specimens were cut from forgings with different cross-sections at a depth of 1/6 of the material thickness and the transition temperatures were determined by means of CVN specimens. The material properties used in this study are shown in Table 2.

Drop weight tests were performed on full size U-sections commonly used in vehicle frames. Three micro-alloyed steel grades were evaluated, one being in the normalized state and two in a thermo-mechanically treated state. The material properties are given in Table 3. The dimensions of the U-sections tested were 70 x 265 x 7.8 mm, and a test length of 1.5 m. Notches in the test pieces were made by cutting with a 45° milling cutter to a depth of 4.6 mm and additionally applying a sharp-edge Schnadt notch to a depth of 5 mm. The load was applied by means of a drop weight with an energy of 4000 Nm. Figure 1 shows the shape of the specimen with the notch and the test setup. The temperatures at which the fracture changed from ductile to brittle was determined as the transition temperature between the mode where a crack was arrested and the mode where the crack continued until complete failure of the test piece occurred.

For a supplementary assessment CVN specimens, with the specimen width reduced according to the plate thickness, were cut from the U-sections and the transition temperatures determined. Due to the small plate thickness of 7.8 mm, a transition temperature at an energy absorption of 50% of that measured on the upper shelf was defined (TT 50%) instead of the FATT 50.

Tab.2 German steels for testing the influence of material thickness

Designation	Name	Standard	Condition	Type	Diameter (D) or Thickness (T) [mm]	Yield Strength [MPa]	Tensile Strength [MPa]	Chemical Composition [in weight %]							
								C	Si	Mn	P	S	Cr	Ni	Mo
S	42CrMoS4	DIN 17 200	Q + T ¹⁾	round bar	50 D	750	875	according to Standard							
				round bar	120 D	610	820								
				round bar	270 D	550	780								
				bar	220 T	535	760								
T	34CrNiMo6	DIN 17 200	Q + T	round bar	50 D	830	955	according to Standard							
				round bar	120 D	830	970								
				bar	200 T	630	820								
				round bar	400 D	695	880								
U	16MnCr5	DIN 17 210	2)	round bar	100 D	600	850	0,20	0,29	1,21	<0,025	0,025	0,88	—	—
				round bar	250 D	465	720	0,19	0,25	1,11	<0,025	0,012	0,98	—	—
V	17CrNiMo6	DIN 17 210	2)	round bar	100 D	870	1115	0,18	0,33	0,48	<0,025	0,022	1,68	1,7	0,32
				round bar	250 D	760	1000	0,18	0,32	0,50	<0,025	0,010	1,68	1,6	0,32
				round bar	350 D	680	1005	0,18	0,23	0,56	<0,025	0,032	1,68	1,47	0,27

1) Quenched and tempered

2) Heat treated corresponding to case hardening

Tab.3 Steels for impact test on full-size profiles

Designation	Name	Condition	Type	Thickness [mm]	Yield Strength [MPa]	Tensile Strength [MPa]	Chemical Composition								
							C	Si	Mn	P	S	Ti	Nb	V	Al
							[in weight %]								
W	PAS 42 ¹⁾	TM ³⁾	plate	7,8	445	515	0,07	0,35	0,94	<0,025	0,011	—	0,025	—	0,03
X	Alform 43 ²⁾	N ⁴⁾	plate	7,8	440	555	0,14	0,24	1,24	<0,03	<0,03	0,10	0,02	—	0,014
Y	PAS 55 ¹⁾	TM	plate	7,8	565	640	0,07	0,38	0,85	<0,025	0,014	0,2	—	0,05	0,07
¹⁾ Trade mark Thyssen AG							³⁾ Thermomechanical treatment								
²⁾ Trade mark Voest Alpine							⁴⁾ Normalized								

1) Trade mark Thyssen AG

2) Trade mark Voest Alpine

3) Thermomechanical treatment

4) Normalized

Test results:

Both laboratories at M.A.N. and U of A determined the transition temperatures for an energy absorption of 27 J (TT 27) as well as FATT 50. The results are shown in Table 4 as well as in Fig. 2. Satisfactory agreement did not appear to exist in all cases. For TT 27 this applied especially to the 17CrNiMo6 steel (F). However, it can be seen from Fig. 3 that the intersections of the transition temperature curves and the 27 J straight line are on the lower flat end of the curves. It is here where small differences in the curve pattern have a pronounced effect on the temperature. The GS-52.3 steel (H) was studied as an example of a steel where differences in the readings of the two laboratories were small. In this case, the intersections with the 27 J straight lines occurred in the steeper part of the curves. The test points indicated represent the mean of only three specimens. One of the reasons for the wide scatter of the readings in the case of TTStE 36 plate (B) appeared to be in the irregular micro-structure (ferrite-pearlite banding) observed.

Tab.4 Notched bar impact test results Comparative tests M.A.N./U.A.

Designation	TT 27 [°C]		ΔT [K]	FATT 50 [°C]		ΔT [K]
	results M.A.N.	results U.A.		results M.A.N.	results U.A.	
A	-86	< -60	—	-85	< -60	—
B	-69	(-64)	5	-58	-29	29
C	-88	(-78)	8	-22	-22	0
D	-7	-10	3	+35	(+28)	7
E	-83	(-73)	10	-44	-26	18
F	-40	-22	18	+5	+7	2
G	+33	(+34)	1	(+55)	> 20	—
H	-1	+5	6	+50	(+25)	25
I	-28	-26	2	+10	+8	4
J	-38	-30	8	-21	-15	6
K	+41	(+35)	6	(+85)	> 20	—

() extrapolated, outside test temperature range

Table 5 shows a comparison of the transition temperatures and the NDT temperatures. For the purpose of a comparison with the measured NDT temperatures, it was decided to use the mean values of the CVN transition temperatures obtained in the tests made by the two laboratories. In Fig. 4, the TT 27 has been plotted versus the NDT temperature and in Fig. 5 the FATT 50 versus the NDT temperature. This graph shows that if all the test points are considered there is unsatisfactory agreement between the TT 27 and the NDT temperature and between the FATT 50 and the NDT temperature. The scatter is too great to merit the use of the curves in

practice. If however, the three groups of plates, forged parts and steel castings are considered separately, there is a satisfactory correlation. Exceptions are the two plate materials TTStE 26 (A) and TTStE 36 (B) which, for the same NDT temperatures, showed a distinct difference in the CVN transition temperatures. This is well illustrated in Fig. 6. It is obvious from this that the energy absorption in the CVN test at the NDT temperatures is higher for those materials with greater energy absorption on the upper shelf. In the case of steels with values of more than 100 J on the upper shelf, the NDT temperatures increasingly diverged from those obtained at the intersection of the 27 J straight line and the transition temperature curves.

Tab.5 Comparison of TT 27 Joule and FATT 50 transition temperature with NDT-temperature

Designation	TT 27 [°C]		FATT 50 [°C]		Mean Value M.A.N./U.A		NDT-Temp [°C]
	results M.A.N	results U.A	results M.A.N	results U.A	TT 27 [°C]	FATT 50 [°C]	
A	-86	< -60	-85	< -60	-	-	-45
B	-69	(-64)	-58	-29	-67	-44	-45
C	-86	(-78)	-22	-22	-82	-22	-35
D	-7	-10	+35	(+28)	-9	+32	+10
E	-83	(-73)	-44	-25	-78	-35	-40
F	-40	-22	+5	+7	-31	+8	-20
G	+33	(+34)	(+55)	> 20	+34	-	+10
H	-1	+5	+50	(+25)	-3	+50	-20
I	-28	-26	+10	+6	-27	+8	-30
J	-38	-30	-21	-15	-34	-18	-40
K	+41	(+35)	(+65)	> 20	+38	-	+15

Figure 7 shows the influence of the diameter on the transition temperature TT 27. The transition temperatures of the case-hardening steels 16MnCr5 (U) and 17CrNiMo6 (V) heat treated corresponding to case hardening did not depend significantly on the diameter in the thickness range investigated. The transition temperatures were relatively high. In the case of the two heat-treatable steels 42CrMoS4 (S) and 34CrNiMo6 (T), the influence of the diameter was also relatively small in the case of steel T, but with distinctly lower transition temperatures. In contrast to this, the influence of the diameter was pronounced in the case of steel S. In general, its suitability for use at low temperatures is limited to relatively small diameters.

For the case-hardening steels 16MnCr5 (U) and 17CrNiMo6 (V), micrographs were taken at the locations where the notched-bar specimens (1/6 diameter) had been cut as well as from the centre of the cross section. It was found that there was practically no difference in the microstructure of the two steels over the cross section. Whereas the microstructure of steel U consisted of coarse-grain ferrite and pearlite with fractions of upper bainite, steel V consisted of bainite with small fractions of ferrite. This explains the lower transition temperatures observed in the case of steel V.

In the case of the heat-treatable steels 42CrMoS4 (S) and 34CrNiMo6 (T), the micrographic specimens were taken only at 1/6 the diameter. At 50 mm diameter, steel S showed a very fine bainite structure. At 270 mm diameter, however, fairly coarse bainite with embedded ferrite could be observed. This microstructure was probably responsible for the unsatisfactory transition temperature. Steel T showed very fine grained bainite up to 200 mm diameter. Only with 400 mm diameter was there a noticeable coarsening of the bainite which, however, had not yet led to a noticeable deterioration of the transition temperature. These findings confirm the observations of Habraken and Economopoulos (1967) and Piehl (1978) that transition temperatures tend to improve as faster cooling rates are applied and transformation as plotted in the TTT diagram shifts from ferrite/pearlite via upper bainite to lower bainite and martensite.

The results obtained from impact tests of full size U-sections are presented in Fig. 8. It was found that when the steels PAS 42 (W) and Alform 43 (X) with comparable strength were compared, the normalized Alform 43 (X) showed a better transition temperature behaviour from the drop-weight test than the thermo-mechanically treated steel PAS 55 (Y). The higher strength thermo-mechanically treated steel PAS 55 (Y) compared favorably with the PAS 42 (W) in respect of the transition temperature. Comparing the transition temperatures TT 27 and TT 50%, a different picture was obtained. Here, the thermo-mechanically treated steel W showed the lowest transition temperature TT 27 as well as the lowest TT 50%. These tests failed to establish a sufficiently accurate correlation between the drop-weight test transition temperature and the transition temperatures obtained in the notched-bar impact test. The latter can be looked upon only as a guide.

Discussion:

The results of the tests carried out in parallel in the two laboratories showed relatively good agreement. The maximum difference for TT 27 was 18°C in a single case. As regards the FATT 50, the maximum deviation was slightly higher in two cases at 29°C and 25°C. However, here there was a pronounced scatter of the test results in the transition temperature range.

In order to permit a comparison of the transition temperatures of the same steels, but from different

melts, it was found that for the 34CrNiMo6 steel between specimens T and E there was excellent agreement, whereas there was wide scatter in comparing specimens S and D for the 42CrMoS4 and for comparing specimens V and F for the 17CrNiMo6 steels.

The agreement of the transition temperature TT 27 as determined in both laboratories with the NDT-temperature was sufficient for a preliminary selection of the steels for use at low temperatures. This was only true, however, if the forged bars and steel castings were considered separately. Exceptions were the two plate materials TTStE26 (A) and TTStE36 (B) where no clear correlation was discernible.

The results of an appraisal of the steels tested for their suitability to meet an NDT-temperature of - 40°C indicated that the case-hardening steel 17CrNiMo6 (F), the plain steels Ck45 (G) and GS-52.3 (H) as well as the alloyed cast steel GS-42CrMo4 (K) failed to meet this requirement. The use of the other steels is limited owing to the varying degree to which they are amenable to through quenching and subsequent tempering. If larger thicknesses are called for in practice, heat treatable steels with a higher content of nickel have to be used.

Owing to the heat treatment, case-hardening steels 16MnCr5 (U) and 17CrNiMo6 (V,F) will not afford such low transition temperatures as would be adequate for safety against fracture at low temperatures. It is customary practice, though, for gear units to be equipped with a heating system in order to maintain sufficient lubrication so that the operating temperature would always be distinctly above the ambient temperature.

In studying the low-alloy CrMo steels it was noted that the 42CrMoS4 (D,K) steels with higher carbon contents had less favourable transition temperatures than the 26CrMo4 (C,I) steels with lower carbon contents. This cannot be explained on the strength of light-optical microstructures and has been attributed to an enhanced precipitation density of carbides (Meyers,1977).

The materials used for the full-size U-profiles tested are suitable without any qualification for the range of operating temperatures considered in this investigation.

Acknowledgements:

The authors express their appreciation to Thyssen AG and Voest Alpine for their assistance in conducting the drop-weight tests on full-size profiles and to D. Pridie and R. Carlson for the work carried out at the University of Alberta.

References:

- ASTM Standard E 208-69, (1969). Standard method for conducting drop-weight-test to determine nil ductility transition temperature of ferritic steels. Annual Book of ASTM-Standards, Part 10.
- ASTM Standard E23-81, (1981). Notched bar impact testing of metallic materials.
- Baumgardt, H., Rohde, M., Schulz, L., (1982). Herstellung und mechanische Eigenschaften von thermomechanisch gewalzten Grobblechen. Thyssen Techn. Berichte, Heft 2.
- Habraken, L.I., Economopoulos, M., (1967). Bainitic microstructures in low-carbon alloy steels and their mechanical properties. Symposium Transformation and Hardenability in Steels, University of Michigan.
- Meyer, L., de Boer, H., (1977). Überblick über hochfeste niedriglegierte Stähle. Thyssen Technische Berichte 1.
- Pellini, W.S. Eschbacher, E.W., (1954). Ductility of weld metal. Weld J. 33(1), 165-205.
- Pellini, W.S., Puzak, P.P., (1963). Fracture analysis diagram. Procedures for the fracture safe engineering design of steel structures. NRL-Report 5920.
- Pense, A.W. (1983). Factors controlling fracture behaviour of cold temperature structures. Proceedings of the Study Session on Fracture Toughness Evaluation of Steels for Arctic Marine Use, CANMET, Ottawa.
- Piehl, K.H. (1978). Einflub von chemischer Zusammensetzung und Gefüge auf die Eigenschaften von Nickel-Chrom-Molybdän-Vanadin-Vergütungsstählen für schwere Schmiedestücke, besonders für Niederdruck-Turbinen- und Generatorwellen, Stahl und Eisen 95.
- Puzak, P.P., Babecki, A.I., Pellini, W.S., (1958). Correlation of brittle-fracture service failures with laboratory notch-ductility tests. Weld. J. 37 (9), pp. 391-410.
- Puzak, P.P., Pellini, W.S., (1962). Standard method for NRL-drop-weight-test. NRL-Report 5831.
- Robertson, T.S. (1953). Propagation of brittle fracture in steel. J. Iron Steel Inst., 12, pp. 361-374.

Wells, A.A. (1956). Experiments on the arrest of brittle cracks in 36 in. wide steel plates. Brit. Weld. J., 3 (11).

Wells, A.A. (1961). Brittle fracture in welded structures. A contemporary view. Weld. Metal Fabr., 29, pp. 89-94.

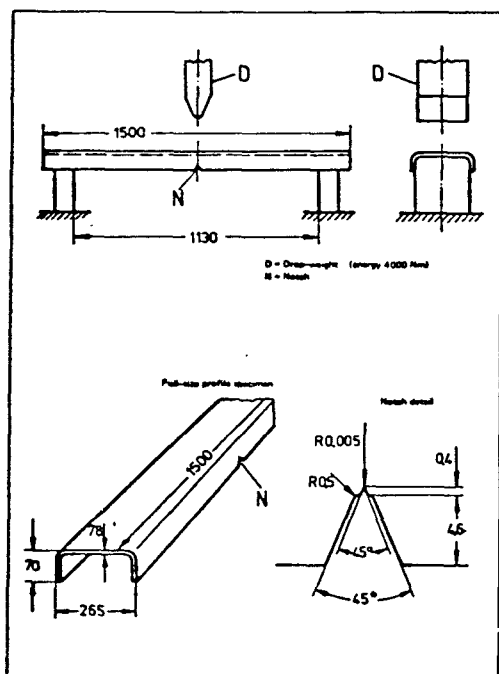


Fig. 1 Full-size profile specimen and jig for impact tests

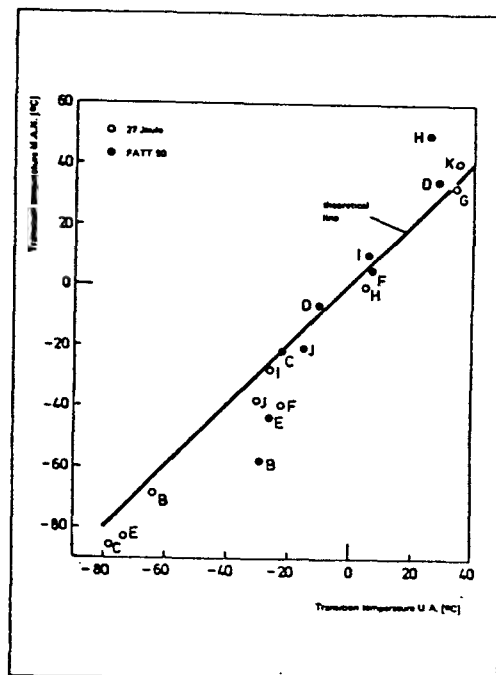


Fig. 2 Comparison between M.A.N. and U.A. notched bar impact test results

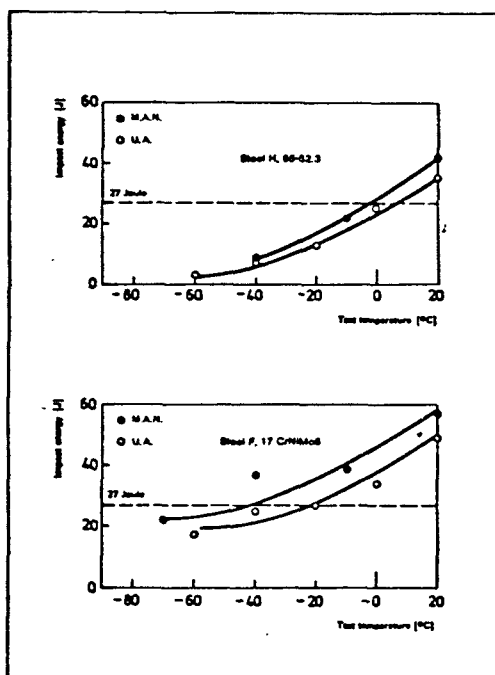


Fig. 3 Transition temperature curves for different steels

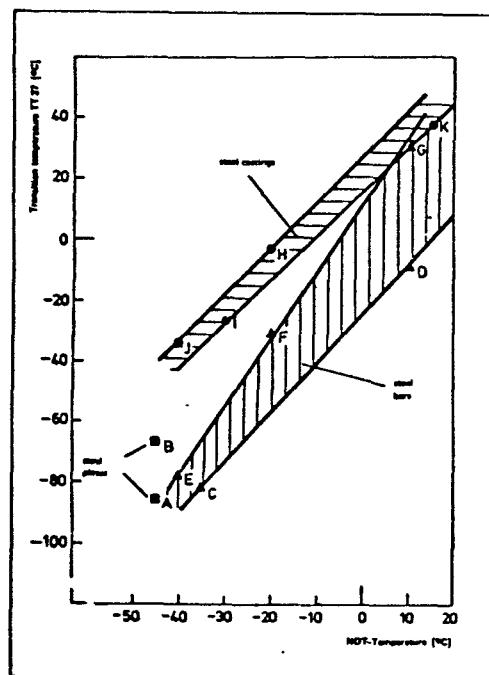


Fig. 4 Comparison between transition temperature TT 27 and NDT-temperature.
German Stahl

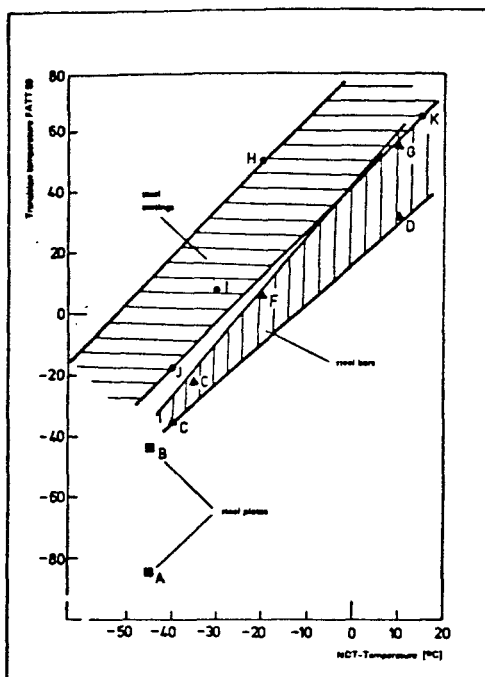


Fig. 5 Comparison between transition temperature FATT 50 and NT-temperature, German steels

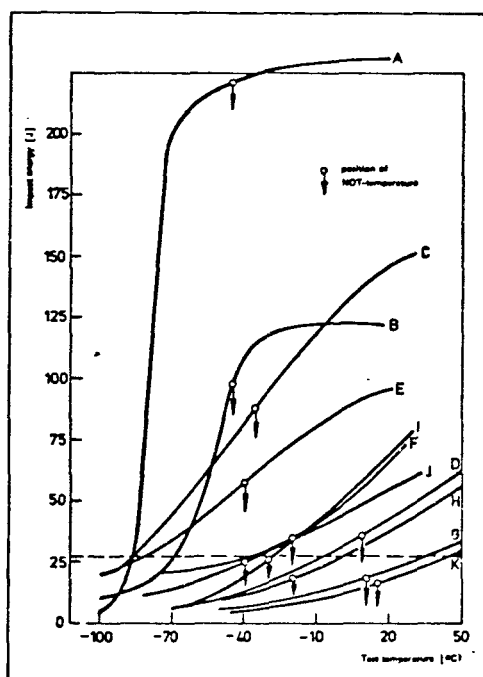


Fig. 6 Impact energy (CVN-specimen) at NDT-temperature

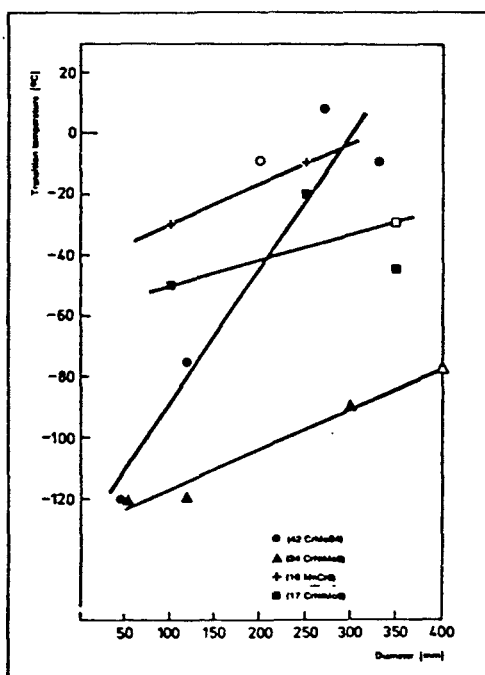


Fig. 7 Effect of material diameter on transition temperature TT 27

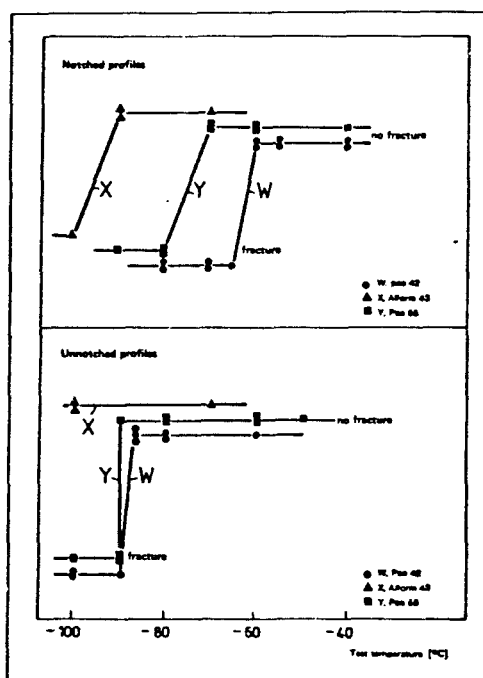


Fig. 8 Full-size profiles of drop-weight transition temperature

THE EFFECT OF MATERIAL THICKNESS ON FRACTURE TOUGHNESS

D.G. Bellow, Professor

Department of Mechanical Engineering
University of Alberta
Edmonton, Alberta, Canada

E.F. Klotzbucher and H.E. Kraft

Maschinenfabrik Augsburg-Nürnberg, A. G.
Nürnberg, West Germany

ABSTRACT

This paper discusses the influence of material thickness on the transition temperature as determined by Charpy V-notch testing. A variety of low alloy steels were evaluated and the CVN results compared with the nil ductility transition temperatures. A method is shown for estimating the maximum possible thickness or diameter to ensure a NDT of -40°C . A second study compared CVN results to full scale tests on U-profile steel sections. It was concluded, for the microalloyed steels tested, that there was no effective correlation between CVN results and full scale tests and that, for assurance, full scale tests are warranted.

INTRODUCTION

In designing equipment for low temperature service for the Arctic or offshore special attention must be given to the selection of materials for fracture resistance as well as to the fabrication techniques employed in the application of these materials.

In determining the fracture characteristics for materials a number of standards are available in which the applicable testing procedures are described. For reasons of economy normally small size specimens which have been machined from full size components are tested. The most common small specimen is the Charpy V-notch specimen according to ASTM:E23-81 [1]. However, the results obtained with this test have no direct relation with the fracture behaviour of full size components. From experience it has been found that the drop weight test as proposed by Pellini and set out in ASTM:E208 [2] is suitable in this way. In this test the nil ductility transition temperature (NDTT) is defined as the temperature below which brittle fracture is liable to occur and propagate. This test, however, is relatively costly. Thus, it is desirable to find a relationship between the NDT temperature and the simple notch impact test (CVN). The transition temperature of the notched impact test and the NDT temperature are each dependent on the microstructure of the material, and for quenched and tempered steels, also dependent on the thickness of the material.

This paper describes a study which undertook to evaluate the effects of material thickness on the CVN transition temperature and the nil ductility transition temperature (NDTT) for forgings and castings from different low alloyed steels. A second study investigated the results of full scale impact tests on truck U-profile underframe members. These results are also compared with CVN data.

EXPERIMENTAL PROCEDURE

Influence of Material Thickness on Transition Temperature of Forgings

In order to determine the influence of material thickness of forged bars on the transition temperature, CVN specimens were cut from forged bars with different cross sections at a depth of $1/6$ of the material thicknesses as shown in Fig 1. Specimens were machined and tested according to ASTM:E23-81 [1] and the transition temperature determined at an energy absorption of 27 J (TT27). Also, the fracture appearance transition temperature (FATT 50) was measured from the broken Charpy specimens. Three specimens were tested per temperature with specimens tested down to -100°C .

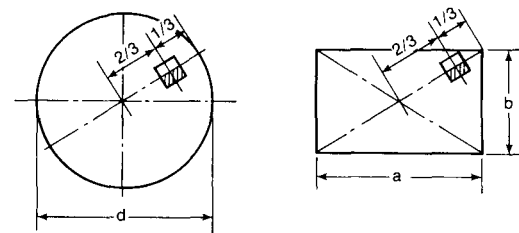


Fig. 1 Location of impact specimens in the cross section

Table 1 Composition and details of materials tested

Designation	Name	Standard	Condition	Type	Diameter D or Thickness T mm	Yield Strength MPa	Ultimate Strength MPa	Chemical Composition (in weight %)										
								C	Si	Mn	P	S	Cr	Mo	Ni	N _B	Al	
A	TTS26	DIN17102	normalized	plate	20T	320	430	0.08	0.24	1.27	0.025	0.01	—	—	—	0.05 ³	—	
B	TTS36	DIN17102	normalized	plate	20T	402	536	0.15	0.37	1.47	0.017	0.009	—	—	—	0.035	0.042	
C	26CrMo4	SEW680 ⁴	Q & T ¹	round bar	200D	478	656	0.27	0.22	0.76	0.02	0.014	1.11	0.23	—	—	—	
C1	26CrMo4	SEW680	Q & T	round bar	100D	468	628	0.27	0.32	0.72	0.006	0.025	1.06	0.17	—	—	—	
D	42CrMoS4	DIN17200	Q & T	round bar	200D	550	756	0.43	0.35	0.57	0.03	0.021	1.14	0.17	—	—	—	
D1	42CrMoS4	DIN17200	Q & T	round bar	100D	761	932	0.45	0.30	0.67	0.024	0.033	1.09	0.20	—	—	—	
E	34CrNiMo6	DIN17200	Q & T	round bar	400D	697	883	0.37	0.28	0.54	0.01	0.007	1.54	0.26	1.55	—	—	
E1	34CrNiMo6	DIN17200	Q & T	round bar	200D	715	886	0.34	0.30	0.53	0.013	1.7	0.23	1.56	—	—	—	
F	17CrNiMo6	DIN17210	Note 2	round bar	350D	608	1010	0.18	0.32	0.56	0.009	0.032	1.69	0.27	1.47	—	—	
G	Ck45	DIN17200	normalized	round bar	100D	358	659	0.49	0.25	0.72	0.007	0.012	—	—	—	—	—	
H	GS523	DIN1681	normalized	cast plate	80T	334	569	0.31	0.53	0.83	0.006	0.009	0.12	0.02	0.06	—	—	
I	GS26CrMo4	SEW685 ⁴	Q & T	cast plate	100T	461	641	0.26	0.42	0.70	0.004	0.011	1.04	0.26	0.06	—	—	
J	GS36CrNiMo4	SEW515 ⁴	Q & T	cast plate	150T	697	871	0.32	0.48	0.64	0.007	0.01	1.5	0.21	1.5	—	—	
K	GS42CrMo4	SEW510 ⁴	Q & T	cast plate	100T	474	711	0.41	0.43	0.81	0.005	0.01	1.12	0.26	0.07	—	—	
L	28NiCrMoV55		Q & T	round bar	500T	561	695	0.27	0.04	0.40	0.008	0.007	1.24	0.43	1.24	5)	—	
S	42CrMoS4	DIN 17200	Q & T	round bar	50D	750	875	0.38-0.45 0.40 max 0.40 max 0.40 max 0.40 max	0.38-0.45 0.40 max 0.40 max 0.40 max 0.40 max	0.69 0.69 0.69 0.69 0.69	0.035 max 0.035 max 0.035 max 0.035 max 0.035 max	0.03 max 0.03 max 0.03 max 0.03 max 0.03 max	14-17 14-17 14-17 14-17 14-17	0.15-0.30 0.15-0.30 0.15-0.30 0.15-0.30 0.15-0.30	— — — — —	— — — — —	— — — — —	
			round bar	120D	610	820												
			round bar	270D	550	780												
			bar	220T	535	760												
			round bar	50D	830	955												
T	34CrNiMo6	DIN 17200	Q & T	round bar	120D	830	970	0.3-0.38 0.40 max 0.4-0.7 0.035 max 0.03 max	0.3-0.38 0.40 max 0.4-0.7 0.035 max 0.03 max	0.3-0.38 0.40 max 0.4-0.7 0.035 max 0.03 max	0.03 max 0.03 max 0.03 max 0.03 max 0.03 max	14-17 14-17 14-17 14-17 14-17	0.15-0.30 0.15-0.30 0.15-0.30 0.15-0.30 0.15-0.30	— — — — —	— — — — —	— — — — —	— — — — —	
			round bar	200T	630	820												
			round bar	400D	695	880												
			round bar	100D	600	850												
			round bar	250D	465	720												
U	16MnCr5	DIN 17210	Note 2	round bar	100D	870	1115	0.18	0.29	1.21	0.025	0.025	0.88	—	—	—	—	
V	17CrNiMo6	DIN 17210	Note 2	round bar	250D	465	720	0.19	0.25	1.11	0.025	0.012	0.98	—	—	—	—	
				round bar	100D	870	1115	0.18	0.33	0.48	0.025	0.022	1.68	0.32	—	—	—	
				round bar	250D	760	1000	0.18	0.32	0.50	0.025	0.010	1.68	0.32	—	—	—	
				round bar	350D	680	1005	0.18	0.23	0.56	0.025	0.032	1.68	0.27	—	—	—	

1) Quenched and tempered

2) Heat treated according to case hardening

3) Also 0.5V

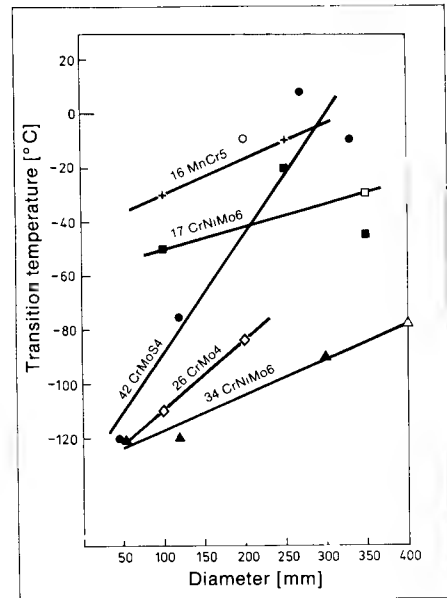
4) Stahl-Eisen-Werkstoffblatt

5) Also 0.1V

Table 2 Effect of material diameter on transition temperature TT₂₇

Name	Diameter [mm]	Transition temperature TT 27 [°C]
26 CrMo4	100	- 110
	200	- 86
42 CrMoS4	50	- 120
	100	- 100
	120	75
	270	+ 8
	330 1)	- 10
	200	9
34 CrNiMo6	50	120
	120	- 120
	200	100
	300 1)	- 90
	400	- 78
16 MnCr5	100	- 30
	250	10
17 CrNiMo6	100	- 50
	250	- 20
	350	- 45
	350	- 31

1) Square bar thickness x 1,5 equivalent diameter

Fig. 2 Effect of material diameter on transition temperature TT₂₇

The forged materials that were tested were made from five different low alloyed steels ranging in diameter from 50 to 400 mm. The chemical compositions of the forged materials tested are shown in Table 1. Three of the steels were quenched and tempered and two were heat treated corresponding to case hardening as noted in Table 1.

The results of the CVN tests on the forged materials described in Table 1 are shown in Table 2 and Fig. 2. The influence of the diameter of the forgings on the transition temperature TT₂₇ was very little for the case hardened steels 16MnCr5 and 17CrNiMo6 over the range of diameters 100 to 350 mm. The transition temperatures were relatively high with -30°C to -10°C in the case of 16MnCr5 and -50°C to -20°C in the case of 17CrNiMo6. For the quenched and tempered steels the influence of the diameter on the 34CrNiMo6 steel was small as evidenced by the shallow sloped line in Fig. 2 whereas a very steep line indicating significant influence of diameter on the transition temperature was noted for the 42CrMoS4 material. For these steels the transition temperatures were generally lower than for the case hardened steels.

For the two case hardened steels 16MnCr5 and 17CrNiMo6 micrographs were taken at the locations where the notched bar specimens had been cut (at 1/6 the diameter) as well as from the center of the forging cross section. There was practically no difference in the microstructure of these two steels over their respective cross sections. However, for the 16MnCr5 steel, the microstructure consisted of coarse grain ferrite and pearlite with fractions of upper bainite whereas the 17CrNiMo6 steel consisted primarily of bainite with small fractions of ferrite as seen in Fig. 3. This explains the lower transition temperatures measured for the 17CrNiMo6 steel.

For the quenched and tempered steels 26CrMo4, 42CrMoS4 and 34CrNiMo6 micrographs were taken only at the 1/6 diameter location. At 50 mm diameter the 42CrMoS4 steel showed a very fine bainite whereas at 270 mm diameter a fairly coarse bainite with embedded ferrite was observed as seen in Fig. 4. This microstructure was responsible for the unsatisfactory transition temperature shown in Fig. 2. For the 34CrNiMo6 steel, a very fine grained bainite structure was present for forgings up to 200 mm. At a diameter of 400 mm there appeared a coarsening of the bainite but which had not yet led to a noticeable deterioration in the transition temperature. The microstructure of the 26CrMo4 steel consisted of bainite with embedded ferrite. The difference in microstructure between the 100 and

200 mm diameters was not marked. Fig. 5 shows the microstructures of the 34CrNiMo6 steels for two diameters. These results confirm the observations in the published literature of Habracken and Economopoulos [3] and Piehl [4] where it is noted that the transition temperature tends to improve as faster cooling rates are applied and transformation, as plotted on the TTT diagram, shifts from ferrite/pearlite via upper bainite to lower bainite and martensite.

Drop Weight Tests on Full size U-Profiles

Drop weight tests were conducted on full size U-profiles of truck underframe members. The object was to determine the temperature range where the fracture starting from the notched or unnotched edge of the section changed from a ductile to a brittle appearance. For the U-profiles tested this was equivalent to determining the transition between the mode where a crack started by the impact was arrested to the mode where the crack continued until complete failure of the part occurred.

The composition of the three microalloyed steels evaluated are shown in Table 3. One test was conducted on a steel which had been normalized and the other two tests were conducted on steels which had been thermo-mechanically treated [5].

The full size drop weight tests were conducted on pieces 1.5 m long. The U-profile dimensions were 70 X 265 X 7.8 mm. There were test pieces with notches cut in the legs of the sections and others without notches. The notches were made by cutting with a 45° milling cutter to a depth of 4.6 mm and additionally applying a sharp-edge Schnadt notch to a depth of 5 mm. The load was applied by means of a drop weight with an impact energy of 4000 Nm. The specimen dimensions and loading configuration are shown in Fig. 6. In addition, CVN specimens were cut from the U-profile sections. However, because of the reduced wall thickness of the U-profiles of 7.8 mm, the specimen width had to be reduced. Consequently, the transition temperature was defined as the energy absorption of 50% (TT 50%) of that measured on the upper shelf rather than the conventional FATT50.

The results of the drop weight tests are shown in Table 4 and Fig. 7. From Fig. 7, it is seen that for the unnotched specimens the transition temperatures were about the same for the microalloyed steels PAS42 and PAS55 whereas a transition temperature of less than -100°C was indicated for the Alform 43 steel. However, for the notched specimens, a different observation was

Table 3 Steels for impact test on full-size profiles

Designation	Name	Condition	Type	Thickness [mm]	Yield Strength [MPa]	Tensile Strength [MPa]	Chemical Composition									
							C	Si	Mn	P	S	Ti	Nb	V	Al	
										[in weight %]						
W	PAS 42 1)	TM 3)	plate	7,8	445	515	0,07	0,35	0,94	<0,025	0,011	—	0,025	—	0,03	
X	Alform 43 2)	N 4)	plate	7,8	440	555	0,14	0,24	1,24	<0,03	<0,03	0,10	0,02	—	0,014	
Y	PAS 55 1)	TM	plate	7,8	565	640	0,07	0,38	0,85	<0,025	0,014	0,2		0,05	0,07	
1) Trade mark Thyssen AG					3) Thermomechanical treatment											
2) Trade mark Voest Alpine					4) Normalized											

1) Trade mark Thyssen AG
2) Trade mark Voest Alpine

3) Thermomechanical treatment
4) Normalized

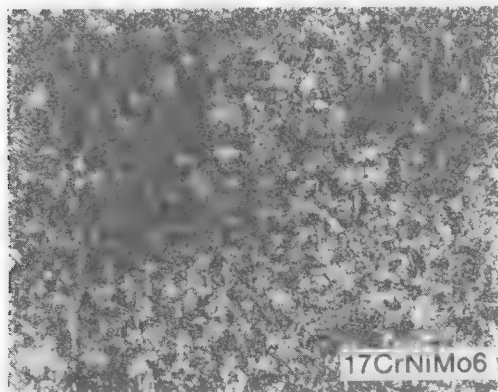
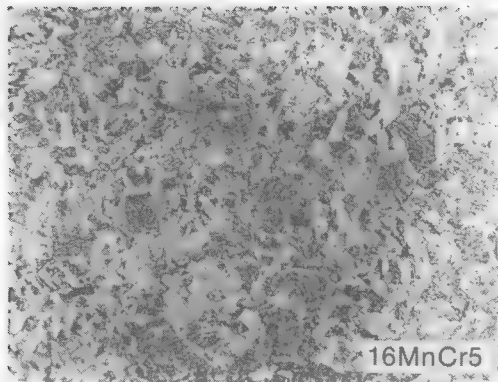


Fig. 3 Microstructure of steels 16MnCr5 and 17CrNiMo6

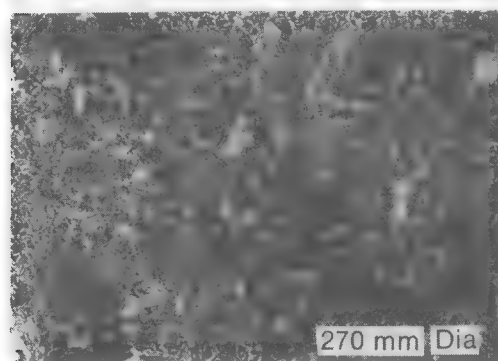
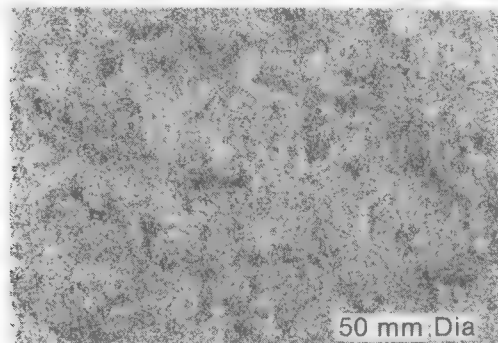


Fig. 4 Microstructure at two diameters for steel 42CrMoS4

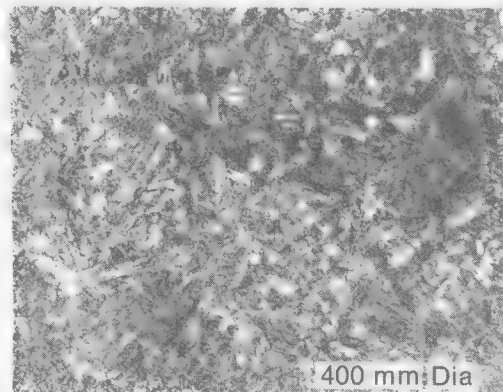
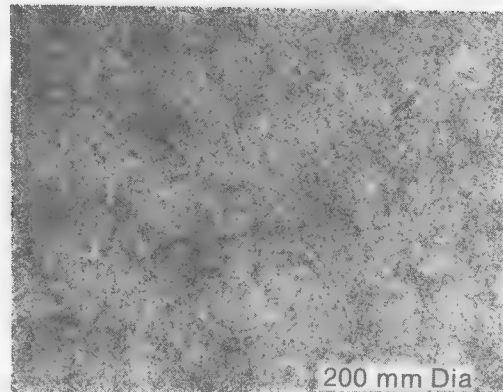


Fig. 5 Microstructure at two diameters for steel 34CrNiMo6

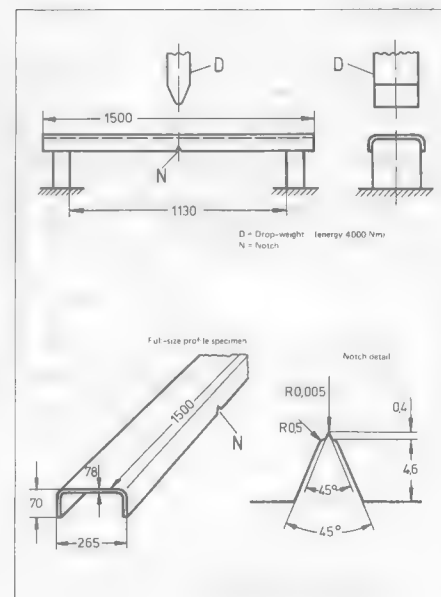


Fig. 6 Full size profile specimen and jig for impact test

made where each of the three steels tested showed distinctly different transition temperatures. The transition temperature was determined as the middle temperature between the temperature at which brittle fracture occurred and the temperature at which no fracture occurred. Usually this was within an interval of 10°C. Micrographs of the fractured surfaces for the PAS42 steel obtained with a scanning electron microscope are shown in Fig. 8 which confirmed the transition from ductile to brittle failure. These results indicated that all three materials had a very narrow temperature range between brittle and ductile failure not unlike that experienced with the Pellini nil ductility test. Comparing the transition temperatures TT27 and TT50% in Table 4 shows that the thermomechanically treated steel PAS42 had the lowest transition temperature TT27 as well as the lowest TT50%. However, it is evident that there was not a strong correlation between the drop weight transition temperature and the transition temperatures obtained in the notched-bar (CVN) impact test. Further investigation along these lines is required. Until such time, if cold service is expected for large structural sections which may encounter impact or dynamic loads, then full size component testing is warranted.

MATERIAL SELECTION CONSIDERATIONS

In another study by the authors [6] a variety of steels were evaluated to determine the correlation between the nil ductility transition temperature (NDTT) and the Charpy V notch transition temperature at an energy level of 27J. The chemical compositions and specifications are shown in Table 1 and designated A through K. Also, from the same reference and shown in Fig. 9 is a comparison of the TT27 with the NDTT for the materials in Table 1. It was found that if the materials were grouped according to forged parts and steel castings there was a reasonable correlation between the NDTT and the TT27 data. In Fig. 10, the CVN data for the alloys A through K is shown with the measured NDT temperatures indicated by arrows. It can be observed that the energy absorbed in the CVN test at the NDT temperature was higher for those materials with greater energy absorption on the upper shelf. For steels with values of 100J or greater on the upper shelf there were greater differences between the NDT temperature and the TT27 as obtained from the Charpy test.

On the basis of the testing program and results presented it was clear there was a linkage between the NDTT, TT27 and thickness parameters. In the following discussion a methodology is described which shows how materials can be selected for a specified design temperature. For purposes of discussion a criterion of -40°C NDTT was chosen. A different NDTT can be used depending on the anticipated service conditions and previous experience with known materials.

In Table 5 are listed the materials, the diameter or thickness and the NDT temperatures. For some steels, the NDTT was measured at or near -40°C so that the corresponding measured TT27 required for an NDTT of -40°C was readily apparent. For other steels, the TT27 required for obtaining a NDTT of -40°C was estimated from Figs. 2 and 9. For example, for the 42CrMoS4 steel, the NDTT was measured at +10°C. Using the lower bound line for "steel bars" in Fig. 8, the TT27 was estimated at -100°C for a NDTT of -40°C.

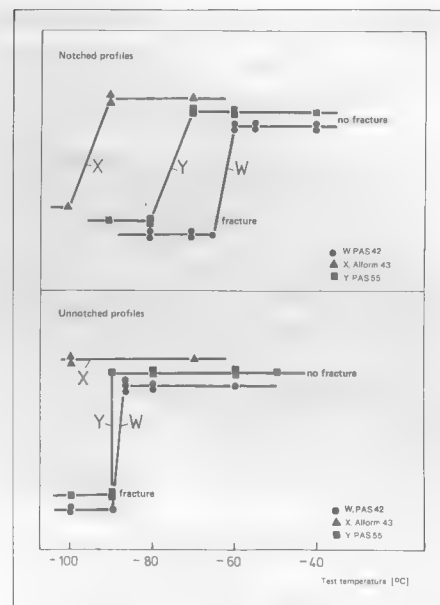


Fig. 7 Fracture test results for full size profiles

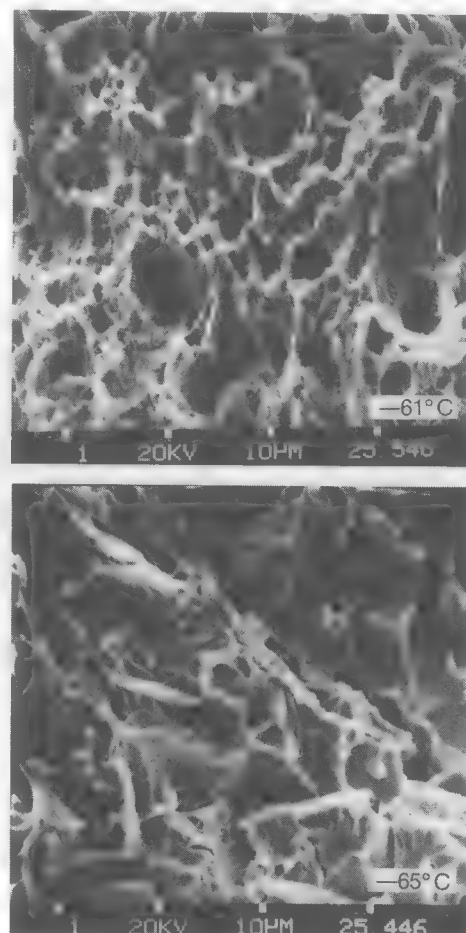


Fig. 8 Fracture appearance under scanning electron microscope for PAS42 (X2000)

Table 4 Comparison of transition temperatures TT27 and TT50% with drop weight transition temperature of full size profiles

Designation	Name	Transition temperature [°C]				Drop-weight transition temperature [°C]	
		TT 27		TT 50 %		Notched profile	Unnotched profile
		long	transv	long	transv		
W	PAS 42	-110	-65	-80	-70	-62	-87
X	Alform 43	-95	-65	-65	-65	-95	< -100
Y	PAS 55	-75	-75	60	-65	-70	-80

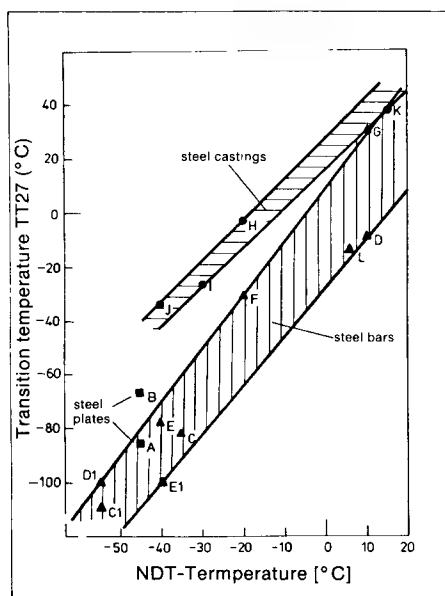


Fig. 9 Comparison between transition temperatures TT27 and NDT temperatures

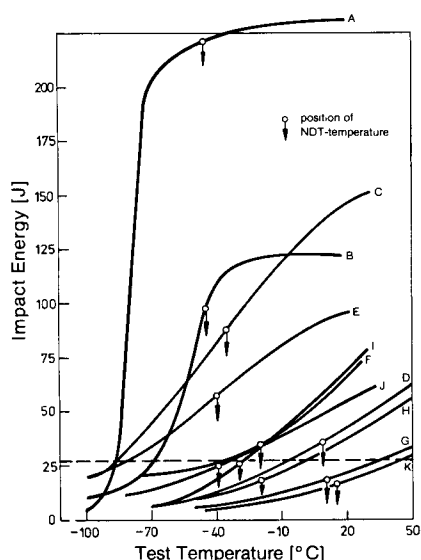


Fig. 10 Impact energy (CVN specimen) at NDT temperature

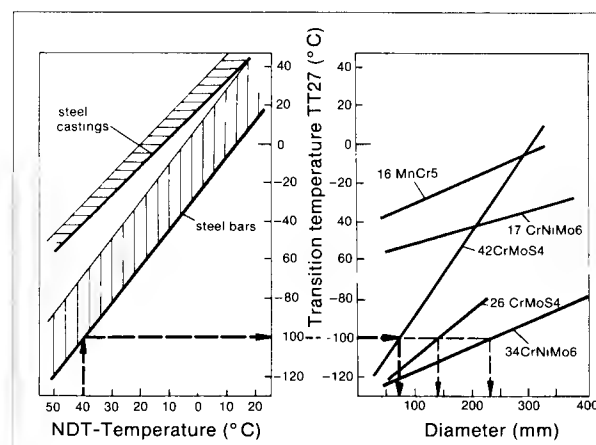


Fig. 11 Estimating maximum possible diameter/thickness for NDTT of -40°C

If Figs. 2 and 9 are combined as shown in Fig. 11 estimates can also be made of the maximum possible thickness or diameter for a given steel to meet or exceed a NDTT of -40°C. For example, as shown on the left hand graph of Fig. 11, for the 42CrMoS4 to have a NDTT of -40°C, the corresponding TT27 was estimated at -100°C. Referring to the graph on the right hand side of Fig. 10 it is seen that at a TT27 of -100°C, the maximum thickness is estimated to be 80 mm, 140 mm and 230 mm for 42CrMoS4, 26CrMo4 and 34CrNiMo4 respectively. These are conservative estimates using the lower bounds of the scattering ranges.

The last column on the right in Table 5 indicates the maximum diameter or thickness that is possible for the alloys evaluated if an NDTT of -40°C is to be achieved. For the case hardened steels 16MnCr5 and 17CrNiMo6, the plain steels Ck 45 and GS-52.3 as well as the alloyed cast steel GS-42CrMoS4 there was no material thickness which would suggest a NDTT of -40°C, thus, these steels have been judged as not suitable for low temperature service.

Because of the heat treatment subjected to the case hardened steels 16MnCr and 17CrNiMo6, these materials will not be suitable for arbitrary application in cold environments. However, as these materials are used mainly for gears, and such installations are usually accompanied by heating units, applications under these circumstances should be satisfactory.

While the above estimating methods cannot be described as absolute they can serve a useful purpose in limiting the sizes and kinds of materials for detailed examination.

Table 5 Steels for a NDTT requirement of -40°C with maximum possible diameter/thickness

Name	Diameter (D) or Thickness (T) [mm]	NDT-Temp. [$^{\circ}\text{C}$]	TT 27 required for getting a NDTT of -40°C [$^{\circ}\text{C}$]	Max. possible diameter or thickness for getting a NDTT of -40°C [mm]
TTS126	20 T	-45	-85	about 20
TTS136	20 T	-45	-67	about 20
26CrMo4	200 D	35	-100	< 200
42CrMoS4	200 D	+10	-100 est	80
34CrNiMo6	400 D	-40	-78	400
17CrNiMo6	350 D	-20	100 est	material not suitable
Ck45	100 D	+10	100	material not suitable
28NiCrMoV55	500 D	+10	100	material not suitable
GS52.3	80 T	20	-40	material not suitable
GS26CrMo4	100 T	-30	-40	< 100
GS36CrNiMo6	150 T	-40	35	150
GS42CrMo4	100 T	+15	-40	material not suitable

SUMMARY

This paper presents the results of an investigation into the effect of material size on the transition temperature as determined by CVN testing. It was found that for some alloys size does influence the CVN results. It was concluded that for some of the steels tested that they would not be satisfactory for service at -40°C because of either the size or because of the alloy type.

For full scale tests on truck underframes it was found there was little confidence in correlating CVN data transition temperature with drop weight test data conducted on full size components. It was concluded, that for such applications, full scale testing should be included in order to provide a complete evaluation of the cold temperature properties of the materials since CVN testing can lead to erroneous results.

REFERENCES

1. ASTM Standard E23-81, "Notched bar impact testing of metallic materials," Annual Book of ASTM Standards, Part 10, 1981.
2. ASTM Standard E208-69 "Standard method for conducting drop weight test to determine nil ductility transition temperature of ferritic steels," Annual Book of ASTM Standards, Part 10, 1969.
3. Habracken, L.I. and Economopoulos, M., "Bainitic microstructures in low carbon alloy steels and their mechanical properties," Symp. Trans. and Hardenability in Steels, Univ. Mich., 1967
4. Piehl, K.H., "Einfluss von chemischer Zusammensetzung und Gefüge auf die Eigenschaften von Nickel-Chrom-Molybdän-Vanadin-Vergütungsstählen für schwere Schmiedestücke, besonders für Niederdruck-Turbinen und Generatorwellen," Stahl und Eisen, Vol. 95, No. 18, 1978.
5. Baumardt, H., Rohde, M., Schulz, L., "Herstellung und mechanische Eigenschaften von thermomechanisch gewalzten Grobblechen," Thyssen Techn. Berichte, Heft 2, 1982.
6. Bellow, D.G., Klotzbücher, E.F., Kraft, H.E., "On the selection of materials for cold temperature service," Proc. Soc. Exp. Mech., Las Vegas, 1985 pp. 428-434.

ACKNOWLEDGEMENTS

The authors wish to thank their respective organizations for the support of this project. Appreciation is also acknowledged to the Natural Sciences and Engineering Research Council under Grant A-2705.

THE EFFECT OF PRECRACKING PARAMETERS ON FRACTURE TOUGHNESS TESTING

D.G. Bellow, Professor
Mechanical Engineering Department

A. Budhiman
Former Graduate Student in Mechanical Engineering Department

D.R. Budney, Professor
Mechanical Engineering Department
University of Alberta, Edmonton, Alberta, Canada

ABSTRACT

Procedures for preparation of test specimens for fracture toughness testing are prescribed by standards ASTM:E399:1981 and BS:5447:1977. These standards include restrictions on the values of K_{fmax} and R ratio during fatigue pre-cracking. The purpose of this investigation was to examine these restrictions. Experimental evidence shows that these restrictions serve the purpose of maximizing the crack propagation rate.

From fracture tests, it was found for the AISI 4140 steel evaluated that K_{fmax} should be less than $0.42 (\sigma_{y1}/\sigma_{y2}) K_q$ which suggests that the above standards could be more stringent. Further, it is shown that at higher R values a sharper crack tip is formed with less blunting. These results suggest the R-ratio restriction needs further study.

NOMENCLATURE

a	Crack length
B	Specimen thickness
K_C	Plane stress fracture toughness
K_{IC}	Plane strain fracture toughness (ASTM:E-399:1978, BS:5447:1977)
K_{fmax}	Maximum fatigue stress intensity factor
K_q	Provisional value of K_{IC}
ΔK	Stress intensity range ($K_{fmax} - K_{fmin}$)
N	Number of cycles
N_r	Number of ring down counts
N_t	Number of cycles to achieve fatigue crack of 0.5W
R	Stress ratio K_{fmin}/K_{fmax}
W	Specimen width
da/dn	Crack propagation rate
α, α_1	Proportionality values
σ_y	Yield stress

INTRODUCTION

Material toughness can be described in terms of the critical stress intensity factor under conditions of plane stress (K_C) or plane strain (K_{IC}) for slow loading and linear elastic behaviour.

Standards developed for K_{IC} (ASTM:E-399:1981, BS:5447:1977) give guidelines and restrictions in preparing specimens for testing. For fatigue pre-cracking of test specimens the standards express the stress intensity factor as

$$K_{fmax} \leq \alpha (\sigma_{y1}/\sigma_{y2}) K_q$$

where K_q is the provisional value of K_{IC} and α is a constant determined experimentally. The yield stress ratio σ_{y1}/σ_{y2} is equal to one if the specimen is prepared at the same temperature as it is tested. Based on the experiments by Brown and Srawley (1970) the ASTM:Standard E-399:1978 specifies $\alpha = 0.60$, whereas based on experiments by May (1970) the British Standard BS:5447:1977 states that $\alpha = 0.70$. These restrictions were imposed to avoid overestimating K_{IC} as a result of a large plastic zone ahead of the crack during fatigue precracking.

An additional restriction for the above standards is that the stress ratio R for fatigue precracking should be $0 < R \leq 0.1$ for BS:5447 and should be $-1 \leq R \leq 0.1$ for ASTM:E-399.

The purpose of this paper is to discuss the results of an experimental program conducted to evaluate the effect of K_{fmax} on K_q and the effect of R-ratio on K_q .

EXPERIMENTAL PROCEDURE

Specimen and Loading Conditions

A total of 98 tests were carried out on AISI 4140 steel which in an as-received condition had a yield stress of 760 MPa (115 ksi) and an estimated K_{IC} value of 45 to 64 MPa \sqrt{m} (50 to 70 ksi \sqrt{in}). Three point bend specimens were machined in accordance with ASTM:E-399:1981 and BS:5447:1977. Prior to fatigue precracking, stress relieving was carried out on the specimens at 650°C (1200°F) for 45 min as required by BS:5447.

Fatigue precracks were developed for the fracture tests under various maximum bending loads and three different stress ratios R (0.1, 0.3 and 0.5). Fatigue precracking was halted when the fatigue crack reached a length of 0.5W (one-half the specimen width). Values of K_{fmax} from 22 to 64 MPa \sqrt{m} (25 to 70 ksi \sqrt{in}) were determined. For each of these combinations a total of five specimens were tested. All fatigue precracking was performed at room temperature on an Amsler Vibrophore. The specimens resonated between 80 and 90 Hz depending on the length of the crack in the specimen.

During the fatigue precracking test the crack length was monitored until it reached a target line of 0.5W by means of a clip gauge located across the milled slot of the specimen. Although the clip gauge reading correlated well with a resistance grid crack gauge, accurate measurements of the crack length of fractured specimens was carried out using a measuring microscope in accordance with the above standards.

Acoustic emission was monitored throughout fatigue precracking. To avoid overloading the acoustic emission measuring system a special resetting circuitry was designed which reset the system after every 500 cycles of load and enabled the data to be recorded and stored at each 500 cycle interval.

Fracture tests were conducted on an Instron universal testing machine at a cross head rate of 1.3 mm/sec (0.05 in/sec). Load, clip gauge displacement and acoustic emission counts were recorded during each test.

From a total of 117 specimens, only ninety-eight specimens tested were considered valid. Some specimens were rejected because of overloading during precracking and others were considered invalid by the appropriate standards due to sloping crack plane and uneven crack length. The valid specimens were fatigue precracked with six different K_{fmax} values and three different R ratios. For each combination five test specimens were evaluated. The values of K_{fmax} were computed according to the appropriate standards.

Experimental Results

In Fig. 1 it is seen that the number of cycles to reach the terminal value N_f (for a fatigue crack of 0.5W) at a constant K_{fmax} increased with increasing R ratio. Replotting the data as a function of the stress intensity range ΔK ($\Delta K = K_{fmax} - K_{fmin}$) in Fig. 2 showed that the speed of crack propagation was a function of the stress intensity range as reported by Paris and Erdogan (1963).

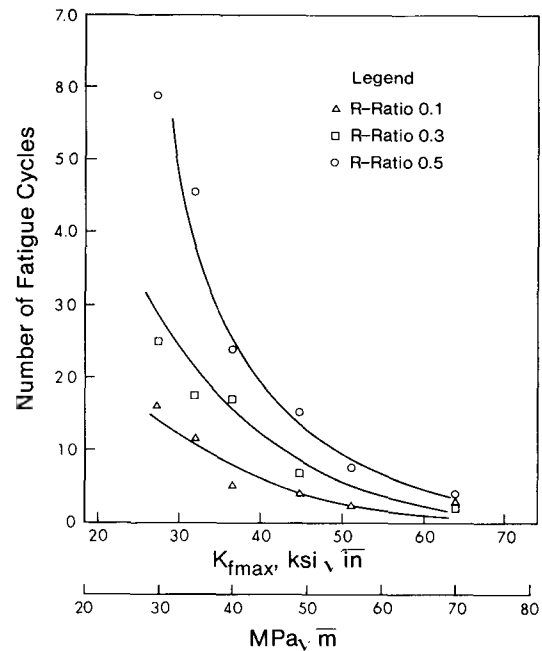


Fig. 1 Number of cycles for 0.5W crack length as a function of K_{fmax}

At intervals of 500 load cycles, the crack length was determined using the clip gauge. From this measurement, the crack propagation rate was calculated and plotted against stress intensity range ΔK ($\Delta K = K_{fmax} - K_{fmin}$) as shown in Fig. 3. From Fig. 3 it is evident that the crack propagation rate changed rapidly for a small change of ΔK near the threshold value of ΔK_{th} .

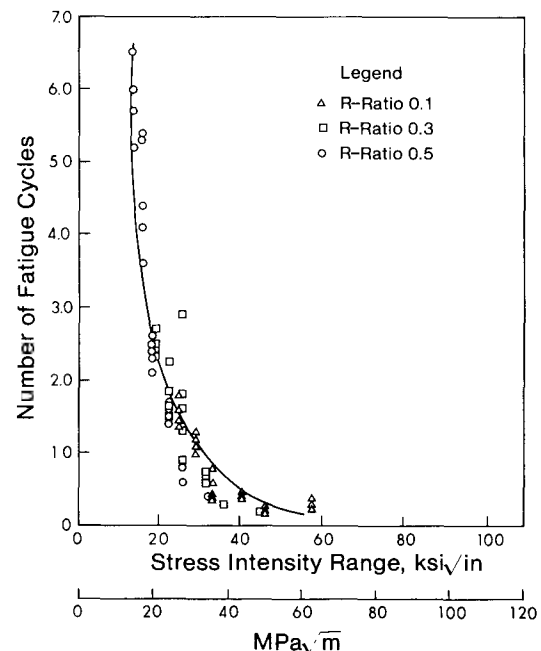


Fig. 2 Number of cycles for 0.5W crack length as a function of the stress intensity range ΔK

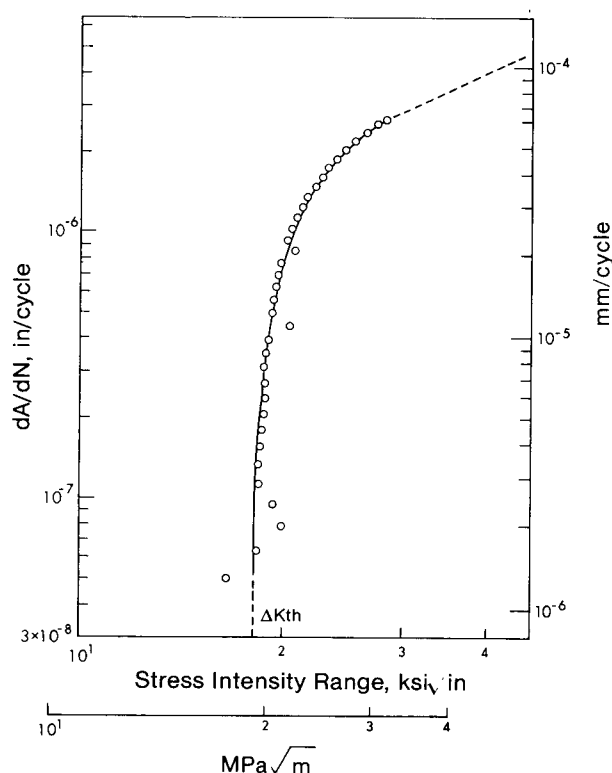


Fig. 3 Crack propagation rate as a function of stress intensity range ΔK

Direct correlation of crack length with acoustic emission counts was considered poor because of the randomness in the data for specimens tested under identical conditions. However, the total acoustic emission counts for crack lengths of 0.5W were all of the same order of magnitude. To obtain an average number of counts per cycle the total number of acoustic emission counts N_T was divided by the number of fatigue cycles N_f . This was continued until the required crack length of 0.5W was attained. These results are plotted in Fig. 4 for three R-ratios as a function of the K_{fmax} values. From Fig. 4 it can be seen that the number of acoustic counts increased rapidly for K_{fmax} greater than about 35 MPa/m (40 ksi/in). This was also observed by Lindley and others (1978) where it was shown that

$$\frac{dN_r}{dN} \propto (\Delta K)^{m+2}$$

The results in Fig. 4 also show that for a constant K_{fmax} the material damage was greater at lower R-ratios resulting in a higher crack propagation rate.

Fracture Testing

The test results of K_Q are plotted (in terms of mean value and range) with respect to K_{fmax} for three R-ratios in Fig. 5. Despite the scatter in data, these results exhibit some important features. It is apparent that K_Q increases with increasing K_{fmax} to a limit at around 55 MPa/m (60 ksi/in) for all R-ratios.

It can also be seen there was less effect of K_{fmax} on K_Q at higher R-ratios. For a constant K_{fmax} , K_Q increased with ΔK . For the lowest K_{fmax} values used in these tests, (approximately 28 MPa/m (30 ksi/in), a mean value of K_Q of 65 MPa/m (70 ksi/in) was determined for all R-ratios. In general, at constant K_{fmax} , K_Q increased with increasing ΔK (decreasing R-ratio). Some low K_Q values at R-ratios of 0.3 and 0.5 suggest that it is possible to produce sharper fatigue cracks for higher R-ratios. This could, in all likelihood, mean that the plastic zone size is smaller at a higher R-ratio. This observation is consistent with the knowledge that the effective stress range decreased with increasing R-ratio. At a K_{fmax} value of 65 MPa/m (70 ksi/in), K_Q is over-estimated at all R-ratios. This again, is probably due to the large plastic zone developed in all specimens.

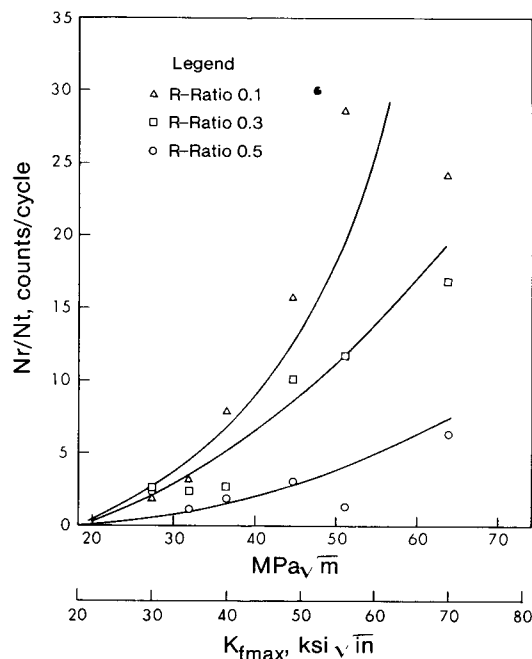


Fig. 4 Acoustic emission counts as a function of K_{fmax} and R-ratio

Assuming a lower limit for K_Q of 67 MPa/m (74 ksi/in) the limiting K_{fmax} value is $0.6 \times 67 = 38$ MPa/m (42 ksi/in) for the ASTM:E-399 Standard and $0.7 \times 64 = 45$ MPa/m (49 ksi/in) for the BS:5447 Standard. As seen from Fig. 5 the restrictions imposed by both standards do not ensure evaluation of the lowest K_Q value. A lower K_{fmax} value of 0.42 K_Q is suggested from the results of this experiment.

An equal number of tests was performed for the COD test (B.S.:5762:1979) and the J_{IC} test (ASTM: E-813:1981) to determine the effect of R-ratio and K_{fmax} on the C.O.D. The experimental data featured considerable scatter with inconclusive results. More experiments are to be performed.

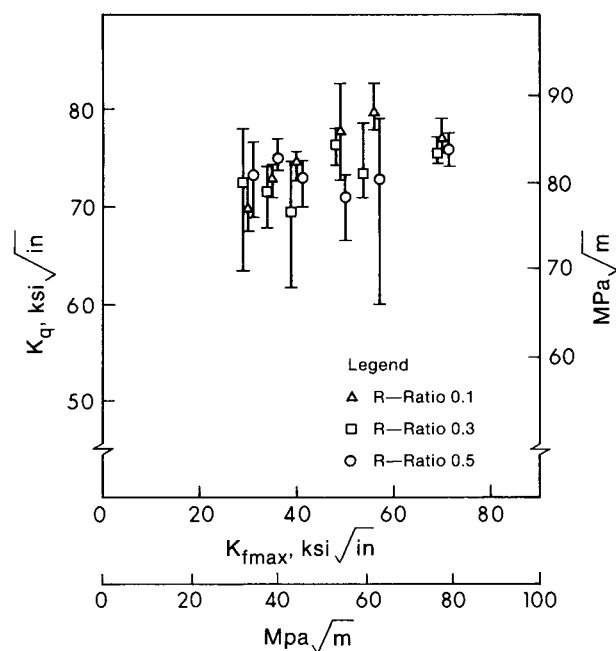


Fig. 5 Effect of K_{fmax} on K_q

DISCUSSION

The crack propagation rate increased with increasing K_{fmax} . For a constant K_{fmax} , da/dN decreased as R increased. Thus, the requirement in the standards for K_{IC} that $R < 0.1$ ensures a rapid crack propagation rate.

The results of this investigation suggest that limiting $R < 0.1$ for a constant K_{fmax} results in a large stress intensity range which may produce a large plastic zone ahead of the crack tip which is not an ideal plane crack. Decreasing R increased the crack propagation rate, the use of higher R values may reduce the size of the plastic zone.

For the AISI 4140 steel evaluated K_q increased with K_{fmax} until a limit was reached. It was found that a lower limit of K_q could be determined if $K_{fmax} < 0.42 K_q$, which is less than the standards allow. This suggests that the K_{fmax} restriction contained in BS:5762 may be too high. However, the production of a sharp fatigue crack is necessary and the K_{fmax} restriction may be justified.

REFERENCES

- ASTM E399. Standard Test Method for Plane Strain Fracture Toughness of Metallic Materials, 1981.
- ASTM E813. Standard Test Method for J_{IC} . A measure of fracture toughness, 1981.
- BS 5447. Methods of Test for Plane Strain Fracture Toughness (K_{IC}) of Metallic Materials, 1979.
- BS 5762. Methods of Crack Opening Displacement (COD) Testing, 1979.
- Brown, W.F. and Srawley, J.E. Commentary on Present Practice: ASTM STP 463, pp. 216-248, 1970.
- Clark, G. Significance of Fatigue Stress Intensity in Fracture Toughness Testing. Int. Jour. of Fracture, Vol. 15, pp. R179-181, 1979.
- Kaufman, J.G. Experience in Plane Strain Fracture Toughness Testing per ASTM Method E 399, ASTM STP 632, pp. 33-34, 1977.
- Lindley, T.C., Palmer, I.G. and Richards, C.E. Acoustic Emission Monitoring of Fatigue Crack Growth, Mat'l Sci. and Eng., Vol. 32, pp. 1-15, 1978.
- May, M.J. British Experience with Plane Strain Fracture Toughness (K_{IC}) Testing, ASTM STP 463, pp. 41-62, 1970.
- Paris, P.C. and Erodogan, F. A Critical Analysis of Crack Propagation Laws, Jour. of Basic Eng., Vol. 85, No. 3, 1963.
- Yeh, T. and Bruck, L.H. Cyclic Crack Opening Displacement Behaviour During High Amplitude Block Loading, Eng. Frac. Mech., Vol. 12, pp. 541-549, 1979.

ACKNOWLEDGEMENTS

The authors wish to thank the Natural Sciences and Engineering Research Council for assistance under Grants A-2705 and A-1376. Thanks are also due to the technicians of the Mechanical Engineering Department who assisted with the experimental work.

On the Selection of Steels for Mining Equipment Operating under Arctic Conditions

E.F. Klotzbücher and H.E. Kraft, F.R. Germany
D.G. Bellow, Canada

Introduction

The design of mining equipment for operation at subzero temperatures requires that special consideration be given to the selection of suitable materials. In addition to the customary selection criteria such as strength, weldability and cost, it is of particular importance that the steels remain ductile at low temperatures.

It is known that the toughness of ferritic steels is liable to suffer a critical reduction at low temperatures. At decreasing temperature the toughness drops within a more or less limited temperature range from an upper shelf to a lower shelf. This transition temperature provides a measure for the brittle fracture behaviour of the components and depends on numerous factors.

Steel components can become brittle at a nominal stress far below the yield stress in the presence of sharp notches, weld flaws or fatigue cracks, which in machinery and equipment cannot be ruled out completely. In the presence of such notches it is possible that stress peaks will combine with residual stresses and thermal stresses which can lead to plastic deformation. The material can only resist this if it still has adequate inherent toughness, i.e. ductility.

The following paper describes various considerations and investigations which were made to establish a basis for the selection of steels for mining equipment operating in subzero temperature areas of Canada.

Methods for Investigation of Brittle Fracture Behaviour

In past years a multiplicity of papers have been published on the brittle fracture behaviour of materials. Mention need only be made of guiding literature by Pellini and others in the U.S.A. [1, 2, 3, 4, 5] as well as by Robertson and Wells in England [6, 7, 8] on the subject of crack initiation and crack arrest. Further references will be found in ASTM E 208 [9]. Research into linear elastic and elastoplastic fracture mechanics, [10, 11, 12, 13] has resulted in great progress in the possibility of making a quantitative appraisal of flaws. This approach can also be helpful for the selection of materials for cold temperature service.

In spite of this abundant information there is no hard-and-fast rule to assist the designer in selecting materials for mining equipment when required to operate at subzero temperatures. Function and safety of a machine are factors of doubt if existing flaws can spread spontaneously. On the basis of earlier experience it was therefore decided to give preference to the drop weight test to determine the *NDT* temperature according to ASTM E 208 [9] (Fig. 1). This test was originally introduced for use as an appraisal of structural steels. However, it has also been adopted for the evaluation of forged and cast materials [9].

The *NDT* temperature is the temperature below which an existing small crack is liable to propagate in an unstable manner at a nominal stress equal to the yield stress. In the presence of a major flaw, as shown in Fig. 1, the nominal stress required to trigger a fracture is distinctly lower than the yield stress. When the nominal stress is equal to the yield stress, and in the presence of a major flaw, the crack initiation temperature (transition temperature) rises.

Dipl.-Ing. E.F. Klotzbücher, Chief Metallurgist and Dipl.-Ing. H.E. Kraft, Metallurgist, MAN-GHH GmbH, Postfach, D-8500 Nürnberg, Federal Republic of Germany; Dr. D.G. Bellow, Professor of Mechanical Engineering, University of Alberta, Edmonton, Canada



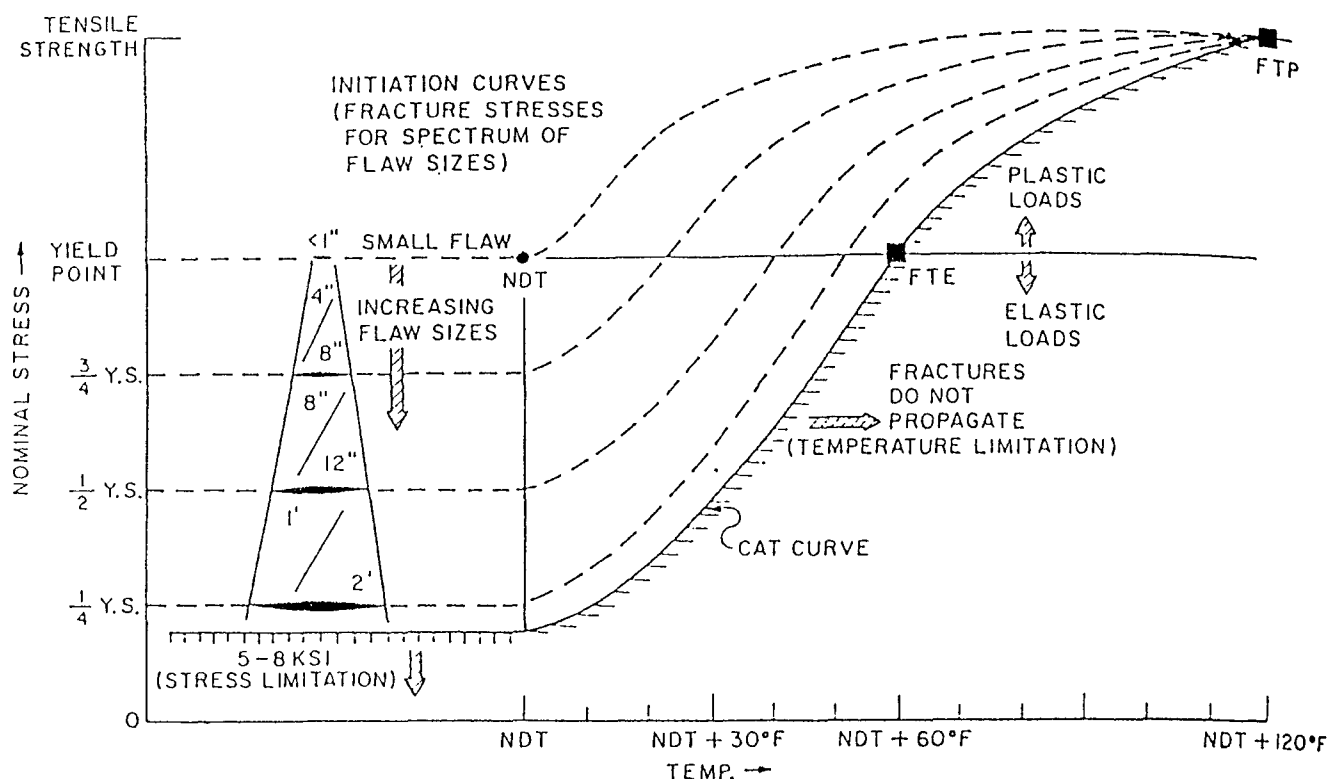


Fig. 1: Generalized fracture analysis diagram indicating the approximate range of flaw sizes required initiation at various levels of nominal stress, as referenced by the *NDT*-temperature (from ASTM E 208/9).

However, due to modern inspection technology the presence of major flaws can be minimized and, as a result, the *NDT* temperature can be considered to be the permissible minimum operating temperature. As it is relatively complicated to determine the *NDT* temperature — in fact, this is not possible for all material thicknesses [14] — a relationship to the transition temperature has been sought, as can be determined with notched-bar impact bending specimens. Charpy-V-notch (CVN) specimens according to ASTM E 23 [15] were used.

Following a review of the test results and their application, details are given regarding the possibilities of applying linear-elastic fracture mechanics (LEFM) for checking and evaluating the results of tests on forged parts.

Test Program

Materials

Tests were carried out using steels which are customarily found in welded steel structures and in mechanical components of mining equipment. In particular, the structural steels TT St E 26 and TT St E 36 and the cast material GS-13 MnNi64 were included in the test program in view of their excellent low temperature mechanical properties.

The X 22 CrMoV 121 steel is a stainless steel and is used occasionally for hinge pins where corrosion pro-

tection is required. Tests were carried out on heavy-gauge steel plates, forged round bars and on cast steel in the form of plates.

The materials were in a heat treated condition as typical for their application. Due to different hardening and tempering conditions of the alloyed steels it was expected [14] that the material thickness would have a major influence on the toughness properties. Consequently, the forged steels were tested in different thicknesses. The steels which were evaluated along with their mechanical properties and metallurgical compositions are listed in Table 1.

Test Procedures

CVN notched-bar impact test specimens were used to determine the transition temperatures according to two customary criteria; energy absorption of 27 J (TT 27) and 50% brittle fracture area (FATT 50). Three specimens were tested for each test temperature.

The *NDT* temperature was determined with Pellini drop weight specimens [4]. Six specimens were used in each case. In addition, microscopic examinations were made of the structure for a better understanding of the test results.

Specimen Location

The CVN specimens were taken in the form of longitudinal specimens from the plates directly underneath the surface, in the case of forged round bars (as longitudinal

Table 1: Steels evaluated.

Designation	Standard	Condition	Type	Diameter (D) or Thickness (T) (mm)	Yield Strength (MPa)	Tensile Strength (MPa)	Chemical Composition (in weight %)											
							C	Si	Mn	P	S	Cr	Mo	Ni	Nb	Al	V	
St 52-3	DIN 17 100	Normalized	plate	40 T	403	593	0,22	0,35	1,55	<0,03	0,012	-	-	-	-	0,03	-	
11StE 26	DIN 17 102	Normalized	"	20 T	320	430	0,08	0,24	1,27	0,025	0,010	-	-	-	0,05	-	0,05	
11StE 36	DIN 17 102	Normalized	"	20 T	402	536	0,15	0,37	1,47	0,017	0,009	-	-	-	0,035	0,042	-	
StE 690	1)	Q + T 2)	"	22 T	840	880	0,19	0,64	1,0	<0,025	0,014	0,69	0,35	0,10	<0,01	-	<0,05	
Ck 45	DIN 17 200	Normalized	round bar	100 D	558	659	0,49	0,25	0,72	0,007	0,012	-	-	-	-	-	-	
26 CrMo 4	SEW 680 5)	Q + T	round bar	100 D	468	628	0,27	0,32	0,72	0,006	0,025	1,06	0,17	-	-	-	-	
			round bar	200 D	478	656	0,27	0,22	0,76	0,02	0,014	1,11	0,23	-	-	-	-	
42 CrMoS 4	DIN 12 200	Q + T	round bar	50 D	750	875	according to Standard DIN 17 200											
			round bar	100 D	761	932	0,45	0,30	0,67	0,024	0,033	1,09	0,20	-	-	-	-	
			round bar	120 D	610	820	according to Standard DIN 17 200											
			round bar	200 D	550	756	0,43	0,35	0,57	0,019	0,021	1,14	0,17	-	-	-	-	
			round bar	270 D	550	780	according to Standard DIN 17 200											
			plate	220 T	535	760	according to Standard DIN 17 200											
34 CrNiMo 6	DIN 17 200	Q + T	round bar	50 D	830	955	according to Standard DIN 17 200											
			round bar	120 D	830	970	according to Standard DIN 17 200											
			round bar	200 D	715	886	0,34	0,30	0,53	0,022	0,013	1,70	0,29	1,70	-	-	-	
			plate	200 T	630	820	according to Standard DIN 17 200											
			round bar	400 D	695	880	0,37	0,28	0,54	0,01	0,007	1,54	0,26	1,55	-	-	-	
X 22 CrMoV 121	DIN 17 240	Q + T	round bar	100 D	669	874	0,24	0,38	0,71	-	-	12,4	1,02	0,75	-	-	0,29	
				200 D	724	911	0,25	0,33	0,48	-	-	12,2	0,93	0,63	-	-	0,60	
16 MnCr 5	DIN 17 210	C.H. 3)	round bar	100 D	600	850	0,20	0,29	1,21	<0,025	0,025	0,88	-	-	-	-	-	
				250 D	465	720	0,19	0,25	1,11	<0,025	0,012	0,98	-	-	-	-	-	
17 CrNiMo 6	DIN 17 210	C.H. 3)	round bar	100 D	870	1115	0,18	0,33	0,48	<0,025	0,022	1,68	0,32	1,7	-	-	-	
				250 D	760	1000	0,18	0,32	0,50	<0,025	0,010	1,68	0,32	1,6	-	-	-	
				350 D	680	1005	0,18	0,23	0,56	<0,025	0,032	1,69	0,27	1,47	-	-	-	
				350 D	608	1010	0,18	0,23	0,56	0,009	0,032	1,69	0,27	1,47	-	-	-	
GS-52.3	DIN 1681	Normalized	casting	80 T	334	569	0,31	0,53	0,83	0,006	0,009	0,12	0,02	0,06	-	-	-	
GS-13 MnNi 64	4)	Q + T	casting	100 T	344	518	0,13	0,40	1,62	0,017	0,012	-	-	1,0	-	0,06	-	
GS-26 CrMo 4	SEW 685	Q + T	casting	100 T	461	641	0,26	0,42	0,70	0,004	0,011	1,04	0,26	0,06	-	-	-	
GS-42 CrMo 4	SEW 515	Q + T	casting	100 T	474	711	0,41	0,53	0,81	0,005	0,01	1,12	0,26	0,07	-	-	-	
GS-34 CrNiMo 6	SEW 510	Q + T	casting	150 T	697	871	0,32	0,48	0,64	0,007	0,01	1,50	0,21	1,50	-	-	-	
1) Steel not standardized, corresponds to NAXTRA 70							4) Steel not standardized, produced by Hoesch AG/Dortmund											
2) Quenched and tempered							5) Stahl-Eisen-Werkstoffblatt											
3) Heat treated corresponding to case hardening																		

1) Steel not standardized, corresponds to NAXTRA 70
 2) Quenched and tempered
 3) Heat treated corresponding to case hardening

4) Steel not standardized, produced by Hoesch AG/Dortmund
 5) Stahl-Eisen-Werkstoffblatt

specimens) and in the case of cast steel from a depth of one sixth of the material thickness in compliance with German (D.I.N.) Standards. The drop weight specimens, as longitudinal specimens, were obtained in the same manner. The specimens for examination of the microscopic structure were taken from the same locations as the mechanical specimens (Fig. 2).

Test Results

Transition Temperatures CVN

Table 2 plots the transition temperatures TT 27 and FATT 50 evaluated on the basis of the notch impact energy temperature curves. In determining the TT 27 a problem arises in that the intersecting points of the 27 Joule line and the notch impact energy temperature curve are located on the lower flat part of the curve. As a result, minor differences in the plotted curve can have a distinct influence on the TT 27 values.

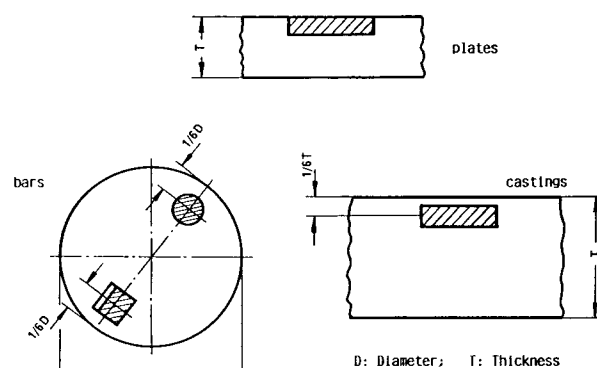


Fig. 2: Location of specimens in the cross-section of the materials tested.

NDT Temperatures

The *NDT* temperatures determined in the tests are also shown in Table 2. They were determined for only some of the materials tested.

Relationship between Transition Temperatures and *NDT* Temperatures

One objective of the tests was to determine whether a correlation exists between the transition temperatures and the *NDTT* which would be useful for practical application. Consequently, both the TT 27 and also the

FATT 50 were plotted versus the *NDTT*. It was found that the relationship was very unsatisfactory [16]. However, if plates and forgings are plotted separately from castings there is a reasonable correlation between TT 27 and *NDTT* as shown in Fig. 3. By comparison, the relationship between FATT 50 and *NDTT* was less satisfactory. This observation was somewhat surprising because according to Fig. 4 the energy absorption of the CVN specimens was found, for the measured *NDTT* temperatures, to be generally higher the higher the energy absorption in the upper shelf of the transition temperature curve and, consequently, a closer relationship was expected between the FATT 50 and the *NDTT*.

Table 2: Test results.

Name	Condition	Diameter (D) or Thickness (T) (mm)	Transition Temp. TT 27 (°C)	Transition Temp. FATT 50 (°C)	NDT-Temp. (°C)
St 52-3	N ¹⁾	40 T	-92	-45	-45
TTStE 26	N	20 T	-86	-85	-45
TTStE 36	N	20 T	-69	-58	-45
StE 690	Q + T ²⁾	22 T	-115	-	-60
Ck 45	N	100 D	+33	+55	+10
26 CrMo 4	Q + T	100 D	-110	-95	-55
		200 D	-86	-22	-35
42 CrMoS 4	Q + T	50 D	-120	-	-
		100 D	-100	-33	-55
		120 D	-75	-	-
		200 D	-7	+35	+10
		270 D	+8	-	-
		220 T	-10	-	-
34 CrNiMo 6	Q + T	50 D	-120	-	-
		120 D	-120	-	-
		200 D	-100	-30	-40
		200 T	-90	-	-
		400 D	-83	-44	-40
X 22 CrMoV 121	Q + T	100 D	-10	+25	-10
		200 D	0	+25	-10
16 MnCr 5	C.H. ³⁾	100 D	-30	-	-
		250 D	-10	-	-
17 CrNiMo 6	C.H.	100 D	-50	-	-
		250 D	-20	-	-
		350 D	-45	-	-
		350 D	-40	+5	-20
GS-52.3	N	80 T	-1	+50	-20
GS-13 MnNi 64	Q + T	100 T	-60	-	-50
GS-26 CrMo 4	Q + T	100 T	-28	+10	-30
GS-42 CrMo 4	Q + T	100 T	+41	+65	+15
GS-34 CrNiMo 6	Q + T	150 T	-38	-21	-40
1) Normalized 2) Quenched and tempered 3) Heat treated corresponding to case hardening					

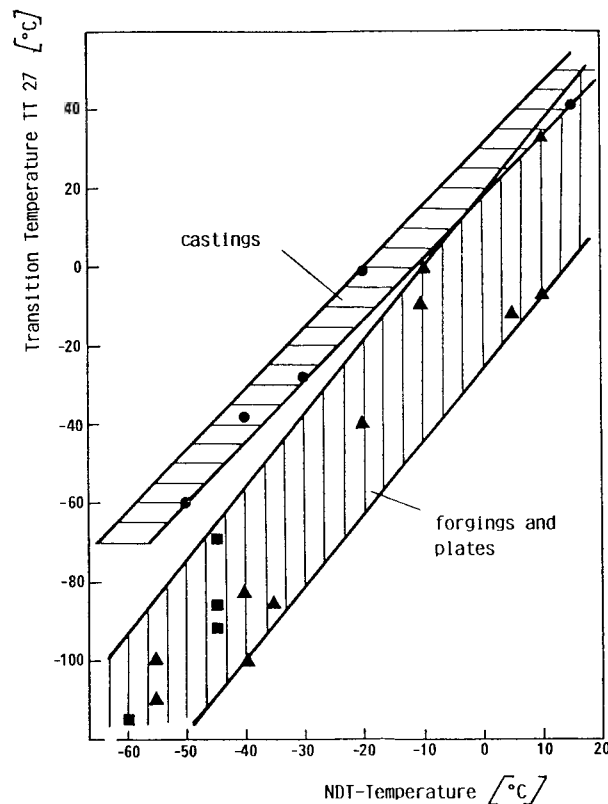


Fig. 3: Correlation between transition temperature TT 27 and NDT-temperature for castings, plates and forgings.

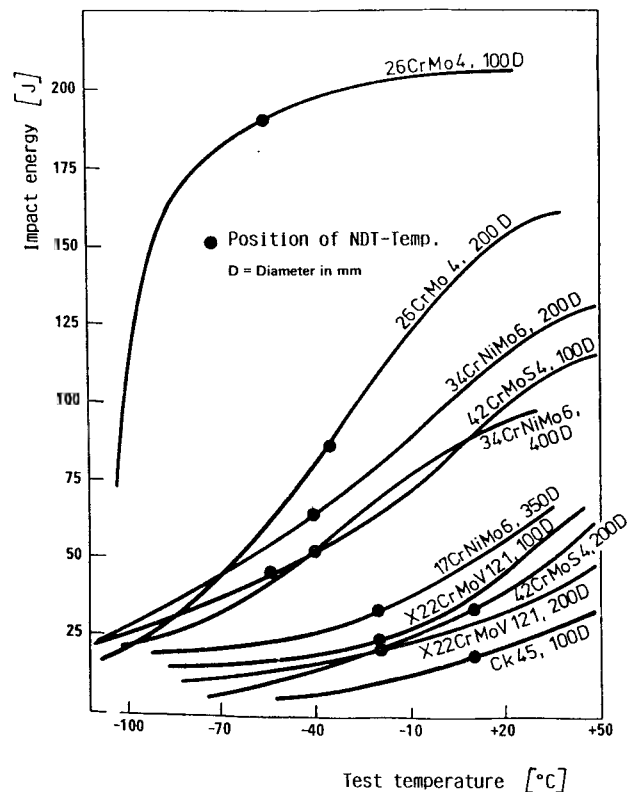


Fig. 4: Impact energy (CVN specimen) at NDT-temperature.

Influence of Material Thickness on CVN Transition Temperature for Forged Steels

With increasing material thickness the toughness values tend to change on account of the differences in the microstructure. This is shown in Fig. 5 for some forged steels where the TT 27 is plotted versus the material thickness. It is clearly seen that for case-hardening steels 16 MnCr 5 and 17 CrNiMo 6 and for the stainless steel X 22 CrMoV 121 the TT 27 is relatively independent of the thickness. And, the transition temperatures are relatively high.

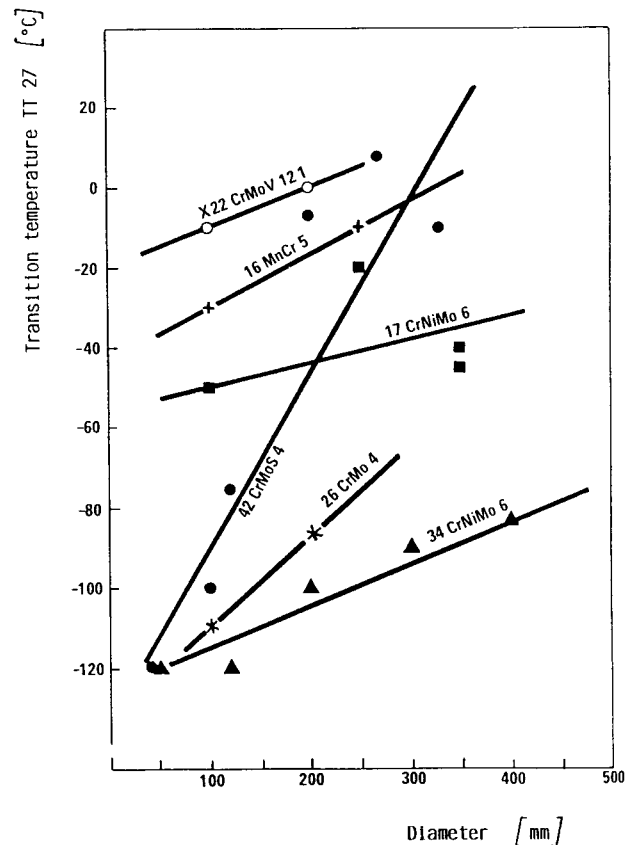


Fig. 5: Forged steels. Effect of material diameter on transition temperature TT 27.

The heat treatable steels 42 CrMoS 4, 26 CrMo 4 and 34 CrNiMo 6 behaved differently. For small thicknesses the TT 27 was very low. For the three steels the TT 27 increased with increasing thickness although not all the same degree. For the steel 42 CrMoS 4 thickness had a pronounced influence and, as a result, its application for low temperatures would be limited to relatively small cross-sections. This observation can be explained by the differences in the microscopic structure of the steels. The 16 MnCr 5 steel was found to contain coarse grained ferrite and pearlite with fractions of upper bainite and the 17 CrNiMo 6 steel contained upper bainite with slight fractions of ferrite. This applied to all material thicknesses. The X 22 CrMoV 121 steel contained practically identical bainite structures in both thicknesses which were tested.

Very fine tempered martensite was observed in the 42 CrMoS 4 at a 50 mm thickness. At greater thicknesses the structure changed from fine bainite into

coarser bainite and ferrite. This is the result of transformation in the upper bainite range. Fine-grained bainite was observed in the 34 CrNiMo 6 steel up to 200 mm thickness. Only at a thickness of 400 mm was a distinctly greater coarseness of the bainite found.

It is known from the literature [17, 18] that the microstructures developing under conditions of an increasingly accelerated cooling rate result in lower transition temperatures. From ferrite-pearlite, via upper bainite, lower bainite to martensite with subsequent tempering, the transition temperature is improved. A comparison between the 42 CrMoS 4 and 26 CrMo 4 steels shows that the steel with the higher carbon content had poorer TT 27 values. An appraisal of the structure under an optical microscope did not provide an explanation for this. According to the literature this is attributable to the negative effect of increased precipitation of carbides at grain boundaries of the steel with the higher carbon content [19]. The steel 26 CrMo 4 is therefore included in a German standard for steels with subzero temperature properties (see Table 1).

Application of Test Results

Observations Regarding Selection of Materials

Combining Figs. 3 and 5 into Fig. 6 enables a determination of the maximum possible thickness of a material for a specific *NDT* temperature. If the lowest operating temperature is specified to satisfy an *NDT* temperature of -40°C for the 42 CrMoS 4 steel, for example, the lower boundary line in Fig. 3 indicates a necessary TT 27 of -100°C and thus from Fig. 5 a maximum possi-

ble thickness of 80 mm may be used. For the 26 CrMo 4 steel the maximum thickness is 140 mm and for the 34 CrNiMo 6 steel the maximum thickness is 240 mm. Table 3 shows the permissible thicknesses of materials for different *NDT* temperatures corresponding to specific operating temperatures between -40°C and 20°C .

To obtain comparable details for cast steel it would be necessary to make additional investigations on the influence of the thickness of the material on the transition temperature TT 27.

For steel plates the test results are adequate to make a realistic appraisal of the possibilities for application. For an *NDT* temperature of -40°C Table 4 gives a list of the tested materials which can be used. Where possible, the maximum possible thicknesses have been indicated. In the case of normalized steel plates it is very difficult to determine the upper boundary thickness. However, it should be distinctly above the tested plate thicknesses shown.

Application of Linear Elastic Fracture Mechanics

Introduction

On the basis of the *NDT* concept it was possible to establish a limiting temperature below which, under certain conditions (i.e., small flaws and nominal stress equal to the yield stress) a brittle failure must be expected. Fracture mechanics offer the possibility of establishing the interaction of nominal stress and flaw size in a quantitative manner to assist in evaluating the test results.

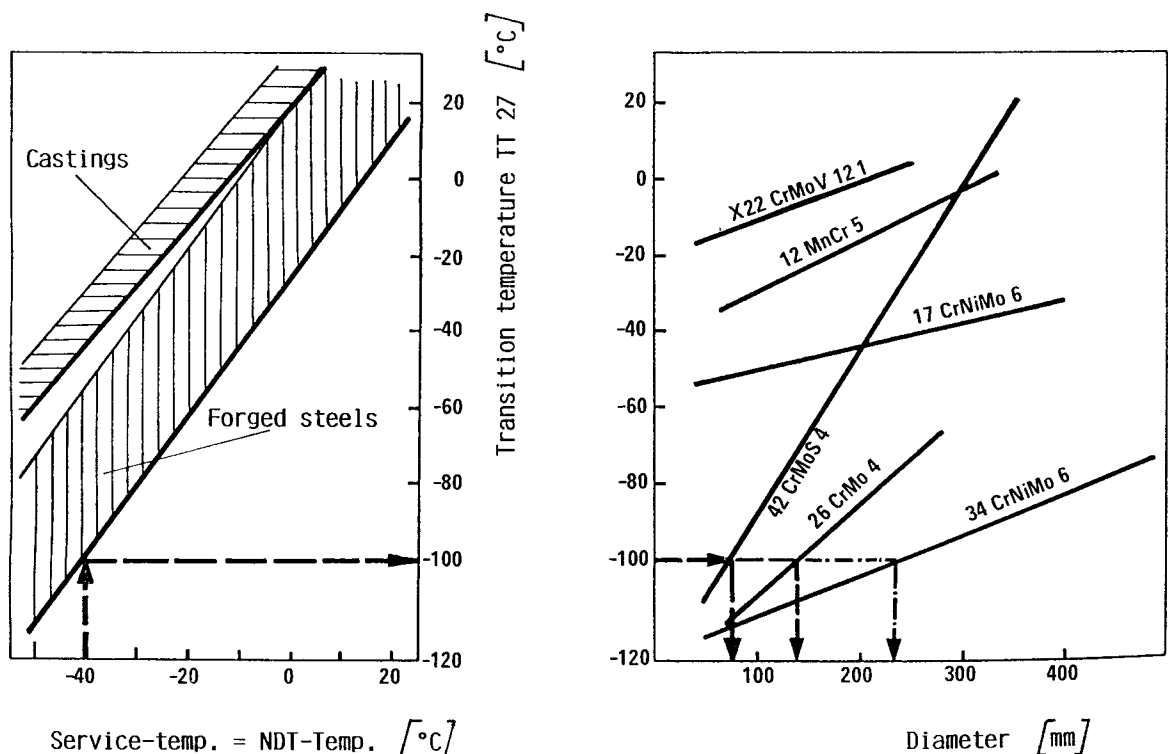


Fig. 6: Forged steels. Estimating maximum possible diameters for a particular *NDT*-(-service) temperature (shown for *NDT* = -40°C).

Table 3: Forged Steels. Estimating maximum possible diameters for different *NDT*-temperatures.

Designation	Maximal possible diameter (mm) for getting a <i>NDT</i> -Temp. of				
	-40 °C	-30 °C	-20 °C	0 °C	+20 °C
Ck 45	1)	1)	1)	1)	100
26 CrMo 4	140	220	300	450	500
42 CrMoS 4	80	120	160	250	320
34 CrNiMo 6	240	420	500	500	500
X 22 CrMoV 121	1)	1)	1)	1)	300
16 MnCr 5	1)	1)	1)	140	400
17 CrNiMo 6	1)	1)	1)	450	500
1) Material not suitable in a practical thickness					

The principles of linear-elastic fracture mechanics (LEFM) are based on the assumption that a cracklike flaw will always propagate when the change in the elastic energy stored in the component is equivalent to the surface energy required for the growth of the fractured surface. On the basis of this analysis the fracture toughness may be written as

$$K_{Ic} = f \times \sigma(\pi a_c)^{0.5} \quad (1)$$

where

K_{Ic} = fracture toughness

σ = nominal stress, vertical to flaw surface

a_c = critical flaw depth, and

f = a correction function depending on crack geometry and stress conditions.

For the practical case of the semi-elliptical surface crack

$$K_{Ic} = 1.1 \times \sigma(\pi a_c/Q)^{0.5} \quad (2)$$

where Q is the flaw shape parameter, evaluated in the literature [10, 11], depending on the flaw aspect ratio and on the ratio of the nominal stress to the yield stress.

Equation 2 was used to calculate the critical flaw depth. It should be noted that LEFM is only suitable to describe the fracture behaviour if the stress is essentially elastic, and the plastic zone at the end of the crack is small in comparison to the dimensions of the component (plane strain condition). This means that the components must have a certain thickness to permit the use of LEFM. The mechanical components of mining equipment generally consist of thick-walled forgings and castings which satisfy the criteria for the application of LEFM [10, 11].

Appraisal of Test Results

Rather than determining the fracture toughness K_{Ic} according to ASTM E 399 [20] by experiment, reference was made to the literature [21, 22] for the relationship

between the *NDT* temperature and the K_{Ic} value for a variety of forging steels, where K_{Ic} is plotted versus the temperature difference $\Delta T = T - NDTT$. For each specific application T is the temperature for which the K_{Ic} value is sought (Fig. 7). Determining the fracture toughness K_{Ic} via the *NDT* temperature offers an advantage in that it also takes into account the influence of thickness due to different states of hardening and tempering conditions. If K_{Ic} were determined according to ASTM E 399, or if the value were known from other sources, it would first have to be clarified whether the specimens used for the measurement actually originated from a test specimen with a thickness equivalent to that of the forging or casting to be evaluated.

Listed in Table 5 are various forging steels with the maximum thicknesses for which, according to Fig. 6 an *NDTT* of -40°C is achievable (Column II, Table 5). On the assumption that the operating temperature $T = NDTT = -40^\circ\text{C}$, it is shown in Fig. 7 that $\Delta T = T - NDTT = 0$. On this basis we can derive the fracture toughness K_{Ic} from Fig. 7 (Column III, Table 5). From K_{Ic} the critical crack depth a_c can be calculated using Eq. 2 for the two arbitrary nominal stresses of 100% and 50% of the yield stress (Column IV, Table 5). This is assuming a depth/length ratio of the semi-elliptical surface flaw of 0.2. Finally, on the arbitrary assumption that non-destructive testing will reliably detect a critical crack depth a_c of 2 or 4 mm, the necessary K_{Ic} values according to Eq. 2 are calculated (Column V, Table 5). A critical review can thus be made of the results obtained with the *NDT* concept.

Referring the calculated K_{Ic} values back into Fig. 7, it is possible to obtain other ΔT values on the abscissa (Column VI, Table 5). As the operating temperature ($T = \Delta T + NDTT$) is constant, new *NDT* temperatures can be calculated on this basis which, according to Fig. 6, result in other maximum possible thicknesses (Column VII, Table 5). The procedure described is shown

Table 4: Maximum possible diameter or thickness for a *NDTT* requirement of -40°C .

Designation	Maximal possible diameter or thickness for getting a NDT temperature of -40°	
St 52-3	40	1)
TTStE 26	20	1)
TTStE 36	20	1)
StE 690	22	1)
Ck 45	not suitable	
26 CrMo 4	140	
42 CrMoS 4	80	
34 CrNiMo 6	240	
X 22 CrMoV 121	not suitable	
16 MnCr 5	not suitable	
17 CrNiMo 6	not suitable	
GS-52.3	not suitable	2)
GS-13 MnNi 63	600	3)
GS-26 CrMo 4	100	2)
GS-42 CrMo 4	not suitable	2)
GS-34 CrNiMo 6	150	2)
<p>1) These thickness were tested. The materials can also be used for greater thicknesses. An upper limit cannot be indicated.</p> <p>2) The influence of thickness has not been investigated. Therefore, only qualitative statements are possible.</p> <p>3) The maker of this special grade guarantees a NDT temperature of -40°C for wall thicknesses up to 600 mm.</p>		

Table 5: Forged steels. Determination of permissible maximum diameters for different critical flaws and nominal stresses using fracture mechanics.

I	II	III	IV		V		VI		VII	
Material	Max. Diameter for NDT temp. – -40°C according to Fig. 6	Fracture toughness K_{IC} at NDT temp. 40°C according to Fig. 7	Critical crack depth a_c calculated with K_{IC} (1) according to III at nominal stress of		K_{IC} value calculated from equation 1 for $a_c = 2.0$ mm (2) ($a_c = 4.0$ mm) at nominal stress of		Permissible change in NDTT to obtain safety against brittle fracture at -40°C (according to Fig. 8)		Maximum thickness taking into account Column VI and Fig. 6	
			50% R p0.2	100% R p0.2	50% R p0.2	100% R p0.2	50% R p0.2	100% R p0.2	50% R p0.2	100% R p0.2
	(mm)	(N/mm ^{3/2})	(mm)		(N/mm ^{3/2}) (3)		(K) (3)		(mm) (3)	
26 CrMo 4	140	1850	23.0	5.0	550 (770)	1170 (1650)	>160 (>160)	60 (10)	>500 (>500)	~500 (220)
42 CrMoS 4	80	1850	17.4	3.8	630 (890)	1340 (1900)	>160 (140)	40 (-5)	>500 (>500)	250 (50)
34 CrNiMo 6	240	1850	13.0	2.8	720 (1020)	1550 (2190)	>160 (100)	20 (-20)	>500 (>500)	~500 (not suit.)
X 22 CrMoV 121	not suitable	1850	—	—	720 (1020)	1550 (2190)	>160 (100)	20 (-20)	>500 (>500)	not suit. (not suit.)
16 MnCr 5	not suitable	1850	—	—	560 (800)	1210 (1710)	>160 (160)	60 (10)	>500 (>500)	420 not suit.
17 CrNiMo 6	not suitable	1850	—	—	930 (1320)	2000 (2830)	110 (45)	-10 (-35)	>500 (~500)	not suit. (not suit.)

(1) The yield point applied is the value guaranteed according to standard for thicknesses – 250 mm. No standard values exist for case-hardening steels. In this case, actually measured values have been used.
(2) Assumed: semi-elliptical surface crack with crack depth-to-crack length ratio $a/c = 0.2$.
(3) Bracketed values are for a critical crack depth $a/c = 4.0$ mm.

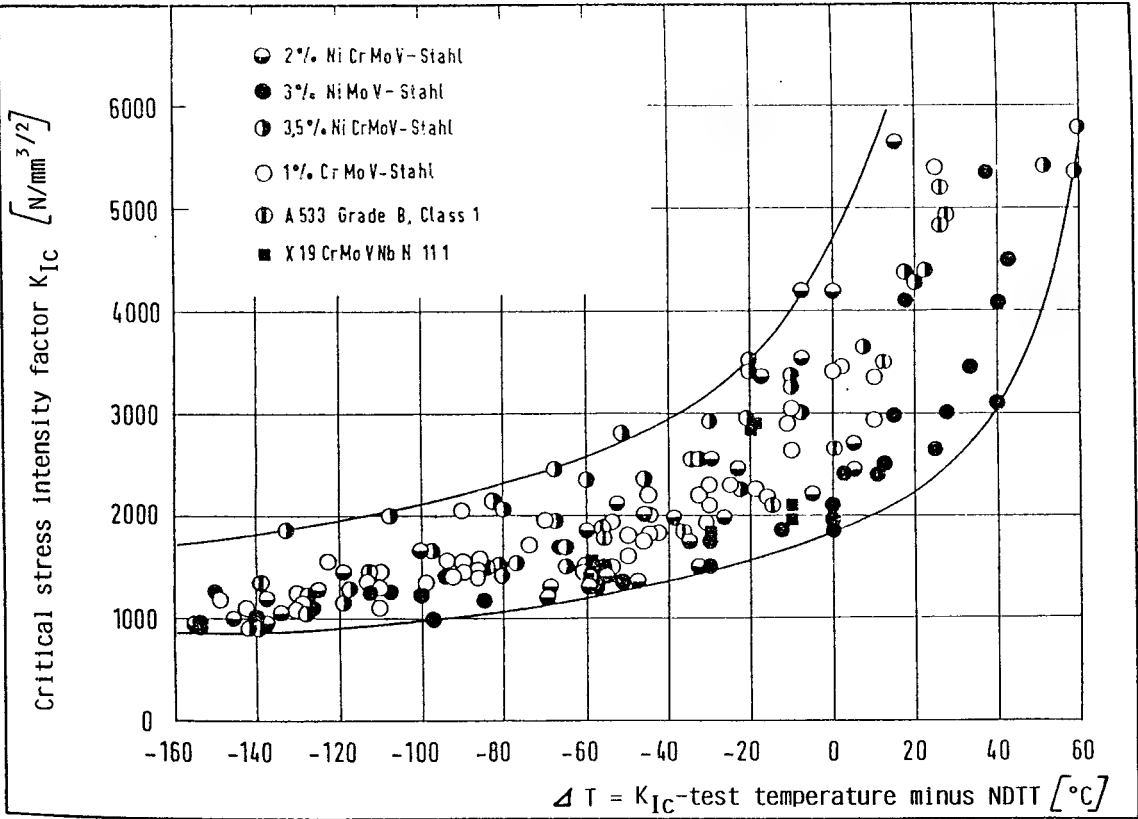


Fig. 7: Critical stress intensity factor K_{IC} vs the temperature difference K_{IC} test temperature minus $NDTT$ for various forging steels according to (19).

schematically in Fig. 8. It is clearly seen that the analysis by fracture mechanics leads to other limiting thicknesses and also to a different grading of the steels than shown in Table 3 on the basis of the *NDT* concept.

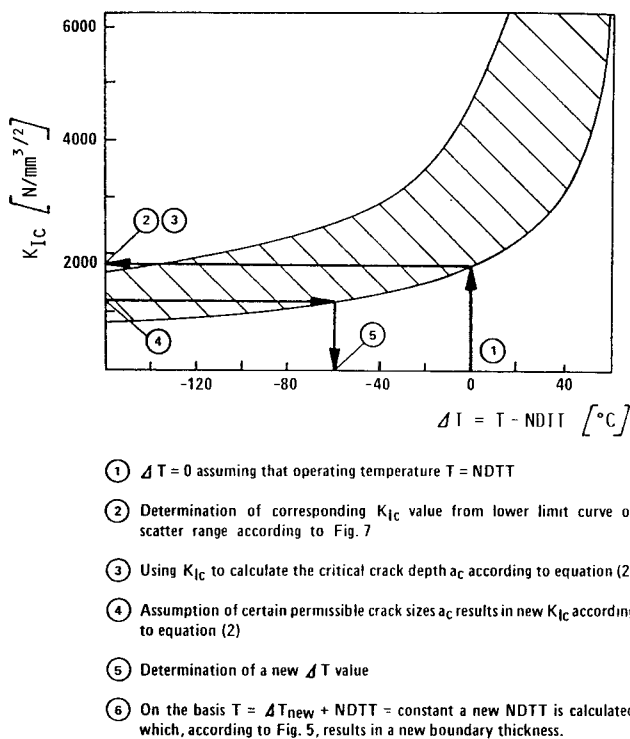


Fig. 8: Explanation for the determination of permissible diameters with the aid of fracture mechanics, basing on the assumption that the operating temperature is equal to *NDT* temperature.

If the nominal stress is assumed to be only 50% of the yield stress the steels can be used at -40°C in all thicknesses required in practice. This shows the strong influence of the nominal stress to which the components are subjected. The high-strength steels, on account of their high yield limit, are rated distinctly lower than according to the *NDT* concept.

Discussion and Conclusion

Plate Materials

The applied *NDTT* concept is well suited for an appraisal of the brittle fracture behaviour of plate materials because in welded structures, due to the influence of residual stresses, the stress level can readily reach the magnitude of the yield limit. Also, weld faults cannot be ruled out with all certainty.

The plate materials evaluated in this study can be used for welded structures down to temperatures of -40°C . For the normalized plates, owing to the low influence of heat treatment, the maximum permissible plate thickness at -40°C should be distinctly above that of the tested plate thicknesses. The structural steel St 52-3 calls for a certain amount of caution. This plate material

revealed extraordinarily good toughness properties. However, in general practice, substantial differences must be expected in low-temperature behaviour because the melting process can vary. Strong desulphurization, as in the case of the tested plate, and the degassing process carried out by some steelworks, can contribute to very good toughness values. However, this is not the rule. Whenever necessary, it might therefore be advisable to consult the steelworks regarding the proposed melting procedure.

To achieve the toughness properties of the parent metal in the weld zone it is important to observe the welding parameters given by the steel manufacturers and/or the material standards. This applies in particular to liquid-quenched steel St E 690 which reacts very strongly to this.

Forged Materials

In the case of forged materials the *NDTT* concept leads to a simple, but very conservative, appraisal which can impose distinct limitations on the feasibility and economy of the structure. This is shown by the relatively small permissible thickness and by the fact that individual materials cannot be used at all at temperatures of -40°C . For instance, on the basis of this concept, the two steels 16 MnCr 5 and 17 CrNiMo 6 generally used for the internals of gearboxes are unsuitable for application at subzero temperatures. However, in general practice, the gearboxes would under such conditions be equipped with heating facilities. Similarly, according to this concept, the stainless steel X 22 CrMoV 121 also fails to offer safety against brittle failure. However, as it is generally only used for hinge pins with little or no notch effect, the risk may be acceptable.

The question which arises is whether better utilization of the material is possible for machinery components where stress conditions can be calculated relatively accurately and generally good access is available for non-destructive examination. Assuming the presence of realistic flaw sizes which nowadays are readily detectable with the aid of non-destructive inspection techniques, as well as realistic nominal stresses in the component, it is possible to make an evaluation by fracture mechanics. This permits the use of lower alloyed materials and of greater thicknesses. Where flaws are very small and stresses are low it is possible to use all the tested materials at -40°C . In the case of the non-alloyed steel Ck 45 a further investigation would be required.

In so far as fatigue-stressed machinery components are concerned the assumed crack sizes are liable to be exceeded due to stable crack growth and, as a result, the assumptions on which the fracture mechanics analysis is based lose their validity. These considerations call for a structure with minimum notch effect, thereby counteracting the development of fatigue cracks.

References

- [1] Pellini, W.S., and Eschenbacher, E.W., "Ductility Transition of Weld Metal," *Weld J.* 33 (1), 1954, pp. 165-205.
- [2] Puzak, P.P., Babecki, A.I., and Pellini, W.S., "Correlation of Brittle Fracture Service Failures with Laboratory Notch-ductility Tests," *Weld. J.* 37 (9), 1958, pp. 391-410.
- [3] Pellini, W.S., and Puzak, P.P., "Fracture analysis diagram. Procedures for the fracture safe engineering design of steel structures.", NRL Report 5920, March 15, 1963.
- [4] Puzak, P.P., and Pellini, W.S., "Standard Method for NRL Drop Weight Test." NRL Report 5831, August 21, 1962.
- [5] Pense, A.W., "Factors Controlling Fracture Behaviour of Cold Temperature Structures." *Proceedings on Fracture Toughness Evaluation of Steels for Arctic Marine Use.* CANMET, Ottawa, 1983.
- [6] Wells, A.A., "Experiments on the Arrest of Brittle Cracks in 36 in. Wide Steel Plates." *Brit. Weld. J.*, 3 (11) 1956.
- [7] Wells, A.A., "Brittle Fracture in Welded Structures. A Contemporary View." *Weld. Metal Fabr.*, 29 (3) 1961, pp. 89-94.
- [8] Robertson, T.S., "Propagation of Brittle Fracture in Steel," *J. Iron Steel Ins.*, 12, 1953, pp. 361-374.
- [9] ASTM E 208-6, "Standard Method for Conducting Drop Weight Test to Determine Nil-ductility Transition Temperature of Ferritic Steels." *Annual book of ASTM Standards*, Part 10.
- [10] Heckel, K., *Einführung in die technische Anwendung der Bruchmechanik* (Introduction into the technical application of fracture mechanics), Carl Hanser Verlag, München, 1970.
- [11] ISI Publication *Fracture Toughness*. The Iron and Steel Institute, London, 1968.
- [12] BS 5762:1979 Methods of crack opening displacement (COD) testing. British Standards Institution.
- [13] PD 6493:1980 Guidance on some methods for the derivation of acceptance levels for defects in fusion welded joints. British Standards Institution.
- [14] Bellow, D.G., Klotzbücher, E.F. and Kraft, H.E., "The Influence of Thickness on Fracture Toughness Testing," 5th Int. Offshore Mechanics and Arctic Engineering Symposium, Tokyo, 1986, pp. 197-203.
- [15] ASTM E 23-81 Notched-bar impact testing of metallic materials.
- [16] Bellow, D.G., Klotzbücher, E.F., and Kraft, H.E., "On the Selection of Materials for Cold Temperature Service," *Proc. Exp. Mech.*, Las Vegas, 1985, pp. 428-434.
- [17] Habracken, L.I., and Economopoulos, M., "Bainitic microstructures in low carbon alloy steel and their mechanical properties." Symposium Transformation and Hardenability in Steels, University of Michigan, Feb. 1967.
- [18] Piehl, K.H., "Einfluß von chemischer Zusammensetzung und Gefüge auf die Eigenschaften von Nickel-Chrom-Molybdän-Vanadin-Vergütungsstählen für schwere Schmiedestücke, besonders für Niederdruck-Turbinen und Generatorwellen" (Influence of chemical composition and microstructure on the properties of nickel chromium molybdenum vanadium heat treatable steels for heavy forgings, especially for low-pressure turbine and generator shafts), *Stahl und Eisen* 95 (18), 1978.
- [19] Meyer, L., and de Boer, H., "Überblick über hochfeste niedrig-legierte Stähle" (Overview of high-strength low-alloyed steels), *Thyssen Technische Berichte* 1, 1977.
- [20] ASTM E 399 *Plane Strain Fracture Toughness of Metallic Materials*.
- [21] Wellinger, K., "Sprödbbruchuntersuchungen an warmfesten Schraubenwerkstoffen" (Brittle fracture analysis of heat-resistant bolt materials), *VGB Kraftwerkstechnik*, No. 7, July 1975, pp. 455-466.
- [22] ASME Code Sect. III, Div. 1, Subsection NA, Fig. G-2110.1.

Start here for second page
Début de la deuxième page

COMPUTER CONTROL FOR FRACTURE TOUGHNESS TESTING

V. Morgenstern and R. Herrera
University of Mar del Plata
Argentina

B.M. Patchett, D.G. Bellow and I.A. Buttar
University of Alberta
Edmonton, Alberta, Canada

Begin page 1
Début du texte

Introduction

Measurement of toughness is often expensive, time consuming and fraught with error due to the type of test employed and the amount of data required to be processed and analyzed. Prediction of the behaviour of a pre-existing crack in a structural element under given loading conditions is essential for the analysis of overall structural integrity. In high fracture toughness steels a large scale yielding situation will appear before fracture occurs. The usual linear-elastic theory must be replaced by an elastic-plastic approach in which either the J integral (Rice, 1) or Crack Tip Opening Displacement (CTOD, 2) may be used for the prediction of crack tip behaviour.

The fracture toughness J_{1c} and δ_1 are the critical values of J and CTOD that need be determined as a crack extends from a pre-existing crack. The unloading compliance method can be used to determine the onset of crack extension. The values of J and δ can be calculated and the amount of crack extension determined by measuring the load, clip gauge displacement and load line displacement.

This report describes a low cost interactive computer control and data processing system used to determine J-R and CTOD-R curves following the method described by Clarke and Brown (3). The J_{1c} values were determined according to ASTM E813-81(4) and the critical CTOD values at initiation according to BS 5762-79(5). Results were obtained initially for the base metal (BM), weld metal (WM) and heat-affected zone (HAZ) regions on an A36 structural steel.

Computerized Testing System

A computer controlled and monitored system was developed on the basis of a post testing system whereby the load and displacement data is recorded and the fracture toughness calculations are carried out after the test is completed. The objectives of the data reduction computer program were to

- 1) Calculate the areas under the load-displacement curve up to each unloading point.
- 2) Determine the clip gauge and load coordinates corresponding to each unloading.
- 3) Find the load and clip gauge coordinates corresponding to the critical value of CTOD as defined by BS5762-79 (5).
- 4) Determine the slope of each unloading curve with a least squares fit.

The areas were measured using displacement increments of 0.01 mm and the trapezoidal rule. The data were taken every 0.5s during the loading portion of the test. During the partial unloadings the data were taken at the rate of 15 per sec. The control and data acquisition system is shown in Fig. 1. The calculation sub-routine is shown in Fig. 2. Three other subroutines, not shown, were used to calculate the area under the curves, a least squares subroutine, and a filter subroutine which was used to reject meaningless load extension values which sometimes occur at the low end of the J-curve.

The final J-R curves were constructed using recalculated values of the crack extension Δ_a from

$$\Delta_a = a_1 - a_0 + \text{offset}$$

where the offset was the shift along the Δ_a axis. An offset was sometimes required due to slight systematic differences between the initial crack length measurement made during the tests. Only offsets of less than one percent of the initial crack length were considered acceptable.

The computer system upon which the program was based used an IBM PC and a Data Translation DT 2805 12 bit interface to an MTS testing machine. An alternate system using a Commodore 128 with a Microtech "Fast Diadic" 12 bit interface was developed to further reduce costs. Both systems use the same logic and flow chart progression.

Experimental

The welded test specimens were fabricated from 38 mm thick A 36 structural plate. The rolling direction of the plate was transverse to the weld joint and the overall dimensions were 1.2 m long by 420 mm wide. The edges of the joint were machined flat at 90° to the plate surface. The joint was a square butt narrow-gap design with a 13 mm gap. The welding was carried out in the flat position using a High Speed Rotating Arc (HSRA) GMAW process developed in Japan by Nippon Kokan.

Two specimen types were utilized; compact tension (CT) and single edge notch bending (SENB). All specimens were precracked in fatigue before testing. After precracking the specimens were side grooved to a depth of 20 percent of the original thickness.

Centre title in CAPITALS
Arrange authors names, titles and addresses uniformly in this space

Titre en MAJUSCULES (au centre)
Noms, Titres et adresses des auteurs (au centre)

The specimens were slowly loaded in stroke control at a rate less than 0.01xW per min. controlled by the computer program. At the end of the test each specimen was heat tinted (to expose the area of fracture) and then broken open. The fatigue crack length and final crack extension were measured.

Results

Figure 3 shows a typical J-R curve for the WM, BM and HAZ. The black dots indicate the points of evaluation corresponding to each unloading.

Conclusions

1. The computer program developed CTOD-R and J-R integral curves facilitated an estimation of δ_i and J_1 as well as the critical value of CTOD according to BS5762:79 and J_{1c} to E813:81.
2. Both the IBM and Commodore systems were easily adaptable to the testing procedure required. Where funding is a problem the Commodore system may be of advantage from a cost point of view.

References

1. Rice, J.R., "A Path Independent Integral and Approximate Analysis of Strain Concentration by Notches and Cracks", *Jour. Ap. Mech* 35, 379-386, 1968.
2. Burdekin, F.M. and Stone, D.E., "The Crack Opening Displacement Approach to Fracture Mechanics in Yielding Materials", *Jour. Strain Analy.* 1(2), 145-153, 1966.
3. Clarke, G.A. and Brown, G.M., "Computerized Methods for J_{1c} Determination using Unloading Compliance Techniques", *ASTM STP 710*, 110-126, 1980.
4. ASTM E 318-81, "Standard Test for J_{1c} . A Measure of Fracture Toughness," 1981.
5. BS5762-79, "Method for Crack Opening Displacement CTOD", *British Stand. Inst.*, 1979.

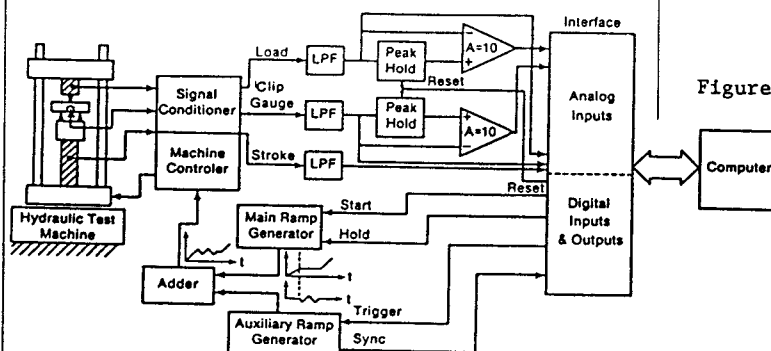


Figure 1. Block diagram for equipment computer interface

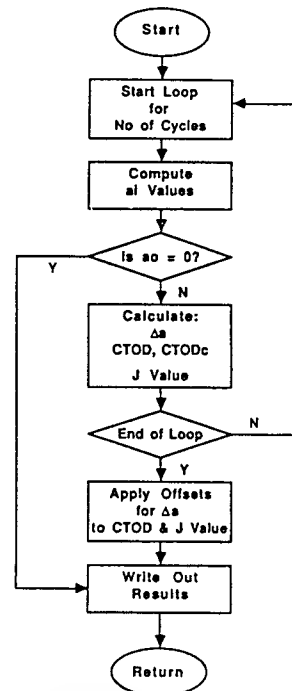


Figure 2. Calculation Subroutine

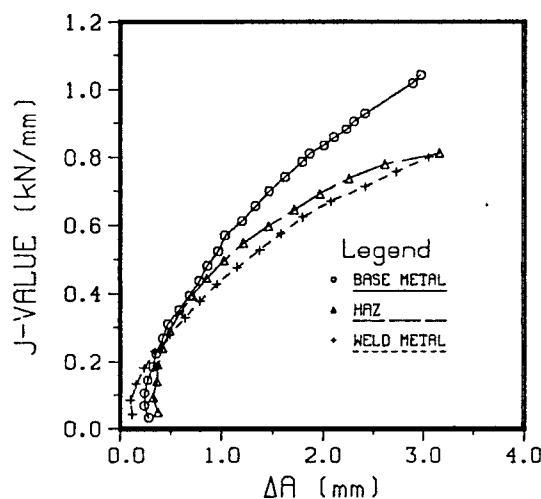


Figure 3. J-R curves for A-36 structural steel



PRODUCTION OPERATIONS

Bending stresses in otherwise straight sucker rods

D.G. BELLOW and R.K. HOWE
University of Alberta

ABSTRACT

In many cases sucker rods fail in the upset portion near the pin end. This may be due to bending stresses resulting from lack of straightness in the rod, even though it was manufactured to be within the API Specification 11B. A number of new, unused rod coupling pairs were analyzed for straightness and a model was developed to predict the bending stresses. It was found, that for some rod coupling configurations, there existed bending stresses as high as 68% of the axial stress. This suggests that the API 11B Specification may not be stringent enough.

Introduction

Research into sucker-rod problems has been ongoing for 50 years or more, resulting in several significant improvements in rod-coupling performance. Nevertheless, failures of rod strings continue to be a problem for the oil producer. As down-hole components get older and well conditions become more corrosive this problem will become more severe. However, there are three avenues which can be followed to alleviate the problem:

1. Reduce the loads on rods appropriate to the specific well conditions (dog-leg, etc.) and environment (i.e. apply more stringent design service factors).
 2. Replace current rods using materials with improved properties.
 3. Improve the current design and manufacturing techniques to eliminate the weaknesses inherent in existing rod strings.
- While (1) above may not be practical except under a total replacement program and (2) requires long-term research and careful examination, (3) may provide the most benefit in the short term but, like (1), would only apply to replacement rods and strings.

The purpose of this paper is to describe a problem related to the third category involving the lack of straightness in sucker-rods which are made within API 11B Specification⁽¹⁾. It will be shown that non-straight rod ends can lead to undesirable bending stresses near the upset pin-end.

Statement of Problem

For the purpose of this study, a rod end is defined as the length from the pin end to a point 860 mm (34 in.) back towards the

rod body. The rod end is defined as non-straight if its centre line deviates from a theoretical centre line with extends through the pin.

To examine bending stresses in non-straight rod ends, a dimensionless bending stress ratio (DB) is defined as:

$$DB = \frac{\text{bending stress}}{\text{axial stress}}$$

The dimensionless bending ratio (DB) can be defined in terms of the axial load P , second moment of area I , cross-sectional area A , and y the distance from the theoretical straight line to the rod centre. Thus,

$$DB = (Py/I)/(P/A) = 4y/r$$

In an earlier work⁽²⁾ it was shown that bending stresses can be determined in rods of uniform cross section with sharp bends in them by considering elementary beam theory where the bending moment M is given by

$$M = EI \frac{d^2(y_0 - y)}{dz^2}$$

and $y_0 - y$ = deflection of bar from the unloaded position, EI is the rod stiffness and z the distance along the rod as measured from the pin end.

By equating the moments and rearranging terms it can be shown that the governing differential equations in the x and y directions can be written as

$$\frac{d^2y}{dz^2} - \frac{P}{EI} y = \frac{d^2y_0}{dz^2}$$

and

$$\frac{d^2x}{dz^2} - \frac{P}{EI} x = \frac{d^2x_0}{dz^2}$$

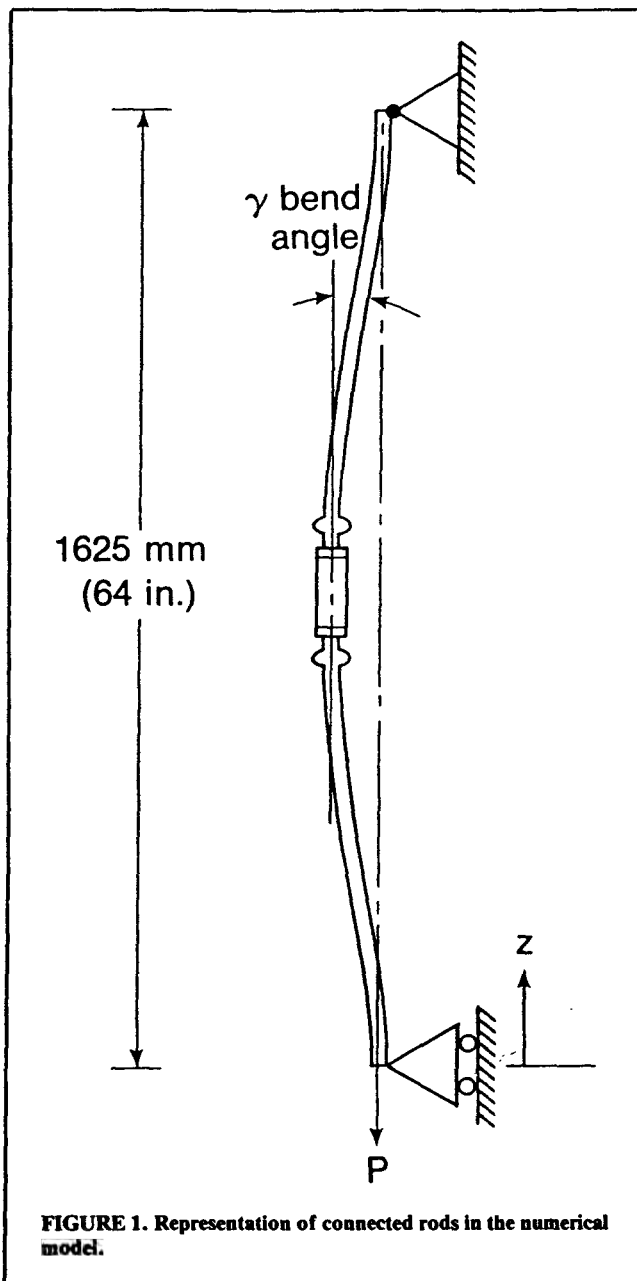
For a non-straight rod the bending stress ratio at any cross section can be determined from the final deflected position with

$$DB = (4/r)(x^2 + y^2)^{1/2}$$

In order to analyze the stresses in a non-straight rod the differential equation must be solved for the case of a changing cross section, which occurs in the upset end, and any bend in three dimensions. It is appropriate to use a numerical solution and cast the equations into finite difference form. That is

Keywords: Sucker rods, Axial stress, Bending stress, Dimensionless bending ratio (DB), Total indicated run out (TIR), Angle of bend.

Paper reviewed and accepted for publication by the Editorial Board of The Journal of Canadian Petroleum Technology.



$$\frac{y_{i+1}}{h_{i+1}} + \frac{y_{i-1}}{h_i} - \left(\frac{h_i + h_{i+1}}{h_i h_{i+1}} + \frac{h_i l_{i+1} + h_{i+1} l_i}{2EI_i l_{i+1}} P \right) Y_i$$

$$= \frac{Y_{oi+1}}{h_{i+1}} + \frac{Y_{oi-1}}{h_i} - \frac{h_i + h_{i+1}}{h_i h_{i+1}} Y_{oi}$$

A similar equation can be written for the x-direction. This analysis assumes that no moments are applied at the ends of the rods and that the boundary conditions can be represented as

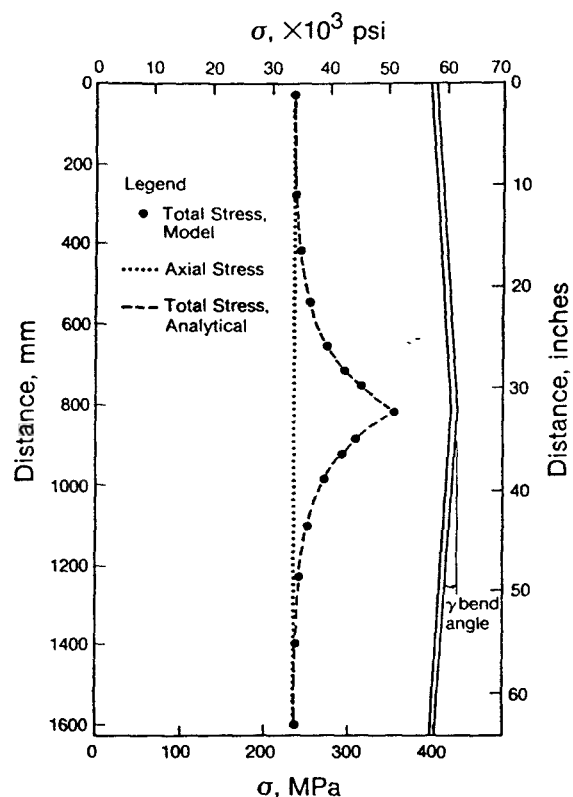
$$y = 0 \text{ at } z = z_1 \text{ and } z = z_2$$

For an "n" element model the solution involves two independent sets of (n-1) linear equations each with (n-1) unknowns.

A computer program was developed to analyze the connection of two rods utilizing seventy elements of unequal size; small elements were used in the upset end of rapidly changing cross section, larger elements were used in the other areas. The model idealizes the connection of two rods as a 1625 mm (64 in.) long non-uniform bar loaded axially as shown in Figure 1.

The model was checked with an analytical solution of a

Sharp Bend, $\gamma = 0.5$ Deg, 67000 N Load (15000 lbs)



sharply bent bar of uniform cross section. The analytical solution, which was verified by back substitution, is

$$\left(\frac{EI}{P} \right)^{1/2} \gamma \exp \left\{ - \left(\frac{P}{EI} \right)^{1/2} z \right\} = y$$

where

$$\frac{d^2 y}{dz^2} = 0, \quad \frac{dy}{dz} = -\gamma \text{ at } z = 0 \text{ and } y = 0 \text{ at } z = \infty$$

and γ in the angle of the bend as shown in Figure 1.

In Figure 2 it is shown that there was good agreement between the two solutions, indicating that the use of a shortened section of a rod to model a longer rod-string is valid providing the bend (after deflection) is confined to the central section of a coupled rod pair (including the joint).

Experimental Procedure

The experimental program consisted of a random selection of finished sucker rods for which the centre line (outward bend) deviation of the rod from the centre line was measured for a number of rotational angles of the rod. The magnitude and angle of deviation for a given cross section was then obtained using a least squares-fit procedure with the centre line deviation data. The technique resulted in an approximation of the true deviation of the centroid as long as the asymmetry of the cross section was small.

The centre line deviations were determined at six different angles requiring a total of 12 measurements at each location along the rod axis. The angle and radius of deviation were then calculated using the least squares analysis, and the entire procedure repeated for each of 32 locations along the rod length. The measurements were made using a LVDT (linear voltage differential transformer) connected to a digital data acquisition

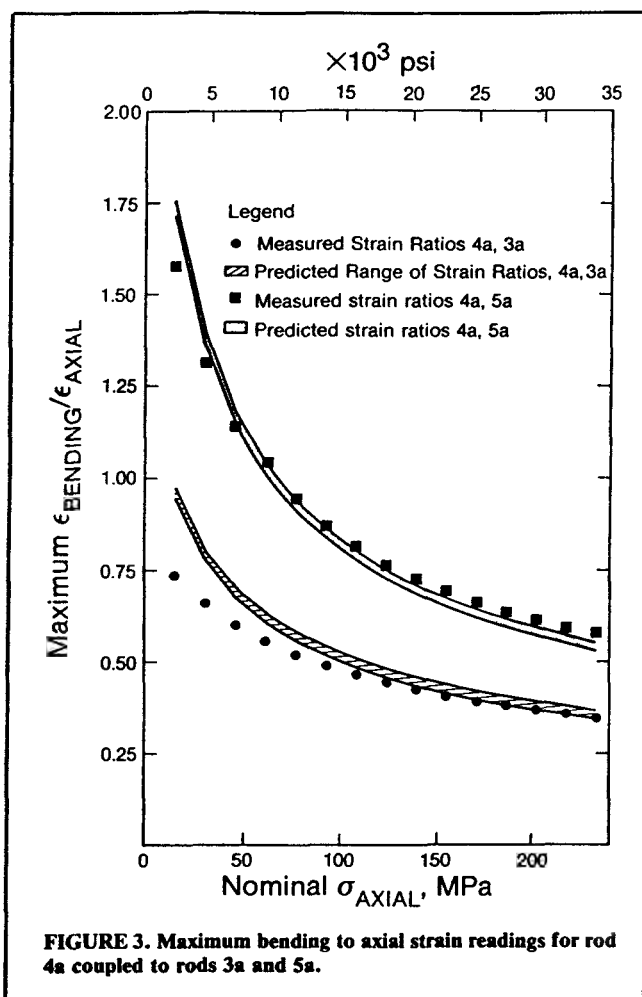


FIGURE 3. Maximum bending to axial strain readings for rod 4a coupled to rods 3a and 5a.

system which carried out the least squares analysis. This procedure was compared with measurements using a dial gauge with vertical deviations measured at 18 different rotation angles. For a 95% confidence level the procedure was deemed to be accurate (as compared with the dial gauge) to ± 0.03 mm (± 0.001 in.) in measuring the magnitude of deviation and ± 4 degrees in measuring the angle of deviation.

An experiment was designed to check the theory. From a production batch of 1830 mm (6 ft) long, 19 mm ($3/4$ in.), grade C quench and tempered sucker rods, five sucker rods were selected at random. The rods were cut in half to provide 10 rod ends 915 mm (3 ft) in length so as to fit in the limited space of the testing machine.

Ten rod ends represented 45 possible rod connection pairs each of which could be connected with a multitude of angles*. This enabled a large number of different rod connections to be analyzed using the mathematical model. The analysis was used to examine the stresses occurring throughout the possible range of rod combinations.

After the rods were measured by the techniques described above, a rod and coupling joint was torqued according to the Specification API 11-B. Electrical resistance strain gauges were applied to the rod along the body and on the upset end. The rod joint consisted of the test rod, a standard coupling and a calibration rod. The calibration rod was measured to have no centre line deviation. This rod string combination was axially loaded in an Tinius Olsen testing machine to 67 kN (15 000 lb) in load increments of 4.5 kN (1000 lb). At each load increment the strain gauge readings were recorded.

Experimental Results

A representative set of results of the load tests are plotted in Figure 3 along with the predictive values derived from the theoretical model. In Figure 3 a rod end 4a was coupled in turn

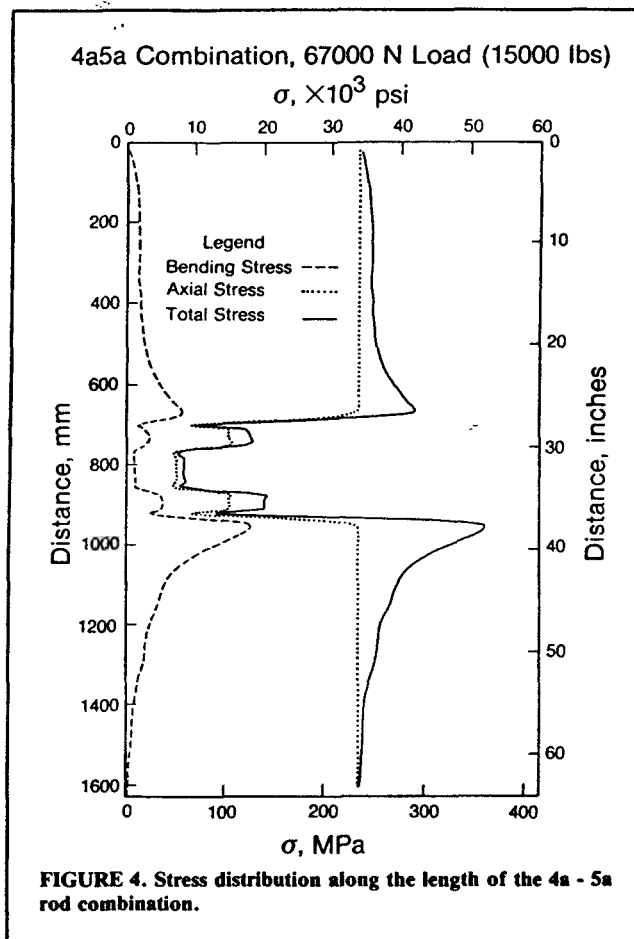


FIGURE 4. Stress distribution along the length of the 4a - 5a rod combination.

with a rod end 3a and then with a rod end 5a. Rod 4a was measured to be straight with no centre line deviation. It is seen that there is good agreement between theory and experiment. In these figures the strain ratio (bending strain divided by axial strain, which for a constant modulus of elasticity, is equivalent to DB) was plotted as a function of the nominal axial stress (applied load divided by nominal cross-sectional area of rod body).

For the stress distribution along the rod length Figure 4 plots theoretical values obtained from the model. The data was calculated for an axial load of 67 kN (15 000 lb). This produces an axial stress of 23 MPa (34 000 psi). For a different axial stress DB becomes

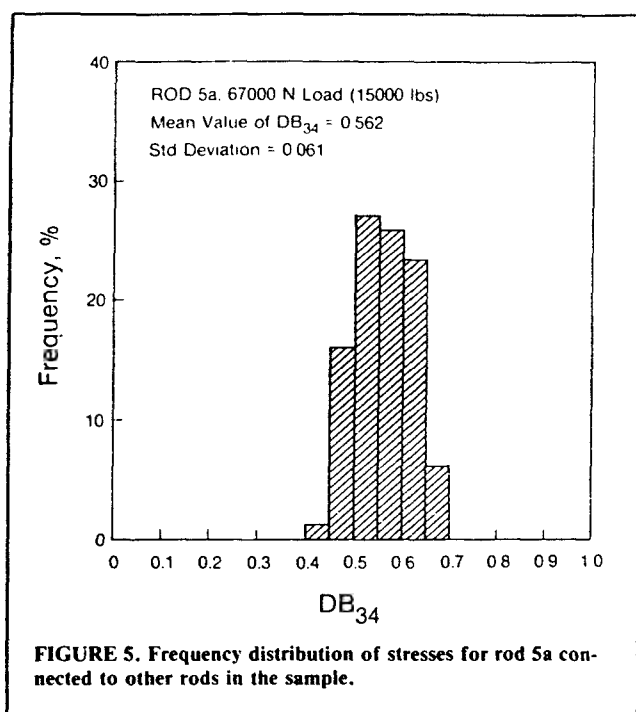
$$DB = DB_{34} (234 \text{ MPa} / \sigma_{\text{axial}})^{1/2}.$$

In all rod combinations studied the maximum bending stress occurred in the vicinity of the transition between the upset end and the rod body as can be seen in Figure 4. This is the location of many sucker rod failures⁽³⁾. The bending stress diminishes rapidly away from this point. It is interesting to note that even a straight rod (4a) can have significant bending stresses when connected to a rod with some deviation (5a).

Discussion of Results

Because the bending stress in one rod is influenced by the bend in the adjacent rod and the axial load, it is not possible to assign a single value which describes the deviation of a non-straight rod. To illustrate this, Figure 5 shows a frequency plot of the result of DB ranging from 0.4 to 0.65 that occurs in a single rod (5a) when connected to different rods at a number of angles. Even when a given combination of two rods is connected, the angle of the connection can affect the DB, as seen in Figure 6. The DB that occurs when a rod end is coupled to a straight rod can be used as a

* This assumes that the final torque angular position is determined by the API-11B Specification and the position of the start of the first thread on the pin end is chosen arbitrarily in the machining of the thread.



measure of straightness but this may underestimate the DB that can occur in actual practice.

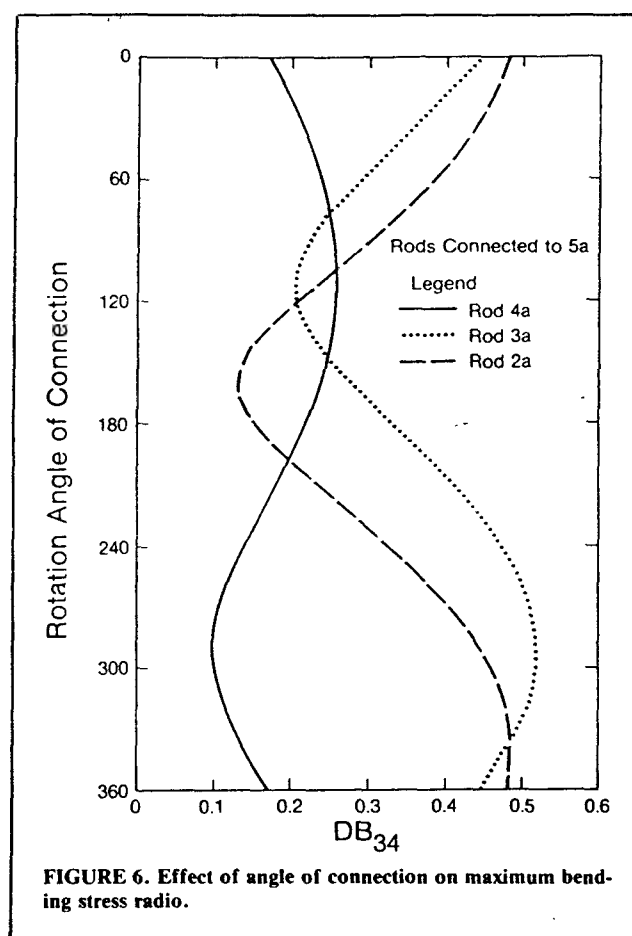
An interesting finding from the computer analysis was the extent to which stresses were increased by small deviations in the rod end. In Figure 7 a frequency distribution was constructed by analyzing each of the possible 45 rod pair combinations at twelve different angles of joint make-up for a 234 MPa (34 000 psi) axial stress. The values of DB_{34} [i.e. DB at an axial stress of 234 MPa (34 000 psi)] ranged up to 0.68 with a mean value of 0.29 yet all the rods in the sample were manufactured to within the API Specifications for straightness. In a rod string loaded to a nominal stress of 234 MPa (34 000 psi) a connection with a DB of 0.68 would be loaded to a total stress of 393 MPa (57 000 psi). That is, the axial stress of 234 MPa (34 000 psi) would also have a bending stress of 0.68×234 or 159 MPa (23 000 psi) added to it bringing the sum to 393 MPa (57 000 psi). This could overstress the rod leading to premature failure.

API Specification for Straightness

One difficulty with the API Specification is that it measures straightness on the rod end in isolation to any connected rod. It has been shown in this paper that DB_{34} is significantly affected by the adjoining coupled rod. However, it would not be practical to measure straightness using a coupled rod. In addition, the API Specification does not correlate with the stresses predicted to occur in the bent rod ends.

Using the API method⁽¹⁾ to measure straightness the rod is centred in a lathe 457 mm (18 in.) from the rod shoulder. The rod is then rotated through 360 degrees while a dial gauge is used to measure the deviation or total indicated run out (TIR) at the shoulder. For rods to be within API Specifications the TIR must be less than 5.1 mm (0.2 in.).

In Figure 8, the TIR is plotted against DB_{34} for the 10 rod ends evaluated in the sample. As can be seen there is little correlation between the TIR and DB_{34} . For example, if the specification for an acceptable TIR was reduced from 5.1 mm (0.2 in.) to 2.5 mm (0.1 in.), the mean value of DB_{34} would remain the same. At best, modifying the standard would just eliminate the worst case in the sample analyzed. While it would screen out 70% of the rods in the sample the average DB_{34} would remain unaffected. In an attempt to improve the correlation, the API method was modified by measuring TIR with the rods clamped 100 mm (4 in.) from the shoulder. This



reduced the scatter by about 50%, but the correlation between DB and TIR was still judged as poor.

Despite the limitations of the API method using TIR a better alternative for measuring straightness is not obvious. As the results of this study show the straightness of a coupled pair should really be evaluated to estimate the effects on bending stresses. But this is not practical as there is no way to know which rod pairs will be coupled together in the field.

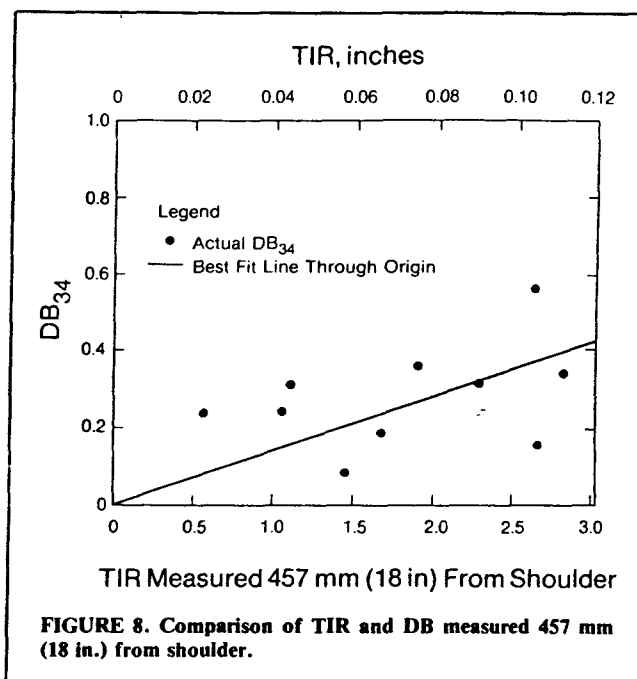
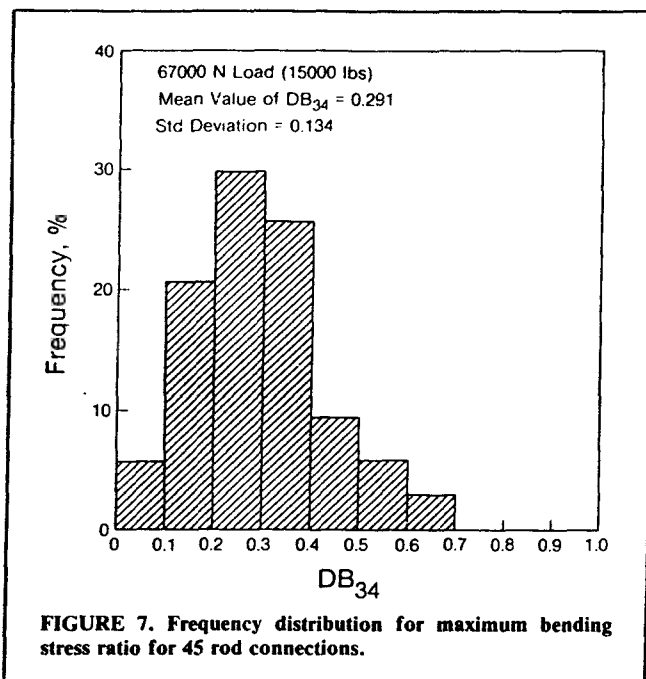
Clearly the manufacturer must adopt techniques which will reduce the deviations in the rod ends. This may be accomplished by replacing manual operations with precisely locating transfer mechanisms in the forging process. A second approach would be to replace the current API Specification with an "Evaluation Report" detailing the expected stresses for a sample batch of rod pairs. The third approach would be to recognize the limitations of the existing method of measuring TIR and adopt a more stringent specification which will effectively lower the possible DB's.

If the current standard for TIR was set a 2 mm (0.08 in.) with the rods clamped 100 mm (4 in.) from the shoulder the worst cases would be screened out. While this may not change the average bending stress in a large sucker rod string with many hundreds of connections, this change could result in an over-all improvement in the life of the sucker rod string.

Conclusions

The mathematical model was an appropriate method for evaluating bending stresses that can occur in imperfect sucker rod ends. It was found that the maximum dimensionless bending stress ratio (DB) occurred at the transition between the rod body and the upset end. The DB was influenced both by the geometry of the adjoining rod and the applied axial load.

It is suggested that there be an over-all improvement to sucker rod service life if the current API standard for TIR were changed to 2 mm (0.08 in.) with rods clamped 100 mm (4 in.) from the shoulder.



It is suggested that there be an over-all improvement to sucker rod service life if the current API standard for TIR were changed to 2 mm (0.08 in.) with rods clamped 100 mm (4 in.) from the shoulder.

NOMENCLATURE

A	= Area of cross section.
DB	= Dimensionless bending stress defined as $q_{bending}/q_{axial}$.
DB_{34}	= Dimensionless bending stress for an axial stress 234 MPa (34 000 psi).
E	= Modulus of elasticity.
I, I_i	= Moment of inertia at a cross section and at a cross section in element i .
LVDT	= Linear variable differential transformer (displacement sensor).
M	= Bending moment.
P	= Axial load.
R	= Magnitude of deviation of a centroid of a cross section from the centre line through the pin.
TIR	= Total indicated runout, API measure of rod end straightness.
X_o, Y_o	= Deviation in the x and y directions of the cross section centroid from the global z axis for the undeflected position of the rod.
X_{oi}, Y_{oi}	= Deviation in the x and y directions of the cross section centroid of node i from the global z axis for the undeflected position of the rod.
(X_o-X)	= Deflection of a cross section centroid from the undeflected.
(Y_o, Y)	= position (X_o, Y_o) in the x and y directions.
a	= Distance from end of bar to sharp bend in bar.
h_i	= Length of element i .
l	= Length of bar

n	= Number of elements in numerical model
r	= Radius of a cross section.
x, y	= Deviation in the x and y directions of the cross section centroid from the global z axis for the deflected position of the rod.
x_i, y_i	= Deviation in the x and y directions of the cross section centroid of node i from the global z axis for the deflected position of the rod.
z	= Distance along the length of the bar from the origin.
ϵ_{axial}	= Tensile strain due to axial load, P .
$\epsilon_{bending}$	= Tensile strain due to bending moment, M .
$\epsilon_{bending}/\epsilon_{axial}$	= Strain ratio.
γ	= Angle (in radians) of a sharp bend in a bar measured from the centre line through the ends.
σ_{axial}	= Tensile stress due to axial loading.
$\sigma_{bending}$	= Tensile stress due to bending moment.
σ_{total}	= Total tensile stress due to both the axial load and the bending moment.

Acknowledgment

The authors express their sincere appreciation to the Natural Sciences and Engineering Research Council (Ottawa) for the financial assistance received in support of this project (Grant A-2705).

REFERENCES

1. API-11B Specifications for Sucker Rods, Section 9, 1984.
2. BELLOW, D.G., and KUMAR, A., Stress Analysis of Bent Sucker Rods; *JCPT*, Vol. 17, No. 3, 1978, pp. 76-81.
3. BELLOW, D.G., Stress and Corrosion Fatigue Experiments on Oil Field Components, SESA/JSME Proc. Hawaii, Part 2, 1981, pp. 651-655.

The Effect of Residual Stresses on the Improvement of Fatigue Life of Medium Strength Butt-Welded Steel Structures

M.A. WAHAB

Lecturer, Mechanical Engineering, University of Tasmania

D.G. BELLOW

Professor of Mechanical Engineering, University of Alberta, Canada

M.G. FAULKNER

Professor of Mechanical Engineering, University of Alberta, Canada

SUMMARY A theoretical analysis of the effect of residual stresses on the fatigue life of butt-welded low-alloy medium strength steel structures is presented. For the theoretical analysis of fatigue crack propagation life Forman's equation with an appropriate combination of effective stress-ratios, combined effect of axial and bending stresses along with the effects of residual stresses was considered. The theoretical model was used to illustrate the interaction of initial residual stress, nominal stress-range and nominal stress-ratios (pulsating, alternating and half-tensile cases) on the fatigue life of steel weldments.

The theory was compared with fatigue experiments calculated on butt-welded steel specimens subjected to various forms of mechanical and thermal treatments. The results showed good agreement between theory and experiment for all treatments evaluated.

INTRODUCTION

The development of residual stresses in welded construction is intrinsic to the welding process. This can be extremely important in determining the behaviour of a structure under static and dynamic loads. In the welding processes high residual stresses are inevitably setup and often cannot be entirely removed by post welding heat treatment. The increased use of welding as a joining technique accentuates the need for a thorough investigation of the problems of relating the influence of residual stresses to the fatigue behaviour of welded structures. The presence of these "locked-in" stresses frequently threatens the reliability of structures.

The welding process is complex and therefore in the prediction of the fatigue life of welded structures, many variables must be considered: e.g., geometry of the weld, methods of welding, variable material properties of heat-affected zone, weld-metal, base metal, and distribution of the residual stresses.

There have been some work on the predictive model of crack initiation and crack propagation life but these have not included the influence of residual stresses although recent experiments have shown how the fatigue life can be influenced by residual stresses (1). The possible reasons for not understanding the influence of residual stresses on the fatigue life of welded structures may be due to the limitations of the methods for their determinations and their changes throughout the fatigue life. A recent study (2,3) shows the comparison of the theory and fatigue experiments on butt-welded specimens subjected to various forms of surface and mechanical treatments.

In this study a closer look on the influence of the residual stresses, stress-ratios, loading conditions and stress-relieving by various mechanical surface treatments on the prediction of fatigue crack propagation will be considered.

METHOD OF ANALYSIS FOR FATIGUE LIFE

Fatigue Crack Initiation Life

The total fatigue life of a butt-weld containing

residual stresses was estimated as a combination of crack initiation and crack propagation life. The detailed description of crack initiation life was described in an earlier work by the authors (2).

Independent estimates of the fatigue crack initiation can be based on the "strain-life" properties and cumulative fatigue damage. The low-cycle fatigue concept for the estimation of crack initiation life considers the basic material properties and overall stress-strain analysis relating local and nominal stress-strain condition. "Local stress-strain" analysis simulates the notch root stress-strain which determines the change in the initial residual stress pattern upon loading. The simulation of the actual effect of residual stress at the weld toe, cyclic and fatigue material properties and damage accumulation model determine the crack initiation life (2).

Fatigue Crack Propagation Life for a Weld

Application of fracture mechanics concepts are used for estimation of the crack propagation life of the welded structures (N_p). The fatigue crack propagation life for a butt-weld was estimated by using Forman's equation of crack propagation (4). This assumes that the crack tip stress intensity factor range ΔK is the controlling variable for analyzing crack-extension rates. This also takes into account the effective load ratio R_{eff} and the instability when the stress-intensity factor approaches the fracture toughness of the material K_{IC} . Forman's equation is modified and written in the form below:

$$\frac{da}{dN_p} = \frac{C_R (\Delta K_{eff})^m}{(1-R_{eff})^{K_c} - \Delta K_{eff}} \quad (1)$$

where

- a = half crack length,
- K_{IC} = critical stress intensity factor for fracture,
- $\bar{K} = YS\sqrt{\pi a}$ (fracture mechanics stress intensity factor),
- ΔK = range of stress-intensity factor ($K_{max} - K_{min}$),
- m, C_R = crack growth exponent and coefficient respectively,
- R_{eff} = fracture mechanics effective stress ratio,

$$R_{eff} = \frac{\sigma_{r,i} + S_{min}}{\sigma_{r,i} + S_{max}}$$

Y = generalized correction factor (function of crack length and specimen geometry,
 $\sigma_{r,i}$ = initial residual stress,

S_{max}, S_{min} = maximum and minimum nominal stress.

From Eq. (1) the cycles required to propagate a crack of initial size a_i to a final crack length a_f are then

$$N_P = \int_{a_i}^{a_f} \left[\frac{(1-R_{eff})K_C - \Delta K_{eff}}{C_R(\Delta K_{eff})^m} \right] da \quad (2)$$

Eq. (2) can be integrated numerically to obtain the fatigue crack propagation life. As ΔK is decreased below the ΔK_{th} , the threshold stress intensity factor range, the crack propagation rate diminishes rapidly. The empirical relationship used by Garwood (5) for $\Delta K_{th} = (190-144R)N_{mm}^{-3/2}$.

The initial crack length a_i is taken as the crack size when the initiation life is complete (2). The initial crack length for welds may be taken as the length of some pre-existent weld defect but a_i should not be smaller than a_{th} , threshold crack size (6);

$$a_{th} \geq \left[\frac{1}{(\pi A)^2} \frac{\Delta K_{th}}{\Delta S} \right]$$

The initial crack length can also be approximated as (7) $a_i = 0.1878 \sqrt{t}/AS_u$.

Estimations of the total fatigue life from propagation theory above assumes that there exists a small initial defect resulting from the fabrication process at the weld toe and may require a_i less than a_{th} especially for long fatigue lives.

The stress intensity factor was modified by superposing the effects of remote axial and bending stresses along with the effect of residual stress intensity factor $K_R = \Delta K_A + \Delta K_B + K_R$ where,

$\Delta K_A, \Delta K_B$ = range of stress intensity factor for axial and pure bending stresses respectively,

$$\Delta K_A = \Delta S_A \sqrt{\pi a} f(c/t, \theta, \phi),$$

$$\Delta K_B = \Delta S_B \sqrt{\pi a} f(b/t, \theta, \phi).$$

$\Delta S_A, \Delta S_B$ are the remote axial and bending component of load; $f(c/t, \theta, \phi)$ and $f(b/t, \theta, \phi)$ are correction factor for weld geometry, loading type, thickness and crack length.

$$K_R = \int_{x=-a}^{x=a} \sigma_r(x) G(x) dx$$

where $G(x)$ is a function of half crack length a and the specimen shape. It is zero at $x = -a$ and goes to infinity at $x = +a$.

$$G(x) = \left[\frac{2 \sin \pi(a+x)/W}{W \sin(2\pi a)/W \cdot \sin \pi(a-x)/W} \right]^{\frac{1}{2}},$$

σ_r = actual residual stress distribution near the weld toe.

It was assumed that the distribution of residual stress at the weld toe is a cosine shape in the middle and sloping downwards at the ends (Fig. 1) and remain unchanged under the fatigue loading. The actual shape of the residual stress level after several cycles is shown in Fig. 2. These assumptions may overestimate the effect of residual stress because the residual stress redistributes after fatigue cycling (Fig. 2).

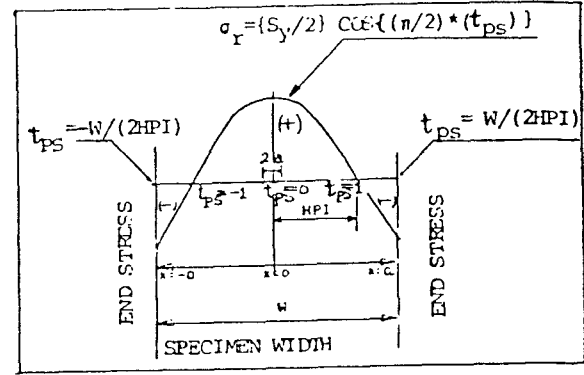


Fig.1. Distribution of residual stress at the weld toe.

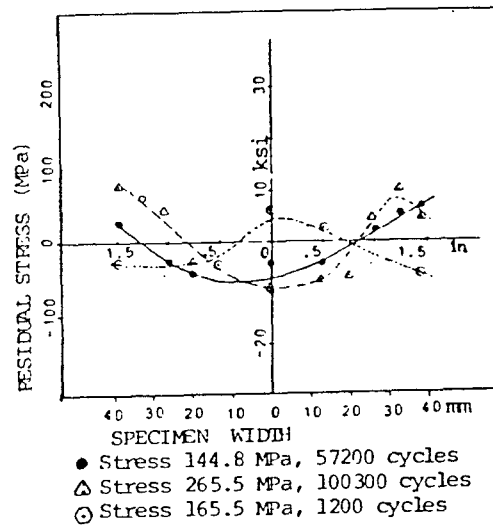


Fig.2. Distribution of residual stresses after fatigue cycling.

The distribution of residual stress shown in Fig. 1 correlates closely with the actual shape found from experiments. From Fig. 1 the non-dimensional term t_{ps} is written as:

$$t_{ps} = \left[\frac{\bar{x} + CDIFF}{HPI} \right] \text{ where}$$

CDIFF = distance between centre of specimen and centre of crack.

\bar{x} = distance from centre of the crack to the intersection of the residual stress distribution.
HPI = a constant according to the distribution of residual stress.

The distribution of residual stress from $t_{ps} = -1$ to $+1$ can be taken as:

$$\sigma_r = \left[S_y/2 \right] \cos \left\{ (\pi/2) + (t_{ps}) \right\}$$

For the straight line portion i.e. $t_{ps} = +1$ to $W/(2HPI)$,

$$\sigma_r(t_{ps} - 1) \left[\frac{-\sigma_E}{W/(2HPI) - 1} \right] \text{ and}$$

from $t_{ps} = -1$ to $-W/(2HPI)$,

$$\sigma_r(t_{ps} + 1) \left[\frac{\sigma_E}{W/(2HPI) - 1} \right] \text{ where}$$

σ_E is the end stress.

The ΔK_{eff} is written in terms of crack-opening factor as:

$$\Delta K_{eff} = C_f \Delta K \quad \text{where}$$

$$C_f(R) = \frac{\Delta K - \Delta K_{open}}{\Delta K} \quad \text{when } \Delta K_{open} < \Delta K$$

$$= 0.4 \text{ to } 1.0 \quad \text{when } \Delta K_{open} \geq \Delta K$$

$$C_f(R = 0.0) \approx 0.5 \text{ for steel.}$$

ΔK_{open} is the crack opening stress intensity factor range,

$$\Delta K_{open} = K_R + \Delta K_B + (S_{max} - S_{op}) f(c/t, \theta, \phi).$$

The crack opening stress, S_{op} , can be approximated as (8) $S_{min} = 1.25 (1.6 S_{op}^2 - 0.79 S_{max}^2) - 0.1 S_{max}$.

The above equation can be solved iteratively for S_{op} . The crack growth coefficient considering the crack opening concept can be found as (9).

$$C_R = C \left[C_f(R) / C_f(R = 0.0) \right]^m \quad \text{where } C \text{ is the}$$

crack growth rate/constant for materials at the crack initiation sites. The fatigue-crack propagation properties K_R , m and c are assumed on the basis of material properties (3). Finally, the crack propagation life (N_p) can be estimated by integrating Eq. (1) over the crack length.

RESULTS OF THEORETICAL STUDY FROM THE CRACK PROPAGATION MODEL

The theoretical predictions on the study of crack propagation life of a butt-weld was made according to the analysis as discussed above. It is also assumed that a crack can occur anywhere along the strained region (toe of the weld) due to the application of tensile residual stress. To apply compressive stresses for peening, the negative compressive stresses were superimposed on the applied stresses taking the initial residual stress as zero.

Fig. 3 shows the predictions of the half crack length "a" as a function of crack propagation life N_p for three stress ratios of $R = \pm \frac{1}{2}$ and 0. It was observed that for the same crack length the propagation life increased as the stress ratio increased. It can be seen that with the increase of stress range ΔS the crack propagation life decreased for the same crack length.

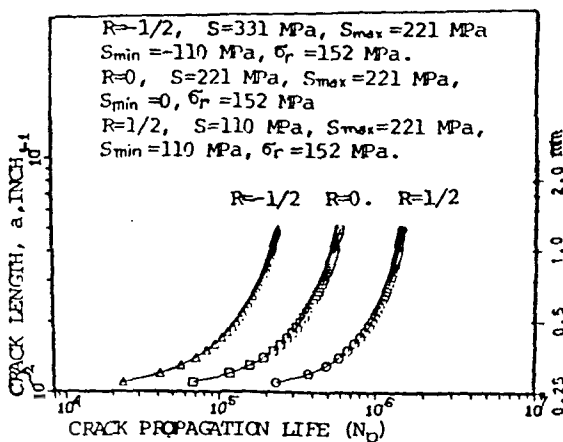


Fig.3. Theoretical predictions of crack propagation life and crack length.

The effect of the range of stress intensity factor ΔK as a function of the fatigue crack growth rate da/dN is shown in Fig. 4. It shows that positive R values lead to slightly higher growth rates than does $R = 0.0$ for the same value of ΔK . As R ratios become increasingly negative the growth rate drops because only stresses which open the crack are capable of driving it. It could be said that any compressive component in a stress cycle will be ineffective in driving the crack because it will cause the crack to close.

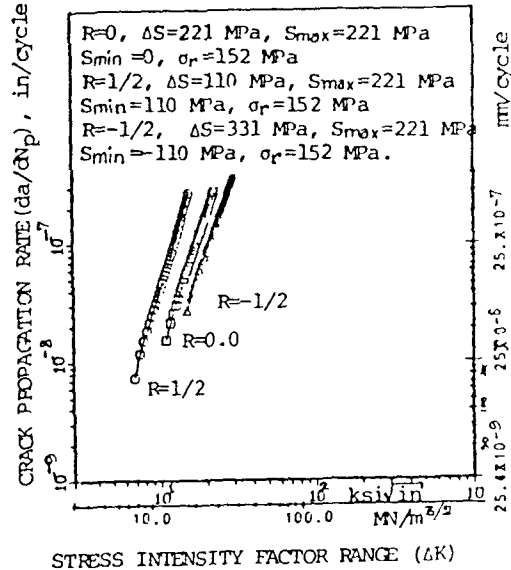


Fig.4. Calculated value of the range of stress intensity factor and rate of crack propagation.

The effect of residual stress intensity factor on the rate of crack propagation (da/dN) is shown in Fig. 5. It can be seen that higher the applied stress range the lower the residual stress intensity factor for the same rate of crack propagation. This suggests that higher applied load caused greater relaxation of residual stresses. This also shows the tendency that the residual stress intensity factor increased the rate of crack propagation almost becomes the same for the three stress ratios studied.

The behaviour of the range of stress intensity factor (ΔK) with the residual stress intensity factor (K_R) is shown in Fig. 6. For the same ΔK , the residual stress intensity factor was greater for positive R ratio. For the same residual stress intensity factor the range of stress intensity factor was largest for $R = -\frac{1}{2}$, therefore crack propagation life decreased with negative stress ratio. On the other hand, stress ratio $R = \frac{1}{2}$ produced lower ΔK which in turn, increased the crack propagation life.

Fig. 7 shows the effect of initial residual stress, stress relieving and the induced compressive residual stress in a plot of ΔK and fatigue crack growth rate da/dN_p .

The effect of stress relieving on growth rate from tensile to zero residual stress is comparatively more than that due to the application of surface compressive stresses. For the same fatigue crack growth rate the stress intensity factor range ΔK increases for the tensile residual stresses and

therefore, the crack propagation life decreased. The improvement of fatigue crack propagation was small with the application of compressive residual stresses as can be seen from Fig. 7 for Columbium-50 Steel.

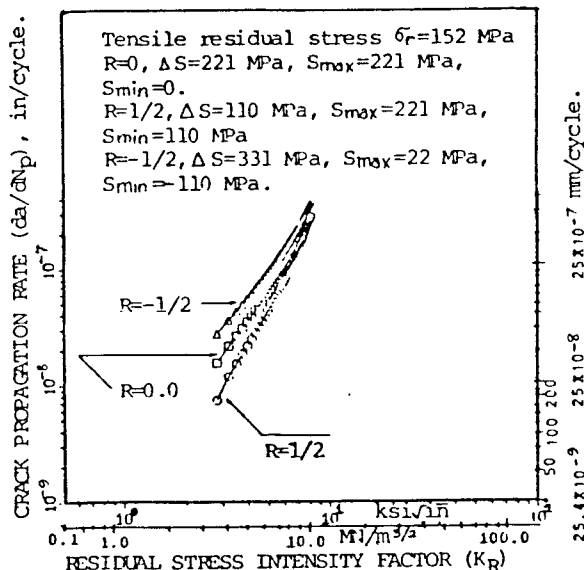


Fig. 5. Calculated value of residual stress intensity factor and rate of crack propagation.

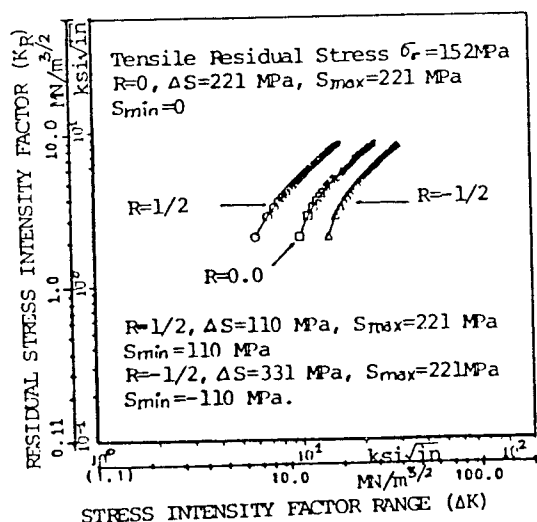


Fig. 6. Calculated value of range of stress intensity factor and residual stress intensity factor.

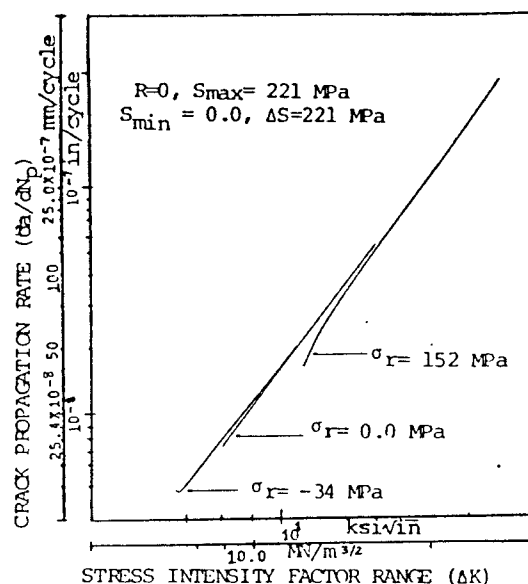


Fig. 7. Effect of stress relieving and induced compressive stress as a function of range of stress intensity factor and rate of crack propagation.

Figs. 8 and 9 are plots of the nominal stress range S as a function of total life for butt-welded specimens which were subjected to a variety of surface treatments as indicated. For each case the residual stress at the toe of the weld was measured by X-ray diffraction and shown on the graphs. The predictions indicate that the induced surface compressive residual stress only influenced total fatigue life in excess of 10^5 cycles. Various techniques are predicted to be most effective at low stresses or at long lives. Overall the experimental results compared well with theory for residual stresses in the range of 14 MPa to 172 MPa.

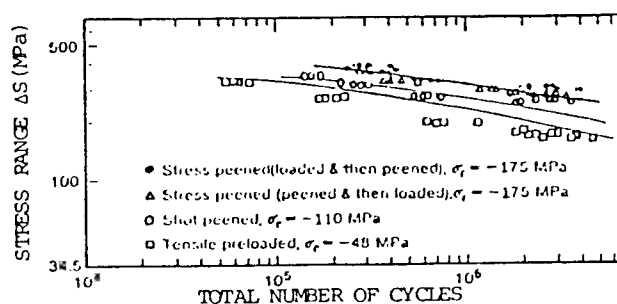


Fig. 8. Theory and Experiment for stress peened, shot peened and tensile preloaded butt-welded specimens.

CONCLUSIONS

This study leads to the following conclusions:

- (1) It was found that stress relieving or introduction of compressive stresses by mechanical means improved the fatigue life in the long life regime. The percentage improvement in the applied stress range as-welded condition at long life (2×10^6 cycles) varied up to 45% whereas at life less than 10^5 cycles it was only 20%.
- (2) Beneficial surface compressive stresses by tensile preloading, glass and steel shot peening, single and multiple point hammer peening, stress-

peening and stress relief by annealing gave large improvements for lives exceeding 5×10^5 cycles with maximum improvement in the case of multiple point hammer peening and stress-peening. The single point hammer peening caused unacceptable surface damage and modification of the weld-toe root radius.

(3) Stress relieving was found to be more beneficial for zero or a positive stress ratio than under alternating loading.

(4) The effect of residual stress on the rate of fatigue crack propagation depended on the applied stress range and the stress ratio. The tensile residual stress, stress-relief and compressive surface residual stresses played a minor role in the propagation life regime.

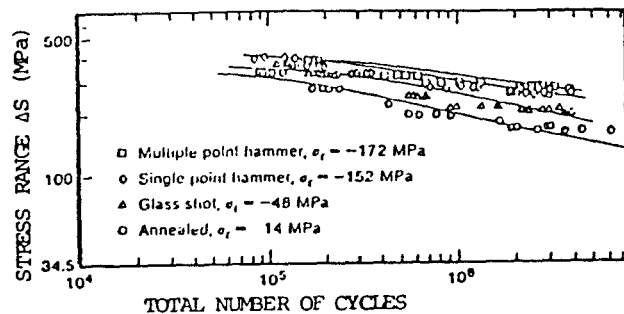


Fig.9. Theory and Experiment for annealed, glass shot, single and multiple point hammer peened butt-welded specimens.

ACKNOWLEDGEMENT

The authors wish to thank the National Sciences and Engineering Research Council (Canada) grants A-2705 and A-7514 and Australian Research Grants 625/018/415-02 for their financial support.

REFERENCES

1. D.G. Bellow, M. Wahab, and M.G. Faulkner, "Residual Stresses and Fatigue of Surface Treated Specimens", Advances in Surface Treatments - II, Pergamon Press, pp. 85-94, 1985.
2. D.G. Bellow, M. Wahab and M.G. Faulkner, "Prediction of Fatigue Crack initiation and propagation of Welded Joints", Advances in Surface Treatments - III, Pergamon Press. pp. 27-40, 1986.
3. M.A. Wahab, Model Analysis of Fatigue Life Estimation of Welded Structures, Ph.D Thesis, Univ. of Alberta, Canada, 1984.
4. Forman, R.G., Kearney, V.E., and Engle, R.M., "Numerical Analysis of Crack Propagation in Cyclic Loaded Structures". Journal of Basic Engineering, Trans. of ASME, pp. 459 - 464, Sept. 1967.
5. Garwood, S.J., "Cumulative Damage of Welded Structures", Welding Institute Report # 3477/8/78, January 1978.
6. Mattos, R.J. and Lawrence Jr., F.V., "Estimation of Fatigue crack initiation life in welds using low cycle fatigue concept".
7. Lawrence Jr., F.V., H.O.N.J. and Mazumds, P.K., "Predicting the fatigue resistance of welds", Ann. Rev. Material Science, 11: 401-425, 1981.

(8) Socie, D.F., "Estimating fatigue crackinitiation and propagation lives in notched plates under variable loading histories", AM report # 417, Univ. of Illinois at Urbana - Champaign, 1975.

(9) Elber, W., "Equivalent constant-amplitude concept for crack growth under spectrum loading, "ASTM, STP 595, pp. 236-250, 1976.

Measurements of Residual Stresses and Their Uncertainties

M.A. WAHAB, B.Sc.E., M.Sc.E., Ph.D., M.I.E.Aust., Lecturer, Mechanical Engineering, Capricornia Institute, Rockhampton, Qld. 4702, Australia.

D.G. BELLOW, B.A.Sc., M.Sc., Ph.D., Professor, Mechanical Engineering, University of Alberta, Edmonton, Canada T6G 2G8.

M.G. FAULKNER, M.Sc., Ph.D., Professor, Mechanical Engineering, University of Alberta, Edmonton, Canada T6G 2G8.

Australasian Instrumentation and Measurement Conference
Adelaide, Australia, 1989, pp39-44

ABSTRACT

The development of residual stresses in welded construction is intrinsic to the welding process. This can be extremely important in determining the behaviour of a structure under static and dynamic loads. The increased use of welding accentuates the need for a thorough investigation of the problems of relating the influence of residual stresses to the fatigue behaviour of welded structure. The reliable measurements of these "locked-in" stresses are quite complex and the fatigue life prediction depends on the accurate measurements of these residual stresses.

In this study the problems arising from measurements of initial and redistributed surface residual stresses by mechanical and thermal treatments are discussed. The relevant stress measurements near heat-affected-zone area were performed by using X-ray diffraction technique, Blind-Hole-drilling method, Sectioning method, Plastic strain measurement by strain-gauging and plastic strain measurements using an extensometer. A close correlation was obtained among the various methods. Discussions are made to improve the accuracy and validity of those methods. Those measurements of residual stresses were taken to predict theoretically the fatigue lives of welded joints and compared with the experimental fatigue lives. The conclusions from these results confirm the validity of these techniques of residual stress measurements.

KEYWORDS: Butt-welds, Heat-Affected-Zone, Peening, Residual Stress, Fatigue Strength, X-ray Diffraction, Hole-drilling, Sectioning

1. INTRODUCTION

The development of residual stresses in welded construction is intrinsic to the welding process. This can be extremely important in determining the behaviour of a structure under static and dynamic loads. In the welding process high residual stresses are set up and often cannot be entirely removed by post welding heat treatments (1).

The increased use of welding as a joining technique accentuates the need for a thorough investigation of the problems of relating the influence of residual stresses to the fatigue behaviour of welded structures. The presence of these "locked-in" stresses frequently threatens the reliability of structures. The accurate determination of these "locked-in" stresses are crucial in the prediction of fatigue life. The investigation requires the study of two phenomena and their mutual interaction. These are:

the influence of residual stresses on the fatigue limits; and

the influence of stresses induced by loading on the magnitude of the residual stresses.

In this study the measurements of residual stresses were taken in the vicinity of the butt-welded joint (submerged-arc welding method) to indicate the distribution of initial residual stresses. Measurements were also taken after the application of cyclic load to predict any correlation of stress patterns. Also, surface compressive stresses by various mechanical and thermal means were introduced on the surface of the butt-welded specimens with the goal of improving its fatigue life. Measurements were taken due to shot-peening, stress-peening, tensile preloading and post-weld thermal treatments on the welded specimens and percentage improvement on the fatigue lives were measured and calculated.

All the relevant stress measurements were performed by using the "Thomas Method-B" double exposure X-ray diffraction technique.

To calibrate the X-ray diffraction method a semi-destructive (blind-hole drilling) and destructive methods were used as well as calibrating against strain-gauge readings and strain measurements by using an extensometer.

2. MEASUREMENTS OF RESIDUAL STRESSES

2.1 Measurement of Stresses by X-Ray Diffraction

The X-ray diffraction technique has two advantages: first, it is non-destructive, and secondly, the measurement need not be in a reference condition of zero-stress (measurement on unstressed metal) which

allows one to measure the applied stress, the residual stress or the combined effect of both. The method is based on the principle that changes in atomic spacing in a metal are proportional to applied loads.

To measure the distribution of residual stress present in the Columbium-50 steel transverse butt-welded specimens a flat camera "Kristalloflex-2" (Siemens Ltd.) X-ray diffraction unit with AgCr30 tube was used. Although many techniques of X-ray diffraction are available the technique used in this study was the double-exposure "Thomas method B" for its known better accuracy. Vanadium filtered chromium K α radiation (35 KV, 18 ma) diffracted from the {211} crystallographic planes provided the sharp deflection lines on the photographic film. The developed negatives were then scanned with the microdensitometer (Joyce, Loebel & Co.) for the "Debye-Scherrer" ring diameters.

"Thomas method B" (2, 3) requires two exposures at the same point "O" with different known camera inclinations α_1 and α_2 to the normal "ON" as shown in Figure 1.

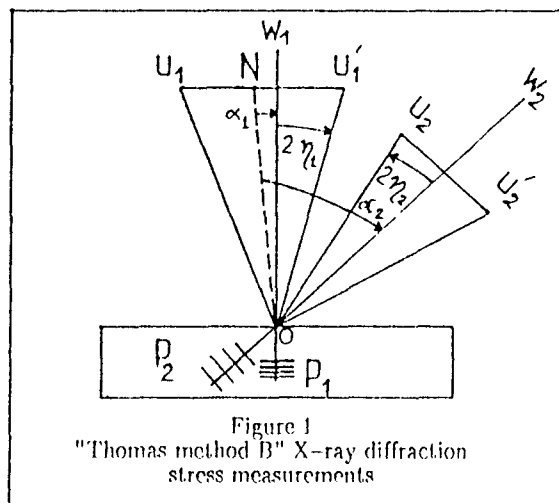


Figure 1
"Thomas method B" X-ray diffraction stress measurements

If η_1 and η_2 are small angles the spacing computed from the diameter U_1U_1' may be taken as representative of the {211} planes for chromium radiation, planes P_1 normal to the primary beam W_1O and the spacing computed from the ring diameter U_2U_2' as representative of the same set of P_2 normal to the primary beam W_2O . Applying stress-strain relation and using elastic theory (2, 3) the residual stress σ_r can be calculated from:

$$\sigma_r = \frac{E (U_1 - U_2) \tan \eta \cos^2 2\eta}{4D (1 + \gamma) (\sin^2 \alpha_2 - \sin^2 \alpha_1)}$$

where

σ_r = stress at target location,
 E = modulus of elasticity for steel,
 γ = Poisson's ratio, 0.28 for steel,
 $\eta = 90^\circ - \text{Bragg's angle} = 11.8025^\circ$ degrees for Chromium radiation on steel,
 D = film to specimen distance,
 α_1 = normal exposure angle, 0 degree,
 α_2 = inclined exposure angle, 45 degrees,
 U_1 = stress ring diameter on normal exposure
 U_2 = stress ring diameter on inclined exposure.

Butt-welded specimens made from Columbium-50 steel were polished in areas close to the toe of the welds with 400/600 micron emery paper to remove any adhering binder. It was then treated with 35 percent hydrochloric acid and greased lightly for preventing renewed oxidation. Calibration powders (Iron, Silver and Gold) were used with vaseline as a thin coat on the specimen for determining the film to specimen distance, the film centroid and to compare the intensity of the diffraction lines. The true σ_r was calculated from the following relationship:

True stress = Indicated stress X (Measured distance)/Actual film to specimen distance.

D_{true} = the actual film to specimen distance,
 D_{cal} = calibration ring diameter.

2.2 Measurements of Residual Stresses by the Blind-Hole Drilling Technique

Residual stresses near the weld toe and on the surface of the specimens were also measured by the blind-hole drilling technique and used to compare with the X-ray diffraction measurement. A 45° rectangular strain rosette (Micro-measurement type EAXX-062RE (Figure 2)) was applied to the surface on which the residual stresses were to be measured. A small hole was drilled (1.71 mm) at the rosette centre. This drilling relaxed the radial stresses at the edge of the hole and caused a local redistribution of the stresses. The resulting strain changes were detected by the gauges. These strain changes could be related to residual stresses in the material by an equation which was developed by Beaney and Proctor (4).

$$\sigma_{1,2} = -(E/2K_1) \left[\frac{\epsilon_1 + \epsilon_3}{1 - \gamma K_2/K_1} \pm \frac{1}{1 + \gamma K_2/K_1} \sqrt{(\epsilon_1 - \epsilon_3)^2 + (2\epsilon_2 - \epsilon_1 - \epsilon_3)^2} \right]$$

and

$$\alpha = -(1/2) \tan^{-1} \left[\frac{\epsilon_1 - 2\epsilon_2 + \epsilon_3}{\epsilon_1 - \epsilon_3} \right]$$

where

$\sigma_{1,2}$ = principal stresses,
 K_1, K_2 = constants,
 E = Young's Modulus,
 $\epsilon_1, \epsilon_2, \epsilon_3$ = relaxed strains,
 γ = Poisson's ratio,
 α = angle between gauge 1 and principle stress direction
 $1/K_1$ and $\gamma K_2/K_1$ can be found by measuring the relaxed strain in any known stress field.

Bathgate (5) showed there was a good correlation between conventional gauges and hole drilling using milling cutters and standard loading equipment. Other researchers have also shown good results using an air-abrasion technique to drill the hole. But for this study a standard milling machine was used to drill the holes. To correct any error due to milling, one gauge

was first applied to a specimen of known stress (annealed specimen) a hole drilled and relaxed strains recorded. This gave the stress due to the milling operation. Other gauges were then used to measure the stresses near the weld toe and at various points on the specimen and which were then corrected by the amount found from the first test.

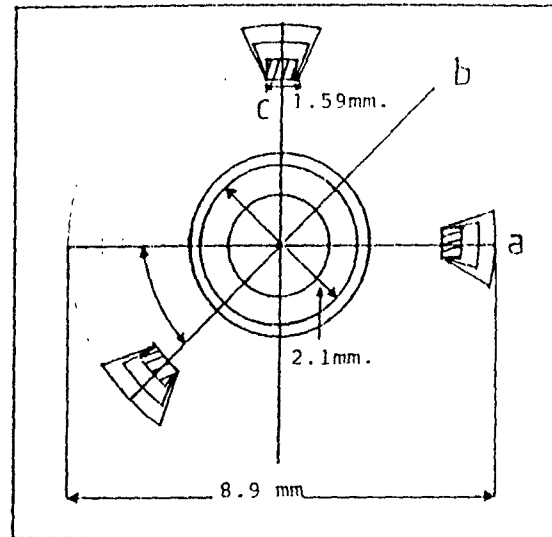


Figure 2
Rectangular rosette for residual stress measurement (Micro-measurement type EAXX-062RE)

2.3 Stress Measurements by Sectioning

Residual stress measurements were made both on annealed and cold-rolled Columbium-50 steel base material by the sectioning method. Strain gauges were attached to the lower and upper surfaces of the cold-rolled flat plate specimen as shown in Figure 3. Before sectioning initial strain readings were taken from the gauges. Following this, the bar was sawn across 12.7 mm away from the centre of the strain gauge grid and the length of the bar not supporting the gauge was discarded. The strain gauge readings were recorded. The gauge bearing block was removed from the bar as shown in Figure 4 and the thickness of the block was measured. Metal was then progressively removed from the inner block faces by careful milling and filing where necessary. This was done in small increments to avoid plastic bending of the remaining shim. Using a high speed cutting saw (5 teeth/mm) and a cutting speed of 52.5 m/min gave consistent strain readings. At each stage thickness and strain measurements were made.

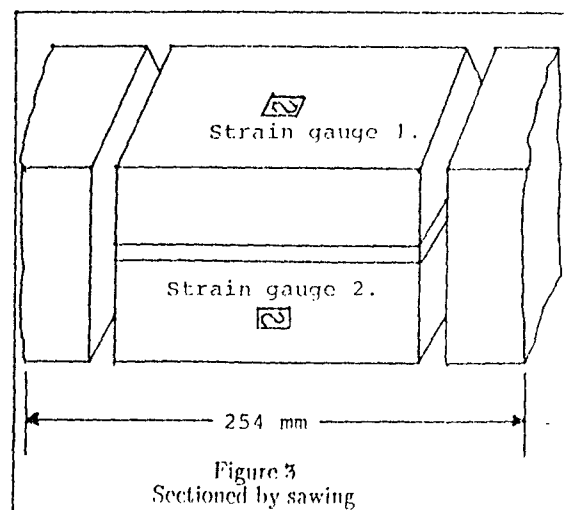


Figure 3
Sectioned by sawing

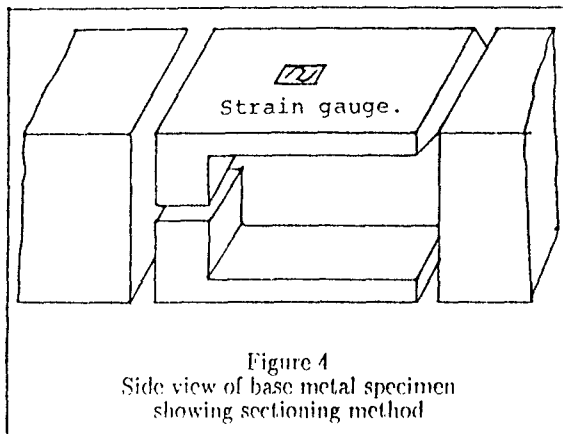


Figure 4
Side view of base metal specimen
showing sectioning method

This modified sectioning method of Rosenthal and Norton (6) requires three sets of data to predict the complete residual stress pattern through the specimen thickness. The first was the change in gauge readings when the first and second cuts were made across the specimen on either side of the gauges. The second was the strain changes after making the longitudinal slit in the middle. The third was a plot of strain changes versus shim thickness as the blocks were milled out to become thin shims.

For the second case of annealed specimens three strain gauges were mounted on the surface of the specimen and the first cut was made 25.4 mm away from the gauges whereas the second and third cut were made 6.35 mm away from the gauges (Figure 5). The changes in the strain readings were noted. Before the sectioning X-ray diffraction stress measurements were taken close to the strain gauges.

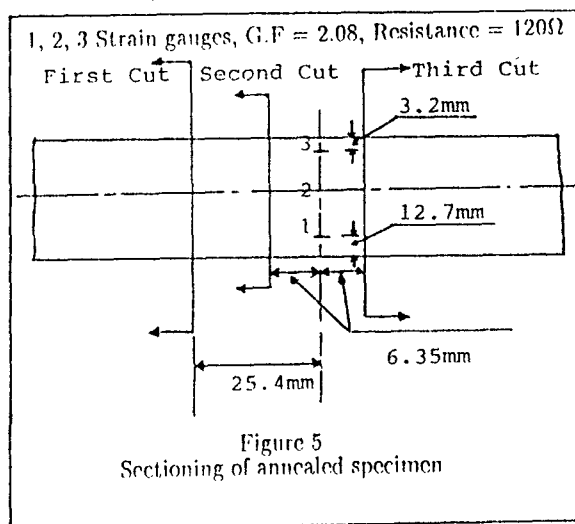


Figure 5
Sectioning of annealed specimen

2.4 Stress Measurements by a Strain Gauging

Calibration of X-ray stress measurements using a single strain gauge and a longitudinal bar of Columbium-50 steel are shown in Figure 6. The longitudinal bar was annealed for stress relaxation. It was sanded and cleaned with 35% HCl. A strain gauge was mounted after the surface preparation. Tensile forces were applied to the bar by a screw arrangement and strain gauge readings and X-ray stress measurements were taken.

It was assumed that the depth of penetration of X-rays was of order 0.0254 mm, the stress was uniaxial and parallel to the longitudinal axis of the bar and was in pure tension. The stress along the thickness was zero as the stress is measured only on the top surface.

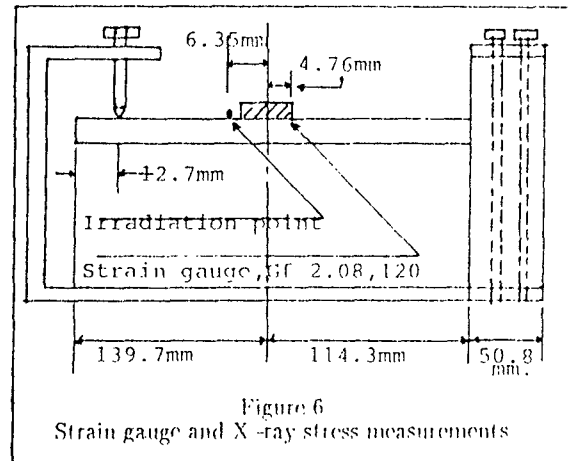


Figure 6
Strain gauge and X-ray stress measurements

2.5 Plastic Strain Measurements by Strain Gauging

The annealed specimens with two strain gauges mounted on the top and bottom surfaces were loaded slowly in the Instron testing machine and yielded to the plastic ranges of the material and then unloaded. Stress readings were taken by X-ray diffraction near the strain gauges of the specimen before gripping the specimen in the testing machine. Initial strain readings were also taken after gripping the specimen. After unloading X-ray stress measurements and strain gauge readings were noted. There was, however, no control on the amount of plastic strain after the yielding of the material.

2.6 Plastic Strain Measurements Using an Extensometer

The extensometer method in combination with hole-drilling method was used to calibrate the X ray diffraction stress measurements. Base material specimens were loaded beyond the elastic limit and strains were measured using a 2.54 mm extensometer. From load and strain measurements and using stress-strain relationships in the plastic range the amount of induced plastic stress was obtained. Later on, a special purpose 45° rectangular rosette was mounted on the yielded specimen and a hole was drilled at small increments and the stress relaxation was noted. X-ray diffraction stress measurements were also taken before and after the yielding of the specimen.

3. EXPERIMENTAL VERIFICATION OF THE WELDING RESIDUAL STRESSES

3.1 Introduction

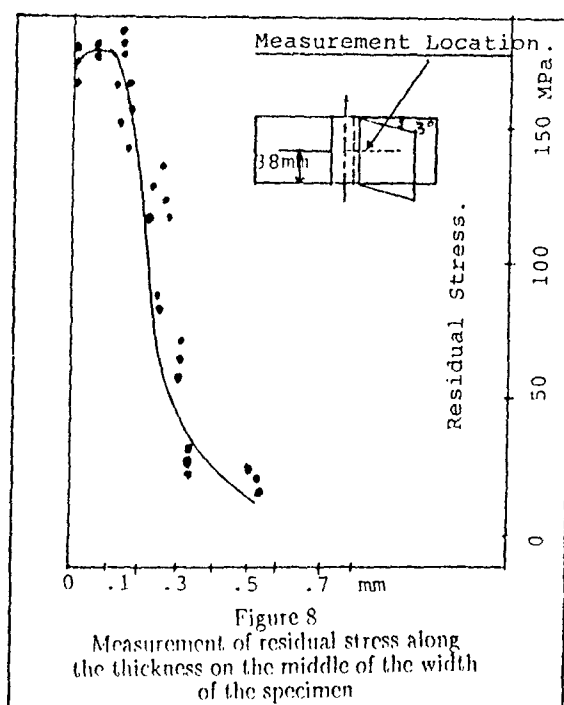
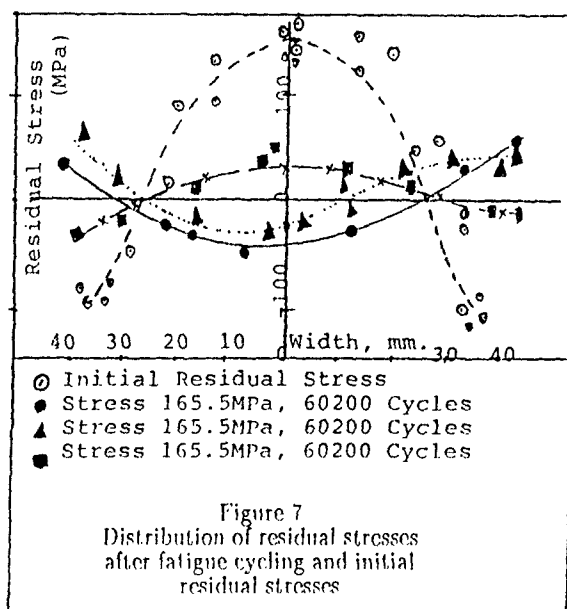
Experimental stress measurements were made along the toe of the weld before fatigue cycling of the specimens to show the presence of the welding residual stresses. A few of the specimens were measured before and after fatigue cycling to demonstrate the redistribution of residual stresses. Stress measurements were also taken across the thickness of both the parent material and transverse butt-welded specimens to examine the presence of a stress gradient due to welding.

Several mechanical treatments for the improvement of weld fatigue life were studied. Stress measurements on the surface of these treated specimens showed that there was a variation of compressive stress level due to each method of treatment.

3.2 Distribution of Welding Residual Stresses

Residual stresses near the weld toe in welded joints were assumed to be the cause of the reduction in fatigue strength of the welded joints. Consequently, the

distribution of welding residual stresses near the weld toe was investigated and are shown in Figure 7. It was observed that away from the weld toe the residual stresses decreased abruptly. This indicated that residual stresses due to welding exist very close to the weld toe. A tensile residual stress of 138 MPa to 172 MPa was observed to exist in the middle near the weld toe and a compressive stress of -90 MPa to -117 MPa was obtained at the end of the specimen. The effect of this positive tensile residual stress was considered in the evaluation of theoretical fatigue life. A few of the welded specimens were stress cycled between 0 to 145 MPa, 0 to 165 MPa and 0 to 265 MPa in the as-welded condition. Residual stress measurements at several locations were performed before and after fatigue cycling at various ranges of cycles. From Figure 7 it can be seen that the magnitude of the initial residual stresses are the same whereas the residual stress pattern changed considerably after cycling. This shows that the residual stress redistributes during fatigue cycling but its pattern is not well known or predictable.



Two welded specimens in the as-welded condition were used to perform the stress measurements through the thickness as shown in Figure 8. The specimens were milled out at an angle of three degrees along the width from the weld toe. The milling operation was performed very slowly and in small increments. Care was taken not to introduce extra machining stresses by allowing sufficient cooling time between operation. The results showed that a sharp stress gradient exists through the thickness. The maximum stress near the weld toe exists mainly on the surface and up to a depth of 0.127 mm.

3.3 Surface Compressive Stress Measurements of Treated Welded Specimens

The X-ray diffraction stress measurements were made near the weld toe for all of surface treatments studied. For the annealed specimen the stress level varied from 0 to 21 MPa. For the case of tensile preloading stress measurements were taken near the weld toe before and after the application of preload. The preload was controlled by the ramp generator settings of the Universal testing machine. Figure 9 shows the data obtained by an application of a single preloading. It can be seen that the initial residual stresses were redistributed and a compressive residual stress of approximately -48 MPa was imposed near the weld toe. It can be observed that although the initial tensile residual stress changes to compressive values at the toe of the weld the stress pattern after the preloading was not consistent. The method of tensile preloading introduces the compressive residual stresses at the weld toe without the modification of the weld toe root radius.

X-ray diffraction stress measurements were also made on the glass and steel shot peened multiple and single point hammer peened and stress peened specimens. It was observed (Figure 9) that glass shot peened introduced approximately -62 MPa compressive surface residual stress whereas steel shot peened, -110 MPa; single-point hammer peened, -152 MPa; and multiple point hammer peening and stress peening produced a surface compressive stress level of -172 MPa. Figure 9 shows that the two types of stress peening introduced almost the same level of residual stresses.

The foregoing levels of surface residual stresses were used to calculate the total fatigue life of the welded treated specimens. The method of analysis of fatigue life which included these surface compressive residual stresses are described in Author's earlier works (7, 8, 9).

4. RESULTS AND DISCUSSIONS

4.1 Calibration of X-ray Stress Measurements

The experimental results obtained from various measurement techniques are plotted in Figure 10 and showed a good correlation between X-ray diffraction and other measuring techniques. The measurements of stress by X-ray diffraction at a low stress range was not very accurate because of the small difference in "Debye-Scherrer" ring diameter. The central hole drilling technique is assumed to be an accurate method of surface stress-measuring technique. In comparison to blind-hole drilling, the X-ray technique gave good results (variation of 5% to 11%) as shown in Figure 10. The variation from different methods could result because of the misalignment of the point of irradiation in determining the film to specimen distance for X-ray stress measurements and measurements in the difference in "Debye-Scherrer" ring diameter or due to the selective action of X-rays.

4.2 Prediction of Fatigue Lives on the Basis of Residual Stresses

The comparisons of predicted and measured fatigue life

are given in Figures 11 and 12. This includes the results for the as-welded specimens as well as those for the various surface treatments described above.

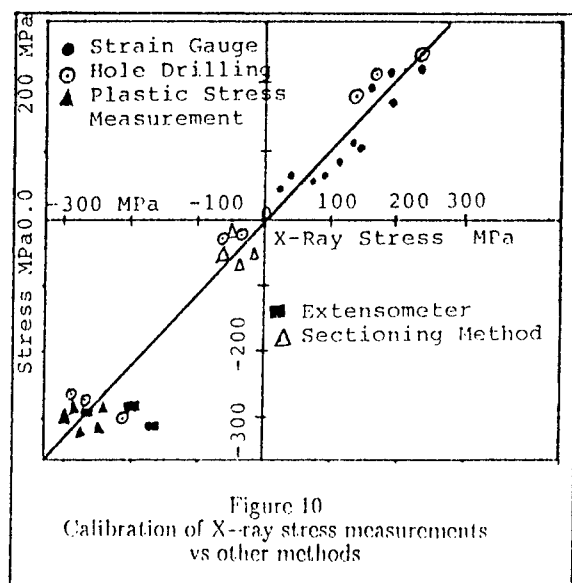
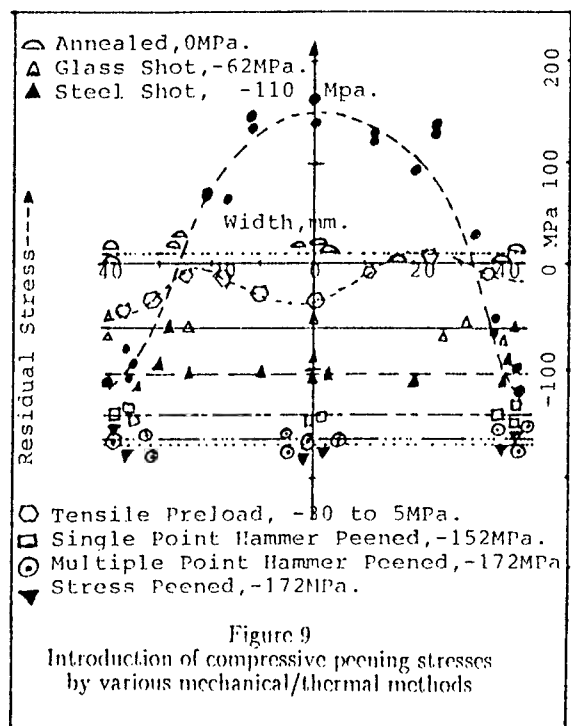


Figure 11 showed the plot of stress range versus total number of cycles to failure for the theory and experimental data points for the as-welded condition. It can be seen that the theory correlated closely with experimental results. The percentage error in stress range at 10^6 cycles between theory and experimental results was 5%. From Figure 11 it was found the variation in percentage stress range was 8% for annealed specimen. For the Tensile preloaded cases, the percentage error in stress range between predictions and experimental results was 14%. It was found that generation of compressive residual stress were uniform for the tensile preloaded cases.

This non-uniform distribution of initial tensile residual stresses due to preloading might have caused the discrepancy between theory and experiment. For glass shot peened specimens the percentage error in applied stress range between predictions and the experimental results was about 14%. It is assumed in the prediction

that stresses due to peening was uniform throughout the peened area but the measurements (Figure 9) showed that there was variation in the surface compressive stress levels due to peening. The percentage errors in the applied stress range between theoretical predictions and experimental results were 5%, 6%, 9% and 1% for steel shot, single point hammer, multiple point hammer and stress peened specimen respectively.

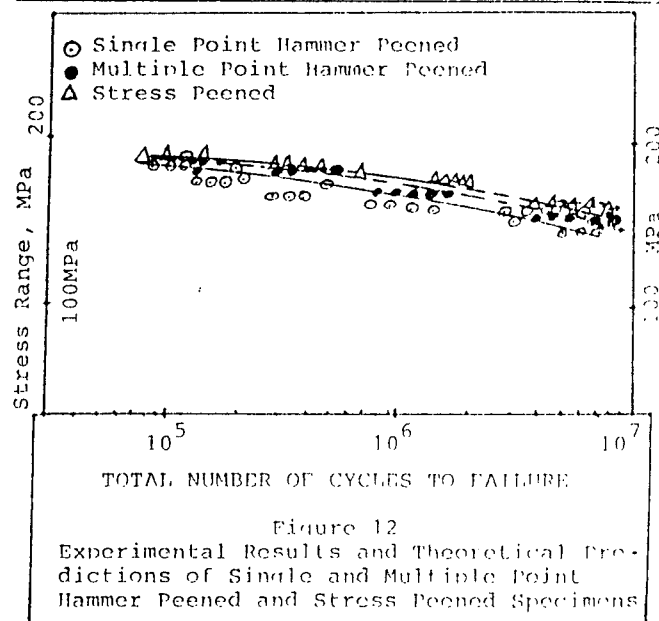
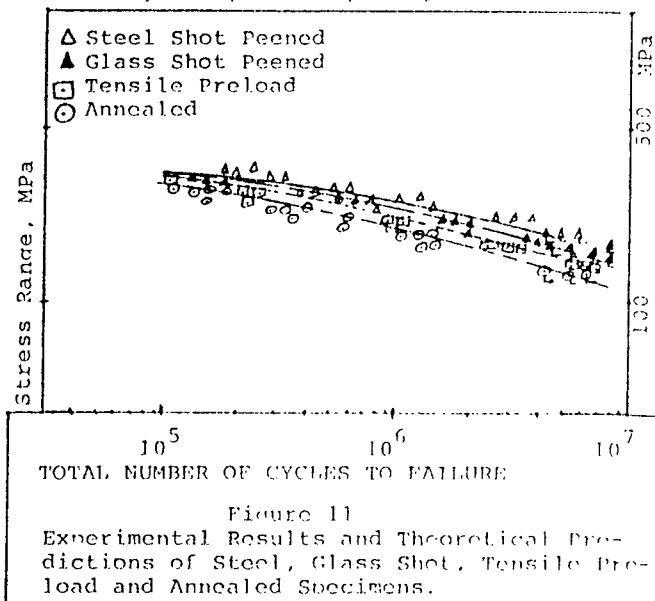


Figure 13 shows the modified Goodman diagram for as-welded condition (initial residual stress 152 MPa) and complete stress relieved condition. This shows the dependence of the maximum and minimum applied stresses on mean stress. For each value of mean stress there is a different value of the limiting range of stress which can be withstood without failure. The stress relieved (dotted lines) and as-welded condition (solid line) show the improvement of stress relieving of Columbian-50 butt-welds at particular fatigue lives of 10^6 , 2×10^6 and 10^7 cycles. the modified Goodman criterion predicts the fatigue resistance of the welded joints when subjected to both varying mean stress and the stress amplitude under fatigue cyclic conditions

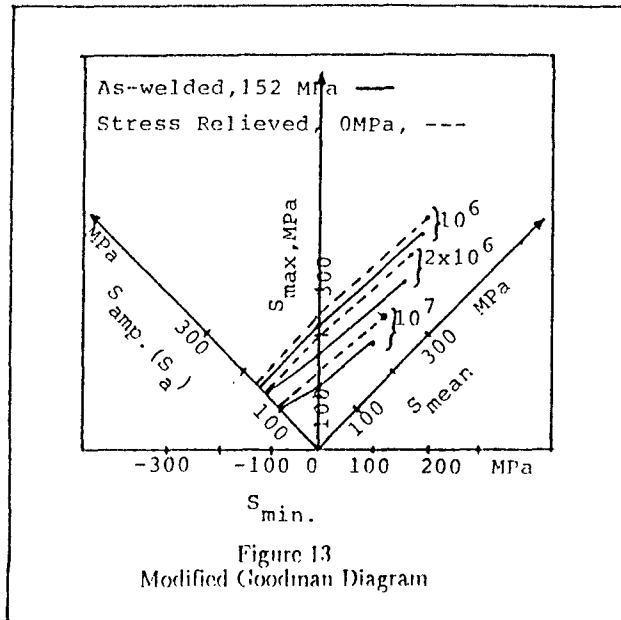


Figure 13
Modified Goodman Diagram

5. CONCLUSIONS

The theoretical approach to the estimation of the fatigue life of welded structure depends on the accurate determination of initial residual stress present in the specimen. The results of theoretical calculations were compared to experimental results for welds which have been mechanically and thermally treated. All the relevant stress measurements were performed by using X-ray diffraction technique. Those measurements of residual stresses were taken to predict theoretically the fatigue lives of welded joints and compared with experimental results. The conclusions from these results confirm the validity of the above mentioned techniques of residual stress measurements.

A close correlation in stress measurements was obtained among the various methods which are discussed earlier. The percentage errors at 138 MPa (X-ray stress) between upper and lower ranges of scattered data from the line of calibration was found to be 26.5%.

To improve the accuracy and to compensate for the selective action of the X-rays at least three to four exposures of each setting should be taken.

Blind-hole drilling technique showed a good correlation between X-ray diffraction and other conventional measurements. To correct any error due to milling operation, the method has to be calibrated against a known stress level and actual stress level on the welded specimen could then be corrected by the amount found from calibration test.

The effect of localized plasticity due to hole-drilling has to be considered in interpreting the results in this hole drilling technique. It was found that surface residual stress could be measured within an accuracy of ± 5 to 11%.

Stress measurements by sectioning method was found to be tedious and requires careful milling and filing. The sectioning has to be done in small increments to avoid temperature rising and plastic bending of the remaining shim. The method was found to be time consuming.

Stress measurements by Strain Gauging gave good results and only tensile stresses could be measured effectively. Plastic strain measurement by strain-gauging and by using an extensometer gave reasonable results; but there was no control on the amount of plastic strain after the yielding of the material. The methods may not be convenient for large specimens and real structures.

6. REFERENCES

1. Gurney, T.R. "Some Recent Work Relating to the Influence of Residual Stresses on Fatigue Strength", Welding Inst. Conf. on "Residual Stresses in Welded Construction and Their Effects". London. p151-163, Nov. 1977.
2. Spronll, X-rays in Practice, McGraw-Hill Book Company. New York, 1946.
3. Cullity, B.D. Elements of X-ray Diffraction, Addison-Wesley Publishing Company Inc. 1978.
4. Beancy, E.M. & Proctor, E. "A Critical Evaluation of the Centre-Hole Technique for Measurement of Residual Stresses", Strain, 7-14, Jan 1974.
5. Bathgate, R.G. "The Collection, Processing, and Application of Data Obtained by the Hole-Drilling Technique", Fulmer Research Institute, April 23, 1974.
6. Rosenthal, D. and Norton, J.T. "A Method of Measuring Triaxial Residual Stresses in Plates", J. of Am. Welding Society, Welding Suppl. V.21, 295-307, 1945.
7. Bellow, D.G., Wahab, M.A. and Faulkner, M.G. "Residual Stresses and Fatigue of Surface Treated Specimens", Advances in Surface Treatments - II, Pergamon Press, 85-94, 1985.
8. Bellow, D.G., Wahab, M.A. and Faulkner, M.G. "Prediction of Fatigue Crack Initiation and Propagation of Welded Joints", Advances in Surface Treatments - III, Pergamon Press, 27-40, 1986.
9. Wahab, M.A., Bellow, D.G. and Faulkner, M.G. "The Effect of Residual Stresses on the Improvement of Fatigue Life of Medium Strength Butt-Welded Steel Structures", Institute of Engineers, Publication 88/4, 16-20, 1988.

FATIGUE & STRESS

FATIGUE LIFE OF SUCKER RODS WITH EPOXY COATINGS

Donald G. Bellow

Professor of Mechanical Engineering, University of Alberta,
Edmonton, Alberta, Canada.

John E. Hood

Research Manager, Product Development, Stelco Inc., Hamilton,
Ontario, Canada.

Kenneth S. Roberts

Manager, Edmonton Finishing Works, Stelco Inc., Edmonton,
Alberta, Canada.

*Paper presented at I.I.T.T. Fatigue and Stress Conference, Paris,
September 1987, to be published by Pergamon Press.*

ABSTRACT

The work described in this paper concerns the effect of heat used to apply an epoxy coating on a shot peened upset forged oil field sucker rod. It is shown that if the heat of application of the epoxy coating is such as to lower the compressive residual stresses then the fatigue life of the sucker rod will be reduced significantly. It is recommended that manufacturers of sucker rods take special steps to monitor and control the residual stresses on the rod surface and, if the rods are to be epoxy coated using an elevated temperature process, steps should be taken to ensure that the process does not adversely affect the residual stresses on the surface.

INTRODUCTION

In recovering oil from wells many thousands of meters below the surface of the earth the conventional method is to actuate a plunger type pump situated at the bottom of the well by means of a string of rods coupled together by threaded couplings. This series of rods and couplings is called a sucker rod string. The sucker rod consists of a 25 ft (7.6 m) length of rod of various diameters ($1/2$ to $1\ 1/16$ in., 12.7 - 26.9 mm) which is upset forged at each end, heat treated and shot blasted. The ends are then threaded using a cold rolling process. A typical oil field installation is schematically shown in Fig. 1. and a detailed view of a sucker rod and the upset end is shown in Fig. 2. Either by the heat treating process or in combination with the shot blasting process (depending on the manufacturer) the surface of the rod is given a residual compressive stress. This residual compressive stress can be as high as -150,000 psi (-1034 MPa) and is effective in resisting the initiation of fatigue cracks. Following the heat treatment the sucker rod is usually painted and then packed for shipping.

IITT-International
40, promenade Marx-Dormoy
F-93460 GOURNAY-SUR-MARNE France

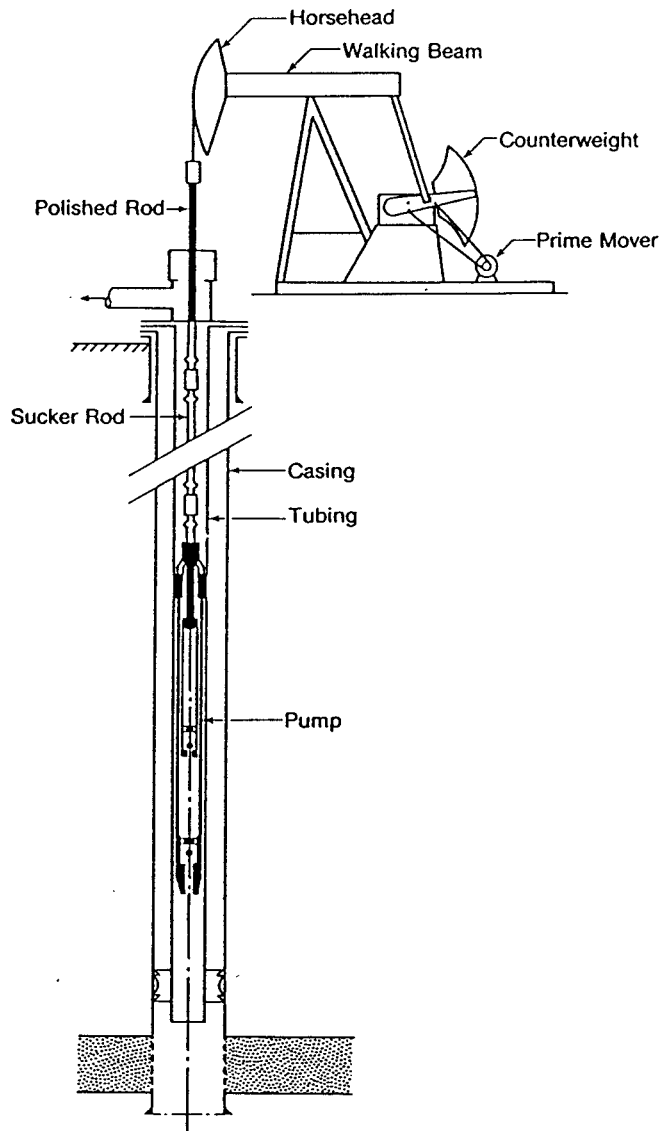


Figure 1. Schematic of oil well pumping unit.

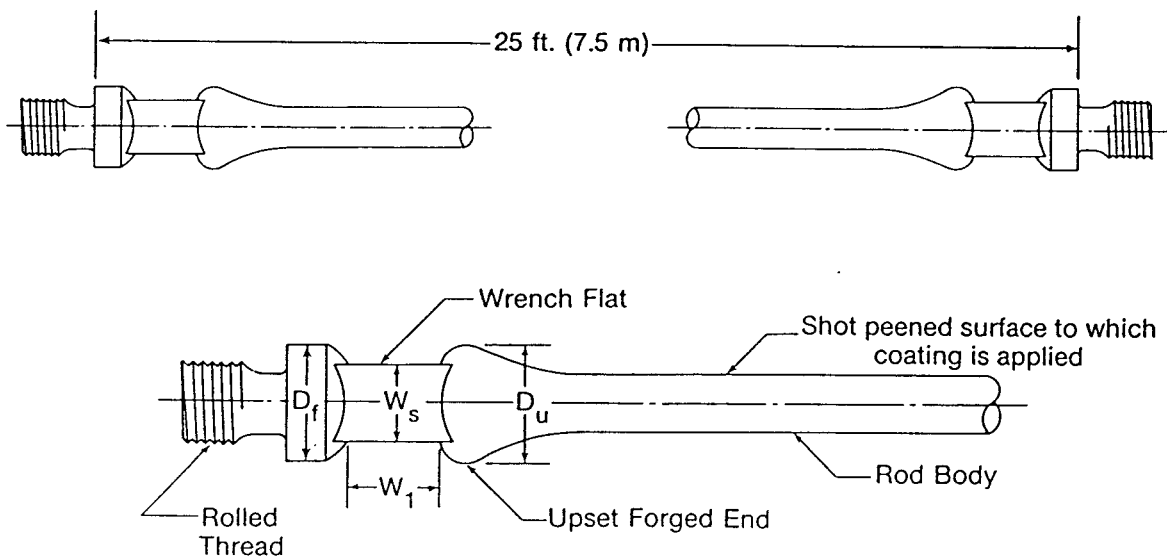


Figure 2. Sucker rod details.

In an oil field installation sucker rods reciprocate up and down with a frequency depending on the depth of the well and the capacity of the pool but usually between 0.01 and 0.2 Hz. For straight wells the load (upward stroke) on the sucker rod string is axial and consists of the weight of the sucker rod string below the point of consideration, plus the fluid load, plus the inertia load, plus friction forces and minus the buoyant forces. In most cases the axial stress varies between a minimum positive stress to a maximum positive stress although in some cases the minimum stress can be negative. Wells which are not straight are called deviated and for such wells the sucker rod strings can have a bending stress superimposed on the axial stress.

Most oil wells are corrosive containing salt water in combination with either (or both) hydrogen sulphide or carbon dioxide. Failure by fatigue is usually in combination with corrosion. There are three types of corrosion; pitting corrosion, crevice corrosion and general corrosion.

Oil producers attempt to resist the effects of corrosion by either designing the size of the sucker rod string for lower stresses than would be normal in a non-corrosive well, or by adding corrosion inhibitors to the well fluid where practical, or by coating the rod with a protective epoxy coating, or by any combination of these.

In many cases (but not all) sucker rods are given a protective epoxy coating by a service company not associated with the original producer of the sucker rod. This operation consists of removing any paint and dirt using a grit blast followed by a combination shot and grit blast. The latter treatment is to provide a suitable surface profile to assist in bonding the epoxy to the rod surface. The application of the epoxy normally occurs by rapidly heating the rod in an induction furnace, electrostatically charging the rod and passing the rod through an atomized atmosphere of epoxy particles. By controlling the pressure of the atomizers, the speed of the rod through the epoxy mist and the temperature, a controlled and uniform thickness of epoxy can be applied.

The object of this paper is to discuss the effects of this corrosion protective coating on the fatigue life of a sucker rod. The results should be applicable to any forging for which a beneficial compressive residual stress has been produced to inhibit the initiation of fatigue cracks.

RESIDUAL STRESSES

Compressive residual stresses are imparted to the surface of the rod either through the heat treating process or through the shot blasting process or a combination of both. In many cases the primary purpose of the shot blasting is to remove scale which occurs following the heat treatment process. The resulting residual compressive stresses are neither measured nor controlled and, for some, not understood.

The beneficial effects of residual compressive stresses in inhibiting fatigue crack initiation have been well documented. The major reference

of A. Niku Lari (1) as well as work on peening intensity and residual stresses by one of the authors of this work (2,3) describe this technique in detail. More specifically, a paper by Makarov et al (4) discusses the effects of surface residual stresses on the fatigue life of sucker rods. Surface residual stresses can also be influenced by phase transformation as described in a paper by Ishii et al (5).

Because of the corrosive environment into which sucker rods must operate there can be a concern that sucker rods with surface residual stresses can be subjected to accelerated corrosion which can promote fatigue crack initiation. In a paper by one of the authors (6) it was shown that the beneficial effects of residual stresses far outweighed the disadvantages in accelerated corrosion and, in fact, specimens with extreme work hardened surfaces had longer fatigue lives than non-work hardened surfaces even though the work hardened surfaces showed more evidence of corrosion pitting. Notwithstanding this, at least one manufacturer (7) offers a stress relieved sucker rod presumably to reduce the susceptibility to corrosion pitting.

STATEMENT OF THE PROBLEM

The work described in this paper was prompted by an oil company which was experiencing premature failures with API Grade D (quenched and tempered) sucker rods. The failures all occurred in the upset forged end. These rods were in corrosive wells but the conditions were not considered excessively corrosive. All the rods had been coated with epoxy using the methods described earlier in this paper. It was required to determine the cause of these failures and make recommendations as to how the problems could be avoided in the future.

In the beginning it was not known whether the problems were the result of improper application or assembly by the oil company or whether there were material defects in the rods themselves. It was determined that the first step in analyzing this problem was to test sucker rods which had come from the same batch which had experienced problems in the field but had not been used in service. Because the failures in the field had occurred in a relatively short time corrosion was ruled out as having a major influence so that a testing program of fatigue in air was justified.

SPECIMEN PREPARATION AND TESTING PROCEDURE

The sucker rods in question were 25 ft long (7.6 m) and had to be shortened so that they could fit into a standard type fatigue machine. Accordingly, the rods were cut and the two ends rejoined by welding to form shortened rods approximately 15 in. (0.4 m) long. This enabled two rods to be tested in tandem as shown in Fig. 3. The weld joining the two ends was peened with a multiple point pneumatic peening tool.

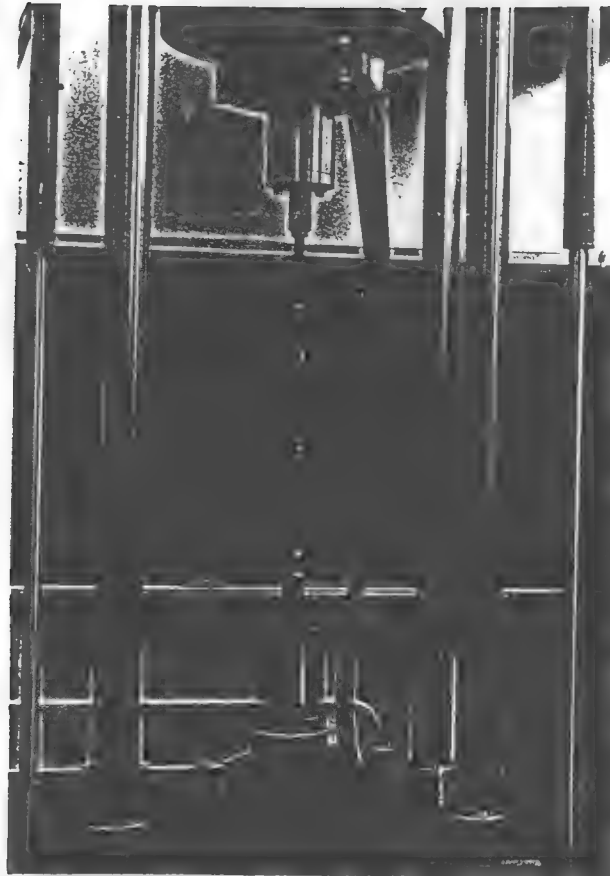


Figure 3. Fatigue testing of two rods in tandem.

The welding of the rods was far enough away from the forged ends so that the heat of the welding did not affect the microstructure of the forged ends. All rods tested were welded and had been shortened from standard 25 ft (7.6 m) long rods.

The shortened rods were torqued into the threaded couplings according to the schedule published by the American Petroleum Institute (API RP BR-1984) (8). The rods were then loaded in fatigue between 40 - 20 ksi (275 - 138 MPa) and the machine was started which resonated at about 75 Hz. The controls of the machine were set so that the machine would stop upon complete fracture of the specimen. It has been found from previous testing (9) that the number of cycles for crack propagation to failure is a small percentage of the number of cycles for crack initiation. No attempt was made to distinguish the onset of crack initiation in this

study.

If a specimen did not fail the test was terminated after 2.5×10^7 cycles. At a typical oil field cyclic rate of 10 cycles per minute 2.5×10^7 cycles represents approximately five years of service life. Although sucker rods can and do last much longer, it was believed 2.5×10^7 cycles was a sufficient period in which to evaluate the integrity of the upset forged ends. In some cases rods were fatigued as long as 4×10^7 cycles without failure.

RESULTS

All the sucker rods tested were manufactured from the same heat of steel although the rods were not all finished at the same time. In the beginning it was not known what was the cause of the premature failures experienced in the field so the first results were obtained to establish a data base from which further tests could be compared as well as replicating the failure lives experienced in the field. Table 1 lists the fatigue life distribution of nine sucker rods taken from the field but which had not been put into service. All the nine rods broke in the upset end in the wrench flat area with an average fatigue life of 9.59×10^6 cycles at 40-20 ksi (275 - 138 MPa). Also shown in Table 1 are the fatigue lives of uncoated rods of which none broke. Fatigue lives of 23.28×10^6 to 35.54×10^6 cycles were recorded. Clearly there was a difference in fatigue life between sucker rods which had been coated with epoxy and those which had not.

EPOXY COATING

The epoxy coating on the sucker rods tested was applied using a rapid heating process and passing the electrostatically charged rods through an atomized mist of epoxy particles. The particles adhered to the rod surface, melted and then solidified as the rod was passed through a water spray. It was found that the temperature of the rod was controlled and monitored on the rod body (narrowest diameter) for a temperature of $475 \pm 5^\circ\text{F}$ ($246 \pm 2^\circ\text{C}$). Because the induction furnace heats according to the distance from the rod surface to the surface of the induction coils, the upset forged end being of a larger diameter than the rod body experienced a higher temperature than the rod body. This was accounted for in part by passing the upset forged ends more rapidly through the induction coil than for the rod body. Nevertheless, excessive heating of the upset forged ends occurred as evidenced by discoloration of the threads which varied between a straw color to a blue color ($450^\circ - 550^\circ\text{F}$, $230^\circ - 290^\circ\text{C}$). This excessive heating would affect the compressive residual stresses existing in the rod prior to the coating process as explained below.

If one considers a circular rod which is rapidly heated so that a temperature gradient is created between the surface and the core, the surface will expand relative to the core and, restrained by it, will develop compressive stresses. Simple calculations show that the maximum possible temperature differential between the surface and core

Table 1 Summary of Fatigue Results

-all tested at 40 - 20 ksi (275 - 138 MPa)

	Cycles to Failure	Remarks
Epoxy Coated Rods	3.05 X 10 ⁶	All Failed in Wrench flat
	3.25 X 10 ⁶	
	4.16 X 10 ⁶	
	7.53 X 10 ⁶	
	13.05 X 10 ⁶	
	4.06 X 10 ⁶	
	15.55 X 10 ⁶	
	26.14 X 10 ⁶	
	8.74 X 10 ⁶	
Uncoated Rods	35.54 X 10 ⁶	No failure, tests stopped arbitrarily
	29.92 X 10 ⁶	
	23.89 X 10 ⁶	
	23.89 X 10 ⁶	
	23.28 X 10 ⁶	
	29.93 X 10 ⁶	
	24.38 X 10 ⁶	
	24.38 X 10 ⁶	

in the epoxy coating process was sufficient to create compressive stresses at the surface exceeding the yield stress. Surface yielding will be enhanced by preexisting compressive residual stresses due to shot peening and a high temperature gradient. Subsequent rapid cooling of the rod will now create higher contraction strains in the surface than the core and leave the surface in a state of relatively higher tensile residual stress than before the thermal cycle.

To determine whether temperature alone was causing the loss in fatigue life a series of rods taken from the same heat of steel were heated in an induction furnace and held at 475°F (246°C) for 10 min. Of four rods

tested none broke in fatigue and the tests were arbitrarily terminated at between 25.7×10^6 and 31.4×10^6 cycles.

After all other possible causes had been eliminated it was agreed, along with the manufacturer of the epoxy coating, to epoxy coat a series of rods using a reduced 350 - 400°F (177-200°C) temperature of application in the vicinity of the upset end. Eight rods were tested, none of which failed in the upset end, four failed in the weld at 1.6×10^6 , 24.3×10^6 , 26×10^6 and 30.7×10^7 , and the tests were arbitrarily stopped for the others at between 30.7×10^6 and 48.7×10^6 cycles. These results confirm that the loss of fatigue life was due to the localized surface heating (475°F, 246°C) used in the application of the epoxy coating.

MEASURED RESIDUAL STRESSES

In an unpublished work (10) surface residual stresses were recorded for a number of API grades of uncoated sucker rods. Compressive residual stresses in the range -4 to -92 ksi (-27 to 634 MPa) were recorded for both quenched and tempered and normalized and tempered rods. For a quenched and tempered rod which had been stressed relieved to 1256°F (680°C) for 30 minutes and air cooled the residual compressive stress was measured at -14 ksi (-96 MPa).

For the sucker rods tested in this study surface residual stresses of the upset portion were measured using a back-scatter X-ray diffraction technique. These results are shown in Table 2. It was found that rods which were uncoated had a residual compressive stress on average at -25.5 ksi (-175 MPa) whereas rods which were coated with epoxy using the method described earlier had residual stresses on average of -11.6 ksi (-80 MPa). For rods which had been heated to 475°F (246°C) for 10 min. the residual stresses were measured on average of -23.9 ksi (-165 MPa). For rods which had been coated using a reduced temperature of 350 - 400°F (172 - 200°C) the surface residual stresses were measured at -3.1 to + 4.1 ksi (-21 to + 28 MPa). This was unexpected in that these rods had long fatigue lives. A 0.003 in. (0.08 mm) layer of the surface was chemically etched away and at this depth the residual stresses were measured at -7.2 ksi (-50 MPa). A check at a 0.005 in (.13 mm) depth for the coated rods using the higher temperature of application showed the residual stresses to be tensile at + 10.3 ksi (+71 MPa). A close inspection of the surface of the fatigued coated specimens, for both the higher and lower temperature coatings, showed evidence of fatigue cracks on the surface. However, for the lower temperature coating the surface cracks propagated to but not through the compressive layer which existed 0.003 in. (0.08 mm) below the surface. For all residual stress measurements there was considerable scatter in the data depending where on the forging the measurement was taken. It was also found that the shot peened surface which was irregular rather than smooth also contributed to the scatter.

Table 2 Measured Residual Stresses

Rod Condition	Number of Readings	Stress Range	Average
Uncoated	10	-9 to -33ksi (-62 to -228MPa)	-25.45 ksi (-175MPa)
Coated	11	+5.5 to -33 ksi (+38 to -228 MPa)	-11.6 ksi (-80 MPa)
Uncoated but heated to 475°/10min	7	-5 to -39.5 ksi (-34 to -272 MPa)	-23.9 ksi (-165 MPa)

SUMMARY

The work described in this paper shows the importance of compressive residual stresses and their influence on the fatigue life of sucker rods. It is reasonable to suspect that most sucker rod manufacturers use the shot blasting process to remove mill scale and prepare the surface for painting or coating. They do not control or monitor the peening intensity to achieve an optimum residual compressive stress at the surface. More work needs to be done in this area.

The other important point this work has shown is that, in the sucker rod industry at least, when sucker rods are subsequently coated and handled by a manufacturer who is not the primary producer of the rod the beneficial effects of heat treatment and residual stresses can be unknowingly altered and yet failures of sucker rods in the field may be attributed to the primary manufacturing process. It is thus incumbent upon the primary manufacturer to ensure that secondary processes do not adversely affect the surface residual stresses which have been imparted to enhance the fatigue life of sucker rods.

REFERENCES

1. Niku-Lari, A. Shot Peening, Pergamon Press, 1982.
2. Faulkner, M.G. and Bellow, D.G., "Improving the Fatigue Strength of Butt Welded Steel Joints by Peening", Weld Res. Int., Vol. 5, No. 3, 1975, pp. 64-72.
3. Bellow, D.G., Wahab, M and Faulkner, M.G., "Residual Stresses and Fatigue of Surface Treated Welded Specimens", Advances in Surface Treatments, Vol.2 pp.85-94, 1985.
4. Makarov, B.H., Saveljev, B.T., Mukhamadeeva, H.H., "Causes of Premature Fatigue Failure of Sucker Rods, Oil and Gas Industry, No. 11, 1981, pp 40 - 42 (in Russian).
5. Ishii, K., Iwamoto, M., Shiraiwa, T. and Sakamoto, Y., "Residual Stress in the Induction Hardened Surface of Steel," SAE Trans, 1969, pp. 1765-1771.
6. Bellow, D.G., and Faulkner, M.G., "Salt Water and Hydrogen Sulphide Corrosion Fatigue of Work Hardened Threaded Elements," JTEVA, Jour. Testing & Eval; Vol.4, No. 2, 1976, pp 141-147.
7. Sumitomo Sucker Rods - catalog, Sumitomo Metal Industries Ltd. 1982.
8. API Specification RP 11BR, American Petroleum Institute, 19th Edition, 1982.
9. Bellow, D.G., and Faulkner, M.G., "Fatigue of Threaded Sucker Rod Couplings" Jour. Can. Pet. Tech., Vol. 11, No. 1, 1972, pp 67-74.
10. "Fatigue Performance of Sucker Rod for Oil Production," unpublished research report of Sumitomo Metal Industries Ltd., 1985.

FATIGUE & STRESS

The role of residual stresses in the development of oilfield sucker rod strings.

Donald G. Bellow (Canada)

published by :

**IITT-International
40, promenade Marx-Dormoy
F-93460 GOURNAY-SUR-MARNE France**

ABSTRACT

Sucker rods used in pumping crude oil are subjected to alternating stresses in combination with corrosive environments. This paper reviews some of the work which has been directed to improving the service life of sucker rods by considering the important role played by residual stresses.

It is shown that cold worked (rolled) threads are superior to cut threads in the sucker rod joint and that the surface compressive residual stresses can markedly influence the corrosion fatigue life of the sucker rod body.

The primary focus of the work described in this paper has been to evaluate various parameters on the fatigue and corrosion fatigue behaviour of sucker rod strings. The work has application to any components for which fatigue and corrosion fatigue are significant design considerations.

KEYWORDS

sucker rods, couplings, residual stresses, shot peening, corrosion, corrosion fatigue, cold worked, surface finish, induction heating.

INTRODUCTION

Conventional crude oil is commonly pumped from pools located many hundreds and often thousands of meters below the surface of the earth. A typical pumping system consists of a double acting pump located at the bottom of the well which is connected to a reciprocating type walking beam apparatus on the surface of the earth. The series of steel rods and couplings which connects the pump to the walking beam is called a sucker rod string. This type of pumping system, but using wooden rods, dates back to the first century where it was used by the Romans to pump water (1,2). Nowadays, sucker rods are also being made as a continuous string, where the coupling is eliminated. In other cases composite materials are replacing steel in downhole components. Alternatively to a plunger pump, rotary pumps are installed at the bottom of the well where the sucker rod

string acts as a torsional element. Despite these alternatives at least 70 to 80 percent of all crude oil is pumped in the conventional manner of using a bottom hole plunger pump actuated by a series of rods and couplings connected to a walking beam on the surface.

In the early days of oil production the wells were not deep, usually not corrosive and, as a result, little attention was paid to the design of the sucker rod string except for standardization of sizes and thread configurations. Even today there is a lack of identifying severe environmental conditions beyond the classifications of sweet (CO_2) and sour (H_2S) service, and yet many wells contain a combination of CO_2 and H_2S as well as a high concentration of chlorides. However, oil producers are finding that sucker rod strings often fail prematurely, and that wells are becoming more and more corrosive due to bacterial growth in older wells and increasing amounts of water which have to be pumped out in order to extract the oil. In some cases 99% of the fluid which is pumped is water. Along with the fact that sucker rods strings are cyclically loaded these rod coupling strings are vulnerable to failure by corrosion-fatigue often in combination with general corrosion, pitting corrosion or crevice corrosion.

To enhance oil recovery in some areas steam flooding is used in a "huff and puff" sequence. In other areas CO_2 injection is used. All of these methods put additional, and sometimes, unknown demands on the conventional materials used down hole. Little attention has been given to what effects these environments have on the sucker rods strings.

In order to overcome frequent failures some oil companies coat their sucker rods and tubing with epoxy resin. Others use inhibitors in the well fluids to counteract the effects of the corrosive environments. As it stands today, no single remedy solves all problems and many oil companies are coping with downhole problems by trial and error and spending millions of dollars in the process.

From what appears to be a very simple machine element the sucker-rod string is probably the longest mechanical transmission link in existence. Its simplicity of design and manufacture sometimes beguiles its users into believing it to be rugged and not harmed by abuse. While the failure of a sucker rod string in service is probably the least costly downhole component to replace, its failure can result in costly downtime and result in high field service costs.

This paper will describe the manufacture of sucker rods and couplings and the problems that are encountered during the manufacturing process and in service in the field. It is shown that residual stresses play an important role in the successful operation of oil field sucker rod strings.

MANUFACTURING PROCESS

The material used for making sucker rods usually comes from a steel mill hot rolled to the approximate diameter required for the finished rod. In a finishing works the rods are cold drawn to the required nominal diameter and then the ends of each rod are heated and upset forged to form the shape shown in Fig. 1. Each end is forged separately through a series of die shapes to form the transition length, the wrench flat area and the thread area. In many cases the forging operation uses five

successive die shapes but one manufacturer is successful in accomplishing the forming operation in only two die shapes. After the rod is forged at the ends the entire rod is subjected to a heat treatment. The heat treatment can consist of a quench and tempered, normalized, normalized and tempered or a case hardened microstructure, depending on the manufacturer. At this point the rods are inspected for straightness and either reprocessed if they do not meet the API-11B Specification (3) for straightness, or are cold straightened. One manufacturer subjects the rods to a twisting/stretching process to straighten the rods.

Following the heat treatment/inspection/straightening the rods are steel shot peened. The principal reason for doing this is to remove mill scale but one manufacturer applies sufficient peening in combination with the heat treatment to produce compressive residual stresses on the surface in excess of 830 MPa (-120,000 psi) (4). After the shot peening operation the rod ends are machined and rolled threads are applied. The rods are inspected, painted or coated and crated in boxes for shipping.

The above is a brief description of the standard manufacturing processes as they exist today. There are variations to this such as continuous sucker rods which are manufactured to an elliptical cross section, which eliminate the couplings except at the top and the bottom, and rods which are coated with epoxy resin as well as fiberglass rods. Couplings as shown in Fig. 1 are made from a higher strength steel, usually AISI 8635 or similar and can be coated with epoxy for corrosion protection or "Ultraprene" or with hard metal spray powders for abrasive resistance.

THE ROLE OF RESIDUAL STRESSES

Over the years many changes have been made to the sucker rod string to improve its performance. For example, to assist in torquing up a sucker rod string the couplings had machined wrench flats on the sides. It was found that these, as well as manufacturers stampings, were the cause of many fatigue failures in the field. Wrench flats on couplings have now been eliminated.

In the 1960's rolled threads replaced cut threads in both the pin end of the sucker rod and the coupling. Manufacturers had more difficulty in producing an internal rolled thread than an external rolled thread but the results shown in Fig. 2 clearly show the superior fatigue performance of a fully cold rolled thread compared with a cut thread (5,6). As seen in Fig. 3 the root of a fully rolled thread has a considerable degree of deformation whereas for a cut thread there is no realignment of the fibres at the thread root. The effect of the plastic deformation on the fatigue life in forming the threads is shown in Fig. 4 where the fatigue notch factor for a fully cold worked thread at 10^6 cycles is 1×10^4 compared to 2.7 for a simple cut thread.

The improved fatigue results for the cold work hardened rolled thread was also borne out in the presence of a corrosive environment. It was shown (7) that if the fatigue life of a simple cut thread at 10^6 cycles was normalized at unity then a fully rolled thread would have a life factor of 37 in air. Even though this was reduced to 0.41 in a solution of H_2S , CH_3COOH and 5% $NaCl$ the simple cut thread had a life factor considerably less at 0.08. The life factors of the various thread forms analyzed in corrosive environments is shown in Table I.

Table I

Based on unity life for cut thread tested in air. Life factor for cut thread and fully cold worked thread at 435 MPa - AISI 8635

Thread Type	Environment	Life Factor
Cold Worked	Air	37
Cold Worked	3.5% NaCl + O ₂	3.1
Simple Cut	Air	1.0
Simple Cut	3.5% NaCl + O ₂	0.43
Cold Worked	H ₂ S + CH ₃ COOH + 5% NaCl	0.41
Simple Cut	H ₂ S + CH ₃ COOH + 5% NaCl	0.08

While all sucker rod manufacturers shot peen their rods after heat treating, the process is used primarily to rid the surface of mill scale prior to painting. One manufacturer follows a more rigorous approach to this and claims to produce surface residual compressive stresses on the rods as high as -830 MPa (-120,000 psi). This is achieved by a combination of surface induction hardening and shot peening. With such a high compressive residual stress on the surface, a nominal tensile stress of 345 MPa (50,000 psi) applied to the rod does not cause any tensile stresses on the surface. This not only enhances the fatigue life but also reduces the susceptibility to corrosion fatigue and stress corrosion cracking.

When a rod string is cyclically loaded in service the compressive residual stresses will be reduced by 30-40 percent. Thus, a rod which has received only superficial shot peening and then subjected to fatigue loading may end up with very little compressive residual stresses, or worse, have residual tensile stresses on the surface after only a few load cycles.

In a paper by Makarov et. al. (8), it was shown that fatigue failure in the upset zone was caused by residual tensile stresses which were not eliminated by subsequent heat treatment, and the resulting grain growth led to a reduction in fatigue life. These researchers found that in the upset end the material had an endurance stress about 18 percent less than that occurring in the main rod body material. They measured residual tensile stresses as high as $0.7\sigma_{ult}$ in the upset area. The highest residual tensile stresses were located about 100 mm (4 in.) from the pin end of the rod.

The effects of induction hardening can induce tensile residual stresses as shown by Ishii (9) but if followed with shot peening, compressive residual stresses can be obtained.

In research conducted by Sumitomo Metal Industries Ltd. in Japan (10) it was shown that if sucker rods were peened the fatigue limit could be increased by 30 percent over an unpeened rod containing mill scale. This observation was based on bending fatigue experiments. A regression analysis was applied to the data to relate fatigue strength σ_f , with tensile strength σ_T , residual stress σ_R , and surface finish R_z (measured in μm)

$$\sigma_f = -0.41\sigma_R - 0.1 R_z + 0.04\sigma_T \quad \text{kgf/mm}^2$$

It is interesting to note that their results showed that the influence of residual stresses on fatigue strength of the unpeened rod was an order of magnitude greater than the influence of the tensile strength of the material.

The residual stresses that have been discussed thus far have dealt with their beneficial effects. If sucker rods are bent or distorted during manufacturing or during installation then localized residual stresses that result from cold straightening the rod can lead to failure of the rod when an axial load is applied. From an investigation into the effect of bends on the stress distribution it was shown (11) that the residual stresses present in a rod which has been bent after heat treatment could be predicted reasonably accurately if the bend was simple and confined to the rod body away from the upset end. Figure 5 shows the extent of residual stresses in a rod as a function of the bend to diameter ratio. For the case of a rod which is initially bent during the manufacturing process, with no residual stresses, and then loaded axially in the field it has been found (11) that the bending stresses caused by straightening the rod can be as high as 68 percent of the axial stress. It was also shown (12) that meeting the API-11 Specification for straightness does not eliminate significant bending stresses.

For a conventional sucker rod and coupling string the stress distribution is complex in the vicinity of the joint (12). Figure 6 shows a typical elastic stress distribution as measured by electrical resistance strain gauges applied to the surface. In particular, there is a large stress gradient in the upset forged end. In Fig. 7 the location of failures is noted. The letter G refers to a ground surface and the letter P refers to a shot peened surface. This particular study (13) showed that there was no difference in the corrosion fatigue life between a ground surface and a peened surface. The peened surface evaluated was used to remove millscale, and as such, produced residual compressive stresses not unlike those produced by a ground surface. The concentration of failure locations in the upset end was due to the sharp stress gradient and superimposed bending stresses. The latter due to eccentricities in the rod geometry.

Mention has been made that some oil producers coat their rods with epoxy resin to prevent corrosive attack in wells with high concentrations of CO_2 , H_2S and/or chlorides. It was shown in a recent paper (14) that if the application of the epoxy coating is such as to lower the compressive residual stresses then the fatigue life of the sucker rod would be reduced significantly. This was explained by noting that if the rod is heated by an induction coil, a temperature gradient is created between the surface and the core. This causes the surface to expand relative to the core and, restrained by it, will develop compressive stresses. Surface yielding will be enhanced by pre-existing compressive residual

stresses due to shot peening and a high temperature gradient. Subsequent rapid cooling of the rod leads to higher contraction strains on the surface than the core which leaves the surface in a relatively high state of residual tensile stress. This problem was resolved by lowering the surface temperature during the coating process from 245°C to 190°C.

Subsequent to the work published in Ref. 14 it was found that the epoxy coating on the rods, which had been applied at the lower temperature of 190°C, severely blistered when in contact with a hydrogen sulphide environment. Apparently to achieve an adequate bond between the metal and the epoxy a 245°C temperature of application is required. Further investigation into this problem showed that the frequency of the current supplied to the induction heater influences the depth of heat penetration and the compressive residual stresses on the surface. This can be understood from the following relationship.

$$p = \frac{5}{\pi} \left[\frac{10^5 \rho}{f \mu} \right]^{1/2}$$

where p is the depth of heat penetration, ρ is the resistivity of the material ($\mu\Omega\text{m}$), μ the magnetic permeability (H/m) and f is the current frequency (Hz). If it is assumed that μ and ρ remain constant then the depth of heat penetration at a current frequency of 1000 Hz will be 3.2 times that at a current frequency of 10,000 Hz. A number of sucker rods coated with epoxy using an induction furnace with a current frequency of 1000 Hz were subjected to cyclic loading between 275 - 140 MPa. No rods failed and the tests were stopped after $30\text{-}46 \times 10^6$ cycles. Residual stresses were measured before and after fatigue loading and were found to be -215 MPa and -175 MPa respectively. Thus, it was shown that the residual stress pattern is relatively unaffected if there is sufficient depth of heating in applying an epoxy coating. The heating used to apply an epoxy resin coating should not be confined to a thin layer on the surface.

CONCLUDING REMARKS

There has been much progress in the manufacture of sucker rods over the past 50 or so years. Nevertheless, there is still more that can be done to ensure a failure free sucker rod string. It will take a combination of efforts between the manufacturer and user to reach this objective. Even if a perfect rod could be made it can fail if it is mishandled such as allowing the surface to be nicked which causes stress risers, or if the joints are improperly made up with insufficient preload. Another problem facing the user is how to combat the effects of corrosion fatigue. Chrome nickel alloyed steels can be employed but these are costly. However, there may be some alloys which can be economically used under severe corrosive conditions providing a proper "matching" can be obtained. Coatings are relatively inexpensive but it is difficult to achieve a "holiday free" coating. Using inhibitors in the well fluid is being used with success in some situations but it is also costly and requires frequent monitoring. The use of composite materials in place of steel eliminates corrosion but introduces dynamic problems and, because of the lighter weight, at least half of the sucker rod string still must be steel in order to prevent the rod string from buckling.

This survey has focussed on the role residual stresses play in the successful operation of a sucker rod string. If sufficient compressive residual stresses can be "manufactured" into the rod initially and if the users would pay close attention to make up procedures in the field, along with a judicious selection of design factors to account for loading and corrosive conditions, then trouble free performance of a sucker rod string may become a reality.

ACKNOWLEDGEMENTS

The author expresses appreciation to the many co-workers who contributed to some of the work described in this paper as well as to those industries who freely exchanged information with the author. Financial assistance received from the Natural Science and Engineering Research Council (Grant A-2705) is gratefully acknowledged.

REFERENCES

1. Sucker Rod Handbook, No. 489, Bethlehem Steel Co., 1952.
2. Zaba, J., Modern Oil-Well Pumping, Petroleum Publishing Co., 1962.
3. API-11B Specification, Sucker Rods (Pony Rods, Polished Rods, Couplings and Subcouplings), American Petroleum Institute, 1984.
4. U.S. Patent #3489620 "Method of Processing Sucker Rods and Resulting Article", 1970.
5. Bellow, D.G. and Faulkner, M.G., "Development of an Improved Thread for the Petroleum Industry", Closed Loop 8(1), 1978.
6. Bellow, D.G. and Faulkner, M.G., "Fatigue of Internally Threaded Machine Elements," Trans. Can. Soc. Mech. Eng. (CSME) 29 (12), 1973.
7. Bellow, D.G. and Faulkner, M.G., "Salt Water and Hydrogen Sulphide Corrosion Fatigue of Work Hardened Threaded Elements," Journ. Testing and Eval. JTEVA, 4(2), 1976.
8. Makarov, V.H., Saveljev, V.F. and Mukhamadeeva, N.N., "Causes of Premature Fatigue Failure of Sucker Rods," Oil and Gas Industry, II, 1981. (in Russian).
9. Ishii, K., Iwamoto, M., Shiraiwa, T. and Sakamoto, Y., "Residual Stresses in the Induction Hardened Surface of Steel," SAE Trans., 1969.
10. Unpublished report, "Fatigue Performance of Sucker Rod for Oil Production", Sumitomo Metal Industries, Ltd. Central Research Laboratories, 1985.
11. Bellow, D.G. and Kumar, A., "Stress Analysis of Bent Sucker Rods", Jour. Can. Pet. Tech., 17(3), 1978.
12. Bellow, D.G. and Howe, R.K., "Bending Stresses in Otherwise Straight Sucker Rods", Jour. Can. Pet. Tech., 1988, in press.

13. Bellow, D.G., "Stress and Corrosion Fatigue Experiments on Oil Field Components", SESA/JSME Proceedings, Hawaii, 1981.

14. Bellow, D.G., Hood, J.E. and Roberts, K.S., "Fatigue Life of Sucker Rods with Epoxy Coatings," 2nd Int. Conf. on Fatigue and Stress, Paris, 1987, in press.

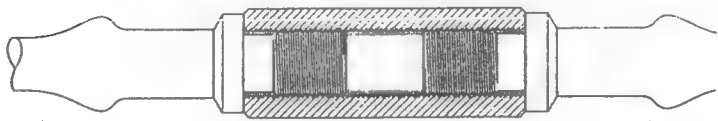


Figure 1. Sucker Rod Joint Configuration.

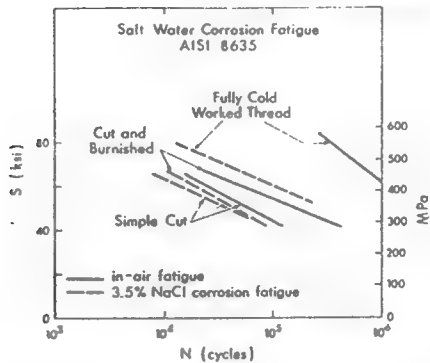
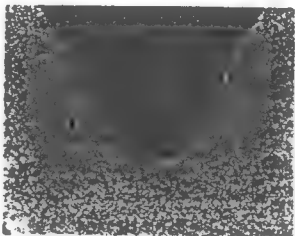
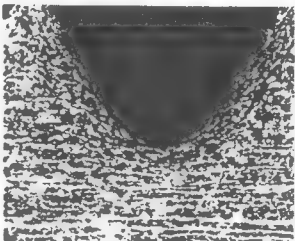


Figure 2. Fatigue Results of Couplings with Different Thread Configurations.



Simple Cut Thread



Fully Cold Worked Thread

Figure 3. Macrographs of Thread Roots.

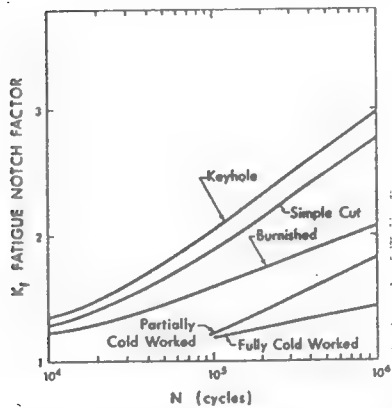


Figure 4. Fatigue Notch Factor for Thread Root Forms.

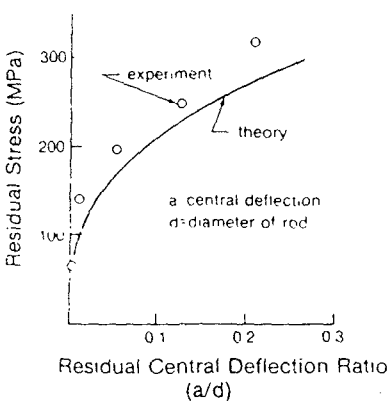


Figure 5 Residual Stresses Due to Bend in the Rod.

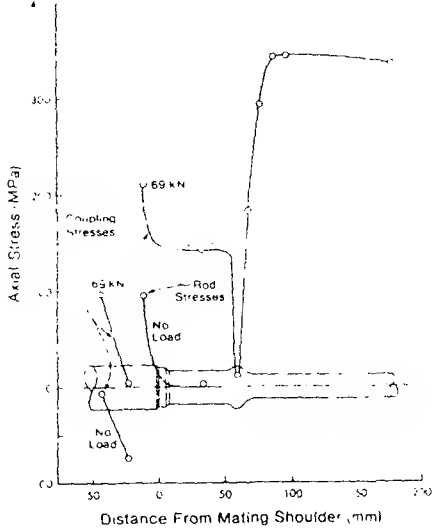


Figure 6. Stress Distribution Across a Sucker Rod Joint.

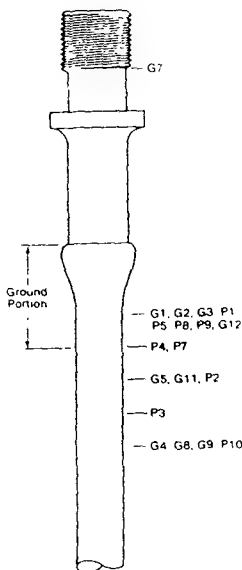


Figure 7. Location of Failures (8.4% NaCl).

FATIGUE & STRESS

H.P. LIEURADE
(IRSID, France)

High temperature fatigue of furnace tray alloys.
D.G. Bellow (Canada)

ABSTRACT

Cast ferrous alloyed trays used in heat treating furnaces are subjected to cyclic heating to 1000°C and cooling to 250°C during the normal course of operation. After a period of time, cracks leading to complete fracture render the trays useless. The purpose of this study was to investigate the cause of these cracks and determine what alloying could be used to minimize or eliminate the problem. A special testing facility was designed which thermally fatigued tensile specimens that were clamped between fixed ends. Of the cast alloys investigated, it was found that an alloy type 49k + Co gave the longest fatigue life closely followed by a 49k + Ni alloy. However, it was apparent that a high nickel content alone did not yield improved thermal fatigue properties.

INTRODUCTION

The purpose of this project was to study the thermal fatigue characteristics of a number of different alloys which could be used as furnace trays in a heat treatment furnace. A large manufacturing company had been experiencing frequent cracking and fracture of furnace trays used in the heat treatment of grinding balls. These trays were cast in the shape of a honeycomb structure and were breaking in the webs after limited use. While a plant testing program was initiated to evaluate trays of different materials and design it was desired to conduct independent laboratory trials under closely controlled conditions on the base material to determine whether or not any one material was superior.

TESTING PROGRAM

In order to evaluate the thermal fatigue properties of alloys a special loading and testing frame is required. It can be seen in the literature that there are a variety of ways in which this test can be carried out but all essentially use the same principle. A test sample is clamped at the ends and a heat source is cyclically applied to the middle of the specimen between a maximum and minimum temperature. A common method of heating is to use an electric induction furnace with cooling using a stream of cold air. The number of thermal cycles to failure is recorded for a specific maximum - minimum range of temperatures. After a crack appears, failure of the specimen follows shortly with complete fracture of the specimen.

IIT-International
40, promenade Marx-Dormoy
F-93460 GOURNAY-SUR-MARNE France

It has been found by previous investigators that the maximum temperature significantly affects the thermal fatigue life more than the temperature range. Also, if the thermal cycle dwells at the maximum temperature creep can occur which may weaken or strengthen the material for fatigue resistance depending on the alloy and the maximum temperature in the thermal cycle (Yen, 1961).

The basic mechanism for a thermally cycled specimen clamped at both ends with no initial load is as follows. Upon heating, the specimen attempts to expand but cannot because of the constraints at the ends. This puts the specimen into compression, but because of the elevated temperature, the yield stress is lowered and plastic flow occurs at the center of the specimen causing a thickening of the specimen due to the plastic upsetting of the material. Upon cooling, the specimen contracts but the upset portion does not recover because the stress is lower now because of the larger cross-sectional area. Thus, as the specimen further contracts the plastic flow stress increases and a tensile stress is imposed on the specimen. Plastic flow can also occur in tension. For each thermal cycle the process is repeated until eventual failure occurs, generally adjacent to the upset center section of the specimen. The center section of the specimen upsets because it is here that the specimen has the smallest cross section and where the heating is the greatest. The upset portion occurs during the first cycle and is stabilized in size just after a few cycles.

To construct a suitable piece of testing equipment a variety of electrical heating sources were tried. Because of limited capacity they failed to heat the specimen adequately or fast enough. In order to provide a reasonably inexpensive heating source a gas fired furnace was constructed. This had the added advantage in that a gas flame directed at a test specimen would more closely model the actual conditions in a gas fired heat treatment furnace. Another advantage was that alternating the gas flame with an air blast the cyclic time could be significantly reduced from what had been reported in the literature. The cycle rate depended on the rate of heating and cooling. The maximum and minimum temperatures were controlled at 1000°C and 250°C respectively. This resulted in a cycle rate of 0.4 cycles/min.

EXPERIMENTAL APPARATUS

The specimen was 45 mm long and approximately 8 mm in diameter at its narrowest section. In Fig. 1 the specimen and testing configuration is shown. The specimen was threaded at both ends and screwed tightly into the end fixtures which were held rigid by the cross-heads of a 50,000 lb. capacity Instron Universal Testing machine. In order to protect the cross-heads, and notably the load cell, water jackets were placed on either side of the specimen. This also had the effect of keeping the specimen ends cooled so that the yield stress in this area would not be affected by temperature and lead to premature failure of the specimen in the threads. A temperature controller was connected to an infrared thermometer focused at, but remote from, the center of the specimen. The two gas jets were ignited and the temperature of the specimen rose quickly to a preset limit in the controller which then shut off the gas jets. Cold air was then

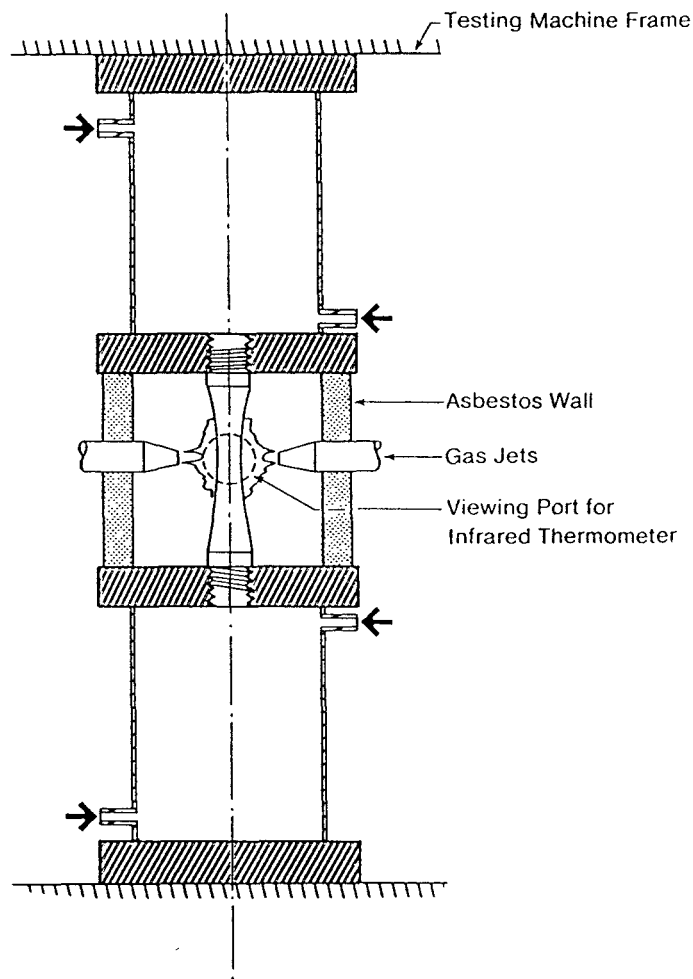


Fig. 1. Thermal fatigue apparatus

directed at the specimen causing it to cool rapidly. The temperature vs. time was recorded as well as the load vs. time. When the lower preset temperature was reached the gas jets were automatically re-ignited. This cyclic process was continued until a specimen failed. A small pilot flame was used to ignite the main jets when the valve on the gas line was opened.

The system was calibrated for temperature by imbedding a thermocouple in a dummy specimen and adjusting the emissivity of the infrared thermometer to match the output of the thermocouple. This method assumed the emissivity of the specimen did not change with temperature and that no scaling of the specimen would occur to interfere with the infrared measurements.

The specimen dimensions were chosen to allow for a rapid rise and fall of temperatures, thus the mass was kept small. A small size was chosen also so that specimens could be machined from the webs of existing furnace trays.

When the apparatus was constructed it was tested out using stainless steel specimens, type 304 and 316. These materials produced scaling and thus the temperature was difficult to control without constant removal of the scale. They did, however, prove useful in developing the experimental procedure.

Before thermal fatiguing, all specimens were aged for 24 hours at 760°C and furnace cooled. This was done because it had been reported by previous investigators that for accelerated thermal fatigue tests insufficient time occurs at the maximum temperatures for equilibrium of carbide precipitation. This occurs naturally in a furnace situation but will not occur in the test specimen during the course of thermal fatigue unless specifically aged before hand. It has been found that by aging the specimens that the thermal fatigue results more closely resemble those which can be expected in the field (Yen, 1961).

TEST RESULTS

A typical load versus temperature curve is shown in Fig. 2. This was observed after a few cycles occurred and after the thermal upsetting had stabilized. This figure shows that upon heating the specimen relaxes with the load dropping off to zero at a temperature of about 870°C. Further heating puts the specimen into compression, because of the end constraints. Upon cooling, the specimen begins to contract and passes through zero at approximately 565°C whereupon it begins to go into tension. For each cycle where the yield stress is exceeded plastic flow occurs.

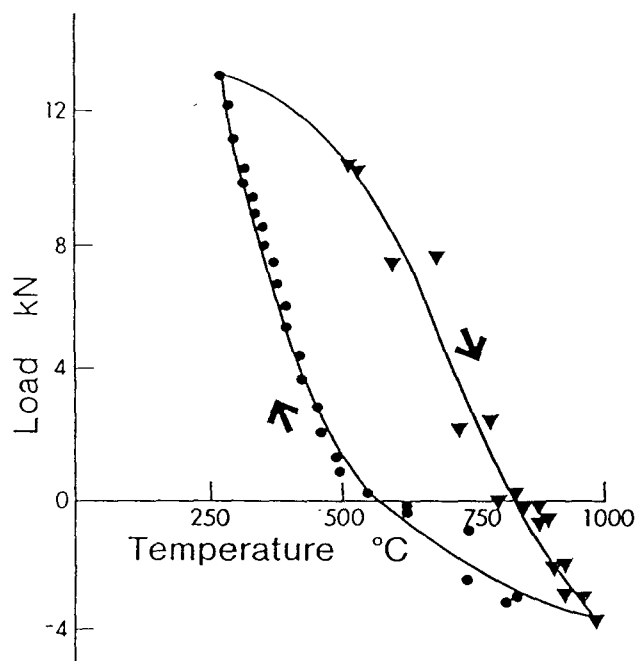


Fig. 2. A single thermal fatigue cycle

As the maximum and minimum temperatures appear to be critical in the thermal fatigue life it was considered that the stress at the maximum and minimum temperatures should be used in comparing the data. Consequently, the thermal fatigue life shown in Fig. 3 was plotted for each specimen tested. Where specimens broke in the threads or the test was accidentally interrupted the results were discarded. The stress was calculated on the basis of the narrowest cross-section adjacent to the thermally upset portion at the center of the specimen. The maximum and minimum loads were averaged for the entire number of thermal cycles except for the first few cycles where equilibrium was being established and also for the last few prior to fracture where the load fell off rapidly. Ignoring these few cycles was less than one percent. The chemical composition of the specimens tested is shown in Tables 1 and the fatigue data is listed in Table 2.

In general, the results showed that, of the five alloy types tested, the X4054A (49k + Co) gave the longest fatigue life followed closely by the X4050 (49k + Ni) and the HN(Fe-Ni-Cr). The alloy material cut from keel blocks #288 and #388 (HT type) had approximately half the fatigue life of the others.

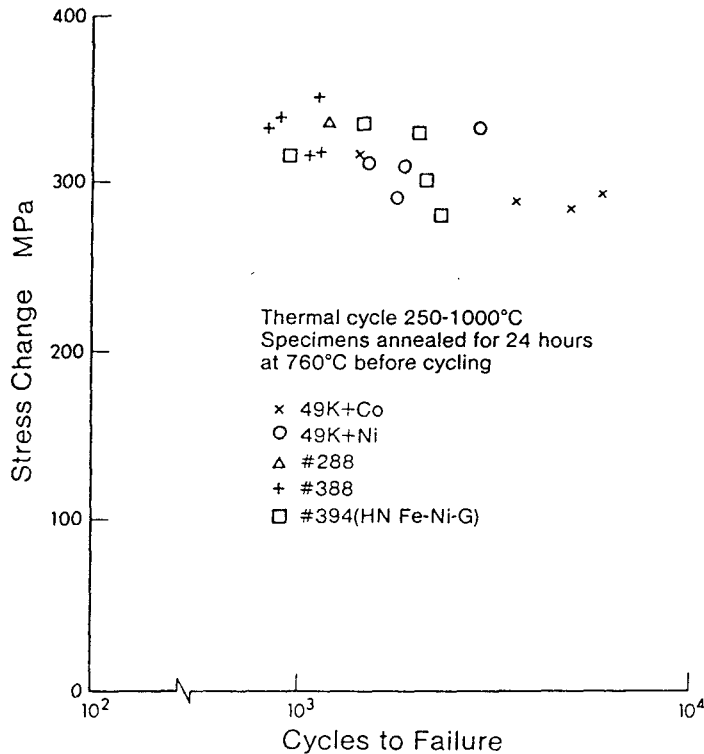


Fig. 3. Thermal fatigue data for five cast alloys

Table 1. Alloy Descriptions

Specimen	Analysis						Notes
	C	Co	Si	Mn	Ni	Cr	
A X4054 49k+Co	0.4	4.25	0.4	0.4	4.5	21.5	
B X4050 49k+Ni	0.4		0.4	0.4	8.0	21.5	
C 43H-type	0.2-0.6*		0.2 max	0.2 max	11-14	24-28	Keel block 288
D Fe-Ni-Cr(HT type)	0.503		1.39	1.30	36.81	17.76	Keel block 388
E Fe-Ni-Cr(HN type)	0.370		1.39	0.93	25.16	22.18	Keel block 394

*Alloy not analyzed - suggested ranges for this type given

For the alloys tested the chromium content ranged between 17.76 and 28% whereas the percentage nickel varied between 4.5 and 36.8%. As already noted the X4054 Alloy with a combination of 4.5% nickel and 4.25% cobalt (Specimen A) gave a better thermal fatigue life than did X4050 which had 8% nickel alloy with no cobalt added (Specimen B). Of particular interest to note is that the HT alloy (Specimen D) which had 36.81% nickel along with 17.76% chromium, had the poorest thermal fatigue life of all alloys tested. A qualification to this statement must be made in that for Specimen D the stress range applied to the specimen was higher, on average, than for the other specimens tested. This could have been due to a more precise setting of the specimens in the test fixture than was carried out for the earlier test specimens (A,B and C). It also could have been due to differences in the thermal expansion coefficient and differences in thermal conductivity of the different alloys tested. Even so there seems to be sufficient data to indicate that the additional nickel contained in Specimen D did not lead to improved thermal fatigue over that obtained for the alloys with lower nickel content.

A metallurgical examination of furnace trays which had failed in service showed that thermal fatigue cracks had occurred ahead of the main fatigue crack and along the grain boundaries. In the test specimens thermal fatigue cracks were observed to have formed in a similar way. It was also observed that as these cavities developed at the grain boundaries, due to the thermal cycling, they joined to form cracks which propagated by progressive tearing of the ligaments between the cavities.

SUMMARY

The results of this testing program have shown that the experimental technique and apparatus described can be used successfully to determine the fatigue life of high temperature cast alloys. Differences in thermal fatigue behaviour were detected in five alloy types investigated. It was found that a high nickel content does not, in itself, yield improved

Table 2. Fatigue Data for Alloys Tested

Specimen	Average Loads lbs.			Dia. at Fracture (mm)	Stress Change (MPa)	Cycles to Failure	Notes
	max	min	ΔF				
A1 X4054 49k+Co	11.62	2.91	14.54	8.00	289	3558	
A2 X4054 49k+Co	13.41	3.52	16.92	-	-	2772	Failure in threads*
A3 X4054 49k+Co	11.36	2.94	14.31	8.00	285	5002	
A4 X4054 49k+Co	10.23	3.14	13.38	7.62	293	~ 6000	Pen failed, cycles est.
B1 X4050 49k+Ni	12.45	3.20	15.66	8.26	292		
B3 X4050 49k+Ni	13.25	3.43	16.67	8.00	332		
B4 X4050 49k+Ni	13.39	3.20	15.66	8.26	309		
C1 #288 43H	11.12	2.72	13.84	-	-	1091	Failure in threads
C2 #288 43H	13.40	2.89	13.84	7.87	334	1180	
D1 #388 HT	12.85	3.51	16.37	8.13	315	1058	
D2 #388 HT	12.09	3.31	15.40	7.87	316	1144	
D3 #388 HT	13.20	3.47	16.68	8.00	332	829	
D4 #388 HT	13.20	3.39	16.58	7.90	338	882	
D5 #388 HT	14.39	3.56	17.95	8.08	350	1126	
E1 #394 HN	13.07	3.83	16.90	8.26	316	948	
E2 #394 HN	10.31	3.02	15.09	8.31	278	2318	
E3 #394 HN	15.52	3.01	15.53	7.75	330	2021	
E4 #394 HN	12.32	2.94	15.26	8.05	300	2145	
E5 #394 HN	13.36	3.16	16.52	7.92	335	1483	

* Except where noted, all failures occurred in the thermally upset portion at the midpoint of the specimen.

thermal fatigue characteristics. Of the alloys tested, the 49k + Co displayed the longest fatigue life followed closely by the 49k + Ni alloy. These results were obtained by cycling between 250 and 1000°C at a rate of 0.4 cycles/min.

While this program was developed to obtain fatigue data for five cast alloys the honeycomb design of the furnace trays themselves probably contributed, in part, to the failure of these trays in service. More work could be undertaken to investigate the ideal tray shape to reduce the constraints at the nodes of the tray webs.

ACKNOWLEDGMENTS

The author expresses appreciation to Stelco Inc. for permission to use the data and to Mr. John Foy of the Mechanical Engineering Department who assisted in the experimental program.

REFERENCES

- Avery, H.S. (1959), "The Mechanism of Thermal Fatigue", Metal Progress, pp. 67-70.
- Avery, H.S. (1969), "Alloys for High Temperatures", Weld. Res. Council Bull. No. 143, pp. 44-48.
- Manson, S.S. (1966), Thermal Stress and Low-Cycle Fatigue, McGraw-Hill, Chap. 6.
- Yen, T.C. (1961), "Thermal Fatigue - A Critical Review", Weld. Res. Council Bull., No. 72, pp. 1-12.



The American Society of
Mechanical Engineers

Reprinted From
Eighth International Conference on Offshore
Mechanics and Arctic Engineering — Vol. III
Editors: M. M. Salama, N. V. Bangaru, R. Denys
H. C. Rhee, and M. Toyoda
Book No. I0285C—1989

ON THE SELECTION OF STEEL ALLOYS FOR CORROSIVE SERVICE

D. G. Bellow and I. Smuga-Otto
Department of Mechanical Engineering
University of Alberta
Edmonton, Alberta, Canada

ABSTRACT

A recent survey of oil field practices and experiences indicated that many downhole failures of sucker rods and couplings are the result of corrosion and corrosion fatigue. An electrochemical testing program was developed to evaluate the corrosion resistance of steel alloys used in sucker rods which could provide the basis for a future corrosion fatigue study. Three different sucker rods types were studied and it was shown that the use of polarization curves obtained from potentiodynamic studies can yield important information about the corrosion behaviour of steel alloys including the tendency for crevice corrosion and pitting to occur. Of the three rod types investigated it was found that the one with a hardened surface was the most resistant to corrosion in both a deaerated 3.5% NaCl solution and an 8% NaCl solution saturated with CO₂.

INTRODUCTION

A recent survey of oil field practices and experiences (Bellow and Smuga-Otto, 1986) showed that downhole failures of sucker rods and couplings could be attributed to one of a number of causes; corrosion fatigue, wear, improper joint makeup or overstressing.

Corrosion fatigue failures were found to be related to pitting corrosion and crevice corrosion as they act as stress risers on the metal surface and are potential sites for fatigue cracks (Bucaram and others, 1973; Chitton, 1968). On sucker rod strings where plastic centralizers are used, crevice corrosion can occur. Therefore, besides evaluating general corrosion rates, it is of interest to evaluate the inclusion-pitting and crevice corrosion relationship and their influence on the development of corrosion and corrosion-fatigue.

In the field survey conducted (Bellow and Smuga-Otto, 1986) it was difficult to get reliable

water analyses to enable an accurate assessment of the worse well conditions and obtain a correlation of wells experiencing frequent failures with a particular fluid chemistry. Nevertheless, it was clear that salt water in the presence of carbon dioxide or hydrogen sulphide, or both, were present in so-called "troublesome" wells.

In order to combat the effects of corrosion, oil companies use a variety of techniques such as inhibiting the well fluid, coating the rods with epoxy (Bellow and others, 1987), employing corrosion resistant alloys, and lowering the operating stresses. In many cases it was found that the oil producers relied on previous experience to combat new and difficult situations, often with less than satisfactory results. The equipment suppliers offer sucker rods for application in sweet or sour service usually with recommended inhibition, which may not be successful. Even when the fluid corrosivity is known, variations in operation conditions can lead to premature failures. Under such conditions oil producers may "switch brands" of sucker rods in the hopes of effecting a solution.

Attempts to improve the corrosion fatigue resistance of sucker rods has been the focus of several research studies. Low alloy steel containing 1.3-1.8% Ni and/or ~0.8% Cr was reported to be inferior to C-Mn steels (Bucaram and others, 1973; Mehdizadeh, 1974). In other studies (Dvoracek, 1973; Snape and Dooyen, 1969) it was found that sucker rods containing Ni and Cr were superior to C-Mn rods. The effect of heat treatment has also received attention where it was shown (Dvoracek, 1973) that for a Grade D sucker rod the heat treatment had no influence on the corrosion-fatigue performance whereas for Grades C and K a normalized and tempered microstructure was better than a quenched and tempered one. And, Mehdizadeh (1974, 1966) reported that corrosion fatigue resistance was unaffected by heat treatment for low alloy steels up to a hardness of 21Rc.

It is evident that a better understanding of the corrosion and corrosive-fatigue behaviour of commercially available sucker-rod alloys is desirable so that oil producers can better match the sucker rods to specific well conditions. This will avoid premature failures and lead to more economical operations. The present study was undertaken to classify the corrosion performance of commercially available sucker rods in selected corrosive environments. This will serve as a basis for future work which will include investigating the corrosion-fatigue behaviour of those alloys which appear to be suitable for corrosive service.

EXPERIMENTAL PROCEDURE

Alloys and Environments

Three different sucker rod types from different manufacturers were selected (see Table I) for evaluation in two corrosive environments; 3.5% NaCl deaerated solution (mild corrosion) and 8% NaCl solution deaerated and saturated with CO₂ (severe corrosion). These rods were selected on the basis that their carbon contents are similar and they were produced by different heat treatment methods. Two of them were alloyed with nickel and chromium and one had an addition of vanadium.

Further testing is planned for aerated solutions in combination with CO₂ and H₂S. The 8% NaCl deaerated with CO₂ was chosen to represent a low pH pitting type environment which was believed to have occurred on many rods that had been examined after failing in service.

Electrochemical Testing

Electrochemical tests were conducted on the sucker rod alloys across the diameter prepared with a 600 grit SiC emery paper and on the "as-is" surface. Cyclic polarization with two scan rates of 0.1 mV/sec (slow scan) on one hour equilibrated specimens and 5 mV/sec (fast scan) on 16 hours equilibrated specimens were conducted.

The rapid sweep of the potential rate had the objective of minimizing film formation so that the current observed related to a film free or at least a thin film condition. The objective of the slow sweep rate was to allow surface films to develop as well as enable local corrosion to occur. The fast scan did not provide a particularly stable metal surface but did maintain a reasonably stable surrounding environment. On the other hand, the slow scan rate provided a reasonably stable metal surface but the pH of the environment was found to increase by two units.

Tafel slopes β_A and β_C were evaluated using cyclic polarization curves. Corrosion rates were calculated for specimens equilibrated for one hour and 16.5 hours. Corrosion rates were also calculated from the polarization resistance R_p which was obtained by determining the specimen polarization at ± 20 mV with respect to E_{corr} at a scanning rate of 0.1 mV/s after one hour and 16 and 17 hours of specimen equilibrium. Data acquisition and calculations were carried out using an IBM PC and "SoftcorrM 342" program (Ref. 9).

All tests were performed in a 1000 ml glass ASTM standard corrosion cell using a 273 EG&G potentiostat/galvanostat with calomel reference electrode and two high density graphite electrodes as auxiliary electrodes.

The rods to be corroded in an "as received" state were carefully prepared first with a glass shot blast, followed by a five minute degreasing in boiling benzene, five minute ultrasonic cleaning in acetone, five minute ultrasonic cleaning in ethanol and rinsed in distilled water immediately prior to testing. The base alloy testing was performed on flat specimens, wet polished with 600 grit SiC paper, followed by rinsing in ethanol, distilled water and dried immediately prior to testing.

EXPERIMENTAL RESULTS

From the electrochemical perspective, a system can be excited by various means including potentiodynamically and galvanodynamically using different scanning rates. It has been recommended by Siebert (1985) that a variety of techniques should be employed to overcome the limitations associated with any one method. For the purpose of this study the corrosion rates were evaluated by five independent electrochemical tests (two cyclic polarization tests and three polarization resistance tests) varied by two scanning rates and different specimen equilibrium times. The general corrosion rates were calculated separately for base alloy and surface in the "as is" condition for two environments. The same technique was used to evaluate crevice corrosion.

It is the authors' experience that the scanning rate in a potentiodynamic experiment can influence the localized corrosion of low carbon steels which, in turn, results in a characteristic cyclic polarization hysteresis loop. However, similar results for the ranking of alloys by general corrosion can be obtained independently of the scanning rate chosen. As the assessment of pitting and crevice corrosion is a major point of interest in this study it is believed that generating cyclic polarization using a slow scan rate (0.1 mV/s) provided sufficient time for pitting and/or crevice corrosion to occur. The slow scan test took 2.5 hours whereas the fast scan test took three minutes. For all investigated cases the resulting current of forward and backward polarization displayed characteristic patterns which were specific to the alloy under investigation, surface preparation, corrosive medium and scan rate. It is suggested that the shape of the hysteresis loop may provide information about the electrolytic formation of the corrosive products on the exposed metal surface which can inhibit the corrosion current and the development of localized corrosion sites such as pitting and crevice. These in turn can be the sources of additional current. By examining the nature of the hysteresis loops and correlating it with the corrosion currents calculated from all electrochemical tests it may be possible to determine, at a particular stage of the applied anodic potential, which corrosion process, general or localized, is prevalent. It was found that the hysteresis loops were reproducible. Two or more tests were repeated for each test condition and the results were almost always identical.

Figure 1 shows six cyclic polarization curves for Test Rods A, B and C in a 3.5% NaCl deaerated solution using a scan rate of 1mV/s and one hour specimen equilibrium. The blocks of curves on the left hand side of Fig. 1 refer to the base alloy with 600 grit SiC emery paper finish whereas on the right hand side the curves are for the "as is" surface of the sucker rods. The arrows indicate the backward polarization. It is seen from Fig. 1 that the polarization curves for the scan rate of 0.1 mV/s are considerably different in shape for each alloy and surface, showing for all rod types and "as is" surfaces, higher currents as a result of backward anodic polarization less than -650 mV/s of applied potential. This may be due to the development of localized corrosion on the "as is" surface as compared with the 600 grit finished surface. The difference in anodic currents between forward and backward polarization was most pronounced for Rod A.

For the 5mV/s polarization curves (not shown) it was observed that all three rod types exhibited positive loops (i.e. the backward branch of the polarization curve was located to the right of the forward branch). It was also observed that the forward and backward polarization currents were higher for the upper part of the loops for the "as is" surfaces than for the base alloys.

If the base alloy curves in Fig. 1 are superimposed upon one another it is evident that Rod A generated higher currents for both forward and backward polarization. Similar results were obtained for the "as is" surface of Rod A. This indicates that Rod A would be expected to be more susceptible to corrosion in the field than either Rods B or C. This is due to the localized corrosion which developed on Rod A and was less evident on Rods B and C.

In Table II the test results obtained from the cyclic polarization experiments for crevice free specimens have been summarized for the three sucker rods evaluated. It is seen that the corrosion current density (Ref. 11) was about the same for a 0.1 mV/s scan rate regardless of whether the surface "as is" or the base alloy was being investigated in a 3.5% NaCl deaerated solution. However, there were more pronounced differences in corrosion rates between the alloy and surface in an 8% NaCl deaerated solution saturated with CO₂. On the basis of the 5 mV/s scan rate and 16h equilibrium time, the corrosion current was lowest for Test Rod C followed by Rod B and A when polarized in an 8% NaCl deaerated solution saturated with CO₂. This might be explained by referring to Table I which shows Test Rod C to contain chromium and nickel which is absent in Test Rod A. The same ranking was obtained from a statistical assessment of the corrosion rates of all five electrochemical experiments (Table IV). The reason Test Rod C appears to have a better corrosion resistance than Test Rod B, which has similar chromium and nickel content, may be due to the heat treatment used in the manufacture of the rod. Test Rod C was case hardened and Test Rod B was normalized and tempered. It is also of interest to note that Test Rod A had about the same I in a 3.5% NaCl deaerated solution as Test Rods B and C, although there was neither nickel nor chromium in Test Rod A.

Test Rod A displayed the highest negative values of corrosion potential for all environments and surface finishes.

From the photomicrographs shown in Fig. 2 it is seen that for Test Rod C the formation of pits were primarily associated with the presence of inclusions when subjected to 0.1 mV/s scan rate polarization in a 3.5% NaCl deaerated solution. A similar result was observed for Test Rods A and B. However, for the same rods tested in an 8% NaCl deaerated solution saturated with CO₂, pitting did not appear to be associated with inclusions as can be seen in Fig. 3.

Figure 4 shows a clear difference in corrosive attack in an 8% NaCl, CO₂ saturated solution between the hardened surface of Rod C and its softer inner core. The hardened part shown in the upper part of Fig. 4 retained the scratches caused in polishing whereas the scratches were corroded away on the lower half which was the inner core.

Crevice corrosion resistance was evaluated by running cyclic polarization and polarization resistance tests on specimens equipped with crevice making devices which consisted of elastic rubber bands wrapped around the circular specimens and, for flat specimens, pieces of teflon mounted to the surface. All physical and electrochemical parameters were the same as for the general corrosion rate experiments. The values of corrosion current densities obtained in the cyclic polarization experiments as well as the percentage of current changes, relative to crevice free specimens, are shown in Table III.

An overall ranking of the test rods was based on a statistical assessment of five electrochemical experiments and is shown in Table IV. In the majority of cases, crevice specimens produced lower corrosion current densities than the crevice-free specimens. This was due to the restricted corrosion fluid flow to the corroded surfaces by the crevice generating attachments. The greater the difference in corrosion rates between the non-crevice and crevice specimen, the lesser susceptibility to crevice corrosion may be expected. The highest crevice corrosion activity was found on the base alloy (600 grit finish) for Rod A in a 3.5% NaCl deaerated environment. Here, crevice corrosion generated a 22% higher current than for the non-crevice specimen. This was also confirmed by the polarization graph obtained after 16h free corrosion of crevice specimen compared with non-crevice graph (Fig. 5).

The polarization currents shown in Fig. 5 are equal or higher along the whole polarization range for crevice corrosion of the base alloy - 600 grit (solid line) than for non-crevice (dotted line) specimen. This behaviour was not so evident for the cyclic polarization curves obtained after 1 hour equilibration, probably due to an insufficient time for the crevice corrosion to develop. The "as is" surface crevice investigation showed that Rod A had the least crevice corrosion susceptibility, followed by rod C and B for both environments.

The pitting depth was assessed on flat specimens which were previously exposed to a six day free

corrosion in a deaerated 8% NaCl/CO₂ environment, and further anodically activated by a potentiodynamic scan rate of 1mv/sec to the 5000 $\mu\text{A}/\text{cm}^2$ current and returned to E_{corr} . The pitting depths were measured using an optical microscope and a Micro Validator Coordinate measuring machine with a measurement accuracy of $\pm 0.001\text{mm}$. The results presented in Table IV show that Test rod C had the lowest pit depth, followed by the other two rods which had similar depths of pitting.

SUMMARY

A testing procedure for evaluating steel alloys for corrosive service has been described. It has been shown that the use of polarization curves obtained from potentiodynamic studies can yield important information about the corrosion behaviour of steel alloys. It is suggested that the shape of the hysteresis loops of polarization curves may be used to detect and/or rank alloys on the effects of localized pitting and crevice corrosion. Optical micrographs of pitted surfaces and base material confirmed the observations made from the potentiodynamic studies.

Five independent electrochemical tests were conducted on three sucker rod alloys and "as is" surfaces. It was found that in a 3.5% deaerated solution there was little difference in corrosion currents for Test Rods A and B but that Test Rod C exhibited better corrosion resistance. An analysis of the cyclic polarization curves for the same environment indicated that Test Rod A had a higher current activity for forward and backward anodic polarization, thus suggesting a more pronounced development of localized corrosion.

Of the three test rods investigated, it was found the one with a hardened surface was the most resistant to corrosion as measured in an 8% NaCl deaerated solution saturated with CO₂. The ranking of alloys on the basis of general corrosion is insufficient if pitting corrosion and/or crevice corrosion in 8% NaCl/CO₂ solution is associated with the failure modes observed in the field. From the crevice corrosion experiments it was found that for the "as is" surface of Rod A there was less tendency for crevice corrosion to occur and yet this alloy had the poorest resistance to general corrosion. By evaluating fast and slow scan rates, additional information may indicate whether or not localized corrosion effects are present. This should lead to a more informed ranking of alloys for oil field service.

ACKNOWLEDGEMENT

The authors express their appreciation to the Natural Sciences and Engineering Research Council (Ottawa) for their support in obtaining the equipment used in this study (Grant E-5259).

REFERENCES

1. Bellow, D.G. and Smuga-Otto, I., 1986, "Survey of Oil Field Sucker Rod Conditions and Practices", Confidential report.
2. S.M. Bucaram, H.G. Byars, H. Kaplan, 1973, "Selection, Handling and Protection and Downhole Materials": A Practical Approach; Materials Protection and Performance, Vol. 12, p.20.
3. J.F. Chitton, 1968, "Corrosion Fatigue Cracking of Oil Well Sucker Rods", Materials Protection, Vol.7, No. 4, pp. 30-33.
4. Bellow, D.G., Hood, J.E. and Robert, K.S., 1987, "Fatigue Life of Sucker Rods with Epoxy Coatings", 1st Int. Conf. on Fatigue and Stress, Paris, Pergamon Press.
5. P. Mehdizadeh, 1974, "Effect of Metallurgical Variables on Corrosion of Sucker Rods in Salt Water Containing CO₂ and H₂S", Materials Performance, Vol. 13, No. 6, p.13-16.
6. L.M. Dvoracek, 1973, "Corrosion Fatigue Testing of Oil Well Sucker Rods", Material Protection and Performance, Vol. 12, No. 9, 1973, pp.16-19.
7. E. Snape, Van D. Dooyen, 1969, "Sucker Rod Corrosion in Sweet Oil", Canadian Petroleum, p.40.
8. P. Mehdizadeh, R.L. McGasson, J.E. Landers, 1966, "Corrosion Fatigue Performance of Carbon Steel in Brine Containing Air, H₂S and CO₂", Corrosion, p. 325.
9. "Softcorr Corrosion Measurement Software", 1986, EG & G Princeton Applied Research.
10. O.W. Siebert, 1985, "Laboratory Electrochemical Test Methods, ASTM STP 866", American Society for Testing and Materials, Philadelphia, pp. 65-90.
11. Walter, G.W., 1977, "Problems Arising in the Determination of Accurate Corrosion Rates from Polarization Resistance Measurements", Corrosion Science, 17, Pergamon Press.

TABLE I SUCKER ROD ALLOYS INVESTIGATED

Alloy	C	Mn	Ni	Cr	Mo	V	σ yield ksi	σ ult. ksi	Hardness Brinell	Heat Treat.
A	.38-.44	1.3-1.5	-	-	-	.05-.07	110	115-140	241	Q&T
B	.38-.43	.60-.80	1.65-2.00	.79-.90	.20-.30	-	110-115	120	210-265	N&T
C	.31-.38	.61-.90	1.25-1.75	.60-.80	-	-	110	140	280,600*	case hardened

*exterior surface

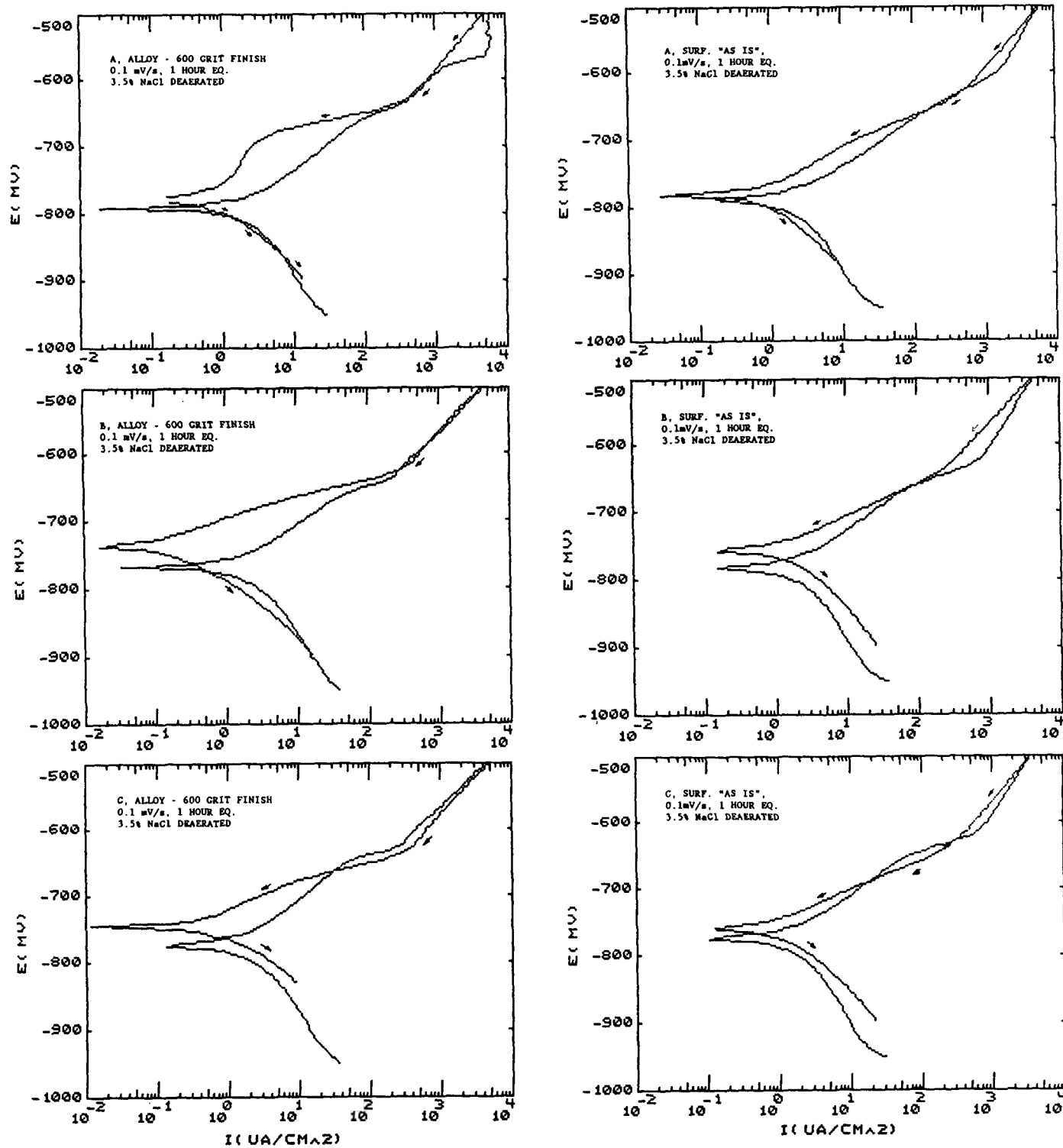


Fig. 1 Cyclic polarization curves for Rod Type A, B & C in 3.5% NaCl deaerated solution, 0.1 mV/s scan rate, 1h equilibrium

TABLE II SUMMARY OF CYCLIC POLARIZATION TESTS

Test Rod	Environment	Surface Condition	E _{corr} mV		I μ A/cm ²		Anodic Tafel mV/dec.		Cathodic Tafel mV/dec.	
			0.1 mV/s	5 mV/s	0.1 mV/s	5 mV/s	0.1 mV/s	5 mV/s	0.1 mV/s	5 mV/s
A	3.5% NaCl deaerated	Alloy 600gr. Surf. "as is"	-790 -775	-791 -770	2.4 2.0	1.6 3.3	74 68	87 149	-145 -157	-97 -93
	8% NaCl deaerated + CO ₂	Alloy 600gr. Surf. "as is"	-712 -711	-707 -699	114 131	96 62	87 73	67 60	+ - ∞ + - ∞	-1017 -1356
B	3.5% NaCl deaerated	Alloy 600gr. Surf. "as is"	-766 -761	-775 -758	2.2 2.1	1.3 2.5	80 75	119 135	-145 -165	-102 -88
	8% NaCl deaerated + CO ₂	Alloy 600gr. Surf. "as is"	-671 -682	-671 -671	155 135	39 32	95 72	64 59	+ - ∞ + - ∞	-196 -169
C	3.5% NaCl deaerated + CO ₂	Alloy 600gr. Surf. "as is"	-769 -759	-771 -755	2.0 1.8	1.9 2.5	89 83	122 138	-149 -169	-118 -103
	8% NaCl deaerated + CO ₂	Alloy 600gr. Surf. "as is"	-676 -678	-680 -673	143 135	28 27	88 86	63 66	+ - ∞ + - ∞	-147 -140

TABLE III CREVICE CORROSION TEST RESULTS

Test Rod	Environment	Surface Condition	I _{cr} [μ A/cm ²]		I-I _{cr} [%]	
			Scan rate 0.1 mV/s 1h eq.	Scan rate 5mV/s 16h eq.	0.1mV/s 1h eq.	5mV/s 16h eq.
A	3.5% NaCl deaerated	alloy, 600grit surface "as is"	1.9 1.3	2.06 2.4	21 40	-22 28
	8% NaCl deaerated + CO ₂	alloy, 600grit surface "as is"	88 74.5	84 28	23 44	15 55
E	3.5% NaCl deaerated	alloy, 600grit surface "as is"	1.6 0.75	1.3 2.4	28 53	15 0
	8% NaCl deaerated + CO ₂	alloy, 600grit surface "as is"	116 74	30 27	26 46	23 16
C	3.5% NaCl deaerated	alloy, 600grit surface "as is"	1.8 0.75	1.5 1.8	8 58	25 28
	8% NaCl deaerated + CO ₂	alloy, 600grit surface "as is"	85 77	21 19	8 39	21 30

TABLE IV RANKING OF TEST RODS ACCORDING TO GENERAL CORROSION RATE,¹⁾ CREVICE CORROSION SUSCEPTIBILITY²⁾ AND PITTING DEPTH.³⁾

Environment	General corrosion rate ranking		Crevice corrosion susceptibility ranking		Pitting depth ranking
	Alloy, 600 grit	Surface "as is"	Alloy 600 grit	Surface "as is"	Alloy 600 grit
3.5% NaCl/N ₂	1 ND	C	ND	A	-
	2 ND	ND	ND	C	-
	3 ND	ND	ND	B	-
8% NaCl/N ₂ /CO ₂	1 C	C	C	A	C
	2 B	B	B	C	ND
	3 A	A	A	B	ND

1) Ranking based on five different electrochemical tests

2) Ranking based on five different electrochemical tests

3) Ranking based on pitting depth statistical assessment measured with 0.001 mm accuracy.

ND - No statistically significant difference found

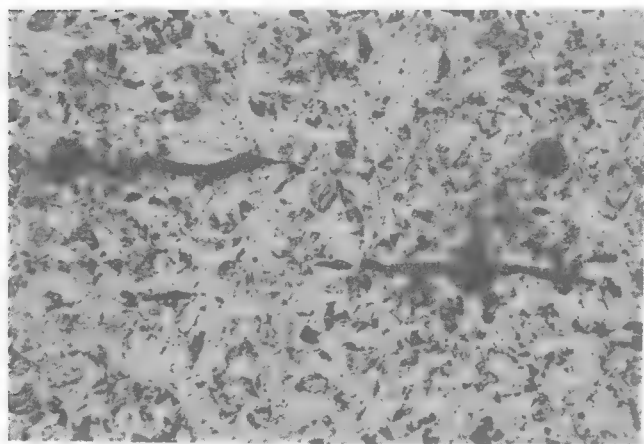


Fig. 2 The presence of corrosion pits in association with inclusions, 0.1 mV/s cyclic polarization, 3.5% NaCl deaerated solution (X800).

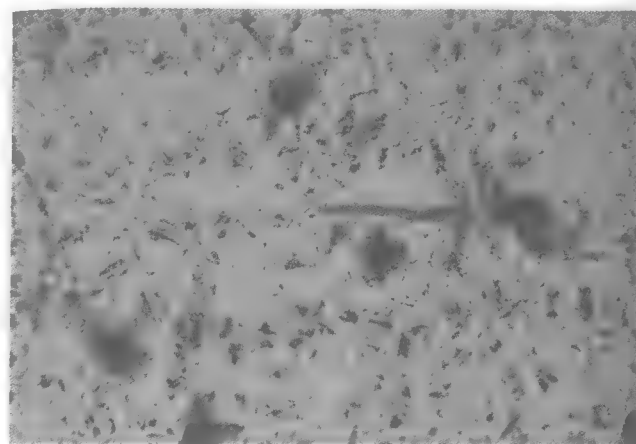
Fig. 3 Absence of pitting along inclusions, 0.1 mV/s cyclic polarization, 8% NaCl. deaerated, solution saturated with CO₂. x 800



Fig. 4 Test Rod C showing boundary between hardening surface (upper) and softer inner core (lower), 8% NaCl, deaerated, saturated with CO_2 (x 80).

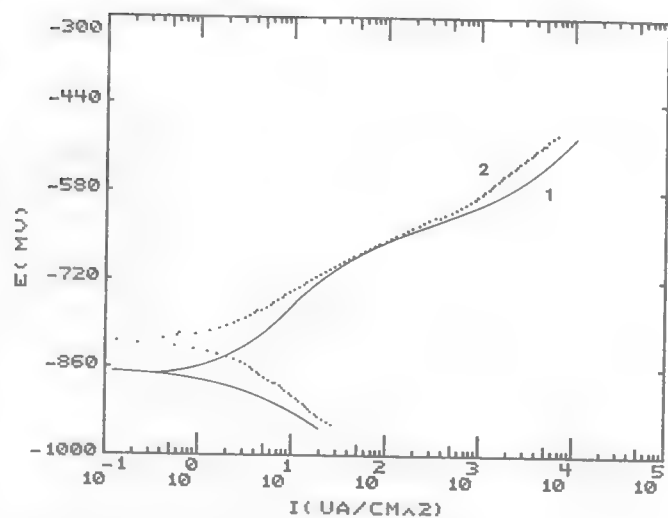


Fig. 5 Forward polarization curves for Rod Type A; 1-crevice, 2-non-crevice specimens tested in 3.5% NaCl deaerated solution with the scan rate 5mv/s.

WEAR OF STANDARD AND HARD-METAL-COATED COUPLINGS WITH OILFIELD TUBING*

DONALD G. BELLOW, D. CRAIG OWENS and I. SMUGA-OTTO

*Department of Mechanical Engineering, University of Alberta, Edmonton, Alberta
T6G 2G8 (Canada)*

Summary

An experimental program was established to determine the wear of down-hole oil field sucker rod couplings and tubing. A special component testing apparatus was designed which enabled a close control of side loads, wear track and frictional forces. It was found that a standard coupling wore more than a hard-metal-coated coupling and that the tubing wore less with the hard-metal-coated coupling. This was explained on the basis that there was a transfer of metal particles from the hard-metal-coated coupling to the softer tubing thus enhancing the wear resistance of the tubing. The way in which the metal surfaces work hardened as the wear process progressed is also explained.

1. Introduction

In a conventional oil well sucker rod string the couplings joining the rods together, being of a larger diameter than the rods, will make contact with the tubing wall causing wear of both the couplings and the tubing as the sucker rod string moves up and down in the tubing. Generally, this causes only mild wear but if the wells are offset, deviated or slanted, then wear of down-hole components can become a significant problem. Even in straight, vertical wells, if the rods go into compression and buckle on the down stroke, side wear of the tubing, rods and couplings can occur. This wear can become excessive in very sandy areas. In particularly bad situations oil field components can wear out in a matter of a few weeks, necessitating replacement of components and a general "workover" for the well.

To lengthen the time between "workovers" and reduce the downtime, oil companies employ a number of devices to reduce down-hole wear problems. Some of these include the use of continuous sucker rods (without couplings), particularly useful in slant wells or deviated wells, injected

*Paper presented at the International Conference on Wear of Materials, Denver, CO, U.S.A., April 8 - 14, 1989.

moulded plastic centralizers placed along the rod to separate the rod from the tubing, plastic-coated couplings, hard-metal-coated couplings and roller couplings. Each of these devices works to a degree but none has so far been able to eliminate wear completely.

When the environmental conditions in an oil well, containing CO_2 , H_2S , chlorides, water and other contaminants, are considered, coupled with indeterminate loading conditions, it is not surprising that there is some confusion as to which methods should be employed in reducing down-hole wear problems.

The work described in this paper was designed to evaluate the basic mechanisms of metal-to-metal wear of oil field components to provide a better understanding of the parameters which influence wear. All wear testing was performed on actual oil field components with the testing variables closely controlled.

2. Experimental procedure

A special wear apparatus was developed to evaluate coupling and tubing wear. Although the velocity-time relationship in a well is sinusoidal the apparatus was designed to provide a square wave form which was essentially constant velocity.

It is very likely that the wear down-hole is accelerated by corrosion so the test apparatus was designed to incorporate a fluid stream to wet the wear contact surfaces continuously. The side load was varied from zero to 2200 N (500 lbf) and the axial force was measured throughout the wear test to evaluate the frictional forces.

The experiments used new J55 with an outer diameter of $2\frac{7}{8}$ in (73 mm) ERW (electrical resistance welded) tubing upon which metal couplings were evaluated for wear. The J55 tubing had a hardness of 225 HV (Vickers' hardness number) and is a low (0.06 - 0.10 wt.%) carbon steel. It is alloyed with manganese (1.1 - 1.3 wt.%) along with columbium (0.033 - 0.047 wt.%) and titanium (0.015 - 0.125 wt.%).

This paper will describe the results obtained from evaluating two different coupling types, a standard coupling and a hardened spray metal coated coupling. The couplings had an outer diameter of $1\frac{3}{4}$ in (44 mm) and 4 in (100 mm) long according to API (American Petroleum Institute) dimensions. The standard coupling was made from a cold extruded tube out of AISI 8630. The surface hardness was measured at 240 HV. The hard metal coupling was a standard coupling to which a hardened layer of metal powder was fused. The nominal composition of the powder before spraying was 12 - 16 wt.% Cr, 4 wt.% Si, 4 wt.% Fe, 2.75 - 3.5 wt.% B and 1 wt.% C or less. The remainder consisted of nickel. After spraying, the surface was ground smooth and the initial surface hardness was measured at 550 HV.

The stroke rate of the test apparatus was set at 25 cycles min^{-1} and the stroke length was 380 mm (15 in). This combination of stroke length and

rate produced 300 000 m of wear path in a period of 11 days. Water was used to represent the “worst case” environment although some oil is present in an oil well. The water flow rate was set at 0.5 l min^{-1} and used fresh non-recirculated tap water at 18°C , pH 7.9.

Wear rates were measured at 10 000 m, and thereafter at longer intervals, depending on the test, up to a total wear path of 300 000 m. Coupling wear was measured by weight loss ($\pm 0.1 \text{ g}$). Tubing wear was determined by measuring the wall thickness at nine equally spaced locations along the center line of the wear path. Wear debris was collected, dried and weighed and inspected using an optical microscope. Tubing wear paths and coupling wear surfaces were inspected using a scanning electron microscope and an optical microscope. The hardness of the surface wear paths was measured with an ultrasonic hardness tester, which used a 7.7 N load on a 136° angle diamond indenter.

On examination after testing the wear surfaces were found to be very similar to wear surfaces of couplings and tubing taken from the field. Thus the testing apparatus appeared to have duplicated accurately the type of wear process experienced in an oil well.

3. Experimental results

3.1. Wear rates

The wear of the standard coupling (240 HV) and the hard-metal-coated coupling (550 HV), as a function of distance travelled in metres, is represented in Fig. 1. Clearly these results show that the hard-metal-coated coupling had greater resistance to wear than the standard coupling.

Figure 2 shows the wear of the J55 tubing which occurred with the standard coupling and the hard-metal-coated coupling. The wear of the tubing was less with the hard-metal-coated coupling, especially at side loads of 890 N (200 lbf) and higher.

The results from a 1335 N (300 lbf) side load are not shown. When the 1335 N (300 lbf) load was applied, the standard coupling wore through the

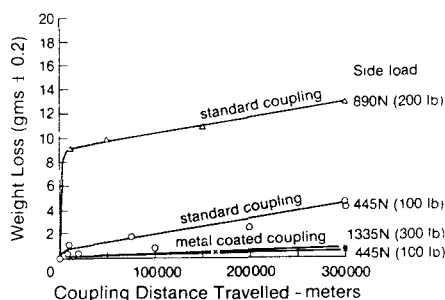


Fig. 1. Coupling weight loss vs. distance travelled, water lubricated.

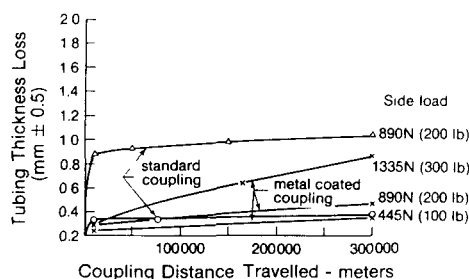


Fig. 2. Tubing thickness loss vs. distance travelled, water lubricated.

tubing after 10 000 m whereas for the hard-metal-coated coupling the wear of the tubing was only 0.66 mm after 300 000 m of travel.

Perhaps an easier way to illustrate the relative wear resistances of the standard coupling and a hard-metal-coated coupling is to compare the wear rates in g per 100 000 m travelled. In Fig. 3 it is seen that the wear rate of the standard coupling increased in a non-linear fashion with side load whereas the wear rate for the hard-metal-coated coupling remained considerably lower and was almost independent of the side load in the range 445 - 890 N (100 - 200 lbf).

Throughout the experiments with both the standard coupling and the hard-metal-coated coupling, it was observed that the wear modes changed from mild to severe with both load and distance travelled. These modes were easily identified by the sound emitted and the type of wear debris collected. The photographs in Fig. 4 illustrate the differences in wear debris produced [1]. For the mild wear mode the debris consisted mainly of small particles,

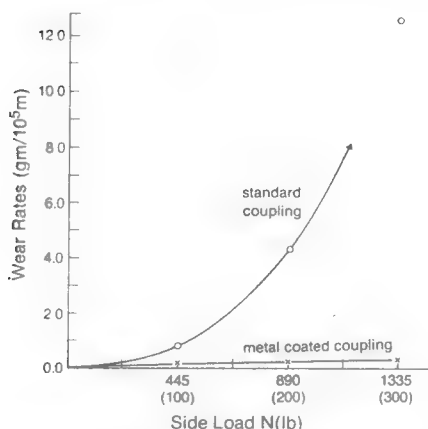
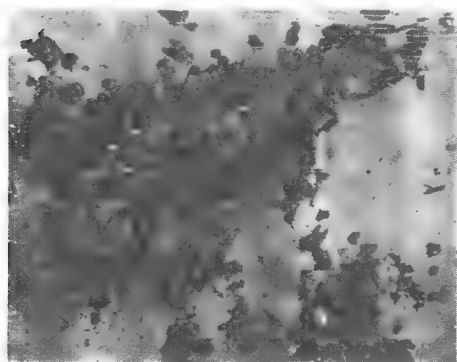
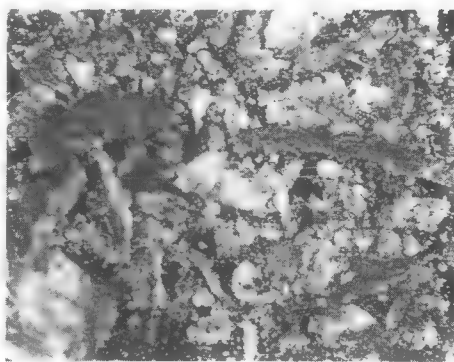


Fig. 3. Coupling wear rates as a function of side load, water lubricated.



(a)



(b)

Fig. 4. Wear debris for the two wear modes observed. (a) Mild wear debris (magnification, 8.75 \times). (b) Severe wear debris (magnification, 8.75 \times).

the majority of which were considerably oxidized. Also, little sound was emitted and the measured frictional force was low. For the severe wear mode the debris consisted of large metal fragments, indicating that a galling action was occurring. These particles were only slightly oxidized. For the severe wear mode the sliding action was noticeably louder and the measured frictional forces were higher than for the mild wear mode.

3.2. Changes in surface hardness

One objective of this study was to determine whether there was any correlation between the two observed wear modes and changes in hardness of the contact surfaces. It was postulated that if hardness variations could be detected this would confirm the hypothesis that work hardening of the surface was occurring.

As the wear was occurring in a water stream it was possible to distinguish the tops of wear tracks from the corroded "valleys". For these measurements, only the tops of the wear paths were measured. Even so, there was considerable scatter of the data so that an average value was computed. A typical hardness analysis is shown in Fig. 5 where the data were reasonably precise; they were less so in Fig. 6. Nevertheless, in comparing Figs. 5 and 6 it is seen that the microhardness of the tubing surface for the mild wear mode, at 445 N (100 lbf) side load, was 244 HV whereas under the severe wear mode, at 1335 N (300 lbf) side load, the tubing surface hardness increased to 433 HV. In each case about 50 readings were taken, and Figs. 5 and 6 show the scatter distribution in these results.

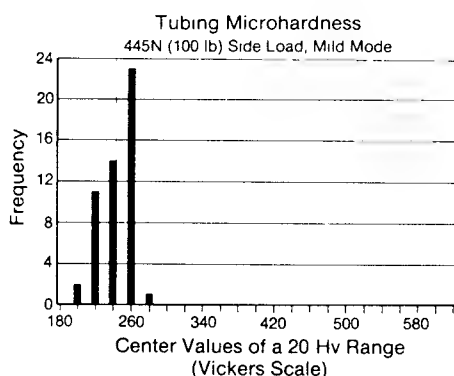


Fig. 5. Tubing microhardness: 445 N (100 lbf) side load.

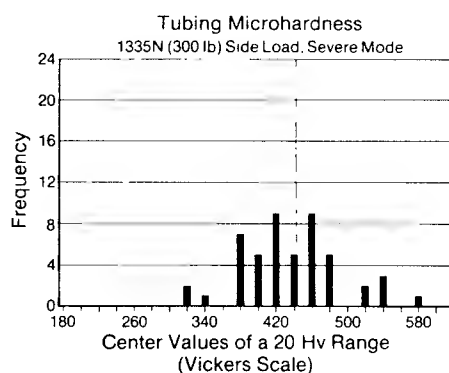


Fig. 6. Tubing microhardness: 1335 N (300 lbf) side load.

The bar chart in Fig. 7 shows the increase in surface hardness of the standard coupling, hard-metal-coated coupling and the J55 tubing as a function of side load. In each case the surface hardness increased with load. Additionally, it was found that during the severe wear mode the work hardening of the surface was much greater than that which occurred during

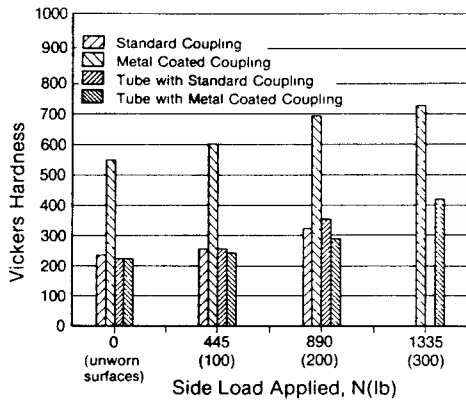


Fig. 7. Vickers' hardness *vs.* side load for mild wear.

the mild wear mode. For example, at an 890 N (200 lbf) side load, the mild wear mode caused the standard coupling surface hardness to increase from 234 to 323 HV whereas under the severe wear mode this increased to 486 HV.

Similar changes in surface hardness were observed with the J55 tubing. Under mild mode conditions the surface hardness of the tubing increased from 222 to 356 HV whereas under severe mode conditions the hardness further increased to 443 HV.

3.3. Wear modes

The mild and severe wear modes were dependent on the nature of the rubbing surfaces and the amount of side load present. This is illustrated in Table 1 where it is seen that at a side load of 445 N (100 lbf) the wear was observed to be both mild and severe. This condition would be observed where normally mild wear was occurring, transferring to severe wear for a short duration, and then returning to mild wear once again. For a side load of (1335 N) the wear was continuously severe.

TABLE 1

Wear modes for side loads

Side load N (lbf)	Standard couplings	Spray metal couplings
445 (100)	0 - 5000 m (Severe) 5000 - 300 000 m (Mild)	0 - 1000 m (Severe/mild) 10 000 - 300 000 m (Mild)
890 (200)	0 - 10 000 m (Severe) 1000 - 615 000 m (Severe/mild)	0 - 20 000 m (Severe/mild) 20 000 - 300 000 m (Mild)
1335 (300)	0 - 10 000 m (Severe) Tubing perforated at 10 000 m	0 - 20 000 m (Severe/mild) 20 000 - 300 000 m (Severe/mild)

Table 1 shows that under a 1335 N (300 lbf) side load the standard coupling experienced severe wear and that only 10 000 m of travel occurred before the tubing wore through. In contrast, the hard-metal-coated coupling, while experiencing both mild and severe wear, did not wear through to the threads of the coupling nor did it wear through the tubing at 300 000 m of travel.

The results in Table 1 also show that at a side load of 890 N (200 lbf) the standard coupling experienced both mild and severe wear in the interval 10 000 - 615 000 m whereas the metal-coated coupling experienced only mild wear in the 20 000 - 300 000 m interval. In the initial 0 - 5000 m interval both standard and spray metal couplings experienced severe wear. This occurred as the wear tracks were being developed and when the contact stresses were the highest for a given coupling side load.

3.4. Coefficients of friction

Electrical resistance strain gauges were mounted to the push rods connecting the couplings to the hydraulic actuator. In this way the force required to slide the coupling along the tubing, as a function of side load and wear mode, could be measured. The coefficient of friction was calculated as the ratio of the push rod force divided by the side load. The results in Fig. 8 were obtained for mild wear conditions. Although the results for the standard coupling are somewhat scattered, it is apparent that the standard coupling had a higher coefficient of friction than did the spray metal coupling. This may be due to the fact, as the next section will show, that the spray metal coupling contained a high percentage of nickel.

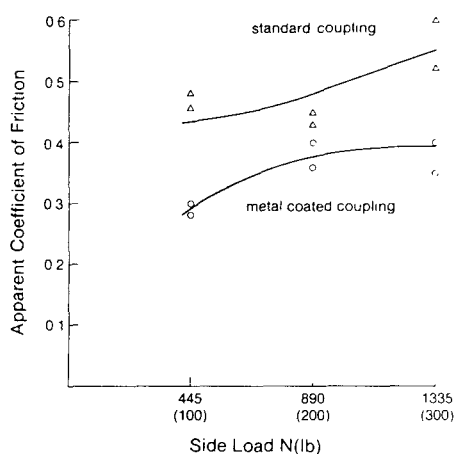


Fig. 8. Friction vs. side load, water lubricated.

3.5. Examination of wear paths

The wear paths of the couplings and tubing were examined by optical and electron microscopy. Figure 9 shows the rapid wear that occurred under



Fig. 9. Coupling-tubing relative wear rates: left-hand side, 445 N (100 lbf) side load, 300 000 m travelled; right-hand side, 1335 N (300 lbf) side load, 10 000 m travelled.

a 1335 N (300 lbf) side load after 10 000 m of travel compared with a 445 N (100 lbf) side load after 300 000 m of travel for a standard coupling and J55 tubing. Viewing a transverse section of the tubing wear path as seen in Fig. 10 the depth of microstructure deformation was measured to be 0.006 mm whereas the average groove depth was measured to be 0.04 mm. This was under a 445 N (100 lbf) load after 300 000 m of travel. Under a 1335 N (300 lbf) load the deformation was more severe as shown in Fig. 11. Here the depth of microstructure deformation was 0.06 mm with the average groove depth measured at 0.08 mm.

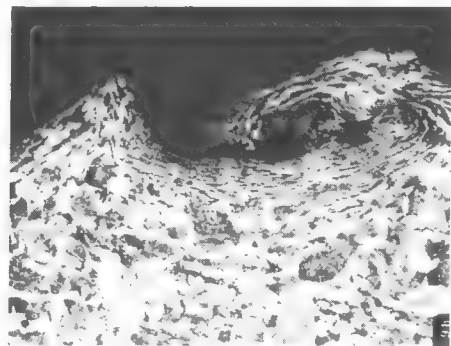
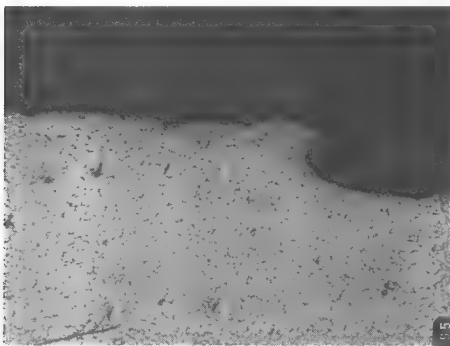


Fig. 10. Transverse surface of tubing under 445 N (100 lbf) side load after 300 000 m of travel (magnification, 170 \times) (2% Nital etchant).

Fig. 11. Transverse surface of tubing under 1335 N (300 lbf) side load after 10 000 m of travel (magnification, 170 \times) (2% Nital etchant).

The wear of the hard-metal-coated coupling was not only less than the standard coupling but it also caused less wear in the J55 tubing. Figure 12 is a micrograph of a cross-section of the hardened surface of the spray metal coupling. This shows the junction between the hard coating and the base material of the coupling. The black spots are voids in the coating. In

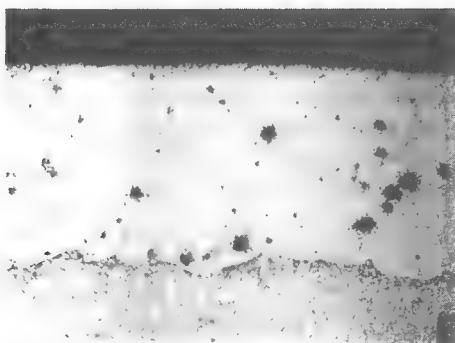


Fig. 12. Micrograph of metal-coated coating (magnification 96 \times).

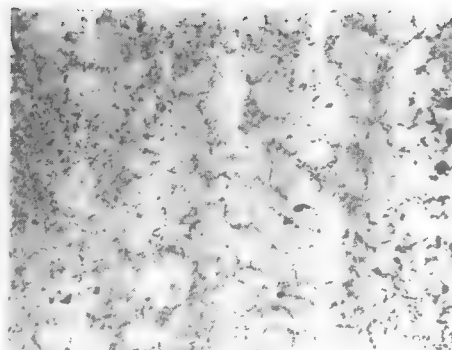


Fig. 13. Scanning electron micrograph of hard spray metal coating (magnification 1500 \times).

Fig. 13 a scanning electron micrograph of the coating indicates a light phase (84 wt.% Ni) and a dark phase (51 wt.% Cr and 45 wt.% Ni). A scanning electron microscopy (SEM) energy-dispersive X-ray analysis (EDXA) spot analysis indicated the constituents listed in Table 2. It should be noted that the constituents in Table 2 are different from those listed for the spray metal powder before application to the coupling. The EDXA spot analysis indicated that the metal powder did not fuse on in a uniform manner but rather the nickel and chromium tended to accumulate preferentially in "light and dark" phases as shown in Fig. 13 [2].

TABLE 2

EDXA spot analysis of spray coating

Phase	Cr (wt.%)	Fe (wt.%)	Ni (wt.%)
Light	9.14	6.30	84.55
Dark	51.50	2.57	45.85

A further examination of the tubing wear path showed a significant transfer of nickel from the hard spray metal coupling to the softer J55 tubing. Figure 14 shows a scanning electron micrograph of a nickel platelet which had been embedded in the tubing surface. This was recorded at a 445 N (100 lbf) side load after 300 000 m of travel. Further evidence of the nickel transfer is shown in the SEM X-ray image shown in Fig. 15. A similar X-ray image failed to detect any chromium transfer.

The SEM analysis was conducted for the side loadings 445, 890 and 1335 N (100, 200, 300 lbf) and each showed a transfer of nickel from the metal-coated coupling to the J55 tubing. A 445 N (100 lbf) side load on the metal-coated coupling did not create the grooved wear path typical of the

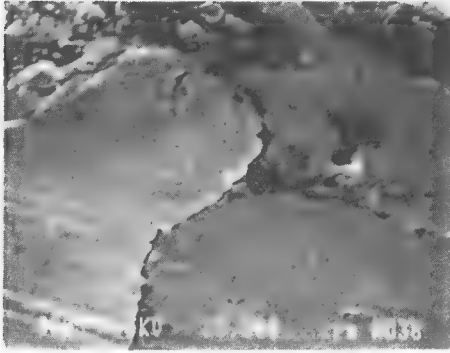
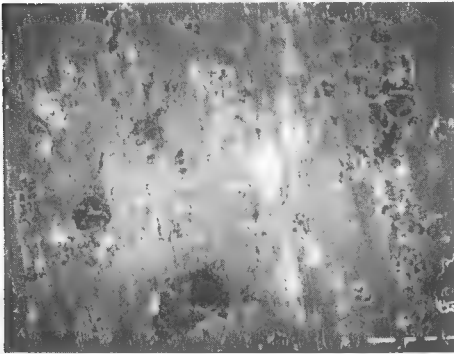
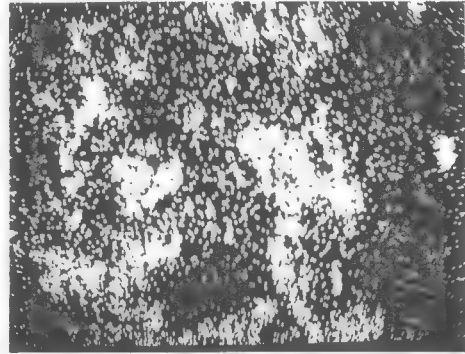


Fig. 14. Scanning electron micrograph of nickel platelet deposited on softer tubing (magnification 2500 \times).



(a)



(b)

Fig. 15. (a) Tubing wear path (magnification 57 \times). (b) X-ray image of nickel distribution.

standard coupling but rather developed a large curved contact area with nickel distributed over the wear path. At higher loads, grooves in the wear path appeared and only on the contact areas was any nickel found. In the grooves, where nickel was not present, oxidation occurred.

4. Discussion

The wear of standard couplings and J55 tubing appears to follow the process of work hardening the surface under load until such time as the surface asperities fracture causing a new and softer surface to be revealed. This process was observed by monitoring the changes in surface hardness and the frictional forces. It was also noted that the process consisted of mild and severe wear and that these modes alternated as the wear continued.

The wear of the hard metal coupling on the J55 tubing was considerably lower than that of the standard coupling and the tubing itself wore less.

Why the hard metal coupling wore less is not clear. SEM analysis of the tubing wear track showed a transfer of nickel platelets but an absence of chromium. Along with the nickel, minute but undetected particles of boron and silicon may also have been transferred to the softer tubing thus increasing its resistance to wear. On the basis of the relative hardnesses of the tubing at a coupling side load of 890 N (200 lbf) the work hardening of the tubing was lower with the hard-metal-coated coupling than with the standard coupling. This suggests that the wear resistance of the tubing was not solely a result of hardness but was also influenced by the metal transfer that occurred.

In a recent paper [3] a series of field measurements on oil field sucker rods and couplings concluded that the tubing wore as much with hard-metal-coated couplings as with standard couplings. However, there is also other evidence from the field which supports the findings in this paper that hard-metal-coated couplings wear the tubing less than do standard couplings. The determining factor behind opposing observations may be whether or not sand is present in an oil well. Although not evaluated as part of this study, it may be that if sand is present between the wear surfaces this may prevent the effective transfer of metal particles and thus diminish the beneficial effects of a hardened metal-coated coupling.

Acknowledgments

The authors express their appreciation to the Natural Sciences and Engineering Research Council (Grant A-2705) and an Imperial Oil Limited University Research Grant for the financial support in aid of this project.

References

- 1 B. J. Nield and O. G. Griffin, Relation between wear rate and debris composition in wear of wrought iron and mild steel, *Wear*, 4 (1961) 111.
- 2 O. Knotek, E. Lugscheider and W. Wichert, On the structure and properties of wear and corrosion resistant nickel-chromium-tungsten carbon (silicon) alloys, *Thin Solid Films*, 53 (1978) 303.
- 3 K. P. McCaslin, A study of the methods of preventing rodwear tubing leaks in sucker rod pumping wells, *Rep. SPE 16198*, 1987 (Society of Petroleum Engineers).

WEAR OF PLASTIC COMPONENTS
USED IN OIL WELLS

Donald G. Bellow*

Allen Chiu**

D. Craig Owens*

An experimental apparatus was used to evaluate the wear of plastic centralizers, and plastic wheels of wheeled couplings used in downhole oil field pumping conditions. It was shown that polyphenylene sulfide (PPS) gave superior wear resistance compared with polyamide (Ny) when used as a centralizer and that the surface roughness of the metal tubing influenced the wear behaviour of these materials in different ways. Two types of plastic wheels, polyamide (Ny) and polyacetal (PA) were evaluated with the polyamide (Ny) showing the most resistance to wear on the inner diameter with the polyacetal (PA) showing better resistance to wear on the outer hole surface.

Introduction

In oil wells, which use a conventional sucker rod and coupling string to operate a reciprocating pump at the bottom of the well, wear of the sucker rods and couplings against the stationary tubing can lead to premature failure of the coupling-rod string and/or the production tubing. These problems can become acute when the wells contain corrosive fluids, sand particles, or are offset, slanted or deviated. Figure 1 shows a typical artificial lift system where the rod string is vertical and where it is slanted and deviated.

In order to minimize wear, oil field operators employ a number of devices to separate the reciprocating (or rotating if a rotary downhole pump is employed) rod string from the tubing. It is common for plastic centralizers or rod guides to be employed of the type shown in Fig. 2.

Some operators are using roller couplings, also shown in Fig. 2, while others believe tubing wear can be minimized with the use of continuous sucker rods (i.e. rods without couplings). In all cases it is more costly to replace the tubing than it is to replace the sucker rod string. As a result, plastic components in different forms have

been used as the wearable material in contact with the metal tubing.

Despite the promise that plastic centralizers and rod guides, roller couplings and plastic coated couplings appear to have, excessive tubing wear is still being encountered. And in some cases, plastic components have accelerated the corrosion-wear of the tubing. In addition, not all plastics stand up to the pressure, temperature, and environmental conditions present in oil wells. Despite the set backs being encountered, in some cases the application of plastics to reduce downhole tubing and rod wear has merit but requires further development.

This paper focuses on the wear of plastic centralizers and plastic wheels used in roller couplings. The wear of these components is discussed in the light of experiments designed to evaluate these under simulated oil field conditions so that judicious choices can be made in selecting plastics for known wear conditions.

Experimental Apparatus

Prior to conducting the relatively expensive wear tests, the injection molded centralizers and rod guides were subjected to shear tests before and after exposure to elevated temperature and pressure conditions. This was done to evaluate their suitability for service environments. Typically, the molded plastic centralizers and rod guides were placed in autoclaves with 1/3 of the plastic

* University of Alberta, Edmonton, Alberta, Canada

** Esso Resources Canada Limited, Calgary, Alberta, Canada

in the aqueous phase, 1/3 in an oil phase and 1/3 in a gaseous phase. The autoclave was pressurized using methane or a gaseous mixture representative of a production well. The test temperature and pressure was typically 93°C and 21 MPa (3000 psi) for 48 hours and then rapidly depressurized within 60s. Upon inspection, if there was evidence of blistering, disbondment, or a shear strength of less than 13 kN, or a 25% reduction in shear strength, the plastic was disqualified for further testing.

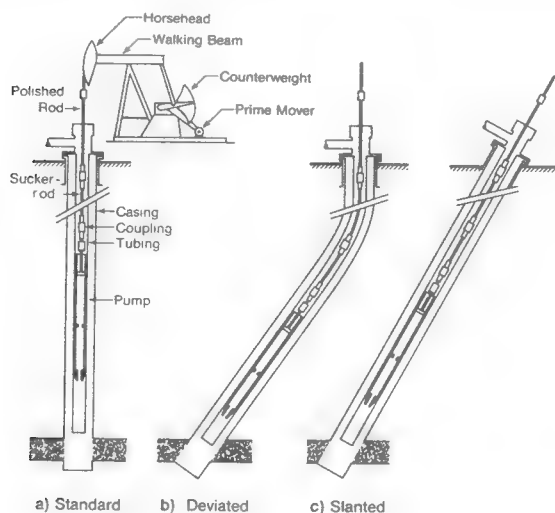


Fig. 1 Schematic of Artificial Lift Oil Wells, Standard, Deviated and Slanted

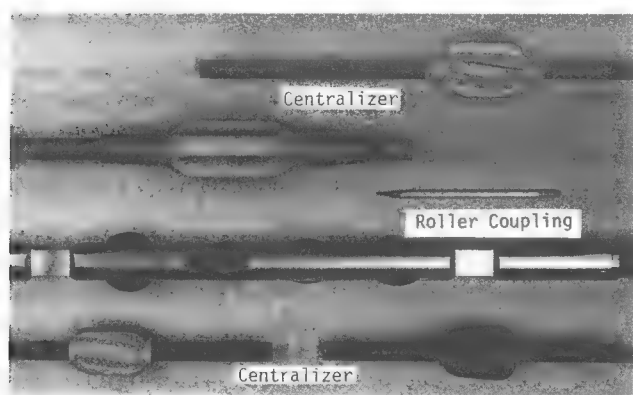


Fig. 2 Plastic Centralizers and Roller Coupling

Initial wear experiments were carried out in a reciprocating wear rig, a detail of which is shown in Fig. 3. This apparatus allowed plastic rod guides and centralizers to wear against a section of a standardized ERW (electrical resistance welded) J55 tubing while being subjected to side loads ranging from 134N (30 lbs) to 1335N (300 lbs) depending on the particular test. While under test the components were subjected to a non-circulating water stream of tap water to

simulate wear of wetted surfaces and to evaluate the effects of mild corrosion. The stroke length and stroke rate was set at 1.0 m (39.4 in.) and 14.1 m/min (555 in./min). The test was stopped at 5000 m, and usually at 25000 m intervals thereafter. At each inspection the dimensions of the centralizer or rod guide were measured for wear and the J55 tubing was visually inspected.

In order to evaluate the effects of sand abrasion, a rubber wheel abrasion tester (ASTM G65-85) was used in its standard configuration, and in a modified configuration. In the standard configuration 10x10x10 mm cubes of plastic were loaded against the revolving (20 rpm) rubber wheel at loads consistent with the contact pressures used with the reciprocating apparatus. In the modified version the rubber wheel was replaced with a steel wheel with known surface roughness.

Roller couplings were evaluated in the reciprocating apparatus and while this showed how the inner diameters of the plastic wheels could wear it gave little information on the wear of the outer diameters. Thus, a special roller coupling wear apparatus was constructed to evaluate roller wheel wear as shown in Fig. 4. This apparatus allowed the plastic wheels to be inclined and/or skewed to the rolling steel surface, permitting both rolling and sliding to occur simultaneously.

For all tests, the wear rate was measured by either monitoring geometrical changes or weight loss. Surface roughness was measured using a Talysurf IV instrument and plastic surfaces were inspected with an optical microscope.

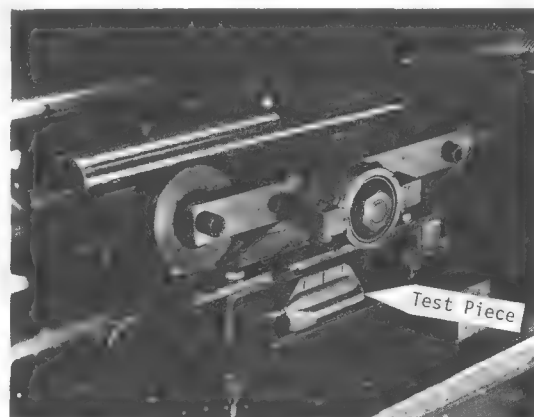


Fig. 3 Reciprocating Wear Apparatus

EXPERIMENTAL RESULTS Plastic Centralizers

Plastic centralizers and scrapers are injection molded on to the bodies of sucker rods to prevent the metal rod body and coupling from making contact with the wall of the

steel tubing. Plastic is used because it is believed it will wear without causing associated wear on the metal tubing. This is only true if the well conditions are not highly corrosive. In corrosive conditions with the plastic centralizer rubbing against the steel tubing, the centralizer can remove the passive films, thus accelerating the corrosive wear of the tubing. However, in the tests described in this paper only mild corrosive conditions existed although it was noted that in some cases the plastic centralizer removed the passive oxide layer causing a minor wear groove to be developed in the steel tubing.

Two different plastic materials used in centralizers were evaluated; a polyphenylene sulphide (PPS) and a polyamide (Ny). The wear was measured by recording the dimensional change in the flute of the centralizer. The PPS centralizer had spiral flutes whereas the Ny centralizer had straight flutes. The centralizers were provided with different side loads and the wear action was subjected to a constant water flood. The wear of these centralizers is shown in Fig. 5 where it is seen that after an initial "break-in" travel of 5000 m the PPS showed very little increase in wear for side loads between 134-800N (30-180 lbs). For the Ny centralizer the wear increased with side load. Thus, under the conditions imposed by the experiment the PPS centralizer had better wear resistance than did the Ny centralizer.

In Fig. 6 the differences in surface roughness of the J55 tubing are shown for 5000 m of wear. Initially the tubing had a CLA (center line average roughness) of $2.5\mu\text{m}$. After 5000 m of wear, with a side load of 134N (30 lbs), the tubing surface roughened to $2.9\mu\text{m}$ with the Ny but the tubing surface smoothed to a CLA of $1.8\mu\text{m}$ with the PPS centralizer. Similar trends were noted for side loads of 267N (60 lbs) and 400N (90 lbs) and at a wear travel of 25000 m. Under the action of a PPS centralizer increased wear travel produced a smoother, and therefore less abrasive, surface on the steel tubing. Whereas for the Ny centralizer, the roughness of the steel tubing surface remained relatively unchanged by the wear travel. The surface hardness of the J55 tubing was measured for each side load and wear travel distance evaluated. The results were scattered but within one standard deviation there was little change in the tubing surface hardness.

The reason for the different wear results reported above may be due to the nature of the centralizer materials. The Ny centralizer was almost entirely polyamide with only about 10% filler material added whereas the PPS had a filler material of about 75% as measured by a thermal gravimetric analysis. Thus, the improved wear resistance of the PPS may have

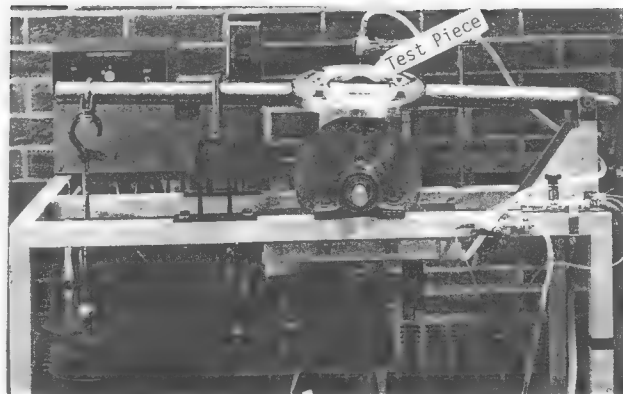


Fig. 4 Roller Wheel Wear Testing Facility

been more the result of the filler material than the type of plastic.

The effect of the PPS in smoothing the surface of the J55 Steel tubing could be diminished if a third body abrasive is present. To evaluate this effect, plastic cubes ($10\times10\times10\text{ mm}$) were cut from the flutes of centralizers and mounted in an ASTM G-65 abrasion tester. This test consisted of pressing the plastic specimens under a fixed load against a rubber wheel rotating at 20 rpm. At the interface between the test specimen and the rubber wheel a steady stream of dry silica sand flowed. The wear was measured, as dimensional changes in the thickness of the plastic specimen, and these results are shown in Fig. 7.

From Fig. 7 it is seen that, with a flow of sand between a rubber wheel and the plastic specimen, the PPS wore more than the Ny with the latter remaining relatively constant over the contact pressures evaluated. This is

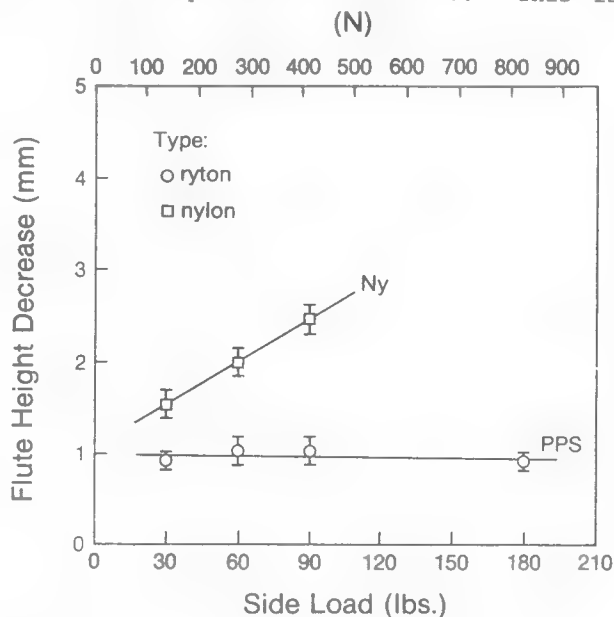


Fig. 5 Wear of Plastic Centralizers on Honed J55 Tubing

opposite to what was observed with the wear of these plastics against the J55 oil field tubing where no sand was present as shown in Fig. 6.

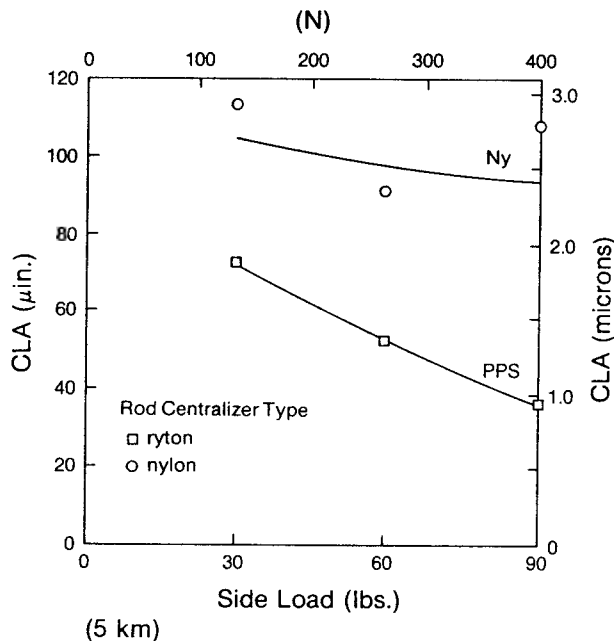


Fig. 6 Surface Roughness Changes of J55 Tubing

Wheeled Couplings

For oil pools which are reached through deviated wells, slant wells, or where there are severe deviations in the oil tubing, considerable friction forces can develop between the sucker rod string and the oil tubing. This causes not only increased power consumption in the pumping system but also can lead to considerable wear of the oil tubing, couplings and sucker rods. A possible remedy to this has been the use of roller or wheeled couplings.

A typical wheeled coupling (Fig. 2) consists of four plastic wheels arranged on axes 45° to each other. When in position in the oil tubing only one of the four wheels may be oriented at 90° to the tangent point of contact with the oil tubing. The other wheels will contact the tubing at angles of 45° and 90° to this tangent point. As the wheel bearing the most load wears down it will cause the other wheels to have a radial downward sliding action superimposed on the longitudinal rolling action.

It was found that under side loads of up to 445N (100 lbs) there was little wear of the outer diameter of the wheels or appreciable wear on the steel tubing. The tubing wear track retained a clean appearance whereas the surrounding tube had built up a significant

oxide layer due to the corrosion caused by the water stream. This showed that the wheel continuously removed the passive oxide layer along the wheel path and, as such, could accelerate the corrosion of the tubing. There was, however, some evidence of wear at the wheel bearings as these were metal and rubbed against the plastic due to the load applied through the wheel.

Field reports of seized wheels and wearing large flat areas on the wheels was not reproduced on the reciprocating wear test rig as long as the wheels were allowed to roll freely. In order to induce the kind of wear experienced in the field a 200 mm (8 in.) diameter steel wheel (which represents the oil tubing) rotated against a single wheel of a wheeled coupling under various bearing loads applied through the fulcrum arrangement shown in Fig. 4. The steel wheel rotated clockwise for $3\frac{1}{2}$ revolutions, stopped, reversed and rotated counterclockwise for another $3\frac{1}{2}$ revolutions, and this was repeated once every 7.5s. This, in effect, simulated an equivalent sucker rod stroke length of 2.2m (7.2 ft) at an average stroke rate of 36 m/min (118 ft/min). The manner in which the wheel of the coupling was mounted allowed it to be skewed and/or inclined to the plane of the steel wheel. In either the case of a skewed or inclined orientation a steady stream of water flowed over the wheel contact surface as well as the bearing surfaces.

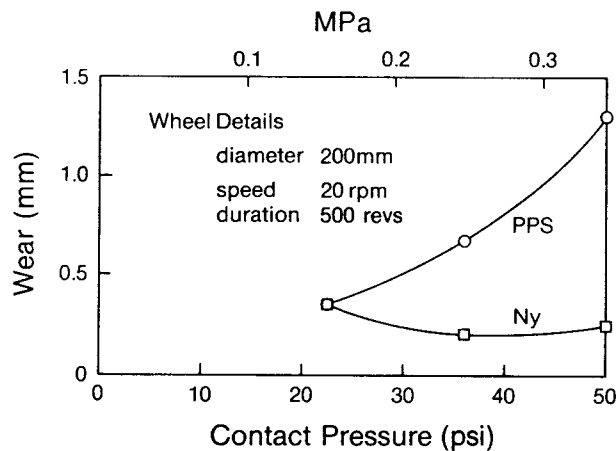


Fig. 7 Abrasion Test of Ryton (PPS) and Nylon (Ny)

Three side loads of 222N (50 lbs), 445N (100 lbs) and 667N (150 lbs) were applied to a single wheel and the wear was measured at different durations up to a wear path of 100,000 m. Before each test the steel wheel was "dressed" with 120 grit emery cloth.

The wear rates were calculated for two types of plastic wheels; polyacetal (PA) and Ny. The wear of the inner diameter for the Ny wheel and for the PA wheel is shown in Fig. 8.

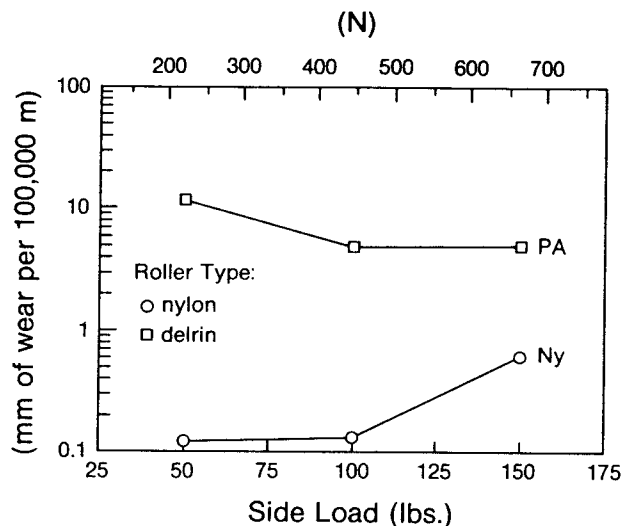


Fig. 8 Wheel Wear vs Bearing Load

This figure shows that the PA wore more than the Ny but at higher side loads the wear of the Ny appeared to increase whereas the PA appeared to be independent of load between 445 and 667N (100 and 150 lbs) side load. At a 222N (50 lbs) side load the wear of the PA wheel was about two orders of magnitude greater than the Ny wheel, whereas at 667N (150 lbs) the difference was about one order of magnitude.

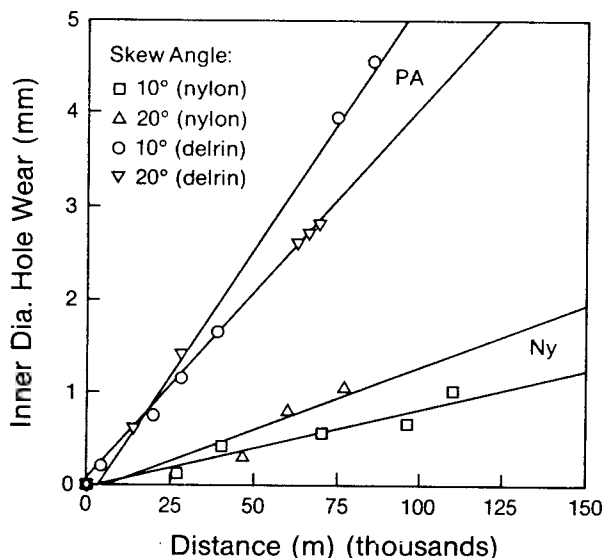


Fig. 9 Inner Hole Diameter Wear as a function of Skew Angle

The wear of the inner hole diameter of the plastic wheels is shown in Fig. 9 as a function of skew angle for a single side load of 222N (50 lbs). In Fig. 10 the inner hole diameter wear for a nylon wheel is shown as a function of the inclination angle at a 222N (50 lbs) side load. In comparing Figs. 9 and

10, for nylon, it is seen that skew angle had about the same influence on wear as did the inclination angle. Also, as the skew angle increased the wear generally increased as might be expected. From Fig. 9 it is seen that the Ny wore less than the PA under identical skew angle conditions. After a wear travel of 100,000m the PA wear was about five times more than with the Ny when the wheels were subjected to a skewing action.

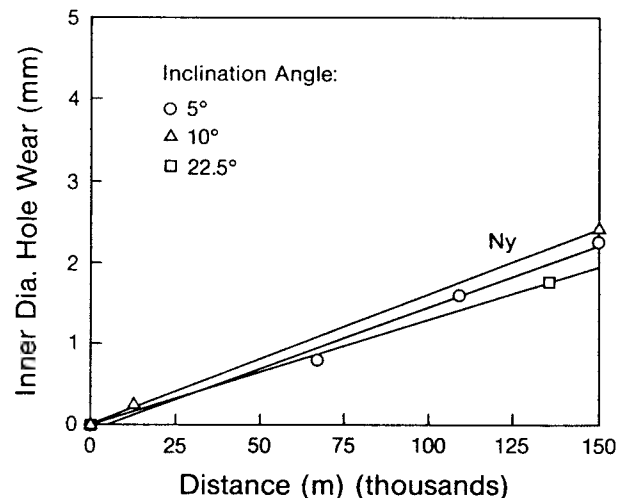


Fig. 10 Inner Hole Diameter Wear as a function of Inclination Angle

The outer diameter wheel wear as a function of skew angle and inclination is shown in Figs. 11 and 12 for a side load of 222N (50 lbs). As before, increasing the skew angle resulted in increased wear, but with the Ny wheel wearing more than the PA wheel under the same side load and wear distance travelled. It is also interesting to note that whereas the inclination angle had only a minor effect on the wear of the inner hole diameter, the inclination angle did affect the outer diameter wheel wear. This is important to note in that a complete assembly of a wheeled coupling consisting of four wheels, at least three of the wheels will be at an inclined orientation which will cause the outer diameters to wear. Although the effect of inclination on wear is about one quarter of that caused by skewing, its effect would be to reduce the overall life of the wheeled coupling.

The observation of better wear performance of PA over Ny in the case of outer hole diameter is contradicted by the observations made on the wear of the inner wheel diameter where Ny was seen to have better wear resistance properties. This example illustrates how wear is influenced by the manner in which components are in contact. In the case of the inner hole the plastic wheel was rubbing in a sliding contact with a non-rotating hardened

steel bushing. For the outer wheel wear the wheel was either purely rolling or under a combination of sliding and rolling (skewing) against a low carbon (0.3%) steel. Thus, the wear processes should not necessarily be expected to be similar.

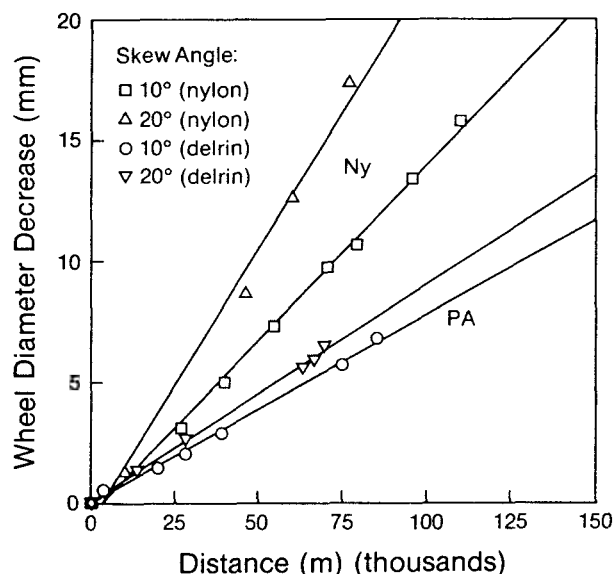


Fig. 11 Outer Diameter Wheel Wear as a function of Skew Angle

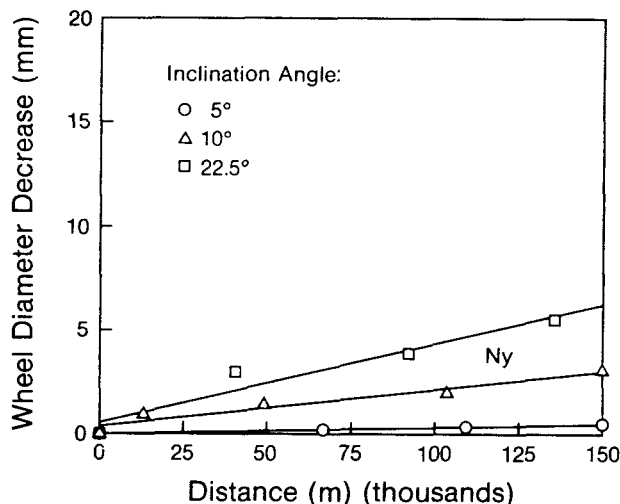


Fig. 12 Outer Diameter Wheel Wear as a function of Inclination Angle.

Discussion

For the plastic centralizers evaluated it was found that, under similar test conditions of contact pressure and distance travelled, that PPS is more resistant to wear than Ny. It was noted that the wear of PPS was independent of load in the load ranges evaluated. This was attributed to the fact that the PPS smoothened the surface of the J55 tubing

whereas this did not occur with the Ny centralizer.

For the case of plastic wheels used with roller couplings recognition must be made of the fact that the inner hole diameter is subjected to different loading characteristics than the outer wheel diameter. This suggests that a different design approach should be used to ensure the outer wheel diameter does not wear more than occurs at the inner hole or vice versa. As seen in this study the choice between PA over Ny is not straightforward. One suggestion that could be explored is, given the purpose of the roller coupling is to reduce wear against the tubing, to design a wheel using Ny for the plastic wheel and use a metal insert to wear against the steel bushing of the inner hole.

In both the cases of centralizers and wheeled couplings the presence of sand will hasten the wear of these components. If sand is not present or can be prevented from contaminating the well then the use of PPS for centralizers and Ny as wheels in roller couplings may provide decided advantages. Although not specifically addressed it was also noted that the surface roughness of the J55 tubing has an influence on the wear of the plastics used and this surface should be as smooth as possible to prevent premature failure, due to wear, of the plastic parts which come into contact with the tubing.

Conclusions

Suitable testing apparatus and procedures have been developed to evaluate commercial products for wear under simulated oil field conditions. This has enabled a comparison of the wear resistance of products to be developed. The next stage of this research will be to investigate further those materials which show superior wear resistance. This will include a more detailed investigation of the wear mechanisms of each plastic on specific metal surfaces. Ultimately, it is desired to know which factors should be considered to enable a particular plastic to be designed for a given downhole oil field situation. This will be a vast improvement over the costly trial and error methods presently being employed in the field.

Acknowledgement

The authors express their thanks to ESSO Resources Canada Ltd. and the Natural Sciences and Engineering Research Council (Canada) for the financial support for the project described in this paper.

Presented at NACE Canadian Region Western Conference, Calgary 1990

Laboratory Simulation of Sucker Rod Downhole Corrosion
Fatigue Type Failures.

Authors: D.G.Bellow, I.Smuga-Otto, D.C.Owens and A.Shirizly.
Mechanical Engineering Department, University of Alberta.
Edmonton, Canada.

ABSTRACT

An experimental program was established to determine the corrosion-fatigue lives of oil field sucker rods under selected environmental and stress range conditions for a sucker rod surface as manufactured and with modified surface treatments. Four point bending fatigue was arranged for the rods with 30 Hz frequency. A corrosion cell was built around the test section of the rod to enable monitoring of the electrochemical parameters. General corrosion rate, air fatigue endurance and corrosion fatigue performance were established for all rods under investigation. No correlation was found between the general corrosion rate, air fatigue endurance limit (evaluated separately) and final sucker rod corrosion-fatigue life performance. The influence of a few environmental parameters (i.e., oxygen presence, carbon dioxide saturation, sodium chloride concentration) under selected stress ranges on rod corrosion-fatigue life was also evaluated.

INTRODUCTION

Corrosion fatigue failures were found as the most frequent cause of oil well sucker rod failures in a recent oil industry survey¹. To eliminate or minimize such failures many attempts have been made both in developing new types of rods on the manufacturer side and reducing the rod stress or controlling downhole corrosion on the user side^{2,3}. The survey¹ also showed that there was insufficient evidence to determine which type of rod performed better in a particular downhole environment and stress condition and what was the effectiveness of corrective actions employed by the field operators to reduce sucker rod failures.

The corrosion fatigue of metals is a complex phenomenon involving metallurgical, mechanical and electrochemical factors. Considerable information is available on air fatigue of alloys separate from their corrosion characteristics in numerous

environments. It is well known that the fatigue action when combined with corrosion causes a corrosion fatigue synergy effect, difficult to predict based on a single characteristic.

In laboratory simulation of corrosion fatigue there is always a question of how much the acceleration of the fatigue disturbs the electrochemical reactions and in turn affects the corrosion fatigue life of investigated components. The frequency effect of applied cyclic stress (alternate bending) of 10, 20 and 30 Hz evaluated on low alloy steels in distilled water, chloride and carbonate water solutions was reported as not causing significant differences with the resulting corrosion fatigue performance⁴, when tested in a particular environment. Major differences noted were referred to the environments used. Also a negligible effect of cyclic loading frequency in the range of 0.1 to 10 Hz on crack propagation in pipeline steel was reported when tested in crude oil containing H_2S ⁵. For the purpose of this study 30 Hz Frequency was utilized whereas a typical oil field cyclic frequency is 0.1Hz.

The majority of the research work reported in the literature concerning corrosion fatigue properties of metals are of limited application to oil field operators because of the test arrangements and environmental conditions being remotely related to the downhole production environment. Only a few publications have appeared covering sucker rod performance as components which were tested under the stress ranges and environments characteristic for downhole service conditions. The conclusions, however, appeared sometimes contradictory, for example, the beneficial effect of nickel and chromium when added to steel to enhance corrosion fatigue performance as suggested by Dvoracek⁶ versus Mehdizadeh⁷ findings which showed that the presence of chromium and nickel in steels made them more susceptible to failure by corrosion fatigue.

The objective of the present work is to evaluate the stress range and various environmental effects such as air presence, concentration of NaCl solution and saturation by carbon dioxide on corrosion fatigue of sucker rods. A comparison is made of corrosion fatigue, general corrosion and air fatigue between the selected rods of similar nominal tensile strength 827/965 MPa (120/140 ksi) commonly used in oil field service.

The correlation is also evaluated between the air fatigue characteristics of a number of selected rod types, their corrosion rates evaluated electrochemically and the corrosion-fatigue lives obtained in the same environments as for the electrochemical tests.

EXPERIMENTAL PROCEDURE.

A special apparatus was developed to evaluate sucker rod corrosion fatigue performance. A four point bending test fixture was designed to cycle sucker rods in bending fatigue utilizing a 30 Hz standard Baldwin Sontag machine. The corrosion cell was designed to enclose over the central portion of the rod. The cell was equipped with electrodes connected to the potentiostat to allow monitoring of electrochemical parameters of the corrosion processes occurring in the corrosion fatigue experiments. Specimens were exposed to the electrolyte solution under open circuit potential and the corrosion potential was continuously recorded during the experiments. The fluid circulation was forced by a peristaltic pump from a 15 liter container to the one liter corrosion cell with the constant flow rate over all experiments. The pH of the testing solution was also recorded. The overall arrangement is shown schematically in Fig.1.

Two commonly used sucker rod types of comparable strength were selected for corrosion fatigue experiments; one being in a quenched and tempered condition (Rod A) and the second normalized and tempered (Rod B). Both rod types were tested with the surface state as manufactured. In addition the surface of the quenched and tempered rod has been subjected to an enhanced mechanical surface treatment and identified as Rod C. The chemical composition and mechanical properties of the rods are provided in Table 1. The geometrical arrangement and dimensions of the test specimens together with the corrosion cell is shown in Fig.2. The undercut was introduced on the compression side of the specimen center in order to generate rod failure in the central part of the corrosion cell.

Verification of rod stress value in the area of maximum stress opposite the undercut was both calculated theoretically and measured experimentally using strain gages. Measured stress values were used to draw load versus stress diagrams characteristic of the four point bending frame and apparatus used. Close agreement between measurement and the theory was obtained and stress values may be considered correct within $\pm 5\%$.

The corrosion fatigue lifetime was defined as the number of cycles required for a crack to progress through $3/4$ of the rod diameter. A testing machine stop was executed by the release of static load triggering a switch located inside the fatigue machine and calibrated accordingly. The number of cycles to failure was an average of the results of a minimum of three experiments performed under the same mechanical and electrochemical conditions. Reproducibility in test results were good and standard deviation did not exceed 10% (of average) in the majority of the cases (Table 2).

Each corrosion fatigue specimen was inspected for crack distribution using nondestructive wet magnetic particle technique and macrophotographed. Cracked specimens were sectioned through the maximum and minimum stress area and were mounted in epoxy, polished and examined using both optical and scanning electron microscopy.

Parallel to the corrosion fatigue tests, the corrosion rate of rods was evaluated electrochemically, utilizing Cyclic Potentiodynamic Polarization and Polarization Resistance techniques. Scanning rates of 0.1mV/sec and 5mV/sec of applied potential with 24 hours intervals starting 1 hour after specimen immersion up to 168 hours were executed. Corrosion tests were performed in the same environments as the corrosion fatigue experiments. Specimens of 15 mm length cut from the rods were tested in the surface state "as manufactured" (Rod A and B) and after being modified (Rod C), preceded by a three stage cleaning including ultrasonic bath in water with detergent, acetone and ethanol respectively and immediately immersed in the ASTM corrosion cell.

The three point bending air fatigue was conducted on 292 mm (11.5 inch) specimens cut from rods A, B and C, utilizing Amsler High Frequency Vibrophore. The experiments were conducted at a frequency of 68 Hz resulting in the fatigue endurance limit evaluation of the three types of rods. Rods were tested with the surface in as manufactured or as modified condition. Load versus stress values was verified by both theory and measurement providing stress value accuracy of $\pm 3\%$.

TESTING ENVIRONMENT

The choice of testing environment for the laboratory experiments to simulate oil field downhole conditions always presents a problem of being sufficiently representative. The concentration of the most crucial element from the corrosion and corrosion fatigue point of view - oxygen - is often not known for many wells, being described by field operators as "possible oxygen entry"¹.

The detrimental effect of dissolved oxygen on corrosion fatigue properties of mild steel has been demonstrated by many workers^{8, 9, 10, 11}. The fatigue resistance substantially decreased for 3-5% NaCl aerated solutions and an endurance limit was no longer observed. An apparent endurance limit was regained in deaerated NaCl water solutions. No difference was recorded in corrosion fatigue performance of low alloy steel between air or oxygen saturated NaCl solutions⁸.

For the purpose of the present study the following

environments were chosen: 8%NaCl (analytical reagent) aqueous solution saturated with carbon dioxide under anaerobic and a separately aerated condition. The pH of this solution was in the range from 4.2 to 5.6 and was representative of a harsh acidic type downhole conditions with a tendency to generate pitting.

The second environment was created by dissolution of 3.5% NaCl (analytical reagent) in distilled water letting free air access to the corrosive solution during the duration of the test. The pH of this solution was in the range from 6.2 to 7.2 representing typical downhole low corrosion condition with the exception that oxygen level is often lower in the field, yet still present in many wells. The presence of chloride ions in all tests assured pit generation and growth, which may act as stress raisers inducing fatigue crack initiation.

The stress range and environment was chosen to cause rod failures within 10 million cycles, the arbitrarily established pass/not pass experiment border line. The stress range was chosen to be within the range (or close to) recommended by the Goodman Diagram. This allowed ranking of relative corrosion fatigue resistance of rods as well as evaluating stress and environmental parameters on rod behavior. Almost all tests were conducted in the presence of oxygen.

RESULTS AND DISCUSSION

All corrosion fatigue experiments were conducted under open circuit corrosion condition. Table 2 provides the summary of these experiments specifying rod type, stress range, environment employed and number of cycles to failure.

NaCl, CO₂ and oxygen concentration effect.

The influence of the corrosive solution composition and concentration has been examined on rod B only. Data obtained in Tests #1 and #2 (Table 2) arranged for 68.7-412.5 MPa (10,000 - 60,000 psi) stress range show that increasing the NaCl concentration from 3.5% to 8% caused a small decrease in the corrosion fatigue life. However, if the amount of carbon dioxide was decreased from the saturation level (pH=4.2-5.6, Test #2) to the equilibrium with the surrounding atmosphere (pH=6.2-7.2, Test #3) in 3.5% NaCl solution, a larger decrease in corrosion fatigue life of rod B was noted (from 7563×10^3 to 1559×10^3 cycles to failure). This phenomenon has been observed previously⁴ and explained on the basis of the passivating effect of the carbonate ions.

The external appearance of the cracks generated during Test #2 and Test #3 which differ by the amount of carbon dioxide concentration level only, is shown in Fig.3 a) and b). The optical microscope investigation of a longitudinal cross section

of the rod indicates that cracks generated in the presence of saturated carbon dioxide solution are densely distributed and shallow (Fig.4a). Figure 4b shows the corrosion fatigue cracks of Test #3 which were almost four times longer and spaced far away from each other after completing 1559×10^3 cycles to failure. The amount of CO_2 available in the corrosive solution seemed to be very influential for the fatigue crack initiation and propagation and the higher the concentration of carbon dioxide, the better the corrosion fatigue performance observed.

It is interesting to note that the general corrosion rate evaluated in a series of electrochemical experiments for rod B in both a 8% NaCl/air saturated by CO_2 (Environment I) and a 3.5% NaCl/free air inlet (Environment II) solutions indicated an increase in corrosion rate for Environment I for all tests performed (see Table 3), hence, presenting much better corrosion fatigue performance.

The influence of oxygen on corrosion fatigue rod life was evaluated by Tests #3 and #4. Rod B tested with the stress range 68.7-412.5 MPa (10,000-60,000 psi) in a 3.5% NaCl solution with free air inlet to the testing environment completed 1559×10^3 number of cycles to failure (Fig.3b) whereas when tested in the same solution under anaerobic condition did not fail within 10 million cycles and almost did not develop any surface cracks (Fig.3c). For a relatively high stress range a complete removal of oxygen from the downhole environment seemed to be the single most effective action to prevent crack nucleation.

For some tests it was noted that numerous cracks were heavily branched, the effect of which was to apparently retard crack propagation. Fig.5 shows examples of crack branching on Rod B. No correlation was found between the rod material, metallurgical or environmental parameters and the susceptibility for branching.

Stress range effect.

The influence of stress range on corrosion fatigue performance may be observed on rod B in Tests #3, #5 and #10. The environment II (3.5% NaCl/air) was employed for the following stress ranges: 68.7-412.5 MPa (10,000-60,000 psi), 68.7-309.4 MPa (10,000-45,000 psi) and 68.7-240.6 MPa (10,000-35,000 psi) which resulted in increasing the number of cycles to failure from 1559×10^3 through 5096×10^3 to no failure over 17 million cycles respectively (Fig.6). Further examination of the crack cross sections of Tests #3 and #5 and #10 did not show any significant difference in crack shape, depth and distribution for the three tests, except test #10 did not develop to final failure. Optical microscope examination of a specimen taken from Test #10 showed, however, one crack located in the specimen center which had progressed to failure.

Rod performance comparison.

The corrosion fatigue performance comparison between the three rod types investigated in Environment I and stress range 68.7-412.5 MPa (10,000-60,000 psi) is shown in Fig.7 and for Environment II and stress range 68.7-309.4 MPa (10,000-45,000 psi) in Fig.8.

Rod B showed superior corrosion fatigue resistance over Rod A when tested in Environment I and 68.7-412.5 MPa (10-60 ksi) stress range. These rods differ in heat treatment (Rod A-quench. and temp., Rod B- norm. and temp.) and by chemical composition (Rod A - having Molybdenum and Rod B - Vanadium). However, if Rod A is tested after modified surface treatment (Rod C) its superiority to other rods is clearly evident. This is also true for Environment II and 68.7-309.4 MPa (10-45 ksi) stress range, where Rod C passed 10 million cycles without developing failure. The Environment II did not produce significant differences in corrosion fatigue performance of Rods A and B.

The crack distribution and shape created on the surface of Rods A and C were examined using Scanning Electron Microscope. Figure 9a shows a micrograph of the surface appearance of Rod A (5.3 million cycles to failure) and Fig.9b of Rod C (10 million cycles without failure). The surface of Rod C seems to be more damaged than Rod A, having larger and more open cracks and still being more corrosion fatigue resistant as a major crack did not develop. The longitudinal cross section of Rods A and C as observed by optical microscope is shown in Fig.10 a and b. Crack shape, depth and distribution seemed to be similar for both rods.

The corrosion fatigue superiority of Rod C over rods A and B showed that the rod surface condition was more important than its differences with heat treatment (different microstructure type and grain size) or small differences with chemical composition (influencing strength and corrosion properties).

There was no correlation found between the general corrosion rate evaluated electrochemically for the three rods in Environments I and II (Table 3) and their corrosion fatigue performance evaluated in the same environments. The Environment I generated the highest corrosion rate for Rod C followed by Rod A and the lowest for Rod B. Environment II did not produce significant differences in corrosion rates for the three rods. These results did not correlate with the ranking obtained for corrosion fatigue experiments which ranked rod C the best, followed by rod B and A.

Environment I (CO_2 saturated) generated larger corrosion rates than Environment II. An opposite effect was obtained on corrosion fatigue performance where CO_2 saturation caused

significant improvement of Rod B fatigue life.

The corrosion rate alone can not serve as an indicator how sucker rods will perform in a corrosion fatigue environment.

The air fatigue results are provided in Table 4 and graphically illustrated in Figures: 11 (Rod A), 12 (Rod B) and 13 (Rod C). Some scatter in air fatigue results may be assigned to the surface imperfections and other related factors which makes exact determination of an air fatigue endurance limit difficult with the number of specimen available for the tests. However the endurance limit (stress value below which no failure occurs) for Rods B and C appeared to be within the same range of 653-672 MPa (95-97.5ksi). The endurance limit range for Rod A was 620-638 MPa (90-92.5 ksi), showing inferiority to both rods B and C.

These results again did not correlate with the ranking obtained for the corrosion fatigue, where the apparent superiority of rod C over Rod B and A was noted.

CONCLUSIONS

1 For fully deaerated water solutions, containing chloride ions (3.5-8%) and with or without carbon dioxide saturation no rod failure was observed below 10 million cycles and no fatigue cracks were noted on the rod surface. Oxygen removal from the environment is the single most effective treatment improving corrosion fatigue performance of rods, within the stress range evaluated.

2. Saturation of the corrosive environment by carbon dioxide substantially improved the corrosion fatigue performance of the sucker rod.

3. For the environments containing oxygen and stress ranges examined, stress range reduction improved corrosion fatigue performance of the rods, however it delayed the failure only, not preventing it.

4. The specific rod surface preparation is very important in regards to its corrosion fatigue resistance and may substantially improve ordinary rod performance for the environments containing oxygen.

5. Knowledge of general corrosion rate or air fatigue endurance limit alone can not serve as an indicator of corrosion fatigue sucker rod performance.

ACKNOWLEDGEMENT

This work was carried out under contract for Stelpipe, a unit of Stelco Inc. The authors express their appreciation to Stelpipe for permission to present these results.

BIBLIOGRAPHY

1. D.G.Bellow, "Sucker Rod Strings - an Overview of Oil Field Practices and Experiences", May, 1987 - Proprietary Information,
2. S.E.Mueller, R.K.O'Neil, "Engineering and Operational Efforts Reduce Sucker Rod Failures", Society of Petroleum Engineers of AIME, Paper 2634, 1969.
3. S.M.Bucaram, H.G.Byars, and M.Kaplan: "Selection, Handling and Protection of Downhole Materials". Materials Protection and Performance, Vol.12, sept.1973, pp.20-26.
4. R.H.Ricci, L.N.Berardo, L.M.Gassa, and J.R.Vilche: "Corrosion Fatigue Behavior of Low Alloy Steels in Aqueous Neutral and Alkaline Electrolytes", Proceedings of International Congress on Metallic Corrosion, Toronto, June 3-7 1984, pp. 161-166.
5. O.Vosikowsky, A.Rivard, "The Effect of Hydrogen Sulfide in Crude Oil on Fatigue Crack Growth in a Pipeline Steel", Corrosion, Vol.38, No.1, p.19-22.
6. L.M.Dvoracek: "Corrosion Fatigue testing of Oil Well Sucker Rods; Materials Performance, Vol.12, Sept.1973, pp 16-19.
7. P.Mehdizadeh, "Effect of Metallurgical Variables on Corrosion of Sucker Rods in Salt Water Containing CO_2 and H_2S ", Materials Performance, Vol.13, No.6, 1974, p.13-16.
8. D.J.Duquette, H.H.Uhlig, "Effect of Dissolved Oxygen and NaCl on Corrosion Fatigue of 0.18% Carbon Steel", Transactions of the ASM, 61, 1968, p.449-456.
9. H.H.Lee and H.H.Uhlig: "Corrosion Fatigue of Type 4140 High Strength Steel"; Metallurgical Transactions, Vol.3, Nov.1971, p.2949
10. D.J.Duquette: "A Review of Aqueous Corrosion Fatigue"; Corrosion Fatigue: Chemistry, Mechanics and Microstructure, NACE 2 Publication, 1972, pp.12-24.
11. P.Mehdizadeh, R.L.Glasson, J.E.Landers, "Corrosion Fatigue Performance of Carbon Steel in Brine Containing Air, H_2S and CO_2 ", Corrosion, Vol.22 No.12, 1966, p.325-335.

Table 1: Properties of Rods A, B & C.

Rod	Chemical Analysis (%)									
Type	C	Mn	P	S	Si	Cr	Ni	Mo	V	
A/C	.33-.38	.65-.95	.04Mx	.04Mx	.15-.35	.70-.90	.40-.70	-	.03-.05	
B	.38-.43	.60-.80	.04Mx	.04Mx	.20-.35	.70-.90	1.25-2.00	.20-.30	-	

Rod	Mechanical Properties		
Type	Yield strength 1000 psi	Tensile strength 1000 psi	Heat treatment
A/C	110 min	120/140	Quenched & Temp.
B	105/120	125/140	Normalized & Temp.

Table 2. Summary of corrosion-fatigue experiments (four point bending fatigue).

Test #	Rod Type	Max. Stress	Min. Stress	Environment	Cycles to Failure $\times 10^3$ *	Comments
1	B	60,000	10,000	8%NaCl/CO2/air	5,653	STD 14% **
2	B	60,000	10,000	3.5%NaCl/CO2/air	7,563	STD 9%
3	B	60,000	10,000	3.5%NaCl/air	1,559	STD 8%
4	B	60,000	10,000	3.5%NaCl/N2	10,898	No Failure
5	B	45,000	10,000	3.5%NaCl/air	5,096	STD 7%
6	A	60,000	10,000	8%NaCl/CO2/air	4,049	STD 8%
7	A	45,000	10,000	3.5%NaCl/air	5,139	STD 22%
8	C	60,000	10,000	8%NaCl/CO2/air	7,419	STD 10%
9	C	45,000	10,000	3.5%NaCl/air	10,610	No Failure
10	B	35,000	10,000	3.5%NaCl/air	17,781	No Failure

* The number of cycles to failure is provided as an average of min. 3 experiments for each test number.

** STD - Standart deviation.

Table 3: Summary of corrosion experiments conducted over 168 hours in two selected environments.

Corrosion rates* are presented as current densities in $\mu\text{A}/\text{cm}^2$ (corrosion current is proportional to the corrosion rate)

Environment	ROD TYPE	EXPERIMENT TYPE					
		Cyclic polarization				Polariz. resistance	
		0.1 mv/sec		5 mv/sec			
		1h	168h	1h	168h	1h	168h
18% NaCl aerated	A	55	222	28	64	58	276
& CO2 saturated	B	40	156	-	48	35	261
	C	133	281	39	74	100	345
	A	31	5	15	11	15	13
3.5% NaCl aerated	B	17	19	12	30	15	19
	C	31	6	8	15	22	17

* calculated as an average of duplicated experiments($\pm 20\%$)

Table 4: Summary of air fatigue experiments.

ROD TYPE	MAXIM STRESS	MIN STRESS	CYCLES TO FAILURE	ROD TYPE	MAXIM STRESS	MIN STRESS	CYCLES TO FAILURE
A	92,500	10,000	1,444,000	B	97,500	10,000	1,054,900
A	90,000	10,000	no failure 10^7 c	B	98,750	10,000	1,111,900
A	92,500	10,000	no failure 10^7 c	B	97,500	10,000	1,470,300
A	100,000	10,000	675,600	B	95,000	10,000	no failure 10^7 c
A	105,000	10,000	789,100	C	95,000	10,000	no failure 10^7 c
A	90,000	10,000	no failure 10^7 c	C	100,000	10,000	no failure 10^7 c
A	90,000	10,000	no failure 10^7 c	C	105,000	10,000	1,191,700
A	95,000	10,000	445,000	C	105,000	10,000	707,800
A	105,000	10,000	435,600	C	102,500	10,000	853,400
B	80,000	10,000	no failure 10^7 c	C	100,000	10,000	1,450,000
B	100,000	10,000	1,005,600	C	97,500	10,000	no failure 10^7 c
B	90,000	10,000	no failure 10^7 c	C	100,000	10,000	1,307,300
B	95,000	10,000	701,200	C	97,500	10,000	no failure 10^7 c
B	95,000	10,000	no failure 10^7 c	C	97,500	10,000	1,000,600
B	97,500	10,000	no failure 10^7 c	C	98,750	10,000	no failure 10^7 c
B	100,000	10,000	956,700	C	96,250	10,000	no failure 10^7 c
B	100,000	10,000	1,229,500	C	96,250	10,000	no failure 10^7 c

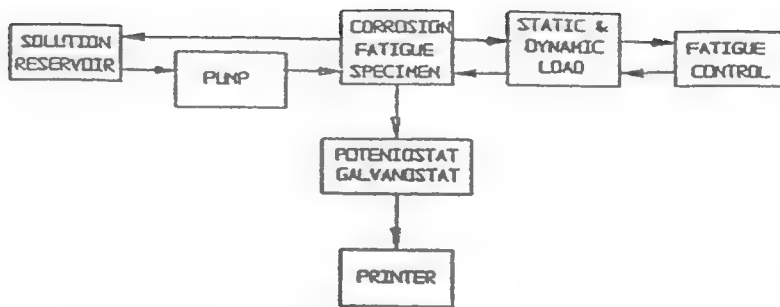


Fig. 1: Schematic representation of corrosion fatigue experiment arrangement.

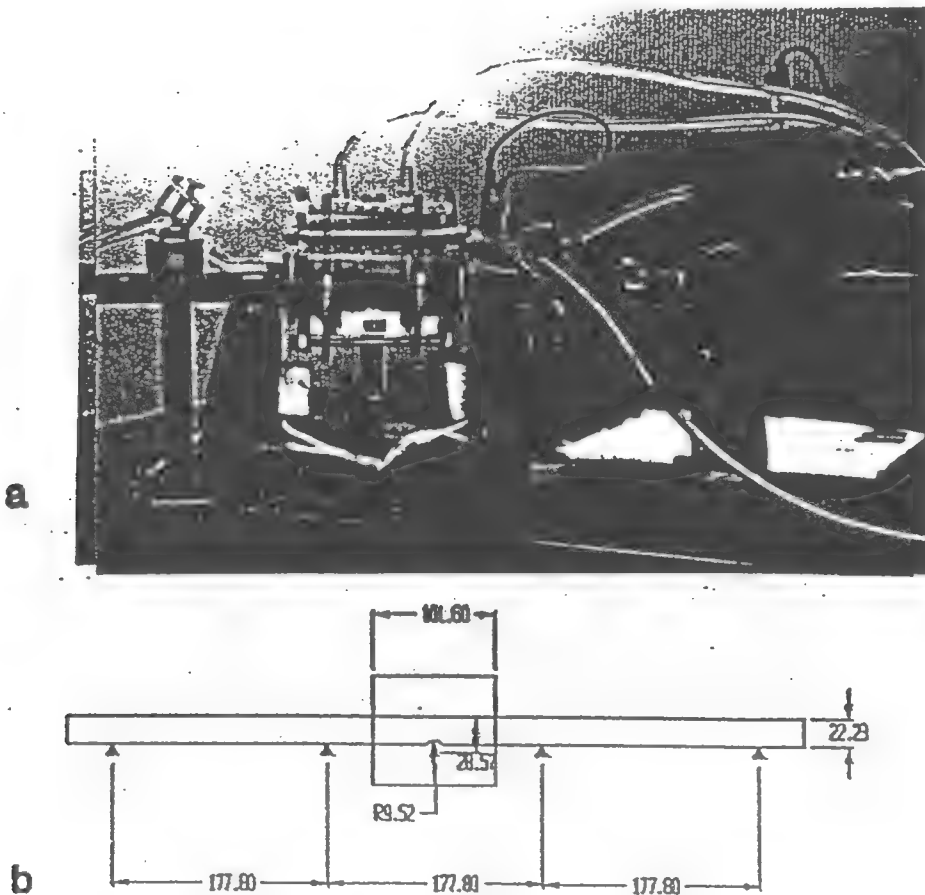


Fig. 2: a) Corrosion-fatigue experiment set up. b) Rod and Cell dimension.

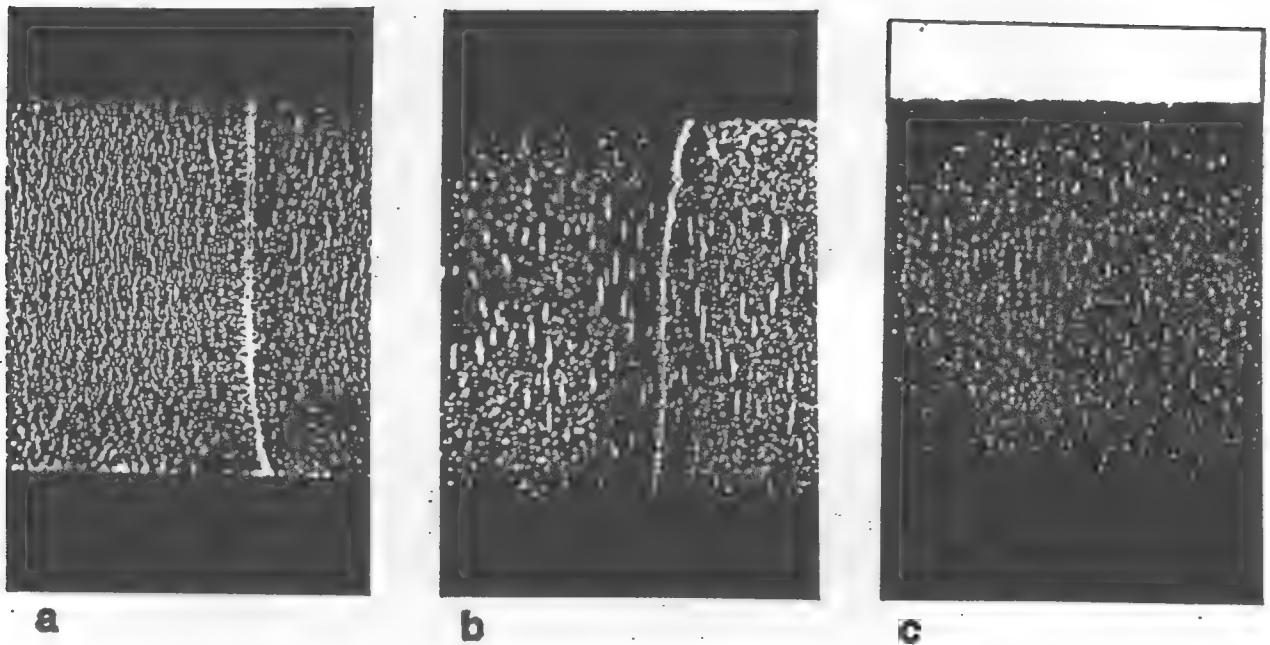


Fig. 3: External appearance of the cracks generated on Rod B tested under 10,000-60,000 psi stress range in 3.5%NaCl solution:

- a) With air access and solution saturated with carbon dioxide (Test #2 , 7,563,000 cycles to failure).
- b) With air access only (Test #3 , 1,559,000 cycles to failure)
- c) With anaerobic condition (Test #4 , no failure and no crack after 10 million cycles).

Cracks are revealed by magnetic particle inspection technique.

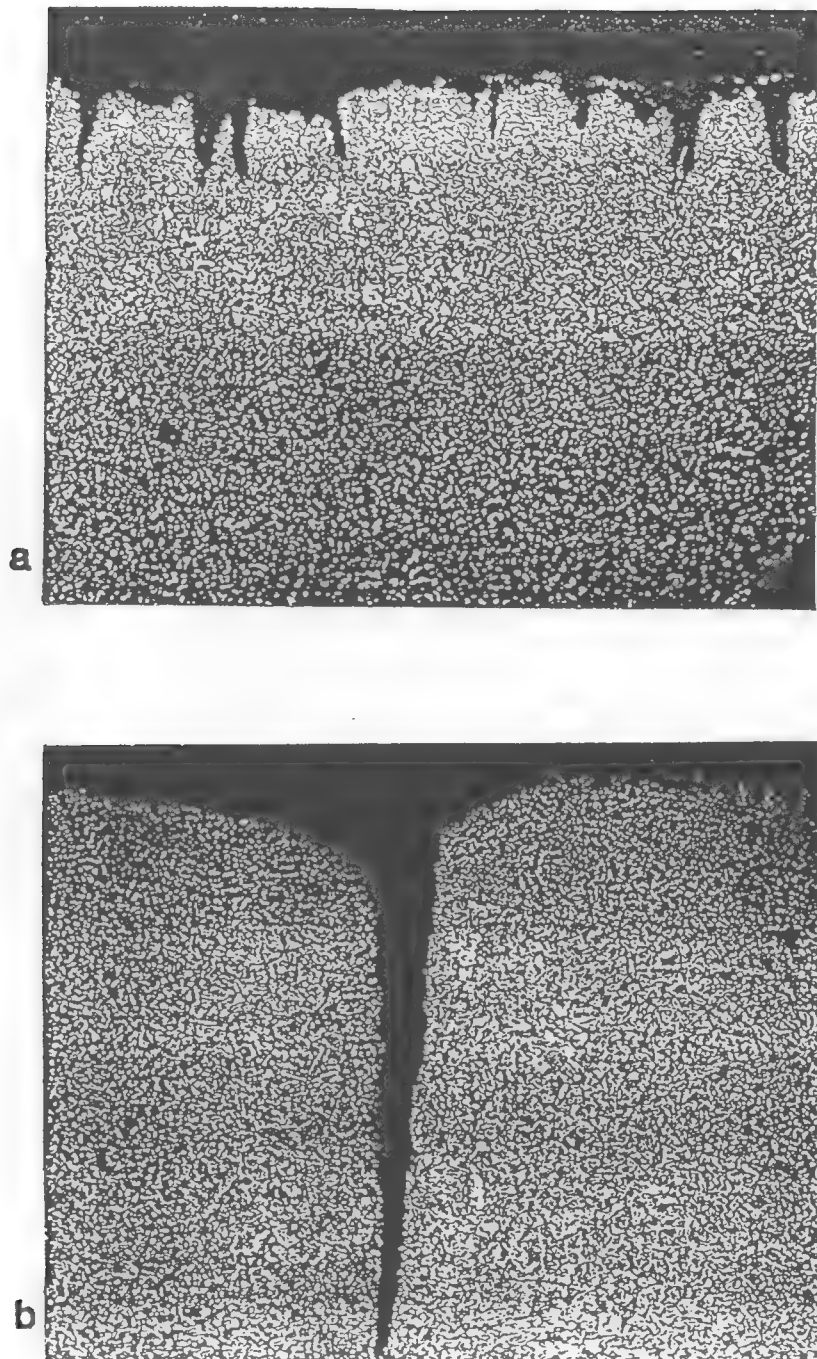


Fig. 4: Longitudinal cross section through the rod B;
10,000-60,000 psi stress range , 3.5% NaCl solution
with free air inlet; Magn. 176x . 2% Nital etch ;
a) Crack distribution after completing 7,563,000 cycles ;
Test #2 , CO₂ saturation.
b) Crack distribution after completing 1,559,000 cycles ;
Test #3.



a



b

Fig. 5: Cross section through the crack branching on Rod B
a) Test #1 (10,000-60,000 psi , 8%NaCl/CO₂/air , 5,653,000 cycles to failuar) Magn. 320x
b) Test #10 (10,000-35,000 psi , 3.5%NaCl/air , no failure at 17,781,000 cycles completed) Magn.176x

Corrosion Fatigue Performance

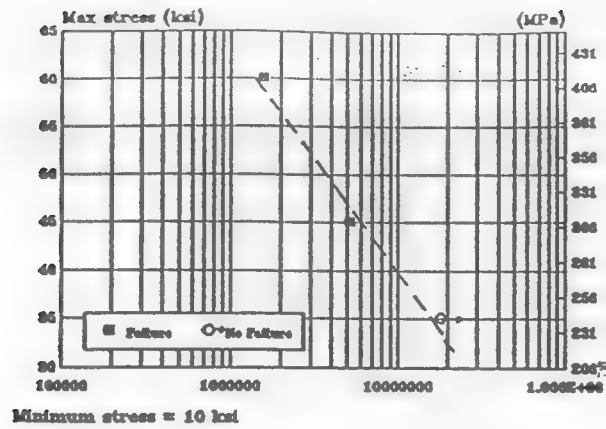
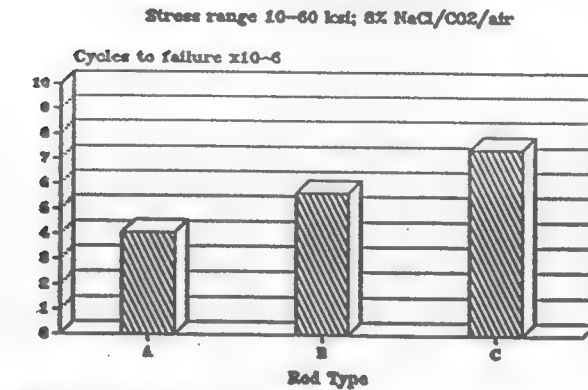
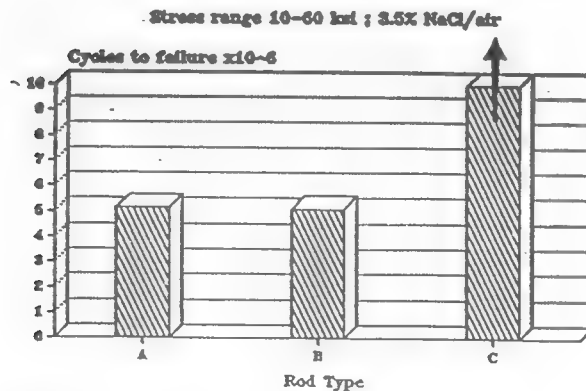


Fig. 6: Stress range influence on corrosion fatigue performance of Rod B in 3.5%NaCl/air environment.



Number of cycles is an average of minimum 3 experiments.

Fig. 7: Comparison of sucker rod corrosion fatigue performance 6%NaCl/CO₂/air, 10,000-60,000 psi stress range.



Number of cycles is an average of minimum 3 experiments.

Fig. 8: Comparison of sucker rod corrosion fatigue performance 3.5%NaCl/air, 10,000-45,000 psi stress range.

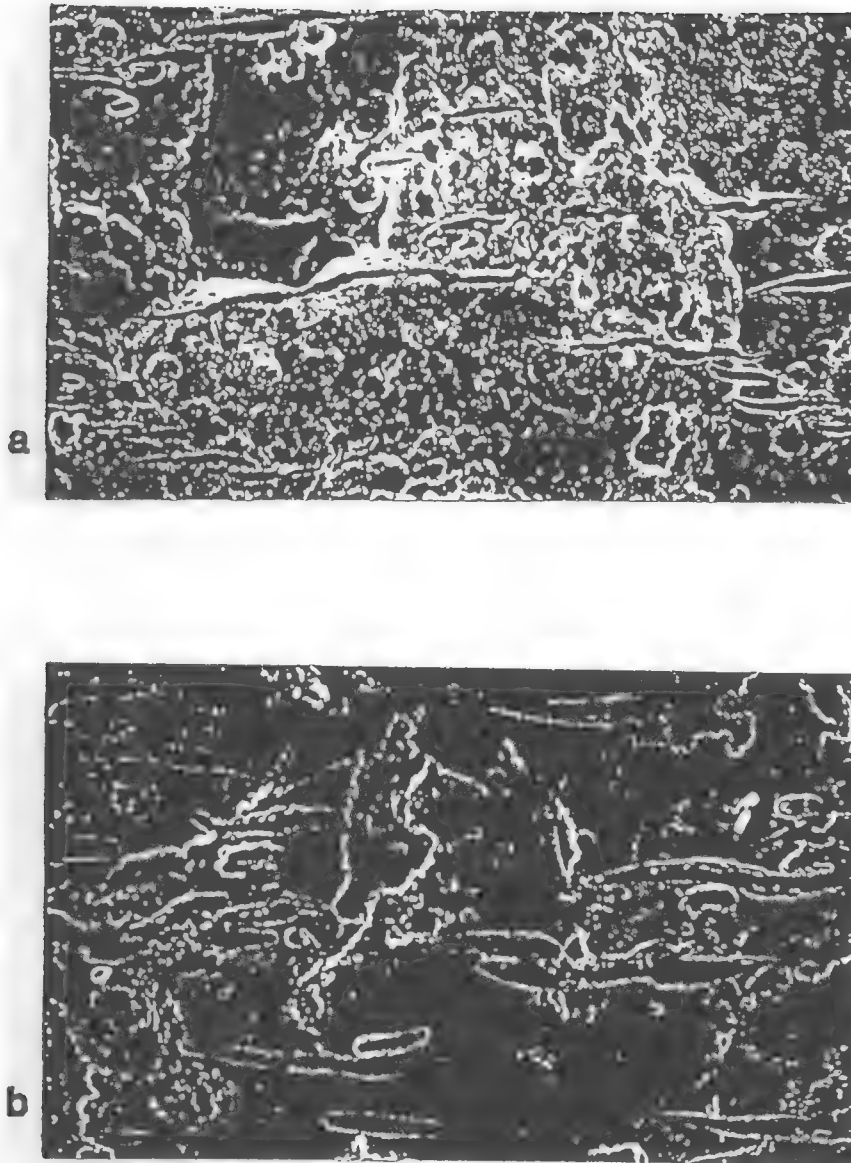


Fig. 9: SEM micrograph of cracks shape and distribution on the surface of:
a) Rod A (5,139,000 cycles to failure).
b) Rod C (10,000,0000 cycles no failure).
Magn. 110x

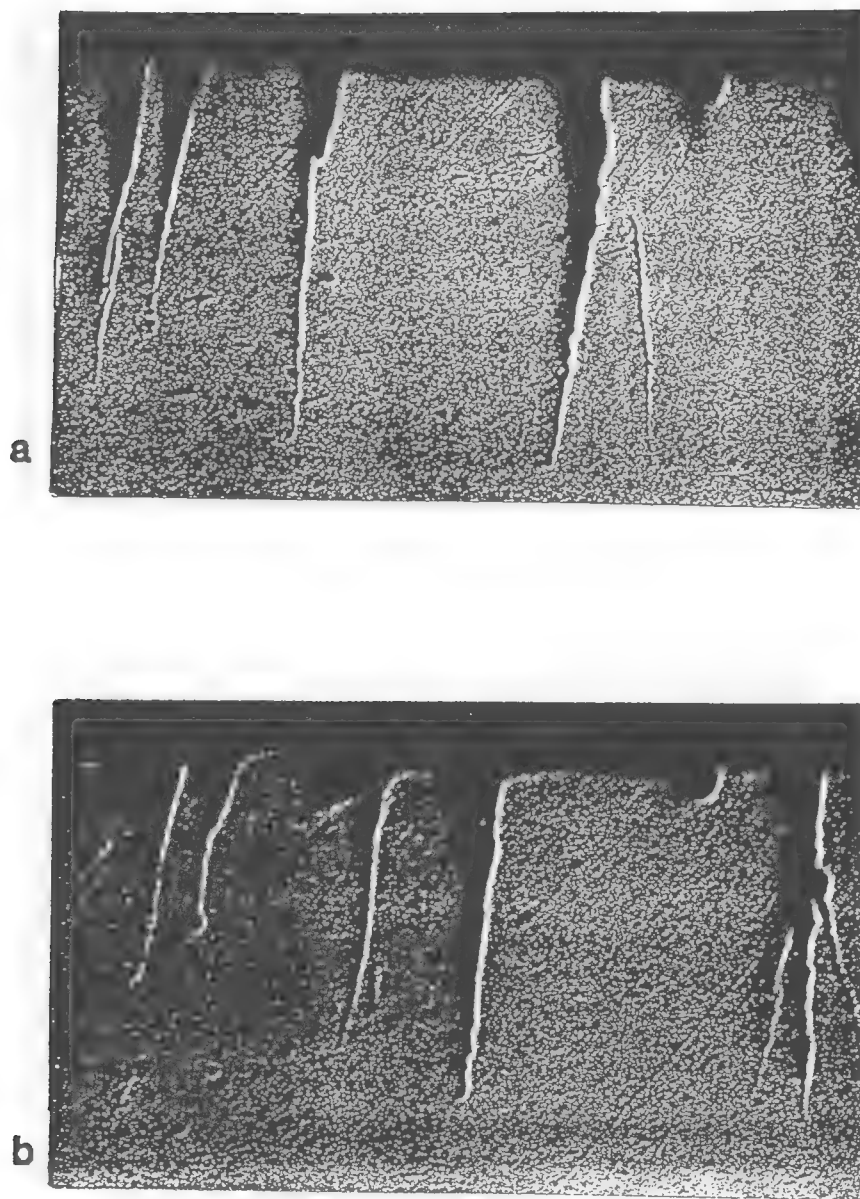


Fig. 10: Longitudinal cross section of areas shown in Fig. 9:
a) Rod A. b) Rod C. Magn. 176x

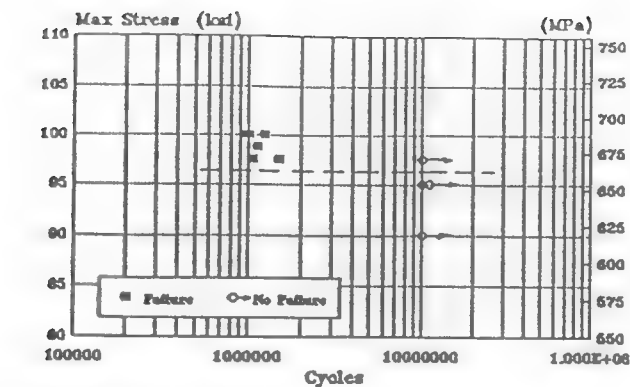


Fig. 11: Air fatigue edurance of Rod A.

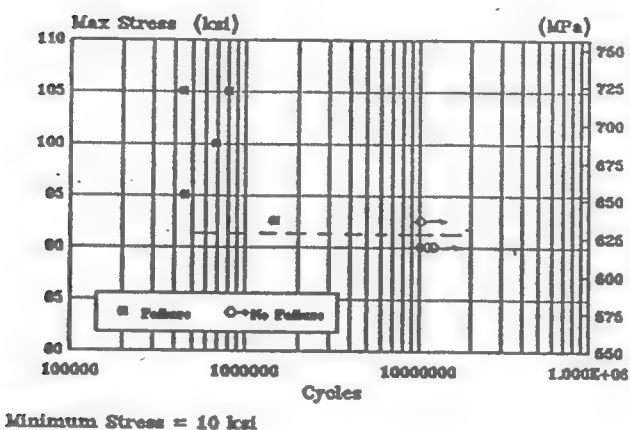


Fig. 12: Air fatigue edurance of Rod B.

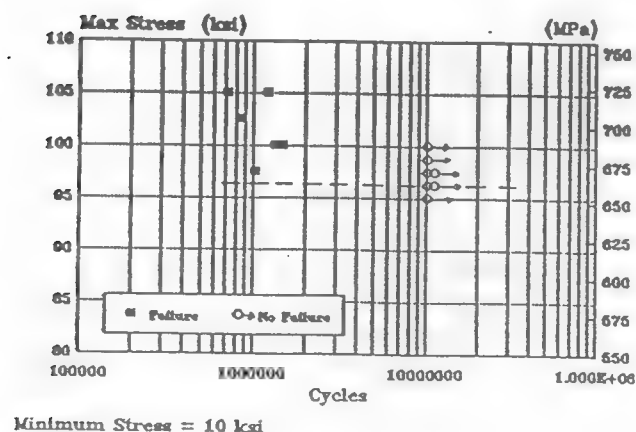


Fig. 13: Air fatigue edurance of Rod C.

CORROSION-FATIGUE OF OIL FIELD SUCKER RODS

Donald G. Bellow
University of Alberta
Edmonton, Alberta, Canada, T6G 2J9

Iwona Smuga-Otto
Centre for Frontier Engineering
Edmonton, Alberta, Canada, T6N 1E2

ABSTRACT

An extensive experimental program was undertaken to evaluate the effects of environment on the fatigue life of oil field sucker rods. A number of different environments were used; 3.5 and 8% NaCl, free of and saturated with CO₂, aerated and deaerated. Cycles to failure as well as microscopic inspection of propagating fatigue cracks were measured. The results showed the influence of air on the corrosion fatigue behaviour and an interesting crack branching development in the presence of CO₂.

From previous work it has been shown how the corrosion behaviour of metals can be evaluated using a potentiostat to measure corrosion currents for specific potentials. This research shows that there was little correlation between such data and the corrosion fatigue results.

Keywords: sucker rods, corrosion-fatigue, NaCl, CO₂, fatigue cracks, surface treatment, potentiodynamic testing.

INTRODUCTION

In artificial lift oil wells, sucker rods are used to impart a reciprocating motion to a pump located at the bottom of the well from the walking beam apparatus situated at the top of the well. A typical oil well configuration is shown schematically in Fig. 1. Because the sucker rod and its couplings are subjected to cyclic stresses, often in the presence of a corrosive environment, failure of the rods can occur due to corrosion-fatigue. Oil producers use a number of different techniques to prevent such failures such as adding corrosion inhibitors to the well fluid, coating the rods with epoxy, using high alloy content in the rod material, using over sized rods to reduce the operating stresses, using non-metallic rods, and so on. All of these preventative measures add to the production costs and none of them can be considered free from fault.

In an extensive study (Ref. 1) conducted by the authors in which over 5000 wells amongst eight producers were analyzed, it was found that the practices of combating corrosion-fatigue varied from one oil producer to the next. Furthermore, the American Petroleum Institute (API) primarily sets guidelines for the chemical composition of sucker rods. It is left for the producer to select and apply sucker rods according to his own field experience and operating goals. It is clear that more information on the corrosion-fatigue susceptibility of existing sucker rods would enable the producers to make a more appropriate selection of sucker rods for wells which are known to contain a high degree of corrosivity.

It was found during the study reported in Reference 1 that an accurate assessment of oil well environments was not possible. Often only the general conditions for a number of adjacent wells is known. Sometimes producers only classify well fluids as sweet (no H₂S) or sour (with H₂S). Thus, it was difficult to relate a particular failure frequency to a specific well environment. It was concluded that to design a specific laboratory experiment to simulate the general oil field conditions would not be possible, nor would there be any merit in designing a laboratory environment to match a specific well condition as there are so many different environments to consider. Instead, it was decided to select environments which had been used by others in evaluating corrosion-fatigue of metals but to use compositions which were common to oil field environments; that is, NaCl, air and CO₂. Hydrogen sulfide, which is commonly found in many oil wells, was not used in the testing reported in this paper because it was not considered to be a primary cause of problems amongst the wells surveyed. It was found that in the presence of H₂S the oil producers took special care to avoid failures whereas in the absence of H₂S no special precautions were taken and, as a result, more failures were experienced. However, it is recognized that a complete evaluation of the corrosion-fatigue susceptibility of sucker rods should also include H₂S as one of the environments evaluated.

ELECTROCHEMICAL TESTING

A study of the selection of corrosive environments was reported by the authors (Ref. 2). In the electrochemical study a potentiostat was used to determine the current densities for a variety of equilibrium times and scanning rates. It was concluded that no single environment, nor given potentiodynamic conditions, had an advantage over any others. It was suggested that a variety of potentiodynamic conditions be used to enable a ranking of materials typically along the lines shown in Fig. 2.

On the basis of the results shown in Fig. 2 it would appear that Rod Type A' was the most affected by the 3.5%NaCl/air environment and that Rod Type A was the least affected. In fact, when these same materials were subjected to corrosion-fatigue it was found that Rod Type A' had the best resistance to corrosion-fatigue. Similar observations were made with other environments tested. It was thus concluded that electrochemical testing in itself would not suffice to determine the resistance of a material to corrosion-fatigue.

CORROSION-FATIGUE LABORATORY CONDITIONS

From the survey reported in Reference 1 it was observed that most of the corrosion-fatigue failures occurred in wells with significant concentrations of CO₂ along with NaCl and water. Hydrogen sulphide was not generally found to be a major contributor although in some known high concentrations it has caused oil producers problems. A more common occurrence was surface pitting caused by CO₂. Thus, the environments used in the laboratory were based on a deaerated NaCl solution along with CO₂.

As the testing proceeded it was found that for the deaerated environments failure did not occur for any of the specimens within 10 million cycles. The stress level could have been increased but it would have been beyond the normal operating stresses prescribed by the Modified Goodman Diagram. It was found that if the environment was exposed to air (but not forceably) then the cycles to failure were reduced significantly. It was decided to conduct all further testing with the environments exposed to air since it is known that many oil wells contain significant amounts of oxygen.

Two levels of salinity, 3.5%NaCl and 8%NaCl were chosen. The latter was saturated with CO₂ and also represented an acidic condition where the pH was 5.7. With this environment it was

expected that the effects of severe pitting, observed on broken rods taken from the field, would manifest in early failure due to corrosion-fatigue.

EXPERIMENTAL TEST ARRANGEMENT

A Baldwin-Sonntag fatigue machine was adapted to apply cyclic bending loads at a testing frequency of 30Hz to 500mm lengths of sucker rods. Although sucker rods in an oil field situation will encounter primarily axial stresses, except at the upset ends where significant bending stresses can occur (see References 3 and 4), the main purpose of the study was to observe the initiation and propagation of surface cracks. It was believed the stress gradient in from the surface was not sufficient to affect the overall assessment of the corrosion-fatigue behaviour of different rods and surface treatments, especially when all rods would be tested under identical loading conditions.

The specimens were cut from sucker rods to the dimensions shown in Fig. 3. The milled notch on the underside was to ensure that failure would occur on the opposite side (maximum tensile stress) and at the midpoint of the rod section. The rod specimen was mounted in a 4-point loading system with the corrosion cell mounted between the inner two supports. The fluid medium was circulated by means of a peristaltic pump.

The stress levels were set so that the minimum stress was tensile at 6ksi (41 MPa) and the maximum stress at the desired level. Limit switches detected minute changes in specimen stiffness, due to a crack being developed, and were set to shut off the machine before the crack had propagated through the specimen. Each day of testing the fluid was changed or whenever a specimen failed, whichever occurred first. The test cell had a volume of one litre and was connected to a main reservoir containing 10 litres of the fluid environment. At the conclusion of a test the fatigued specimens were inspected by magnetic particle and U-V light, and by optical microscopy.

Under the influence of a corrosive environment materials do not exhibit an endurance limit. The scatter in the data is also less than if fatigued in air. Thus, there was close agreement between "identical" tests and that, in most cases, three tests were all that were required. If the scatter was more than deemed acceptable then additional tests were performed.

TEST RESULTS

To illustrate the influence of environment for a given stress level a single grade of sucker rod was fatigued in four different environments. The cycles to failure were averaged and are shown in Fig. 4. In a 3.5% NaCl solution the presence of air yielded a fatigue life of 1.6 million cycles whereas if air was excluded no failures were recorded within 10 million cycles. The interesting result was that when the same environment was saturated with CO₂, even in the presence of air, the fatigue life was extended from 1.6 to 6.9 million cycles. A similar effect was observed with the 8% NaCl solution. The fatigue life was increased from 1.9 million cycles to 5.6 million cycles with the addition of CO₂. The effect of increasing the salinity from 3.5 to 8% NaCl was not significant in the absence of CO₂ for the grade of sucker rod tested.

Microscopic inspection of the surfaces revealed that, in the presence of CO₂, a fatigue crack developed with considerable branching and prevented the crack from propagating much further. What appeared to have occurred was that the fatigue crack propagated in from the surface but was arrested by the compressive residual stress layer. In the presence of CO₂ this arrested crack was subjected to active pitting which had the effect of blunting the tip of the crack. With the progression of time and cyclic stress many cracks initiated from this blunted area but with less intensity than from a single crack as shown in Fig. 5a. In the absence of CO₂ this blunting did not occur and the initial crack propagated, more or less, as a single crack as shown in Fig. 5b.

One of the initial objectives of this study was to evaluate existing sucker rod materials to determine if the higher cost alloy rods gave superior resistance to corrosion-fatigue. It was observed that the fatigue resistance of the lower cost rods could be enhanced if the surfaces were given additional compressive residual stresses, either by thermal or mechanical treatment, or both. In one phase of the testing, eight different rod types were evaluated for corrosion-fatigue using a 3.5% NaCl solution and the results are plotted in Fig. 6. Not suprising, the rod which showed the best resistance to corrosion-fatigue also had the the deepest compressive residual stress profile. However, it was also shown that the rod which had the poorest performance (A in Fig. 6), with additional mechanical treatment, could be made to have the third best performance (A' in Fig. 6). Sucker rod E, whose performance was midpoint in the group, became equal to the best with additional mechanical treatment (E' in Fig. 6). The rods in Fig. 6 were of different chemical compositions as shown in Table 1. Comparing the alloy contents with the results in Fig. 6 it is seen that resistance to corrosion-fatigue was more influenced by surface treatment than by changes in chemical composition.

TABLE 1
CHEMICAL COMPOSITION OF SUCKER RODS EVALUATED

Rod Label	Steel Grade	Tensile Strength ksi	C	Mn	Cr	Ni	Mo	V
A,A'	4617	85/105	.15/.20	.55/.75	--	1.65/2.00	.20/.30	.03/.05
B	special	90/115	.33/.38	.65/.95	.70/.90	.40/.70	--	.03/.05
C	special	140Mx	.28/.33	.80/1.00	.80/1.00	1.65/2.00	.20/.30	.04/.05
D	4340	125/140	.38/.43	.60/.80	.70/.90	1.65/2.00	.20/.30	--
E,E'	special	120/140	.33/.38	.69/.95	.70/.90	.40/.70	--	.03/.05
F	4142	115/140	.40/.45	.75/1.00	.80 /1.10	--	.15/.25	--
G	1541Md	115/140	.38/.44	1.30/1.50	--	--	--	.05/.07
H	special	n.a.	.31/.38	.60/.90	.60/.90	1.25/1.75	--	--

SUMMARY

This paper describes how a simple apparatus can be used to develop an assessment of the corrosion-fatigue behaviour of a number of commercially available sucker rod materials. In using a saline and CO2 environment it is shown that the presence of CO2 actually inhibits the propagation of a fatigue crack by developing branching at the crack front. This was an unexpected result because it is known from field experience that CO2 causes severe pitting of the surface of sucker rods and it was expected that this would lower the resistance to fatigue.

The corrosion-fatigue results were consistent with earlier in-air fatigue testing in that, with the presence of compressive residual stresses on the surface of the rod, the fatigue life is improved. This occurs in a corrosive environment in spite of the fact that the susceptibility to corrosion increases with an increase in the magnitude of the residual stress. The governing factor is that the

resultant stress is less than the applied tensile stress due to the superposition of the compressive stress. Thus, fatigue cracks which are initiated on the surface due to pitting by the corrosive environment are slow to propagate due to the beneficial effects of the compressive residual stresses acting below the surface.

ACKNOWLEDGEMENTS

The authors express their sincere appreciation to Steltech Inc. for permission to include in this paper some of the results of a research contract carried out under their sponsorship. Thanks are also due to the Natural Sciences and Engineering Research Council for their financial support under Grant A-2705.

REFERENCES

1. Bellow, D.G., "Sucker Rod Strings, An Overview of Oil Field Practices and Experiences," Confidential Report for Stelco, Inc., Research and Development, 1987, 39 pages.
2. Bellow, D.G., Smuga-Otto, I., and Owens, D.C., "On the Selection of Steel Alloys for Corrosive Service", 8th International Conference on Offshore Mechanics and Arctic Engineering, " Vol.III, ASME den Haag, 1989, pp. 199-205.
3. Bellow, D.G., and Kumar, A., "Stress Analysis of Bent Sucker Rods," Jour. Can. Pet. Tech., 17(3),1978, pp. 76-81.
4. Bellow, D.G., and Howe, R.K., " Bending Stresses in Otherwise Straight Sucker Rods," Jour. Can. Pet. Tech., 27(5), 1988, pp. 53-57.

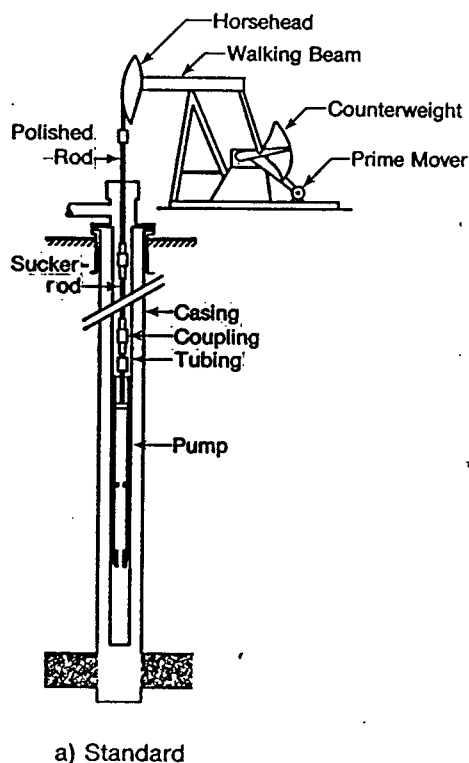


Fig. 1. Schematic of an Artificial Lift Oil Well

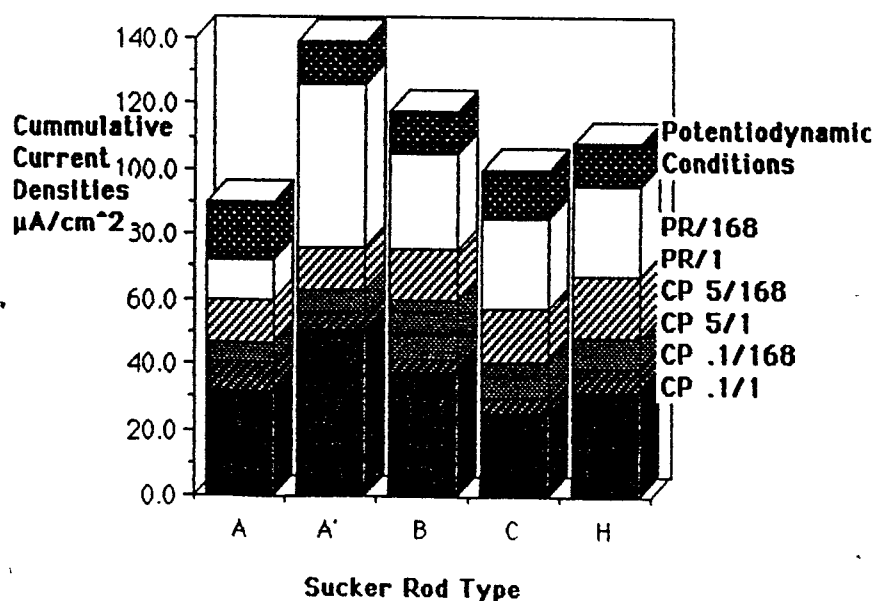


Fig. 2. Electrochemical Testing Results in 3.5% NaCl Solution

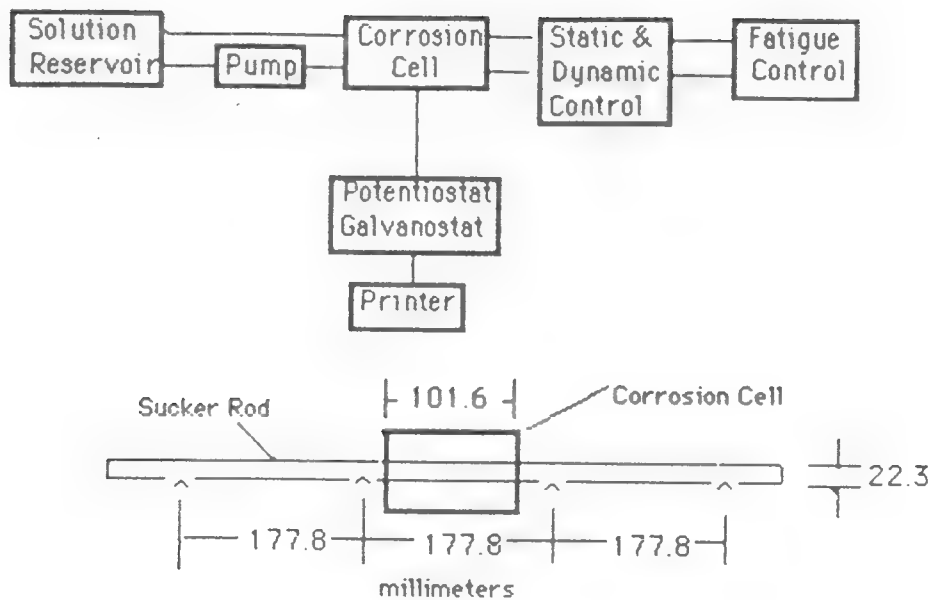


Fig. 3 Experimental Test Arrangement

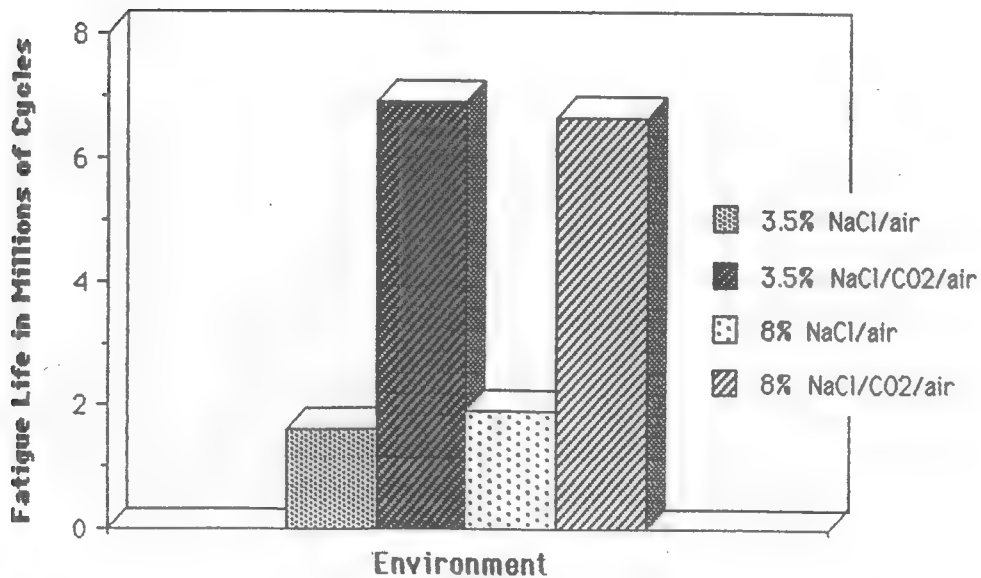


Fig.4 Effect of Environment of Fatigue Life

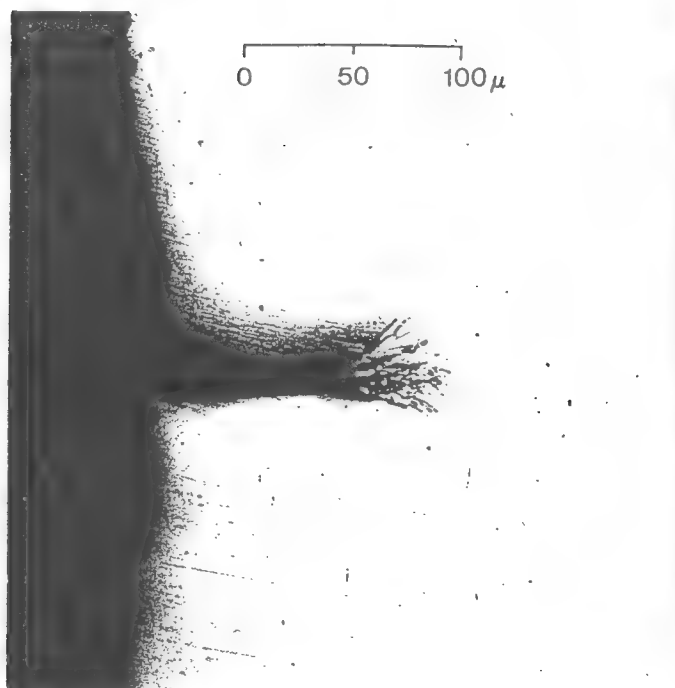


Fig. 5a. Corrosion Fatigue Crack
3.5% NaCl/air/CO₂ (x282)

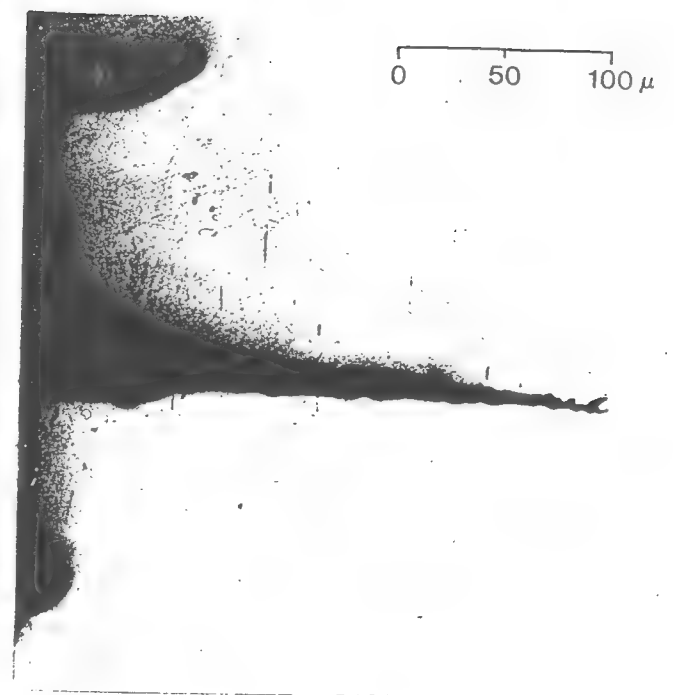


Fig. 5b. Corrosion Fatigue Crack
3.5% NaCl/air/no CO₂ (X282)

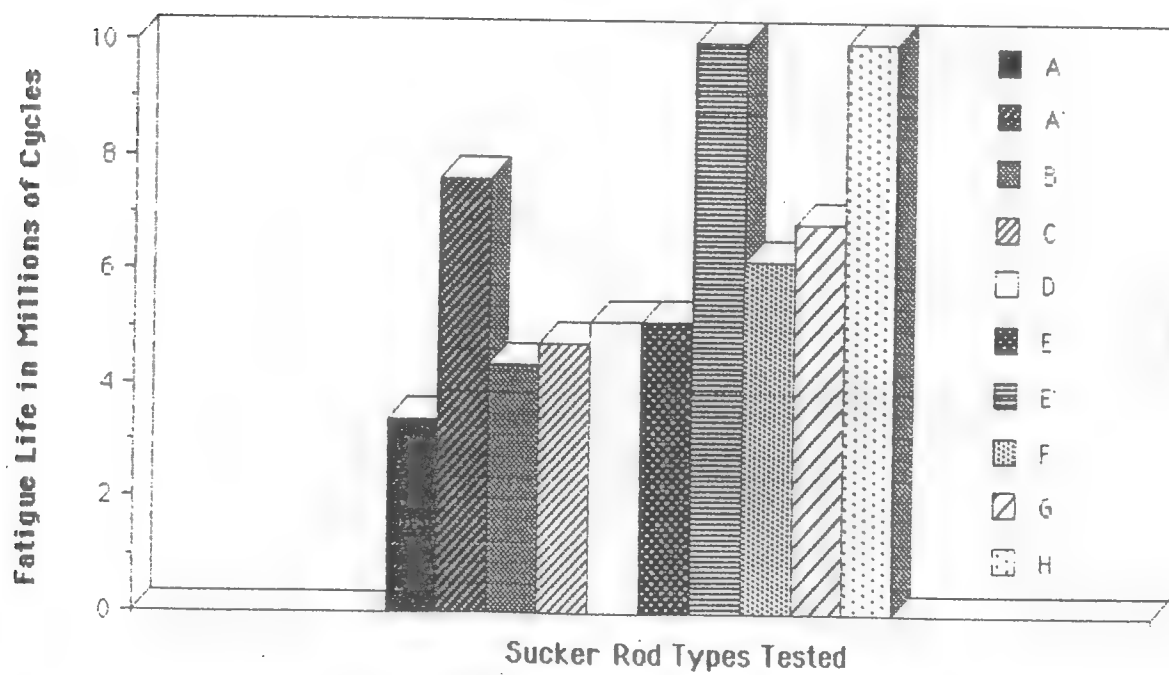


Fig. 6. Comparison of Corrosion-Fatigue Lives for Eight Different Sucker Rod Types in a 3.5% NaCl/air Environment

Case Study

An analysis of the wear of polymers

Donald G. Bellow and Narendra S. Viswanath

*University of Alberta, Department of Mechanical Engineering,
Edmonton, Alta. T6G 2G8 (Canada)*

Abstract

This paper describes an experimental programme used to evaluate the wear characteristics of a number of commercially available polymers when sliding against a steel counterface. A vertical pin-on-disc machine and a horizontal pin-on-disc machine were employed, using discs made from heat-treated, stress-relieved 4140 and AISI 1018 steels. All the tests were conducted at ambient temperature and humidity. The results showed that there is no relationship between wear and friction. The results also showed that the counterface roughness affected the wear behaviour of the polymers tested and that this should be considered in any model being developed for the wear of polymers.

1. Introduction

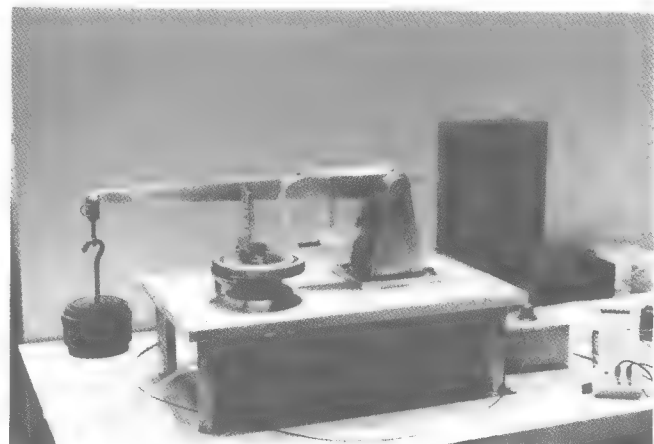
The increasing use of polymers as components in sliding systems has focused research on the modelling of the friction and wear behaviour, since not all polymers exhibit similar wear characteristics. The results of this experimental work are intended to form the basis for a mathematical model which can be used to predict the wear behaviour of polymers, or failing such a generalization, be used to predict the wear behaviour of a class of polymers.

The parameters that were controlled were the contact load, sliding speed, test duration (sliding distance), counterface roughness, counterface material and polymer type. The measured values were the coefficient of dry sliding friction, wear volume and the changes in counterface roughness and hardness. Wear and friction characteristics of polymers, including the effect of sliding speed and sliding distance, have been investigated by a number of authors [1-3]. Counterface roughness has been found to be a critical factor during the wear of polymers [4-6]. Comparisons have revealed that wear factors vary over several orders of magnitude for different polymers [7-9]; similarly, the coefficients of friction of polymers also vary with each other [7, 10] and yet there exists no physical evidence to support a relationship between wear and friction [11].

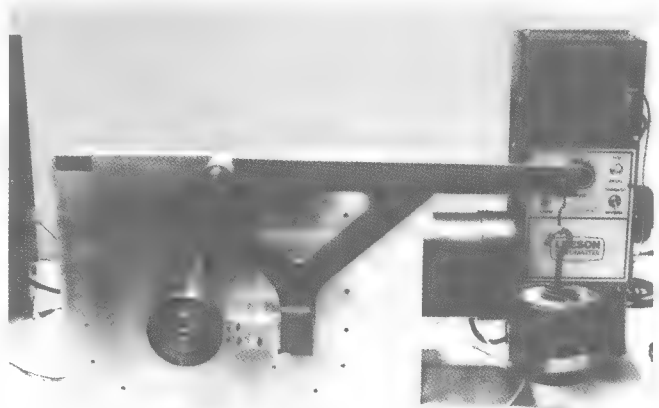
The results presented in this paper are part of ongoing research, where six different polymers were evaluated under identical operating conditions, and their wear factors and coefficients of friction are compared. In addition, the effect of the counterface material is discussed.

2. Experimental procedure

Wear testing was conducted on two pin-on-disc machines, using a variety of polymers as pins on two different steel rotating counterfaces. A photograph of the vertical pin-on-disc machine is shown in Fig. 1(a). The horizontal pin-on-disc machine shown in Fig. 1(b) used the same specimen geometry and loading ar-



(a)



(b)

Fig. 1. (a) Vertical and (b) horizontal pin-on-disc machines.

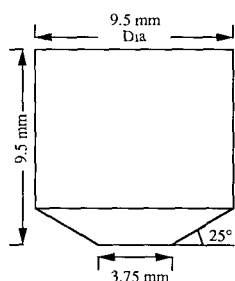


Fig. 2. Shape and dimensions of the polymer pin specimen.

ramentage as for the vertical pin-on-disc, but the metal counterface was the circumferential edge of the disc. For most cases, the relative results from the two machines were approximately the same, although the magnitude of wear was greater on the horizontal pin-on-disc machine.

For each data point, a minimum of three tests were performed. All the testing was conducted in an unlubricated state in ambient air conditions, where the temperature was controlled at $20 \pm 3^\circ\text{C}$ and the relative humidity (RH) did not vary for a given polymer by more than 5%, but over the entire testing programme varied in the range 20% to 50%.

Two different metal counterfaces were used; one was heat-treated, stress-relieved (HTSR) 4140 steel with a hardness of RA 63 and the other was made from cold-rolled AISI 1018 steel with a hardness of RA 47. The steel discs were machined flat, ground and polished for a surface finish in the range of $0.05\text{--}0.40\text{ }\mu\text{m}$. The counterface roughness (CLA) and profile were measured by means of a Talysurf IV instrument. Prior to a test, the disc was cleaned with acetone followed by methanol. The contact load between the pin and the disc was applied by means of a dead weight and lever arm arrangement. A load cell connected to the pin assembly allowed for a measurement of the dynamic friction force.

Some 12 different polymers were chosen for testing; 2 teflon types were used; virgin(v) and mechanical(m). The mechanical(m) type is extruded using recycled Teflon scrap. The specimens were machined to the shape of a truncated cone, as shown in Fig. 2. The end was polished with a 600 grit emery paper, washed in methanol and dried with compressed air. The specimens were weighed before and after testing to an accuracy of $\pm 0.0001\text{ g}$. From the weight difference, the volume of material lost during the test was calculated.

3. Results

Bartenev and Lavrenten [12] state that there is a direct relationship between friction and wear. For this study, a plot of coefficient of friction *vs.* wear volume

is shown in Fig. 3 for polymers under a normal load of 88.96 N, surface speed of 0.5 m s^{-1} , sliding against HTSR 4140 and AISI 1018 counterfaces with a roughness of $0.15\text{ }\mu\text{m}$ in both pin-on-disc machines for a duration of 5 h. From Fig. 3 it is seen that, while the coefficients of friction varied between 0.188 and 0.504, the corresponding wear volumes spanned four orders of magnitude, from a low of $5.31 \times 10^{-11}\text{ m}^3$ for ultrahigh molecular weight polyethylene to $1.47 \times 10^{-7}\text{ m}^3$ for Teflon against AISI 1018. Similar results were obtained for an HTSR 4140 steel counterface, where the coefficient of friction varied in the range 0.186–0.480, with corresponding wear volumes in the range $1.06 \times 10^{-10}\text{--}1.35 \times 10^{-7}\text{ m}^3$. The wear factors were found to be between 3.48×10^{-7} and $8.39 \times 10^{-6}\text{ mm}^3\text{ N}^{-1}\text{ m}^{-1}$ for all the polymers except teflon types, for which they were between 3.06×10^{-4} and $7.66 \times 10^{-4}\text{ mm}^3\text{ N}^{-1}\text{ m}^{-1}$. The wear factors were evaluated by dividing the wear volume by the load and sliding distance.

Figure 4(a) shows some typical wear results as affected by load, sliding speed, sliding length (duration of test) and counterface roughness for four polymer types. Similar results are shown in Fig. 4(b) for Teflon (v and m), whose wear factors were an order of magnitude higher than those of the other polymers tested. The wear factors of Delrin, Rulon and PVC were those least affected by increases in sliding speed, sliding length or counterface roughness. The decrease in the wear

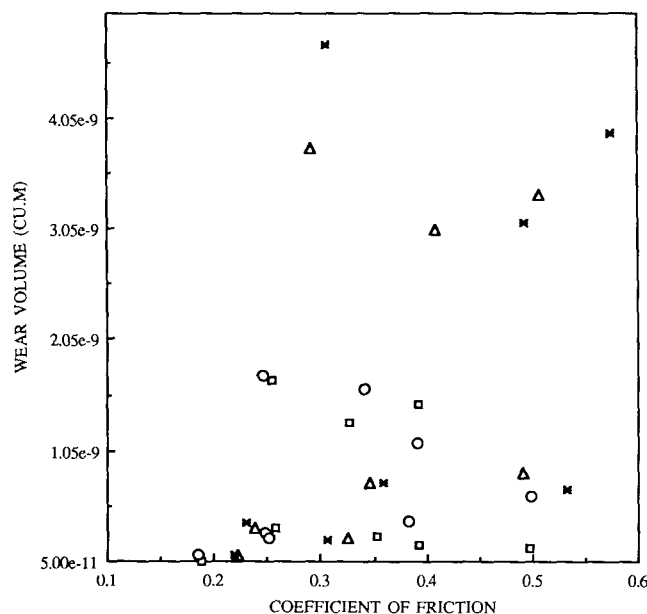


Fig. 3. Wear volume *vs.* coefficient of friction for polymers sliding against AISI 1018 steel and HTSR 4140 steel on horizontal and vertical pin-on-disc machines. Δ , HTSR 4140 steel, horizontal pin-on-disc machine; *, AISI 1018 steel, horizontal pin-on-disc machine; \circ , HTSR 4140 steel, vertical pin-on-disc machine; \square , AISI 1018 steel, vertical pin-on-disc machine.

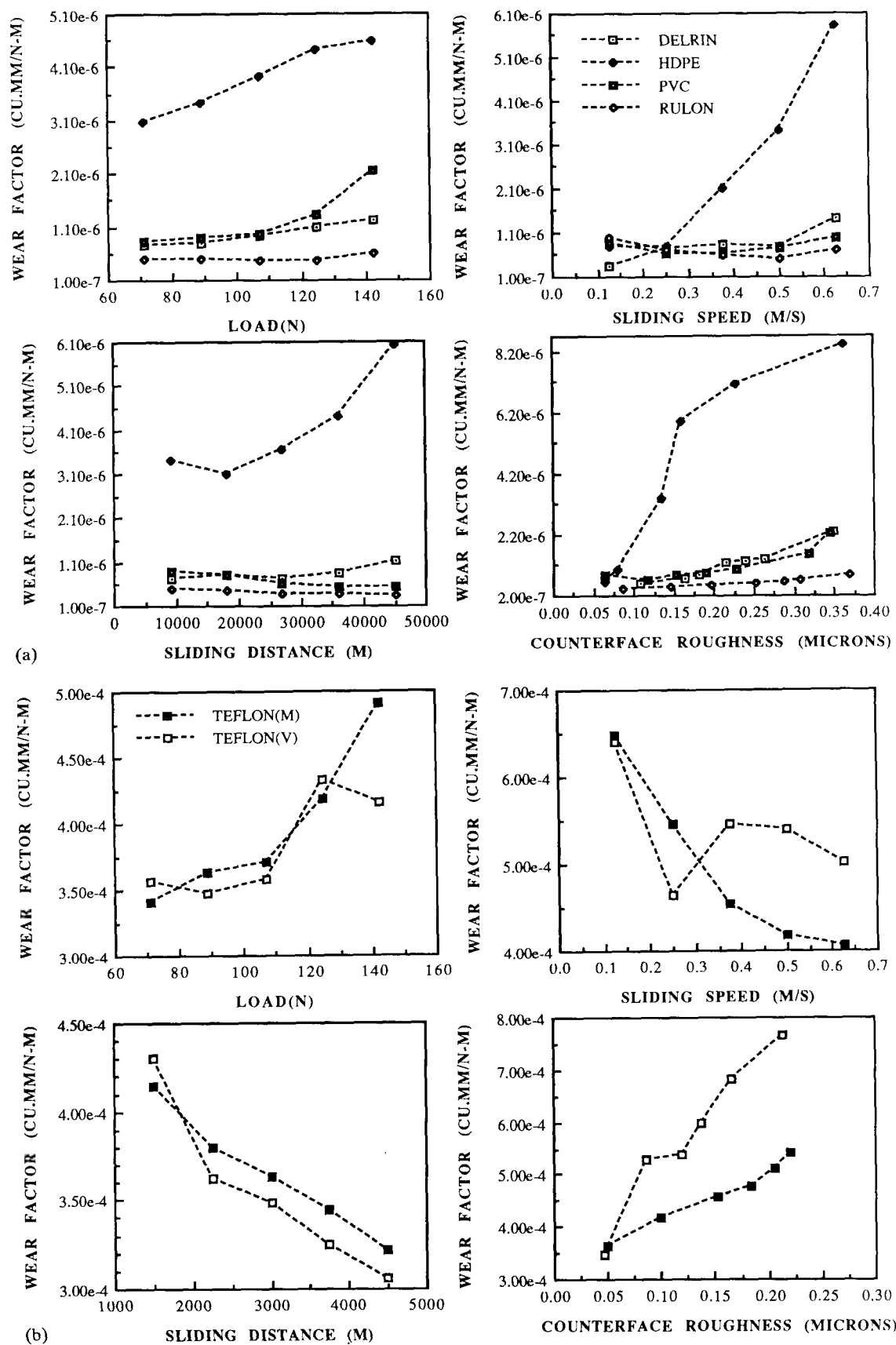


Fig. 4. Wear factor vs. operating variables for (a) different polymers and (b) Teflon (m and v) against AISI 1018 steel.

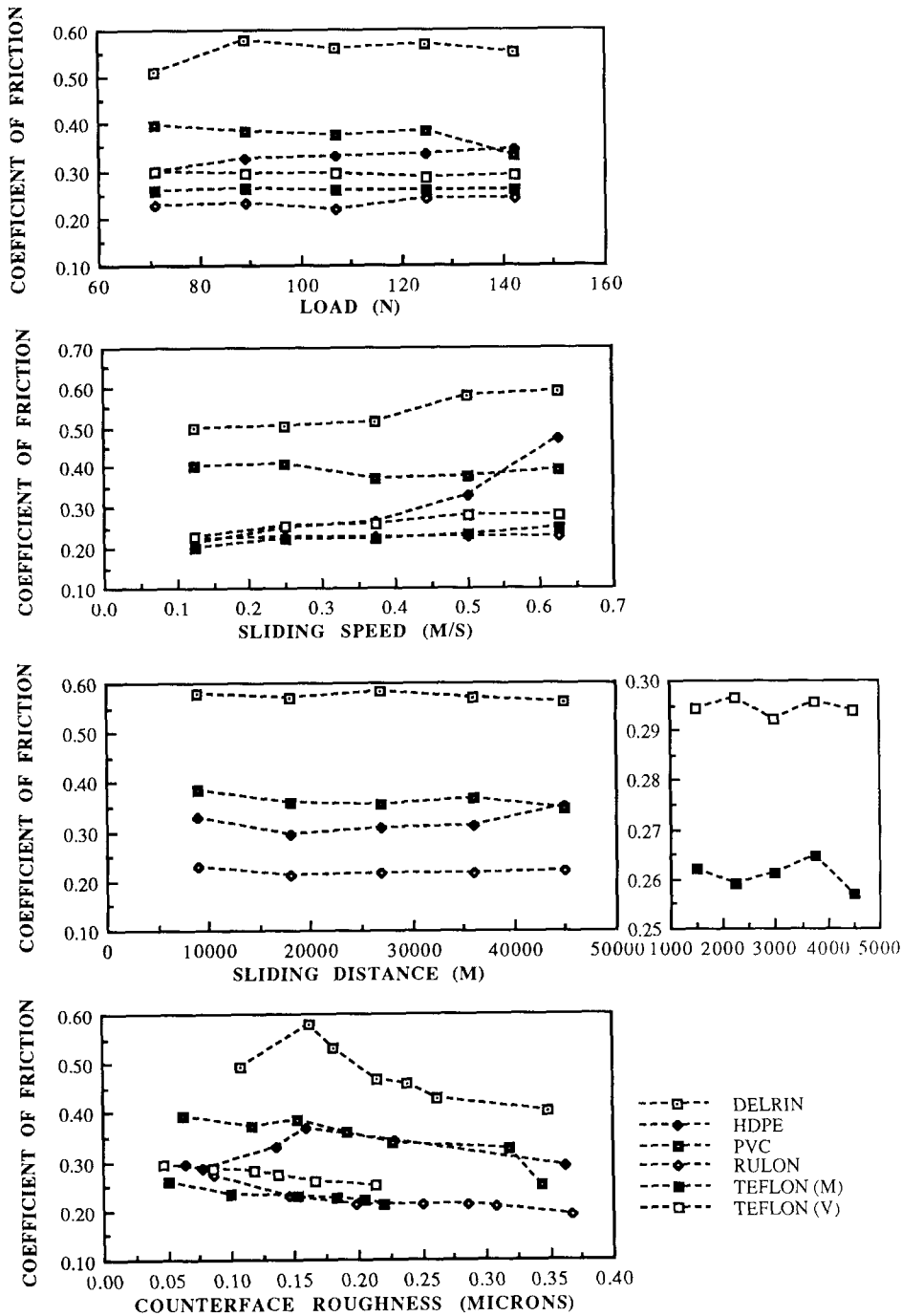


Fig. 5. Coefficient of friction vs. operating variables for different polymers against AISI 1018 steel.

factors of Teflon and no change in the wear factors for HDPE with increasing sliding speed were in agreement with the results of previous investigators. A similar behaviour of a decrease in the wear factors at higher speeds was observed by Dickens *et al.* [2]. The wear factors of both Teflon types increased continuously with increasing counterface roughness in the range up to 0.30 μm . The characteristic trend of an increase in the wear factor with an increase in the counterface rough-

ness was found for high density polyethylene (HDPE). The existence of two roughness ranges *i.e.* up to 0.15 μm and above 0.15 μm , corresponding to the rapid and gradual increase in the wear factor, can be found from Fig. 4(a). This was similar to the results obtained by Tanaka and Yamada [4] for both HDPE and low density polyethylene. No direct relationship between the wear factors and counterface roughness was evident from the test results.

The coefficient of friction remained relatively constant over a range of loads and sliding lengths, as seen in Fig. 5. In the case of HDPE, a relatively small increase in the coefficient of friction with sliding speed was observed, whereas the coefficient of friction decreased for PVC, which was sensitive to the sliding speed. The effect of the counterface roughness was more pronounced, with a decrease in friction occurring with an increase in counterface roughness. The relative order of magnitude of the coefficient of friction of polymers was the same under all operating conditions.

The wear and friction results in Figs. 4(a), 4(b) and 5 were obtained against an AISI 1018 steel counterface. The counterface material also had an effect on the wear of the polymers, as can be seen in Figs. 6 and 7, where the volume loss is plotted for a number of different polymers. The numbers on the bar graphs refer to the coefficients of friction. The two counterfaces, AISI 1018 and HTSR 4140, generally showed, for the same initial roughness, that the AISI 1018 counterface caused greater wear of the polymers than did HTSR 4140, although the AISI 1018 counterface had a hardness of RA 47, whereas the HTSR 4140 had a hardness of RA 63. The surface roughness did not change throughout a test but there appeared to be changes in the surface profile. This may have been due more to the type of measurement; the surface roughness is an averaging measurement, whereas the surface profile is not.

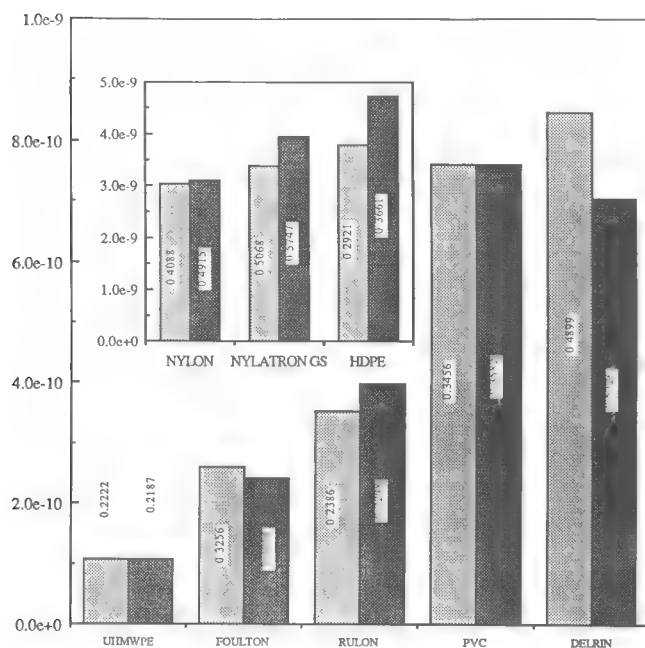


Fig. 6. Comparison of wear volume and coefficient of friction of polymers sliding against AISI 1018 steel and HTSR 4140 steel counterfaces. Sliding speed, 0.5 m s^{-1} ; load, 88.96 N ; time, $18\,000 \text{ s}$; counterface roughness, $0.15 \text{ }\mu\text{m}$; light shading, HTSR 4140; dark shading, AISI 1018.

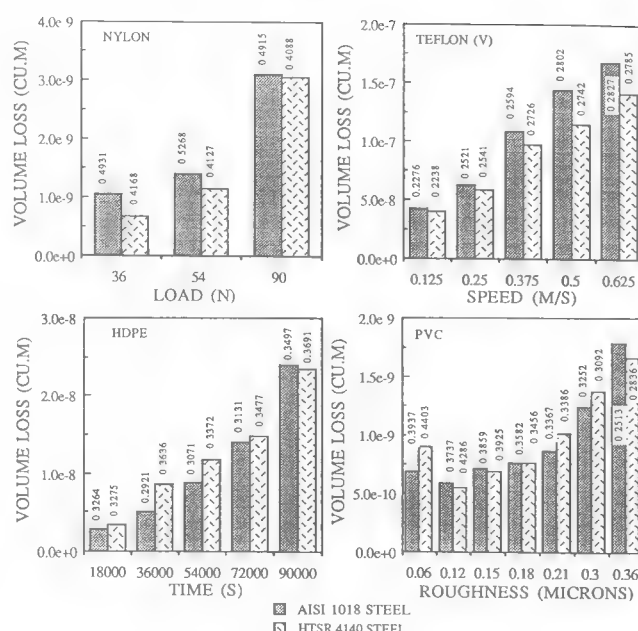


Fig. 7. General comparison of wear volume and coefficient of friction of different polymers sliding against AISI 1018 steel and HTSR 4140 steel counterfaces at different operating variables. Nylon: speed, 0.5 m s^{-1} ; time, $18\,000 \text{ s}$; counterface roughness, $0.15 \text{ }\mu\text{m}$. Teflon(v): load, 88.96 N ; time, 6000 s ; counterface roughness, $0.13 \text{ }\mu\text{m}$. HDPE: load, 88.96 N ; speed, 0.5 m s^{-1} ; counterface roughness, $0.13 \text{ }\mu\text{m}$. PVC: load, 88.96 N ; speed 0.5 m s^{-1} ; time, $18\,000 \text{ s}$.

The polymers tested did not show any single wear mechanism. Scanning electron micrographs were taken of all the worn polymer surfaces, although they are not shown here. It was evident from these micrographs that adhesive junctions had formed, resulting from broken fragments which were transferred to the steel counterface or produced as wear debris. Examples of abrasive wear producing severe gouging of the polymer surface were evident at higher counterface roughnesses. Some of the polymers exhibited delaminations at the interface. Fatigue wear was observed in cases where the counterface roughness was higher than $0.16 \text{ }\mu\text{m}$ (CLA) and with loads of $90\text{--}145 \text{ N}$, 0.5 m s^{-1} and $5\text{--}10 \text{ h}$ test duration.

4. Observations and conclusions

The purpose of this research was to evaluate a number of commercially available polymers which are being used in the oil field industry and to see if these results can be used to develop a useful model to predict the wear behaviour. This analysis is ongoing but the experimental results showed some interesting behaviours, particularly the effect of the metal counterface. More investigation is required on the effect of the counterface material but clearly the counterface roughness is im-

portant. The alloy content and hardness of the counterface also may play a role. The analysis confirmed that the wear volume is affected by the load, sliding speed, sliding length (test duration) and counterface roughness.

(1) The measured coefficient of friction is not related to the resistance to wear for the conditions applied in this research.

(2) For applications in the oil field industry, the wear resistance may be a more important feature than the coefficient of friction. For the polymers tested, the wear volume varied by three orders of magnitude, whereas the coefficient of friction remained within the range of 0.18–0.51.

(3) As the counterface roughness increased, the coefficient of friction was found to decrease but with a resulting increase in wear volume.

(4) An increase in the operating variables had no effect of the wear factor for Delrin, PVC and Rulon, whereas the wear factors varied for other polymers (HDPE, Teflon(m) and Teflon(v)).

(5) During sliding, the polymers were seen to load up the counterface profile but no changes in counterface roughness were detectable.

(6) There did not appear to be a generalized wear behaviour for all the polymers tested.

Acknowledgements

The authors express their appreciation to the Natural Sciences and Engineering Research Council (A2705)

and Esso Resources Canada Ltd., for their financial support.

References

- 1 M. Watanabe and H. Yamaguchi, *Wear*, **110** (1986) 379–388.
- 2 P. M. Dickens, J. L. Sullivan and J. K. Lancaster, *Wear*, **112** (1986) 273–389.
- 3 V. R. Agarwal, U. T. S. Pillai and A. Sethuramaiah, in K. C. Ludema (ed.), *Proc. Int. Conf. on Wear of Materials*, ASME, New York, 1989, pp. 501–506.
- 4 K. Tanaka and Y. Yamada, in K. C. Ludema (ed.), *Proc. Int. Conf. on Wear of Materials*, ASME, New York, 1987, pp. 407–414.
- 5 D. Dowson, S. Taheri and N. C. Wallbridge in K. C. Ludema (ed.), *Proc. Int. Conf. on Wear of Materials*, ASME, New York, 1987, pp. 415–425.
- 6 T. C. Ovaert and H. S. Cheng, *Wear*, **150** (1991) 275–287.
- 7 K. Holmberg and G. Wickstrom, *Wear*, **115** (1987) 95–05.
- 8 J. W. M. Mens and A. W. J. de Gee, *Wear*, **149** (1991) 255–268.
- 9 L. Lavielle, *Wear*, **151** (1991) 63–75.
- 10 M. Vaziri, F. H. Stott and R. T. Spurr, *Wear*, **122** (1988) 313–327.
- 11 V. R. Evans and F. E. Kennedy, in K. C. Ludema (ed.), *Proc. Int. Conf. on Wear of Materials*, ASME, New York, 1987, pp. 427–433.
- 12 G. M. Bartenev and V. V. Lavrenten, *Friction and Wear of Polymers*, Elsevier, Amsterdam, 1981.

EVALUATING THE WEAR OF DOWNHOLE OILFIELD COMPONENTS

Donald G. Bellow
University of Alberta
Edmonton, Canada

ABSTRACT

This paper describes the wear of downhole oilfield components and some of the problems encountered when correlating field tests with laboratory experiments. A number of examples are described whereby field tests have led to erroneous conclusions because all the operating parameters in the field were not known or precisely controlled. It is also shown that it is not always possible to replicate field conditions in the laboratory, and that the wear of components can be different than that predicted by the wear of the materials themselves.

INTRODUCTION

In determining experimental wear characteristics the control of the experiment, and the assumption and conditions imposed, can have a significant influence on the results. Although there are a number of different standards for testing a variety of different materials, no standard exists for the testing of downhole oil-field components. The purpose of this paper is to discuss the merits of simulating actual field conditions in the laboratory, and the difficulties that can arise in relating the results with field observations.

It has often been tried through trial and error to replicate wear rates and produce worn surfaces which are similar to those obtained in the field. However, such observations can lead to erroneous and misleading conclusions. For example, if the wear surface of a laboratory sample appears to be similar to the wear surface of a component taken from the field, it would be incorrect to assume that the surfaces had undergone the same loading and environmental conditions. It would be equally incorrect to assume that the same wear mechanism occurred in each case. To illustrate these points a few examples are taken from the oil producing industry.

A typical artificial lift system for an oil well consists of a double acting pump located at the bottom of the well which is connected to a reciprocating type walking beam apparatus on the surface. A series of rods and couplings, called a sucker rod string, connects the pump to the walking beam. The reciprocating action of the pump causes the couplings and rods to wear against the inner wall of the oil tubing. Eventually, wear can be so severe as to perforate the tubing, and/or wear away the couplings to the point where failure of the system occurs.

Oil producers employ a number of devices and systems to reduce downhole component wear. Plastic centralizers, injection moulded or cast on to the rod, plastic

coated couplings, hard spray metal couplings, continuous sucker rods (ie., no couplings), and wheeled couplings are being used to reduce downhole wear (Ref. 1). One of the biggest difficulties is that the wear of downhole components cannot be observed in situ, nor are the loading or environmental conditions accurately known. Only when the sucker rod string is pulled out of the well can the condition of the components be observed. Such inspections are very costly, and unless there are broken components to repair, the sucker rod string is not pulled to inspect for wear alone.

FIELD OBSERVATIONS

To measure downhole wear under actual operating conditions an experiment was reported (Ref. 2) whereby sucker rod couplings, standard and hard spray metal, were placed alternately along the entire length of the sucker rod string. Two wells were used in close proximity to one another. While the two wells were of similar depth one well was more deviated than the other, so it is suspected that the loading conditions may not have been the same. The pumping systems were put into operation until failure occurred, at which time the strings were pulled out and the tubing wear was measured by calipers. It was observed that the amount of wear was different between the wells, and that the hard spray metal couplings appeared to wear the tubing more in one well than the other. However, since the side loads (interface loads between the couplings and the tubing) were unknown, such observations provided little information in leading to a better understanding of the influence of the parameters on the wear, and in particular, what the wear mechanisms are. Furthermore, it is known that other operators have benefited by using hard spray metal couplings, and opposite to the views expressed in Ref. 2.

LABORATORY EXPERIMENTS

Effect of Third Body Abrasives

To illustrate how different conclusions to the above could be made, a laboratory experiment was devised (Ref. 3) to evaluate the wear of oilfield tubing using standard and hard spray metal couplings. In the laboratory water was used as the fluid medium and no sand or corrosive elements were added. Continuous monitoring of the sliding wear revealed two types of wear mechanisms; mild and severe wear. The debris from each was evaluated as were changes in the surface roughness and hardness at various stages during the experiment. The side loads were prescribed and carefully controlled as was the wear track. The results showed that the hard spray metal couplings had superior wear resistance compared with the standard coupling, but in contradiction to the field results reported in Ref. 1, the metal coated coupling wore the softer tubing less. as well. This can be seen in Fig. 1 where the superior wear resistance of the hard spray metal coupling is compared with the wear of a standard coupling. For example, at a side load of 890N the hard spray metal coupling was shown to have a loss of 2gm/10000m of travel whereas the wear for the standard coupling was 8gm/10000m of travel, or four times more than the hard spray metal coupling. In contrast to the observations made from the field (Ref. 2), the wear of the tubing by the metal coated coupling was less than caused by the standard coupling, as shown in Fig. 2. This was explained in Ref. 3 in that there was a transfer of nickel platelettes from the hard spray metal to the softer tubing, thus imparting an improved wear resistance to the tubing.

The above experiments were repeated with the same materials and loading and conditions except that a small quantity of sand 0.001% by weight (15gm/24hr) was introduced into the water stream to cause third body abrasive action. The wear results

of the standard and spray metal couplings along with the wear of the tubing are shown in Fig. 3 under a constant side load of 890N. The presence of sand increased the wear rates significantly for both coupling types and the tubing. In addition, the hard spray metal coupling caused more wear on the tubing than did the standard coupling. These results showed that the influence of sand prevented the transfer of nickel platelettes to the softer tubing, and thus the tubing wear was greater with a hard spray metal coupling than with the standard coupling. This experiment illustrated the influence of sand on the wear behaviour, and that if sand cannot be prevented from entering the rubbing interfaces, then the beneficial effects of the hard spray metal coupling are lost.

In another set of experiments designed to evaluate the presence of third body abrasives, the wear of plastics used as centralizers/scrapers attached to the sucker rods was investigated. Centralizers/scrapers are 100-150mm lengths of plastic, usually fluted, which are bonded at intervals along the length of the sucker rod string where rubbing of the sucker rod is expected to cause severe wear of the oilfield tubing. The principle is that the plastic will wear, and, being softer than the metal tubing, it will protect the tubing from excessive wear. This is not always successful because the rubbing of the plastic against the metal tubing removes the passive corrosive layer attached to the metal tubing causing accelerated corrosive wear. The other problem encountered is the plastic centralizers/scrapers can wear prematurely, especially in the presence of sand, thus negating their purpose and requiring costly workovers of the sucker rod string assembly.

In Ref. 1 it was shown how various types of plastics used for centralizers/scrapers wear as a function of contact load and distance travelled. A typical set of data is shown in Fig. 4 for two types of materials; nylon and ryton. In the absence of any third body abrasive the ryton scraper wore far less than the nylon scraper, and in fact, for the ryton scraper, the wear appeared to level off and independent of load beyond 133N. On the basis of these tests it could be concluded that the ryton scraper had superior wear resistance when compared to nylon. However, in the presence of a third body abrasive (sand) there appeared some curious, if not conflicting, results. The presence of sand appeared to reduce the wear of the nylon scraper. This is explained by the fact that sand became imbedded in the plastic thus enhancing its surface hardness. This, of course, would lead to accelerated wear of the tubing. For the ryton scraper just the opposite occurred. In the presence of sand the ryton scraper showed increased wear. Finally, from Fig. 4 it is seen that in the presence of sand these two plastics had similar wear rates, although as discussed above, for different reasons.

Effect of Loading Characteristics

In cases where oil wells are deviated, offset, or slanted, some oil producers employ roller or wheeled couplings. A typical design is to use a plastic wheel which rotates on a steel bushing. Four such wheels are mounted in a steel coupling with the wheels arranged so that they are always in contact with the tubing regardless of the orientation of the coupling down the well. When in operation the wheels will be subjected to concentrated radial loads. The outer diameter of the plastic wheel will be subjected to smaller contact pressure than the inner diameter of the plastic wheel. Wheeled couplings taken from the field have shown that they were subjected to sliding, as well as rolling wear. Also, in some cases the wheels had seized which caused them to wear flat on one side. This also caused deep grooves to be worn in the tubing.

In an attempt to evaluate the wear of the plastic wheels used in wheeled couplings a special apparatus was constructed and has been described in Ref. 1. This apparatus

allowed the wheels to roll and slide as the coupling body was simulated in a reciprocating action. Although a variety of wear behaviours were observed there were no experimental conditions which caused the wheels to slide without rolling. This suggested that a sand/tar environment, observed from some specimens taken from the field, would be needed at the interface between the inner diameter of the plastic wheel and the steel bushing in order for the wheel to become seized.

The experimental apparatus allowed the observation of some conflicting results due to the manner in which the load was applied to the plastic wheels. In comparing two plastic materials, nylon and delrin (polyacetate), it was found that the wear behaviour differed depending on whether the inner diameter wear was being measured, which was pure rolling, or the outer diameter wear was being measured, which was a combination of rolling plus sliding. This is illustrated in Figs. 5 & 6. Although the outer diameter wear of the plastic wheels was more than the inner diameter, because of the greater sliding distance travelled, it is interesting to note that if the two plastics evaluated were to have been ranked for wear based on the outer diameter wear, the ranking would have been just opposite on the basis of the inner hole diameter wear.

The wear behaviour of plastic materials is no less complex than that for metals. The wear of plastic on metal is influenced by the initial surface roughness of the metal, more so than for metal-to-metal wear. It has been found that under certain conditions the surface roughness of the metal changes very little under repeated sliding action of a plastic material and the metal surface itself abrades away the plastic material. For other plastics the metal surface is soon "filled" with plastic, and thus a hybrid plastic-metal surface is developed. In such cases further wear of the plastic is retarded. In still other cases the effect of the plastic wearing against the metal tubing, in the presence of a corrosive environment, removes the passive corrosive layer, and thus accelerates the corrosion wear of the metal tubing.

DISCUSSION

The foregoing illustrates some of the difficulties that can be encountered when determining the wear behaviour of materials in a downhole oilfield application. The merits of conducting wear tests in the field are questionable and have little scientific validity when the test conditions are unknown. A more meaningful approach is to conduct laboratory testing under closely controlled and known conditions. The disadvantage of such testing is that the results may not correlate well with field experience. Ideally, laboratory data can be used to rank materials, and then the results can be compared with field experience.

In evaluating wear a number of parameters can be measured such as weight loss and geometrical changes. In the case of metal-to-metal wear the changes in the surface hardness and surface topography (roughness) should also be measured. The wear track should be inspected carefully using optical and scanning electron microscopy as should the wear debris. Also, the effects of corrosion should not be overlooked. Corrosion has a synergistic effect on the wear mechanisms.

It has been shown that the determination of wear of components in an artificial oil well lift system is difficult, whether carried out in the laboratory or conducted in the field. In general, no laboratory experiment can take the place of a properly run field test. However, in the case of an oilfield sucker rod string the wear of the downhole components cannot be related to the operating conditions with any degree of accuracy or precision. Thus, the best and recommended approach, is to conduct laboratory

experiments under a variety of different, but closely controlled, conditions to obtain a ranking of materials or components. The results can be used to select those materials which show merit and then apply these samples in a few test oil wells to confirm or refute the laboratory analysis. It should be emphasized that the more that is known about the field conditions, and the more closely these are followed in the laboratory, the better informed the analysis will become.

ACKNOWLEDGEMENTS

The author wishes to thank Esso Resources Canada Ltd. and the Natural Sciences and Engineering Research Council of Canada for the financial assistance in aid of this research.

REFERENCES

1. Bellow, D.G., Chiu, A.S., and Owens, D.C., "Wear of Plastic Components used in Oil Wells", Proceedings of Japan Tribology Conference, Nagoya, 1990.
2. McCaslin, K.P., "A Study of the Methods of Preventing Rodwear Tubing Leaks in Sucker Rod Pumping Wells," Society of Petroleum Engineers, SPE-16198, pp 125-131, 1987.
3. Bellow, D.G., Owens, D.C., and Smuga-Otto, I., "Wear of Standard and Hard Metal Coated Couplings and Oilfield Tubing", *Wear*, 133, pp 83-93, 1989.

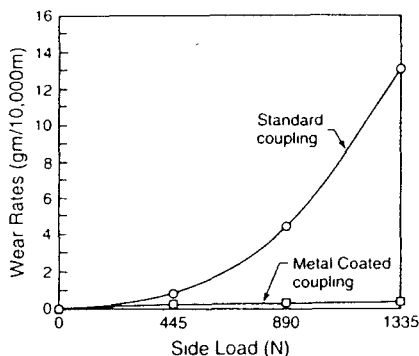


Fig. 1 Wear of Standard and Coated Couplings

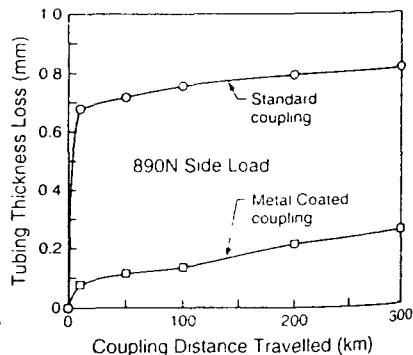


Fig. 2 Wear of Tubing by Couplings

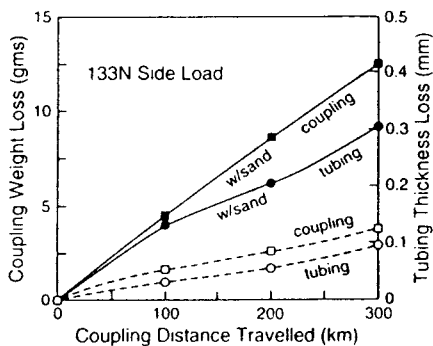


Fig. 3 Wear of Couplings and Tubing - Sand Environment

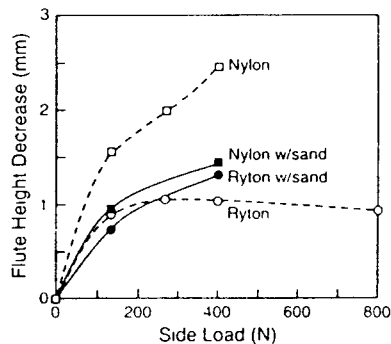


Fig. 4 Wear of Plastic Scrapers with Tubing in Sand.

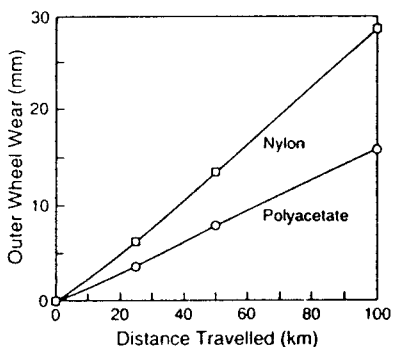


Fig. 5 Outer Diameter Roller Wheel Wear

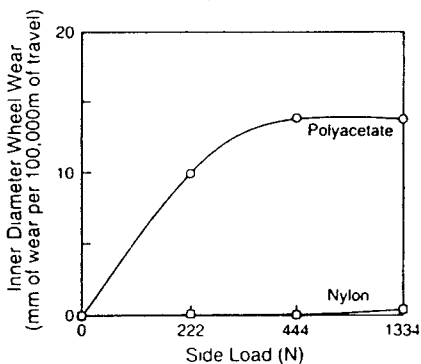


Fig. 6 Inner Diameter Roller Wheel Wear

6TH INTERNATIONAL CONGRESS ON TRIBOLOGY

August 30 - September 2, 1993

Budapest - Hungary

Development of an equation for the wear of polymers

N. Viswanath, D.G. Bellow

Department of Mechanical Engineering, University of Alberta, Edmonton, Alta. T6G 2G8, Canada

Received 26 April 1994; accepted 11 October 1994

Abstract

The aim of this research was to investigate and analyze the wear of polymers by use of an empirical wear equation. A dimensional analysis was carried out to develop an equation in which the volume of polymer material worn during sliding on a horizontal pin-on-disk machine was expressed in terms of the operating conditions, properties of the polymer, and counterface roughness. Both a linear and a non-linear relationship of volume loss with other variables was considered in evaluating a dimensionless wear coefficient. It was concluded that a better correlation with the variables was obtained using a non-linear relationship.

Keywords: Wear model; Dimensional analysis; Polymers; Metal–polymer interface; Countersurface roughness

1. Introduction

The wear of polymers is determined by the nature of the materials, the surface and bulk mechanical, physical and chemical properties of the frictionally interacting bodies, the operating parameters, the macro and micro-geometry, and the working environment. Investigations by Rymuza [1] show that the wear dynamics of polymer–polymer and polymer–metal systems are determined by properties of the polymer such as surface energy, modulus of elasticity, specific heat, thermal conductivity, and various operating conditions.

Ratner et al. [2], Lewis [3], Rhee [4], Lancaster [5], Atkinson et al. [6], Eiss et al. [7], Dowson et al. [8], and others have developed various forms of equations/relationships for the wear of polymers. All these models have expressed wear volume as a function of either the operating variables such as load/pressure, speed, sliding length/duration or include properties such as hardness of the counterface, asperity height, shear strength of the polymer, etc. In 1974 Kar and Bahadur [9] developed a wear equation using a dimensional analysis for adhesive wear of POM and 20% PTFE-filled POM. They considered the experimental variables which appeared to influence the wear process at a polymer–metal sliding interface and to express them as an equation to determine a wear constant. The wear equation was in terms of the sliding variables, pressure P , speed v and time T , and the material properties, modulus of elasticity E , surface energy γ , thermal conductivity K and specific heat C_p . This resulted in

four dimensionless groups. The Kar and Bahadur wear equation was derived as follows:

$$V = k P^x v^{y-z} T^y \gamma^{3-y+z} E^{-3-x+y} \left(\frac{C_p}{K} \right)^z \quad (1)$$

where x , y and z are exponents determined experimentally.

The above equation was based specifically on wear tests from the materials considered but the model could be extended to other materials. It did not include any effects of counterface roughness.

Except for the equation of Kar and Bahadur [9] most of the wear equations have related the volume loss to the operating variables through a wear constant or a wear coefficient. All the uncertainties in other variables are contained within the wear constant k . Because this constant is a combination of all the other uncertainties, it does not describe the influence of the individual factors.

Wear is not an intrinsic material property, rather it depends on physical quantities and/or operating variables. Therefore a reliable relationship between the wear of polymers and both the operating variables and polymer material properties is desirable in order to obtain a better understanding of the wear behaviour of polymers.

2. Development and significance of the wear equation

The concept of dimensional analysis defines in an explicit fashion the operations on a set of dimensional

quantities and was used in developing the wear equation by Kar and Bahadur [9]. Dimensional analysis is based on the hypothesis that the solution of the problem is expressible by means of a dimensionally homogeneous equation in terms of specified variables. This method can be used to characterize a phenomenon in terms of the relationships among dimensionless variables which are fewer in number than the original physical variables. It also helps to predict the qualitative form of the mathematical relationship. Expanding on the work of Kar and Bahadur [9] the present work shows how the wear equation can be modified to include the effects of the roughness of the counterface and be applied to a wide variety of polymers [10].

Wear volume was used as the main dependent variable. Sliding velocity, modulus of elasticity, surface energy and thermal conductivity were used as independent variables. The four primary dimensions were mass (M), length (L), time (T) and temperature (Θ). The dependent variable wear volume V was grouped and expressed as

$$\Psi(V, W, T, \alpha, C_p, \gamma, E, v, K) = 0 \quad (2)$$

where Ψ was some arbitrary function.

The dimensional analysis reduced the number of variables from nine to five dimensionless groups using the Buckingham Pi theorem [11,12] and the physical significance of each of these groups is explained as follows:

$$\left(\frac{VE^3}{\gamma^3}\right) \quad \left(\frac{WE}{\gamma^2}\right) \quad \left(\frac{vTE}{\gamma}\right) \quad \left(\frac{\alpha E}{\gamma}\right) \quad \left(\frac{C_p \gamma}{vK}\right)$$

$$\frac{VE^3}{\gamma^3}$$

This group contains the wear volume as a dependent variable. It represent the significance of interface contact and deformation.

$$\frac{WE}{\gamma^2}$$

This group involves normal load along with the modulus of elasticity and represents deformation under load. Surface energy contributes to interface junction strength. The group can be split as $(W/\gamma)(E/\gamma)$, which represents the influence of normal load on interface contact and its strength characteristics.

$$\frac{vTE}{\gamma}$$

or

$$\left\{\frac{TEC_p}{K}\right\}$$

In this group the speed and duration of a test combine to give sliding distance during the wear process. Along with modulus of elasticity and surface energy, this group represents the distance over which formation and deformation of junctions occur. By combining the $\{vTE/\gamma\}$ and $\{C_p \gamma/vK\}$, a new group $\{TEC_p/K\}$ is obtained, which has duration of test as the operating variable. This group shows that with an increase in time, variation in temperature and thermal factor (C_p/K) will occur.

$$\frac{\alpha E}{\gamma}$$

This group includes the counterface roughness ' α ' which determines the apparent contact area that supports the load and can influence the type of wear process that occurs.

$$\frac{\gamma C_p}{vK}$$

The ratio (C_p/K) is a factor controlling the thermal contribution during interface formation and that this thermal effect is influenced by speed. The group is rewritten as $\{vK/\gamma C_p\}$ to represent velocity as a prime variable.

Redefining Eq. (2) by combining all the groups the following expression containing five dimensionless groups can be obtained:

$$\Psi\left(\frac{VE^3}{\gamma^3}, \frac{WE}{\gamma^2}, \frac{vK}{\gamma C_p}, \frac{TEC_p}{K}, \frac{\alpha E}{\gamma}\right) = 0 \quad (3)$$

The main dependent group $\{VE^3/\gamma^3\}$ was expressed in terms of the undetermined function Ψ comprising the other four groups. The undetermined function Ψ was evaluated from the experiments and then a relationship was established between the main dependent variable, the volume V of the worn polymer material, and the variables influencing the wear of polymers. Eq. (3) was rewritten as

$$\left(\frac{VE^3}{\gamma^3}\right) = \Psi\left(\frac{WE}{\gamma^2}, \frac{vK}{\gamma C_p}, \frac{TEC_p}{K}, \frac{\alpha E}{\gamma}\right) \quad (4)$$

In Eq. (4), the volume of material lost is expressed in terms of the operating variables (normal load, sliding speed, duration of test and counterface roughness) which were controlled during the experiments, and material properties (modulus of elasticity, surface energy, specific heat, and thermal conductivity). To find the undetermined function Ψ in the above equation, a number of experiments were conducted by varying only one operating variable at a time while maintaining the other variables constant. This was the same as controlling the dimensionless groups because each group had only one operating variable and the rest were material properties which were constant for a given polymer.

The undetermined function Ψ was assumed to be either linear or non-linear and the main dependent group with the wear volume in Eq. (4) was expressed as being proportional to the other groups. For the linear relationship

$$\frac{VE^3}{\gamma^3} \propto \left(\frac{WE}{\gamma^2}\right) \left(\frac{vK}{\gamma C_p}\right) \left(\frac{TEC_p}{K}\right) \left(\frac{\alpha E}{\gamma}\right) \quad (5a)$$

For a more generalized relationship, such as non-linear, Eq. (4) was rewritten with exponents p, q, r and s for the dimensionless groups and was expressed as

$$\frac{VE^3}{\gamma^3} \propto \left(\frac{WE}{\gamma^2}\right)^p \left(\frac{vK}{\gamma C_p}\right)^q \left(\frac{TEC_p}{K}\right)^r \left(\frac{\alpha E}{\gamma}\right)^s \quad (5b)$$

Eqs. (5a) and (5b) were simplified and the wear equations were written with k_w as a proportionality dimensionless wear coefficient for both relationships. For the linear relationship

$$V = \frac{k_w W v T \alpha}{\gamma} \quad (6a)$$

and for the non-linear relationship

$$V = k_w W^p v^q T^r \alpha^s E^{-3+p+r+s} \gamma^{3-2p-q-s} (C_p/K)^{r-q} \quad (6b)$$

where the exponents p , q , r and s were to be determined experimentally.

These wear equations in terms of the wear coefficients were used to evaluate the wear coefficients for different polymers and determined whether the linear or non-linear relation was the most appropriate relationship between the wear volume and the other factors.

3. Experimental results

A horizontal pin-on-disk machine was used to develop the experimental data with a polymer pin sliding against the rim of a vertical steel disk [13]. Two types of steel disks were used: AISI 1018 steel and HTSR 4140 steel. Both disks were finished to specific surface roughnesses and tests were conducted at prescribed loads, speeds and test durations. At the end of the test the corresponding volume loss of polymer was measured.

From the test results it was seen that the difference in the volume loss of a polymer when sliding against the two different counterfaces was noticeable but did not vary significantly in magnitude. For the purpose of this analysis a single combined graph for volume loss against each operating variable with both counterfaces of similar roughness was used to represent the relationship.

For a given polymer–steel combination under different operating variables, tests were conducted in the humidity range of $\pm 5\%$ of the mean value. It was believed that the scatter in the experimental results was attributed to other uncertainties in conducting the experiment and not the result of minor changes in humidity.

3.1. Derivation of wear equation exponents

Graphs of volume loss of each polymer against both counterfaces for each set of tests were plotted both on linear and logarithmic (non-linear) co-ordinates for different operating conditions. The non-linear plot of wear volume against each operating variable determined the exponents p , q , r and s for Eq. (6b). An example

is shown for the polymer Delrin (POM) in Figs. 1 and 2. The data from each set of tests were best fit on to a straight line to explore which relationship was the most appropriate for each material combination. The regression coefficients indicated that the non-linear fit of the data provided a better correlation for the variables considered. It was noted that the exponents for operating variables in the case of a linear relationship were equal to one, whereas in the case of a non-linear relationship they were not equal to one. The mean slope of the straight lines were the exponents used in the non-linear model and are tabulated in Table 1.

It is seen from Table 1 that the exponents developed for Eq. 6(b) were different for each polymer and some general comments follow. For the polymers tested the exponent p with contact load was significant and was the highest for each polymer except for HDPE, for which the q exponent with speed was the highest. This suggests that load was the most critical operating variable. The exponent q with speed for Delrin and PVC were also significant. The exponent r with time for

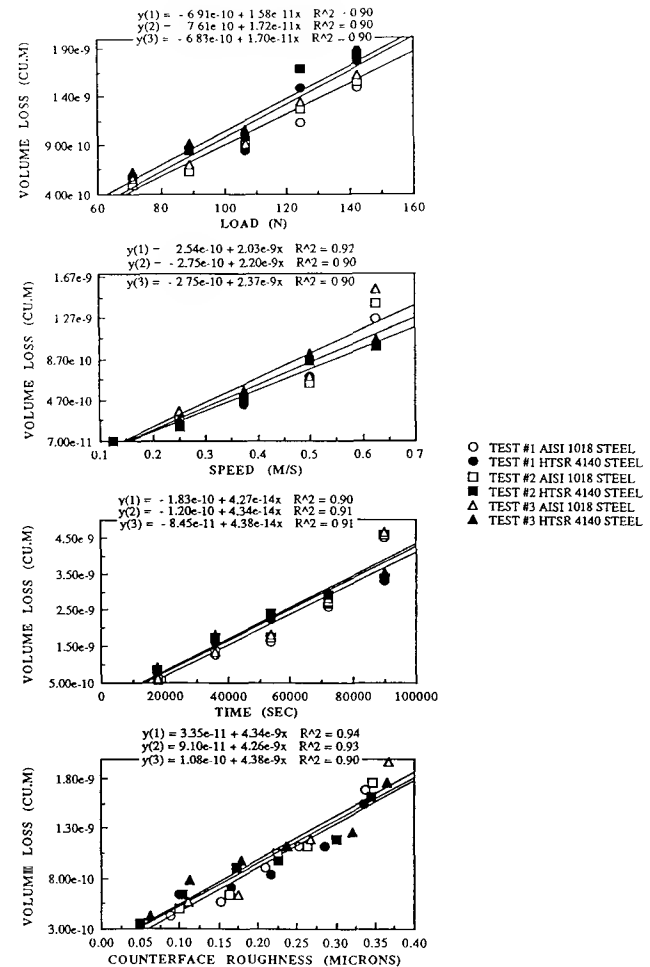


Fig. 1. Volume loss vs. different operating variables for Delrin on linear coordinates with best fit straight lines for each set of tests against both counterfaces.

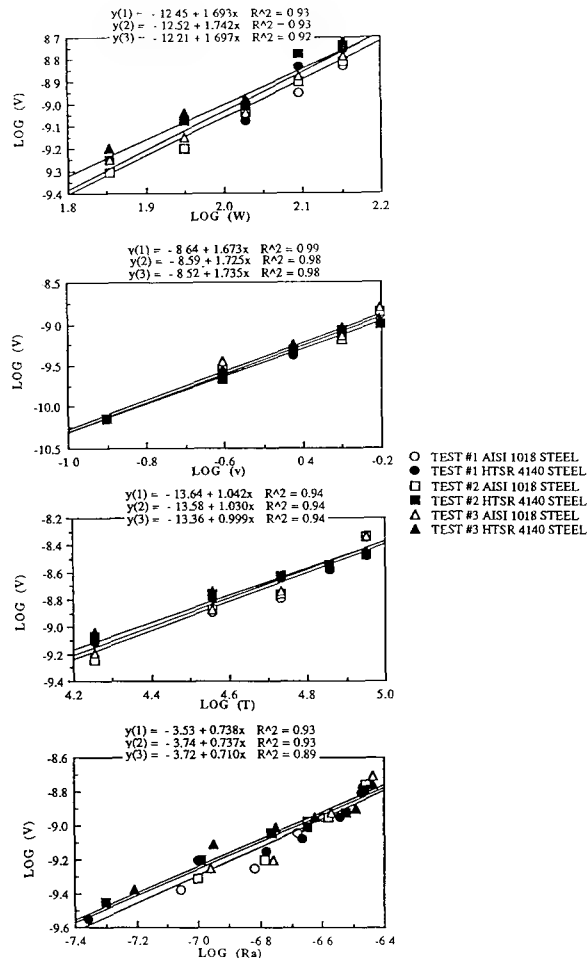


Fig. 2. Volume loss vs. different operating variables for Delrin on logarithmic coordinates with best fit straight lines for each set of tests against both counterfaces.

Delrin and HDPE were higher than the exponents in the same range for the other polymers. The exponents with all the operating variables for HDPE were comparatively higher than the exponents of all other polymers. The exponent s with counterface roughness for Teflon(m) (PTFE) was the lowest among all the exponents of the polymers which means that the wear of Teflon(m) was less affected with the counterface roughness than noted with the other polymers. According to the manufacturer Teflon(m) is processed

using recycled Teflon material. The exponents obtained show that, each operating variable had its own influence on the wear behaviour, which was not seen in the case of a linear relationship. Therefore, this suggests that the wear behaviour of these polymers may be explained better based on the exponents obtained from the non-linear relationship between volume loss of polymers and different operating variables. Thus, it was deemed more appropriate to base the empirical model on the non-linear fit of the data.

In Eq. (6a) the operating variables are directly proportional and surface energy is inversely proportional to the volume loss. Except for the surface energy, not all the other material properties are included in this equation. The wear coefficient is a number representing all the other variables not specified as individual factors in the equation. But this was not the intent as the main objective was to have as many of the known variables included in the equation. Eq. (6a) is written in terms of the wear coefficient as

$$k_w = \frac{V\gamma}{WvT\alpha} \quad (7)$$

From Eq. (7) the wear coefficient is seen as a function of volume loss, operating variables and the surface energy, which is a constant for the given material. Eq. (7) can be reduced to

$$k_w^* = \frac{V}{WvT\alpha} \quad (7a)$$

where k_w^* is the wear coefficient with surface energy included.

Except for the counterface roughness this is the equation developed by Lewis [3]. But this has been shown by other researchers to have limited application since it does not consider all the material properties which are known to influence wear.

With the non-linear representation the wear volume appeared to possess a unique relationship with each operating variable and with other material properties. Eq. (6b) is written in terms of the wear coefficient as

$$k_w = \frac{V}{W^p v^q T^r \alpha^s E^{-3+p+r+s} \gamma^{3-2p-q-s} (C_p/K)^{r-q}} \quad (8)$$

Table 1
Exponential parameters for different polymers against both counterfaces

Polymer	p (load)	q (speed)	r (time)	s (counterface roughness)
Delrin	1.711	1.711	1.024	0.728
High density polyethylene	1.364	2.425	1.229	1.470
Polyvinyl chloride	2.041	1.152	0.679	0.949
Rulon	1.381	0.665	0.764	0.625
Teflon(m)	1.497	0.695	0.772	0.258
Teflon(v)	1.287	0.845	0.681	0.610

Table 2
Material properties of different polymers

Material	Surface energy (N M ⁻¹)	Thermal conductivity (cal s ⁻¹ cm ⁻³ °C ⁻¹ cm ⁻¹)	Specific heat (cal °C ⁻¹ m ⁻¹)	Modulus of elasticity (N m ⁻²)
Delrin	0.0312	5.50×10^{-4}	0.35	3.1061×10^9
HDPE	0.0285	5.20×10^{-4}	0.55	1.0342×10^9
PVC	0.0347	2.80×10^{-4}	0.24	3.5232×10^9
Rulon	0.0184	7.92×10^{-4}	0.24	7.8944×10^8
Teflon(m)	0.0180	5.86×10^{-4}	0.25	6.5128×10^8
Teflon(v)	0.0180	5.86×10^{-4}	0.25	6.5128×10^8

Table 3
Average dimensionless wear coefficient of different polymers for the linear and the non-linear models

Polymer	Wear coefficient $k_w \pm \% \text{ error}$ (linear model)	Wear coefficient $k_w \pm \% \text{ error}$ (non-linear model)
Polyvinyl chloride	$2.08 \times 10^{-10} \pm 4.4\%$	$4.47 \times 10^{-19} \pm 2.1\%$
Delrin	$1.74 \times 10^{-10} \pm 4.0\%$	$3.59 \times 10^{-18} \pm 2.3\%$
High Density Polyethylene	$8.10 \times 10^{-10} \pm 6.1\%$	$1.12 \times 10^{-16} \pm 3.8\%$
Rulon	$6.26 \times 10^{-11} \pm 4.3\%$	$1.03 \times 10^{-11} \pm 2.2\%$
Teflon(m)	$1.07 \times 10^{-7} \pm 6.3\%$	$2.99 \times 10^{-9} \pm 0.7\%$
Teflon(v)	$9.91 \times 10^{-8} \pm 4.5\%$	$1.16 \times 10^{-5} \pm 2.2\%$

Eq. (8) incorporates most of the variables as individual factors and which are believed to be significant in the wear equation. It was expected that, this would yield a better representation of the wear coefficient than obtained from the linear analysis.

By substituting the material properties listed in Table 2 and experimental data into the Eqs. (7) and (8), the wear coefficients from linear and non-linear relationship for each polymer was evaluated. The dimensionless average wear coefficients of all polymers are tabulated in Table 3.

4. Discussion

A wear equation was written for each polymer material. For example, for Delrin sliding against both steel counterfaces, the wear equation for the linear model is given by

$$V = 1.74 \times 10^{-10} W v T \alpha \gamma^{-1} \quad (11a)$$

and for the non-linear model the equation is given by

$$V = 3.59 \times 10^{-18} W^{1.711} v^{1.711} T^{1.024} \alpha^{0.728} E^{0.463} \gamma^{-2.861} \times (C_p/K)^{-0.687} \quad (11b)$$

A similar wear equation can be written for other materials HDPE, PVC, Rulon, Teflon(m) and Teflon(v).

An analysis of the wear coefficients evaluated for all operating variables showed that the percentage error in the mean value of the wear coefficient was less than that found in the linear model. It can be seen from Table 3 that the wear coefficient explicitly represented the wear behaviour and did not mask the influence of

the material properties as they were independently represented in the wear equation. The wear coefficients from the linear model for all the polymers tested except Teflon(m) and Teflon(v) were approximately in the same range $((0.60-8) \times 10^{-10})$. This is because the linear wear equation used the same values for all the terms except surface energy and the wear volume, both of which did not vary largely for the materials evaluated. Therefore, the wear coefficients derived from the linear model provide little insight into the effect of material properties which are known to influence the wear process. From the statistical analysis of the wear coefficients, it was seen that the percentage error in the wear coefficient from the linear model were always higher than the wear coefficients from the non-linear model.

The principle of uncertainty [14] was applied to evaluate the fractional uncertainty in the wear coefficients for both the linear and the non-linear models. Substituting the fractional uncertainties of individual variables, the fractional uncertainty in the wear coefficient from the linear model was found to be to $\pm 10\%$. It was seen that the fractional uncertainties in V , γ , v and T had a negligible effect on the wear coefficient. The mean exponent was used for carrying out the uncertainty analysis of the wear coefficient from the non-linear model. The percentage error for the mean exponent was found to be within $\pm 3\%$ from the statistical analysis. The lowest fractional uncertainty of 4% was found with Teflon(m) and the highest was found for HDPE at 15%. The above analysis predicted different uncertainties in the wear coefficients for dif-

ferent polymers due to the non-linear relation between volume loss and the operating variables, whereas the linear model showed a single uncertainty for all polymers. This is unlikely since the wear coefficients for different polymers are not the same, as the wear coefficient is a unique function of different variables for a given polymer.

To study the sensitivity of the wear coefficients with operating variables, graphs were plotted for wear coefficient vs. operating variable. An example for Delrin is shown in Fig. 3. A large scatter in the wear coefficients from the mean value line was seen in the wear coefficients with each operating variable for most of the polymers tested. In some cases the wear coefficients seemed to be influenced by the variation in the operating variables, but this was not expected for the wear coefficient as they were assumed to be a proportionality

constant for a given polymer. The sensitivity analysis showed less scatter in the individual wear coefficients for each operating variable from the average wear coefficient. Thus, the wear coefficient was not as influenced by a variation in the operating variables. This is a significant and desirable feature of the proposed model. An example of the analysis is shown for Delrin in Fig. 4.

Table 3 shows that the order of the dimensionless wear coefficients from the non-linear model varied significantly for different polymers. This indicated the influence of the material properties (Table 2) which would not be seen in the case of the linear model. Teflon(v) had the highest wear coefficient and PVC the lowest of the polymers tested. In addition, the highest wear volume was seen for Teflon(v), whereas comparatively a lower wear volume was seen for PVC. For both PVC and Delrin the wear coefficients were

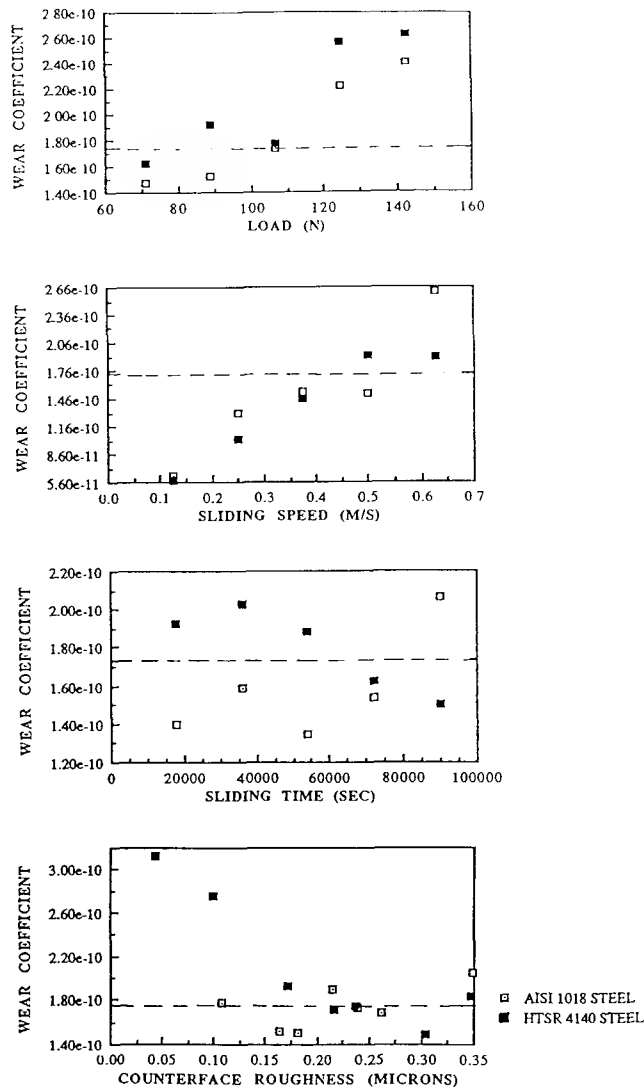


Fig. 3. Sensitivity of the wear coefficient of Delrin with the operating variables and scatter from the average wear coefficient (dotted line) for the linear model.

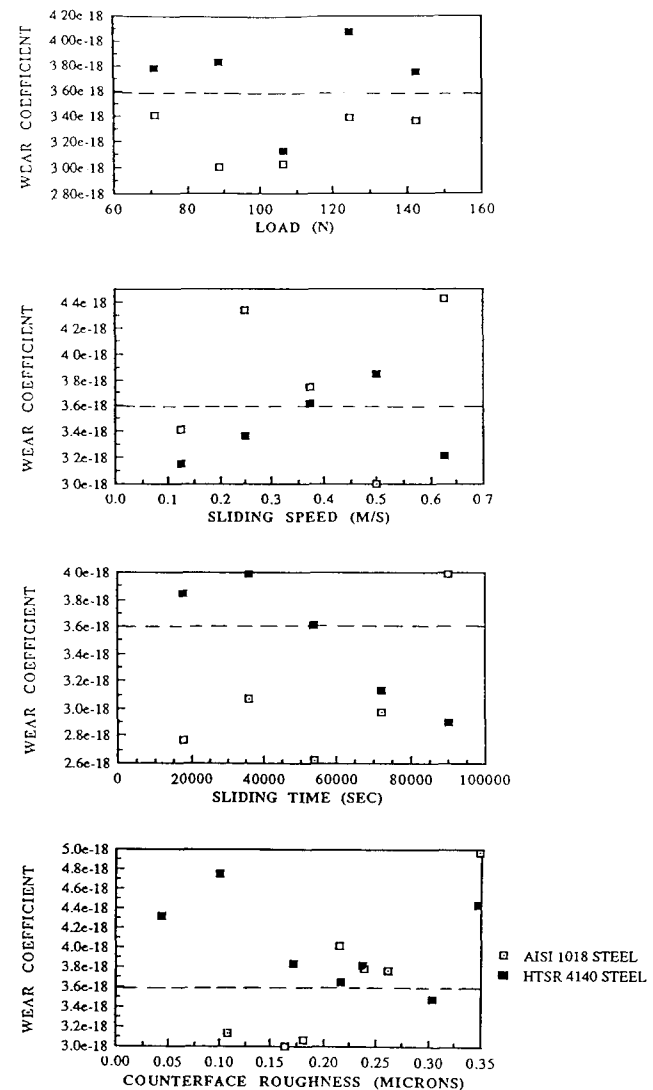


Fig. 4. Sensitivity of the wear coefficient of Delrin with the operating variables and scatter from the average wear coefficient (dotted line) for the non-linear model.

approximately of the same order. One of the important material parameters responsible for the low wear coefficient was their modulus of elasticity, which was the highest for both PVC and Delrin when compared to the other polymers. The same observation applies to HDPE and Rulon where HDPE had a comparatively lower wear coefficient than Rulon. All other material properties in the wear equation differed by a marginal value.

Among the polymers tested, PVC, Delrin and HDPE can be grouped within one category with their wear coefficient varying between three orders of magnitude. Teflon(m), Teflon(v) and Rulon (ceramic-filled fluorocarbon) can be grouped in another category with the wear coefficients of Teflon(m) and Teflon(v) varying between four orders of magnitude and Rulon, a filled fluorocarbon with two orders of magnitude lower than Teflon(m) and Teflon(v). This suggests that polymers having the same molecular structure may possess a common wear coefficient which is applicable under all conditions.

The material properties of Rulon did not vary much compared with those of Teflon whose modulus of elasticity and surface energy were lower than the other polymers considered. Rulon exhibited superior wear resistance compared with ordinary Teflon due to its composition and structure but had a lower coefficient of friction, similar to Teflon. As can be seen from Table 3, Teflon(v) had the highest wear coefficient indicating a higher volume loss. Teflon(m), which was made from recycled Teflon scrap, exhibited a comparatively better wear resistance due to cross linking of the Teflon matrix. The friction and wear results of Teflon(v), Teflon(m) and Rulon obtained during sliding against both counterfaces, along with SEM photographs of the worn surfaces, revealed that they have a unique wear behaviour independent of the counterface not seen with any other polymers. The similarity of the wear coefficients of these suggests these polymers can be considered within a single category.

The above analysis suggests that the wear coefficient can be used to represent the wear volume or wear potential of a particular polymer, but that a universal wear constant or coefficient may not exist for all the polymers.

5. Conclusions

The main aim of this research was to extend a dimensional analysis of wear of polymers to include the effects of counterface roughness. An empirical model in the form of a wear equation was developed based on a non-linear relationship between wear volume and other variables. In particular the following observations and conclusions were made.

- (1) It was shown that an equation for the wear of polymers involving operating variables and material properties could be reasonably represented by five dimensionless groups and that one of the groups contained the influence of counterface roughness.
- (2) A comparison of a linear and a non-linear relationship of volume loss of polymers showed that the wear volume was better represented by a non-linear proportionality with the operating variables.
- (3) Wear coefficients from the non-linear model confirmed that the material properties influenced the wear coefficient.
- (4) The wear coefficients found from the non-linear model had a lower percentage error than with the linear model. The sensitivity of the wear coefficients with changes in the operating variables was less in the case of the non-linear model.
- (5) On the basis of the polymers tested it was found that they could be grouped according to their wear behaviour and molecular structure.

Appendix A: Nomenclature

AISI	American Iron and Steel Institute
HDPE	high density polyethylene
HTSR	heat treated and stress relieved
POM	polyoxymethylene (Delrin)
PTFE	polytetrafluoroethylene
PVC	polyvinyl chloride
SEM	scanning electron microscope
Teflon(m)	Teflon (mechanical)
Teflon(v)	Teflon (virgin)
C_p	specific heat
E	modulus of elasticity
k_w	wear constant or coefficient
K	thermal conductivity
L	sliding length
$\{p, q, r, s\}$	exponential parameters
P	contact pressure
T	duration of test or sliding time
v	sliding speed
V	volume of worn material
W	contact force or normal load at the junction
α	counterface roughness
γ	surface free energy
μ	coefficient of friction

Acknowledgements

The authors express their sincere appreciation to the Natural Sciences and Engineering Research Council of Canada (Grant A-2705) for the financial aid in support of this research.

References

- [1] Z. Rymuza, Wear in polymer micro-pairs, *Proc. 3rd. Int. Conf. on Wear of Materials*, 1981, pp. 125–132.
- [2] S.B. Ratner, I.I. Farberova, O.V. Radyukevich and E.G. Lure, Connection between the wear resistance of plastics and other mechanical properties, *Sov. Plast.*, 7 (1964) 37.
- [3] R.B. Lewis, Predicting the wear of sliding plastic surfaces, *Mech. Eng.*, 86 (1964) 32–35.
- [4] S.K. Rhee, Wear equation for polymers sliding against metal surfaces, *Wear*, 16 (1970) 431–445.
- [5] J.K. Lancaster, Friction and wear, in A.D. Jenkins (ed.), *Polymer Science*, 1972, Chapter 14.
- [6] J.R. Atkinson, K.J. Brown and D. Dowson, The wear of high molecular weight polyethylene, Pt. 1. Isotropic polyethylene against dry stainless steel in unidirectional motion, *Trans. ASME, J. Lubr. Technol.*, 100 (1978) 208–218.
- [7] N.S. Eiss, Jr., K.C. Wood, J.A. Herold and K.A. Smyth, Model for the transfer of polymer to rough hard surfaces, *Trans. ASME, J. Lubr. Technol.*, 101 (1979) 212–219.
- [8] D. Dowson, S. Taheri and N.C. Wallbridge, The role of counterface imperfections in the wear of polyethylene, *Proc. 6th Int. Conf. on Wear of Materials*, 1987, pp. 415–425.
- [9] M.K. Kar and S. Bahadur, The wear equation for unfilled and filled poly oxymethylene, *Wear*, 30 (1974) 337–348.
- [10] N.S. Viswanath, An analysis of the wear of polymers, *Ph.D. Thesis*, University of Alberta, Edmonton, Canada, 1992.
- [11] E. Buckingham, Model experiments and the forms of empirical equations, *Trans. ASME*, 37 (1915) 263–296.
- [12] H.L. Langhaar, *Dimensional Analysis and Theory of Models*, Wiley, New York, 1951.
- [13] D.G. Bellow and N.S. Viswanath, An analysis of the wear of polymers, *Wear*, 162–164 (1993) 1048–1053.
- [14] J.R. Taylor, *An Introduction to Error Analysis—The Study of Uncertainties in Physical Measurements*, Oxford University Press, University Science Books, Mill Valley, CA, USA, 1982.

Selection of Grader Blades for Wear Resistance and Toughness

Donald G. Bellow

University of Alberta, Edmonton, Alberta, Canada, T6G 2J9

ABSTRACT

An experimental investigation was undertaken to evaluate the abrasive resistance and fracture toughness of a variety of steel alloys which can be used, or are being used, in the manufacture of grader blades. Abrasion resistance was determined by ASTM G 65-80 and fracture toughness by ASTM E436. The results indicated that the 1084 as-rolled material had the best wear resistance but the 10B30 through hardened material had the highest toughness, even though the material exhibited brittle behaviour at room temperature. It is suggested that the 5160H steel hardened to HRC 44 is a material that has 69% of the toughness of the 10B30 while it is 21% more wear resistant than the 10B30.

INTRODUCTION

Grader blades used in earth moving equipment and for snow and ice removal on roadways are required to have high resistance to abrasion but at the same time be resistant to fracture under impact loads at low temperatures. Manufacturers provide a variety of steels depending on the users' specifications which usually are based on costs and field experience. There are no standards in the industry for the selection of grader blade materials other than hardness and chemical composition, although sometimes users will specify tensile strength. The objective of this investigation was to evaluate a number of steels as to their abrasion resistance, strength and toughness and to recommend which material(s) are best suited for grader blades.

TESTING PROGRAM

A number of different steels were supplied from a rolling mill which included some identical alloys but from different heats of steel. Table 1 lists the materials tested along with their respective heat treatments and hardnesses of the specimens as tested. The oil quenched specimens were austenitized at 885 °C for 30 min. The water quenched specimens were austenitized at 870 °C. The tensile tests were run according to ASTM E-8. Hardness was measured on the Rockwell C scale. Figure 1 shows the yield and tensile strengths as a function of hardness. Both the yield and the tensile values increased with an increase in hardness in the range HRC 27-37. For hardnesses greater than HRC43 the yield and tensile strengths tended to level off at maximum values of approximately 1475 MPa for the yield stress and 1675 MPa for the tensile strength.

The abrasion tests were conducted according to ASTM G-65-80 standard. Specimens were machined to

25x76x12 mm and the machine used dry silica sand which flowed between a rubber wheel, which rotated at 200 rpm, and the specimen. Each test was terminated after 6000 revolutions of the wheel. The specimens were weighed before and after each test to determine the weight loss in grams. For all abrasion tests six specimens were machined from the steel samples as supplied by a rolling mill; three in the longitudinal

Table 1 Heat Treatment of Grader Blade Materials

Grade	Heat Treatment	Hardness HRC
10B30	water quenched, tempered in salt bath to 227°C for 20 min.	47.5
1045(1)	as rolled	37.5
1045(2)	as rolled; different heat	48
1084	as rolled	27.5
1541(1)	as rolled	37
1541(2)	as rolled; different heat	47.5
4140(1)	oil quenched and tempered at 316°C for 30 min.	31
4140(2)	oil quenched and tempered at 649°C for 30 min.	47
5160H(1)	oil quenched and tempered at 399°C for 20 min.	29.5
5160H(2)	oil quenched and tempered at 603°C for 20 min.	44
8640(1)	oil quenched and tempered at 316°C for 20 min.	33
8640(2)	oil quenched and tempered at 621°C for 30 min.	46

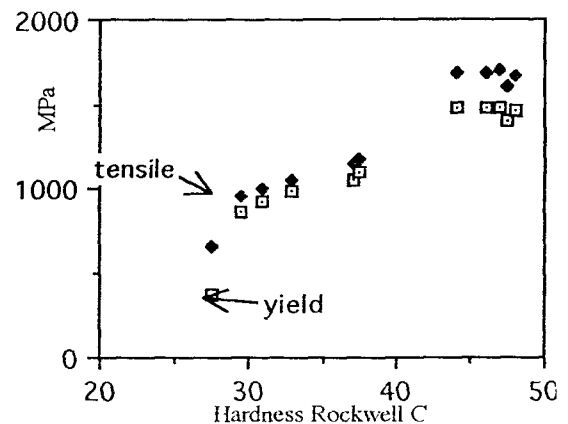


Fig. 1 Yield and tensile stress as a function of hardness.

direction and three in the transverse direction. There was no significant difference in the abrasion resistance in these two directions. Similarly, there was no difference in the yield and tensile values in the two directions.

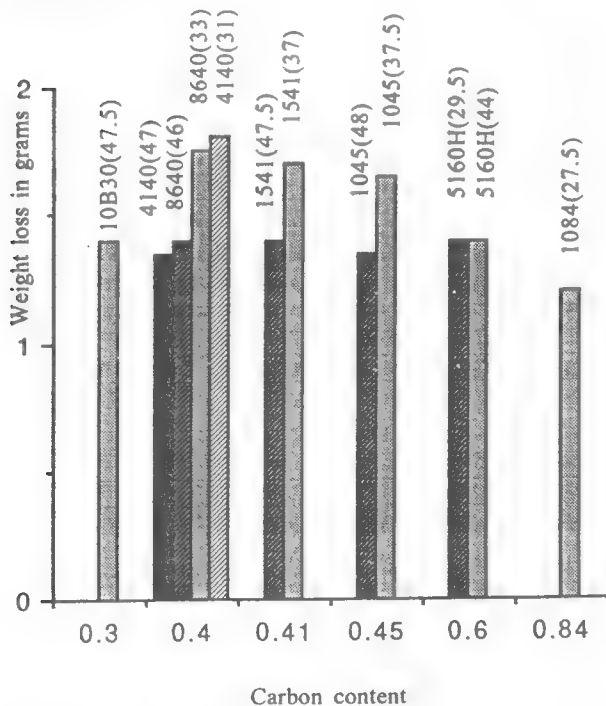


Fig. 2 Wear as a function of carbon content.

Figure 2 shows the ranking of materials with respect to abrasive wear and carbon content. Atop each bargraph, after the alloy type, is the hardness value. It is seen from this figure that hardness alone does not determine the abrasion resistance. Also, it is noted that the lower the carbon content the harder the material. For the alloys with 0.4 and 0.41 carbon content it is clear that hardness influenced the abrasive wear. Better wear resistance was obtained from the harder material. However, for the 5160H material there did not seem to be any benefit to the resistance to wear by increasing the hardness from 29.5 to 44 HRC. The 1084 material had the best resistance to abrasion although its hardness was only 27.5 HRC. One characteristic of this alloy which may explain this, in part, is that its combined carbon and manganese content was higher than the other materials evaluated.

Considerable difficulty was experienced in determining a suitable test for toughness. A number of ASTM Standards were considered and evaluated. As a preliminary evaluation, standard size Charpy specimens were tested with the 10B30 and 1084 materials in an attempt to determine the brittle to ductile transition temperature. Full thickness specimens were also

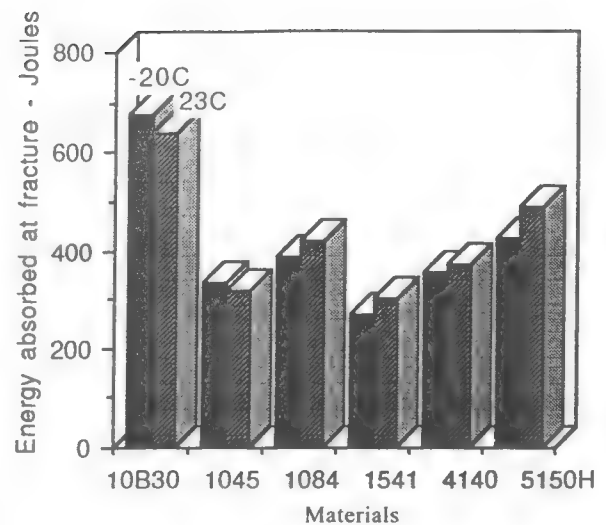


Fig. 3 Fracture toughness of steel alloys.

prepared and tested according to ASTM E436. From these tests it was clear that a transition temperature was not evident at room temperature or less and that brittle behaviour was prevalent. In other words, the energy absorbed at fracture was from the "lower shelf" of the energy-transition temperature diagram. Fortunately, access to a large Charpy machine at a pipe mill enabled specimens 75x305x12.5mm to be tested. These specimens had an edge notch pressed according to ASTM E436. The specimens were supported at the ends (on the edges) and the impact was applied to the edge opposite to the notch. Two testing temperatures were used, 23°C and -20°C, to confirm that the measured energy values were from the "lower shelf". Averaged results for the fracture tests are plotted in Fig. 3 which show that the highest energy levels were obtained from the 10B30 steel followed by 5160H (HRC 44), 1084 (HRC 27.5) and 4140 (HRC 47). The lowest toughness was exhibited by 1045 (HRC 48) and 1541 (HRC 47.5).

CONCLUSIONS

Of the alloys tested there was no material which combined both the highest toughness with the best abrasion resistance. Field experience will determine whether wear resistance or toughness should be the primary specification. Where breakage is commonplace then the 10B30 material may be preferred. On the other hand, it is seen that superior wear resistance can be obtained from an as-rolled 1084 material. It is suggested that a compromise material that combines both good wear resistance with toughness is 5160H hardened to HRC 44. This material possesses 69% of the toughness of the 10B30 but is 21% more wear resistant than the 10B30 and is 13% tougher than 1084.

EFFECT OF SAND CONTAMINATION ON SLIDING WEAR

Donald G. BELLOW¹ and Gaby H. SONEGO²

¹*University of Alberta, Edmonton, CANADA*

²*Black Max-Downhole Tool Ltd., Nisku, Alberta, CANADA*

This paper describes the results of an experiment to determine the influence of the degree of sand contamination on the wear of pairs of sliding components. The results are applicable to down hole oil field components where sand contamination is often encountered between sucker rod couplings and oil well tubing. Five different sand rates of contamination were evaluated and it was found that there was an approximate linear relationship between the wear of the sliding surfaces with the amount of sand introduced into the wear process. Even with a relatively small amount of sand contamination of 15 g/day it is shown that at a sliding distance of 300,000m the wear of both the coupling and the tubing was more than double that if no sand were present.

Keywords: Sliding wear, sand contamination, sucker rod couplings, oil well tubing

1. INTRODUCTION

In evaluating the sliding wear of metal surfaces in the laboratory third body abrasives are sometimes introduced. This is done especially where the presence of such contaminants may be found in practice. One case in point is the evaluation of the wear of down hole oil field components. In oil wells requiring an artificial lift system a plunger type pump at the bottom of the well is activated by a walking beam apparatus on the surface attached to a series of sucker rods and couplings which reciprocate up and down within a steel oil well tubing. During the pumping operation the sucker rods and couplings rub against the tubing which can lead to severe wear causing either the sucker rod string to break or the tubing to perforate. In either case a loss of oil production results. These problems are exacerbated when the well is slanted or deviated or when the fluid being pumped is corrosive or abrasive.

In oil wells sand is often encountered which can lead to excessive wear between the couplings and the oil well tubing. To simulate oil field conditions in the laboratory is difficult at best, and to take into account the effect of sand contamination only adds to the problem. However, laboratory tests are useful in understanding the down hole wear behaviour of tubing and couplings without resorting to costly and often inconclusive field trials.

In many experiments incorporating a third body abrasive the apparatus has been designed to use a sand slurry. This usually consists of surrounding the wear specimens in a water solution in which a known quantity of sand is kept in suspension by means of vigorous agitation. This adequately serves the purpose of evaluating the effect of sand on the sliding wear of two interfaces in a

"worst case" scenario. However, unless a fresh solution is prepared for each test and each test is of a relatively short duration the sand, eventually, is reduced in particle size and its influence is also reduced. Under field conditions the sand is not thought to recirculate but rather pass through a sliding interface only once. On the other hand, experiments which introduce sand onto the sliding interfaces in a continuous fashion are thought to be less severe although they avoid recirculating the sand debris of reduced particle size.

In actual oil field practice third body abrasives are avoided if at all possible. Unfortunately, in some oil wells sand contamination does occur and excessive wear is accepted as a cost of producing oil in such situations. It is of interest to know, therefore, if under such conditions whether or not the wear of sliding surfaces is affected by the degree of sand contamination, or if there is any correlation with the amount of wear recorded. It is also desirable to determine the most appropriate way to evaluate the wear of down hole oil field components subjected to sand contamination.

A number of research studies on sucker-rod/coupling and tubing wear have been reported in the literature (1-3). A recent paper (4) describes the difficulties in equating field experience with laboratory results. The correlation of results between the field and the laboratory is improved if the laboratory conditions can more closely represent the conditions in the field. Thus, it follows that if sliding wear of oil field components is to be evaluated in the presence of a third body abrasive, which may occur in minute quantities, it is important to evaluate such wear in the laboratory under conditions similar to known field conditions. The purpose of this paper is to evaluate the

sliding wear of sucker rod couplings with oil well tubing using different rates of sand contamination.

2. EXPERIMENTAL PROCEDURE

Sucker rod coupling and oil well tubing wear has been successfully carried out (1) using the apparatus shown in Fig.1. Oil well tubing was cut lengthwise and formed the stationary base upon which sucker rod couplings reciprocated back and forth under predetermined contact loads. The oil well tubing was of a type J55 ERW (electrical resistance welded) and was prepared for testing by honing to an initial surface roughness of 3.7 microns. The initial hardness of the tubing was 180HV measured using a 785g indenter.

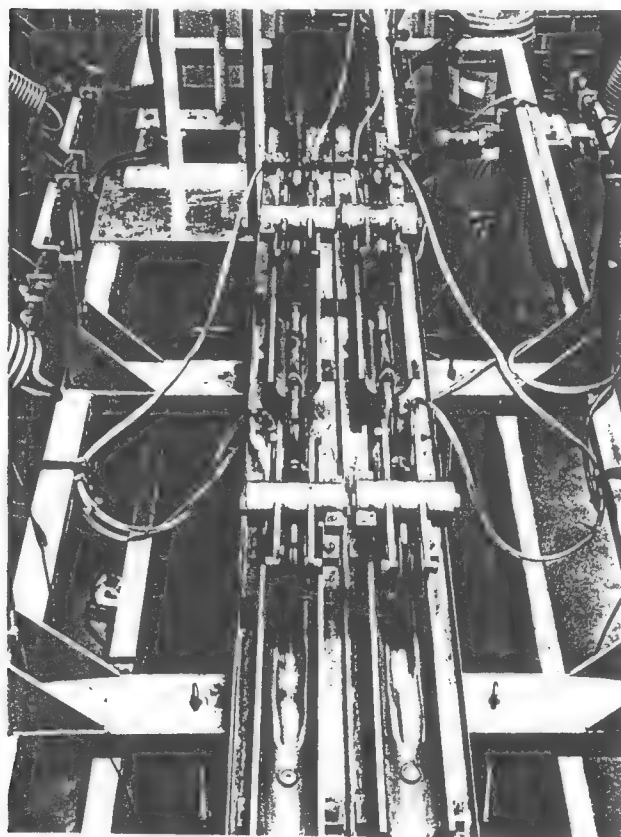


Fig. 1 Overall view of the wear apparatus

The testing procedure consisted of reciprocating the couplings back and forth along the tubing at a stroke rate of 44 strokes/min over a stroke length of 0.41m. A constant contact load was applied by means of a calibrated spring loaded carriage atop the couplings. The stroke speed used in the laboratory was 18m/min which compares with oil field conditions varying anywhere from 5-25 strokes/min, 0.3-1.5m stroke length, or stroke speeds of 1.5-37.5 strokes/min. A typical laboratory test was run for 11-1/2 days during which time a total accumulated sliding distance of 300,000m occurred. Wear measurements in terms of coupling weight loss and tubing thickness loss were recorded at intermediate intervals of distance traveled.

The sliding wear experiments were conducted with water as the medium of lubrication. Water was chosen

rather than oil because it added an element of corrosivity to the wear process, and represents more closely many older wells where more than 95% of the fluid being pumped is water.

With reference to Fig. 1, a constant stream of domestic water (0.5 l/min) was introduced at one end (top end of the photograph) and was allowed by gravity to flow down the oil field tubing which was set at an incline. In this way the surfaces of the tubing and the couplings were constantly wet. Wear tracks on the tubing surfaces are visible in Fig.1.

In order to evaluate the wear of the couplings and tubing in a sand environment a sand dispensing apparatus was designed and built as shown in Fig. 2. Dry sand, which was continuously stirred in a hopper, was gravity fed through a tube to the side of a cavity milled into a Teflon block. A 4.5mm thick metal disc with a series of 2mm holes drilled around its perimeter rotated between a pair of Teflon blocks. As the disc rotated, the holes filled with sand and were carried to an exit point where a small jet of air blew the sand out of the hole in the disc into a hole in a second Teflon block on the opposite side and then into a vertical tube which conveyed the sand onto the wear track. By varying the rotational speed of the disc a precise amount of sand could be introduced onto the wear track of the sliding pairs. Sand entered the water flow upstream of the wear track between the couplings and the oil well tubing. Neither the water, the sand, nor the metal debris were recirculated and allowed to re-enter the wear track. Of course, not all sand thus dispensed into the water stream would find its way between the sliding pairs. However, the manner in which the sand was introduced was the same for all experiments and repeated tests confirmed the precision of the system. The sand grit was Ottawa 50-70.

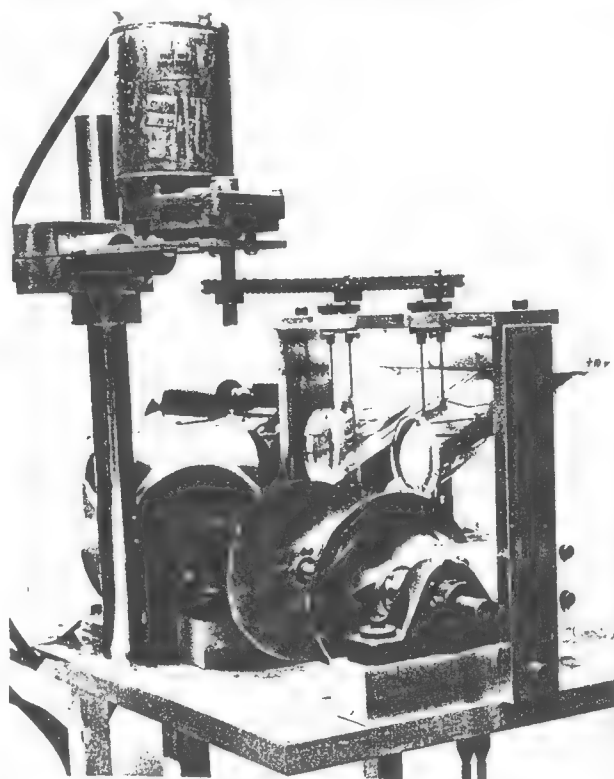


Fig. 2 Detailed view of the sand metering device

The test specimens used a standard type sucker rod coupling, 46mm in diameter and 100mm long, made from cold extruded AISI 8630 steel with an initial hardness of 190 HV (785g).

EXPERIMENTAL RESULTS

The experimental results presented in Figs. 3 and 4 show the coupling weight loss and tubing thickness loss for five sand rates of contamination (0, 15, 100, 165, and 180 g/day) at a constant contact load of 133.5N. Wear was measured at intervals of 10,000, 100,000, 200,000 and 300,000 meters of travel. As might be expected, the wear of both the coupling and the tubing increased with an increase in sand contamination.

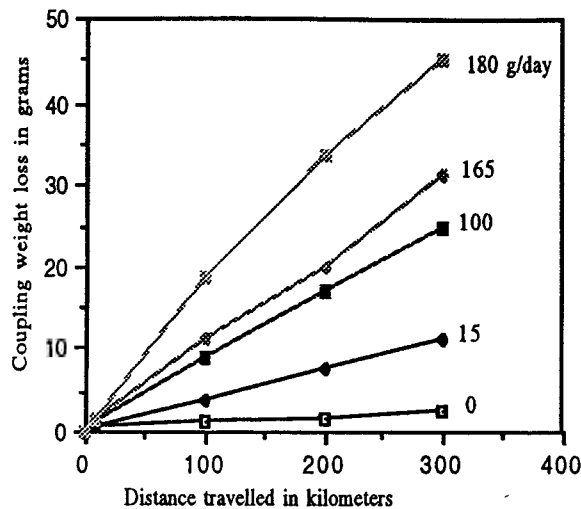


Fig. 3 Coupling weight loss for different sand rates of contamination

Calculating the wear rate of the couplings, as volume of material removed per distance-force, shows in Fig. 5 that at the low sand rate of 15g/day, the wear rate was approximately constant, but at higher sand rates the sand rate decreased with increased distance traveled. This was probably because of the geometrical shape of the sliding surfaces which increased in contact area as the wear traveled increased. As the contact load was kept constant throughout the test the result of increasing the contact area reduced the contact pressure, thus reducing the wear

Figure 6 shows the effect of the rate of sand contamination on the weight loss of the coupling. These results were obtained at a contact load of 133.5N after 300,000m of wear travel. The results show an almost linear weight loss with the degree of sand contamination.

In the absence of sand the wear mechanism was observed to be primarily caused by adhesion as can be seen from the SEM of the tubing wear in Fig. 7. Although at higher contact loads a certain amount of abrasive wear also occurred. This was probably caused by the length of the wear specimen which enabled metal debris to be trapped between the contact surfaces. When sand was present the wear mechanism was abrasive as can be seen in Fig. 8.

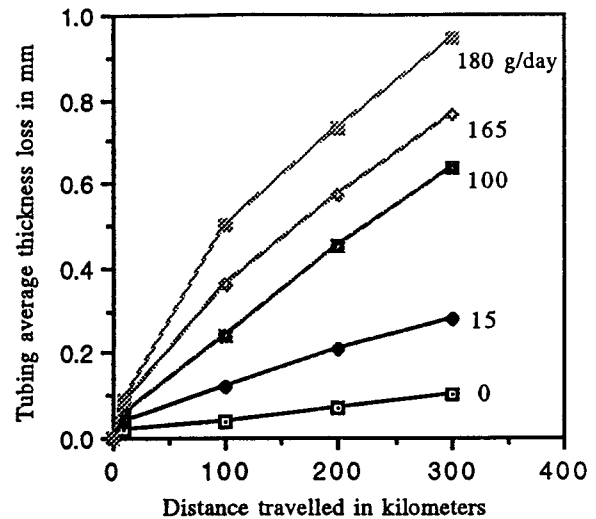


Fig. 4 Tubing average thickness loss for different sand rates

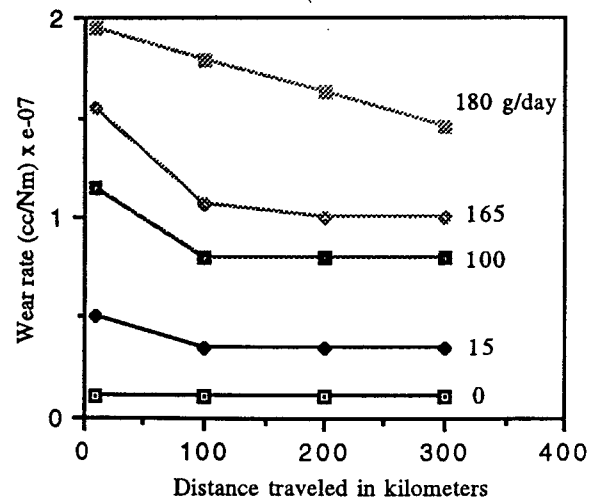


Fig. 5 Coupling wear rate for different rates of sand contamination

Both the SEM's in Figs. 7 and 8 also show evidence of corrosion products and fatigue cracks. The SEM in Fig.9 shows a silica sand particle that was imbedded into the tubing surface. This would have contributed to excessive wear of the coupling and indicates also that not all the sand that entered the wear track passed through quickly. Figure 10 shows the end view of a coupling and the tubing after an 11-1/2 day test period (300,000m of wear travel) at a contact load of 445N. This was at a sand rate of 165g/day. The coupling had worn almost through to the internal thread roots. This wear is typical of specimens taken from the field where sand is known to be prevalent in the well. When such wear occurs

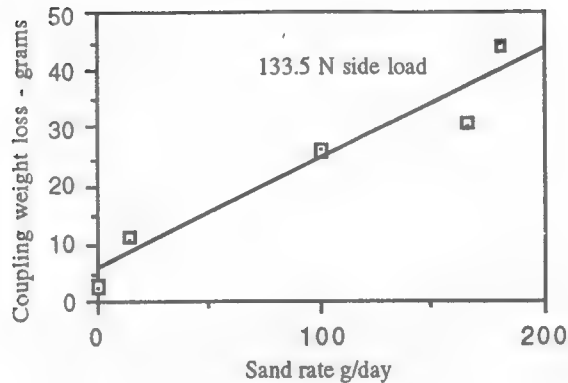


Fig. 6 Coupling weight loss after 300,000m of wear travel for different sand rates of contamination

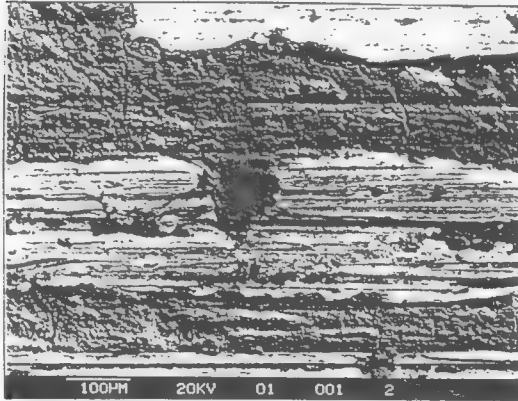


Fig. 7 SEM of tubing wear track, no sand contamination, x120

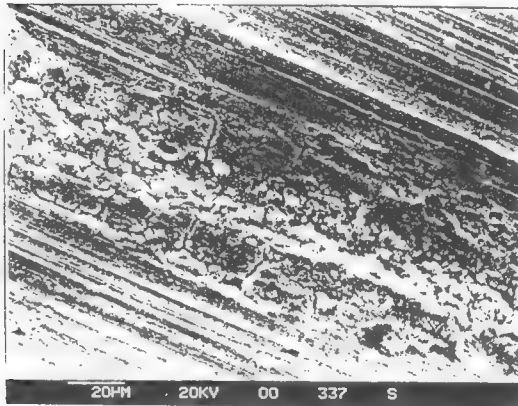


Fig. 8 SEM of tubing wear track with sand contamination, x350

in an oil well it often leads to failure of the sucker rod string due to the reduced cross-sectional area causing the axial stresses to exceed the ultimate tensile strength.

Previous research (1) has shown that the wear of the sucker rod couplings and the tubing leads to work hardening as well as changing the profile and roughness of the surfaces. In Fig. 11 it is shown how the surface roughness changed, measured in microns (μm). Generally speaking, for a given sand rate, the surface roughness decreased with an increase in the length of wear travel. This was opposite to what was expected in that if the sand rate of contamination was increased it was expected that the surface roughness would also increase. This may be partly explained by the fact that full size couplings were used in the experiment and, because of their relatively large size, and despite the extra care taken in measuring, it was difficult to obtain a truly representative measurement of the surface roughness. Also, there were local areas which work hardened differently than adjacent areas, although all were within the overall contact area. Surface roughness was measured using a stylus and Talysurf IV instrument. Such a measurement is very dependent on the alignment of the stylus along the wear track and from Figs. 7-9 it is easy to see how different roughness readings could be obtained depending on the placement of the stylus.

It is evident from Fig. 12 that the surface hardness of the tubing increased with an increase in distance traveled and with an increase in the rate of sand contamination. Similar results were observed with changes in the hardness of the coupling. At the higher sand rates the surface had more work hardening after 300,000m of wear travel. For example, at a contact load of 133.5N, with no sand present, the Vickers hardness increased from 180 to 220 VHN after 300,000m of wear travel. With the introduction of sand at a rate of 180g/day the surface hardness of the coupling increased from 180 to 300 VHN under the same load and distance traveled. Clearly, the surface work hardened as a result of a plowing action of the sand in addition to its abrasive effects.

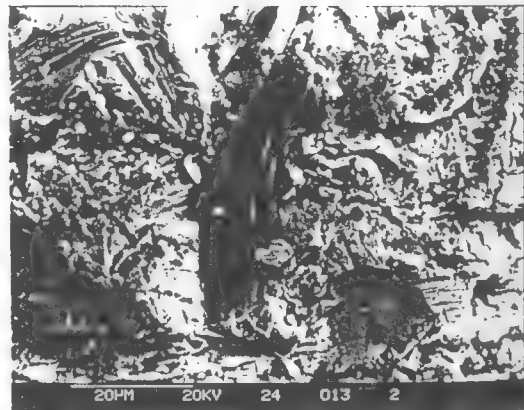


Fig. 9 Imbedded sand particle in tubing surface, x1000

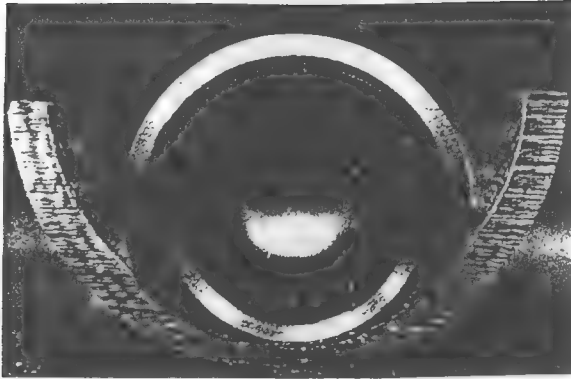


Fig. 10 End view of worn coupling and tubing

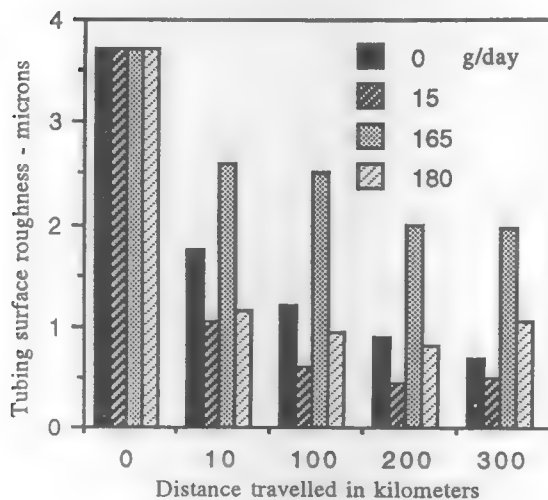


Fig. 11 Tubing surface roughness at different sand rates of contamination

4. SUMMARY

Ideally no sand should be allowed to contaminate a sliding pair. However, in oil wells sand contamination is sometimes unavoidable and it is therefore necessary to determine the effect this contamination has on the wear of components such as sucker rod couplings sliding against oil well tubing.

The wear of components subjected to sand contamination is evaluated in the laboratory by either the use of a sand slurry or by metering small amounts of sand into a fluid medium such as described in this paper. The introduction of sand through a dispensing system which meters the sand in precise amounts is thought to be preferable because it can more closely evaluate the minute effects of sand as a contaminate that occurs in actual down hole oil well conditions. Sand slurries are useful in ranking materials but this testing procedure does not necessarily represent actual oil well conditions.

Even if the sand is metered out in precise amounts, as described in this paper, there is no guarantee that all the sand will enter the wear track between the sliding surfaces. As the data of these experiments show,

some unexpected results were obtained relative to surface roughness and hardness changes with increased sand rates. These anomalies may have been due to the surface profiles that were developed during the wear process which, in some cases, allowed more or less sand to intervene between the sliding pairs.

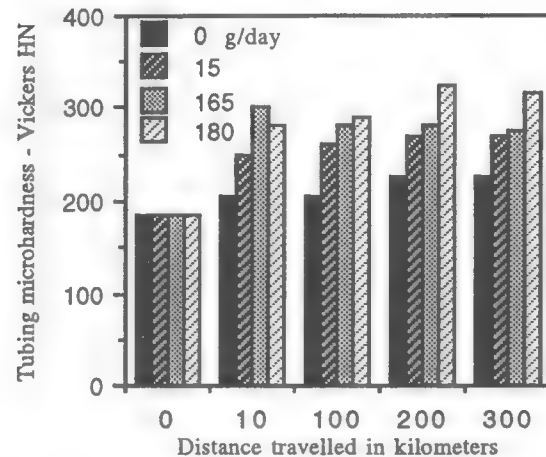


Fig. 12 Tubing micro hardness for different rates of sand contamination

Overall the experiment was considered successful in that it demonstrated that even with a small amount of sand contamination, i.e., as little as 15g/day, over a sliding distance of 300,000m and at a contact load of 133.5N, the wear of oil well sucker couplings and tubing was more than double that when no sand was present.

The results of this investigation can be applied to those experiments which use a sand slurry in as much as the percentage of sand per volume of water will influence the amount of wear to be expected. For example, it should be expected that an eight percent concentration of sand will cause about twice the amount of wear as a four percent solution.

5. ACKNOWLEDGMENTS

The authors express their appreciation for the assistance given to this project by the Natural Sciences and Engineering Research Council of Canada (A-2705). Thanks are also due to the staff in the Department of Mechanical Engineering machine shop; to Mr. Bernie Faulkner, Mr. Al Muir and Mr. Max Schubert for their assistance and helpful suggestions in building the apparatus, and to Mr. John Foy for his help in photography.

6. REFERENCES

1. Bellow, D.G., Owen, D.C. and Smuga-Otto, I., *Wear*, Vol.133, Elsevier (1989) 83-93.
2. Ko, P.L. Humphries, K. and Mathews, C., *Wear of Metals*, ASME (1989) 681-687.
3. Schumacher, W.J., *Matls. Conf. NACE*, Vol. 30 No. 9 (1991) 62-64.
4. Bellow, D.G. *Eurotrib'93*, Budapest, Vol. 5 (1993) 417-421.

DATE DUE SLIP

F255

University of Alberta Library



0 1620 0613 9628